

FINAL REPORT
LONG-TERM MONITORING GROUNDWATER OPTIMIZATION
AT OU-12 LORING AFB, MAINE USING THE GEOSTATISTICAL
TEMPORAL/SPATIAL (GTS) ALGORITHM

CONTRACT NUMBER: F41624-00-D-8030
TASK ORDER 0062
TASK 4

May 2004

Submitted to:

HQ AFCEE/BCE
3300 Sidney Brooks Road
Brooks City-Base TX 78235

Submitted by:

Science Applications International Corporation
11251 Roger Bacon Drive
Reston, VA 20190

SAIC Project No. 06-6312-04-4567-004

This page left intentionally blank for duplicating purposes.

Table of Contents

Introduction	1
Section 1. Executive Summary	2
Section 2. Description of Site OU-12, Loring AFB	3
Section 2.1. Site Hydrogeology and Contaminant Sources	3
Flow Field 1	4
Flow Field 2	4
Flow Field 3	5
Flow Field 6	6
Flow Field 8	6
Section 2.2. Monitoring Network	6
Section 3. Temporal Optimization at Site OU-12	9
Section 3.1. Data Preparation.....	9
Section 3.2. Temporal Methodology	11
Section 3.2.1. Temporal Variograms	11
Section 3.2.2. Iterative Thinning.....	14
Section 3.3. Trend Mapping.....	20
Section 3.4. Temporal Optimization Results	21
Section 3.4.1. Temporal Variograms	21
Section 3.4.2. Iterative Thinning.....	22
Section 3.4.3. Trend Maps	27
Section 4. Spatial Optimization	47
Section 4.1. Data Preparation.....	47
Section 4.2. Methodology	48
Section 4.2.1. Declustered CDF.....	48
Section 4.2.2. Spatial Bandwidth and Search Radius	51
Section 4.2.3. Creating Base Maps with LWQR	52
Section 4.2.4. Constructing the Base Map.....	54
Section 4.2.5. Global Regression Weights.....	56
Section 4.2.6. Local and Global Variance Measures	57
Section 4.2.7. Iterative Elimination of Wells.....	58
Section 4.3. Spatial Optimization Results.....	58
Section 4.3.1. Global Measures of Redundancy	59
Section 4.3.2. Local Indications of Redundancy	61
Section 4.3.3. Base Map Accuracy	62
Section 5. Recommendations for Loring AFB, Site OU-12	63
Section 5.1 Recommendations Regarding Sampling Frequency	63
Section 5.2 Recommendations Regarding Spatial Redundancy	65
Section 5.3 Recommendations Regarding Siting of New Wells	71
Section 5.4. Cost Analysis and Costing Methodology	74
Section 5.4.1. Initial Monitoring and Cost Information.....	74

Section 5.4.2. Creating the Baseline 74
 Section 5.4.3. Scenario Cost Estimates..... 75
 Section 5.4.4. Resulting Costs Savings..... 76
Section 6. References 77

Appendixes

Appendix 3-1 Temporal Optimization: Temporal Variograms
 Appendix 3-2 Temporal Optimization: Benzene Iterative Fitting Overlays
 Appendix 3-2 Temporal Optimization: FE Iterative Fitting Overlays
 Appendix 3-2 Temporal Optimization: MN Iterative Fitting Overlays
 Appendix 3-3 Temporal Optimization: BZ Iterative Fitting Results
 Appendix 3-3 Temporal Optimization: FE Iterative Fitting Results
 Appendix 3-3 Temporal Optimization: MN Iterative Fitting Results
 Appendix 3-4 Temporal Optimization: Trend Maps
 Appendix 4-1 Spatial Optimization: Global Redundancy Measures
 Appendix 4-2 Spatial Optimization: BZ Indicator Difference Maps
 Appendix 4-2 Spatial Optimization: FE Indicator Difference Maps
 Appendix 4-2 Spatial Optimization: MN Indicator Difference Maps
 Appendix 4-3 Spatial Optimization: BZ Local Variance Maps
 Appendix 4-3 Spatial Optimization: FE Local Variance Maps
 Appendix 4-3 Spatial Optimization: MN Local Variance Maps
 Appendix 4-4 Spatial Optimization: BZ Base Concentration Maps
 Appendix 4-4 Spatial Optimization: FE Base Concentration Maps
 Appendix 4-4 Spatial Optimization: MN Base Concentration Maps
 Appendix 5-1 Estimate of Cost Savings (MS Excel file)

Figures

Figure 5-1. Approximate Locations of Greatest Local Uncertainty 73

Tables

Table 2-1. Existing OU-12 Baseline LTM Network (all measurements in feet)..... 7

Table 3-1. COC Detection Frequencies 10

Table 3-2. Well Detection Rates for Selected COCs 10

Table 3-3. Temporal Variogram Ranges and Recommended Sampling Interval 22

Table 3-4. Summary of Iterative Thinning Results, By COC and Well Location 23

Table 3-5. Optimal Sampling Intervals and Frequencies Measured Across All COCs.... 26

Table 3-6. Estimated Trend Magnitudes and Confidence Intervals by COC and Well Location 29

Table 4-1. Parameters of Final Spatial Correlation Models 50

Table 4-2. Reference Concentrations and Corresponding Percentiles of Declustered CDF for Each COC 53

Table 4-3. Boundaries of Optimization Box 55

Table 4-4. Hypothetical LWQR Results for Benzene 55

Table 5-1. Example Sampling Plan for the First Year of the Optimized LTM Sampling Program 65

Table 5-2. Essential Monitoring Network Based on Analysis of All COCs (All measurements in ft) 67

Table 5-3. Redundant Monitoring Wells Based on Analysis of All COCs (All measurements in ft) 69

Table 5-4. Essential Monitoring Network Based on Benzene Analysis (All measurements in ft) 69

Table 5-5. Redundant Monitoring Wells Based on Benzene Analysis (All measurements in ft) 71

Table 5-6. Approximate Well Locations of Greatest Local Relative Uncertainty 73

Table 5-7. Estimate of Cost Savings 77

This page left intentionally blank for duplicating purposes.

Long-Term Monitoring Groundwater Optimization at OU-12 Loring AFB, Maine Using the Geostatistical Temporal/Spatial (GTS) Algorithm

Prepared by SAIC and MacStat Consulting, Ltd., May 2004

Introduction

This report summarizes the effort to optimize the existing long-term groundwater monitoring (LTM) network at site OU-12 on Loring Air Force Base in Maine. The optimization analysis is based on an application of the Geostatistical Temporal/Spatial (GTS) algorithm, which was designed for the Air Force Center for Environmental Excellence (AFCEE) by MacStat Consulting, Ltd. The analysis and the algorithm consist of two basic parts: a temporal optimization component and a spatial optimization component. The twin goals of the study are to determine, based on the existing sampling data and sampling network, 1) to what extent sampling frequencies at the site can be optimized so as to pare sampling and analysis budgets efficiently, and 2) to what extent locations within the sampling network can be optimized so that sampling information is not being collected at statistically redundant groundwater wells. Set against these goals is the overriding mandate that information critical to the success of the LTM program at site OU-12 should not be sacrificed.

It should be noted that GTS is not designed around a traditional hypothesis testing framework. As an example, considering the spatial analysis, rather than deciding whether or not the mean concentration level at the site is above or below a fixed concentration limit, and then designing the monitoring network with the goal of balancing the risks of false positive and false negative decision errors, GTS is fundamentally aimed at balancing a different kind of trade-off. In particular, GTS assumes that the existing network of sampling locations is the 'most informative' available, and that a map of the spatial distribution of concentration levels based on all the existing sampling information is the most accurate map that can be estimated barring significant numbers of additional well locations. Under this presumption, GTS then balances the information lost in map accuracy against the savings in sampling and monitoring resources that otherwise would be spent maintaining the current network. Optimization is thus defined with respect to this accuracy-cost trade-off and not with respect to the false negative-false positive trade-off common to hypothesis testing.

The report is organized into six major sections. The first section is the executive summary of the optimization results and recommendations. The second section provides a brief description of the site and its existing groundwater monitoring scheme. The next two sections correspond to the temporal and spatial analyses respectively. As explained below, the temporal component is further divided into three parts: temporal variogram analysis, iterative fitting of individual wells, and trend mapping. The spatial analysis

consists of a series of iterative steps. The site maps corresponding to these iterations are collected in appendices to the report. The fifth section of the report summarizes the conclusions of the optimization effort, offers a number of recommendations, and provides a cost analysis at the site based on the optimization results. The final section provides relevant technical references.

Section 1. Executive Summary

After using the Geostatistical Temporal/Spatial (GTS) algorithm to optimize the long-term monitoring network at Site OU-12 on Loring AFB, the following key results were found:

- GTS exploratory analyses were used to determine 2 to 3 ‘best’ candidates for the optimization routine. The COCs were not chosen *primarily* on the basis of regulatory concern or health risk-exposure (although these factors were considered), but rather with the intent to include those parameters in the optimization routine that offered *the most statistical information* concerning temporal and spatial redundancy. The best such parameters typically exhibit larger detection rates and more widespread spatial occurrence. At Site OU-12, based on detection frequencies, per-well ‘hit’ rates, and spatial plotting of the maximum per-well concentration values, the most promising candidates appeared to be manganese (MN), iron (FE), trichloroethylene (TCE), and benzene (BZ). From this list, since BTEX parameters were of particular concern at Loring AFB, and because many of the wells did not have any TCE ‘hits’ and there were very few wells with large TCE concentrations, benzene was included over TCE in the optimization analysis. It also showed a fairly widespread spatial distribution at the site. The final three optimization candidates were thus MN, FE, and BZ.
- The *common* sampling schedule for Site OU-12 as a whole ought to be adjusted. Temporal variograms generated by combining all the available sampling information indicate that the common sampling interval could be set to one sampling event every 2 quarters with little loss of statistical information, compared to current quarterly sampling regimen (3 events per year excluding Winter).
- The recommended operational sampling interval for those wells analyzed by Iterative Fitting is generally 2 quarters (i.e., semi-annually). This is very consistent with the recommended sampling interval from the Temporal Variograms of approximately 2 to 3 quarters. It is also the case that at least three-quarters of the wells could have their sampling frequencies reduced by 20%, and at least half could be reduced by 25%, without any significant loss of statistical trend information.
- If the results of the GTS optimization analysis are implemented at Site OU-12, there ought to be a similar follow-up analysis conducted after 3 to 5 years in order to assess whether or not the same recommendations would still hold. However,

any new sampling schedules should be implemented with care. The Temporal Variograms, for instance, depend significantly on having pairs of measurements from any given well with a variety of inter-event time intervals. If all wells are sampled from the same quarters each year after implementation, the range of between-sample intervals will be reduced, and consequently it will be much harder to construct a future Temporal Variogram to test the original recommendation. Instead, it is recommended the overall set of wells be divided in half, and that two quarters from each calendar year (excluding Winter due to logistical constraints) be selected at random for the sampling of each half-group. Thus, on a given year, one half the wells might be sampled in Spring and Fall, while the other half is sampled in Summer and Fall. The next year a possibly different pair of quarters would be selected for each half-group, and so on. This approach will allow some inter-event times to be as short as the current quarterly sampling, even though each well would only be sampled twice a year. **Table 5-1 in Section 5.1** provides a possible schedule for the first five years after implementation.

- The spatial optimization analysis at Site OU-12 reveals varying levels of spatial redundancy. For the benzene data, a ‘safe’ level of redundancy appeared to be about 30% of the total well network. For manganese, this safe level dropped to about 20% of the wells. Iron fell in-between the other two at 20-30%.
- 17 wells were commonly listed as potentially redundant across all three candidate COCs, amounting to 15 percent of the total baseline well set. However, when considering the highest priority COC of these three, benzene, 29 wells were considered redundant or 25% of the baseline LTM network.
- The GTS optimization algorithm can offer potentially significant cost savings over the existing LTM program at OU-12. Accurate estimates of plume magnitude and extent can be made using fewer wells than the current network and sampling at a lower frequency than presently in place. Estimates of specific potential cost savings off the total annual project budget range from 33–39%, amounting to between \$306,000 and \$358,000 per year.

Section 2. Description of Site OU-12, Loring AFB

Section 2.1. Site Hydrogeology and Contaminant Sources

Operable Unit (OU) 12 consists of the groundwater underlying Loring Air Force Base, with the exception of groundwater underlying OU 2 (underneath Landfills 2 and 3) and OU 2A (underneath Landfill 1, the Coal Ash Pile, Drum Disposal Area, and Paint Can Disposal Area). The subsurface geology of OU 12 varies across the site. The bedrock at the site was identified as low-grade metamorphic pelitic limestone. The depth to bedrock varies from zero to greater than 60 feet. Depending on location and depth, the bedrock varies from lightly fractured to well fractured. There are also three distinct overburden units at the site: glaciofluvial deposits (sands and gravels), till, and fill. Both an

overburden and deeper regional groundwater system exist at the site. Groundwater flow in the overburden/shallow groundwater system at the site is from source areas to nearby surface water bodies. Groundwater flow in the bedrock system depends on fracture orientation.

Groundwater contamination was detected at the site as the result of an investigation conducted in 1986 under the Department of Defense's Installation Restoration Program. As the result of further investigations conducted as part of a Bottom Up Program Review in 1994, thirty contamination sources or plumes were identified as part of OU 12. Due to the large area encompassed by OU 12 and the number of plume sources identified, OU 12 was subdivided into ten overlapping flow fields. However, not all of these sources or plumes were found to pose a significant risk to human health or the environment, and so were removed from further consideration. The contamination sources or plumes requiring further remediation are found primarily in five flow fields (1–3, 6, and 8).

Flow Field 1

Flow Field 1 contains one contaminant source. The RMSA site includes Building 7600 and a nearby parking area and covers approximately six acres in the southern part of the site. Building 7600 was historically used for maintenance of fuel bowser trucks. Likely sources of contamination at the site include an oil interceptor, underground storage tank, and a dry well used for the interceptor effluent. There is no overburden groundwater below the RMSA site, but a chlorinated solvent contamination plume has been detected in bedrock groundwater underneath the site. This plume is approximately 10 acres in size and extends to the west of the RMSA site.

Flow Field 2

Flow Field 2 contains three significant contamination sources: the Vehicle Maintenance Building (VMB), the Fuels Tank Farm (FTF), and the Base Laundry (BL).

The VMB site includes Buildings 7500 and 7501, located southeast of the intersection of Pennsylvania and South Carolina Roads. Building 7500 was used for maintenance of USAF vehicles. Building 7501 was a vehicle parking building. Likely sources of contamination at the site include waste oil, antifreeze, solvents, Speedy-Dry, and battery electrolyte in building floor drains, a sand and gas trap, an oil/water separator, a waste oil UST, and spill-contaminated soils. The VMB plume consists of chlorinated and fuel-related contaminants in both overburden and bedrock groundwater underneath the site. This plume is approximately 13 acres in size and migrates in a westerly direction from the source.

The FTF site is approximately 35 acres in size, and is located south of the Flight Line Area. It was used for bulk fuel storage, in aboveground storage tanks. Contamination at the site has occurred as the result of fuel spills and underground fuel line leaks. The FTF South plume consists of chlorinated and fuel-related contaminants in overburden groundwater underneath the site. This plume is approximately 0.3 acres in size and migrates in a southwesterly direction from the source.

The BL site includes Building 7330 the surrounding area, located northeast of the intersection of Pennsylvania and South Carolina Roads. Building 7330 was used for laundry, including dry cleaning. Contamination at the site has occurred as the result of PCE leaks or spills at the site. The BL plume consists of PCE in bedrock groundwater underneath the site. This plume is approximately 11 acres in size and migrates in a southwesterly direction from the source.

Flow Field 3

Flow Field 3 contains five significant contamination sources: the Former Solvent Storage Building (FSSB), Pumphouse (PH) 8210, the Entomology Shop (ES), the Jet Engine Build-up Shop (JEBS), and the Contract Storage Shed (CSS). All overburden groundwater flow underneath Flow Field 3 is to the south/southwest.

The FSSB site includes a building used to store paint thinner and solvents used for aircraft maintenance, located near the northeast corner of the Arch Hangar. Likely sources of contamination at the site include small spills or releases of thinners or solvents. The FSSB plume is approximately 3 acres in size and consists of chlorinated solvents in overburden groundwater underneath the site.

The PH 8210 site is approximately five acres in size and consists of a reinforced concrete building, six USTs, a defueling tank, a collection tank, and associated piping, located adjacent to the runway, west of the Kilo Ramp and south of the Crash Fire Station. Likely sources of contamination at the site include releases from the pumphouse and adjacent valve pits and transfer pipelines. The PH 8210 plume is approximately 11 acres in size and consists of fuel-related compounds and chloromethane in both overburden and, to a limited extent, bedrock groundwater underneath the site.

The ES site is approximately one acre in size and consists of a small building, a drainage ditch north of the building, an AST, and pipes connecting the ES to other base locations, located east of Arizona Road. The ES was used as a wastewater treatment facility for the JEBS, the DC hangar, and the Snow Building, prior to its conversion for pesticide and herbicide preparation and storage. The likely source of contamination at the site is residual wastewater from the hangars and the JEBS. The ES/JEBS South plume consists of chlorinated and fuel-related compounds in bedrock groundwater. It is approximately 11 acres in size and extends northward to the southwest corner of the JEBS.

The JEBS site is located west of the Flightline Area, in the central industrial area of the base. It was used for draining, maintenance, repair, teardown, and modification of jet engines. Likely sources of contamination include a washrack, floor drains, oil and grease trap, oil/water separator, and spills from paint, chemical, and mixed petroleum wastes stored at the site. The JEBS North plume is approximately 18 acres in size and consists of chlorinated and fuel-related compounds in bedrock groundwater underneath the site.

The CSS site is located in the northeast quadrant of the intersection of Weinman and Kansas roads, west of the railroad tracks. It includes a shed used for the storage of waste oil, waste chemical drums, and electrical transformers. It was also reported to have been used for pesticide mixing and as a parking lot and storage area for grounds-keeping

equipment. Likely sources of contamination at the site include a former UST and past activities and small spills at the site. The CSS plume is approximately 1.5 acres in size and consists of xylene contamination in bedrock groundwater and chlorinated and fuel-related compounds in overburden groundwater underneath the site.

Flow Field 6

Flow Field 6 contains one contaminant source. The Base Exchange Service Station (BXSS) site is approximately 2.5 acres in size and includes a single building and a large paved area used for the dispensing of leaded and unleaded fuel from several USTs. It is located in the central portion of the base, at the intersection of Texas and Cupp Roads. There are two contamination plumes originating from the BXSS site. The BXSS plume consists of fuel-related overburden groundwater contamination. Likely sources of this plume include small spills and leakage from the USTs. The BXSS plume is approximately three acres in size and flows in a westerly direction from the BXSS site. The Upgradient BXSS plume consists of TCE bedrock groundwater contamination. The source of the TCE is believed to be upgradient of the BXSS site, but is not identified. The Upgradient BXSS plume is approximately 37 acres in size and migrates in a west/southwesterly direction.

Flow Field 8

Flow Field 8 also contains one contaminant source. The 12-acre Quarry site consists of a former rock quarry located near the northwestern boundary of the base, adjacent to the NDA. Waste materials from construction projects, industrial and maintenance shops, and other base activities were stored and disposed of at the quarry. Overburden groundwater at the site flows downward into the bedrock groundwater, which migrates southwestward. The Quarry plume is approximately 16 acres in size and consists of chlorinated and fuel-related bedrock groundwater contamination.

Section 2.2. Monitoring Network

The existing monitoring network used as a baseline for the optimization analyses at Site OU-12 includes 115 wells as listed in **Table 2-1**. This set of locations covers an area that is roughly physically contiguous, but excludes two subsets of wells separately located farther to the north and northeast. The wells included in the analysis are currently sampled three times per year, in the spring, summer, and fall. Available data for this analysis covered the period from 1988 to 2002. The most typical constituents of concern (COCs) collected at the site are listed in **Section 3.1, Data Preparation**.

Groundwater is collected at OU-12 from both overburden and bedrock wells. The depths of screened intervals range from approximately 10 feet to almost 390 feet below ground surface (bgs). The ground surface itself varies across well locations by approximately 160 feet. The deepest overburden wells are located about 50 feet bgs, while the shallowest bedrock wells are located approximately 30 feet bgs. Probably due to the nature of the subsurface geology, there were few statistically reliable or clear-cut distinctions in contaminant patterns between the overburden and bedrock zones. Instead the distributions tended to substantially overlap, with some obvious differences in upper concentration extremes. For this reason, the spatial optimization analysis was carried out

on the data set as a whole, considered as three-dimensional site volume, rather than as separate two-dimensional (areal) horizons.

Table 2-1. Existing OU-12 Baseline LTM Network (all measurements in feet)

Note: Screen Elevation is recorded as the midpoint depth of a screen typically 10 feet in length

WELL_ID	EASTING	NORTHING	DEPTH	SCREEN ELEVATION
056MW02	110269.46	12297.76	25	675.28
056MW04	110130.1	12294.51	18	679
AR25	109037	11902	153.25	518.92
BMW712	107428.49	16287.99	21	680.93
BMW715	107439.45	16139.85	45	656.97
BMW717	107613.87	16146.84	37	666.71
JBW7101	108258.77	9885.66	85.5	563.86
JBW7102	109201.33	8769.83	33	630.78
JBW7106A	105746.65	8560.7	125.4	490.44
JBW7106B	105746.65	8561.7	62.2	553.64
JBW7203A	108468.08	10501.33	79.1	562.43
JBW7203B	108468.08	10502.33	53	588.53
JBW7204A	108133.57	10239.05	302	329.67
JBW7212A	109634	10474	189	477.36
JBW7212B	109634	10475	40	626.36
JBW7213A	109465.95	11143.64	199	469.06
JBW7213B	109465.95	11144.64	83	585.06
JBW7215B	109929.84	11368.79	80	608.76
JBW7309	107579.17	11409.42	33	613.39
JBW7317	112089.57	15002.11	40	688.74
JBW7326A	108222.3	10888.36	88	550.18
JBW7326B	108222.3	10889.36	41	597.18
JBW7328	110684.04	14780.69	35	686.78
JBW7330A	109964.67	13026.8	387.3	309.71
JBW7333	110584.22	13306.8	50	663.82
JBW7336A	110531.15	13035.23	83	629.3
JBW7336B	110531.15	13036.23	57	655.3
JBW7338A	110830.36	13609.17	111	610.71
JBW7338B	110830.36	13610.17	40	681.71
JBW7340B	110361.54	13210.74	47	659.68
JBW7344	110987.6	13622.38	32.5	690.05
JBW7345A	110554.5	13806.74	93	619.39
JBW7345B	110554.5	13807.74	34	678.39
JBW7347B	110460.02	14624.9	34	678.24
JBW7348	110802.02	13966.56	46.6	675.08
JBW7350	111365.86	14160.19	48.225	677.215
JBW7607	107063.59	15642.68	39	635.27
JBW7617B	106434.87	15543.05	50.9	617.97
JBW7710	109834.07	15664.23	50	657.89
JBW7725	109695.14	17708.18	35	693.48
JBW7737A	107734	17185	200	501.02
JBW7737B	107734	17186	38	663.02
JBW7738A	106930.24	16925.75	100	575.16
JBW7742B	109908.62	16530.1	94	623.17
JBW7752	108375.42	16683.09	31.75	687.05
JBW7806	107716.95	20532.58	37	679.26
JBW7809	109112.81	21161.11	43	725.95
JBW7812B	108332.56	20848.69	71	637.41
JBW7816	108577.94	20890.92	59	682.08
JMW0201A	108502.6	20874.6	76	664.31
JMW0201C	108503.6	20874.6	41	699.31
JMW0301C	109861	13420	59	634.47
JMW0401	108432.9	20095	66	701.77
JMW0503	111069.89	14733.53	69.6	651.8
JMW0505	111132.9	14617.51	29	691.13

WELL_ID	EASTING	NORTHING	DEPTH	SCREEN ELEVATION
JMW0542	109338.8	12434.2	23	654.26
JMW0603	110871.7	9324.6	41	637.86
JMW0604	111650.6	8969.9	96	597.76
JMW0701	107403.43	16369.68	27	671.03
JMW1562	111523.51	14976.24	23	698.44
JMW1564	111324.2	14979.63	34	683.92
JMW1565	111522.3	14964.19	44	678
JMW1860	108944.86	9032.97	29	630.73
JMW1881	108936.65	9301.22	51	604.53
JMW1960	109086.09	10613.03	35	621.03
JMW1963	109286.98	10487.77	26	629.53
JMW1964	109282.91	10966.36	37	622.41
JMW1966	109099.64	10610.39	15	641.57
JMW3082	109539.7	12427.4	30	650.58
JMW3202	110684.15	13404.85	46	668.09
JMW35X2	110127.97	10067.32	17.5	656.09
JMW3601	109694.87	11278.81	48	628.12
JMW6001	109866.12	16952.71	15	702.39
JMW6105	108145.33	17187.8	25	692.779
JMW7332	107984.11	11714.85	14	633.11
JMW7612	106986.73	16453.32	17	656.29
JPZ0340	109561.37	13962.51	40	631.71
JPZ0341	109554.37	13917.07	15.2	657.43
JPZ0342	109510.08	14069.1	38	634.18
JPZ0343	109503.35	14073.53	20	652.04
JPZ0344	108969.07	12592.36	61	612.46
JPZ0348	108885.33	12194.33	50	616.6
JPZ0349	108892.85	12200.73	29	637.63
JPZ1586	111185.59	15286.16	27	683.8
JPZ1780	109521.51	12824.33	30	646.97
JPZ1781	109931.54	12811.71	41	653.33
JPZ7208	108141.92	10243.38	15	617.52
JPZ7312	109847.28	15397.09	19	679.02
JPZ7601	106807.89	16674.53	15	662.75
JPZ7807	107539.3	20443.3	31	674.55
MMW0003	106376.08	15069.79	40	629.78
MMW0004	108965.36	14148.06	59.2	629.05
MMW0005	110994.15	14918.82	32.65	687.72
MMW0006	106091.03	15467.33	38	620.94
MMW0007A	105635.89	8867.39	137	465.21
MMW0007B	105635.89	8869.39	52	550.21
MMW0008	105643.92	8869.73	9	592.97
MMW0009	107189.78	20000.95	44	658.77
MMW0010	107230.49	9847.09	67.5	552.56
MMW0011	107224.74	9841.5	24	595.57
MMW0012	108059.46	10484.21	75	556.84
MMW0013	108066.33	10492.6	28	603.32
MMW0016	107858.21	10022.92	14.5	608.43
MMW0017	107038.16	9401.65	20.5	602.96
MMW0019	105655.31	8657.3	9.4	594.52
MMW0020	106299.33	19477.31	150	565.27
MMW0124	109448.8	11150.7	33.25	634.48
MMW0125	109628.4	11203.7	30.75	641.63
MMW0421A	106411.06	19294.66	92	619.6
MMW0421B	106411.06	19295.66	41	670.6
MMW0422	107002	19354.37	64	638
MMW0423	107000.5	19350.93	30	672.4
MMW1560	111365.14	15129.42	25	691.99
MMW7330	109964.67	13027.8	121	576.2
USMW025	109706	17772	35	692.05

Section 3. Temporal Optimization at Site OU-12

Section 3.1. Data Preparation

Data queries were made by AFCEE and Montgomery Watson of all available electronic sampling records from Site OU-12. Data covered the period from 1988 until late 2002. In order to better gauge sources of variability — especially spatial variation — among the chemical data, data queries specifically asked for field duplicates as well as normal environmental samples.

Included in the database were a number of sets of multiple records associated with the same sampling date and sample type. Each set apparently represented multiple laboratory runs on the same sample. To ensure that only one sample result of a given type (field duplicate or normal) was kept per sampling date (at a given location and depth), all of the sets of multiples were screened by manual inspection. Although this screening process was somewhat subjective and imperfect, a list of rules and priorities was developed to make the screening as consistent as possible. These rules included giving priority to sampling records with lower dilution factors (when dilution information was available) or lower reporting limits (“RLs”); and quantified concentrations (“hits”) over estimated concentrations (“J” values) or non-detects (NDs). In addition, even when dilution factors were present, priority was given to hits with higher dilution over either J values or NDs with lower dilution, and J values with higher dilution over NDs with lower dilution.

Another issue corrected within the database was that of records with a quality control flag of “R.” These records were deemed unusable by Montgomery Watson, and they, along with any wells missing easting and northing coordinates or labeled as vapor wells, were eliminated prior to analysis. Also eliminated for the metals data, in particular, were any field-filtered samples.

Overall, the subsequent database included almost 22,000 records covering the following fifteen constituents of concern (COC): benzene (BZ), toluene (BZME), cadmium (CD), 1,2-dichloroethane (DCA12), 1,2-c-dichloroethene (DCE12C), ethylbenzene (EBZ), iron (FE), manganese (MN), naphthalene (NAPH), lead (PB), perchloroethene (PCE), antimony (SB), trichloroethene (TCE), vinyl chloride (VC), and total xylenes (XYLENES). These COCs were noted in site documents and reports as chemicals being monitored at Site OU-12 and that had been detected in laboratory analyses of sampling data. Initial detection rates by sample record for these COCs are given in **Table 3-1**:

Table 3-1. COC Detection Frequencies

COC	Rate of Detection (%)
MN	91.2
FE	85.0
TCE	50.2
PB	47.4
DCE12C	46.4
BZ	25.5
CD	24.7
PCE	23.4
VC	16.6
XYLENES	14.0
EBZ	13.6
SB	13.2
BZME	11.7
NAPH	11.6
DCA12	2.3

Based on these detection rates and initial time series plots of the raw data, eight COCs were initially eliminated from consideration as not exhibiting enough statistical variation for meaningful analysis: BZME, DCA12, EBZ, NAPH, PCE, SB, VC, and XYLENES.

The remaining constituents were further examined by computing per-well detection rates, that is, the fraction of wells for a given compound with at least one detection, along with per-well detection rates above specific concentration levels of interest (usually a primary or secondary MCL). Summaries of these statistics are given in **Table 3-2** below:

Table 3-2. Well Detection Rates for Selected COCs

COC	Well Hit Rate (%)	MCL (ppb)	Hits > MCL (%)
BZ	37.2	5	28.2
CD	74.5	5	10.0
DCE12C	51.0	7	25.8
FE	98.9	300	65.1
MN	100.0	50	65.5
PB	88.3	15	11.7
TCE	54.5	5	39.1

Based on these summaries and additional time series plots of the remaining COCs, the most promising candidates for the GTS optimization routine appeared to be MN, FE, TCE, and BZ. Spatial plotting of the maximum per-well concentration values was then conducted to determine the crude spatial distribution of the hits for each parameter. These plots generally confirmed that the most frequently detected COCs also had the most

widespread spatial distribution at Site OU-12. This would have narrowed the list to MN, FE, and TCE. However, since BTEX parameters were of particular concern at Loring AFB, and because many of the wells did not have any TCE ‘hits’ and there were very few wells with large TCE concentrations, benzene was included over TCE in the optimization analysis. It also showed a fairly widespread spatial distribution at the site. Thus, the final three optimization candidates were MN, FE, and BZ.

Note in this regard that one of the purposes of the initial exploratory analysis was to determine 2 to 3 ‘best’ candidates for the optimization routine. Including a larger number of COCs significantly increases the amount of work required to run the GTS algorithm without typically improving the results. The aim is *not* to determine which COCs to monitor, but rather to include only those parameters in the optimization routine that offer *the most statistical information* concerning temporal and spatial redundancy. The best such parameters typically exhibit larger detection rates and more widespread spatial occurrence.

Another preparation step that was taken to prepare the remaining data for temporal optimization was to average values for a given sampling date by duplicate status and across multiple depths (when they existed). That is, if a given well on a given date had both normal samples and field duplicates and/or had multiple samples collected at different depths, all of these values were averaged in order to create a single analysis value for that well and sampling event. The major reason for doing this was to ensure that estimates of the typical interval between samples were not biased downward by the presence of multiple samples on a given date. Most of the wells and sampling dates only included a single sample at depth, so to include all the sample records without this averaging step would tend to skew the results.

As a final note, non-detects were handled prior to analysis by converting them to half the listed reporting limit (RL). In addition, part of the temporal analysis required keeping track of which samples were non-detects and which were detections. For single, non-averaged samples this posed no difficulty. But for values that were averaged across duplicate status and/or depth, if any of the samples to be averaged were ‘hits,’ the average value was also considered a hit. If all were non-detects, the average value was also labeled a non-detect.

Section 3.2. Temporal Methodology

The temporal optimization analysis in GTS consists of three basic components: 1) temporal variograms applied to groups of wells, 2) iterative thinning of individual wells, and 3) trend mapping over specific time periods. Each of these components is explained below. Note again that the temporal analysis is *not* designed to determine which well locations might be redundant and perhaps unnecessary to the LTM program. Rather, the major goal of the temporal portion of GTS is to examine and optimize well sampling frequencies for *currently existing* locations.

Section 3.2.1. Temporal Variograms

The first piece of the GTS temporal puzzle is the Temporal Variogram. The Temporal Variogram technique is designed to optimize sampling frequencies simultaneously over a

group of well locations. These locations might represent all wells at a given site, those connected with a particular regulatory unit, or even selected wells that are part of a treatment system network. Whatever the grouping, the Temporal Variogram aims to provide a single optimal sampling interval that can be applied to every well within the group. Thus, this technique can be particularly helpful when a site manager wants to establish uniform operational sampling schedules at the site, and the optimization of individual well frequencies is not deemed as high a priority.

Results from the Temporal Variogram should not be viewed as optimal for any *single* well. The Temporal Variogram in GTS combines data from all wells in the group in its construction. Consequently, it attempts to find an optimal sampling interval, *on average*, for the group. Some individual wells might be better optimized with shorter or longer sampling intervals. Nevertheless, when a uniform sampling frequency is desired, the Temporal Variogram can provide a reasonable way to estimate it for the well group simultaneously.

Another advantage of the Temporal Variogram as employed in GTS is that even wells with very little sampling data can be included in its construction. The trend fitting methods for individual wells explained in **Section 3.2.2** generally require at least 8 or more distinct sampling events to provide a reasonable fit. With the temporal variogram, any well with at least two distinct sampling events can be included.

The Temporal Variogram is constructed using nested pairs of concentration measurements from each well in the group. By nested what is meant is that given a particular location, all pairs of measurements are formed for that well and one-half the squared difference is then computed for each pair. Pairs are never formed *across* distinct wells, which would introduce unwanted spatial variability, but rather are *nested within* wells. This allows an independent estimate of temporal variability from each well. Then, to allow the inclusion of wells with only minimal amounts of sampling data, and to gauge average temporal variation for the group as a whole, the squared differences are amalgamated together into a single set of *pair differences* for the entire group.

In previous versions of GTS, a Temporal Variogram was actually constructed for each well, but then a weighted average of the individual variograms was formed to get the final overall Temporal Variogram. In the current version of GTS, this process is streamlined by simply estimating the final variogram from the entire unweighted set of half-squared pair differences. In this fashion, wells with more data are naturally given greater weight in the final Temporal Variogram (since they contribute more pairs), while well locations with less data are given some, but lesser weight.

The Temporal Variogram itself is simply a graph of a unitless variogram measure plotted against time, or more specifically, against the time lag between successive sampling events. It is estimated using locally-weighted quadratic regression (LWQR), taking the half-squared difference pairs as the *y*-variable and the time lag or time difference between sampling event pairs as the *x*-variable. All sampling dates at Site OU-12 were converted into number of weeks since a reference date prior to any actual historical sampling. The time lag differences were thus expressed in number of *weeks* between sampling events.

As explained in more detail in **Section 3.2.2** on the use of LWQR in Iterative Fitting, the GTS analyst must choose an appropriate bandwidth parameter prior to estimating the Temporal Variogram. However, testing of various data sets has shown that smaller bandwidths do not do a good job of capturing the most important features of the variogram. Instead, larger bandwidths provide better and more interpretable results.

For this reason, all the Site OU-12 Temporal Variograms were computed at two larger bandwidths: 50% and 70%. Both of these estimated fits are graphed for each constituent in **Appendix 3-1**. The use of LWQR also allowed the estimation of confidence bands around the fit, in order to better gauge possible variation in the estimate. Confidence bands were constructed for both bandwidths; however, for visual clarity only the 50% bandwidth confidence bands are actually plotted on the graphs in **Appendix 3-1**. Sometimes the LWQR fit at the 70% bandwidth is different enough from the 50% bandwidth fit as to make the former estimate fall outside the confidence bands. Nonetheless, as described below, the key to comparing results at different bandwidths is not whether the *magnitude* of the Temporal Variogram differs from one bandwidth to the next, but instead whether the fundamental *shapes* of the variograms differ. Generally, at Site OU-12 they did not.

A couple of additional technical points are important to the Temporal Variogram methodology. First, concentration outliers can skew the results of the Temporal Variogram as much as they can skew the Iterative Thinning routine (as explained in **Section 3.2.2**). Because of this possibility, Tukey's box plot rule (also described in **Section 3.2.2**) was run on the concentration data from each well, both on the raw and logged scales of measurement. Again, as with Iterative Thinning, only data values that were tagged as outliers on *both* scales were excluded from the Temporal Variogram computations.

In addition, to avoid the problem of some wells having vastly different average concentration levels (and thus contributing vastly different squared-difference pair contributions to the Temporal Variogram), each well's data was temporarily re-scaled to have a maximum of one before doing the Temporal Variogram calculations and fitting. Thus, every well in the group was put more or less on an 'equal footing' in terms of its concentration range.

Another potential problem involved non-detects. Prior testing of the Temporal Variogram has shown that wells with too many non-detects exhibit too little temporal variation to be of help in estimating the Temporal Variogram. For this reason, all wells with less than a 30% detection rate are excluded from the variogram computations.

Finally, two different types of Temporal Variograms were computed on the Site OU-12 data: the *mean* variogram and the *median* variogram. In each case, the LWQR procedure looks at a neighborhood of half-squared-difference pairs surrounding a time lag point to be estimated. However, in the case of the mean variogram, the local regression estimate attempts to pinpoint the arithmetic average of the difference pairs, while in the case of the median variogram, a similar estimate is made on the *ranks* of the set of difference pairs

rather than the pair values themselves. Comparisons of these variogram types showed that the mean variogram rarely offered interpretable results, mainly because it was too erratic, while the median variogram was typically more promising and well-behaved. Consequently, the Temporal Variograms of **Appendix 3-1** only include the median variogram results.

The ultimate goal when analyzing a Temporal Variogram is to identify an approximate *range* in its structure. That is, at what point (if any) does the variogram start to ‘level out’ and remain at roughly a constant level? Ideally, any variogram offers a measure of correlation between the measured data and either time or space. For cases of positive temporal or spatial correlation, such a linkage is evidenced on the variogram by small values for small lags (either *time* lags between sampling events for the Temporal Variogram or, more commonly, *distance* lags between well locations when constructing variograms for a geostatistical analysis) and larger values for large lags. Small values on a variogram are typically indicative of a high degree of correlation, while higher values represent a loss of correlation and greater statistical independence.

On many variograms, there is a point at which larger lags no longer lead to larger variogram values. It is at this point that the range is identified. The magnitude of the leveled-out portion of the variogram is known as its *sill*. Lags at least as large as the range — and thereby associated with the sill — are thought to represent sampling pairs having essentially no statistical correlation. Smaller lags on the other hand, having variogram values smaller than the sill, represent pairs which are correlated to some degree and therefore contain a certain level of statistical redundancy in the information they offer.

It is for this reason that GTS sets the optimal sampling interval for a group of wells as the *range* of the Temporal Variogram, if it can be identified. Sampling intervals smaller than the range are associated with somewhat correlated, and therefore redundant, sampling results. On the other hand, sampling intervals at least as large as the range tend to be uncorrelated, and therefore — from a statistical standpoint — optimal in the sense that consecutive samples collected at such lags will provide the shortest sampling interval at which the maximal statistical information per sample is achieved.

Bear in mind that while the Temporal Variogram is a useful tool, it is not without its caveats. Sometimes a range cannot be reliably identified, often because some of the wells in the group do not possess the same basic temporal correlation structure as other wells. In other cases, a range may be identified, yet the result is different from that estimated via Iterative Thinning. This can happen in part because the Temporal Variogram tries to optimize a group of locations *on average*, rather than individually. It can also occur if only a smaller number of wells have enough sampling data to be included in the Iterative Fitting analysis, yet are included in the Temporal Variogram computations.

Section 3.2.2. Iterative Thinning

Iterative Thinning refers to the technique by which the well sampling frequencies at *individual* wells are optimized. Because each location is analyzed separately, it is quite possible to have a different optimal sampling interval for each well after applying the

Iterative Thinning routine. Nevertheless, GTS looks at the optimized sampling intervals as a whole and adjusts the recommended common operational sampling frequency for either all the wells treated as a single group, or each subgroup of related wells, based on the median optimal sampling interval for that group or subgroup.

The Iterative Thinning process is based on a relatively simple idea: 1) take the existing, historical data for a given well location and constituent, 2) determine the current average sampling frequency and sampling interval, 3) fit a trend to these initial data along with statistical confidence bounds around this trend, 4) iteratively remove, at random, certain fractions of the original data, and 5) re-estimate the trend based on the reduced dataset to determine whether or not the trend still lies within the original confidence bounds. If too much of the new trend falls outside the confidence limits, stop removing data and compute a new, optimized sampling frequency and sampling interval based on the portion of data removed.

The original version of GTS fit trends during Iterative Thinning by way of Sen's slope statistic, a non-parametric estimate of the slope of a linear trend. Although useful, Sen's statistic is not highly informative for cases of more complicated, non-linear trends. Previously, this meant that the GTS analyst would have to 'screen out' those wells which did not exhibit roughly linear trends over time. Since then, GTS has been modified to estimate the initial trend via a statistical technique known as locally-weighted quadratic regression (LWQR; see Loader, 1999). This procedure is readily able to fit complex trends and confidence bounds around those trends. Moreover, the data requirements for using LWQR are quite similar to Sen's slope method, and the process can be automated to essentially the same degree.

To perform the Iterative Thinning, LWQR was used to construct an initial trend and 90% confidence bounds around this trend. Also, the baseline sampling frequency was computed over the entire record of sampling at the well, and the baseline sampling interval was estimated by averaging the set of intervals between consecutive samples. As will be noted below, greater emphasis was given to more recent sampling information when constructing these baselines, especially if any large gaps appeared within the sampling record. Still, it is quite possible that the baseline sampling interval for a given well may not directly correspond to the nominal operational sampling schedule currently being used. The Iterative Thinning routine is data driven, and includes as much useful trend information as is possible, even if contributed by, for instance, multiple contractors operating under different sampling schedules or goals.

Once the initial trend was fit, data points were removed at random in systematic increments of 5% at each level, up to a maximum of 95%. At each stage, the trend was re-estimated on the reduced dataset and then compared to the initial confidence bounds. Since data points were removed randomly, and it was therefore possible that only points from one portion of the existing sampling record might be removed, the same removal process was repeated 500 times at each removal level, each iteration with a new set of randomly chosen points. This step helped to ensure that the trend results were not artifacts of the removal process, but really reflected what kind of trend estimate was possible at each stage of removal.

Another advantage to using LWQR in this way is that it can readily account for seasonal fluctuations or seasonal trends. Because local regression is used to estimate non-linear trends in the original or baseline data at a given well, it does a good job of identifying seasonal patterns in the initial estimate. Then, since subsequent trends computed on the reduced data-sets are compared to the baseline estimate, if a dominant seasonal fluctuation cannot be identified in the reduced data, the iterative fitting procedure will register such a result as a loss of accuracy and perhaps conclude that too much data has been removed from that well.

Because 500 new trends were fit to the reduced data at each removal level, key statistical summaries were used to express the results. These include the median trend value (calculated at a series of dates throughout the sampling record), the lower quartile (i.e., 25th percentile) trend value, and the upper quartile (i.e., 75th percentile) trend value. The median trend summaries are plotted on the graphs in **Appendix 3-2** for two specific removal levels: the percentage at which too much data has been removed to adequately reconstruct the original trend, and the removal level just below this, which represents the optimal stopping point for the Iterative Thinning algorithm. Thus, for example, at well 056MW04 for BZ, the initial trend is plotted in blue with 90% confidence bounds around this trend shaded in light blue, the median fit of the set of new trends when 25% of the data has been removed is plotted in red, and the median fit of the optimal stopping point of 20% removal is plotted in green. This same pattern and color scheme was used for all of the **Appendix 3-2** graphs.

The other summary plotted on each **Appendix 3-2** graph is the pair of upper and lower quartile fits (identified by red dashed traces) on the reduced data when too much sampling information was removed. These statistics are quite important for a couple of reasons. First, the upper quartile represents the point which is exceeded by 25% of all the new trend values (and the same for the lower quartile on the low end of the concentration range). If this trace falls outside the original confidence bounds, it demonstrates that at least a quarter of the new trend values constructed from the reduced data were outside the initial confidence limits. This can happen even when the *median* trend fit doesn't look that bad, especially in the case where the new trend value is 'swinging wildly' from iteration to iteration above and below the initial fit, causing the median fit to fall somewhere near the original trend, but at the expense of substantial variability in the 500 trend fits at that removal level. Therefore it can be quite informative to compare the lower and upper quartile fit traces against the original confidence bounds. Sometimes there are key stretches of the data record where these fits lie outside the confidence band, indicating too much variability in the fitting process to allow for reliable trend reconstruction.

Second, the difference between the upper and lower quartile fits — also known as the *interquartile range* or IQR — was computed at each fitting point along the sampling record and averaged across the fitting points to form the *average* IQR. This statistic offers a numerical indication of the typical level of variation exhibited among the 500 trend fits computed at a given removal level. It is also plotted against removal level (i.e., fraction of data removed) for each well and parameter in the graphs of **Appendix 3-3**.

There the average IQR typically increases as more of the data is removed, up until and often beyond the optimal stopping point.

Note however that the average IQR is not a fail-safe indicator. In some cases, this statistic begins to *drop* near to or beyond the optimal stopping point, rather than continuing to increase. The primary reason for such behavior is that when enough data is removed — and depending on the configuration of the original time series — the re-estimated trend can, instead of ‘swinging’ above and below the initial fit, merely stay either consistently above or below the original trend, leading to a lower than expected difference between the upper and lower quartile fits.

It is for this reason that the optimal stopping point was chosen not on the basis of the average IQR, but rather by determining what fraction of the new trend values fell outside the original 90% confidence band. For Site OU-12, a threshold of 25% was chosen, meaning that too much removal was judged to have occurred whenever at least 25% of the reduced-data trend values fell beyond the initial confidence bounds. While the choice of threshold is somewhat arbitrary, tests of the data at Site OU-12 and at other sites have shown that it gives generally good results. However, it may not be the *ideal* threshold for each and every time series. Remember, the overall goal in Iterative Thinning is to determine how much data can be removed (and thus how much the interval between sampling events can be lengthened) and still allow one to reconstruct the *major* features of the original trend. Some ‘finer’ features of the time series trend are undoubtedly lost when less data is collected, but often it is quite difficult to determine whether these features are ‘real’ or simply due to measurement and/or field variation in the data. It may also be the case that certain transient features are less important to the needs of the long-term monitoring program and therefore do not need to be estimated as carefully.

To graphically illustrate at what point the ‘out-of-bounds’ fraction of new trend values exceeded the threshold of 25%, a graph of this measure plotted against removal level is provided for each well and COC in **Appendix 3-3**. Both this graph and the plot of the average IQR are denoted by red traces and set in the top panel of the page for each well. Also on these graphs is a vertical reference line indicating the optimal stopping point of data removal as determined by the Iterative Thinning routine. In the bottom panel are two graphs representing optimal sampling interval (in green) and optimal sampling frequency (in blue). These graphs were constructed by adjusting the baseline sampling interval and baseline frequency according to the amount of data ‘thinned’ at each removal level. Also included are two reference lines indicating the optimal stopping point and the optimal interval or sampling frequency associated with that stopping point. Hence, again referring to BZ at well 056MW04, the baseline sampling interval is just over 17 weeks between sampling events, while the optimal interval is found to be almost 22 weeks. Conversely, the baseline sampling frequency at this well is approximately 0.0558 samples per week (approximately 2.9 samples per year), compared to a recommended optimal frequency of approximately 0.0457 samples per week (2.4 samples per year).

Data Screening prior to LWQR

It is important to note certain steps that were necessary to apply the locally-weighted quadratic regression technique. While extremely flexible as a statistical tool, its flexibility

comes with certain restrictions and assumptions. First, prior testing of the GTS algorithm has demonstrated that reliable fitting of an initial trend, and especially, confidence bounds around that trend, are almost impossible with less than 8 to 10 sample measurements (that is, data from distinct sampling events). Because of this, well locations with fewer sampling events at Site OU-12 were automatically screened out of the Iterative Thinning routine and do not appear in the graphs of **Appendices 3-2** and **3-3**.

Furthermore, large data gaps in the sampling record are also troublesome to the LWQR algorithm and tend to cause artifactual looking trends. For this reason, historical sampling data prior to a large gap were screened from that well's time series before fitting. In this case, a large gap was defined as an outlier among the set of time-lags between consecutive sampling events using *Tukey's box plot outlier rule*, where a sampling gap outlier is identified whenever the lag exceeds the upper 'hinge' of the box plot of time-lags. (The upper hinge is defined as the upper quartile plus 1.5 times the interquartile range [IQR] of the box plot.)

Another data feature that can significantly affect the trend estimate is the presence of concentration outliers. The modified GTS algorithm screens these values prior to fitting with LWQR by again using Tukey's box plot rule, this time on the concentration values. To ensure that only very significant outliers are identified and removed, two passes of the box plot test are run, once on the raw data and once on the logged concentrations. Only samples that are identified as outliers on *both* scales are screened from the time series prior to fitting.

A final screening check is made for wells with no observable variation, typically in the case where all the data for a time series are non-detects with a common reporting limit (RL). Although LWQR can estimate a (flat) trend to such data, it is impossible to construct a confidence band around the trend or to determine an optimal stopping point for data removal. These latter statistics require the measurements to exhibit some variation (the same is true of other trend estimation methods). Because of this, wells with no observable variation are screened from the Iterative Thinning routine. In addition, the data at some wells — after removing apparent concentration outliers and sampling events prior to large data gaps — only consist of a string of identically-valued non-detects. These wells are consequently also screened from Iterative Thinning.

After running these automated checks, the results are re-checked manually by the GTS analyst by examining a time series plot of each well with possible outliers, data gaps, and stretches of no variation identified. Occasionally, it is necessary to add or remove one or more outliers or data gaps, in order to improve the fitting process.

Trend Fitting with LWQR

After screening the time series measurements for data gaps, concentration outliers, and observable variation, one final step was needed before constructing the initial trend estimates. That step was to choose a *bandwidth* for fitting. LWQR works by estimating the trend value at a given fitting point (i.e., a particular date within the range of dates between the start and end of the sampling record) using a weighted linear combination of the known sample values close to the fitting point. What must be selected by the analyst

is how many neighboring sample measurements to use. In GTS this is done by selecting a *bandwidth parameter* that represents the fraction of known samples to be included in the neighborhood of any given fitting point. These bandwidths typically range from 40% to 80%, depending, among other things, on the number of points in the time series and its shape.

In order to automate the GTS routines as much as possible, especially when there are a large number of wells to analyze, every attempt is made to simplify the choice of bandwidth. In general, the higher the bandwidth, the greater the amount of ‘smoothing’ that will occur within the fitted trend. Too high a bandwidth and the trend may ‘miss’ important peaks and valleys in the time series. Too low a bandwidth and the trend may exhibit artifactual jumps and/or dips between known sample values. It can also occur that the fitted trend mostly ‘disregards’ the known data altogether, leading to highly inaccurate trend estimates.

To guard against these scenarios, it is important to run a ‘pre-flight’ check of the LWQR fits at several possible bandwidths prior to running the Iterative Thinning routine. This pre-flighting is done in two basic ways: 1) visually comparing the estimated fits obtained by systematically changing the bandwidth for each well, and 2) computing diagnostic checks of the *residuals* obtained when the trend is estimated at each known sample value and the known value is subtracted from this estimate. Again the goal is to automate this process as much as possible. However, some visual inspection of the pre-flight results at each well is still necessary.

As to the first pre-flight check, plots of the known sampling data can be overlaid with LWQR trend estimates at several possible bandwidths. In this setting, one should look for a ‘visually pleasing’ fit, one that captures the major features of the overall trend, and especially to exclude fits that are clearly bad.

The second pre-flight check, that of residuals, includes the following calculations: Mallow’s CP statistic, correlation of the residuals with date of sampling, skewness of the residuals, and Filliben’s probability plot correlation coefficient. Each of these statistics is designed to provide a numerical indication of the goodness of the estimated trend relative to a given bandwidth. In GTS, these residual diagnostic measures are plotted simultaneously against bandwidth in order to search for the most appropriate fitting neighborhood. None of them, however, is fail-safe by themselves.

Mallow’s CP statistic is a scaled measure of the sum of squared residuals. Lower values of Mallow’s CP usually indicate a better fit. However, it is possible to have a very low Mallow’s CP and yet a visually unacceptable fit between known sample values. This occurs for instance when the estimated trend ‘goes right through’ each known sampling value, yet has improbable ‘squiggles’ or curves *between* sampling points. The correlation with sampling date is used to check whether the fit is worse over certain portions of the sampling record than others. Values close to zero are best. The skewness coefficient is used to check for ‘lopsidedness’ in the distribution of residuals. LWQR works best when the *residual* distribution is symmetric and normally distributed, so skewness values closer to zero are better. Along the same lines, Filliben’s correlation coefficient is a test of

normality that can be used to check the shape of the residual distribution. Coefficient values closer to one are best.

As noted, none of the residual diagnostic measures are fool-proof by themselves. They can even give conflicting indications for the same time series in some situations. Nevertheless, examined together along with graphs of the possible fits by bandwidth, an acceptable initial trend estimate can almost always be found.

Section 3.3. Trend Mapping

One of the natural by-products of constructing the initial trend fits at each well location during Iterative Fitting is the ability to create a *map* of the trend estimates for any specific time period. In order to construct the confidence band around the initial fit on the known sample data, LWQR creates an estimate not only of the trend value at each fitting point, but also the local *first derivative* or *slope*. These local slopes can then be averaged in an appropriate way to determine the general direction and magnitude of the trend for a given portion of the sampling record.

At Site OU-12, three different time windows were chosen for estimating average trend slopes: 1) the historical trend, based on all the available and usable data at a well location, 2) the recent trend, based on data collected since the start of 2000, and 3) the newest trend, based on the four latest sampling measurements. Each of these trends was also characterized as increasing (with an average slope > 0) or decreasing/flat (with an average slope no greater than 0).

To actually estimate the typical slope, the *median* slope value is selected from the set of fitting points falling within the specified time period. This is done to ensure that the dominant trend direction is identified. With non-linear trends, there can be short periods of very steep trends that do not represent the dominant direction of the trend over the time interval in question. The *mean* slope can be then skewed by a few very large local slope values, whereas the *median* slope tends to be resistant to this problem.

In addition, it is possible to compute a non-parametric confidence interval around the median slope, in order to characterize the *strength* of each trend. Using a 95% nominal target confidence level, each trend can then be characterized as either fairly 'sure' or 'unsure,' depending on whether the confidence interval around the slope contained the value zero.

Finally, all of this trend information can be mapped by well location. The maps presented in **Appendix 3-4** offer for each COC and designated time period a spatial representation of the types of trends at Site OU-12, along with an indication of their strength and relative magnitude. Specifically, increasing trends are listed in red and pink, with trends surely above 0 identified in red, and less sure increases in pink. Flat or decreasing trends are colored in blue and light blue, with surely decreasing trends in blue and less sure trends (including flat trends) in light blue.

Also on these maps is an indication of the *relative* magnitude of each trend. To do this, the actual slope estimates were divided into quintiles (each quintile representing 20% of

the ranked slope estimates). Then, an increasing series of symbol sizes was assigned to the set of quintiles for plotting purposes. Consequently, the largest red symbols on the trend maps, for example, represent increases in the top 20% of magnitude, while the smallest red symbols designate increases in the lowest 20% of magnitude. The same patterns apply to the other trends. The largest blue symbols represent those trends that exhibited the largest decreases, while the smallest blue symbols represent the smallest downward trends. And so on.

It is important to note that the trend maps do not provide information specific to the optimal adjustment of sampling frequencies. Rather, the maps provide an overview of where at the site different kinds of trends are occurring and how probable it is that the trends represent something ‘real.’ They can also be used to potentially augment or confirm patterns of plume movement or change over time, and perhaps to help identify areas of the site where additional sampling might be helpful. Still, it must be remembered that the LWQR fits are only constructed at wells with at least 8 usable sampling events. At Site OU-12, this included the vast majority of the wells with usable data.

Section 3.4. Temporal Optimization Results

The temporal optimization results at Site OU-12 are contained in a series of graphs and tables. Overall, there is room to adjust and optimize sampling frequencies within the long-term monitoring (LTM) program. A number of the monitoring wells could have their sampling frequencies reduced by at least 20-30% yet retain the most useful statistical information concerning their long-term trends. It would also be possible to adjust the *common* sampling schedule for Site OU-12 as a whole. Temporal variograms generated by combining all the available sampling information indicate that the common sampling interval could be set to one sampling event every 2 or 3 quarters with little loss of statistical information, compared to current quarterly sampling regimen (3 events per year excluding Winter).

Section 3.4.1. Temporal Variograms

The Temporal Variograms for Site OU-12 are contained in the graphs of **Appendix 3-1**. There is one Temporal Variogram per COC. As can be seen from each of these graphs, there appears to be an initial leveling off of the variogram at a lag of approximately 40 weeks. Each graph then ultimately continues to rise slowly out to a period of at least 130 to 140 weeks, meaning that a small degree of apparent correlation remains for at intervals greater than 40 weeks. Nevertheless, the vast majority of the statistical correlation, and therefore statistical redundancy, disappears for pairs of samples collected after this initial 40 week lag. In fact, the initial leveling off is consistent enough across the COCs to recommend an optimal sampling interval for Site OU-12 of approximately one sampling event every two or three quarters. Results by COC are listed in table below.

It should be noted that the recommendations on sampling frequency for Site OU-12 are strictly data driven. Other regulatory or engineering considerations may need to be accommodated in the assignment of final sampling schedules. Still, the sampling intervals listed below in **Table 3-3** offer a summary of the statistical information provided by the available data, and how that information can be used to adjust operations at the site.

Table 3-3. Temporal Variogram Ranges and Recommended Sampling Interval

Temporal Variogram Range			Optimal Sampling Interval
BZ	FE	MN	
30-40 wks	30-40 wks	30-40 wks	2-3 qtrs

Section 3.4.2. Iterative Thinning

Mention has already been made of the graphs in **Appendices 3-2** and **3-3**. These appendices provide the visual results of the Iterative Thinning process. As described above, **Appendix 3-2** includes a time series graph of each eligible well, overlaid with the initial trend fit, a confidence band around that trend, and selected results of the Iterative Thinning routine, including an indication of the optimal stopping point for data removal. These results are further detailed in the graphs of **Appendix 3-3**, where for each well and COC there are four plots: 1) the percentage of trend fits on the reduced data that fall outside the initial confidence band, plotted against the percent of data removed; 2) the average interquartile range (IQR) of the reduced-data trend fits, plotted against percent of data removed; 3) the optimal average sampling interval, plotted against percent of data removed; and 4) the optimal average sampling frequency, plotted against percent of data removed.

Key numerical portions of this same information are summarized in **Table 3-4**. There for each well, the optimal and recommended sampling intervals and frequencies are summarized for the three COCs input into GTS. It will be noted that different stopping points sometimes occur for the same well depending on the COC utilized. Operationally, the minimum data removal percentage across the COCs could be chosen to select the optimal sampling interval and frequency, as shown in **Table 3-5**.

As is seen in this latter table, the suggested operational sampling interval for the wells that could be analyzed by Iterative Fitting is generally 2 quarters. This is very consistent with the recommended sampling interval from the Temporal Variograms of approximately 2 to 3 quarters. It is also the case that at least three-quarters of the wells could have their sampling frequencies reduced by 20%, and at least half could be reduced by 25%, without any significant loss of statistical trend information.

Table 3-4. Summary of Iterative Thinning Results, By COC and Well Location

Notes: CUT = optimal data removal percentage; OUTPCT = fraction of estimated trend pts on reduced data falling outside baseline trend confidence bands; INTERVAL = optimal sampling interval (in weeks); FREQ = optimal sampling frequency per week; AVE-IQR = average interquartile range across 500 iterative LWQR fits on reduced dataset at specified removal level

WELL_ID	EASTING (ft)	NORTHING (ft)	COC	CUT	OUTPCT	INTERVAL (wks)	FREQ (#/wk)	AVE-IQR (ppb)
056MW02	110269.46	12297.76	FE	0.25	0.241	22.96	0.0440	152.200
056MW02	110269.46	12297.76	MN	0.25	0.171	22.62	0.0446	739.100
056MW04	110130.10	12294.51	BZ	0.20	0.212	21.65	0.0468	3.518
056MW04	110130.10	12294.51	FE	0.30	0.224	24.40	0.0417	2952.000
056MW04	110130.10	12294.51	MN	0.25	0.226	22.87	0.0443	2304.000
AR25	109037.00	11902.00	FE	0.25	0.202	22.53	0.0447	58.460
AR25	109037.00	11902.00	MN	0.25	0.234	22.43	0.0450	20.990
FMW3413	111995.35	22114.24	FE	0.45	0.246	31.29	0.0319	43.490
FMW3413	111995.35	22114.24	MN	0.15	0.165	19.95	0.0507	0.174
JBW7101	108258.77	9885.66	FE	0.25	0.223	20.37	0.0489	151.700
JBW7101	108258.77	9885.66	MN	0.20	0.236	19.42	0.0515	3.531
JBW7102	109201.33	8769.83	FE	0.50	0.207	33.19	0.0301	69.160
JBW7102	109201.33	8769.83	MN	0.50	0.209	34.11	0.0301	5.203
JBW7106A	105746.65	8560.70	FE	0.25	0.244	21.80	0.0464	30.060
JBW7106A	105746.65	8560.70	MN	0.35	0.244	25.61	0.0398	2.261
JBW7106B	105746.65	8561.70	FE	0.15	0.174	19.30	0.0523	123.300
JBW7106B	105746.65	8561.70	MN	0.25	0.210	21.71	0.0464	3.949
JBW7203A	108468.08	10501.33	FE	0.30	0.235	20.65	0.0488	33.170
JBW7203A	108468.08	10501.33	MN	0.30	0.209	20.62	0.0494	6.692
JBW7203B	108468.08	10502.33	FE	0.35	0.243	23.76	0.0417	65.550
JBW7203B	108468.08	10502.33	MN	0.35	0.235	22.40	0.0454	2.531
JBW7204A	108133.57	10239.05	FE	0.20	0.195	21.69	0.0466	76.580
JBW7204A	108133.57	10239.05	MN	0.20	0.226	21.59	0.0469	2.441
JBW7212A	109634.00	10474.00	FE	0.10	0.197	24.36	0.0427	3.377
JBW7212A	109634.00	10474.00	MN	0.30	0.209	24.22	0.0414	0.883
JBW7212B	109634.00	10475.00	BZ	0.30	0.218	24.57	0.0411	1.398
JBW7212B	109634.00	10475.00	FE	0.35	0.242	26.63	0.0376	287.900
JBW7212B	109634.00	10475.00	MN	0.30	0.202	23.58	0.0437	2.611
JBW7213A	109465.95	11143.64	BZ	0.15	0.187	20.30	0.0498	0.461
JBW7213A	109465.95	11143.64	FE	0.40	0.237	28.57	0.0353	25.330
JBW7213A	109465.95	11143.64	MN	0.35	0.219	26.35	0.0384	60.770
JBW7213B	109465.95	11144.64	BZ	0.25	0.225	22.56	0.0445	0.436
JBW7213B	109465.95	11144.64	FE	0.35	0.243	26.54	0.0379	12.550
JBW7213B	109465.95	11144.64	MN	0.30	0.219	24.91	0.0411	46.090
JBW7215B	109929.84	11368.79	FE	0.25	0.245	26.25	0.0392	28.960
JBW7215B	109929.84	11368.79	MN	0.30	0.228	24.90	0.0408	0.995
JBW7317	112089.57	15002.11	FE	0.40	0.246	28.11	0.0356	341.800
JBW7317	112089.57	15002.11	MN	0.35	0.206	26.20	0.0382	81.280
JBW7326A	108222.30	10888.36	FE	0.30	0.180	24.27	0.0416	28.240
JBW7326A	108222.30	10888.36	MN	0.20	0.198	21.73	0.0465	6.892
JBW7326B	108222.30	10889.36	FE	0.25	0.215	23.03	0.0440	16.620
JBW7326B	108222.30	10889.36	MN	0.25	0.224	22.81	0.0444	2.004
JBW7328	110684.04	14780.69	FE	0.50	0.248	33.95	0.0290	293.000
JBW7328	110684.04	14780.69	MN	0.30	0.228	24.43	0.0414	32.380
JBW7330A	109964.67	13026.80	BZ	0.30	0.247	24.57	0.0416	0.185
JBW7330A	109964.67	13026.80	FE	0.30	0.215	24.18	0.0415	27.470
JBW7330A	109964.67	13026.80	MN	0.35	0.216	26.04	0.0390	1.325
JBW7333	110584.22	13306.80	BZ	0.20	0.194	21.71	0.0466	4.049
JBW7333	110584.22	13306.80	FE	0.20	0.206	21.71	0.0467	43.150
JBW7333	110584.22	13306.80	MN	0.10	0.200	20.16	0.0510	62.110
JBW7338A	110830.36	13609.17	BZ	0.35	0.250	26.40	0.0380	3.393
JBW7338A	110830.36	13609.17	FE	0.30	0.247	23.95	0.0419	832.600
JBW7338A	110830.36	13609.17	MN	0.25	0.245	26.17	0.0392	278.300
JBW7338B	110830.36	13610.17	BZ	0.35	0.234	26.43	0.0376	16.330
JBW7338B	110830.36	13610.17	FE	0.50	0.238	33.40	0.0297	31.840
JBW7338B	110830.36	13610.17	MN	0.05	0.136	19.56	0.0533	0.397

WELL_ID	EASTING (ft)	NORTHING (ft)	COC	CUT	OUTPCT	INTERVAL (wks)	FREQ (#/wk)	AVE-IQR (ppb)
JBW7340B	110361.54	13210.74	BZ	0.15	0.235	20.40	0.0497	1.413
JBW7340B	110361.54	13210.74	FE	0.20	0.191	21.58	0.0466	159.600
JBW7340B	110361.54	13210.74	MN	0.20	0.201	21.52	0.0467	84.590
JBW7344	110987.60	13622.38	BZ	0.30	0.197	27.38	0.0372	5.026
JBW7344	110987.60	13622.38	FE	0.10	0.230	21.68	0.0471	662.500
JBW7344	110987.60	13622.38	MN	0.15	0.247	22.91	0.0446	99.030
JBW7345A	110554.50	13806.74	BZ	0.25	0.206	22.72	0.0442	0.718
JBW7345A	110554.50	13806.74	FE	0.30	0.229	24.82	0.0408	17.760
JBW7345A	110554.50	13806.74	MN	0.20	0.208	21.55	0.0469	0.816
JBW7347B	110460.02	14624.90	FE	0.30	0.229	24.09	0.0416	203.200
JBW7347B	110460.02	14624.90	MN	0.25	0.224	23.04	0.0437	1.470
JBW7348	110802.02	13966.56	BZ	0.45	0.161	30.68	0.0324	5.833
JBW7348	110802.02	13966.56	FE	0.25	0.231	23.18	0.0437	23.930
JBW7348	110802.02	13966.56	MN	0.20	0.221	21.35	0.0470	47.360
JBW7350	111365.86	14160.19	BZ	0.30	0.250	24.72	0.0411	0.118
JBW7350	111365.86	14160.19	FE	0.35	0.225	26.93	0.0374	36.050
JBW7350	111365.86	14160.19	MN	0.30	0.212	24.49	0.0410	3.665
JBW7710	109834.07	15664.23	BZ	0.35	0.218	26.41	0.0383	3.155
JBW7806	107716.95	20532.58	FE	0.20	0.207	21.46	0.0472	138.500
JBW7806	107716.95	20532.58	MN	0.25	0.223	22.91	0.0442	43.350
JBW7809	109112.81	21161.11	FE	0.25	0.206	22.83	0.0444	16.530
JBW7809	109112.81	21161.11	MN	0.30	0.196	24.09	0.0418	0.893
JBW7812B	108332.56	20848.69	BZ	0.20	0.211	21.16	0.0475	2.207
JBW7812B	108332.56	20848.69	FE	0.25	0.165	22.75	0.0444	16.590
JBW7812B	108332.56	20848.69	MN	0.20	0.206	21.67	0.0465	8.103
JBW8003B	115426.83	21756.94	FE	0.30	0.228	23.93	0.0420	111.900
JBW8003B	115426.83	21756.94	MN	0.20	0.197	21.04	0.0481	16.820
JBW8004B	116178.78	22363.68	FE	0.30	0.234	24.54	0.0411	126.300
JBW8004B	116178.78	22363.68	MN	0.25	0.185	22.67	0.0445	1.085
JBW8009	113487.91	21023.48	FE	0.25	0.208	22.84	0.0446	91.990
JBW8009	113487.91	21023.48	MN	0.25	0.236	22.60	0.0450	12.340
JMW0201A	108502.60	20874.60	BZ	0.15	0.232	70.62	0.0140	25.720
JMW0301C	109861.00	13420.00	FE	0.20	0.202	21.70	0.0468	68.390
JMW0301C	109861.00	13420.00	MN	0.30	0.206	24.13	0.0419	12.470
JMW0503	111069.89	14733.53	FE	0.40	0.241	28.33	0.0354	399.400
JMW0503	111069.89	14733.53	MN	0.35	0.227	26.03	0.0385	27.640
JMW0505	111132.90	14617.51	BZ	0.15	0.246	58.35	0.0166	2.019
JMW0505	111132.90	14617.51	FE	0.40	0.230	29.10	0.0350	185.700
JMW0505	111132.90	14617.51	MN	0.45	0.228	31.28	0.0320	4.373
JMW0542	109338.80	12434.20	BZ	0.25	0.199	22.48	0.0445	0.107
JMW0542	109338.80	12434.20	FE	0.20	0.240	21.76	0.0467	273.200
JMW0542	109338.80	12434.20	MN	0.30	0.222	23.94	0.0419	191.600
JMW0604	111650.60	8969.90	BZ	0.30	0.235	92.43	0.0107	0.647
JMW0701	107403.43	16369.68	BZ	0.45	0.214	30.08	0.0327	8.448
JMW1103D	114886.70	21449.90	BZ	0.40	0.222	57.64	0.0168	4.621
JMW1103D	114886.70	21449.90	FE	0.30	0.212	24.29	0.0416	2327.000
JMW1103D	114886.70	21449.90	MN	0.20	0.242	19.59	0.0518	33.560
JMW1562	111523.51	14976.24	BZ	0.10	0.155	69.23	0.0146	323.800
JMW1564	111324.20	14979.63	BZ	0.20	0.170	27.35	0.0382	5.599
JMW1564	111324.20	14979.63	FE	0.30	0.199	24.05	0.0419	1208.000
JMW1565	111522.30	14964.19	BZ	0.10	0.169	20.52	0.0509	212.400
JMW1565	111522.30	14964.19	FE	0.25	0.176	22.95	0.0443	5530.000
JMW1565	111522.30	14964.19	MN	0.25	0.232	23.06	0.0436	749.300
JMW1860	108944.86	9032.97	BZ	0.15	0.217	20.12	0.0501	0.093
JMW1860	108944.86	9032.97	FE	0.25	0.192	22.89	0.0445	965.500
JMW1860	108944.86	9032.97	MN	0.20	0.231	21.68	0.0465	48.630
JMW1881	108936.65	9301.22	BZ	0.25	0.223	22.60	0.0447	0.670
JMW1881	108936.65	9301.22	FE	0.10	0.159	19.04	0.0530	0.716
JMW1881	108936.65	9301.22	MN	0.20	0.236	21.28	0.0474	14.740
JMW1960	109086.09	10613.03	BZ	0.25	0.216	85.02	0.0119	354.200
JMW1960	109086.09	10613.03	FE	0.30	0.215	91.64	0.0111	1549.000
JMW1963	109286.98	10487.77	BZ	0.25	0.238	25.55	0.0403	1.492
JMW1963	109286.98	10487.77	FE	0.25	0.173	22.88	0.0445	46.600
JMW1963	109286.98	10487.77	MN	0.35	0.223	26.57	0.0378	44.190
JMW1964	109282.91	10966.36	BZ	0.25	0.211	22.98	0.0437	2.157
JMW1964	109282.91	10966.36	FE	0.40	0.237	32.60	0.0311	16.170
JMW1964	109282.91	10966.36	MN	0.15	0.241	22.44	0.0457	0.134

WELL_ID	EASTING (ft)	NORTHING (ft)	COC	CUT	OUTPCT	INTERVAL (wks)	FREQ (#/wk)	AVE-IQR (ppb)
JMW1966	109099.64	10610.39	BZ	0.30	0.236	25.00	0.0406	4.826
JMW1966	109099.64	10610.39	FE	0.50	0.225	34.97	0.0292	315.100
JMW1966	109099.64	10610.39	MN	0.35	0.241	26.59	0.0383	243.500
JMW3202	110684.15	13404.85	BZ	0.55	0.217	69.63	0.0143	8.030
JMW3202	110684.15	13404.85	FE	0.20	0.203	21.60	0.0467	711.200
JMW3202	110684.15	13404.85	MN	0.30	0.245	24.94	0.0404	293.800
JMW35X2	110127.97	10067.32	FE	0.45	0.219	31.52	0.0319	87.660
JMW35X2	110127.97	10067.32	MN	0.25	0.247	22.77	0.0444	1.503
JMW6001	109866.12	16952.71	BZ	0.50	0.242	34.39	0.0294	1.864
JMW7332	107984.11	11714.85	FE	0.30	0.247	24.16	0.0417	306.400
JMW7332	107984.11	11714.85	MN	0.35	0.201	26.42	0.0382	1179.000
JMW7612	106986.73	16453.32	BZ	0.25	0.208	23.10	0.0441	0.974
JMW8011	116191.11	22376.38	FE	0.25	0.221	22.45	0.0450	118.000
JMW8011	116191.11	22376.38	MN	0.55	0.237	38.08	0.0270	134.300
JPZ0340	109561.37	13962.51	BZ	0.30	0.180	24.45	0.0411	0.388
JPZ0340	109561.37	13962.51	FE	0.15	0.201	20.00	0.0505	5.981
JPZ0340	109561.37	13962.51	MN	0.10	0.178	21.07	0.0486	27.660
JPZ0341	109554.37	13917.07	FE	0.15	0.177	20.05	0.0503	57.030
JPZ0341	109554.37	13917.07	MN	0.15	0.181	22.51	0.0455	127.400
JPZ0342	109510.08	14069.10	BZ	0.70	0.166	104.97	0.0092	0.676
JPZ0342	109510.08	14069.10	FE	0.25	0.214	23.13	0.0440	68.750
JPZ0342	109510.08	14069.10	MN	0.20	0.217	21.30	0.0473	16.130
JPZ0343	109503.35	14073.53	BZ	0.10	0.203	34.77	0.0291	1.937
JPZ0343	109503.35	14073.53	FE	0.20	0.205	21.10	0.0478	450.200
JPZ0343	109503.35	14073.53	MN	0.20	0.240	21.52	0.0467	108.500
JPZ0348	108885.33	12194.33	BZ	0.35	0.220	26.45	0.0384	0.625
JPZ0348	108885.33	12194.33	FE	0.35	0.206	26.52	0.0381	21.010
JPZ0348	108885.33	12194.33	MN	0.35	0.244	26.61	0.0380	1.112
JPZ0349	108892.85	12200.73	FE	0.40	0.244	29.42	0.0343	32.950
JPZ0349	108892.85	12200.73	MN	0.25	0.236	22.90	0.0440	20.520
JPZ1780	109521.51	12824.33	FE	0.35	0.246	26.55	0.0379	30.980
JPZ1780	109521.51	12824.33	MN	0.35	0.200	26.06	0.0387	1.806
JPZ7208	108141.92	10243.38	FE	0.45	0.233	31.00	0.0323	40.410
JPZ7208	108141.92	10243.38	MN	0.25	0.230	23.38	0.0435	94.460
JPZ7312	109847.28	15397.09	BZ	0.25	0.189	22.66	0.0447	2.741
JPZ7807	107539.30	20443.30	FE	0.30	0.243	24.31	0.0413	14.040
JPZ7807	107539.30	20443.30	MN	0.30	0.243	24.43	0.0414	1.008
MMW0005	110994.15	14918.82	BZ	0.30	0.245	24.31	0.0413	36.920
MMW0005	110994.15	14918.82	FE	0.25	0.227	21.78	0.0468	2124.000
MMW0005	110994.15	14918.82	MN	0.20	0.175	20.01	0.0511	156.800
MMW0007A	105635.89	8867.39	FE	0.25	0.213	22.48	0.0454	22.190
MMW0007A	105635.89	8867.39	MN	0.20	0.201	20.79	0.0485	2.384
MMW0007B	105635.89	8869.39	FE	0.20	0.234	23.17	0.0439	11.120
MMW0007B	105635.89	8869.39	MN	0.45	0.228	29.92	0.0338	2.289
MMW0008	105643.92	8869.73	FE	0.25	0.243	25.83	0.0401	6.638
MMW0008	105643.92	8869.73	MN	0.35	0.235	25.82	0.0390	1.488
MMW0009	107189.78	20000.95	BZ	0.25	0.191	22.59	0.0448	0.213
MMW0009	107189.78	20000.95	FE	0.40	0.247	28.12	0.0356	109.600
MMW0009	107189.78	20000.95	MN	0.30	0.202	23.51	0.0425	7.100
MMW0010	107230.49	9847.09	FE	0.30	0.246	27.58	0.0374	11.660
MMW0010	107230.49	9847.09	MN	0.55	0.247	37.89	0.0270	0.599
MMW0011	107224.74	9841.50	FE	0.30	0.208	24.08	0.0420	11.680
MMW0011	107224.74	9841.50	MN	0.20	0.250	24.13	0.0424	0.562
MMW0012	108059.46	10484.21	FE	0.25	0.247	22.70	0.0447	10.140
MMW0012	108059.46	10484.21	MN	0.35	0.240	25.94	0.0388	0.885
MMW0013	108066.33	10492.60	FE	0.30	0.192	24.12	0.0416	17.410
MMW0013	108066.33	10492.60	MN	0.20	0.217	21.13	0.0476	28.940
MMW0016	107858.21	10022.92	FE	0.40	0.222	28.89	0.0356	47.900
MMW0016	107858.21	10022.92	MN	0.25	0.220	22.50	0.0449	1.033
MMW0017	107038.16	9401.65	FE	0.30	0.218	24.06	0.0417	1710.000
MMW0017	107038.16	9401.65	MN	0.25	0.225	22.75	0.0445	24.070
MMW0019	105655.31	8657.30	FE	0.25	0.222	21.45	0.0478	82.620
MMW0019	105655.31	8657.30	MN	0.25	0.232	21.86	0.0466	37.830
MMW1560	111365.14	15129.42	BZ	0.25	0.239	22.70	0.0446	1078.000
MMW1560	111365.14	15129.42	FE	0.20	0.216	21.29	0.0477	437.900
MMW1560	111365.14	15129.42	MN	0.25	0.248	22.63	0.0446	1265.000
MMW7330	109964.67	13027.80	BZ	0.10	0.205	19.26	0.0525	0.122

WELL_ID	EASTING (ft)	NORTHING (ft)	COC	CUT	OUTPCT	INTERVAL (wks)	FREQ (#/wk)	AVE-IQR (ppb)
MMW7330	109964.67	13027.80	FE	0.30	0.193	24.25	0.0415	505.200
MMW7330	109964.67	13027.80	MN	0.25	0.212	22.38	0.0447	24.700
MMW8015	116664.03	22451.10	BZ	0.20	0.199	20.76	0.0485	0.191
MMW8015	116664.03	22451.10	FE	0.20	0.204	20.72	0.0487	703.200
MMW8015	116664.03	22451.10	MN	0.20	0.196	20.60	0.0491	240.200
RFW1144	114680.90	21344.90	BZ	0.30	0.222	24.41	0.0414	2.052
RFW1144	114680.90	21344.90	FE	0.25	0.218	22.54	0.0448	749.300
RFW1144	114680.90	21344.90	MN	0.20	0.191	21.10	0.0480	119.800
RFW1147	114493.70	21230.60	BZ	0.25	0.162	22.34	0.0452	1.320
RFW1147	114493.70	21230.60	FE	0.15	0.162	19.71	0.0512	1579.000
RFW1147	114493.70	21230.60	MN	0.20	0.213	21.00	0.0479	243.500

Table 3-5. Optimal Sampling Intervals and Frequencies Measured Across All COCs

Notes: N-COCs = Number of COCs with Results; REMOVAL = Minimum fraction of data removed; INTERVAL = Minimum Optimal Sampling Interval (in weeks); FREQ = Maximum Optimal Sampling Frequency (samples/week); PROPOSED = closest operational sampling interval (in quarters) to the minimum optimal sampling interval (e.g., 3Q = 3 quarters)

WELLID	EASTING	NORTHING	N-COCs	REMOVAL	INTERVAL (wks)	FREQ (#/wk)	PROPOSED
056MW02	110269.46	12297.76	2	0.25	22.62	0.0446	2Q
056MW04	110130.10	12294.51	3	0.20	21.65	0.0468	2Q
AR25	109037.00	11902.00	2	0.25	22.43	0.0450	2Q
FMW3413	111995.35	22114.24	2	0.15	19.95	0.0507	2Q
JBW7101	108258.77	9885.66	2	0.20	19.42	0.0515	1Q
JBW7102	109201.33	8769.83	2	0.50	33.19	0.0301	3Q
JBW7106A	105746.65	8560.70	2	0.25	21.80	0.0464	2Q
JBW7106B	105746.65	8561.70	2	0.15	19.30	0.0523	1Q
JBW7203A	108468.08	10501.33	2	0.30	20.62	0.0494	2Q
JBW7203B	108468.08	10502.33	2	0.35	22.40	0.0454	2Q
JBW7204A	108133.57	10239.05	2	0.20	21.59	0.0469	2Q
JBW7212A	109634.00	10474.00	2	0.10	24.22	0.0427	2Q
JBW7212B	109634.00	10475.00	3	0.30	23.58	0.0437	2Q
JBW7213A	109465.95	11143.64	3	0.15	20.30	0.0498	2Q
JBW7213B	109465.95	11144.64	3	0.25	22.56	0.0445	2Q
JBW7215B	109929.84	11368.79	2	0.25	24.90	0.0408	2Q
JBW7317	112089.57	15002.11	2	0.35	26.20	0.0382	2Q
JBW7326A	108222.30	10888.36	2	0.20	21.73	0.0465	2Q
JBW7326B	108222.30	10889.36	2	0.25	22.81	0.0444	2Q
JBW7328	110684.04	14780.69	2	0.30	24.43	0.0414	2Q
JBW7330A	109964.67	13026.80	3	0.30	24.18	0.0416	2Q
JBW7333	110584.22	13306.80	3	0.10	20.16	0.0510	2Q
JBW7338A	110830.36	13609.17	3	0.25	23.95	0.0419	2Q
JBW7338B	110830.36	13610.17	3	0.05	19.56	0.0533	2Q
JBW7340B	110361.54	13210.74	3	0.15	20.40	0.0497	2Q
JBW7344	110987.60	13622.38	3	0.10	21.68	0.0471	2Q
JBW7345A	110554.50	13806.74	3	0.20	21.55	0.0469	2Q
JBW7347B	110460.02	14624.90	2	0.25	23.04	0.0437	2Q
JBW7348	110802.02	13966.56	3	0.20	21.35	0.0470	2Q
JBW7350	111365.86	14160.19	3	0.30	24.49	0.0411	2Q
JBW7710	109834.07	15664.23	1	0.35	26.41	0.0383	2Q
JBW7806	107716.95	20532.58	2	0.20	21.46	0.0472	2Q
JBW7809	109112.81	21161.11	2	0.25	22.83	0.0444	2Q
JBW7812B	108332.56	20848.69	3	0.20	21.16	0.0475	2Q
JBW8003B	115426.83	21756.94	2	0.20	21.04	0.0481	2Q
JBW8004B	116178.78	22363.68	2	0.25	22.67	0.0445	2Q
JBW8009	113487.91	21023.48	2	0.25	22.60	0.0450	2Q
JMW0201A	108502.60	20874.60	1	0.15	70.62	0.0140	5Q
JMW0301C	109861.00	13420.00	2	0.20	21.70	0.0468	2Q
JMW0503	111069.89	14733.53	2	0.35	26.03	0.0385	2Q

WELLID	EASTING	NORTHING	N-COCS	REMOVAL	INTERVAL (wks)	FREQ (#/wk)	PROPOSED
JMW0505	111132.90	14617.51	3	0.15	29.10	0.0350	2Q
JMW0542	109338.80	12434.20	3	0.20	21.76	0.0467	2Q
JMW0604	111650.60	8969.90	1	0.30	92.43	0.0107	7Q
JMW0701	107403.43	16369.68	1	0.45	30.08	0.0327	2Q
JMW1103D	114886.70	21449.90	3	0.20	19.59	0.0518	2Q
JMW1562	111523.51	14976.24	1	0.10	69.23	0.0146	5Q
JMW1564	111324.20	14979.63	2	0.20	24.05	0.0419	2Q
JMW1565	111522.30	14964.19	3	0.10	20.52	0.0509	2Q
JMW1860	108944.86	9032.97	3	0.15	20.12	0.0501	2Q
JMW1881	108936.65	9301.22	3	0.10	19.04	0.0530	1Q
JMW1960	109086.09	10613.03	2	0.25	85.02	0.0119	7Q
JMW1963	109286.98	10487.77	3	0.25	22.88	0.0445	2Q
JMW1964	109282.91	10966.36	3	0.15	22.44	0.0457	2Q
JMW1966	109099.64	10610.39	3	0.30	25.00	0.0406	2Q
JMW3202	110684.15	13404.85	3	0.20	21.60	0.0467	2Q
JMW35X2	110127.97	10067.32	2	0.25	22.77	0.0444	2Q
JMW6001	109866.12	16952.71	1	0.50	34.39	0.0294	3Q
JMW7332	107984.11	11714.85	2	0.30	24.16	0.0417	2Q
JMW7612	106986.73	16453.32	1	0.25	23.10	0.0441	2Q
JMW8011	116191.11	22376.38	2	0.25	22.45	0.0450	2Q
JPZ0340	109561.37	13962.51	3	0.10	20.00	0.0505	2Q
JPZ0341	109554.37	13917.07	2	0.15	20.05	0.0503	2Q
JPZ0342	109510.08	14069.10	3	0.20	21.30	0.0473	2Q
JPZ0343	109503.35	14073.53	3	0.10	21.10	0.0478	2Q
JPZ0348	108885.33	12194.33	3	0.35	26.45	0.0384	2Q
JPZ0349	108892.85	12200.73	2	0.25	22.90	0.0440	2Q
JPZ1780	109521.51	12824.33	2	0.35	26.06	0.0387	2Q
JPZ7208	108141.92	10243.38	2	0.25	23.38	0.0435	2Q
JPZ7312	109847.28	15397.09	1	0.25	22.66	0.0447	2Q
JPZ7807	107539.30	20443.30	2	0.30	24.31	0.0414	2Q
MMW0005	110994.15	14918.82	3	0.20	20.01	0.0511	2Q
MMW0007A	105635.89	8867.39	2	0.20	20.79	0.0485	2Q
MMW0007B	105635.89	8869.39	2	0.20	23.17	0.0439	2Q
MMW0008	105643.92	8869.73	2	0.25	25.82	0.0401	2Q
MMW0009	107189.78	20000.95	3	0.25	22.59	0.0448	2Q
MMW0010	107230.49	9847.09	2	0.30	27.58	0.0374	2Q
MMW0011	107224.74	9841.50	2	0.20	24.08	0.0424	2Q
MMW0012	108059.46	10484.21	2	0.25	22.70	0.0447	2Q
MMW0013	108066.33	10492.60	2	0.20	21.13	0.0476	2Q
MMW0016	107858.21	10022.92	2	0.25	22.50	0.0449	2Q
MMW0017	107038.16	9401.65	2	0.25	22.75	0.0445	2Q
MMW0019	105655.31	8657.30	2	0.25	21.45	0.0478	2Q
MMW1560	111365.14	15129.42	3	0.20	21.29	0.0477	2Q
MMW7330	109964.67	13027.80	3	0.10	19.26	0.0525	1Q
MMW8015	116664.03	22451.10	3	0.20	20.60	0.0491	2Q
RFW1144	114680.90	21344.90	3	0.20	21.10	0.0480	2Q
RFW1147	114493.70	21230.60	3	0.15	19.71	0.0512	2Q

Section 3.4.3. Trend Maps

The trend maps themselves have been described above (a graph for each COC and each time period is contained in **Appendix 3-4**). It is clear from these maps that most of the estimated trends in either direction are not ‘certain’ in a statistical sense, as denoted by the light pink and light blue shading. That is, they could possibly be artifacts of sampling variation. However, it is also apparent that certain ‘hot spots’ around the site have existed and may still exist for these COCs.

Benzene shows up with less certainty in the most recent sampling events, but hot spots of increasing benzene concentration seem to have existed near the Central NDA and FSSB areas in somewhat older data. There is also a fairly certain downward trend, both historically and more recently, at a cluster of wells located near the BL and VMB areas, and probably near the UPGRADIENT BXSS area.

With respect to the metals, iron shows historical and fairly recent increases at wells located near the Central NDA, FSSB, and East Loring Lake areas. Very recently, there is also an indication of increasing iron near FLDD SOUTH. The trends in manganese are similar to iron, except that the evidence is less strong for samples from the East Loring Lake area, and that there is another more recent increase in manganese suggested near the FLDD NORTH area.

Specific numerical information about the estimated trend magnitudes — including confidence bounds around each trend — by well and COC is listed in **Table 3-6**.

Table 3-6. Estimated Trend Magnitudes and Confidence Intervals by COC and Well Location

Notes: Historical = all data; Latest = last 4 sampling events
 CONF-LEV = Achieved confidence level of non-parametric confidence interval around median slope
 TREND = estimated magnitude of median slope (ppb/week);
 LOWER-LIMIT = lower 95% confidence bound on trend magnitude (ppb/week)
 UPPER-LIMIT = upper 95% confidence bound on trend magnitude (ppb/week)

WELLID	EASTING	NORTHING	COC	TYPE	CONF-LEV	TREND	LOWER-LIMIT	UPPER-LIMIT
056MW02	110269.46	12297.76	BZ	Historical	0.953	0.0000	0.0000	0.0000
056MW02	110269.46	12297.76	BZ	Post-1999	0.959	0.0000	0.0000	0.0000
056MW02	110269.46	12297.76	BZ	Latest	0.978	0.0000	0.0000	0.0000
056MW02	110269.46	12297.76	FE	Historical	0.953	-1.2809	-7.8915	-0.5672
056MW02	110269.46	12297.76	FE	Post-1999	0.959	-1.1097	-5.1672	-0.5464
056MW02	110269.46	12297.76	FE	Latest	0.978	1.9364	-0.3592	7.8657
056MW02	110269.46	12297.76	MN	Historical	0.953	-2.3554	-13.2236	34.3546
056MW02	110269.46	12297.76	MN	Post-1999	0.959	-4.2593	-13.6912	31.2714
056MW02	110269.46	12297.76	MN	Latest	0.978	89.6971	5.8200	240.8873
056MW04	110130.10	12294.51	BZ	Historical	0.953	-0.0056	-0.1476	0.0558
056MW04	110130.10	12294.51	BZ	Post-1999	0.959	0.0130	-0.0833	0.0623
056MW04	110130.10	12294.51	BZ	Latest	0.978	-0.1476	-0.5434	0.0130
056MW04	110130.10	12294.51	FE	Historical	0.953	-15.9485	-34.4114	5.4018
056MW04	110130.10	12294.51	FE	Post-1999	0.959	-17.0481	-40.0089	3.7415
056MW04	110130.10	12294.51	FE	Latest	0.978	17.8635	-17.0481	45.2509
056MW04	110130.10	12294.51	MN	Historical	0.953	0.2094	-15.4145	16.9294
056MW04	110130.10	12294.51	MN	Post-1999	0.959	3.9743	-11.0809	17.4117
056MW04	110130.10	12294.51	MN	Latest	0.978	4.2654	-81.8914	19.9349
AR25	109037.00	11902.00	BZ	Historical	0.953	0.0000	0.0000	0.0000
AR25	109037.00	11902.00	BZ	Post-1999	0.959	0.0000	0.0000	0.0000
AR25	109037.00	11902.00	BZ	Latest	0.978	0.0000	0.0000	0.0000
AR25	109037.00	11902.00	FE	Historical	0.953	-1.9346	-2.7109	-0.7012
AR25	109037.00	11902.00	FE	Post-1999	0.959	-1.8077	-2.6939	0.0331
AR25	109037.00	11902.00	FE	Latest	0.978	-1.7924	-4.9831	2.3092
AR25	109037.00	11902.00	MN	Historical	0.953	-0.7208	-1.1422	-0.2990
AR25	109037.00	11902.00	MN	Post-1999	0.959	-0.5969	-1.1337	-0.2605
AR25	109037.00	11902.00	MN	Latest	0.978	-0.2303	-0.5969	0.1726
BMW715	107439.45	16139.85	BZ	Historical	0.953	0.0000	0.0000	0.0000
BMW715	107439.45	16139.85	BZ	Post-1999	0.959	0.0000	0.0000	0.0000
BMW715	107439.45	16139.85	BZ	Latest	0.978	0.0000	0.0000	0.0000
BMW717	107613.87	16146.84	BZ	Historical	0.953	0.0000	0.0000	0.0000
BMW717	107613.87	16146.84	BZ	Post-1999	0.959	0.0000	0.0000	0.0000
BMW717	107613.87	16146.84	BZ	Latest	0.978	0.0000	0.0000	0.0000
FMW3413	111995.35	22114.24	BZ	Historical	0.965	0.0000	0.0000	0.0000

WELLID	EASTING	NORTHING	COC	TYPE	CONF-LEV	TREND	LOWER-LIMIT	UPPER-LIMIT
FMW3413	111995.35	22114.24	BZ	Post-1999	0.971	0.0000	0.0000	0.0000
FMW3413	111995.35	22114.24	BZ	Latest	0.988	0.0000	0.0000	0.0000
FMW3413	111995.35	22114.24	FE	Historical	0.953	-0.4854	-0.6496	0.2520
FMW3413	111995.35	22114.24	FE	Post-1999	0.959	-0.4854	-0.6496	0.4528
FMW3413	111995.35	22114.24	FE	Latest	0.978	-0.4854	-0.5880	0.2520
FMW3413	111995.35	22114.24	MN	Historical	0.953	0.0075	-0.0065	0.0214
FMW3413	111995.35	22114.24	MN	Post-1999	0.959	0.0083	-0.0056	0.0215
FMW3413	111995.35	22114.24	MN	Latest	0.978	0.0214	-0.0101	0.1181
JBW7101	108258.77	9885.66	BZ	Historical	0.953	0.0000	0.0000	0.0000
JBW7101	108258.77	9885.66	BZ	Post-1999	0.959	0.0000	0.0000	0.0000
JBW7101	108258.77	9885.66	BZ	Latest	0.978	0.0000	0.0000	0.0000
JBW7101	108258.77	9885.66	FE	Historical	0.962	-0.9660	-1.3362	-0.1908
JBW7101	108258.77	9885.66	FE	Post-1999	0.966	-0.9710	-1.3384	-0.8054
JBW7101	108258.77	9885.66	FE	Latest	0.987	-2.1444	-3.2758	-0.9786
JBW7101	108258.77	9885.66	MN	Historical	0.962	0.0031	-0.0256	0.0138
JBW7101	108258.77	9885.66	MN	Post-1999	0.966	0.0004	-0.0321	0.0135
JBW7101	108258.77	9885.66	MN	Latest	0.987	-0.0708	-0.0781	-0.0420
JBW7102	109201.33	8769.83	BZ	Historical	0.953	0.0000	0.0000	0.0000
JBW7102	109201.33	8769.83	BZ	Post-1999	0.959	0.0000	0.0000	0.0000
JBW7102	109201.33	8769.83	BZ	Latest	0.978	0.0000	0.0000	0.0000
JBW7102	109201.33	8769.83	FE	Historical	0.953	0.5252	-0.9157	2.1921
JBW7102	109201.33	8769.83	FE	Post-1999	0.959	0.6297	-0.6488	2.6816
JBW7102	109201.33	8769.83	FE	Latest	0.978	1.7241	-0.9157	6.1195
JBW7102	109201.33	8769.83	MN	Historical	0.953	0.0266	0.0108	0.0530
JBW7102	109201.33	8769.83	MN	Post-1999	0.959	0.0285	0.0135	0.0575
JBW7102	109201.33	8769.83	MN	Latest	0.978	0.1222	0.0500	0.2415
JBW7106A	105746.65	8560.70	BZ	Historical	0.953	0.0000	0.0000	0.0000
JBW7106A	105746.65	8560.70	BZ	Post-1999	0.971	0.0000	0.0000	0.0000
JBW7106A	105746.65	8560.70	BZ	Latest	0.978	0.0000	0.0000	0.0000
JBW7106A	105746.65	8560.70	FE	Historical	0.953	-1.1932	-2.8235	-0.2980
JBW7106A	105746.65	8560.70	FE	Post-1999	0.971	-1.1282	-2.8235	-0.0845
JBW7106A	105746.65	8560.70	FE	Latest	0.978	-0.2980	-1.3474	0.5291
JBW7106A	105746.65	8560.70	MN	Historical	0.953	-0.0144	-0.0525	0.0047
JBW7106A	105746.65	8560.70	MN	Post-1999	0.971	-0.0124	-0.0525	0.0069
JBW7106A	105746.65	8560.70	MN	Latest	0.978	0.0047	-0.0232	0.0216
JBW7106B	105746.65	8561.70	BZ	Historical	0.953	0.0000	0.0000	0.0000
JBW7106B	105746.65	8561.70	BZ	Post-1999	0.971	0.0000	0.0000	0.0000
JBW7106B	105746.65	8561.70	BZ	Latest	0.978	0.0000	0.0000	0.0000
JBW7106B	105746.65	8561.70	FE	Historical	0.953	0.2441	-8.3748	8.6529
JBW7106B	105746.65	8561.70	FE	Post-1999	0.971	0.9494	-8.3748	10.0362
JBW7106B	105746.65	8561.70	FE	Latest	0.978	0.2441	-35.4373	15.1735
JBW7106B	105746.65	8561.70	MN	Historical	0.953	-0.0067	-0.1679	0.1271
JBW7106B	105746.65	8561.70	MN	Post-1999	0.971	0.0034	-0.1679	0.1602
JBW7106B	105746.65	8561.70	MN	Latest	0.978	-0.0067	-0.6976	0.2289

WELLID	EASTING	NORTHING	COC	TYPE	CONF-LEV	TREND	LOWER-LIMIT	UPPER-LIMIT
JBW7203A	108468.08	10501.33	BZ	Historical	0.953	0.0000	0.0000	0.0000
JBW7203A	108468.08	10501.33	BZ	Post-1999	0.959	0.0000	0.0000	0.0000
JBW7203A	108468.08	10501.33	BZ	Latest	0.978	0.0000	0.0000	0.0000
JBW7203A	108468.08	10501.33	FE	Historical	0.953	0.4177	-0.1203	0.8217
JBW7203A	108468.08	10501.33	FE	Post-1999	0.976	0.2475	-0.4830	0.8217
JBW7203A	108468.08	10501.33	FE	Latest	0.965	1.1874	0.2475	4.2081
JBW7203A	108468.08	10501.33	MN	Historical	0.953	-0.1247	-0.1773	-0.0774
JBW7203A	108468.08	10501.33	MN	Post-1999	0.976	-0.1589	-0.2155	-0.0774
JBW7203A	108468.08	10501.33	MN	Latest	0.965	-0.1589	-0.4006	-0.0822
JBW7203B	108468.08	10502.33	BZ	Historical	0.953	0.0000	0.0000	0.0000
JBW7203B	108468.08	10502.33	BZ	Post-1999	0.959	0.0000	0.0000	0.0000
JBW7203B	108468.08	10502.33	BZ	Latest	0.978	0.0000	0.0000	0.0000
JBW7203B	108468.08	10502.33	FE	Historical	0.962	-0.6566	-1.3722	-0.2598
JBW7203B	108468.08	10502.33	FE	Post-1999	0.966	-0.5828	-1.3705	0.1320
JBW7203B	108468.08	10502.33	FE	Latest	0.987	-0.8085	-1.6169	0.1320
JBW7203B	108468.08	10502.33	MN	Historical	0.953	0.0144	0.0075	0.0428
JBW7203B	108468.08	10502.33	MN	Post-1999	0.976	0.0271	0.0075	0.0448
JBW7203B	108468.08	10502.33	MN	Latest	0.965	0.0144	-0.0146	0.0361
JBW7204A	108133.57	10239.05	BZ	Historical	0.953	0.0000	0.0000	0.0000
JBW7204A	108133.57	10239.05	BZ	Post-1999	0.959	0.0000	0.0000	0.0000
JBW7204A	108133.57	10239.05	BZ	Latest	0.978	0.0000	0.0000	0.0000
JBW7204A	108133.57	10239.05	FE	Historical	0.953	-2.5419	-6.6887	0.4249
JBW7204A	108133.57	10239.05	FE	Post-1999	0.959	-3.6958	-7.1544	0.3183
JBW7204A	108133.57	10239.05	FE	Latest	0.978	-3.6958	-6.6887	0.3183
JBW7204A	108133.57	10239.05	MN	Historical	0.953	-0.1460	-0.1924	-0.0686
JBW7204A	108133.57	10239.05	MN	Post-1999	0.959	-0.1404	-0.1924	-0.0612
JBW7204A	108133.57	10239.05	MN	Latest	0.978	-0.0954	-0.1865	-0.0156
JBW7212A	109634.00	10474.00	BZ	Historical	0.953	0.0000	0.0000	0.0000
JBW7212A	109634.00	10474.00	BZ	Post-1999	0.959	0.0000	0.0000	0.0000
JBW7212A	109634.00	10474.00	BZ	Latest	0.978	0.0000	0.0000	0.0000
JBW7212A	109634.00	10474.00	FE	Historical	0.976	0.0364	-0.0478	0.0778
JBW7212A	109634.00	10474.00	FE	Post-1999	0.964	0.0368	-0.0462	0.0778
JBW7212A	109634.00	10474.00	FE	Latest	0.987	0.0407	-0.0890	0.2011
JBW7212A	109634.00	10474.00	MN	Historical	0.953	0.0094	-0.0049	0.0219
JBW7212A	109634.00	10474.00	MN	Post-1999	0.959	0.0082	-0.0069	0.0205
JBW7212A	109634.00	10474.00	MN	Latest	0.978	0.0205	0.0094	0.0467
JBW7212B	109634.00	10475.00	BZ	Historical	0.953	-0.0216	-0.0236	-0.0205
JBW7212B	109634.00	10475.00	BZ	Post-1999	0.959	-0.0225	-0.0238	-0.0206
JBW7212B	109634.00	10475.00	BZ	Latest	0.978	-0.0392	-0.0857	-0.0227
JBW7212B	109634.00	10475.00	FE	Historical	0.953	-2.7632	-6.4445	0.0093
JBW7212B	109634.00	10475.00	FE	Post-1999	0.959	-2.0289	-4.2854	0.1797
JBW7212B	109634.00	10475.00	FE	Latest	0.978	-0.3741	-7.1469	2.4299
JBW7212B	109634.00	10475.00	MN	Historical	0.965	-0.0035	-0.0583	0.0156
JBW7212B	109634.00	10475.00	MN	Post-1999	0.959	-0.0035	-0.0578	0.0156

WELLID	EASTING	NORTHING	COC	TYPE	CONF-LEV	TREND	LOWER-LIMIT	UPPER-LIMIT
JBW7212B	109634.00	10475.00	MN	Latest	0.978	-0.0268	-0.1256	0.0513
JBW7213A	109465.95	11143.64	BZ	Historical	0.953	-0.0319	-0.0562	-0.0102
JBW7213A	109465.95	11143.64	BZ	Post-1999	0.959	-0.0332	-0.0630	-0.0136
JBW7213A	109465.95	11143.64	BZ	Latest	0.978	-0.0562	-0.1914	-0.0165
JBW7213A	109465.95	11143.64	FE	Historical	0.953	-0.1847	-0.2163	0.0636
JBW7213A	109465.95	11143.64	FE	Post-1999	0.959	-0.1789	-0.2147	0.1813
JBW7213A	109465.95	11143.64	FE	Latest	0.978	0.0636	-0.1847	0.7551
JBW7213A	109465.95	11143.64	MN	Historical	0.953	-0.1940	-0.8101	0.1261
JBW7213A	109465.95	11143.64	MN	Post-1999	0.959	-0.2291	-0.9925	0.1058
JBW7213A	109465.95	11143.64	MN	Latest	0.978	0.5888	0.1058	1.6643
JBW7213B	109465.95	11144.64	BZ	Historical	0.953	-0.0042	-0.0099	0.0013
JBW7213B	109465.95	11144.64	BZ	Post-1999	0.959	-0.0057	-0.0114	-0.0010
JBW7213B	109465.95	11144.64	BZ	Latest	0.978	-0.0061	-0.0147	-0.0010
JBW7213B	109465.95	11144.64	FE	Historical	0.953	0.1223	0.0770	0.2158
JBW7213B	109465.95	11144.64	FE	Post-1999	0.959	0.1351	0.0828	0.2265
JBW7213B	109465.95	11144.64	FE	Latest	0.978	0.1772	0.1137	0.5090
JBW7213B	109465.95	11144.64	MN	Historical	0.953	0.1946	-0.4776	0.8575
JBW7213B	109465.95	11144.64	MN	Post-1999	0.959	0.3979	-0.3436	0.8873
JBW7213B	109465.95	11144.64	MN	Latest	0.978	2.4049	0.3979	7.3878
JBW7215B	109929.84	11368.79	BZ	Historical	0.953	0.0000	0.0000	0.0000
JBW7215B	109929.84	11368.79	BZ	Post-1999	0.959	0.0000	0.0000	0.0000
JBW7215B	109929.84	11368.79	BZ	Latest	0.978	0.0000	0.0000	0.0000
JBW7215B	109929.84	11368.79	FE	Historical	0.965	-0.0039	-0.2137	1.0486
JBW7215B	109929.84	11368.79	FE	Post-1999	0.971	-0.0302	-0.2301	0.4062
JBW7215B	109929.84	11368.79	FE	Latest	0.987	0.9596	-0.0039	3.8384
JBW7215B	109929.84	11368.79	MN	Historical	0.953	0.0051	0.0017	0.0102
JBW7215B	109929.84	11368.79	MN	Post-1999	0.959	0.0049	-0.0022	0.0069
JBW7215B	109929.84	11368.79	MN	Latest	0.978	0.0248	0.0060	0.0721
JBW7317	112089.57	15002.11	BZ	Historical	0.953	0.0000	0.0000	0.0000
JBW7317	112089.57	15002.11	BZ	Post-1999	0.959	0.0000	0.0000	0.0000
JBW7317	112089.57	15002.11	BZ	Latest	0.978	0.0000	0.0000	0.0000
JBW7317	112089.57	15002.11	FE	Historical	0.953	2.6718	-2.1152	10.3353
JBW7317	112089.57	15002.11	FE	Post-1999	0.959	2.2614	-3.3904	11.8610
JBW7317	112089.57	15002.11	FE	Latest	0.978	-9.2215	-13.9272	-0.5738
JBW7317	112089.57	15002.11	MN	Historical	0.953	-0.4458	-1.1558	0.0963
JBW7317	112089.57	15002.11	MN	Post-1999	0.959	-0.1738	-1.1369	0.2722
JBW7317	112089.57	15002.11	MN	Latest	0.978	-2.7556	-4.4059	0.7695
JBW7326A	108222.30	10888.36	BZ	Historical	0.953	0.0000	0.0000	0.0000
JBW7326A	108222.30	10888.36	BZ	Post-1999	0.959	0.0000	0.0000	0.0000
JBW7326A	108222.30	10888.36	BZ	Latest	0.978	0.0000	0.0000	0.0000
JBW7326A	108222.30	10888.36	FE	Historical	0.953	-0.0640	-0.5236	0.1008
JBW7326A	108222.30	10888.36	FE	Post-1999	0.959	-0.0381	-0.4997	0.1340
JBW7326A	108222.30	10888.36	FE	Latest	0.978	-0.7688	-2.1931	0.1380
JBW7326A	108222.30	10888.36	MN	Historical	0.953	0.0176	-0.0065	0.0865

WELLID	EASTING	NORTHING	COC	TYPE	CONF-LEV	TREND	LOWER-LIMIT	UPPER-LIMIT
JBW7326A	108222.30	10888.36	MN	Post-1999	0.959	0.0187	-0.0052	0.0945
JBW7326A	108222.30	10888.36	MN	Latest	0.978	0.0589	-0.0052	0.1544
JBW7326B	108222.30	10889.36	BZ	Historical	0.953	0.0000	0.0000	0.0000
JBW7326B	108222.30	10889.36	BZ	Post-1999	0.959	0.0000	0.0000	0.0000
JBW7326B	108222.30	10889.36	BZ	Latest	0.978	0.0000	0.0000	0.0000
JBW7326B	108222.30	10889.36	FE	Historical	0.953	-0.0812	-0.3961	0.2873
JBW7326B	108222.30	10889.36	FE	Post-1999	0.959	-0.0879	-0.5561	0.2602
JBW7326B	108222.30	10889.36	FE	Latest	0.978	0.1095	-0.0933	0.3804
JBW7326B	108222.30	10889.36	MN	Historical	0.953	-0.0269	-0.0791	0.0114
JBW7326B	108222.30	10889.36	MN	Post-1999	0.959	-0.0218	-0.0763	0.0160
JBW7326B	108222.30	10889.36	MN	Latest	0.978	0.0160	-0.0269	0.1010
JBW7328	110684.04	14780.69	BZ	Historical	0.953	0.0000	0.0000	0.0000
JBW7328	110684.04	14780.69	BZ	Post-1999	0.959	0.0000	0.0000	0.0000
JBW7328	110684.04	14780.69	BZ	Latest	0.978	0.0000	0.0000	0.0000
JBW7328	110684.04	14780.69	FE	Historical	0.953	-0.6186	-3.7941	4.9132
JBW7328	110684.04	14780.69	FE	Post-1999	0.959	-0.4285	-2.9796	6.0673
JBW7328	110684.04	14780.69	FE	Latest	0.978	6.0673	-79.2982	24.4704
JBW7328	110684.04	14780.69	MN	Historical	0.953	-0.5990	-1.1156	-0.0483
JBW7328	110684.04	14780.69	MN	Post-1999	0.959	-0.5689	-0.9222	-0.0393
JBW7328	110684.04	14780.69	MN	Latest	0.978	0.0353	-2.4578	0.2760
JBW7330A	109964.67	13026.80	BZ	Historical	0.953	0.0012	0.0004	0.0020
JBW7330A	109964.67	13026.80	BZ	Post-1999	0.959	0.0014	0.0006	0.0023
JBW7330A	109964.67	13026.80	BZ	Latest	0.978	0.0019	-0.0041	0.0027
JBW7330A	109964.67	13026.80	FE	Historical	0.953	0.0134	-0.2220	0.3090
JBW7330A	109964.67	13026.80	FE	Post-1999	0.959	-0.0493	-0.2401	0.2380
JBW7330A	109964.67	13026.80	FE	Latest	0.978	-0.0493	-0.2401	0.2265
JBW7330A	109964.67	13026.80	MN	Historical	0.953	0.0110	0.0014	0.0132
JBW7330A	109964.67	13026.80	MN	Post-1999	0.959	0.0110	0.0005	0.0124
JBW7330A	109964.67	13026.80	MN	Latest	0.978	0.0116	0.0061	0.0150
JBW7333	110584.22	13306.80	BZ	Historical	0.953	-0.0818	-0.1290	-0.0378
JBW7333	110584.22	13306.80	BZ	Post-1999	0.959	-0.0692	-0.1173	-0.0232
JBW7333	110584.22	13306.80	BZ	Latest	0.978	-0.0232	-0.0956	0.0406
JBW7333	110584.22	13306.80	FE	Historical	0.953	2.0240	1.5486	3.9402
JBW7333	110584.22	13306.80	FE	Post-1999	0.959	1.9903	1.3630	3.7908
JBW7333	110584.22	13306.80	FE	Latest	0.978	0.9150	-0.3234	1.7520
JBW7333	110584.22	13306.80	MN	Historical	0.976	-0.7343	-1.0547	-0.5650
JBW7333	110584.22	13306.80	MN	Post-1999	0.971	-0.7411	-1.0899	-0.6199
JBW7333	110584.22	13306.80	MN	Latest	0.961	-0.3681	-0.7411	-0.1194
JBW7338A	110830.36	13609.17	BZ	Historical	0.953	0.0527	-0.0150	0.1104
JBW7338A	110830.36	13609.17	BZ	Post-1999	0.959	0.0388	-0.0360	0.0948
JBW7338A	110830.36	13609.17	BZ	Latest	0.978	-0.0564	-0.1316	0.0948
JBW7338A	110830.36	13609.17	FE	Historical	0.953	-7.3660	-8.9216	-5.3220
JBW7338A	110830.36	13609.17	FE	Post-1999	0.959	-7.3975	-9.1864	-5.4616
JBW7338A	110830.36	13609.17	FE	Latest	0.978	-8.2125	-9.3249	-6.8121

WELLID	EASTING	NORTHING	COC	TYPE	CONF-LEV	TREND	LOWER-LIMIT	UPPER-LIMIT
JBW7338A	110830.36	13609.17	MN	Historical	0.965	-1.3987	-2.6187	0.4694
JBW7338A	110830.36	13609.17	MN	Post-1999	0.971	-1.3349	-2.3628	0.9851
JBW7338A	110830.36	13609.17	MN	Latest	0.988	-1.3987	-3.6554	0.4694
JBW7338B	110830.36	13610.17	BZ	Historical	0.953	-0.0016	-0.4945	0.4197
JBW7338B	110830.36	13610.17	BZ	Post-1999	0.959	-0.1391	-0.5318	0.4450
JBW7338B	110830.36	13610.17	BZ	Latest	0.978	-0.6048	-0.6312	-0.4945
JBW7338B	110830.36	13610.17	FE	Historical	0.953	0.2204	-0.5291	0.3522
JBW7338B	110830.36	13610.17	FE	Post-1999	0.959	0.2803	-0.2321	0.3837
JBW7338B	110830.36	13610.17	FE	Latest	0.978	-0.5574	-1.0548	0.7054
JBW7338B	110830.36	13610.17	MN	Historical	0.976	0.0046	-0.0355	0.0203
JBW7338B	110830.36	13610.17	MN	Post-1999	0.971	-0.0090	-0.0367	0.0199
JBW7338B	110830.36	13610.17	MN	Latest	0.965	-0.0301	-0.0409	0.0094
JBW7340B	110361.54	13210.74	BZ	Historical	0.953	-0.0124	-0.0278	0.0000
JBW7340B	110361.54	13210.74	BZ	Post-1999	0.959	-0.0087	-0.0250	0.0000
JBW7340B	110361.54	13210.74	BZ	Latest	0.978	-0.0126	-0.0278	0.0000
JBW7340B	110361.54	13210.74	FE	Historical	0.953	-0.3103	-1.5510	1.3034
JBW7340B	110361.54	13210.74	FE	Post-1999	0.959	-0.2958	-1.5255	1.3294
JBW7340B	110361.54	13210.74	FE	Latest	0.978	1.3294	-1.5749	8.7502
JBW7340B	110361.54	13210.74	MN	Historical	0.953	-1.0005	-2.0441	-0.5198
JBW7340B	110361.54	13210.74	MN	Post-1999	0.959	-0.9871	-2.0272	-0.4866
JBW7340B	110361.54	13210.74	MN	Latest	0.978	-0.5607	-2.0441	0.0791
JBW7344	110987.60	13622.38	BZ	Historical	0.965	0.0854	0.0231	0.1380
JBW7344	110987.60	13622.38	BZ	Post-1999	0.971	0.1035	0.0234	0.1463
JBW7344	110987.60	13622.38	BZ	Latest	0.988	0.2232	-0.0243	1.2518
JBW7344	110987.60	13622.38	FE	Historical	0.965	-1.2675	-37.0779	15.0670
JBW7344	110987.60	13622.38	FE	Post-1999	0.971	-0.5491	-36.4927	16.3098
JBW7344	110987.60	13622.38	FE	Latest	0.988	17.0984	-69.7666	24.4701
JBW7344	110987.60	13622.38	MN	Historical	0.965	-2.2567	-11.7169	7.2843
JBW7344	110987.60	13622.38	MN	Post-1999	0.971	-1.3779	-11.1982	7.6340
JBW7344	110987.60	13622.38	MN	Latest	0.988	-2.2567	-14.0127	30.5029
JBW7345A	110554.50	13806.74	BZ	Historical	0.953	-0.0092	-0.0253	0.0183
JBW7345A	110554.50	13806.74	BZ	Post-1999	0.959	-0.0095	-0.0266	0.0164
JBW7345A	110554.50	13806.74	BZ	Latest	0.978	-0.0266	-0.0988	0.0291
JBW7345A	110554.50	13806.74	FE	Historical	0.953	0.0814	-0.2681	0.2098
JBW7345A	110554.50	13806.74	FE	Post-1999	0.959	0.0964	-0.1630	0.2158
JBW7345A	110554.50	13806.74	FE	Latest	0.978	-0.3748	-0.5453	0.4501
JBW7345A	110554.50	13806.74	MN	Historical	0.953	-0.0191	-0.0433	0.0011
JBW7345A	110554.50	13806.74	MN	Post-1999	0.959	-0.0138	-0.0367	0.0035
JBW7345A	110554.50	13806.74	MN	Latest	0.978	-0.0351	-0.0519	0.0393
JBW7347B	110460.02	14624.90	BZ	Historical	0.953	0.0000	0.0000	0.0000
JBW7347B	110460.02	14624.90	BZ	Post-1999	0.959	0.0000	0.0000	0.0000
JBW7347B	110460.02	14624.90	BZ	Latest	0.978	0.0000	0.0000	0.0000
JBW7347B	110460.02	14624.90	FE	Historical	0.953	0.3961	-2.0256	3.2193
JBW7347B	110460.02	14624.90	FE	Post-1999	0.959	0.3331	-2.0437	1.9416

WELLID	EASTING	NORTHING	COC	TYPE	CONF-LEV	TREND	LOWER-LIMIT	UPPER-LIMIT
JBW7347B	110460.02	14624.90	FE	Latest	0.978	-2.0256	-4.8535	0.3331
JBW7347B	110460.02	14624.90	MN	Historical	0.953	-0.0136	-0.0350	0.0109
JBW7347B	110460.02	14624.90	MN	Post-1999	0.959	-0.0193	-0.0371	0.0044
JBW7347B	110460.02	14624.90	MN	Latest	0.978	-0.0350	-0.0998	-0.0136
JBW7348	110802.02	13966.56	BZ	Historical	0.953	-0.0688	-0.3158	0.3342
JBW7348	110802.02	13966.56	BZ	Post-1999	0.959	-0.0701	-0.4039	0.1857
JBW7348	110802.02	13966.56	BZ	Latest	0.978	-0.0959	-0.4937	0.0373
JBW7348	110802.02	13966.56	FE	Historical	0.953	-0.0523	-0.4786	0.2029
JBW7348	110802.02	13966.56	FE	Post-1999	0.959	-0.0552	-0.5195	0.1962
JBW7348	110802.02	13966.56	FE	Latest	0.978	0.2282	-0.0523	0.3289
JBW7348	110802.02	13966.56	MN	Historical	0.953	-0.1941	-1.9446	-0.0382
JBW7348	110802.02	13966.56	MN	Post-1999	0.959	-0.3357	-2.9982	-0.0397
JBW7348	110802.02	13966.56	MN	Latest	0.978	-0.0279	-0.0554	-0.0179
JBW7350	111365.86	14160.19	BZ	Historical	0.953	-0.0010	-0.0020	0.0000
JBW7350	111365.86	14160.19	BZ	Post-1999	0.959	-0.0010	-0.0026	0.0000
JBW7350	111365.86	14160.19	BZ	Latest	0.978	-0.0026	-0.0040	-0.0010
JBW7350	111365.86	14160.19	FE	Historical	0.953	-0.1877	-0.4800	-0.0224
JBW7350	111365.86	14160.19	FE	Post-1999	0.959	-0.1607	-0.3753	0.0012
JBW7350	111365.86	14160.19	FE	Latest	0.978	0.0822	0.0012	0.1738
JBW7350	111365.86	14160.19	MN	Historical	0.953	-0.0157	-0.1010	0.0664
JBW7350	111365.86	14160.19	MN	Post-1999	0.959	-0.0584	-0.1032	0.0683
JBW7350	111365.86	14160.19	MN	Latest	0.978	-0.0910	-0.1140	-0.0009
JBW7607	107063.59	15642.68	BZ	Historical	0.953	0.0000	0.0000	0.0000
JBW7607	107063.59	15642.68	BZ	Post-1999	0.959	0.0000	0.0000	0.0000
JBW7607	107063.59	15642.68	BZ	Latest	0.978	0.0000	0.0000	0.0000
JBW7617B	106434.87	15543.05	BZ	Historical	0.953	0.0000	0.0000	0.0000
JBW7617B	106434.87	15543.05	BZ	Post-1999	0.959	0.0000	0.0000	0.0000
JBW7617B	106434.87	15543.05	BZ	Latest	0.978	0.0000	0.0000	0.0000
JBW7710	109834.07	15664.23	BZ	Historical	0.953	-0.0559	-0.1090	-0.0108
JBW7710	109834.07	15664.23	BZ	Post-1999	0.959	-0.0462	-0.0941	-0.0081
JBW7710	109834.07	15664.23	BZ	Latest	0.978	-0.0005	-0.0931	0.0190
JBW7725	109695.14	17708.18	BZ	Historical	0.953	0.0000	0.0000	0.0000
JBW7725	109695.14	17708.18	BZ	Post-1999	0.959	0.0000	0.0000	0.0000
JBW7725	109695.14	17708.18	BZ	Latest	0.978	0.0000	0.0000	0.0000
JBW7737A	107734.00	17185.00	BZ	Historical	0.953	0.0000	0.0000	0.0000
JBW7737A	107734.00	17185.00	BZ	Post-1999	0.959	0.0000	0.0000	0.0000
JBW7737A	107734.00	17185.00	BZ	Latest	0.978	0.0000	0.0000	0.0000
JBW7737B	107734.00	17186.00	BZ	Historical	0.953	0.0000	0.0000	0.0000
JBW7737B	107734.00	17186.00	BZ	Post-1999	0.959	0.0000	0.0000	0.0000
JBW7737B	107734.00	17186.00	BZ	Latest	0.978	0.0000	0.0000	0.0000
JBW7738A	106930.24	16925.75	BZ	Historical	0.953	0.0000	0.0000	0.0000
JBW7738A	106930.24	16925.75	BZ	Post-1999	0.959	0.0000	0.0000	0.0000
JBW7738A	106930.24	16925.75	BZ	Latest	0.978	0.0000	0.0000	0.0000
JBW7742B	109908.62	16530.10	BZ	Historical	0.953	0.0000	0.0000	0.0000

WELLID	EASTING	NORTHING	COC	TYPE	CONF-LEV	TREND	LOWER-LIMIT	UPPER-LIMIT
JBW7742B	109908.62	16530.10	BZ	Post-1999	0.959	0.0000	0.0000	0.0000
JBW7742B	109908.62	16530.10	BZ	Latest	0.978	0.0000	0.0000	0.0000
JBW7752	108375.42	16683.09	BZ	Historical	0.953	0.0000	0.0000	0.0000
JBW7752	108375.42	16683.09	BZ	Post-1999	0.959	0.0000	0.0000	0.0000
JBW7752	108375.42	16683.09	BZ	Latest	0.978	0.0000	0.0000	0.0000
JBW7806	107716.95	20532.58	BZ	Historical	0.976	0.0000	0.0000	0.0000
JBW7806	107716.95	20532.58	BZ	Post-1999	0.964	0.0000	0.0000	0.0000
JBW7806	107716.95	20532.58	BZ	Latest	0.979	0.0000	0.0000	0.0000
JBW7806	107716.95	20532.58	FE	Historical	0.953	-4.1703	-5.7701	-1.8604
JBW7806	107716.95	20532.58	FE	Post-1999	0.959	-4.2216	-6.0365	-2.8167
JBW7806	107716.95	20532.58	FE	Latest	0.978	-1.2595	-1.8604	-0.4774
JBW7806	107716.95	20532.58	MN	Historical	0.953	-1.0853	-2.2413	0.0245
JBW7806	107716.95	20532.58	MN	Post-1999	0.959	-1.3184	-2.3581	0.0109
JBW7806	107716.95	20532.58	MN	Latest	0.978	-0.8405	-1.7824	0.8838
JBW7809	109112.81	21161.11	BZ	Historical	0.953	0.0000	0.0000	0.0000
JBW7809	109112.81	21161.11	BZ	Post-1999	0.959	0.0000	0.0000	0.0000
JBW7809	109112.81	21161.11	BZ	Latest	0.978	0.0000	0.0000	0.0000
JBW7809	109112.81	21161.11	FE	Historical	0.953	0.0130	-0.0868	0.2236
JBW7809	109112.81	21161.11	FE	Post-1999	0.959	0.0135	-0.0328	0.2653
JBW7809	109112.81	21161.11	FE	Latest	0.978	0.2236	-0.2623	1.4833
JBW7809	109112.81	21161.11	MN	Historical	0.953	0.0113	0.0003	0.0323
JBW7809	109112.81	21161.11	MN	Post-1999	0.959	0.0094	-0.0024	0.0295
JBW7809	109112.81	21161.11	MN	Latest	0.978	0.0113	0.0003	0.0815
JBW7812B	108332.56	20848.69	BZ	Historical	0.953	0.0107	-0.0459	0.0873
JBW7812B	108332.56	20848.69	BZ	Post-1999	0.959	-0.0117	-0.0481	0.0629
JBW7812B	108332.56	20848.69	BZ	Latest	0.978	-0.0319	-0.2296	0.1034
JBW7812B	108332.56	20848.69	FE	Historical	0.953	0.4875	0.1431	0.7947
JBW7812B	108332.56	20848.69	FE	Post-1999	0.959	0.4018	0.1056	0.7669
JBW7812B	108332.56	20848.69	FE	Latest	0.978	-1.1286	-1.6688	0.1517
JBW7812B	108332.56	20848.69	MN	Historical	0.953	-0.1316	-0.2696	0.0876
JBW7812B	108332.56	20848.69	MN	Post-1999	0.959	-0.1542	-0.3023	0.0693
JBW7812B	108332.56	20848.69	MN	Latest	0.978	-0.2032	-0.9178	0.0693
JBW8003B	115426.83	21756.94	BZ	Historical	0.953	0.0000	0.0000	0.0000
JBW8003B	115426.83	21756.94	BZ	Post-1999	0.959	0.0000	0.0000	0.0000
JBW8003B	115426.83	21756.94	BZ	Latest	0.978	0.0000	0.0000	0.0000
JBW8003B	115426.83	21756.94	FE	Historical	0.953	-1.2640	-2.7417	-0.8441
JBW8003B	115426.83	21756.94	FE	Post-1999	0.959	-1.1809	-1.5250	-0.8408
JBW8003B	115426.83	21756.94	FE	Latest	0.978	-1.0768	-1.3904	-0.8408
JBW8003B	115426.83	21756.94	MN	Historical	0.953	-0.2980	-0.6180	-0.2532
JBW8003B	115426.83	21756.94	MN	Post-1999	0.959	-0.2711	-0.4957	-0.2523
JBW8003B	115426.83	21756.94	MN	Latest	0.978	-0.1876	-0.2562	-0.1434
JBW8004B	116178.78	22363.68	BZ	Historical	0.953	0.0000	0.0000	0.0000
JBW8004B	116178.78	22363.68	BZ	Post-1999	0.959	0.0000	0.0000	0.0000
JBW8004B	116178.78	22363.68	BZ	Latest	0.978	0.0000	0.0000	0.0000

WELLID	EASTING	NORTHING	COC	TYPE	CONF-LEV	TREND	LOWER-LIMIT	UPPER-LIMIT
JBW8004B	116178.78	22363.68	FE	Historical	0.953	-1.8165	-2.7449	0.8054
JBW8004B	116178.78	22363.68	FE	Post-1999	0.959	-1.9979	-3.2721	0.2539
JBW8004B	116178.78	22363.68	FE	Latest	0.978	0.2539	-7.4683	1.4122
JBW8004B	116178.78	22363.68	MN	Historical	0.953	-0.0223	-0.0684	0.0140
JBW8004B	116178.78	22363.68	MN	Post-1999	0.959	-0.0297	-0.0754	0.0054
JBW8004B	116178.78	22363.68	MN	Latest	0.978	-0.0629	-0.1120	-0.0223
JBW8009	113487.91	21023.48	BZ	Historical	0.953	0.0000	0.0000	0.0000
JBW8009	113487.91	21023.48	BZ	Post-1999	0.959	0.0000	0.0000	0.0000
JBW8009	113487.91	21023.48	BZ	Latest	0.978	0.0000	0.0000	0.0000
JBW8009	113487.91	21023.48	FE	Historical	0.953	-4.4358	-7.9989	-3.7420
JBW8009	113487.91	21023.48	FE	Post-1999	0.959	-4.4183	-7.6223	-3.0358
JBW8009	113487.91	21023.48	FE	Latest	0.978	-4.4183	-5.7387	-3.7420
JBW8009	113487.91	21023.48	MN	Historical	0.953	0.3563	-0.2784	0.5091
JBW8009	113487.91	21023.48	MN	Post-1999	0.959	0.3784	-0.1302	0.5241
JBW8009	113487.91	21023.48	MN	Latest	0.978	0.4419	0.3313	0.6679
JMW0201A	108502.60	20874.60	BZ	Historical	0.969	0.0764	-0.0417	0.2476
JMW0201A	108502.60	20874.60	BZ	Post-1999	0.875	6.5681	-5.2916	7.7094
JMW0201A	108502.60	20874.60	BZ	Latest	0.750	6.6606	-5.2916	7.7094
JMW0301C	109861.00	13420.00	BZ	Historical	0.965	0.0000	0.0000	0.0000
JMW0301C	109861.00	13420.00	BZ	Post-1999	0.961	0.0000	0.0000	0.0000
JMW0301C	109861.00	13420.00	BZ	Latest	0.992	0.0000	0.0000	0.0000
JMW0301C	109861.00	13420.00	FE	Historical	0.953	-1.2749	-4.1078	0.5187
JMW0301C	109861.00	13420.00	FE	Post-1999	0.959	-2.1258	-4.1521	0.1844
JMW0301C	109861.00	13420.00	FE	Latest	0.978	-4.1078	-6.0369	-1.1026
JMW0301C	109861.00	13420.00	MN	Historical	0.953	-0.0690	-0.4355	0.3110
JMW0301C	109861.00	13420.00	MN	Post-1999	0.959	-0.0593	-0.4838	0.4313
JMW0301C	109861.00	13420.00	MN	Latest	0.978	-0.2146	-0.6344	0.8529
JMW0503	111069.89	14733.53	BZ	Historical	0.953	0.0000	0.0000	0.0000
JMW0503	111069.89	14733.53	BZ	Post-1999	0.959	0.0000	0.0000	0.0000
JMW0503	111069.89	14733.53	BZ	Latest	0.978	0.0000	0.0000	0.0000
JMW0503	111069.89	14733.53	FE	Historical	0.953	-3.0083	-5.1178	-2.5576
JMW0503	111069.89	14733.53	FE	Post-1999	0.959	-3.0847	-8.4993	-2.6594
JMW0503	111069.89	14733.53	FE	Latest	0.978	-2.3786	-2.9216	-1.7596
JMW0503	111069.89	14733.53	MN	Historical	0.953	-0.1674	-0.3089	-0.1517
JMW0503	111069.89	14733.53	MN	Post-1999	0.959	-0.1754	-0.5298	-0.1542
JMW0503	111069.89	14733.53	MN	Latest	0.978	-0.1229	-0.1542	-0.1124
JMW0505	111132.90	14617.51	BZ	Historical	0.964	-0.0034	-0.0198	-0.0006
JMW0505	111132.90	14617.51	BZ	Post-1999	0.961	-0.0004	-0.0032	0.0024
JMW0505	111132.90	14617.51	BZ	Latest	0.938	-0.0032	-0.0197	0.0038
JMW0505	111132.90	14617.51	FE	Historical	0.953	-0.5248	-1.2925	-0.2136
JMW0505	111132.90	14617.51	FE	Post-1999	0.959	-0.5502	-1.6081	-0.3671
JMW0505	111132.90	14617.51	FE	Latest	0.978	-0.2136	-0.8621	0.2071
JMW0505	111132.90	14617.51	MN	Historical	0.953	-0.0062	-0.0137	0.0079
JMW0505	111132.90	14617.51	MN	Post-1999	0.959	-0.0087	-0.0227	0.0046

WELLID	EASTING	NORTHING	COC	TYPE	CONF-LEV	TREND	LOWER-LIMIT	UPPER-LIMIT
JMW0505	111132.90	14617.51	MN	Latest	0.978	-0.0034	-0.0125	0.0252
JMW0542	109338.80	12434.20	BZ	Historical	0.953	0.0000	-0.0070	0.0016
JMW0542	109338.80	12434.20	BZ	Post-1999	0.959	-0.0006	-0.0071	0.0003
JMW0542	109338.80	12434.20	BZ	Latest	0.978	-0.0037	-0.0302	0.0030
JMW0542	109338.80	12434.20	FE	Historical	0.953	-5.8680	-8.5989	3.9812
JMW0542	109338.80	12434.20	FE	Post-1999	0.959	-5.6002	-8.5169	5.0681
JMW0542	109338.80	12434.20	FE	Latest	0.978	-6.8878	-9.3974	-0.7031
JMW0542	109338.80	12434.20	MN	Historical	0.953	2.3138	-2.1295	6.4333
JMW0542	109338.80	12434.20	MN	Post-1999	0.959	2.5587	-1.8967	8.0004
JMW0542	109338.80	12434.20	MN	Latest	0.978	-3.6984	-8.1007	5.6376
JMW0604	111650.60	8969.90	BZ	Historical	0.962	-0.0009	-0.0031	0.0004
JMW0604	111650.60	8969.90	BZ	Post-1999	0.938	0.0000	0.0000	0.0013
JMW0604	111650.60	8969.90	BZ	Latest	0.875	0.0000	0.0000	0.0008
JMW0701	107403.43	16369.68	BZ	Historical	0.953	-0.1485	-0.2278	-0.0348
JMW0701	107403.43	16369.68	BZ	Post-1999	0.959	-0.1188	-0.2154	-0.0271
JMW0701	107403.43	16369.68	BZ	Latest	0.978	-0.1987	-0.3256	-0.0508
JMW1103D	114886.70	21449.90	BZ	Historical	0.970	-0.0221	-0.0309	-0.0146
JMW1103D	114886.70	21449.90	BZ	Post-1999	0.951	-0.0126	-0.0145	0.0081
JMW1103D	114886.70	21449.90	BZ	Latest	0.969	0.0203	-0.0043	0.0334
JMW1103D	114886.70	21449.90	FE	Historical	0.953	25.4203	12.6156	81.3606
JMW1103D	114886.70	21449.90	FE	Post-1999	0.959	24.1259	11.3838	80.7950
JMW1103D	114886.70	21449.90	FE	Latest	0.978	-5.7588	-40.4893	24.1259
JMW1103D	114886.70	21449.90	MN	Historical	0.965	-4.5168	-7.1905	1.7763
JMW1103D	114886.70	21449.90	MN	Post-1999	0.959	-4.6583	-8.9875	0.9761
JMW1103D	114886.70	21449.90	MN	Latest	0.987	-10.0123	-21.3519	-4.5072
JMW1562	111523.51	14976.24	BZ	Historical	0.953	-5.9994	-12.4619	-4.3338
JMW1562	111523.51	14976.24	BZ	Post-1999	0.979	-3.9307	-7.3810	-0.4689
JMW1562	111523.51	14976.24	BZ	Latest	0.984	-1.5456	-12.8250	0.0849
JMW1564	111324.20	14979.63	BZ	Historical	0.976	0.0986	-0.0263	0.1137
JMW1564	111324.20	14979.63	BZ	Post-1999	0.964	0.0936	-0.0263	0.1105
JMW1564	111324.20	14979.63	BZ	Latest	0.979	-0.3204	-1.4250	-0.0263
JMW1564	111324.20	14979.63	FE	Historical	0.953	-18.3482	-39.4649	21.1948
JMW1564	111324.20	14979.63	FE	Post-1999	0.959	-24.8791	-45.8537	15.7929
JMW1564	111324.20	14979.63	FE	Latest	0.978	-50.1981	-155.5583	-28.0362
JMW1565	111522.30	14964.19	BZ	Historical	0.976	-4.2679	-4.6612	-2.4405
JMW1565	111522.30	14964.19	BZ	Post-1999	0.971	-4.3602	-4.7238	-2.6410
JMW1565	111522.30	14964.19	BZ	Latest	0.961	0.0153	-4.8206	6.3628
JMW1565	111522.30	14964.19	FE	Historical	0.953	58.0691	51.7181	77.7083
JMW1565	111522.30	14964.19	FE	Post-1999	0.959	63.0928	52.8291	83.2874
JMW1565	111522.30	14964.19	FE	Latest	0.978	135.8865	-18.8766	403.7204
JMW1565	111522.30	14964.19	MN	Historical	0.953	8.2026	3.1306	10.1418
JMW1565	111522.30	14964.19	MN	Post-1999	0.959	8.5313	3.2636	10.4954
JMW1565	111522.30	14964.19	MN	Latest	0.978	9.6804	-5.0856	36.5897
JMW1860	108944.86	9032.97	BZ	Historical	0.953	-0.0034	-0.0073	0.0017

WELLID	EASTING	NORTHING	COC	TYPE	CONF-LEV	TREND	LOWER-LIMIT	UPPER-LIMIT
JMW1860	108944.86	9032.97	BZ	Post-1999	0.959	-0.0038	-0.0081	0.0015
JMW1860	108944.86	9032.97	BZ	Latest	0.978	-0.0013	-0.0065	0.0052
JMW1860	108944.86	9032.97	FE	Historical	0.953	-7.9900	-18.1822	-2.1451
JMW1860	108944.86	9032.97	FE	Post-1999	0.959	-8.1967	-23.1713	-5.8281
JMW1860	108944.86	9032.97	FE	Latest	0.978	-7.9900	-15.7832	-2.1451
JMW1860	108944.86	9032.97	MN	Historical	0.953	-0.2746	-0.8788	0.0320
JMW1860	108944.86	9032.97	MN	Post-1999	0.959	-0.3375	-1.0107	0.0317
JMW1860	108944.86	9032.97	MN	Latest	0.978	-0.0044	-0.2746	0.6925
JMW1881	108936.65	9301.22	BZ	Historical	0.953	0.0024	-0.0147	0.0106
JMW1881	108936.65	9301.22	BZ	Post-1999	0.959	-0.0027	-0.0184	0.0086
JMW1881	108936.65	9301.22	BZ	Latest	0.978	0.0131	-0.0415	0.0637
JMW1881	108936.65	9301.22	FE	Historical	0.953	0.0912	-0.8805	0.2578
JMW1881	108936.65	9301.22	FE	Post-1999	0.959	0.1090	-0.4579	0.2687
JMW1881	108936.65	9301.22	FE	Latest	0.978	1.3181	0.1090	3.5953
JMW1881	108936.65	9301.22	MN	Historical	0.953	-0.1099	-0.4329	0.1286
JMW1881	108936.65	9301.22	MN	Post-1999	0.959	-0.0452	-0.4030	0.2349
JMW1881	108936.65	9301.22	MN	Latest	0.978	0.4658	-0.0233	0.8760
JMW1960	109086.09	10613.03	BZ	Historical	0.953	0.6785	0.2302	1.0885
JMW1960	109086.09	10613.03	BZ	Post-1999	0.979	-1.8584	-2.7528	0.7878
JMW1960	109086.09	10613.03	BZ	Latest	0.984	-1.6250	-3.2864	0.9773
JMW1960	109086.09	10613.03	FE	Historical	0.953	1.4927	-5.9013	5.8570
JMW1960	109086.09	10613.03	FE	Post-1999	0.979	0.6945	-11.0000	4.1317
JMW1960	109086.09	10613.03	FE	Latest	0.984	-1.1603	-16.7141	1.8046
JMW1963	109286.98	10487.77	BZ	Historical	0.965	-0.0317	-0.0563	-0.0113
JMW1963	109286.98	10487.77	BZ	Post-1999	0.971	-0.0323	-0.0579	-0.0010
JMW1963	109286.98	10487.77	BZ	Latest	0.987	-0.0462	-0.0874	-0.0315
JMW1963	109286.98	10487.77	FE	Historical	0.953	-1.1903	-2.2234	-0.2680
JMW1963	109286.98	10487.77	FE	Post-1999	0.959	-1.0192	-1.8583	-0.2483
JMW1963	109286.98	10487.77	FE	Latest	0.978	-2.2234	-2.8200	-0.2680
JMW1963	109286.98	10487.77	MN	Historical	0.953	0.3563	-0.4728	0.9177
JMW1963	109286.98	10487.77	MN	Post-1999	0.959	0.3746	0.0171	0.9783
JMW1963	109286.98	10487.77	MN	Latest	0.978	-0.4728	-1.3688	1.2196
JMW1964	109282.91	10966.36	BZ	Historical	0.953	-0.0156	-0.0313	-0.0045
JMW1964	109282.91	10966.36	BZ	Post-1999	0.959	-0.0157	-0.0360	-0.0072
JMW1964	109282.91	10966.36	BZ	Latest	0.978	-0.0838	-0.2383	-0.0156
JMW1964	109282.91	10966.36	FE	Historical	0.965	0.0190	-1.3939	1.3076
JMW1964	109282.91	10966.36	FE	Post-1999	0.971	-0.1926	-1.8072	1.3076
JMW1964	109282.91	10966.36	FE	Latest	0.988	-1.0050	-2.7765	0.5661
JMW1964	109282.91	10966.36	MN	Historical	0.965	0.0101	-0.0072	0.0364
JMW1964	109282.91	10966.36	MN	Post-1999	0.971	0.0058	-0.0109	0.0273
JMW1964	109282.91	10966.36	MN	Latest	0.988	-0.0274	-0.1315	0.0575
JMW1966	109099.64	10610.39	BZ	Historical	0.953	0.0659	-0.0862	0.0928
JMW1966	109099.64	10610.39	BZ	Post-1999	0.959	0.0728	-0.0394	0.0990
JMW1966	109099.64	10610.39	BZ	Latest	0.978	-0.1623	-0.3014	-0.0394

WELLID	EASTING	NORTHING	COC	TYPE	CONF-LEV	TREND	LOWER-LIMIT	UPPER-LIMIT
JMW1966	109099.64	10610.39	FE	Historical	0.953	3.6549	0.1479	9.1763
JMW1966	109099.64	10610.39	FE	Post-1999	0.959	4.1254	0.9776	9.8045
JMW1966	109099.64	10610.39	FE	Latest	0.978	-12.3099	-27.7400	9.1539
JMW1966	109099.64	10610.39	MN	Historical	0.953	-0.4753	-4.7512	2.2517
JMW1966	109099.64	10610.39	MN	Post-1999	0.959	-0.3956	-4.7512	2.9836
JMW1966	109099.64	10610.39	MN	Latest	0.978	-6.9367	-10.7843	-2.1940
JMW3202	110684.15	13404.85	BZ	Historical	0.962	-0.0855	-0.1555	0.0071
JMW3202	110684.15	13404.85	BZ	Post-1999	0.959	-0.1159	-0.1868	0.1177
JMW3202	110684.15	13404.85	BZ	Latest	0.984	-0.1797	-0.2500	0.1118
JMW3202	110684.15	13404.85	FE	Historical	0.953	-16.9818	-30.3938	-2.3190
JMW3202	110684.15	13404.85	FE	Post-1999	0.959	-17.9809	-32.2790	-7.7701
JMW3202	110684.15	13404.85	FE	Latest	0.978	-17.9809	-55.9827	-0.3278
JMW3202	110684.15	13404.85	MN	Historical	0.953	-1.1707	-9.7404	0.2417
JMW3202	110684.15	13404.85	MN	Post-1999	0.959	-1.9709	-10.3743	-0.0757
JMW3202	110684.15	13404.85	MN	Latest	0.978	-5.4150	-17.9102	4.6853
JMW35X2	110127.97	10067.32	BZ	Historical	0.953	0.0000	0.0000	0.0000
JMW35X2	110127.97	10067.32	BZ	Post-1999	0.959	0.0000	0.0000	0.0000
JMW35X2	110127.97	10067.32	BZ	Latest	0.978	0.0000	0.0000	0.0000
JMW35X2	110127.97	10067.32	FE	Historical	0.953	0.3404	-0.2699	1.2979
JMW35X2	110127.97	10067.32	FE	Post-1999	0.959	0.3437	-0.1288	1.8461
JMW35X2	110127.97	10067.32	FE	Latest	0.978	-2.0393	-2.7708	0.9557
JMW35X2	110127.97	10067.32	MN	Historical	0.953	-0.0298	-0.0517	-0.0051
JMW35X2	110127.97	10067.32	MN	Post-1999	0.959	-0.0268	-0.0446	-0.0023
JMW35X2	110127.97	10067.32	MN	Latest	0.978	-0.0427	-0.0760	0.0073
JMW6001	109866.12	16952.71	BZ	Historical	0.953	-0.0073	-0.0765	0.0154
JMW6001	109866.12	16952.71	BZ	Post-1999	0.959	-0.0080	-0.1012	0.0091
JMW6001	109866.12	16952.71	BZ	Latest	0.978	-0.0094	-0.1012	0.0010
JMW6105	108145.33	17187.80	BZ	Historical	0.953	0.0000	0.0000	0.0000
JMW6105	108145.33	17187.80	BZ	Post-1999	0.959	0.0000	0.0000	0.0000
JMW6105	108145.33	17187.80	BZ	Latest	0.978	0.0000	0.0000	0.0000
JMW7332	107984.11	11714.85	BZ	Historical	0.953	0.0000	0.0000	0.0000
JMW7332	107984.11	11714.85	BZ	Post-1999	0.959	0.0000	0.0000	0.0000
JMW7332	107984.11	11714.85	BZ	Latest	0.978	0.0000	0.0000	0.0000
JMW7332	107984.11	11714.85	FE	Historical	0.953	1.5208	-9.4590	4.0979
JMW7332	107984.11	11714.85	FE	Post-1999	0.959	1.6064	-8.3679	4.9768
JMW7332	107984.11	11714.85	FE	Latest	0.978	4.0979	1.6064	7.0444
JMW7332	107984.11	11714.85	MN	Historical	0.953	12.1153	8.9675	13.2348
JMW7332	107984.11	11714.85	MN	Post-1999	0.959	12.3950	10.4366	13.3365
JMW7332	107984.11	11714.85	MN	Latest	0.978	16.3185	-46.0135	25.2070
JMW7612	106986.73	16453.32	BZ	Historical	0.953	-0.0364	-0.0483	0.0314
JMW7612	106986.73	16453.32	BZ	Post-1999	0.959	-0.0392	-0.0503	0.0114
JMW7612	106986.73	16453.32	BZ	Latest	0.978	-0.1056	-0.2446	-0.0520
JMW8011	116191.11	22376.38	BZ	Historical	0.953	0.0000	0.0000	0.0000
JMW8011	116191.11	22376.38	BZ	Post-1999	0.959	0.0000	0.0000	0.0000

WELLID	EASTING	NORTHING	COC	TYPE	CONF-LEV	TREND	LOWER-LIMIT	UPPER-LIMIT
JMW8011	116191.11	22376.38	BZ	Latest	0.978	0.0000	0.0000	0.0000
JMW8011	116191.11	22376.38	FE	Historical	0.953	-6.2216	-7.4187	-4.7129
JMW8011	116191.11	22376.38	FE	Post-1999	0.959	-6.1338	-6.7688	-3.9360
JMW8011	116191.11	22376.38	FE	Latest	0.978	-6.2216	-6.5967	-5.5150
JMW8011	116191.11	22376.38	MN	Historical	0.953	-3.8700	-10.1666	1.8024
JMW8011	116191.11	22376.38	MN	Post-1999	0.959	-3.3513	-9.6724	2.4622
JMW8011	116191.11	22376.38	MN	Latest	0.978	-9.6724	-10.3177	-3.3304
JPZ0340	109561.37	13962.51	BZ	Historical	0.953	-0.0023	-0.0065	0.0066
JPZ0340	109561.37	13962.51	BZ	Post-1999	0.959	-0.0006	-0.0063	0.0072
JPZ0340	109561.37	13962.51	BZ	Latest	0.978	-0.0066	-0.0296	-0.0053
JPZ0340	109561.37	13962.51	FE	Historical	0.953	0.2240	-0.0701	0.7067
JPZ0340	109561.37	13962.51	FE	Post-1999	0.959	0.0967	-0.0758	0.6968
JPZ0340	109561.37	13962.51	FE	Latest	0.978	-0.2594	-1.2558	0.7067
JPZ0340	109561.37	13962.51	MN	Historical	0.965	-0.3720	-0.5997	0.0060
JPZ0340	109561.37	13962.51	MN	Post-1999	0.971	-0.2824	-0.5997	0.0692
JPZ0340	109561.37	13962.51	MN	Latest	0.988	-0.6786	-0.7725	-0.5316
JPZ0341	109554.37	13917.07	BZ	Historical	0.965	0.0000	0.0000	0.0000
JPZ0341	109554.37	13917.07	BZ	Post-1999	0.971	0.0000	0.0000	0.0000
JPZ0341	109554.37	13917.07	BZ	Latest	0.988	0.0000	0.0000	0.0000
JPZ0341	109554.37	13917.07	FE	Historical	0.953	-7.4752	-14.7796	-0.6103
JPZ0341	109554.37	13917.07	FE	Post-1999	0.959	-6.0331	-11.7630	0.8683
JPZ0341	109554.37	13917.07	FE	Latest	0.978	-8.8191	-15.3347	-3.1086
JPZ0341	109554.37	13917.07	MN	Historical	0.965	-9.0424	-11.6267	3.3020
JPZ0341	109554.37	13917.07	MN	Post-1999	0.971	-8.3299	-11.1836	4.1033
JPZ0341	109554.37	13917.07	MN	Latest	0.988	-13.9143	-45.6262	-10.6536
JPZ0342	109510.08	14069.10	BZ	Historical	0.970	0.0064	0.0009	0.0090
JPZ0342	109510.08	14069.10	BZ	Post-1999	0.969	0.0055	-0.0072	0.0090
JPZ0342	109510.08	14069.10	BZ	Latest	0.984	-0.0104	-0.0475	-0.0010
JPZ0342	109510.08	14069.10	FE	Historical	0.953	-0.3205	-0.8458	0.4243
JPZ0342	109510.08	14069.10	FE	Post-1999	0.959	-0.3158	-0.8045	0.7221
JPZ0342	109510.08	14069.10	FE	Latest	0.978	0.3984	-0.4947	2.4958
JPZ0342	109510.08	14069.10	MN	Historical	0.953	-0.2976	-0.3737	-0.2228
JPZ0342	109510.08	14069.10	MN	Post-1999	0.959	-0.2976	-0.3628	-0.1955
JPZ0342	109510.08	14069.10	MN	Latest	0.978	-0.1832	-0.3408	0.0137
JPZ0343	109503.35	14073.53	BZ	Historical	0.953	-0.0024	-0.0103	0.0019
JPZ0343	109503.35	14073.53	BZ	Post-1999	0.981	-0.0034	-0.0176	0.0013
JPZ0343	109503.35	14073.53	BZ	Latest	0.992	0.0003	-0.0075	0.0019
JPZ0343	109503.35	14073.53	FE	Historical	0.953	-6.7732	-13.2241	3.0777
JPZ0343	109503.35	14073.53	FE	Post-1999	0.959	-4.0550	-12.2127	3.3310
JPZ0343	109503.35	14073.53	FE	Latest	0.978	-0.5427	-18.7904	8.5231
JPZ0343	109503.35	14073.53	MN	Historical	0.953	1.5473	-1.0125	2.4846
JPZ0343	109503.35	14073.53	MN	Post-1999	0.959	1.5885	-0.7917	2.4887
JPZ0343	109503.35	14073.53	MN	Latest	0.978	1.2739	-3.2439	8.6956
JPZ0348	108885.33	12194.33	BZ	Historical	0.953	-0.0054	-0.0082	-0.0049

WELLID	EASTING	NORTHING	COC	TYPE	CONF-LEV	TREND	LOWER-LIMIT	UPPER-LIMIT
JPZ0348	108885.33	12194.33	BZ	Post-1999	0.959	-0.0054	-0.0077	-0.0044
JPZ0348	108885.33	12194.33	BZ	Latest	0.978	-0.0077	-0.0246	0.0007
JPZ0348	108885.33	12194.33	FE	Historical	0.953	0.0185	-0.0862	0.2394
JPZ0348	108885.33	12194.33	FE	Post-1999	0.959	-0.0086	-0.0914	0.2009
JPZ0348	108885.33	12194.33	FE	Latest	0.978	-0.0727	-0.2458	0.1928
JPZ0348	108885.33	12194.33	MN	Historical	0.953	-0.0092	-0.0132	0.0239
JPZ0348	108885.33	12194.33	MN	Post-1999	0.959	-0.0097	-0.0194	0.0113
JPZ0348	108885.33	12194.33	MN	Latest	0.978	-0.0118	-0.0354	-0.0006
JPZ0349	108892.85	12200.73	BZ	Historical	0.965	0.0000	0.0000	0.0000
JPZ0349	108892.85	12200.73	BZ	Post-1999	0.971	0.0000	0.0000	0.0000
JPZ0349	108892.85	12200.73	BZ	Latest	0.988	0.0000	0.0000	0.0000
JPZ0349	108892.85	12200.73	FE	Historical	0.953	0.1018	-0.1676	0.5733
JPZ0349	108892.85	12200.73	FE	Post-1999	0.959	0.1246	-0.0328	0.6361
JPZ0349	108892.85	12200.73	FE	Latest	0.978	0.1018	-0.6256	2.1559
JPZ0349	108892.85	12200.73	MN	Historical	0.953	-0.0080	-0.4109	0.3653
JPZ0349	108892.85	12200.73	MN	Post-1999	0.959	0.0552	-0.2617	0.4767
JPZ0349	108892.85	12200.73	MN	Latest	0.978	0.2107	-0.2617	1.1641
JPZ1780	109521.51	12824.33	BZ	Historical	0.976	0.0000	0.0000	0.0000
JPZ1780	109521.51	12824.33	BZ	Post-1999	0.981	0.0000	0.0000	0.0000
JPZ1780	109521.51	12824.33	BZ	Latest	0.979	0.0000	0.0000	0.0000
JPZ1780	109521.51	12824.33	FE	Historical	0.953	0.0646	-0.4647	0.3177
JPZ1780	109521.51	12824.33	FE	Post-1999	0.959	0.0015	-0.5403	0.2687
JPZ1780	109521.51	12824.33	FE	Latest	0.978	-0.3564	-0.8434	0.2687
JPZ1780	109521.51	12824.33	MN	Historical	0.953	-0.0022	-0.0323	0.0184
JPZ1780	109521.51	12824.33	MN	Post-1999	0.959	-0.0080	-0.0324	0.0109
JPZ1780	109521.51	12824.33	MN	Latest	0.978	0.0190	-0.0240	0.0422
JPZ7208	108141.92	10243.38	BZ	Historical	0.953	0.0000	0.0000	0.0000
JPZ7208	108141.92	10243.38	BZ	Post-1999	0.959	0.0000	0.0000	0.0000
JPZ7208	108141.92	10243.38	BZ	Latest	0.978	0.0000	0.0000	0.0000
JPZ7208	108141.92	10243.38	FE	Historical	0.953	0.0308	-1.6693	1.6537
JPZ7208	108141.92	10243.38	FE	Post-1999	0.959	-0.1420	-1.7478	1.3752
JPZ7208	108141.92	10243.38	FE	Latest	0.978	-0.1420	-1.7478	1.9842
JPZ7208	108141.92	10243.38	MN	Historical	0.953	-0.2614	-2.0957	1.2762
JPZ7208	108141.92	10243.38	MN	Post-1999	0.959	0.0754	-2.0118	1.9211
JPZ7208	108141.92	10243.38	MN	Latest	0.978	0.5031	-2.0118	5.7259
JPZ7312	109847.28	15397.09	BZ	Historical	0.953	-0.0166	-0.0246	0.0288
JPZ7312	109847.28	15397.09	BZ	Post-1999	0.959	-0.0170	-0.0328	0.0173
JPZ7312	109847.28	15397.09	BZ	Latest	0.978	-0.0393	-0.1212	0.0602
JPZ7601	106807.89	16674.53	BZ	Historical	0.953	0.0000	0.0000	0.0000
JPZ7601	106807.89	16674.53	BZ	Post-1999	0.959	0.0000	0.0000	0.0000
JPZ7601	106807.89	16674.53	BZ	Latest	0.978	0.0000	0.0000	0.0000
JPZ7807	107539.30	20443.30	BZ	Historical	0.953	0.0000	0.0000	0.0000
JPZ7807	107539.30	20443.30	BZ	Post-1999	0.971	0.0000	0.0000	0.0000
JPZ7807	107539.30	20443.30	BZ	Latest	0.979	0.0000	0.0000	0.0000

WELLID	EASTING	NORTHING	COC	TYPE	CONF-LEV	TREND	LOWER-LIMIT	UPPER-LIMIT
JPZ7807	107539.30	20443.30	FE	Historical	0.953	0.1545	-0.1467	0.3568
JPZ7807	107539.30	20443.30	FE	Post-1999	0.959	0.0732	-0.1722	0.3449
JPZ7807	107539.30	20443.30	FE	Latest	0.978	-0.4496	-0.5437	-0.2905
JPZ7807	107539.30	20443.30	MN	Historical	0.953	0.0095	-0.0144	0.0368
JPZ7807	107539.30	20443.30	MN	Post-1999	0.959	0.0013	-0.0161	0.0350
JPZ7807	107539.30	20443.30	MN	Latest	0.978	-0.0074	-0.0231	0.0472
MMW0003	106376.08	15069.79	BZ	Historical	0.953	0.0000	0.0000	0.0000
MMW0003	106376.08	15069.79	BZ	Post-1999	0.959	0.0000	0.0000	0.0000
MMW0003	106376.08	15069.79	BZ	Latest	0.978	0.0000	0.0000	0.0000
MMW0005	110994.15	14918.82	BZ	Historical	0.953	0.7794	0.3026	1.4342
MMW0005	110994.15	14918.82	BZ	Post-1999	0.959	0.9000	0.2575	1.6164
MMW0005	110994.15	14918.82	BZ	Latest	0.978	-0.0092	-1.2140	3.6042
MMW0005	110994.15	14918.82	FE	Historical	0.965	70.7319	35.4099	100.9453
MMW0005	110994.15	14918.82	FE	Post-1999	0.959	60.6591	34.3502	100.1710
MMW0005	110994.15	14918.82	FE	Latest	0.987	27.3581	-39.7564	246.5311
MMW0005	110994.15	14918.82	MN	Historical	0.965	12.2977	7.9720	22.0414
MMW0005	110994.15	14918.82	MN	Post-1999	0.959	12.1143	4.0195	21.2693
MMW0005	110994.15	14918.82	MN	Latest	0.987	2.8989	-9.8822	47.6136
MMW0006	106091.03	15467.33	BZ	Historical	0.953	0.0000	0.0000	0.0000
MMW0006	106091.03	15467.33	BZ	Post-1999	0.959	0.0000	0.0000	0.0000
MMW0006	106091.03	15467.33	BZ	Latest	0.978	0.0000	0.0000	0.0000
MMW0007A	105635.89	8867.39	BZ	Historical	0.953	0.0000	0.0000	0.0000
MMW0007A	105635.89	8867.39	BZ	Post-1999	0.971	0.0000	0.0000	0.0000
MMW0007A	105635.89	8867.39	BZ	Latest	0.978	0.0000	0.0000	0.0000
MMW0007A	105635.89	8867.39	FE	Historical	0.953	-0.1181	-0.6828	0.4201
MMW0007A	105635.89	8867.39	FE	Post-1999	0.971	-0.0837	-0.6828	0.4854
MMW0007A	105635.89	8867.39	FE	Latest	0.978	-0.3208	-0.7339	0.6354
MMW0007A	105635.89	8867.39	MN	Historical	0.953	0.0077	-0.0514	0.0617
MMW0007A	105635.89	8867.39	MN	Post-1999	0.971	0.0095	-0.0514	0.0631
MMW0007A	105635.89	8867.39	MN	Latest	0.978	0.0066	-0.0624	0.0903
MMW0007B	105635.89	8869.39	BZ	Historical	0.953	0.0000	0.0000	0.0000
MMW0007B	105635.89	8869.39	BZ	Post-1999	0.971	0.0000	0.0000	0.0000
MMW0007B	105635.89	8869.39	BZ	Latest	0.978	0.0000	0.0000	0.0000
MMW0007B	105635.89	8869.39	FE	Historical	0.965	-0.2872	-0.5697	-0.0866
MMW0007B	105635.89	8869.39	FE	Post-1999	0.980	-0.2405	-0.5697	-0.0664
MMW0007B	105635.89	8869.39	FE	Latest	0.987	0.1052	-0.1229	0.5304
MMW0007B	105635.89	8869.39	MN	Historical	0.953	-0.0018	-0.0125	0.0256
MMW0007B	105635.89	8869.39	MN	Post-1999	0.971	-0.0030	-0.0155	0.0256
MMW0007B	105635.89	8869.39	MN	Latest	0.978	-0.0348	-0.0607	-0.0058
MMW0008	105643.92	8869.73	BZ	Historical	0.953	0.0000	0.0000	0.0000
MMW0008	105643.92	8869.73	BZ	Post-1999	0.959	0.0000	0.0000	0.0000
MMW0008	105643.92	8869.73	BZ	Latest	0.978	0.0000	0.0000	0.0000
MMW0008	105643.92	8869.73	FE	Historical	0.965	0.1460	0.0296	0.2559
MMW0008	105643.92	8869.73	FE	Post-1999	0.971	0.1308	0.0253	0.2551

WELLID	EASTING	NORTHING	COC	TYPE	CONF-LEV	TREND	LOWER-LIMIT	UPPER-LIMIT
MMW0008	105643.92	8869.73	FE	Latest	0.988	-0.0671	-0.1344	0.3843
MMW0008	105643.92	8869.73	MN	Historical	0.953	0.0033	-0.0126	0.0217
MMW0008	105643.92	8869.73	MN	Post-1999	0.959	-0.0008	-0.0148	0.0077
MMW0008	105643.92	8869.73	MN	Latest	0.978	0.0217	-0.0148	0.0809
MMW0009	107189.78	20000.95	BZ	Historical	0.953	-0.0063	-0.0134	0.0001
MMW0009	107189.78	20000.95	BZ	Post-1999	0.959	-0.0029	-0.0119	0.0004
MMW0009	107189.78	20000.95	BZ	Latest	0.978	-0.0027	-0.0117	0.0001
MMW0009	107189.78	20000.95	FE	Historical	0.953	-1.5940	-2.1515	1.1606
MMW0009	107189.78	20000.95	FE	Post-1999	0.959	-1.0555	-2.0215	1.5229
MMW0009	107189.78	20000.95	FE	Latest	0.978	0.0911	-1.8674	2.2824
MMW0009	107189.78	20000.95	MN	Historical	0.953	-0.0707	-0.1548	-0.0303
MMW0009	107189.78	20000.95	MN	Post-1999	0.959	-0.0702	-0.1276	-0.0115
MMW0009	107189.78	20000.95	MN	Latest	0.978	-0.0115	-0.0682	0.0429
MMW0010	107230.49	9847.09	BZ	Historical	0.953	0.0000	0.0000	0.0000
MMW0010	107230.49	9847.09	BZ	Post-1999	0.959	0.0000	0.0000	0.0000
MMW0010	107230.49	9847.09	BZ	Latest	0.978	0.0000	0.0000	0.0000
MMW0010	107230.49	9847.09	FE	Historical	0.965	0.0902	-0.0002	0.2335
MMW0010	107230.49	9847.09	FE	Post-1999	0.971	0.0750	-0.0150	0.1797
MMW0010	107230.49	9847.09	FE	Latest	0.987	0.0681	-0.1580	0.1735
MMW0010	107230.49	9847.09	MN	Historical	0.953	-0.0266	-0.0407	-0.0108
MMW0010	107230.49	9847.09	MN	Post-1999	0.959	-0.0256	-0.0342	-0.0077
MMW0010	107230.49	9847.09	MN	Latest	0.978	0.0024	-0.1401	0.0373
MMW0011	107224.74	9841.50	BZ	Historical	0.965	0.0000	0.0000	0.0000
MMW0011	107224.74	9841.50	BZ	Post-1999	0.971	0.0000	0.0000	0.0000
MMW0011	107224.74	9841.50	BZ	Latest	0.988	0.0000	0.0000	0.0000
MMW0011	107224.74	9841.50	FE	Historical	0.953	0.0815	-0.0213	0.2327
MMW0011	107224.74	9841.50	FE	Post-1999	0.959	0.0644	-0.0432	0.2214
MMW0011	107224.74	9841.50	FE	Latest	0.978	-0.0213	-0.2220	0.8157
MMW0011	107224.74	9841.50	MN	Historical	0.965	0.0060	-0.0021	0.0111
MMW0011	107224.74	9841.50	MN	Post-1999	0.971	0.0047	-0.0075	0.0096
MMW0011	107224.74	9841.50	MN	Latest	0.988	0.0116	0.0047	0.0626
MMW0012	108059.46	10484.21	BZ	Historical	0.965	0.0000	0.0000	0.0000
MMW0012	108059.46	10484.21	BZ	Post-1999	0.971	0.0000	0.0000	0.0000
MMW0012	108059.46	10484.21	BZ	Latest	0.961	0.0000	0.0000	0.0000
MMW0012	108059.46	10484.21	FE	Historical	0.953	-0.0746	-0.1782	-0.0338
MMW0012	108059.46	10484.21	FE	Post-1999	0.959	-0.0729	-0.1043	-0.0017
MMW0012	108059.46	10484.21	FE	Latest	0.978	0.3071	0.0668	0.4630
MMW0012	108059.46	10484.21	MN	Historical	0.953	0.0050	0.0032	0.0095
MMW0012	108059.46	10484.21	MN	Post-1999	0.959	0.0052	0.0036	0.0118
MMW0012	108059.46	10484.21	MN	Latest	0.978	0.0124	-0.0035	0.0243
MMW0013	108066.33	10492.60	BZ	Historical	0.953	0.0000	0.0000	0.0000
MMW0013	108066.33	10492.60	BZ	Post-1999	0.959	0.0000	0.0000	0.0000
MMW0013	108066.33	10492.60	BZ	Latest	0.978	0.0000	0.0000	0.0000
MMW0013	108066.33	10492.60	FE	Historical	0.953	-0.0837	-0.3425	0.3666

WELLID	EASTING	NORTHING	COC	TYPE	CONF-LEV	TREND	LOWER-LIMIT	UPPER-LIMIT
MMW0013	108066.33	10492.60	FE	Post-1999	0.959	0.0077	-0.3341	0.4693
MMW0013	108066.33	10492.60	FE	Latest	0.978	-0.2152	-0.8286	0.5446
MMW0013	108066.33	10492.60	MN	Historical	0.953	0.6331	0.0792	1.3041
MMW0013	108066.33	10492.60	MN	Post-1999	0.959	0.7286	0.2402	1.3328
MMW0013	108066.33	10492.60	MN	Latest	0.978	0.4825	0.0196	1.0568
MMW0016	107858.21	10022.92	BZ	Historical	0.953	0.0000	0.0000	0.0000
MMW0016	107858.21	10022.92	BZ	Post-1999	0.959	0.0000	0.0000	0.0000
MMW0016	107858.21	10022.92	BZ	Latest	0.978	0.0000	0.0000	0.0000
MMW0016	107858.21	10022.92	FE	Historical	0.953	-0.1037	-0.9017	0.0655
MMW0016	107858.21	10022.92	FE	Post-1999	0.959	-0.1037	-1.1086	0.0655
MMW0016	107858.21	10022.92	FE	Latest	0.978	0.4657	0.0415	0.6363
MMW0016	107858.21	10022.92	MN	Historical	0.953	-0.0239	-0.0322	-0.0068
MMW0016	107858.21	10022.92	MN	Post-1999	0.959	-0.0218	-0.0302	-0.0018
MMW0016	107858.21	10022.92	MN	Latest	0.978	-0.0068	-0.0725	0.0316
MMW0017	107038.16	9401.65	BZ	Historical	0.953	0.0000	0.0000	0.0000
MMW0017	107038.16	9401.65	BZ	Post-1999	0.959	0.0000	0.0000	0.0000
MMW0017	107038.16	9401.65	BZ	Latest	0.978	0.0000	0.0000	0.0000
MMW0017	107038.16	9401.65	FE	Historical	0.953	-28.3403	-63.7828	12.8073
MMW0017	107038.16	9401.65	FE	Post-1999	0.959	-16.6242	-63.5554	13.2810
MMW0017	107038.16	9401.65	FE	Latest	0.978	-16.5856	-181.9737	27.7553
MMW0017	107038.16	9401.65	MN	Historical	0.953	-0.0109	-0.5273	0.4073
MMW0017	107038.16	9401.65	MN	Post-1999	0.959	0.0797	-0.2993	0.4462
MMW0017	107038.16	9401.65	MN	Latest	0.978	-0.5273	-3.3364	0.5313
MMW0019	105655.31	8657.30	BZ	Historical	0.953	0.0000	0.0000	0.0000
MMW0019	105655.31	8657.30	BZ	Post-1999	0.959	0.0000	0.0000	0.0000
MMW0019	105655.31	8657.30	BZ	Latest	0.978	0.0000	0.0000	0.0000
MMW0019	105655.31	8657.30	FE	Historical	0.965	-0.8199	-2.9659	1.5939
MMW0019	105655.31	8657.30	FE	Post-1999	0.959	-0.8381	-3.4351	1.0528
MMW0019	105655.31	8657.30	FE	Latest	0.987	1.4479	-1.9815	3.4394
MMW0019	105655.31	8657.30	MN	Historical	0.965	-0.6988	-0.9066	-0.3757
MMW0019	105655.31	8657.30	MN	Post-1999	0.959	-0.7261	-0.9547	-0.3987
MMW0019	105655.31	8657.30	MN	Latest	0.987	-0.7663	-1.0434	-0.4822
MMW1560	111365.14	15129.42	BZ	Historical	0.953	13.6245	-6.1450	33.9167
MMW1560	111365.14	15129.42	BZ	Post-1999	0.959	19.4032	-3.6233	36.0614
MMW1560	111365.14	15129.42	BZ	Latest	0.978	13.6245	-12.0991	55.1220
MMW1560	111365.14	15129.42	FE	Historical	0.953	20.9848	12.8839	25.5089
MMW1560	111365.14	15129.42	FE	Post-1999	0.959	22.6433	15.3086	25.8559
MMW1560	111365.14	15129.42	FE	Latest	0.978	46.2320	3.4244	100.7457
MMW1560	111365.14	15129.42	MN	Historical	0.953	43.5052	1.4135	70.7520
MMW1560	111365.14	15129.42	MN	Post-1999	0.959	48.8405	12.6073	74.3364
MMW1560	111365.14	15129.42	MN	Latest	0.978	41.5812	-13.6134	155.0779
MMW7330	109964.67	13027.80	BZ	Historical	0.953	0.0000	-0.0030	0.0000
MMW7330	109964.67	13027.80	BZ	Post-1999	0.959	0.0000	-0.0015	0.0000
MMW7330	109964.67	13027.80	BZ	Latest	0.978	0.0000	0.0000	0.0000

WELLID	EASTING	NORTHING	COC	TYPE	CONF-LEV	TREND	LOWER-LIMIT	UPPER-LIMIT
MMW7330	109964.67	13027.80	FE	Historical	0.953	-9.0006	-13.7055	-4.4721
MMW7330	109964.67	13027.80	FE	Post-1999	0.959	-9.9385	-14.0658	-5.5133
MMW7330	109964.67	13027.80	FE	Latest	0.978	-5.7296	-13.1923	4.7322
MMW7330	109964.67	13027.80	MN	Historical	0.953	0.5428	0.1821	1.1855
MMW7330	109964.67	13027.80	MN	Post-1999	0.959	0.6913	0.2023	1.3087
MMW7330	109964.67	13027.80	MN	Latest	0.978	0.1711	0.1440	0.3633
MMW8015	116664.03	22451.10	BZ	Historical	0.953	-0.0042	-0.0047	-0.0027
MMW8015	116664.03	22451.10	BZ	Post-1999	0.971	-0.0040	-0.0047	-0.0025
MMW8015	116664.03	22451.10	BZ	Latest	0.978	0.0001	-0.0085	0.0034
MMW8015	116664.03	22451.10	FE	Historical	0.953	-1.7158	-3.8069	11.0573
MMW8015	116664.03	22451.10	FE	Post-1999	0.971	-1.7203	-4.7312	11.0573
MMW8015	116664.03	22451.10	FE	Latest	0.978	11.0573	-16.3236	21.7876
MMW8015	116664.03	22451.10	MN	Historical	0.953	-1.0405	-3.2680	0.5645
MMW8015	116664.03	22451.10	MN	Post-1999	0.971	-1.2073	-3.4646	0.5645
MMW8015	116664.03	22451.10	MN	Latest	0.978	-2.3504	-7.8979	-0.6896
RFW1144	114680.90	21344.90	BZ	Historical	0.953	0.0042	-0.0257	0.0177
RFW1144	114680.90	21344.90	BZ	Post-1999	0.959	0.0001	-0.0260	0.0140
RFW1144	114680.90	21344.90	BZ	Latest	0.978	-0.0535	-0.2095	-0.0257
RFW1144	114680.90	21344.90	FE	Historical	0.953	-5.0023	-11.1619	-0.1787
RFW1144	114680.90	21344.90	FE	Post-1999	0.959	-6.4406	-12.7450	-0.7906
RFW1144	114680.90	21344.90	FE	Latest	0.978	-0.7906	-3.1768	20.4336
RFW1144	114680.90	21344.90	MN	Historical	0.953	-2.2214	-3.8693	-0.4473
RFW1144	114680.90	21344.90	MN	Post-1999	0.959	-2.4297	-4.4068	-0.7351
RFW1144	114680.90	21344.90	MN	Latest	0.978	-0.7351	-2.2214	0.4694
RFW1147	114493.70	21230.60	BZ	Historical	0.953	0.0092	-0.0075	0.0581
RFW1147	114493.70	21230.60	BZ	Post-1999	0.959	0.0086	-0.0154	0.0552
RFW1147	114493.70	21230.60	BZ	Latest	0.978	0.0086	-0.0075	0.1109
RFW1147	114493.70	21230.60	FE	Historical	0.953	48.4400	10.0155	83.8213
RFW1147	114493.70	21230.60	FE	Post-1999	0.959	56.8190	19.4167	86.7157
RFW1147	114493.70	21230.60	FE	Latest	0.978	48.4400	-33.0375	251.2362
RFW1147	114493.70	21230.60	MN	Historical	0.953	2.5448	-0.9374	7.0637
RFW1147	114493.70	21230.60	MN	Post-1999	0.959	4.2901	-0.8934	9.5311
RFW1147	114493.70	21230.60	MN	Latest	0.978	5.9553	-7.0003	33.2421
USMW025	109706.00	17772.00	BZ	Historical	0.965	0.0000	0.0000	0.0000
USMW025	109706.00	17772.00	BZ	Post-1999	0.971	0.0000	0.0000	0.0000
USMW025	109706.00	17772.00	BZ	Latest	0.988	0.0000	0.0000	0.0000

Section 4. Spatial Optimization

This section summarizes the spatial statistical analyses conducted at Site OU-12 on long-term groundwater monitoring (LTM) data using the spatial component of the GTS algorithm. The main goal of this portion of the study was to determine whether there are statistical redundancies within the spatial network of well locations being monitored at Site OU-12, and to make recommendations as to which current wells might be “pulled out” of the network, or at least sampled very infrequently. The purpose in doing so is to optimize the LTM program by determining whether there are resources being poured into sampling and analysis that might be pared without sacrificing critical information.

A secondary goal of the spatial analysis is to determine whether there are specific areas at Site OU-12 where the siting of additional wells would provide important, unknown information about contaminant extent. By “eliminating” redundant wells from “over-sampled” areas and then potentially adding wells to other areas of “undercoverage,” the spatial network can be optimized in the sense that monitoring wells are effectively placed to capture key information about the contaminant plume(s).

This section includes descriptions of 1) what data preparations were made for input to the GTS spatial algorithm; 2) the GTS spatial algorithm itself, including changes made to the algorithm since the last published version (Cameron and Hunter, 2002); and 3) results of the Site OU-12 spatial analysis.

Section 4.1. Data Preparation

As discussed in **Section 3.1**, data queries were made for all chemical analytical data collected from wells Site OU-12. Exploratory statistical analyses were then performed to pare the initial list of possible constituents to 2 to 3 candidate constituents of concern (COC). As mentioned previously, including a large number of COCs significantly increases the amount of work required to run the GTS algorithm without typically improving the results. So the goal was to include only those parameters in the optimization routine that offer *the most statistical information* concerning temporal and spatial redundancy. The best such parameters typically exhibit larger detection rates and more widespread spatial occurrence.

Overall, the most promising candidates at Site OU-12 were BZ, MN, and FE. These three were chosen for the optimization analysis. Other COCs had much lower detection rates and/or poorer spatial distributions.

Unlike the temporal analysis, where sampling data at a given well and date but collected over multiple depths were averaged so as to ensure that there was only one value per sampling event per well, the spatial analysis was designed to be three-dimensional in nature. What that meant was that every sample measurement was assigned not only an easting and northing, but also a depth and elevation value. Only data that could be placed within three-dimensional space could be utilized in the analysis. Data points missing any of these components were excluded.

Because a small number of existing well locations were either missing the depth or surface elevation component, attempts were made to “fill in” missing information where possible. After obtaining the most up-to-date information from Montgomery Watson, two wells had to be eliminated from the data base due to insufficient information. Surface elevation data were added to three others.

The other major step in the data preparation was to divide the available data for each COC into two separate “time slices” or time periods. The reason for analyzing separate time slices was three-fold: 1) because the character and extent of contamination is likely to change over time, yet maps of a site represent only “snapshots,” it is important to analyze data from a limited time frame in order to create reasonably accurate maps; 2) unless sampling events are highly regimented and all wells are sampled at the same time and during the same sampling event, it may be impossible to include a full representation of the spatial well network if only a specific sampling event is analyzed, as opposed to a “slice” of time that includes a limited range of events; 3) to help ensure that well locations are optimized over the life of the LTM program and not simply for a given sampling event, wells are only identified as potentially redundant if they exhibit redundancy across time slices (note, however, that newer wells might not have any data for earlier time slices; such wells would exhibit redundancy only in more recent time slices).

At OU-12, the first time slice consisted of all measurements procured during 1999 and 2000. The second covered all measurements sampled from 2001 and 2002. Data prior to this were not used in the spatial analysis in part to ensure that the most current well network was optimized.

In practical terms at Site OU-12, with 3 COCs and two time slices per COC, six distinct data sets were analyzed under the spatial optimization algorithm. This allowed for a six-fold comparison of redundancy in identifying wells that were either “essential” or potentially “redundant” in their statistical information. On a final note, as in the temporal analysis, non-detects were handled by converting them to half the listed reporting limit (RL).

Section 4.2. Methodology

The heart of the spatial optimization analysis in GTS consists of the following basic steps: 1) estimation of a declustered, univariate cumulative distribution of concentration values for each COC; 2) determination of an appropriate spatial bandwidth; 3) creation of a base map using locally-weighted quadratic regression and all existing site data; 4) calculation of a global regression weight at each well; and 5) iterative elimination of wells with the lowest global regression weights and re-estimation of the site map based on the reduced data set. Each of these steps is explained below.

Section 4.2.1. Declustered CDF

The first task of the spatial analysis was to determine an appropriate univariate distribution of concentration values for each COC. At many contaminated sites, the measurement data may range over several orders of magnitude. As importantly, there is a

complex, three-dimensional spatial distribution associated with these values, dependent both on the nature of the subsurface and the intensity and location of the contaminant plume(s). High concentrations tend to cluster together, although not uniformly and not necessarily in a predictable fashion. Because of this reality, most standard geospatial techniques, including typical forms of kriging, can suffer in their ability to produce reasonable site maps. Univariate and parametric forms of kriging, in particular, such as ordinary or lognormal kriging, often have great difficulty accurately reproducing the highs and lows of widely spread concentration ranges. Except that is, at known data locations, where kriging “honors” the data by exactly reproducing it.

A better strategy is to use a non-parametric form of spatial analysis, such as probability kriging or perhaps even quantile kriging. Probability kriging transforms the original concentration data into a series of indicator variables and another variable representing the uniform scores of the original data. Each indicator is a binary 0-1 variable associated with a particular reference concentration level. All samples with values no greater than the reference level are converted to ones and all values larger than the reference level are converted to zeros. The basic idea is to convert each data value into known probabilities: if the reference level is, for example, 10 ppb, an indicator value of one means it is certain that the data point in question does not exceed 10 ppb (the probability of not exceeding the reference level being equal to one), while an indicator value of zero means that the actual concentration is certainly greater than 10 ppb (the probability of not exceeding the reference being zero).

Typically in probability kriging a series of increasing reference levels is used to define key portions of the actual concentration range (e.g., 5 ppb, 100 ppb, 1,000 ppb, 5,000 ppb, 10,000 ppb). Indicator variables are defined for each reference level and kriging is performed on each indicator. The ultimate goal at each unknown map location is to form a weighted combination of the known 0's and 1's to estimate a probability that the unknown location does not exceed the reference level. Then, by having such probabilities in hand for the entire series of indicators, a reasonable estimate can be made of the actual concentration at the unknown location (more on that below).

To improve these estimates, probability kriging employs an extra variable computed as the *uniform scores* of the original concentration distribution. This transformation simply orders the data and converts each value to its rank divided by the data set sample size, thus giving a transformed value between 0 and 1. Higher values thus have uniform scores closer to 1 while low values have uniform scores closer to 0.

The same strategy is used in quantile kriging. While no indicator variables are formed as in probability kriging, kriging is performed on the uniform scores directly instead of the actual concentrations, leading to kriged estimates between 0 and 1. These estimates can then be thought of as percentiles, since they represent a probability of not exceeding a certain concentration level. The concentration level itself is known as the *quantile* associated with the particular percentile, hence the name quantile kriging. So for example, if the kriged estimate were 0.7, the estimated value at that location would represent the 70th percentile of the possible distribution of concentration measurements.

To actually re-transform these percentile estimates back to the original concentration scale, some form of the cumulative distribution of concentration measurements must be used. Unfortunately, because sampling in contaminated areas is often done to “chase the plume,” clusters of high values are often over-represented in the raw, univariate concentration distribution, biasing the results. A better solution is to make use of the *declustered cumulative distribution* or declustered CDF for short. The declustered CDF adjusts the raw distribution for spatial clustering and generally offers a more accurate estimate of the true concentration distribution.

While a variety of techniques exist to form the declustered CDF, the one utilized in GTS is based on a method for finding declustering weights (Bourgault, 1999). In this method, simple quantile kriging is performed on the set of known measurements, not to estimate *unknown* locations, but rather to *cross-validate* the *known* ones. This is done by temporarily removing a known value from the data set and then calculating a kriged estimate at that spot using the remaining data (otherwise known as “leave-one-out” cross-validation or jackknifing). As it turns out, the local kriging variance associated with each data location being cross-validated can be considered a *declustering weight*: higher variances represent locations with minimal spatial clustering while lower variances represent locations with significant clustering. By then weighting the original concentrations according to these declustering weights, the declustered CDF is formed as the resulting weighted univariate distribution.

To perform the actual cross-validation and simple quantile kriging, two preparation steps had to be accomplished. One was to convert the original data into uniform scores. The other was to develop a three-dimensional model of spatial covariance for the uniform scores. This was accomplished by analyzing omnidirectional variograms of the uniform scores for each of the three COCs and fitting appropriate nested spatial correlation models to these plots. Parameters for each model are provided in **Table 4-1** below.

Table 4-1. Parameters of Final Spatial Correlation Models

COC	Nugget	Spherical Component		Exponential Component		Gaussian Component	
		Sill	Range	Sill	Range	Sill	Range
BZ	0.77	0.22	1000	0.2	10000	—	—
FE	0.73	0.23	850	0.21	17000	—	—
MN	0.69	0.22	800	0.2	9600	—	—

The result of this step was a declustered univariate CDF for each COC. Note that this cumulative distribution of concentration values was designed to represent the range of concentrations that could be observed at Site OU-12. As such, the declustered CDF includes data from the entire time period under consideration, from 1994 through 2002. Furthermore, as will be explained below, the declustered CDF was ultimately used to derive concentration estimates of each COC along a grid of unknown locations encompassing what will be termed the *optimization box*.

Section 4.2.2. Spatial Bandwidth and Search Radius

An important step to building an estimated site map is to choose a *spatial bandwidth*. The fitting procedure used in the current version of GTS, namely *locally-weighted quadratic regression* (LWQR), works by estimating the surface value at a given unknown grid location using a weighted linear combination of the known sample values close to the grid point. The analyst must select, however, how many neighboring sample measurements to use. In GTS this is done by selecting a *bandwidth parameter* that represents the fraction of known samples to be included in the neighborhood of any given grid point. For a one-dimensional time series, these bandwidths typically range from 40% to 80%. With volumetric or three-dimensional data, roughly equivalent bandwidths (in terms of data density included in the neighborhood per unit of volume) are on the order of 10% to 40%.

In general, the higher the bandwidth, the greater the amount of ‘smoothing’ that will occur over the estimated surface. Too high a bandwidth and the surface trend may ‘miss’ important peaks and valleys. Too low a bandwidth and the surface trend may exhibit artifactual jumps and/or dips between known sample values.

To guard against these scenarios, it is important to run a ‘pre-flight’ check of the LWQR fits at several possible bandwidths prior to constructing a base map of the site. This pre-flighting is done by computing diagnostic checks of the *residuals* obtained when the surface trend is estimated at each known sample location and the known value is subtracted from this estimate.

Using GTS, several tests of the surface residuals are made, including the following calculations: Mallow’s CP statistic, correlation of the residuals with the estimated surface trend, average bias of the residuals, and Filliben’s probability plot correlation coefficient. Each of these statistics is designed to provide a numerical indication of the goodness of the estimated trend relative to a given bandwidth. In GTS, these residual diagnostic measures are plotted simultaneously against bandwidth in order to search for the most appropriate fitting neighborhood. The residuals are also plotted in space to look for obvious anomalies or areas of substantial lack of fit.

Mallow’s CP statistic is a scaled measure of the sum of squared residuals. Lower values of Mallow’s CP usually indicate a better fit. The correlation with the estimated surface trend is used to check whether the fit is worse over certain ranges of the variable being estimated than others. Values close to zero are best. Values close to zero are also good when examining the average bias, which simply measures the average difference between the estimated surface value and the known measurement. Filliben’s correlation coefficient is a test of normality that can be used to check the shape and symmetry of the residual distribution. LWQR works best when the *residual* distribution is symmetric and normally distributed. Coefficient values closer to one are best.

Taken together, it is usually possible to find an acceptable bandwidth with which to construct the surface maps. At Site OU-12, a value of 20% was deemed a reasonably good choice for BZ and FE. That simply means that the nearest one-fifth of the data

measurements were used to help estimate the unknown grid point, regardless of their distance from that location. For MN, a bandwidth of 25% was used.

Section 4.2.3. Creating Base Maps with LWQR

Once a bandwidth is chosen, the next task is to create a three-dimensional base map for each COC and time slice. The base map under GTS serves as the primary means by which degrees of spatial redundancy are assessed. Not only is a baseline established as each COC is mapped across the site area, but measures of local and global variance are also computed. At each further iteration of the GTS algorithm, new maps created from reductions in the original data set are compared to the base map to determine how much plume information has been lost and at what price in increased map uncertainty. For this reason, it is important to try and build as accurate a base map as possible.

The previously published version of GTS employed a fairly simple strategy for creating base maps (and subsequent maps). In order to 1) avoid data complexity, 2) handle large fractions of non-detect values, and to 3) aid in the fitting of spatial covariance models, all measurements were converted to a single indicator variable (i.e., zeros and ones), where the reference concentration level was taken as either the detection/reporting limit or a regulatory limit (such as an MCL). Base maps constructed from these indicators were not re-converted to concentrations, but rather represented maps of the probability that the true concentration was below the reference level. As such, these maps did not provide detailed information about plume intensity, but still were useful for assessing spatial redundancy. However, a significant amount of statistical information concerning the spatial distribution of contaminants was not utilized.

In the current version of GTS, the attempt is made to map the plume or contaminant distribution more completely. This is done by converting the sample concentrations into a series of 10 indicator variables, with each reference concentration representing a key quantile of the original, univariate declustered CDF, as shown in **Table 4-2** below. The goal here is not to choose specific regulatory limits as reference values, but rather levels that adequately 'divide' or 'span' the univariate distribution of COC concentrations, paying particular attention to the often highly skewed upper end of these distributions.

It should also be noted that at the lower end of the concentration range, the reference percentiles are not always equally distributed. At many sites, including Site OU-12, there is often a significant fraction of non-detects at a common reporting limit. This can lead to large jumps in the declustered CDF.

Table 4-2. Reference Concentrations and Corresponding Percentiles of Declustered CDF for Each COC

Indicator Variable	BZ		FE		MN	
	Reference Conc (ppb)	Percentile	Reference Conc (ppb)	Percentile	Reference Conc (ppb)	Percentile
I-1	0.5	0.648	20	0.140	2	0.183
I-2	1	0.739	50	0.408	5	0.368
I-3	5	0.830	125	0.602	35	0.549
I-4	10	0.892	250	0.699	120	0.712
I-5	20	0.915	850	0.797	425	0.799
I-6	40	0.943	1600	0.849	850	0.851
I-7	80	0.951	2500	0.898	1400	0.900
I-8	200	0.967	4000	0.947	2400	0.954
I-9	600	0.975	7000	0.977	5000	0.975
I-10	2000	0.989	20000	0.989	22500	0.990

Another facet of the previous version of GTS was that all analyses were conducted in two-dimensional (2D) space. Depth information was simply ignored or collapsed so that all well locations were treated as if they resided in a 2D plane. Furthermore, the technique used to estimate the base map (and all subsequent maps) was ordinary indicator kriging. Kriging takes a neighborhood of known values around an unknown grid point and solves a set of simultaneous linear equations to find the “best” estimate for that grid point. The known locations are “honored” in the sense that a kriged estimate at a known location returns the original data value. In this way, kriging can be thought of as a kind of *spatial interpolator*, where grid points between known locations are interpolated based on the known values.

A key aspect of the kriging method is that it fundamentally depends on having a spatial covariance model that adequately describes the strength of the spatial correlation between adjacent sample points. Much effort in fact can be devoted to analyzing the empirical spatial correlation measure (typically called the variogram or semi-variogram) and then developing an appropriate mathematical model of the spatial covariance.

In order to streamline this process, a different technique has been incorporated into the GTS algorithm: *locally-weighted quadratic regression* (LWQR). Like kriging, LWQR takes a neighborhood of sample values located near an unknown grid point and solves a system of linear equations to determine the optimal estimate. Like kriging, LWQR is a kind of linear estimator. Both techniques assign numerical weights to the sample values in the neighborhood and form the new estimate as a weighted average of the sample values. However, there are also a number of differences.

For one, kriging requires that all the sample data have distinct locations in space. Otherwise the kriging algorithm does not return a solution. In practice, if some locations have multiple measurements during a given time slice (say from distinct sampling events), these values must first be averaged or pre-processed in such a way that only a

single value is used for kriging. Some information about the individual measurements and data variability is necessarily lost in this step. LWQR has no similar requirement. So multiple values at a given well or given sampling location are OK.

Second, kriging, as mentioned above, is a spatial interpolator which honors the known data values. LWQR is instead a *smoother*. Applied to spatial fields, LWQR attempts to find the best overall surface to *fit* the available sample points, but it does not require that any individual data value be honored. The best analogy is standard linear regression. When a best-fitting line is estimated for a time series or an XY-scatterplot, the line may or may not exactly pass through any given individual value. Nevertheless, the line is chosen to minimize the sum of squared deviations from it and to fit the overall trend. In a similar way, the standard version of LWQR is designed to determine the best-fitting quadratic surface through the sample points, but will not *necessarily* pass through any one of them exactly.

In practical terms, LWQR attempts to fit the best overall surface to the sample data while implicitly assuming that the measured samples may not precisely fit the surface trend either due to error or some other source of variation. Standard forms of kriging basically assume that all sample data are known exactly. Of course, there is no guarantee that some measurements might not include elements of laboratory or sampling error. Variation is also introduced by the fact that the groundwater quality and/or plume intensity may change slightly from one sampling event to the next.

A third difference is that LWQR does not require prior development of a spatial covariance model. With LWQR, a locally-quadratic surface is fit to each grid point. Spatial correlation is incorporated in this method not through an explicit prior correlation model, but rather through the apparent *curvature* in the sample points themselves. The quadratic surface is fit to this curvature, the degree of curvature potentially changing with each grid point. In this way, spatial clustering *is* accommodated by the LWQR technique.

Section 4.2.4. Constructing the Base Map

To actually build the base maps at Site OU-12, a volume surrounding the site was constructed and a rectangular grid imposed on this volume. This volume is termed the *optimization box* in GTS. Often the optimization box will not precisely coincide with the site boundaries, or may not include some peripheral wells, but the aim is to have the box match the site boundaries fairly closely. Peripheral wells are included in the neighborhoods of sample points associated with some of the nearby grid locations. In this way, those wells do get included in the optimization analysis.

The specific coordinate ranges of the optimization box for Site OU-12 are listed in **Table 4-3** below. Note that due to the surface topography, it may occur that nodes on the upper layer of the grid are sometimes higher than ground level. Furthermore, due to the spatial layout of the site, attention was limited to a more compact area. Wells which were located in the far western flank of the area and off-site were excluded from the analysis. The same was true of those wells located near East Loring Lake. This small area was too disconnected from the main site area to be easily analyzed. Overall, as mentioned in **Section 2**, a subset of 115 wells were thus used as a baseline for the optimization.

Table 4-3. Boundaries of Optimization Box

Direction	Minimum	Maximum	Step Size
Easting	105,500 ft	112,000 ft	500 ft
Northing	9000 ft	21,000 ft	500 ft
Elevation	450 ft	700 ft	25 ft

At each grid node, an LWQR estimate was made using each of the ten indicator variables in turn. At each indicator level, the zeros and ones corresponding to the sample data were employed to compute an estimate of the probability that the reference concentration level had not been exceeded. Repeating this process for each indicator then gave a series of ten probability values at each grid node, representing updated information helping to “bracket” the best estimate of the concentration at that node. As an example of this process, consider the following hypothetical results for BZ at node 10 as shown in **Table 4-4**:

Table 4-4. Hypothetical LWQR Results for Benzene

COC	Indicator Variable	Reference Level (ppb)	LWQR Result
BZ	I-1	0.5	0.10
BZ	I-2	1	0.20
BZ	I-3	5	0.25
BZ	I-4	10	0.28
BZ	I-5	20	0.36
BZ	I-6	40	0.45
BZ	I-7	80	0.78
BZ	I-8	200	0.95
BZ	I-9	600	0.99
BZ	I-10	2000	0.99

Based on the LWQR results, there would be only a 10% probability that the true concentration fell below 0.5 ppb, a 20% chance that the true concentration was below 1 ppb, a 25% chance that the true value was below 5 ppb, a 28% chance that the true value was below 10 ppb, a 36% chance that the true value was below 20 ppb, a 45% chance that the true value was below 40 ppb, a 78% chance that the value was below 80 ppb, a 95% chance that the true value was below 200 ppb, and a 99% probability that the value was below 2000 ppb or greater. The most likely range would therefore be between 40 ppb and 80 ppb.

To actually determine a concentration estimate for this hypothetical grid node, the approach taken in GTS is to update the univariate declustered CDF using the LWQR results for the series of indicators. This leads to what is known as the *conditional* cumulative distribution function or CCDF. The basic idea is to *condition* or *adjust* the overall univariate distribution of measured values using the updated information provided by the LWQR indicator results. So, for instance, in the hypothetical example above, the declustered CDF for BZ indicates that 95.1% of all the available BZ measurements at

Site OU-12 were no greater than 80 ppb (see previous table). At the hypothetical grid node being estimated, however, the probability that the true value does not exceed 80 ppb is only 78%. Therefore, the overall univariate CDF must be updated so that values less than 80 ppb only occur 78% of the time *at this grid node*. In this manner, an updated CCDF can be calculated independently for each grid node and estimates of the (locally-varying) true mean concentration made across the site using the formula:

$$\hat{v} = \sum_i v_i (CCDF(v_i) - CCDF(v_{i-1}))$$

where v_i indexes the observed concentration values from the declustered, univariate CDF, and $CCDF(v_i)$ represents the updated or conditional CDF probability associated with v_i .

Section 4.2.5. Global Regression Weights

In addition to the base map built from the LWQR estimates, another key output is the computation of global regression weights. The vector of global regression weights associates each known well location with a numerical index representing that well's overall relative contribution to the base map. Positive global regression weights represent wells that are more influential in the base map estimation; negative or zero weights represent wells which play a smaller, more redundant statistical role in the creation of the map. Thus, the global regression weights serve to identify degrees of spatial redundancy among the set of existing well locations.

The global regression weights are calculated by accumulating in an appropriate way a series of intermediate vectors known as the *local* regression weights. These intermediate weights are a by-product formed when computing the estimated probability of non-exceedance for each indicator variable at a given grid node: the LWQR results are manipulated to compute what is known as the *local weight diagram*. The weight diagram is a vector of numerical weights, one per sample measurement in the search neighborhood, such that the probability of non-exceedance for a specific indicator level is proportional to a weighted average of the product of the sample indicator values and the weight diagram. Thus the weight diagram represents the set of local regression weights that gets applied to the observed indicator data to produce the LWQR estimate.

There are two important things to note about the local weight diagram. First, each grid node involves a different set of neighborhood samples, but across the site as a whole, any given sample value is likely to be used in the neighborhood of a number of distinct grid nodes. Thus, the search neighborhoods tend to overlap as one "moves about" the grid. Second, the local weights in LWQR, while they sum to one, are not necessarily positive.

With these items in mind, how are the global regression weights then computed from the local weights? First, the local weight vectors are augmented to give *zero* weight to any sample location located outside the search neighborhood for that grid node. This numerically represents the fact that samples outside the neighborhood have no influence (positive or negative) on the LWQR result for the node being estimated. Second, the augmented local weight vectors are averaged across all the grid nodes *by* sample location. This means that given a known sample location at well X, the local weights associated with that location (one per grid node, with some possibly equaling zero) are summed and

then divided by the total number of nodes. Finally the averaged weights are adjusted for wells with multiple sampling depths. Here the weights are summed across depths for each well. Weights at wells with only a single sampling depth remain unchanged.

After all these steps are completed, *there is exactly one weight per well location*, and it is this numerical vector that is deemed the set of global regression weights. The term global is used because the final weights are built by averaging the local influence on the base map of each sample across the grid, and hence, across the site as a whole. With this vector in hand, the wells are then ranked according to their statistical influence on the base map. Wells with higher global regression weights are deemed more essential to the map estimate, while those with lower weights are deemed least essential and thus potentially redundant.

Section 4.2.6. Local and Global Variance Measures

In addition to forming the basis for the global regression weights, the local regression weights are also useful for estimating relative local and global variance measures. These measures provide a way to assess the relative degree of statistical uncertainty associated with a given map estimate. First, a local uncertainty measure is computed at each grid node using the local weight diagram and the following formula:

$$locvar(w_k) = \sum_i |lx^i(w_k)|^2$$

where w_k denotes the k th grid node, i indexes the sample values in the search neighborhood around the k th node, and lx represents the local regression weight vector.

Because a different relative local variance is computed at each grid node, the set of local variances can be mapped, much like the base map of concentration estimates. One can also determine from such a variance map whether there are certain areas of the site where the local variance is particularly high, representing places of greater statistical uncertainty connected with the mapped concentration estimate.

With the local variances in hand, GTS also computes a global variance measure for the site as a whole. To do this, the local variances are simply summed across the set of grid nodes, using the following formula:

$$gvar = \sum_k locvar(w_k)$$

where, as before, w_k denotes the k th grid node and the summation is taken over the entire grid.

The reason why the global variance is valuable is that it provides a single numerical summary of the total relative statistical uncertainty associated with a given configuration of well locations. In other words, the global variance from the base map — utilizing all the original well locations — can be compared against the global variance computed from estimating the same map on a reduced or different set of well locations. Increases in global uncertainty then represent configurations that are less statistically reliable.

Section 4.2.7. Iterative Elimination of Wells

Given that the global regression weights provide a *relative* but not an *absolute* measure of spatial redundancy, it is important to use other measures to test how many wells are actually redundant and what degree of redundancy should be tolerated. The global regression weights therefore provide a *strategy* for identifying potentially redundant wells. However, the acid test is to see how accurately maps can be estimated when these possibly redundant wells are temporarily removed from the data set.

To accomplish this goal in a systematic fashion, GTS uses the following procedure. First, at each iterative stage of removal, the remaining wells are sorted by global regression weight. Second, the subset with the lowest five to ten percent of global regression weight scores are flagged and removed from the data. Then LWQR is used on the reduced data set to re-estimate the site map. Comparing this re-estimated map to the original base map, three basic statistical quantities are measured: 1) change in global regression variance; 2) changes in local node-specific variances, including tracking of the percentage of nodes with local variances greater than a pre-defined threshold; and 3) changes in the mapped concentration estimates.

The same process is repeated several times by removing five to ten percent of the lowest ranked well locations (that is, ranked by global regression weight) at each incremental iteration. In this fashion, a small number of wells is temporarily eliminated at each step, until the map estimates show obvious deterioration and the variance measures show substantial change.

The final step in the spatial analysis is to review the results of the iterative well location removal algorithm and to decide at what point the re-estimated maps have deteriorated beyond a reasonable level. Such a decision is necessarily somewhat subjective. However, it is often helpful to examine the rate of deterioration in the maps and the rate of change in the global and local variance measures as a function of the percentage of well locations that has been removed.

Once a “stopping point” has been decided, only wells deemed potentially redundant at the *previous* removal step are ultimately tagged as redundant for that COC and time slice. Then the lists of redundant wells are compared across the COCs and time slices in order to determine that subset of locations which is consistently redundant. These wells then make up the final redundancy list for the site.

One final thing to note is that the global regression weights are recomputed at each stage of removal and therefore are not “fixed” measures of redundancy. Wells with higher global weights at one stage, and thus considered important enough to “keep in the mix” of essential wells, might have low global weights at a subsequent stage. Because of this, rankings based on the global regression weights are only meaningful relative to the particular removal stage at which they are computed.

Section 4.3. Spatial Optimization Results

The spatial optimization results are contained in a series of graphs and tables. Overall, the spatial analysis of the two time slices (1999-2000 and 2001-2002) and the three COCs at

Site OU-12 revealed varying levels of spatial redundancy. For the benzene data, a ‘safe’ level of redundancy appeared to be about 30% of the total well network. For manganese, this safe level dropped to about 20% of the wells. Iron fell in-between the other two at 20-30%. Because of the importance of benzene as a representative of the BTEX plume(s) at OU-12, the overall recommendation from the GTS analysis identifies 30% of the well network as redundant.

When matching lists of redundant wells across the COCs that were analyzed, only 17 wells were commonly listed, amounting to 15 percent of the total baseline well set. However, if only benzene is considered (again, as representative of the BTEX plume(s)), 29 wells might be considered redundant or 25% of the baseline LTM network. Note in this context that the lists of redundant wells also varied somewhat by time slice, so that even though about 30% of the network was redundant for benzene in each time period, the common list amounted to a smaller fraction.

Potentially, *from strictly a statistical point of view*, all of these redundant wells ought to be eliminated from the Site OU-12 LTM network. However, other considerations should also be factored in before making any such decisions. The spatial analysis here only considers statistical contributions of each well to concentration maps of the site. It does not consider other purposes for these wells. Some of them may be essential for other engineering or site characterization reasons. Each potentially redundant well should be reviewed by site geologists and hydrologists to determine if such overriding factors exist.

Section 4.3.1. Global Measures of Redundancy

To help assess redundancy at a global level, the graphs in **Appendix 4-1** were prepared. These graphs plot selected summary statistics from the spatial mapping exercise against the percentage of wells that was removed from the data for each COC. Examination of these graphs can provide one indication of when ‘too much’ data has been removed (that is, when a reasonable level of statistical redundancy has been exceeded), especially if the trend is flat or very gentle at first (say for lower fractions of data removal), but then begins to trend more sharply at some increased level of data removal.

The first measure of global redundancy is given in the first figure for each COC in **Appendix 4-1**. These graphs plot the trend in global variance for each COC and each time slice. In general, the global variance might be expected to increase as more data is removed and the maps are re-estimated. In other words, less data equals less certainty and higher variance. However, this pattern does not always occur. At some grid nodes, the estimated variance tends to ‘blow up,’ leading to a much higher global variance value even at low removal levels. This artifact makes the global variance measures harder to interpret. In other cases, say for manganese, the global variance is essentially flat or dropping slightly at removal levels far greater than a safe level (according to other measures discussed below).

Additional measures of global redundancy are shown the second two figures for each COC in **Appendix 4-1**. The first of these documents the change in two measures: the percentage of voxels (i.e., three-dimensional pixels) with very high grid-node-specific local variances (denoted REDUCED-VARPCT on the plots) and the average level of

difference between the estimated indicator values from the reduced data set and those of the base map (denoted AVE-IDIFF). The first of these (i.e., REDUCED-VARPCT) simply counts across the site grid the percentage of estimated nodes where the local variance value was determined to be in the extreme upper tail of the distribution of local variances. As the fraction of data removal increases, the percentage of extreme local variances would also be expected to increase.

The second measure (i.e., AVE-IDIFF) was computed by taking the difference at each of the five indicator levels between the reduced data set indicator estimate and the corresponding base map indicator estimate. These indicator differences were then averaged across the five indicator levels and finally averaged again across all the nodes on the site grid. The interpretation of the average indicator difference is as follows: each indicator variable corresponds to a particular concentration level from the overall declustered CDF (for instance, the first indicator for FE corresponds to a reference concentration value of 20 ppb). The indicator estimate after mapping the site with LWQR is the probability of not exceeding this reference concentration value. To the extent that the indicator estimates at a particular grid node for both the base map and the reduced-data map are the same, both maps then provide the same statistical information about the expected concentration level at that node. On the other hand, if the indicator estimates differ, the estimated concentration values will also differ, leading the reduced-data map to differ in pattern and magnitude from the base map. Averaged across all the nodes on the site grid, the average indicator difference then provides a summary measure of how much change is to be expected between the base and reduced-data maps.

For none of the COCs is there any particular pattern to the REDUCED-VARPCT measure. In fact it is generally flat to declining in overall trend as more data is removed. The reason for this appears to be connected with how the LWQR method estimates variance. Because the estimated variability depends fundamentally on the observed concentration values, if enough of the pre-existing variation has been removed at a given step (by not including wells with more variable sampling data), the local variances may begin to drop, leading sometimes to a lower overall global variance, and a smaller percentage of grid nodes with very high local variance values. This pattern can be seen for instance in some of the graphs in **Appendix 4-3**.

The average indicator difference measure (AVE-IDIFF) traces a more complicated, but also more informative, pattern. *Negative* values of this measure signify an overall *over*-estimation of the site grid on the reduced-data set compared to the base map. *Positive* values signify an overall *under*-estimation. For all three COCs, low levels of data removal correspond to values of AVE-IDIFF fairly close to zero. With more removal, however, this measure tends to move away from zero in either direction, depending on whether over-estimation or under-estimation of the map is more prevalent.

For benzene, the change in AVE-IDIFF is fairly mild up to about 30% removal, when it then jumps upward more rapidly. For iron, a larger drop in this measure can be seen for time slice one after a 30% removal. For manganese, AVE-IDIFF starts to change rapidly after a 20% removal during both time slices; however, in one case the reduced-data maps tend to be over-estimated and in the other, the maps tend to be under-estimated.

The final set of global redundancy measures are denoted by MEAN-MISCLASS, TRIM-MISCLASS, and PCT-IDIFF. MEAN-MISCLASS refers to the percentage of voxels or nodes that were classified one way relative to a regulatory limit or other pre-specified concentration level on the base map but are classified the *opposite* way on the reduced-data map. For example, using the MCL of 5 ppb for BZ, a little over 20% of all the estimated grid nodes were *misclassified* when 10% of the wells were removed in time slice one. That percentage rises to over 40% by the time 40% of the wells have been removed. TRIM-MISCLASS is a measure closely related to MEAN-MISCLASS, except that instead of classifying voxels on the basis of the estimated mean concentration, the classification is done using the estimated *trimmed mean*, cutting off 10% of the lower and upper tails of the updated, conditional CDF. For the most part, MEAN-MISCLASS and TRIM-MISCLASS tend to give similar results at OU-12.

For all the COCs, while the percentage of such misclassifications increases as expected with increased data removal, the trends generally provide no obvious way to measure a specific degree of acceptable redundancy. Instead of a flat or nearly flat trend followed at greater levels of removal by a sharp increase, the majority of the increase often occurs right away at the lowest removal levels. The only exception to this at Site OU-12 is for manganese, where there appears to be a jump in misclassifications after 20% of the wells have been removed.

PCT-IDIFF is an additional measure of how much the reduced-data map indicator estimates differ from the base map indicator estimates. It counts the percentage of nodes at which at least one reduced-data indicator differs from the corresponding base map indicator by at least 0.5 (remember that all the indicator estimates are between 0 and 1; a difference of at least 0.5 is thus a large change in the estimated probability of non-exceedance for the associated reference concentration level). Unfortunately, while PCT-IDIFF again trends upward with increased data removal for all three COCs and both time slices, there is little evidence of any ‘flat’ portions of the trends upon which to judge degrees of redundancy.

Section 4.3.2. Local Indications of Redundancy

While global measures of redundancy can be useful, they do not provide the full story. Global misclassification rates for example do not indicate *where* the misclassification is occurring or to what degree. Only actual maps of the site can provide this type of information. To this end, two sets of maps are provided for each COC and time slice. The first documents, at each level of data removal, the differences in the local indicator values between the base map and each reduced-data map (see **Appendix 4-2**) Local areas of overestimation (corresponding to *negative* indicator differences) are shaded in orange and red. Local areas of underestimation (corresponding to *positive* indicator differences) are shaded in blue. By comparing these maps relative to the increase in the amount of data removed, one can assess at what point too many local areas of over- and under-estimation ‘pop-up.’

The second set of maps (see **Appendix 4-3**) details in a similar way what changes occur in the local variance with increasing data removal. Are there particular areas of the site at

which the local uncertainty is unacceptably high? Do the areas with high local variance change as more data is removed? Do new areas emerge? All these questions can be assessed by viewing the maps in **Appendix 4-3**.

In general, the maps in **Appendices 4-2** support the conclusion that too much local information is lost from the base map when the data removal fraction rises above approximately 30% for benzene, 20-30% for iron, and 20% for manganese.

The maps in **Appendix 4-3** are more problematic. The overriding pattern exhibited by the local variance maps is an increase in areas of both very high variability and, simultaneously, areas of very low variability. As noted in **Section 4.3.1**, this is probably due to the fact that when a larger percentage of the wells have been removed, there are large swatches of the site where the nearest sample measurements are fairly uniform in concentration level, leading to a low variability estimate. At other locations, there is less data available to use in the estimates (or perhaps the remaining data do not vary in a continuous manner) and so the variation is quite high. In any event, the local variance maps do not provide much help at OU-12 in assessing degrees of redundancy.

One important thing to note about the maps in **Appendices 4-2** and **4-3** is that they are presented as two-dimensional “plan-view” contour surfaces. The actual map estimates at Site OU-12 were three-dimensional, as noted earlier. However, it is difficult to adequately visualize three-dimensional data within a static report. To solve this difficulty, all the indicator difference and local variance maps were first *averaged over depth* in order to provide two-dimensional projections of the three-dimensional surface estimates. Some information is of course lost when such averaging is done. Nevertheless, the results can be presented and visualized much more easily.

Section 4.3.3. Base Map Accuracy

In **Appendix 4-4**, there is a base map of the estimated concentrations for each COC (based on all the data prior to any removal), overlaid with a scatter plot of the actual data locations used in the analysis. Both the base map and the scatter plot of actual data are colored by contour level. One can see from this representation that most of the observed data levels correspond reasonably well with the surrounding nearby base map estimates. There are, however, some notable exceptions.

A couple of major reasons account for areas where there appears to be poor base map accuracy. First, the two-dimensional base map representation is again averaged over depth, but is in reality three-dimensional. Often the plume areas lie below the ground surface, but appear to be at ground level on the 2D surface map. Although unavoidable, this averaging process affects to some degree how well the observed data appear to “match” the estimated contours on the base map. Along the same lines, many more individual samples were used in the base map construction than show up on the base maps in **Appendix 4-4**. Deeper sample values are sometimes ‘hidden’ by shallower, but nearby, locations due to the scaling and size of the maps.

Second, locally-weighted quadratic regression is, as was noted earlier, a smoothing technique rather than a spatial interpolator. Because of this, the estimated surface may not

precisely equal the value of any given observed data point. This will especially be true in those cases where one nearby sample is quite high while its neighbor is quite low. At Site OU-12, there is one noticeable area to the northwest of the Central NDA area toward the Quarry where little sample information is available. In this case, LWQR graduates the estimated plume from the high values near the Central NDA down to the much lower values near the Quarry.

Ultimately, having an accurate base map is an important key to a successful spatial optimization analysis using GTS. As noted, all assessments of redundancy flow from a comparison between the base map and subsequent maps constructed from reduced-data sets. Although it is likely that the GTS algorithm is ‘robust’ to some base map inaccuracy, it is certainly the case that spatial redundancy cannot be judged fairly unless the base map matches the actual data to a reasonable degree.

The base maps generated using LWQR may or may not adequately coincide with similar hand-drawn maps created by project geologists. The estimated base maps from the spatial analysis are strictly data driven and do not account for special features of the terrain or hydrogeology. Again, due to the relative paucity of hard data in areas to the northwest of the Central NDA area, the smoothing process extended and graduated the plume in this direction, in large part because the higher data were still within the search neighborhoods for those grid nodes located between Central NDA and the Quarry, and thus had a significant impact on the grid estimates.

Section 5. Recommendations for Loring AFB, Site OU-12

Section 5.1 Recommendations Regarding Sampling Frequency

It has already been noted in **Section 3** from the temporal analysis that the operational sampling frequency at OU-12 ought to be reduced from quarterly to once every 2 or possibly 3 quarters. This recommendation is based on the overall consistency between the Temporal Variograms discussed in **Section 3.4.1** and the typical Iterative Fitting results discussed in **Section 3.4.2**. What was not discussed is how this sampling schedule can be translated into a site-specific sampling plan. The recommended sampling strategy is discussed in more detail below.

With regard to sampling frequency, construction of the Temporal Variograms requires pairs of measurements from any given well with a variety of inter-event time intervals. If the wells are sampled at regular intervals (e.g., every seven quarters) after implementation, the range of between-sample intervals would not have the required variety of inter-event time intervals, and consequently it would be much harder to construct a future Temporal Variogram to test the original recommendation. Therefore, a key goal of the sampling strategy is to ensure that each well is sampled at irregular intervals over time. This involves ‘mixing up’ or randomizing the distribution of inter-event sampling intervals to facilitate a similar follow-up analysis after 3 to 5 years to assess whether or not the initial recommendations would still hold.

Full implementation of the sampling strategy may not, however, be practical for certain wells that need to be sampled together or in a particular sequence. To make the sampling procedure as operationally efficient as possible, but without sacrificing the goal of at least partially ‘mixing up’ or randomizing the distribution of inter-event sampling intervals, one could also group the wells into clusters that would be sampled simultaneously. This might be needed, for instance, if ‘cleaner’ wells needed to be sampled prior to ‘dirtier’ wells, or perhaps for other logistical reasons. In this case, each cluster would be treated as a single well in the randomization scheme discussed below. Care should be taken, however, to ensure that individual clusters are not so large as to make the final sampling groups highly unbalanced.

It is recommended that a sampling plan be developed using the following three-step process to ensure sufficient variety of inter-event sampling intervals:

Step 1 – Randomly divide the set of essential monitoring wells into two approximately equal-size groups (e.g., Group 1 and Group 2). This process would be akin to representing each well as a ball, and then randomly dropping each ball into one of two different urns, until all the balls are used up. In practical terms, the easiest way to achieve such random assignment — and to ensure that each group is of roughly equal size — is to list the wells in any order (say on a spreadsheet), draw a random number between 0 and 1 for each well from either a computer, calculator, or random number table, list the random numbers beside each well, sort the list in order of the random values, then assign the wells in the top half of the sorted list to the first urn (i.e., Group 1) and the well in the second half of the list to the second urn (i.e., Group 2).

Step 2 - Randomly assign Group 1 wells to two of the three available quarters for sampling (i.e., Spring, Summer, or Fall), and then randomly assign Group 2 wells to two of the three available quarters for sampling. Note that it will be quite possible to have more than one of the well groups sampled during the same quarter. This means, in other words, that the quarter for sampling is chosen independently for each of the seven well groups.

Step 3 – At the start of each successive sampling year, repeat steps 1 and 2. This step ensures that no single well will be sampled at precisely the same time during each sampling round.

Example Sampling Schedule for Wells Listed in Table 5-2 (98 wells):

Step 1- Divide the set of wells (98 wells) into two equal groups. *Note that this table is for illustrative purposes, and site managers should construct their own well grouping to address any site-specific operational considerations (such as the need to sample certain wells together or in a particular sequence).*

Example of Random Grouping of Wells Listed in Table 5-2			
Group 1		Group 2	
JBW7336A	MMW0423	JMW6105	JPZ0344
JBW7215B	JMW3082	MMW0005	JBW7102
JMW3601	JMW1860	JMW1963	MMW0007A
JBW7326B	JBW7348	MMW0124	MMW0020
JBW7203A	JPZ1780	JBW7213B	MMW0422
MMW0011	JMW0505	JBW7203B	JMW0301C
JBW7326A	JBW7812B	JBW7317	JMW0201C
JPZ0340	JBW7333	JPZ0348	JMW1966
JPZ7601	JBW7106A	JBW7737A	JMW6001
JPZ0349	JBW7738A	MMW0010	JBW7809
JMW1562	MMW0016	JMW7332	JBW7338B
MMW0017	MMW0421A	JMW3202	MMW0004
BMW712	JMW0701	JBW7106B	JPZ7312
JPZ0342	MMW0006	MMW0421B	056MW02
JBW7742B	JBW7338A	MMW0125	JBW7213A
JBW7328	JBW7350	JBW7345B	JMW0401
JBW7344	MMW0003	AR25	056MW04
JMW1964	JBW7330A	JBW7204A	JMW35X2
JBW7607	MMW0012	MMW0019	JBW7347B
MMW7330	JMW1960	MMW1560	MMW0007B
JMW1881	MMW0013	JMW0542	JPZ0341
JPZ1781	JBW7340B	JMW0503	JBW7212A
JBW7212B	JBW7101	JMW0604	JBW7617B
JPZ7807	JBW7336B	JBW7309	MMW0008
JMW0603		JPZ7208	

Step 2 – Randomly assign Group 1 wells to two of the three available quarters for sampling (i.e., Spring, Summer, or Fall), and randomly assign Group 2 wells to two of the three available quarters for sampling. See **Table 5-1**. Note that during some quarters, it is possible that no sampling will be required.

Table 5-1. Example Sampling Plan for the First Year of the Optimized LTM Sampling Program

Year	Spring	Summer	Fall
1	Group 1 Group 2	Group 1	Group 2

Thus, all wells will be sampled twice per year. Per **Step 3**, the process is repeated to develop a new sampling schedule each subsequent year.

Section 5.2 Recommendations Regarding Spatial Redundancy

The ultimate decision about when ‘too much’ data has been removed is somewhat subjective. But, based on the GTS spatial analysis, and considering both the global measures of redundancy and the maps of local indicator differences, at least 17 wells and perhaps as many as 29, could be considered as redundant to the OU-12 LTM program. This leaves 86 to 98 wells from the baseline list as ones that should remain in the

monitoring program. Specific lists of wells essential to the LTM program are provided in **Tables 5-2** and **5-4**. **Table 5-2** is a list of *essential* wells based on using all three COCs from the spatial analysis. **Table 5-4** is a similar, but slightly smaller, list based on the results of the benzene analysis. Given the importance of the BTEX contaminants at OU-12, this analysis recommends that the second of these monitoring networks be implemented.

Note that in each of these tables, the last column assigns a relative ranking of the statistical importance of each well, classified as HIGH, MED(IUM), or LOW. These rankings reflect whether or not the well was consistently deemed essential in each time slice for at least one COC and had a positive average global regression weight (HIGH), was consistently deemed essential but had a non-positive average global regression weight (MED), or was deemed essential only in certain time slices (LOW).

Complementing these tables are lists of statistically redundant wells culled from each thread of the analysis. **Table 5-3** lists the redundant wells derived from an analysis using all three COCs, while **Table 5-5** is a longer list of redundant wells derived from the results of the benzene analysis.

It should also be noted that for the purposes of long-term follow-up analysis, if redundant wells are removed from regular long-term monitoring, they should ideally not be decommissioned. Rather, prior to a multi-year follow-up review, the same wells ought to be sampled again to determine whether or not the original recommendations are still valid. Thus, these wells would still be sampled very infrequently, say once every 3 to 5 years.

Lastly, it is important to reiterate that the recommendations concerning redundant wells are highly data-driven. Groundwater wells can serve multiple purposes and may be important for reasons other than long-term monitoring. Because of this, all of the potentially redundant wells should be evaluated by site geologists and regulators to ensure that other goals of the OU-12 LTM program are not compromised.

Table 5-2. Essential Monitoring Network Based on Analysis of All COCs (All measurements in ft)

Note: RANKING refers to relative statistical importance; HIGH = wells deemed essential in both time slices and having positive average global regression weights at optimal removal stage; MED = wells deemed essential in both time slices but having non-positive average global regression weights; LOW = wells deemed essential in only one of two time slices

WELL_ID	EASTING	NORTHING	DEPTH	SCREEN ELEVATION	RANKING
056MW04	110130.1	12294.51	18	679	HIGH
JBW7101	108258.77	9885.66	85.5	563.86	HIGH
JBW7102	109201.33	8769.83	33	630.78	HIGH
JBW7106B	105746.65	8561.7	62.2	553.64	HIGH
JBW7203A	108468.08	10501.33	79.1	562.43	HIGH
JBW7204A	108133.57	10239.05	302	329.67	HIGH
JBW7212A	109634	10474	189	477.36	HIGH
JBW7213A	109465.95	11143.64	199	469.06	HIGH
JBW7215B	109929.84	11368.79	80	608.76	HIGH
JBW7326A	108222.3	10888.36	88	550.18	HIGH
JBW7330A	109964.67	13026.8	387.3	309.71	HIGH
JBW7338A	110830.36	13609.17	111	610.71	HIGH
JBW7338B	110830.36	13610.17	40	681.71	HIGH
JBW7345B	110554.5	13807.74	34	678.39	HIGH
JBW7607	107063.59	15642.68	39	635.27	HIGH
JBW7737A	107734	17185	200	501.02	HIGH
JBW7742B	109908.62	16530.1	94	623.17	HIGH
JBW7812B	108332.56	20848.69	71	637.41	HIGH
JMW0401	108432.9	20095	66	701.77	HIGH
JMW0503	111069.89	14733.53	69.6	651.8	HIGH
JMW0505	111132.9	14617.51	29	691.13	HIGH
JMW0542	109338.8	12434.2	23	654.26	HIGH
JMW0603	110871.7	9324.6	41	637.86	HIGH
JMW1881	108936.65	9301.22	51	604.53	HIGH
JMW1963	109286.98	10487.77	26	629.53	HIGH
JMW1964	109282.91	10966.36	37	622.41	HIGH
JMW1966	109099.64	10610.39	15	641.57	HIGH
JMW6001	109866.12	16952.71	15	702.39	HIGH
JMW7332	107984.11	11714.85	14	633.11	HIGH
JPZ0348	108885.33	12194.33	50	616.6	HIGH
MMW0006	106091.03	15467.33	38	620.94	HIGH
MMW0007A	105635.89	8867.39	137	465.21	HIGH
MMW0008	105643.92	8869.73	9	592.97	HIGH
MMW0010	107230.49	9847.09	67.5	552.56	HIGH
MMW0011	107224.74	9841.5	24	595.57	HIGH
MMW0013	108066.33	10492.6	28	603.32	HIGH
MMW0016	107858.21	10022.92	14.5	608.43	HIGH
MMW7330	109964.67	13027.8	121	576.2	HIGH
056MW02	110269.46	12297.76	25	675.28	MED
AR25	109037	11902	153.25	518.92	MED
JBW7106A	105746.65	8560.7	125.4	490.44	MED
JBW7212B	109634	10475	40	626.36	MED
JBW7213B	109465.95	11144.64	83	585.06	MED
JBW7317	112089.57	15002.11	40	688.74	MED
JBW7340B	110361.54	13210.74	47	659.68	MED
JBW7344	110987.6	13622.38	32.5	690.05	MED
JBW7350	111365.86	14160.19	48.225	677.215	MED
JBW7617B	106434.87	15543.05	50.9	617.97	MED
JBW7738A	106930.24	16925.75	100	575.16	MED
JBW7809	109112.81	21161.11	43	725.95	MED
JMW0301C	109861	13420	59	634.47	MED
JMW0604	111650.6	8969.9	96	597.76	MED

WELL_ID	EASTING	NORTHING	DEPTH	SCREEN ELEVATION	RANKING
JMW1860	108944.86	9032.97	29	630.73	MED
JMW1960	109086.09	10613.03	35	621.03	MED
JMW3202	110684.15	13404.85	46	668.09	MED
JMW35X2	110127.97	10067.32	17.5	656.09	MED
JMW3601	109694.87	11278.81	48	628.12	MED
JMW6105	108145.33	17187.8	25	692.779	MED
JPZ0349	108892.85	12200.73	29	637.63	MED
JPZ1780	109521.51	12824.33	30	646.97	MED
JPZ7208	108141.92	10243.38	15	617.52	MED
JPZ7312	109847.28	15397.09	19	679.02	MED
MMW0007B	105635.89	8869.39	52	550.21	MED
MMW0012	108059.46	10484.21	75	556.84	MED
MMW0017	107038.16	9401.65	20.5	602.96	MED
MMW0019	105655.31	8657.3	9.4	594.52	MED
BMW712	107428.49	16287.99	21	680.93	LOW
JBW7203B	108468.08	10502.33	53	588.53	LOW
JBW7309	107579.17	11409.42	33	613.39	LOW
JBW7326B	108222.3	10889.36	41	597.18	LOW
JBW7328	110684.04	14780.69	35	686.78	LOW
JBW7333	110584.22	13306.8	50	663.82	LOW
JBW7336A	110531.15	13035.23	83	629.3	LOW
JBW7336B	110531.15	13036.23	57	655.3	LOW
JBW7347B	110460.02	14624.9	34	678.24	LOW
JBW7348	110802.02	13966.56	46.6	675.08	LOW
JMW0201C	108503.6	20874.6	41	699.31	LOW
JMW0701	107403.43	16369.68	27	671.03	LOW
JMW1562	111523.51	14976.24	23	698.44	LOW
JMW3082	109539.7	12427.4	30	650.58	LOW
JPZ0340	109561.37	13962.51	40	631.71	LOW
JPZ0341	109554.37	13917.07	15.2	657.43	LOW
JPZ0342	109510.08	14069.1	38	634.18	LOW
JPZ0344	108969.07	12592.36	61	612.46	LOW
JPZ1781	109931.54	12811.71	41	653.33	LOW
JPZ7601	106807.89	16674.53	15	662.75	LOW
JPZ7807	107539.3	20443.3	31	674.55	LOW
MMW0003	106376.08	15069.79	40	629.78	LOW
MMW0004	108965.36	14148.06	59.2	629.05	LOW
MMW0005	110994.15	14918.82	32.65	687.72	LOW
MMW0020	106299.33	19477.31	150	565.27	LOW
MMW0124	109448.8	11150.7	33.25	634.48	LOW
MMW0125	109628.4	11203.7	30.75	641.63	LOW
MMW0421A	106411.06	19294.66	92	619.6	LOW
MMW0421B	106411.06	19295.66	41	670.6	LOW
MMW0422	107002	19354.37	64	638	LOW
MMW0423	107000.5	19350.93	30	672.4	LOW
MMW1560	111365.14	15129.42	25	691.99	LOW

Table 5-3. Redundant Monitoring Wells Based on Analysis of All COCs (All measurements in ft)

WELL_ID	EASTING	NORTHING	DEPTH	SCREEN ELEVATION
BMW715	107439.45	16139.85	45	656.97
BMW717	107613.87	16146.84	37	666.71
JBW7345A	110554.5	13806.74	93	619.39
JBW7710	109834.07	15664.23	50	657.89
JBW7725	109695.14	17708.18	35	693.48
JBW7737B	107734	17186	38	663.02
JBW7752	108375.42	16683.09	31.75	687.05
JBW7806	107716.95	20532.58	37	679.26
JBW7816	108577.94	20890.92	59	682.08
JMW0201A	108502.6	20874.6	76	664.31
JMW1564	111324.2	14979.63	34	683.92
JMW1565	111522.3	14964.19	44	678
JMW7612	106986.73	16453.32	17	656.29
JPZ0343	109503.35	14073.53	20	652.04
JPZ1586	111185.59	15286.16	27	683.8
MMW0009	107189.78	20000.95	44	658.77
USMW025	109706	17772	35	692.05

Table 5-4. Essential Monitoring Network Based on Benzene Analysis (All measurements in ft)

Note: RANKING refers to relative statistical importance; HIGH = wells deemed essential in both time slices and having positive average global regression weights at optimal removal stage; MED = wells deemed essential in both time slices but having non-positive average global regression weights; LOW = wells deemed essential in only one of two time slices

WELL_ID	EASTING	NORTHING	DEPTH	SCREEN ELEVATION	RANKING
056MW02	110269.46	12297.76	25	675.28	HIGH
AR25	109037	11902	153.25	518.92	HIGH
JBW7101	108258.77	9885.66	85.5	563.86	HIGH
JBW7102	109201.33	8769.83	33	630.78	HIGH
JBW7106A	105746.65	8560.7	125.4	490.44	HIGH
JBW7106B	105746.65	8561.7	62.2	553.64	HIGH
JBW7203A	108468.08	10501.33	79.1	562.43	HIGH
JBW7204A	108133.57	10239.05	302	329.67	HIGH
JBW7212A	109634	10474	189	477.36	HIGH
JBW7212B	109634	10475	40	626.36	HIGH
JBW7213A	109465.95	11143.64	199	469.06	HIGH
JBW7215B	109929.84	11368.79	80	608.76	HIGH
JBW7326A	108222.3	10888.36	88	550.18	HIGH
JBW7330A	109964.67	13026.8	387.3	309.71	HIGH
JBW7338A	110830.36	13609.17	111	610.71	HIGH
JBW7607	107063.59	15642.68	39	635.27	HIGH
JBW7737A	107734	17185	200	501.02	HIGH
JBW7742B	109908.62	16530.1	94	623.17	HIGH
JBW7812B	108332.56	20848.69	71	637.41	HIGH
JMW0301C	109861	13420	59	634.47	HIGH
JMW0505	111132.9	14617.51	29	691.13	HIGH
JMW0603	110871.7	9324.6	41	637.86	HIGH
JMW1881	108936.65	9301.22	51	604.53	HIGH
JMW1964	109282.91	10966.36	37	622.41	HIGH
JMW1966	109099.64	10610.39	15	641.57	HIGH
JMW6001	109866.12	16952.71	15	702.39	HIGH
JMW7332	107984.11	11714.85	14	633.11	HIGH
JPZ0348	108885.33	12194.33	50	616.6	HIGH
JPZ1780	109521.51	12824.33	30	646.97	HIGH

WELL_ID	EASTING	NORTHING	DEPTH	SCREEN ELEVATION	RANKING
JPZ7208	108141.92	10243.38	15	617.52	HIGH
JPZ7807	107539.3	20443.3	31	674.55	HIGH
MMW0006	106091.03	15467.33	38	620.94	HIGH
MMW0007A	105635.89	8867.39	137	465.21	HIGH
MMW0008	105643.92	8869.73	9	592.97	HIGH
MMW0010	107230.49	9847.09	67.5	552.56	HIGH
MMW0011	107224.74	9841.5	24	595.57	HIGH
MMW0013	108066.33	10492.6	28	603.32	HIGH
MMW0016	107858.21	10022.92	14.5	608.43	HIGH
MMW0017	107038.16	9401.65	20.5	602.96	HIGH
MMW7330	109964.67	13027.8	121	576.2	HIGH
056MW04	110130.1	12294.51	18	679	MED
JBW7213B	109465.95	11144.64	83	585.06	MED
JBW7326B	108222.3	10889.36	41	597.18	MED
JBW7340B	110361.54	13210.74	47	659.68	MED
JBW7344	110987.6	13622.38	32.5	690.05	MED
JBW7345B	110554.5	13807.74	34	678.39	MED
JBW7617B	106434.87	15543.05	50.9	617.97	MED
JBW7738A	106930.24	16925.75	100	575.16	MED
JBW7809	109112.81	21161.11	43	725.95	MED
JMW0503	111069.89	14733.53	69.6	651.8	MED
JMW0542	109338.8	12434.2	23	654.26	MED
JMW0604	111650.6	8969.9	96	597.76	MED
JMW1860	108944.86	9032.97	29	630.73	MED
JMW1960	109086.09	10613.03	35	621.03	MED
JMW1963	109286.98	10487.77	26	629.53	MED
JMW35X2	110127.97	10067.32	17.5	656.09	MED
JMW3601	109694.87	11278.81	48	628.12	MED
JMW6105	108145.33	17187.8	25	692.779	MED
JPZ7312	109847.28	15397.09	19	679.02	MED
MMW0003	106376.08	15069.79	40	629.78	MED
MMW0007B	105635.89	8869.39	52	550.21	MED
MMW0012	108059.46	10484.21	75	556.84	MED
MMW0019	105655.31	8657.3	9.4	594.52	MED
MMW0423	107000.5	19350.93	30	672.4	MED
BMW712	107428.49	16287.99	21	680.93	LOW
JBW7203B	108468.08	10502.33	53	588.53	LOW
JBW7309	107579.17	11409.42	33	613.39	LOW
JBW7333	110584.22	13306.8	50	663.82	LOW
JBW7336A	110531.15	13035.23	83	629.3	LOW
JBW7336B	110531.15	13036.23	57	655.3	LOW
JBW7347B	110460.02	14624.9	34	678.24	LOW
JMW0701	107403.43	16369.68	27	671.03	LOW
JMW1562	111523.51	14976.24	23	698.44	LOW
JMW3082	109539.7	12427.4	30	650.58	LOW
JPZ0340	109561.37	13962.51	40	631.71	LOW
JPZ0341	109554.37	13917.07	15.2	657.43	LOW
JPZ0344	108969.07	12592.36	61	612.46	LOW
JPZ1781	109931.54	12811.71	41	653.33	LOW
JPZ7601	106807.89	16674.53	15	662.75	LOW
MMW0020	106299.33	19477.31	150	565.27	LOW
MMW0124	109448.8	11150.7	33.25	634.48	LOW
MMW0125	109628.4	11203.7	30.75	641.63	LOW
MMW0421A	106411.06	19294.66	92	619.6	LOW
MMW0421B	106411.06	19295.66	41	670.6	LOW
MMW0422	107002	19354.37	64	638	LOW
MMW1560	111365.14	15129.42	25	691.99	LOW

Table 5-5. Redundant Monitoring Wells Based on Benzene Analysis (All measurements in ft)

WELL_ID	EASTING	NORTHING	DEPTH	SCREEN ELEVATION
BMW715	107439.45	16139.85	45	656.97
BMW717	107613.87	16146.84	37	666.71
JBW7317	112089.57	15002.11	40	688.74
JBW7328	110684.04	14780.69	35	686.78
JBW7338B	110830.36	13610.17	40	681.71
JBW7345A	110554.5	13806.74	93	619.39
JBW7348	110802.02	13966.56	46.6	675.08
JBW7350	111365.86	14160.19	48.225	677.215
JBW7710	109834.07	15664.23	50	657.89
JBW7725	109695.14	17708.18	35	693.48
JBW7737B	107734	17186	38	663.02
JBW7752	108375.42	16683.09	31.75	687.05
JBW7806	107716.95	20532.58	37	679.26
JBW7816	108577.94	20890.92	59	682.08
JMW0201A	108502.6	20874.6	76	664.31
JMW0201C	108503.6	20874.6	41	699.31
JMW0401	108432.9	20095	66	701.77
JMW1564	111324.2	14979.63	34	683.92
JMW1565	111522.3	14964.19	44	678
JMW3202	110684.15	13404.85	46	668.09
JMW7612	106986.73	16453.32	17	656.29
JPZ0342	109510.08	14069.1	38	634.18
JPZ0343	109503.35	14073.53	20	652.04
JPZ0349	108892.85	12200.73	29	637.63
JPZ1586	111185.59	15286.16	27	683.8
MMW0004	108965.36	14148.06	59.2	629.05
MMW0005	110994.15	14918.82	32.65	687.72
MMW0009	107189.78	20000.95	44	658.77
USMW025	109706	17772	35	692.05

Section 5.3 Recommendations Regarding Siting of New Wells

While the primary motivation for the spatial analysis at Site OU-12 was to identify potentially redundant wells, a secondary goal was to locate areas of the site where additional wells might provide significant improvements in accuracy of the estimated site maps and thus improved information on the nature and extent of the groundwater plume(s). In GTS, the most straightforward way to do this is to examine the local variance *base maps* for each time slice and COC. There the local variances offer an indication of the relative *local uncertainty* associated with the mapped grid estimates. The higher the local uncertainty at a particular spot, the greater the benefit to siting a new well in that location.

It should be noted that high local uncertainty arises from two basic sources using the LWQR estimation technique. First, there may be areas of data sparsity, such as the locations northwest of the Central NDA area. Estimates in these spots tend to be uncertain because few wells are sited there. Secondly, there may be areas of data inconsistency, where nearby wells exhibit strongly different concentration levels. This second phenomenon occurs when wells with very low concentrations are located near wells with much higher measurements. High local uncertainty at grid nodes in these areas is then a result of the inconsistency of the known data located within the search

neighborhood. In such cases, it may not be advantageous to site a new well nearby to several existing well locations, especially since the inconsistency might be due to the complex pattern of groundwater flow through the subsurface.

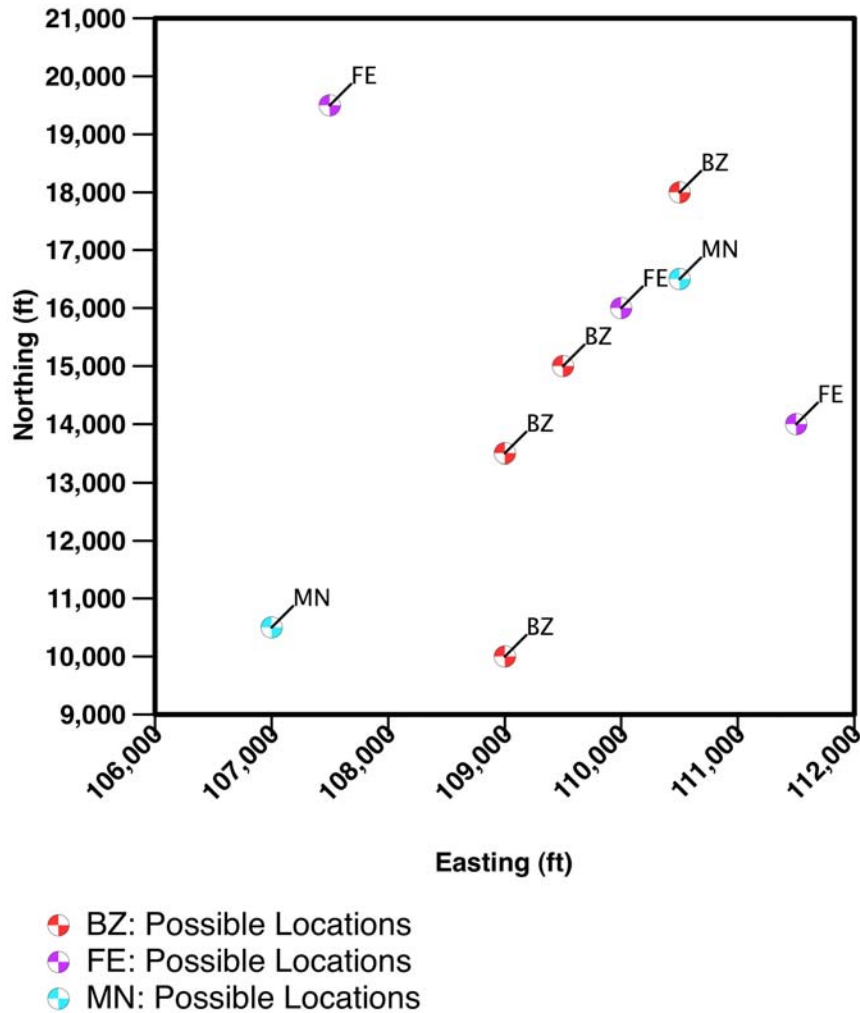
The approximate locations exhibiting the greatest local uncertainty are listed below in **Table 5-6** and graphed in **Figure 5-1**. Any of these spots might serve as locations for the siting of additional wells, but particularly those locations where nearby wells are sparse. Please note, however, that since the determination of local variance depends *both* upon the spatial configuration of the well network *and* the actual concentration values at those locations, it cannot be determined *a priori* exactly which additional sites would provide the greatest informational benefit, nor to what degree the accuracy would be improved. In addition, **Table 5-6** and **Figure 5-1** take no account of physical obstacles at the site (e.g., buildings) that might preclude siting of wells in the listed locations.

It should also be noted that the locations in **Table 5-6** are not ranked in any particular order. Operationally, more weight could be given to those four locations found to exhibit high local uncertainty when using the more recent data of time slice two (2001-2002). At this point, though, there is no reliable way within the GTS algorithm to reliably rank or distinguish between locations of uncertainty found from the benzene analysis versus the iron analysis or the manganese analysis. Furthermore, high local uncertainty, for instance in benzene, does not mean there is high local uncertainty for other COCs not included in the optimization at those locations. However, given the fact that COCs are chosen for optimization in part because they exhibit more frequent and widespread spatial occurrence than other available chemical parameters, it is not unreasonable to assume that these same locations would be good candidates for sampling of other pertinent COCs.

Table 5-6. Approximate Well Locations of Greatest Local Relative Uncertainty

COC	Time Slice	Easting (ft)	Northing (ft)
BZ	1999-2000	109,000	10,000
		109,500	15,000
	2001-2002	110,500	18,000
		109,000	13,500
FE	1999-2000	107,500	19,500
		110,000	16,000
	2001-2002	111,500	14,000
		107,000	11,000
MN	1999-2000	110,500	16,500
	2001-2002	107,000	10,500

Figure 5-1. Approximate Locations of Greatest Local Uncertainty



Section 5.4. Cost Analysis and Costing Methodology

This section describes the methodology for developing credible estimates of annualized cost savings that might result from the implementation of a GTS-optimized monitoring program. The approach is based on a simple cost model. To calculate a cost savings, two cost estimates are required for comparison. The first is the baseline (current) costs, including fixed and variable costs; the second is the projected cost under the optimized program. Cost savings are estimated based on the difference between baseline monitoring costs and project costs under the optimized program, expressed in terms of current dollars and percent reduction from baseline. Initial baseline cost estimates required first developing per sample cost estimates for each contaminant of concern (COC) being sampled, and then estimating the frequency that each COC is sampled for at each well.

Section 5.4.1. Initial Monitoring and Cost Information

The Loring AFB optimization study focused on 115 wells that monitor OU-12. Monitoring data from 2000 to 2003 shows that of the 115 wells only 113 wells are currently being monitored. The estimated monitoring cost for these 113 wells serves as the baseline by which to measure cost savings. The monitoring data identifies which COCs are monitored at each of the 113 wells. There are 112 wells monitored for Volatile Organic Compounds (VOCs), while 93 are monitored for various metals.

The initial (raw) annual costs for the groundwater monitoring programs at Loring AFB were obtained from MWH Americas, Incorporated, an Air Force contractor supporting LTM at the site. The cost information reflected the costs for monitoring at only 106 wells and does not list which specific COCs are monitored at each well. Instead, the cost information provides a count of how many of the 106 wells are monitored for each COC.

The cost information also provides estimates for sampling labor costs, sample cooler shipping charges, as well as the rental and purchase costs of material and equipment. These costs, however, were provided to SAIC on an annual basis rather than per COC sampled basis. **Table 5-7.A1** in **Appendix 5-1** shows the initial sample analysis cost information received from MWH Americas. The cost information also provides estimates of monitoring project costs that are not directly connected with the field sampling and analysis, such as: chemistry data management; monitoring reports and meetings; the updating and revision of documents; and overall project management and administration. These initial cost estimates are found in **Table 5-7.B1** in **Appendix 5-1**.

Section 5.4.2. Creating the Baseline

An estimate of current monitoring costs was needed to serve as a baseline for the purpose of estimating cost savings that might be realized under each optimized plan. The current monitoring costs provided by MWH did not address all of the wells used in the optimization study so adjustments were made to extrapolate the cost data to the number of wells included in the study. In addition, the cost data did not specify which COCs were monitored for at each well. To use the MWH Americas cost information for a baseline it had to be adjusted to match the optimization study data. The cost information showed that there are 12 COCs currently being monitored for at the site, of which one is VOCs and three are metals. As mentioned, the optimization study data lists for each well

if it is monitored for VOCs or metals. However, there were eight COCs listed in the cost information that were not included in the optimization study data. The assumption was made for each of these eight COCs that the ratio of wells monitored for each COC to the total number of wells monitored would remain constant.

In the baseline cost estimate, the costs associated with sample analysis also needs to account for any quality assurance samples taken. To estimate the cost of quality assurance samples taken during future monitoring efforts, the number of quality assurance samples needed to be expressed as a ratio of normal samples taken. Based on the MWH Americas cost information there is one quality assurance sample taken for every six normal samples taken for each COC. **Table 5-7.A2** in **Appendix 5-1** shows the resulting baseline sample analysis cost table.

Section 5.4.3. Scenario Cost Estimates

The optimization study identified specific wells that can be excluded from future monitoring efforts. The study results produced two lists of essential wells. The first list is based on optimizing the monitoring program for the VOC benzene. Under this scenario, 28 of the currently baseline wells were considered redundant. The second scenario optimizes for all three COCs. The resulting scenario calls for the elimination of 16 currently-monitored wells. The first step in estimating cost savings was to reduce the total COC samples taken as a result of the elimination of these specific wells. The second step was to account for any changes in sampling frequency. MWH Americas cost information shows that each well is monitored three times a year. The optimization results suggested monitoring could be reduced to only twice per year. Therefore, for each of the two optimization scenarios the projected number of samples required was adjusted to reflect the reduction in sampling frequency.

Table 5-7.A3 in **Appendix 5-1** shows the reduction in annual samples taken and the resulting sampling cost estimates for the optimization based on benzene. Similarly, **Table 5-7.A4** in **Appendix 5-1** shows annual samples taken and sampling cost estimates for the optimization based on all three COCs. These two tables also show reductions in associated labor, equipment, and shipping costs. Because initial baseline costs for labor, equipment, and shipping were not expressed on a per-sample or per-well basis, assumptions had to be made regarding how much these costs would change under each optimization scenario.

It was assumed that the costs for labor are directly associated with the number of samples taken. Therefore, these costs were reduced proportionally to the total reduction in the number of samples taken annually.

Costs for equipment rental and purchase were considered less sensitive to the number of samples taken, whereas the cost of sample vials will vary proportionately to samples taken. Therefore, the initial baseline equipment and materials cost of \$9,200 was divided into a fixed and a variable cost. One half (\$4,600) is considered a fixed cost that does not vary. The other half of the baseline cost was divided by the total number of baseline samples to derive a per-sample cost (\$1.49). The per-sample cost is then multiplied by the

total samples under each scenario, to derive the variable portion of the equipment and materials cost.

Sample cooler shipping charges were varied by the number of wells monitored rather than with the number of samples taken. The reason is that shipping is typically done at the end of each day after all wells have been sampled for that day. The number of samples in each shipment will vary depending on the number of wells are sampled. Yet the daily number of wells sampled and resulting shipping costs will be relatively the same.

In **Appendix 5-1, Tables 5-7.B2b, 5-7.B3b and 5-7.B4b** show the monitoring project costs not directly related to the collection and laboratory analysis of samples. These costs include costs for chemistry data management, reports and meetings, updates and revisions to documents, professional site visits and QA/QC audits, and project management and administration. Most of these costs are assumed to be less sensitive to the number of samples taken. Chemistry data management cost is the one exception, as it is assumed to vary proportionally to the number of samples taken annually. Monitoring reports and meetings are considered to have both fixed and variable components. So it was assumed that 70% of the initial baseline costs for reports and meetings was fixed, while the other 30% varied directly with the total number of samples taken. The updating and revision of documents was considered a fixed cost regardless of changes to the number of annual samples. Finally, overall project management and administration costs were assumed to be half fixed and half variable, like the equipment and materials costs.

Section 5.4.4. Resulting Costs Savings

Although the measurement data at Site OU-12 are somewhat challenging, the temporal and spatial analyses demonstrate that the GTS optimization algorithm can offer potentially significant cost savings over the existing LTM program. Despite the complexities of the site, reasonably good estimates of plume magnitude and extent can be made using fewer wells than the current network and sampling at a lower frequency than presently in place. Estimates of specific potential cost savings of course depend on how many wells are actually deemed redundant after further review by project managers and regulators, and to what extent sampling frequencies can be reduced to levels recommended in the temporal analysis. Nevertheless, **Table 5-7** below offers two estimates of the savings that might be achieved, based on costs of the current network, and also assuming that one of the two reduced monitoring networks is implemented at OU-12.

The baseline for OU-12 estimates that 3,306 annual samples will be taken from 113 wells annually at a total cost of approximately \$921,000. Under the first optimization scenario 1,690 annual samples would be taken from 85 wells annually for a total cost of approximately \$564,000 (an annual cost savings of 38.8 percent). Under the second optimization scenario an estimated 1,926 annual samples would be taken from 97 wells annually for a total cost of approximately \$616,000 (an annual cost savings of 33.2 percent).

Table 5-7. Estimate of Cost Savings

Loring OU 12 LTM			
	Baseline	Optimization 1 (Benzene)	Optimization 2 (All COCS)
Wells Monitored	113	85	97
Samples Collected Annually	3,306	1,690	1,926
Annual Costs			
Analytical Cost for Annual Sampling	\$177,545	\$90,410	\$102,717
Sampling and Analysis Labor Costs	\$184,787	\$94,443	\$107,660
Sample Shipping Costs	\$16,550	\$8,300	\$9,471
Materials and Equipment Costs	\$9,532	\$7,120	\$7,473
Subtotal Sampling and Analysis Costs	\$388,413	\$200,273	\$227,322
Chemistry Data Management	\$223,851	\$114,408	\$130,420
Reports and Meetings	\$127,090	\$107,529	\$110,391
Update & Revise Documents	\$21,500	\$21,500	\$21,500
Professional Site Visits & QA/QC Audits	\$5,180	\$3,870	\$4,062
Project Management and Administration	\$155,406	\$116,095	\$121,846
Total Annual Project Cost	\$921,442	\$563,674	\$615,541
Potential Cost Savings		\$357,767	\$305,901
Percentage Reduction in Annual Monitoring Costs		38.83%	33.20%

Section 6. References

Bourgault, G. (1997) Spatial declustering weights. *Mathematical Geology*, 29:277-290.

Cameron, K. & Hunter, P. (2002) Using spatial models and kriging techniques to optimize long-term groundwater monitoring networks: a case study. *Environmetrics*, 13:629-656.

EPA (1999) EPA Superfund Record of Decision: Loring Air Force Base OU-12. EPA/ROD/R01-99/118. (www.epa.gov/superfund/sites/rods/fulltext/r0199118.pdf)

EPA (2003) NPL Site Narrative for Loring Air Force Base. (www.epa.gov/superfund/sites/npl/nar38.htm)

Loader, C. (1999) *Local Regression and Likelihood*. New York: Springer-Verlag.

United States Air Force Base Conversion Agency (AFBCA) (2000). First Five-Year Review Report for Loring Air Force Base. (www.epa.gov/region01/superfund/sites/loring/34312.pdf)

Appendix 3-1

Temporal Optimization: Temporal Variograms

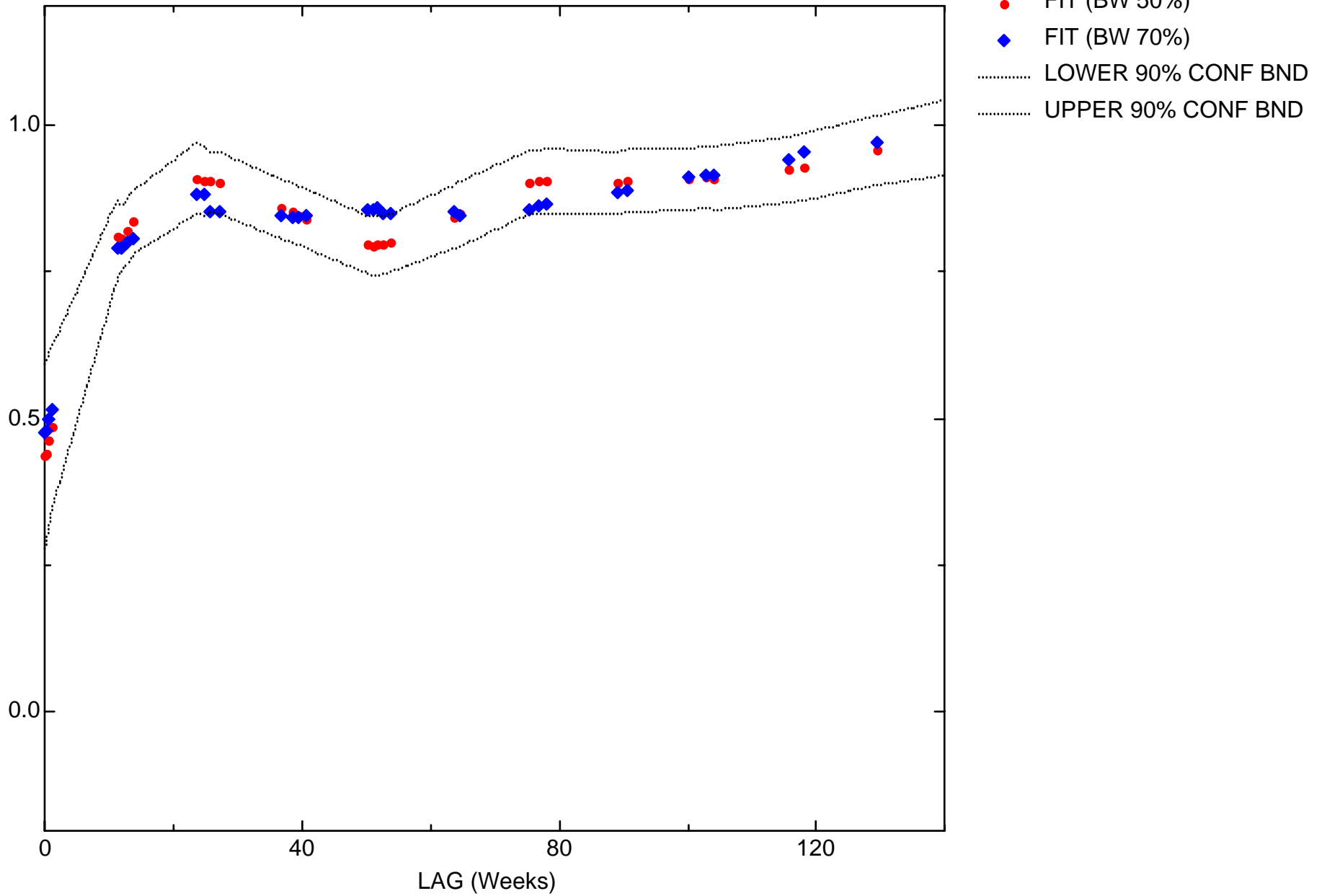
Key to acronyms:

CONF BND = Confidence bound

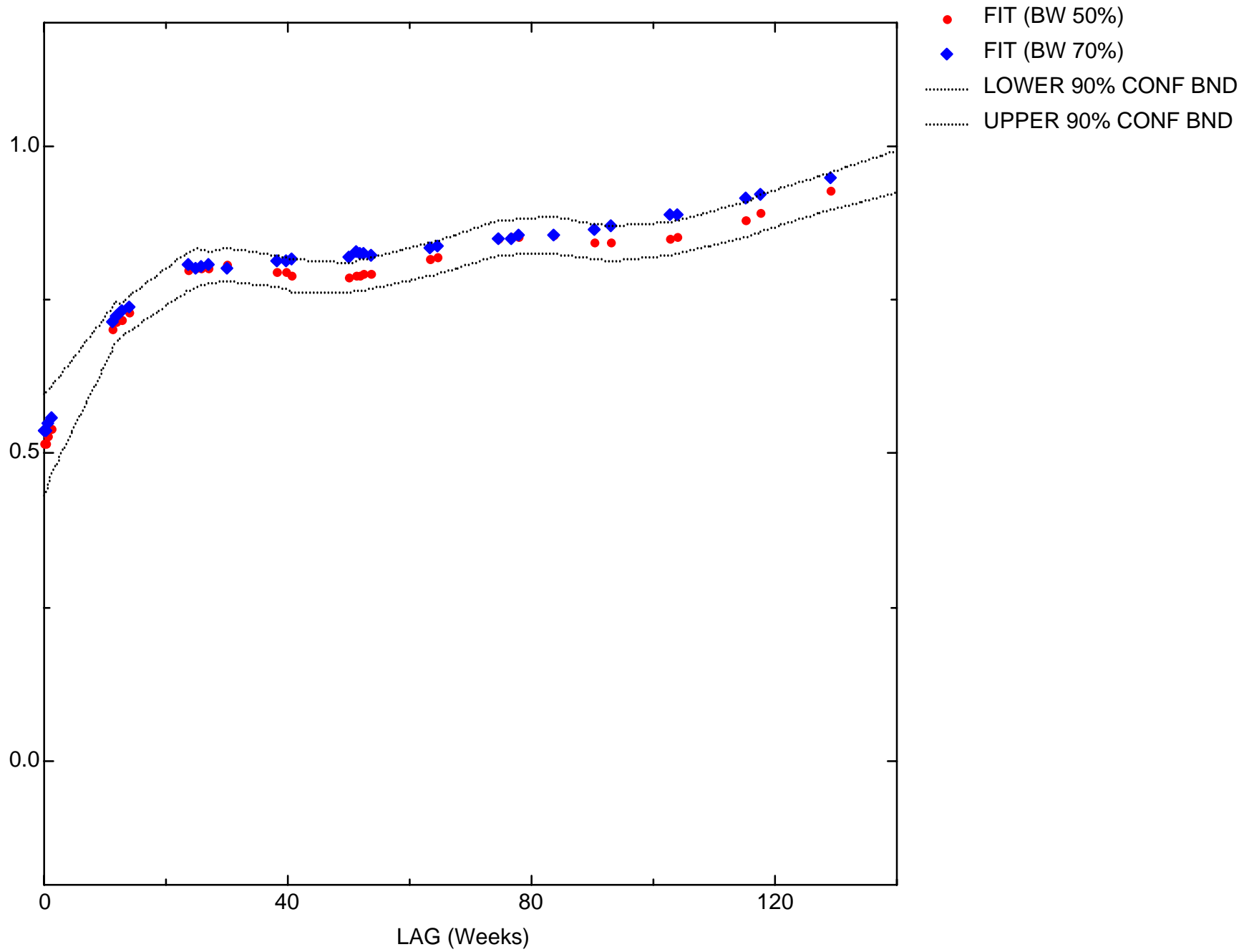
BW = Bandwidth parameter

FIT = Locally-weighted quadratic regression (LWQR) estimate of variogram

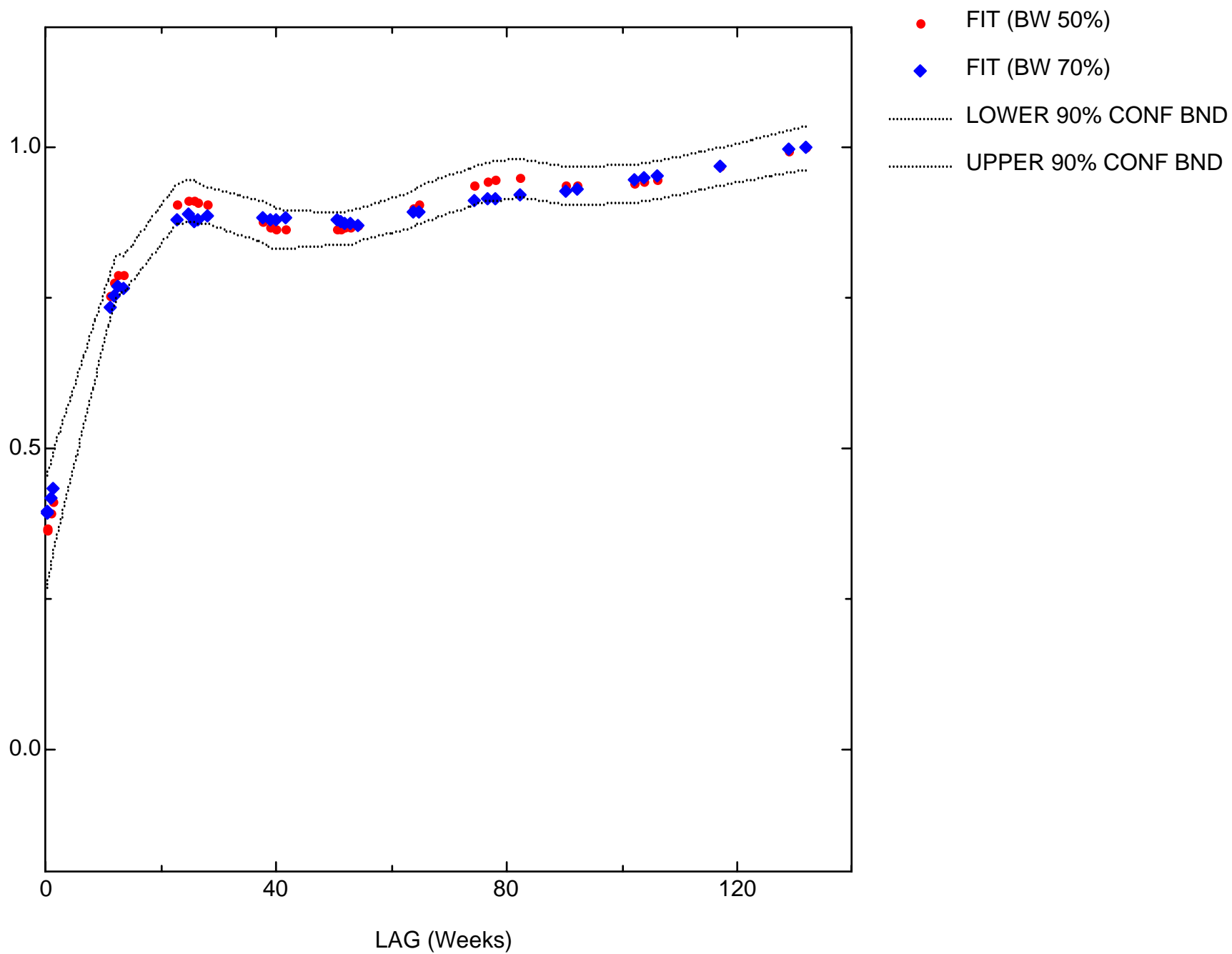
LORING AFB, SITE OU-12: BZ TEMPORAL VARIOGRAM



LORING AFB, SITE OU-12: FE TEMPORAL VARIOGRAM



LORING AFB, SITE OU-12: MN TEMPORAL VARIOGRAM



Appendix 3-2

Temporal Optimization: Benzene Iterative Fitting Overlays

Key to acronyms:

Conf Bnd = Confidence bound

Initial Fit = Locally-weighted quadratic regression (LWQR) estimate on baseline dataset

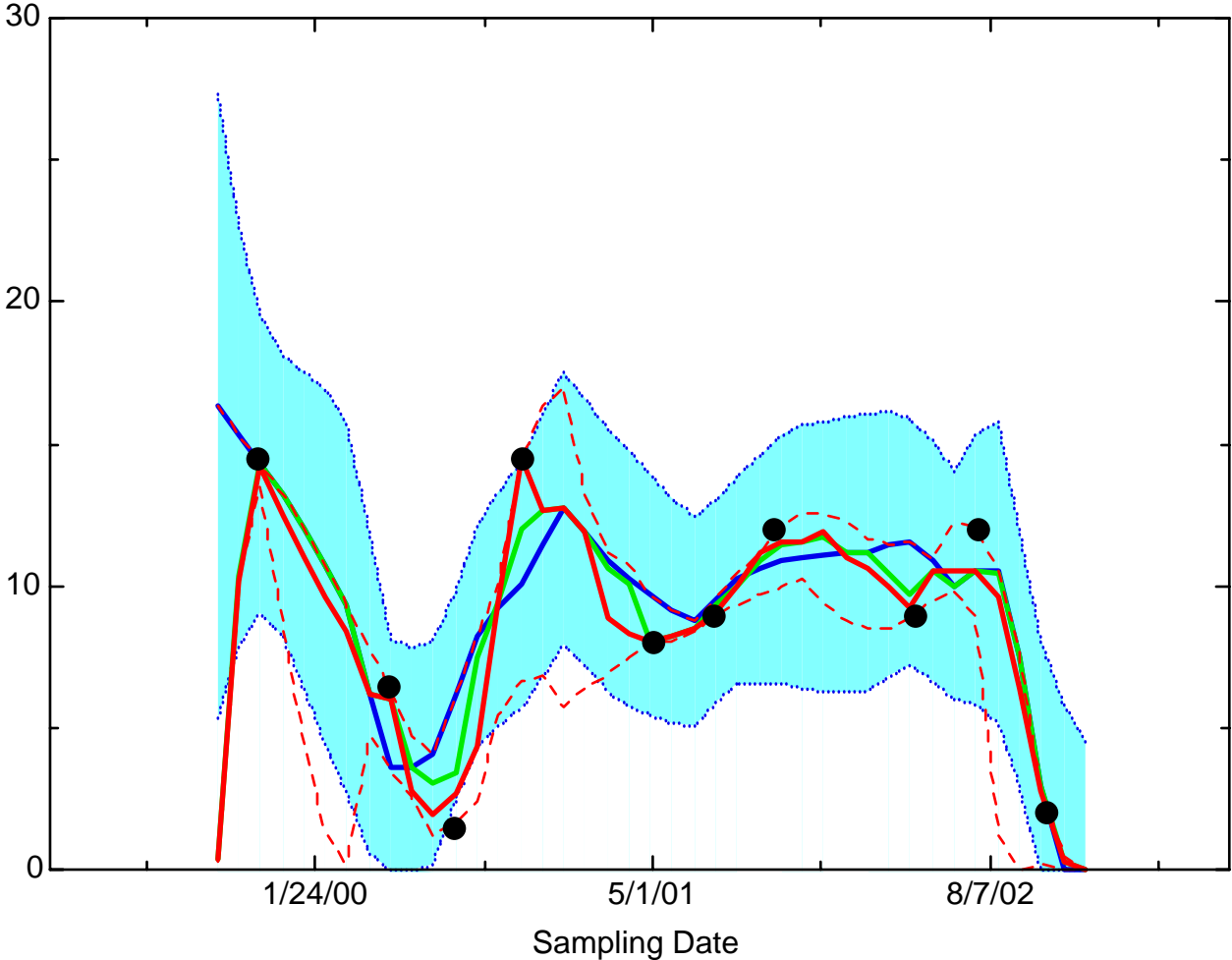
Med Fit = Median of 500 pointwise LWQR estimates on reduced dataset

LQ Fit = Lower quartile of 500 pointwise LWQR estimates on reduced dataset

UQ Fit = Upper quartile of 500 pointwise LWQR estimates on reduced dataset

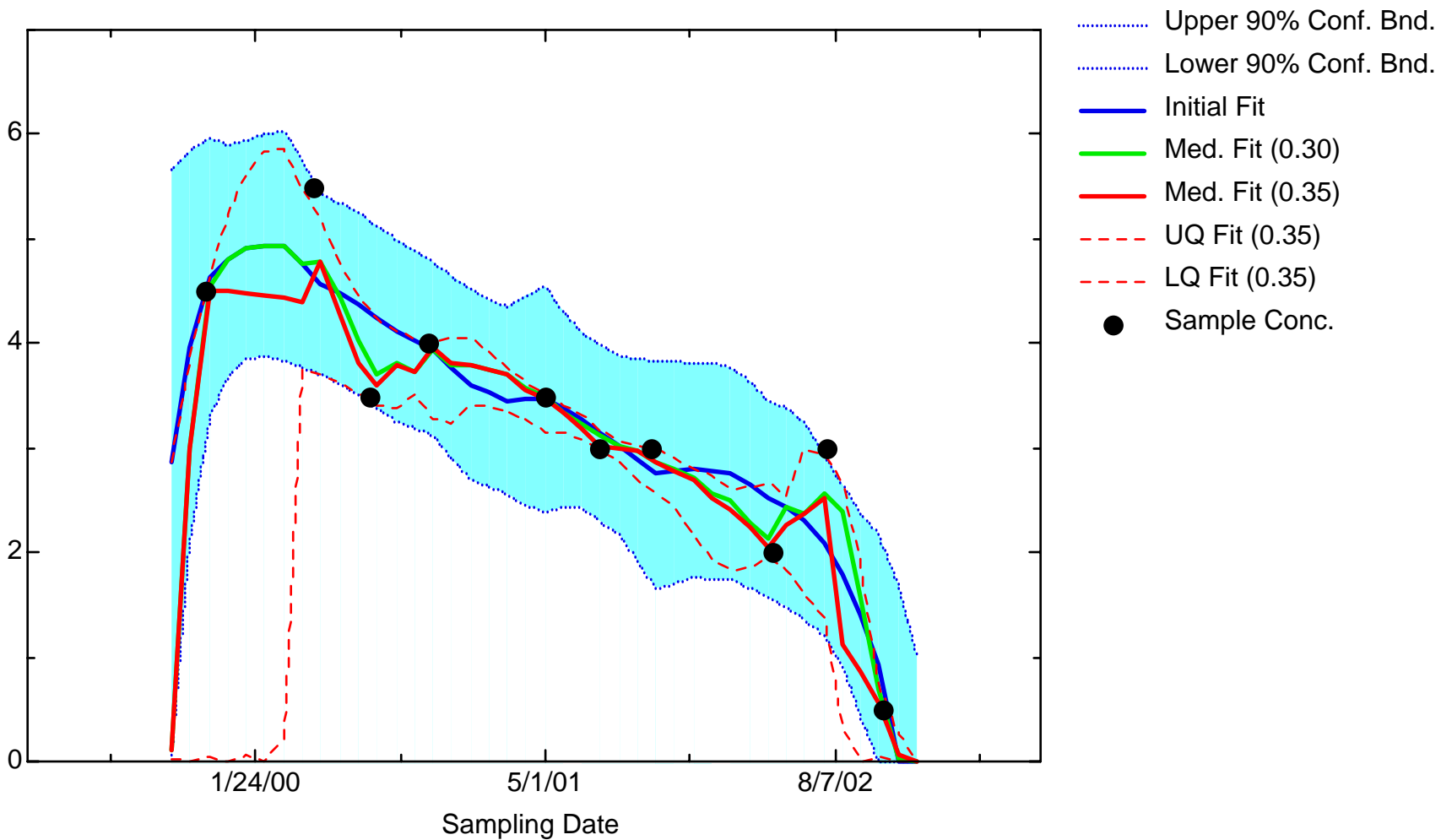
Conc = Concentration

BZ: Well 056MW04

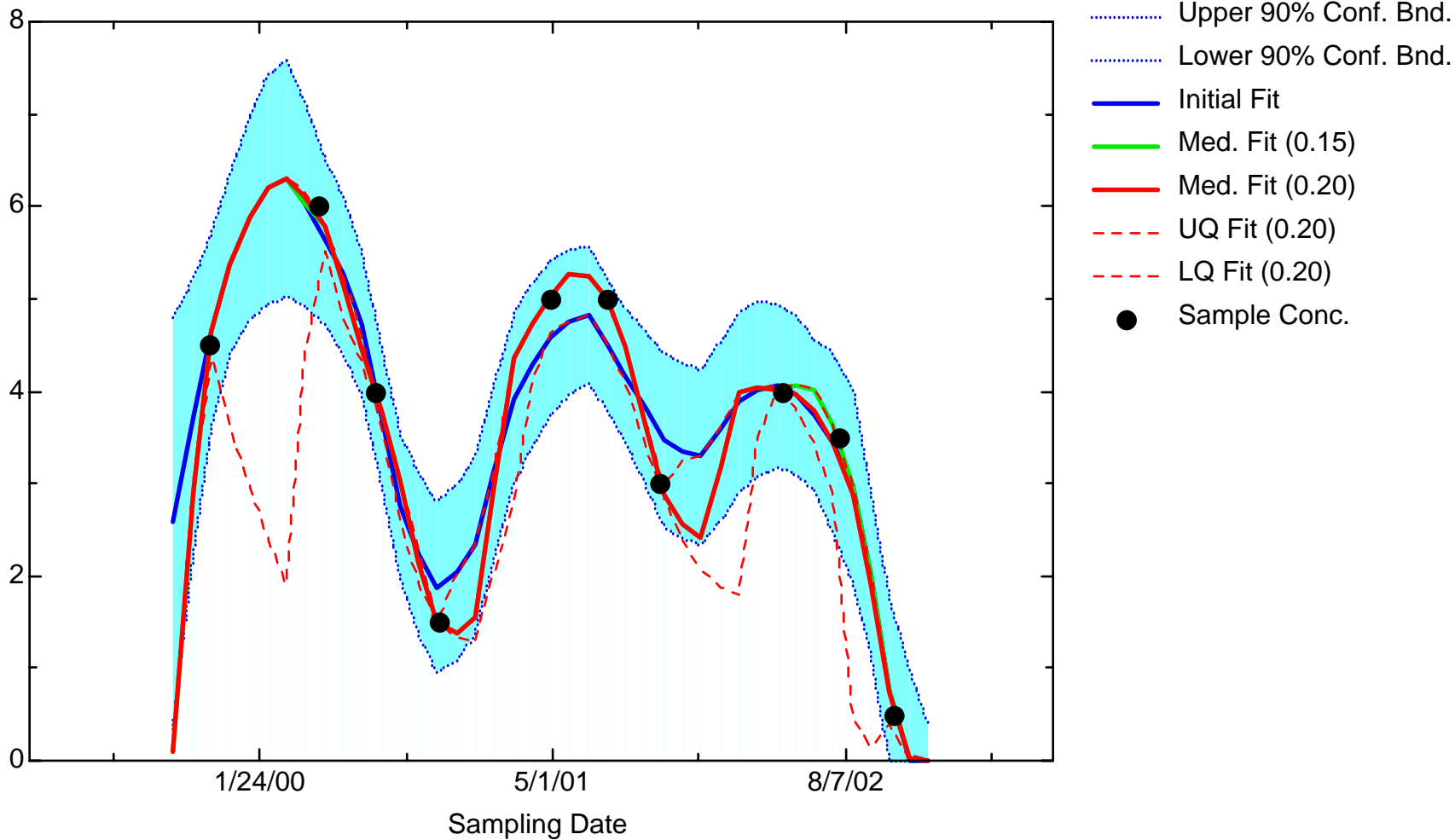


- Upper 90% Conf. Bnd.
- Lower 90% Conf. Bnd.
- Initial Fit
- Med. Fit (0.20)
- Med. Fit (0.25)
- - - UQ Fit (0.25)
- - - LQ Fit (0.25)
- Sample Conc.

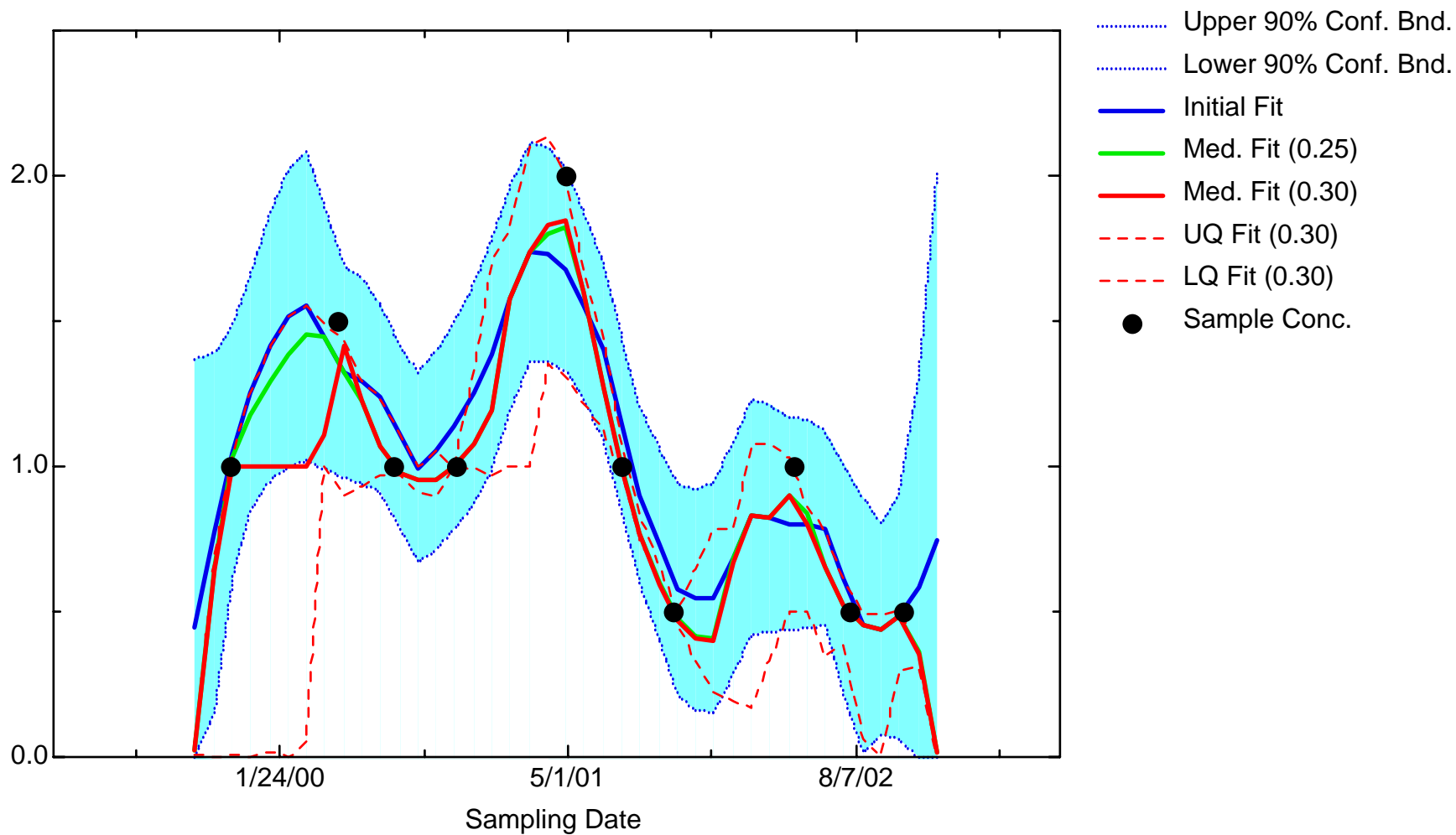
BZ: Well JBW7212B



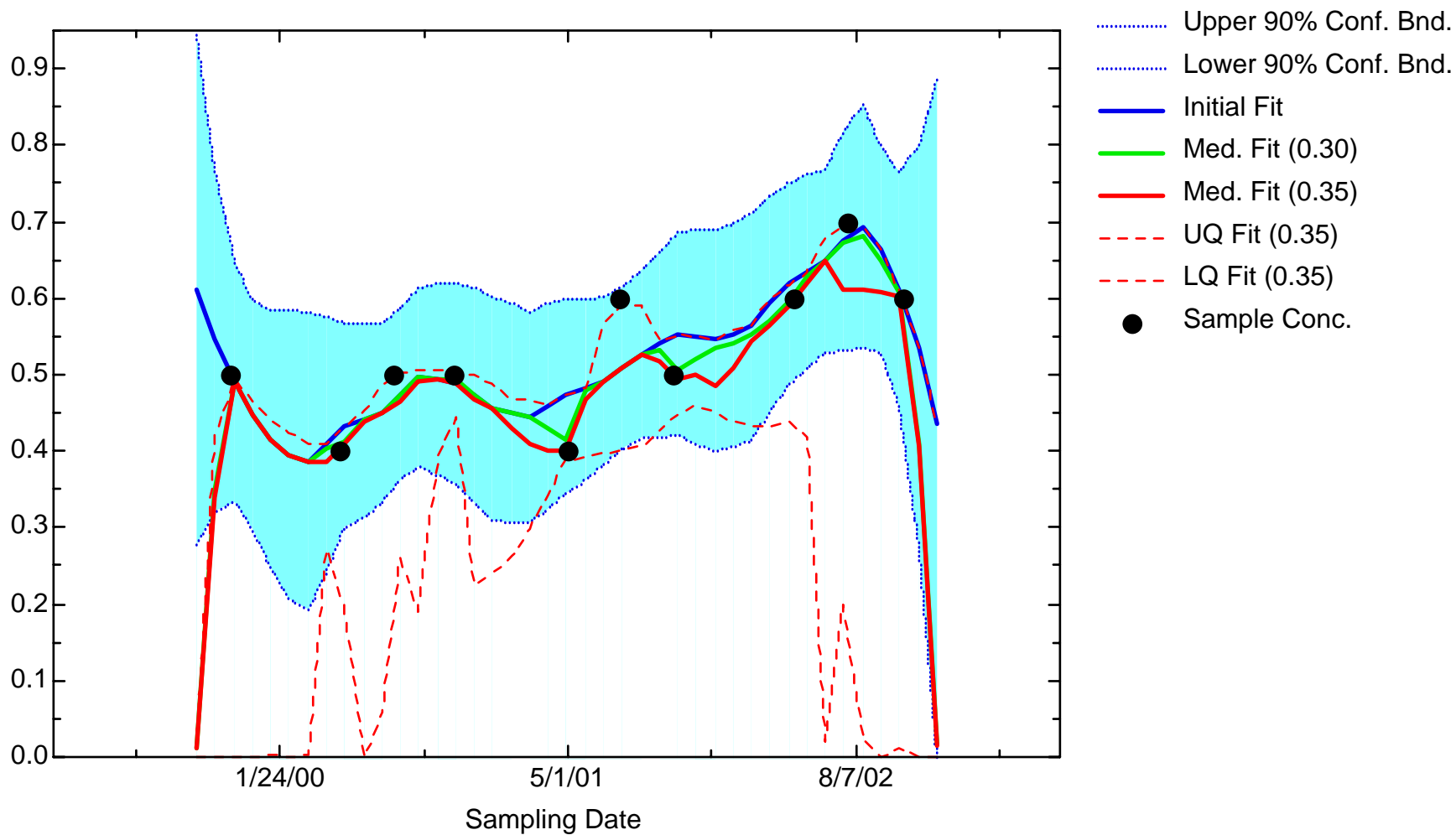
BZ: Well JBW7213A



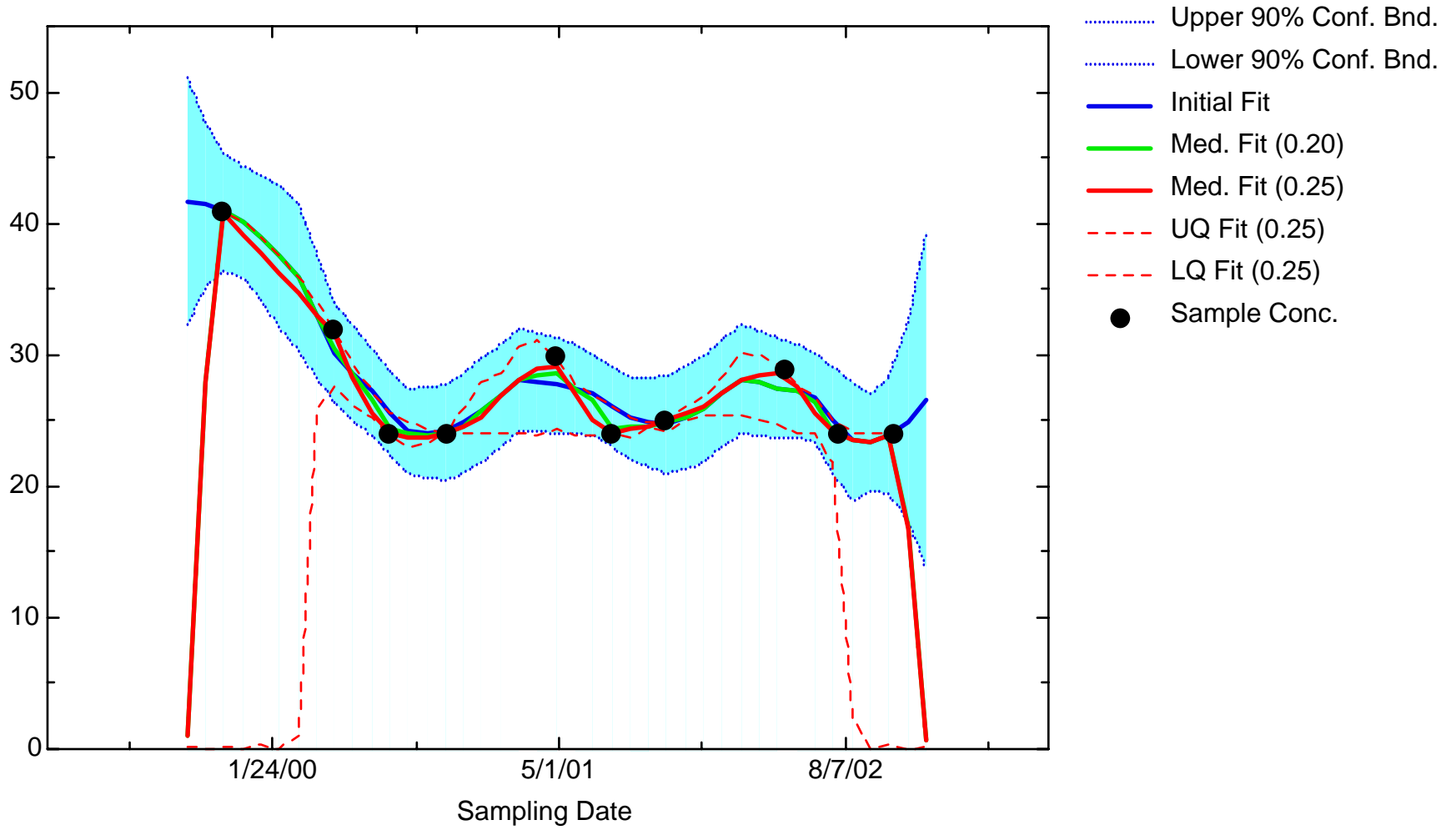
BZ: Well JBW7213B



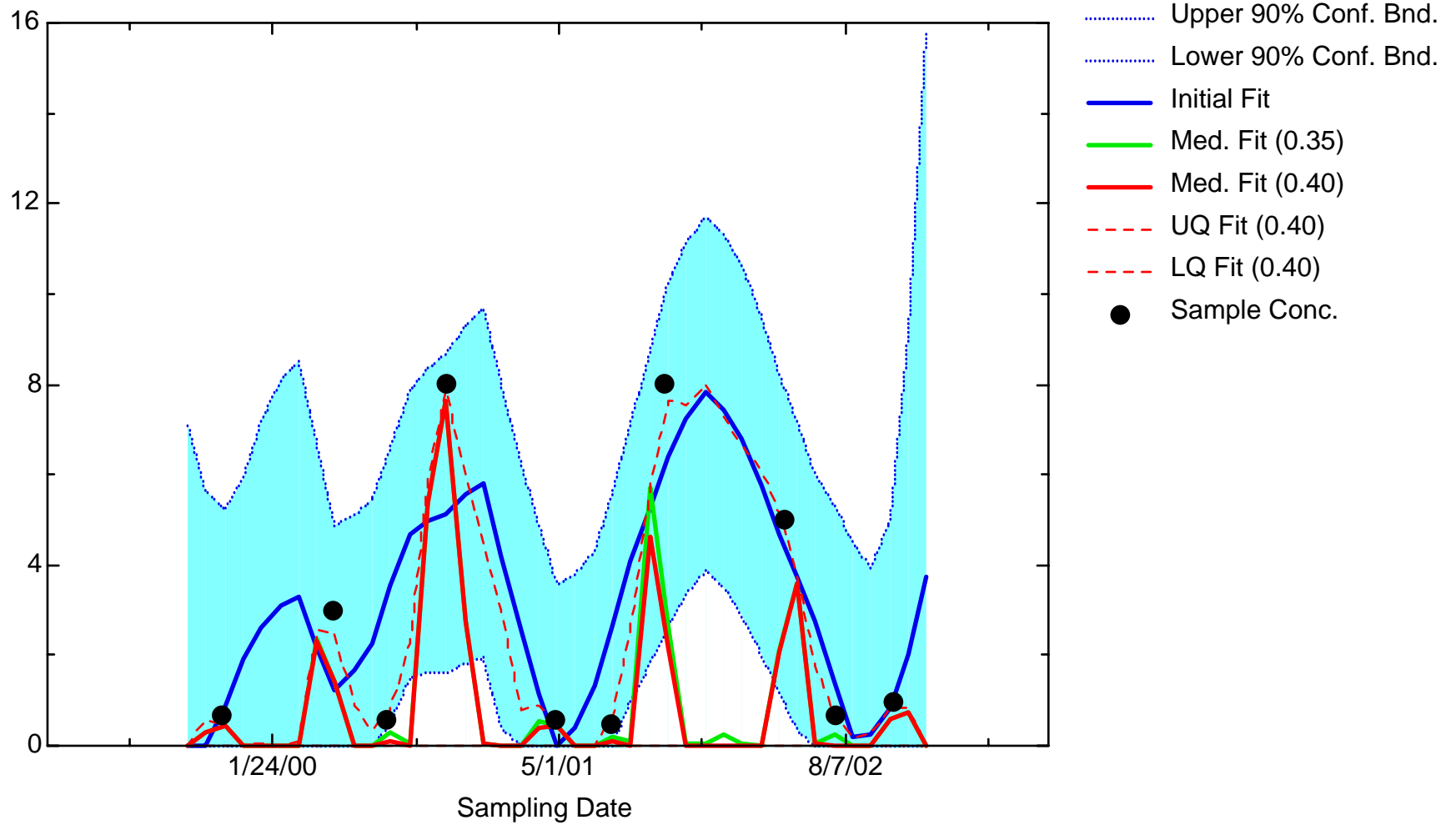
BZ: Well JBW7330A



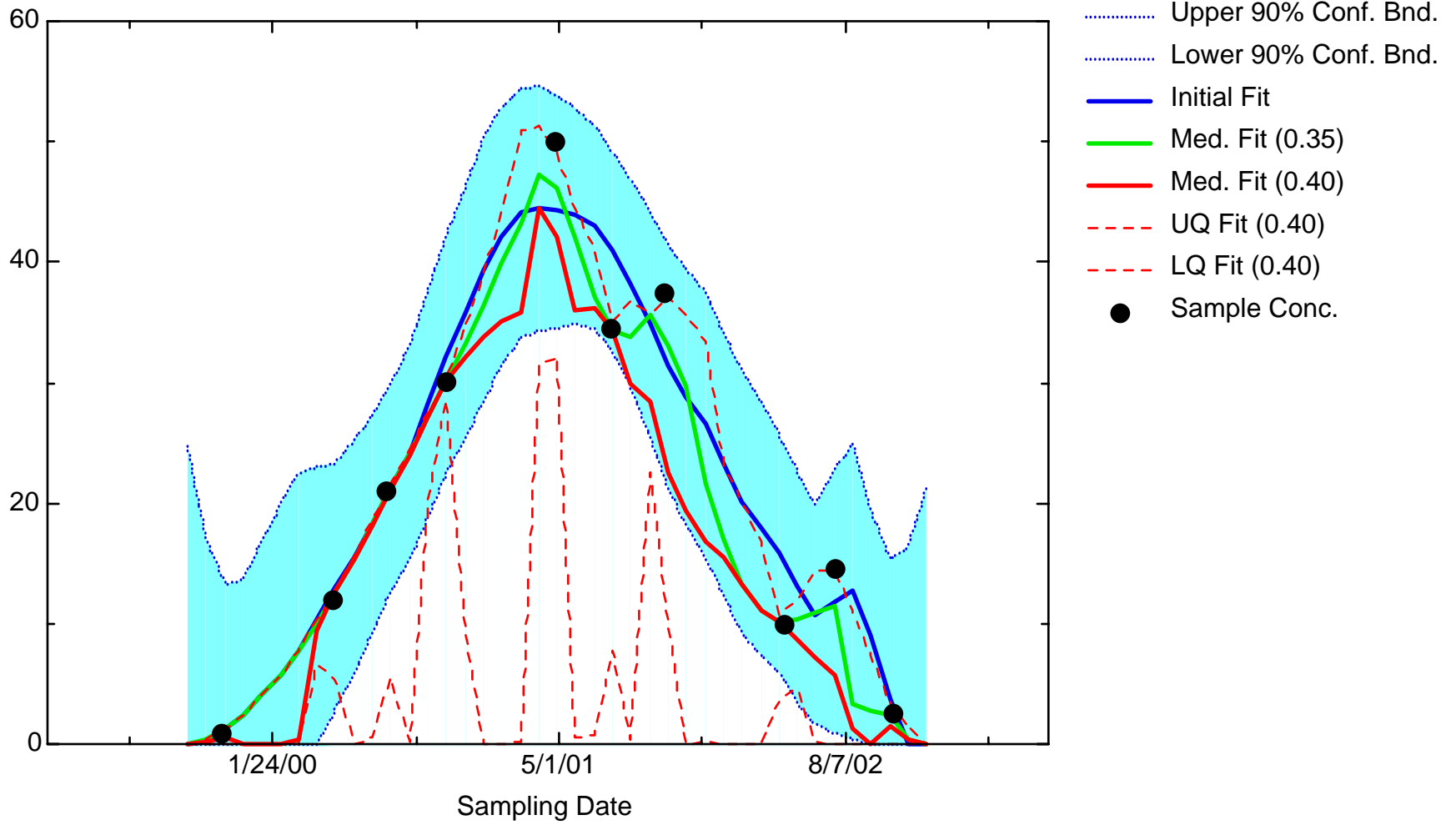
BZ: Well JBW7333



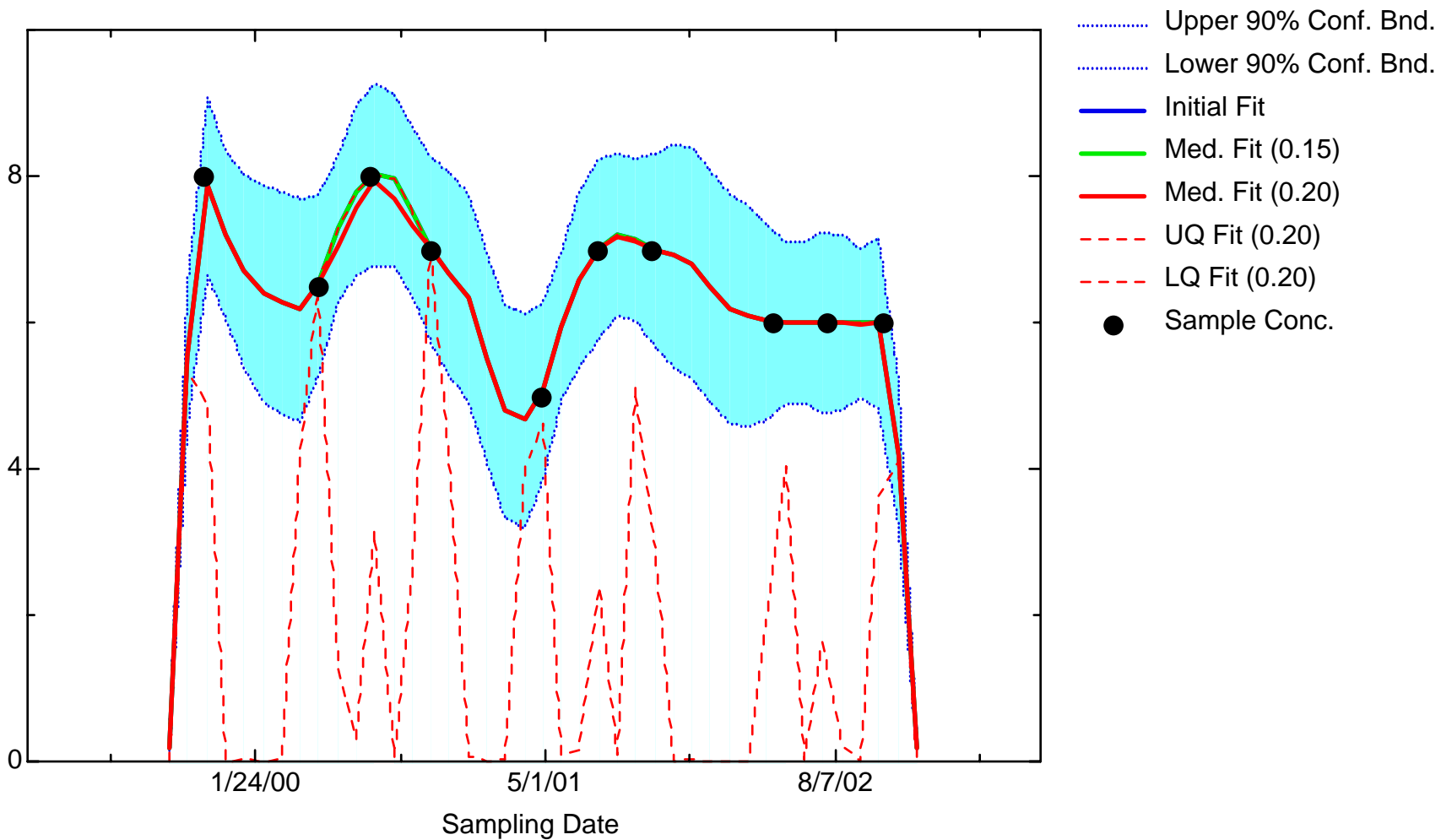
BZ: Well JBW7338A



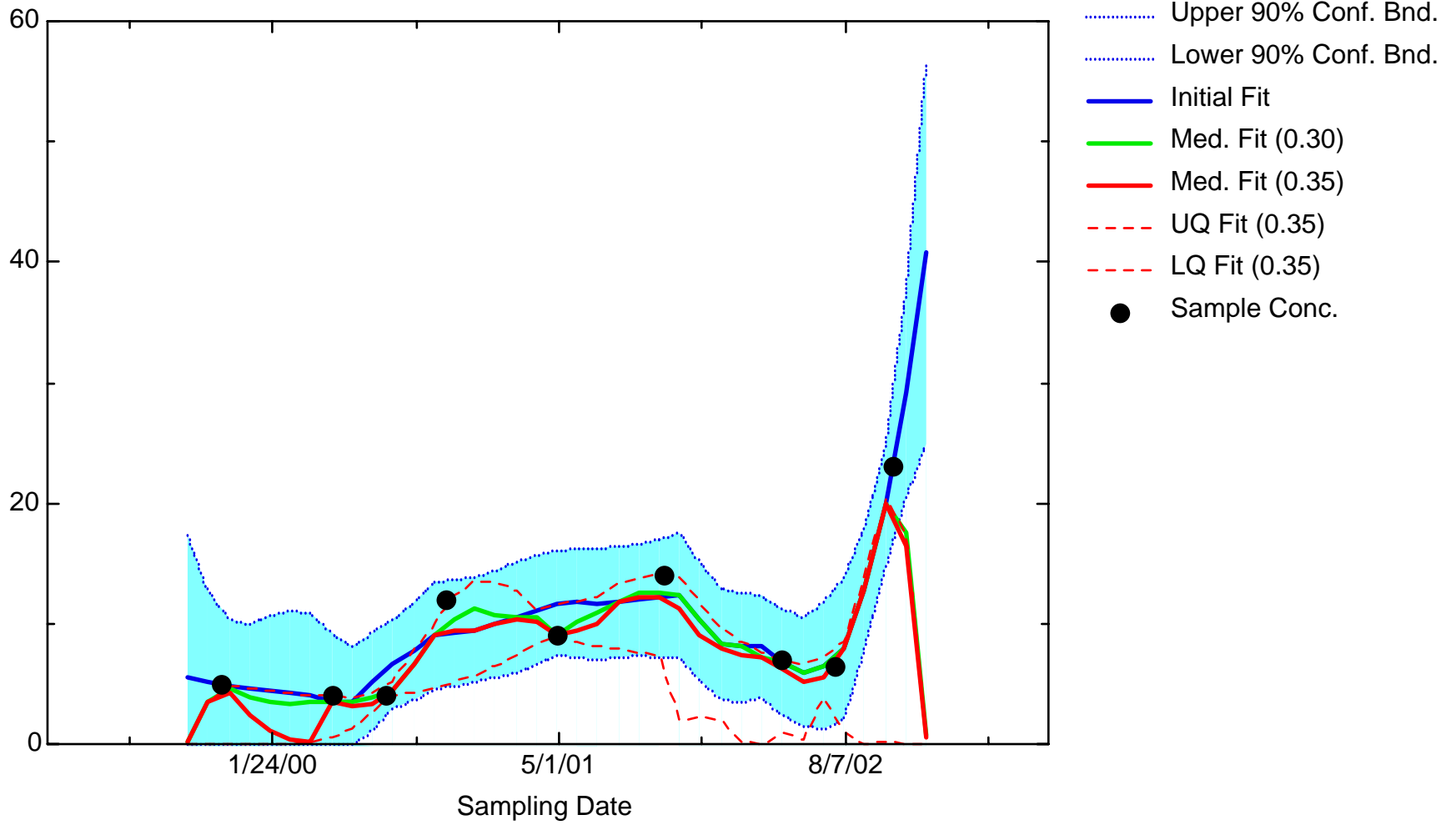
BZ: Well JBW7338B



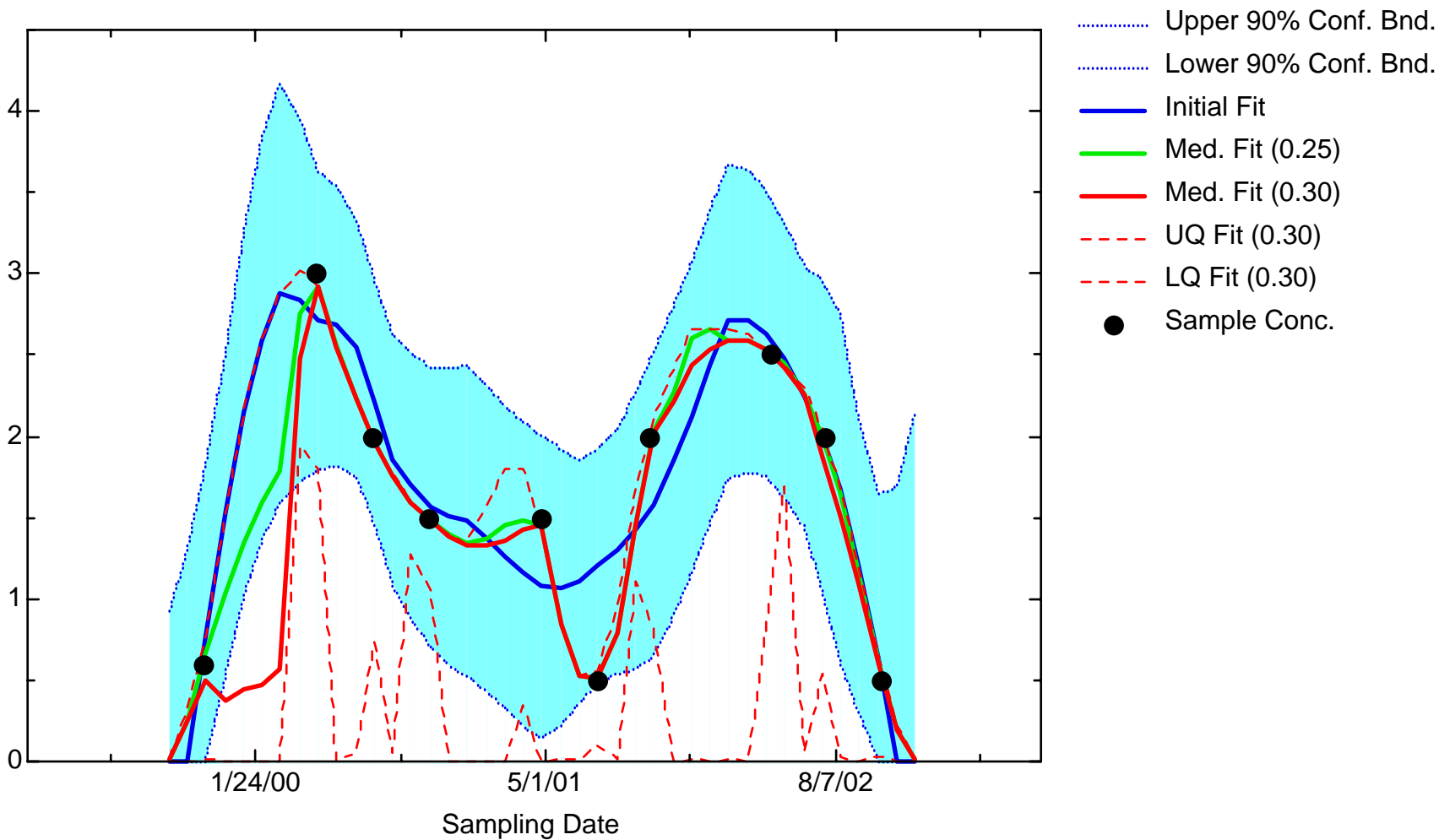
BZ: Well JBW7340B



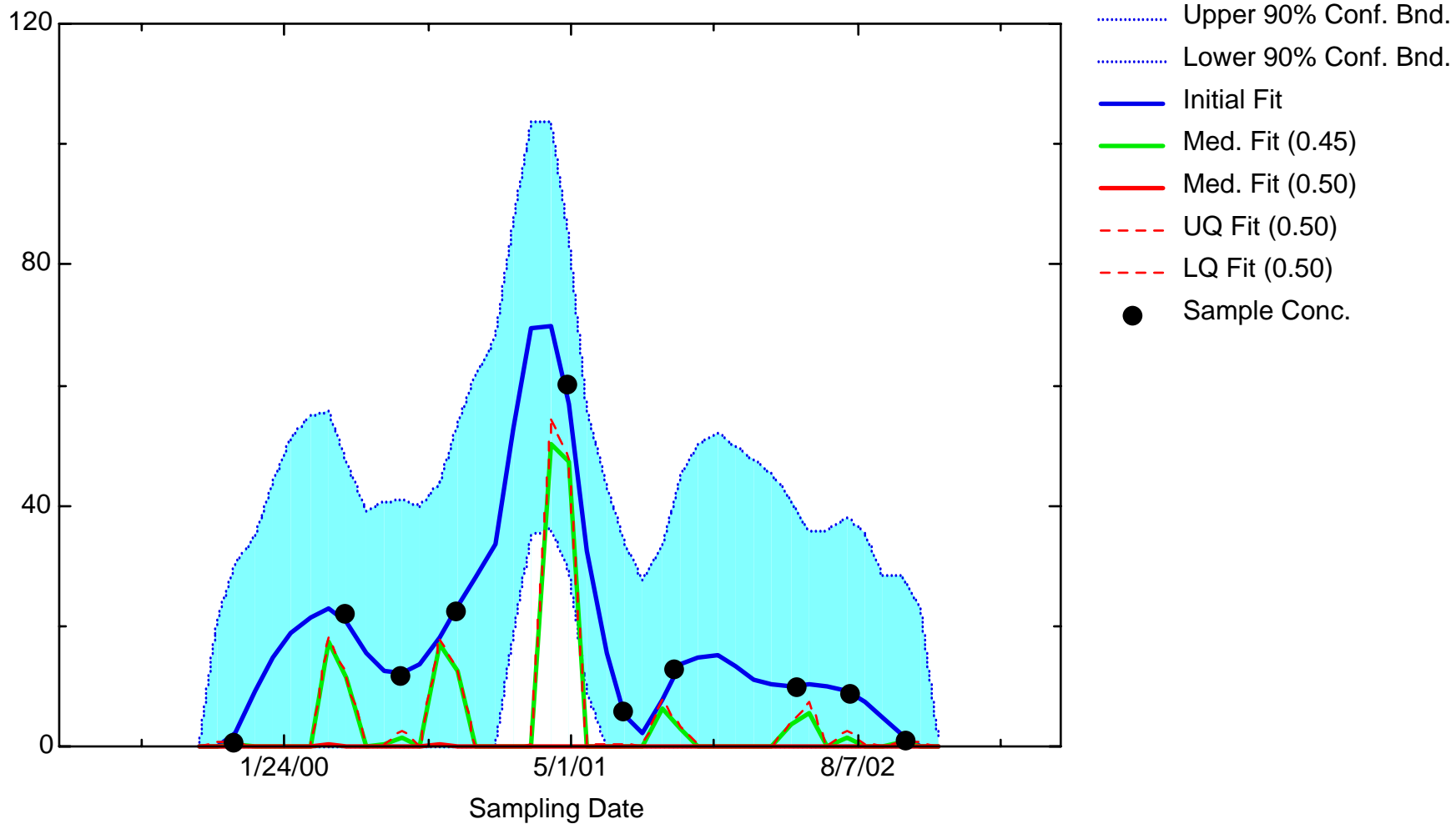
BZ: Well JBW7344



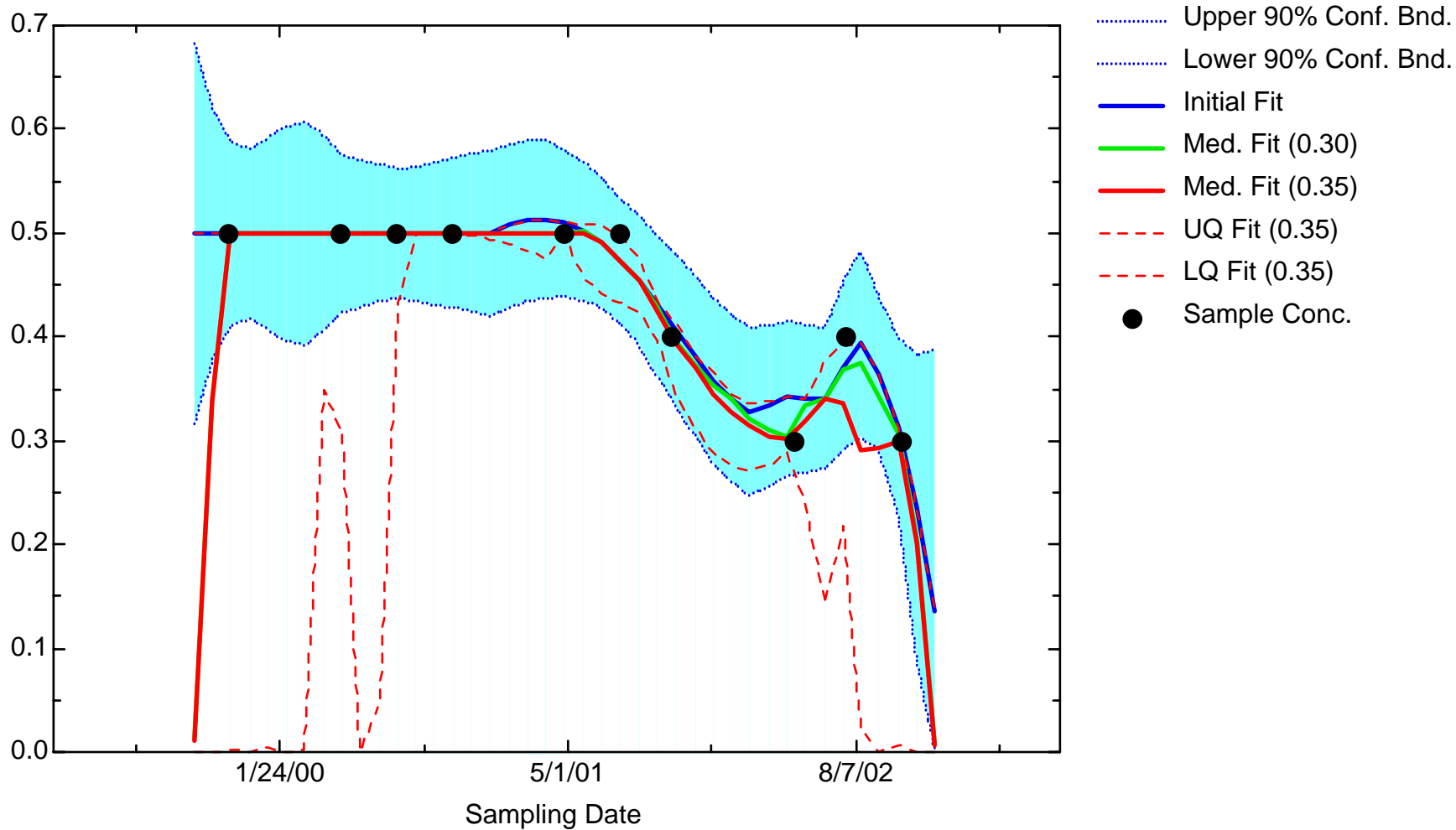
BZ: Well JBW7345A



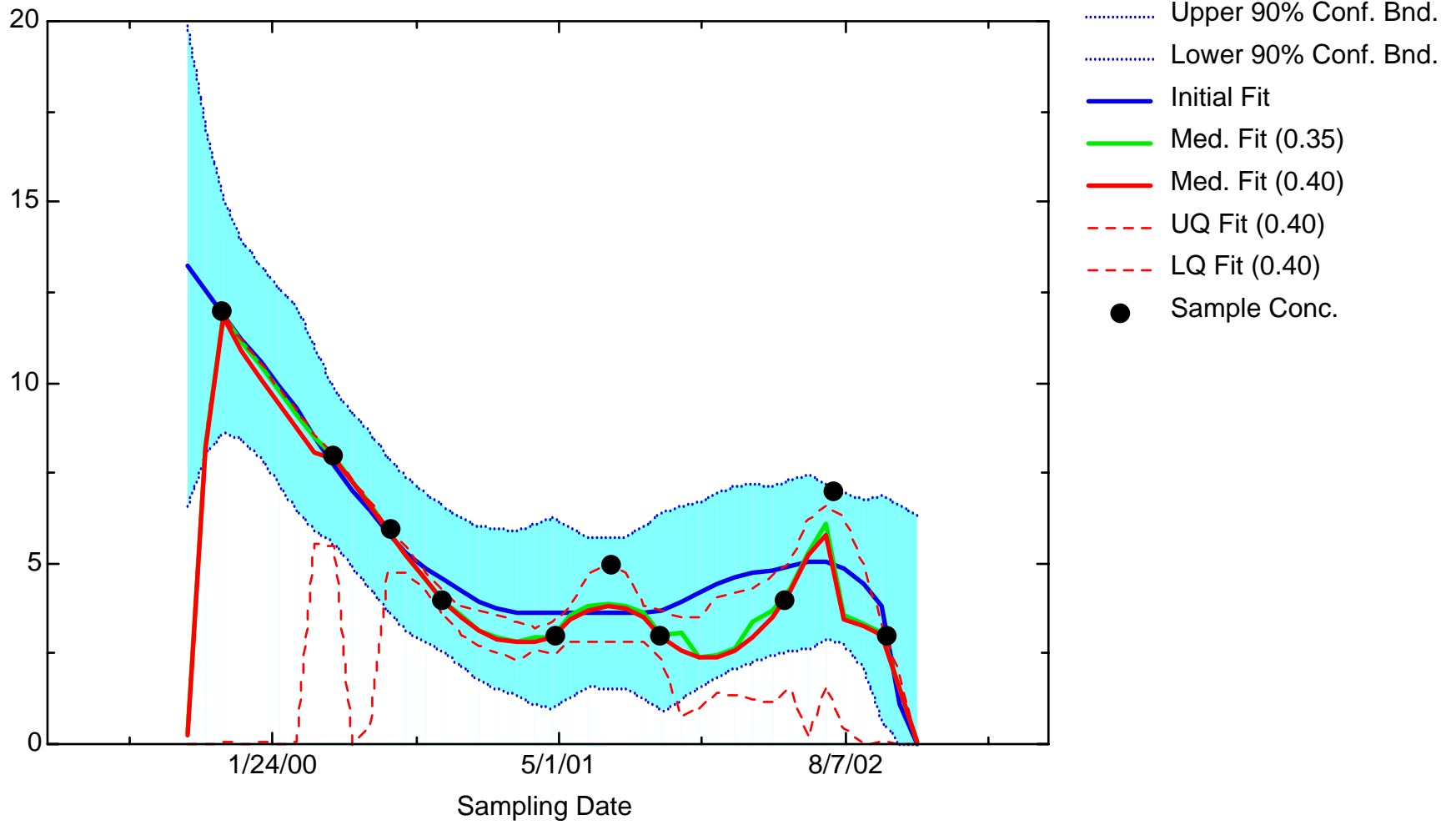
BZ: Well JBW7348



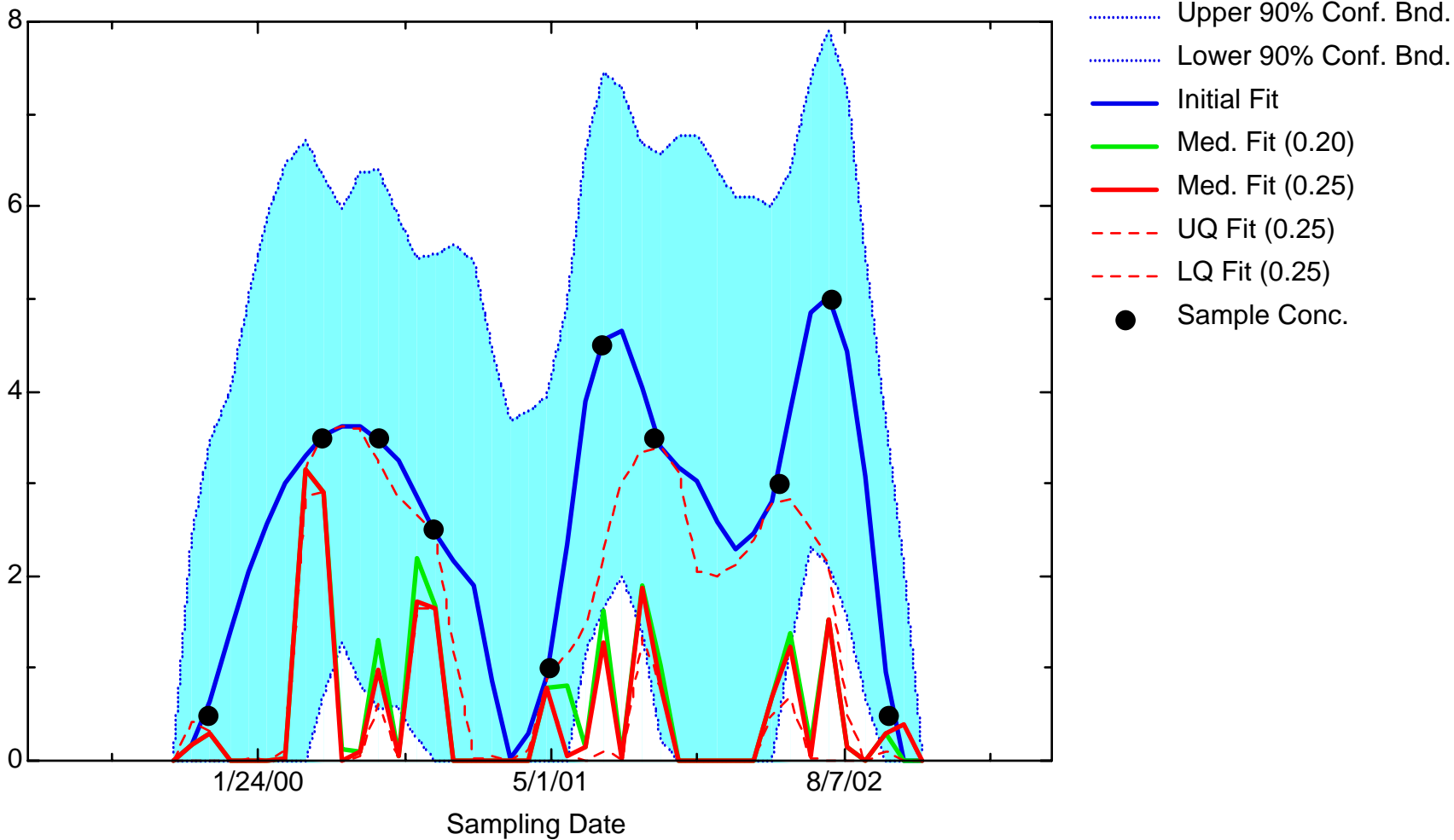
BZ: Well JBW7350



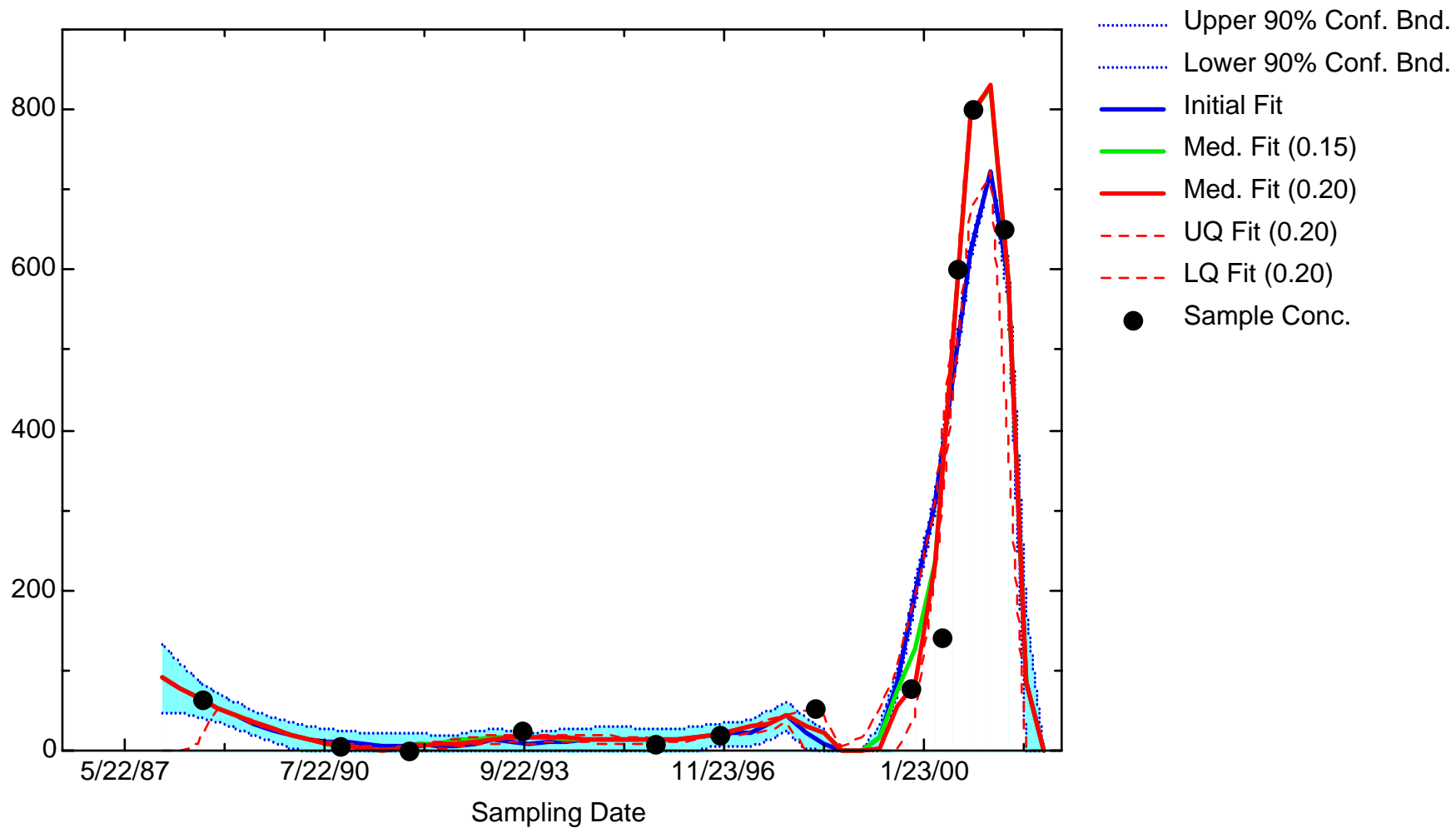
BZ: Well JBW7710



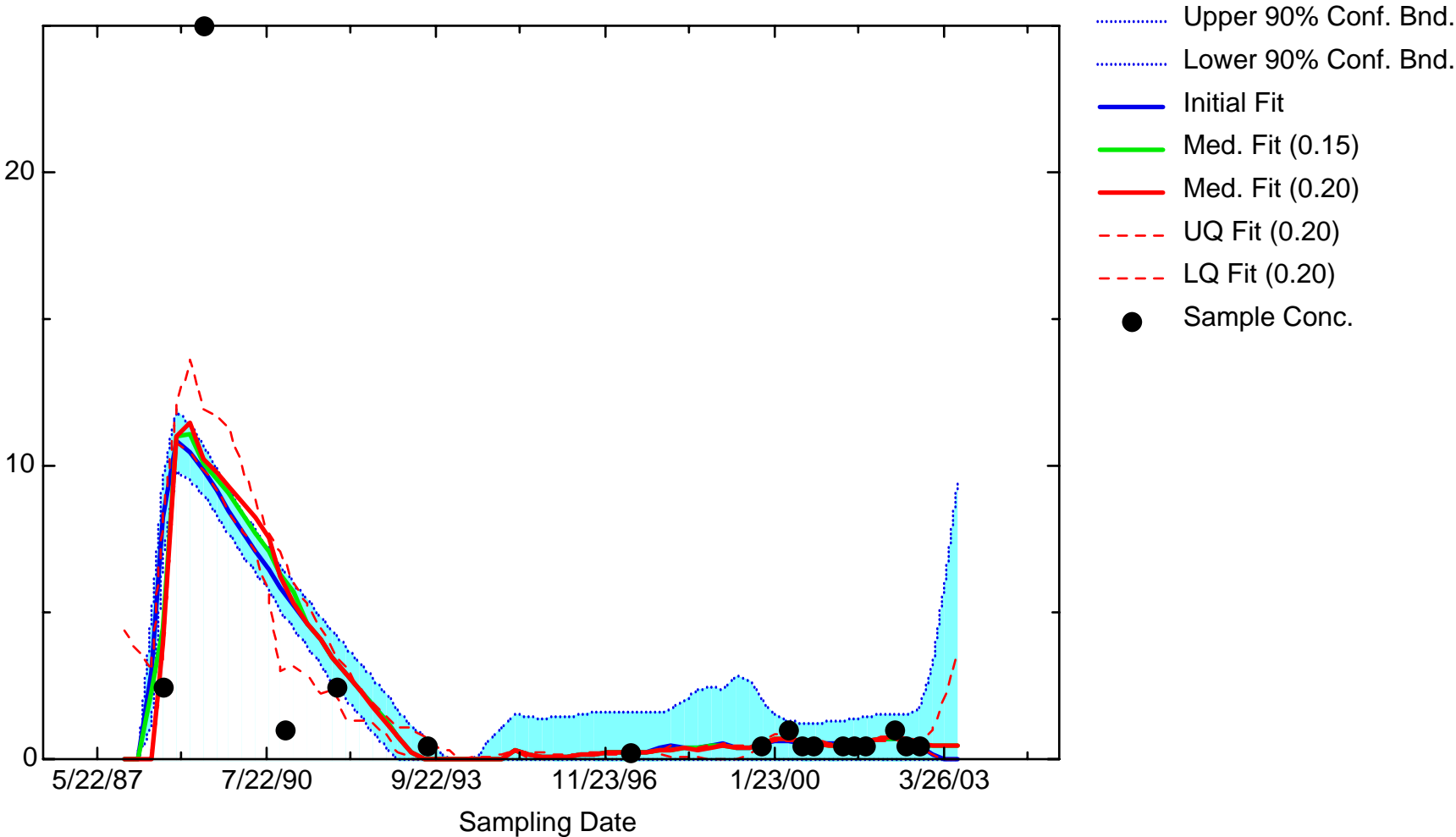
BZ: Well JBW7812B



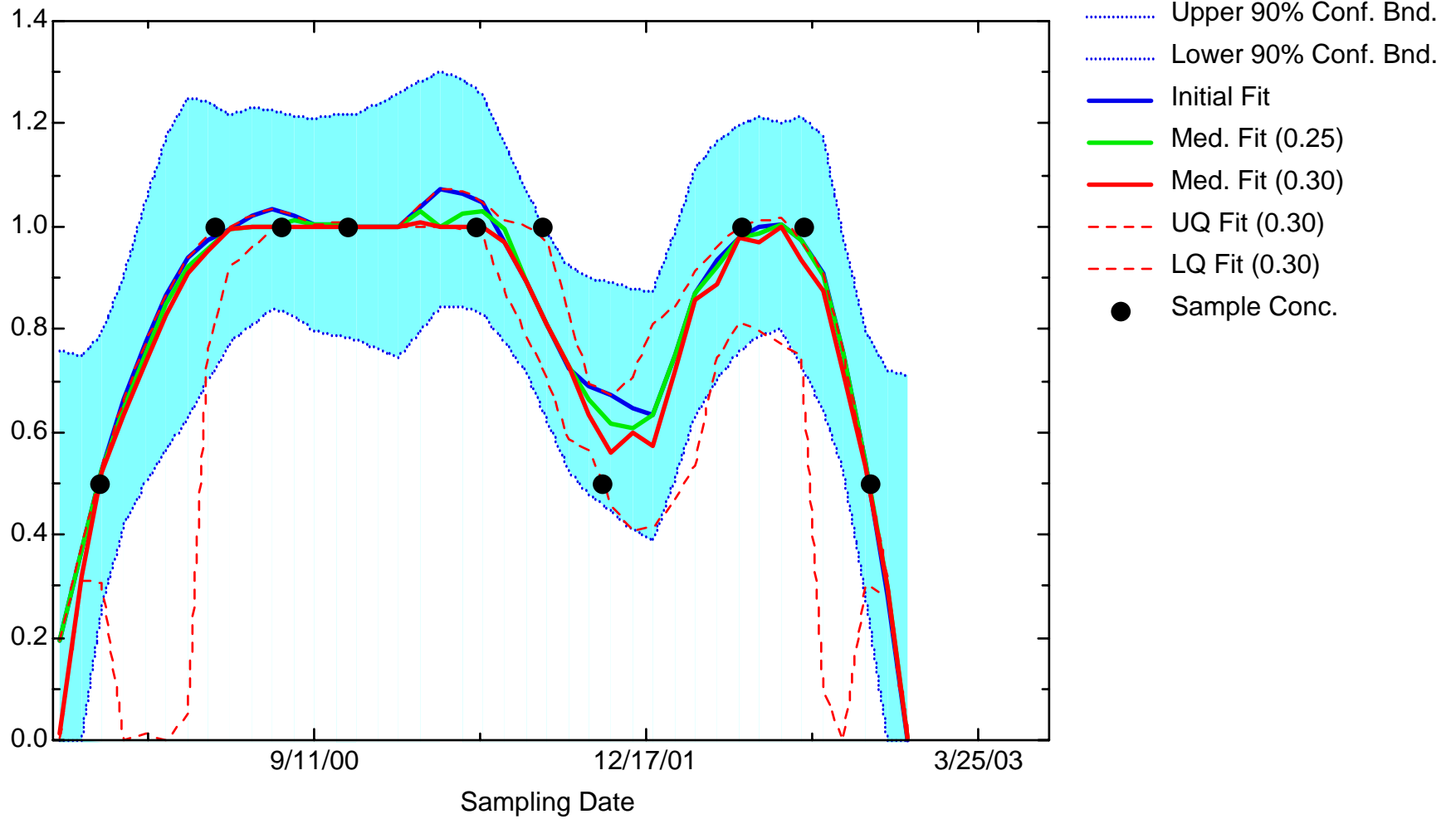
BZ: Well JMW0201A



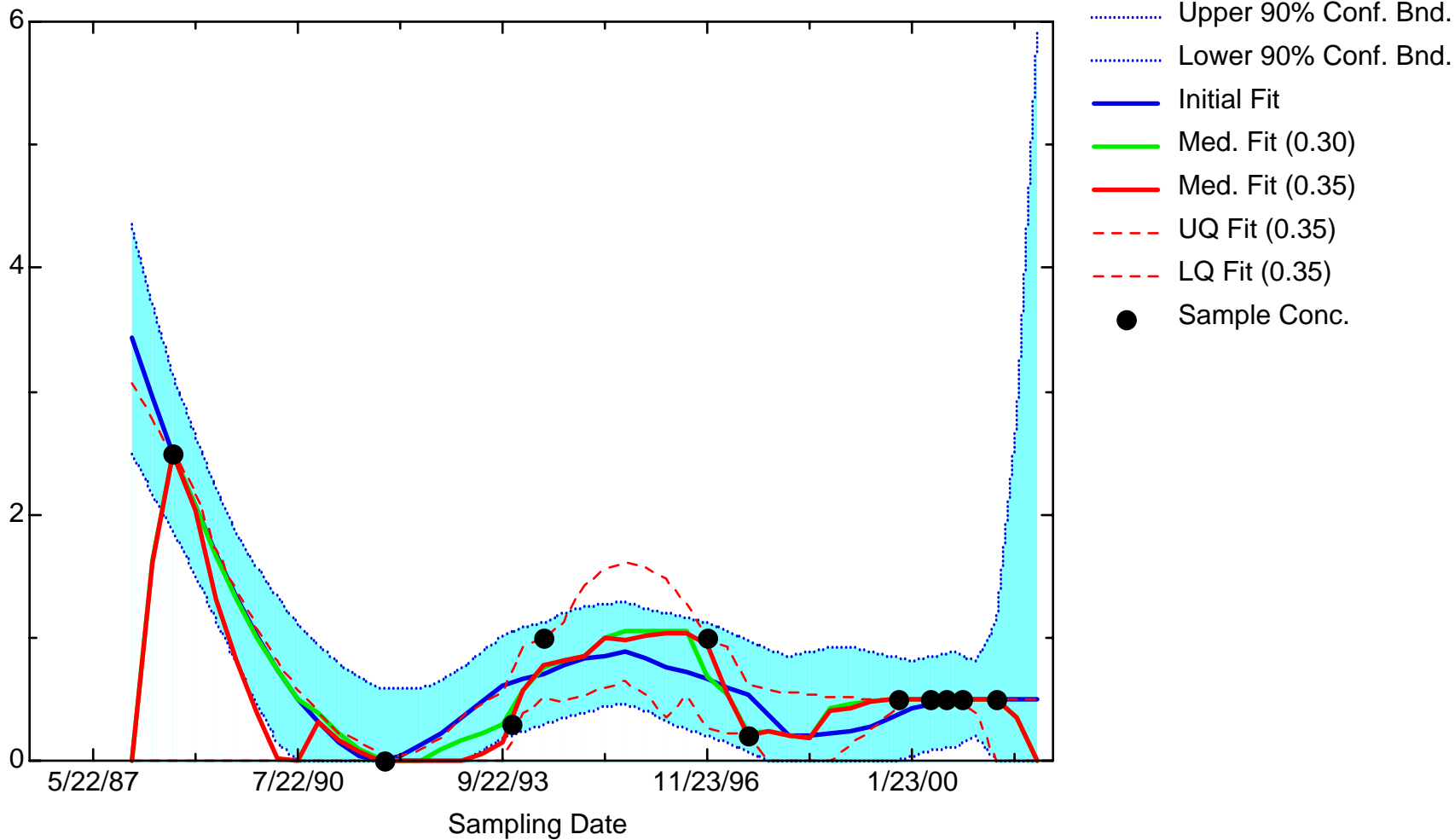
BZ: Well JMW0505



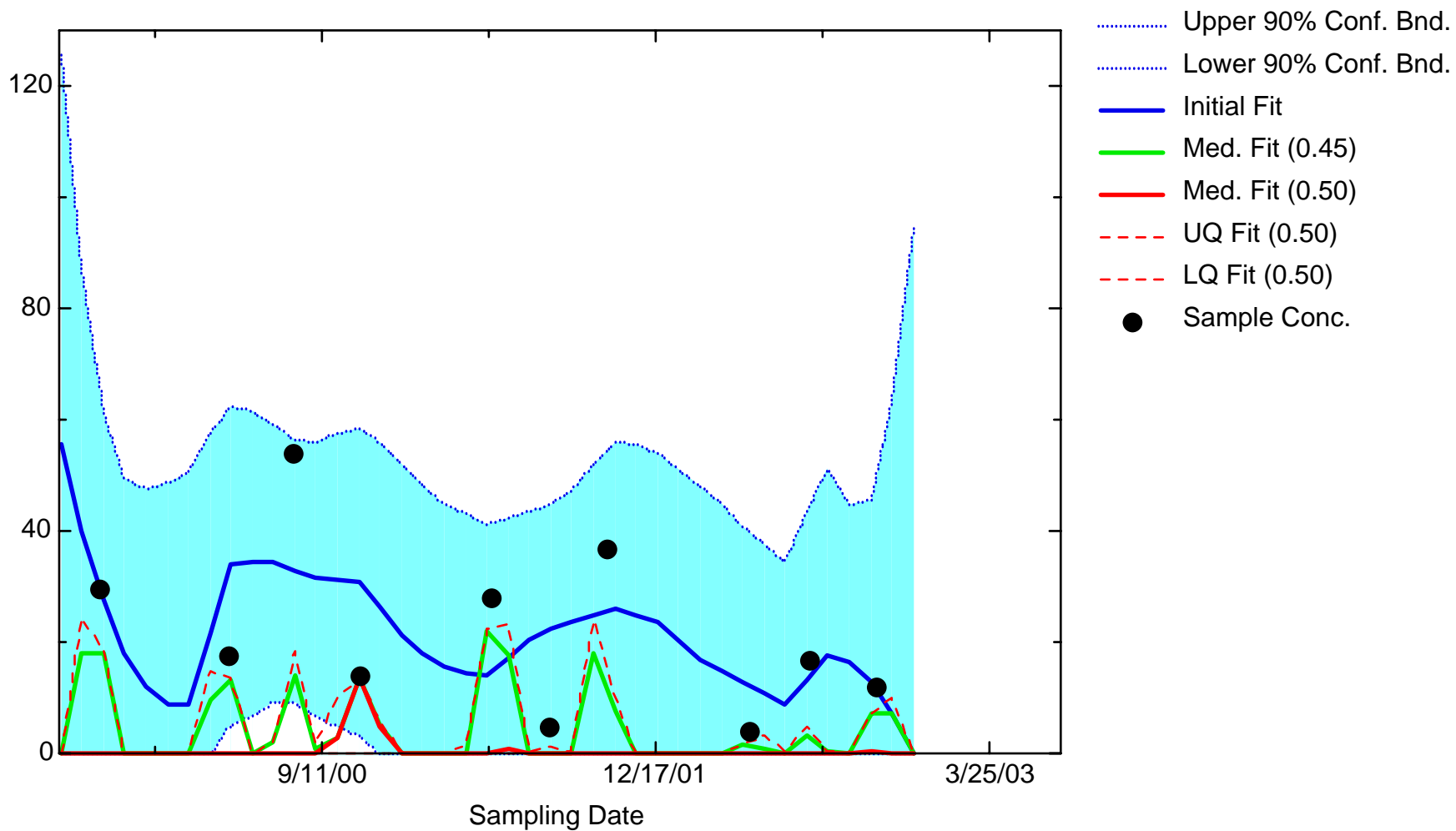
BZ: Well JMW0542



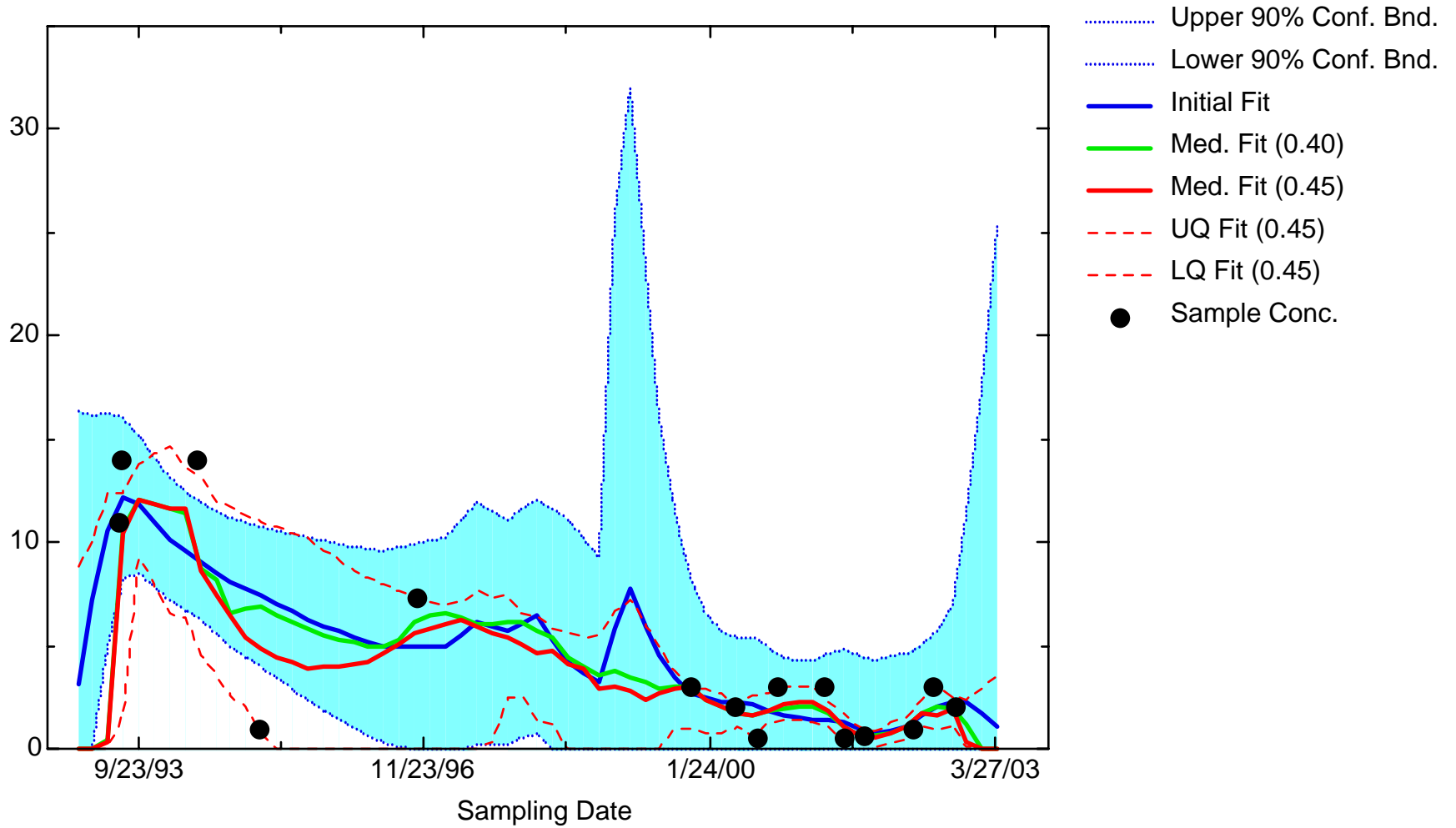
BZ: Well JMW0604



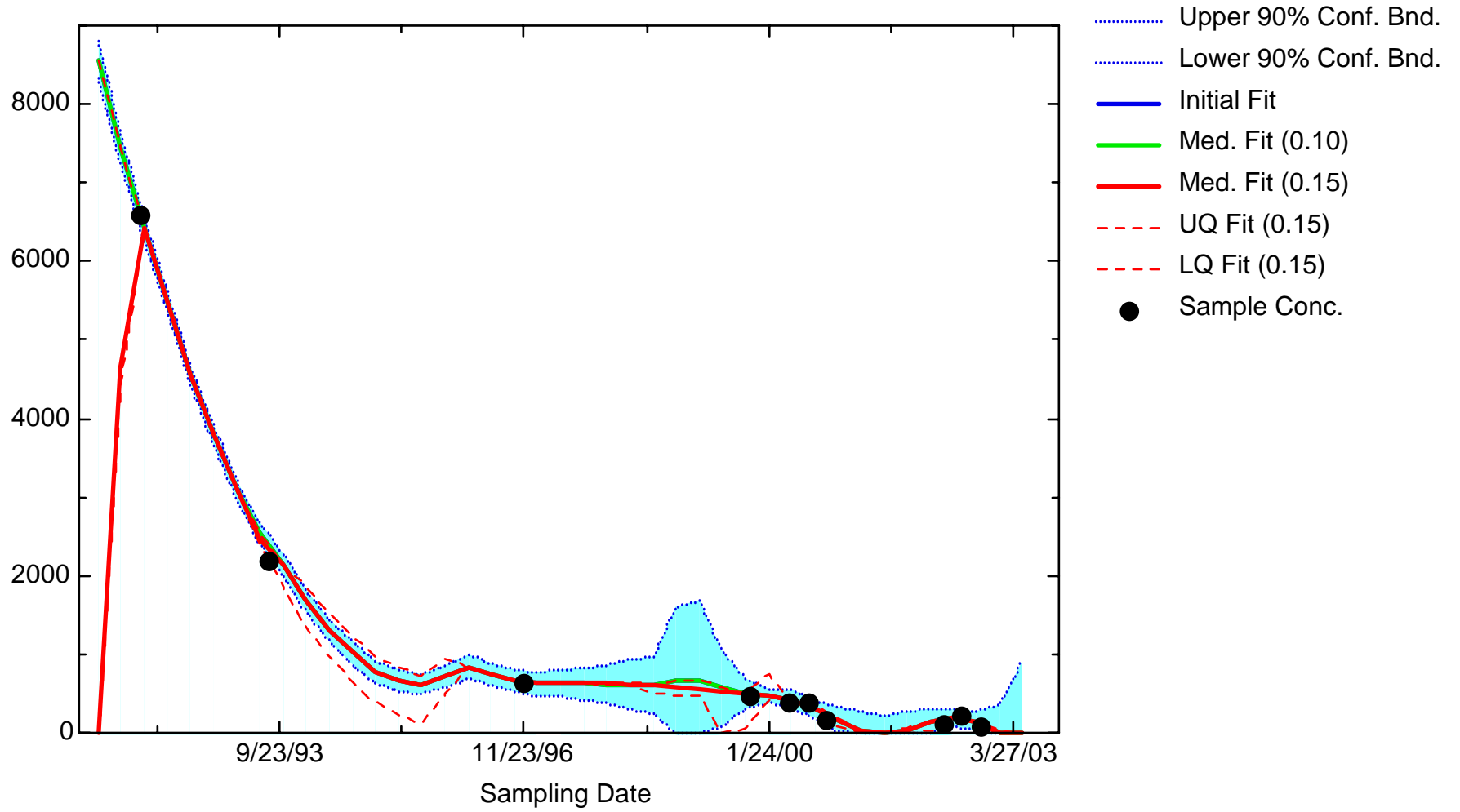
BZ: Well JMW0701



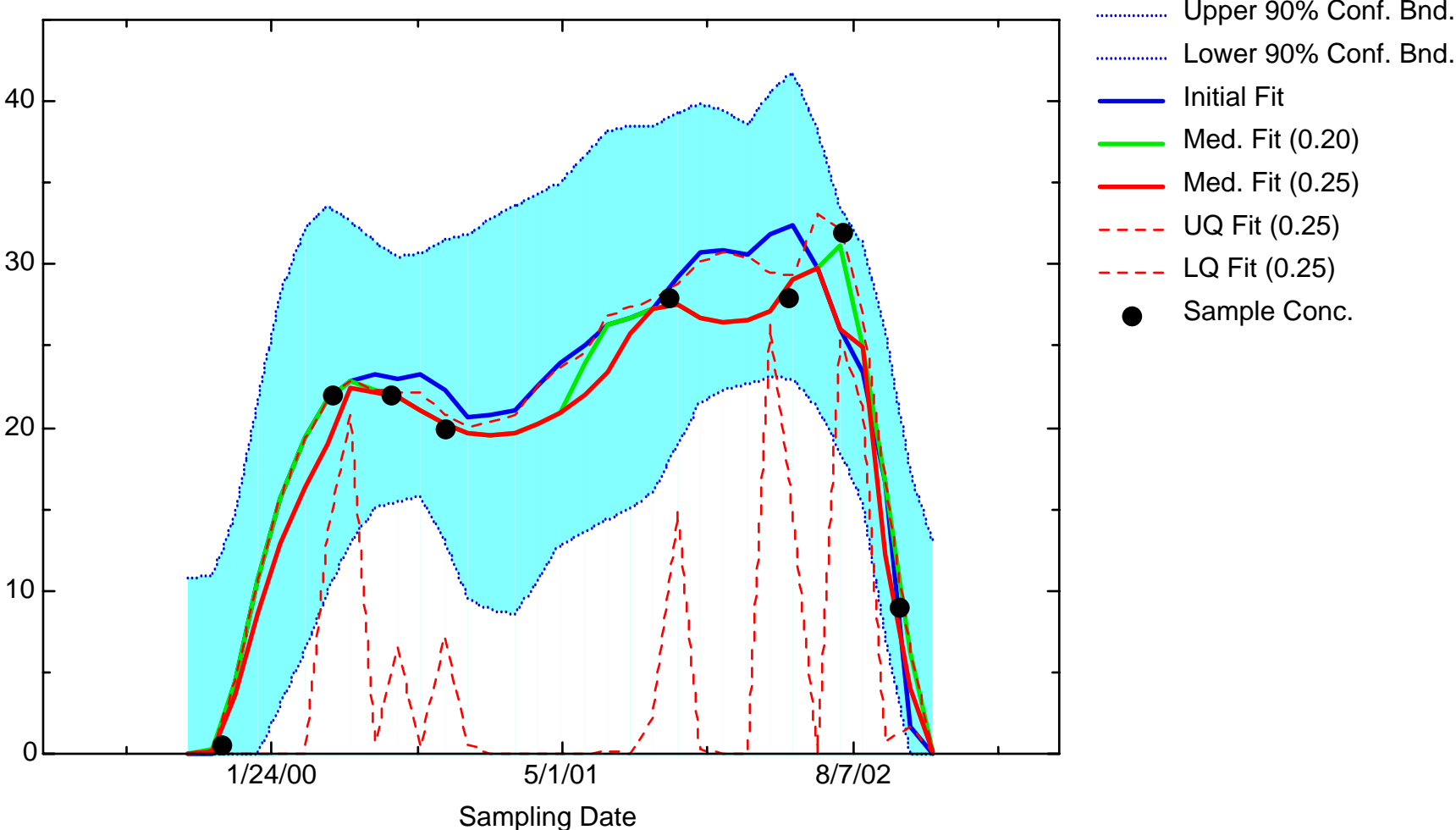
BZ: Well JMW1103D



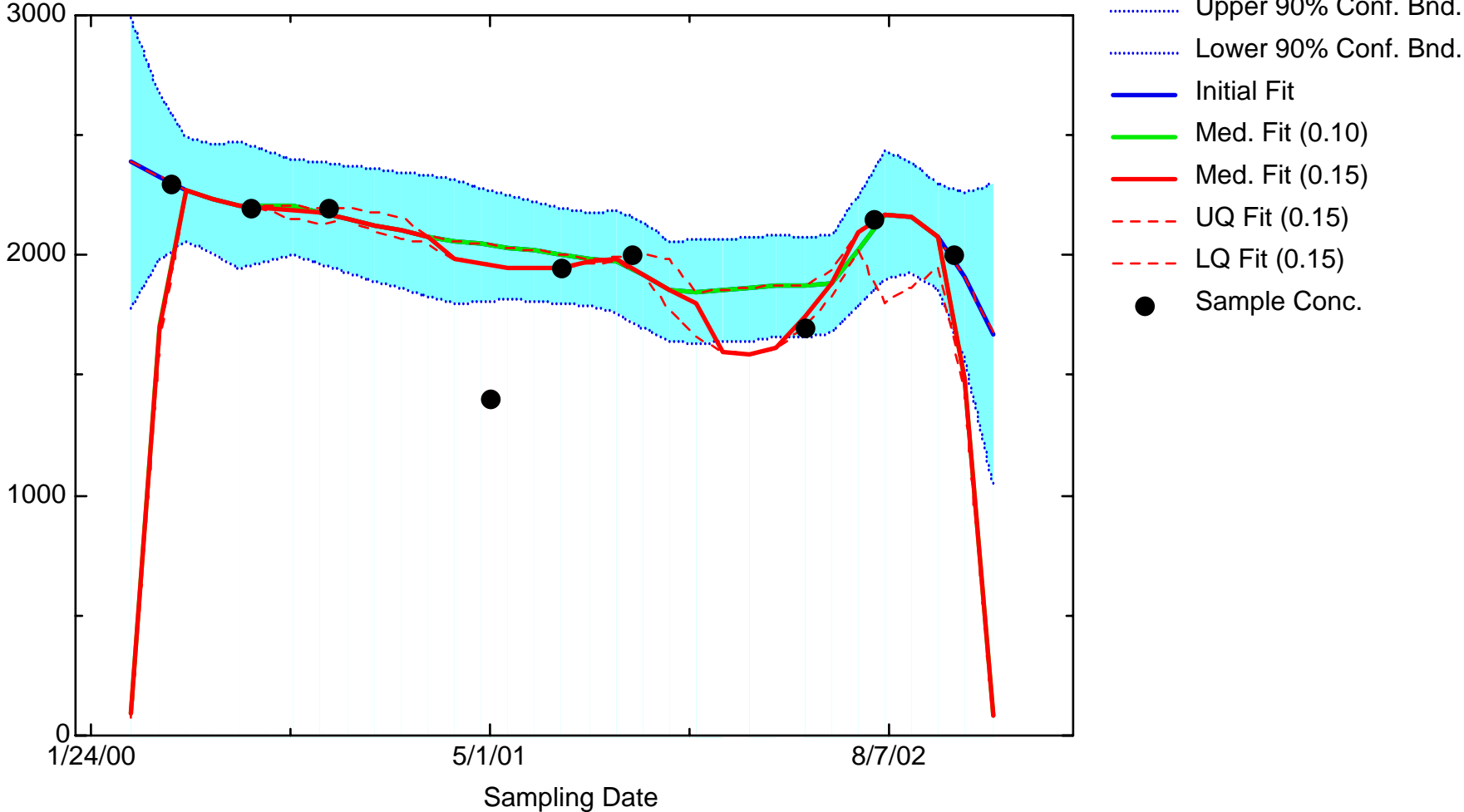
BZ: Well JMW1562



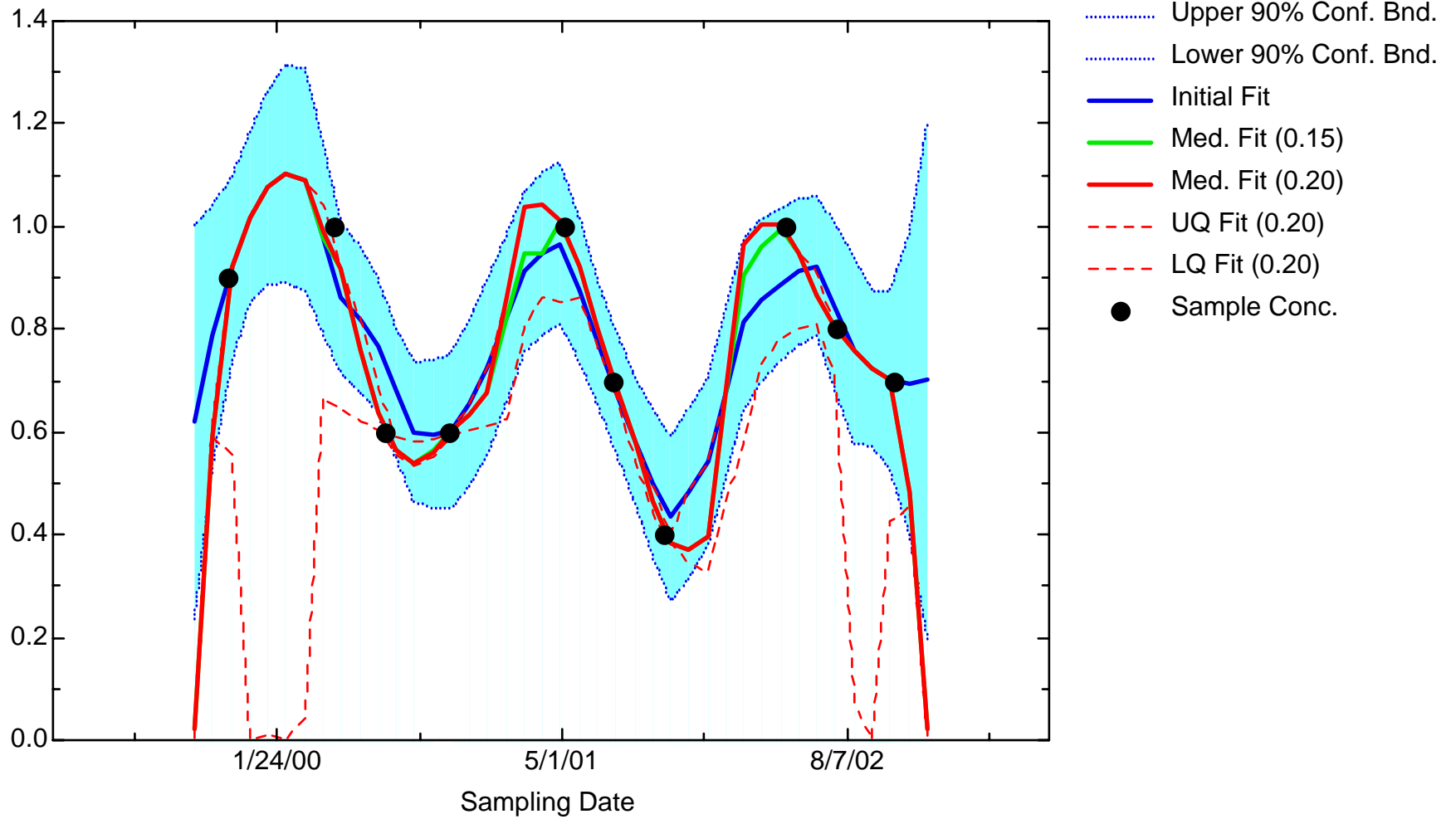
BZ: Well JMW1564



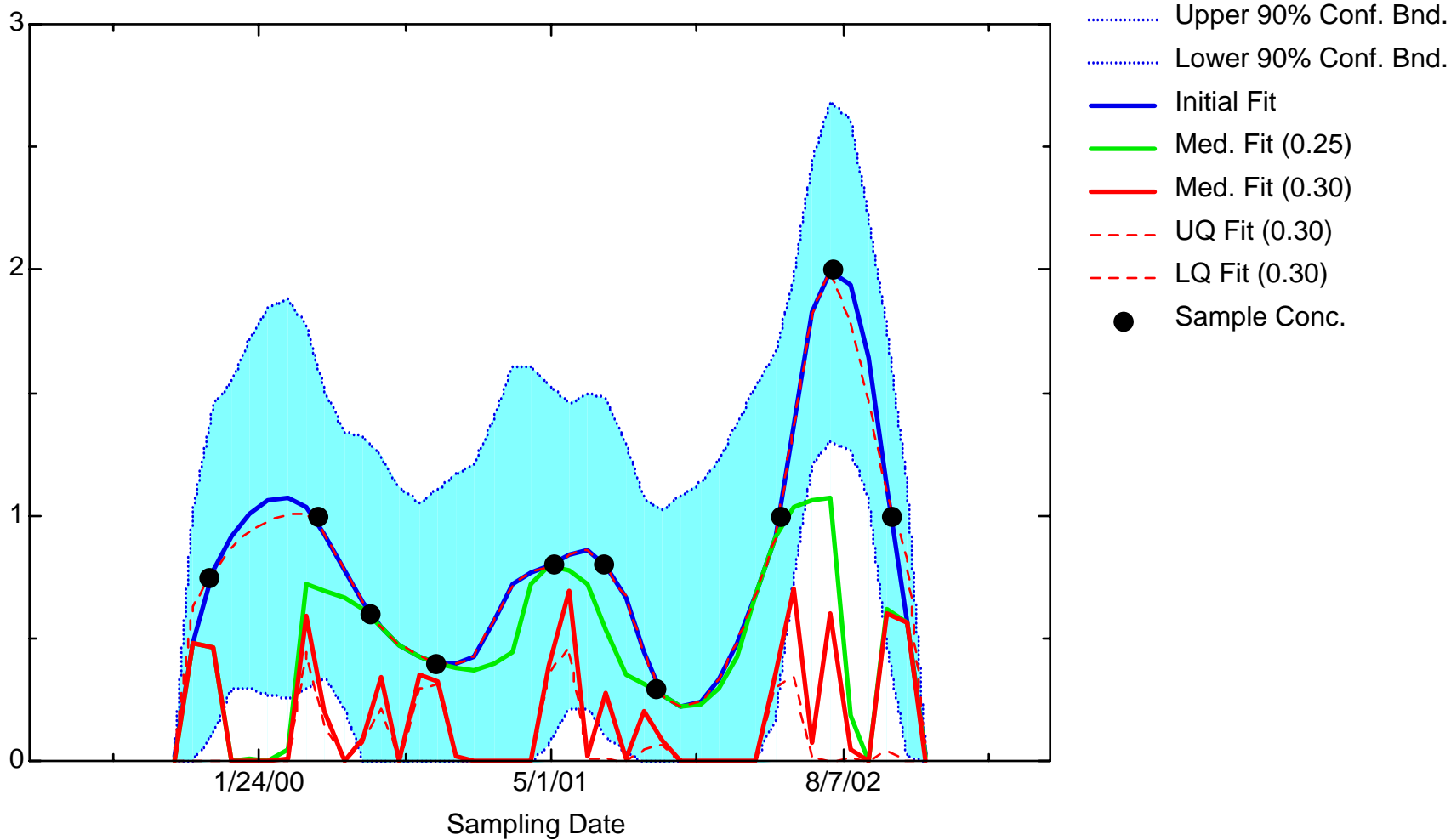
BZ: Well JMW1565



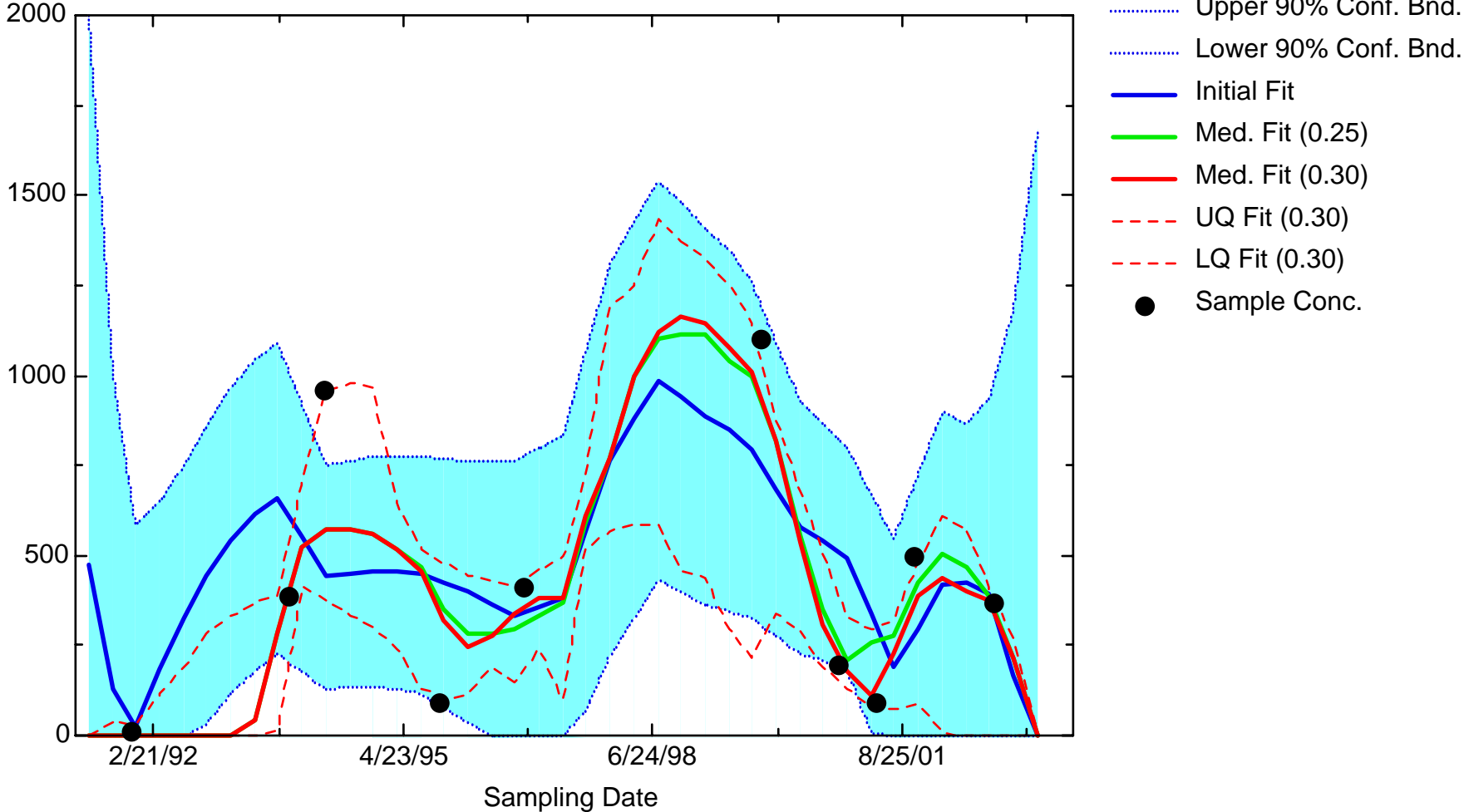
BZ: Well JMW1860



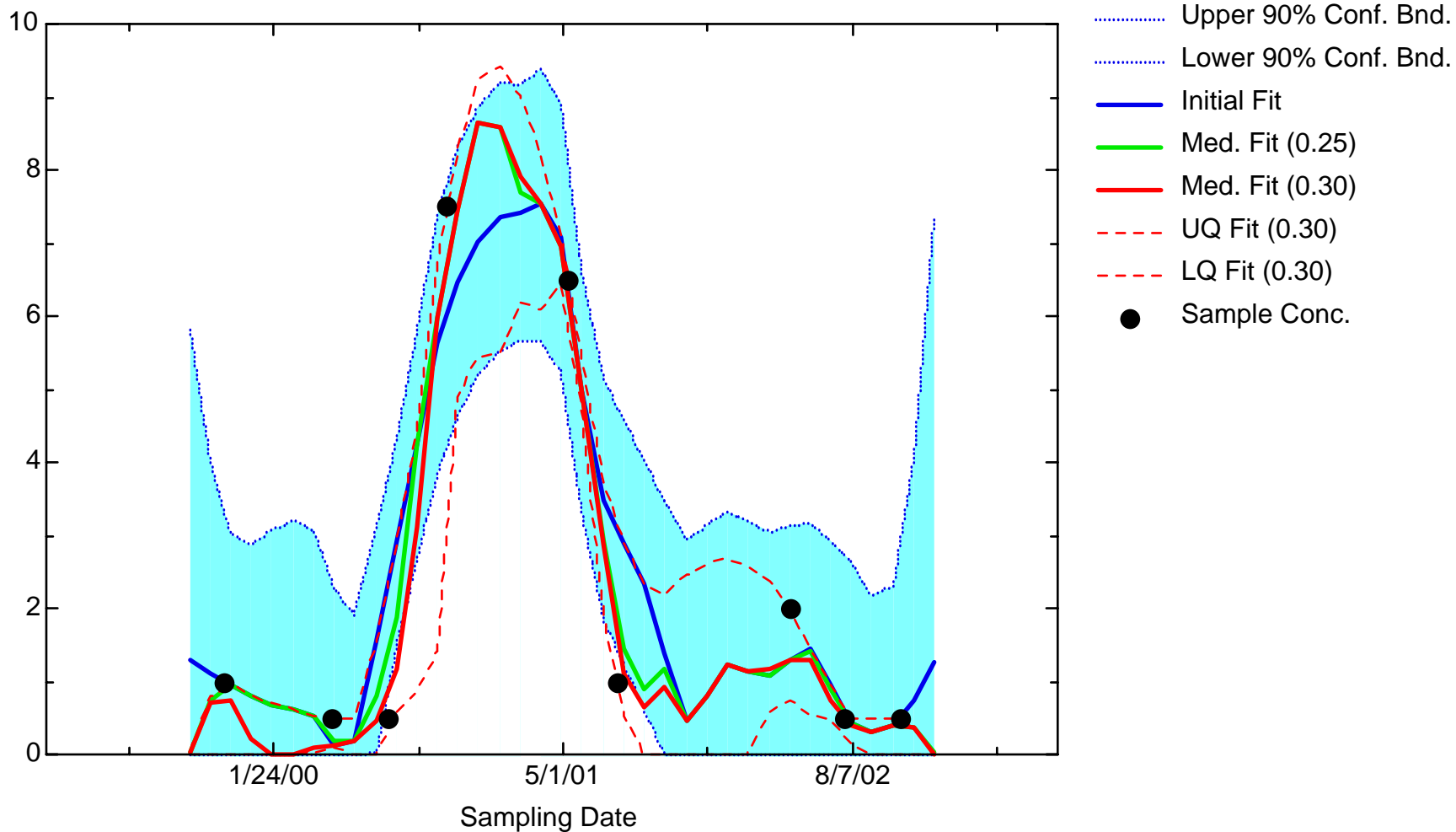
BZ: Well JMW1881



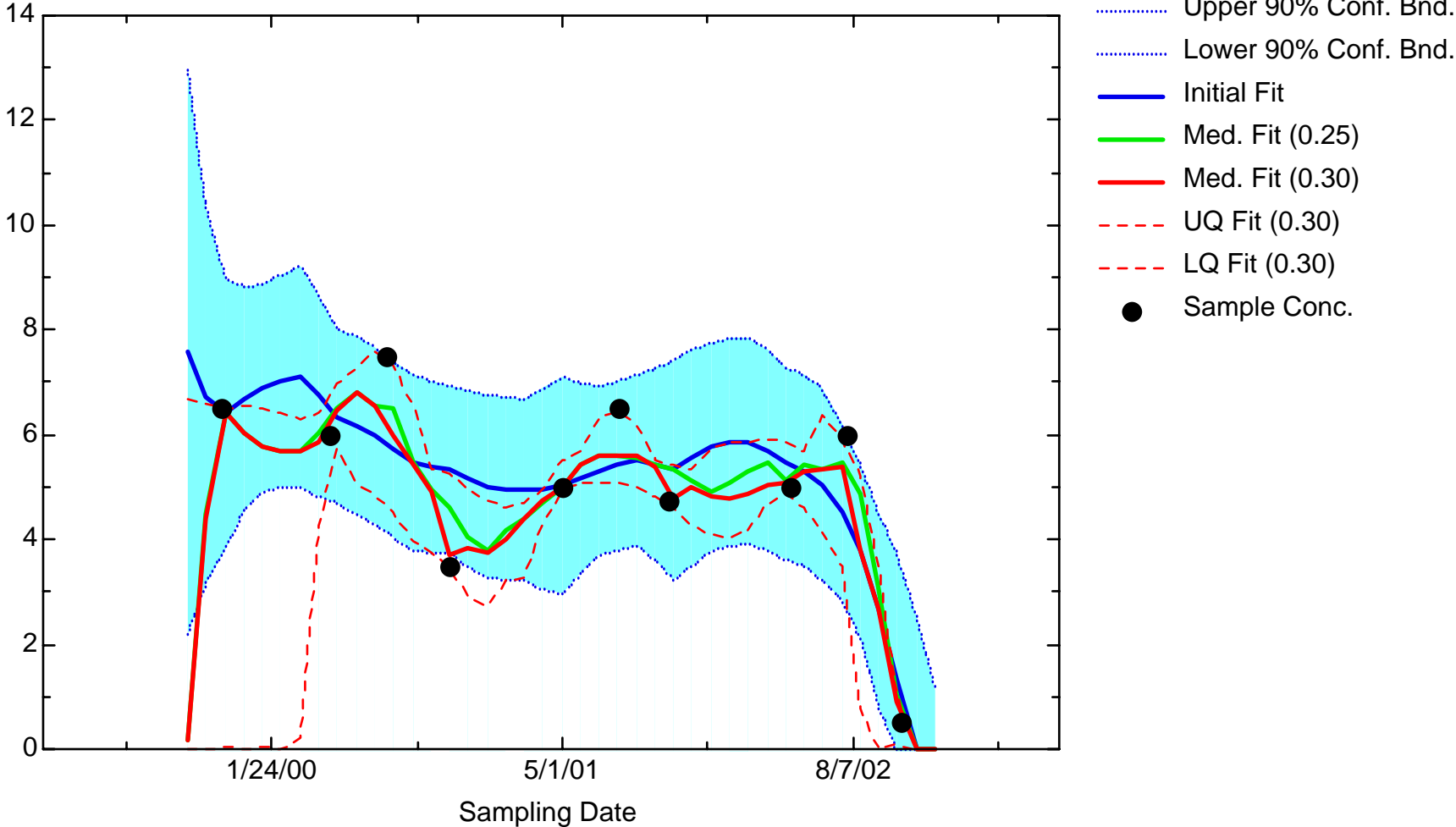
BZ: Well JMW1960



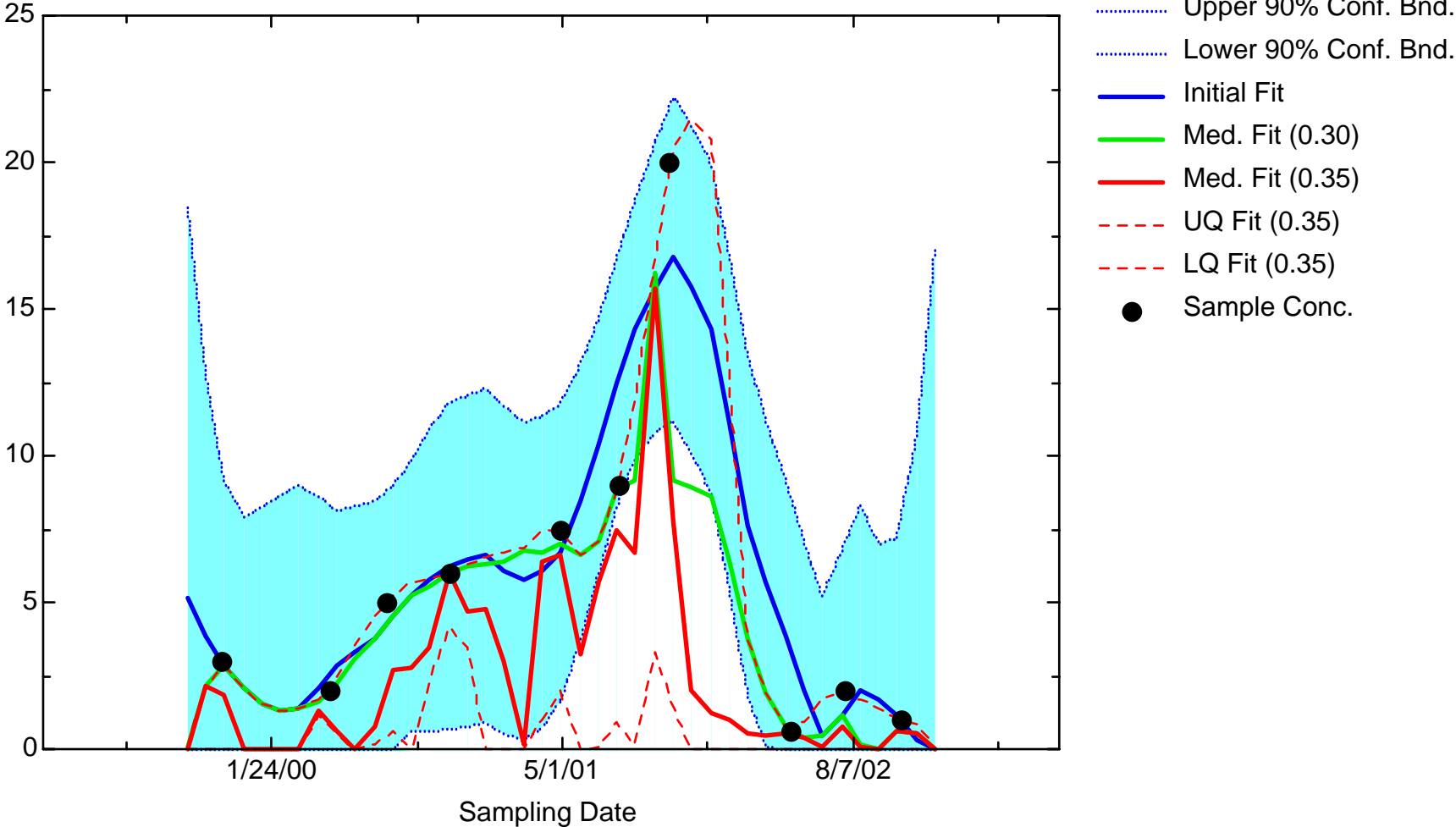
BZ: Well JMW1963



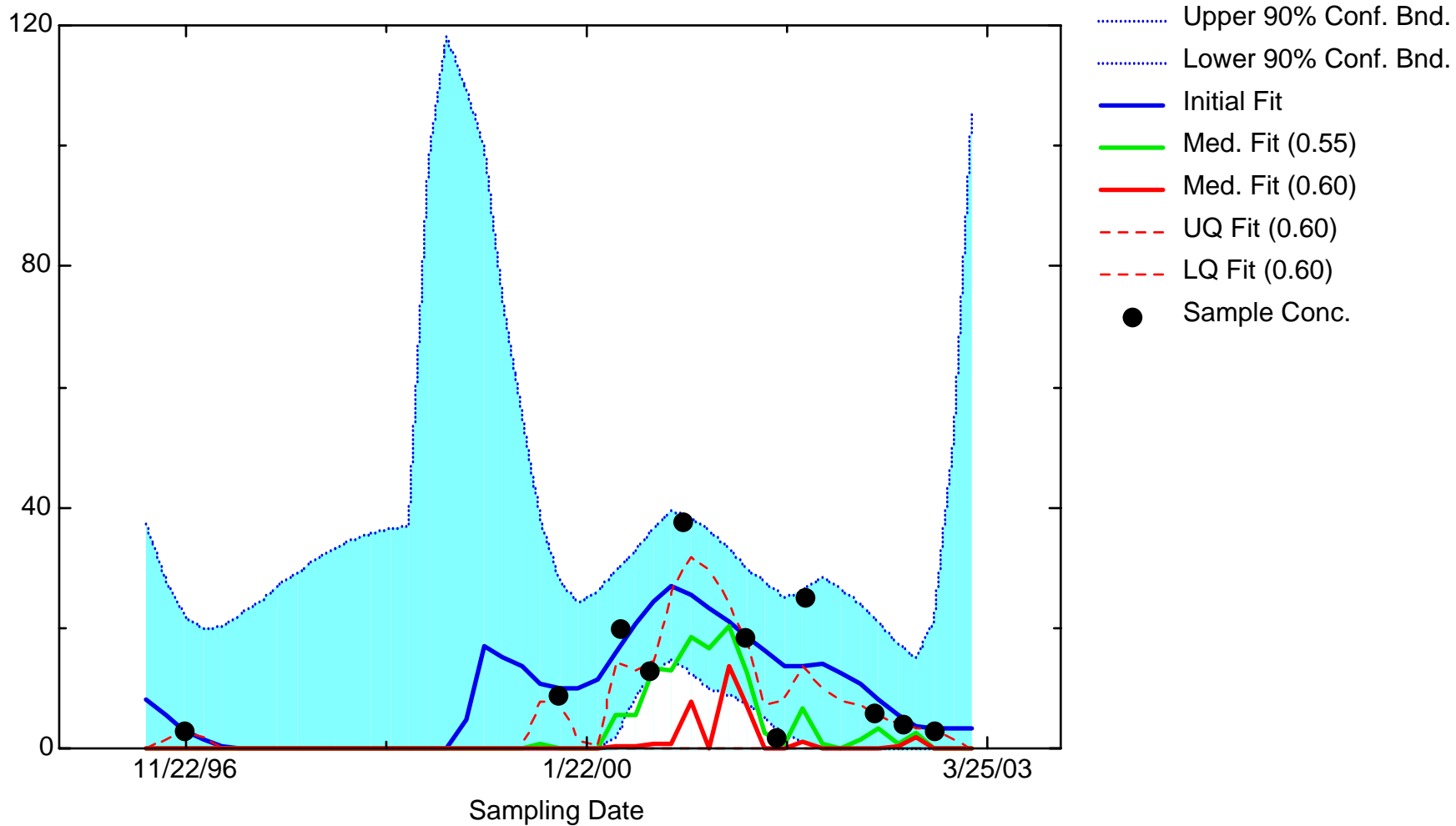
BZ: Well JMW1964



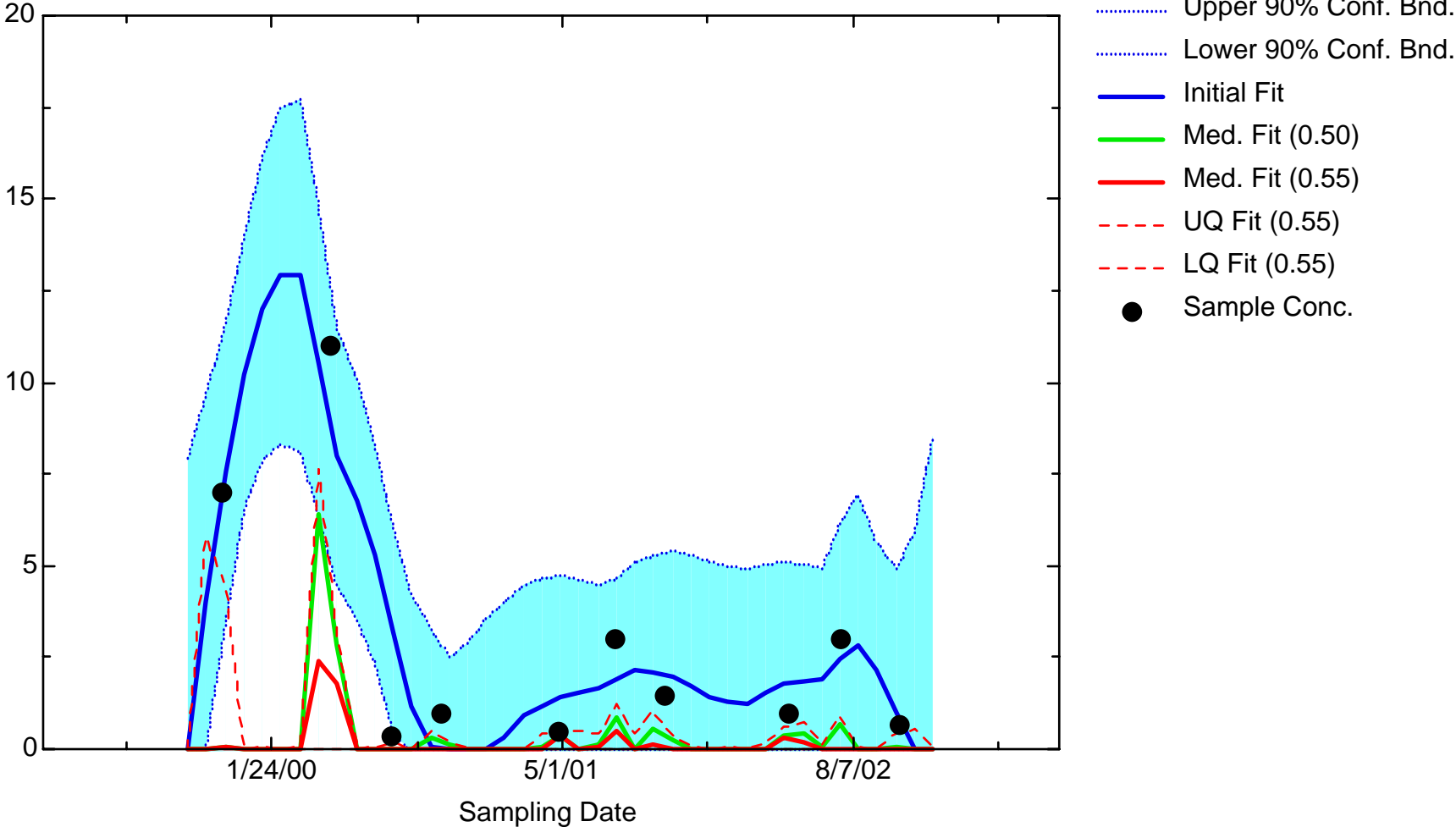
BZ: Well JMW1966



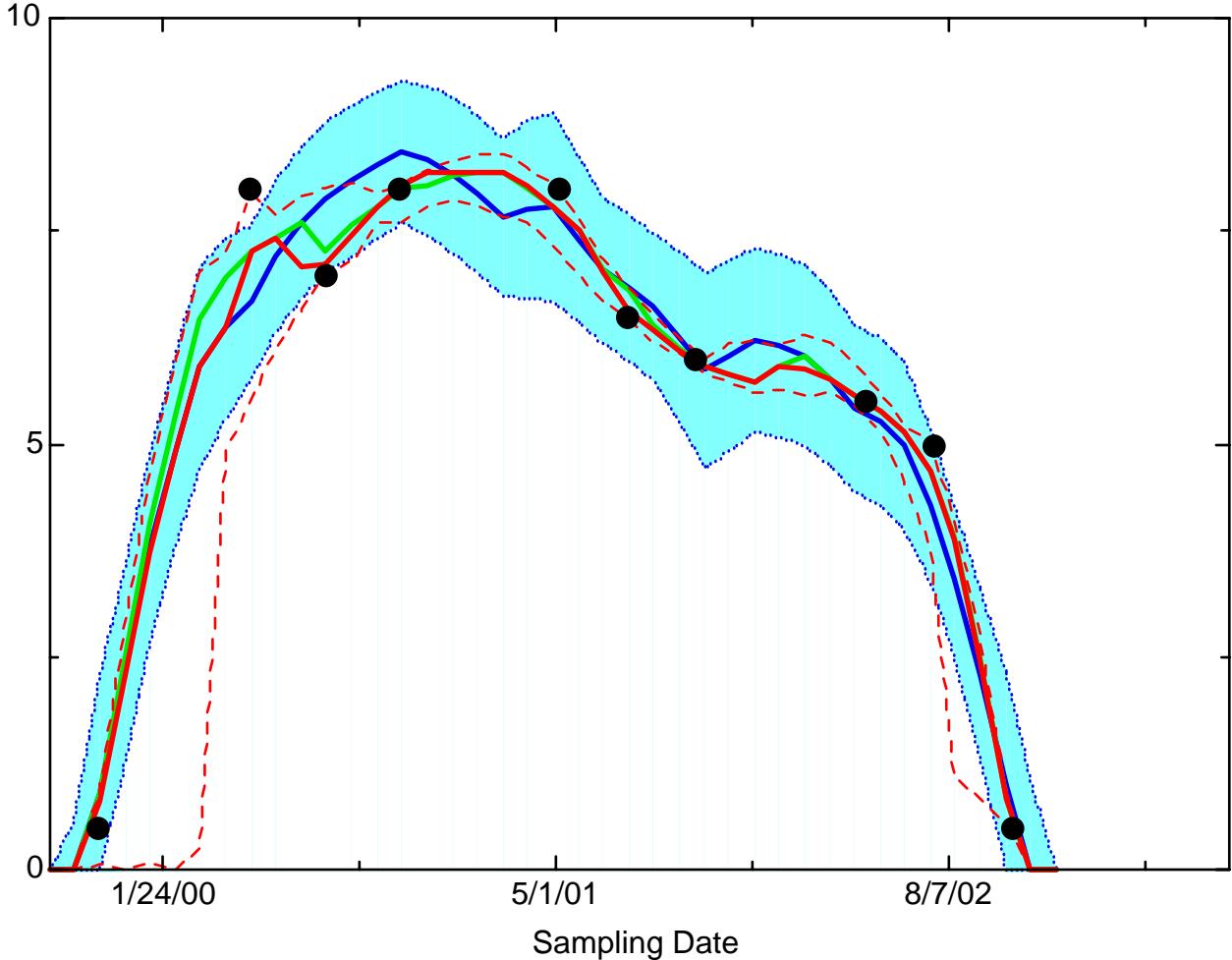
BZ: Well JMW3202



BZ: Well JMW6001

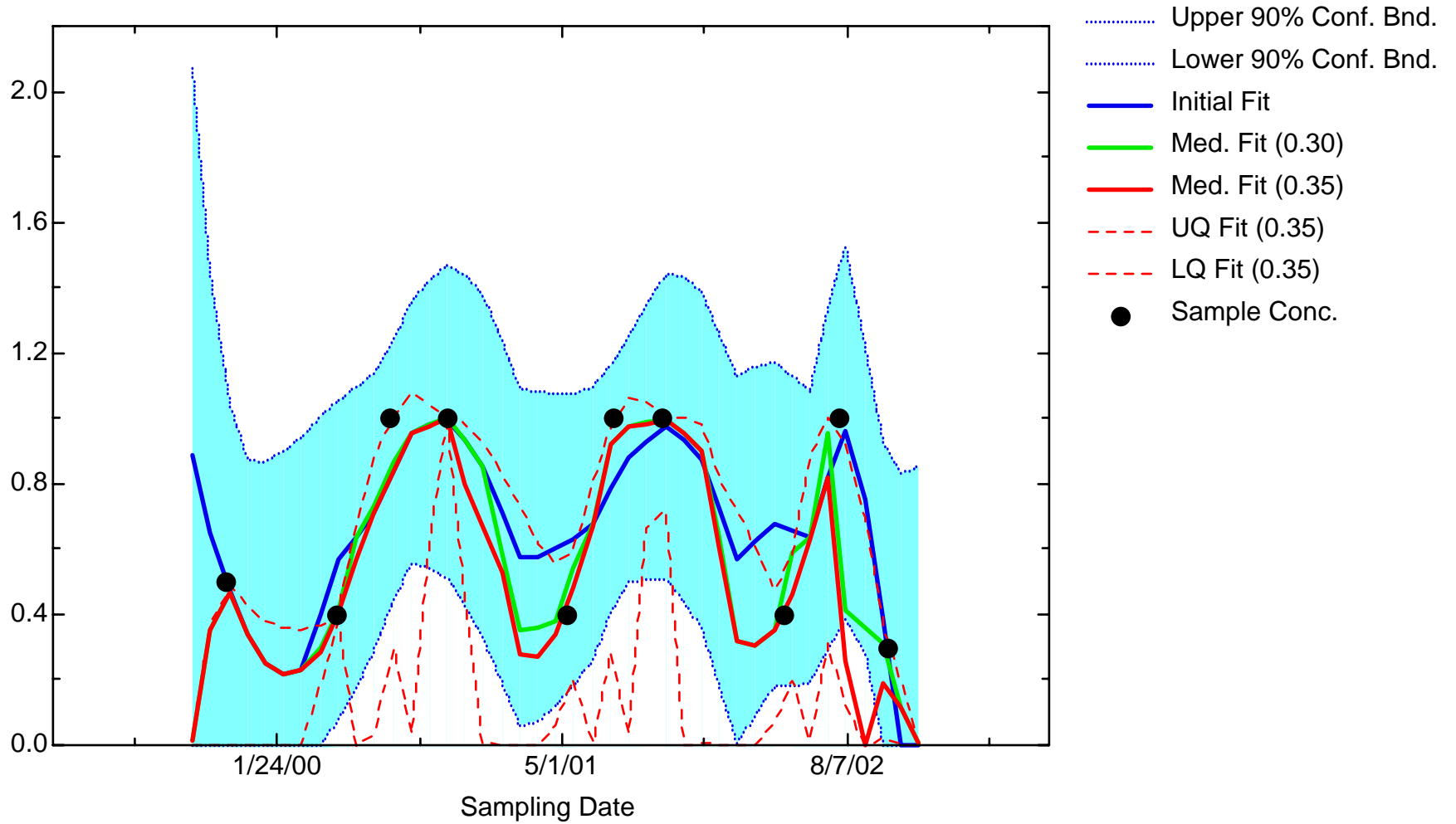


BZ: Well JMW7612

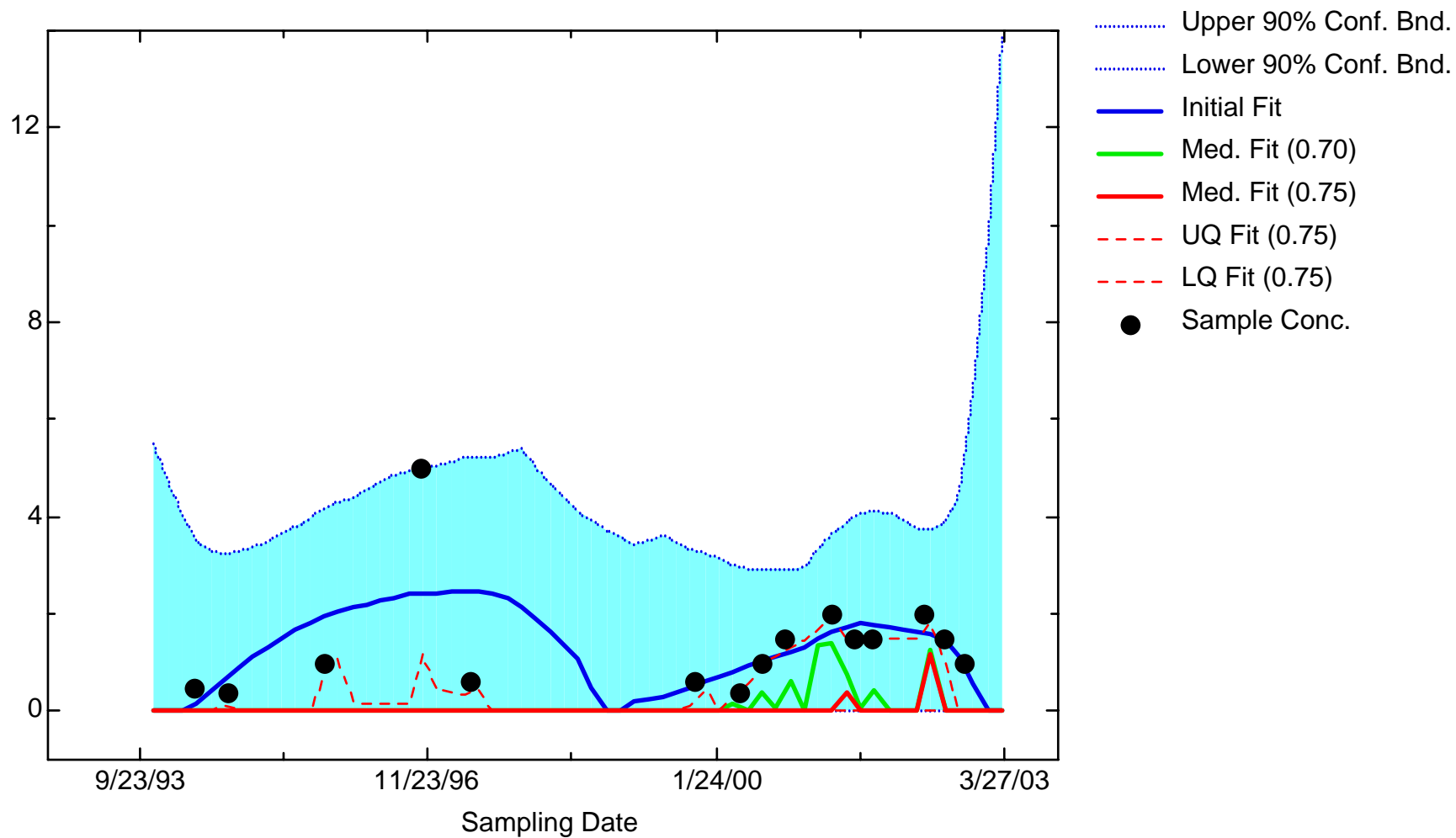


- Upper 90% Conf. Bnd.
- Lower 90% Conf. Bnd.
- Initial Fit
- Med. Fit (0.25)
- Med. Fit (0.30)
- UQ Fit (0.30)
- LQ Fit (0.30)
- Sample Conc.

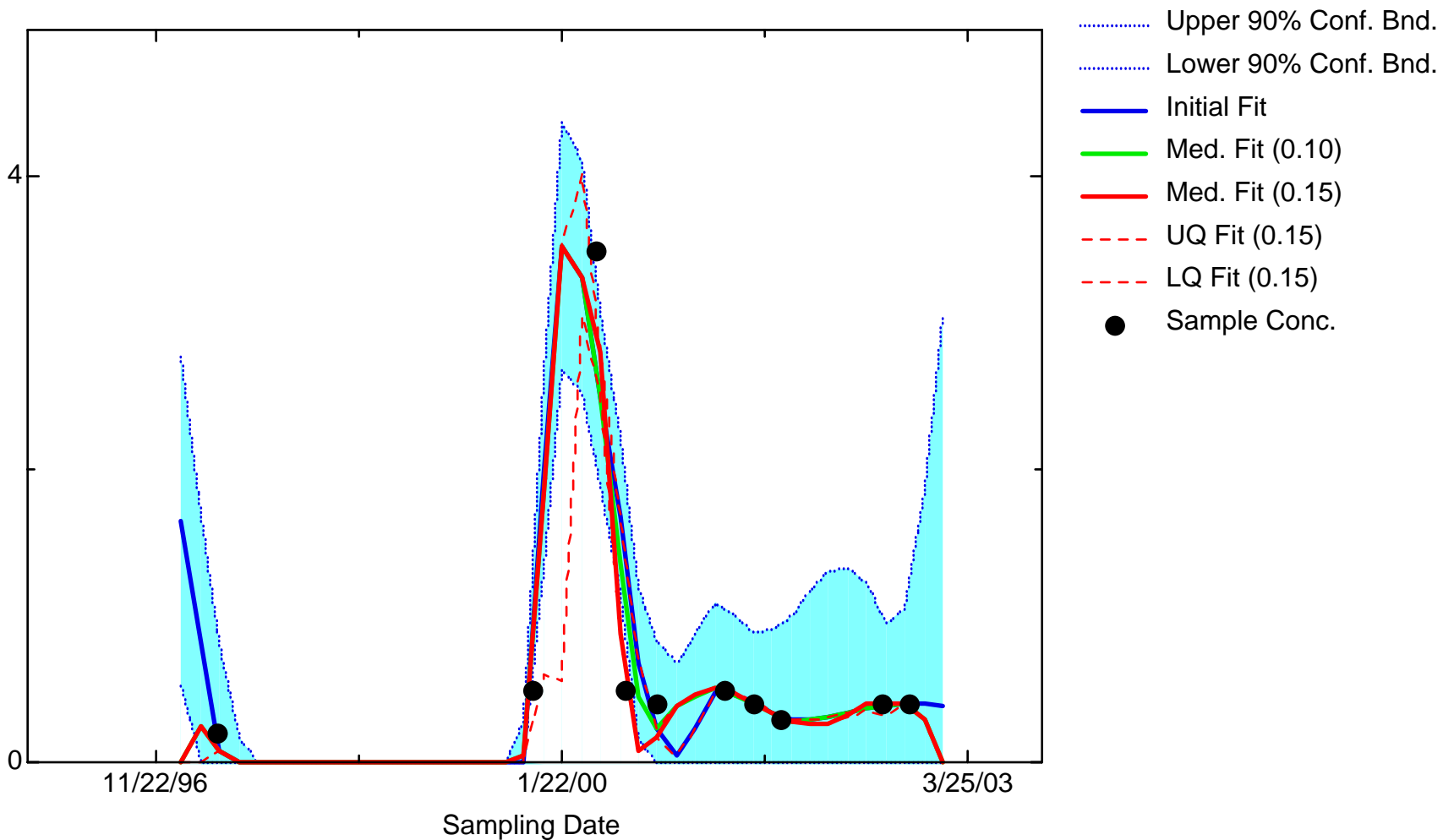
BZ: Well JPZ0340



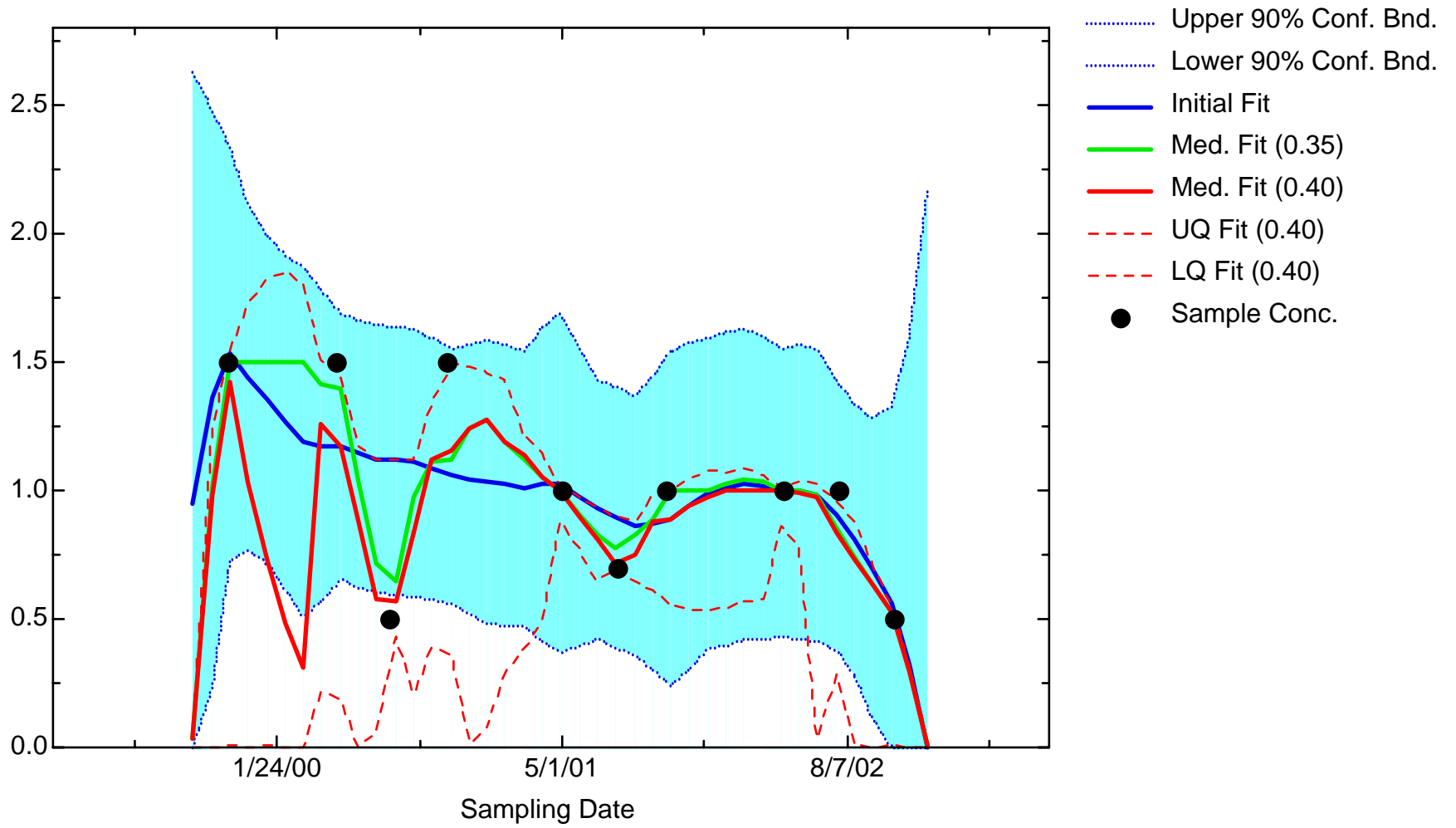
BZ: Well JPZ0342



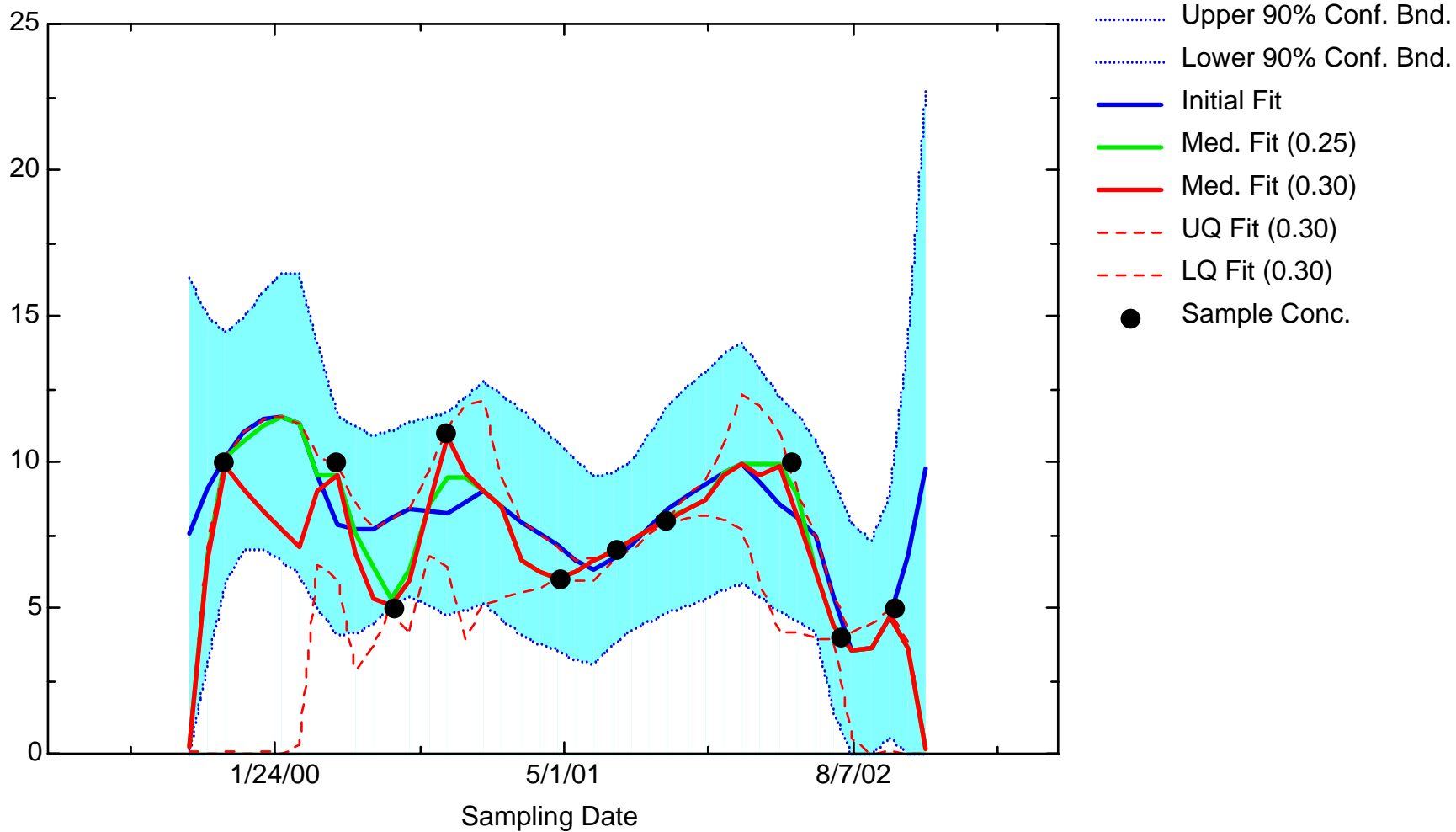
BZ: Well JPZ0343



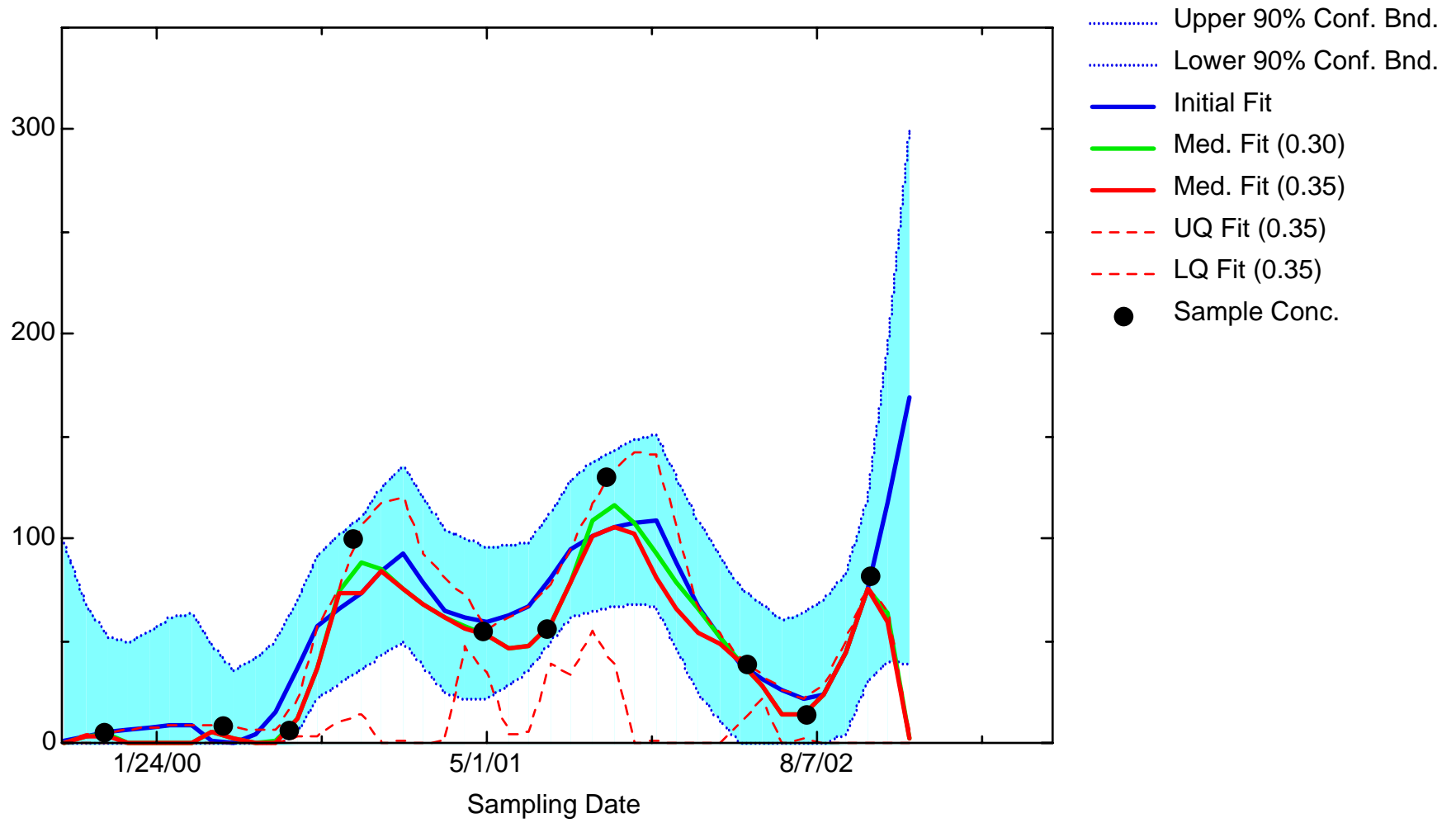
BZ: Well JPZ0348



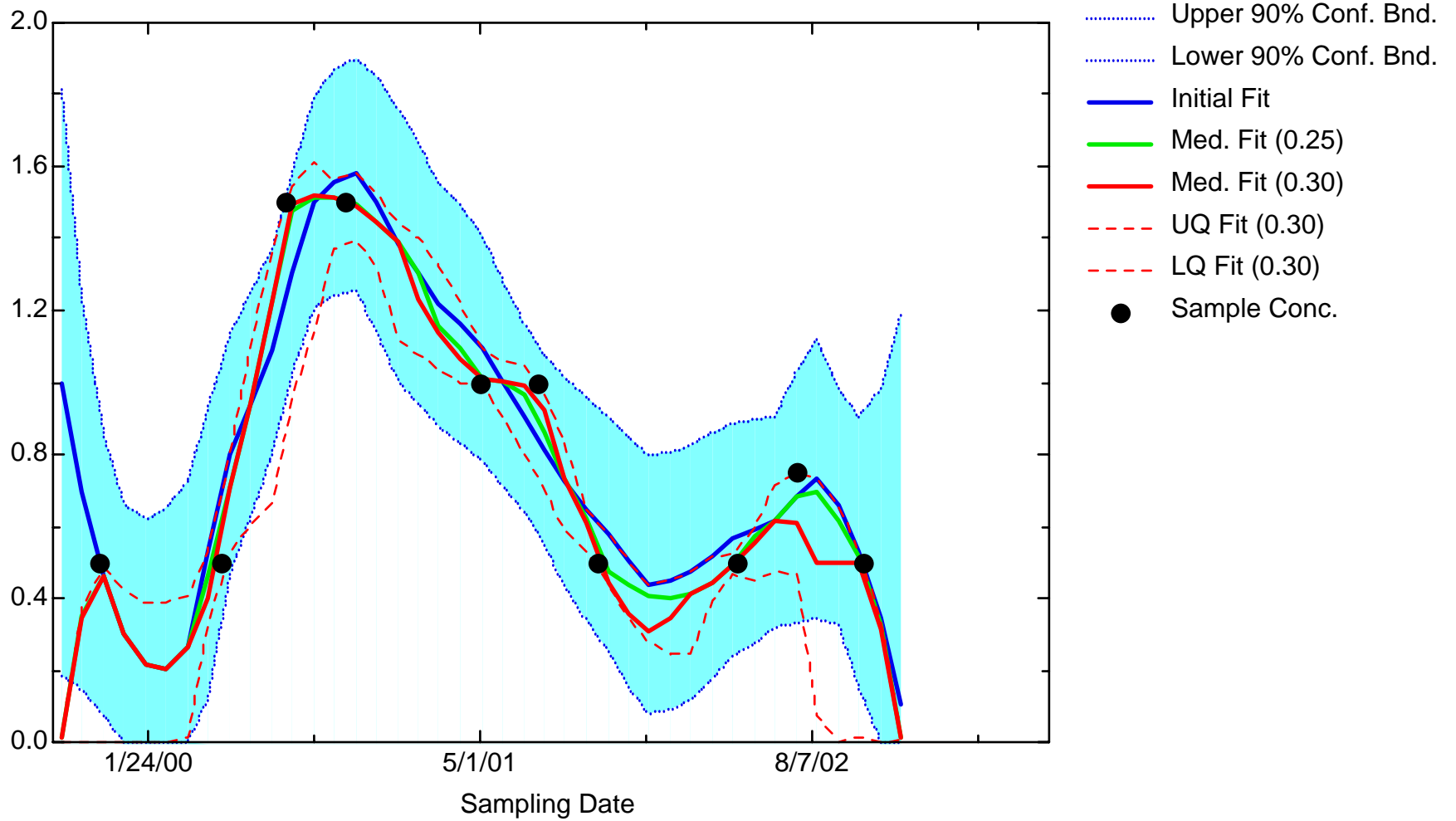
BZ: Well JPZ7312



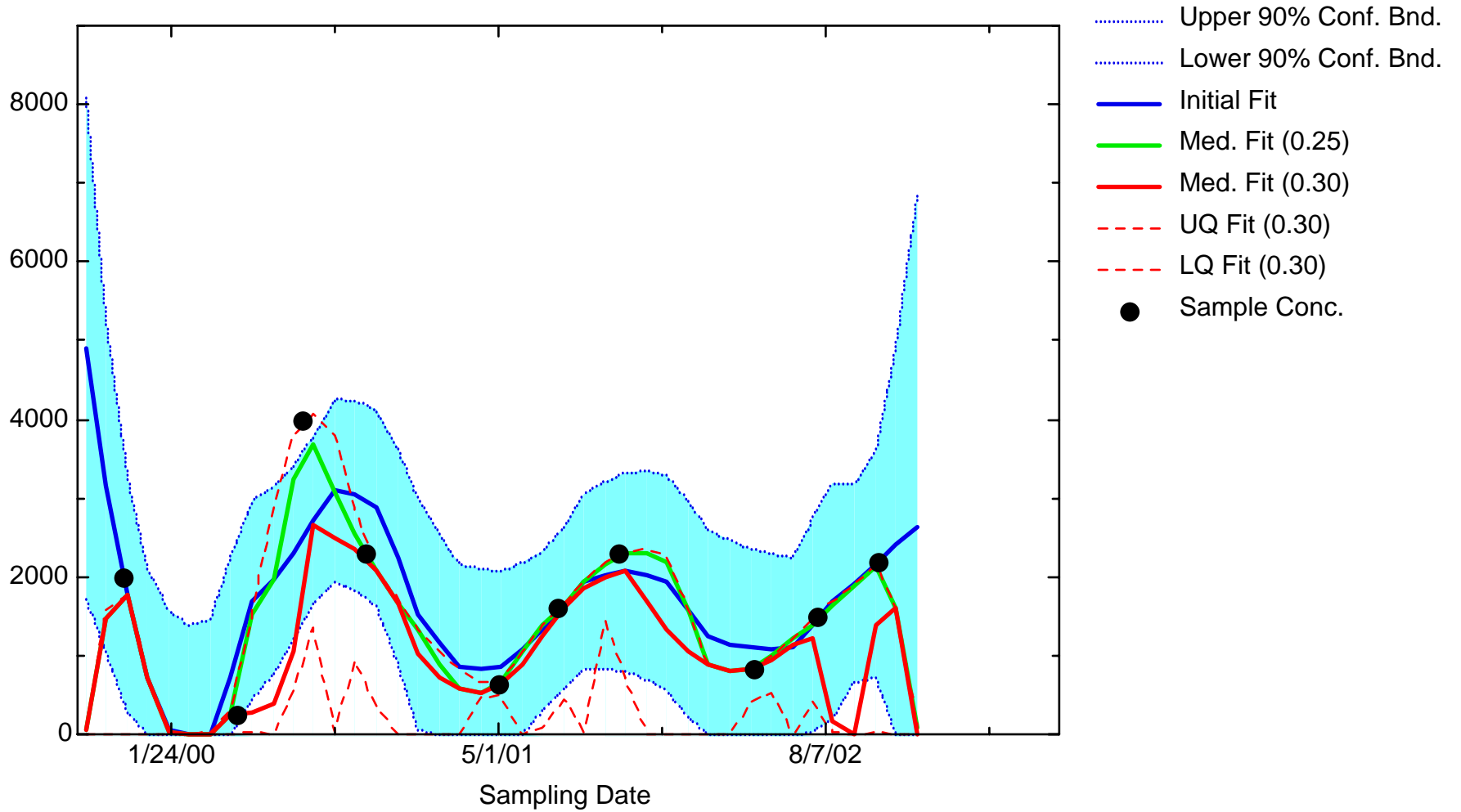
BZ: Well MMW0005



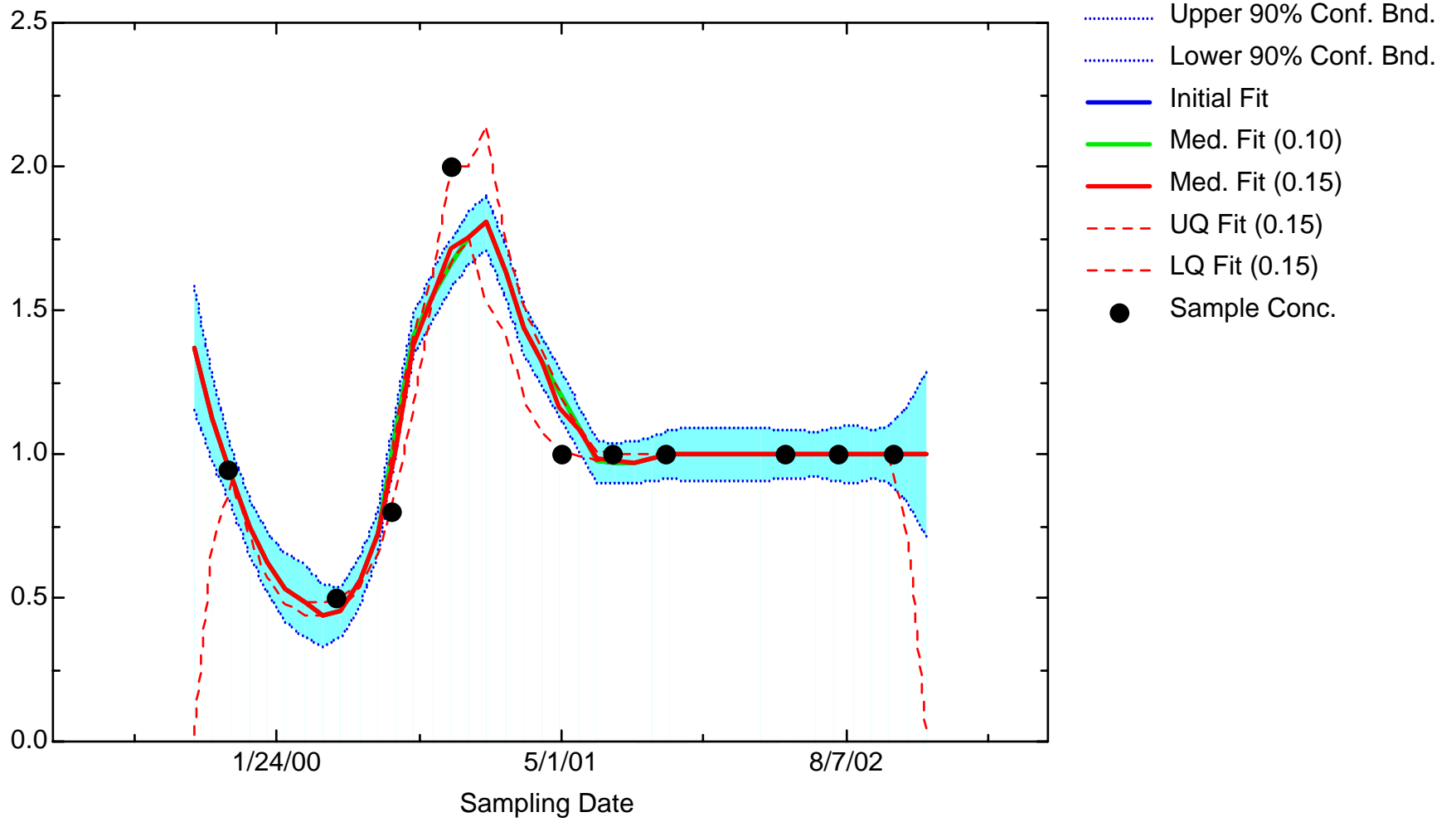
BZ: Well MMW0009



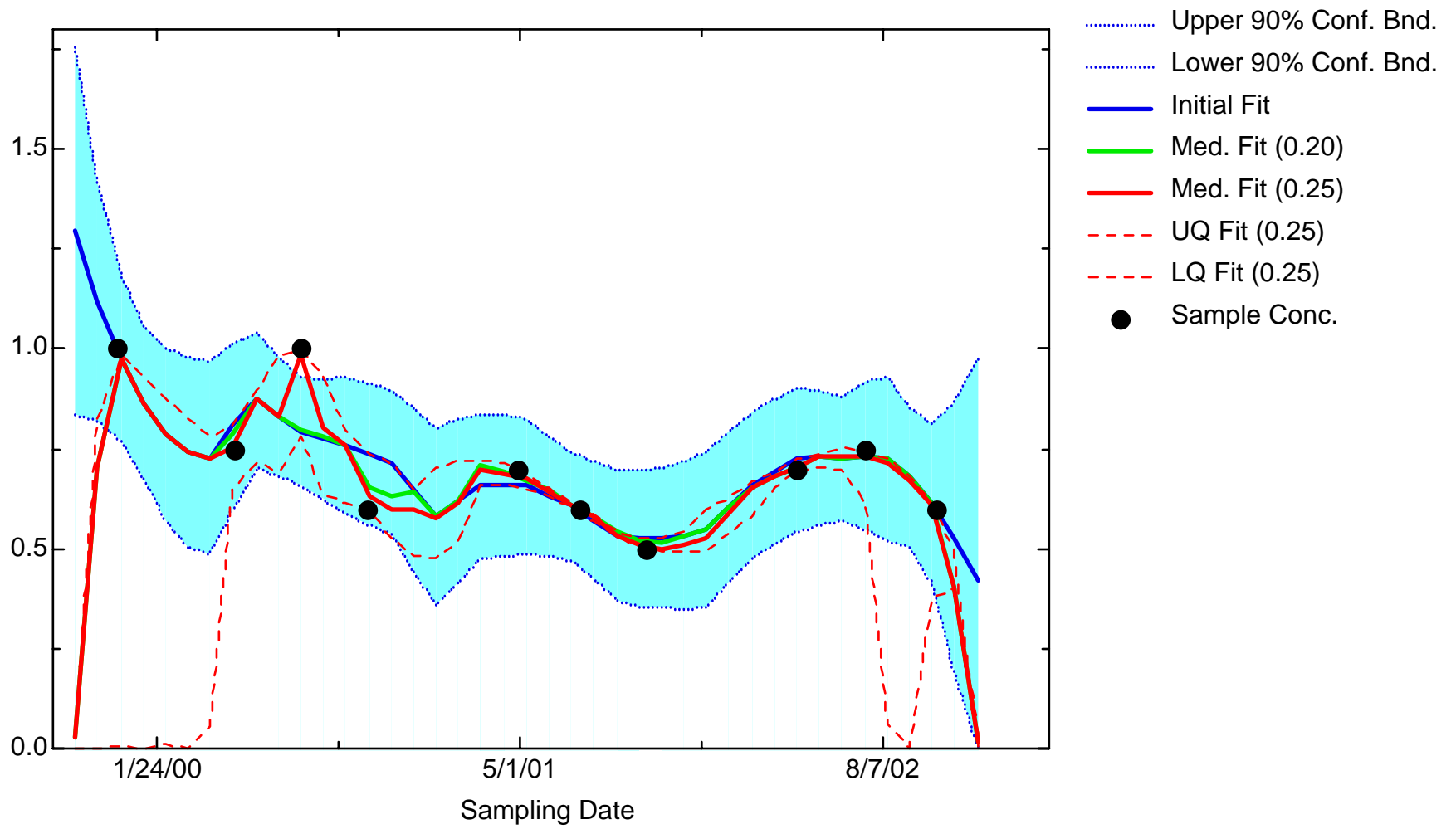
BZ: Well MMW1560



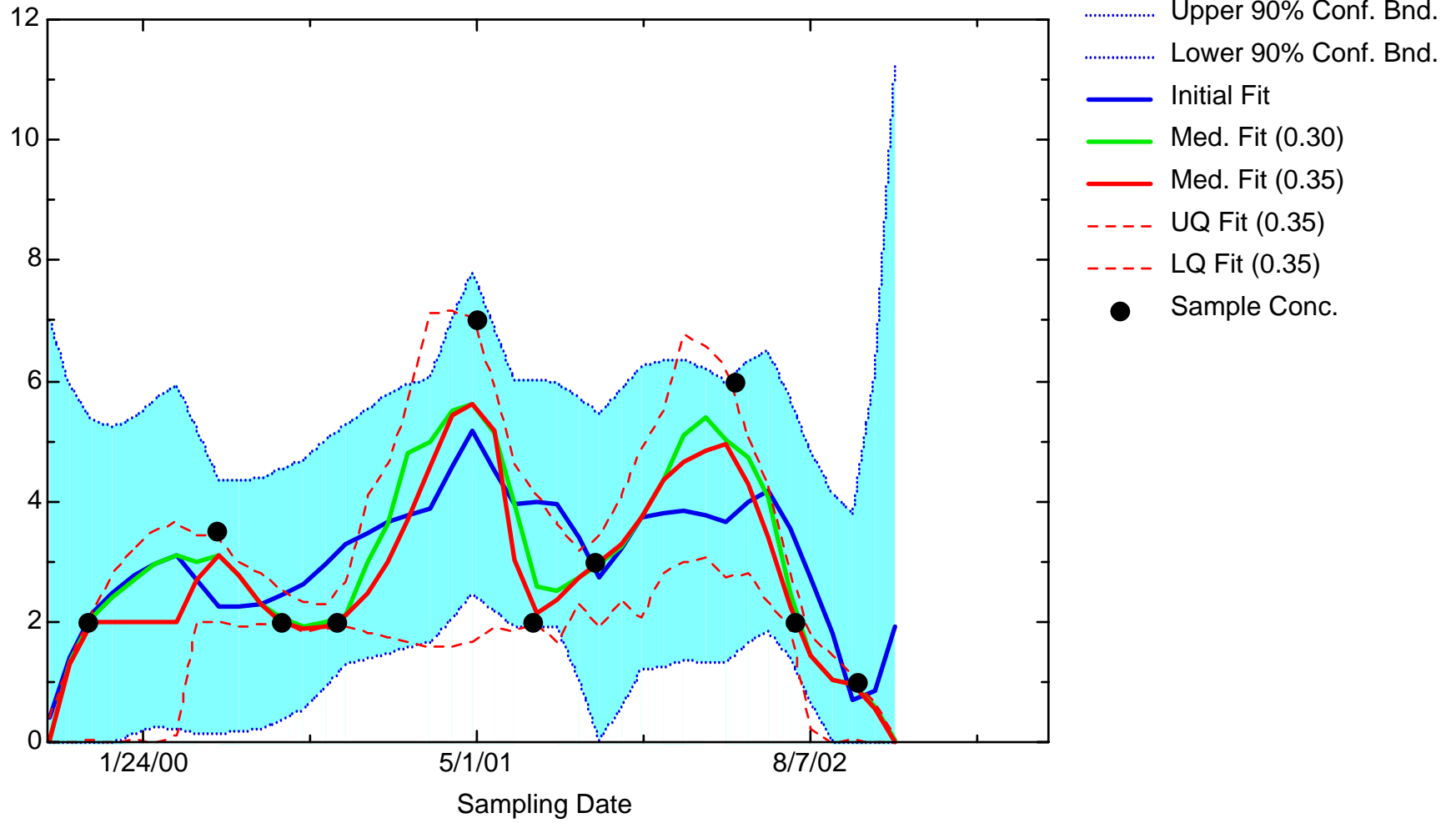
BZ: Well MMW7330



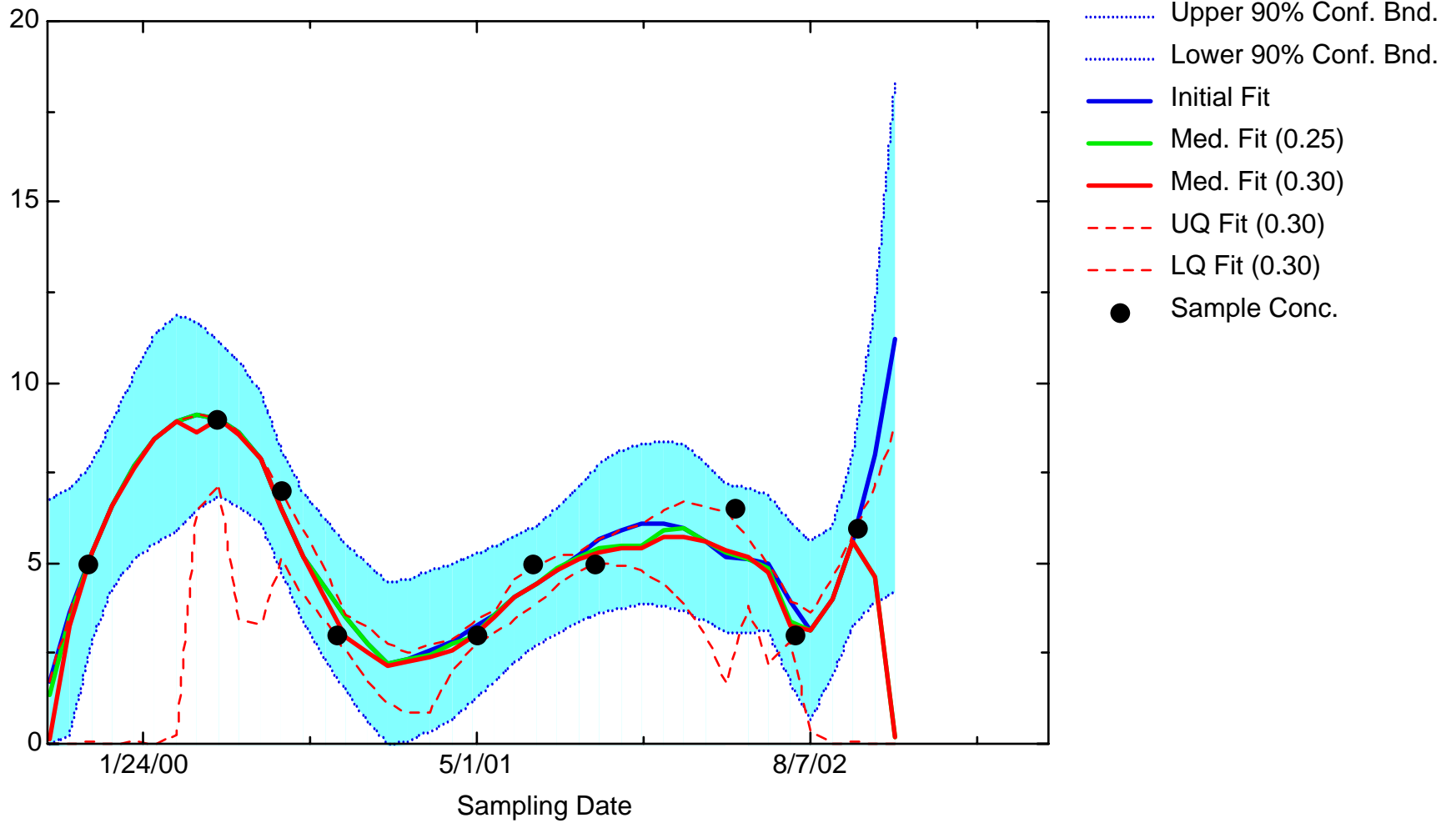
BZ: Well MMW8015



BZ: Well RFW1144



BZ: Well RFW1147



Appendix 3-2

Temporal Optimization: FE Iterative Fitting Overlays

Key to acronyms:

Conf Bnd = Confidence bound

Initial Fit = Locally-weighted quadratic regression (LWQR) estimate on baseline dataset

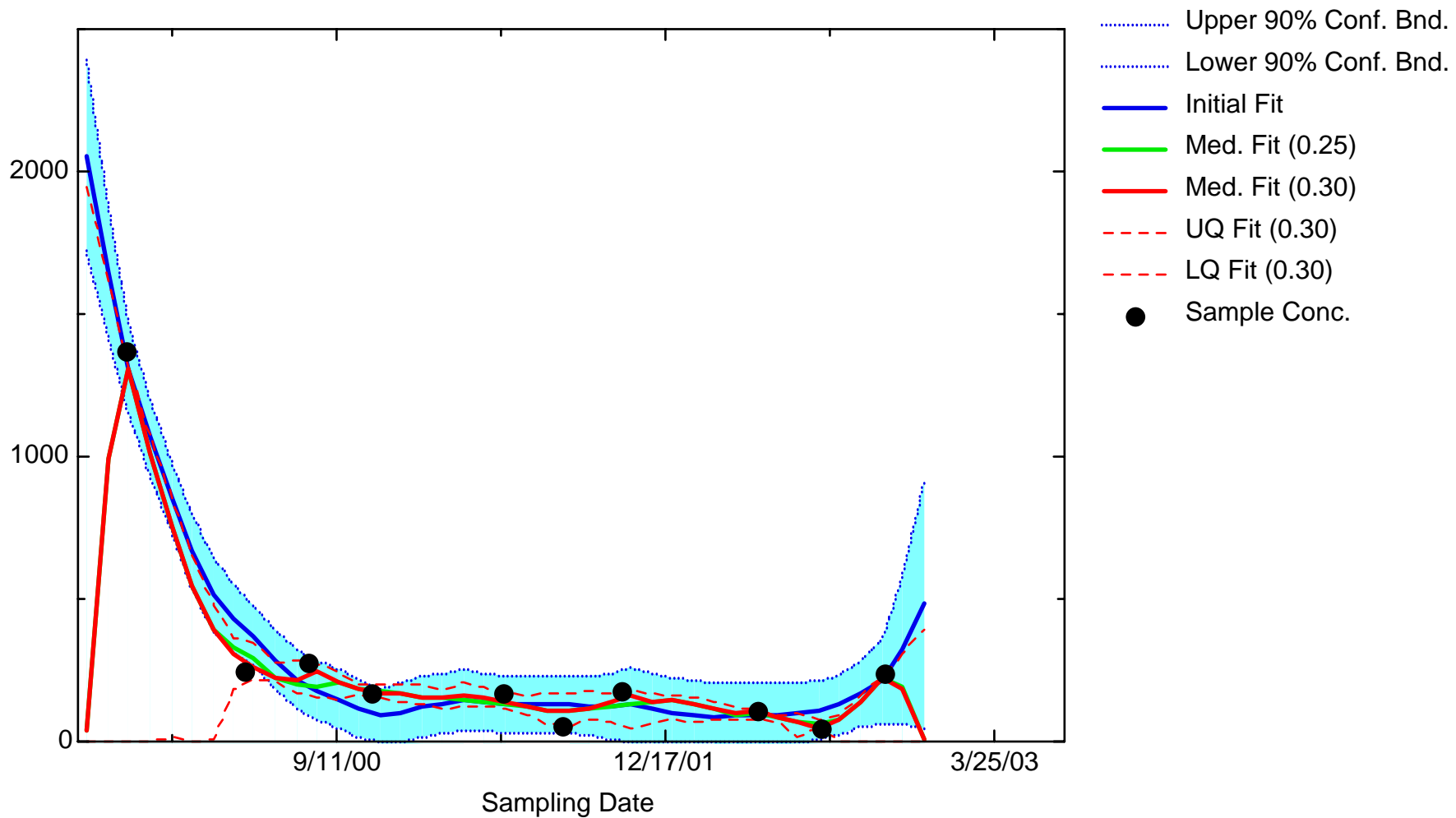
Med Fit = Median of 500 pointwise LWQR estimates on reduced dataset

LQ Fit = Lower quartile of 500 pointwise LWQR estimates on reduced dataset

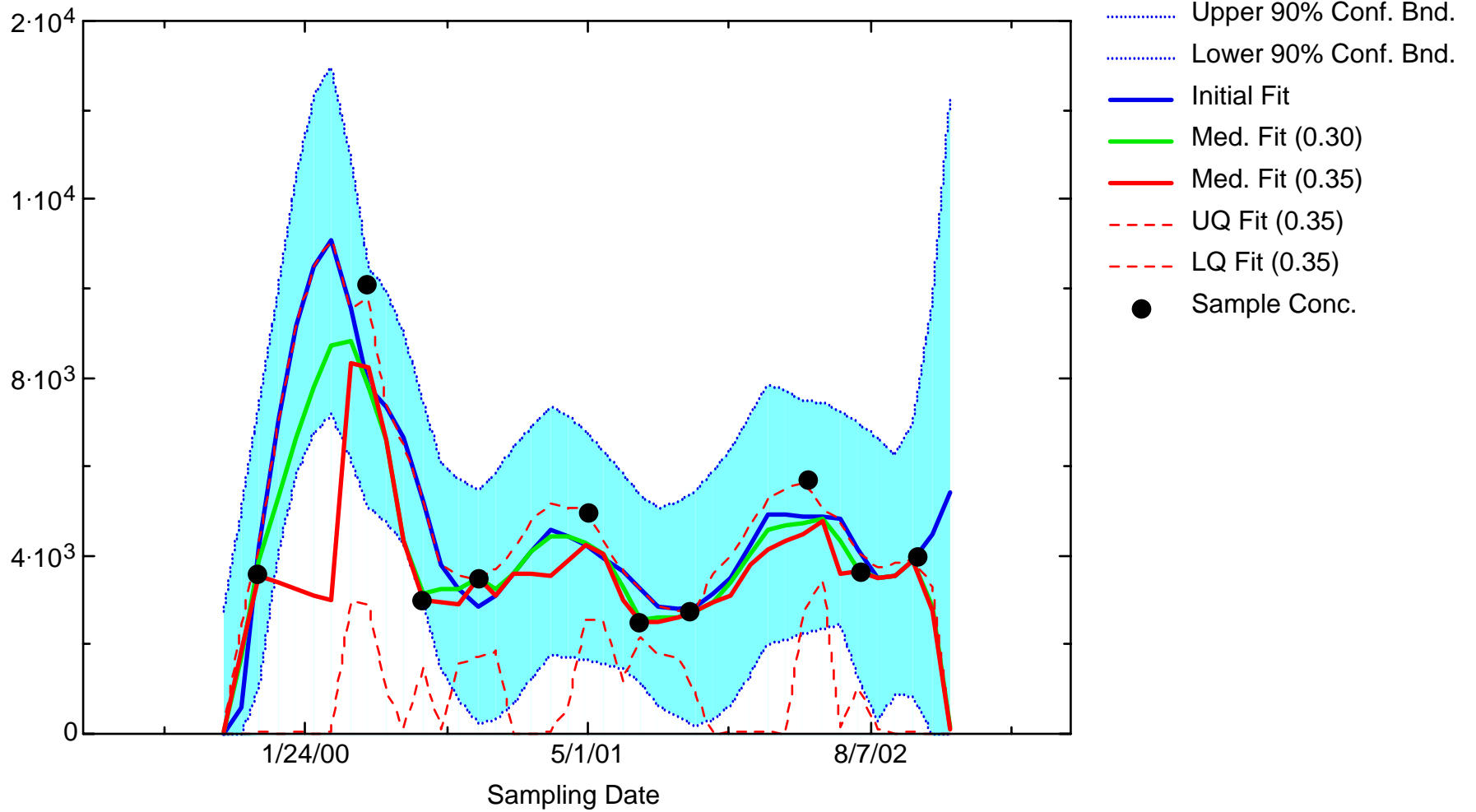
UQ Fit = Upper quartile of 500 pointwise LWQR estimates on reduced dataset

Conc = Concentration

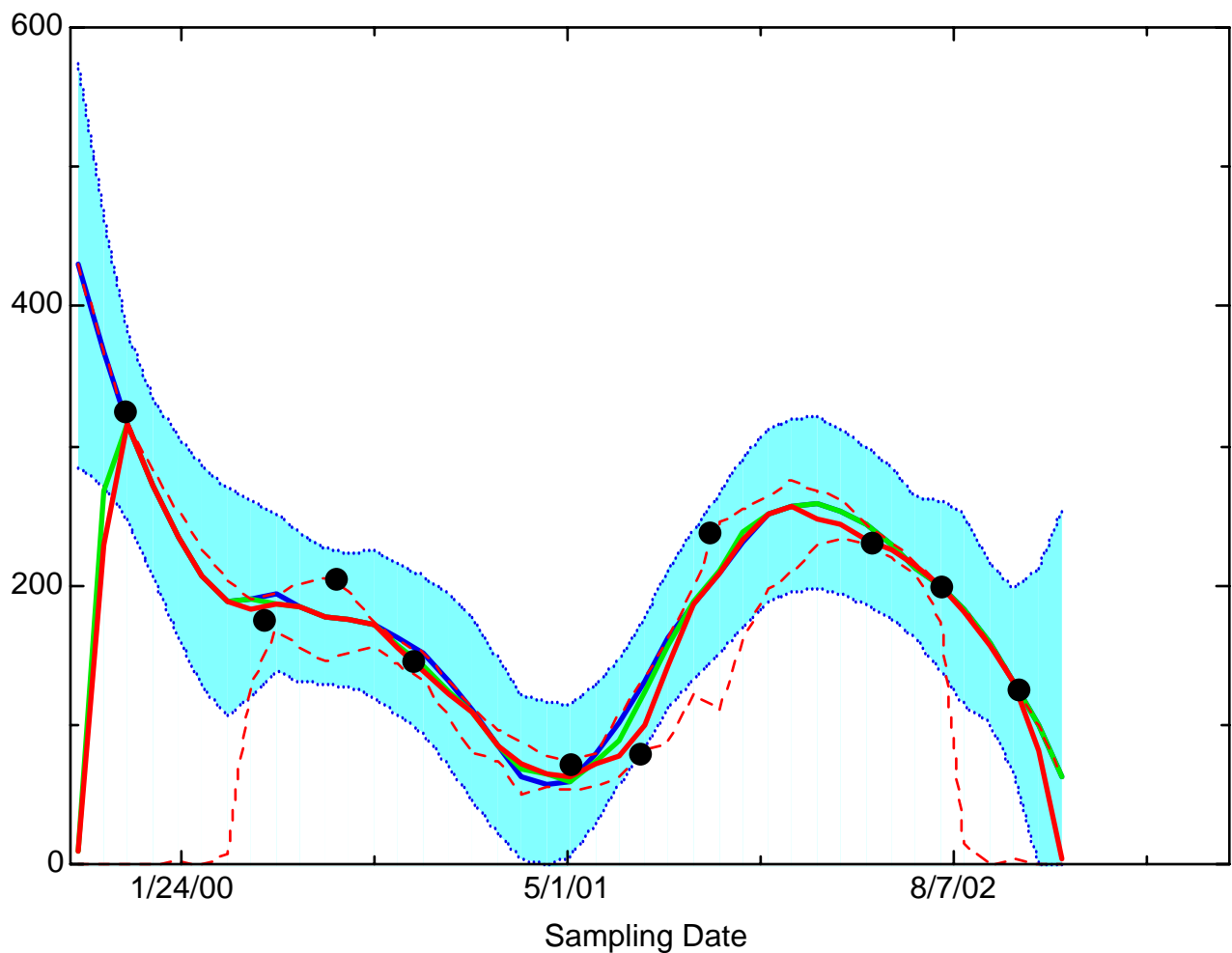
FE: Well 056MW02



FE: Well 056MW04

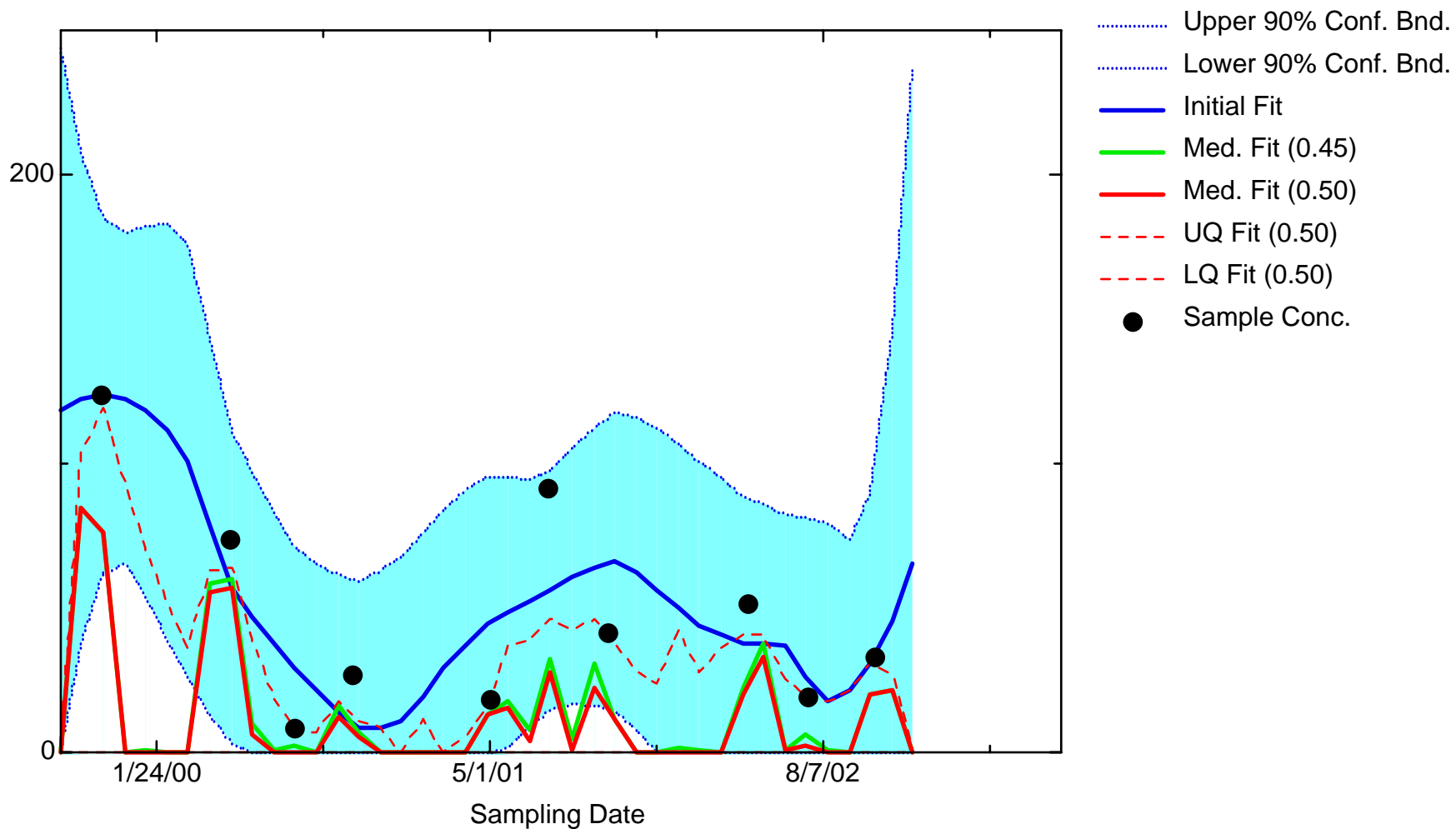


FE: Well AR25

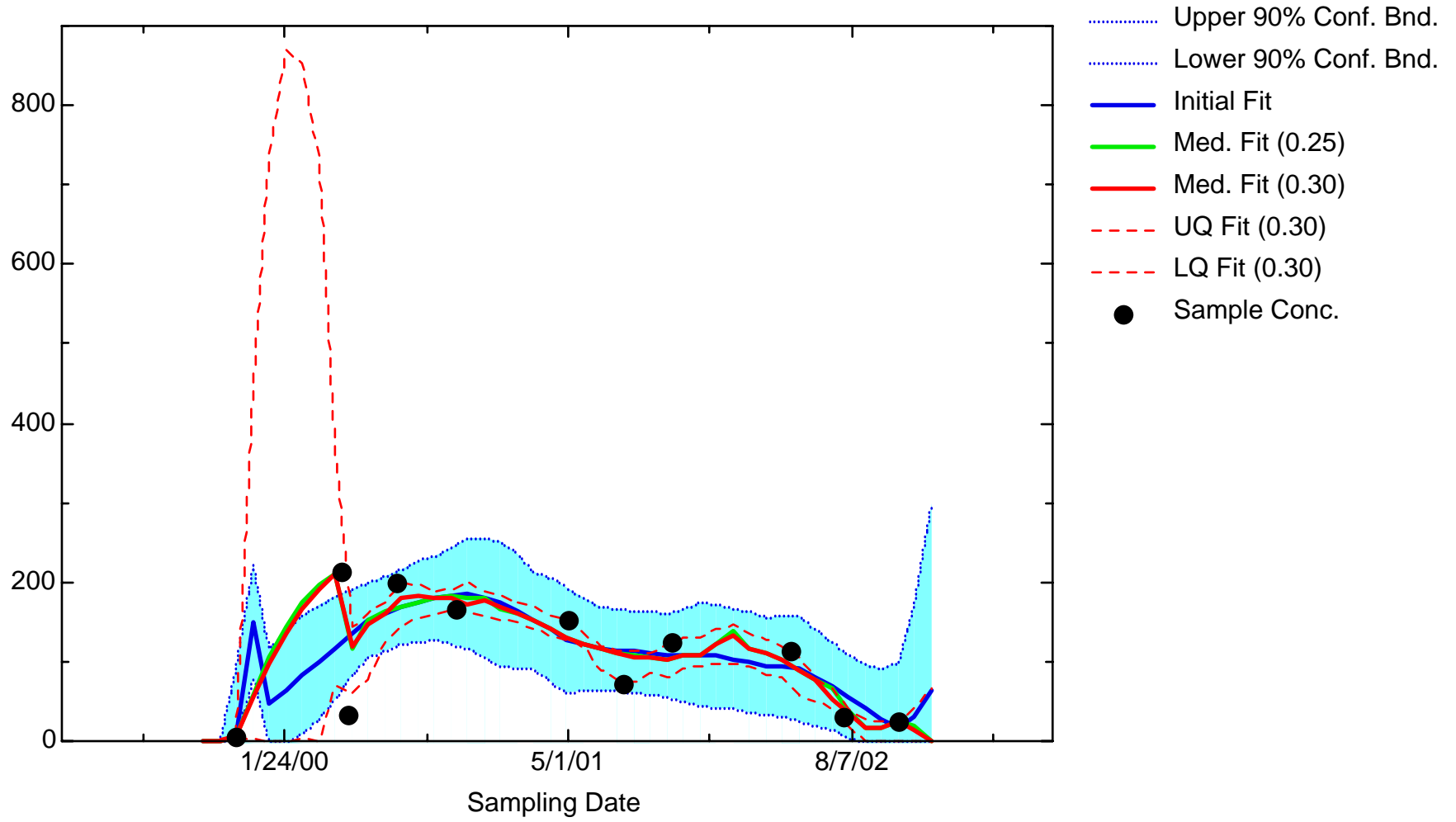


- Upper 90% Conf. Bnd.
- Lower 90% Conf. Bnd.
- Initial Fit
- Med. Fit (0.25)
- Med. Fit (0.30)
- UQ Fit (0.30)
- LQ Fit (0.30)
- Sample Conc.

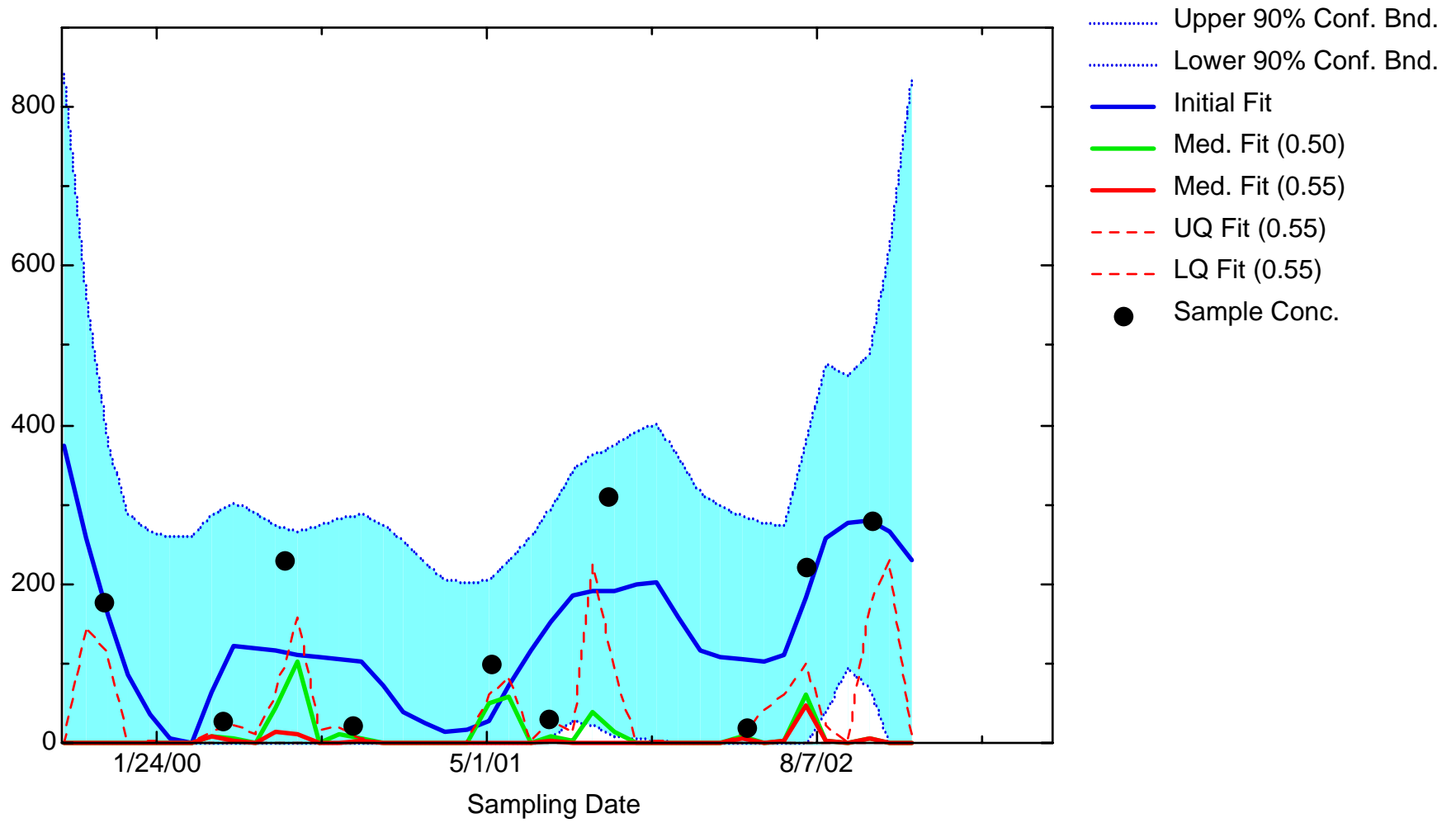
FE: Well FMW3413



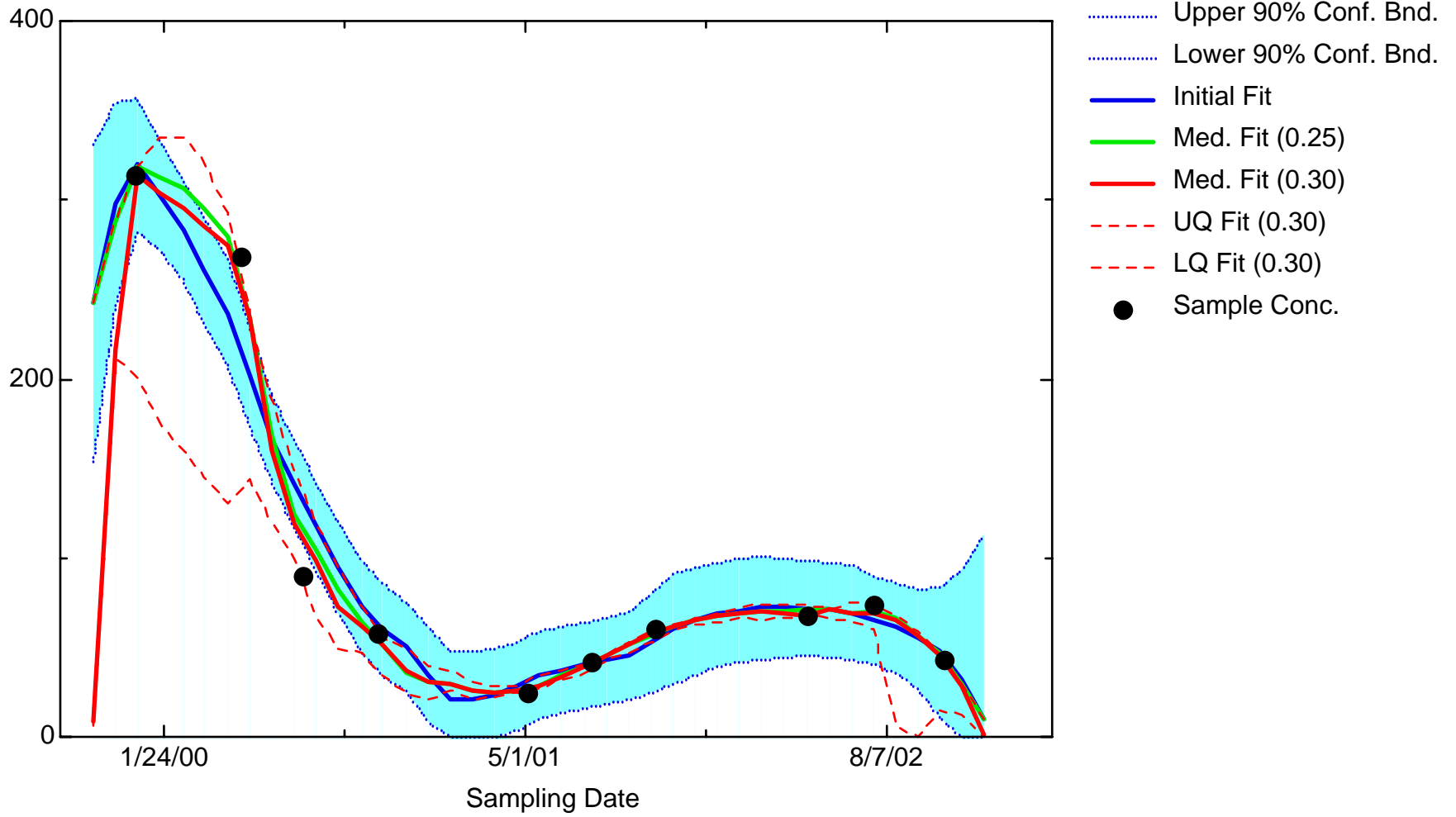
FE: Well JBW7101



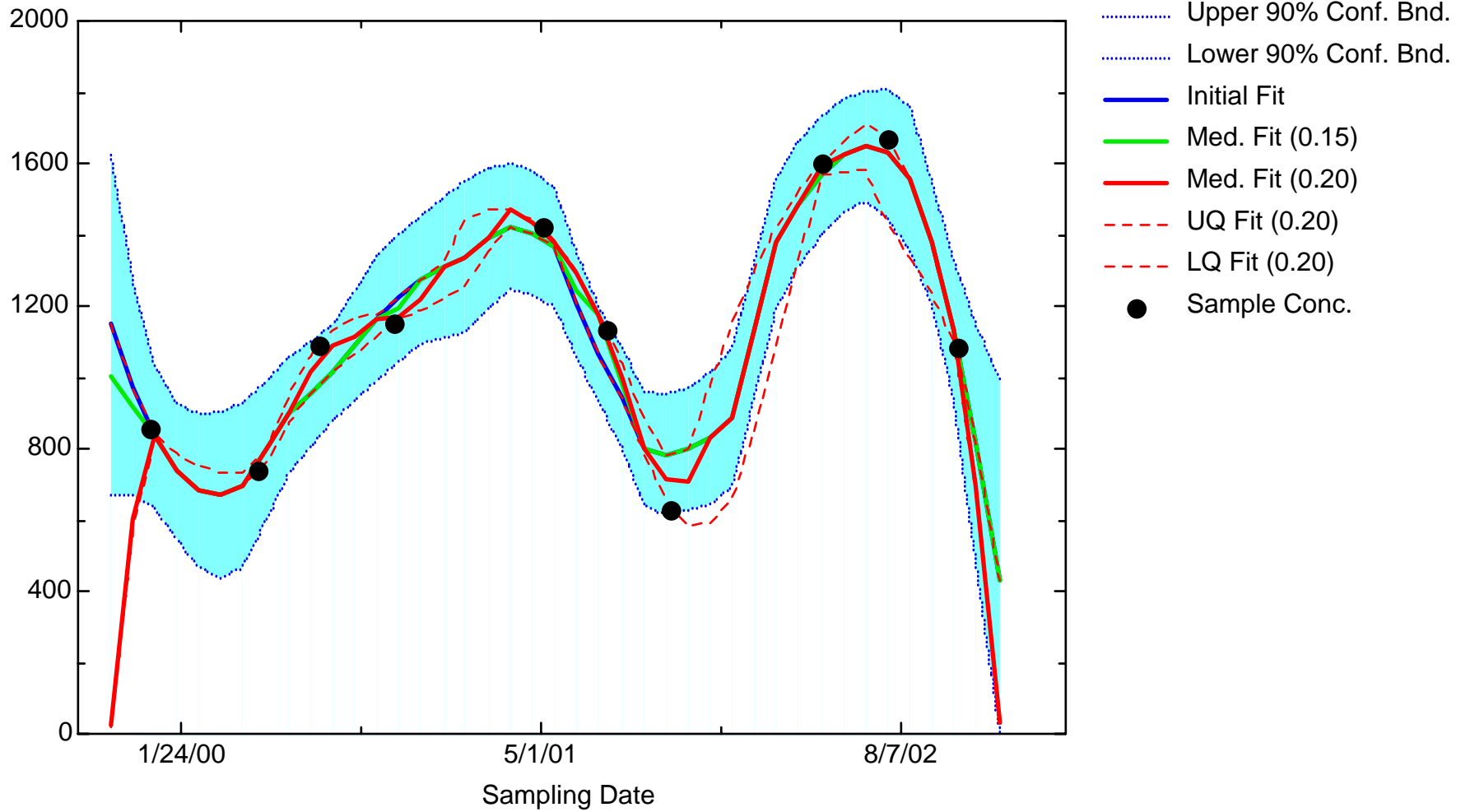
FE: Well JBW7102



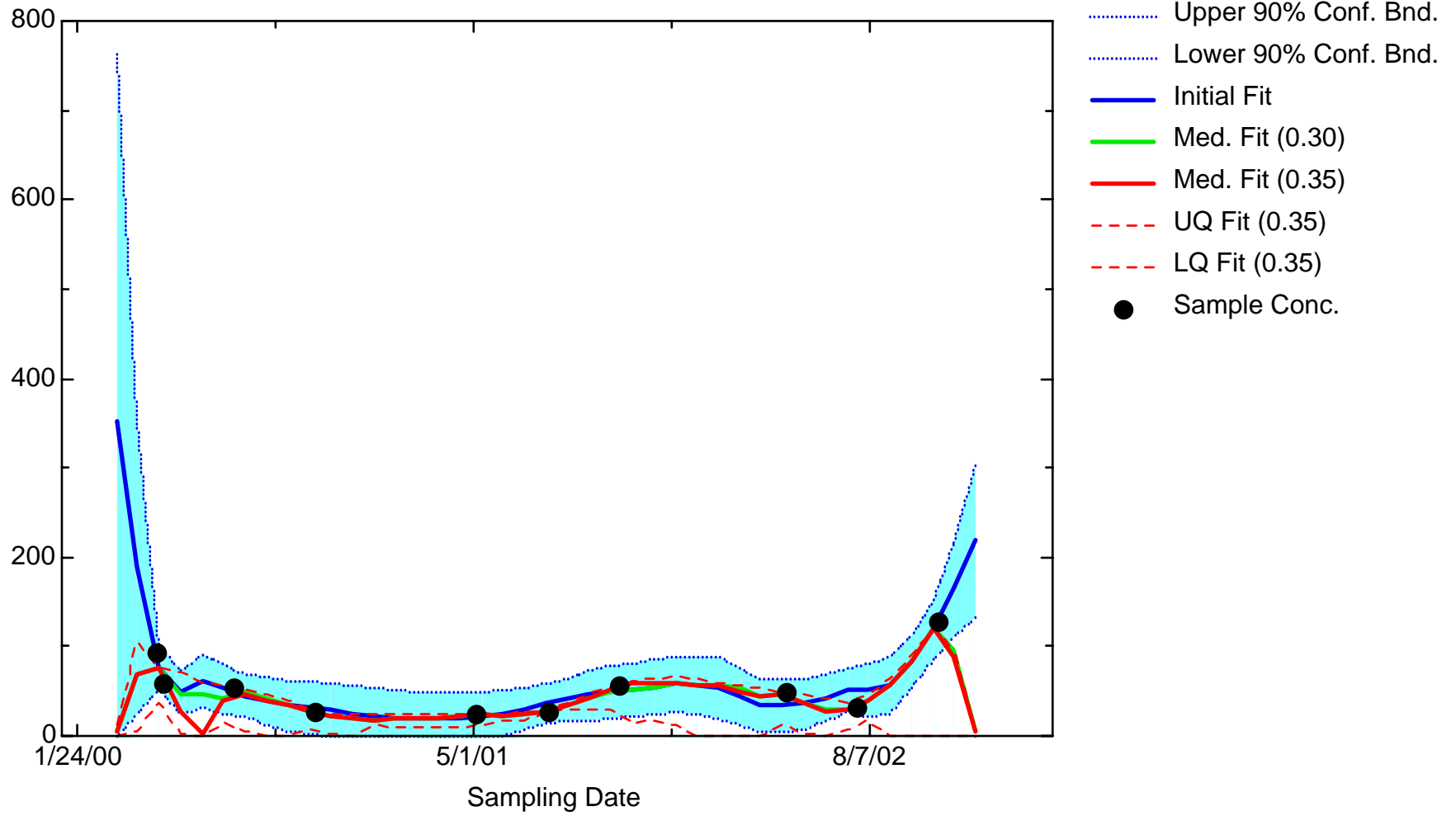
FE: Well JBW7106A



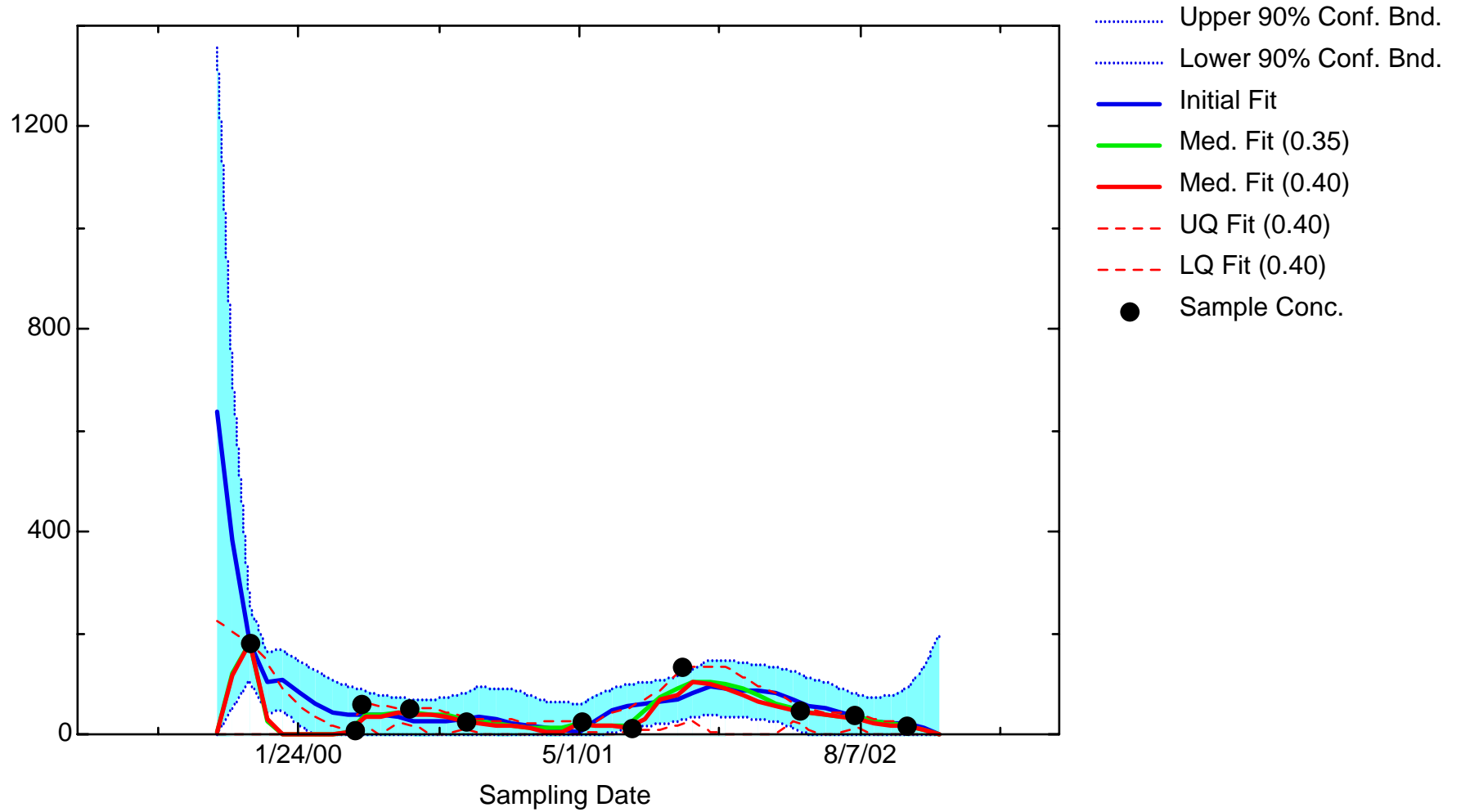
FE: Well JBW7106B



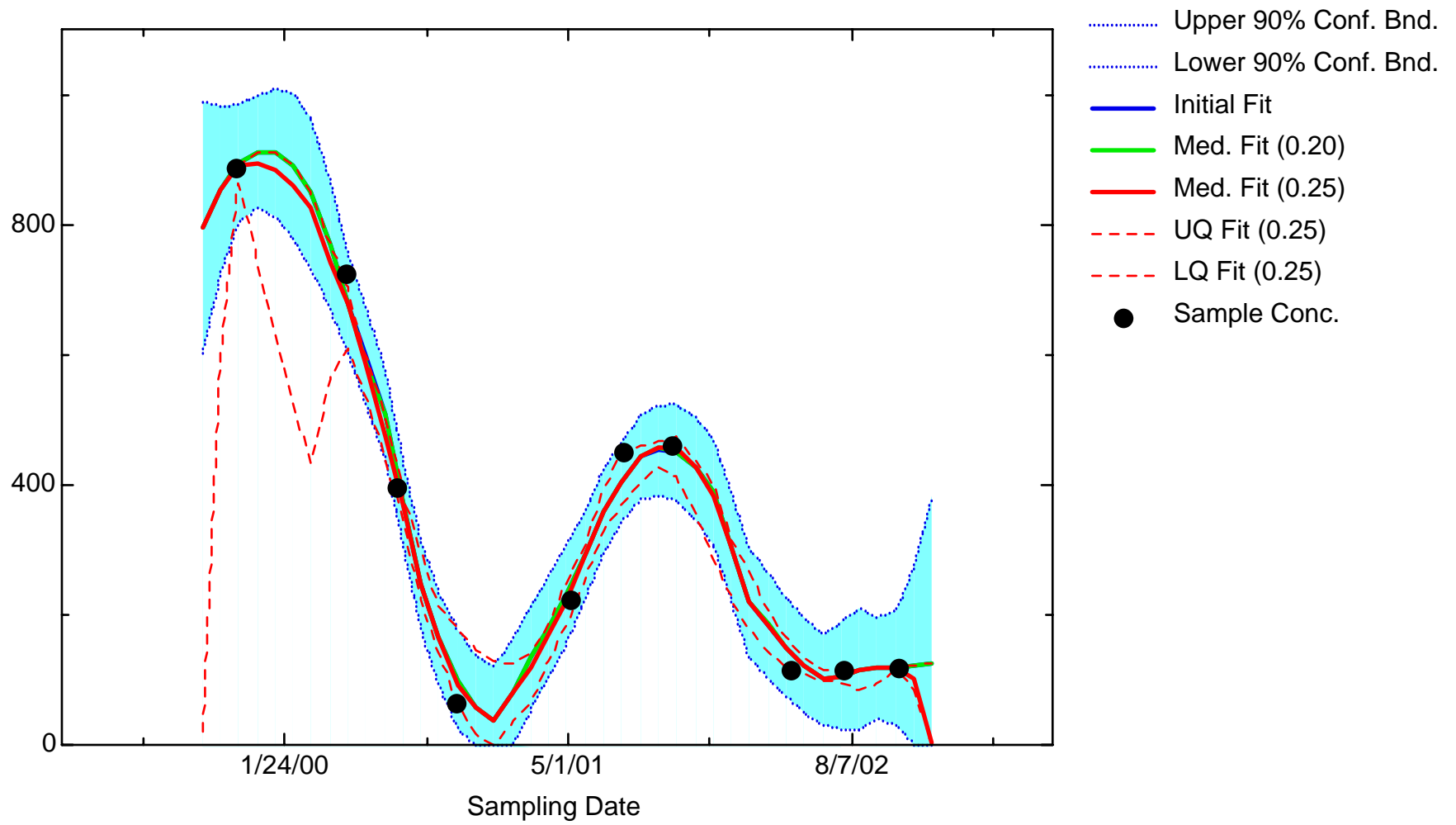
FE: Well JBW7203A



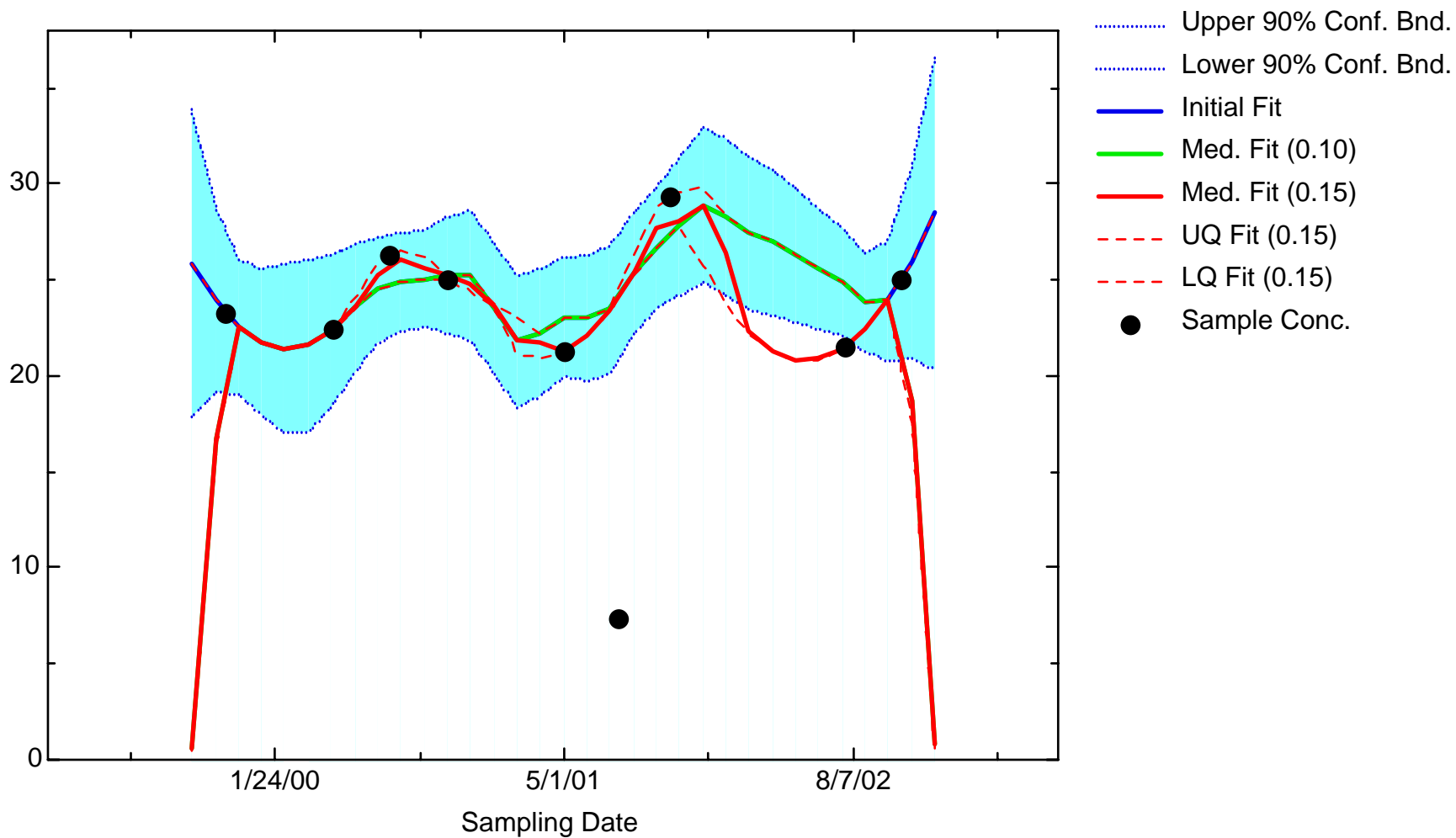
FE: Well JBW7203B



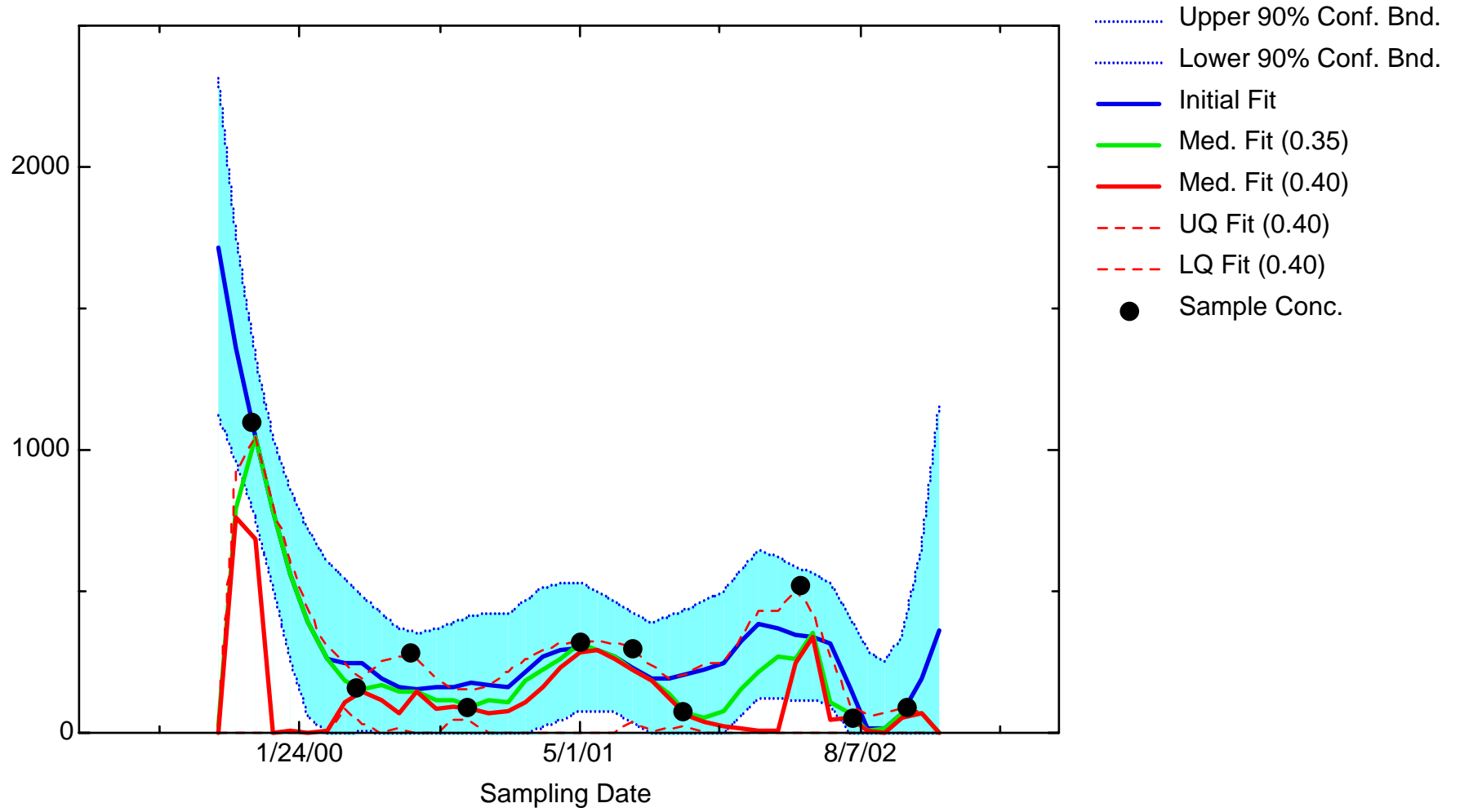
FE: Well JBW7204A



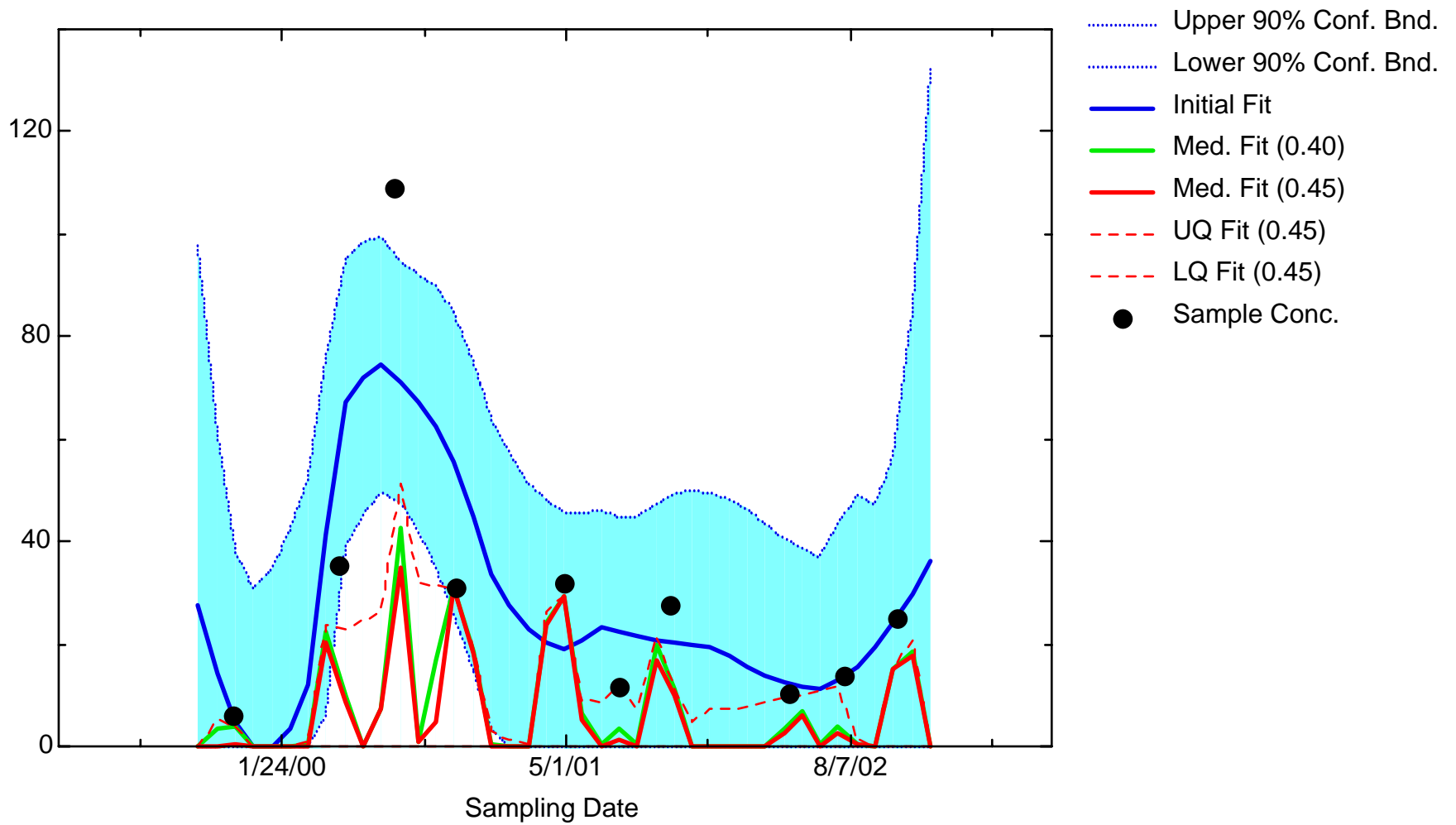
FE: Well JBW7212A



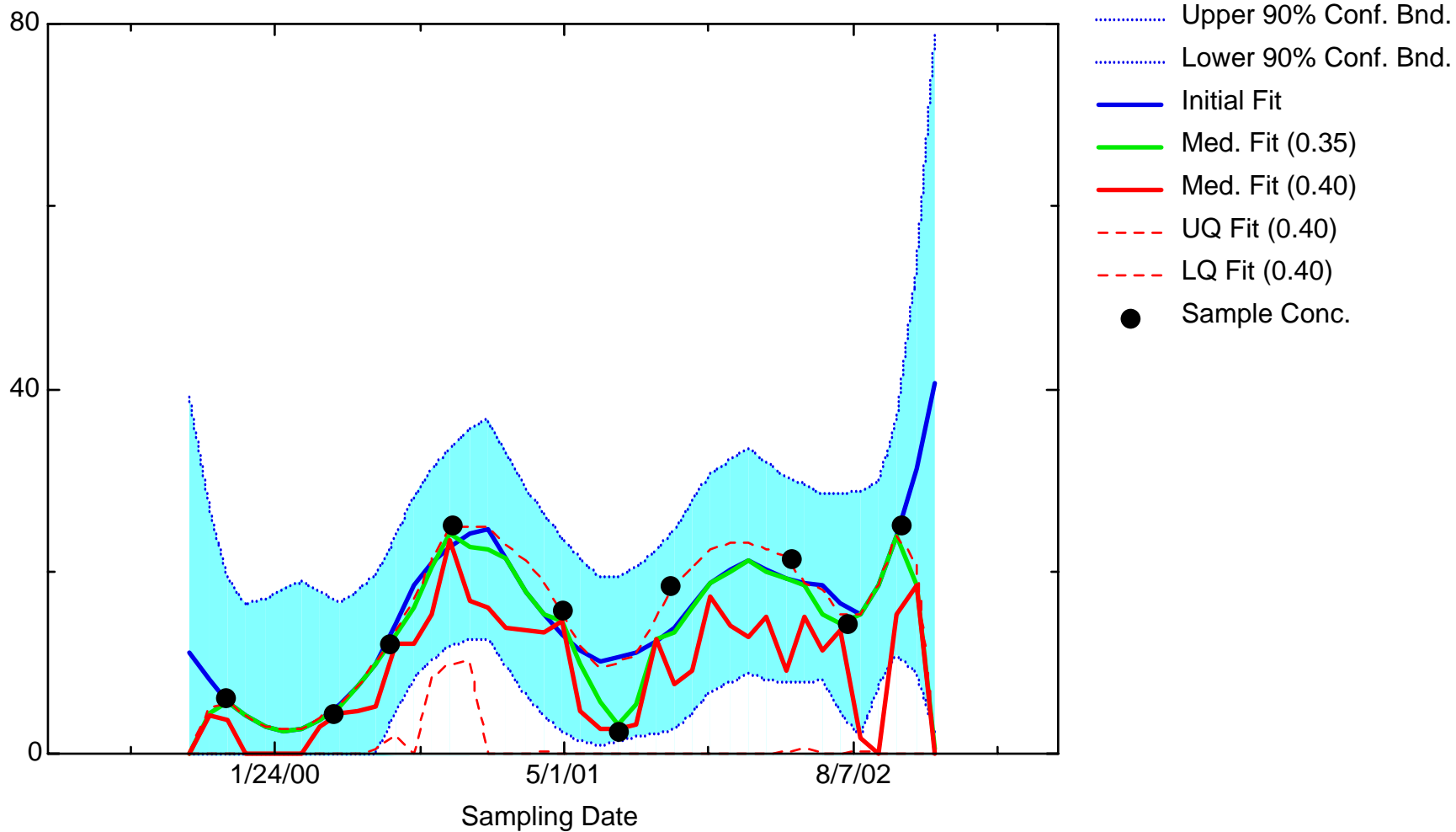
FE: Well JBW7212B



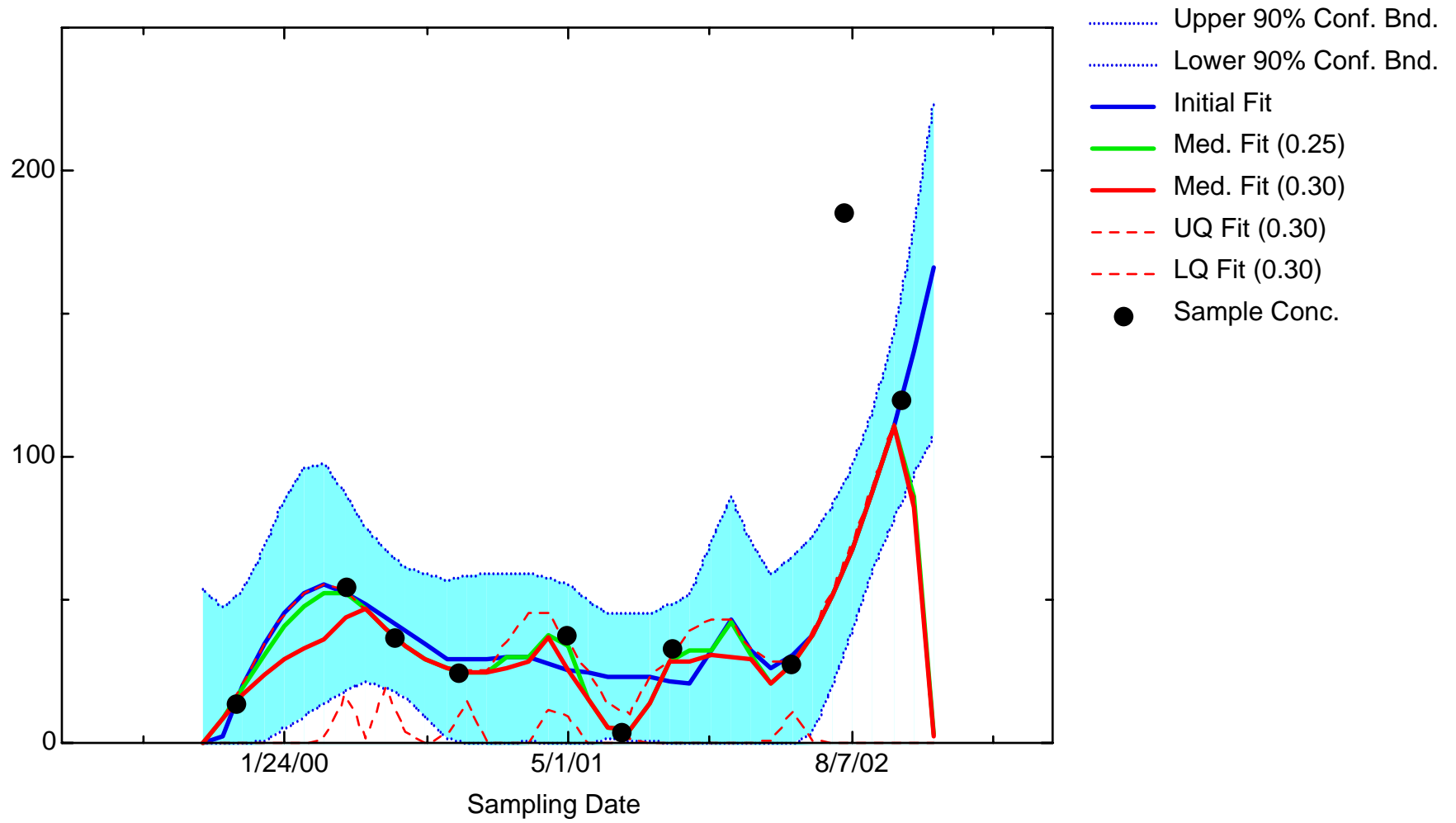
FE: Well JBW7213A



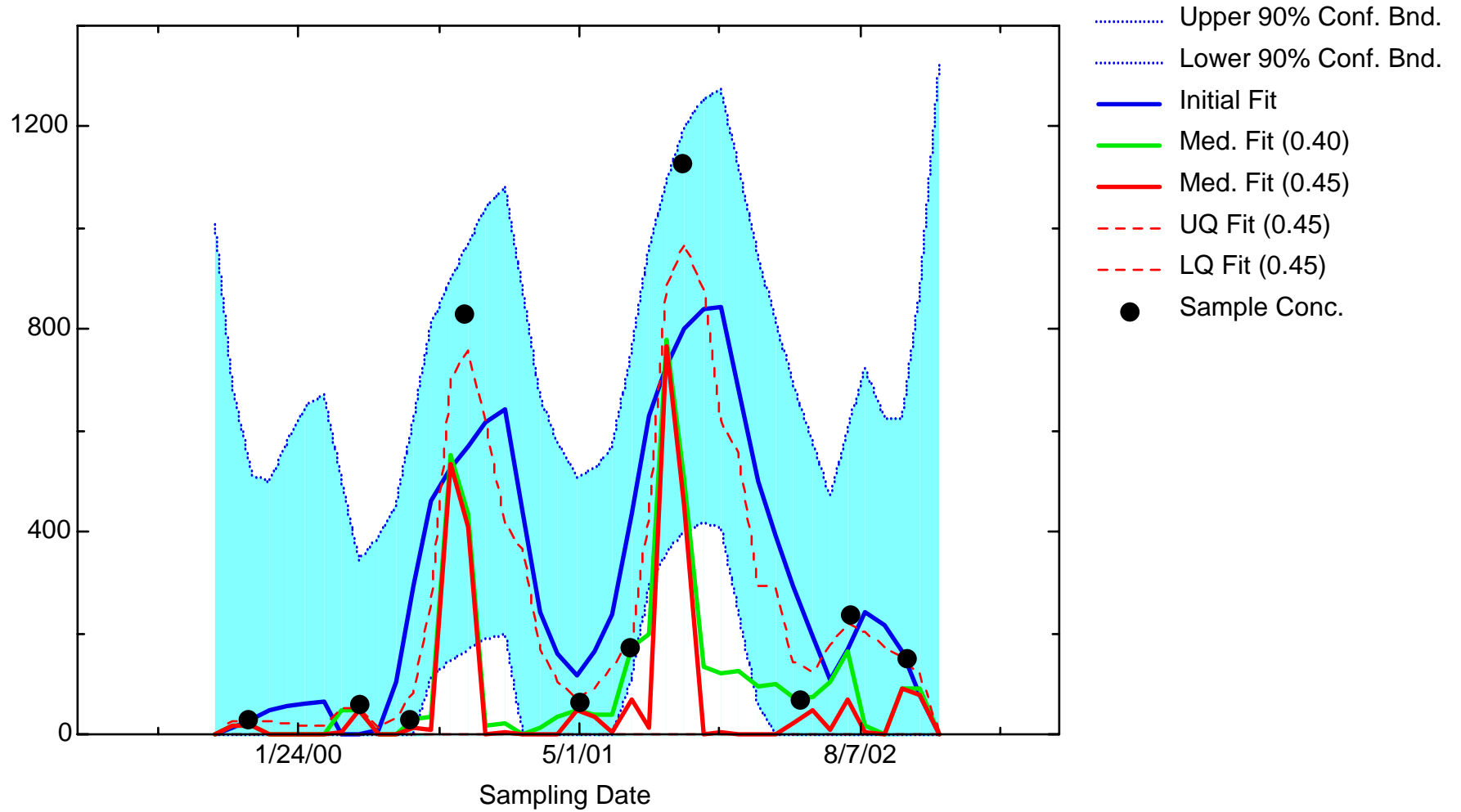
FE: Well JBW7213B



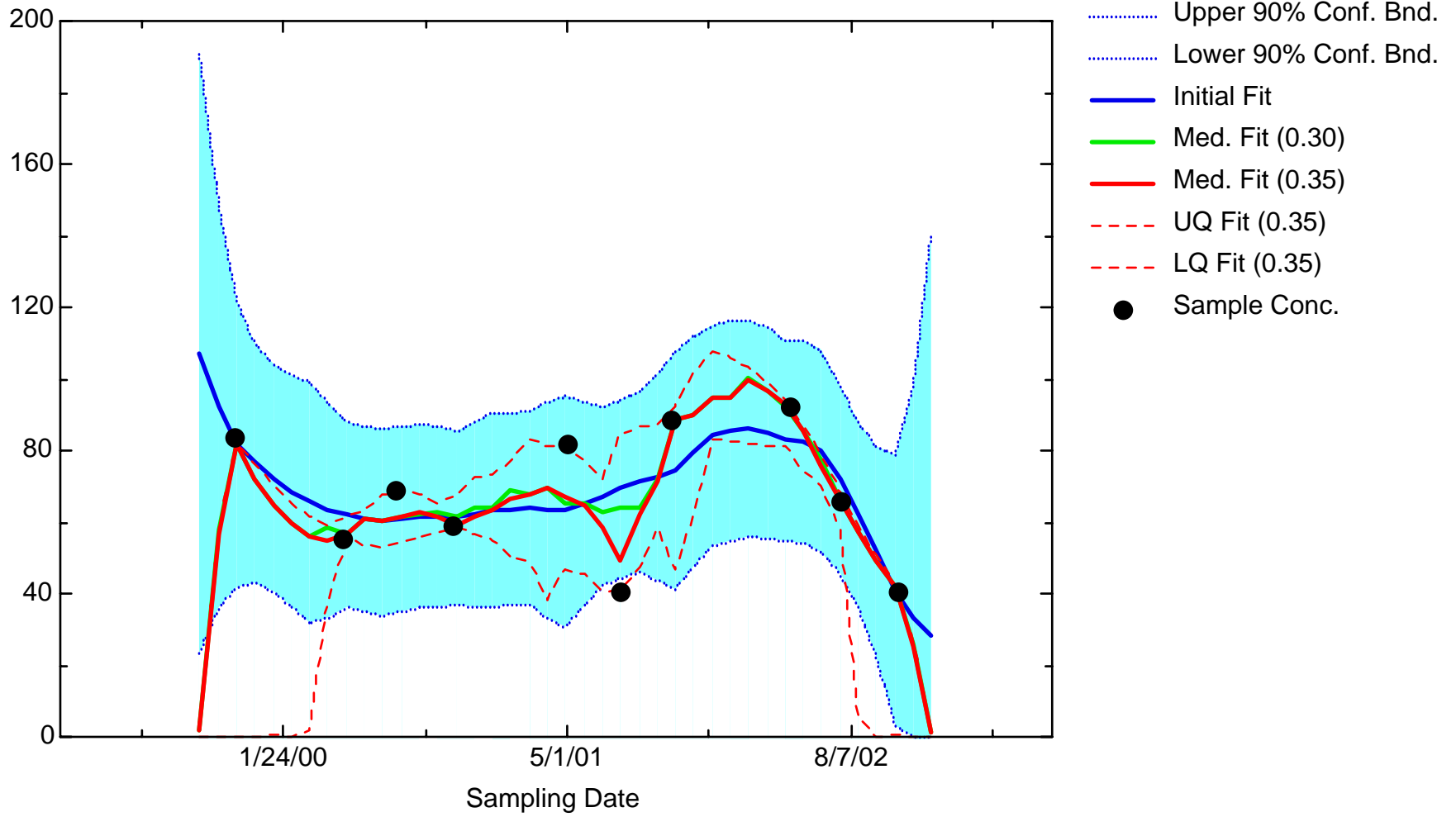
FE: Well JBW7215B



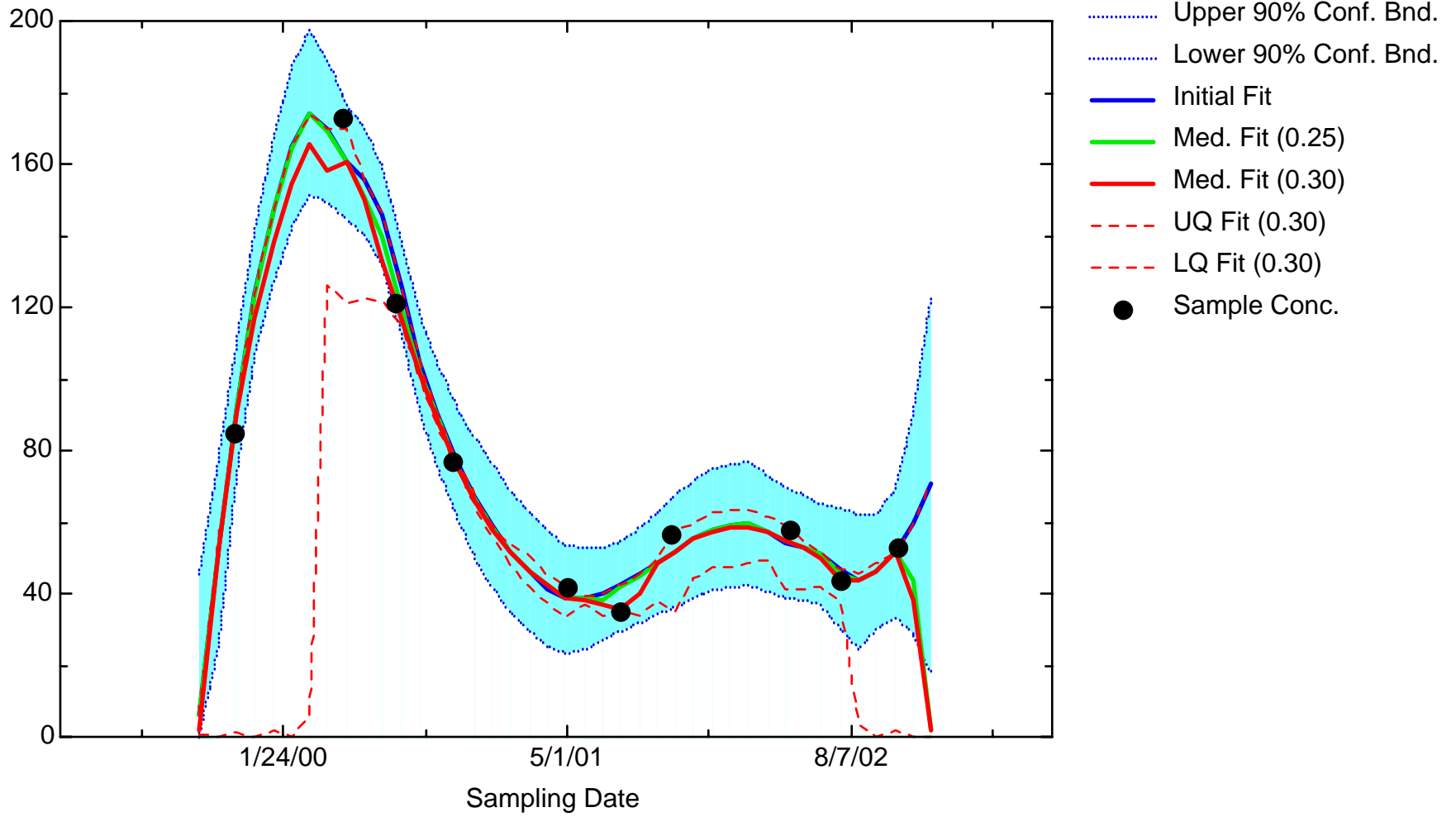
FE: Well JBW7317



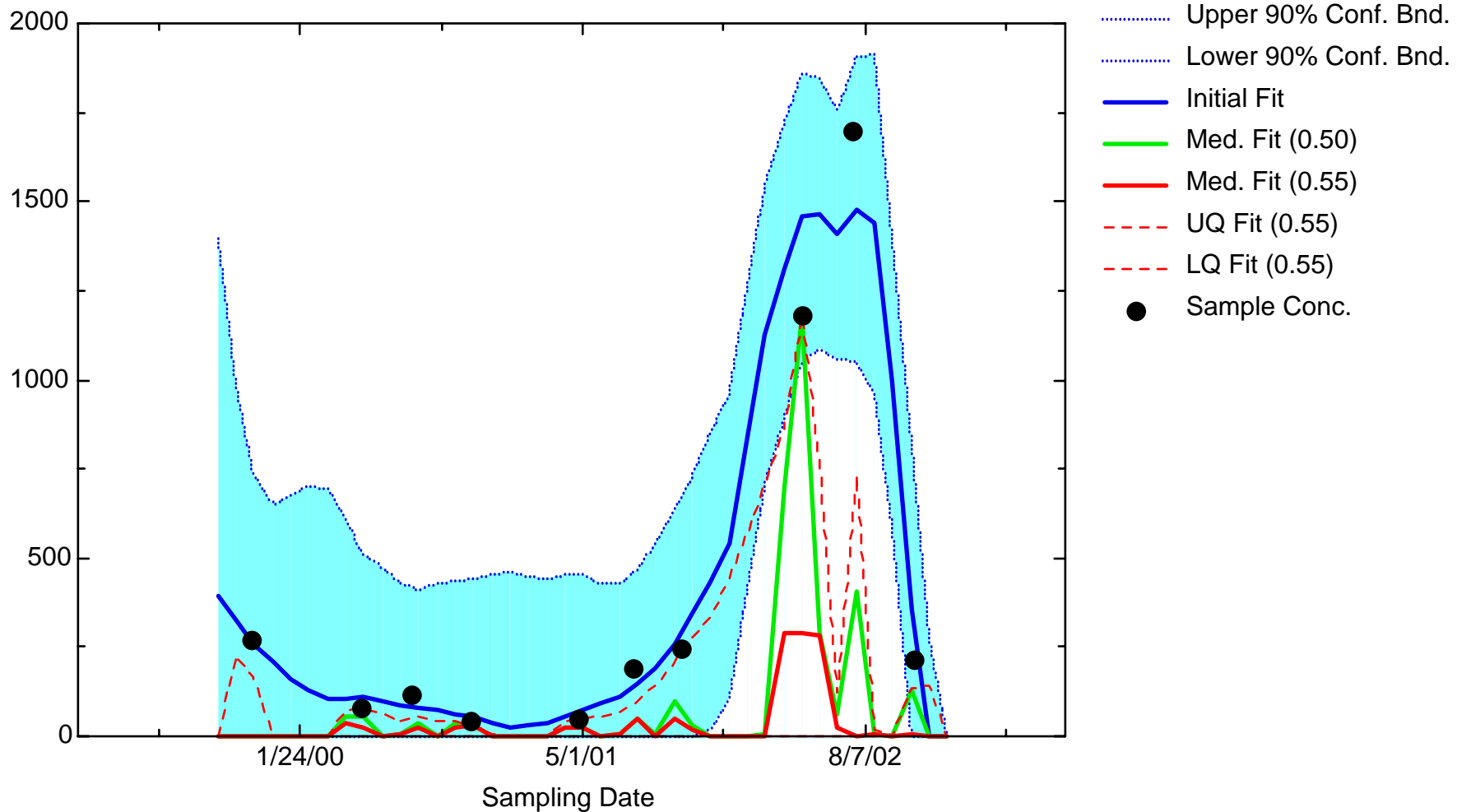
FE: Well JBW7326A



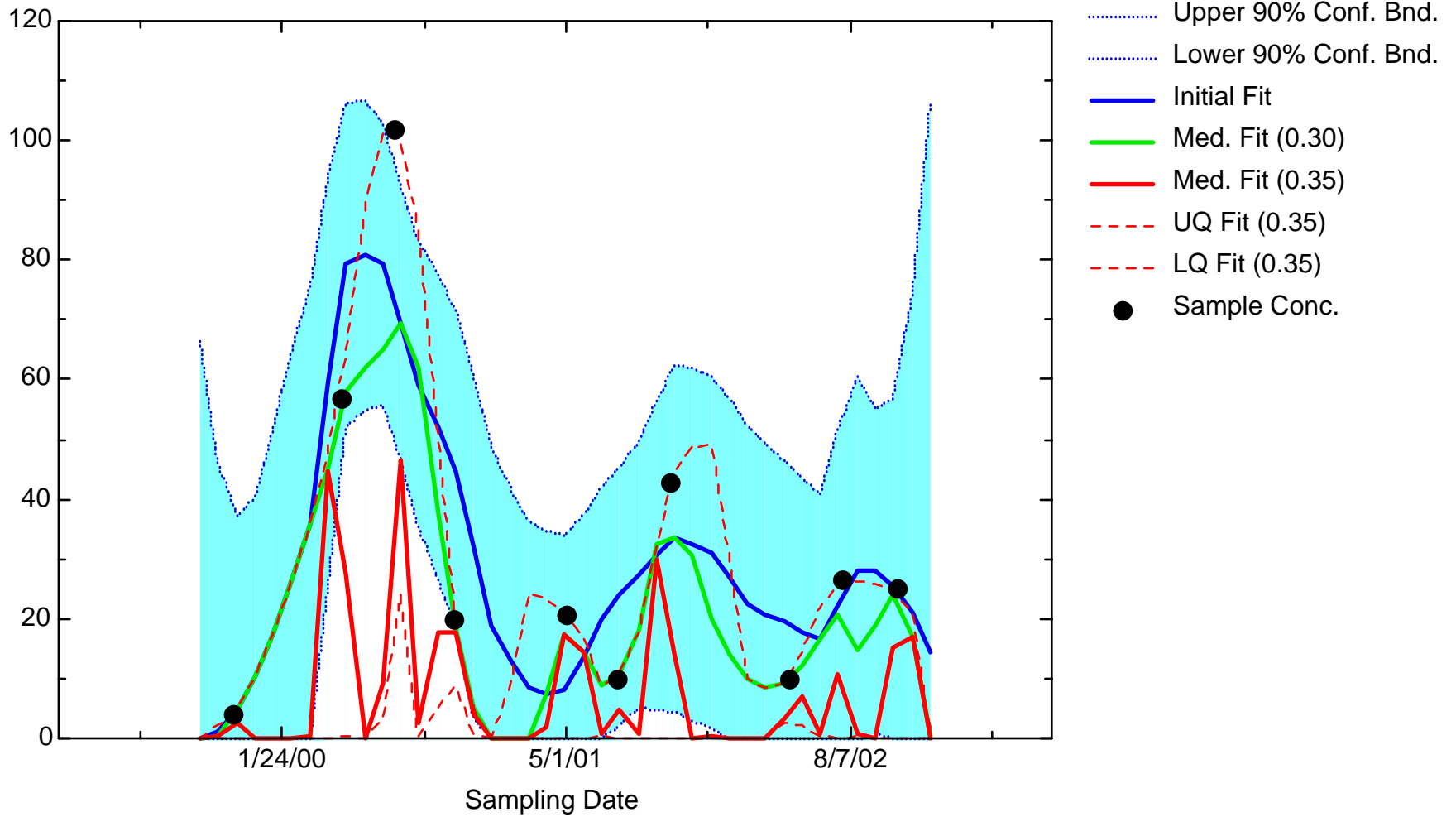
FE: Well JBW7326B



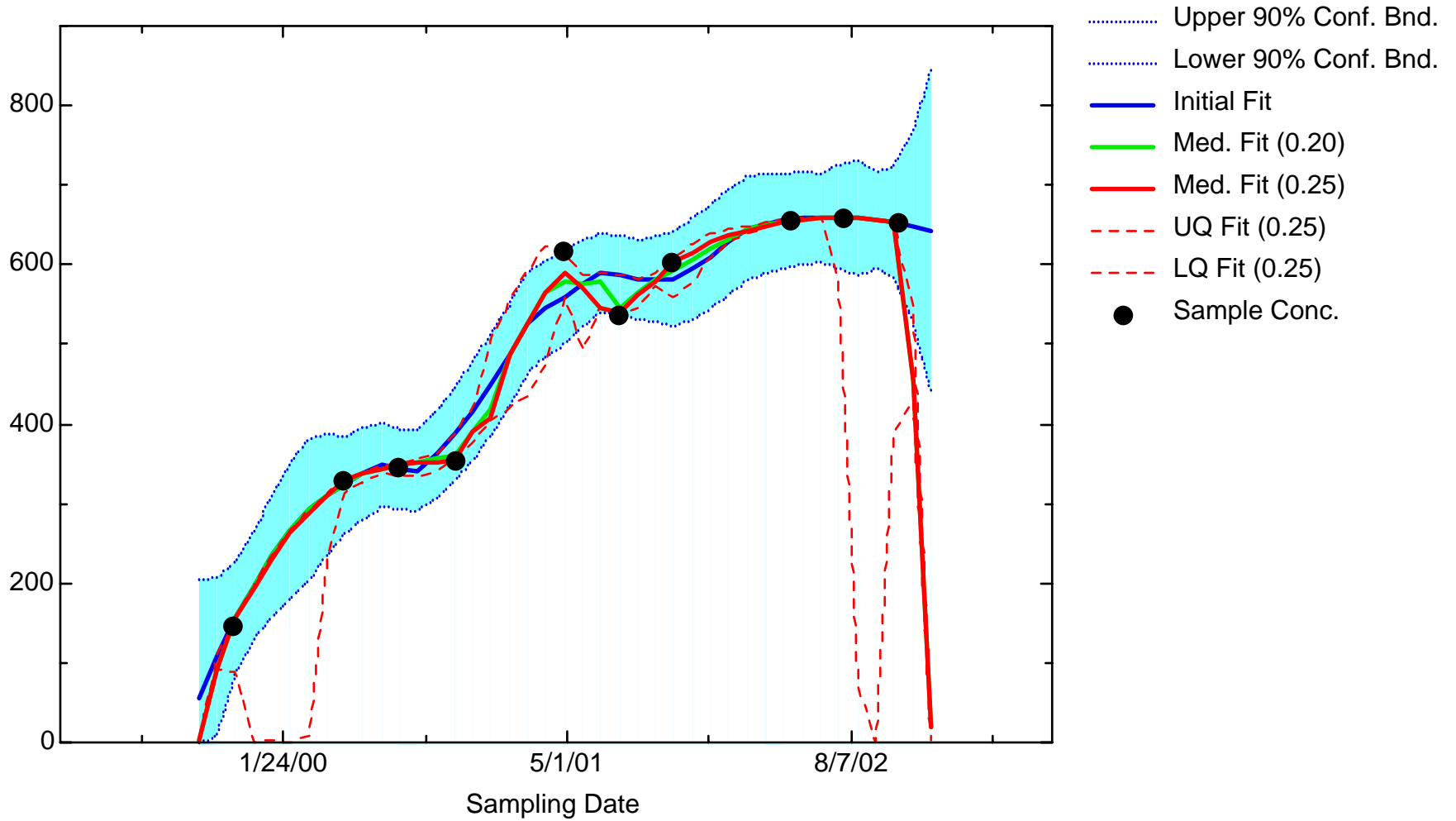
FE: Well JBW7328



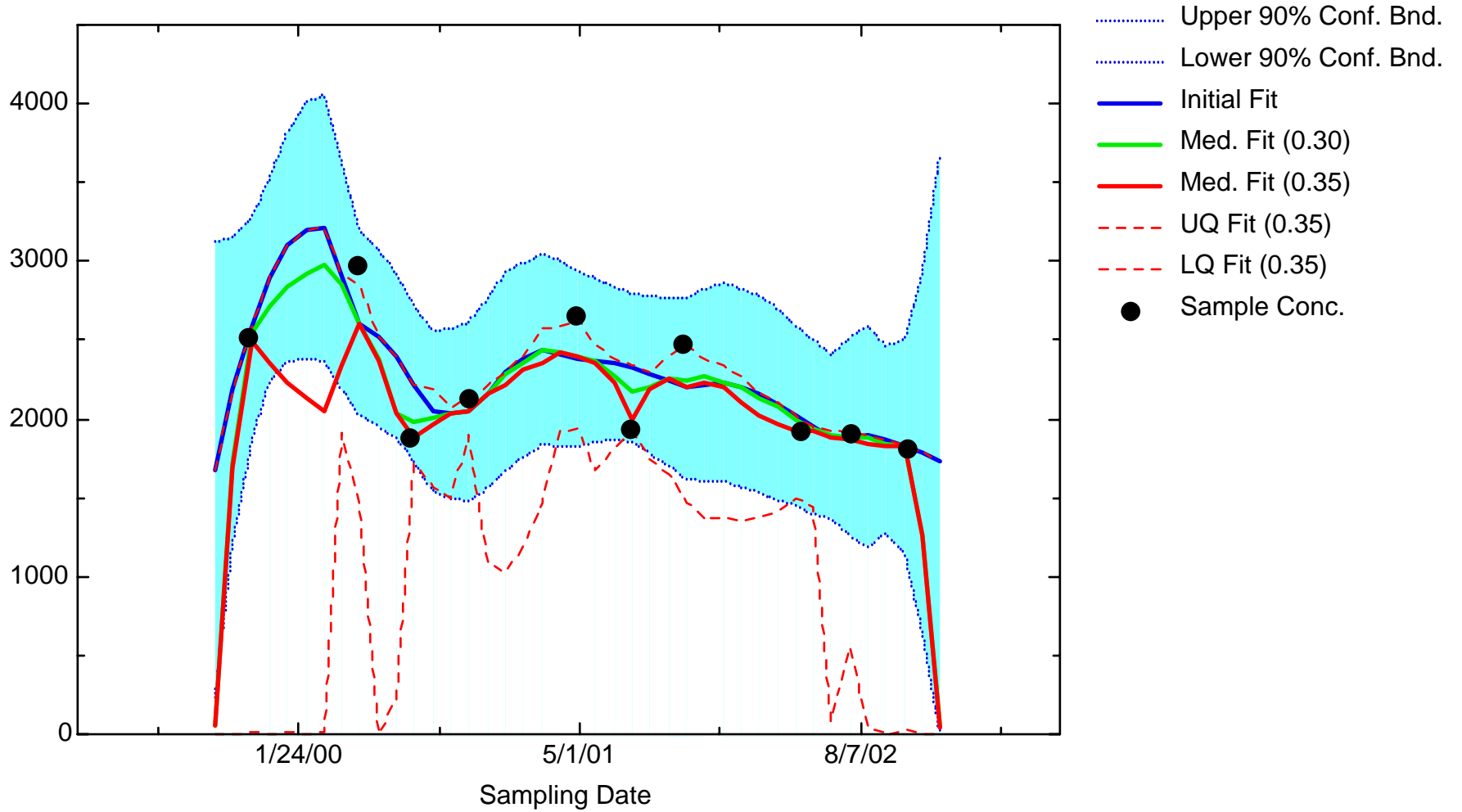
FE: Well JBW7330A



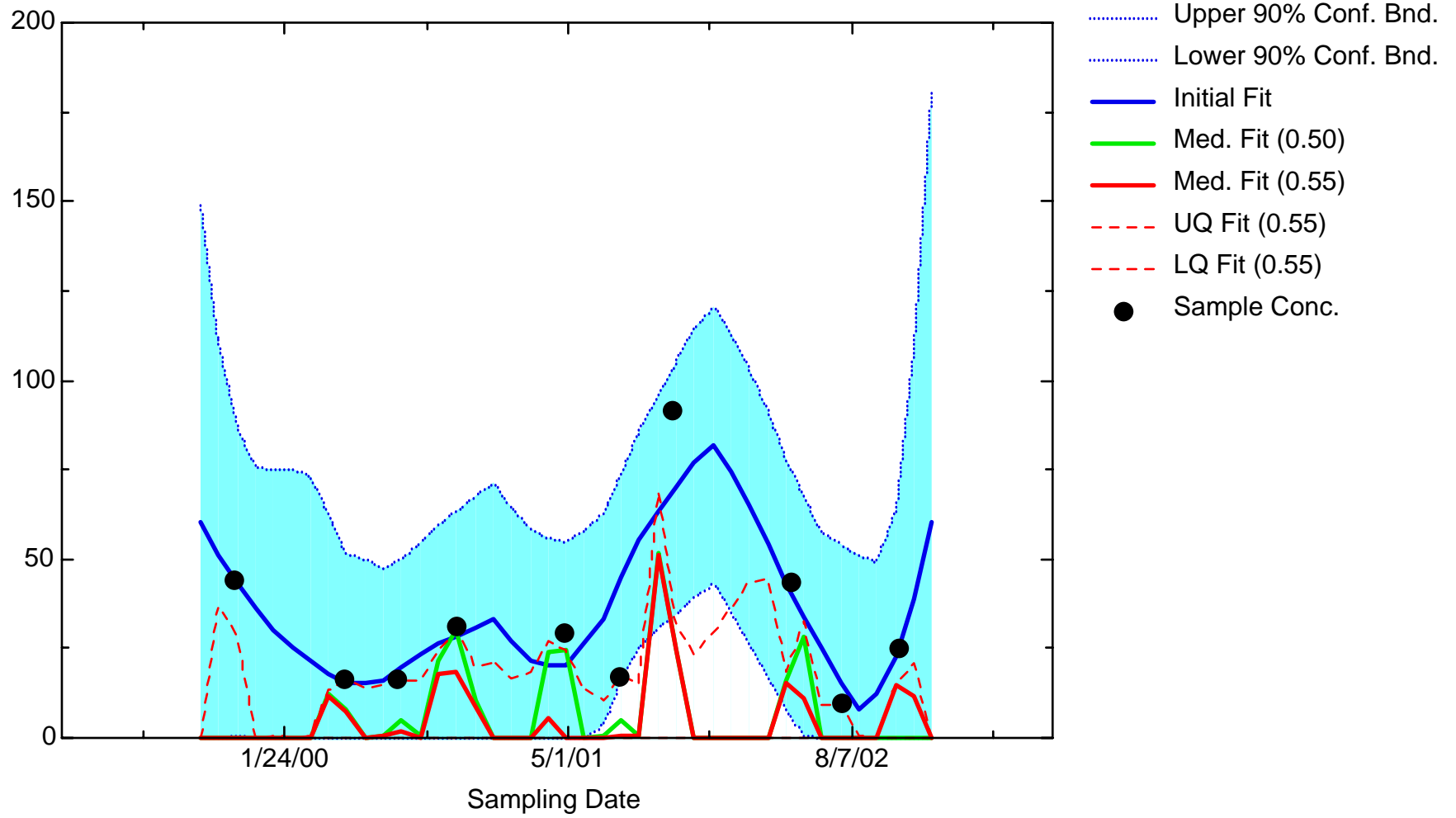
FE: Well JBW7333



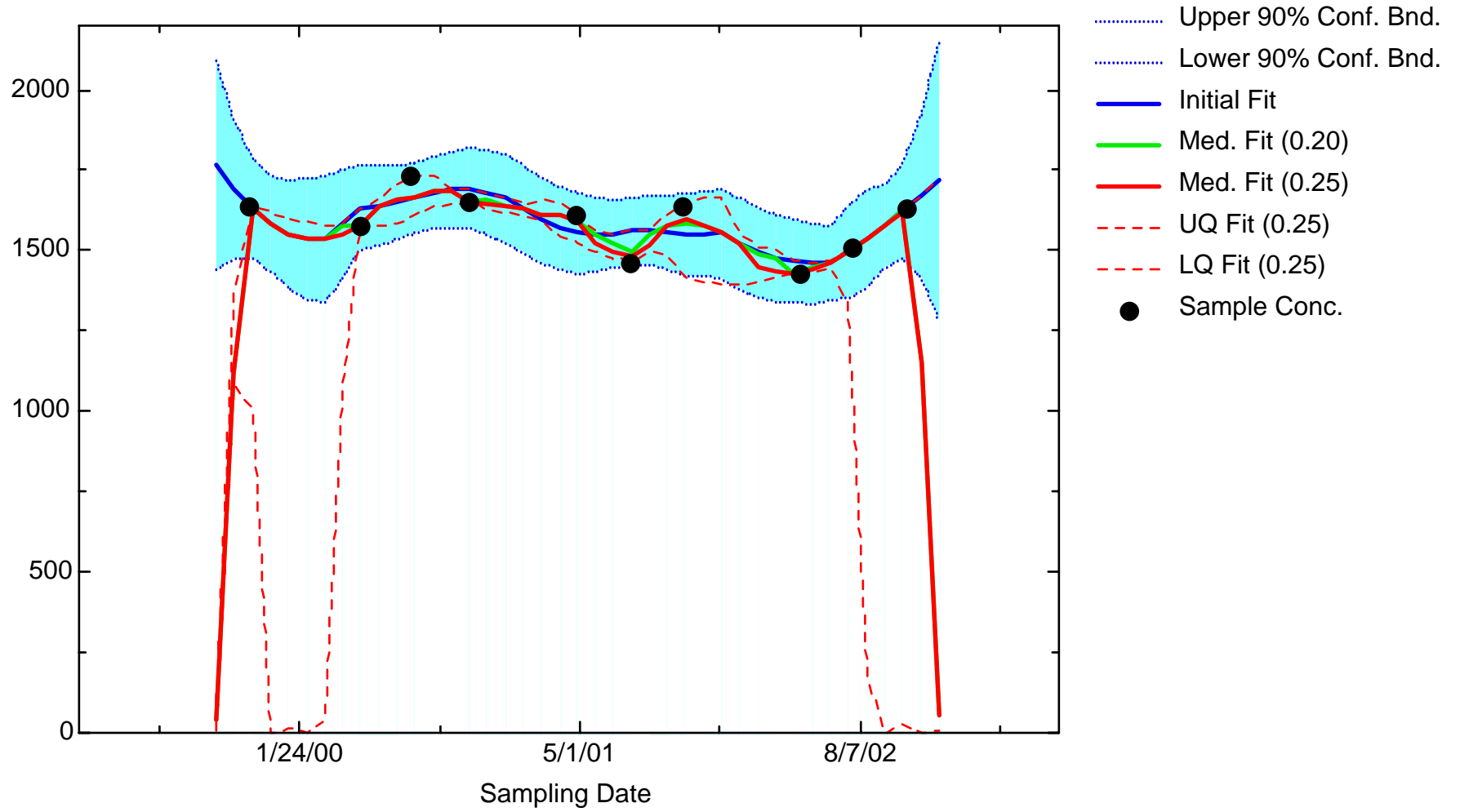
FE: Well JBW7338A



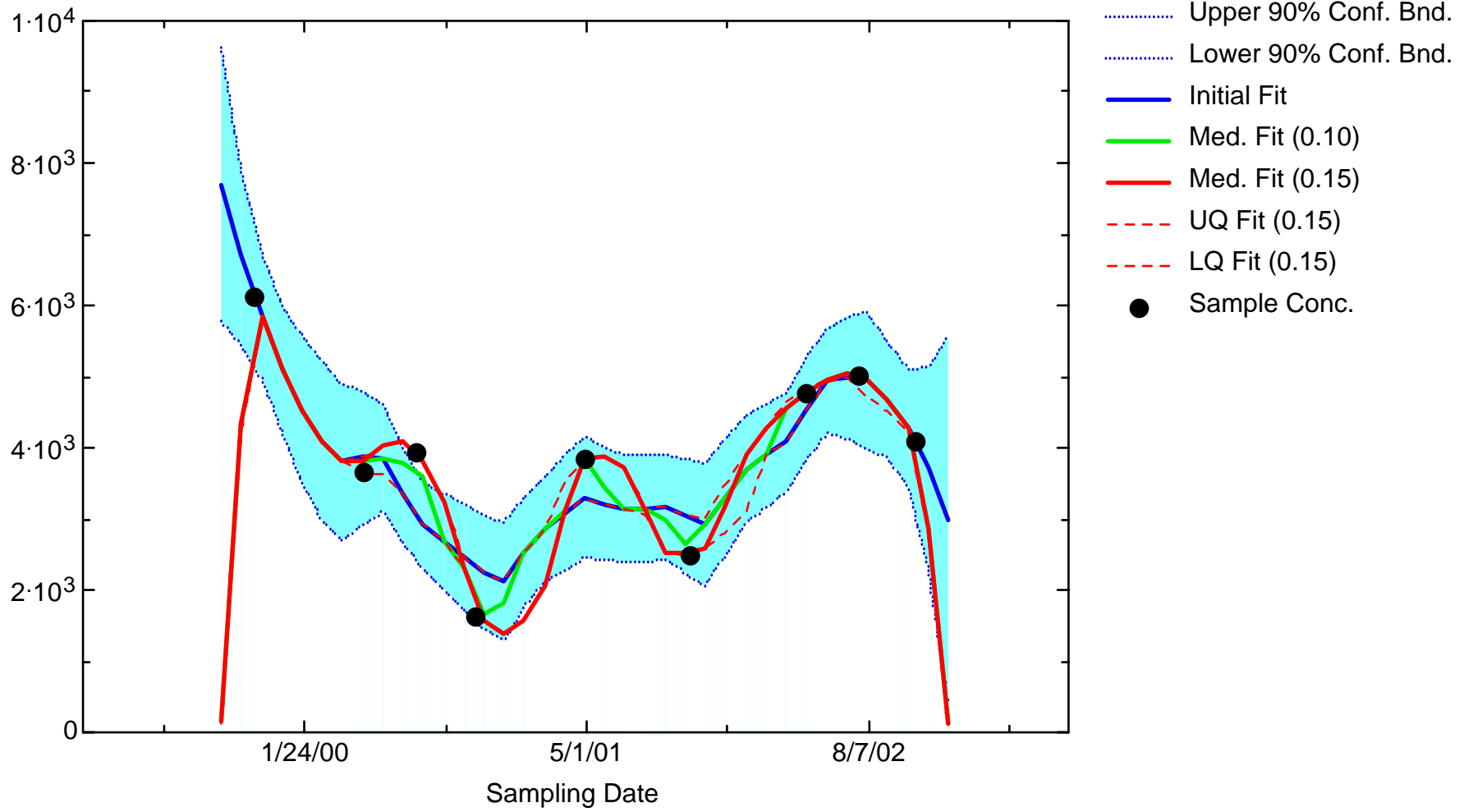
FE: Well JBW7338B



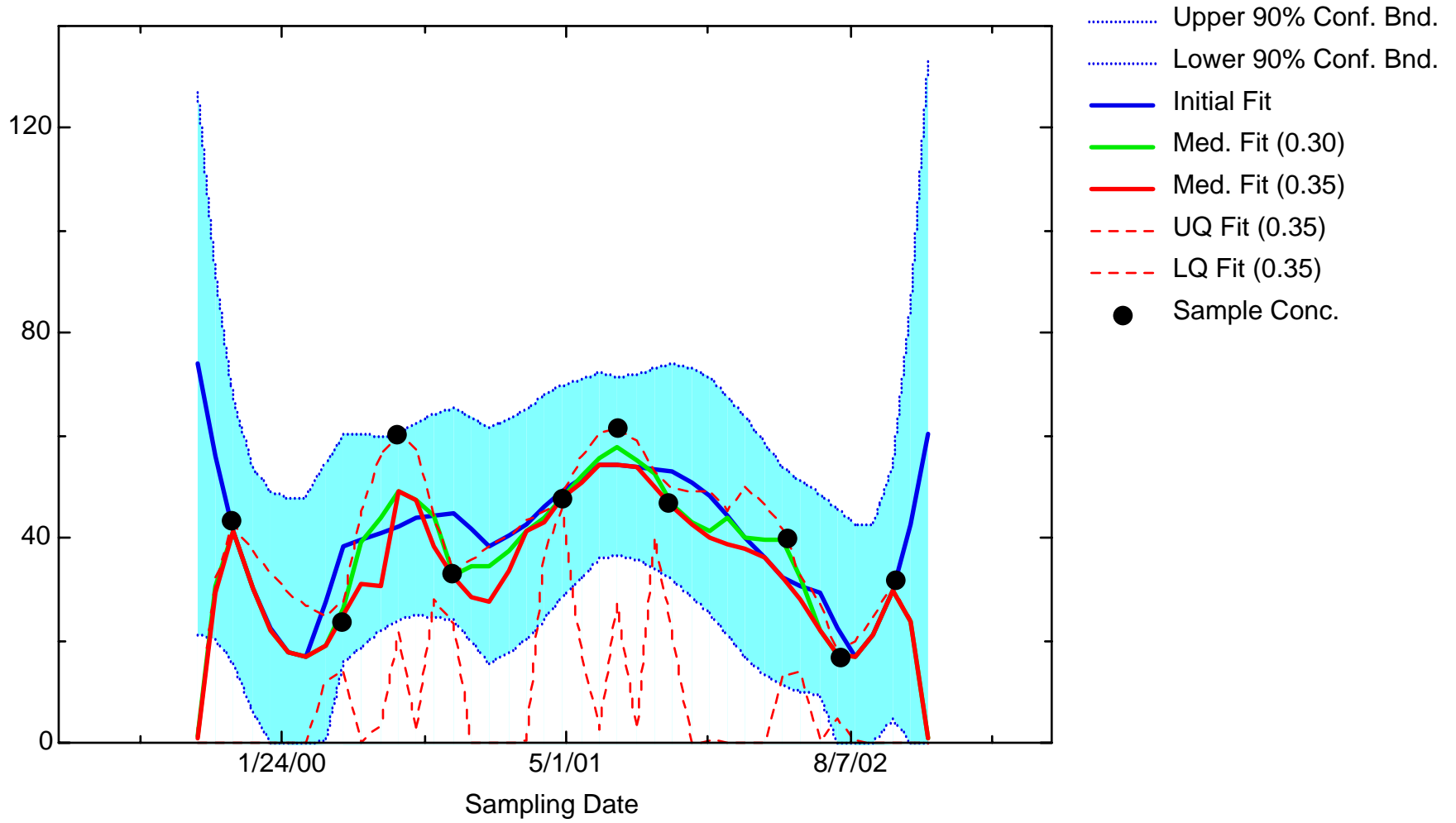
FE: Well JBW7340B



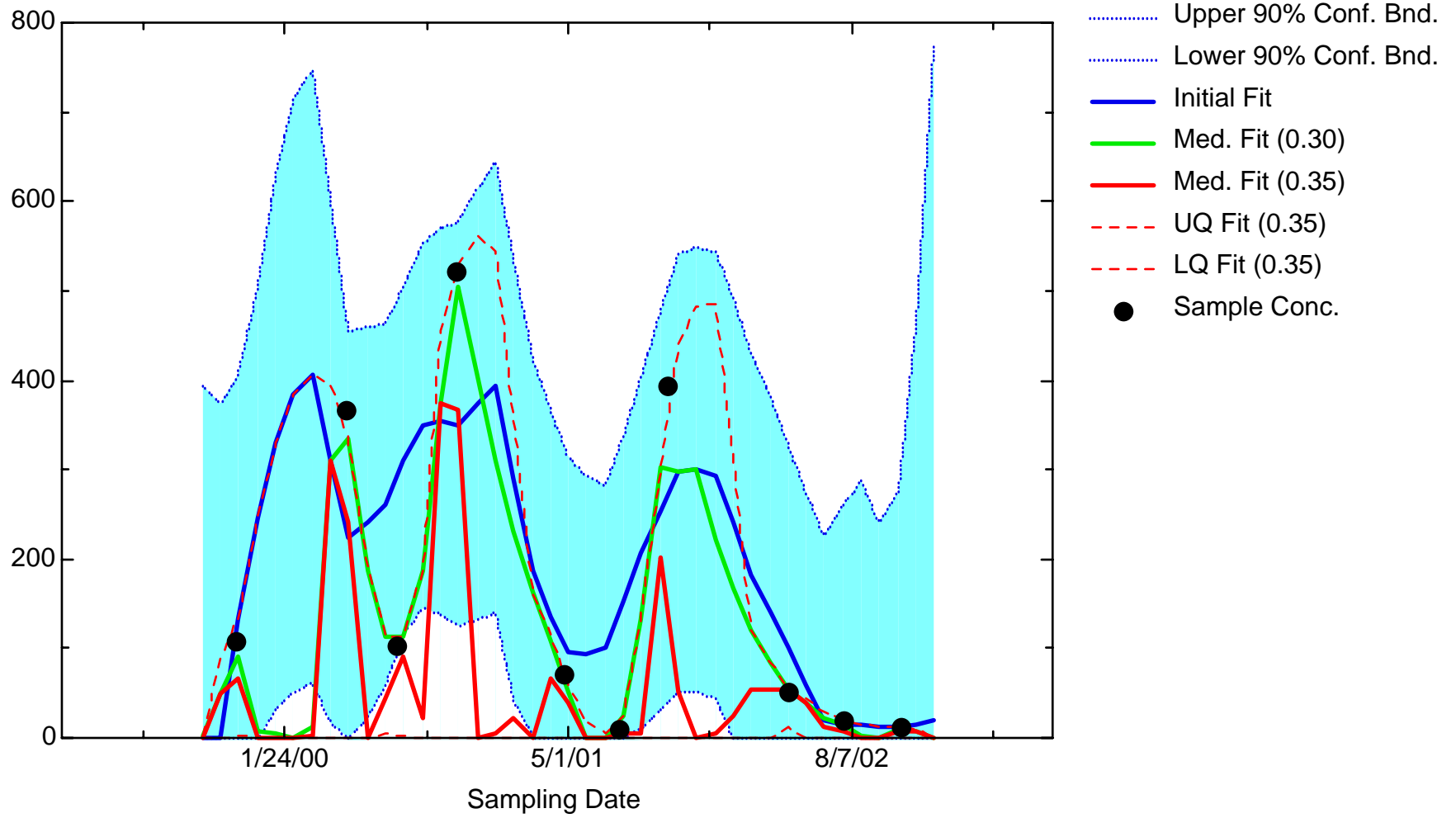
FE: Well JBW7344



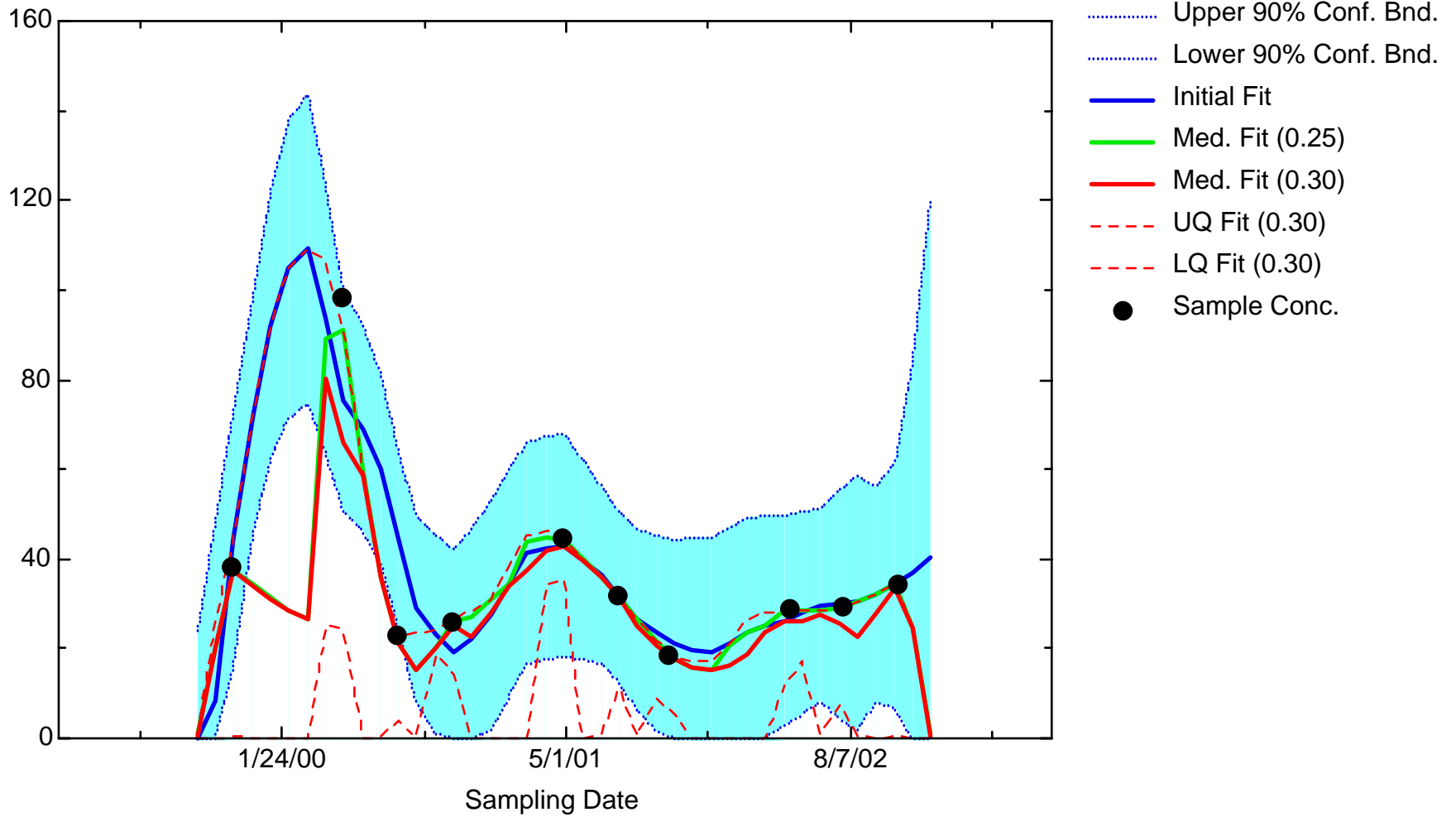
FE: Well JBW7345A



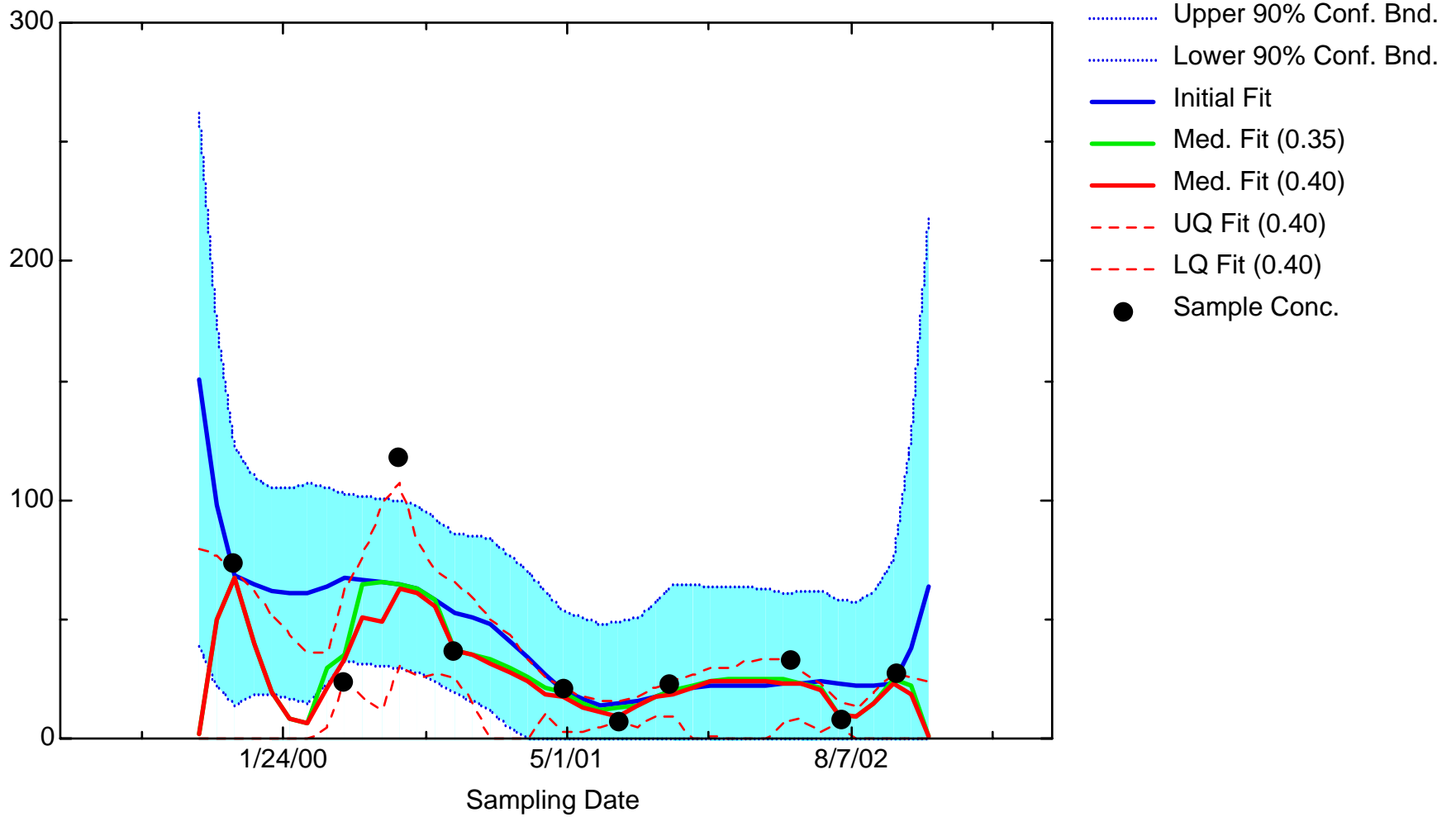
FE: Well JBW7347B



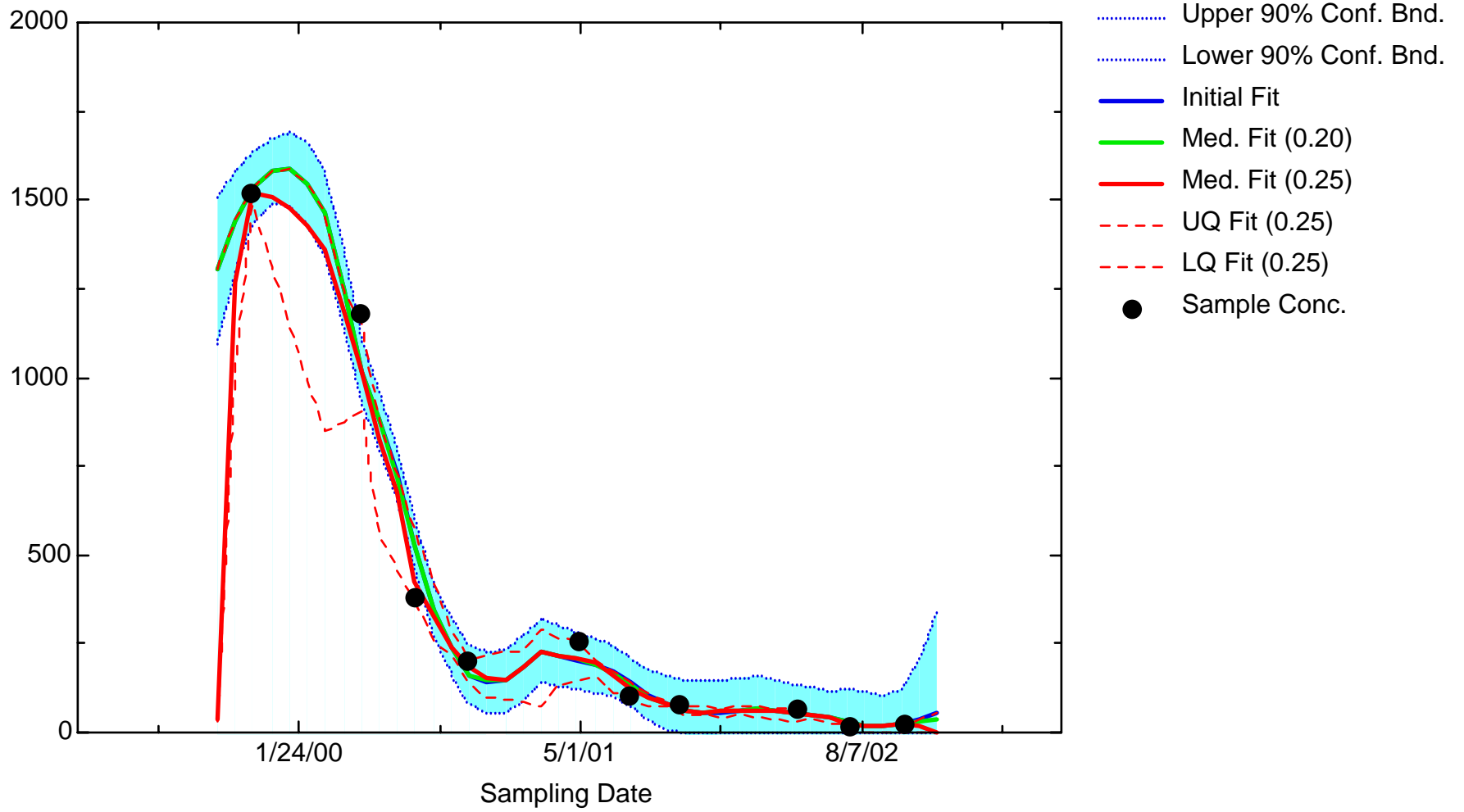
FE: Well JBW7348



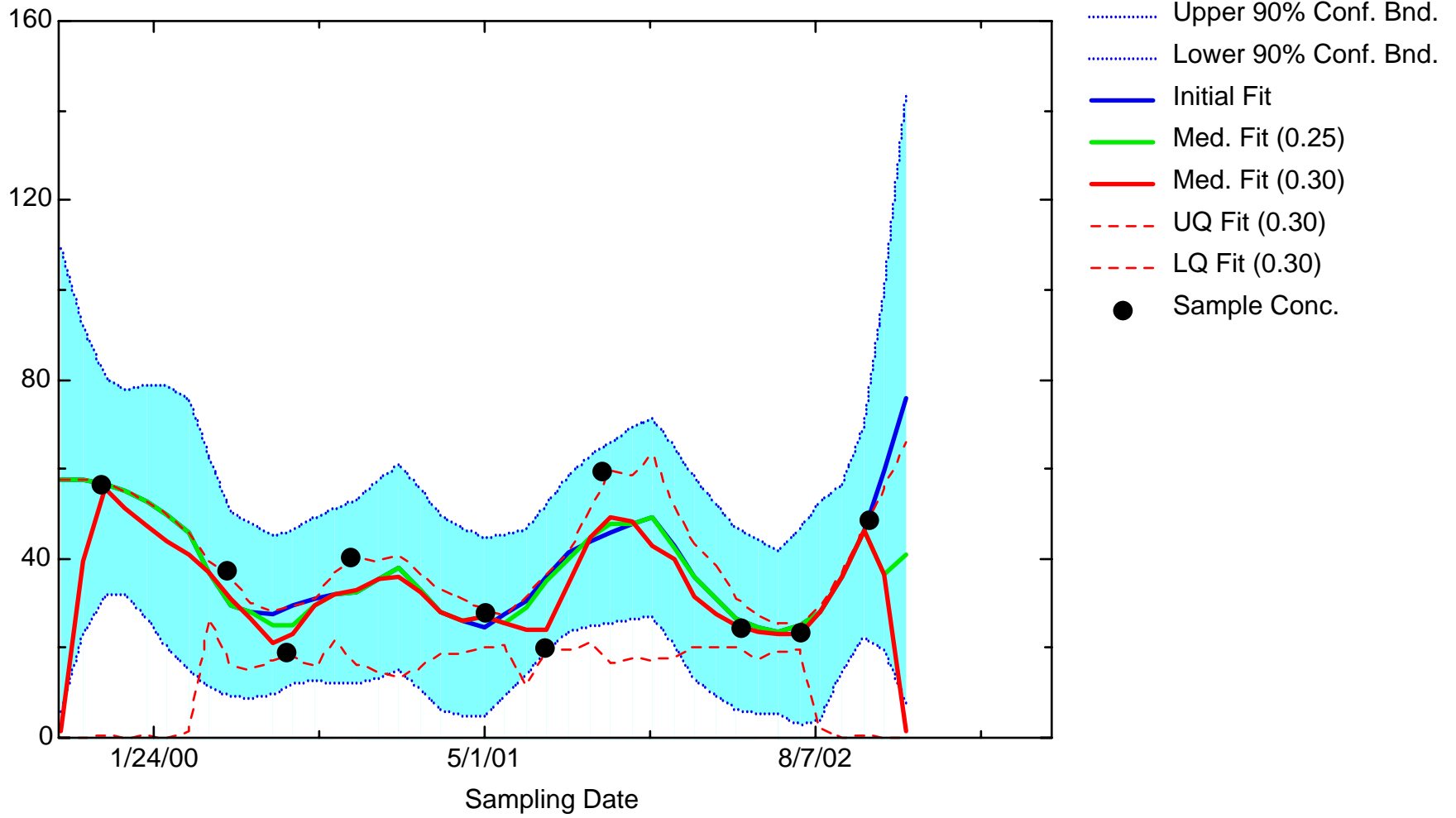
FE: Well JBW7350



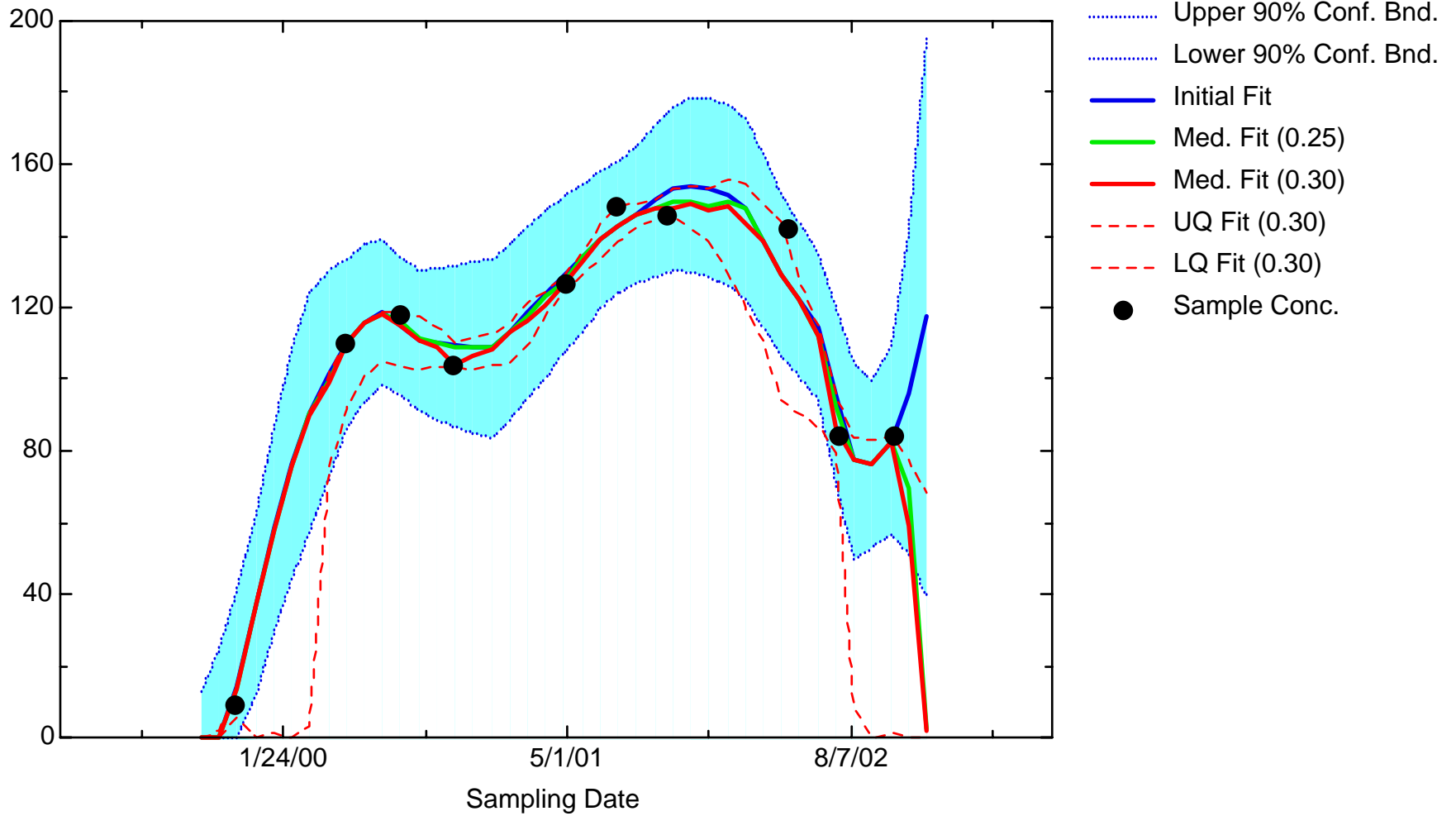
FE: Well JBW7806



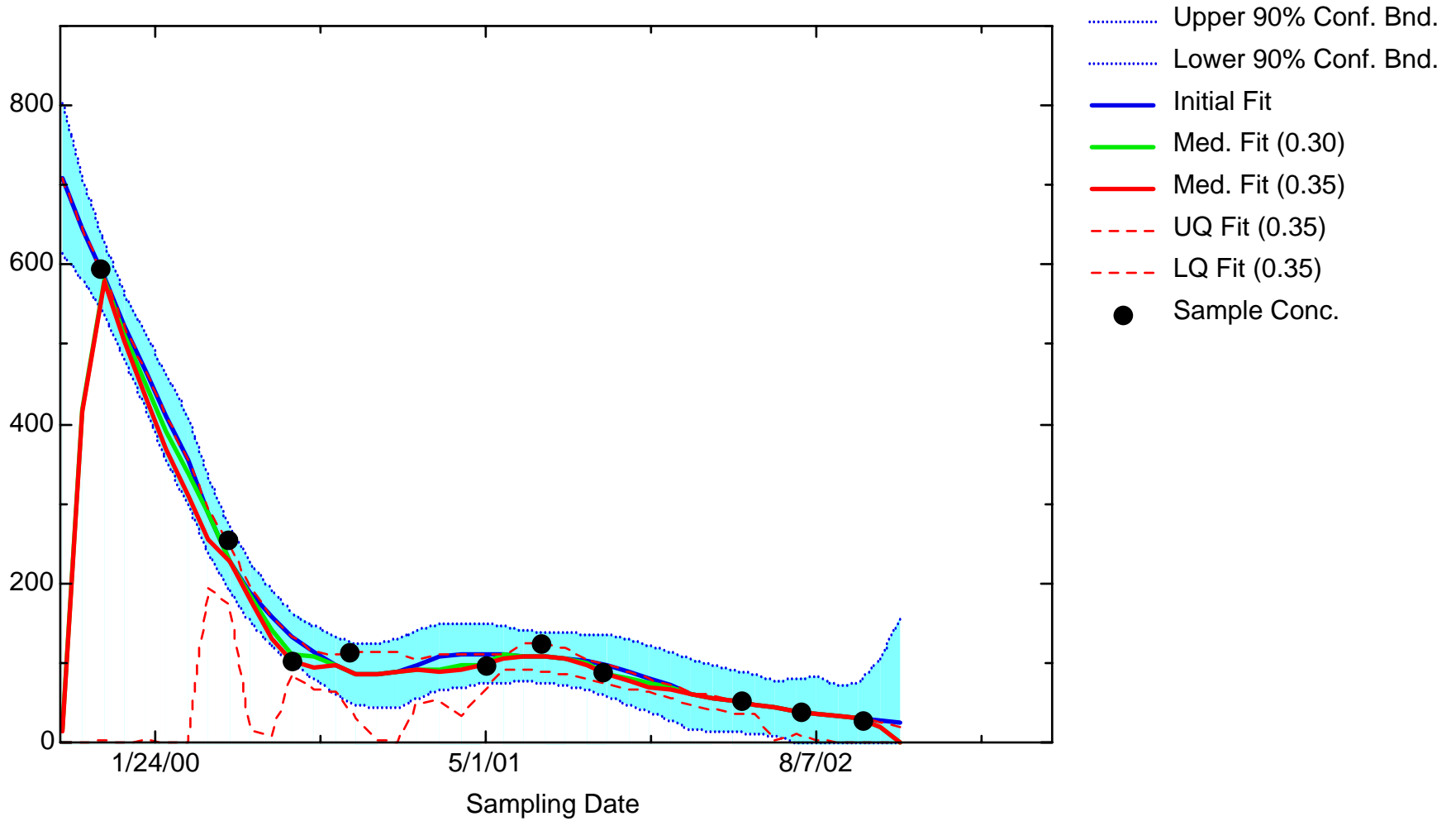
FE: Well JBW7809



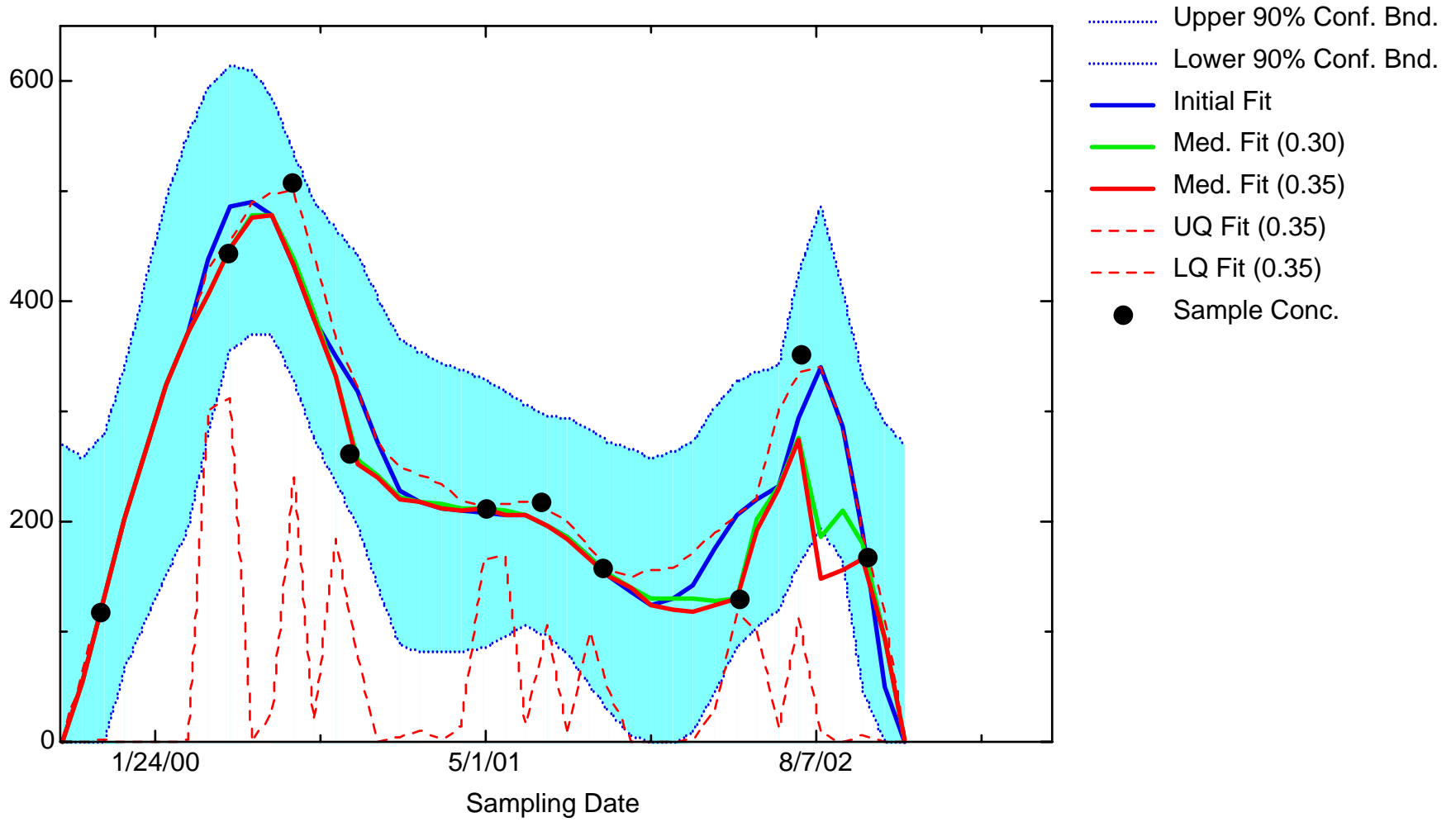
FE: Well JBW7812B



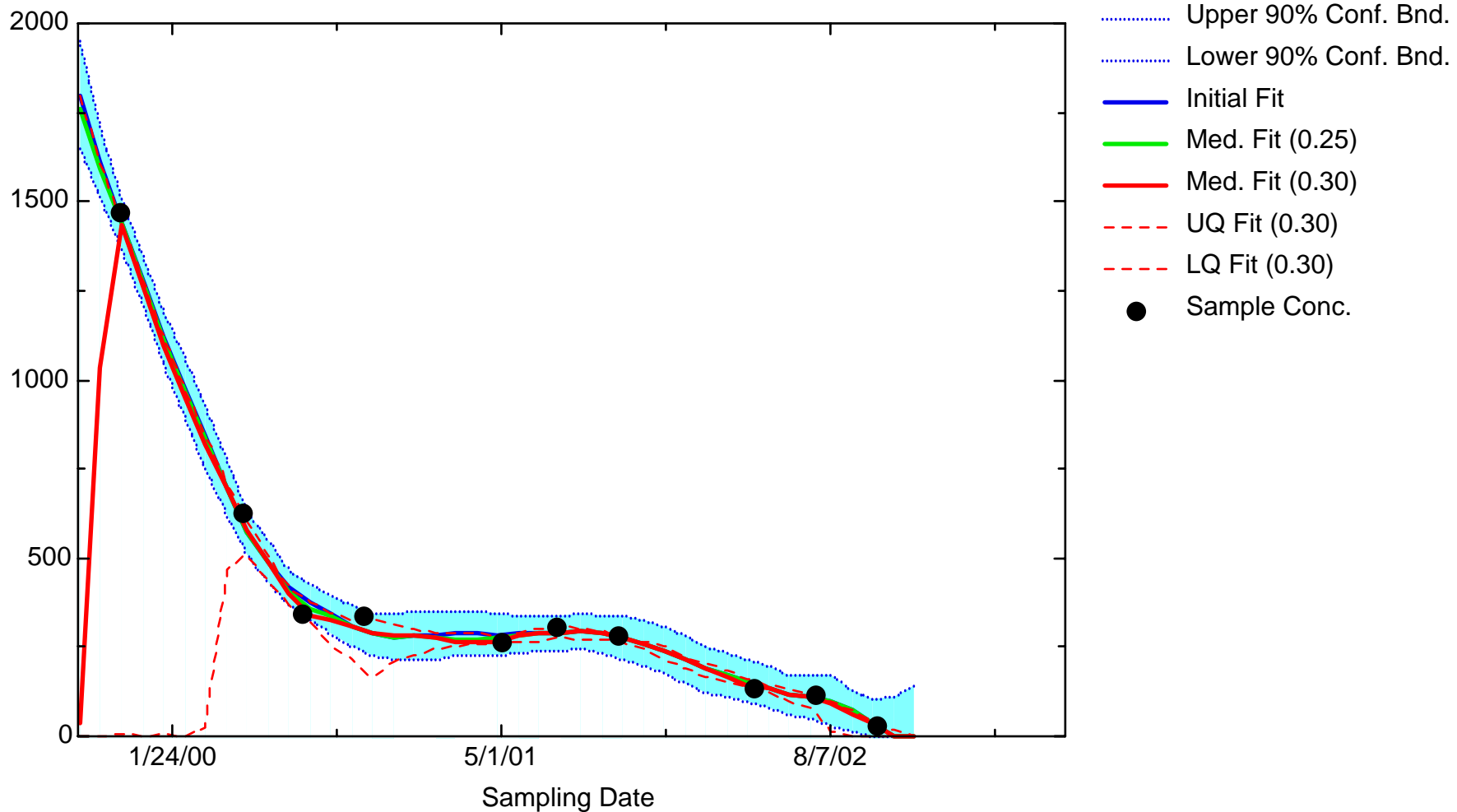
FE: Well JBW8003B



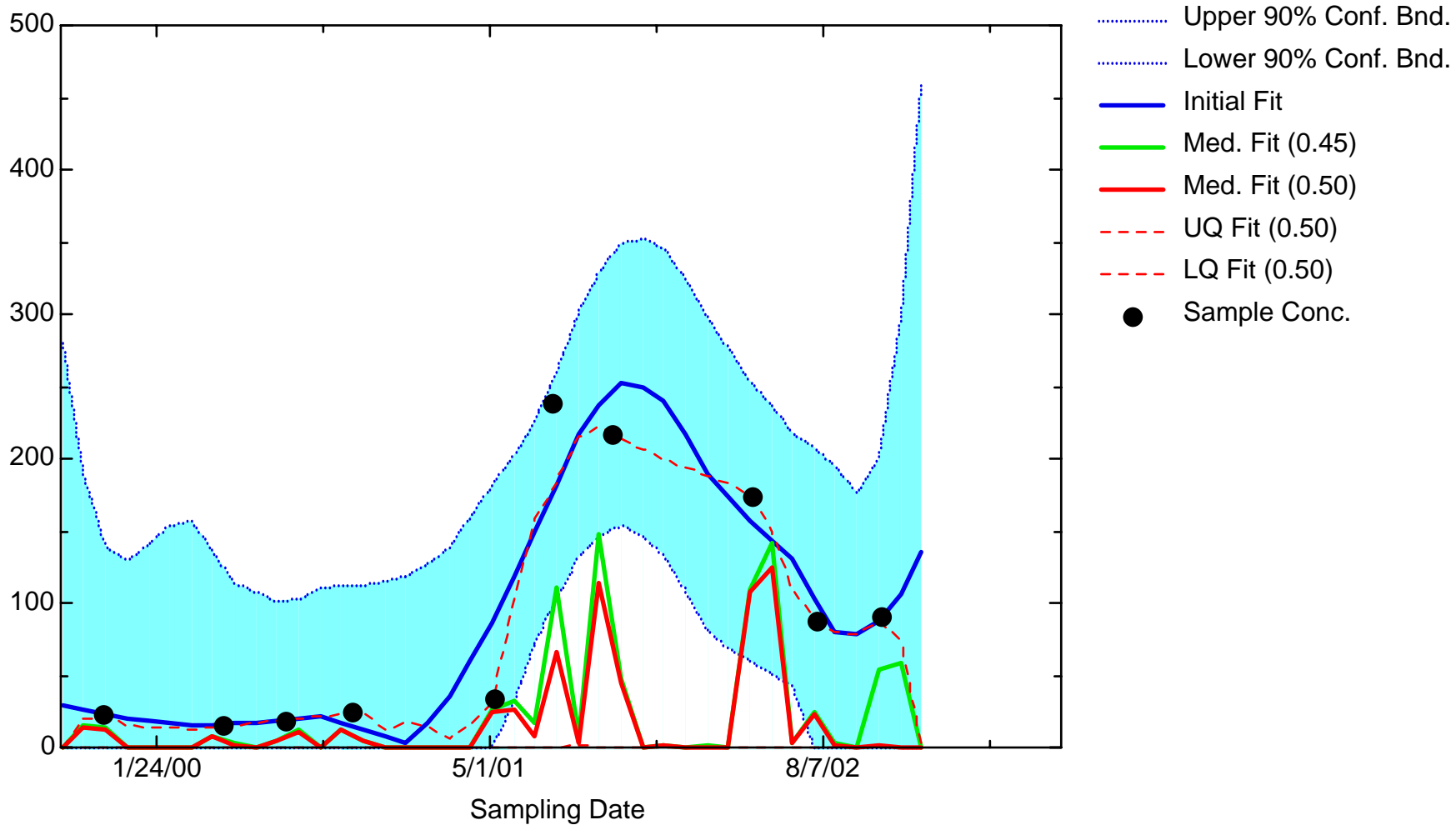
FE: Well JBW8004B



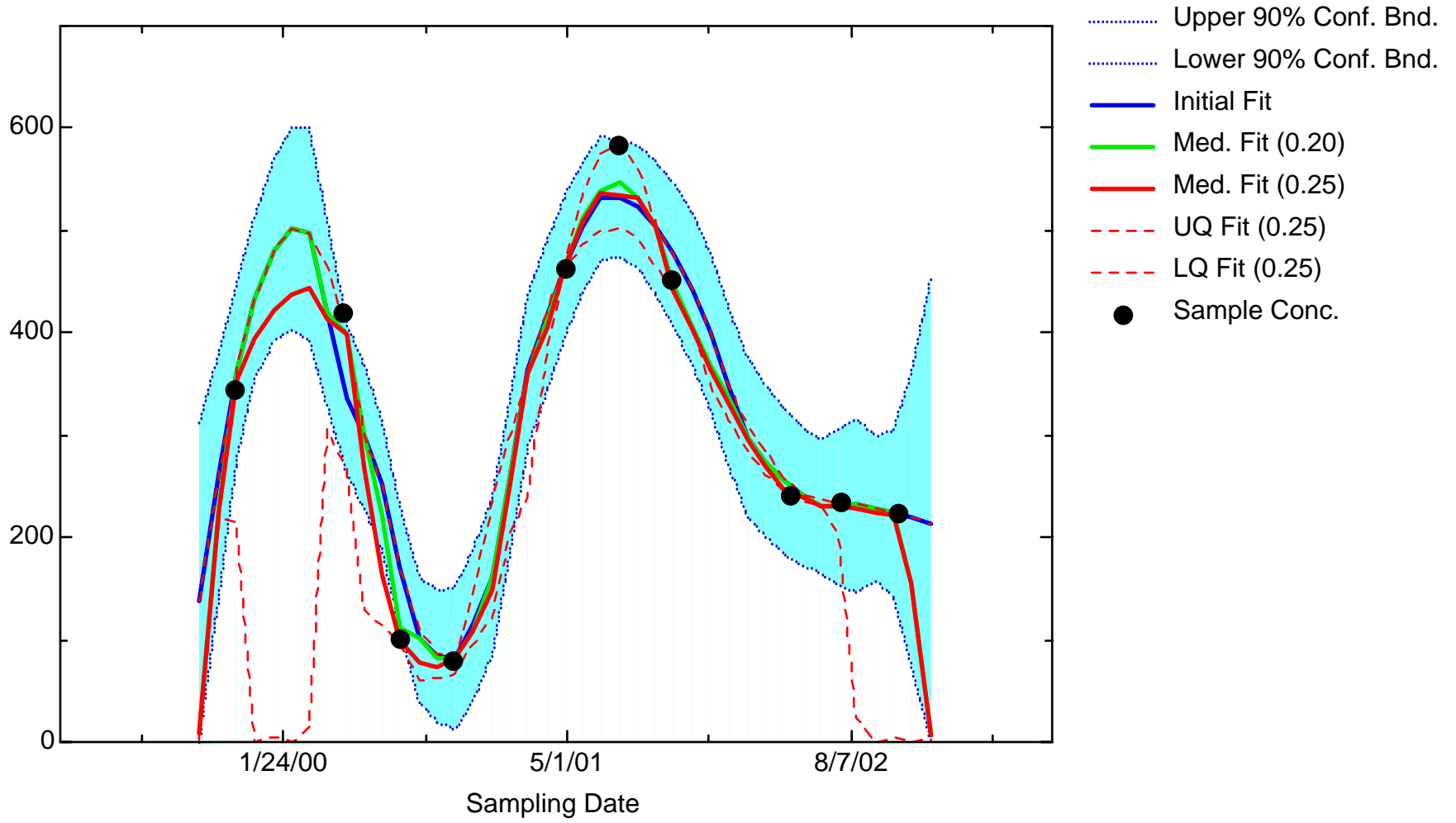
FE: Well JBW8009



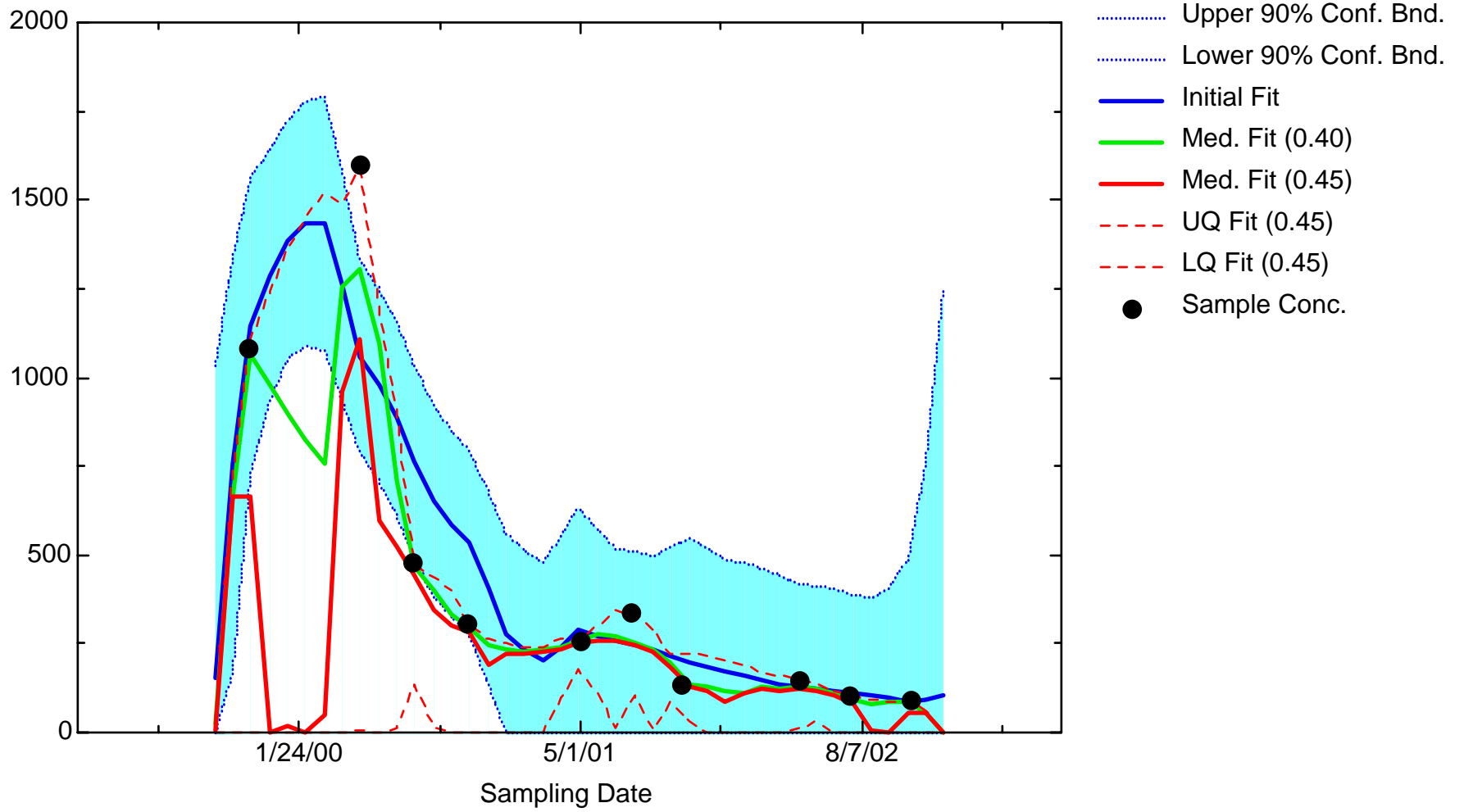
FE: Well JMW35X2



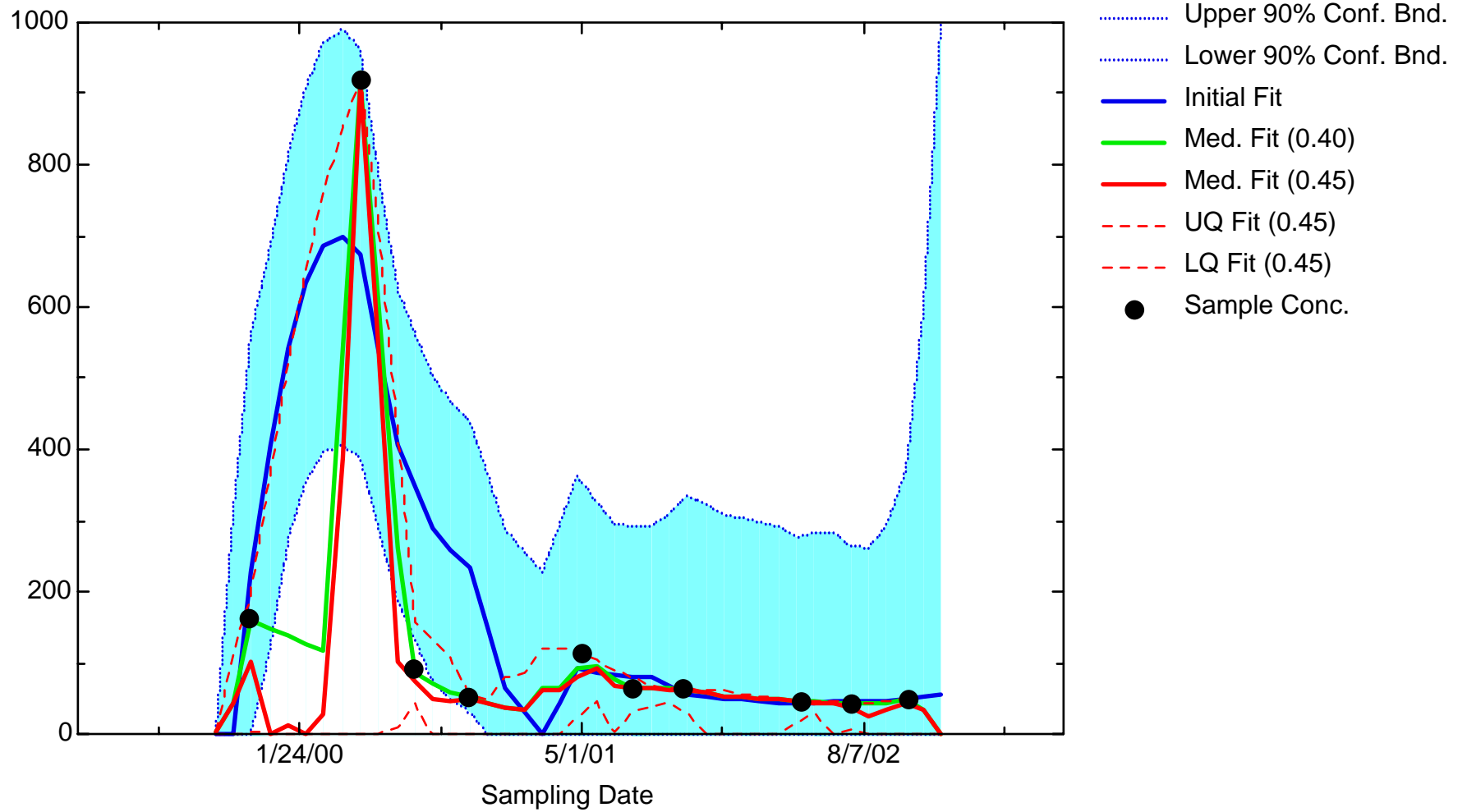
FE: Well JMW0301C



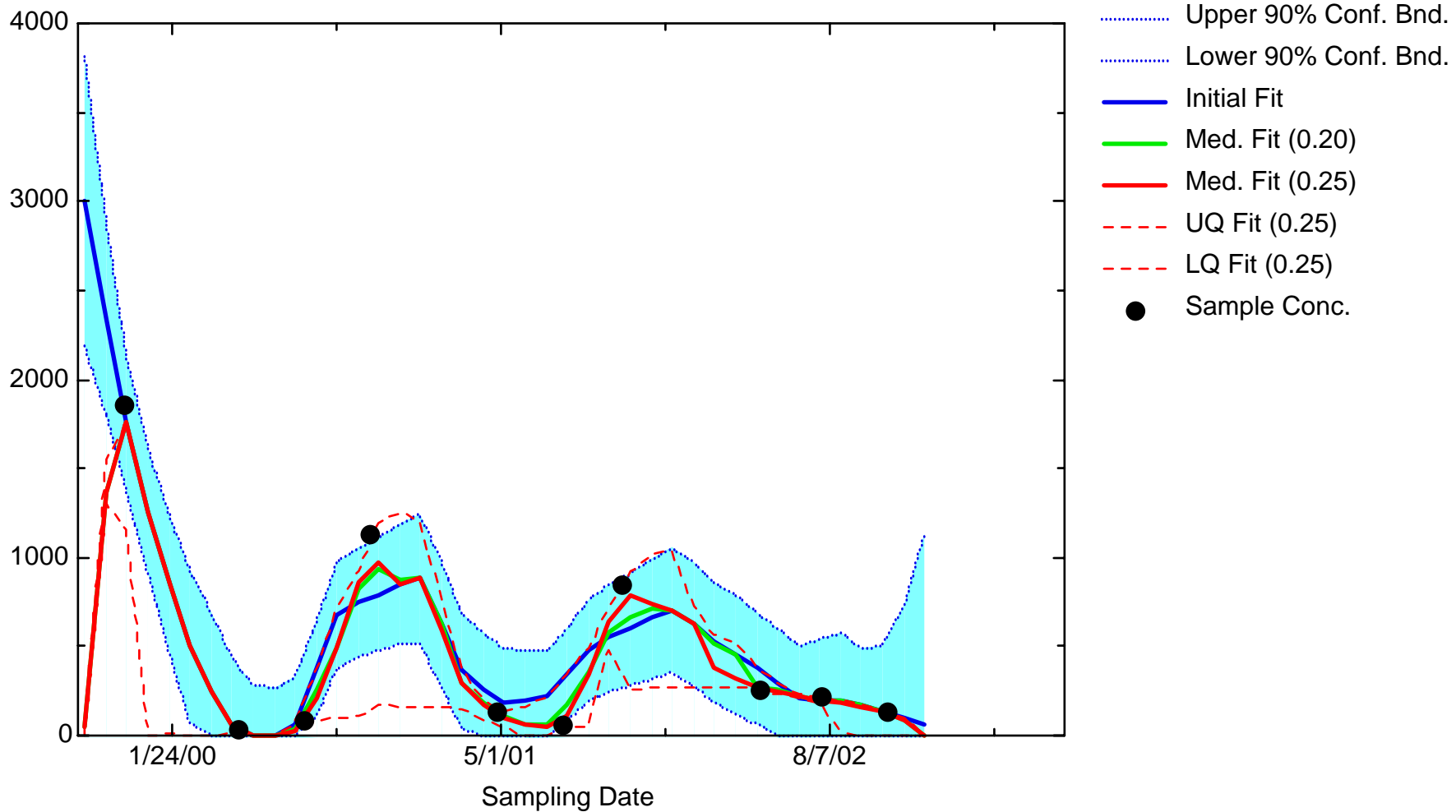
FE: Well JMW0503



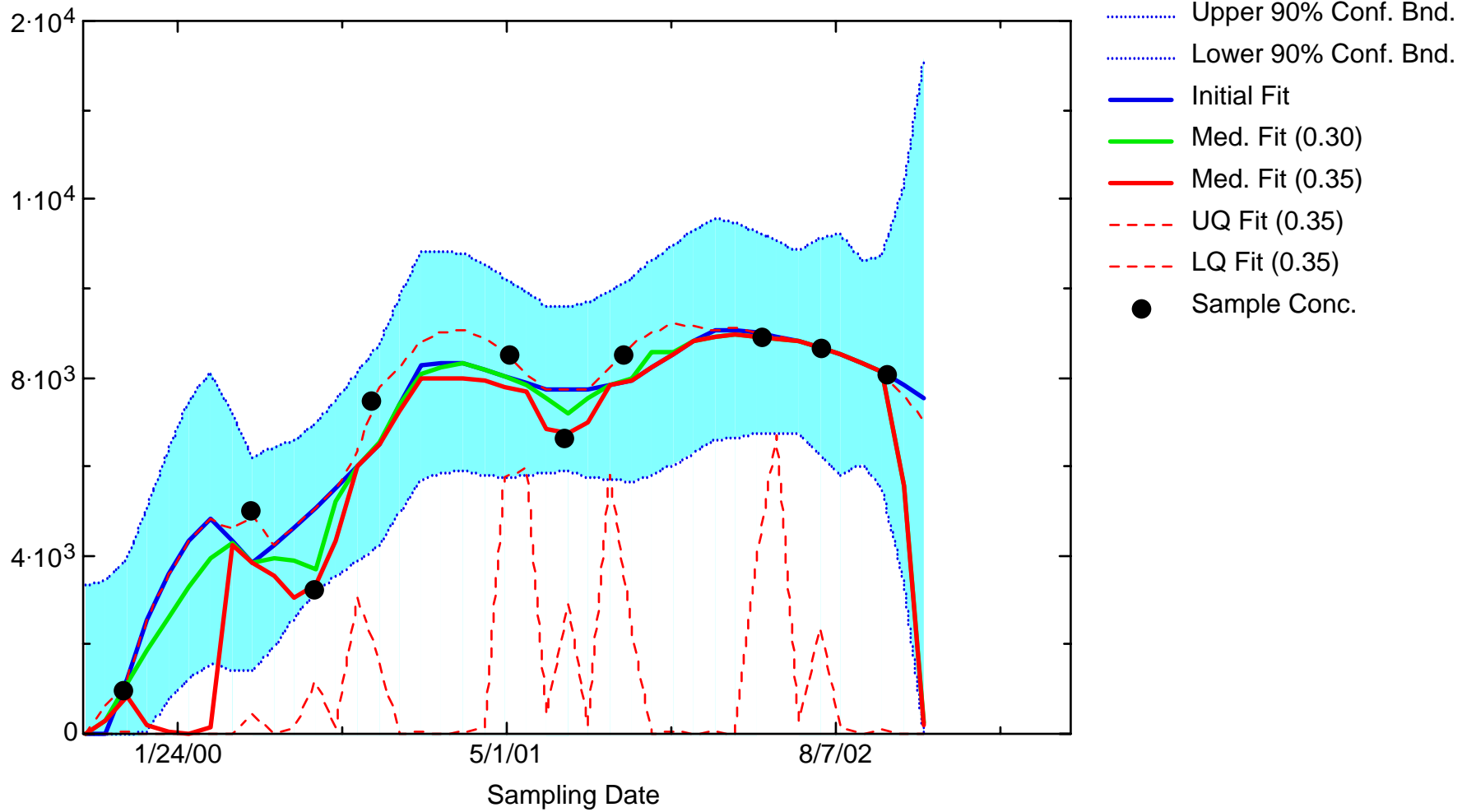
FE: Well JMW0505



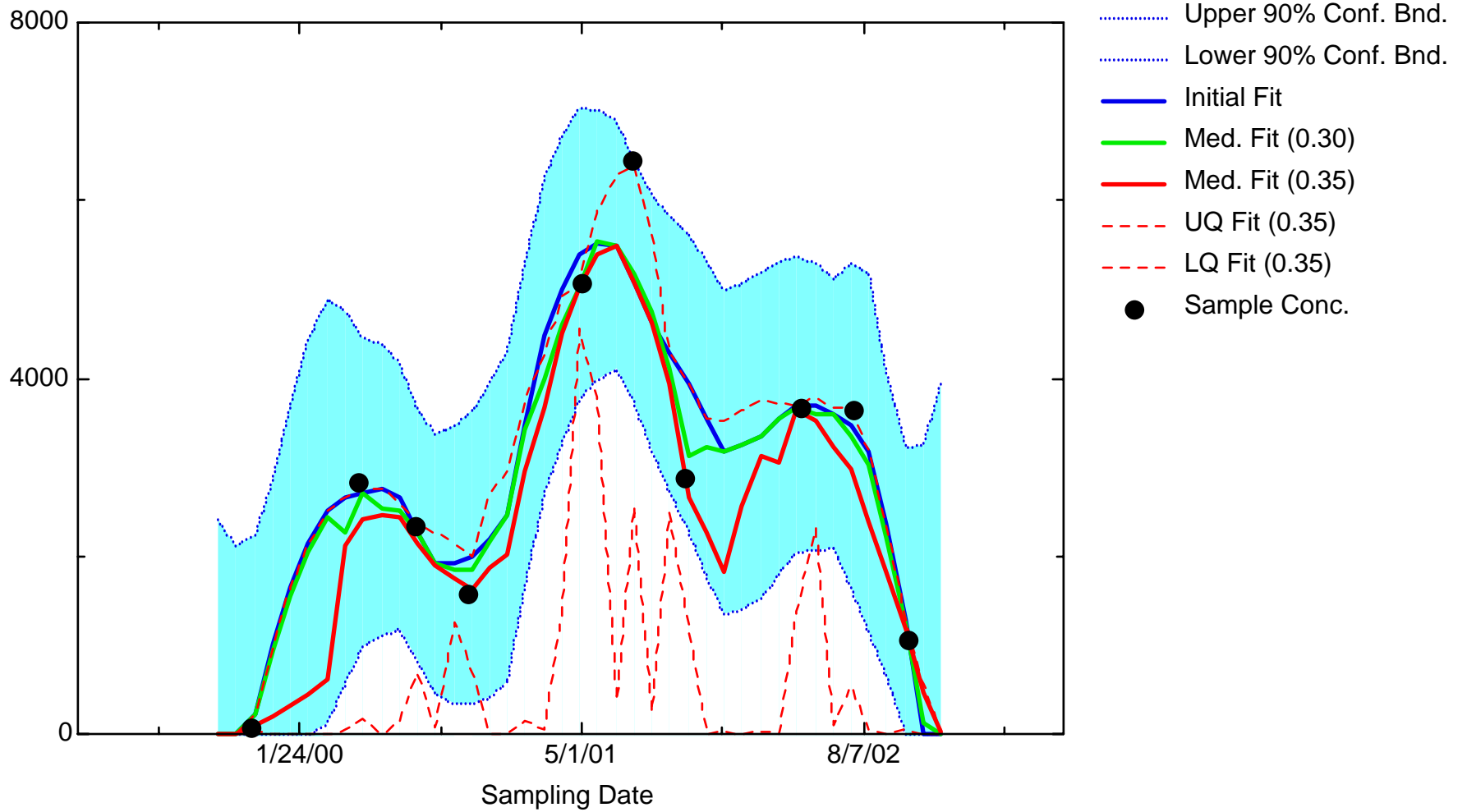
FE: Well JMW0542



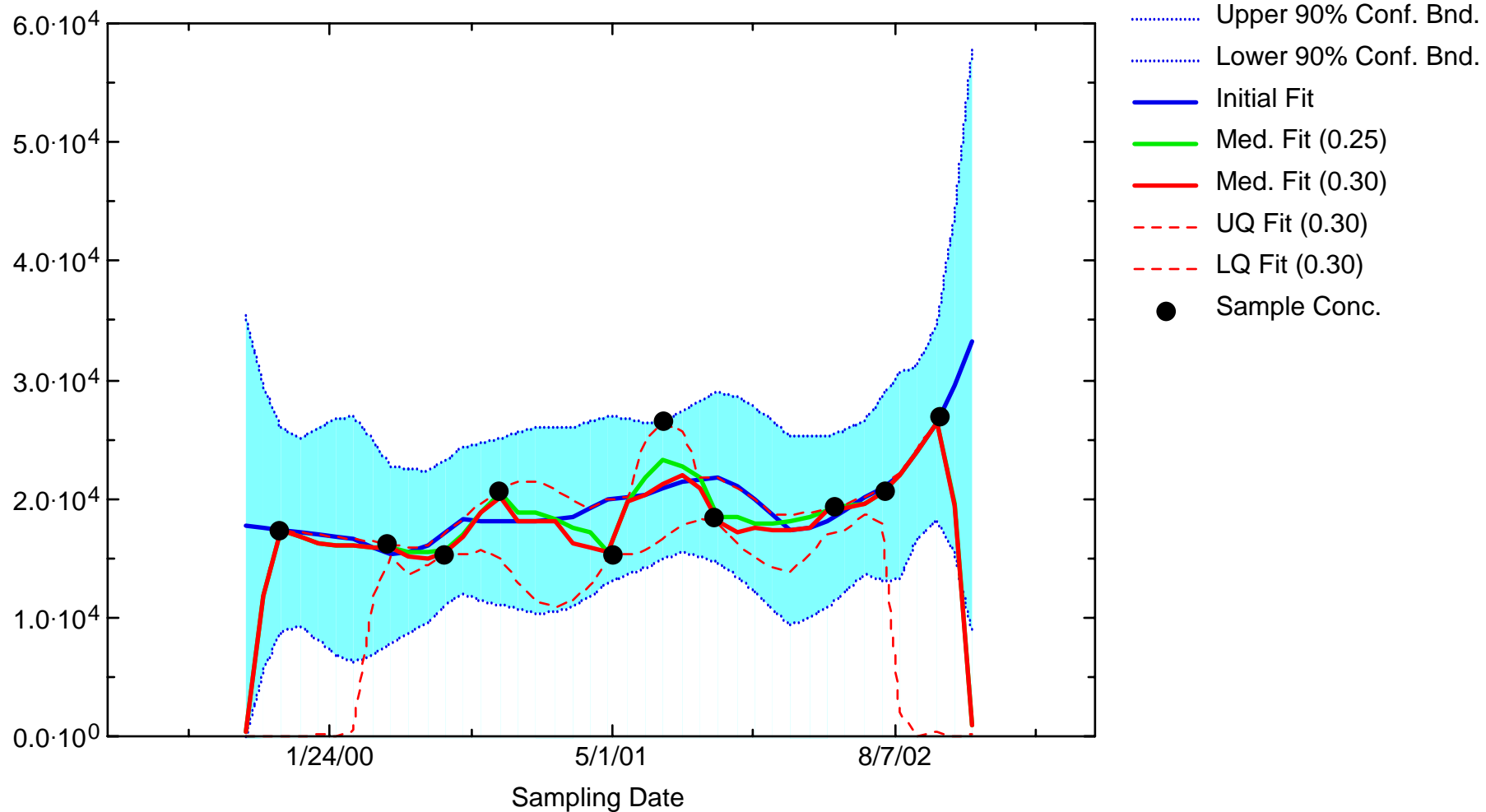
FE: Well JMW1103D



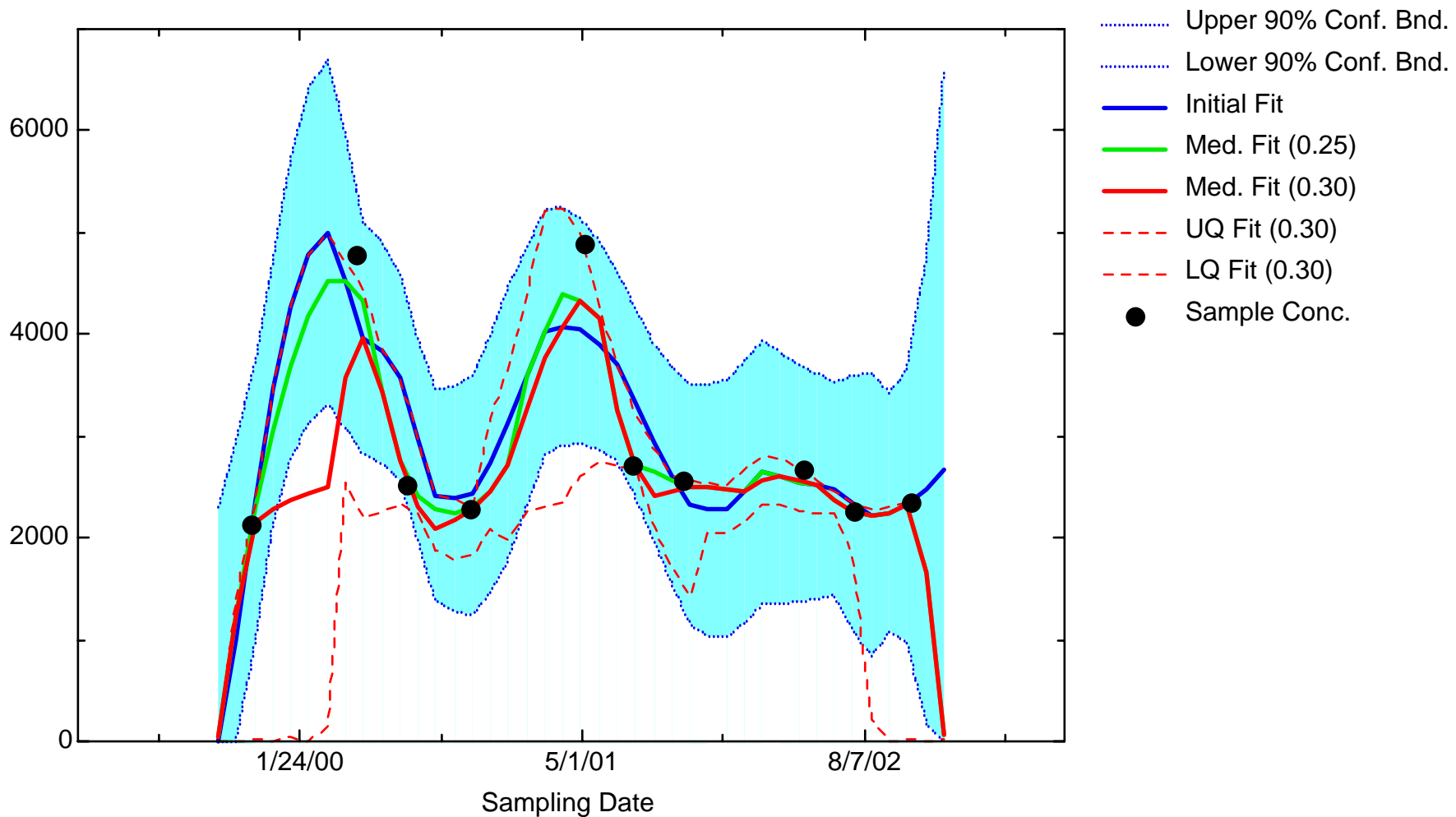
FE: Well JMW1564



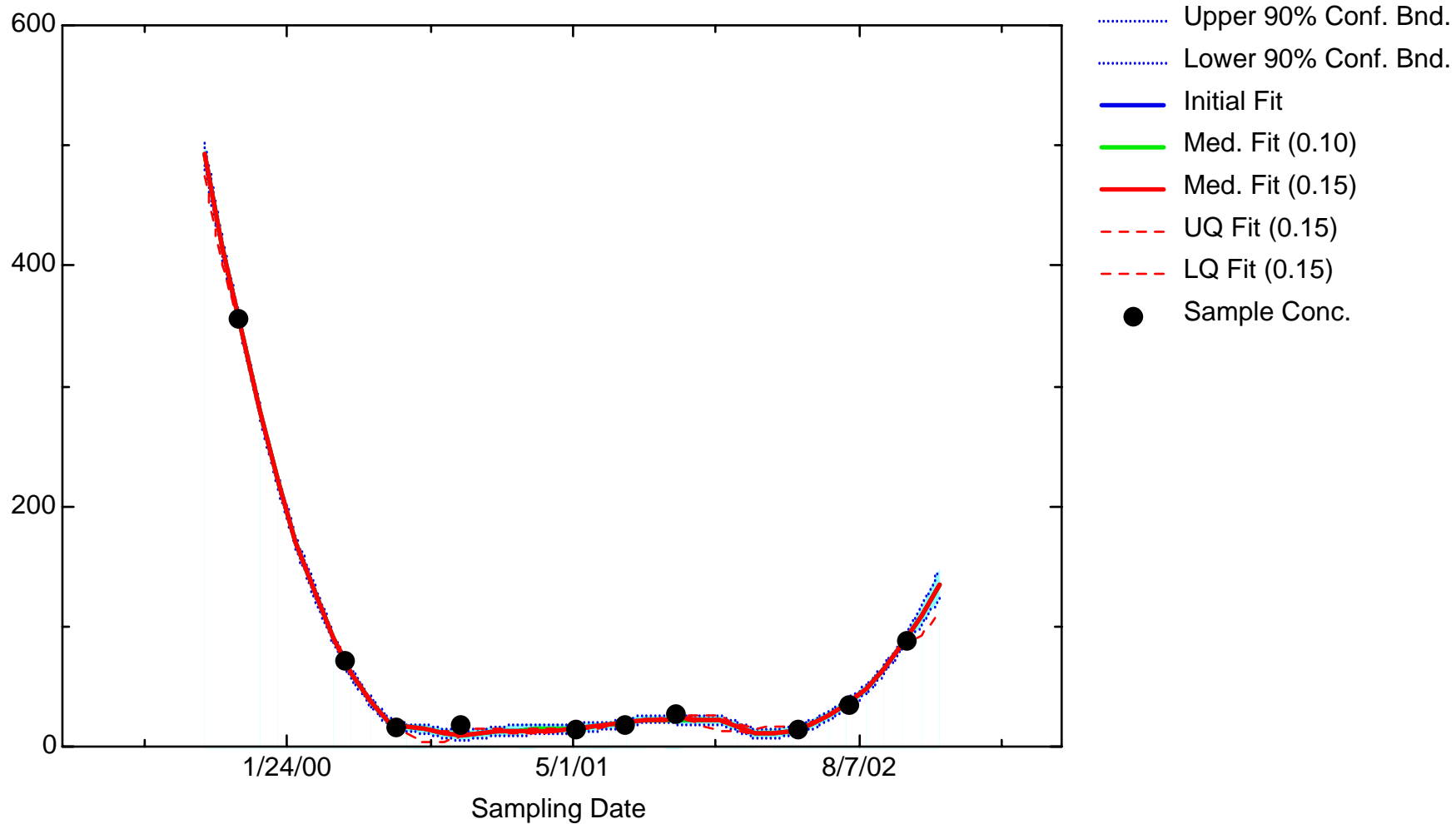
FE: Well JMW1565



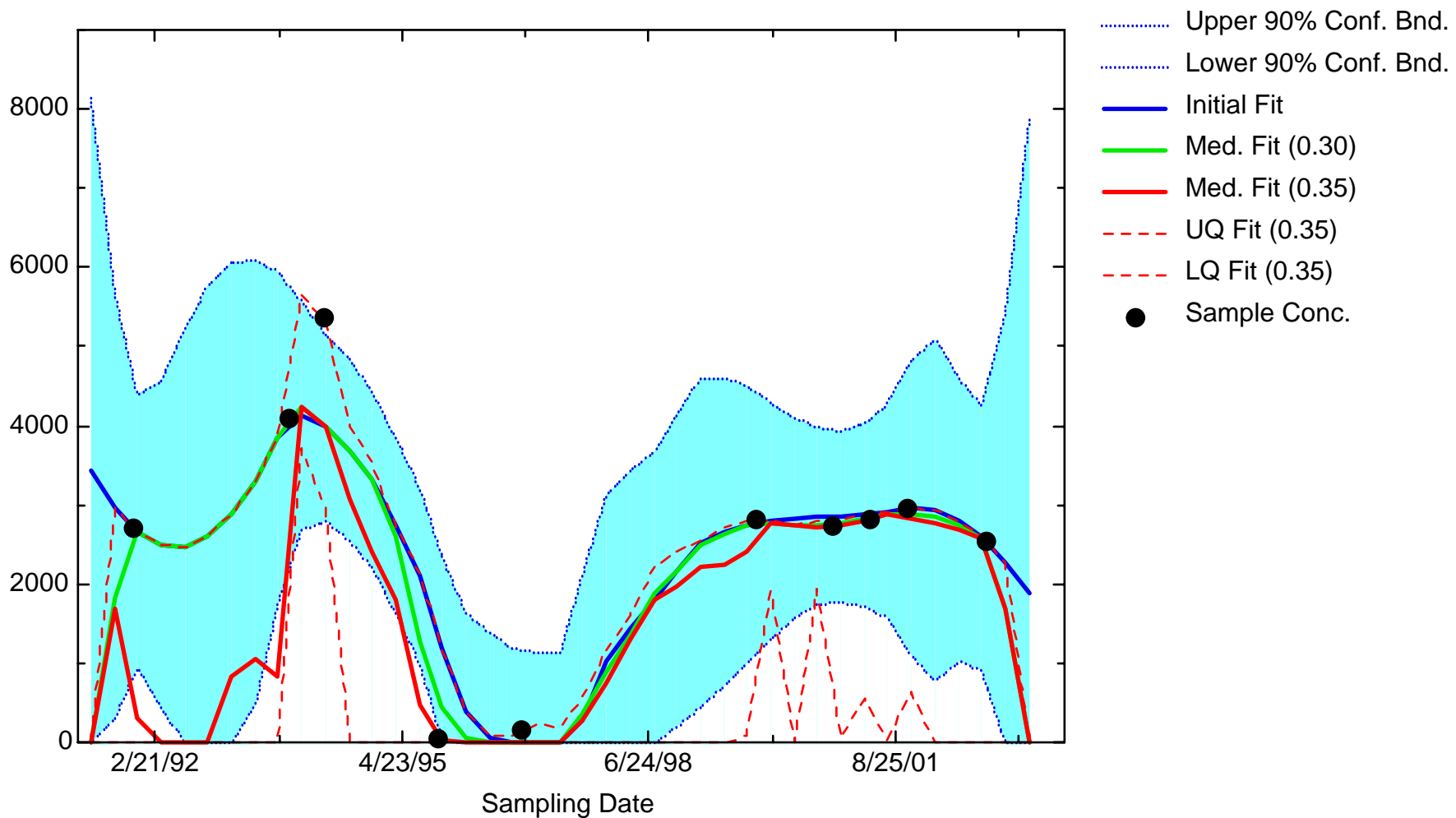
FE: Well JMW1860



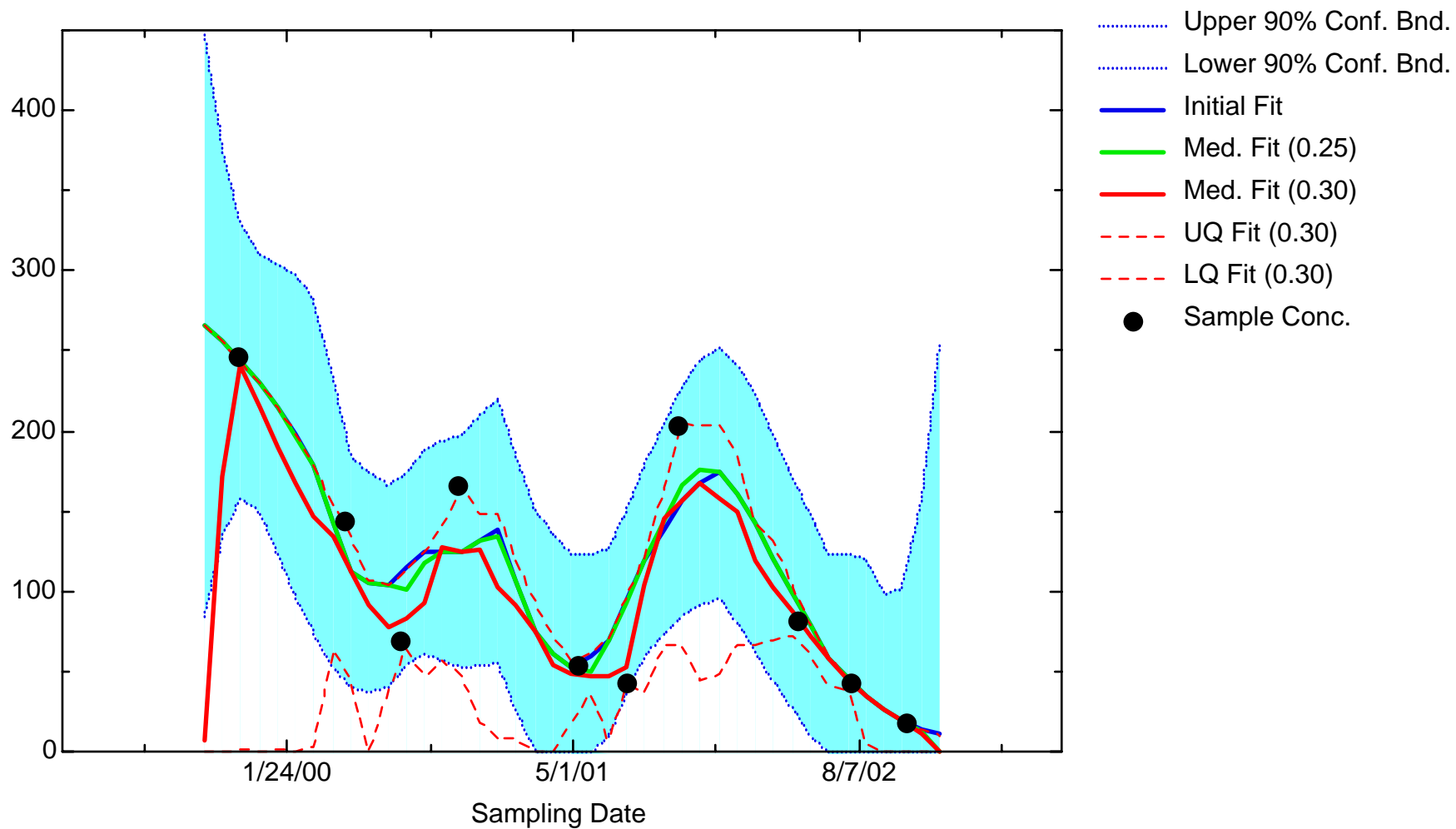
FE: Well JMW1881



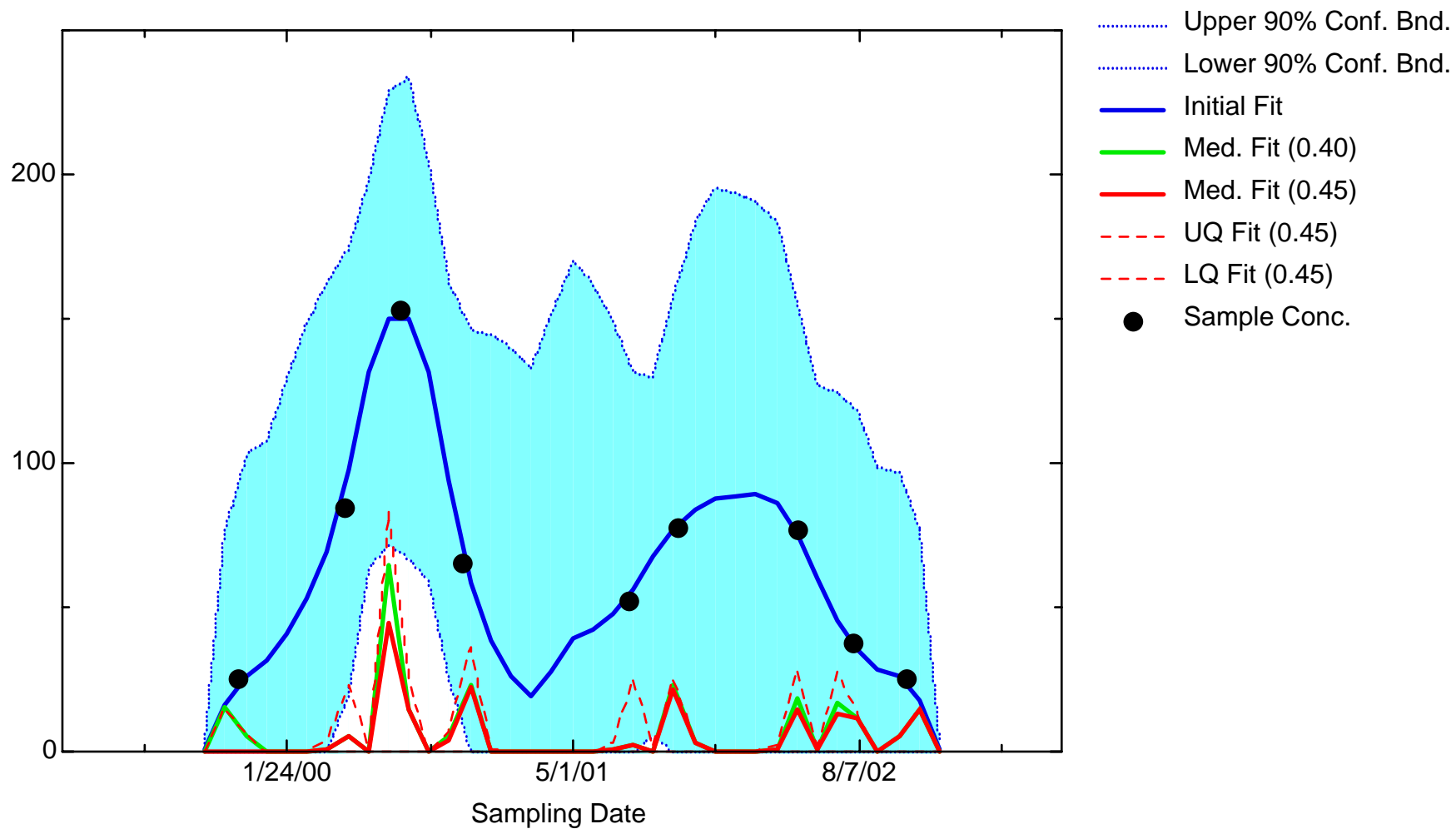
FE: Well JMW1960



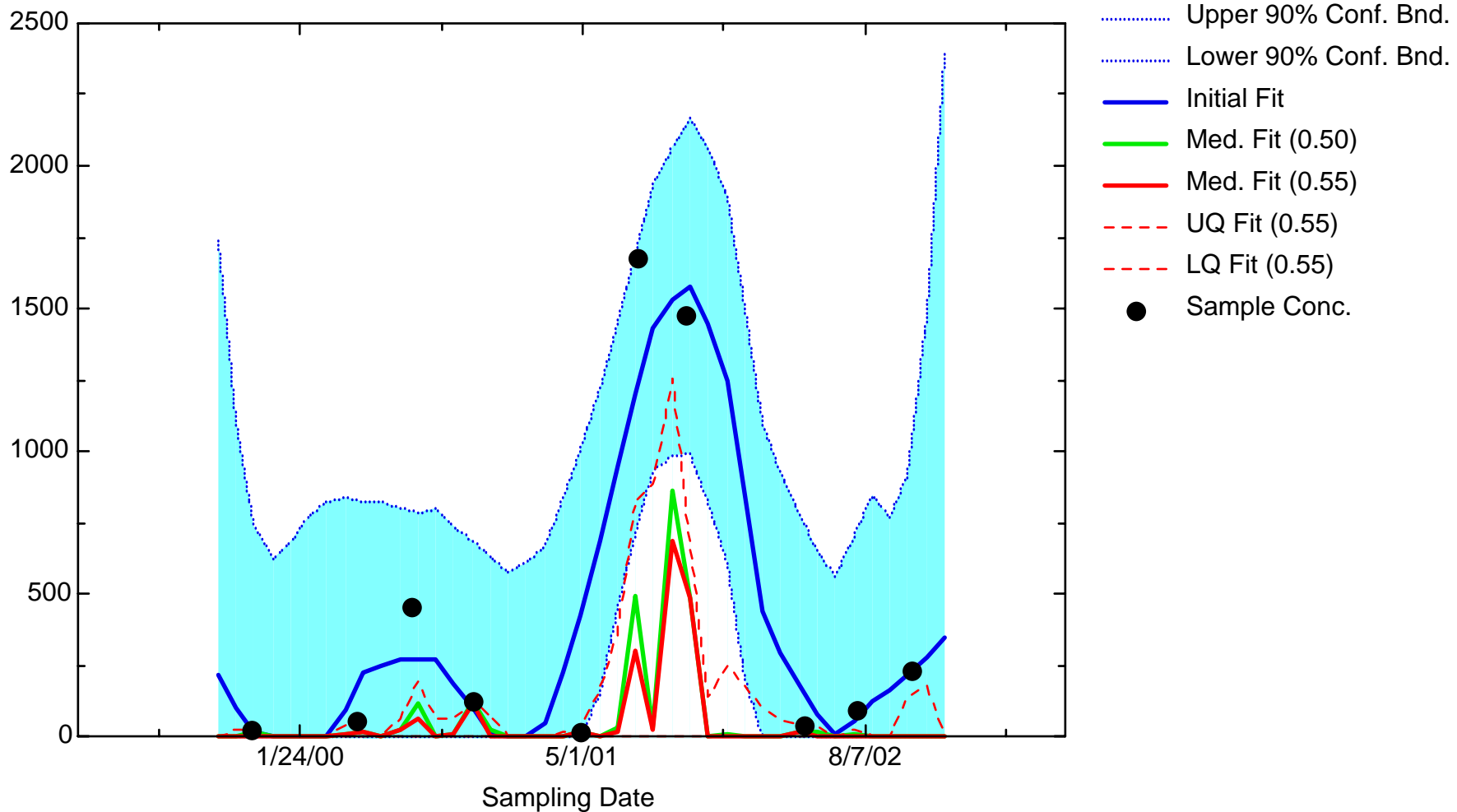
FE: Well JMW1963



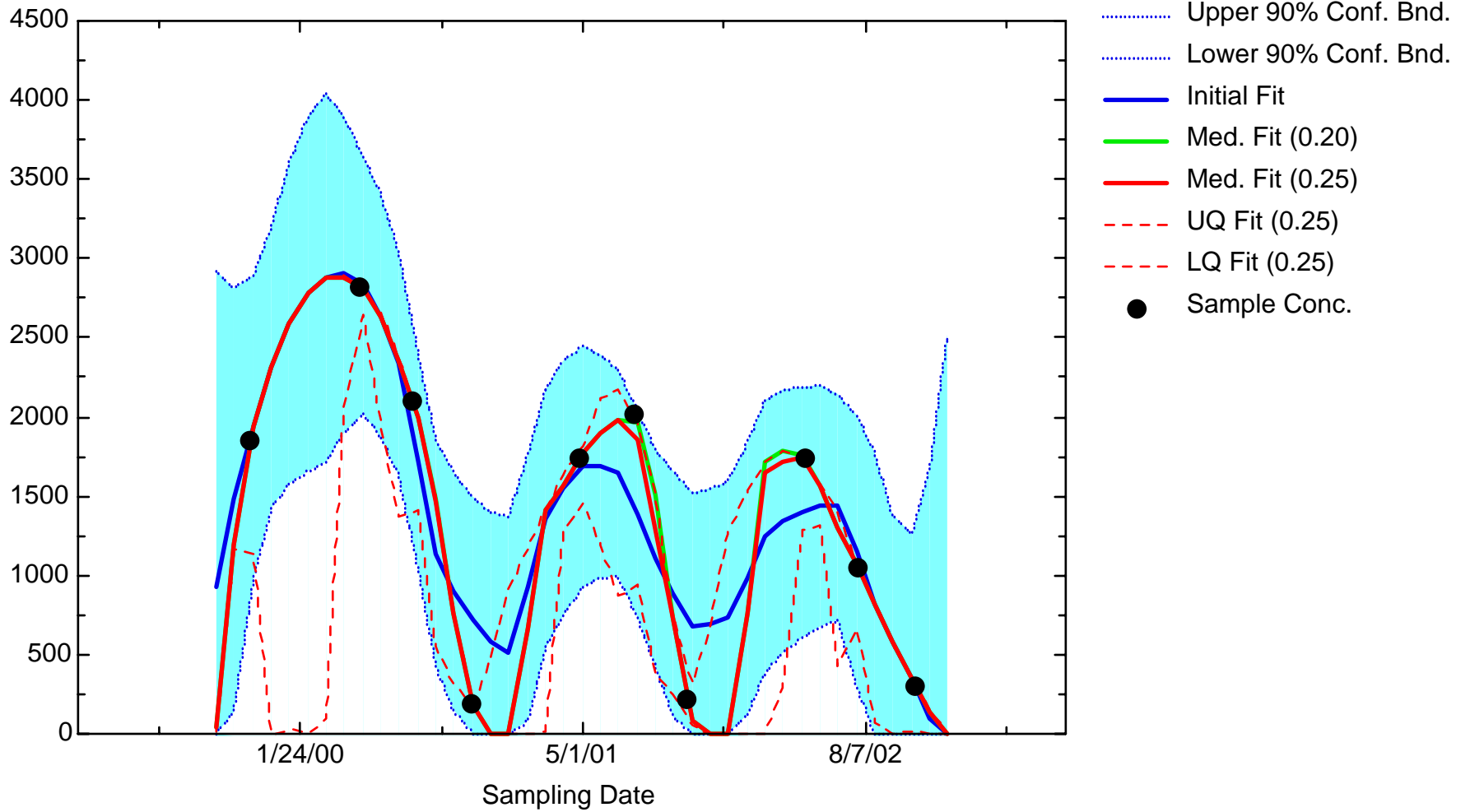
FE: Well JMW1964



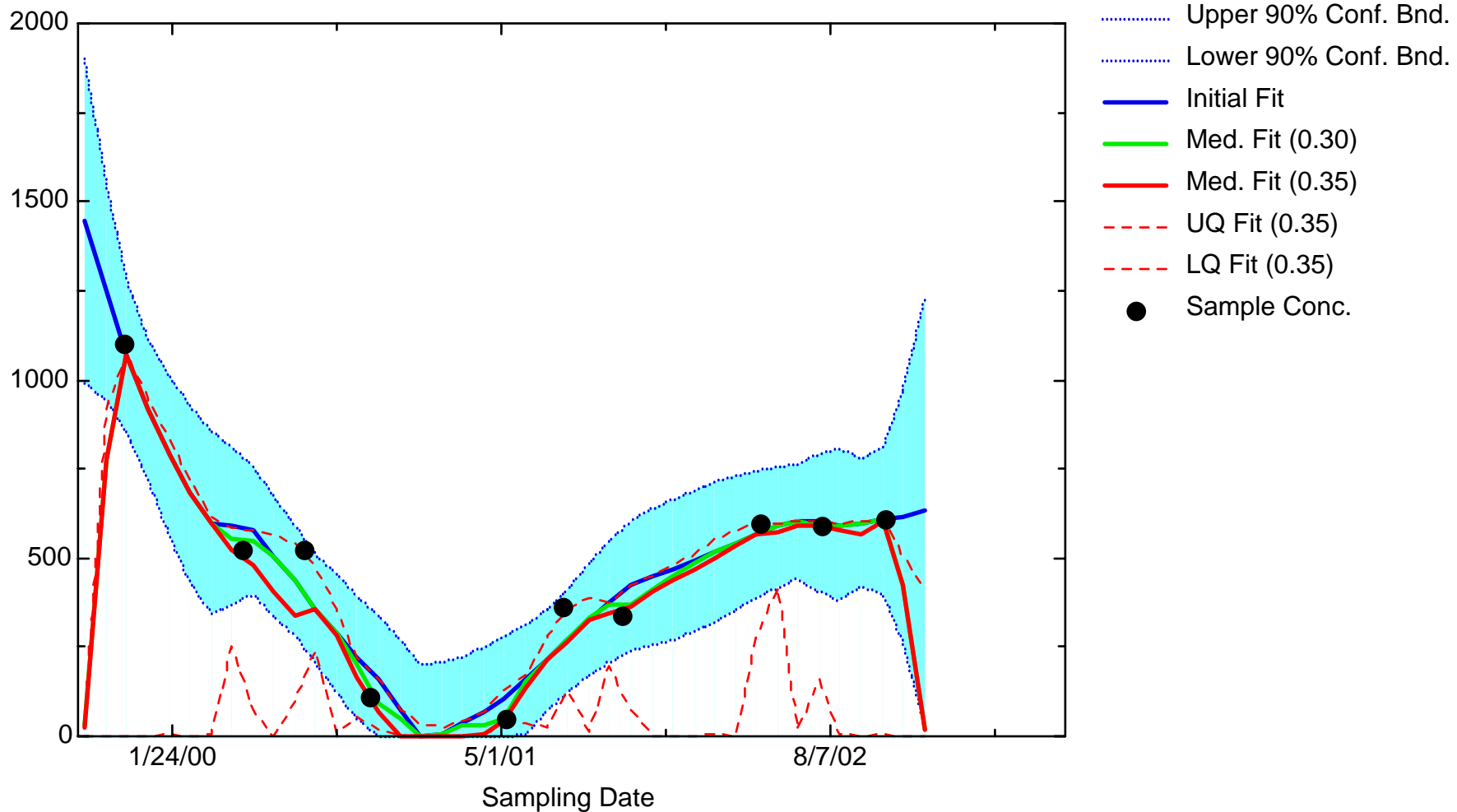
FE: Well JMW1966



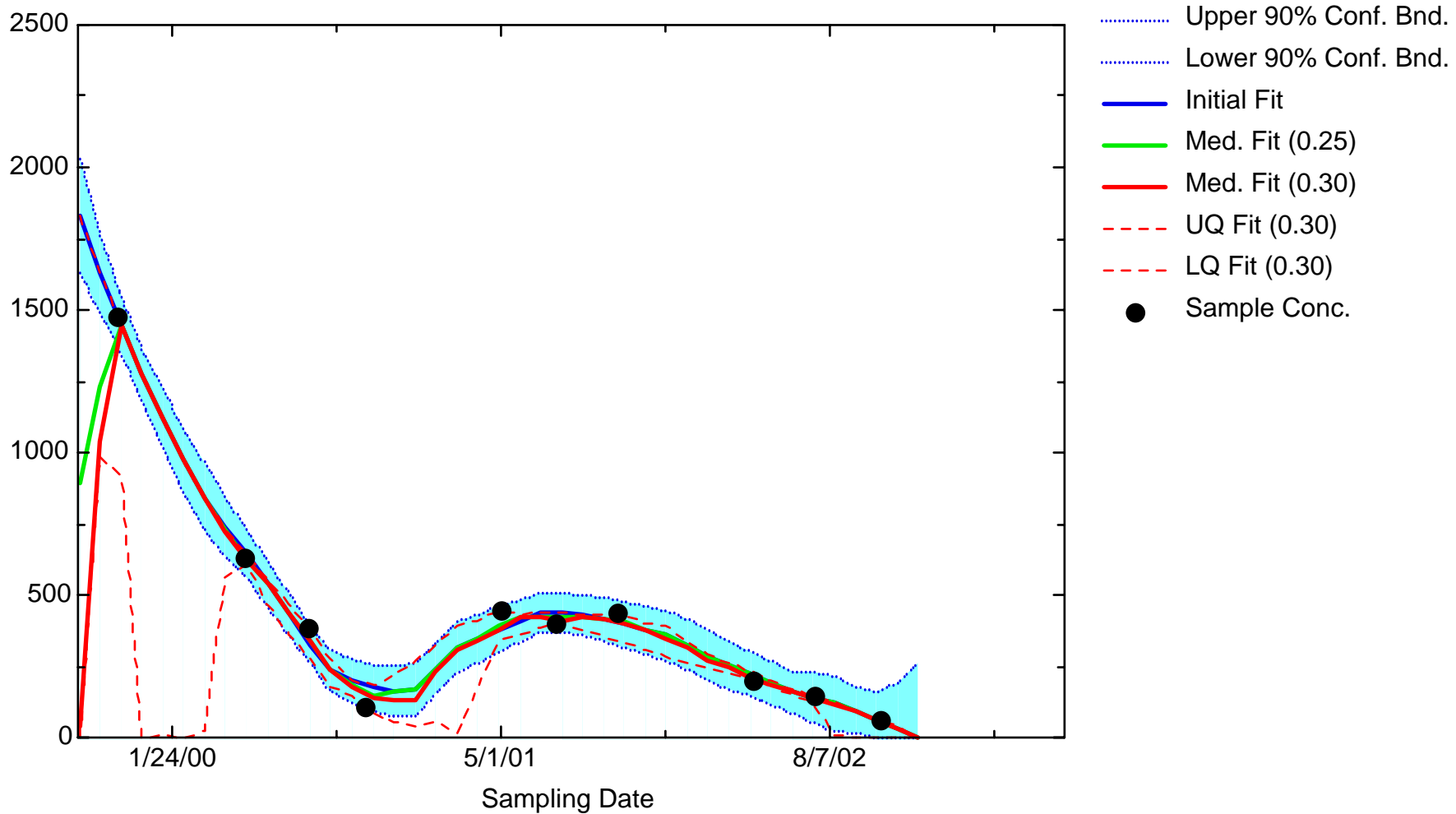
FE: Well JMW3202



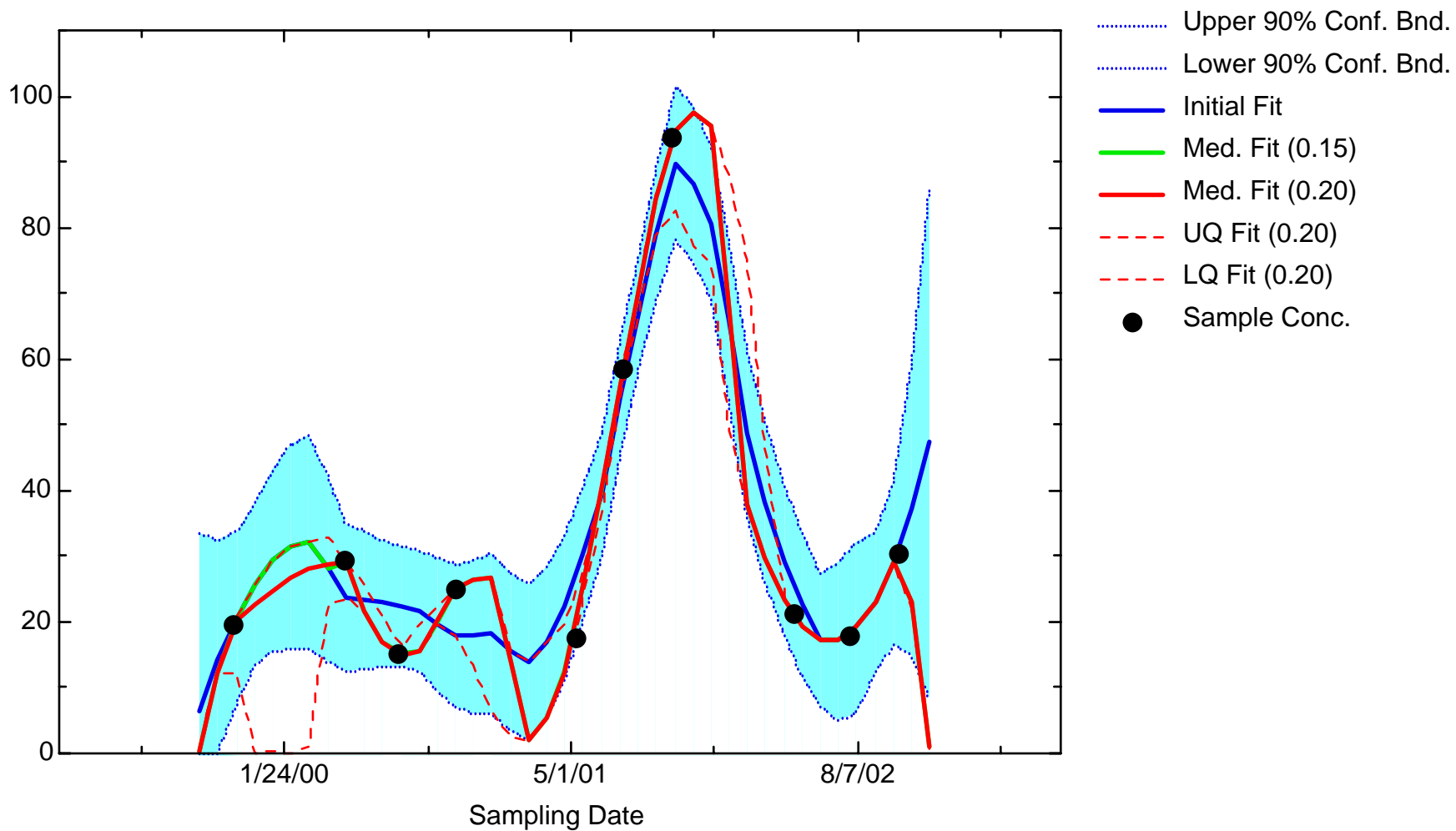
FE: Well JMW7332



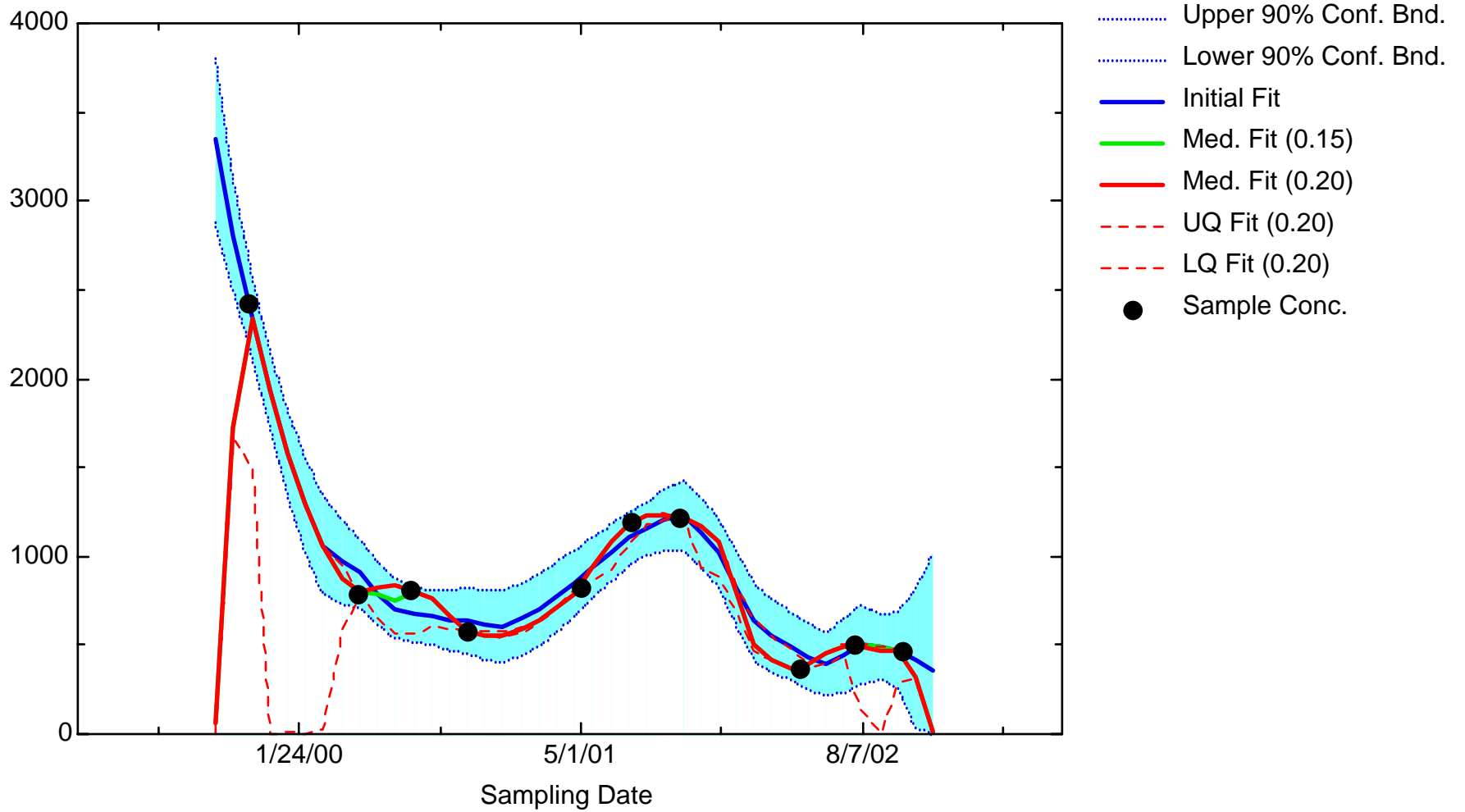
FE: Well JMW8011



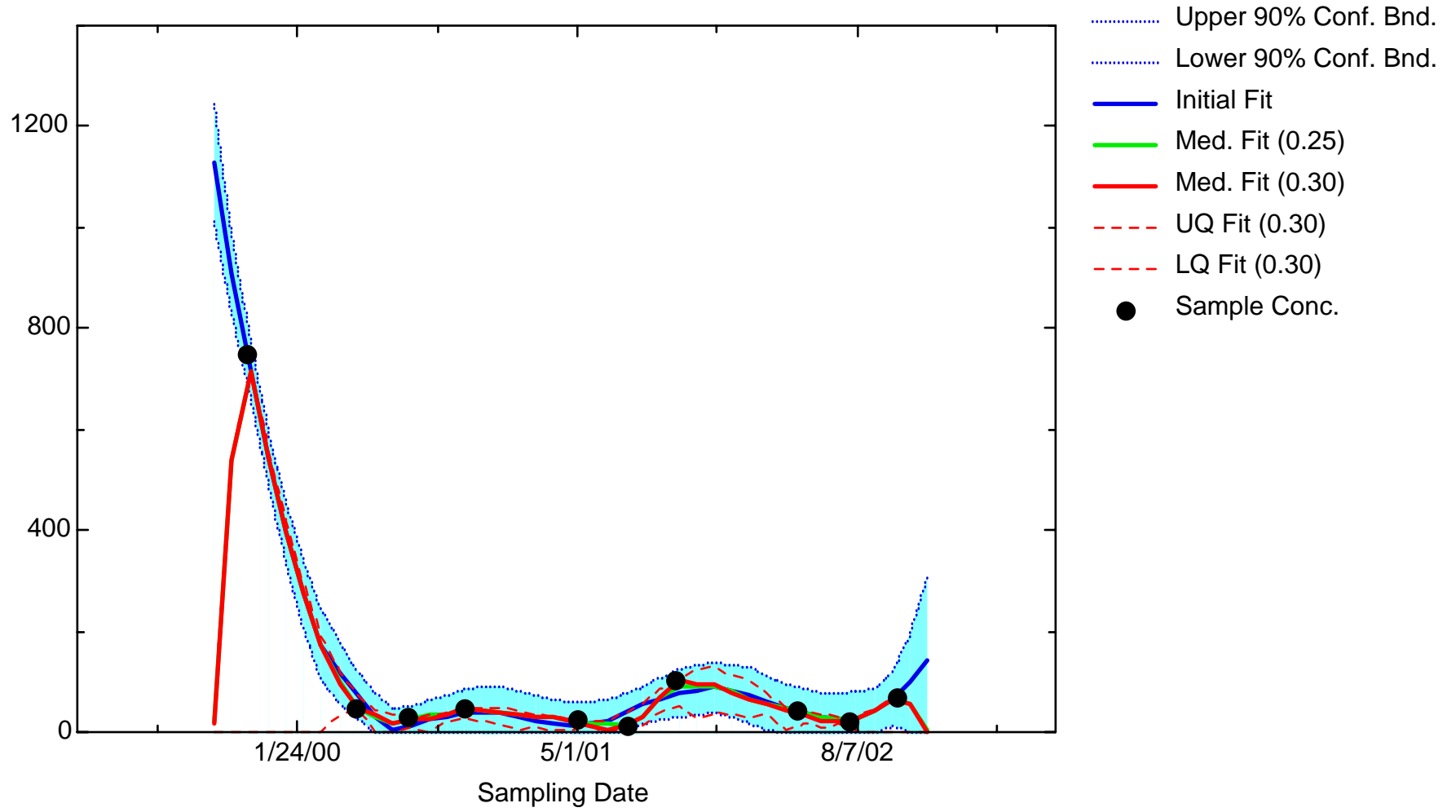
FE: Well JPZ0340



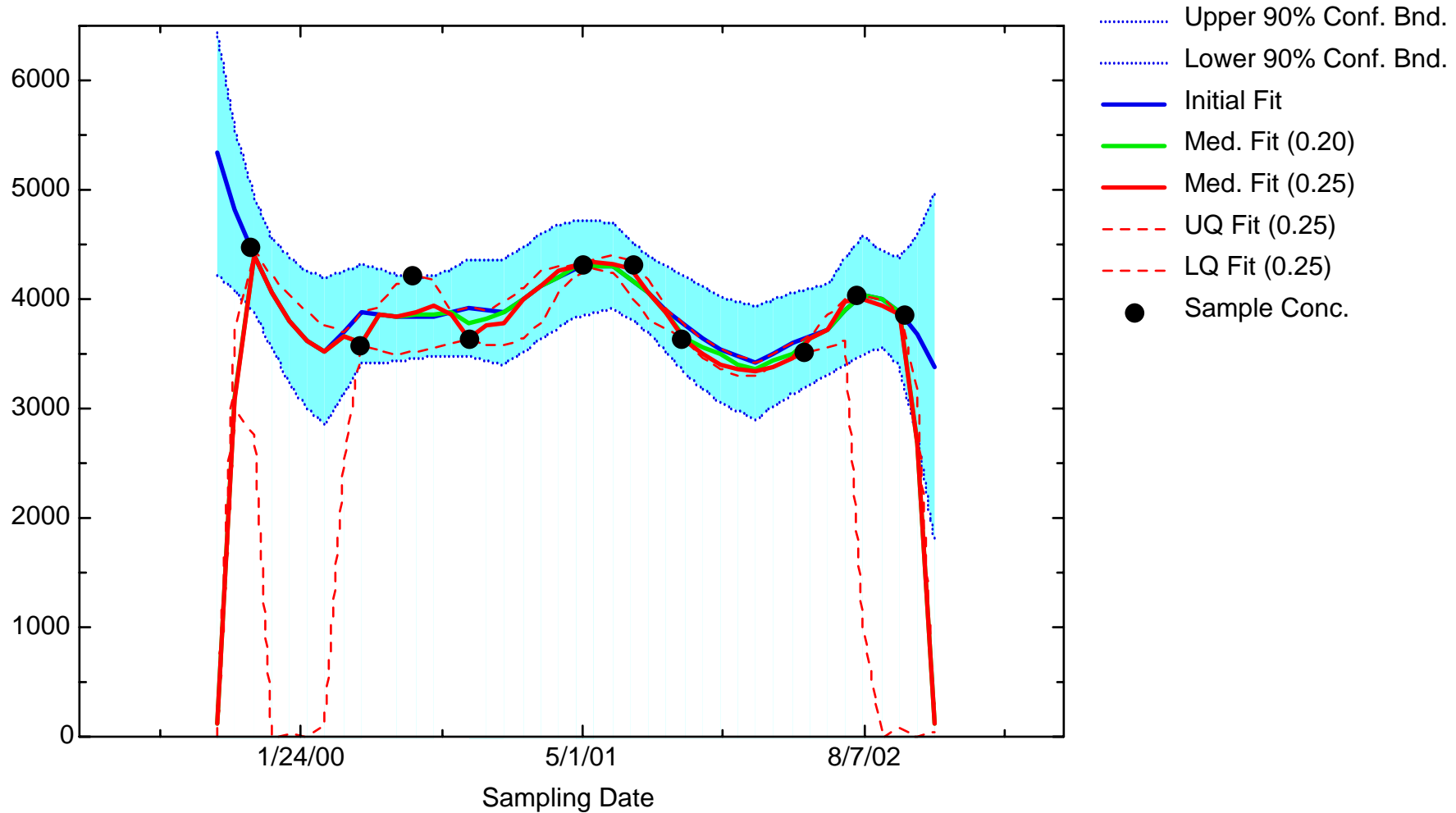
FE: Well JPZ0341



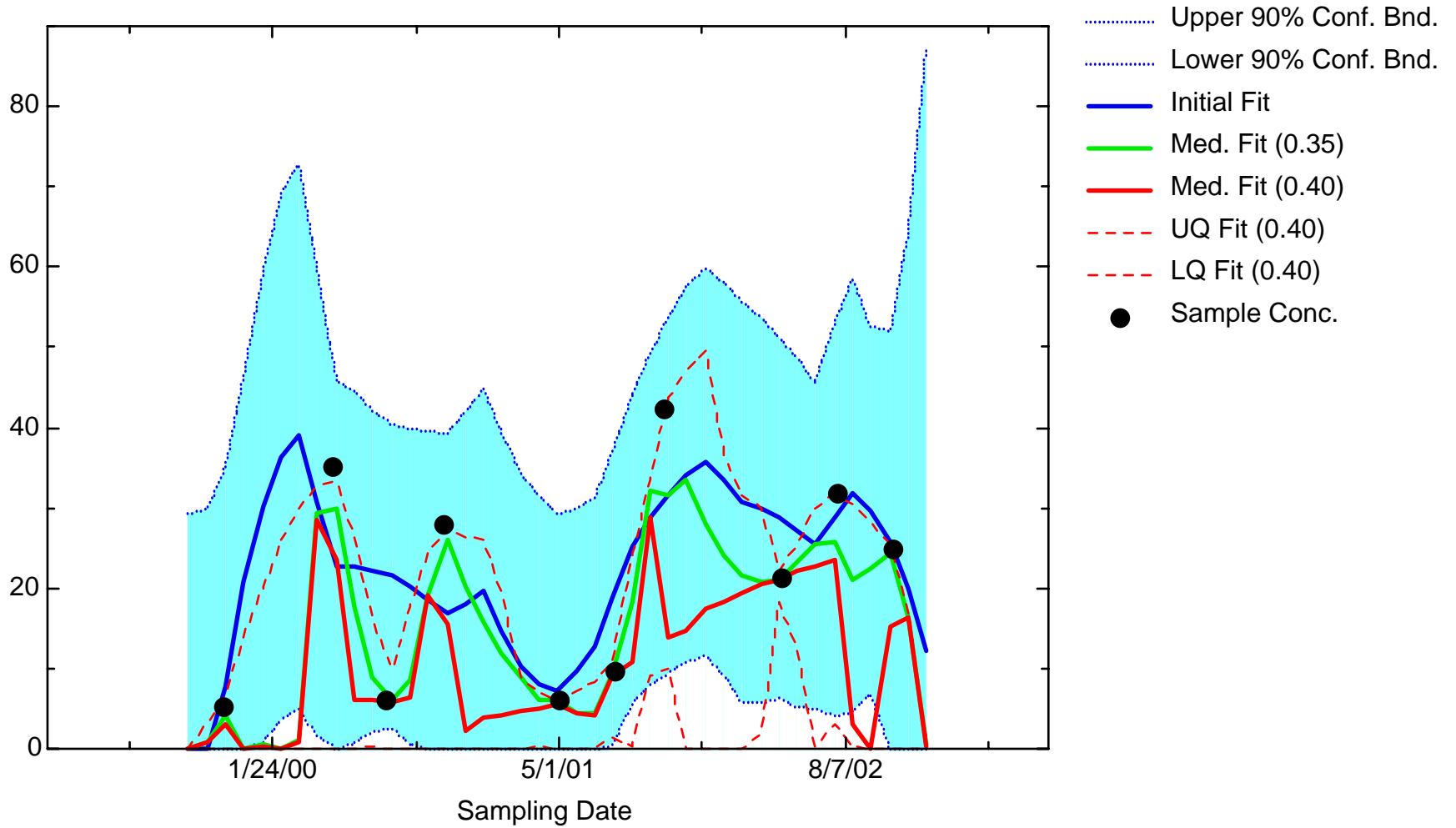
FE: Well JPZ0342



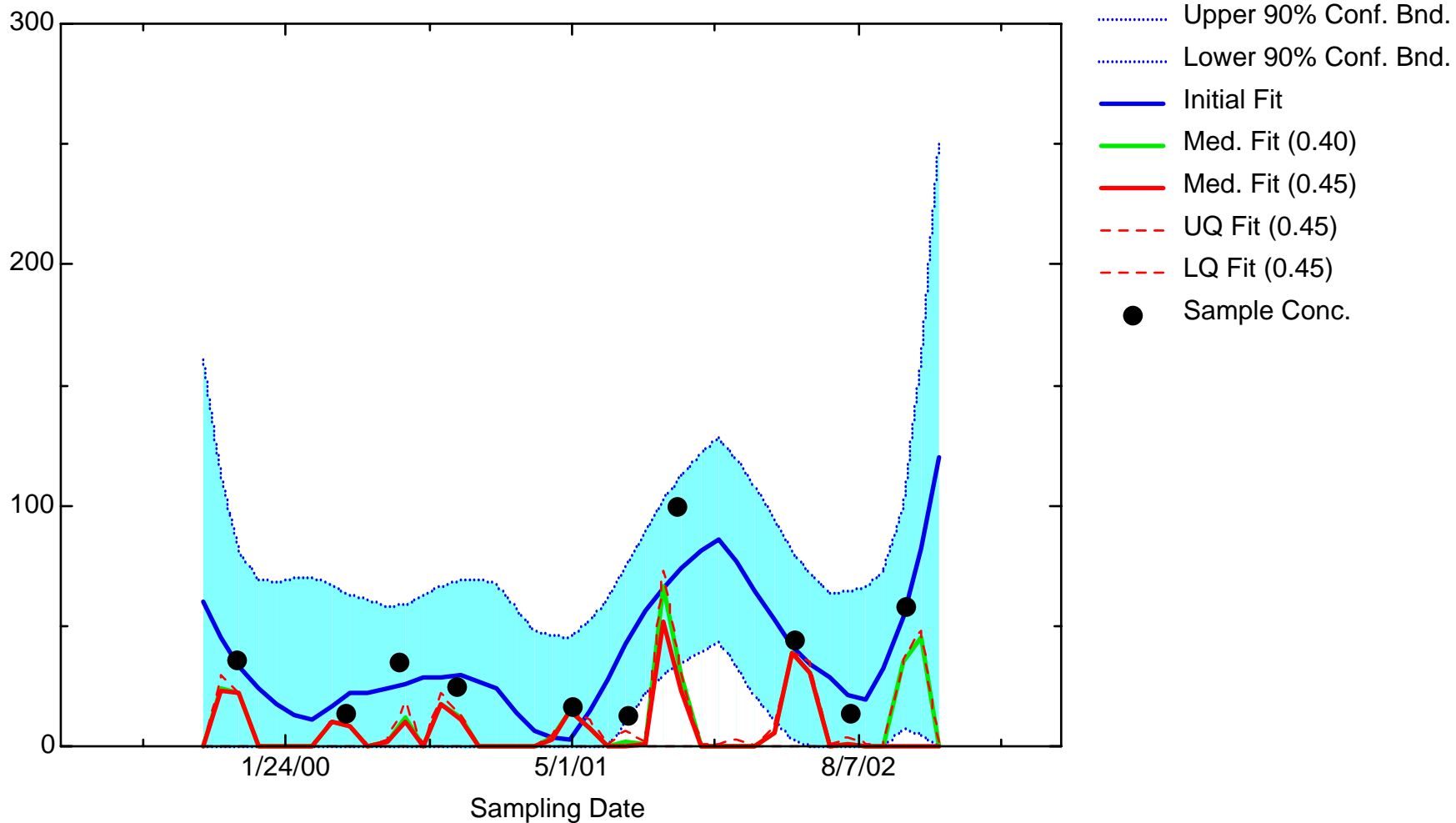
FE: Well JPZ0343



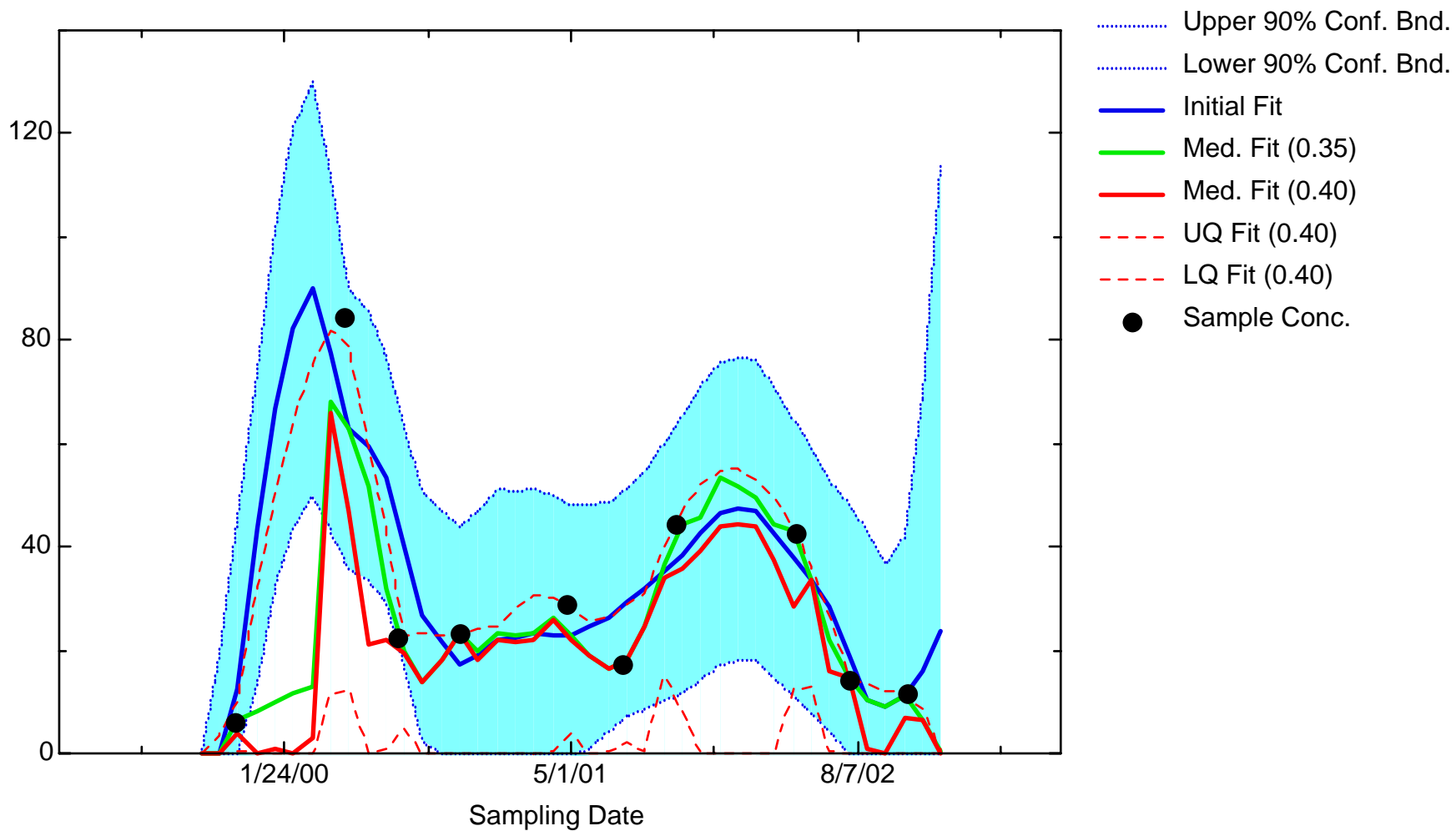
FE: Well JPZ0348



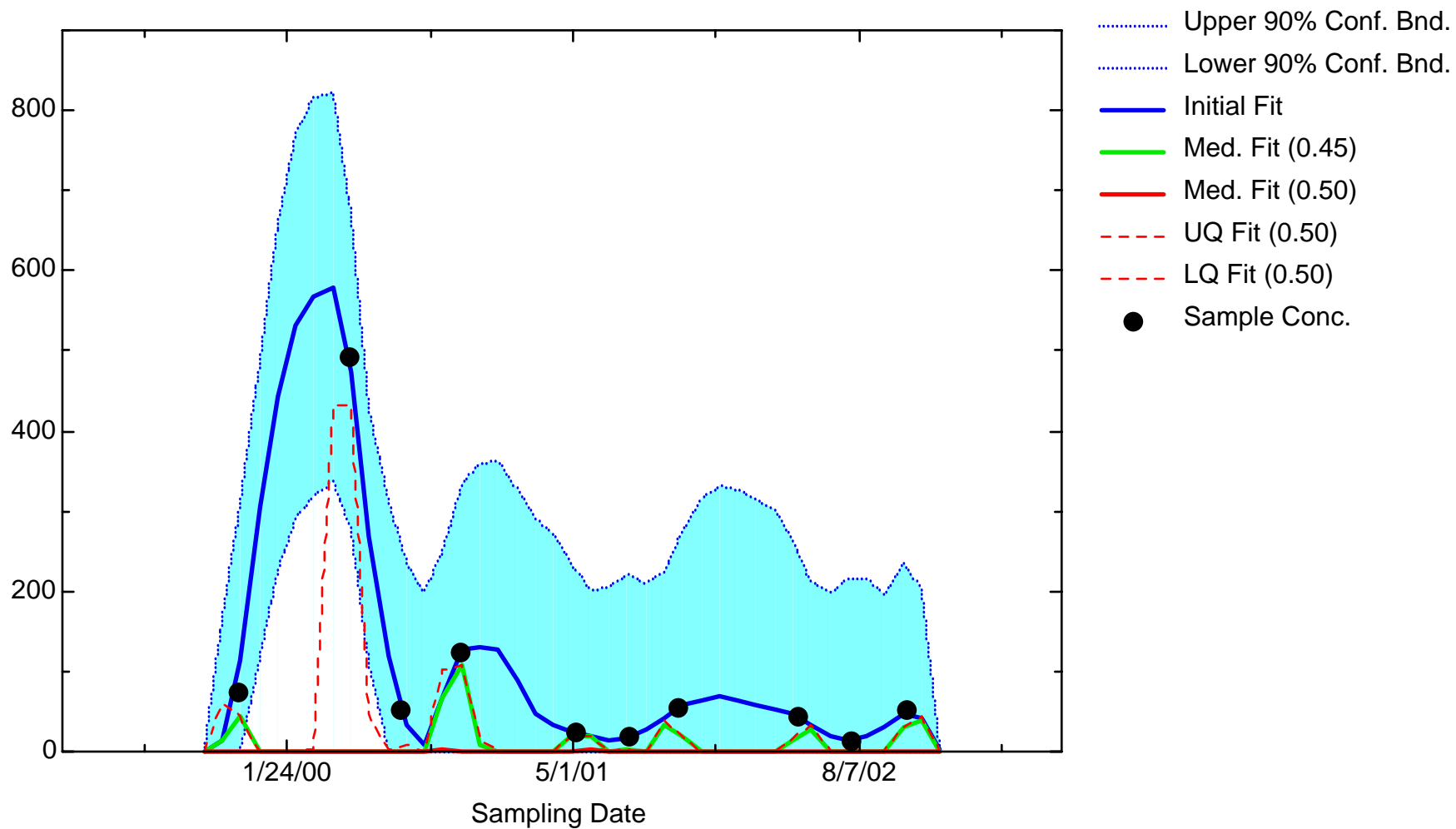
FE: Well JPZ0349



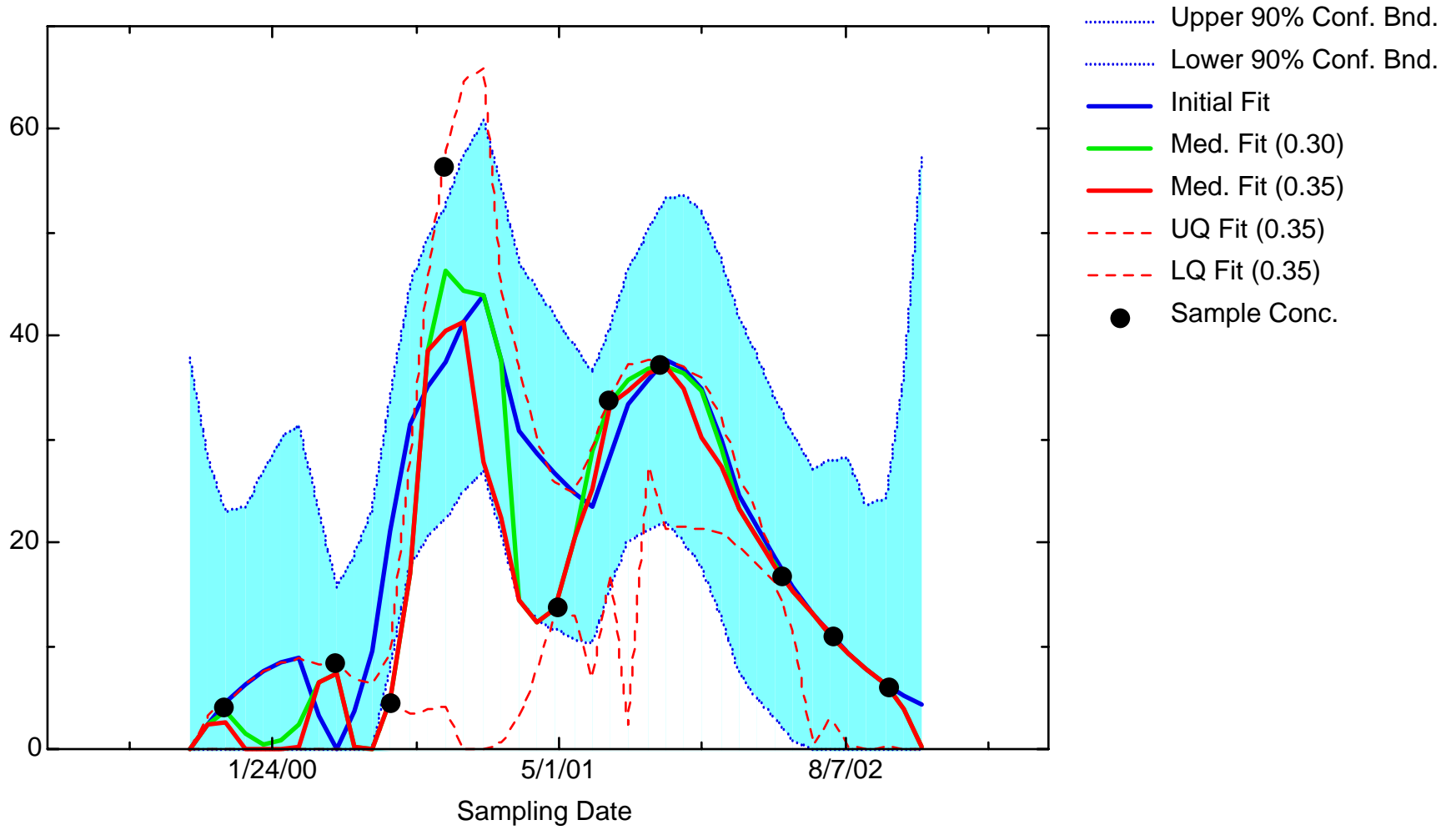
FE: Well JPZ1780



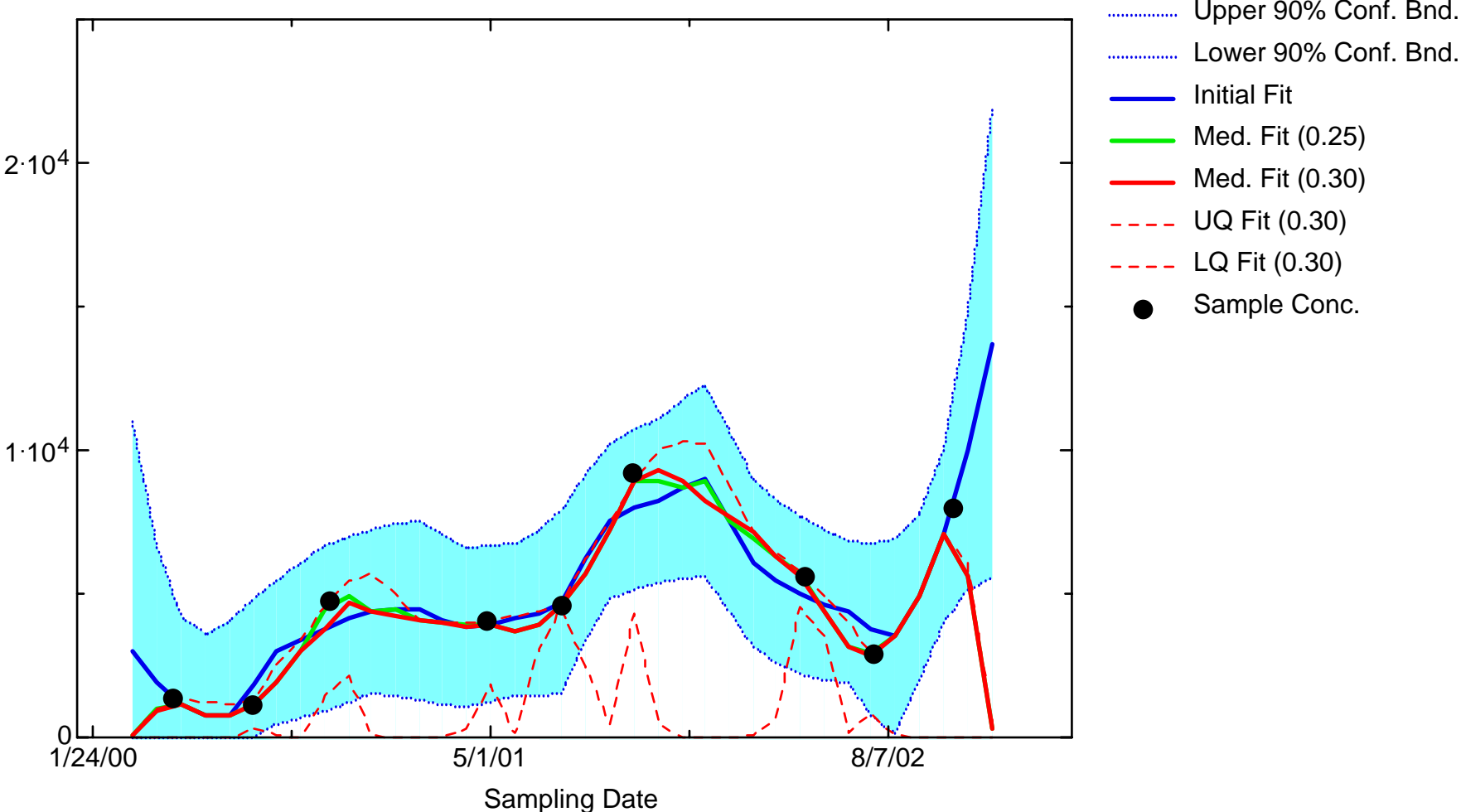
FE: Well JPZ7208



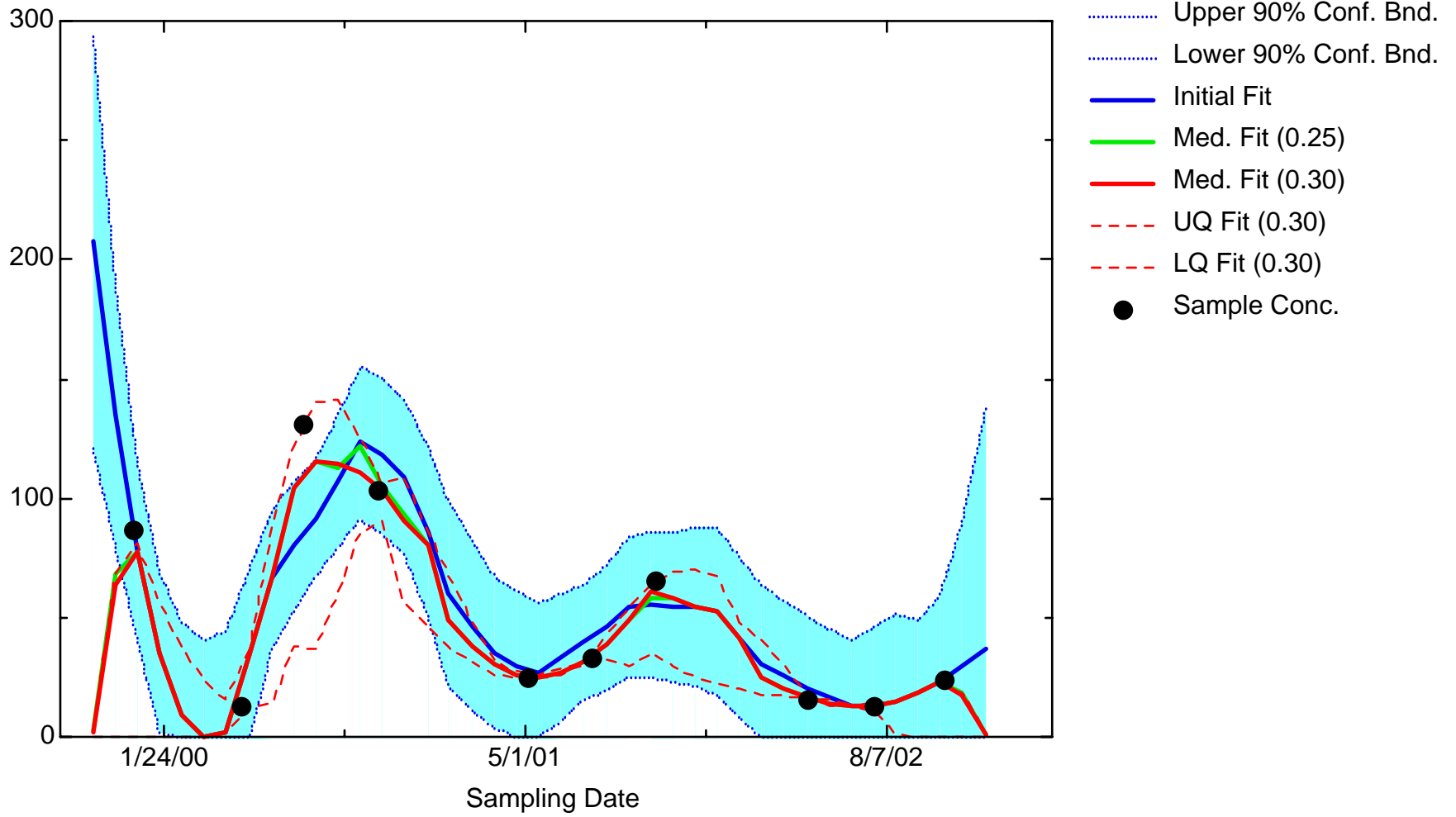
FE: Well JPZ7807



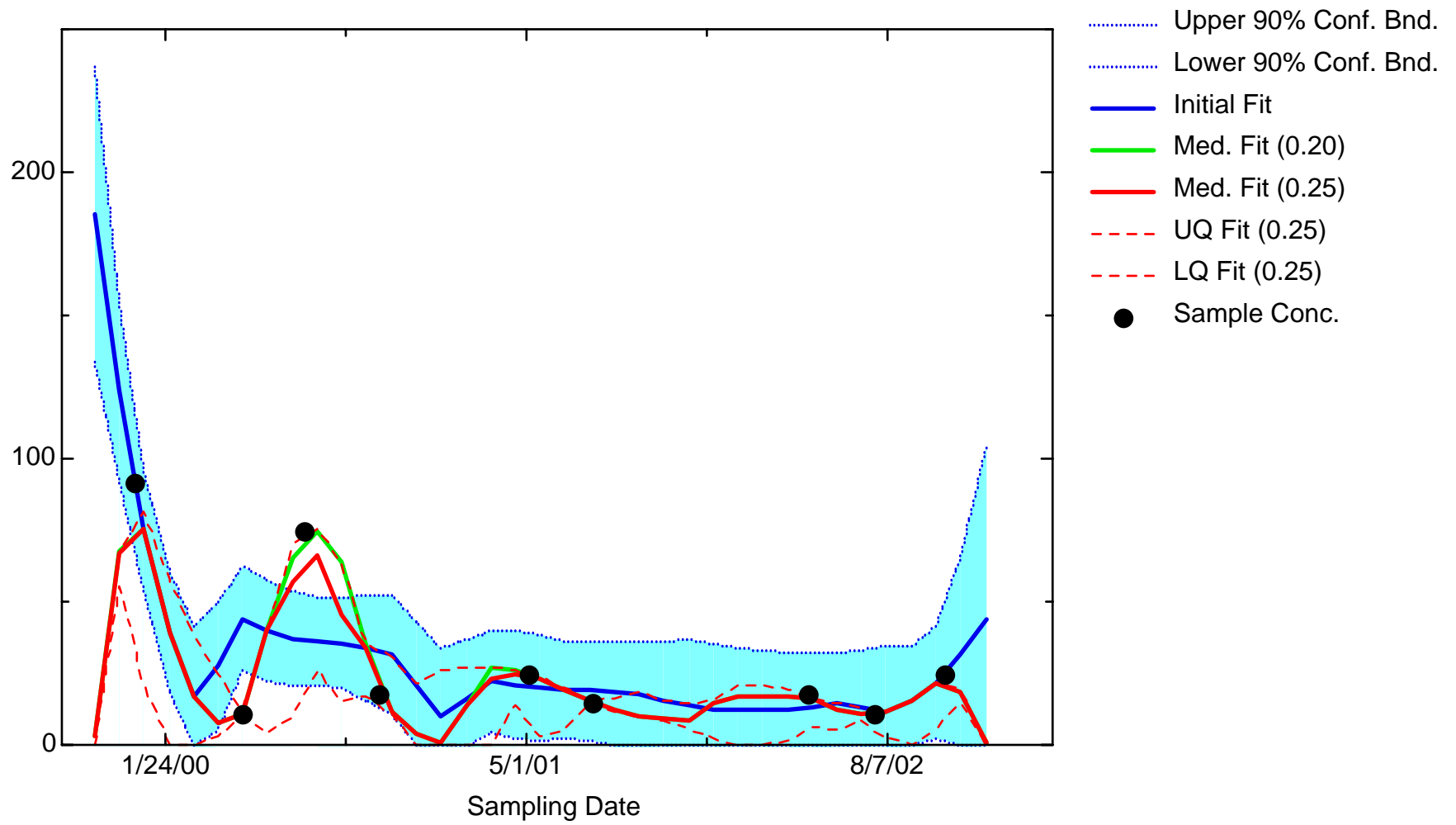
FE: Well MMW0005



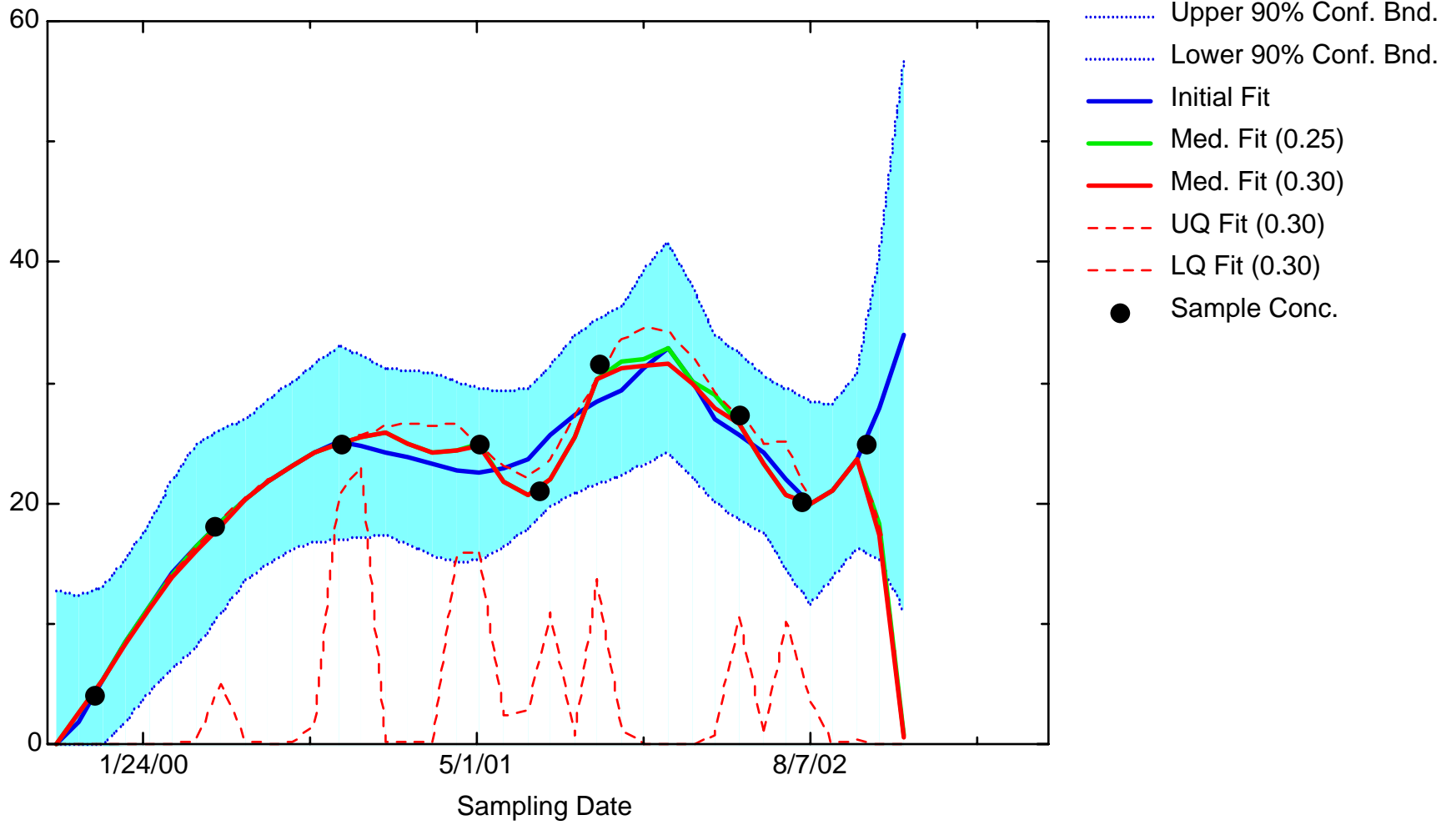
FE: Well MMW0007A



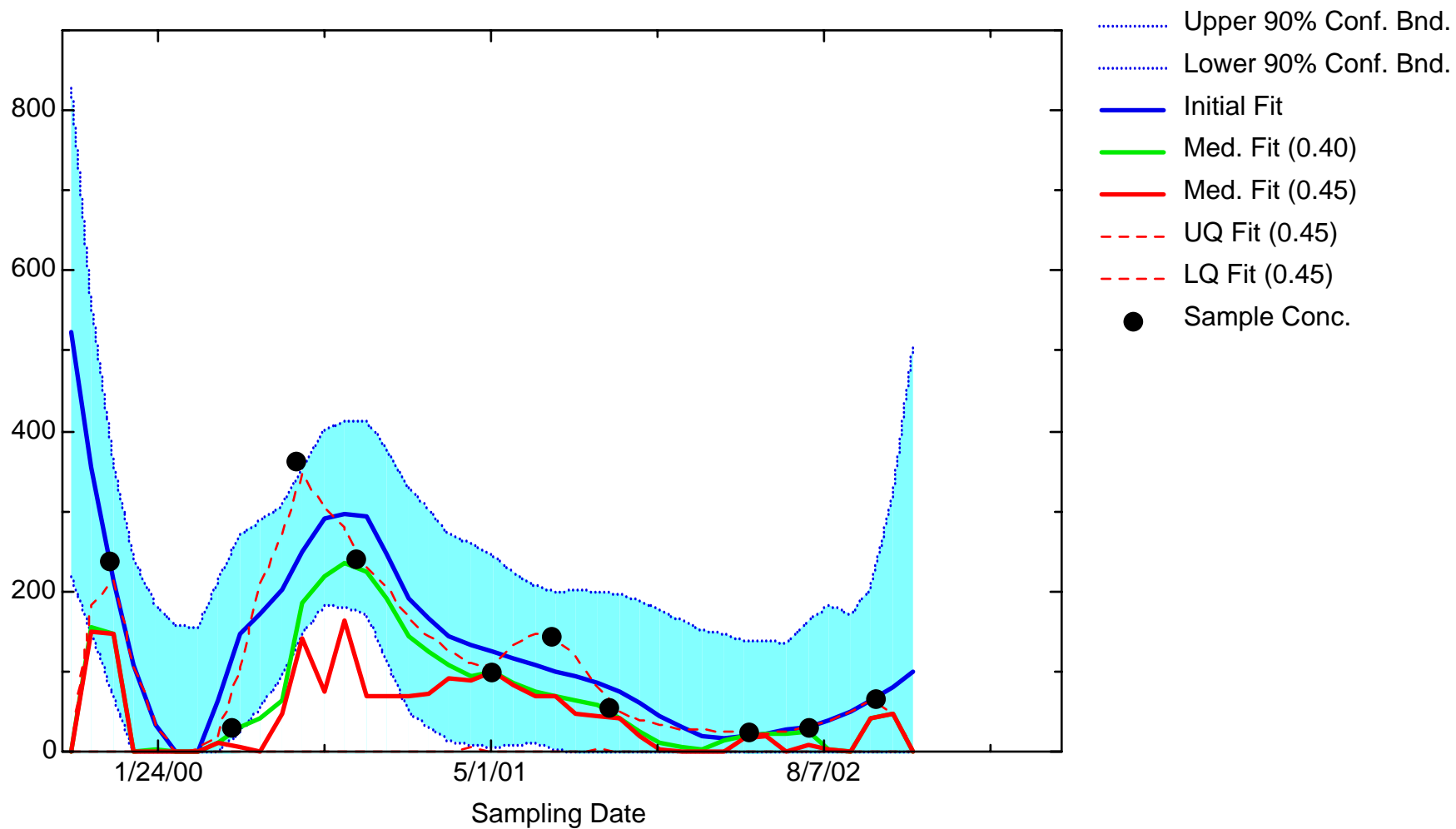
FE: Well MMW0007B



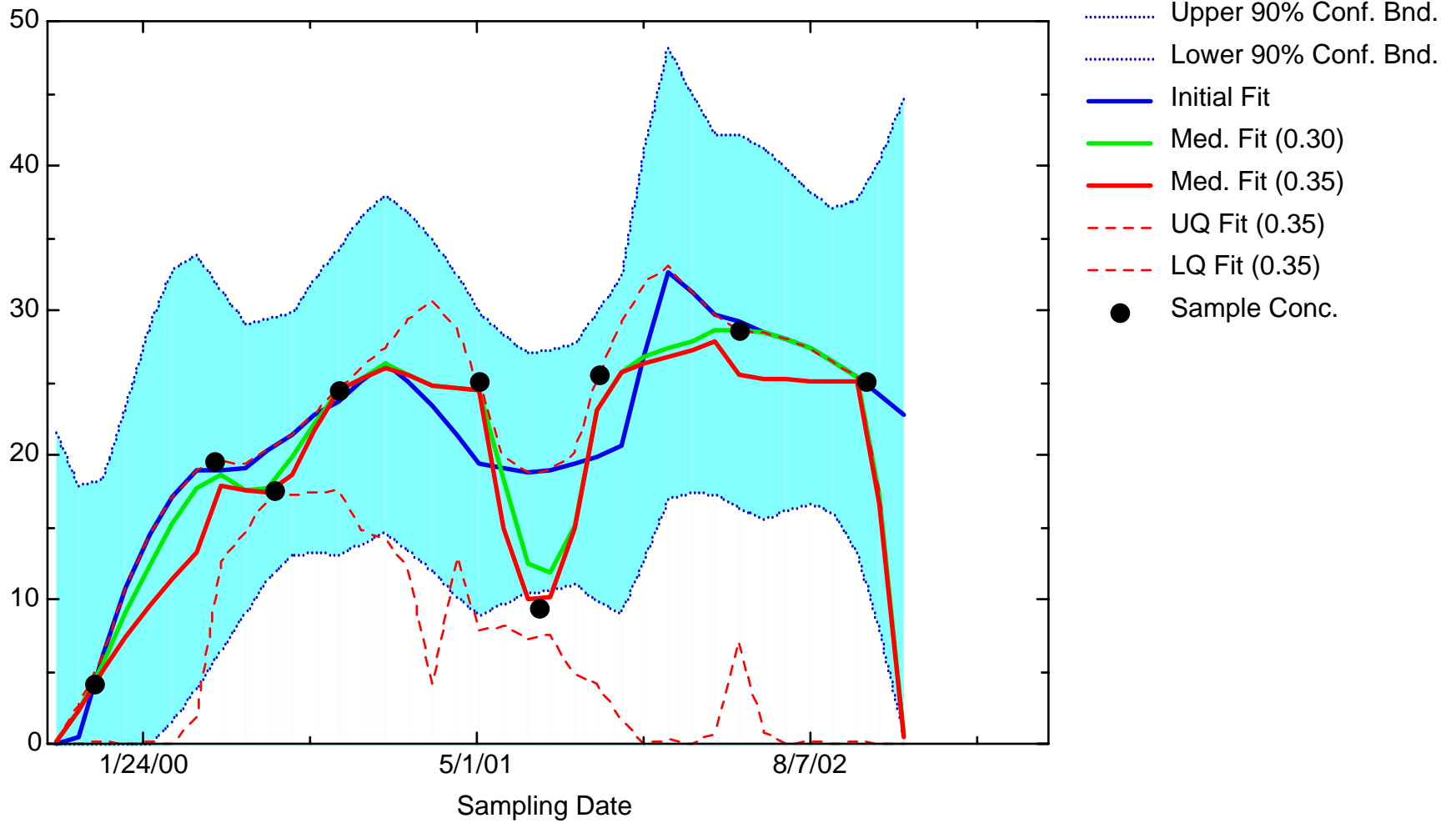
FE: Well MMW0008



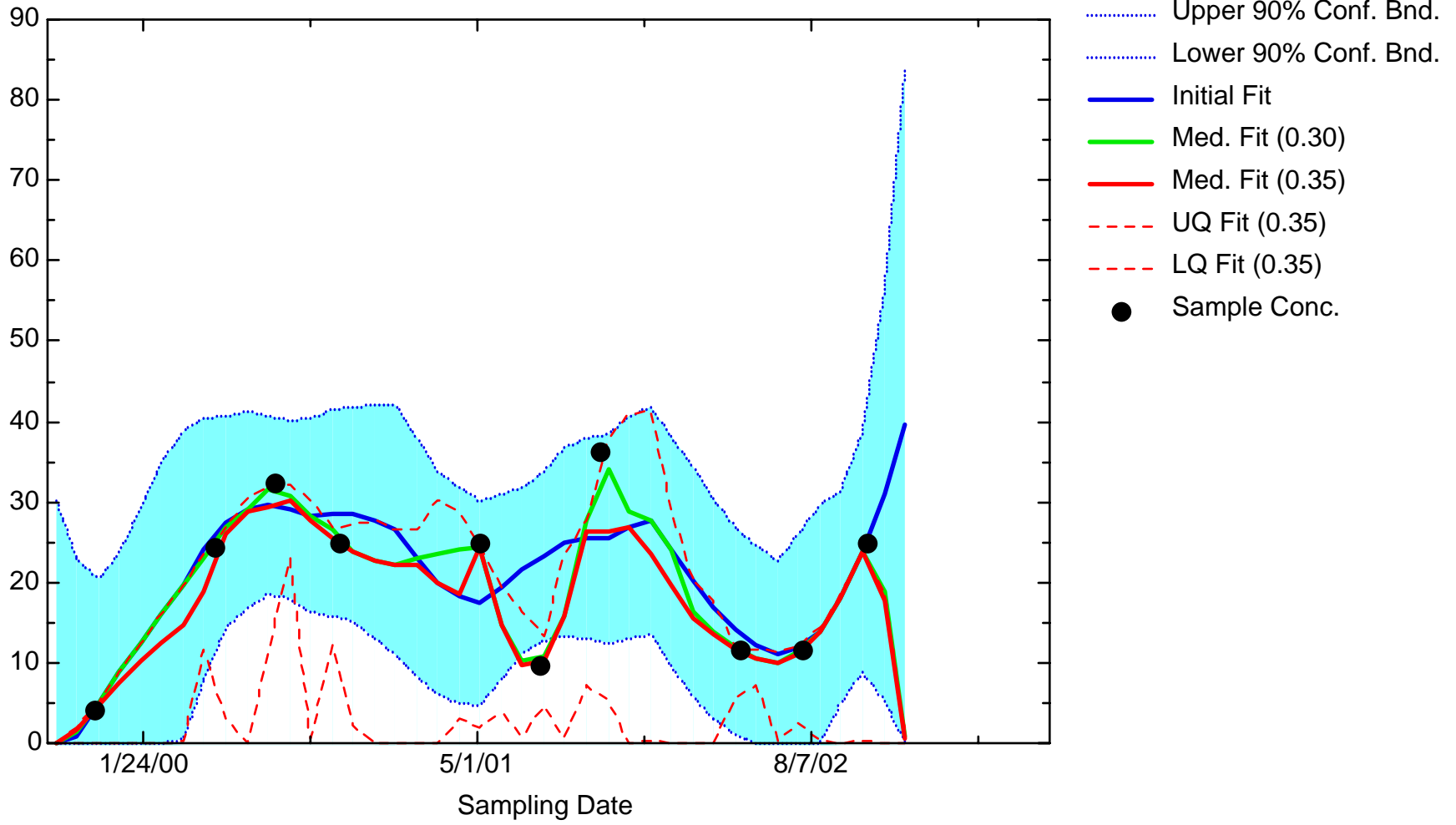
FE: Well MMW0009



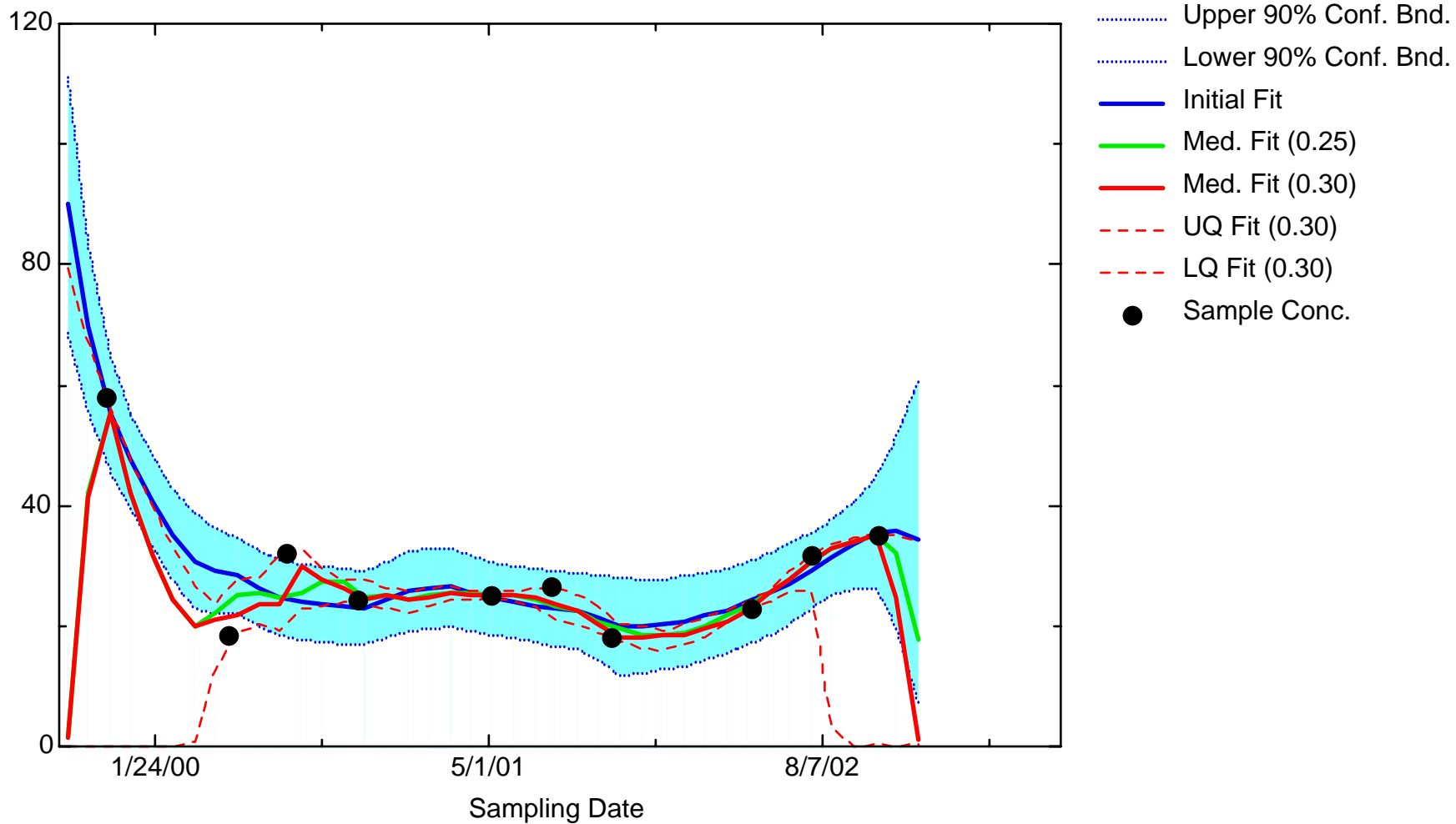
FE: Well MMW0010



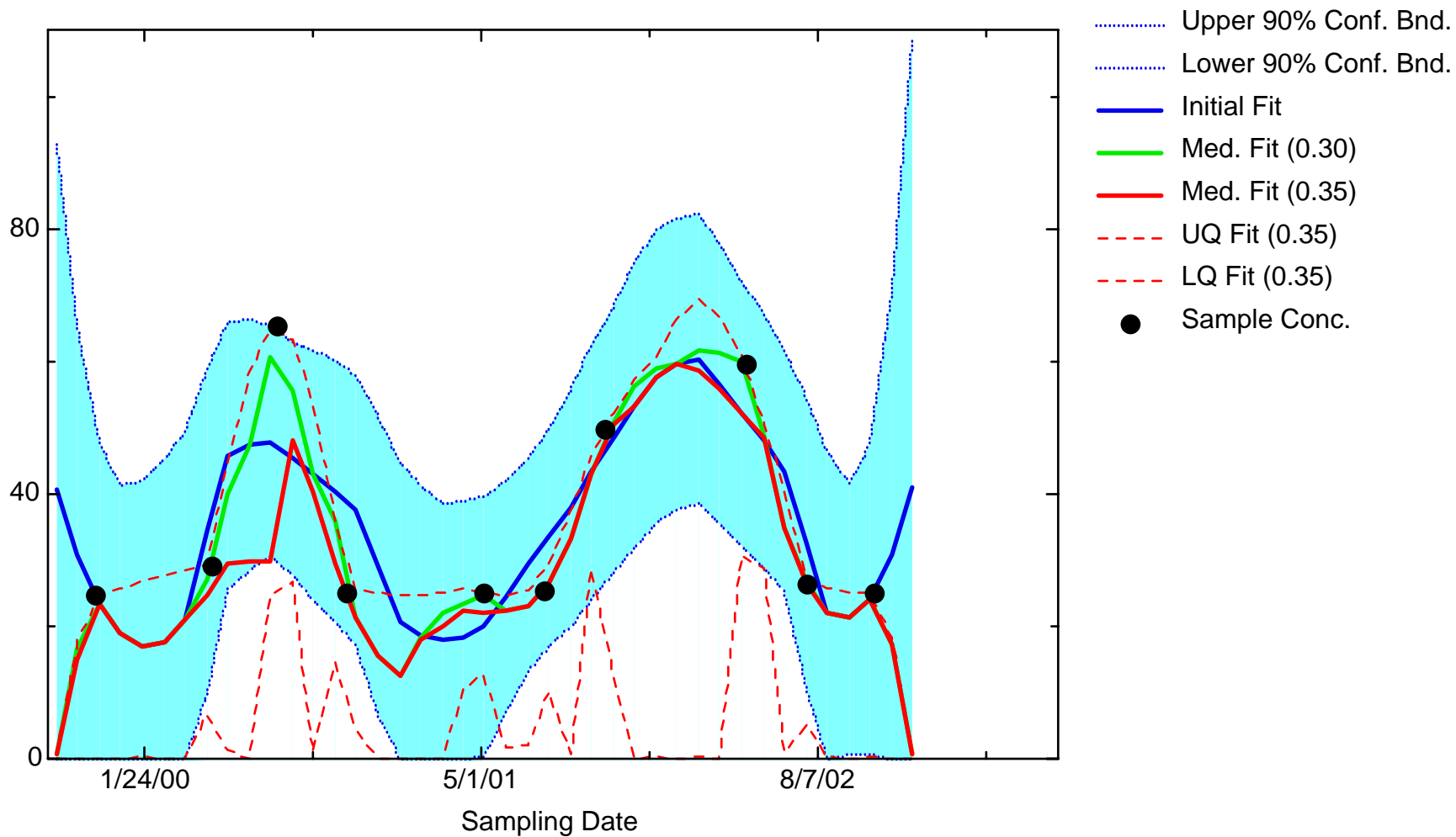
FE: Well MMW0011



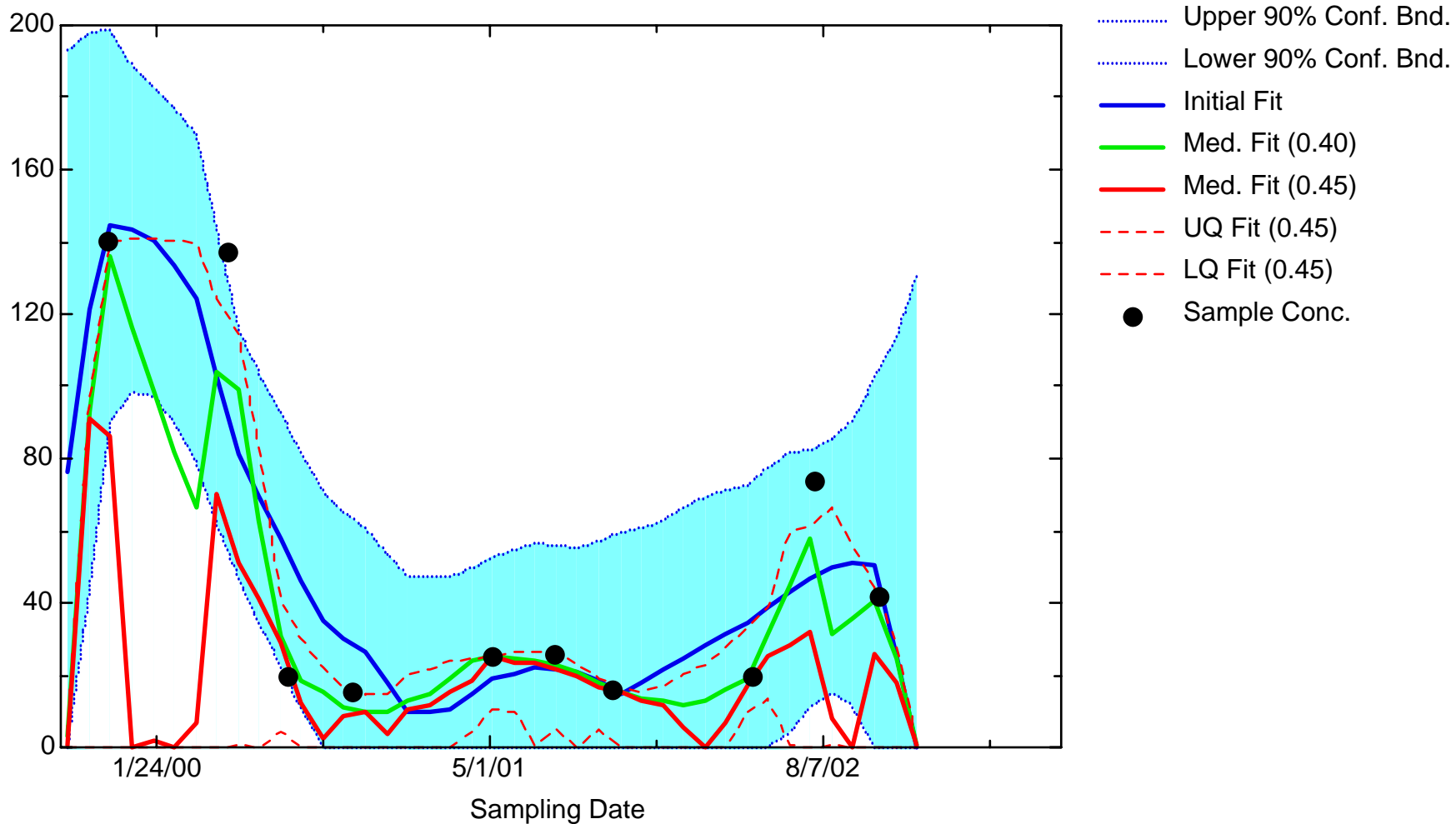
FE: Well MMW0012



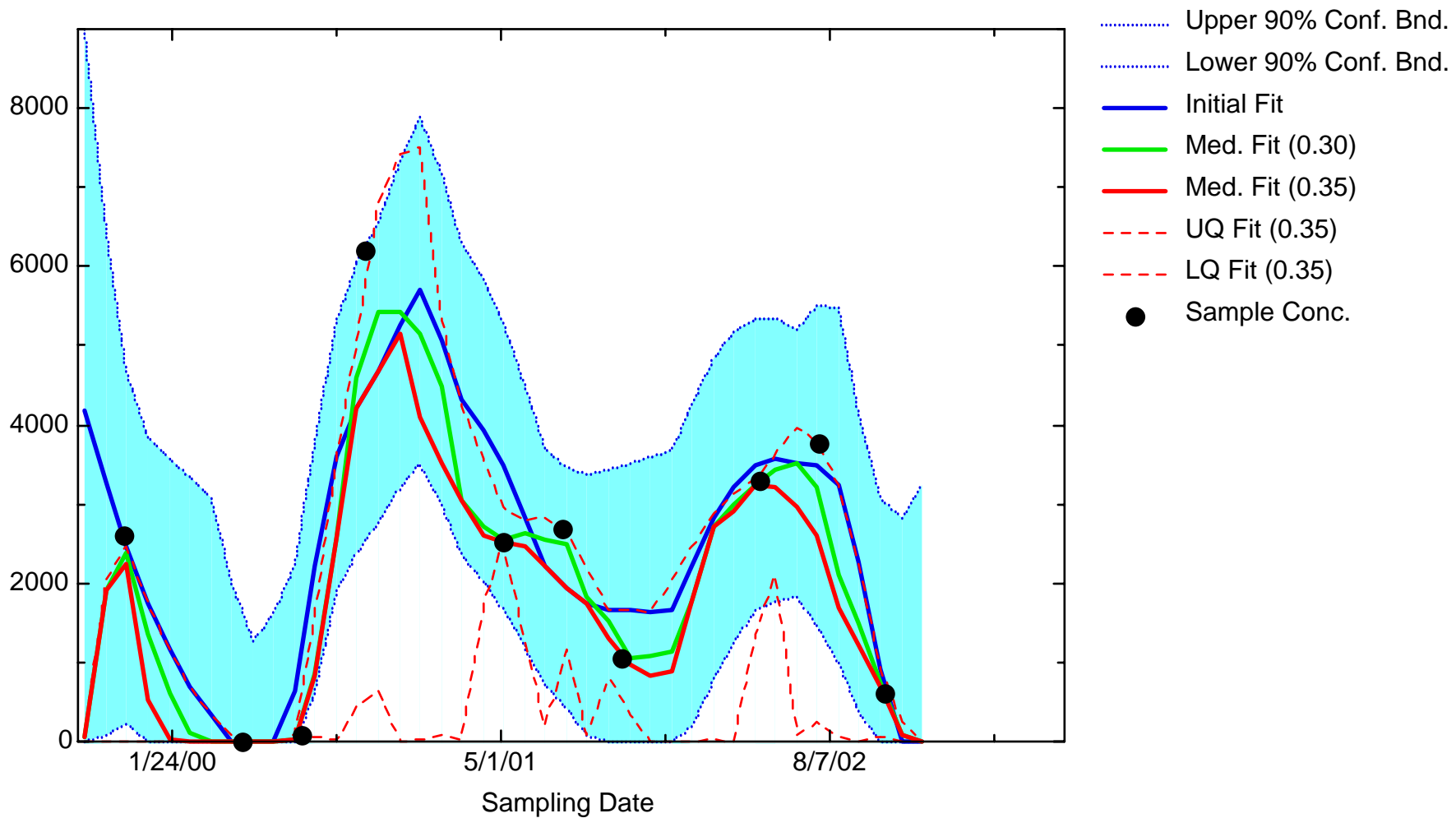
FE: Well MMW0013



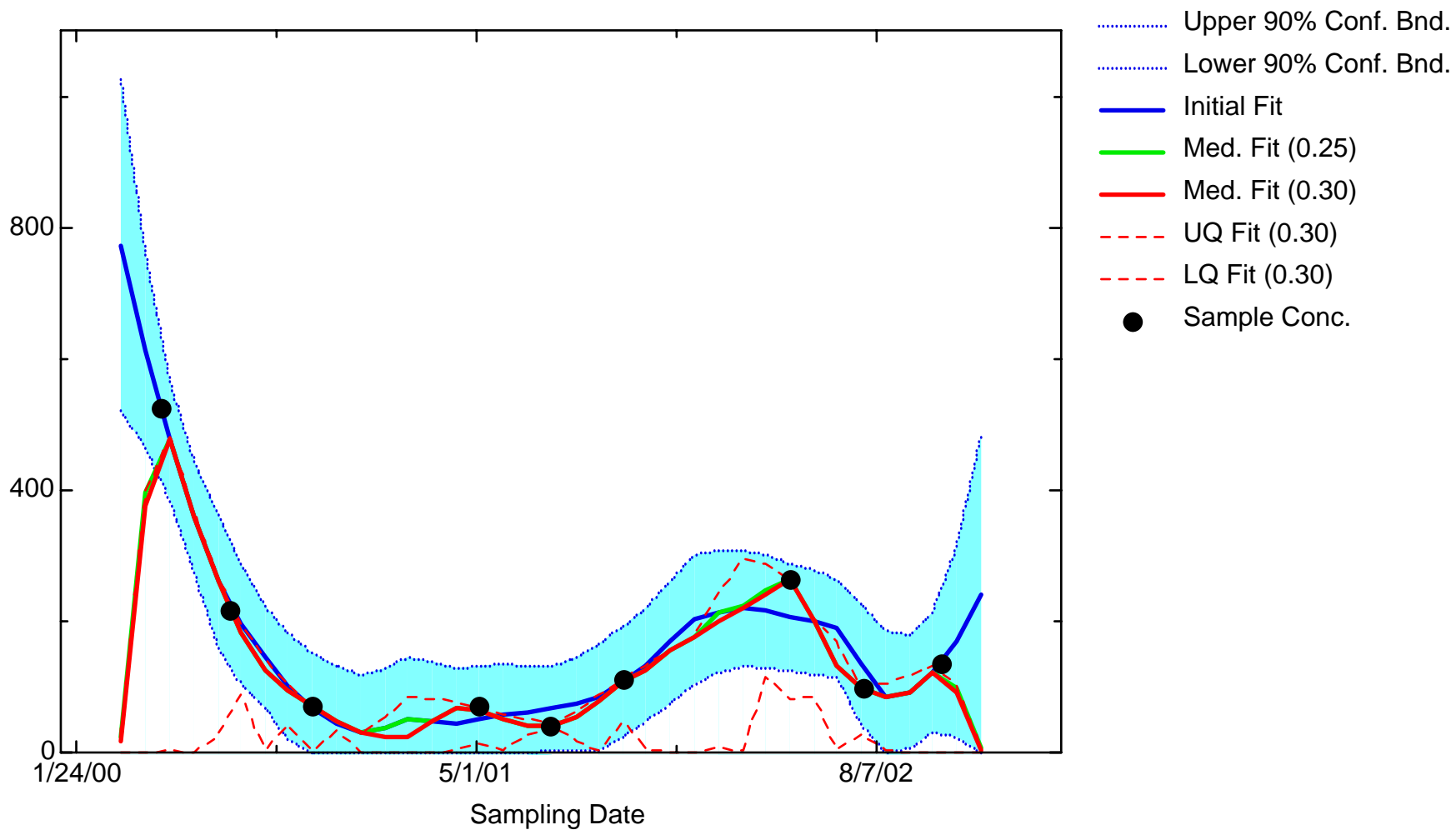
FE: Well MMW0016



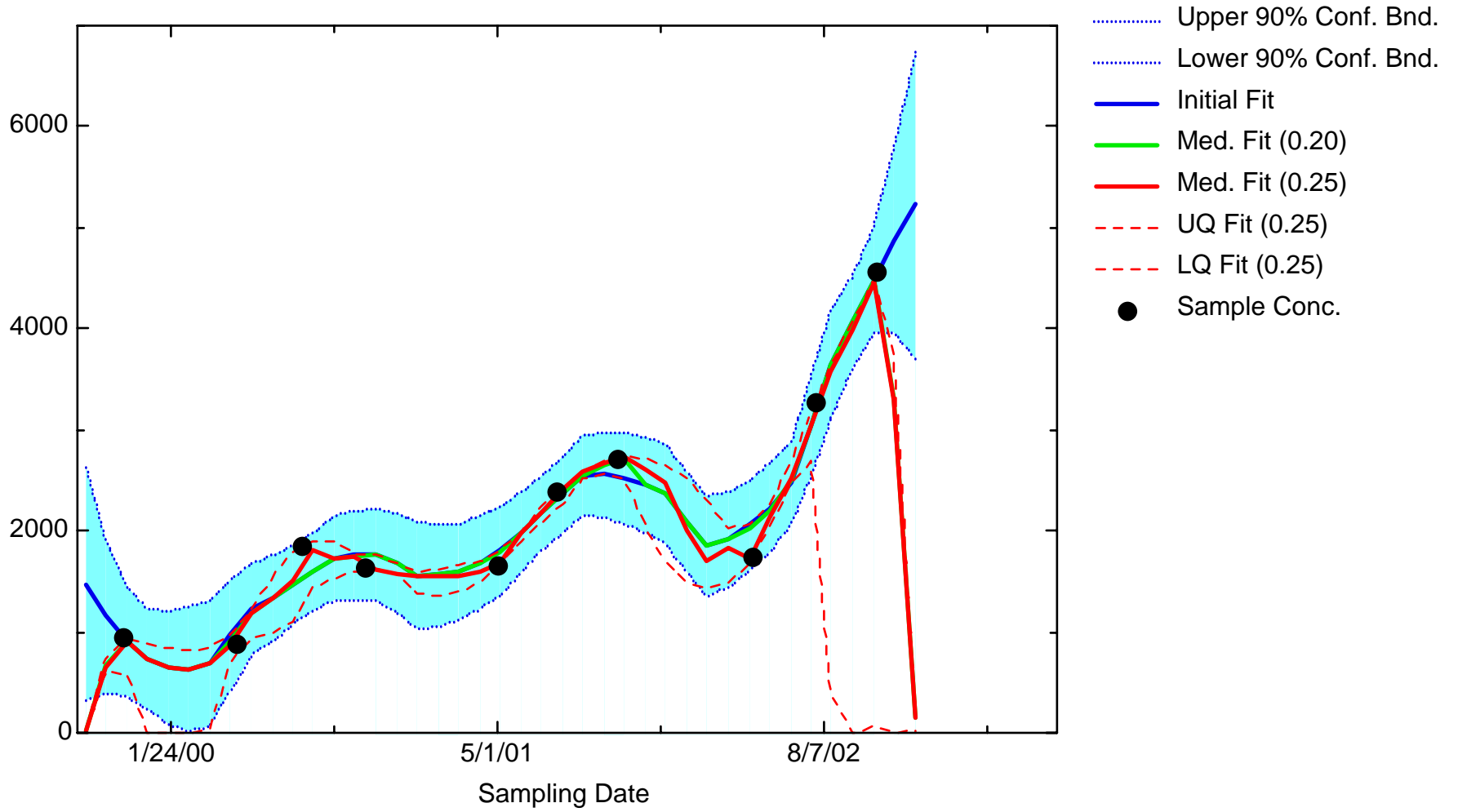
FE: Well MMW0017



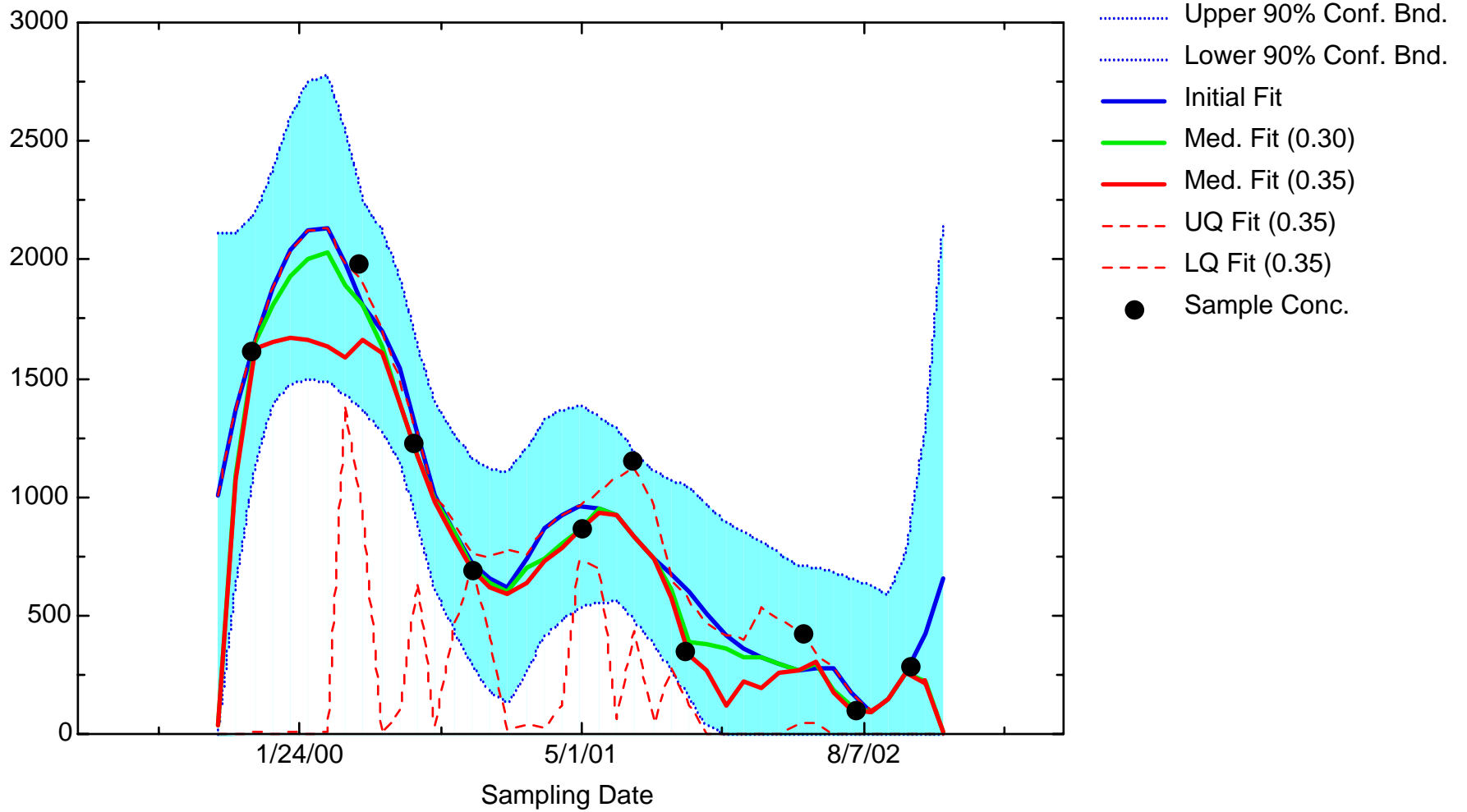
FE: Well MMW0019



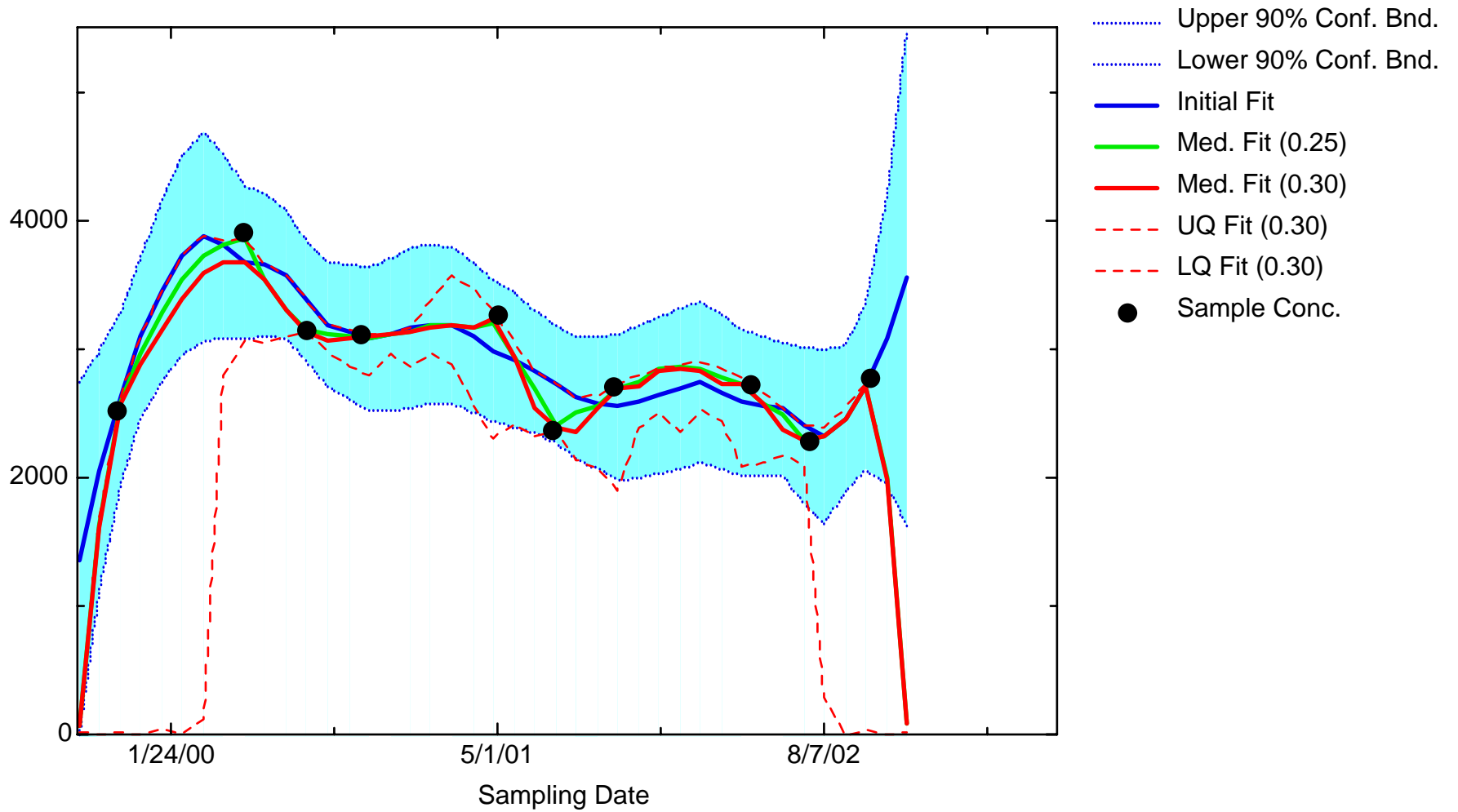
FE: Well MMW1560



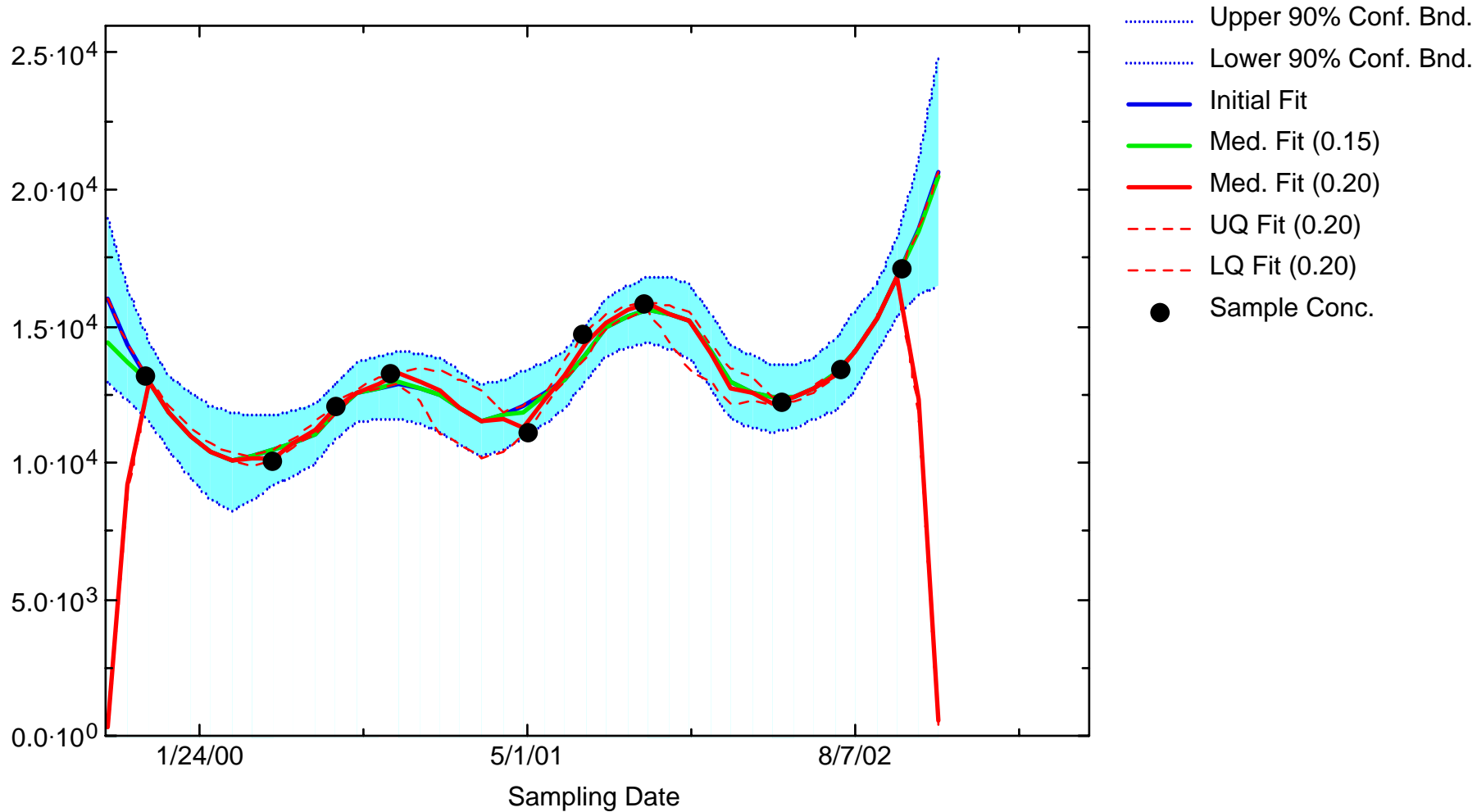
FE: Well MMW7330



FE: Well RFW1144



FE: Well RFW1147



Appendix 3-2

Temporal Optimization: MN Iterative Fitting Overlays

Key to acronyms:

Conf Bnd = Confidence bound

Initial Fit = Locally-weighted quadratic regression (LWQR) estimate on baseline dataset

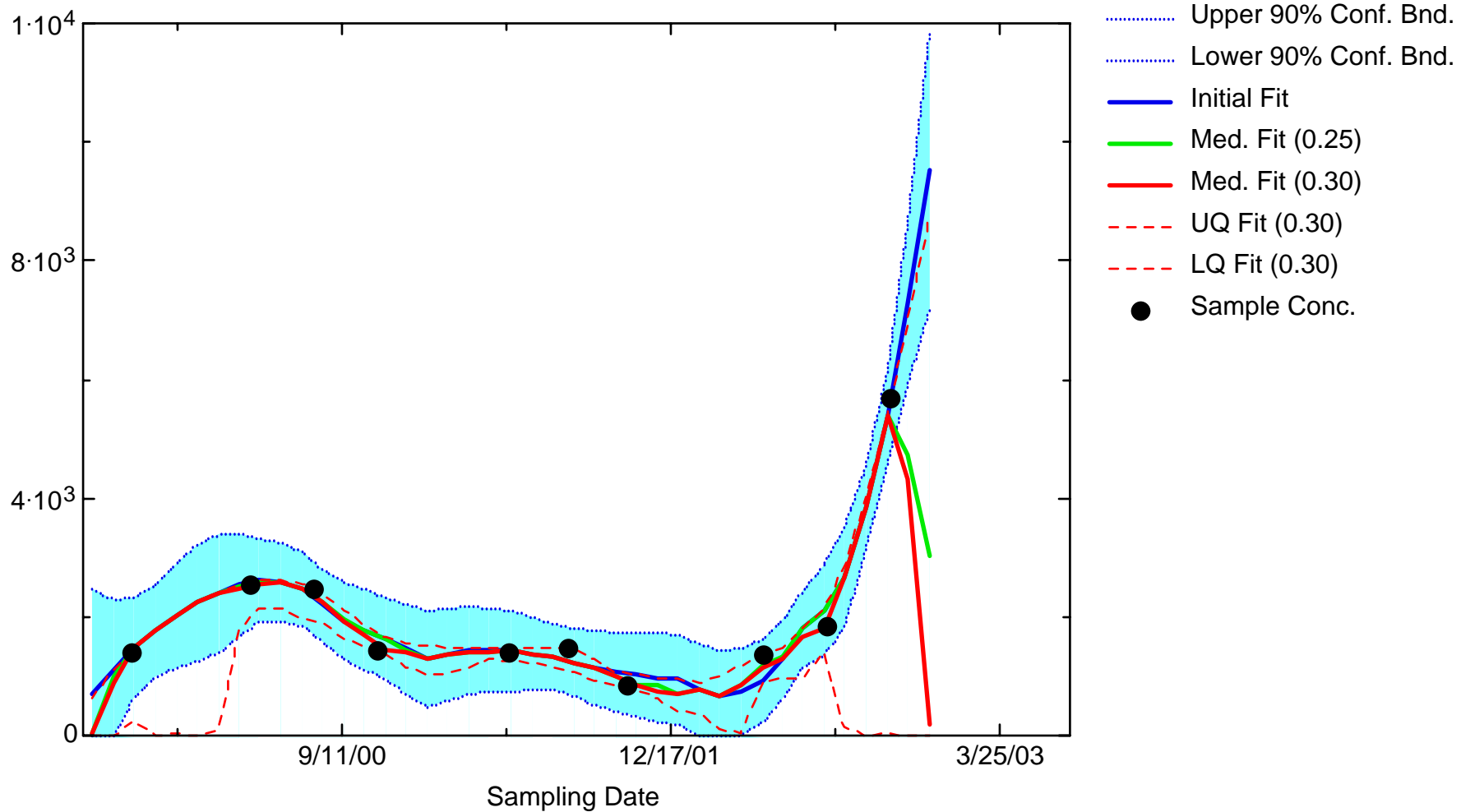
Med Fit = Median of 500 pointwise LWQR estimates on reduced dataset

LQ Fit = Lower quartile of 500 pointwise LWQR estimates on reduced dataset

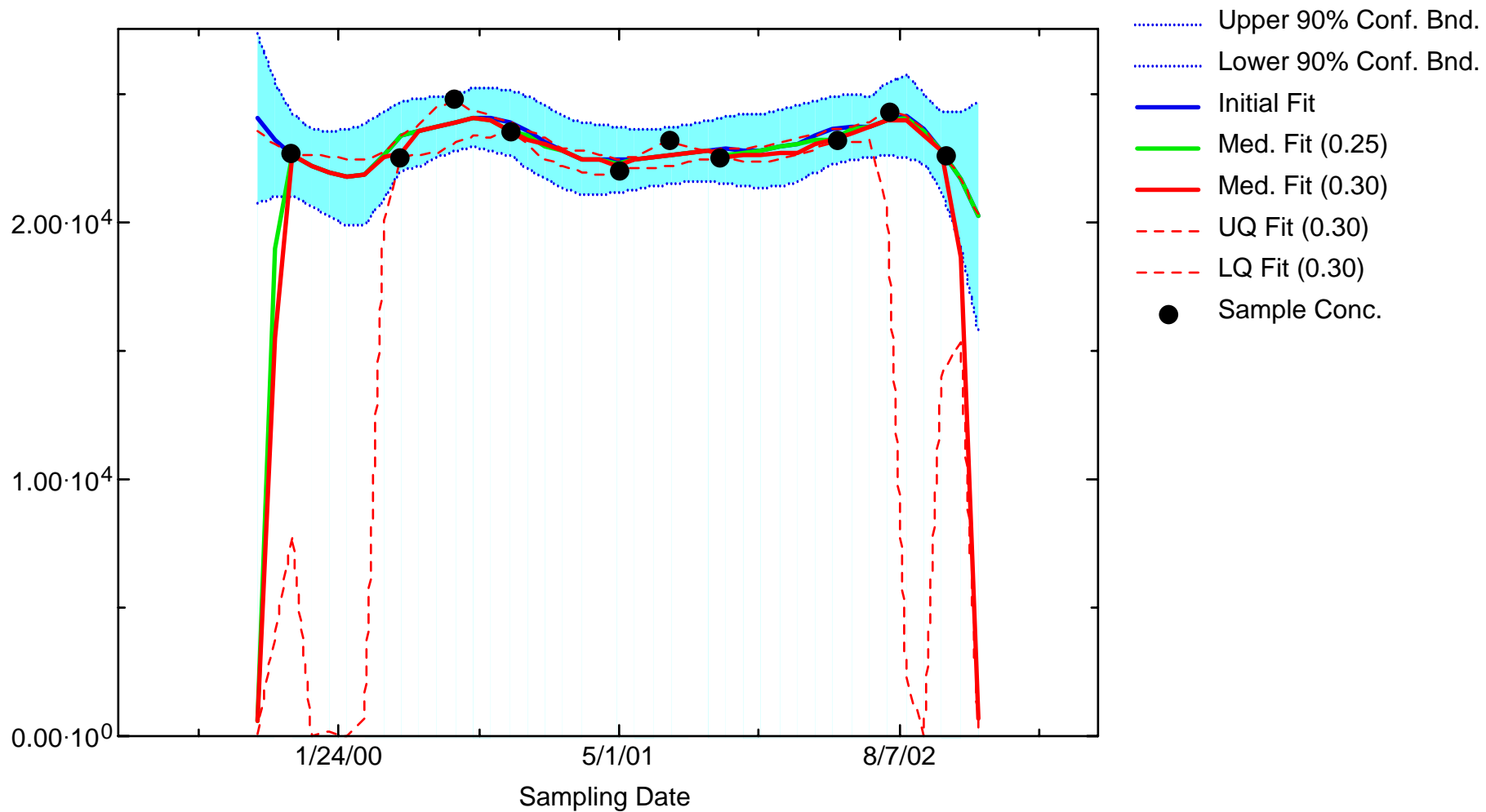
UQ Fit = Upper quartile of 500 pointwise LWQR estimates on reduced dataset

Conc = Concentration

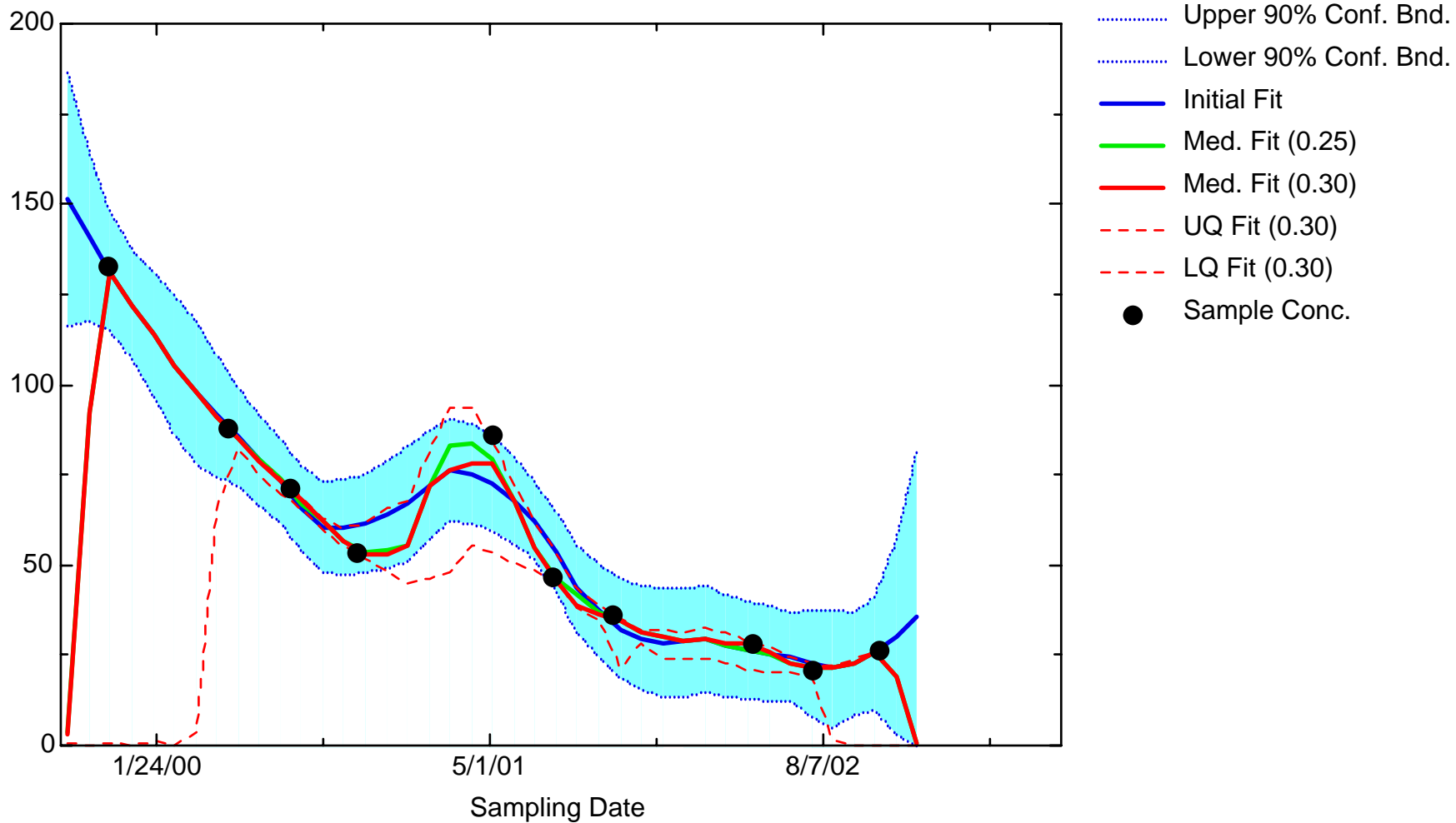
MN: Well 056MW02



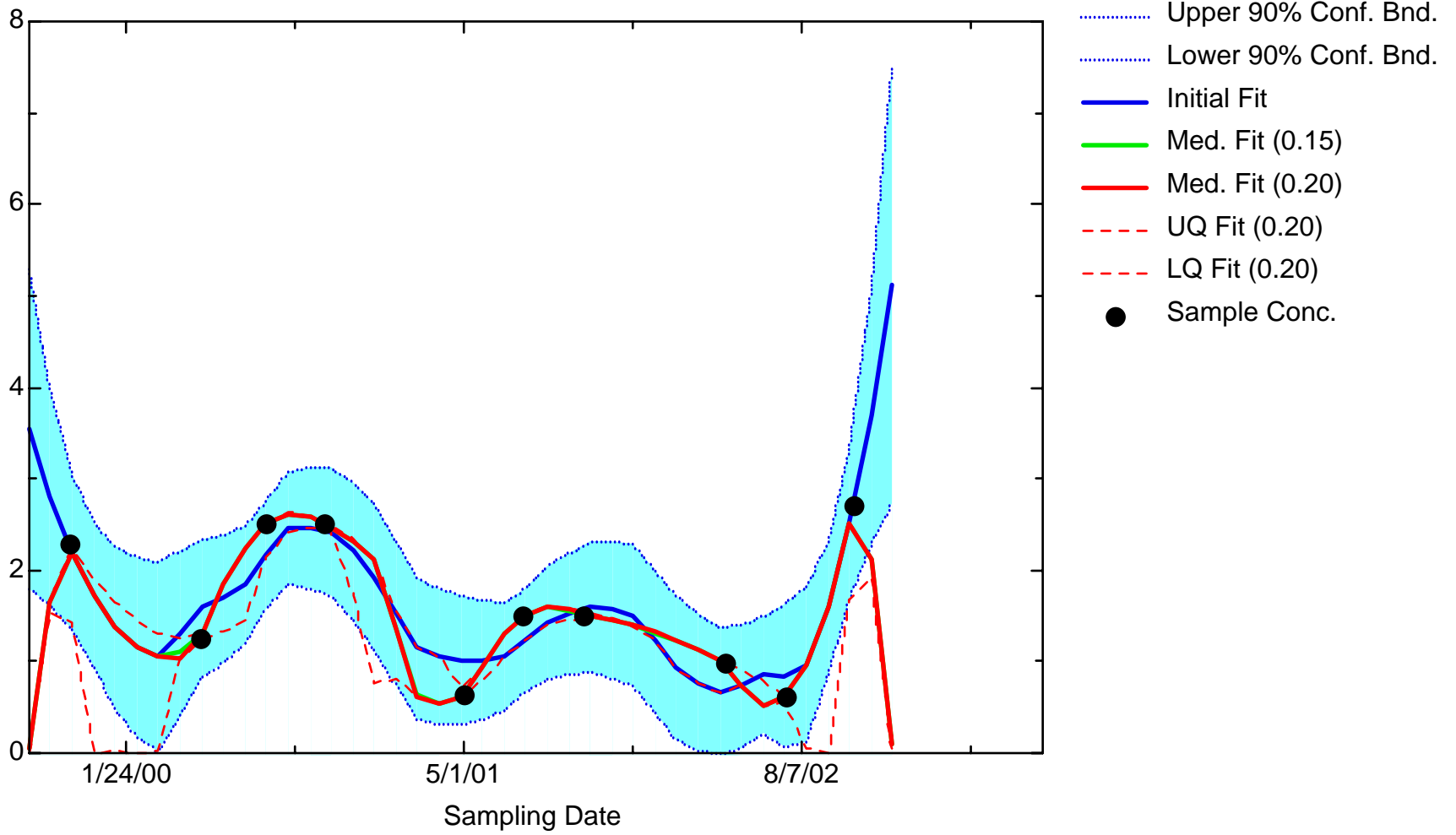
MN: Well 056MW04



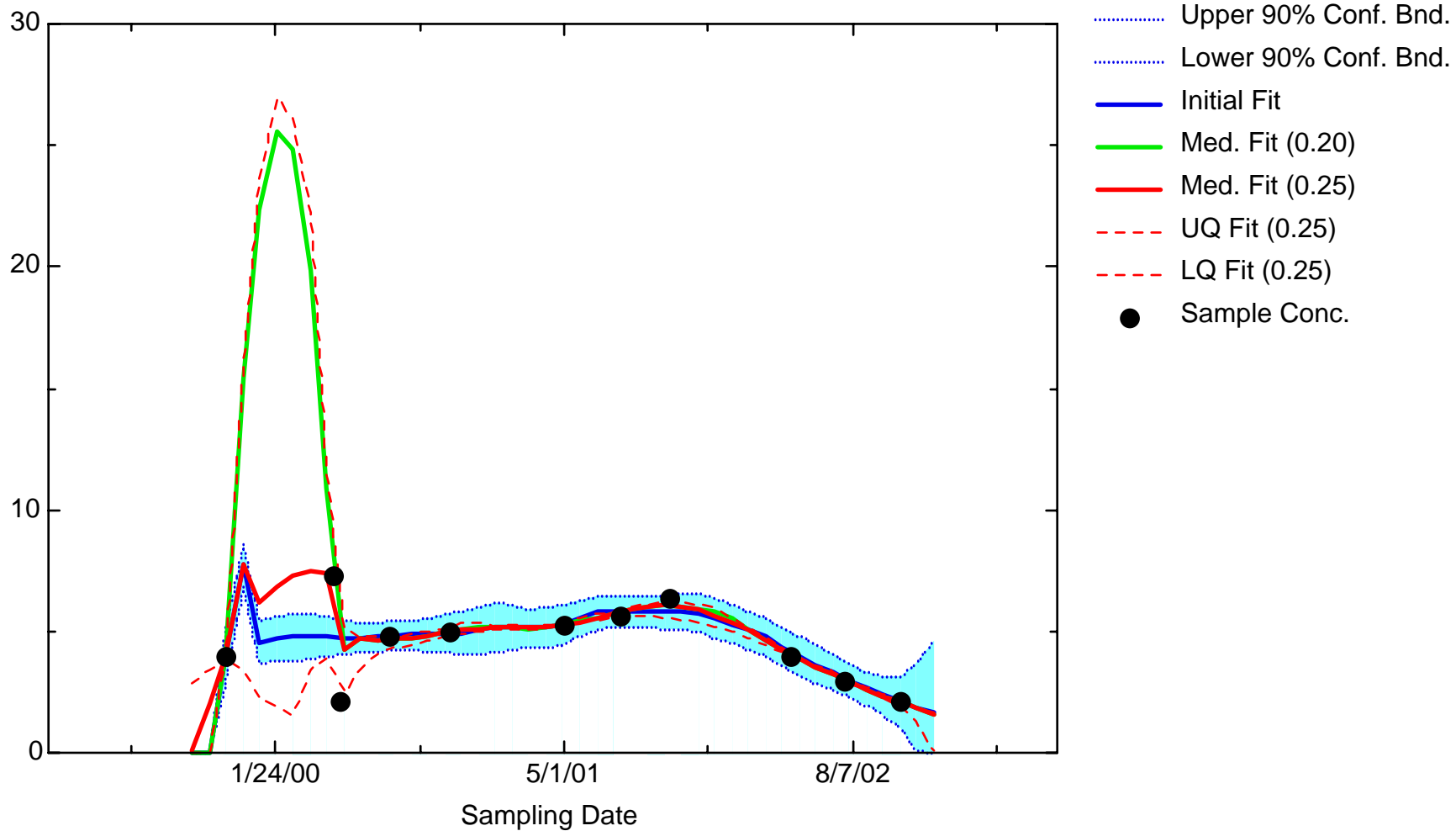
MN: Well AR25



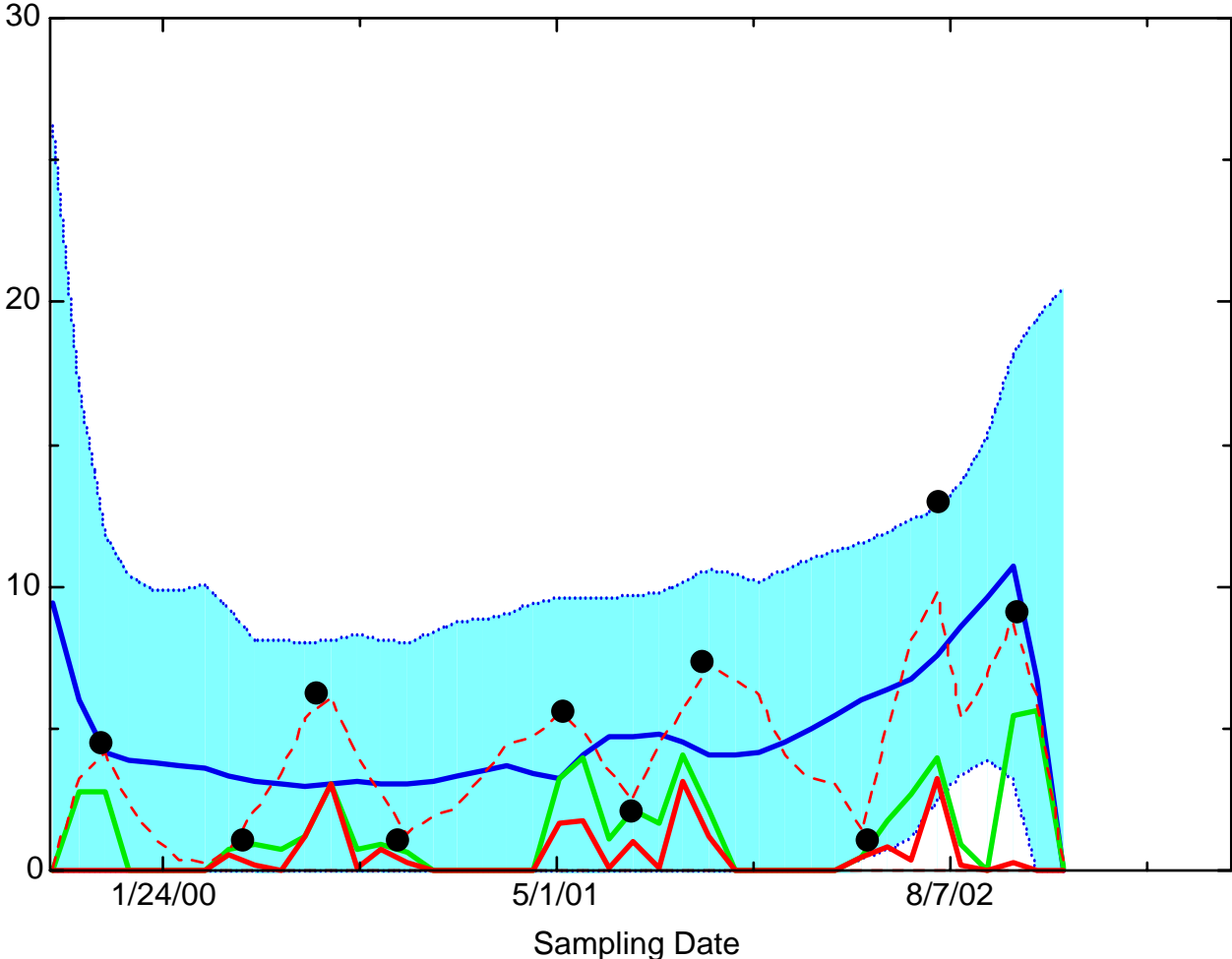
MN: Well FMW3413



MN: Well JBW7101

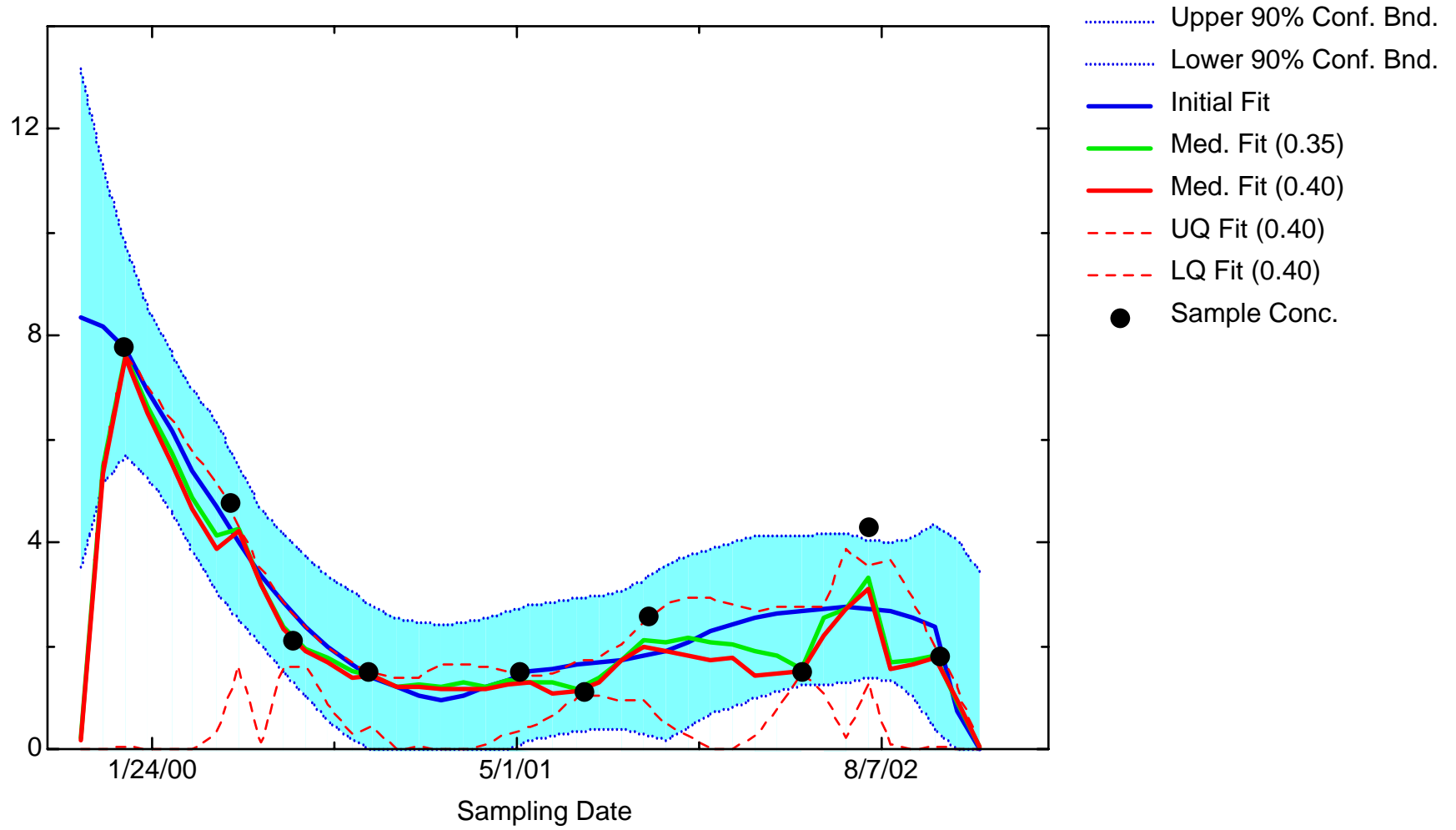


MN: Well JBW7102

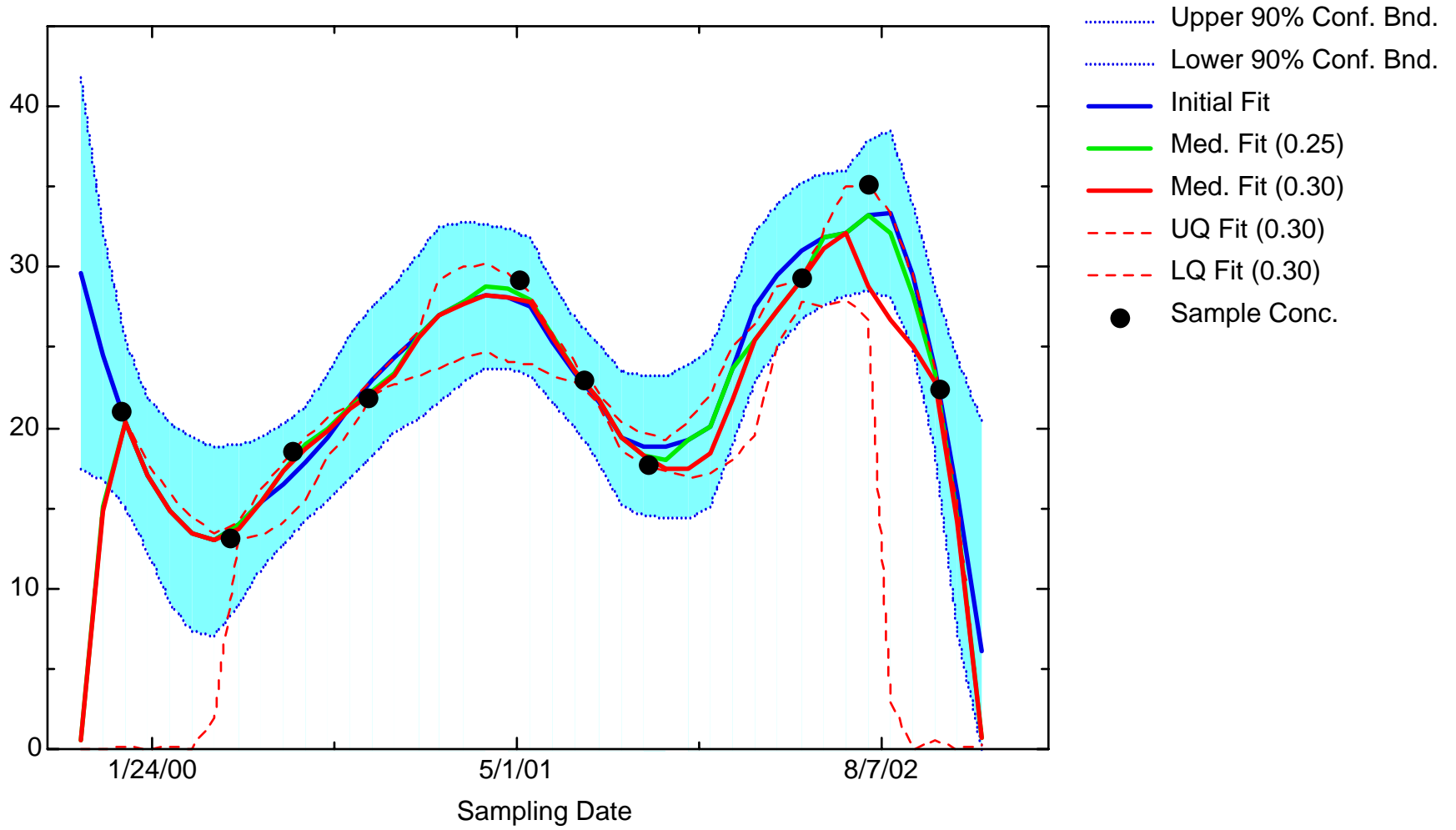


- Upper 90% Conf. Bnd.
- Lower 90% Conf. Bnd.
- Initial Fit
- Med. Fit (0.50)
- Med. Fit (0.55)
- - - UQ Fit (0.55)
- - - LQ Fit (0.55)
- Sample Conc.

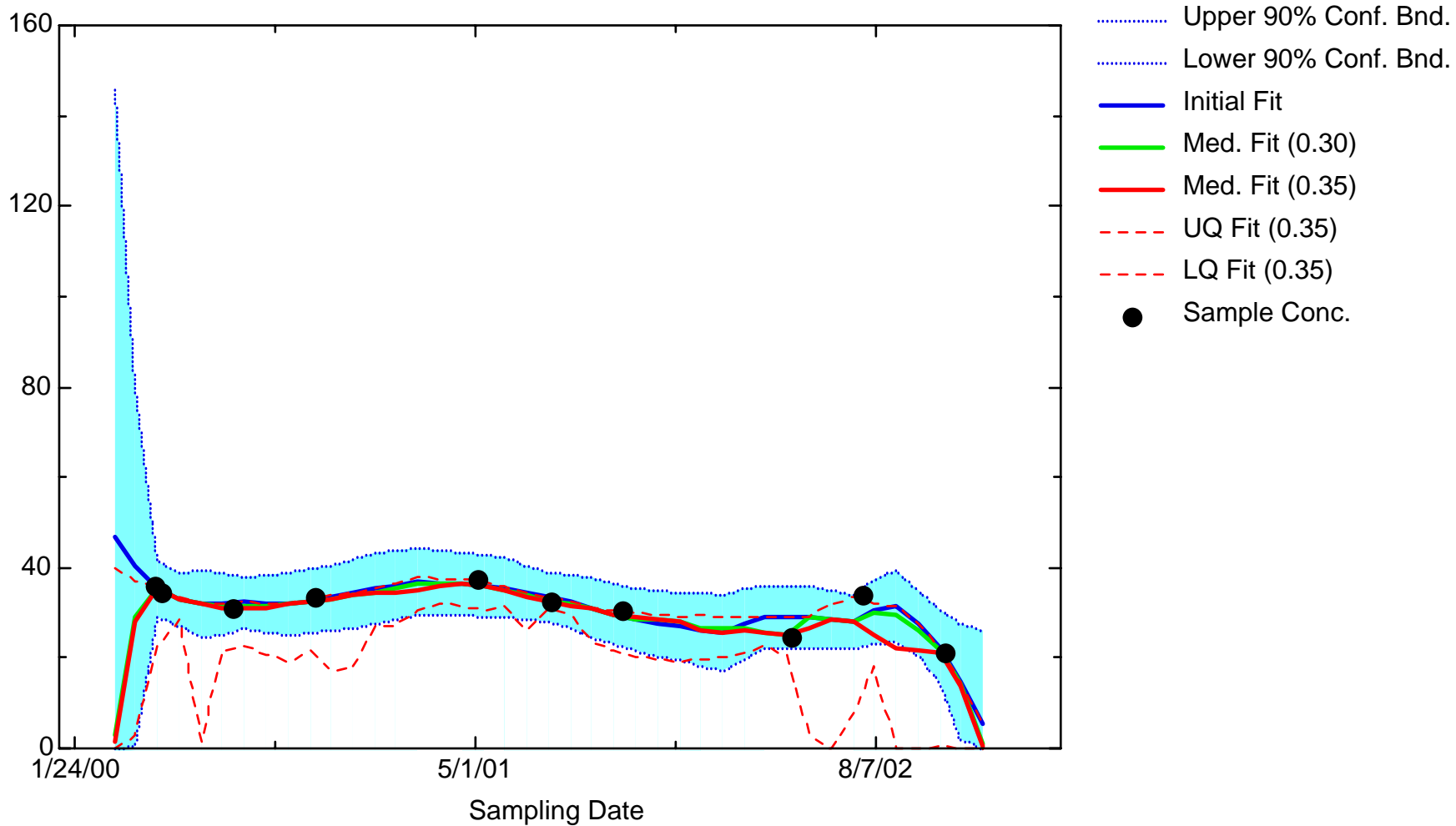
MN: Well JBW7106A



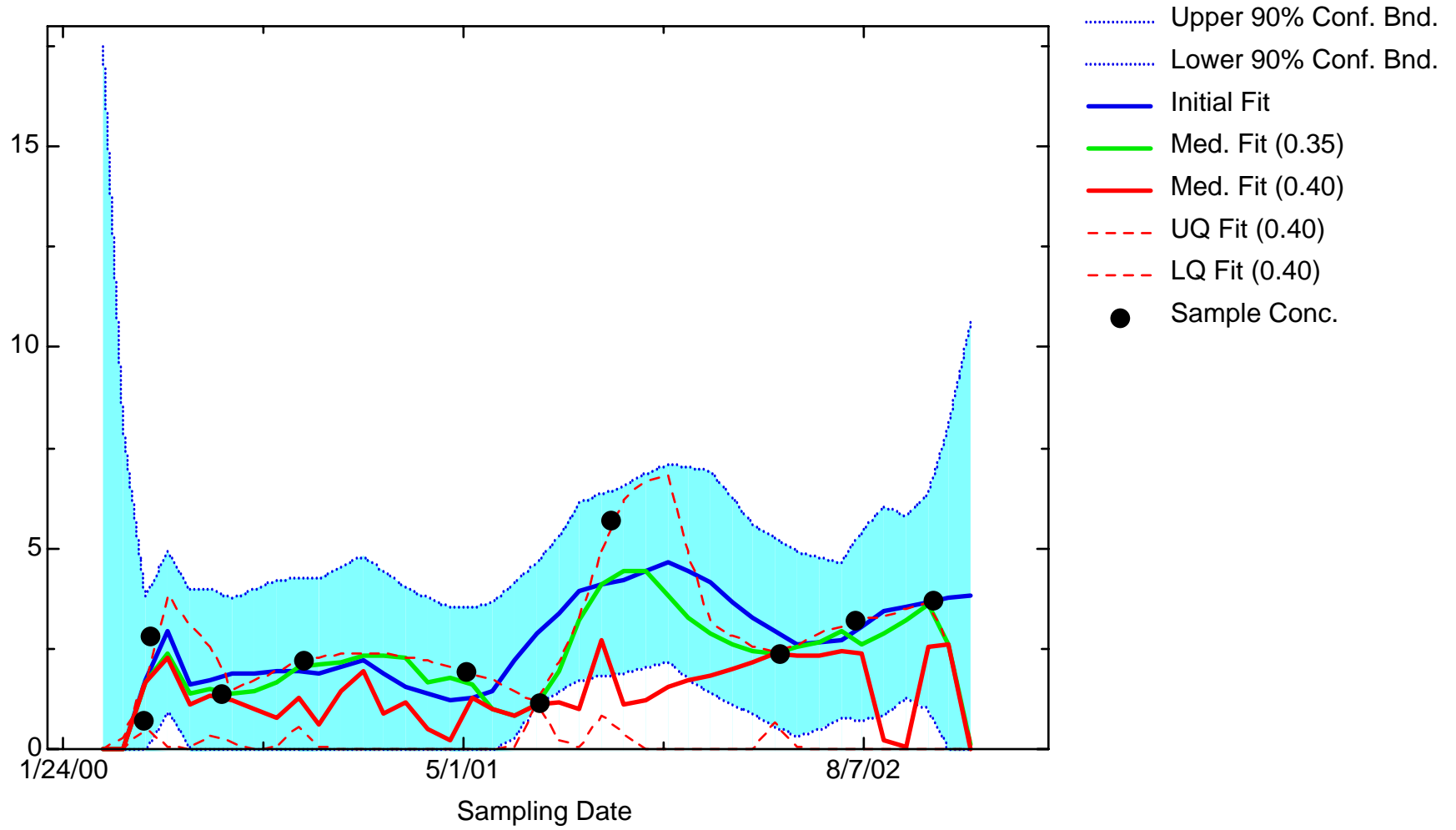
MN: Well JBW7106B



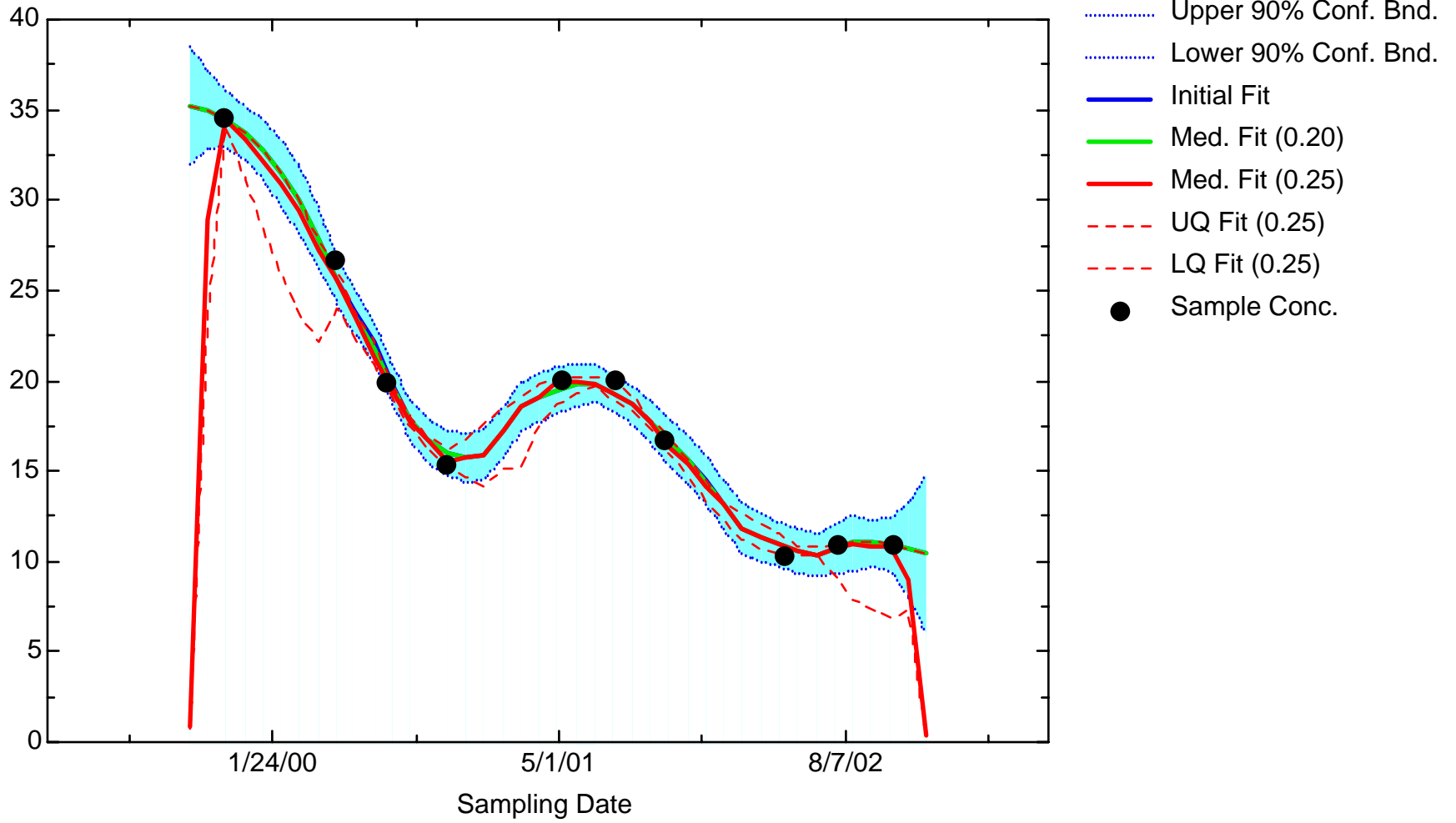
MN: Well JBW7203A



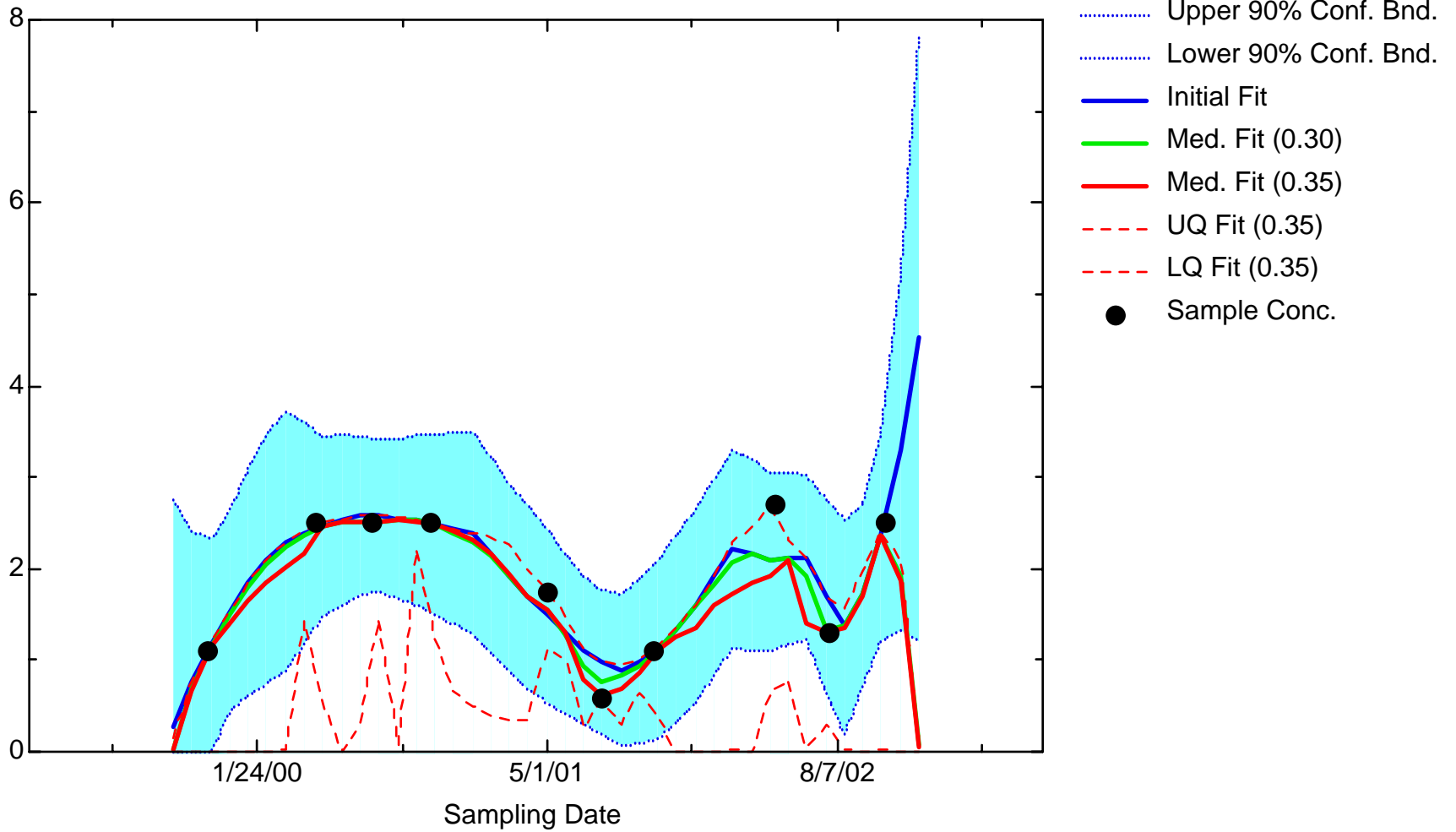
MN: Well JBW7203B



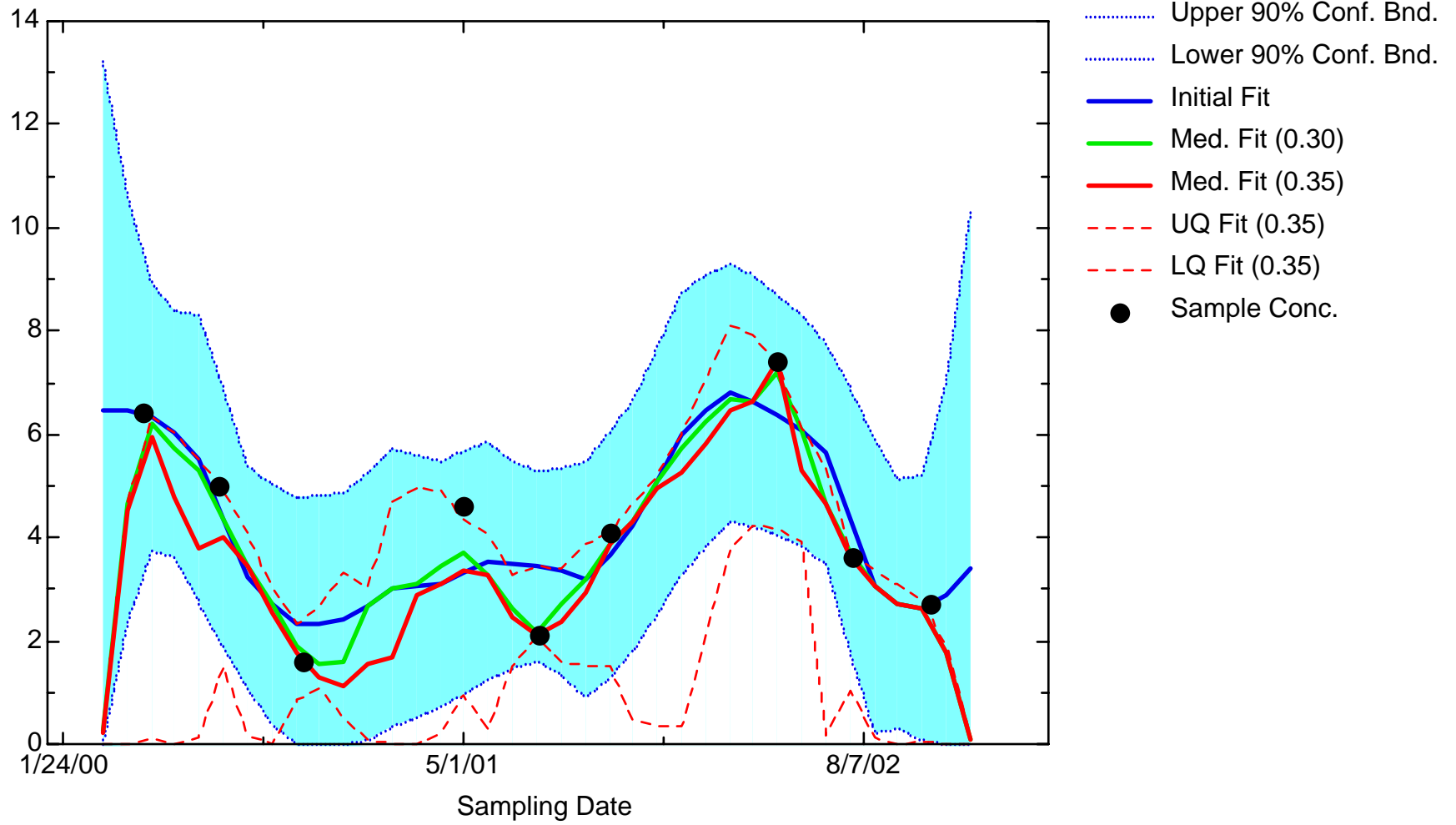
MN: Well JBW7204A



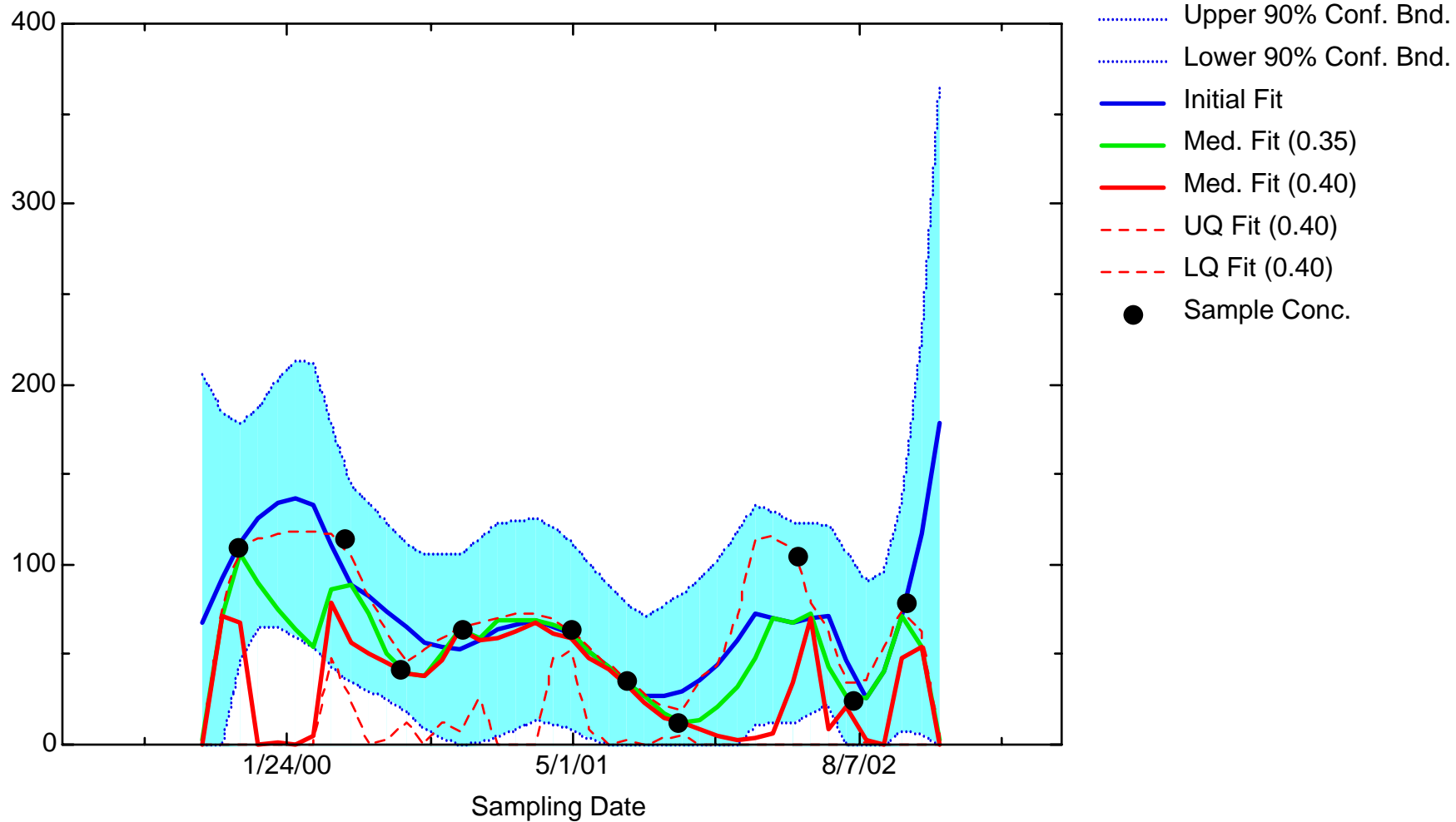
MN: Well JBW7212A



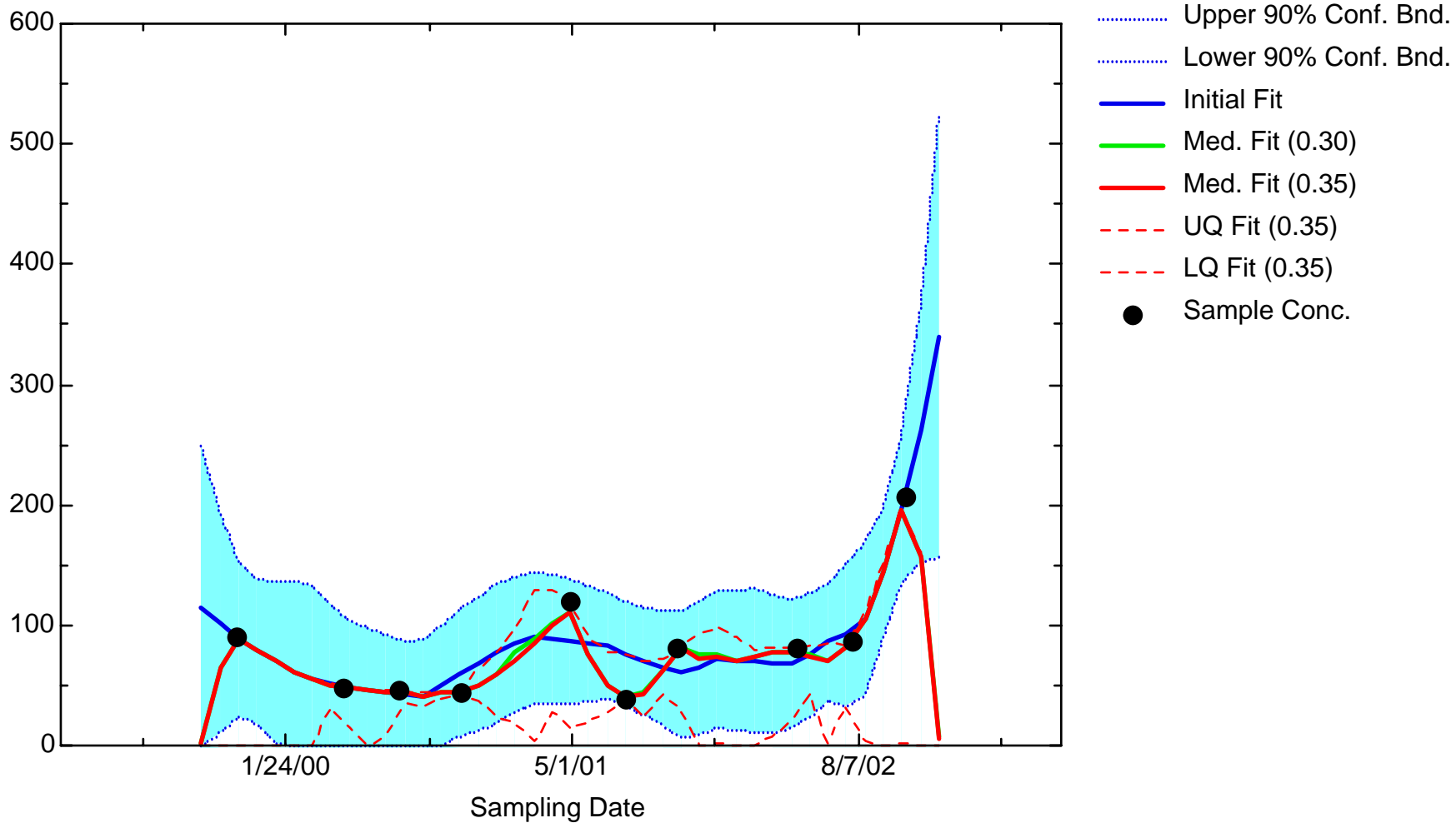
MN: Well JBW7212B



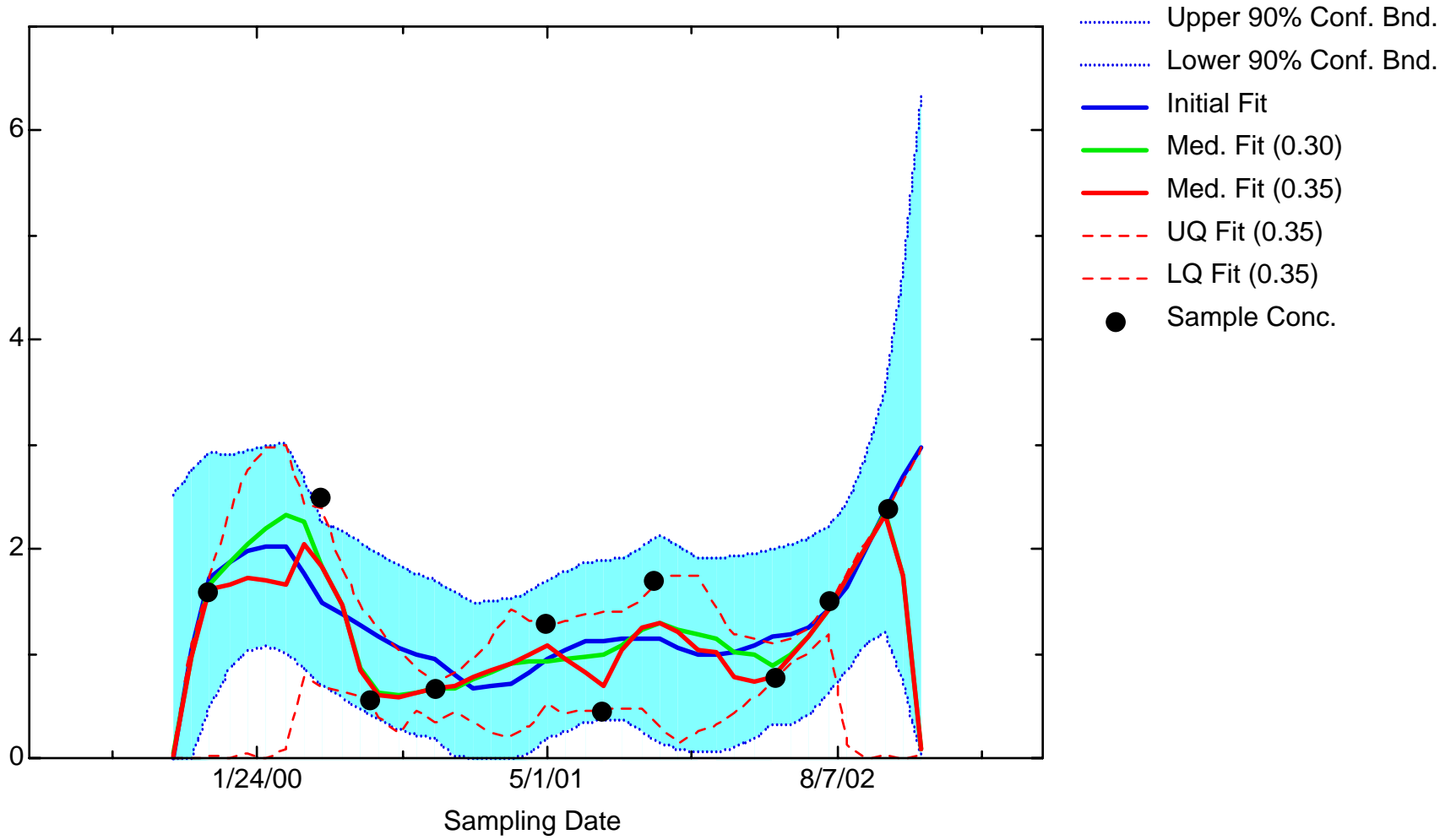
MN: Well JBW7213A



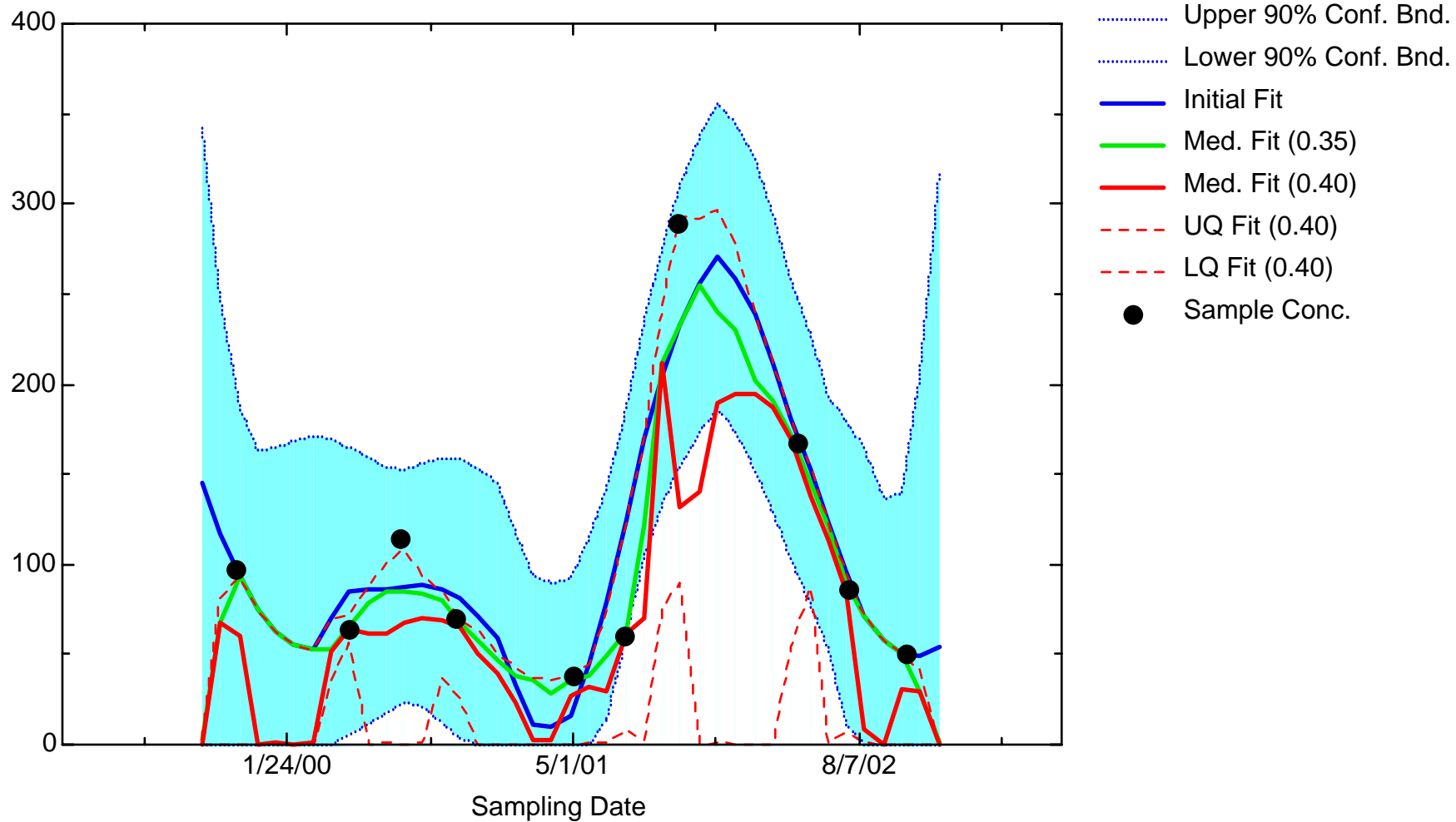
MN: Well JBW7213B



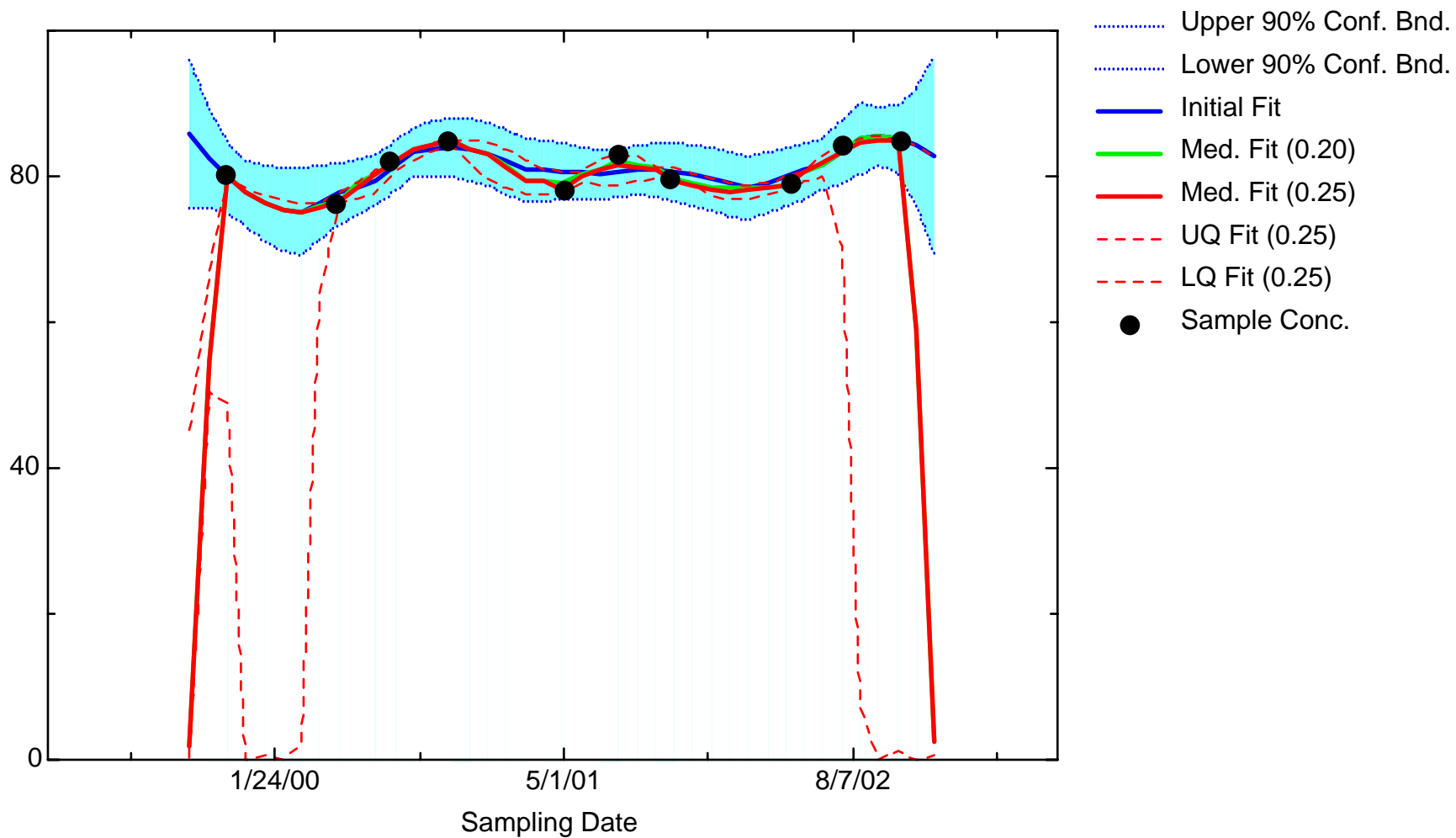
MN: Well JBW7215B



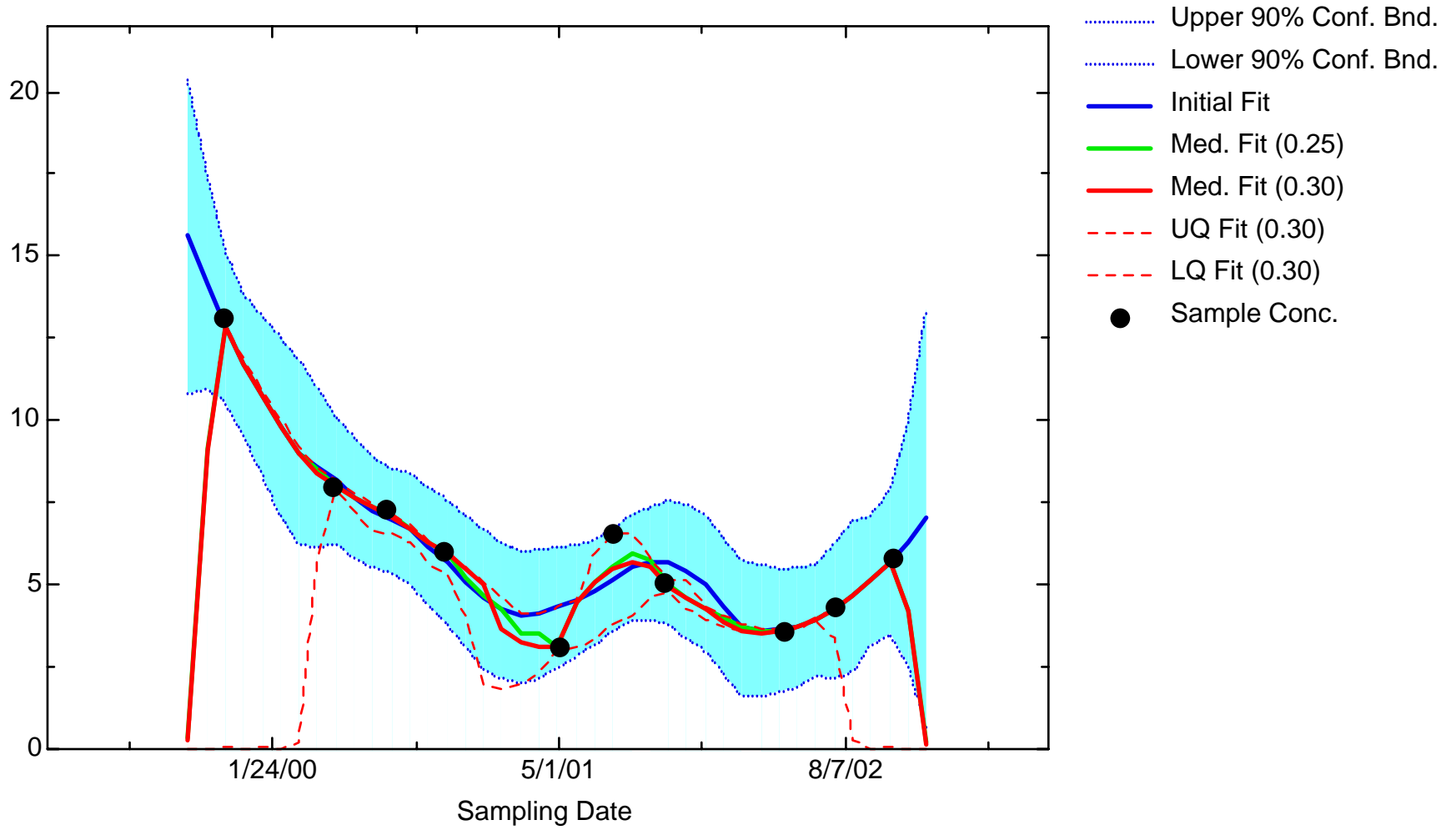
MN: Well JBW7317



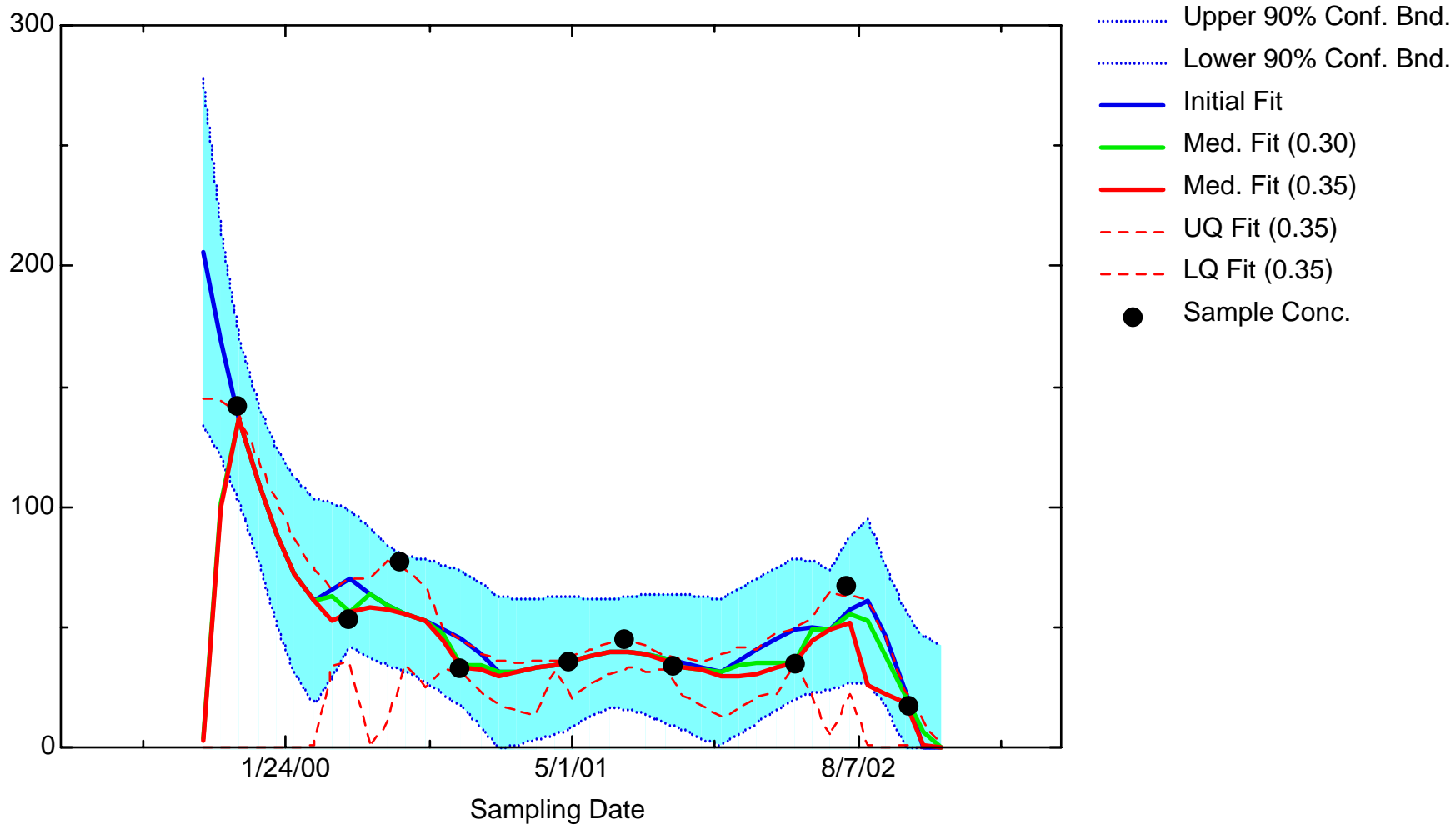
MN: Well JBW7326A



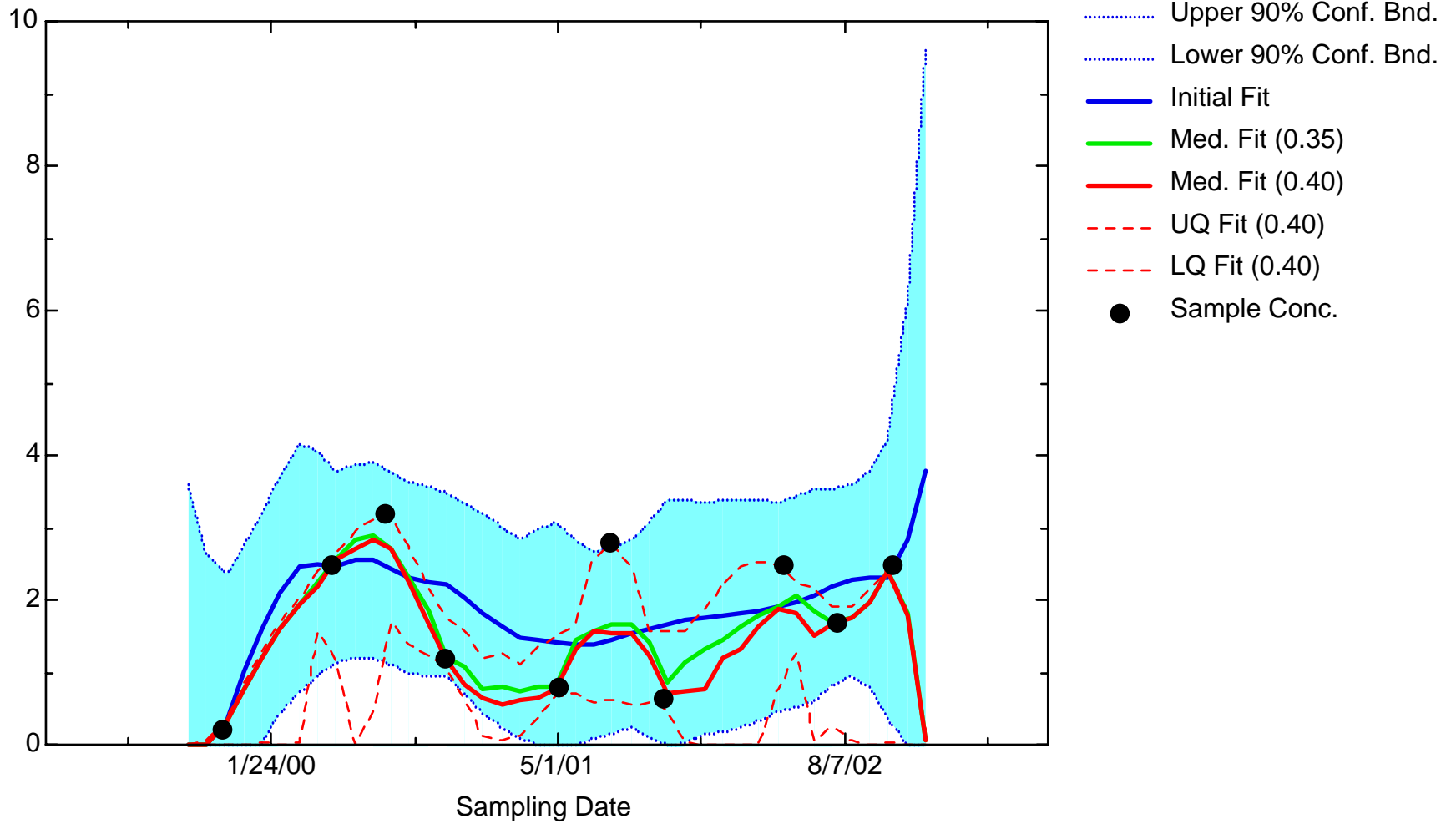
MN: Well JBW7326B



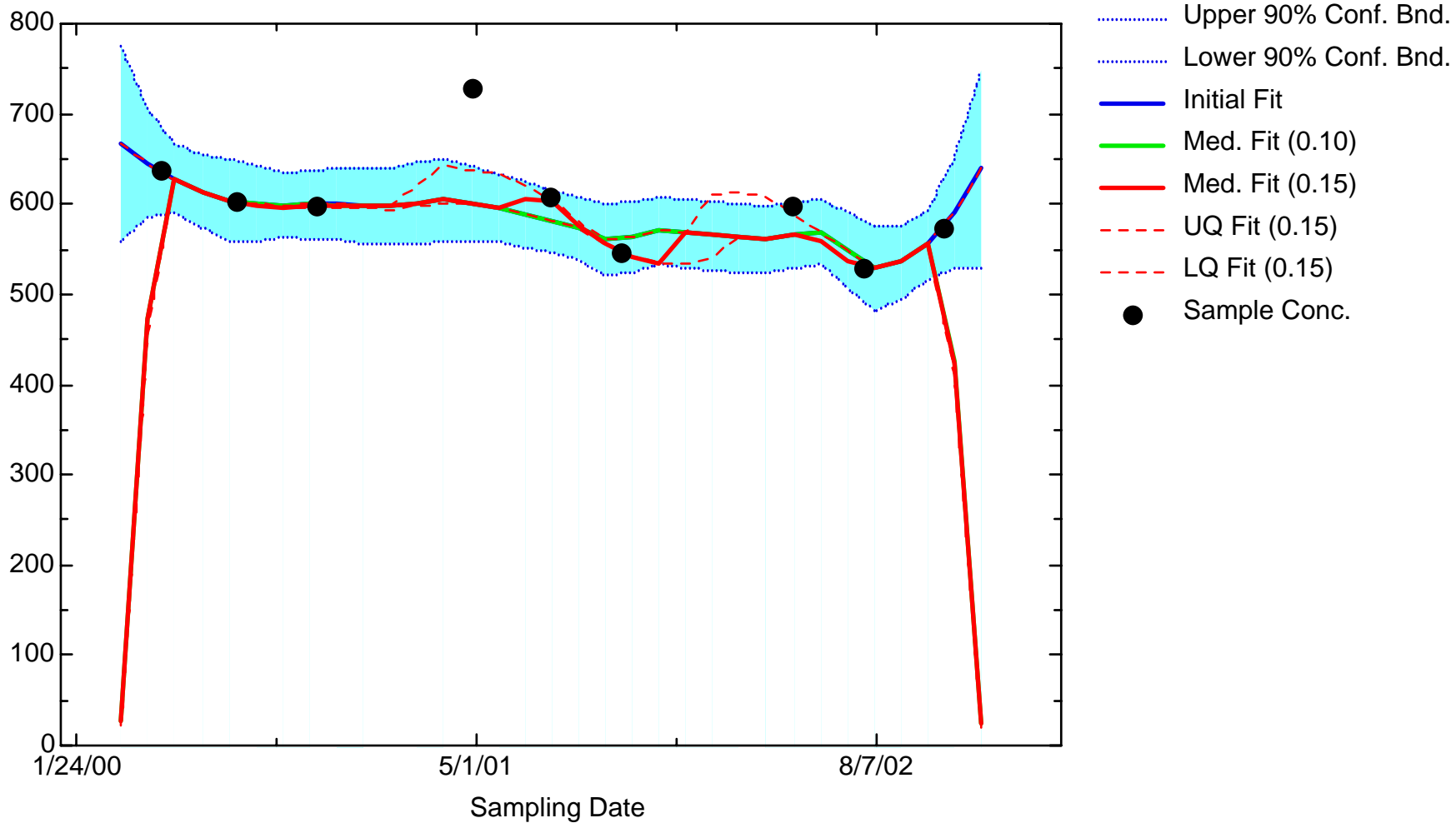
MN: Well JBW7328



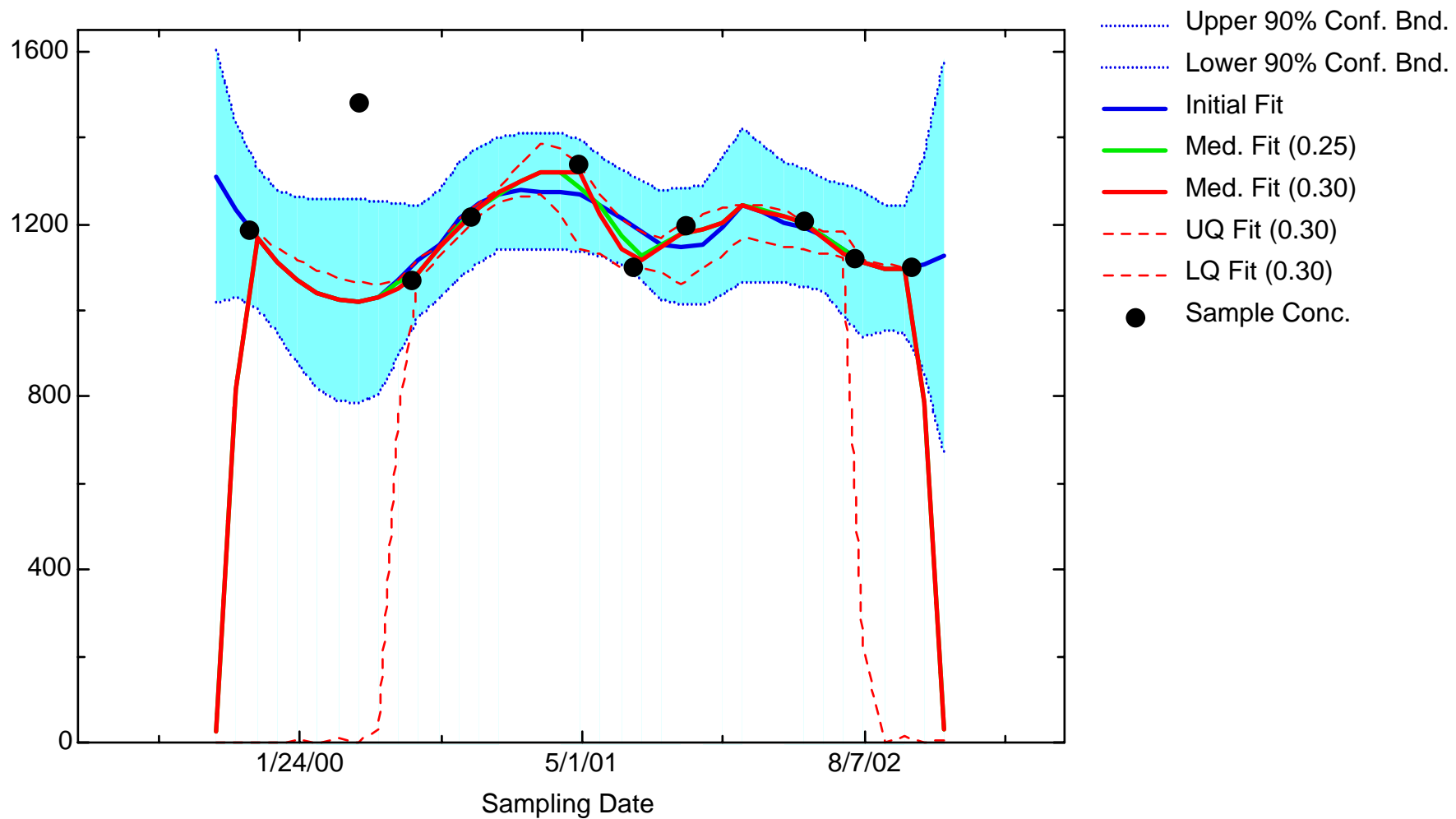
MN: Well JBW7330A



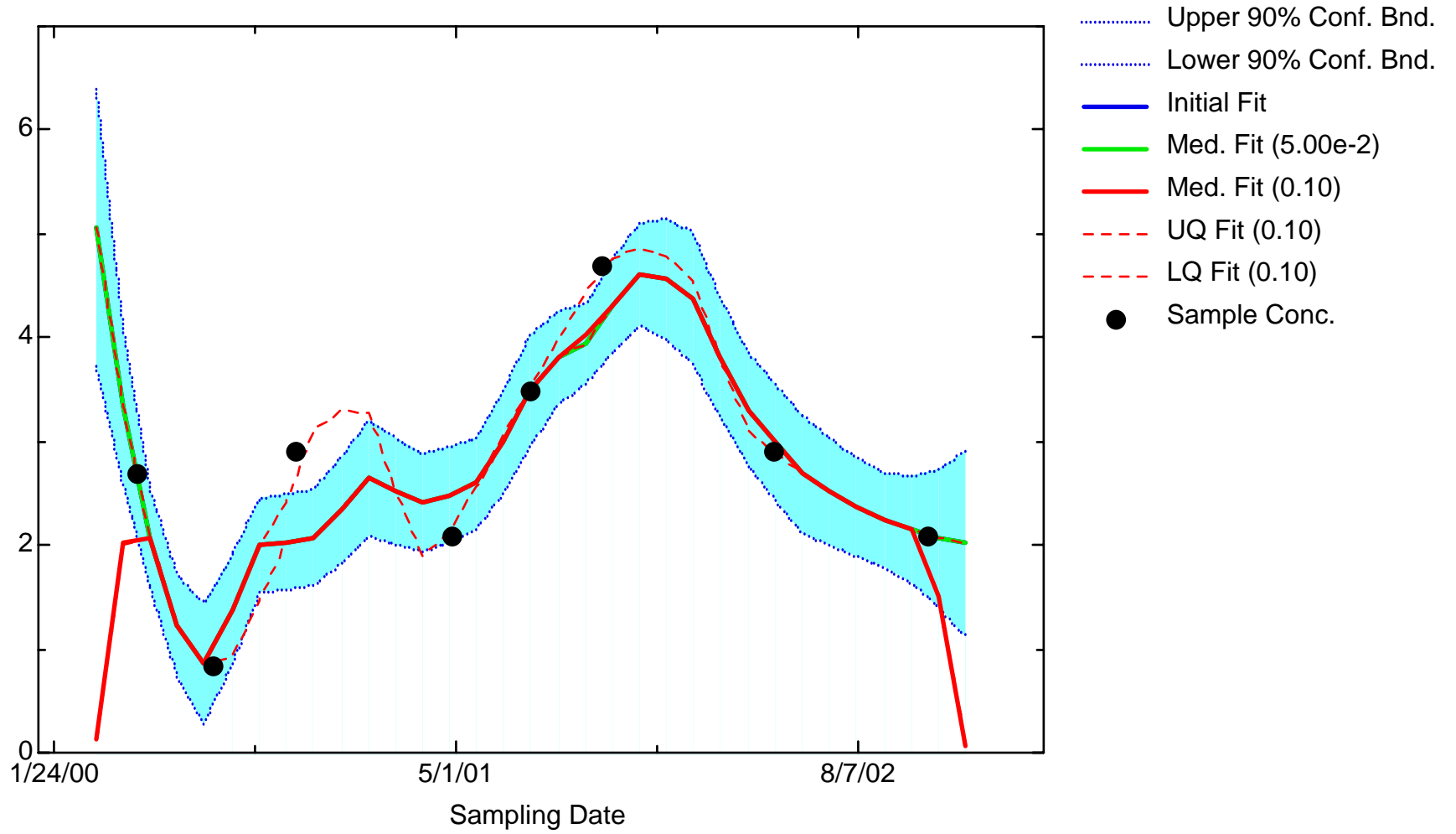
MN: Well JBW7333



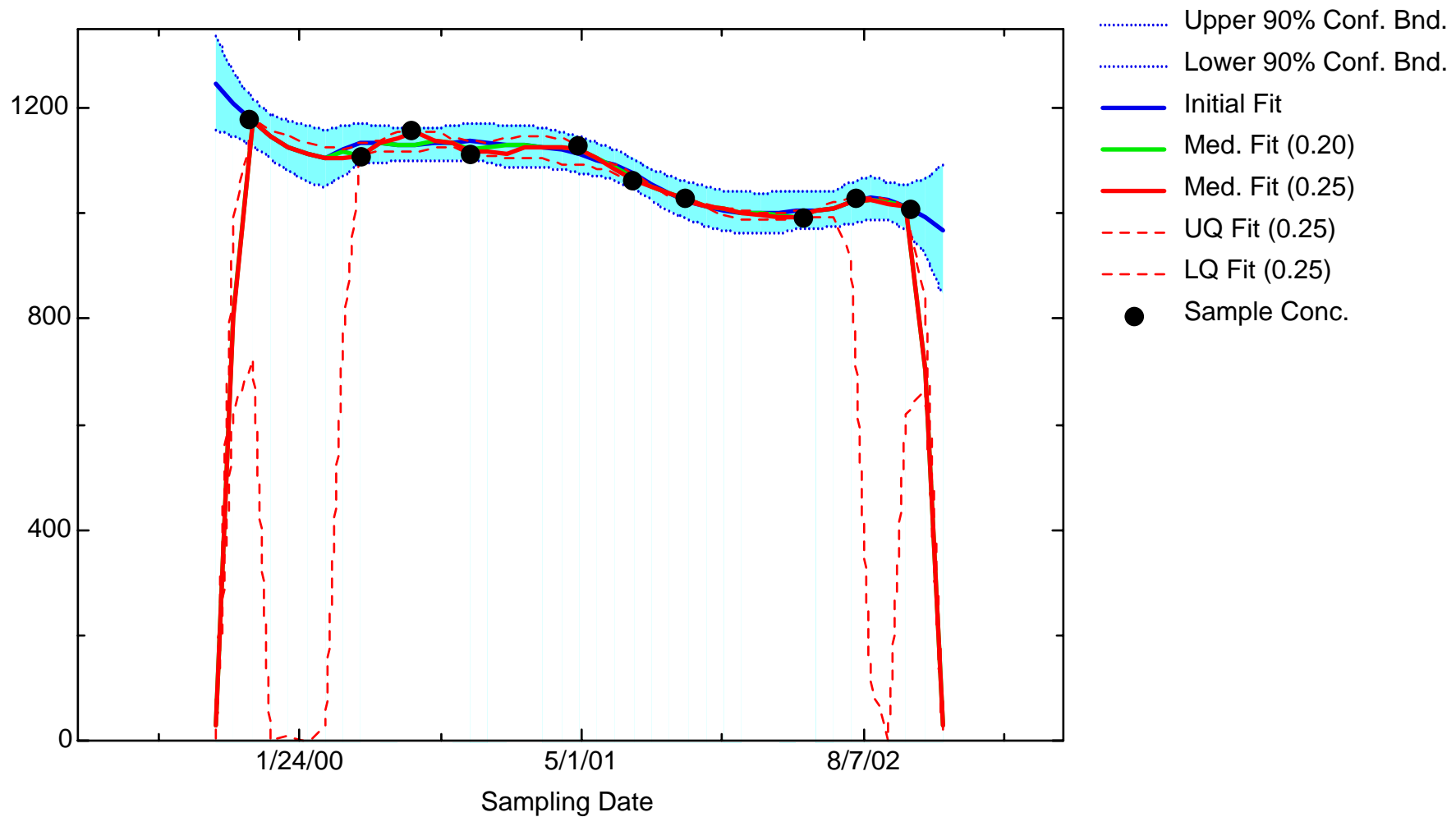
MN: Well JBW7338A



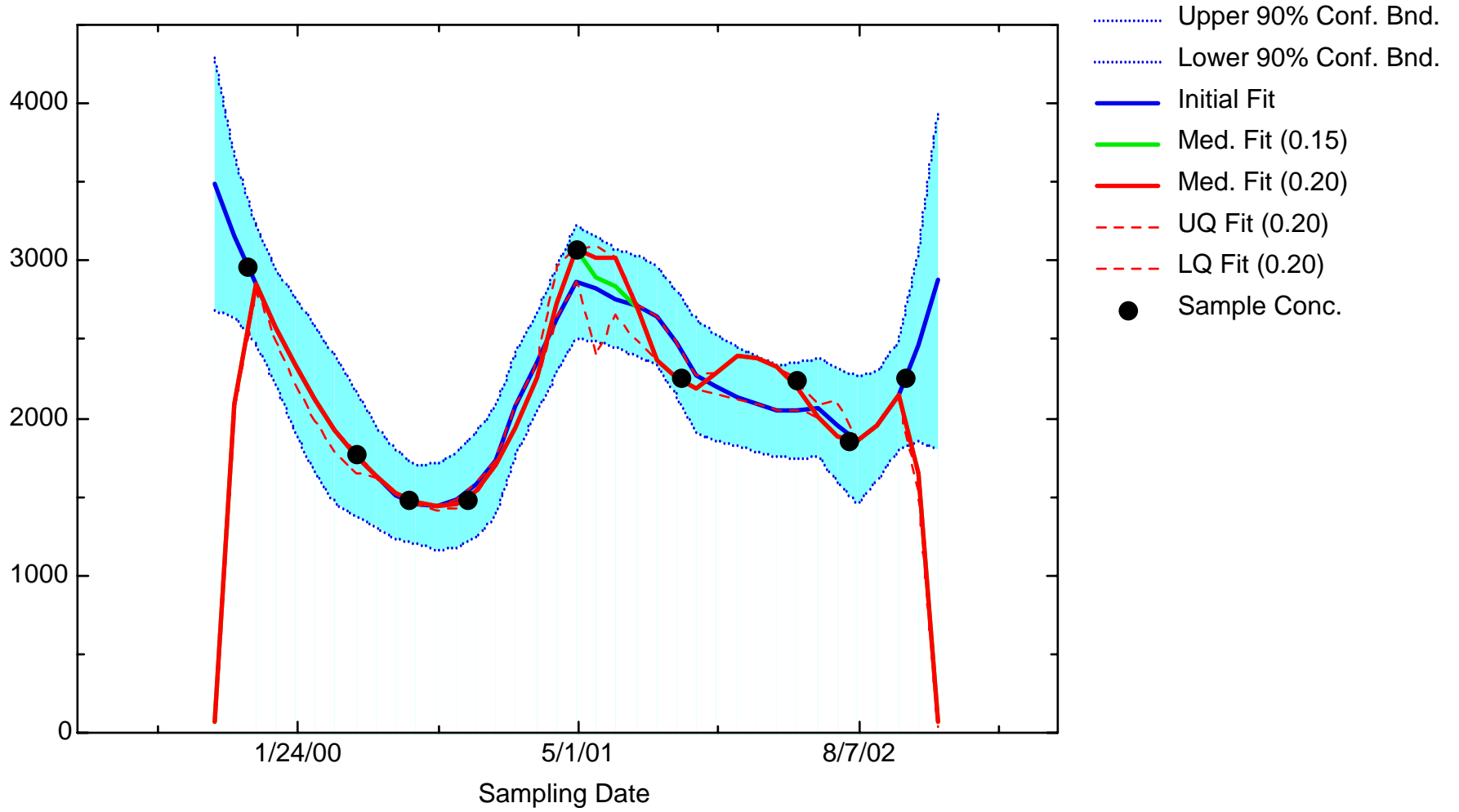
MN: Well JBW7338B



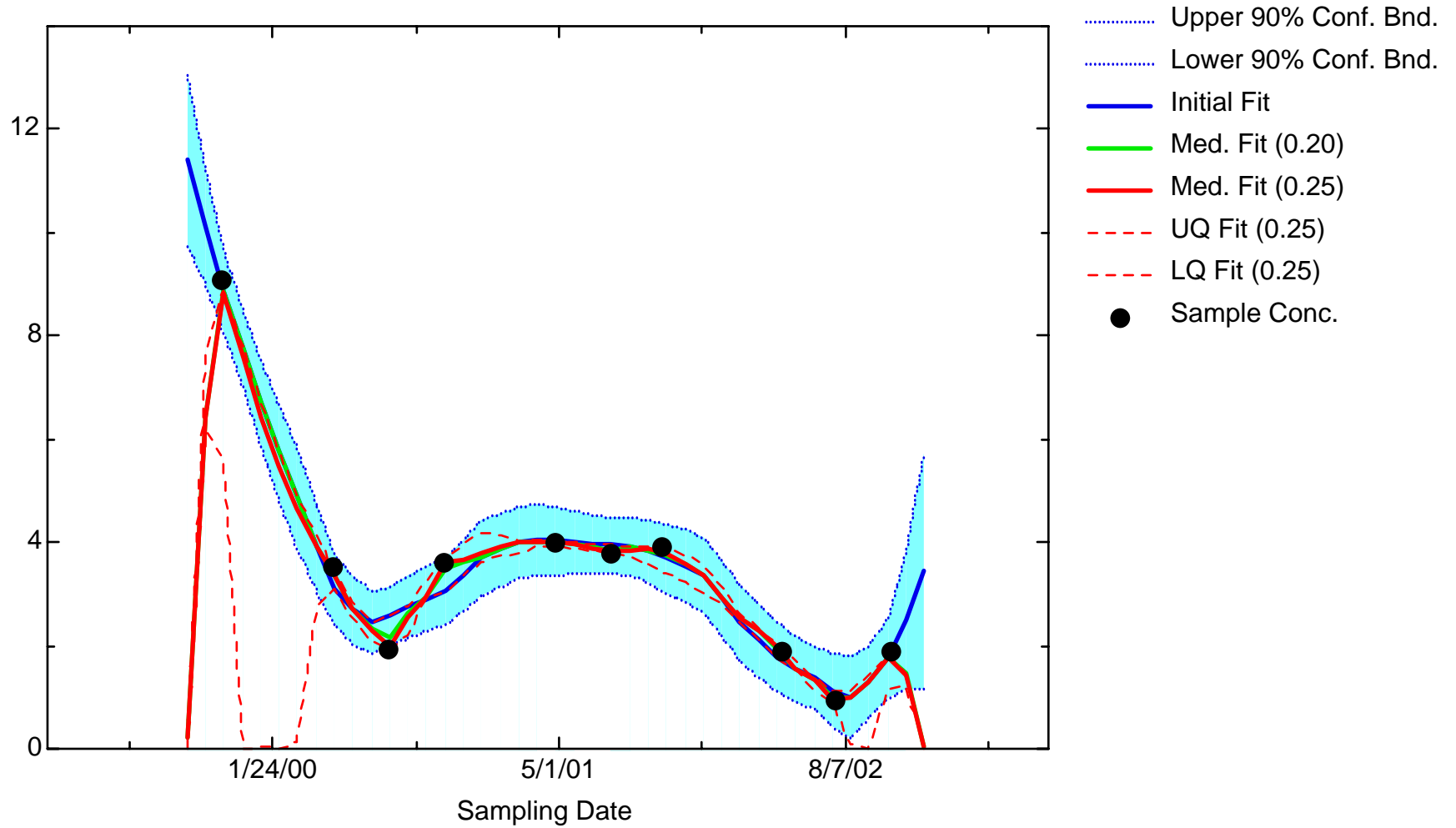
MN: Well JBW7340B



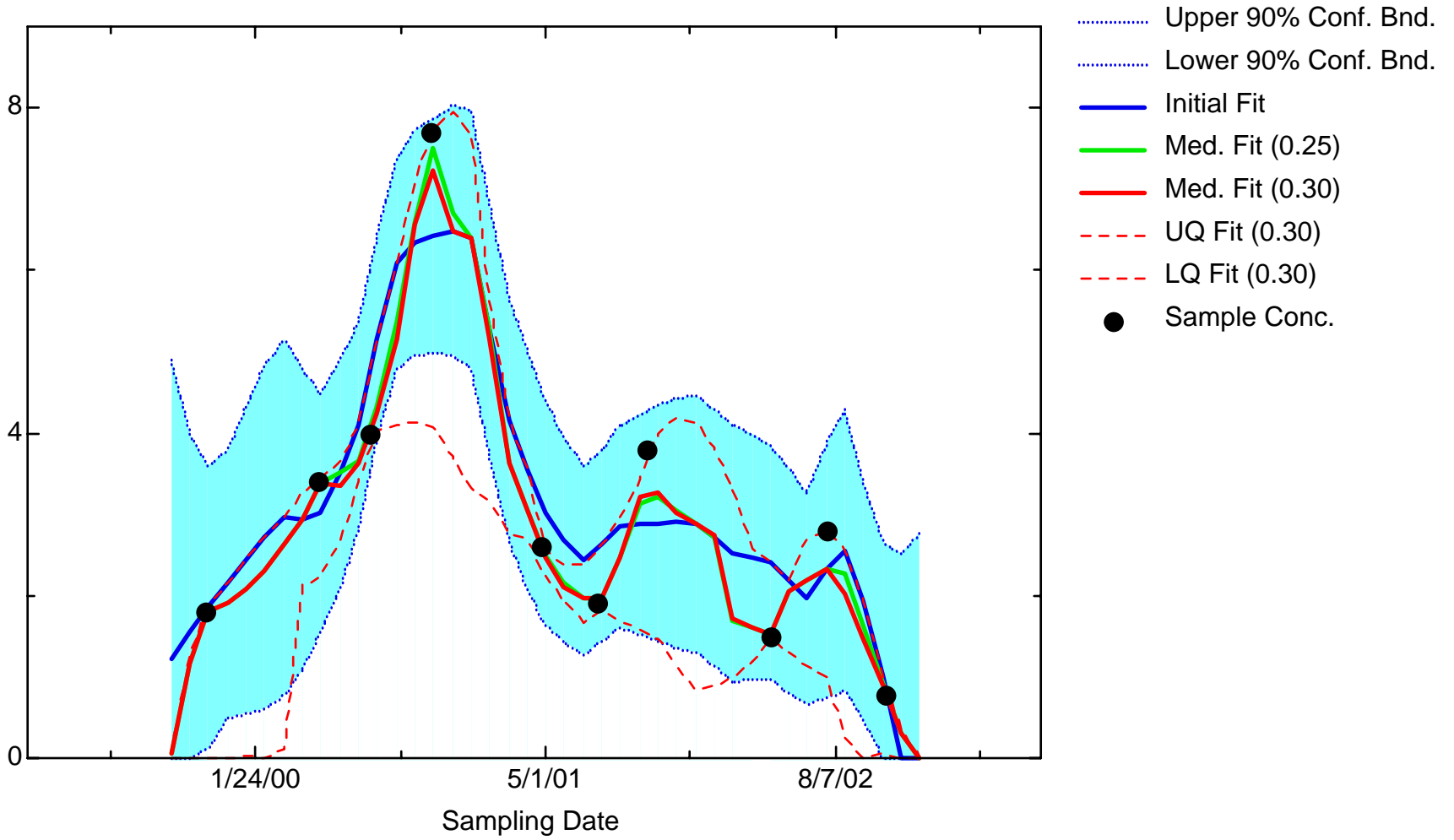
MN: Well JBW7344



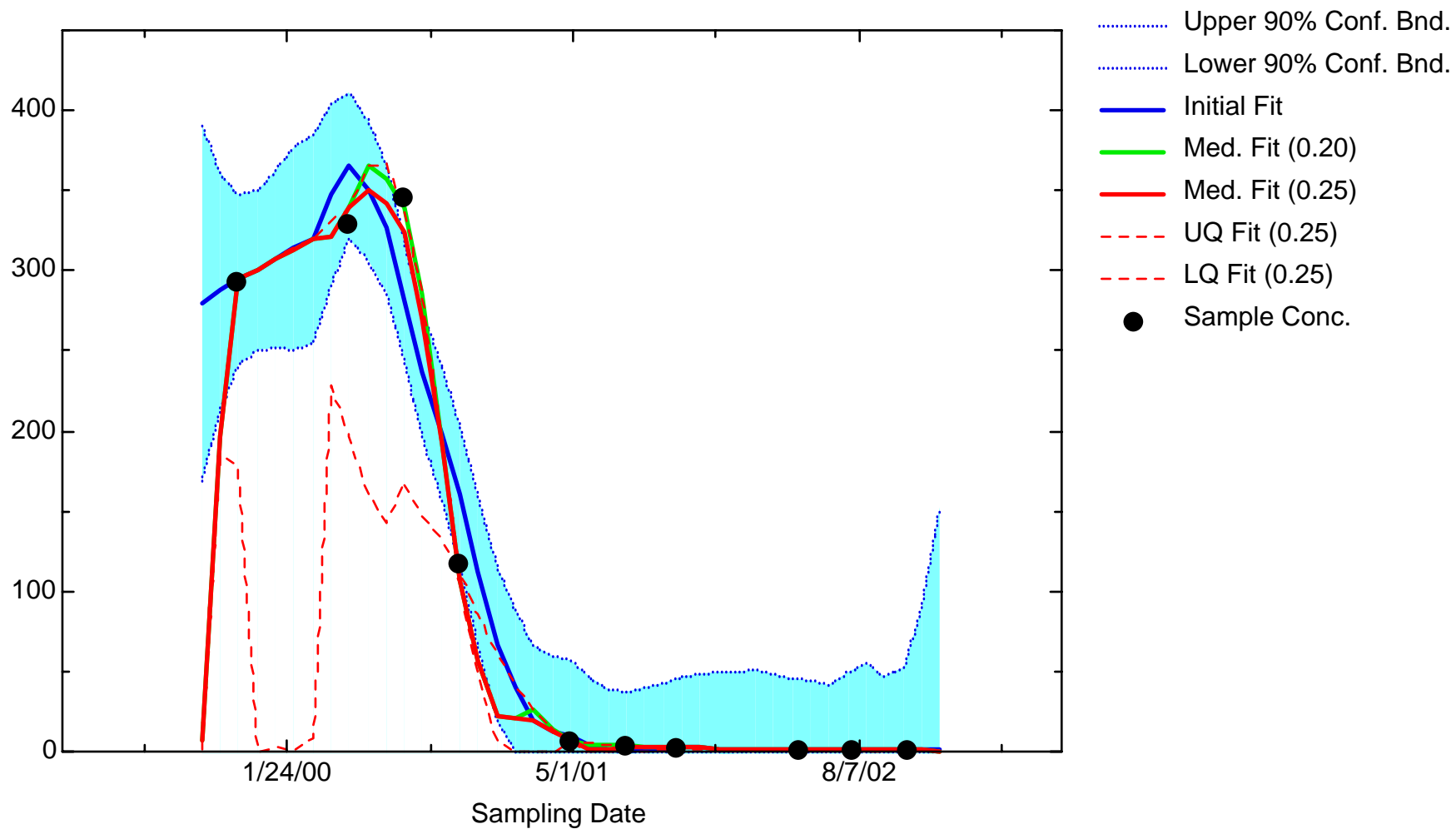
MN: Well JBW7345A



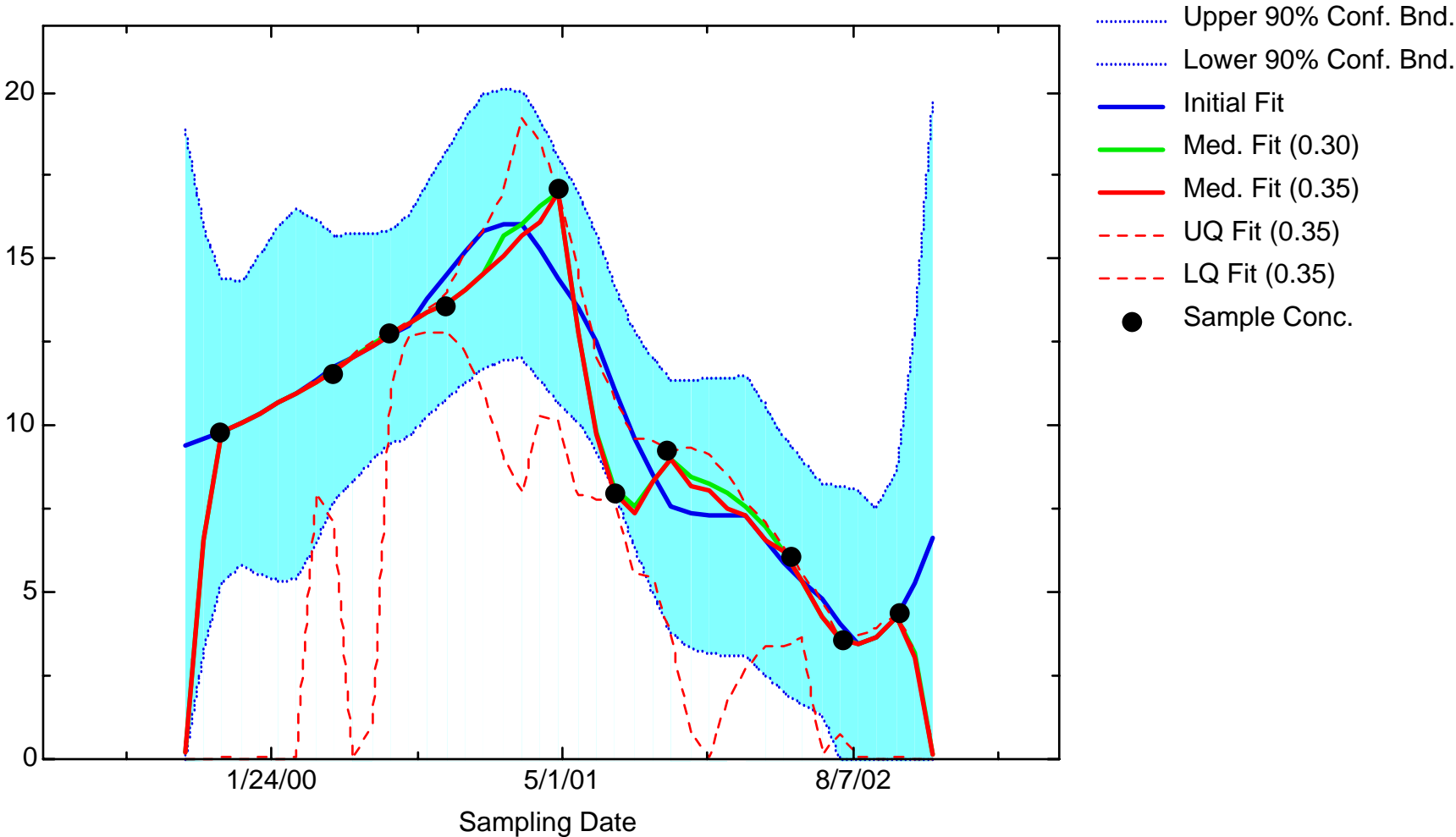
MN: Well JBW7347B



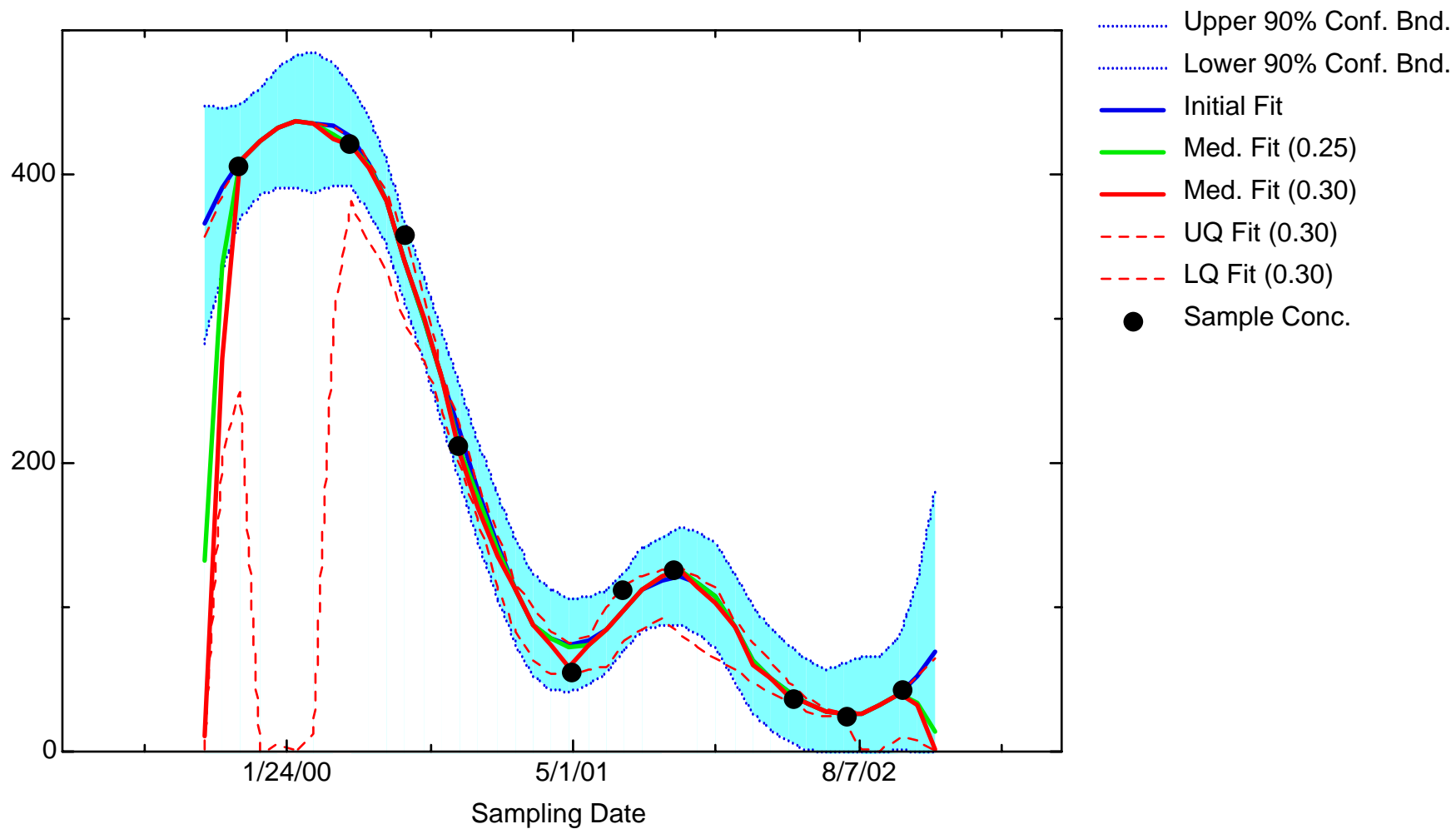
MN: Well JBW7348



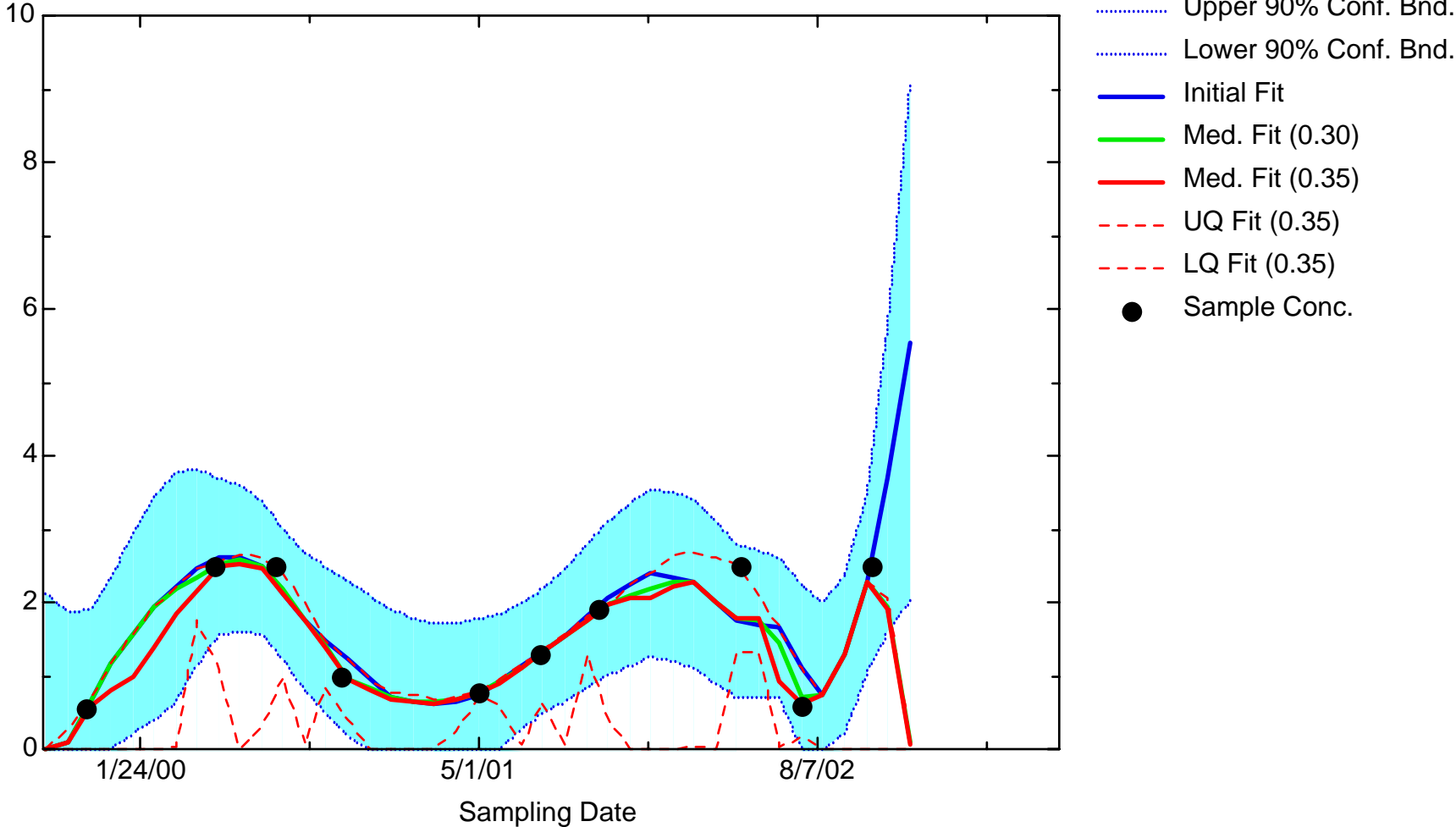
MN: Well JBW7350



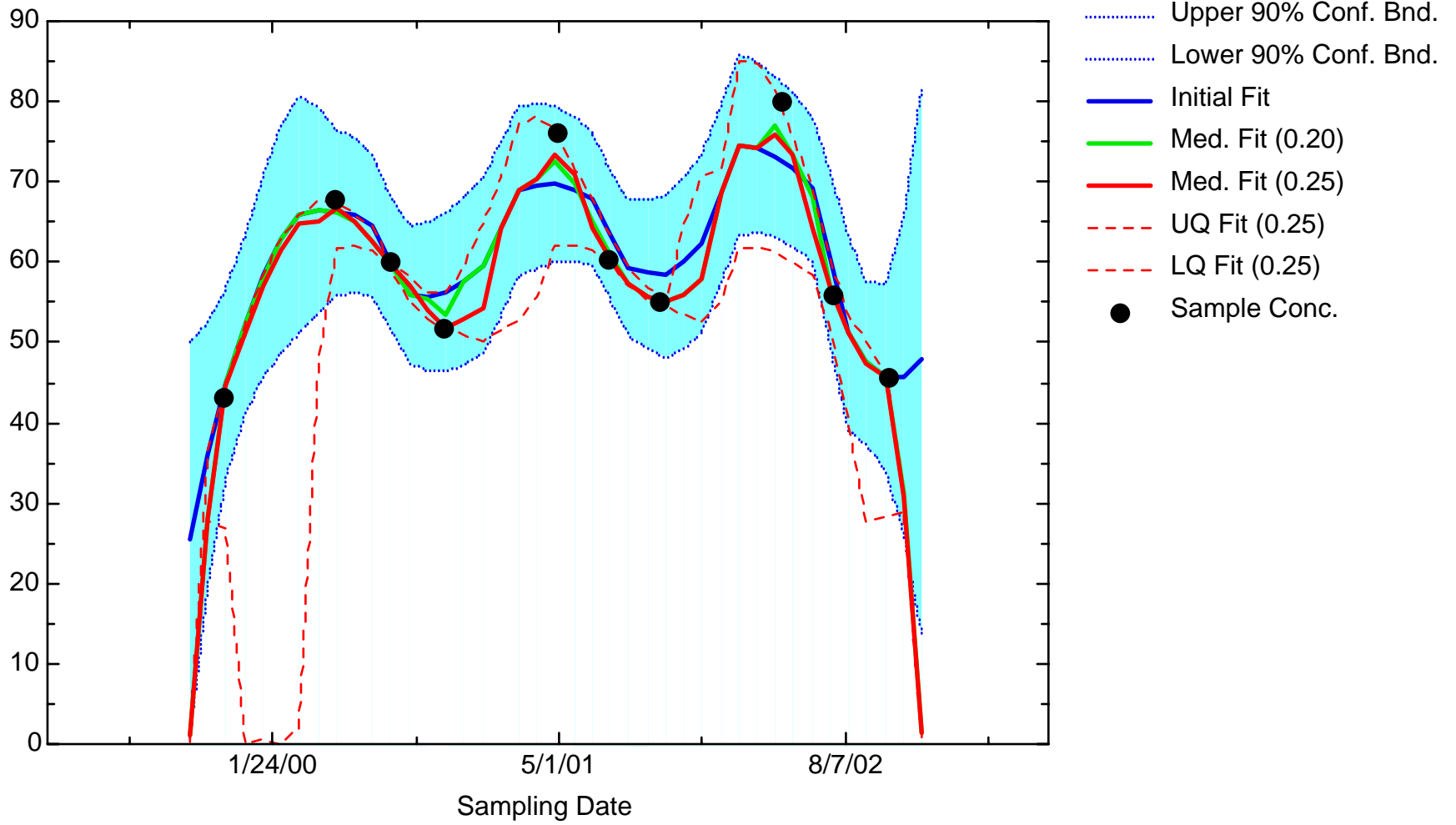
MN: Well JBW7806



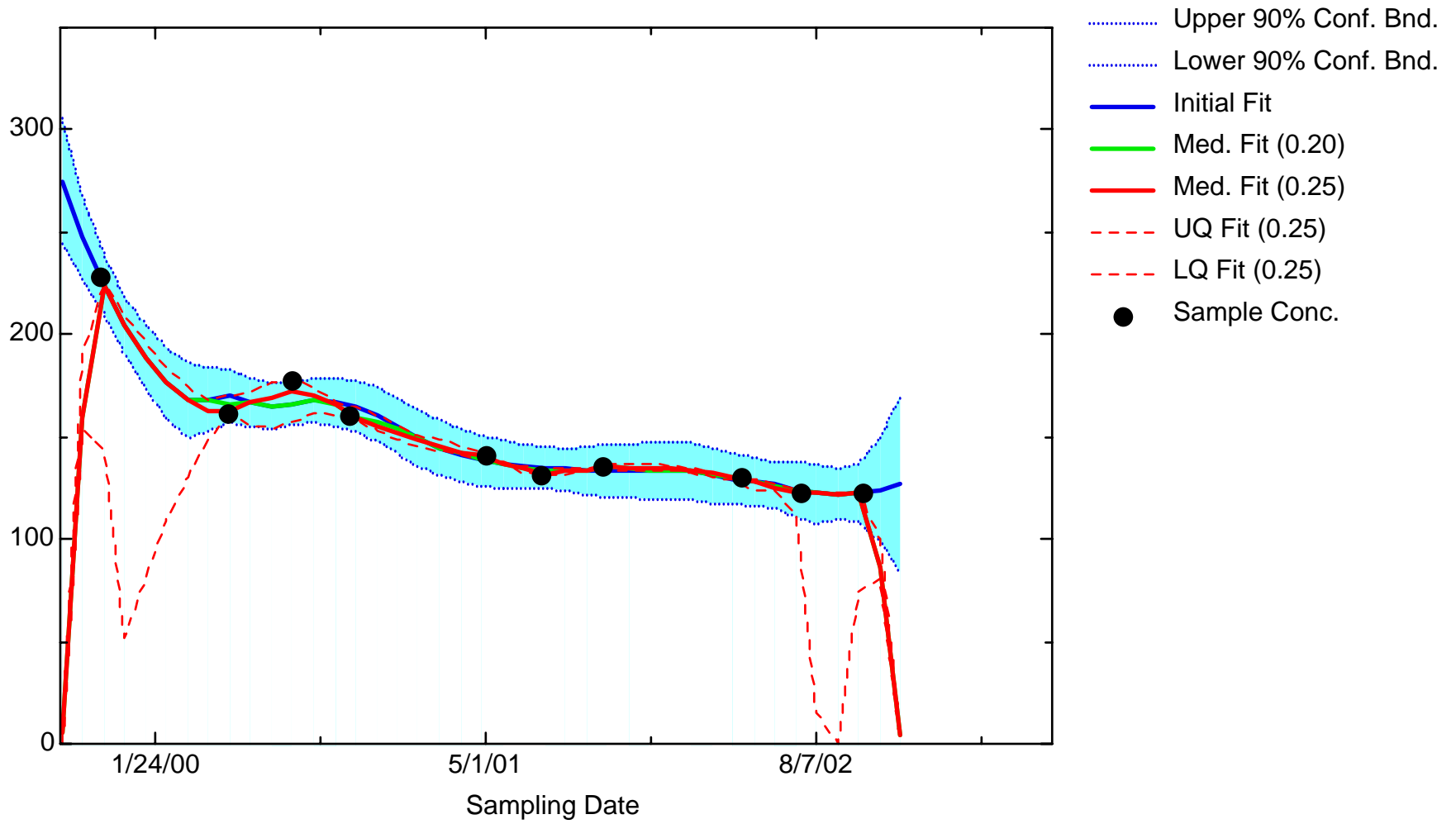
MN: Well JBW7809



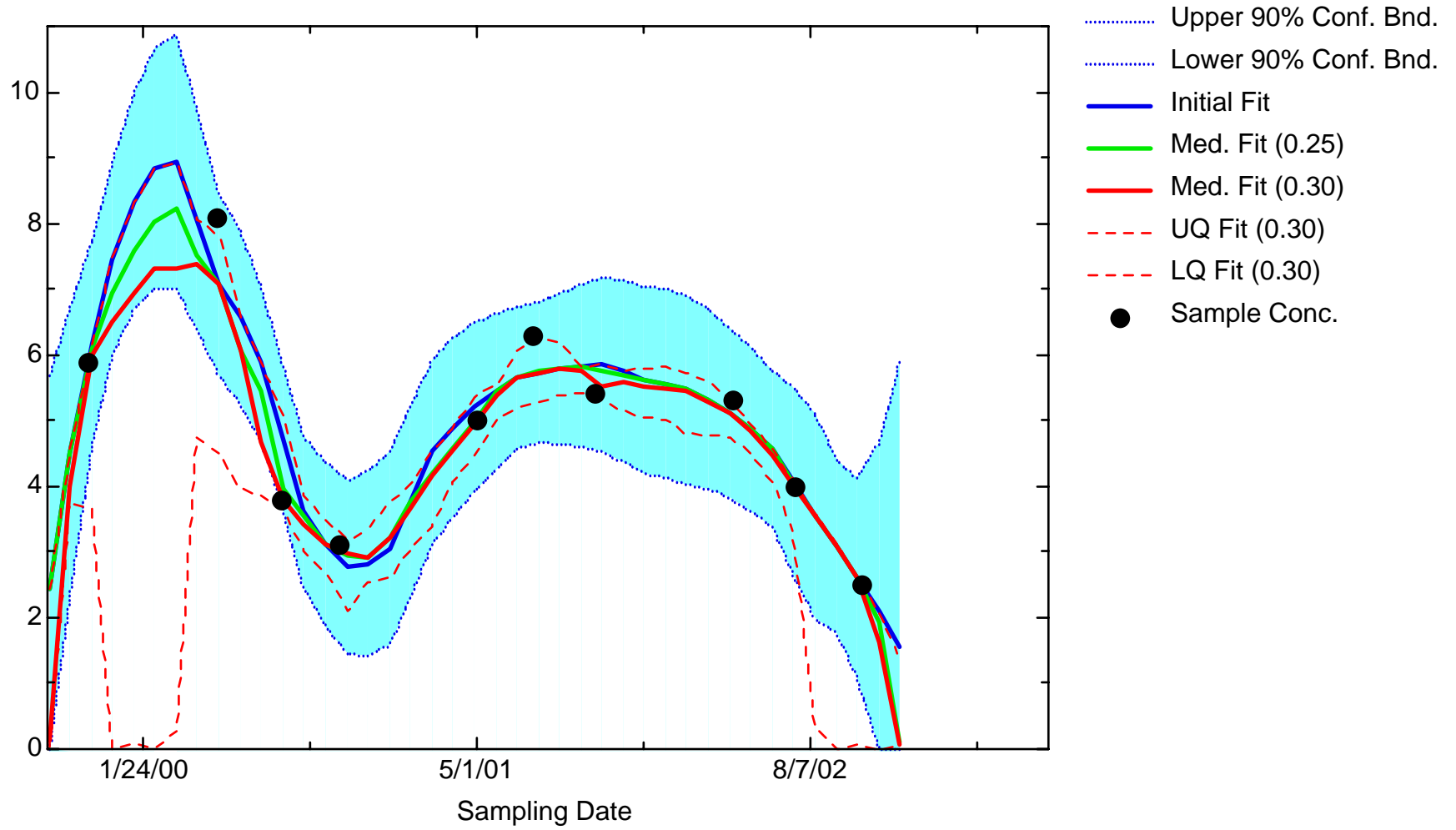
MN: Well JBW7812B



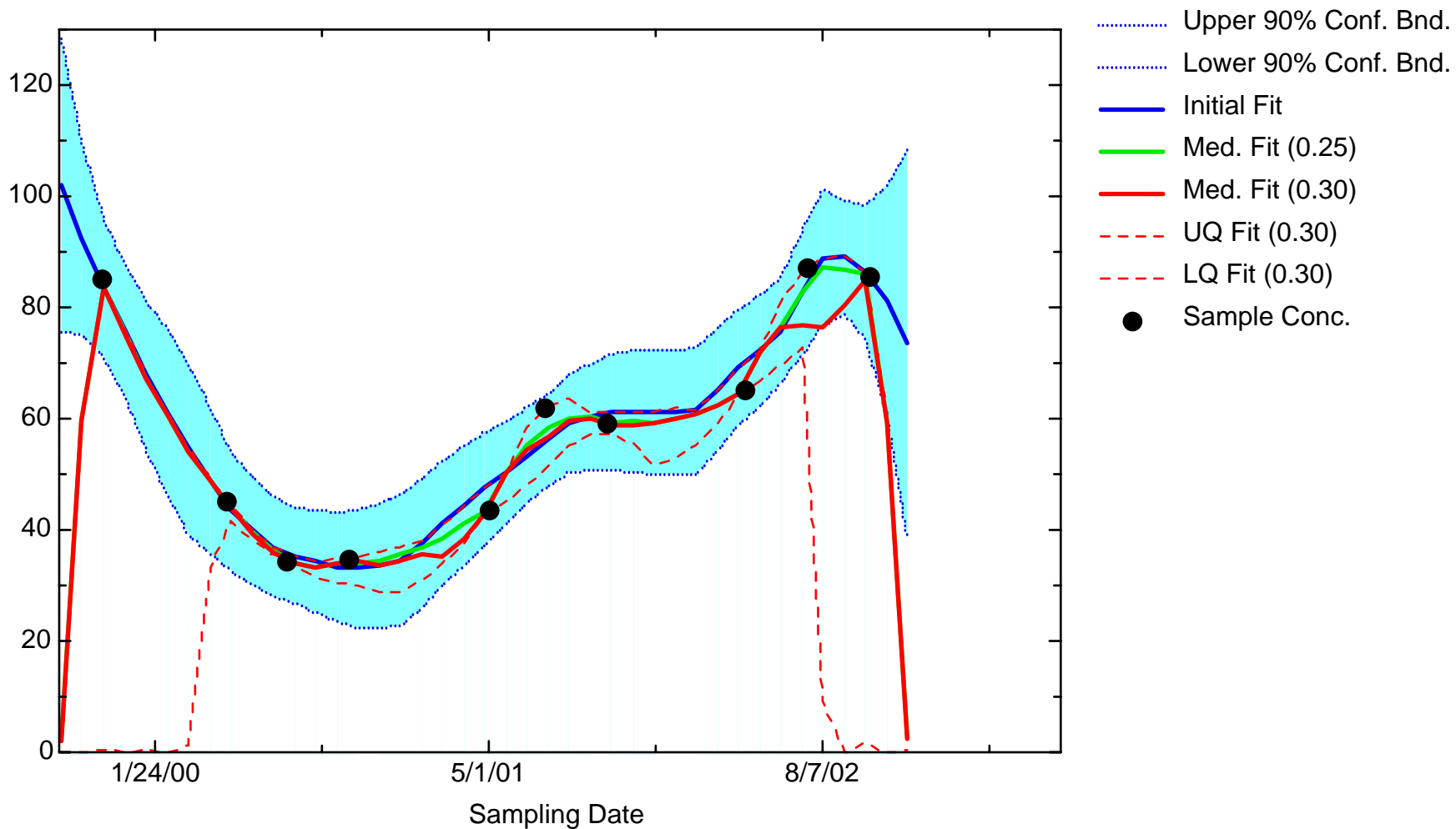
MN: Well JBW8003B



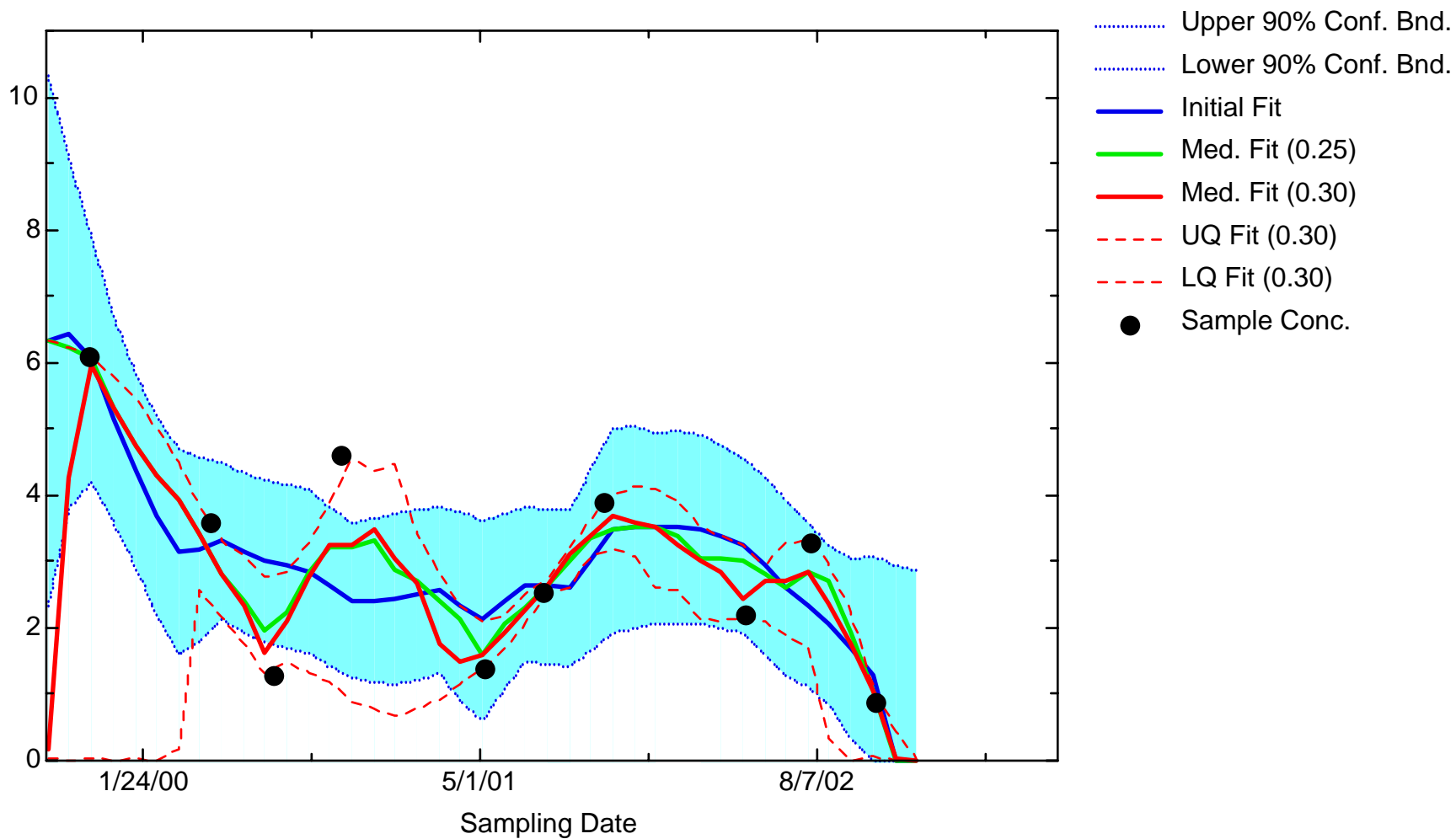
MN: Well JBW8004B



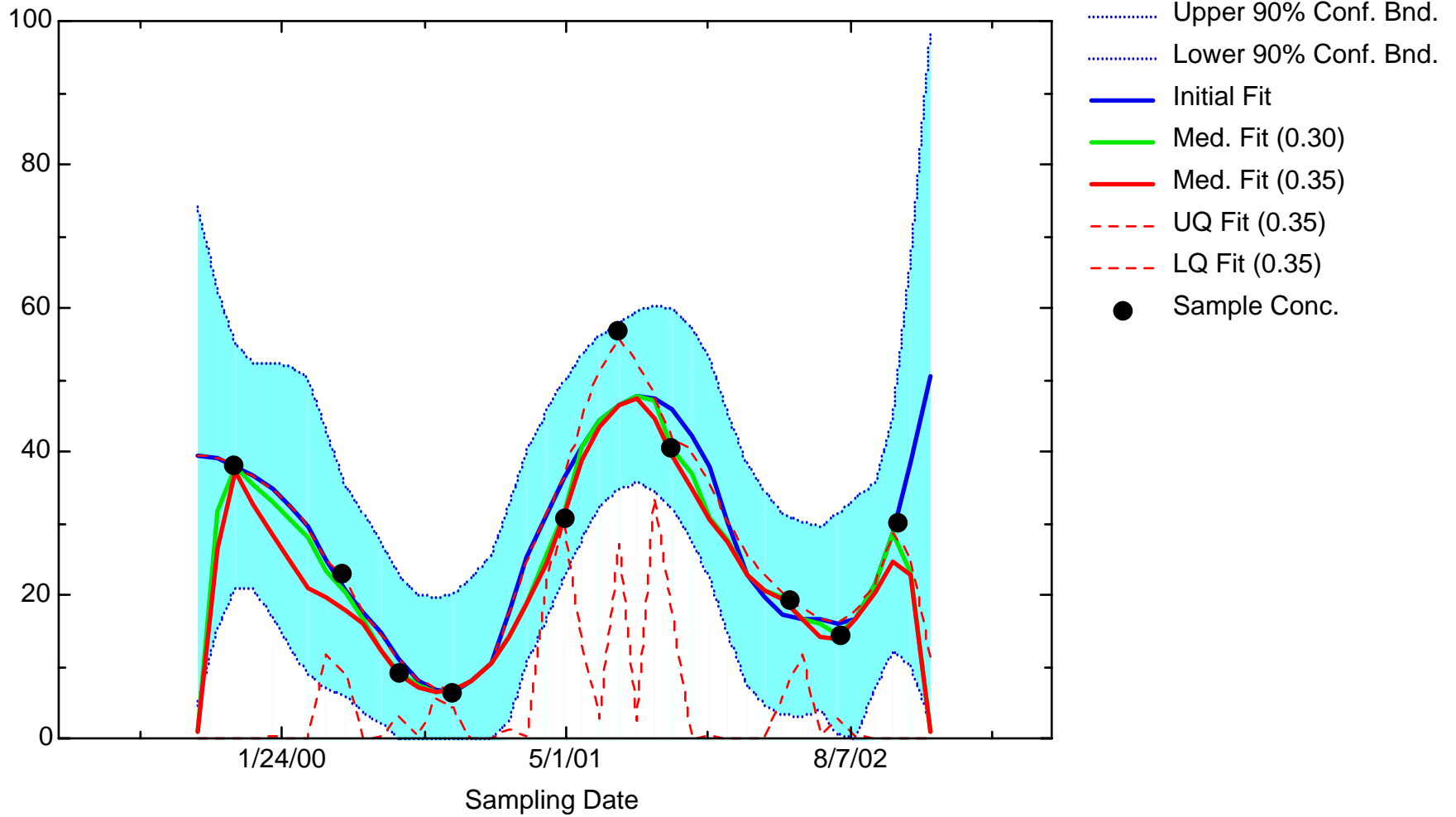
MN: Well JBW8009



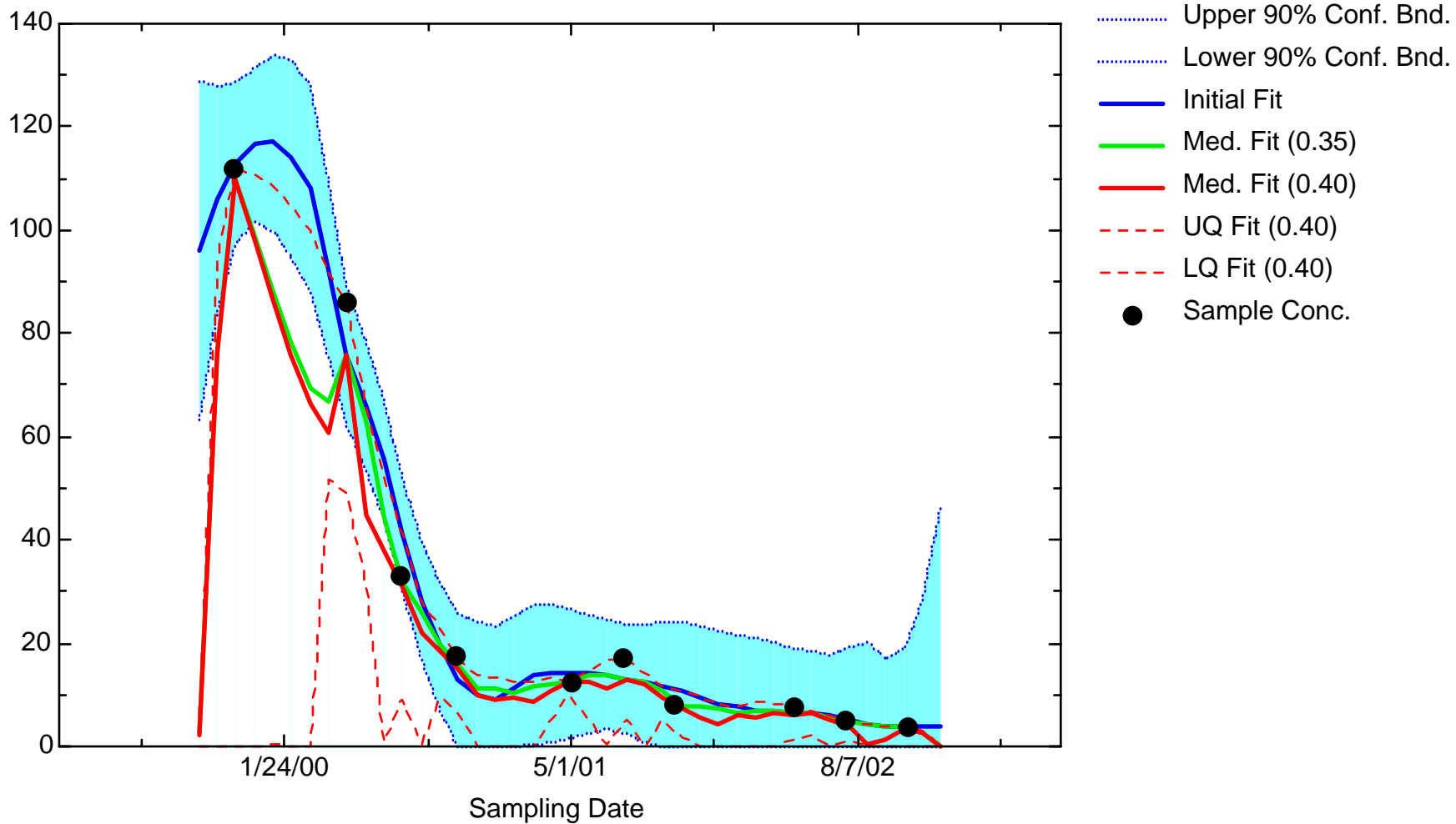
MN: Well JMW35X2



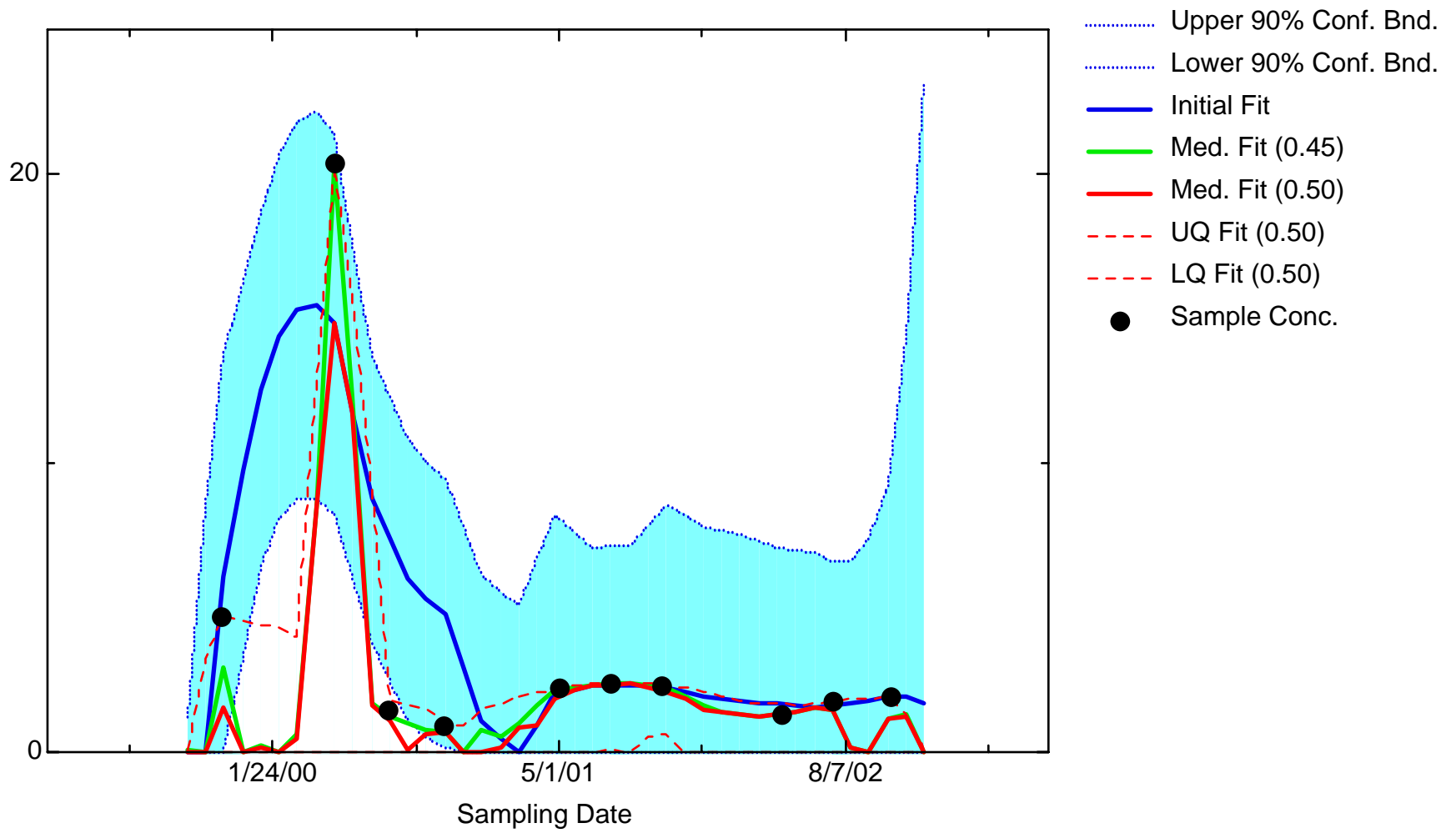
MN: Well JMW0301C



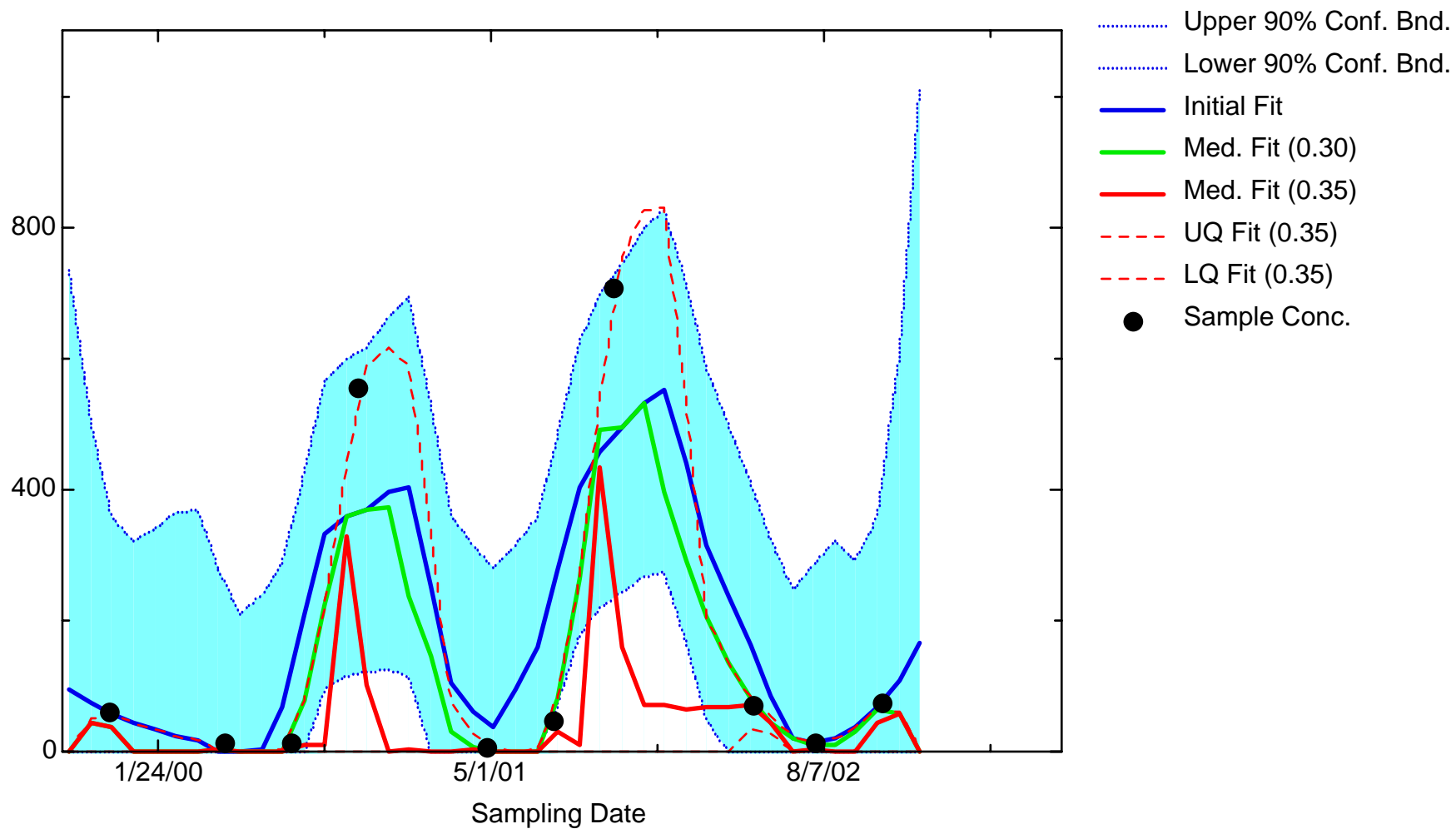
MN: Well JMW0503



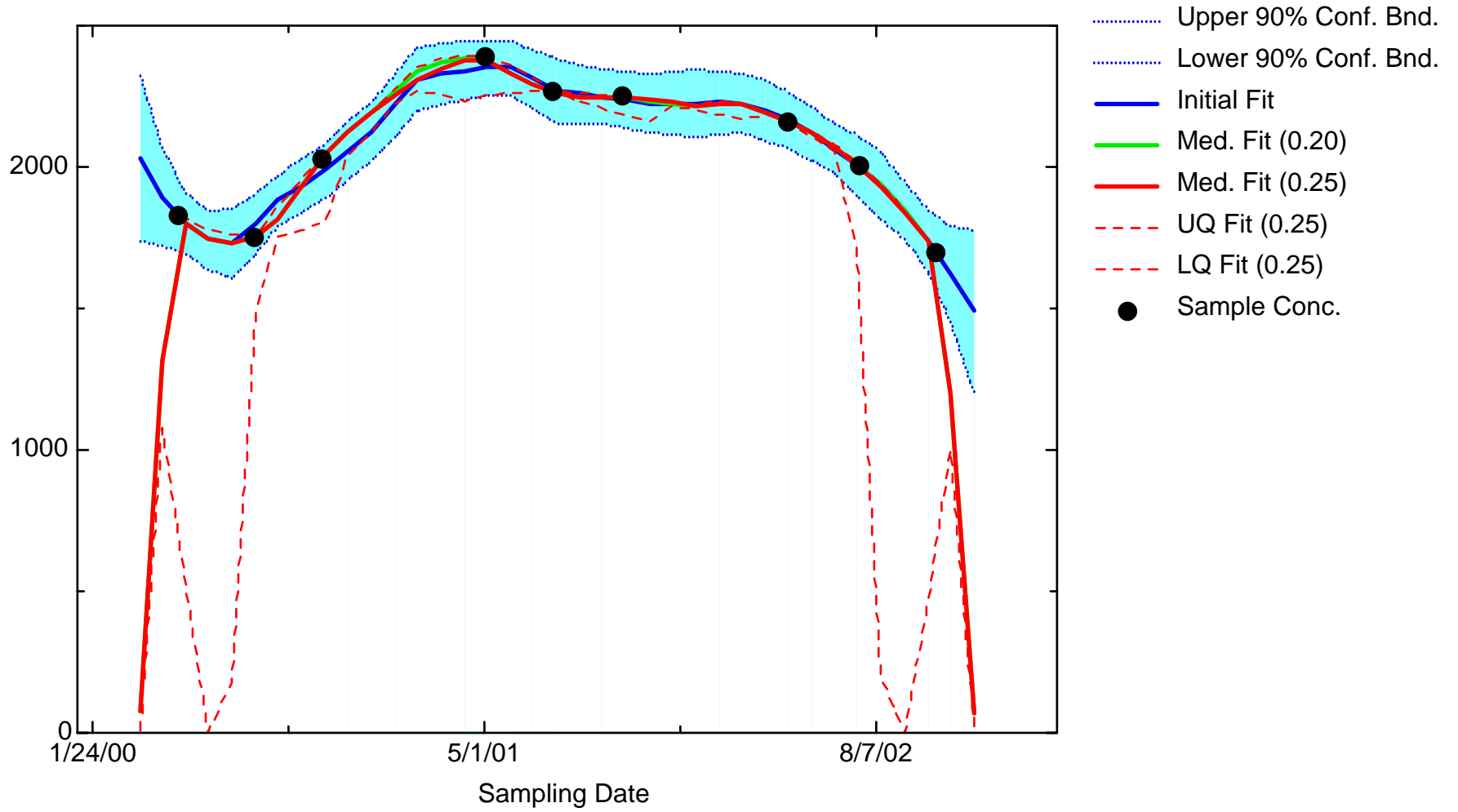
MN: Well JMW0505



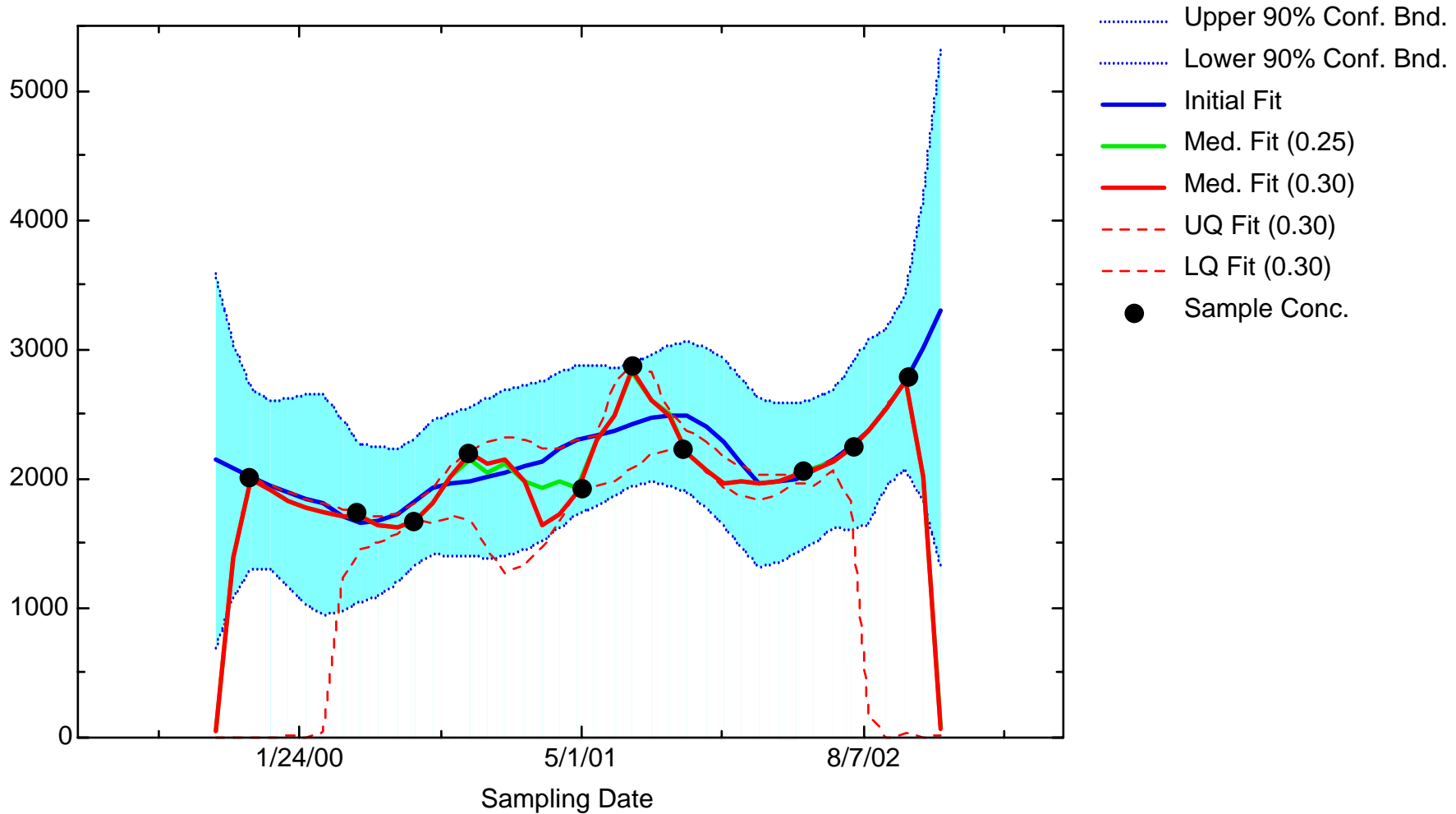
MN: Well JMW0542



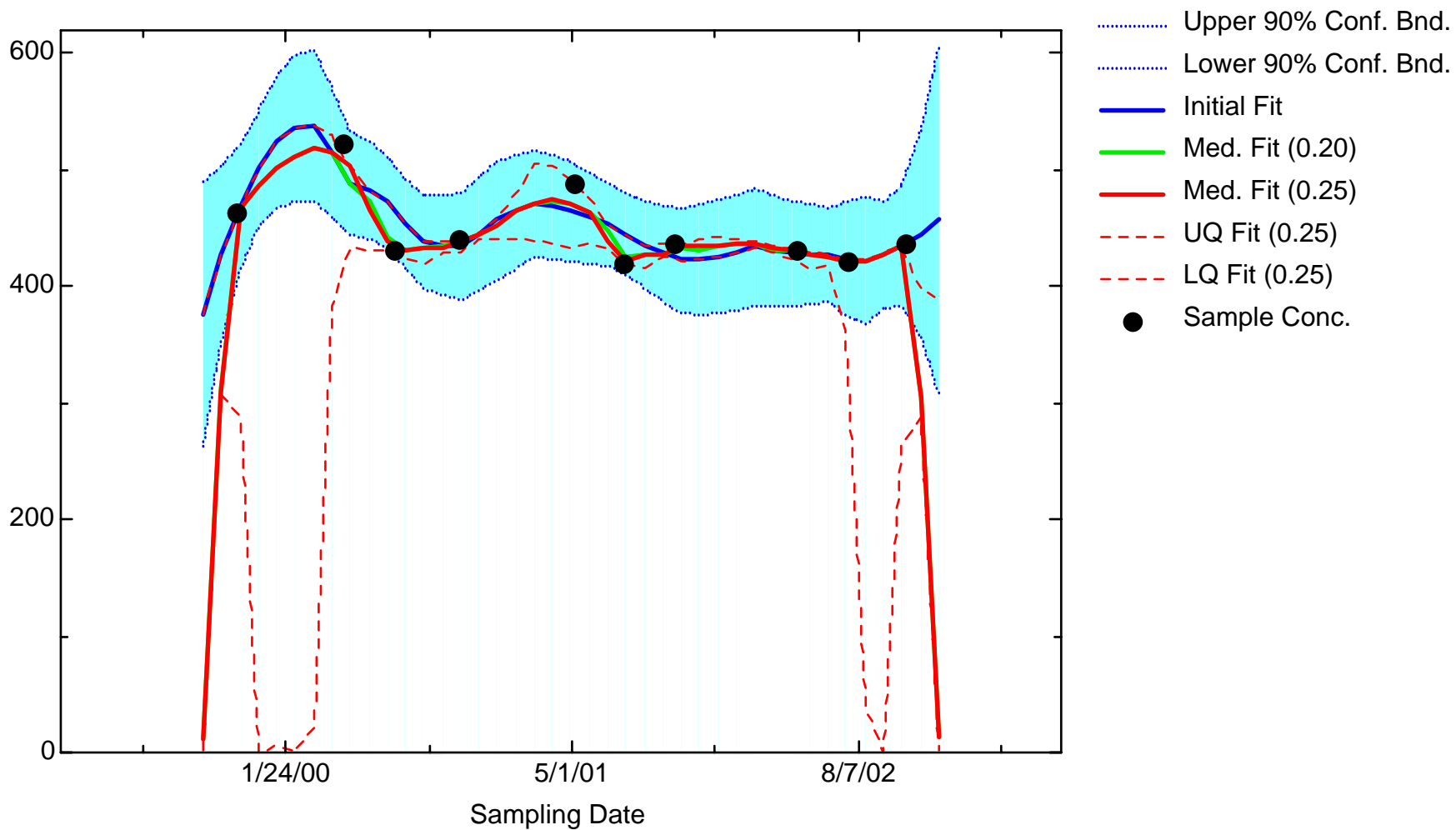
MN: Well JMW1103D



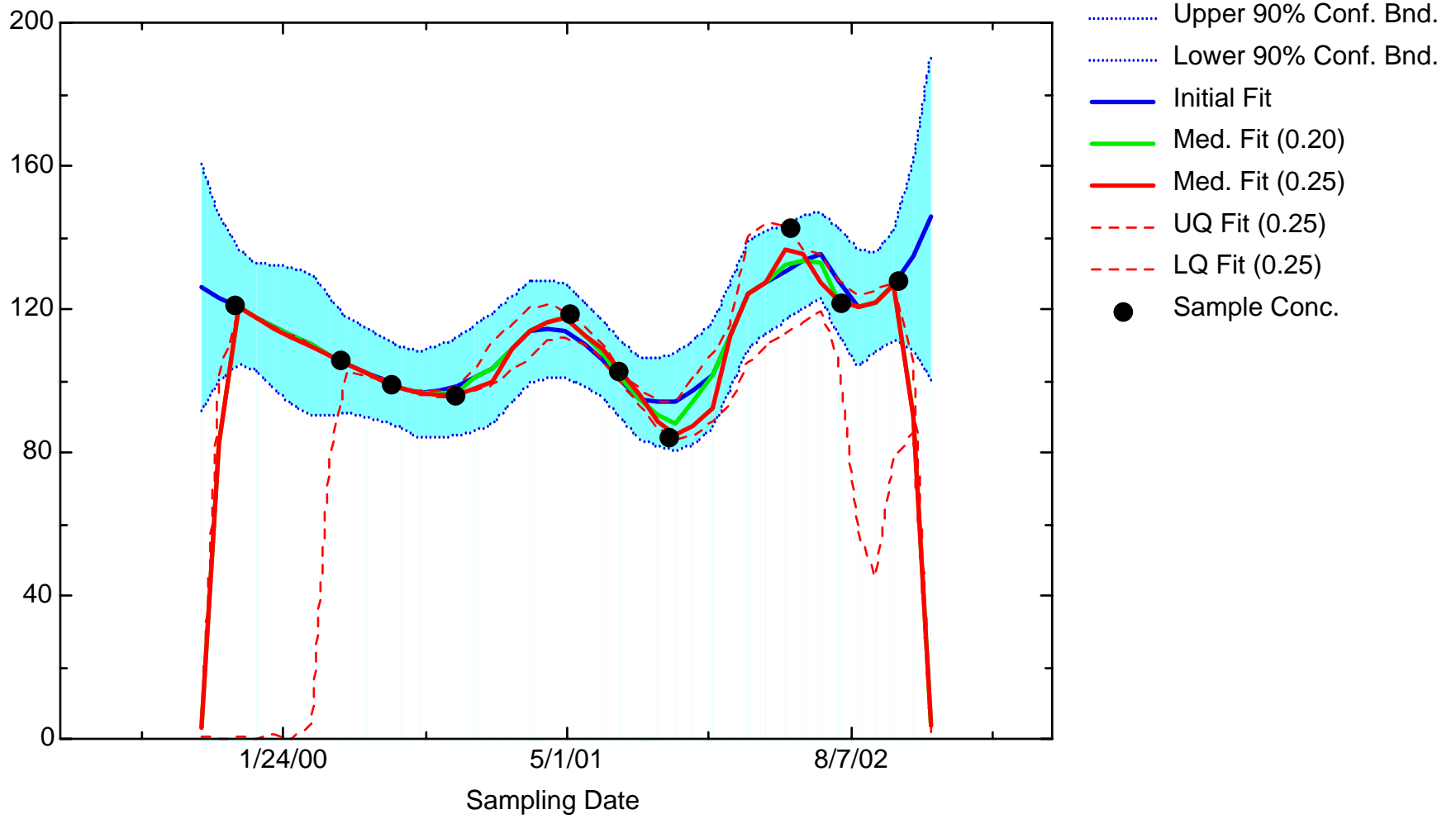
MN: Well JMW1565



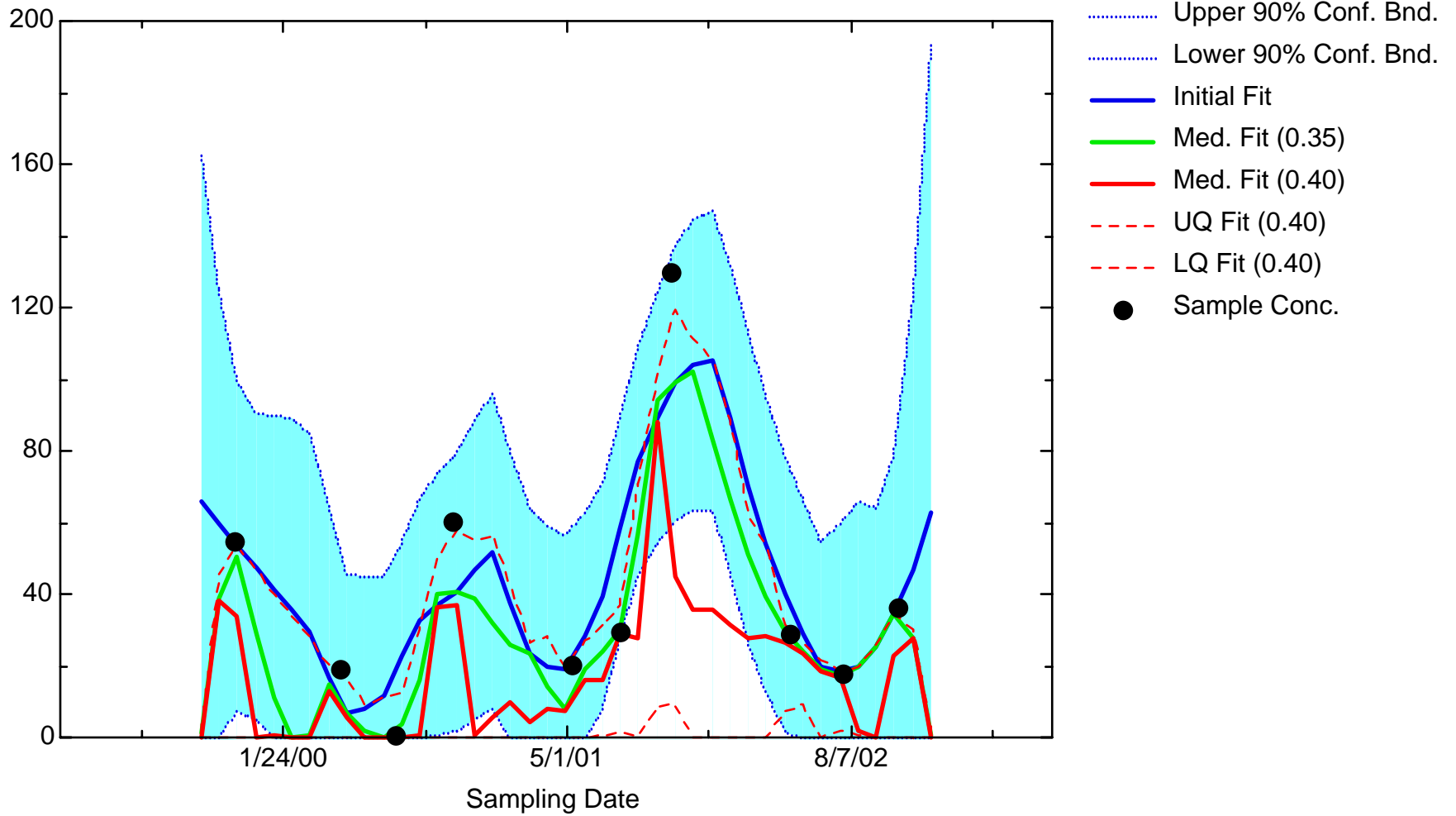
MN: Well JMW1860



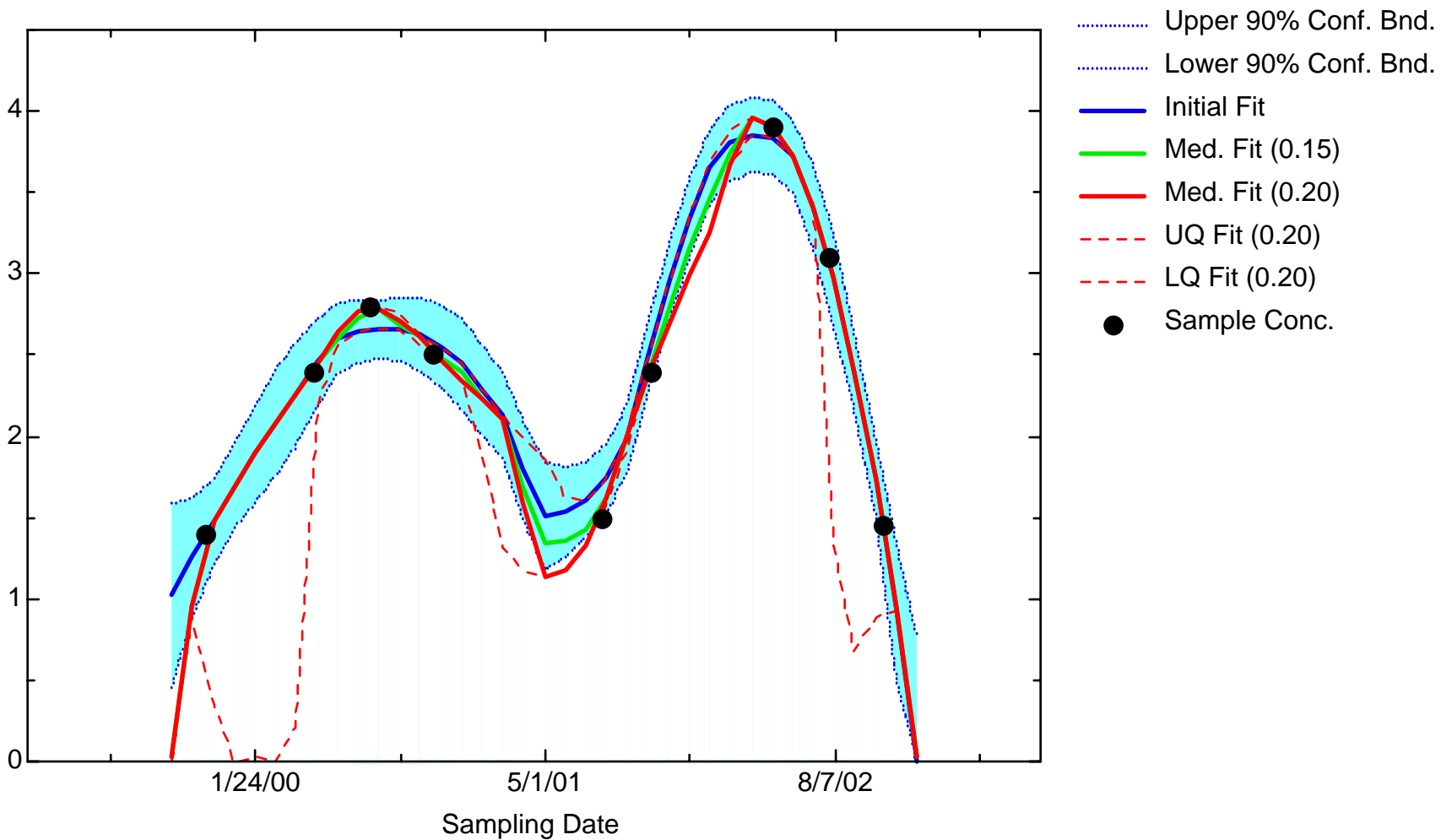
MN: Well JMW1881



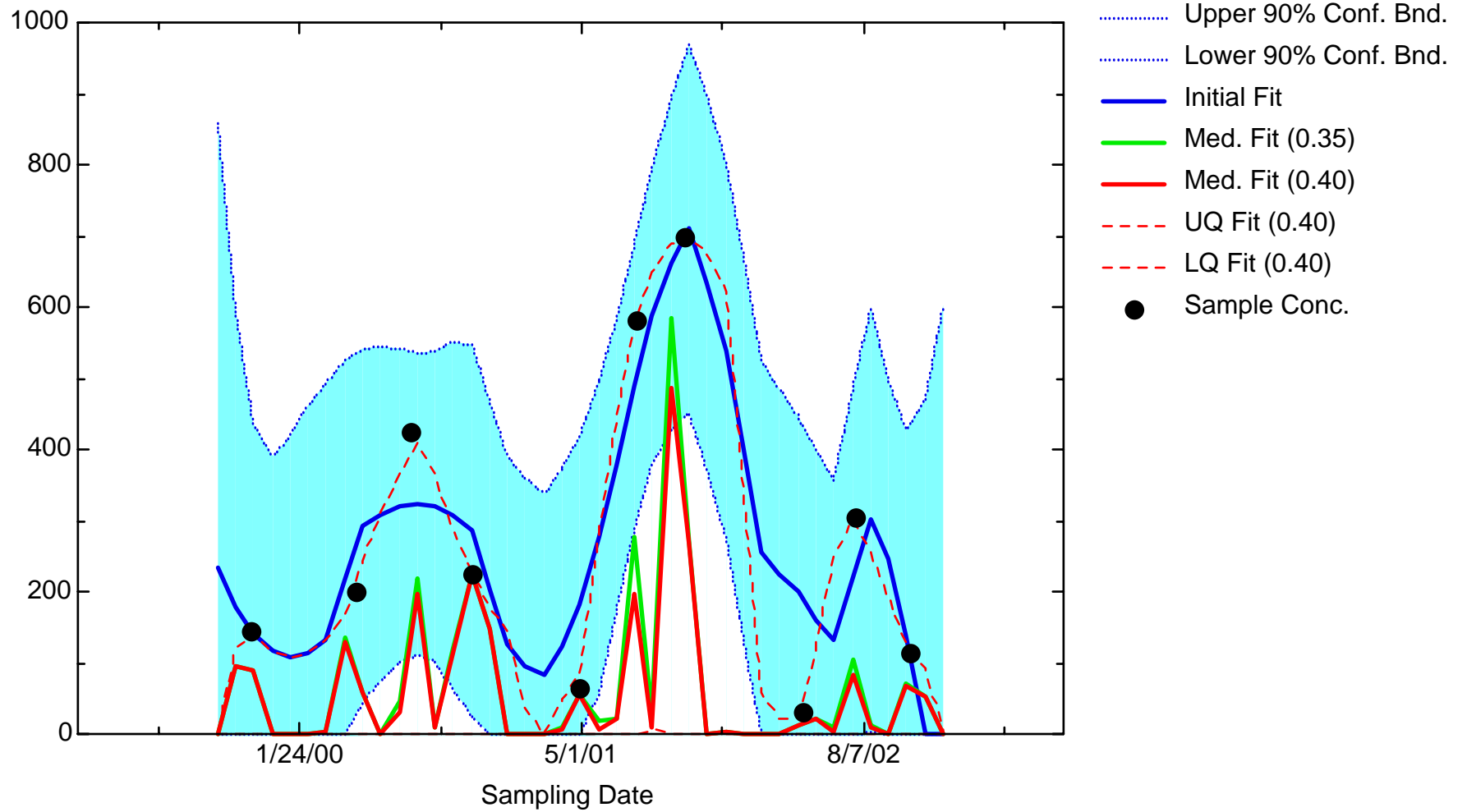
MN: Well JMW1963



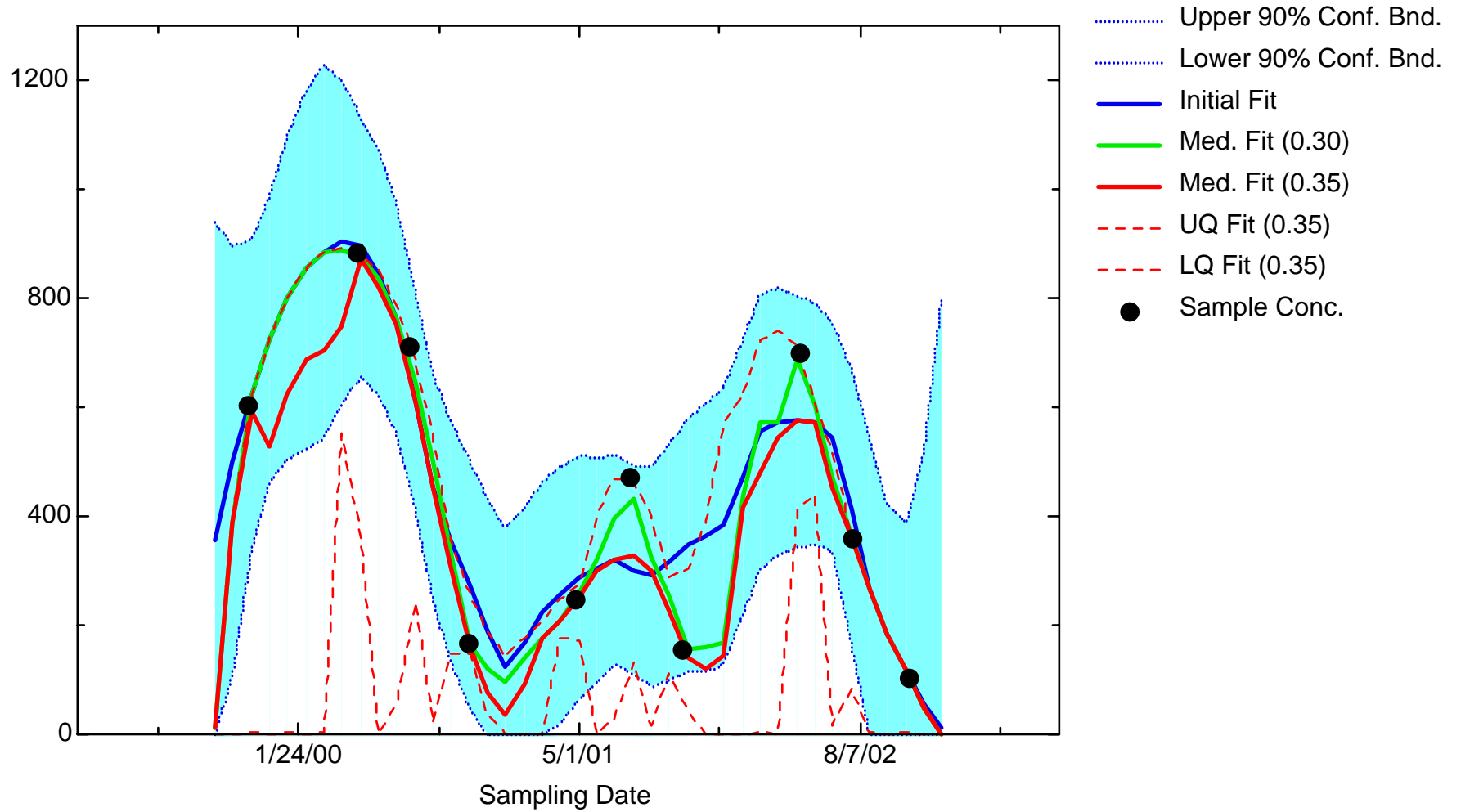
MN: Well JMW1964



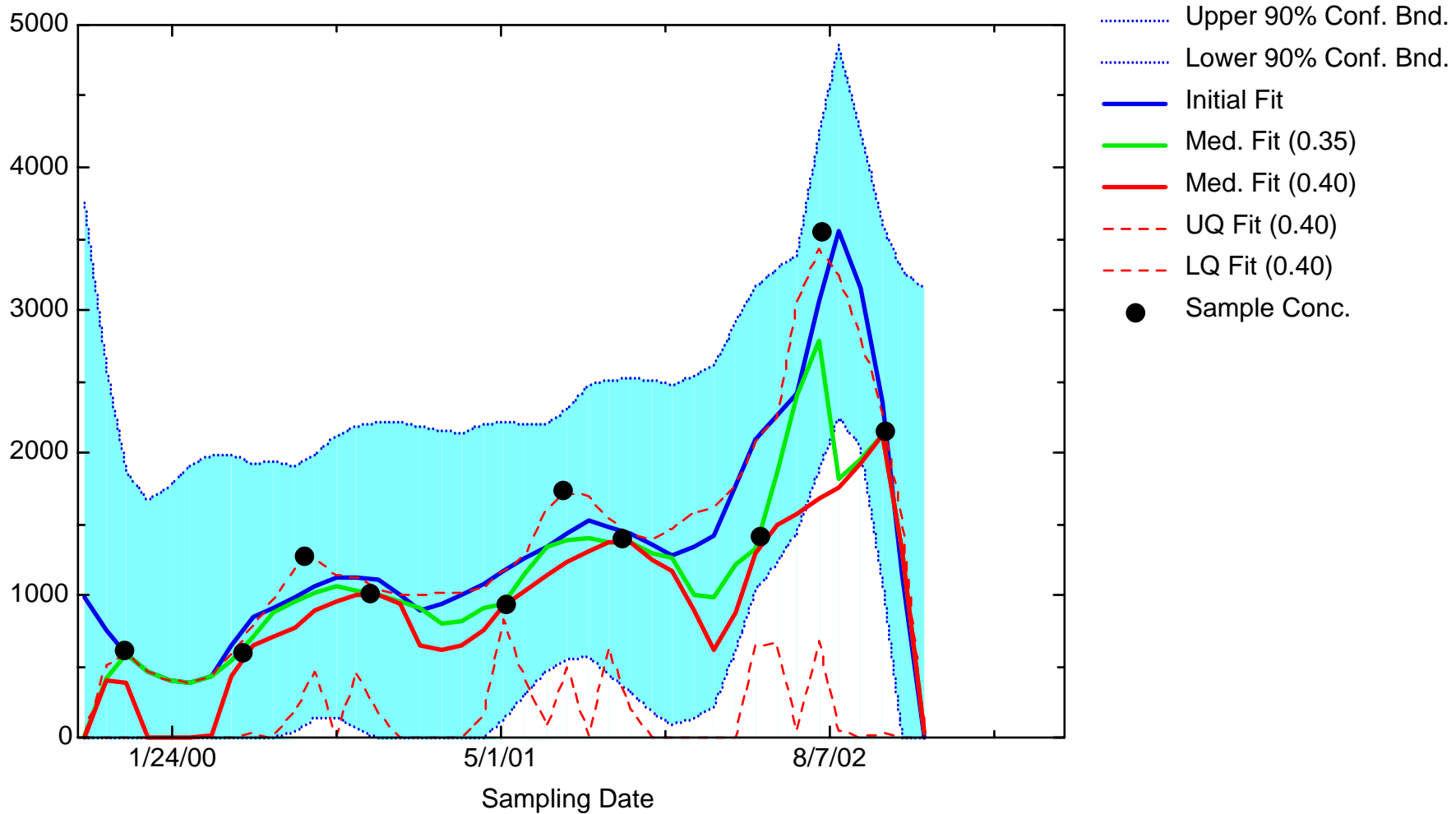
MN: Well JMW1966



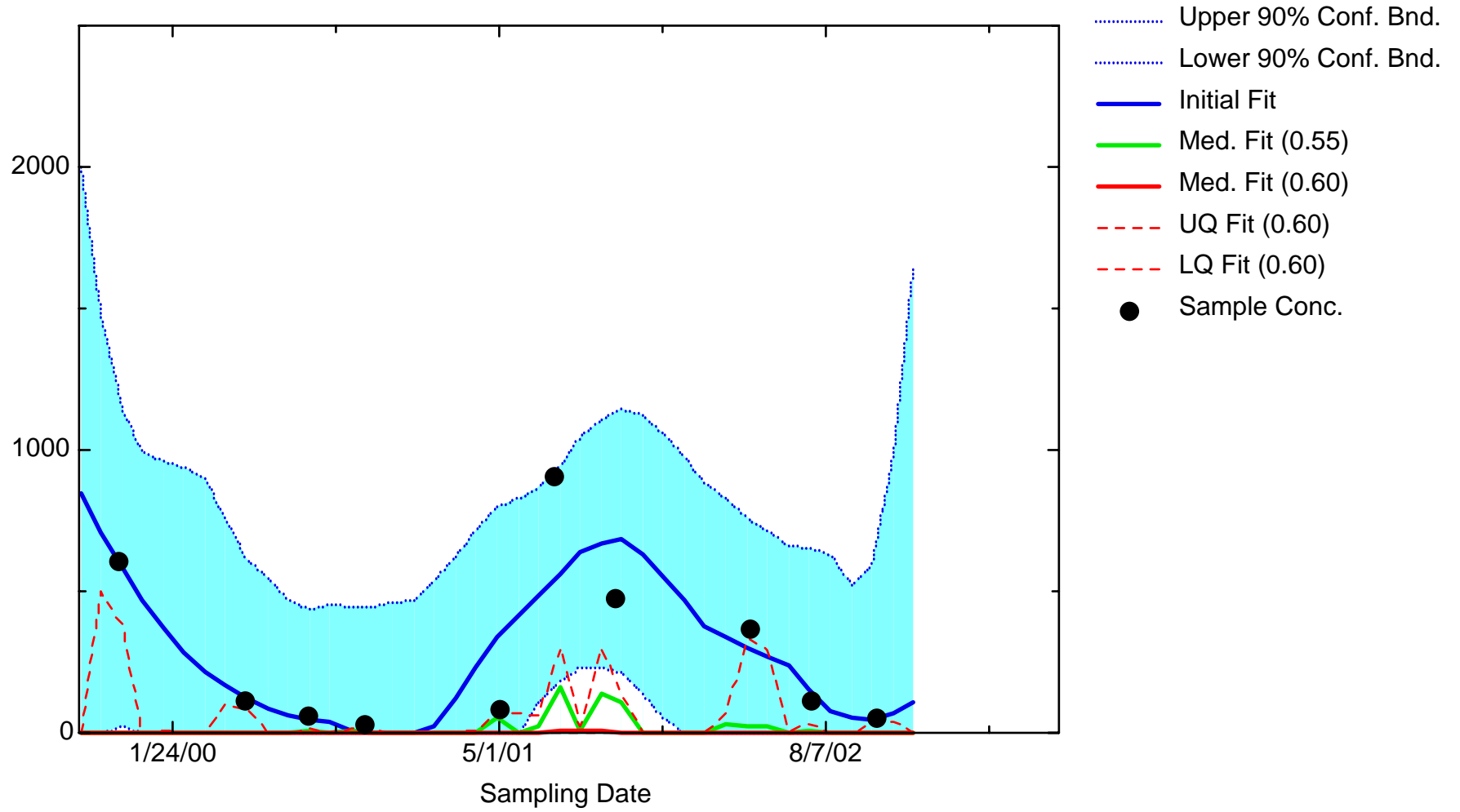
MN: Well JMW3202



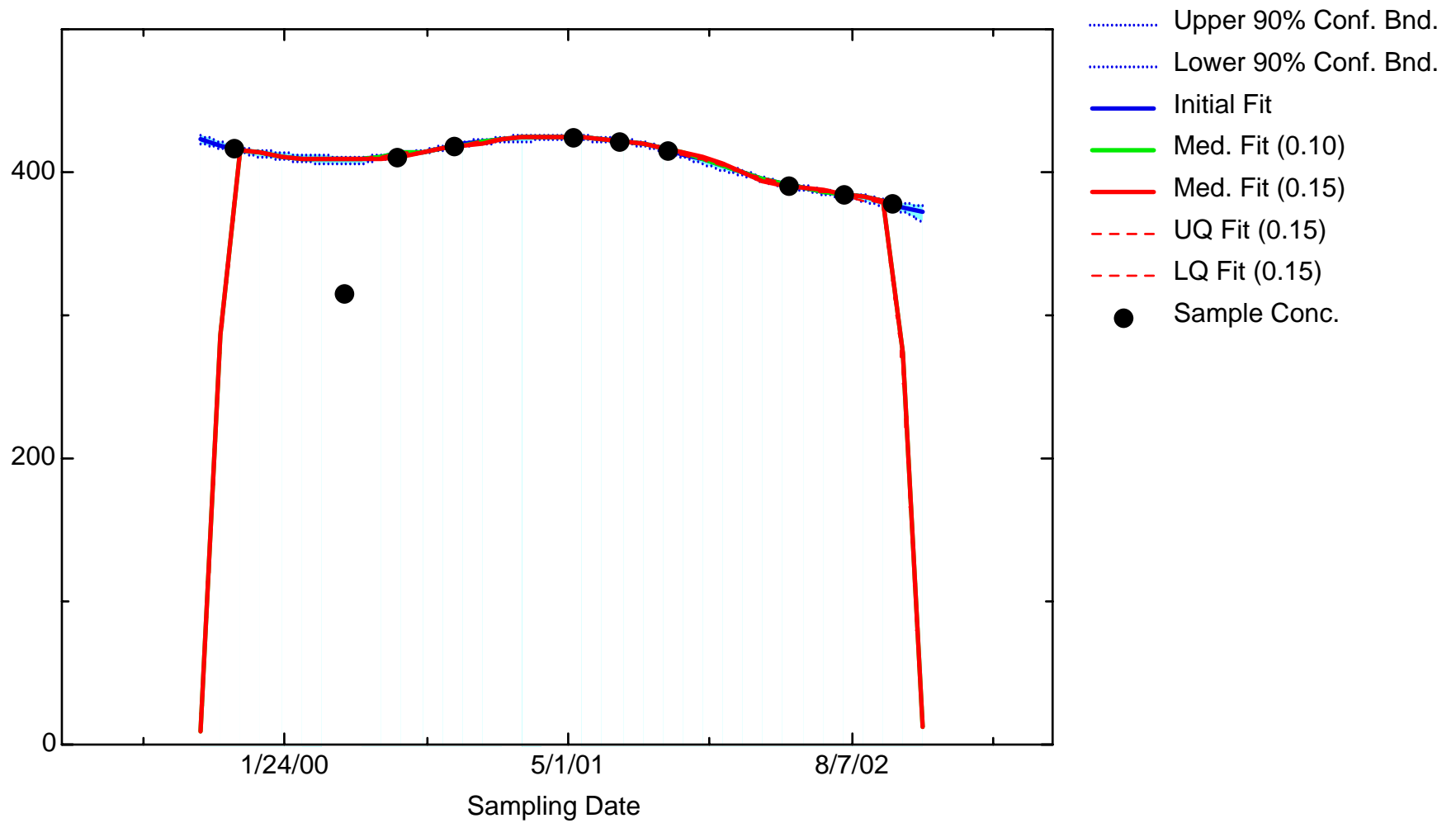
MN: Well JMW7332



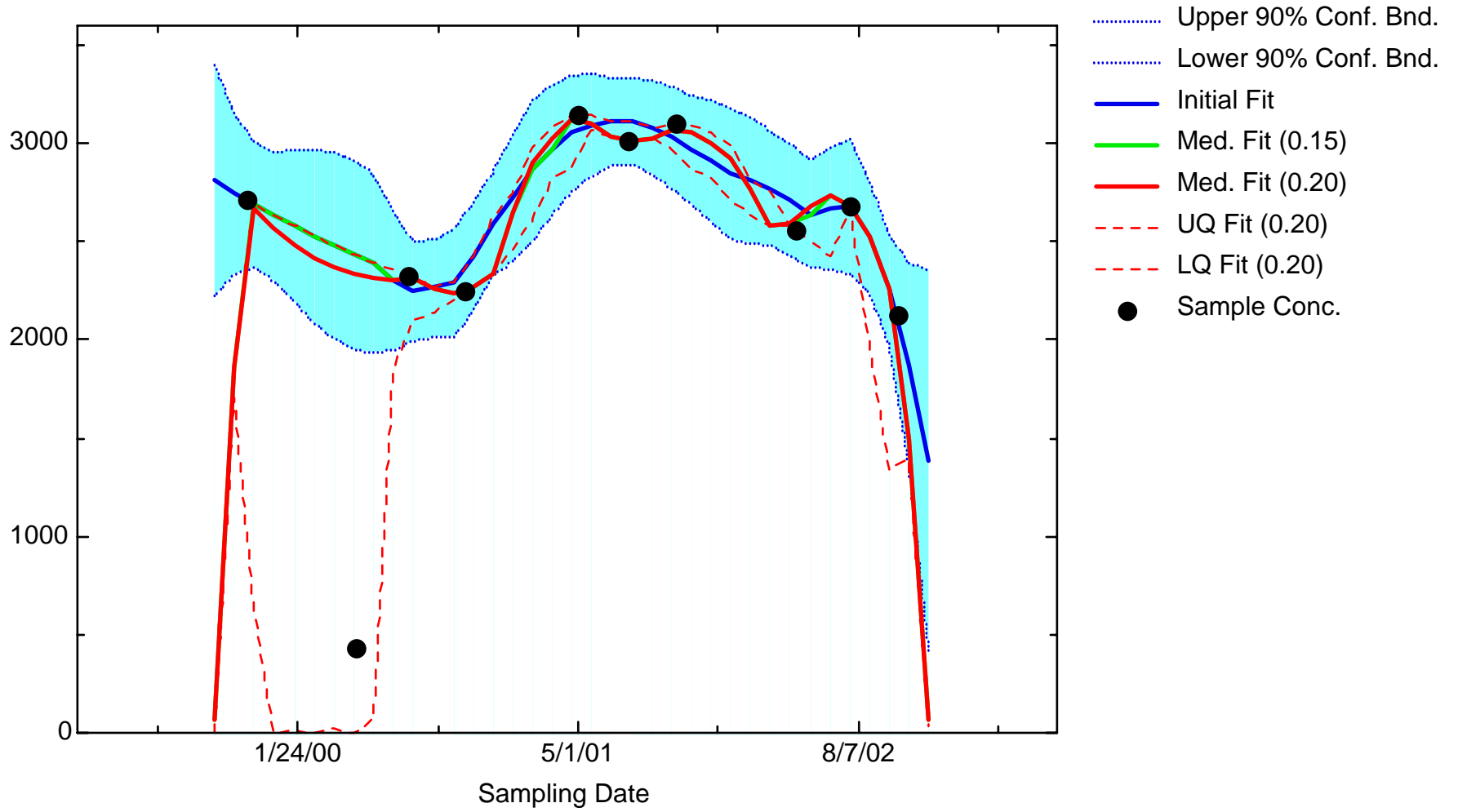
MN: Well JMW8011



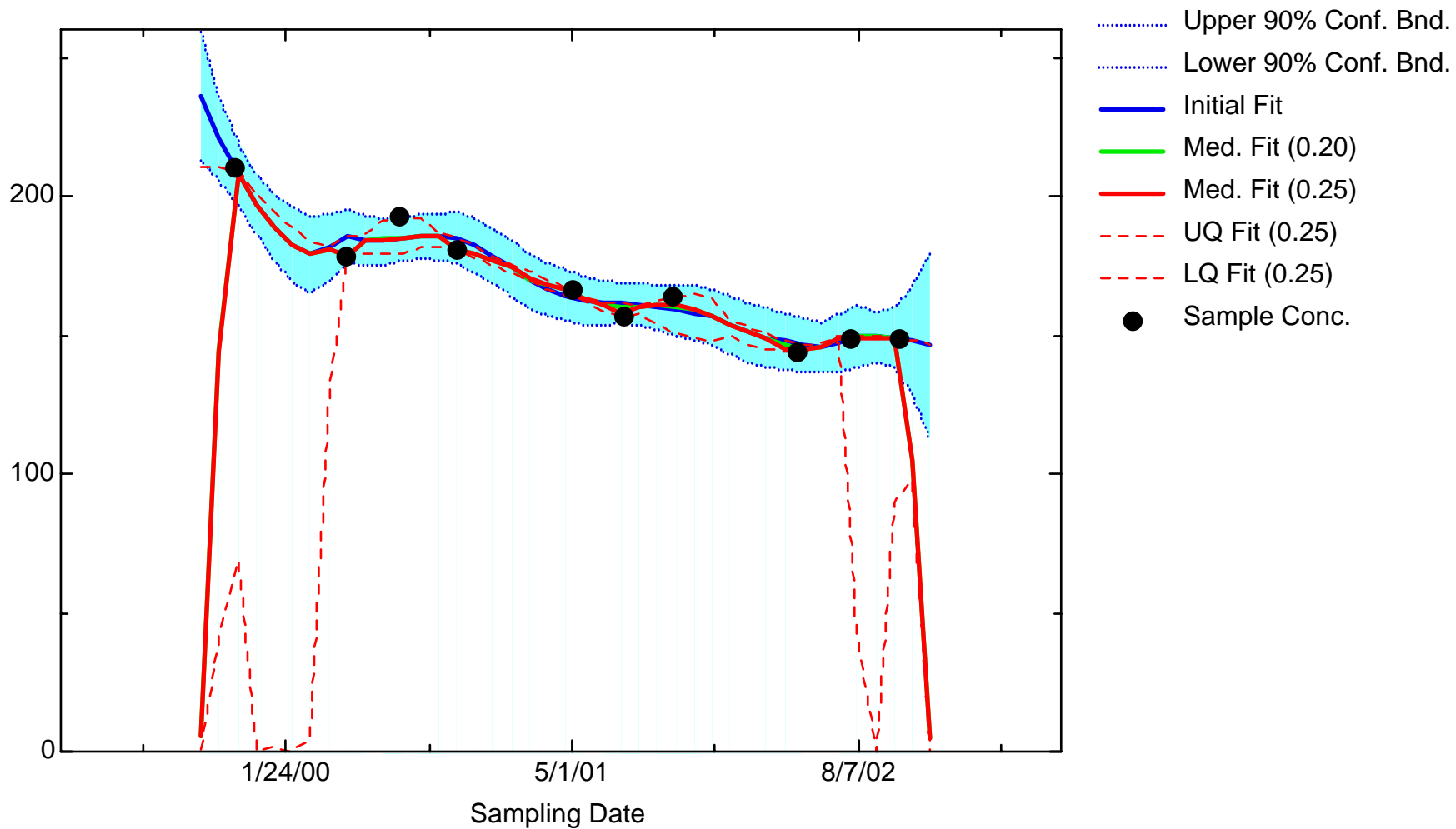
MN: Well JPZ0340



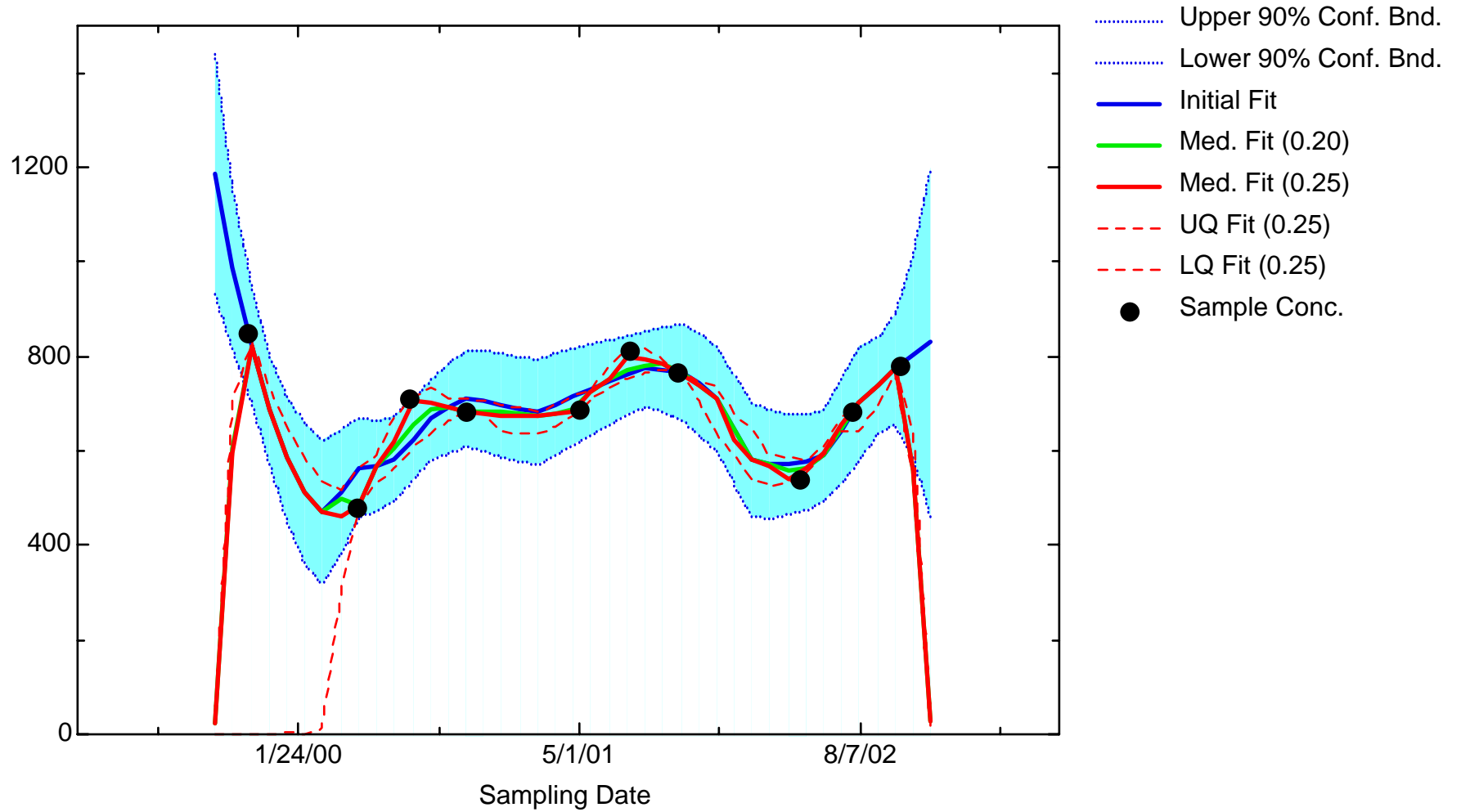
MN: Well JPZ0341



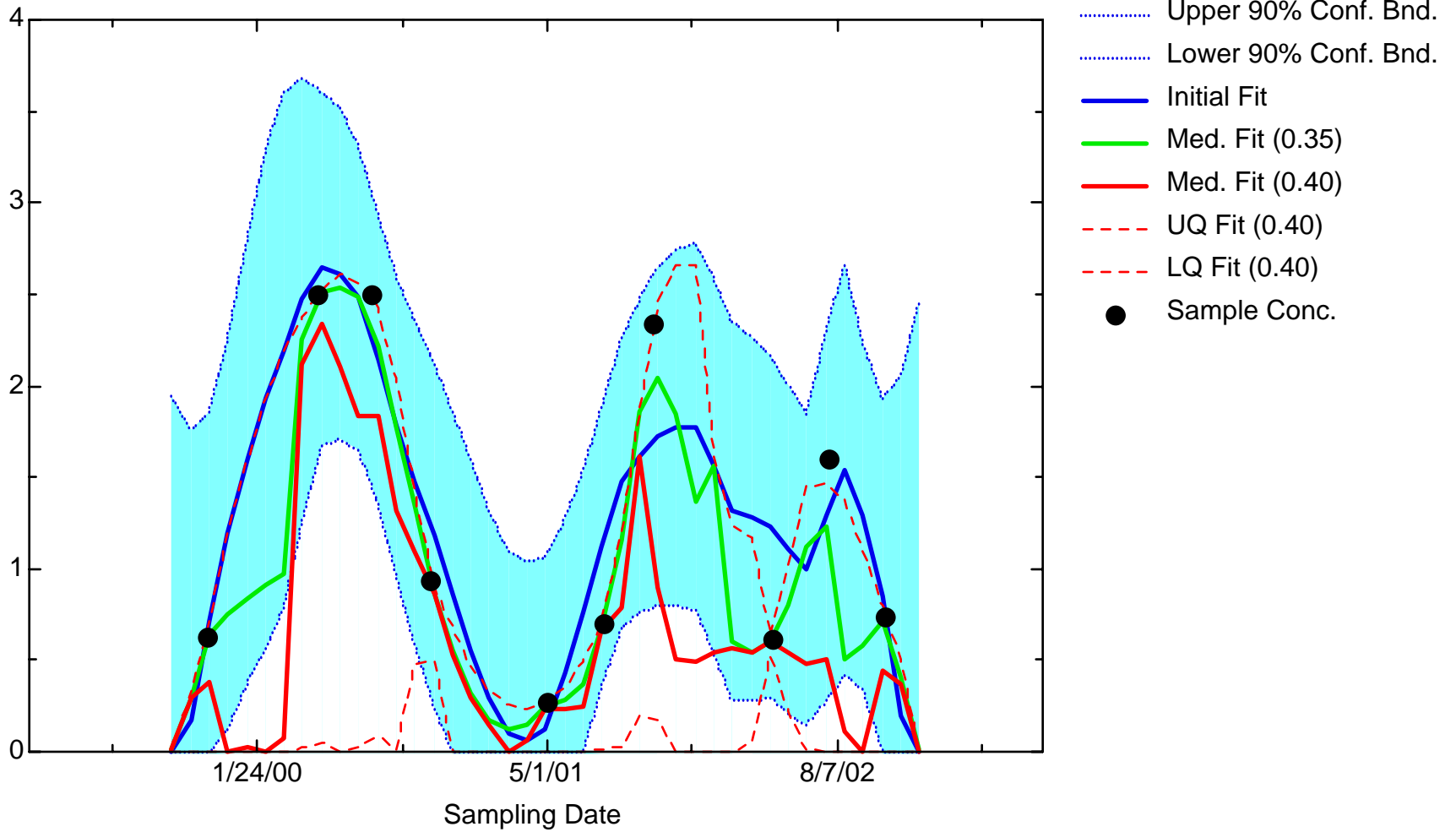
MN: Well JPZ0342



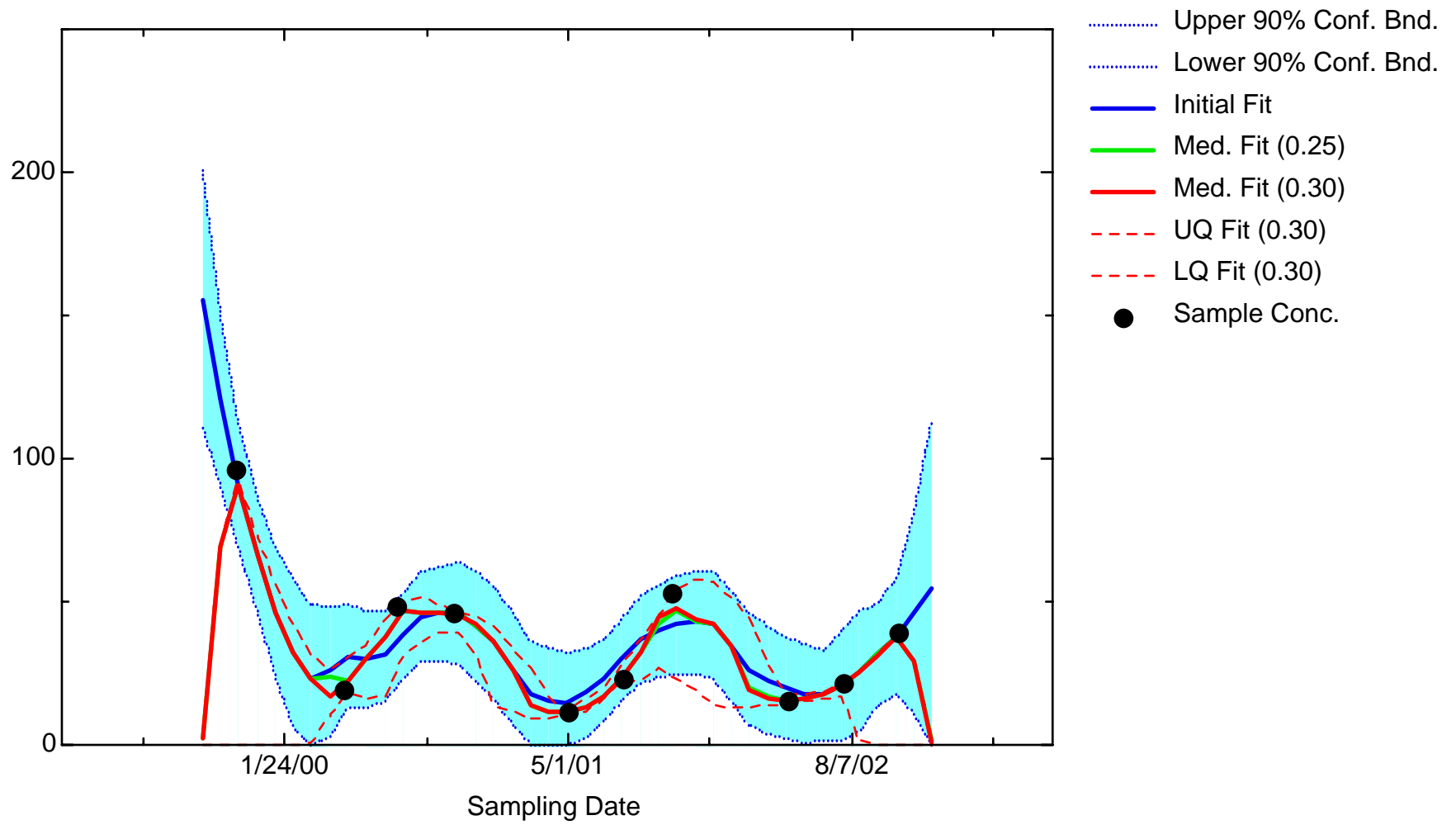
MN: Well JPZ0343



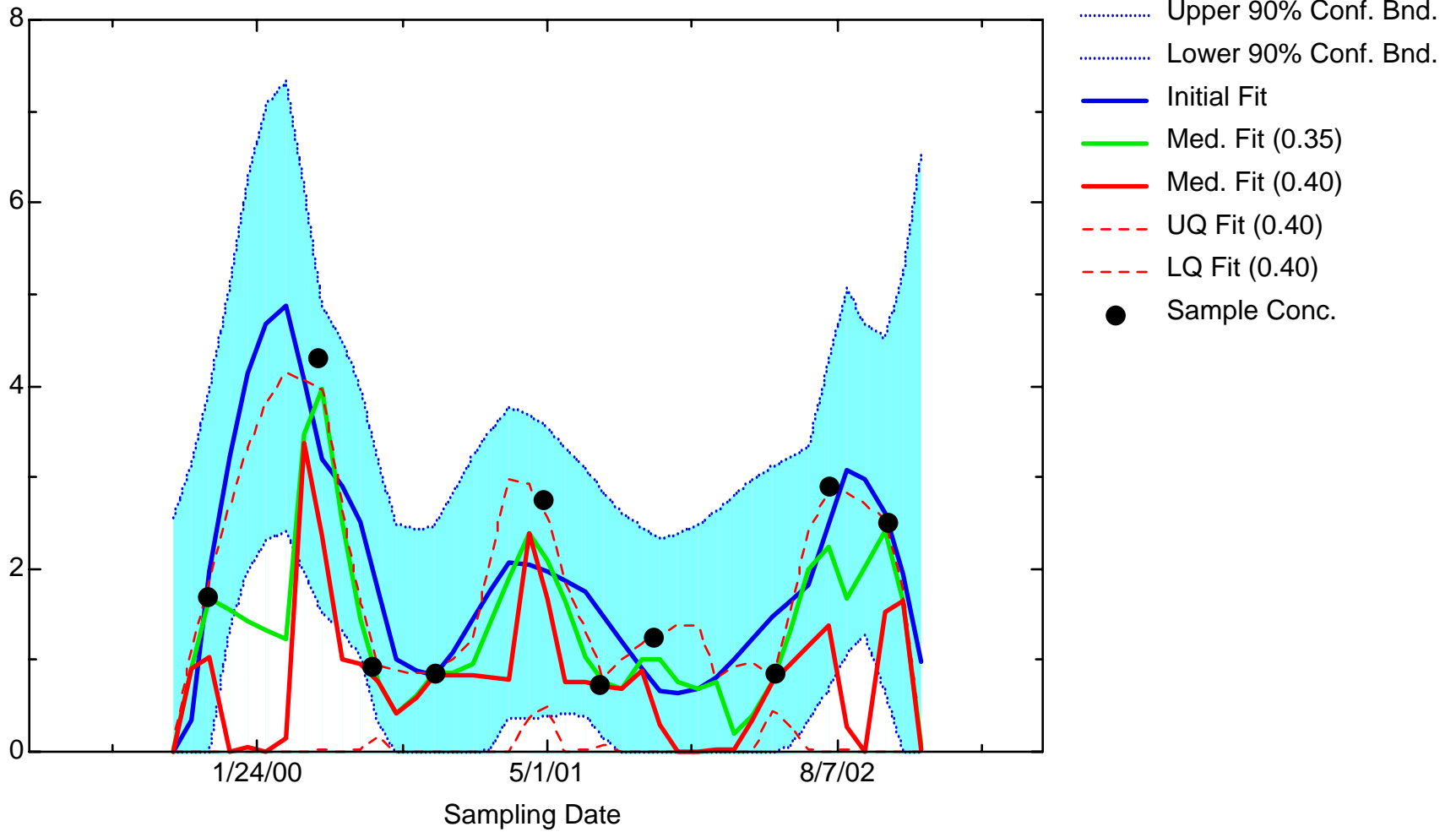
MN: Well JPZ0348



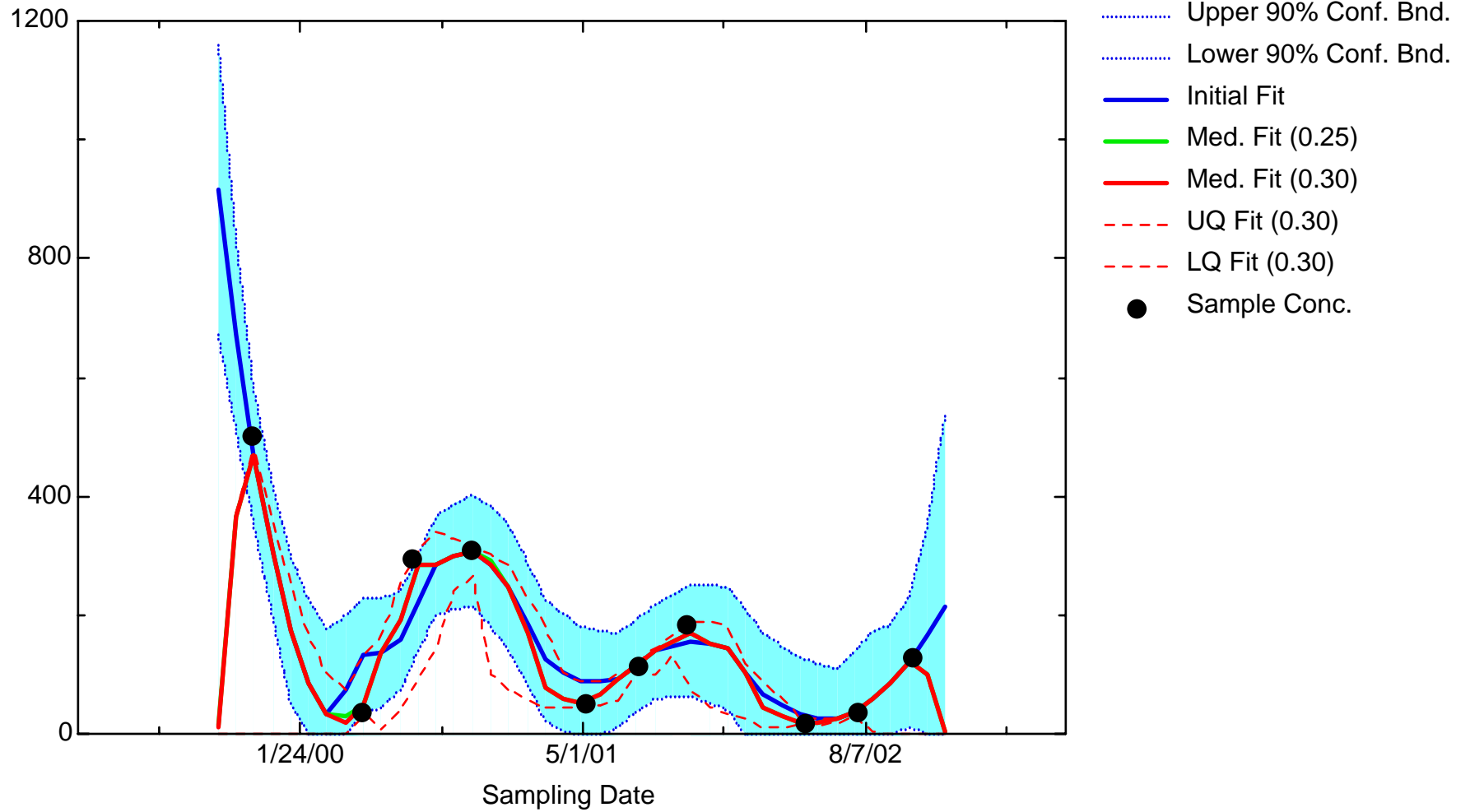
MN: Well JPZ0349



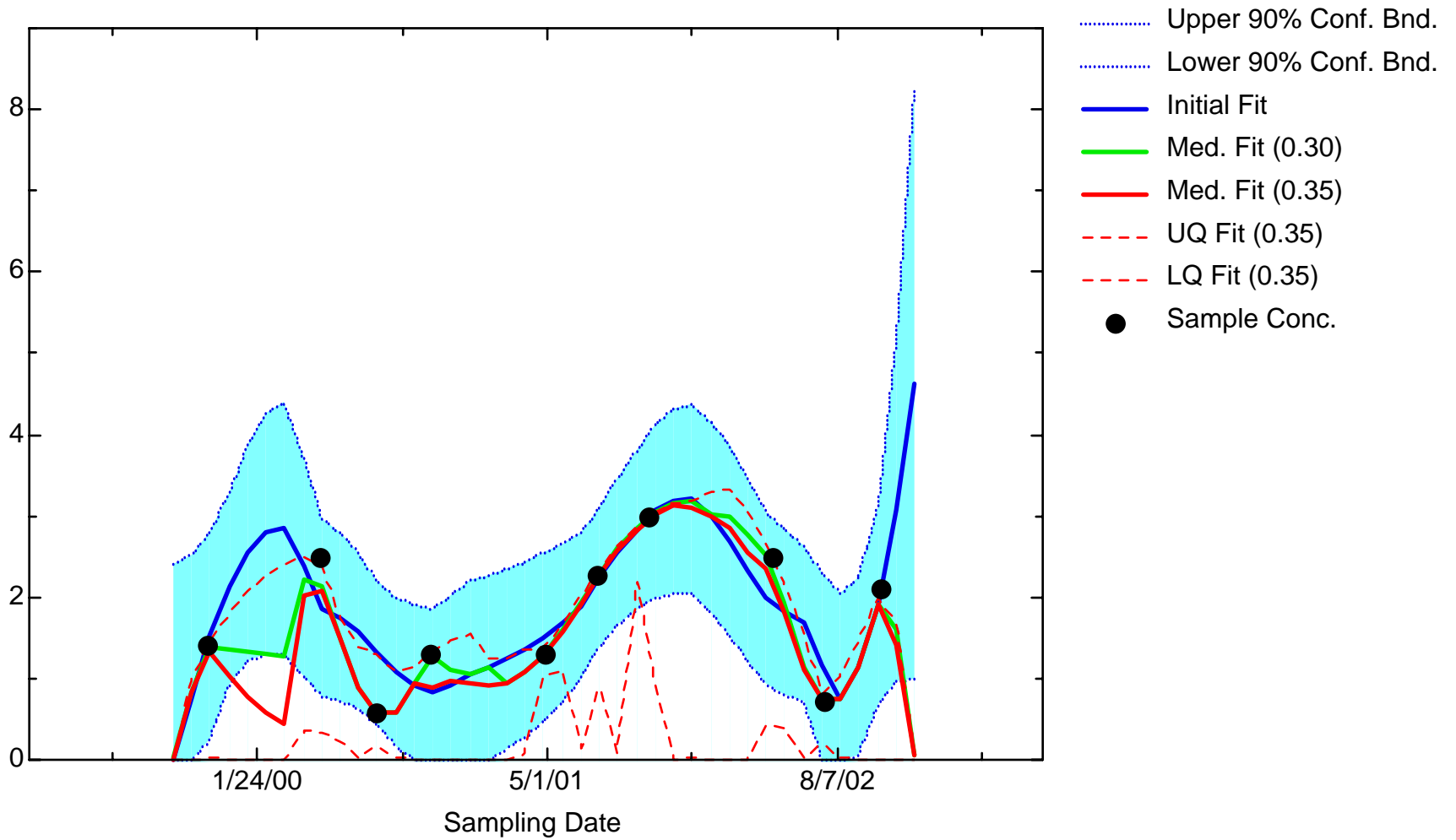
MN: Well JPZ1780



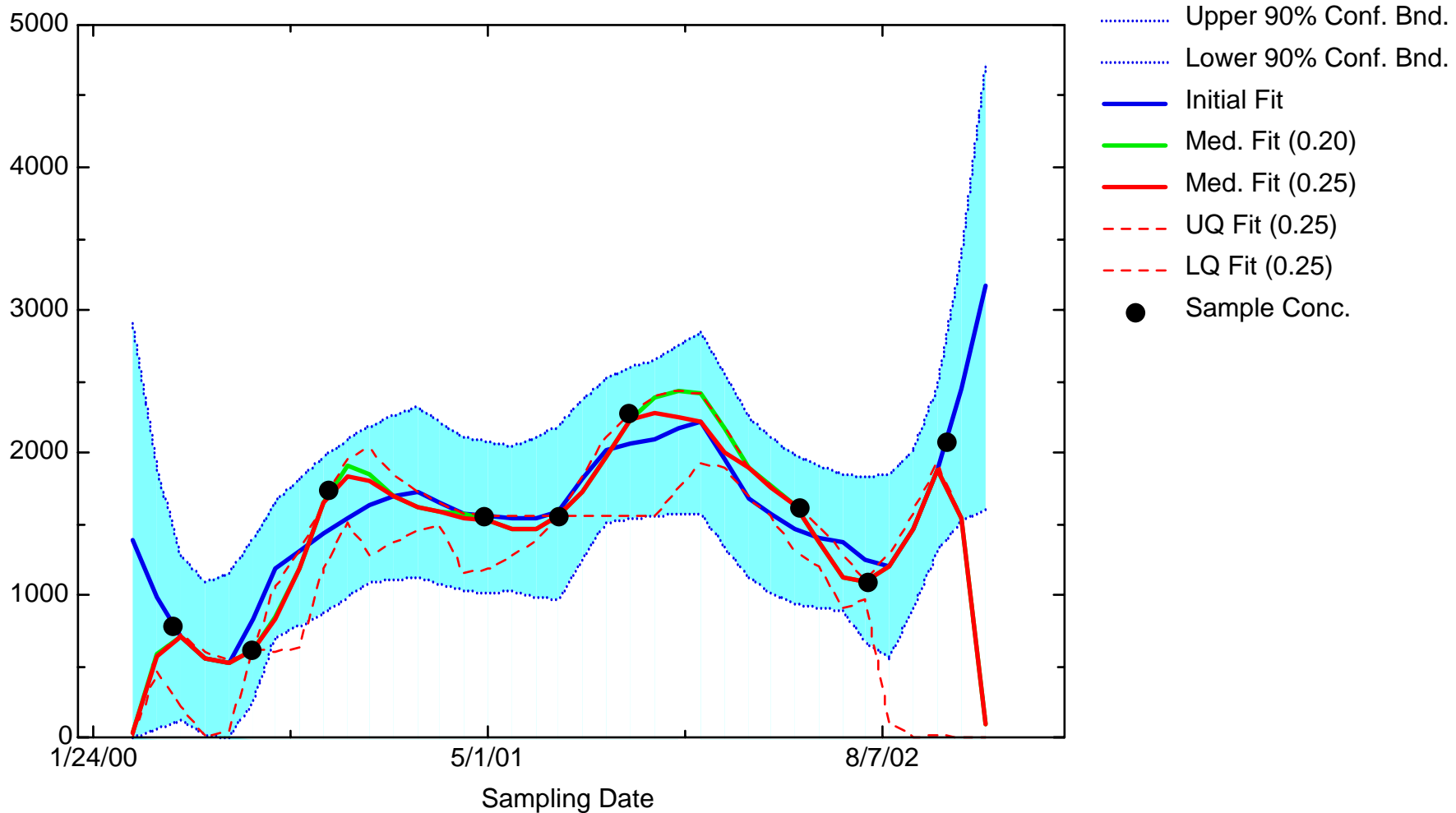
MN: Well JPZ7208



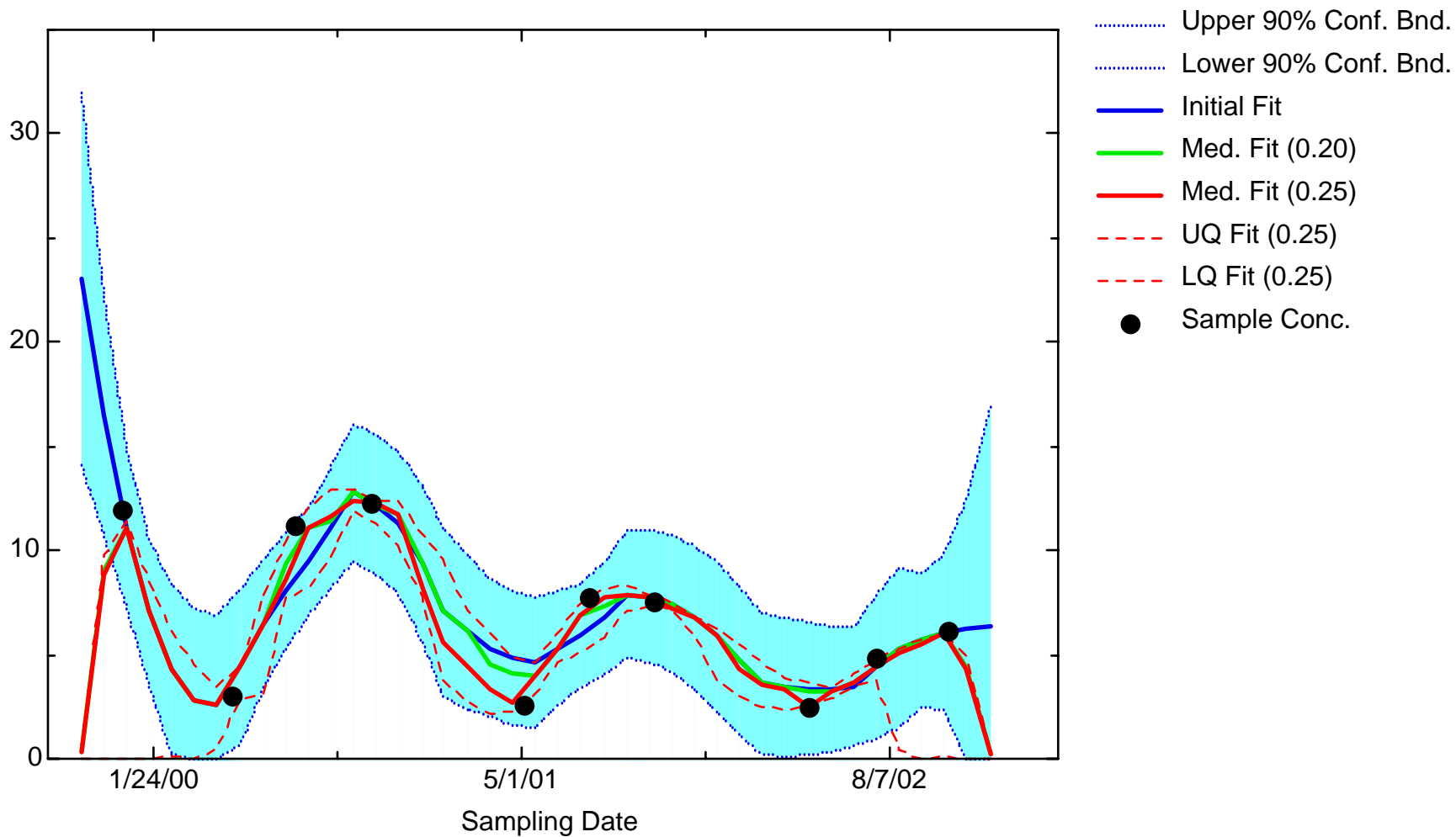
MN: Well JPZ7807



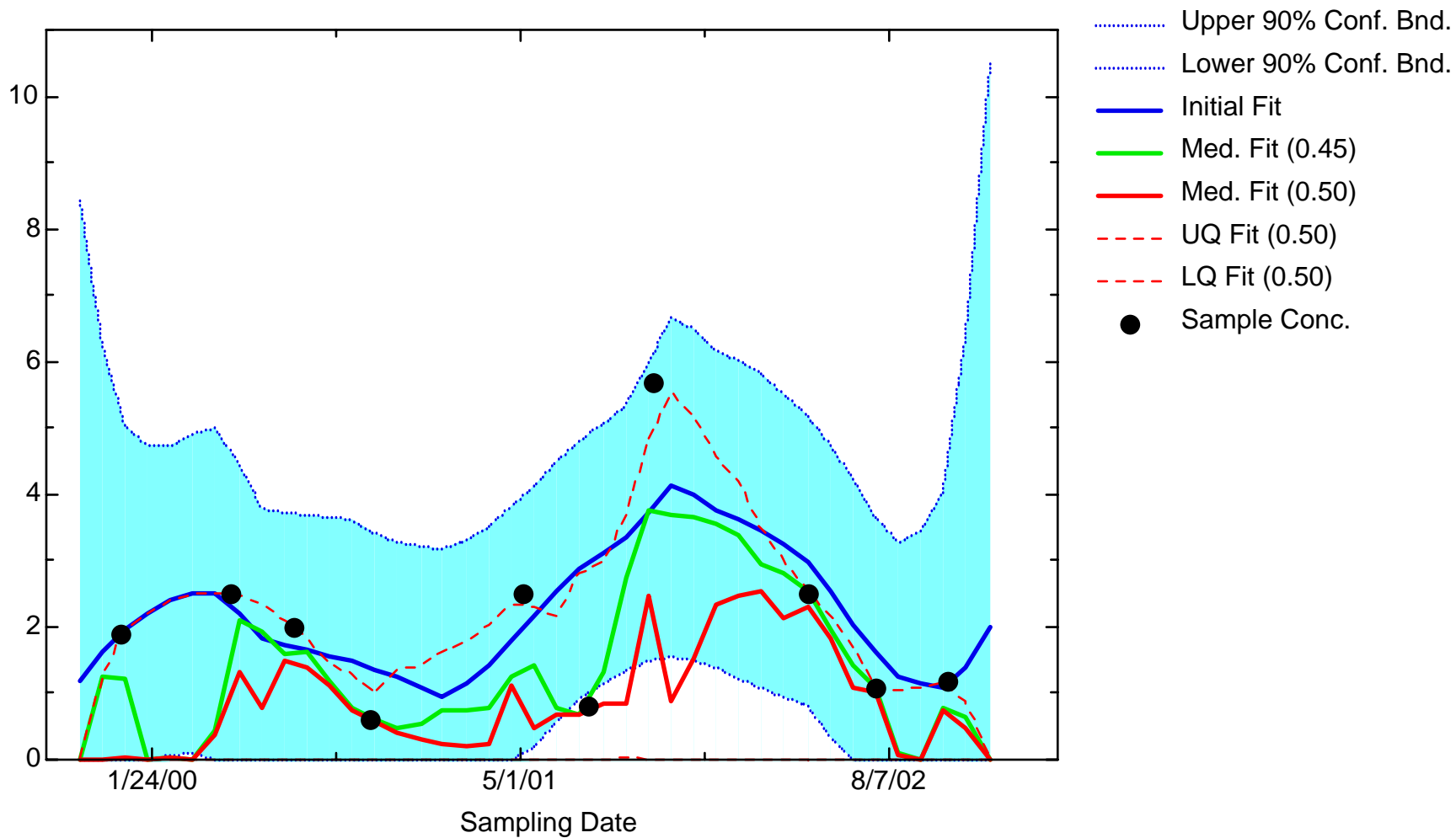
MN: Well MMW0005



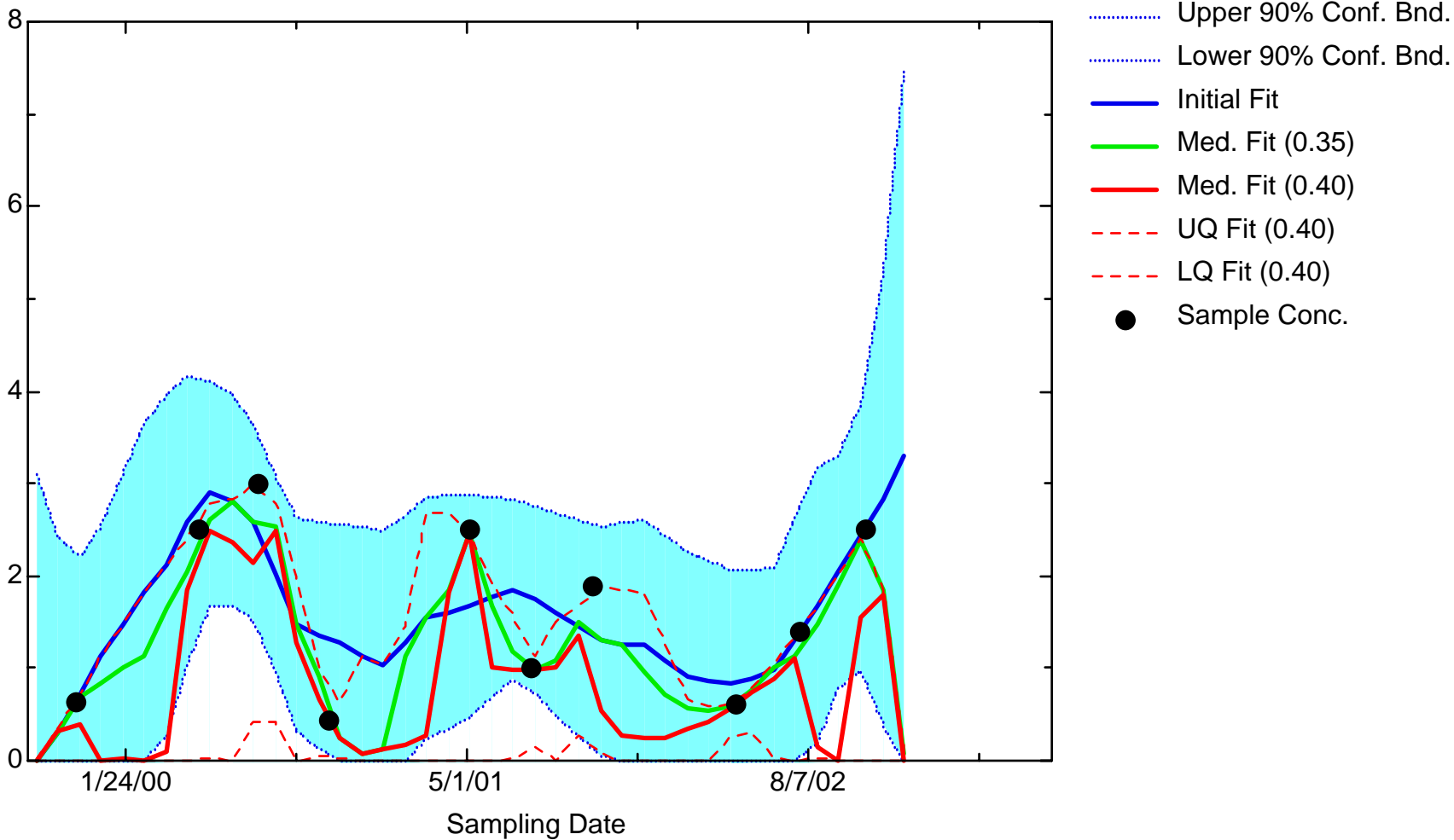
MN: Well MMW0007A



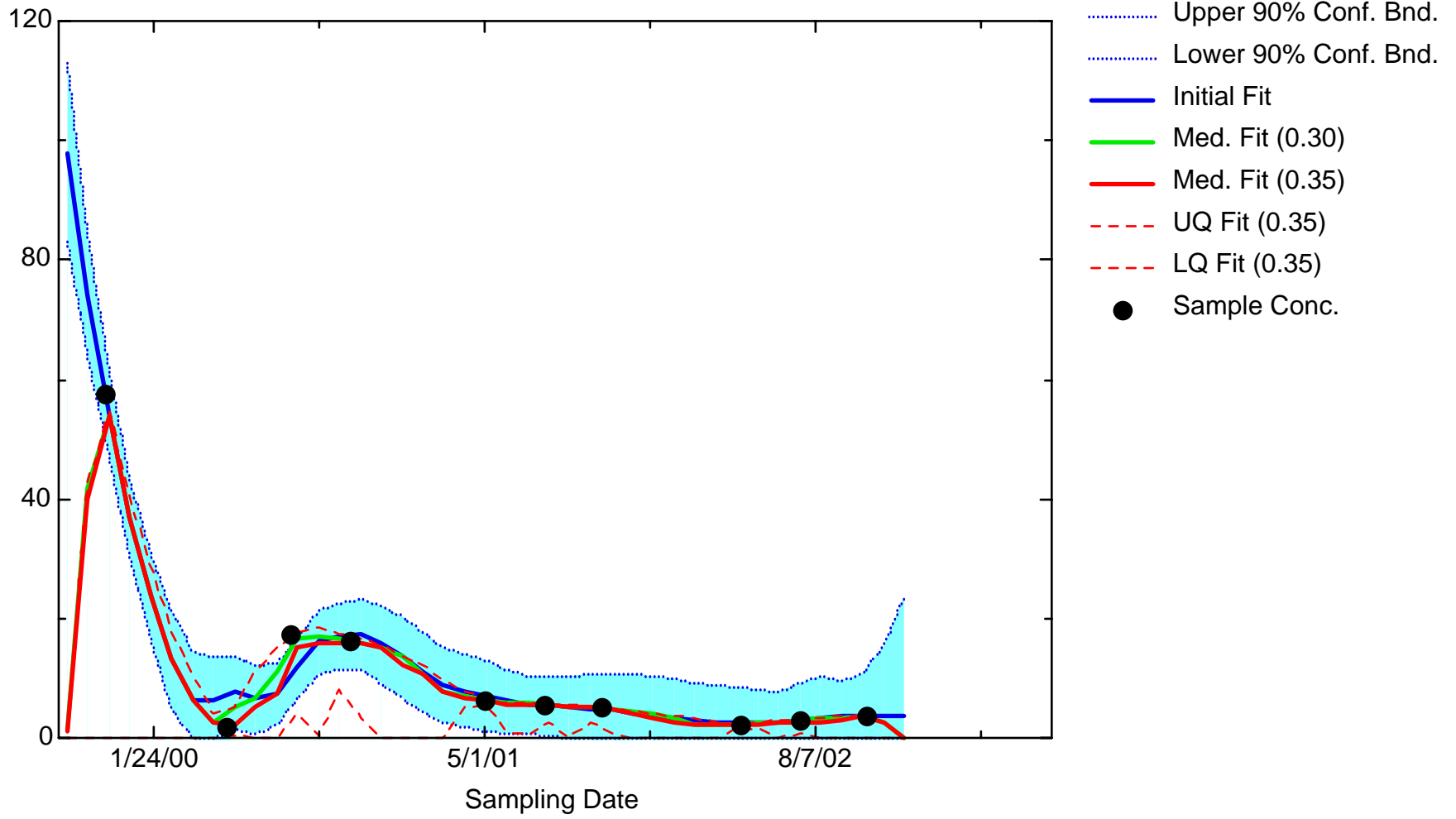
MN: Well MMW0007B



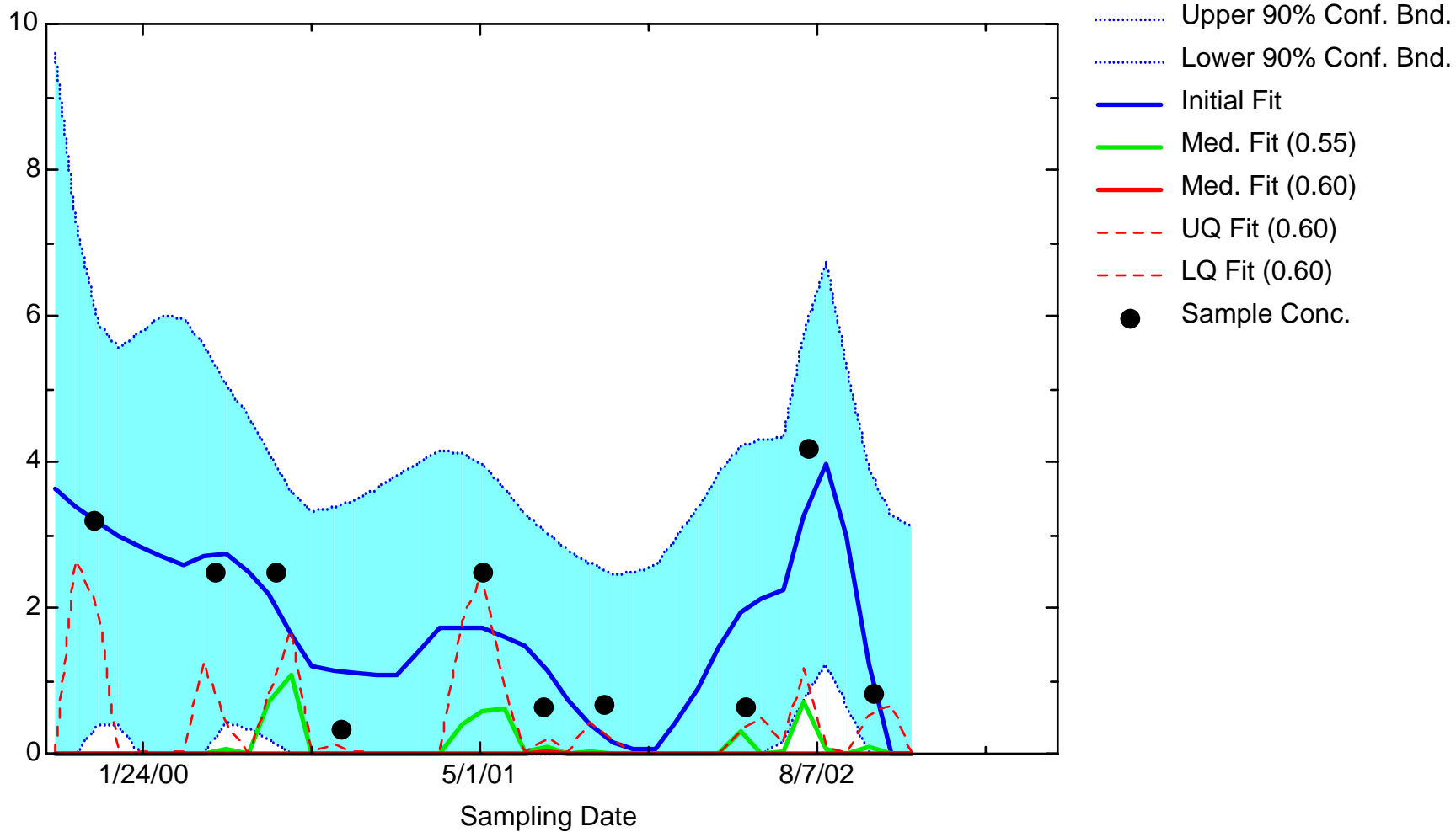
MN: Well MMW0008



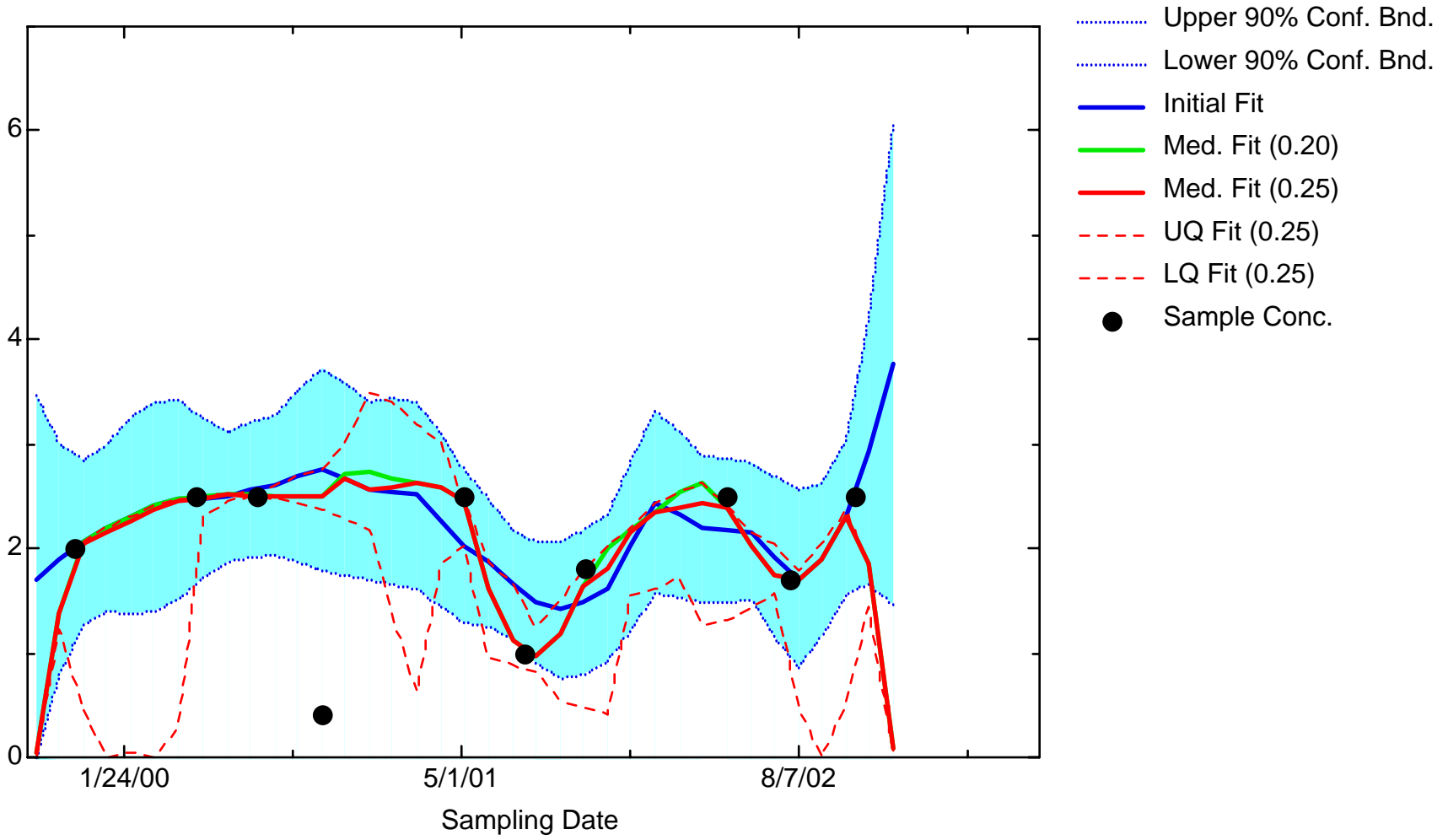
MN: Well MMW0009



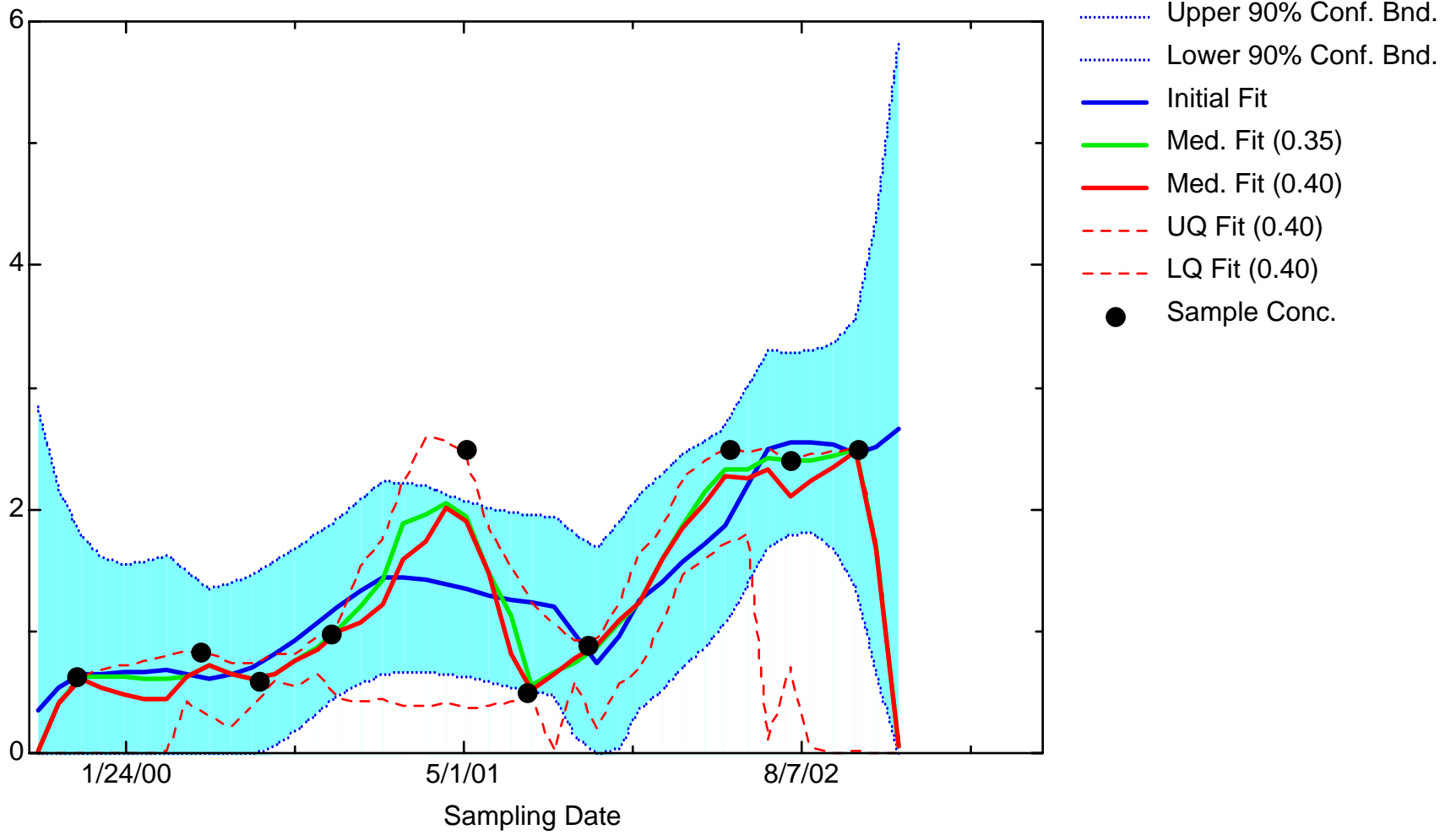
MN: Well MMW0010



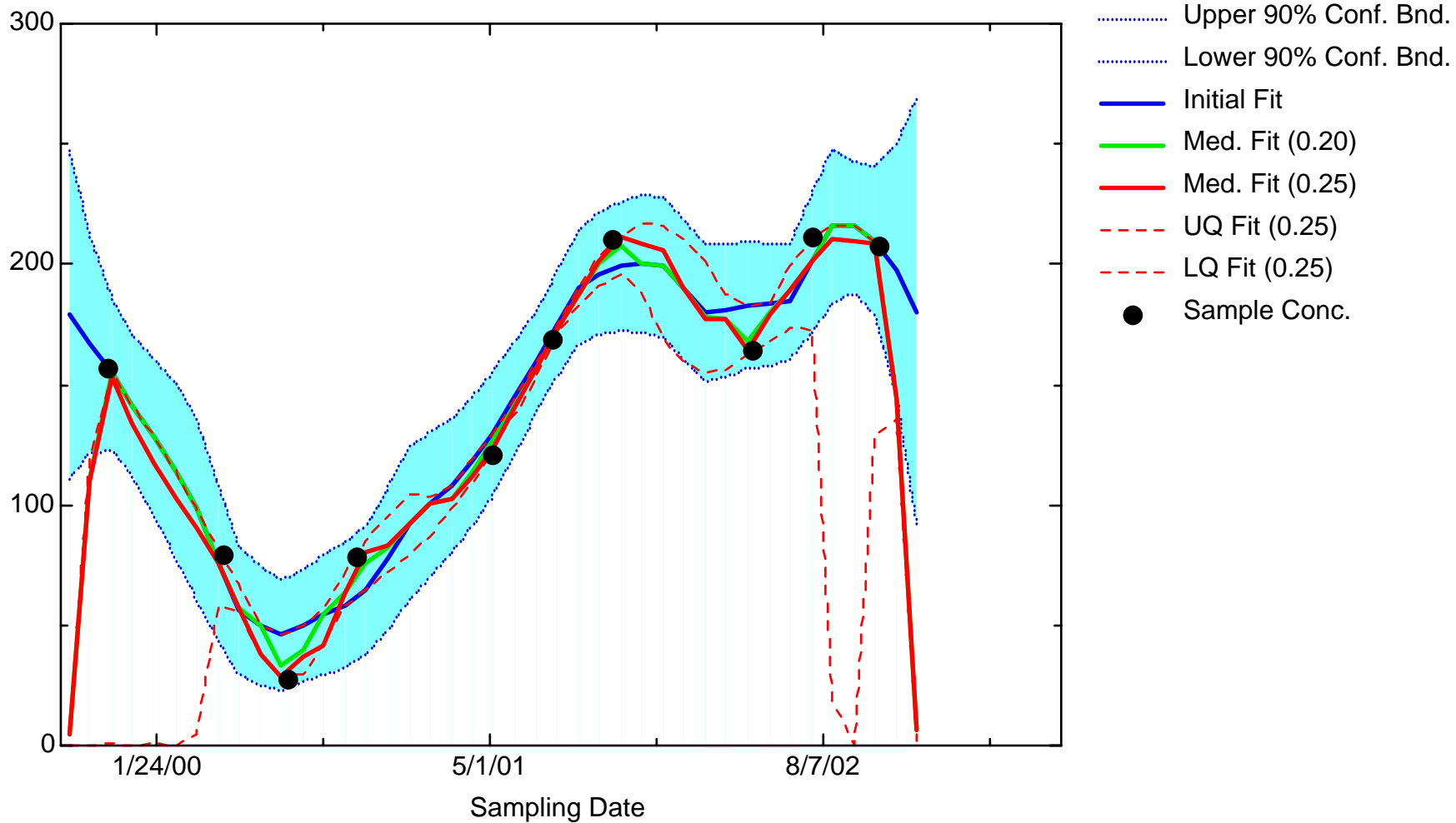
MN: Well MMW0011



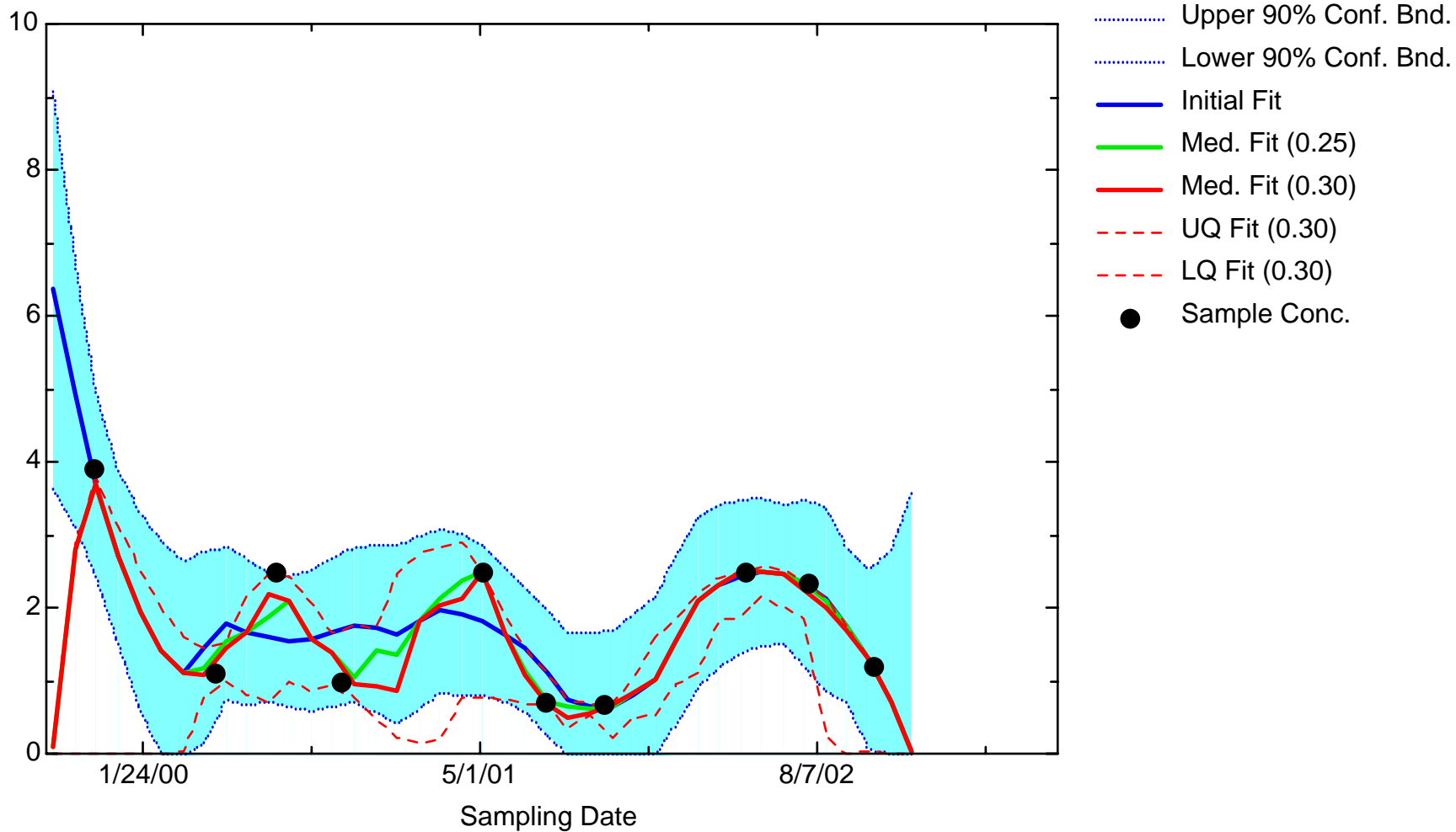
MN: Well MMW0012



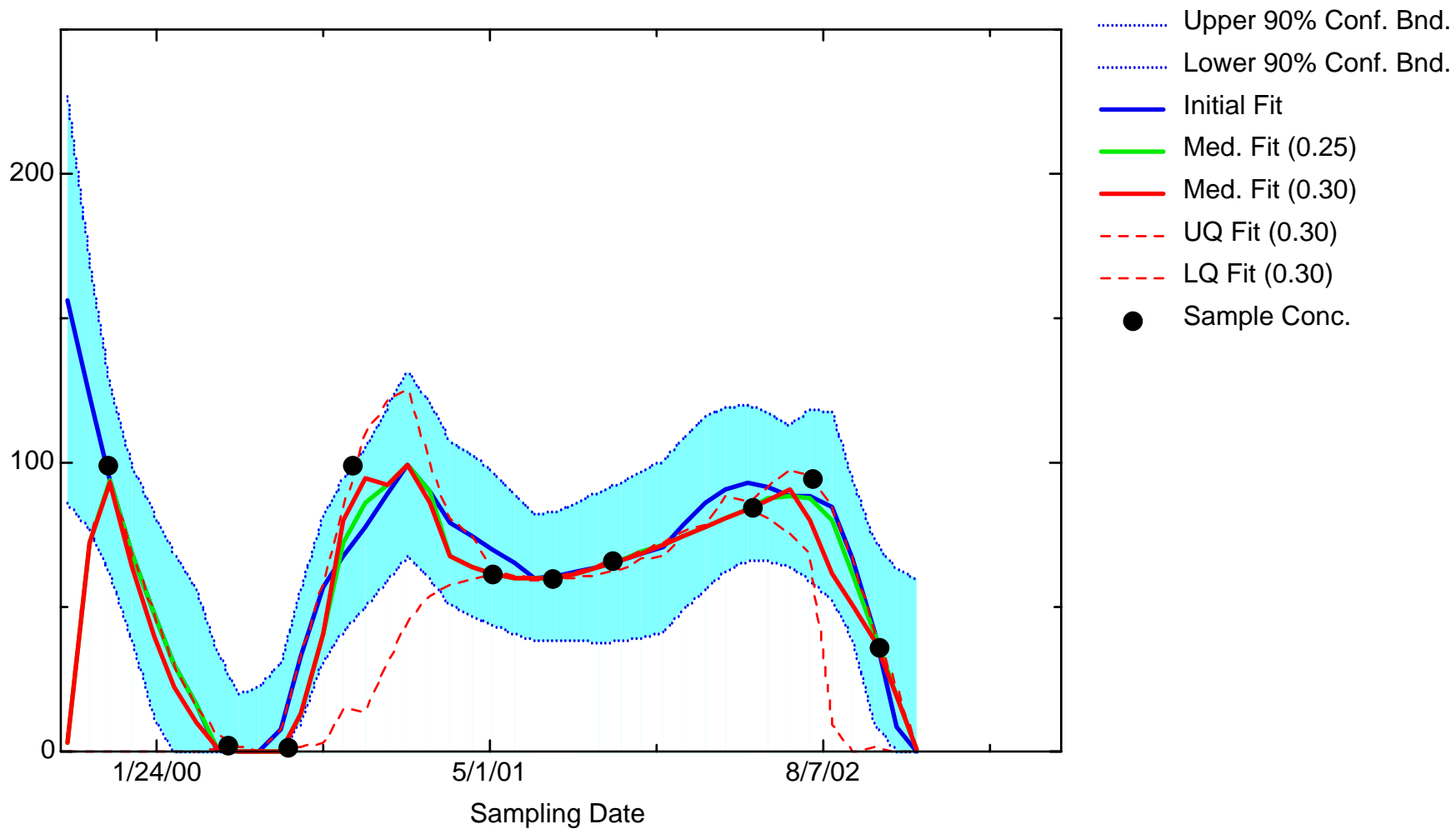
MN: Well MMW0013



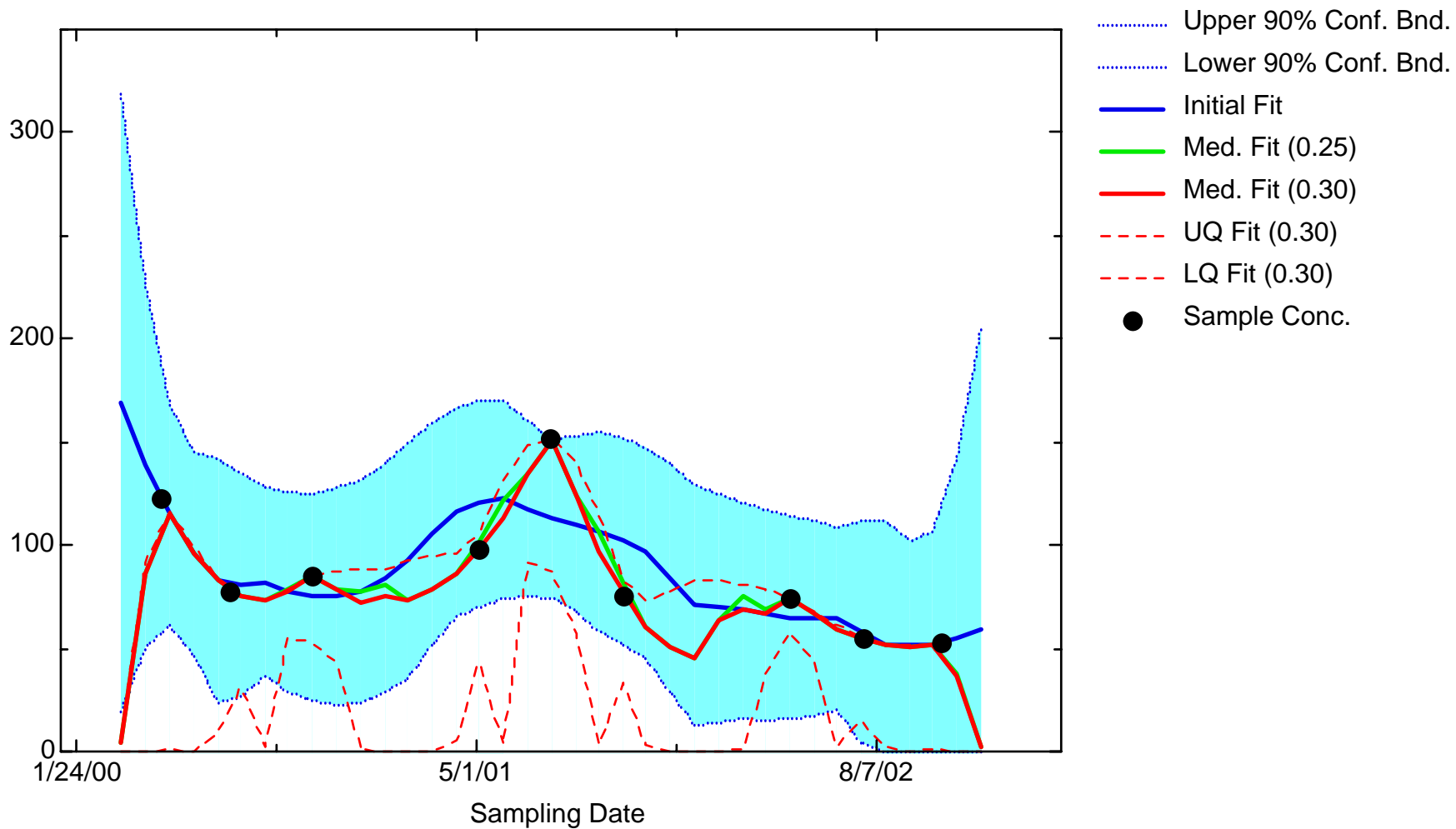
MN: Well MMW0016



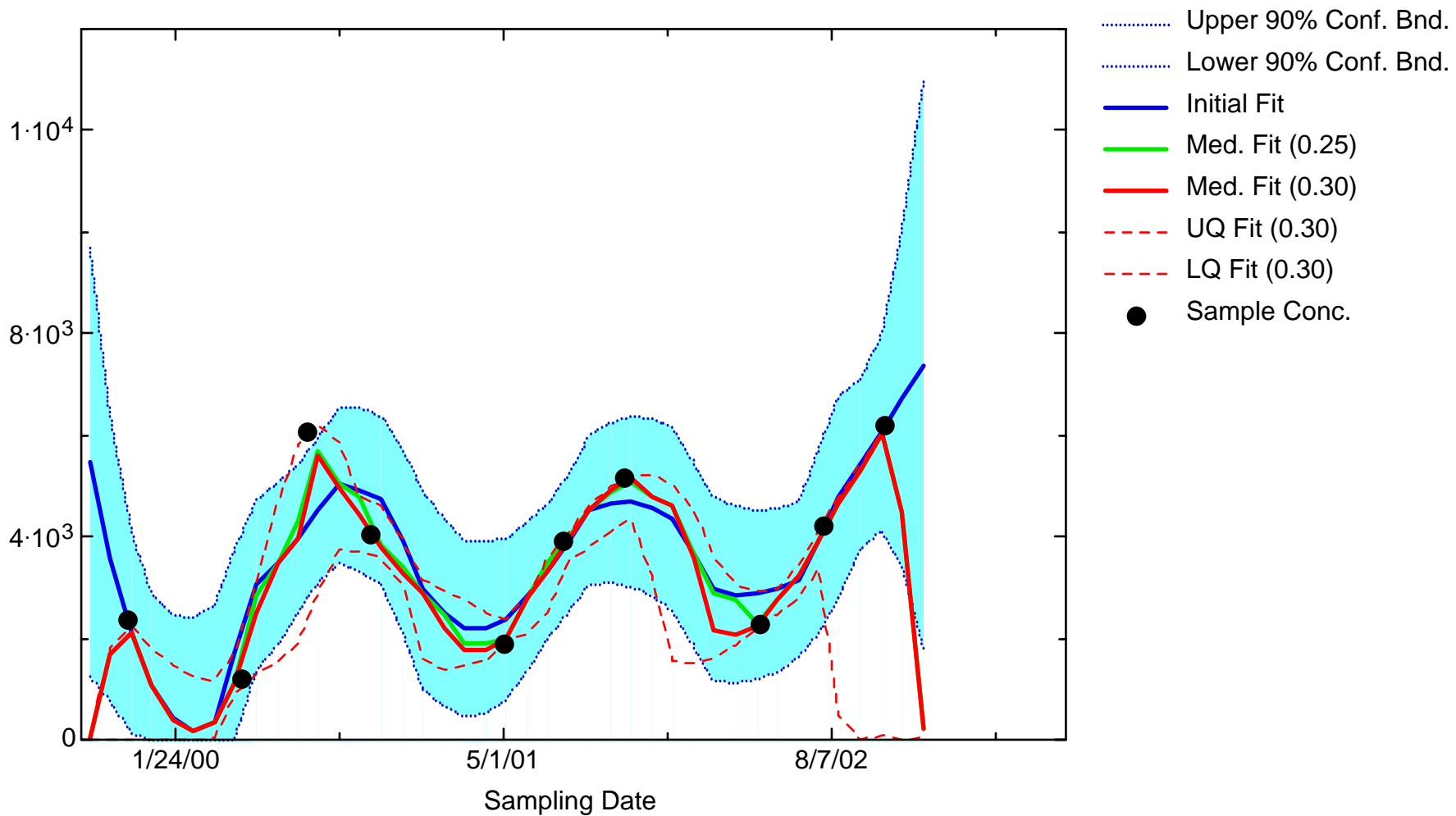
MN: Well MMW0017



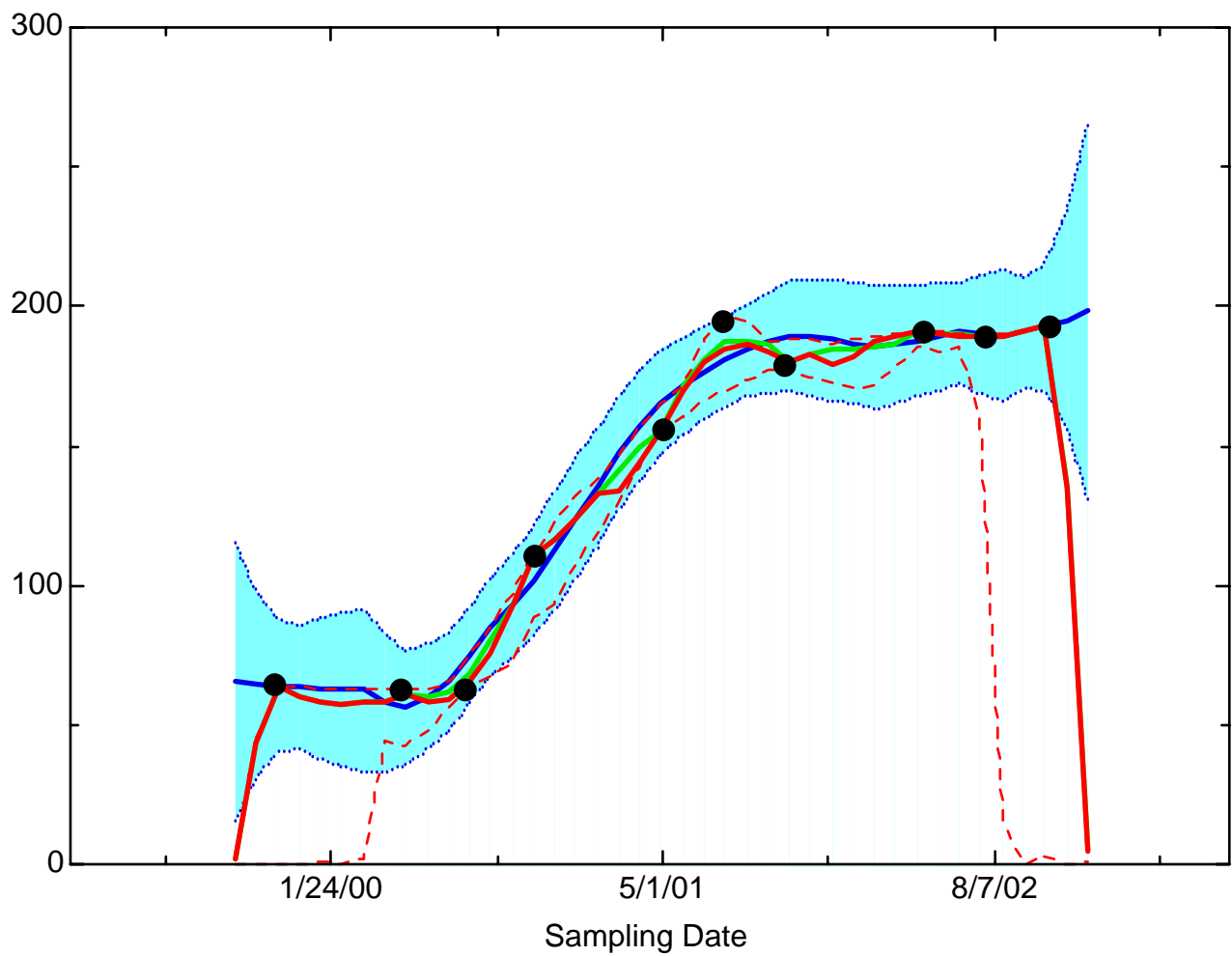
MN: Well MMW0019



MN: Well MMW1560

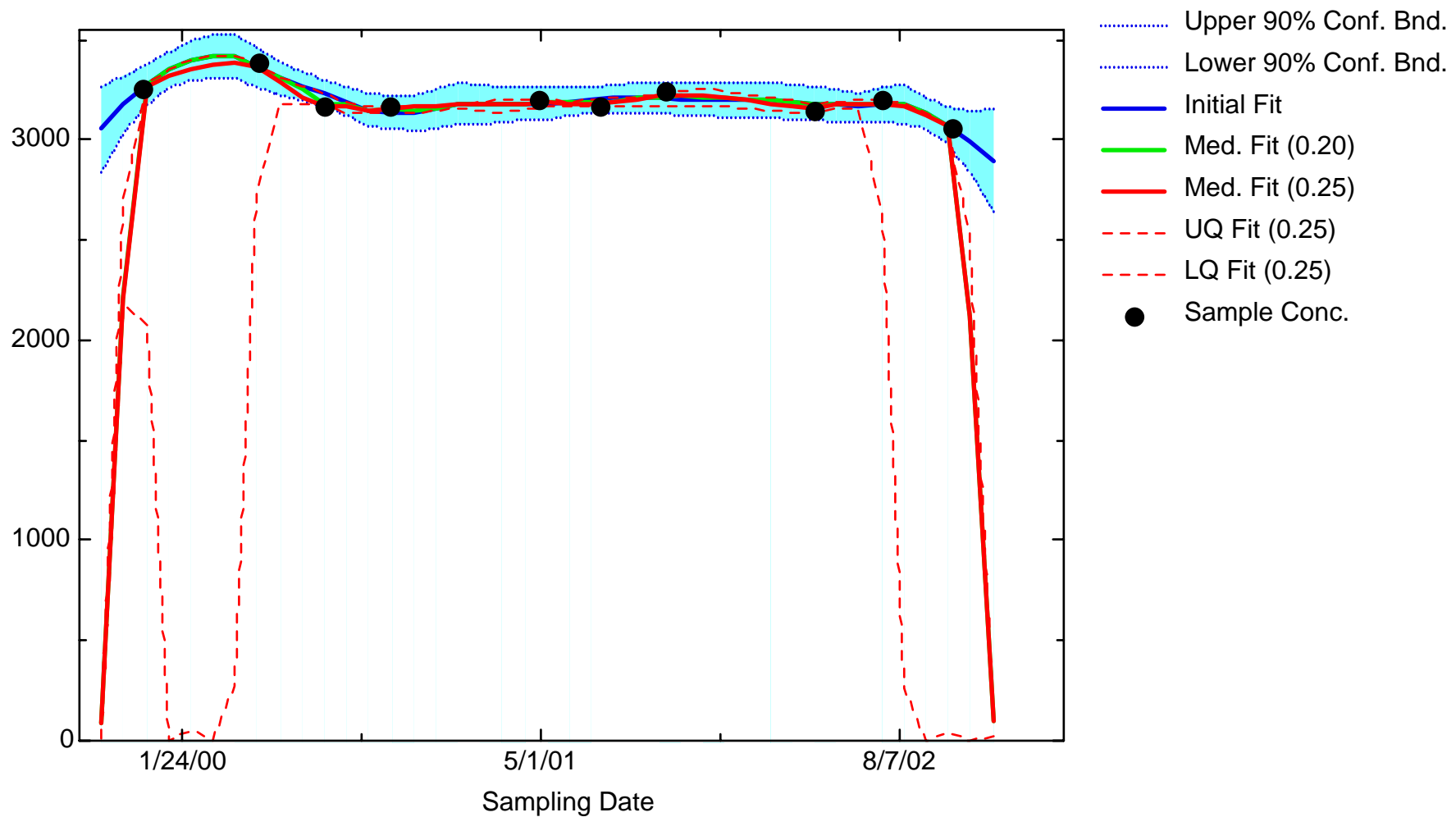


MN: Well MMW7330

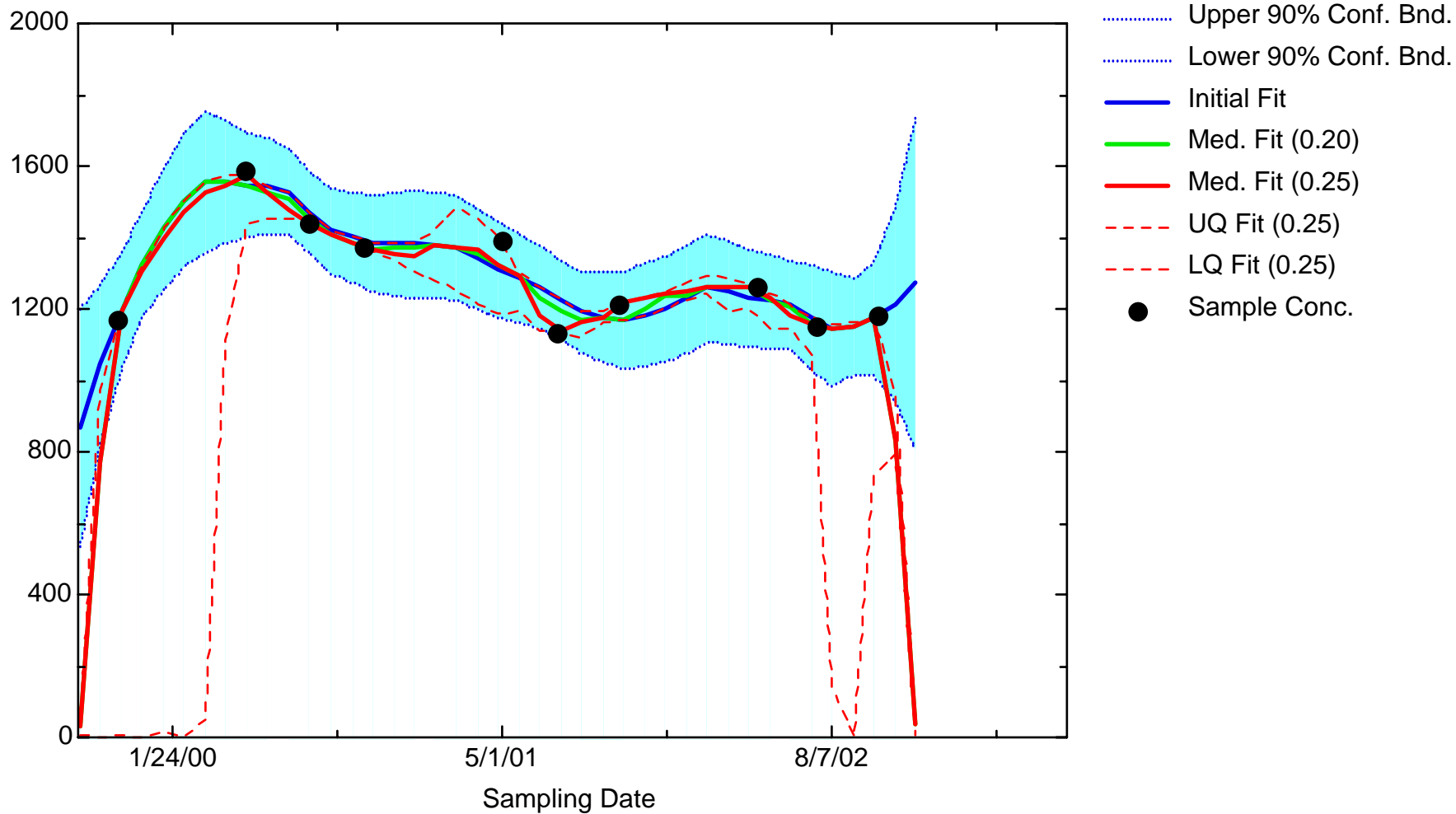


- Upper 90% Conf. Bnd.
- Lower 90% Conf. Bnd.
- Initial Fit
- Med. Fit (0.25)
- Med. Fit (0.30)
- UQ Fit (0.30)
- LQ Fit (0.30)
- Sample Conc.

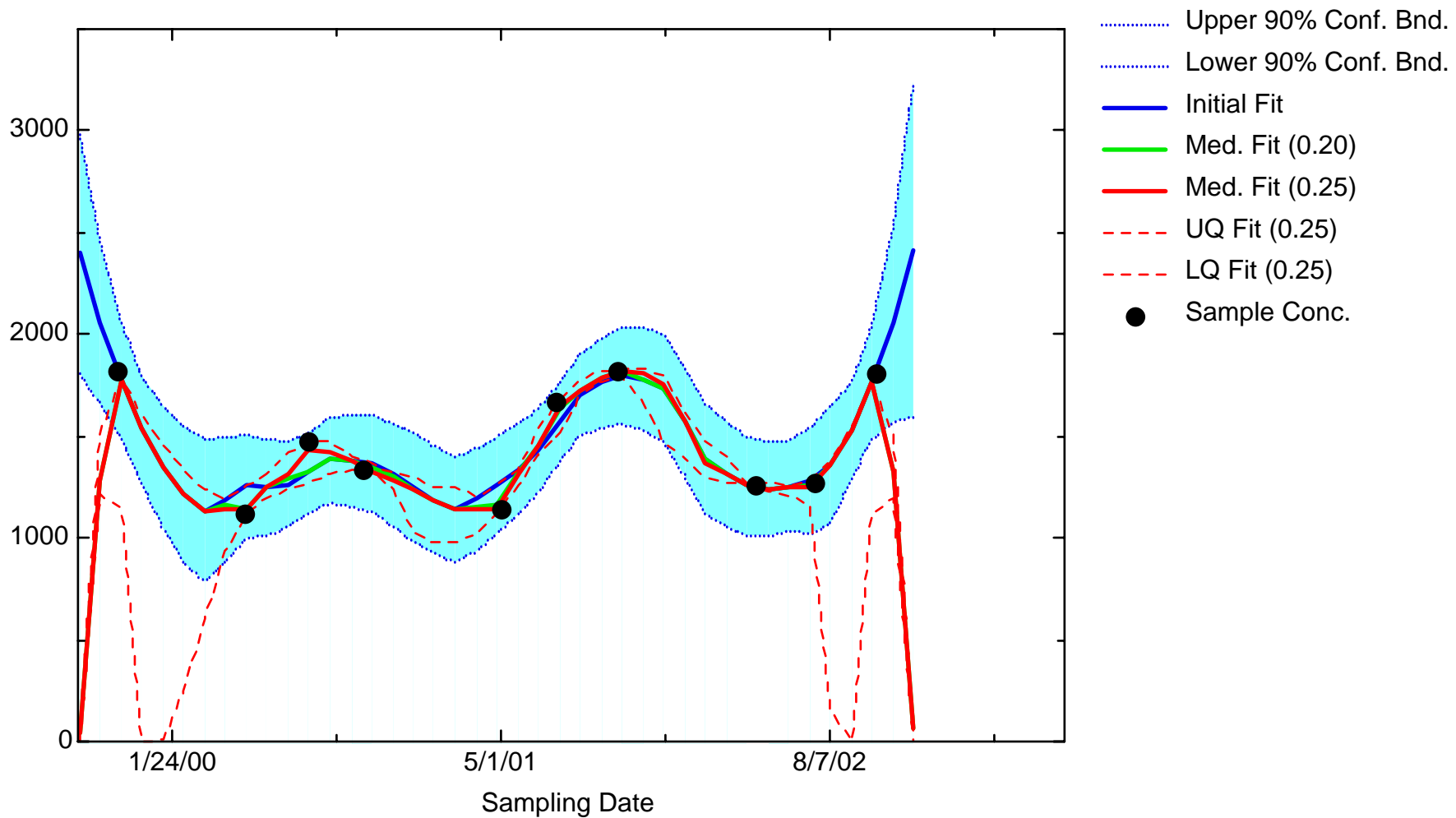
MN: Well MMW8015



MN: Well RFW1144



MN: Well RFW1147



Appendix 3-3

Temporal Optimization: BZ Iterative Fitting Results

Key to acronyms:

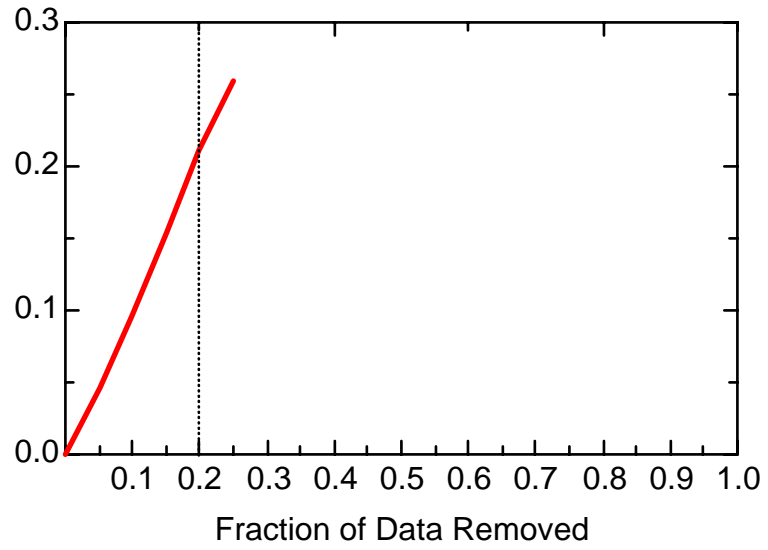
Fraction Outside Conf Bnds = Fraction of pointwise locally-weighted quadratic regression (LWQR) estimates from reduced data located beyond confidence bounds around LWQR fit on baseline data

Ave IQR of Iterative Fits = Mean interquartile range (averaged pointwise along the trend) of 500 LWQR fits computed on reduced dataset

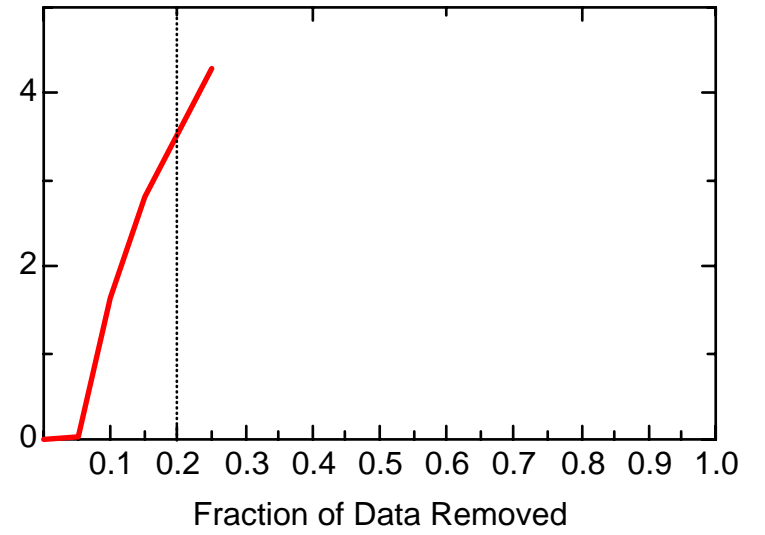
Opt Sampling Int = Optimal sampling interval, given fraction of data removed

Opt Num Samples/Week = Optimal weekly sampling frequency, given fraction of data removed

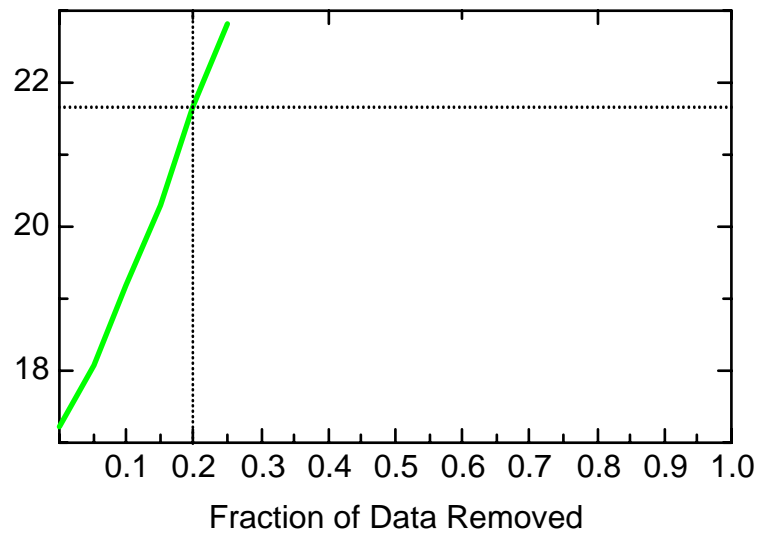
BZ: Well 056MW04



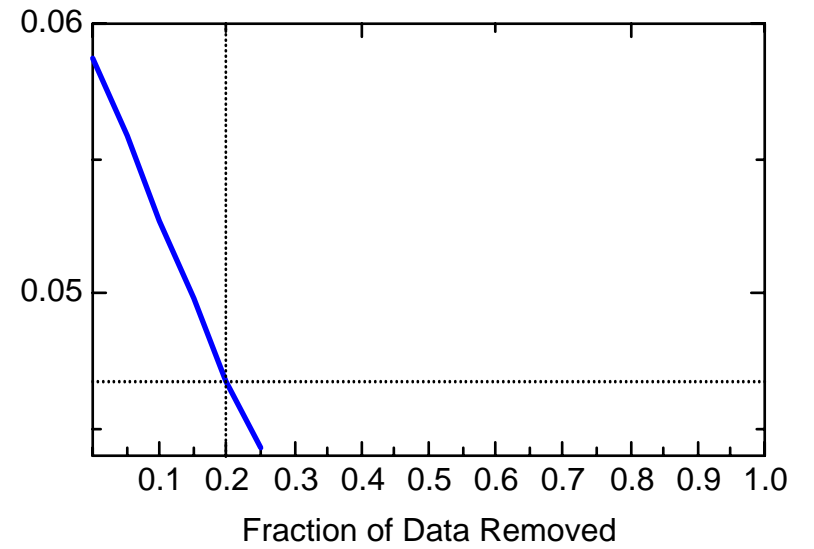
BZ: Well 056MW04



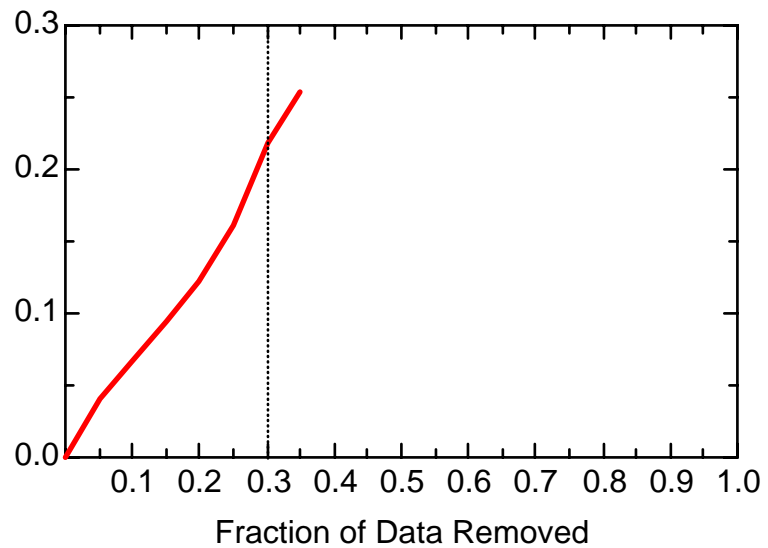
BZ: Well 056MW04



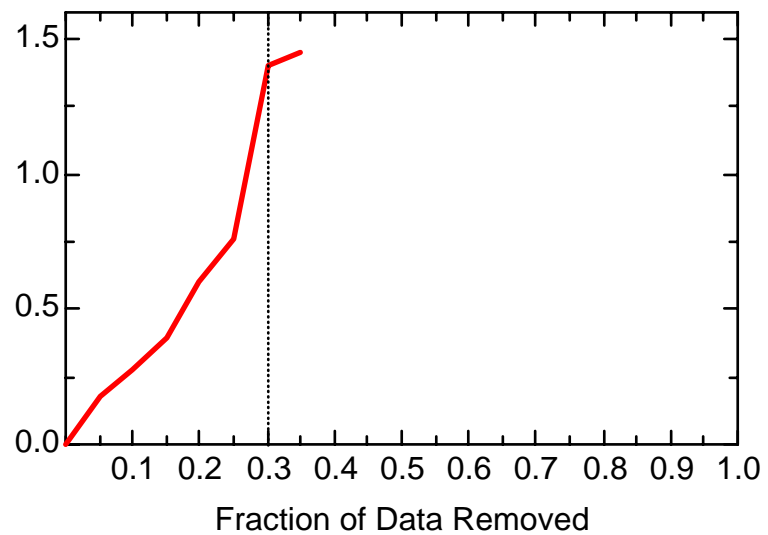
BZ: Well 056MW04



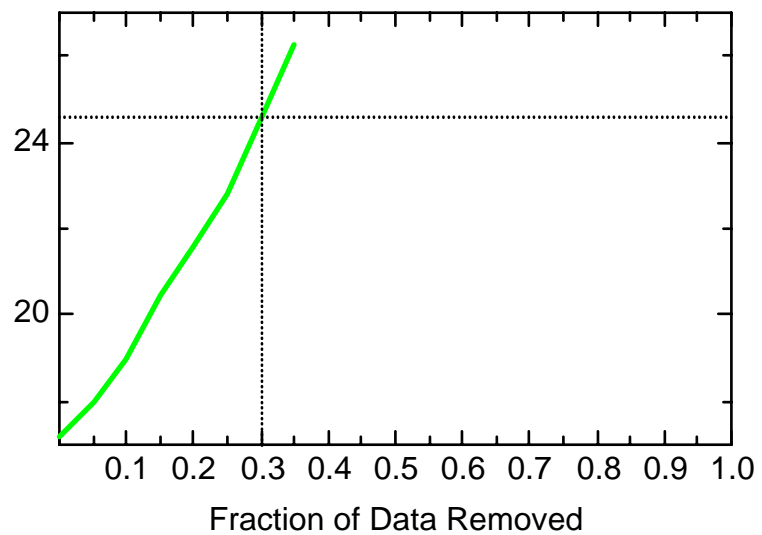
BZ: Well JBW7212B



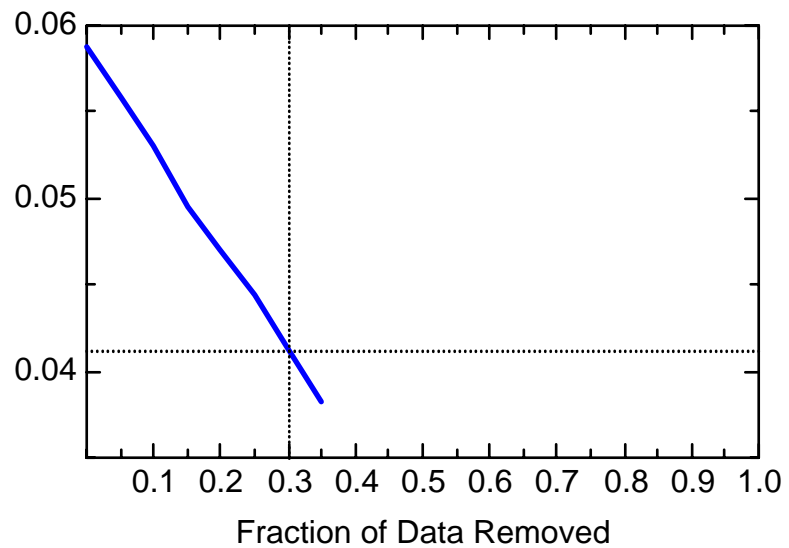
BZ: Well JBW7212B



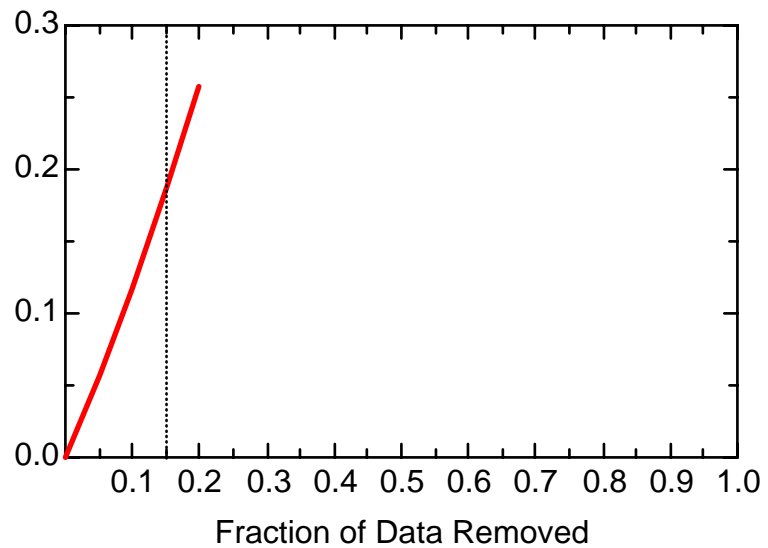
BZ: Well JBW7212B



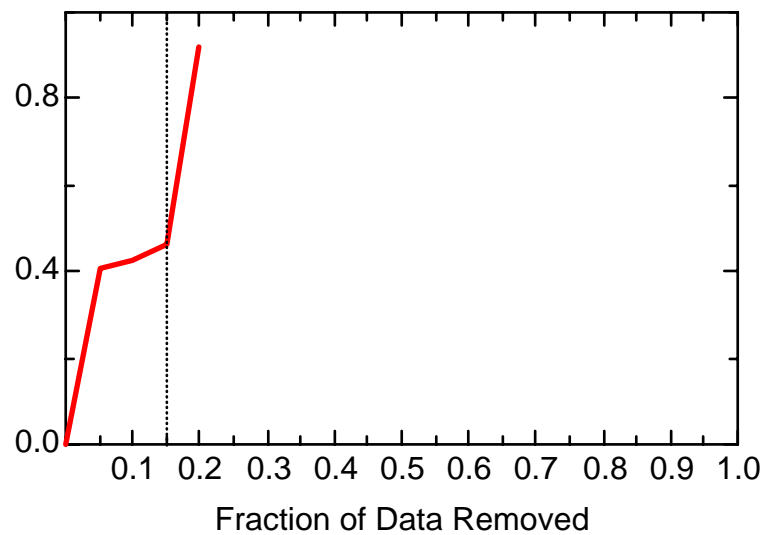
BZ: Well JBW7212B



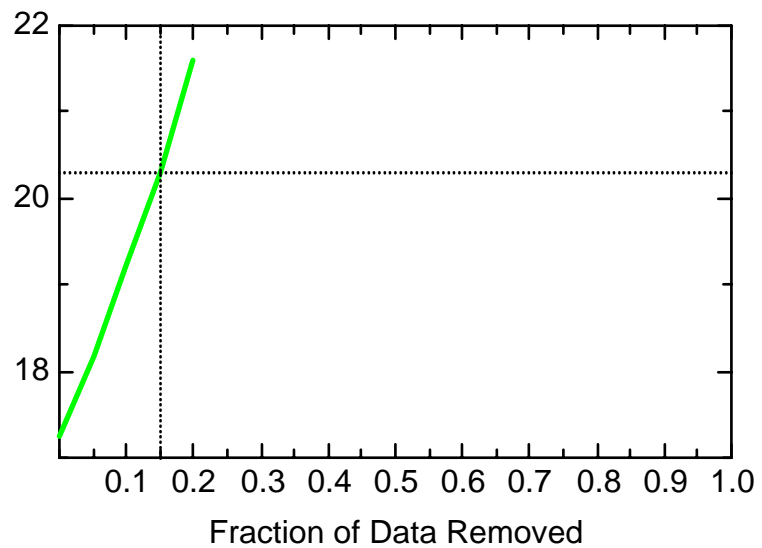
BZ: Well JBW7213A



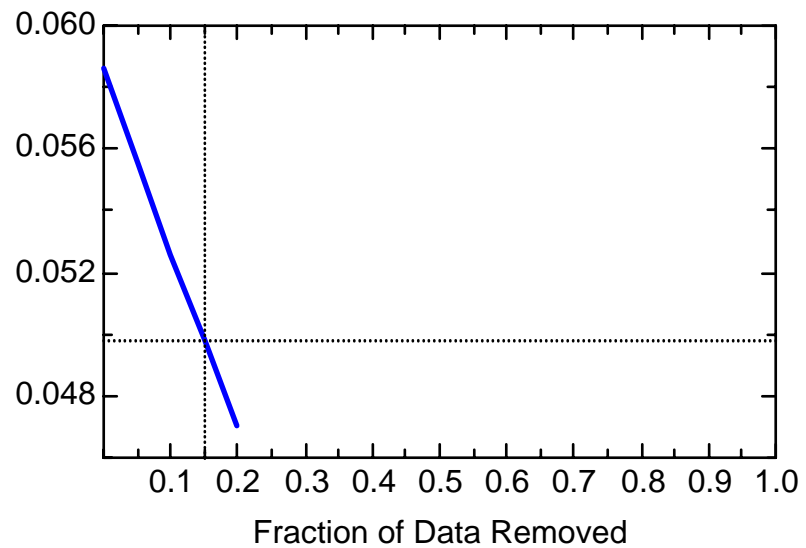
BZ: Well JBW7213A



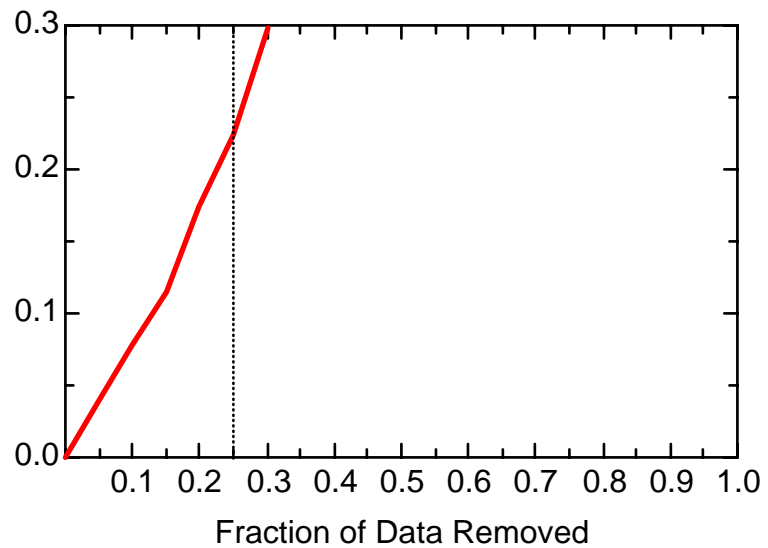
BZ: Well JBW7213A



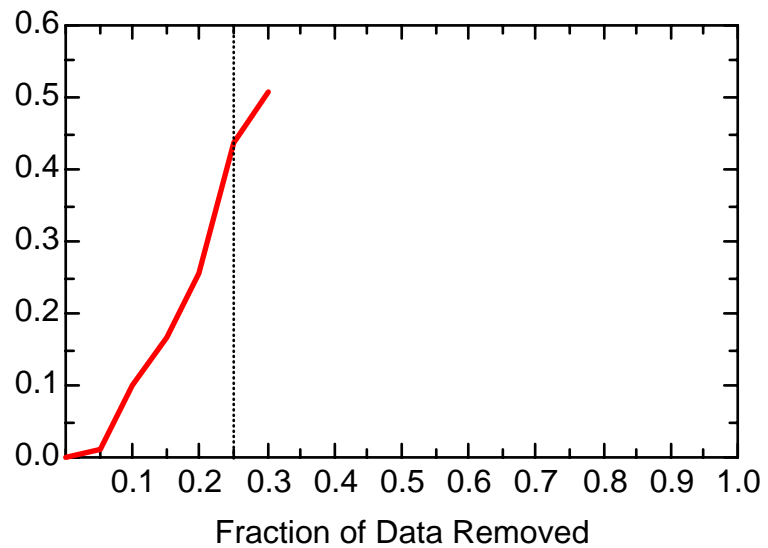
BZ: Well JBW7213A



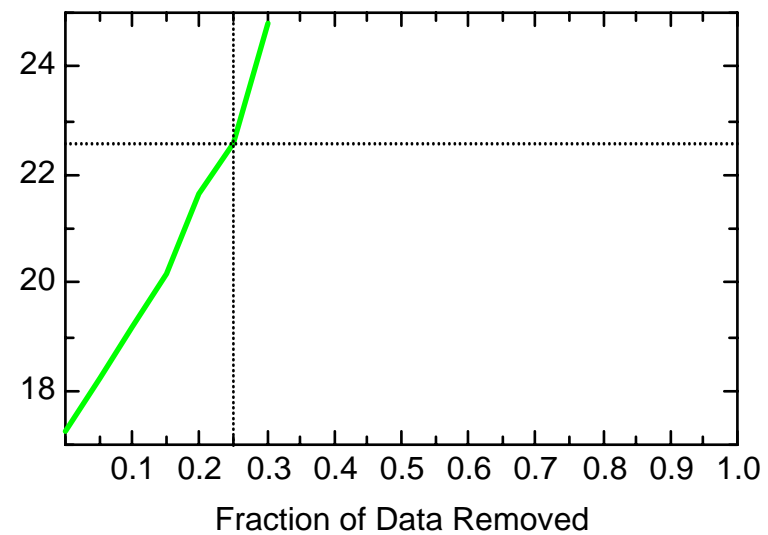
BZ: Well JBW7213B



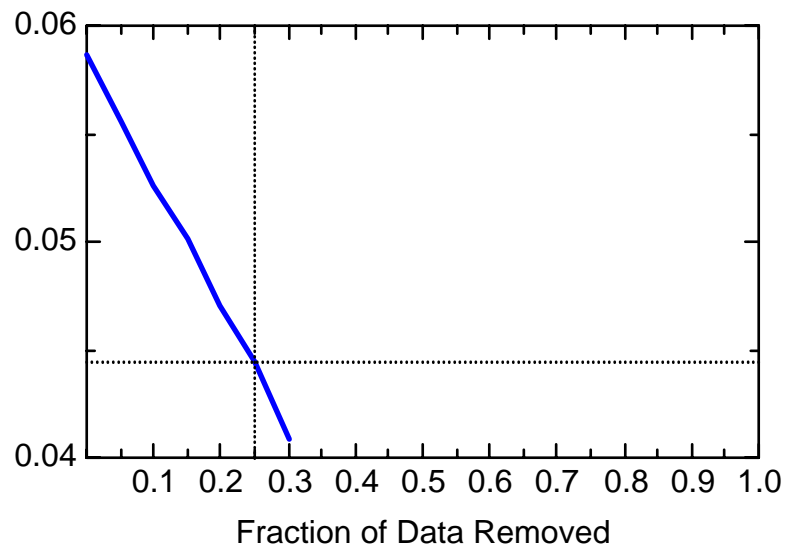
BZ: Well JBW7213B



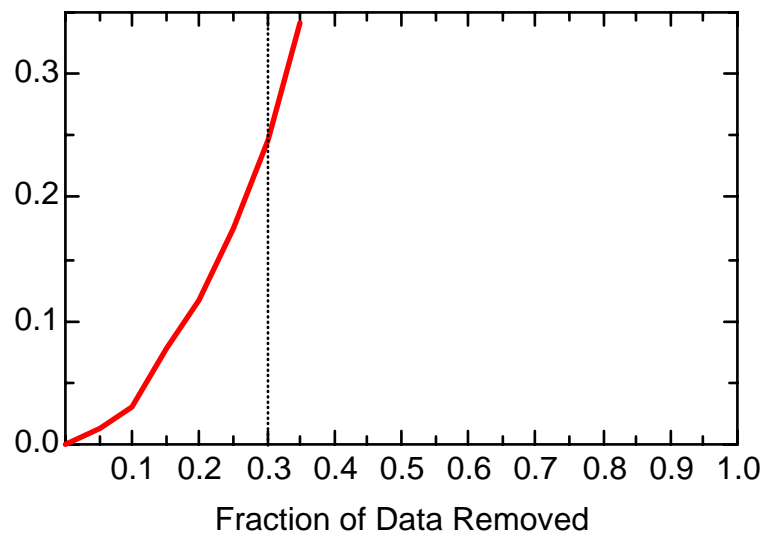
BZ: Well JBW7213B



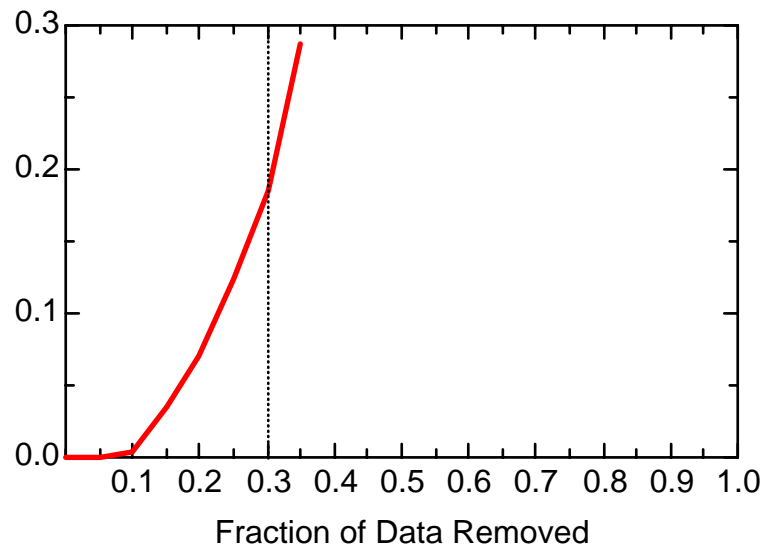
BZ: Well JBW7213B



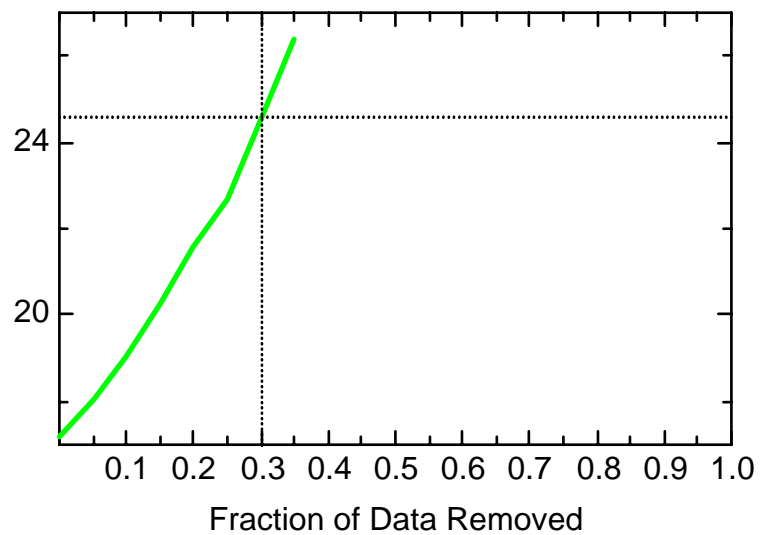
BZ: Well JBW7330A



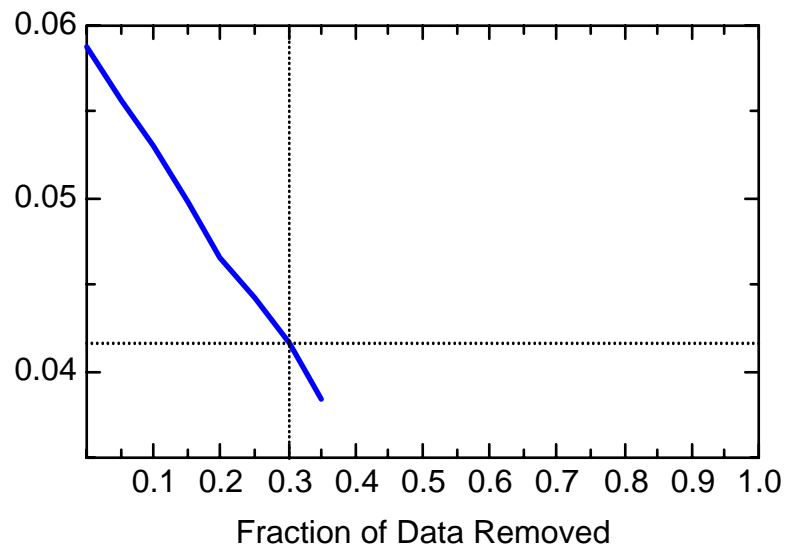
BZ: Well JBW7330A



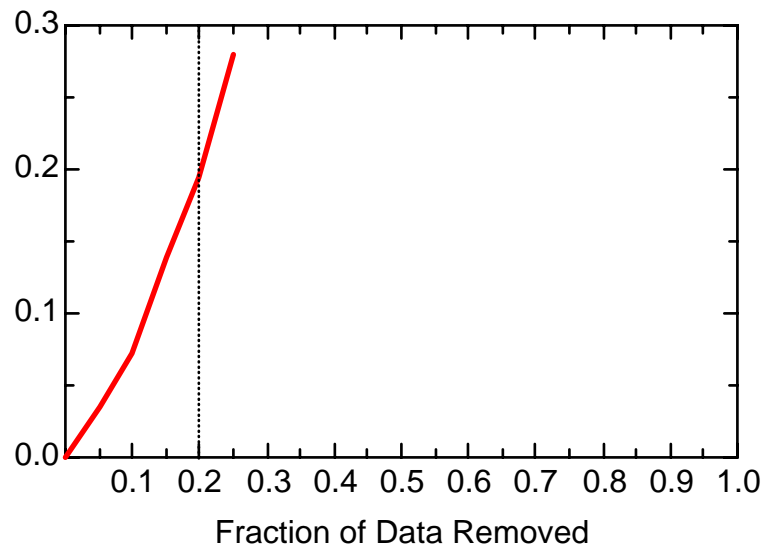
BZ: Well JBW7330A



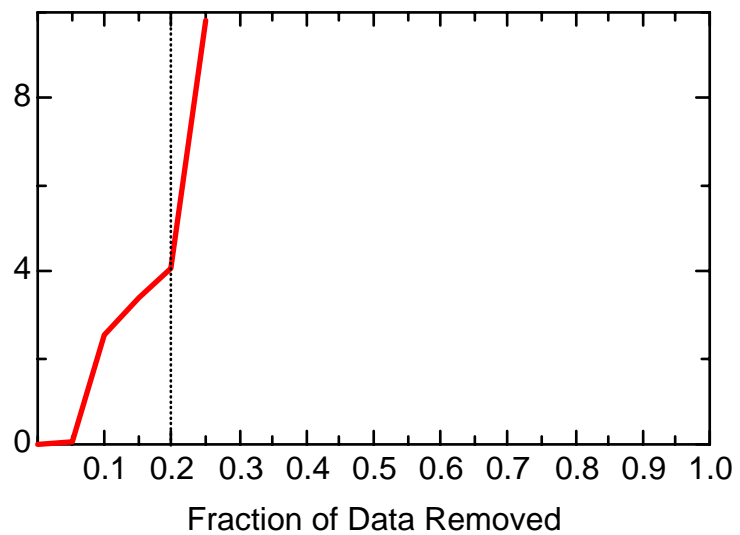
BZ: Well JBW7330A



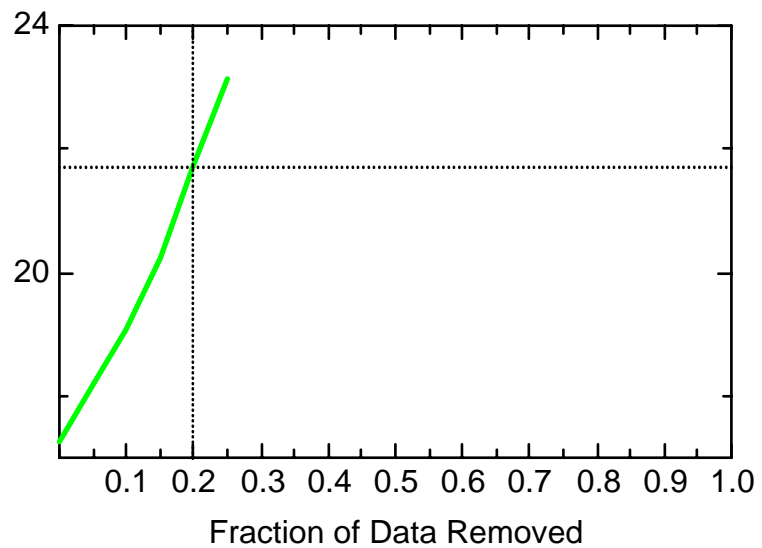
BZ: Well JBW7333



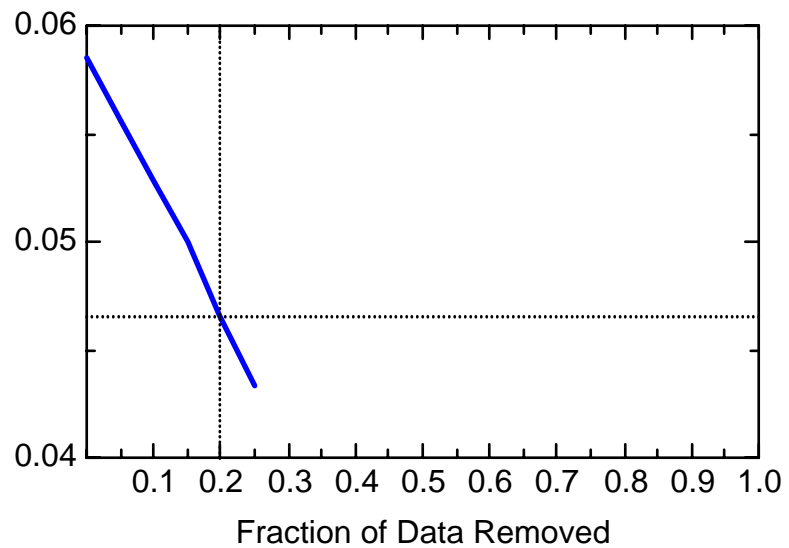
BZ: Well JBW7333



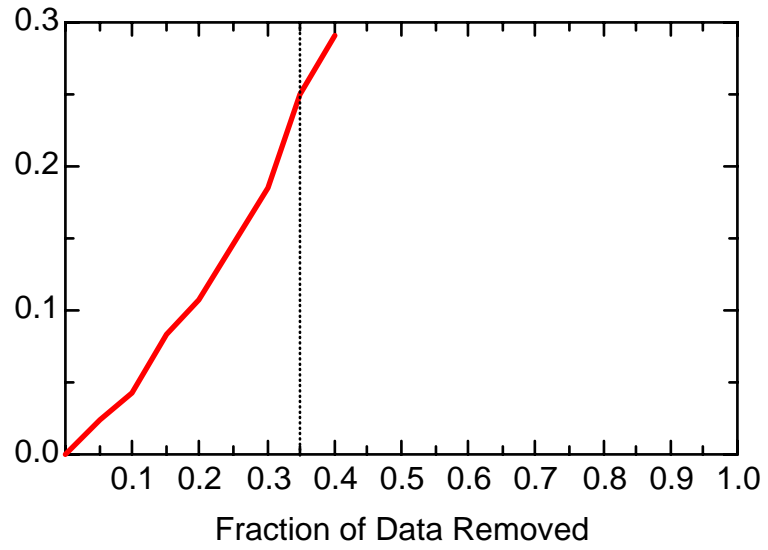
BZ: Well JBW7333



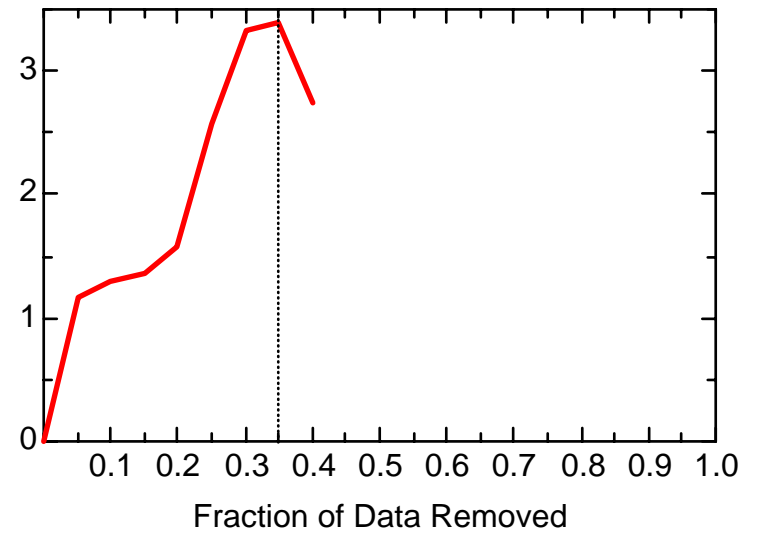
BZ: Well JBW7333



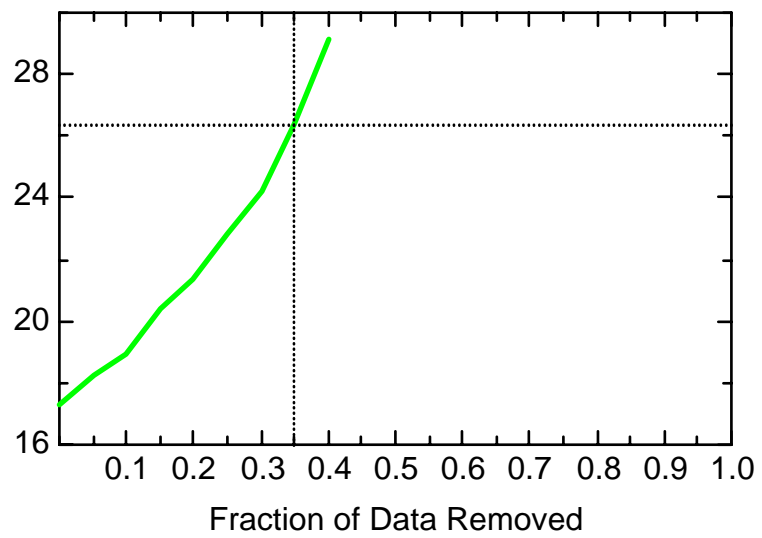
BZ: Well JBW7338A



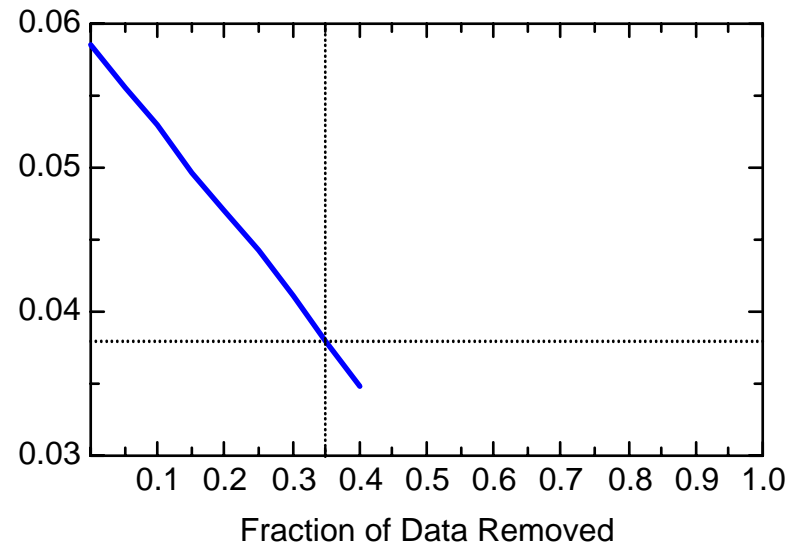
BZ: Well JBW7338A



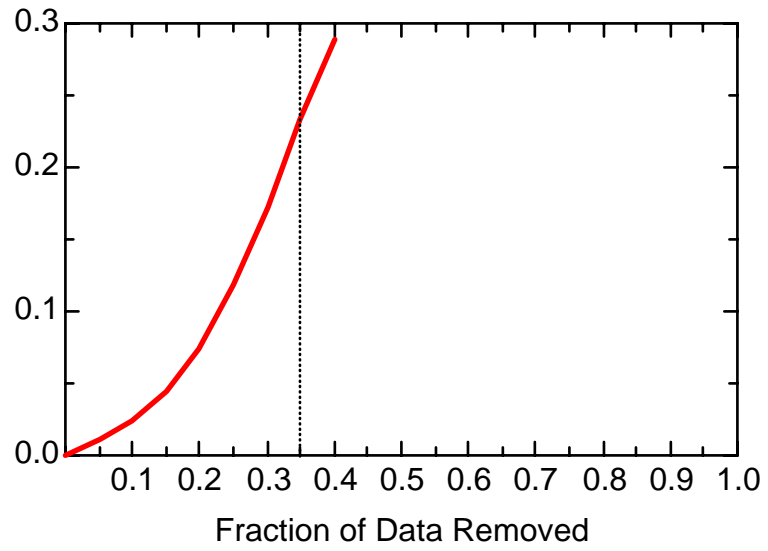
BZ: Well JBW7338A



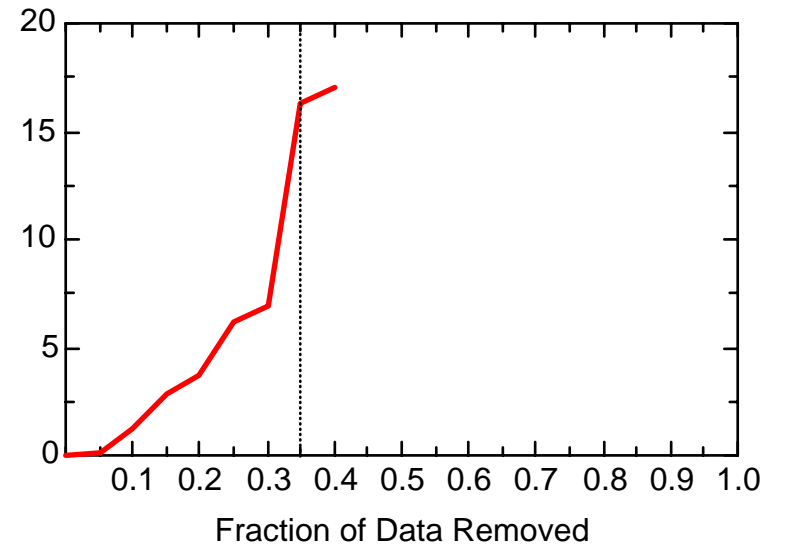
BZ: Well JBW7338A



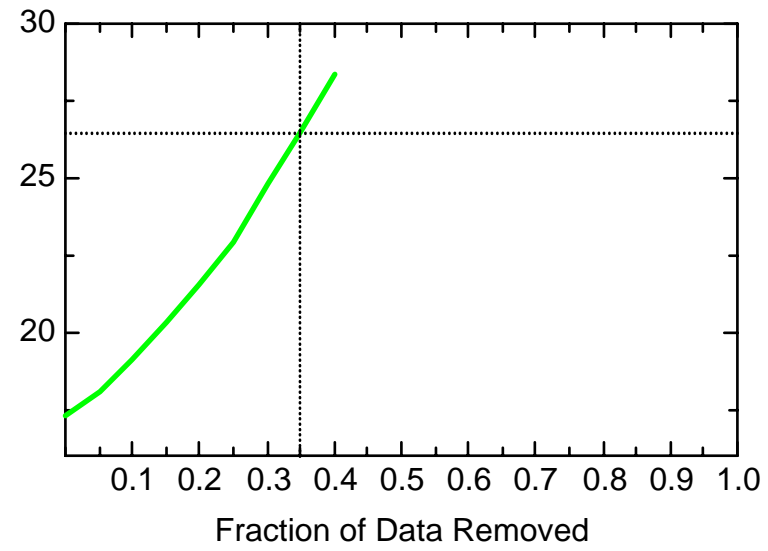
BZ: Well JBW7338B



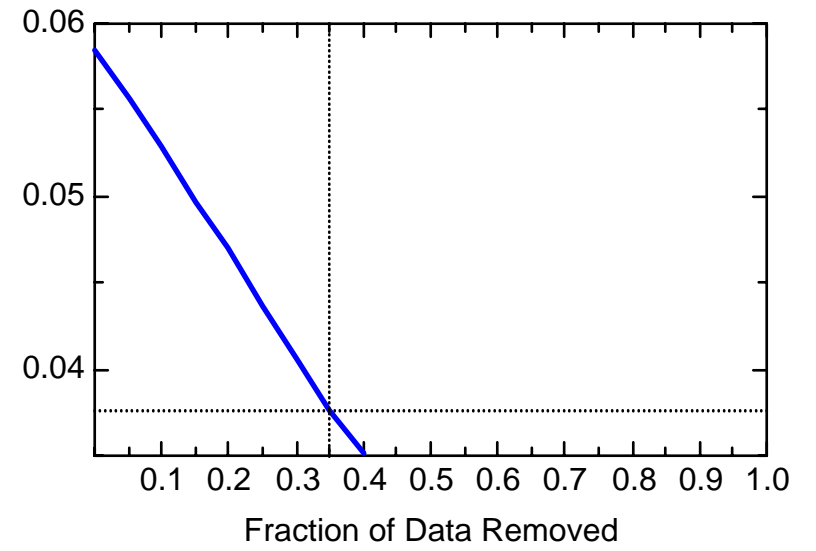
BZ: Well JBW7338B



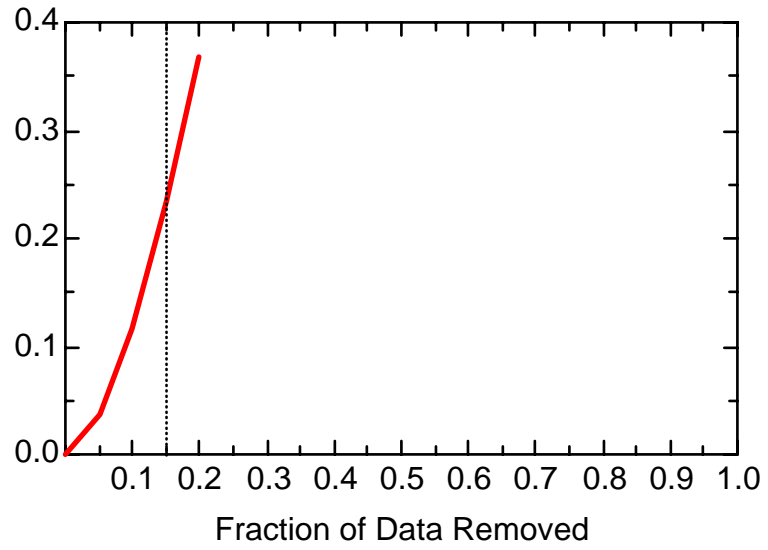
BZ: Well JBW7338B



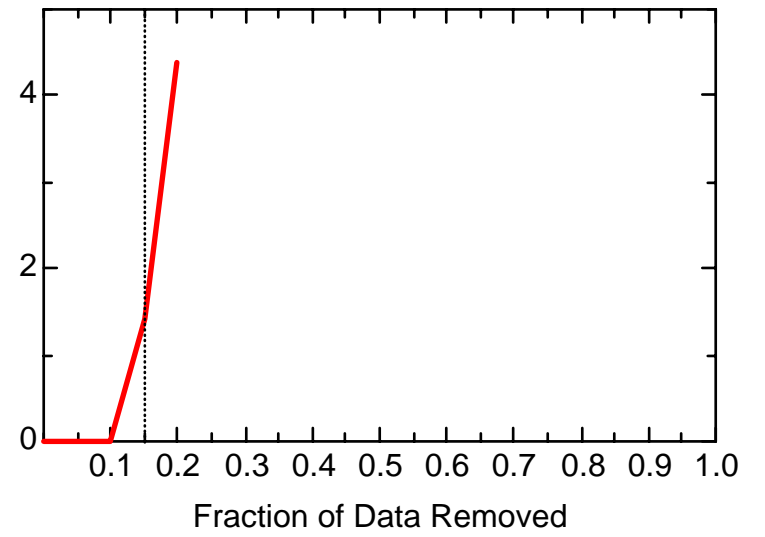
BZ: Well JBW7338B



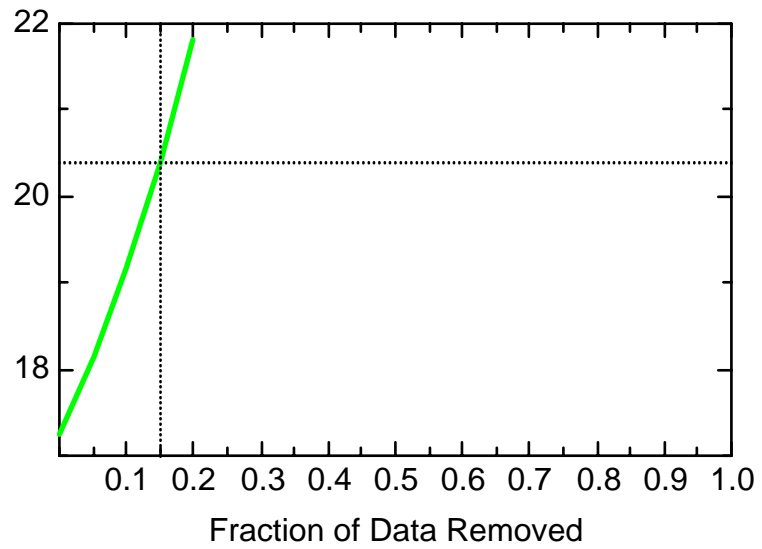
BZ: Well JBW7340B



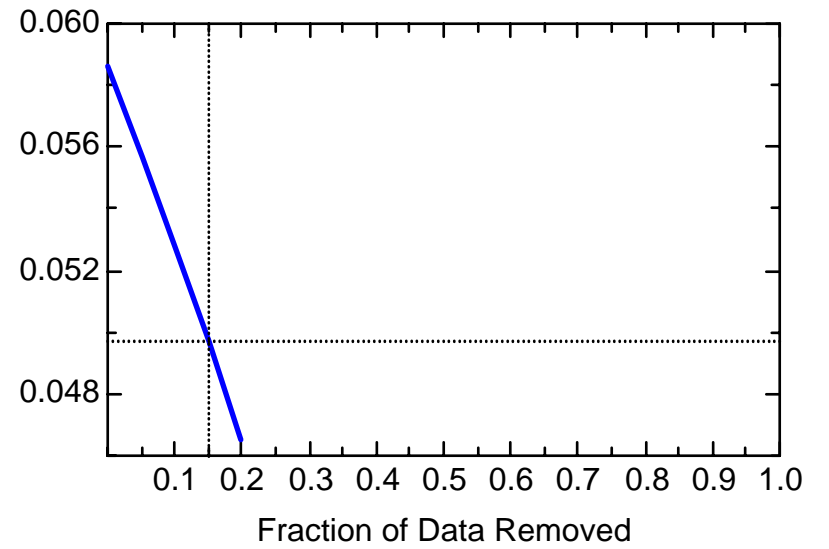
BZ: Well JBW7340B



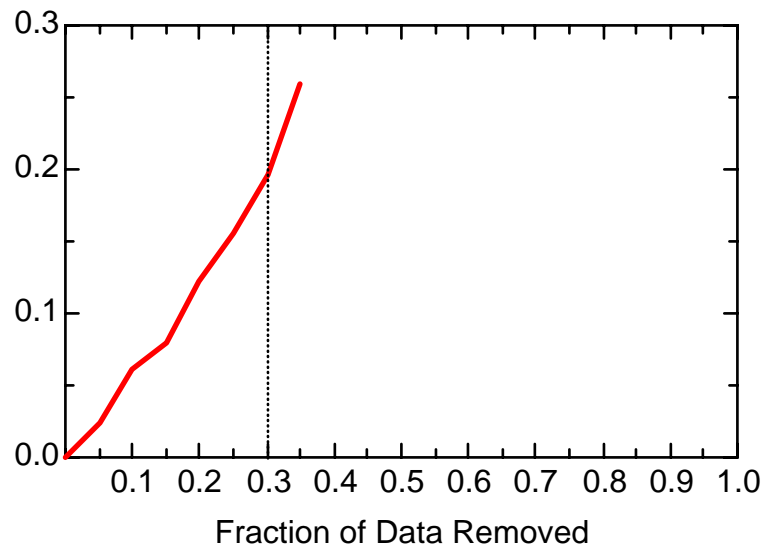
BZ: Well JBW7340B



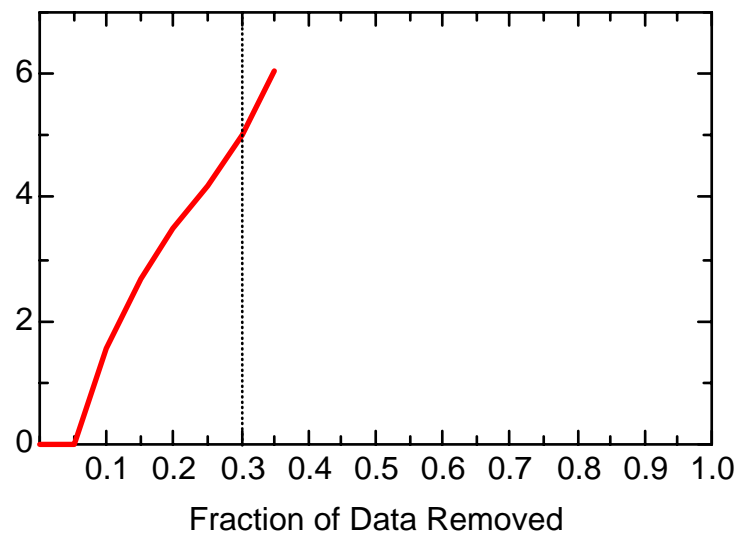
BZ: Well JBW7340B



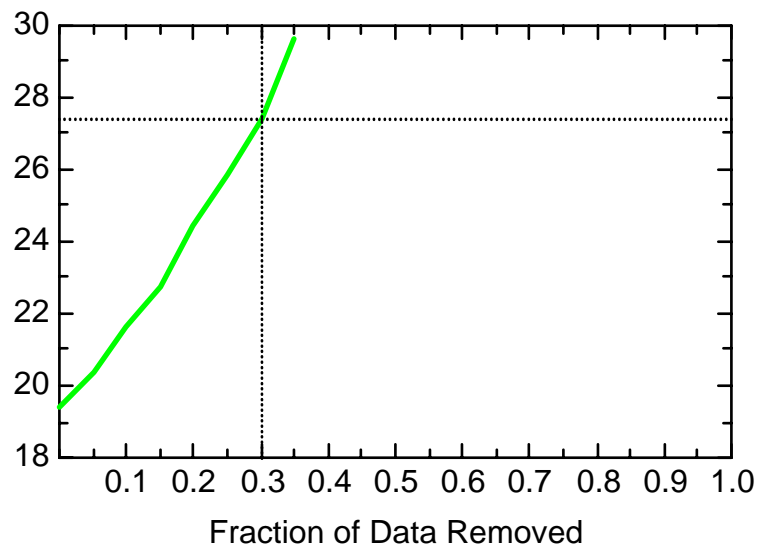
BZ: Well JBW7344



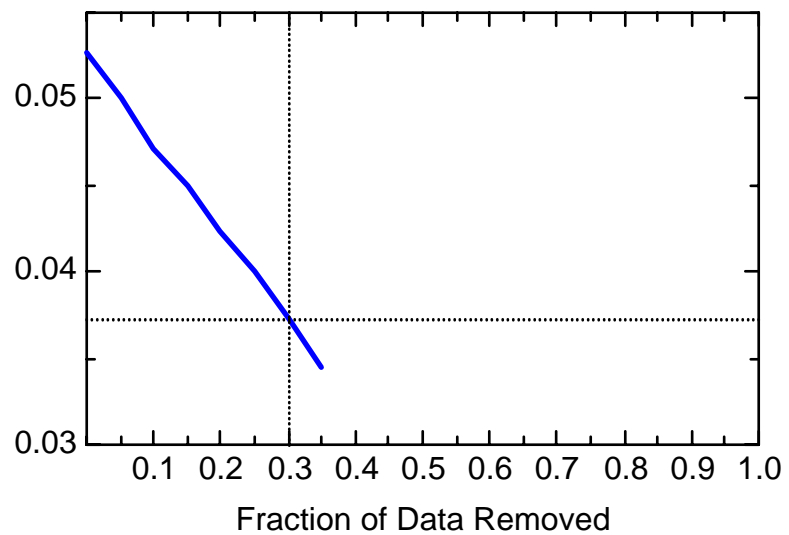
BZ: Well JBW7344



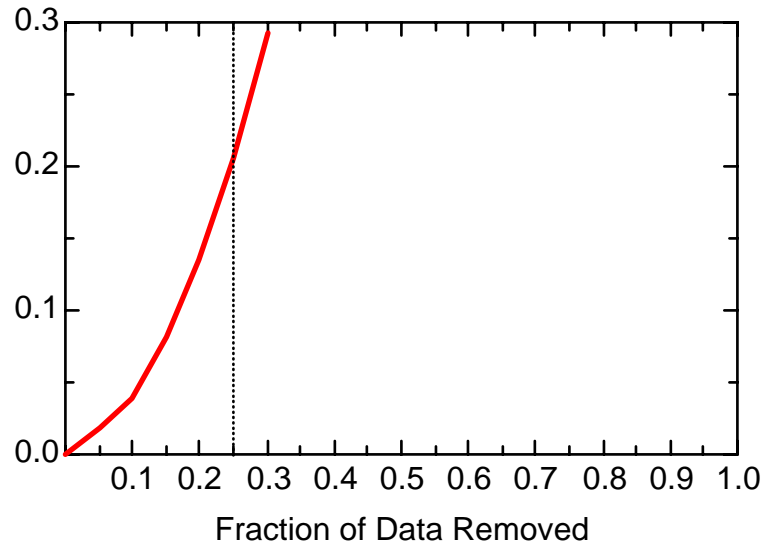
BZ: Well JBW7344



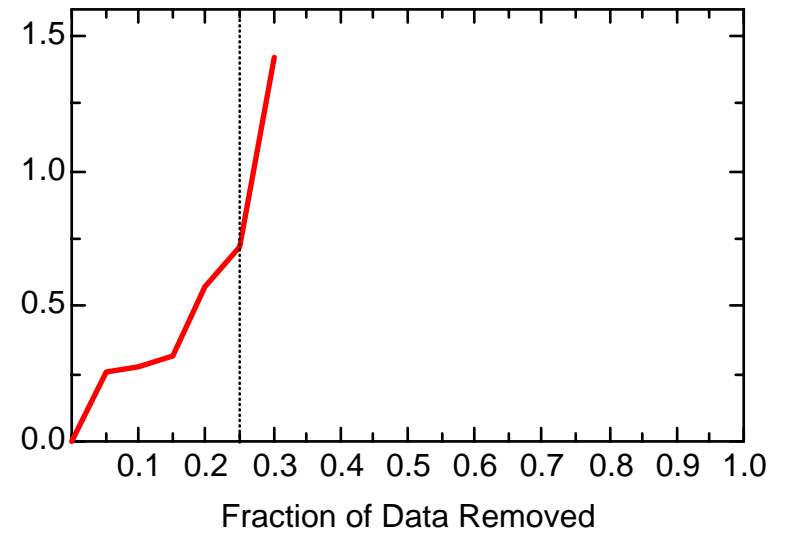
BZ: Well JBW7344



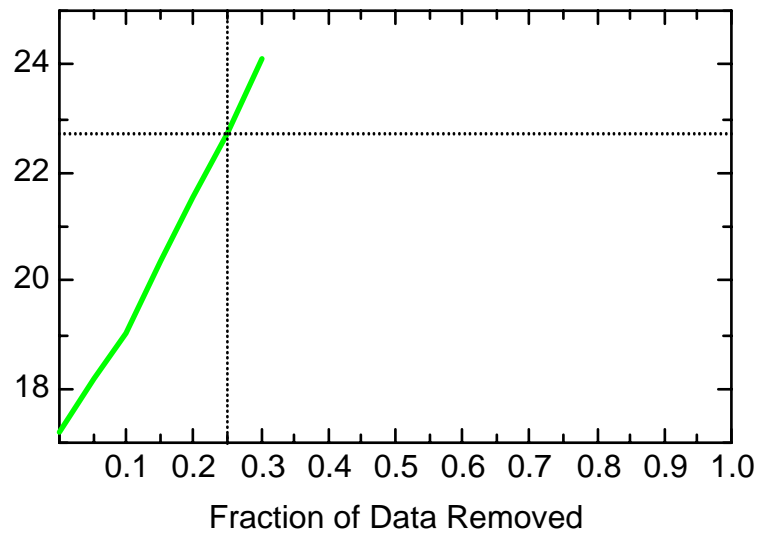
BZ: Well JBW7345A



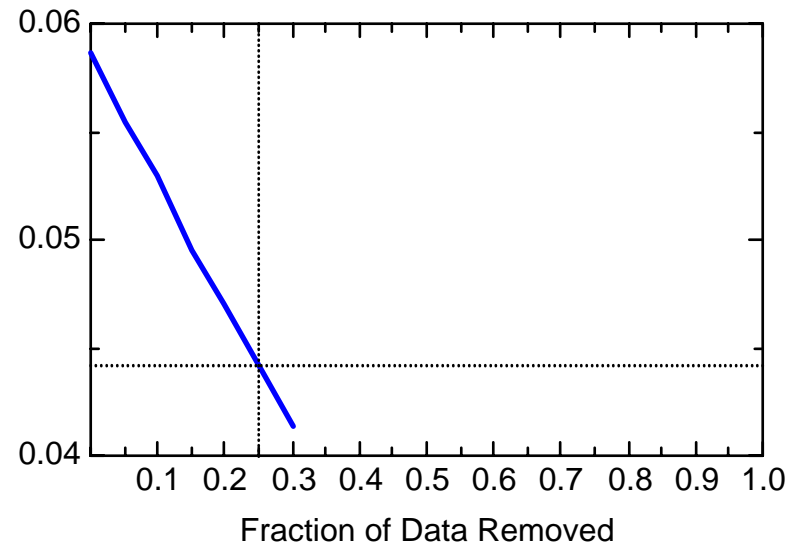
BZ: Well JBW7345A



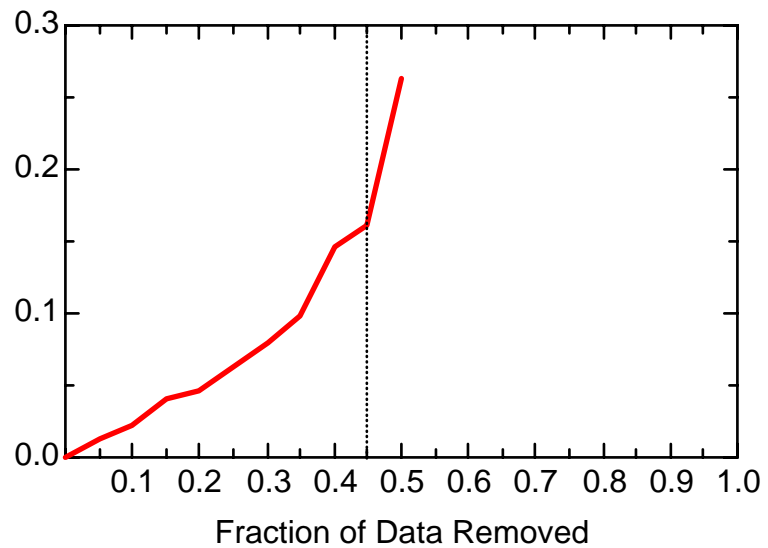
BZ: Well JBW7345A



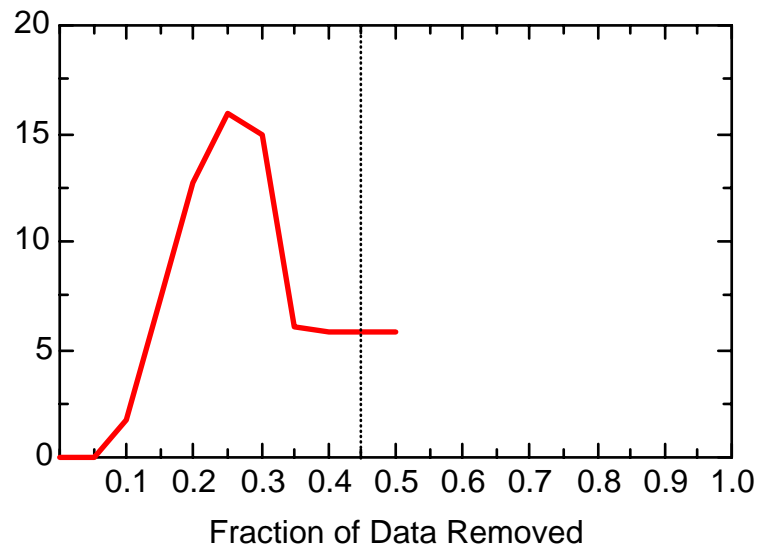
BZ: Well JBW7345A



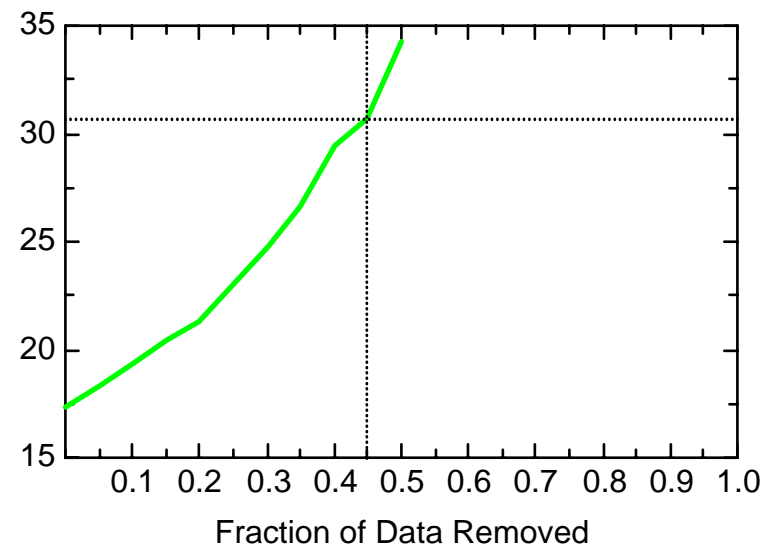
BZ: Well JBW7348



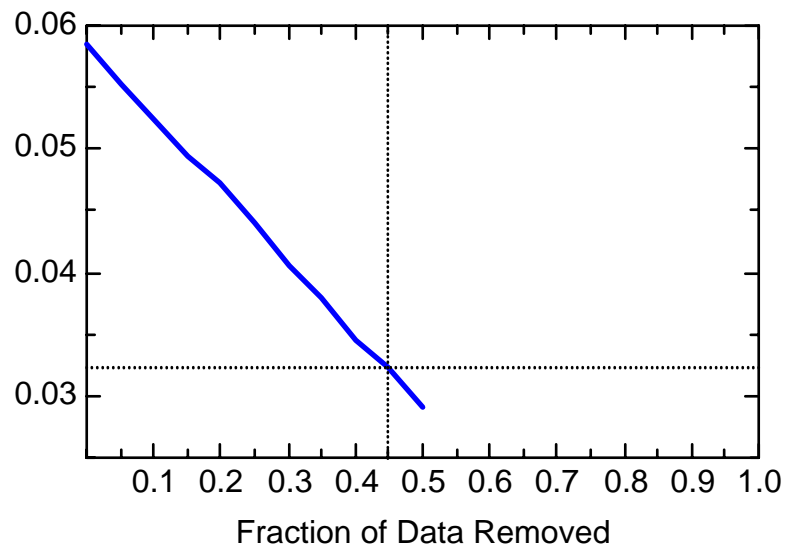
BZ: Well JBW7348



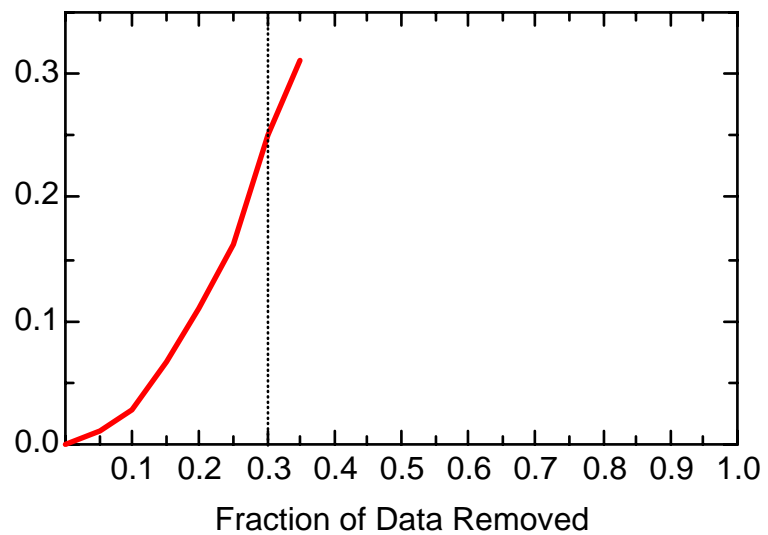
BZ: Well JBW7348



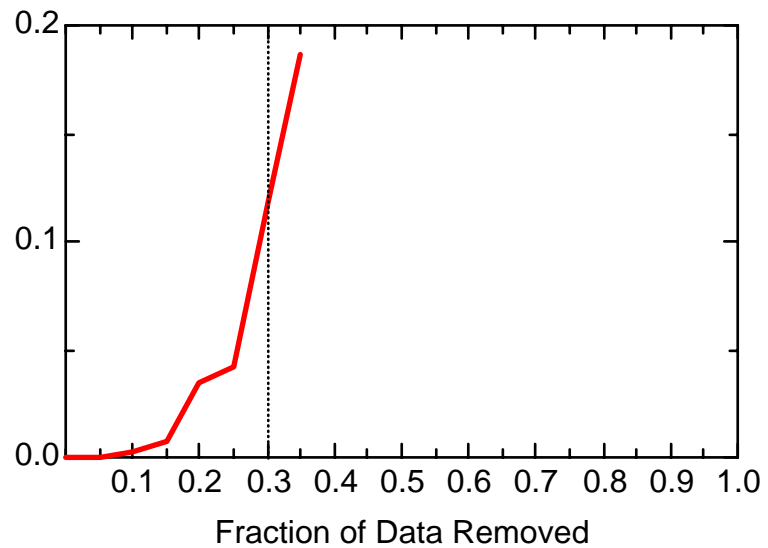
BZ: Well JBW7348



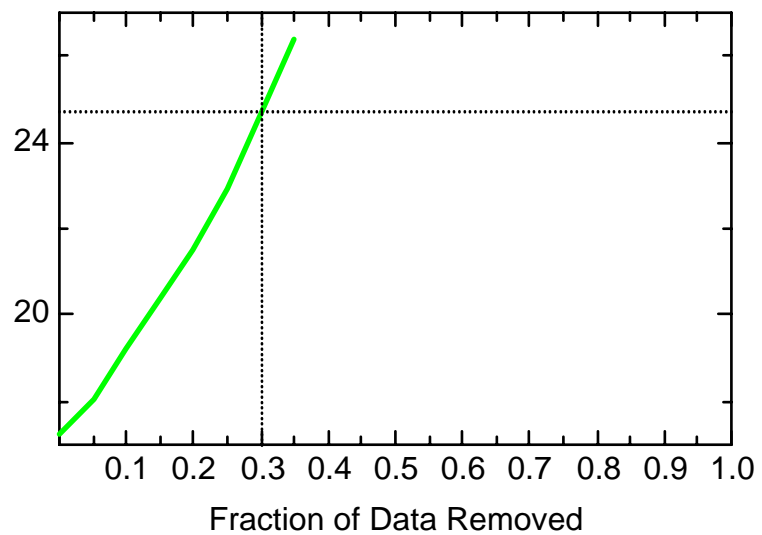
BZ: Well JBW7350



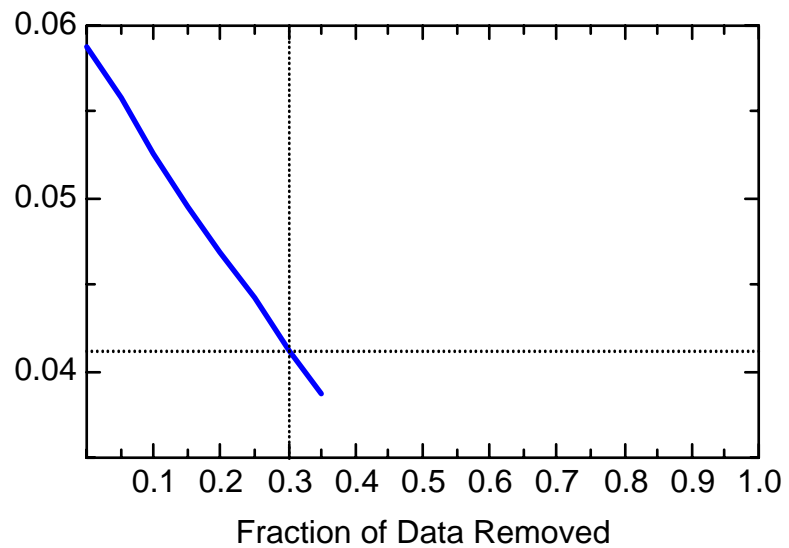
BZ: Well JBW7350



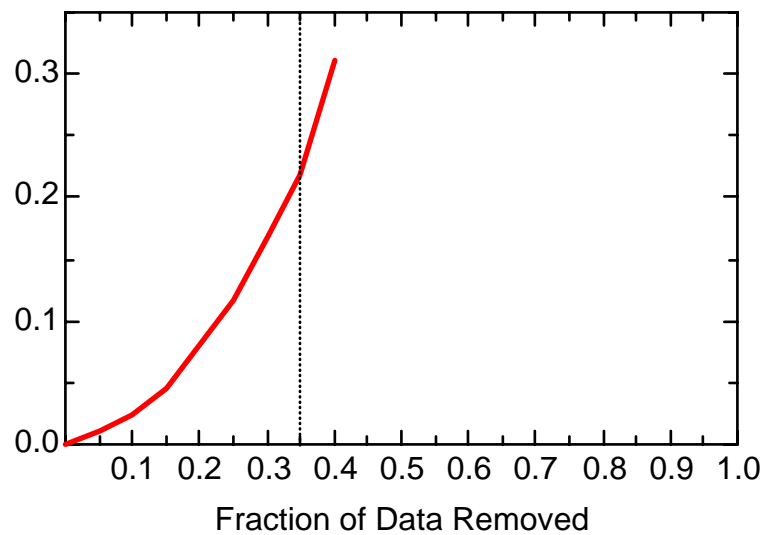
BZ: Well JBW7350



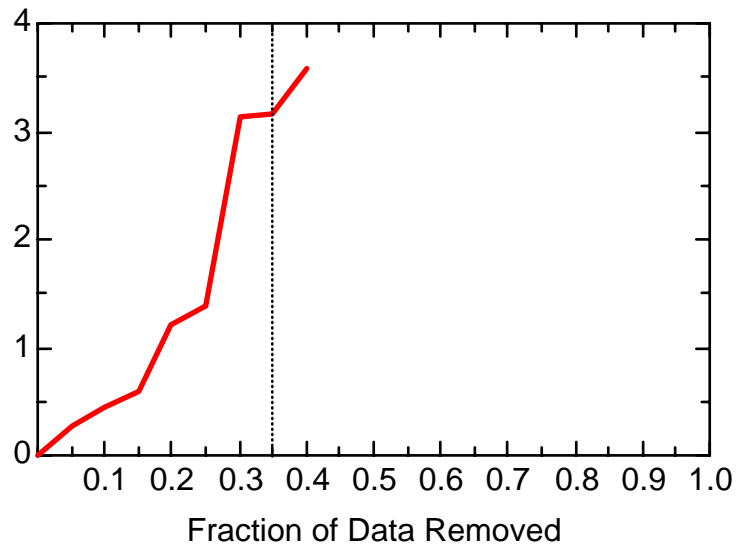
BZ: Well JBW7350



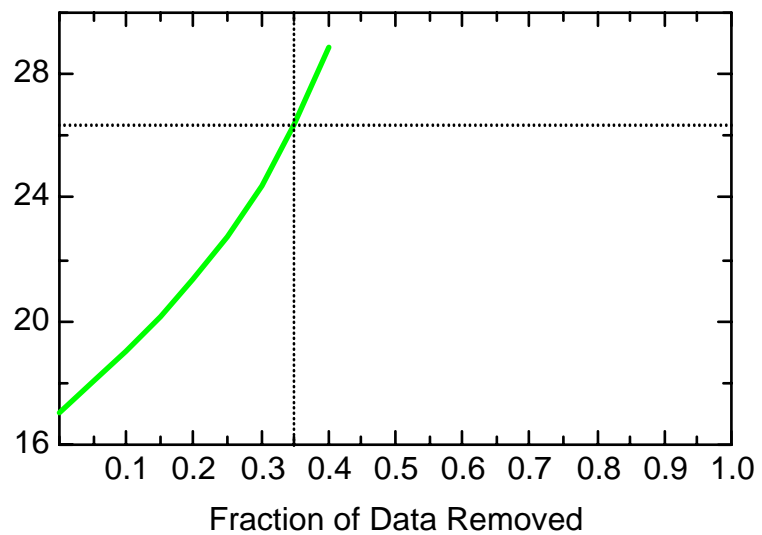
BZ: Well JBW7710



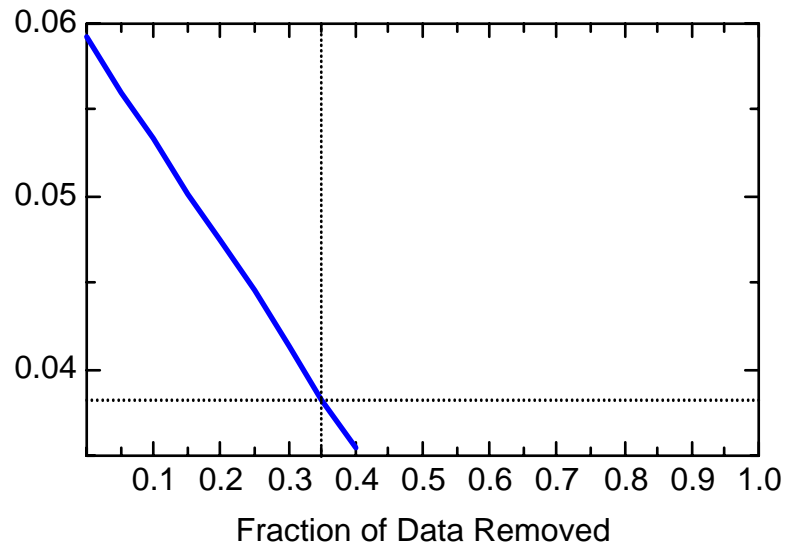
BZ: Well JBW7710



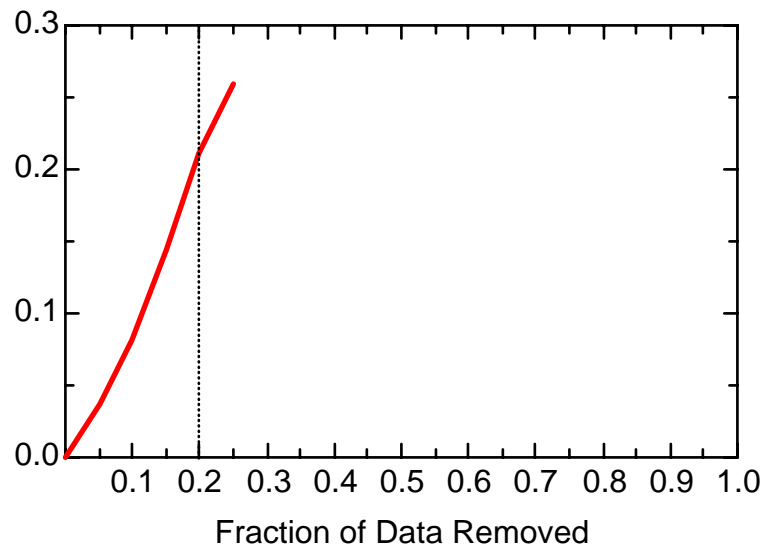
BZ: Well JBW7710



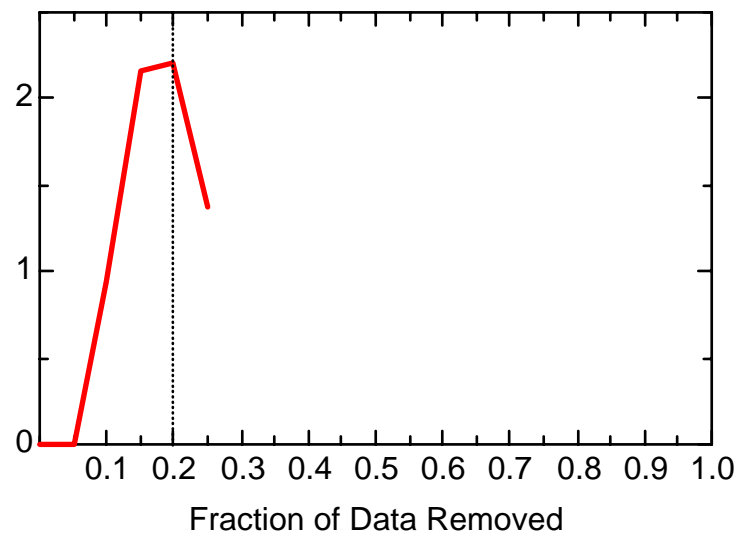
BZ: Well JBW7710



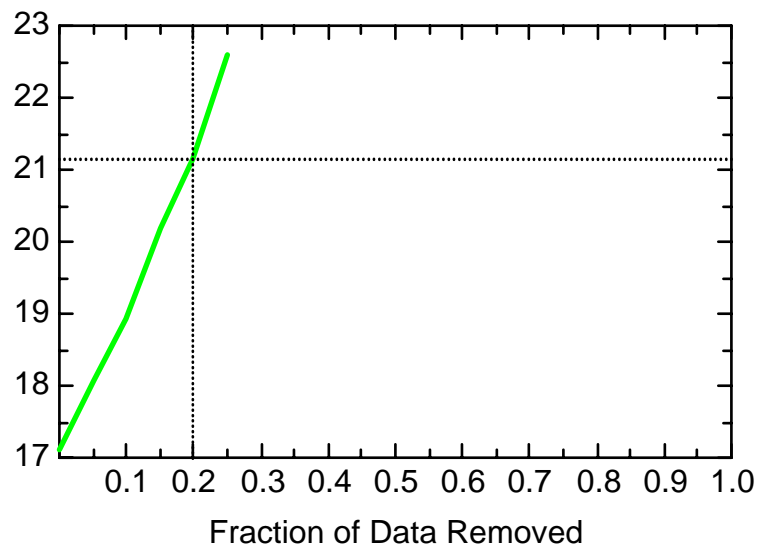
BZ: Well JBW7812B



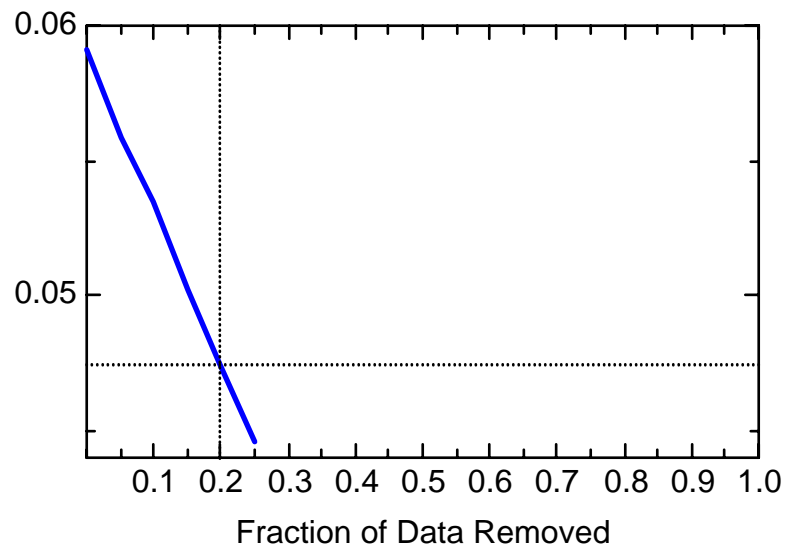
BZ: Well JBW7812B



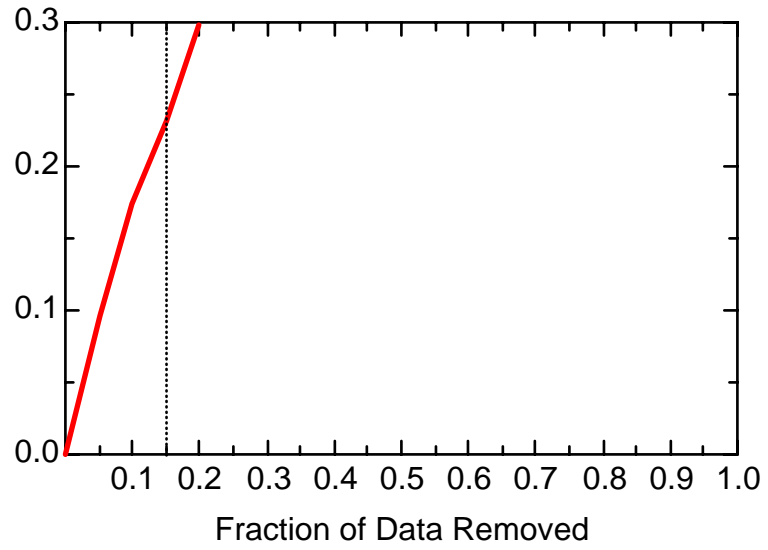
BZ: Well JBW7812B



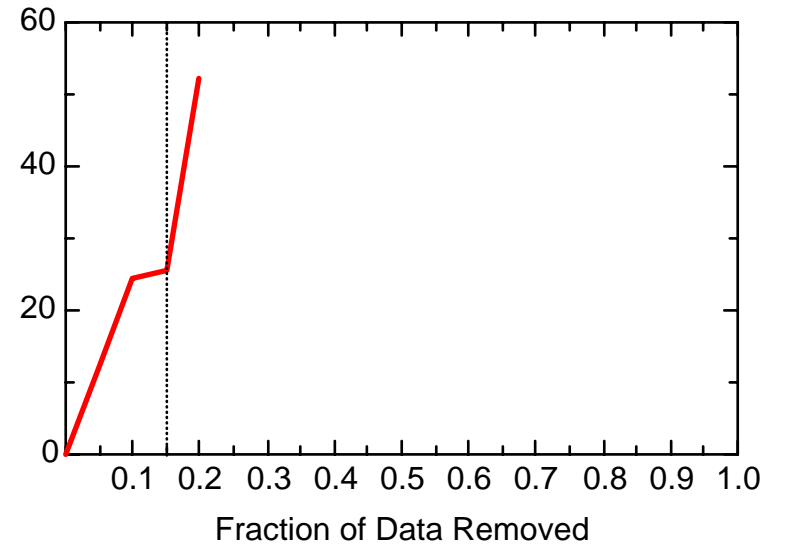
BZ: Well JBW7812B



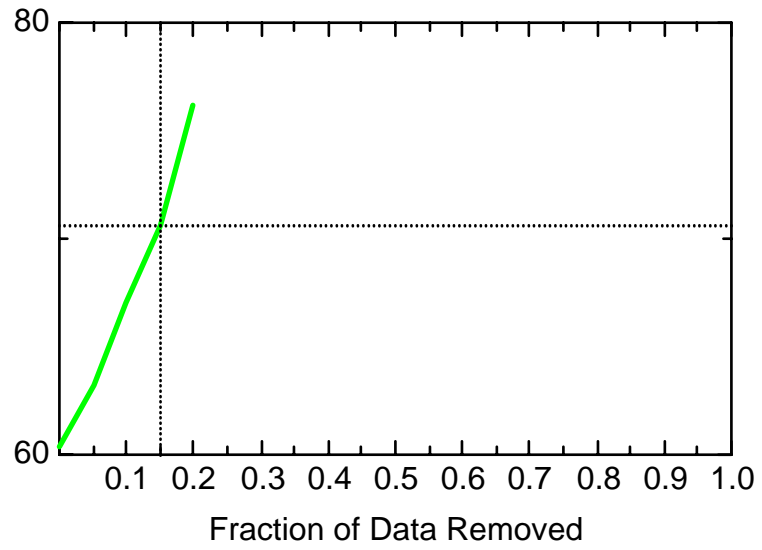
BZ: Well JMW0201A



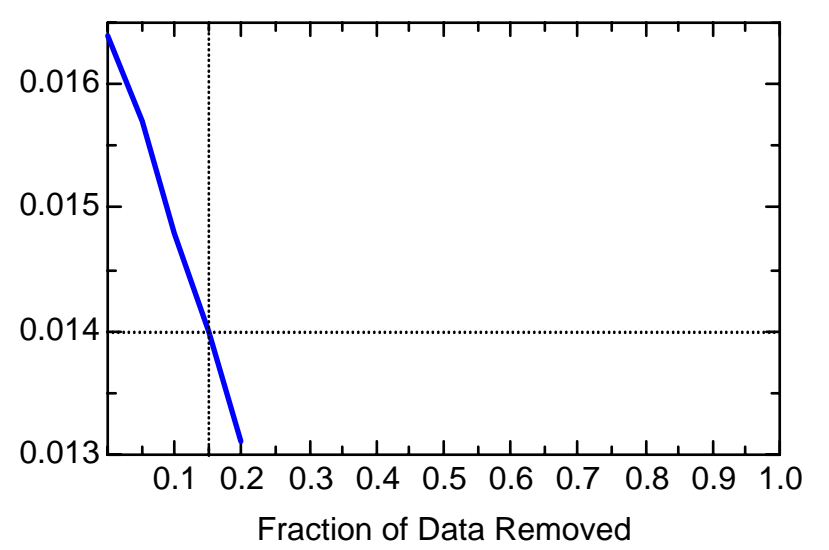
BZ: Well JMW0201A



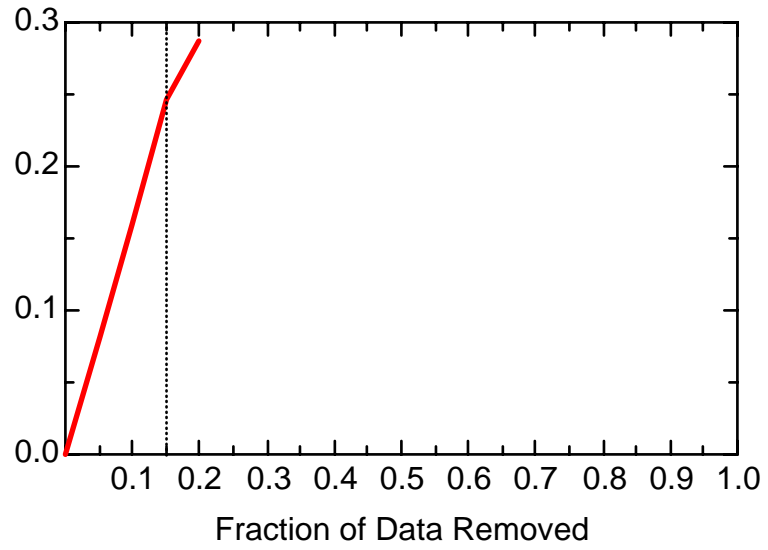
BZ: Well JMW0201A



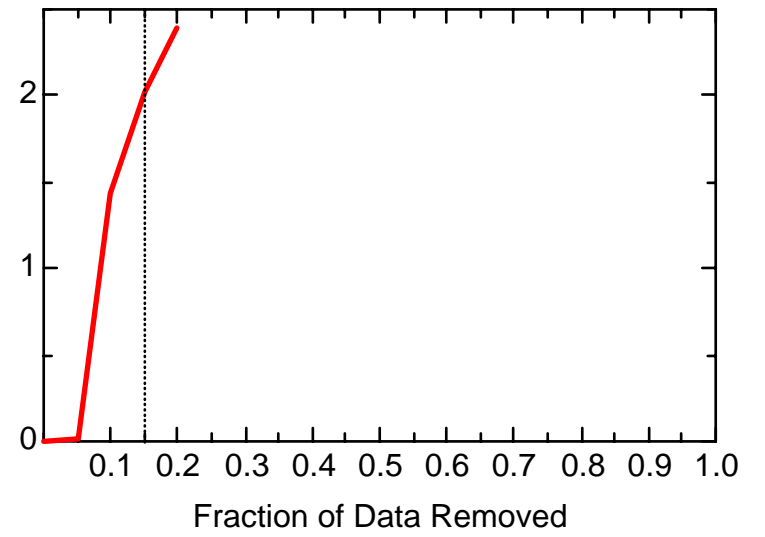
BZ: Well JMW0201A



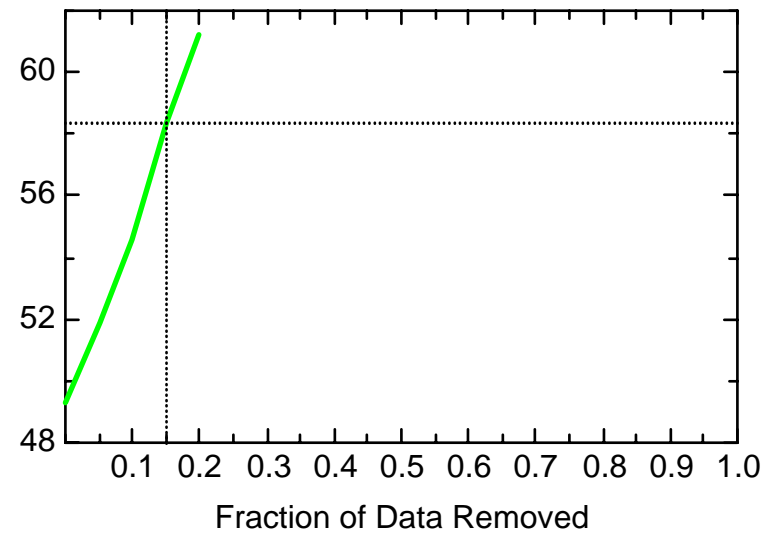
BZ: Well JMW0505



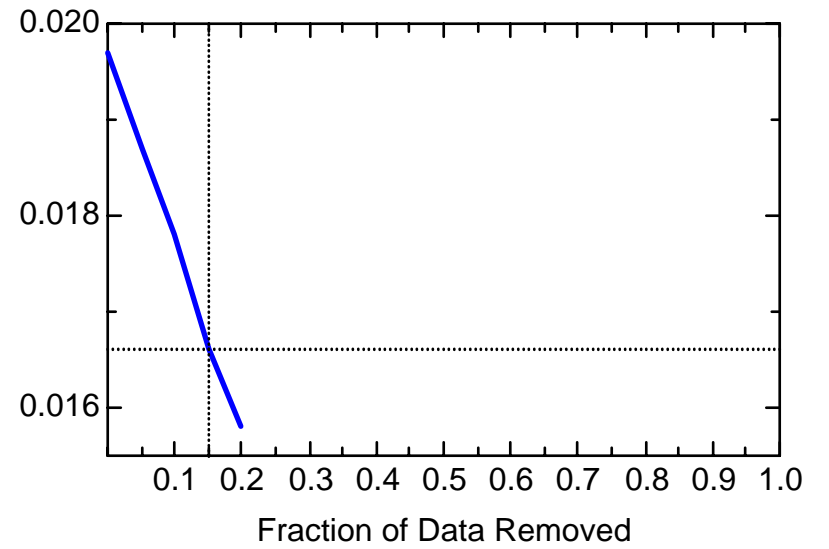
BZ: Well JMW0505



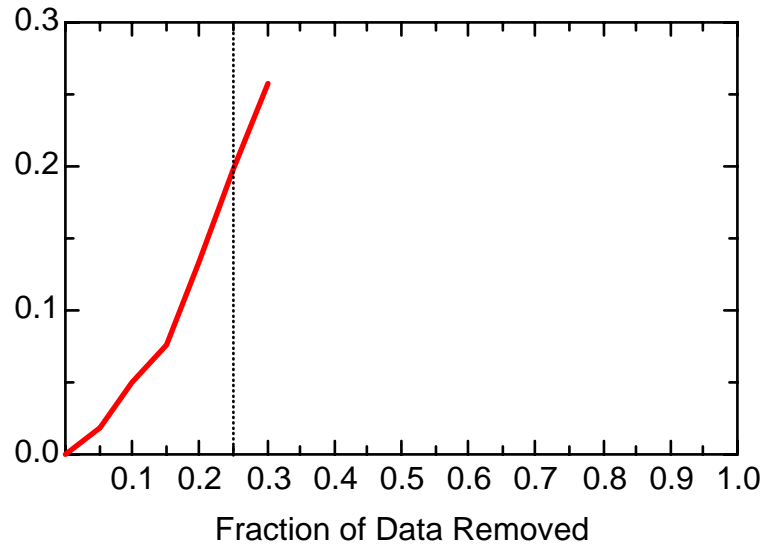
BZ: Well JMW0505



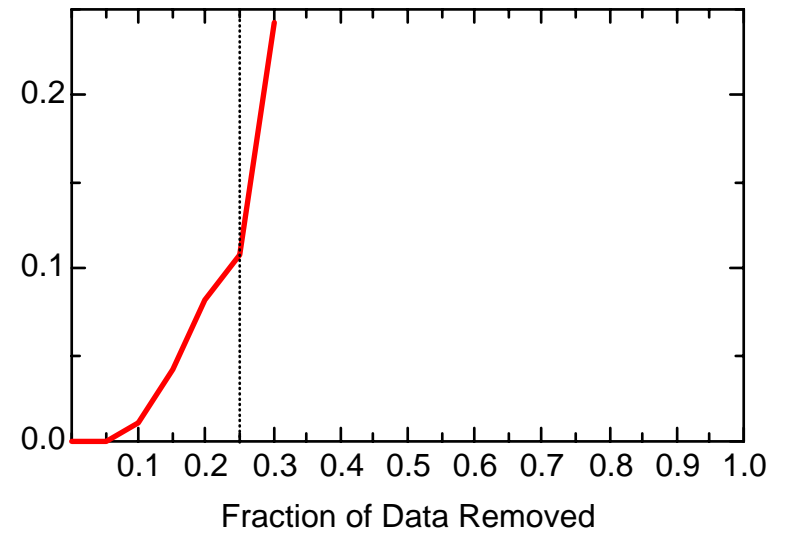
BZ: Well JMW0505



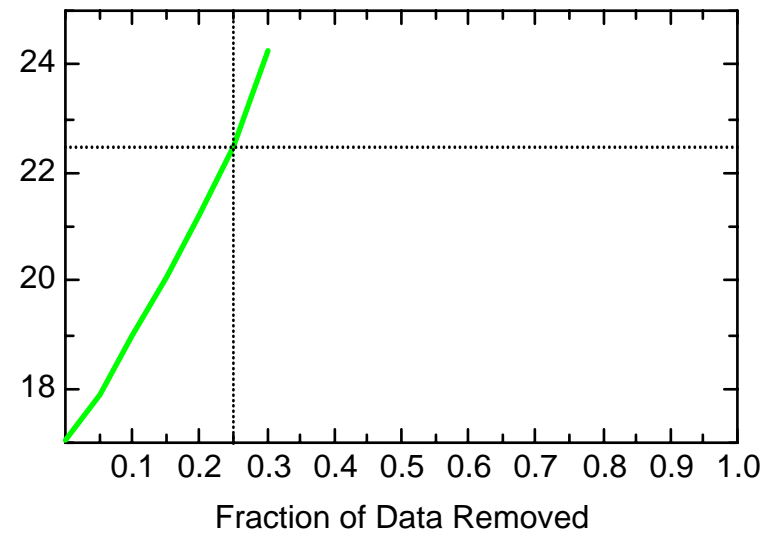
BZ: Well JMW0542



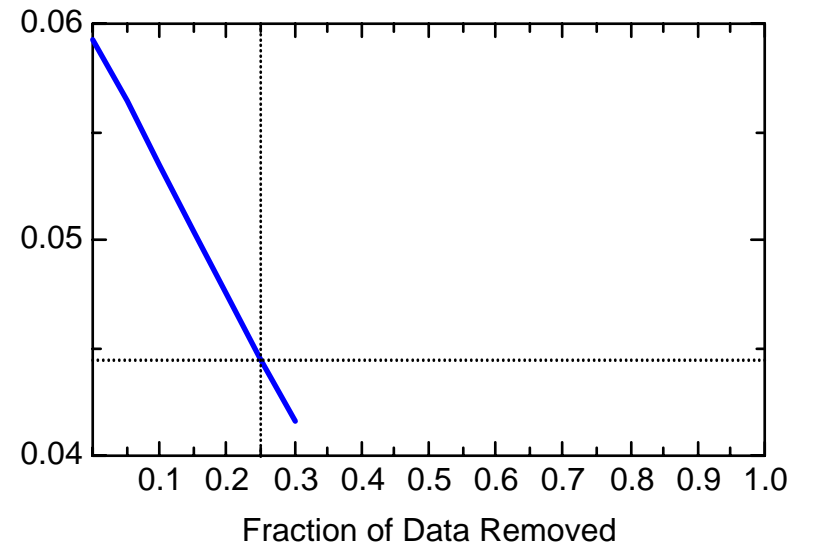
BZ: Well JMW0542



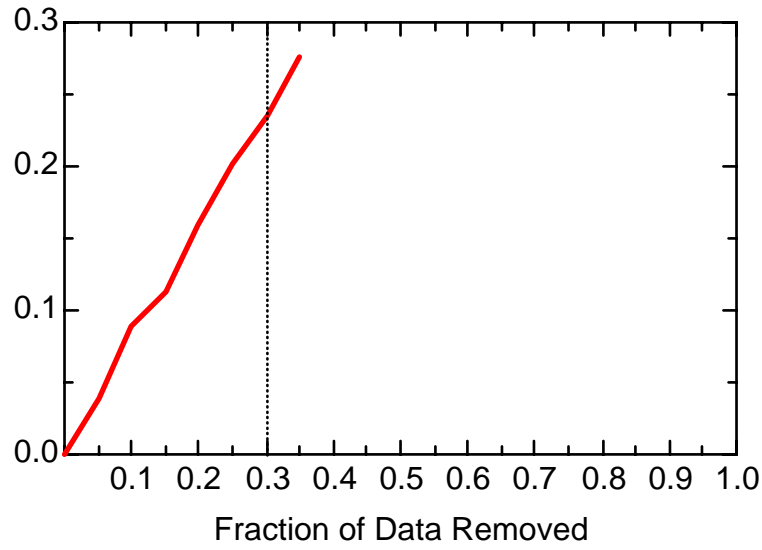
BZ: Well JMW0542



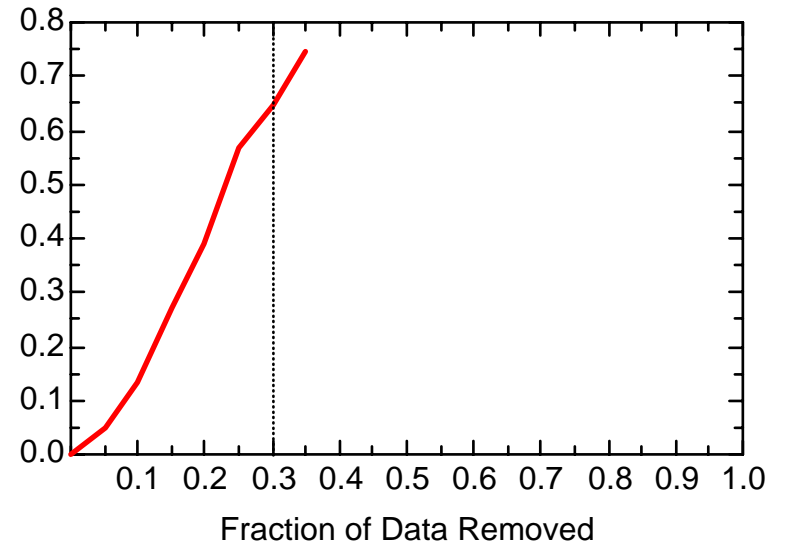
BZ: Well JMW0542



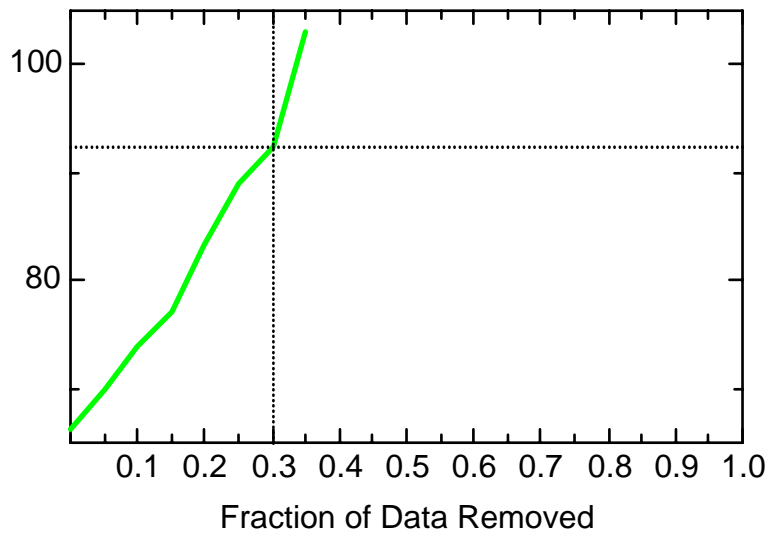
BZ: Well JMW0604



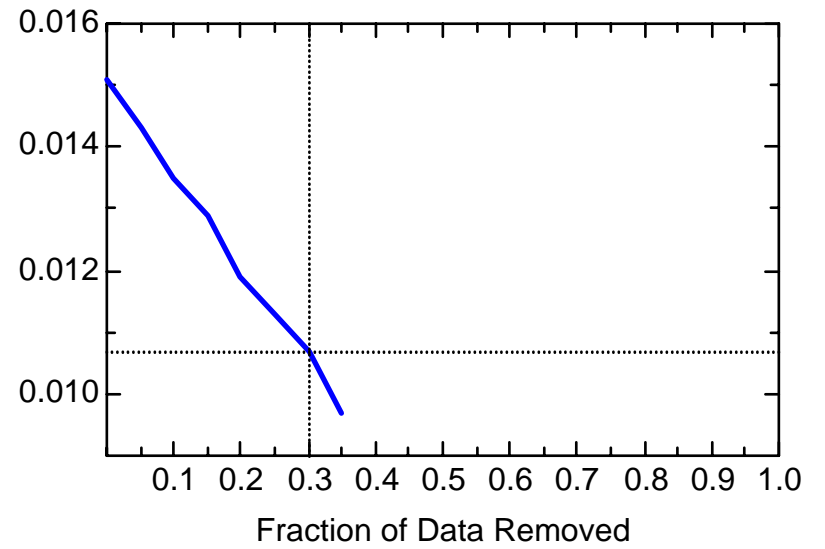
BZ: Well JMW0604



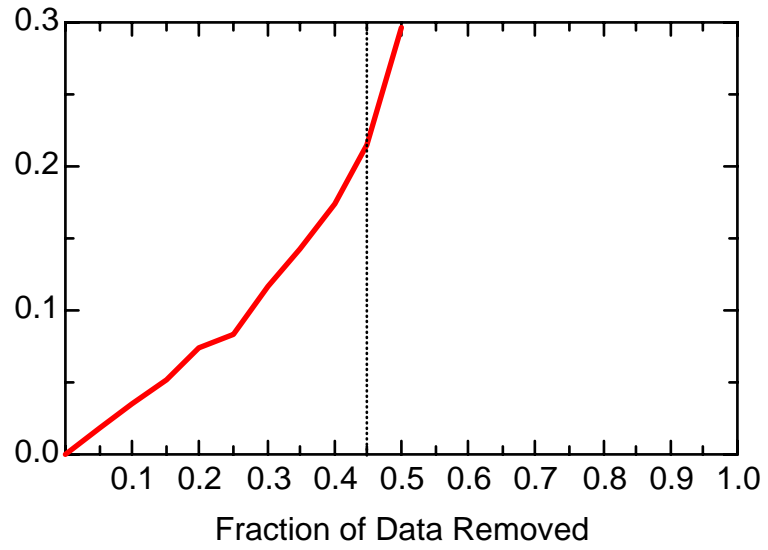
BZ: Well JMW0604



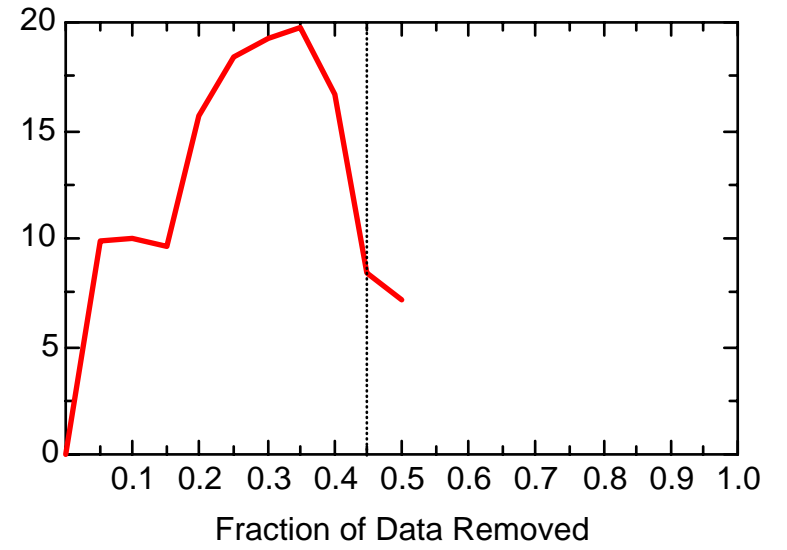
BZ: Well JMW0604



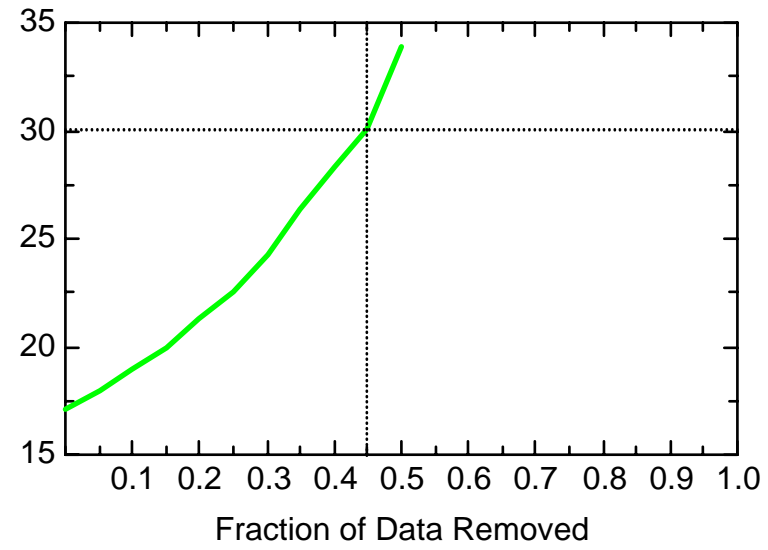
BZ: Well JMW0701



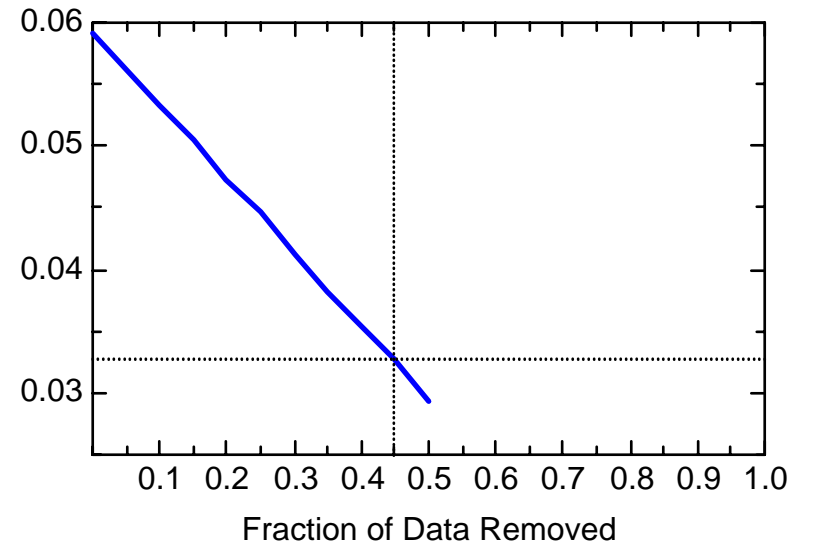
BZ: Well JMW0701



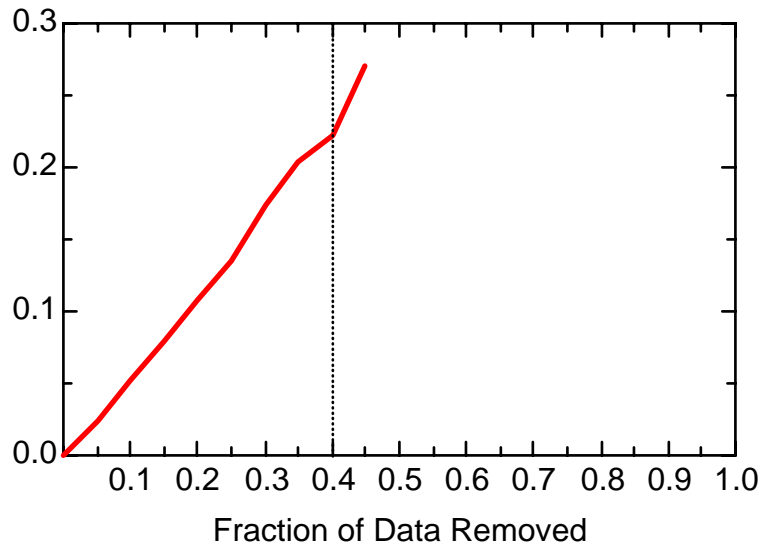
BZ: Well JMW0701



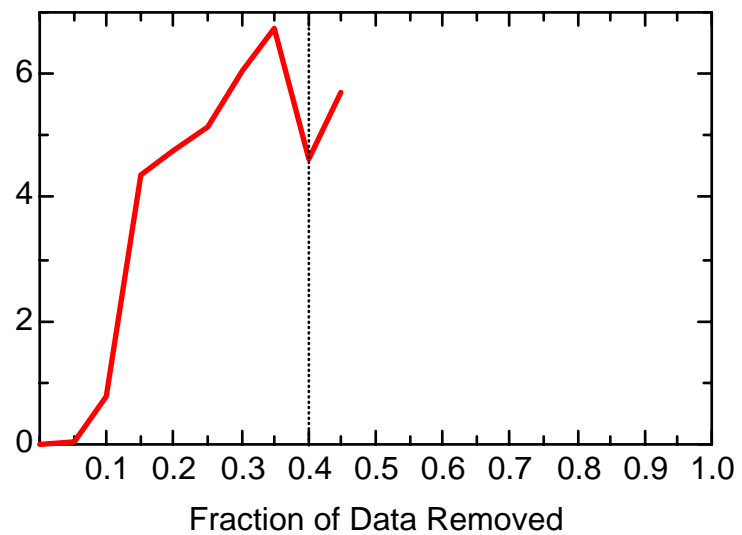
BZ: Well JMW0701



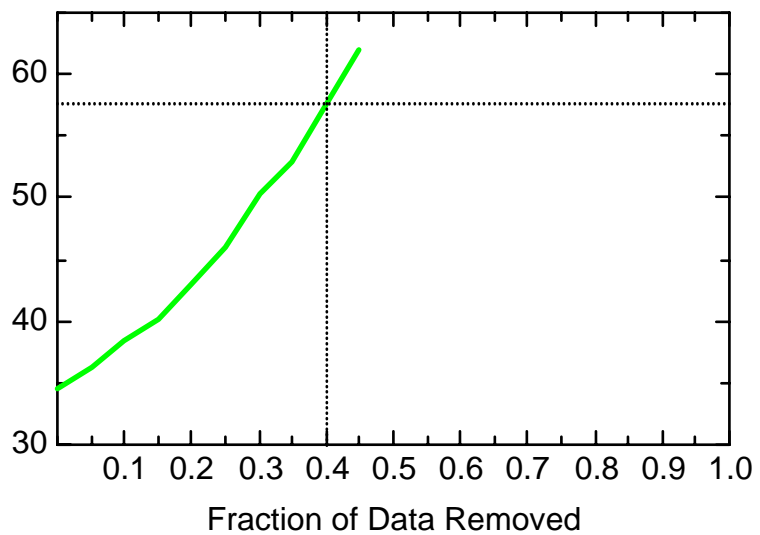
BZ: Well JMW1103D



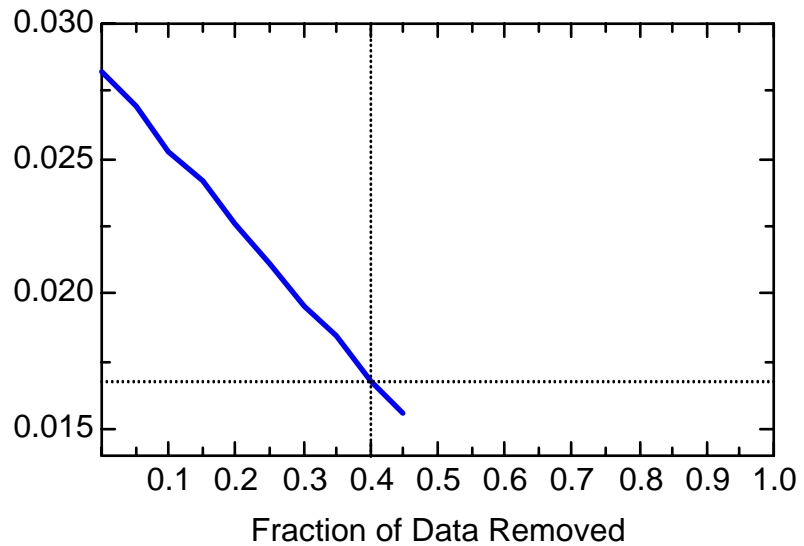
BZ: Well JMW1103D



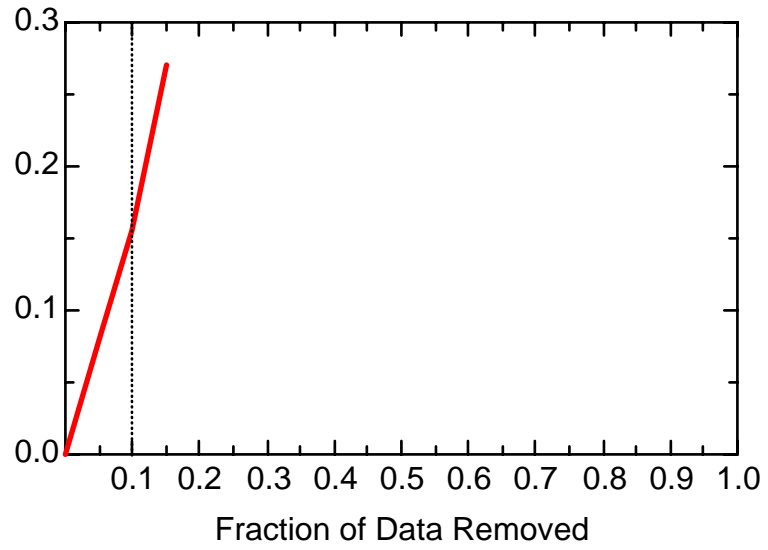
BZ: Well JMW1103D



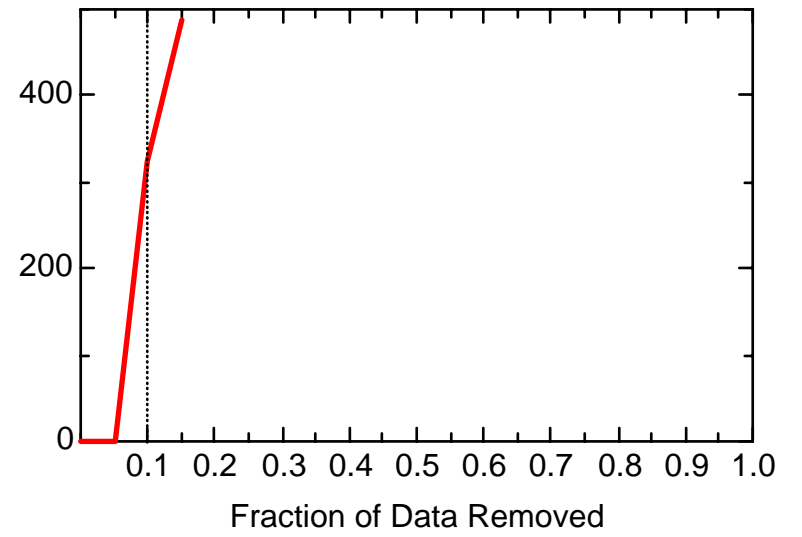
BZ: Well JMW1103D



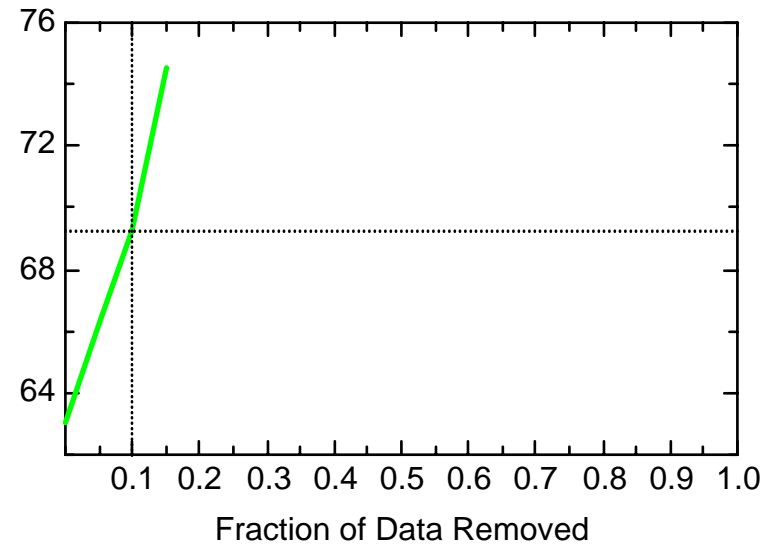
BZ: Well JMW1562



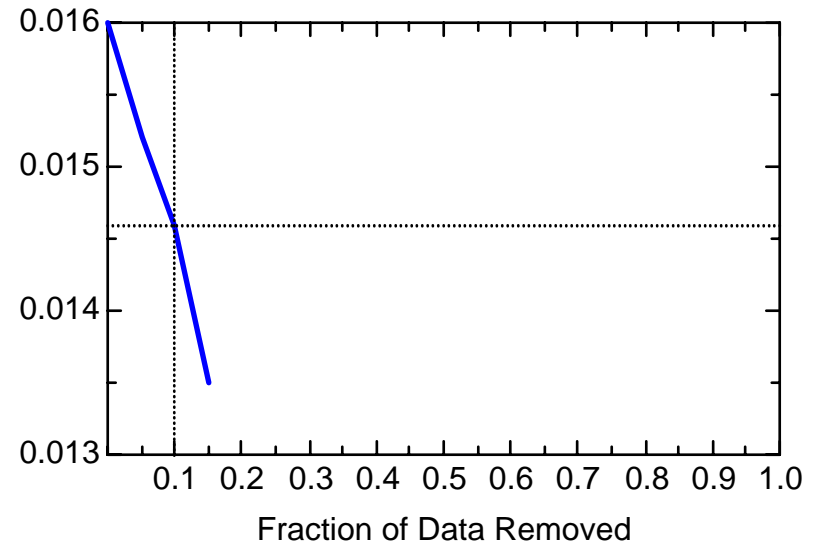
BZ: Well JMW1562



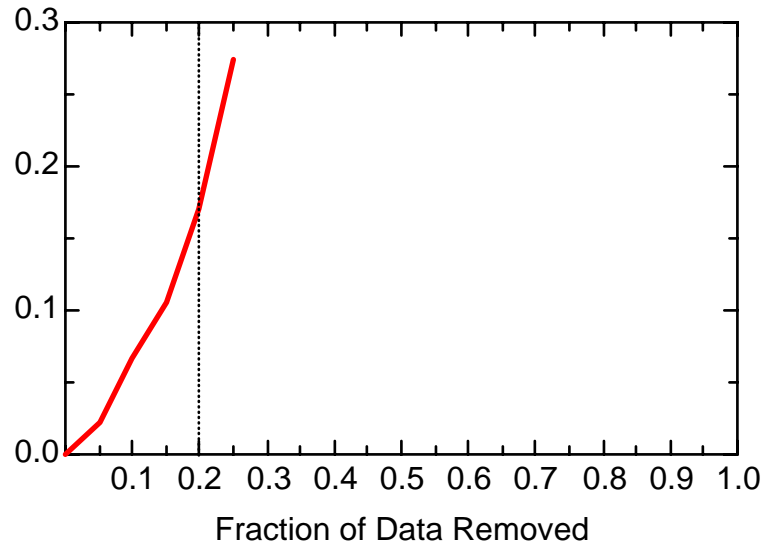
BZ: Well JMW1562



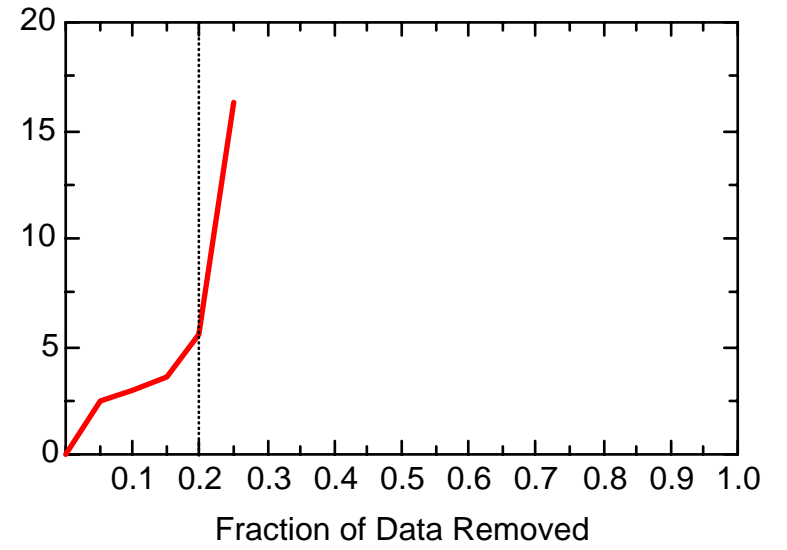
BZ: Well JMW1562



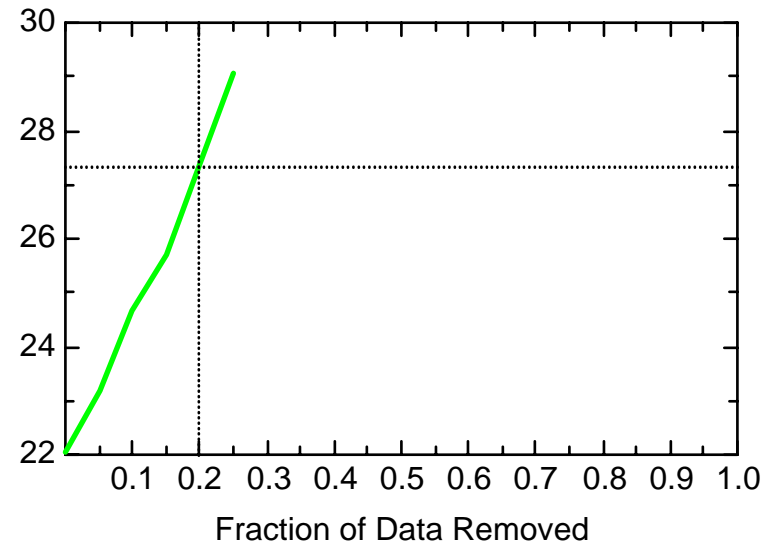
BZ: Well JMW1564



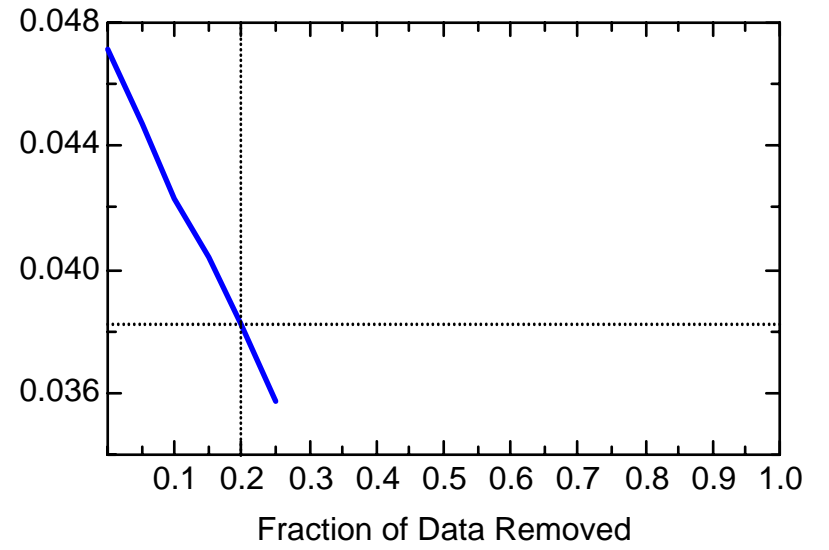
BZ: Well JMW1564



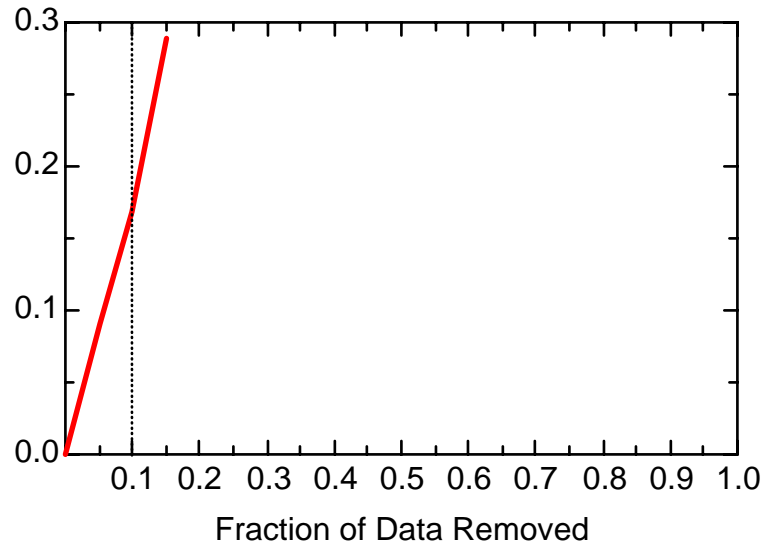
BZ: Well JMW1564



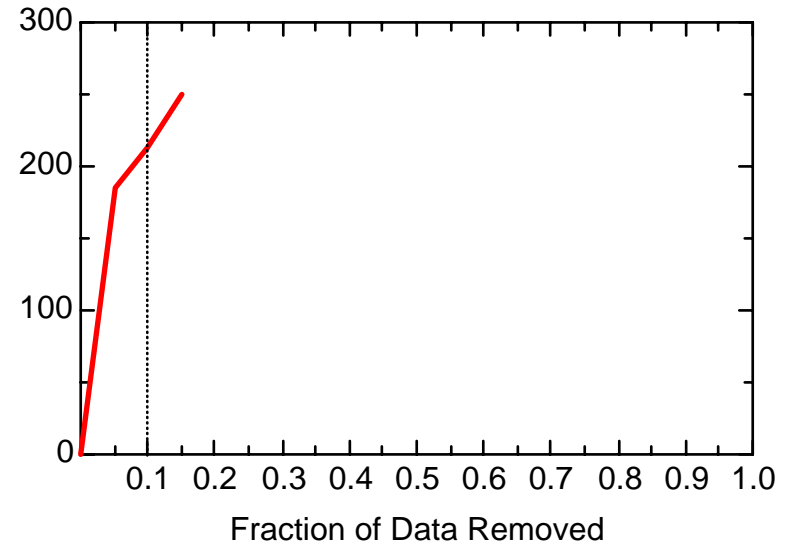
BZ: Well JMW1564



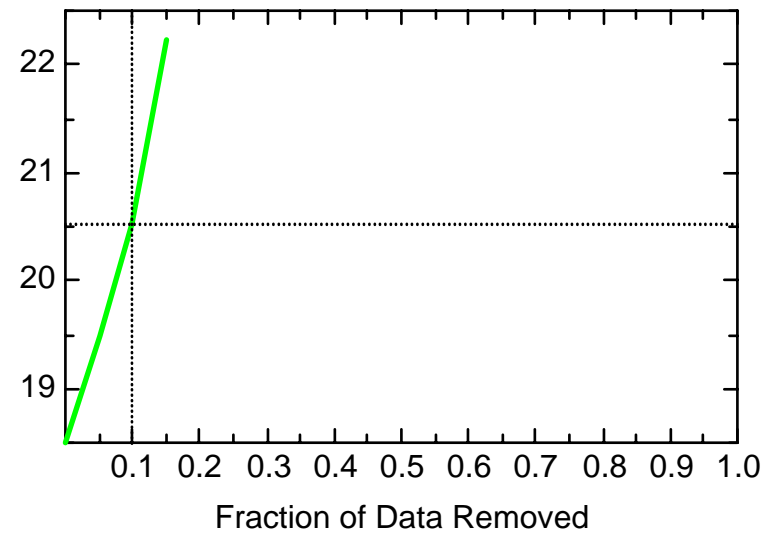
BZ: Well JMW1565



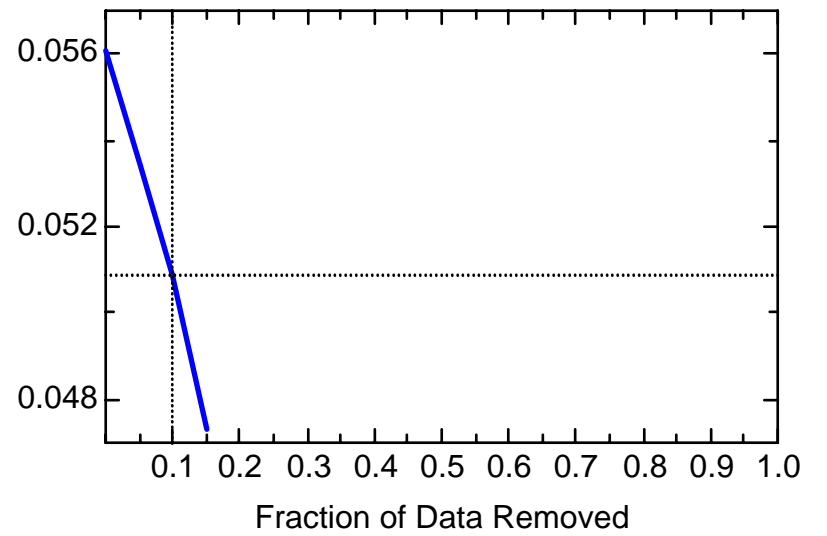
BZ: Well JMW1565



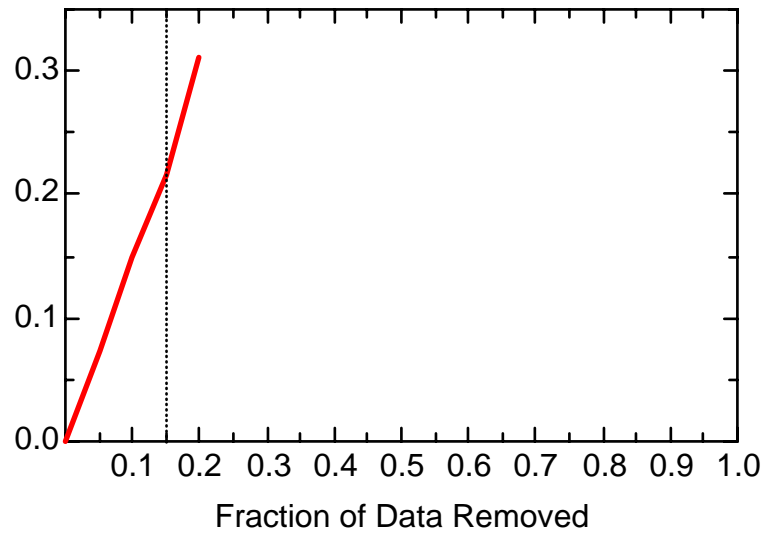
BZ: Well JMW1565



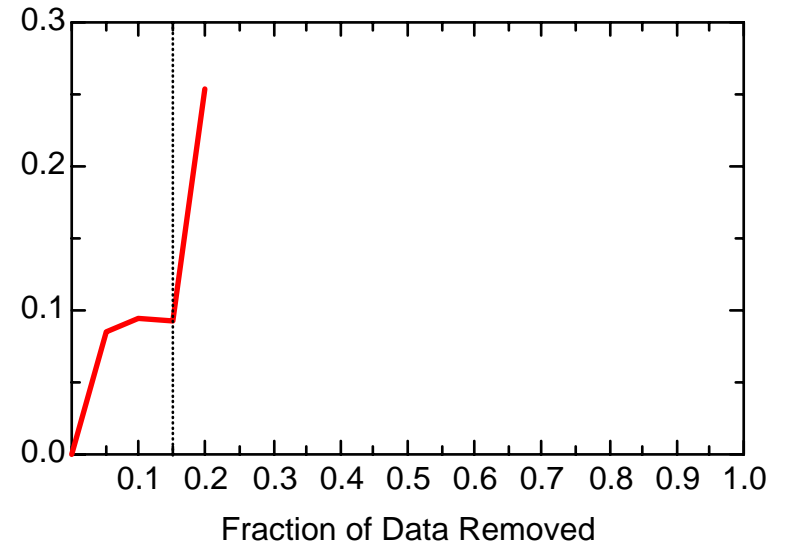
BZ: Well JMW1565



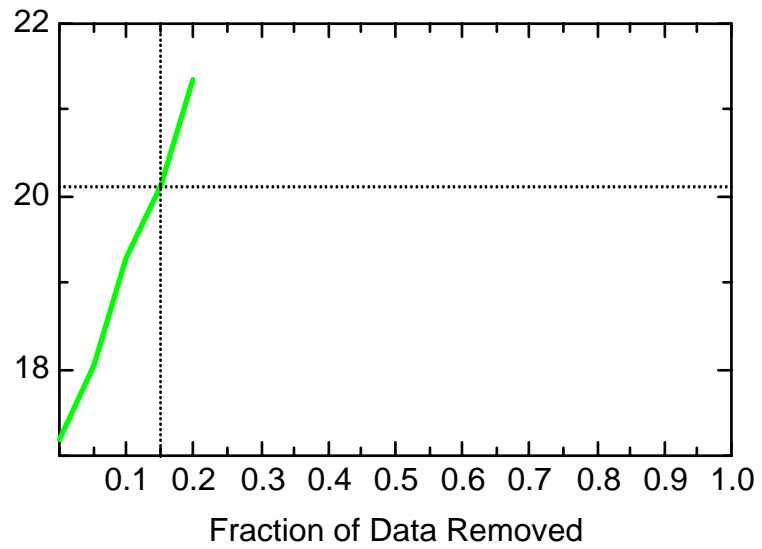
BZ: Well JMW1860



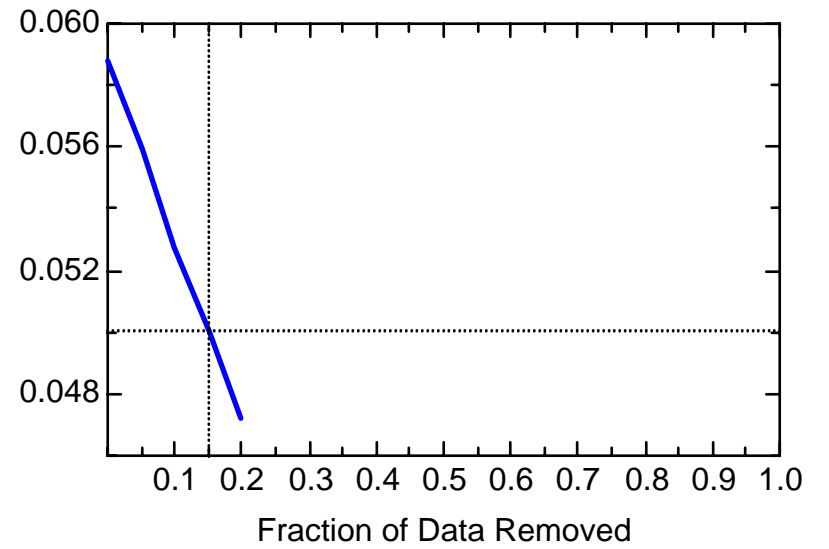
BZ: Well JMW1860



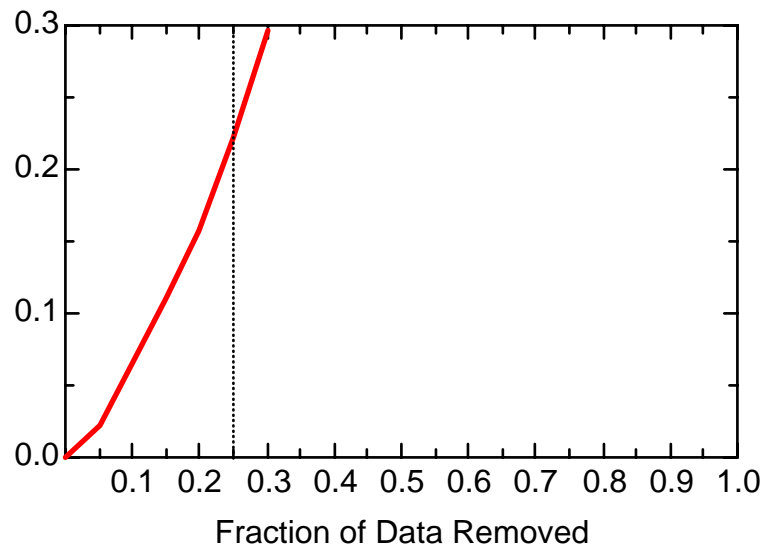
BZ: Well JMW1860



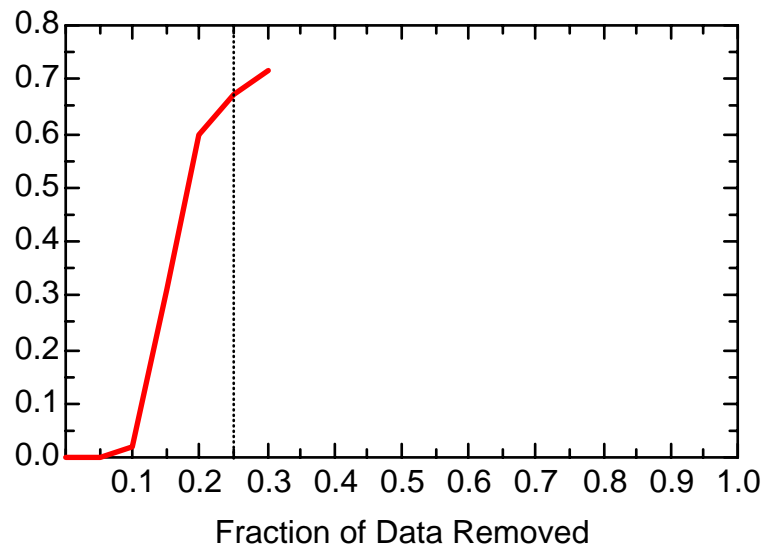
BZ: Well JMW1860



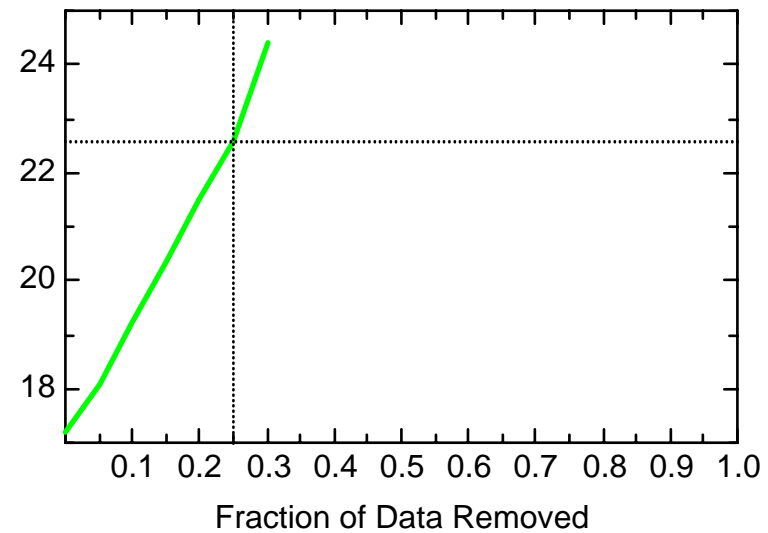
BZ: Well JMW1881



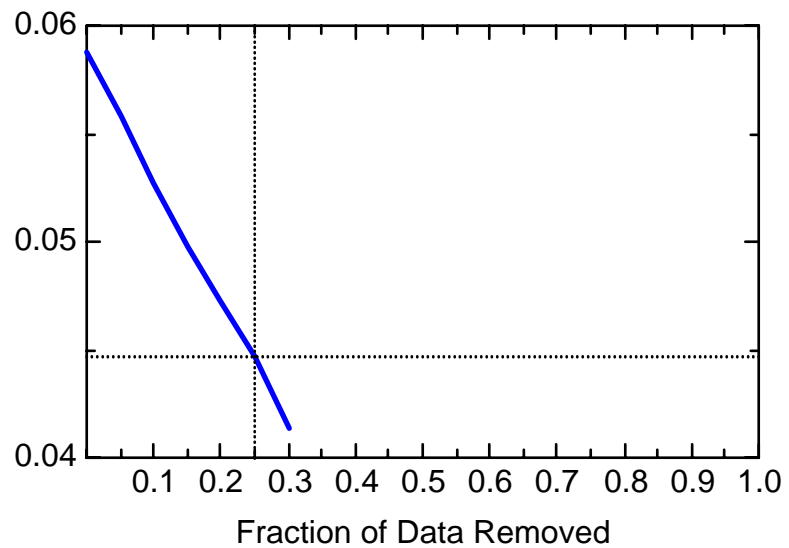
BZ: Well JMW1881



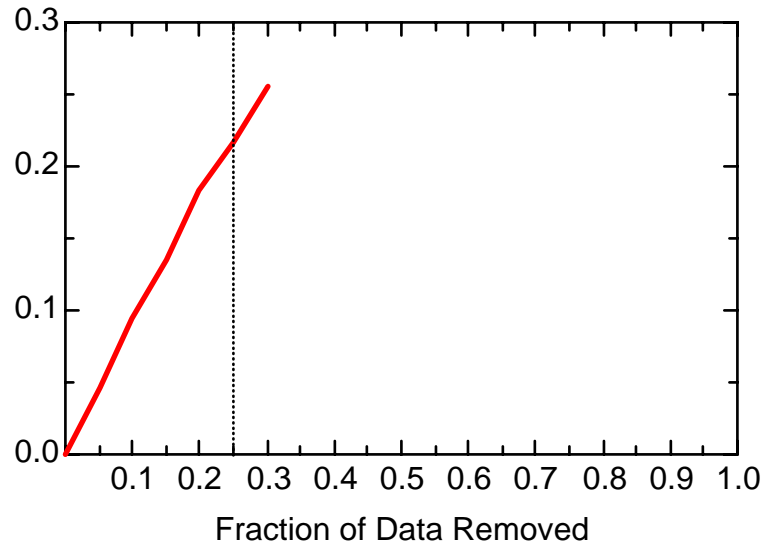
BZ: Well JMW1881



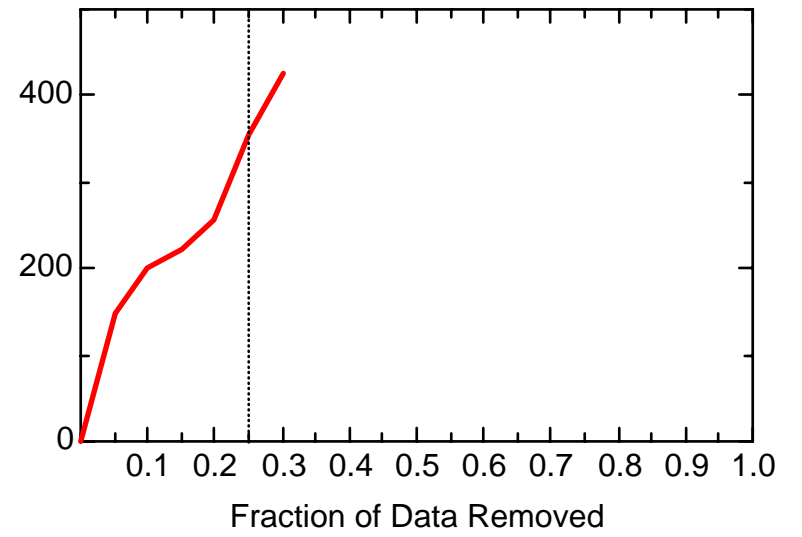
BZ: Well JMW1881



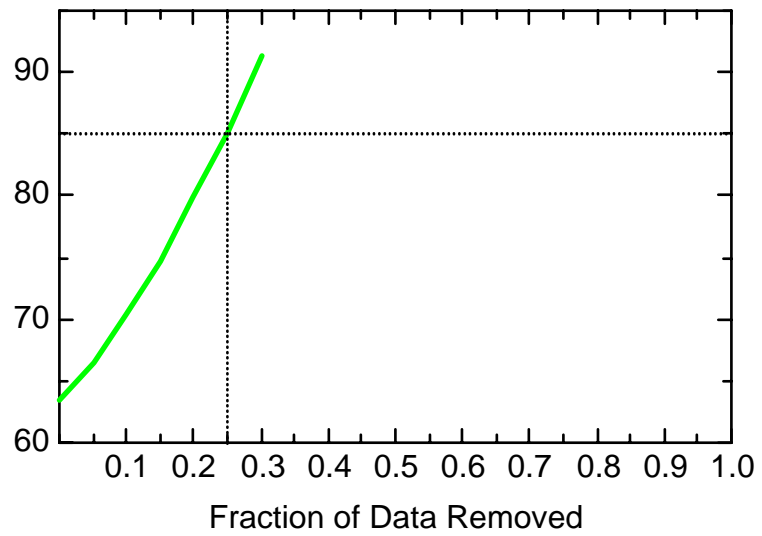
BZ: Well JMW1960



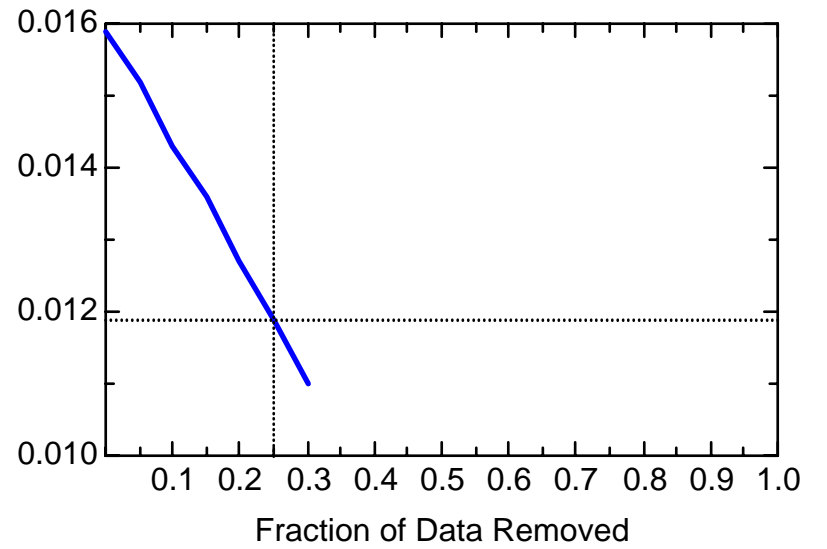
BZ: Well JMW1960



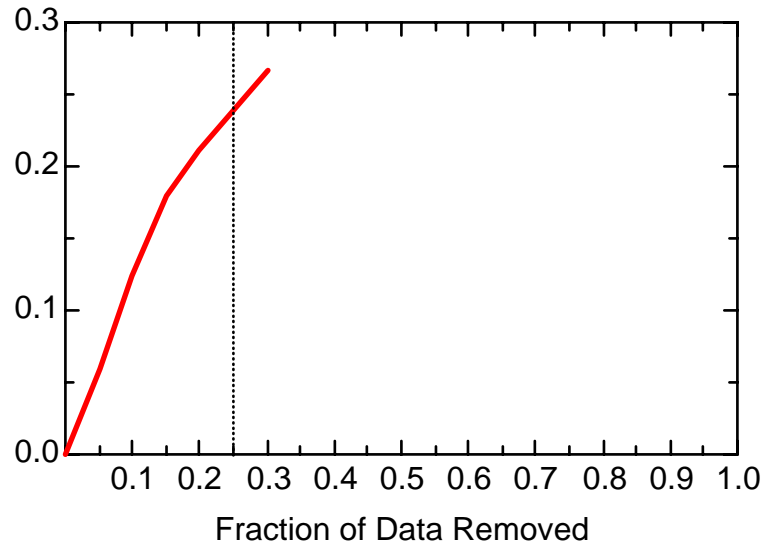
BZ: Well JMW1960



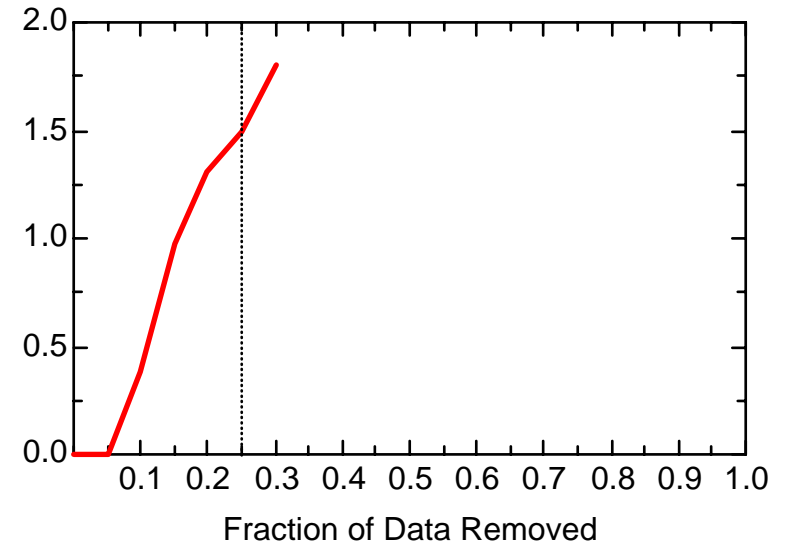
BZ: Well JMW1960



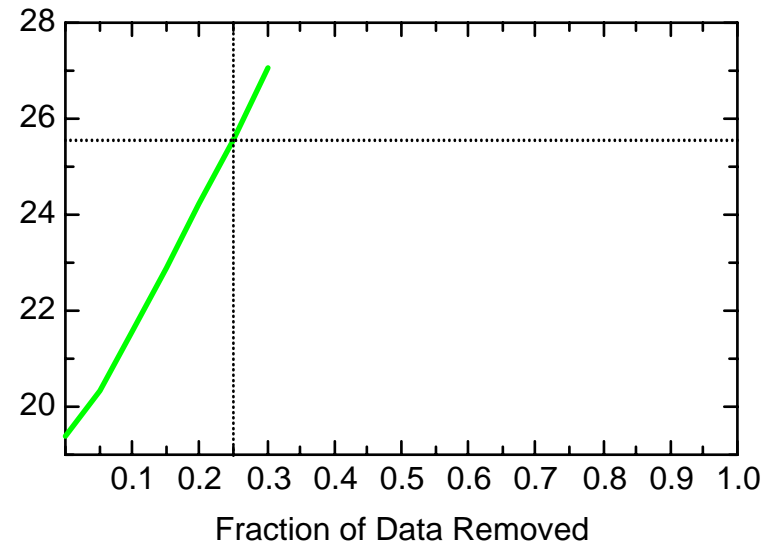
BZ: Well JMW1963



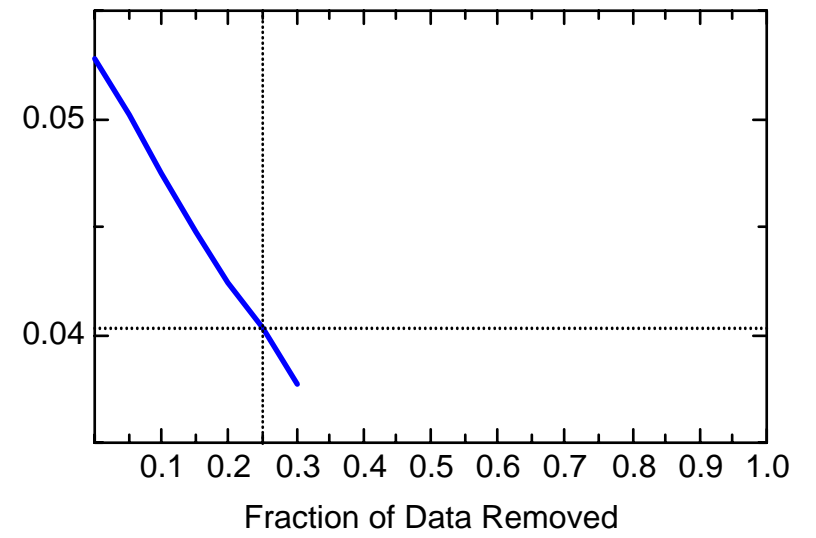
BZ: Well JMW1963



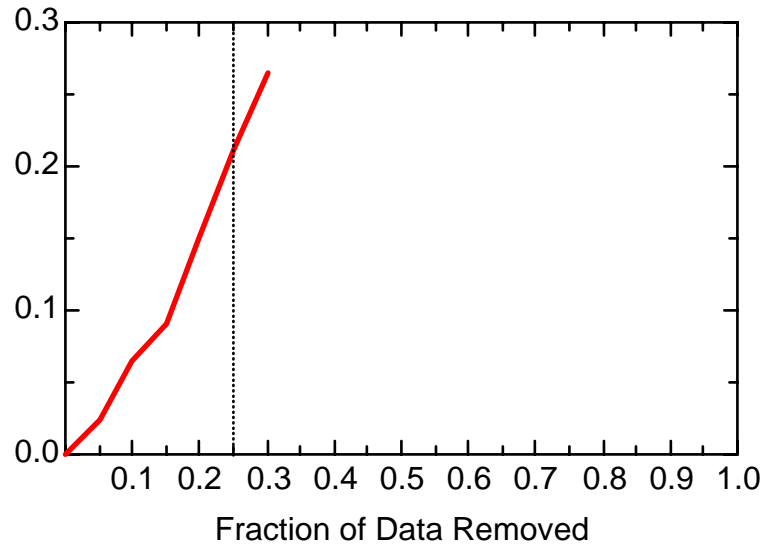
BZ: Well JMW1963



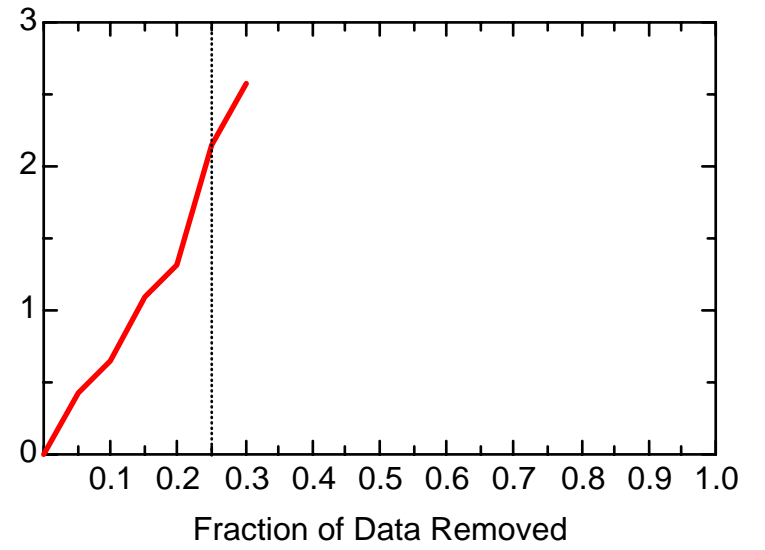
BZ: Well JMW1963



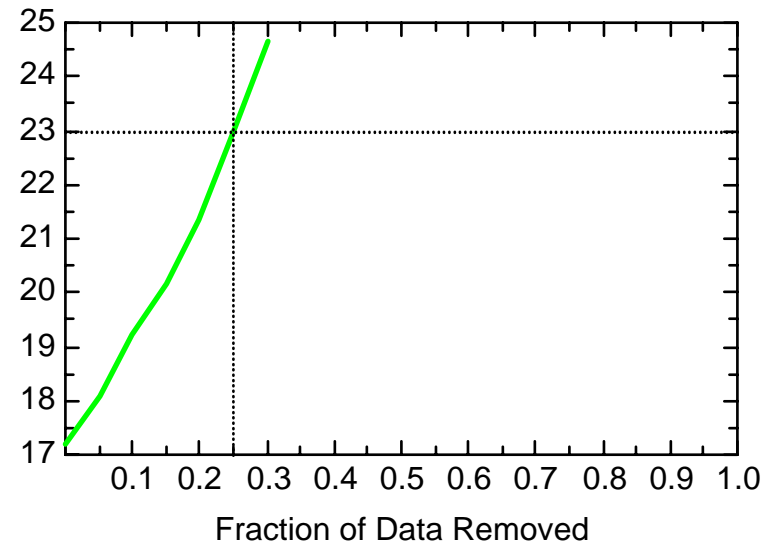
BZ: Well JMW1964



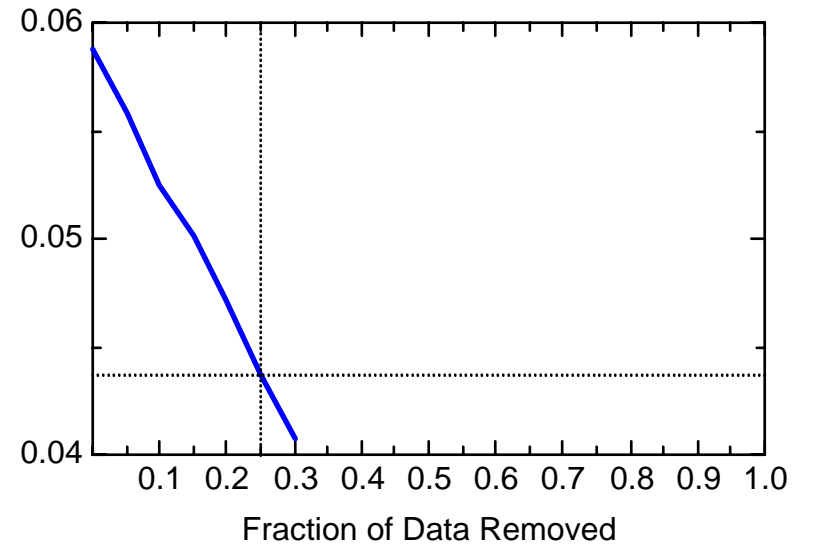
BZ: Well JMW1964



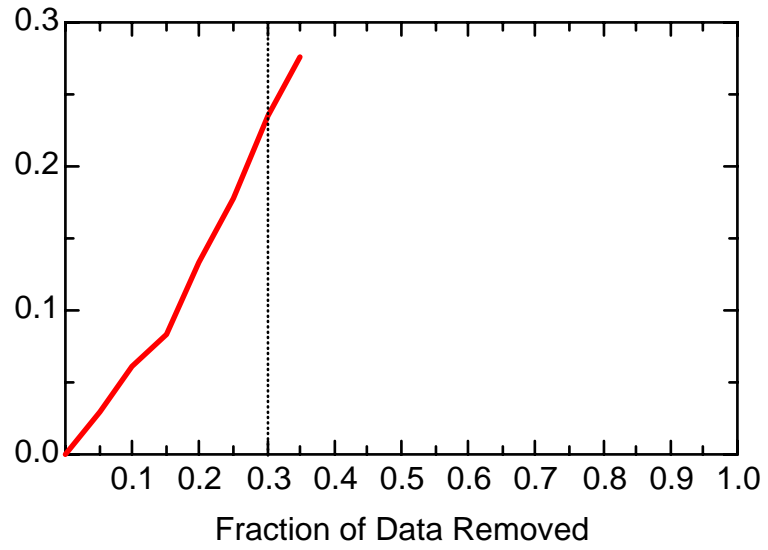
BZ: Well JMW1964



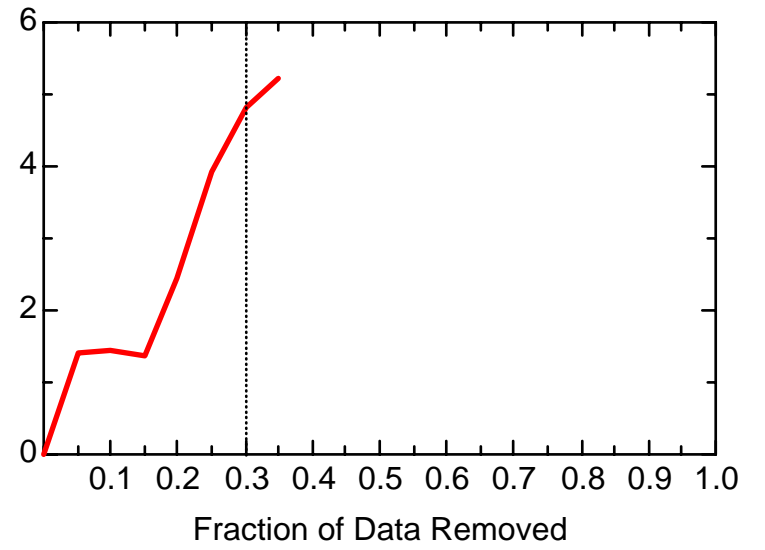
BZ: Well JMW1964



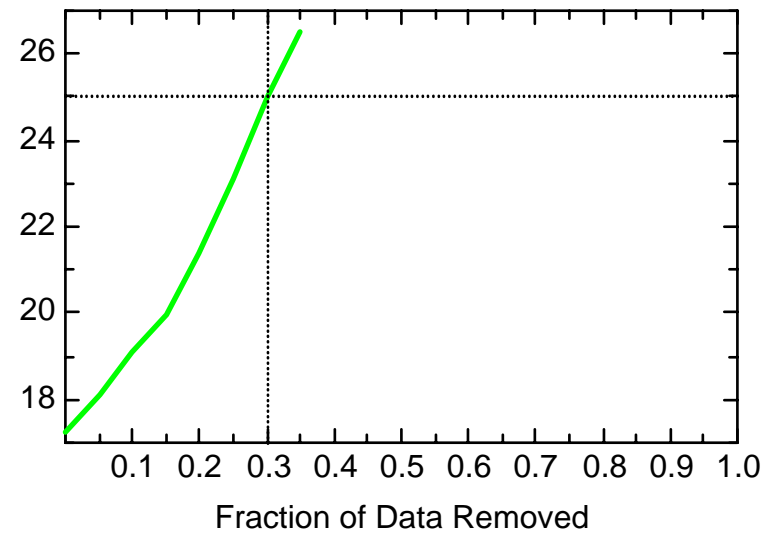
BZ: Well JMW1966



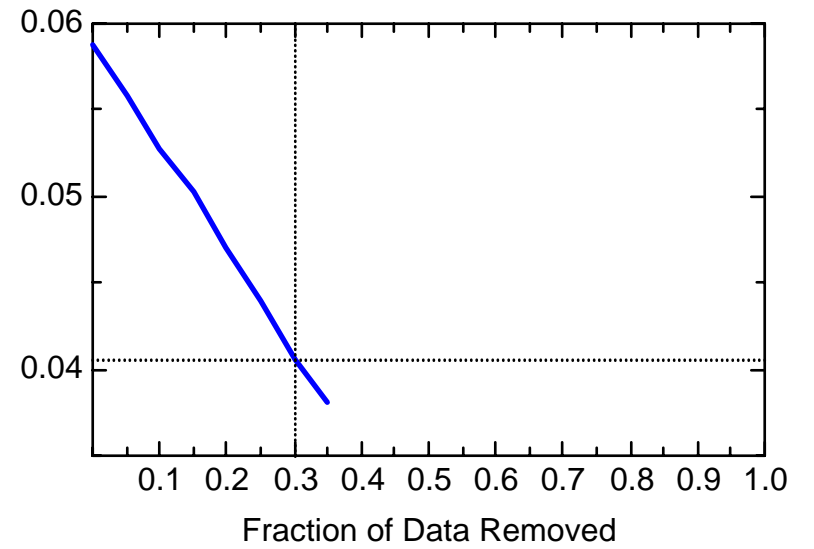
BZ: Well JMW1966



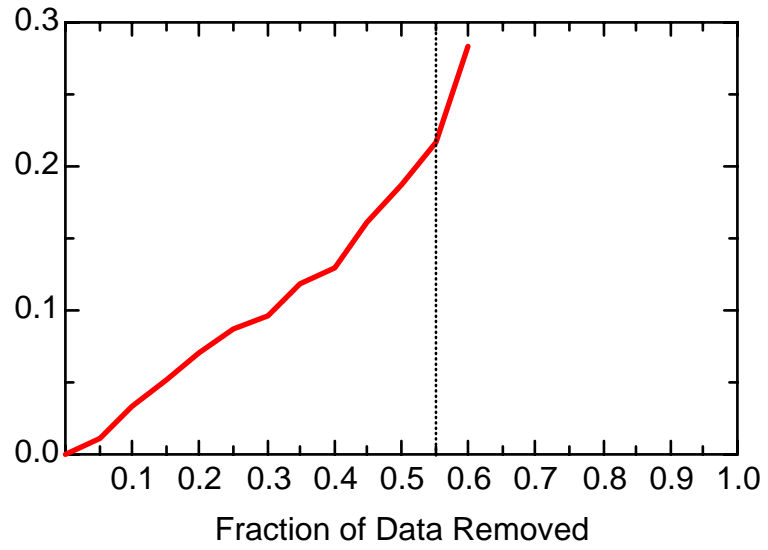
BZ: Well JMW1966



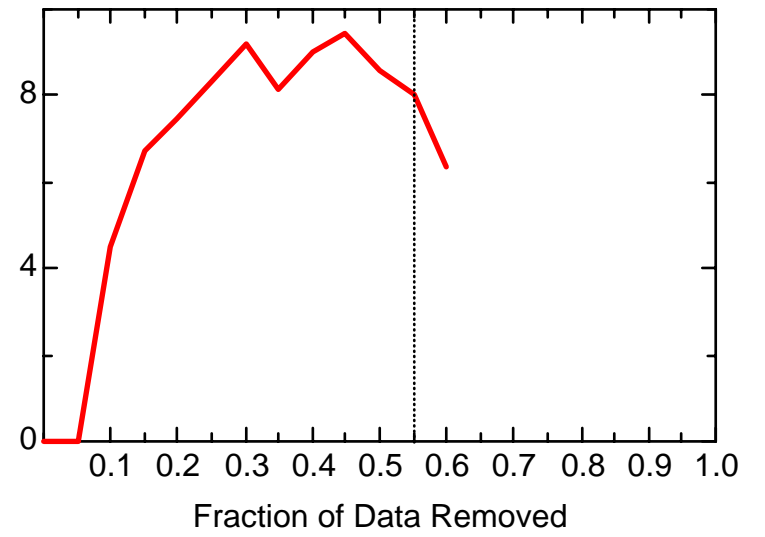
BZ: Well JMW1966



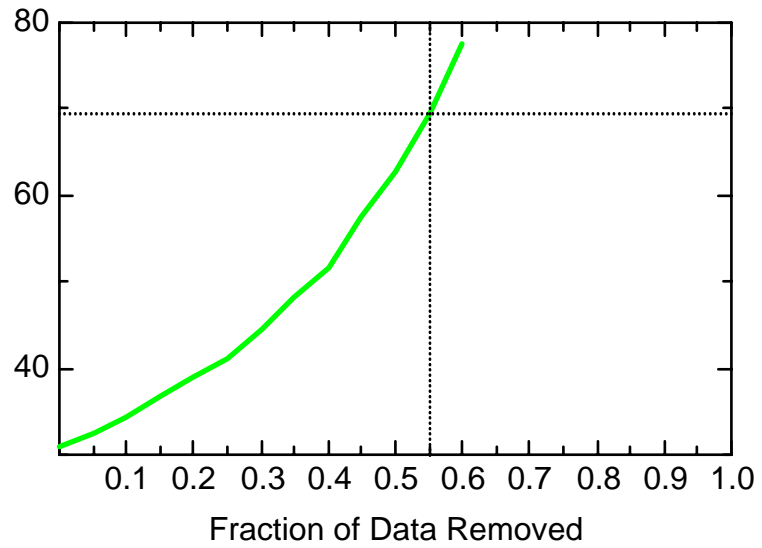
BZ: Well JMW3202



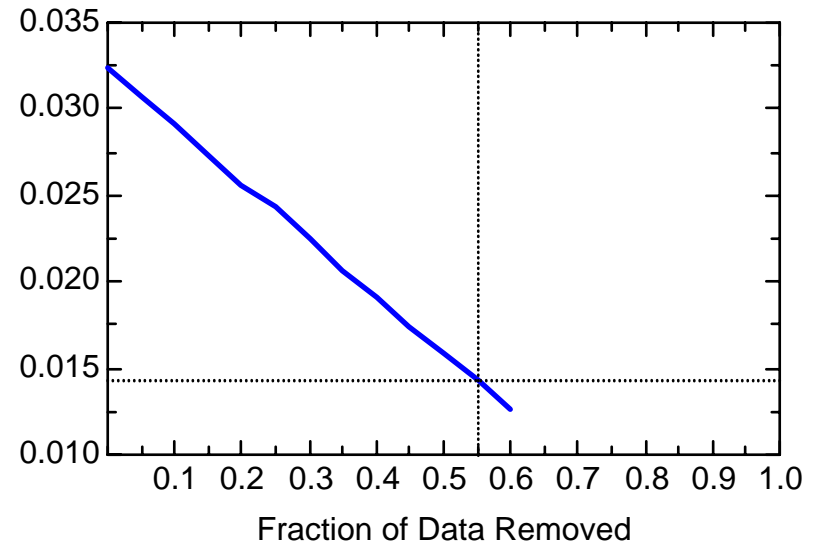
BZ: Well JMW3202



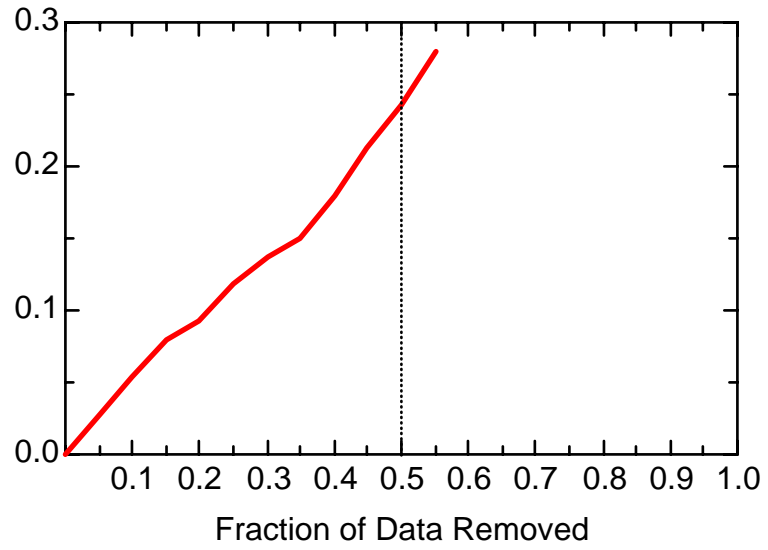
BZ: Well JMW3202



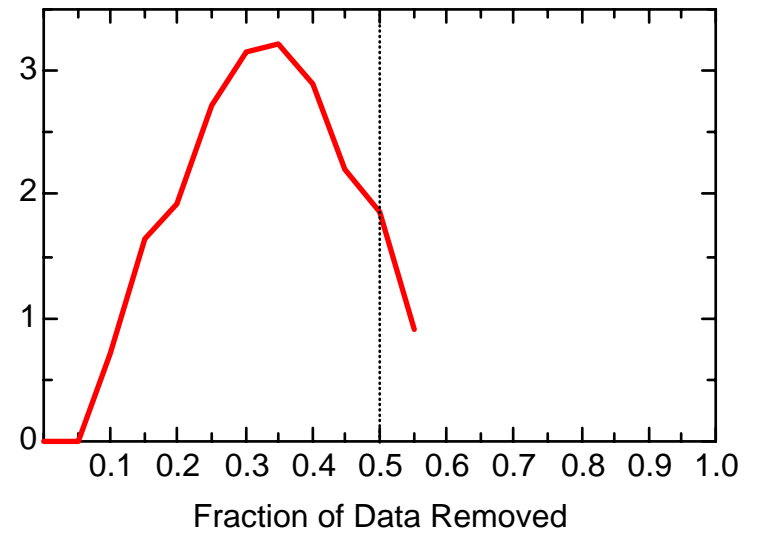
BZ: Well JMW3202



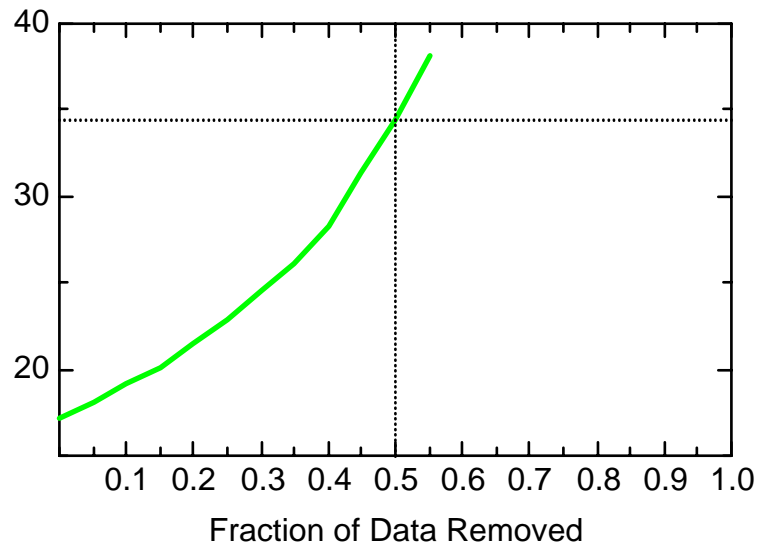
BZ: Well JMW6001



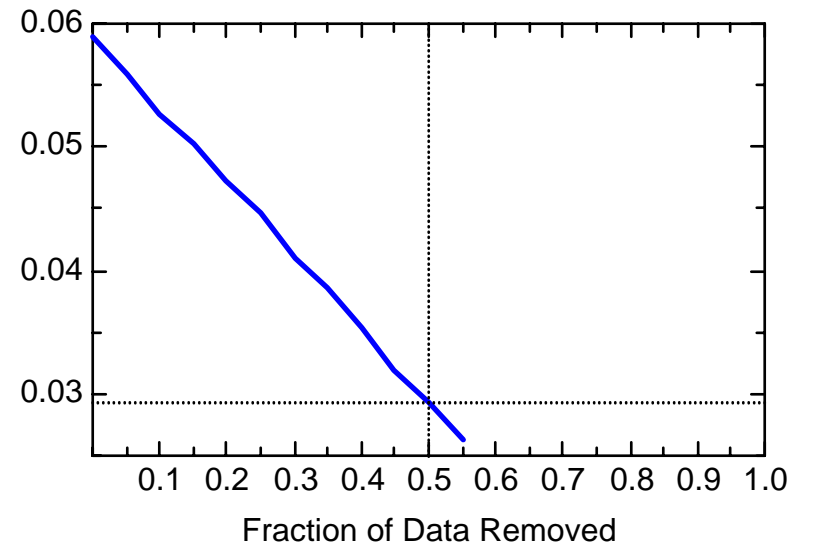
BZ: Well JMW6001



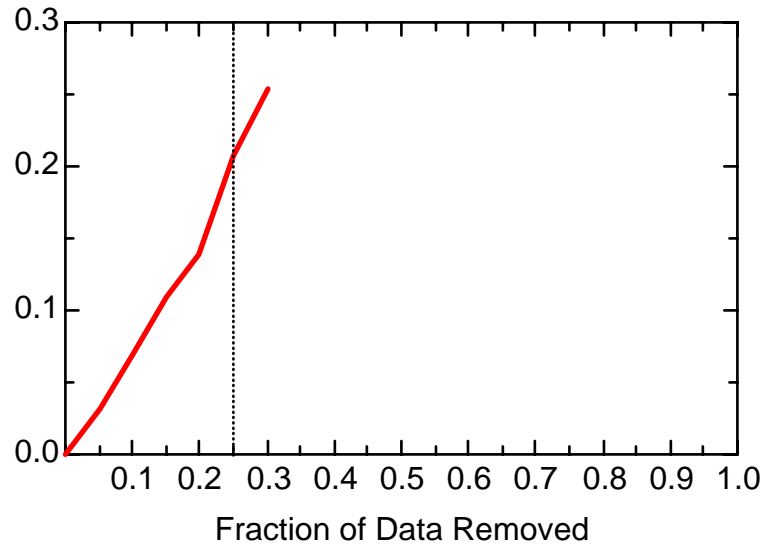
BZ: Well JMW6001



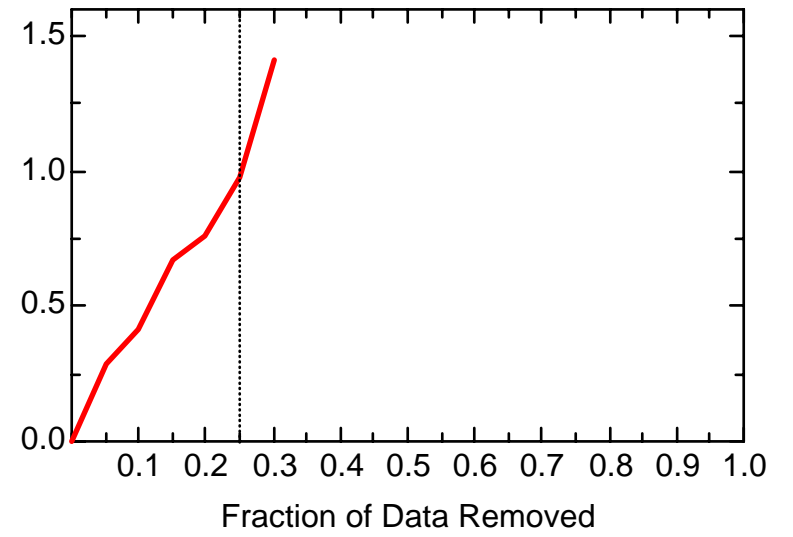
BZ: Well JMW6001



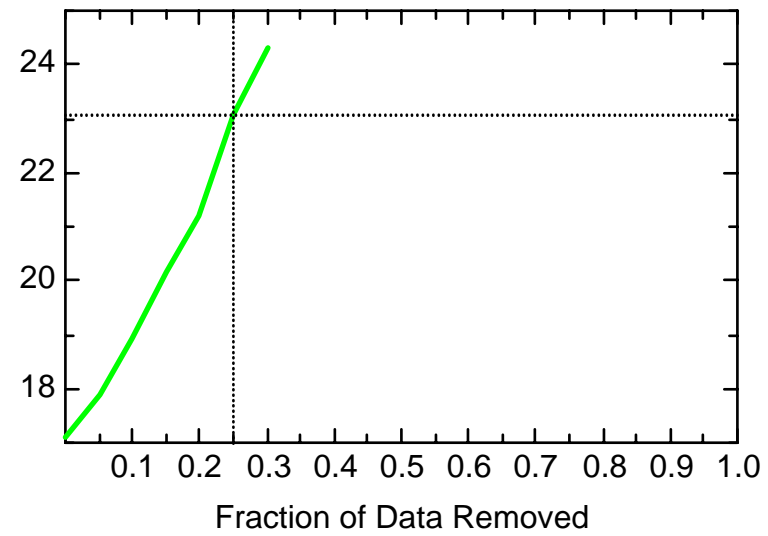
BZ: Well JMW7612



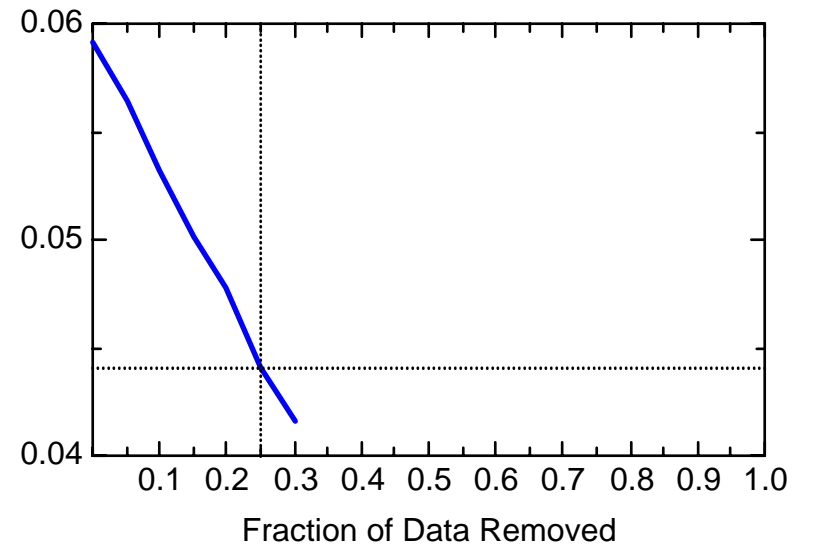
BZ: Well JMW7612



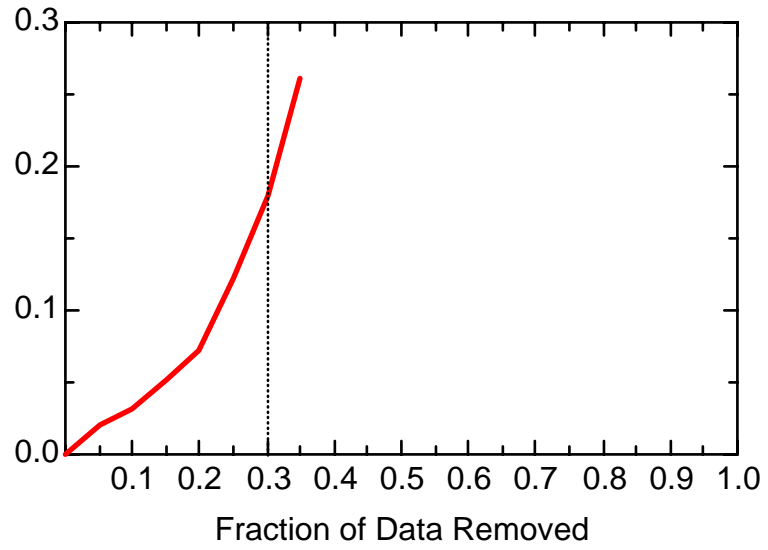
BZ: Well JMW7612



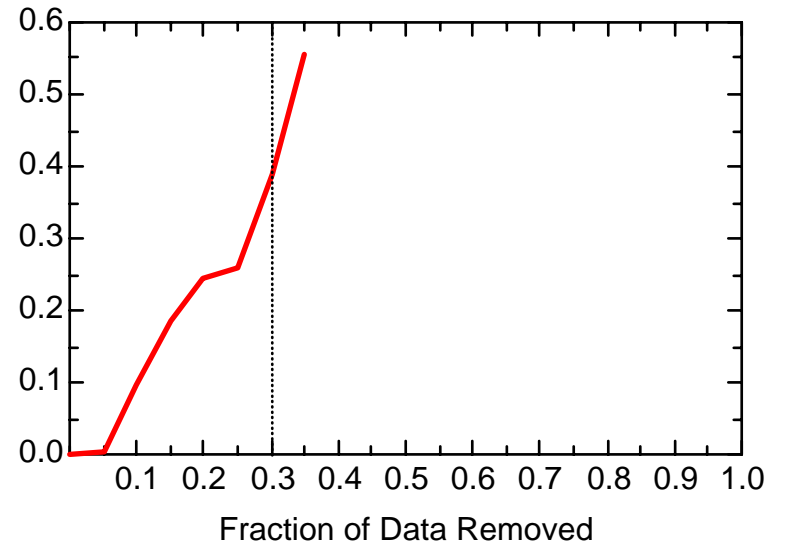
BZ: Well JMW7612



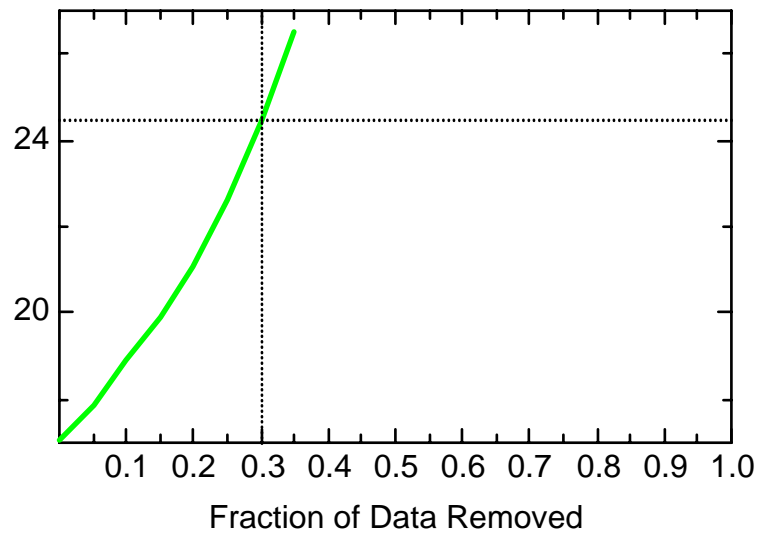
BZ: Well JPZ0340



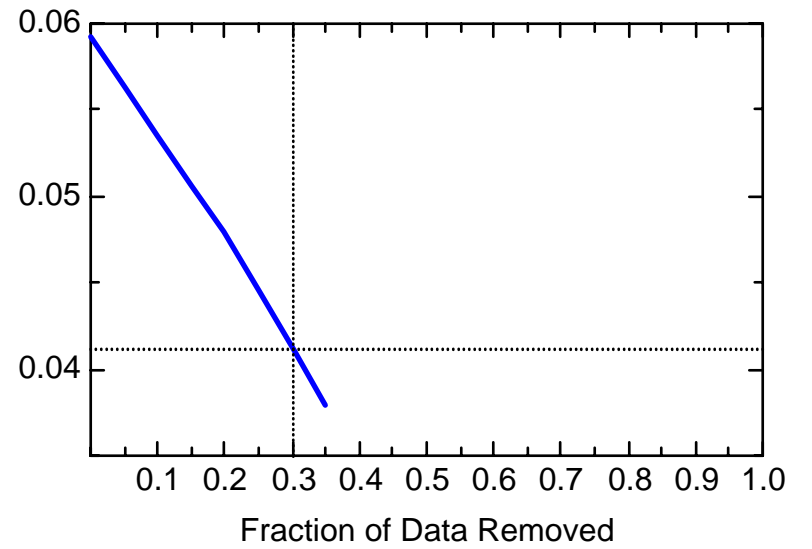
BZ: Well JPZ0340



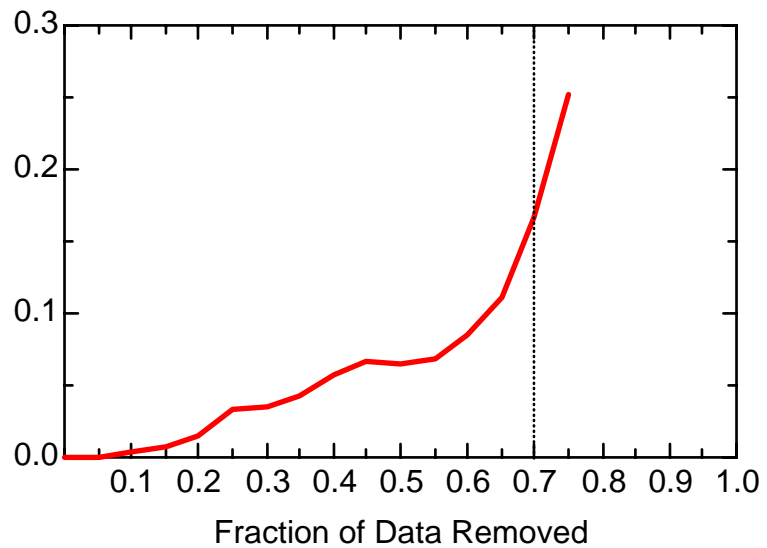
BZ: Well JPZ0340



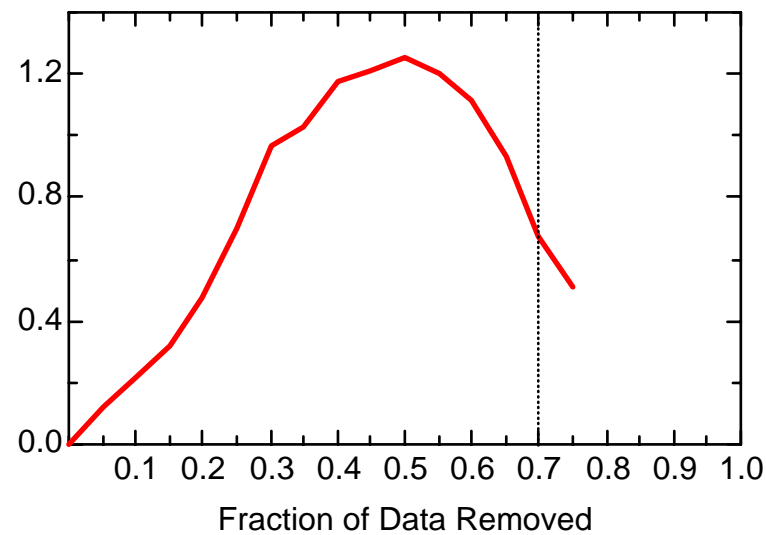
BZ: Well JPZ0340



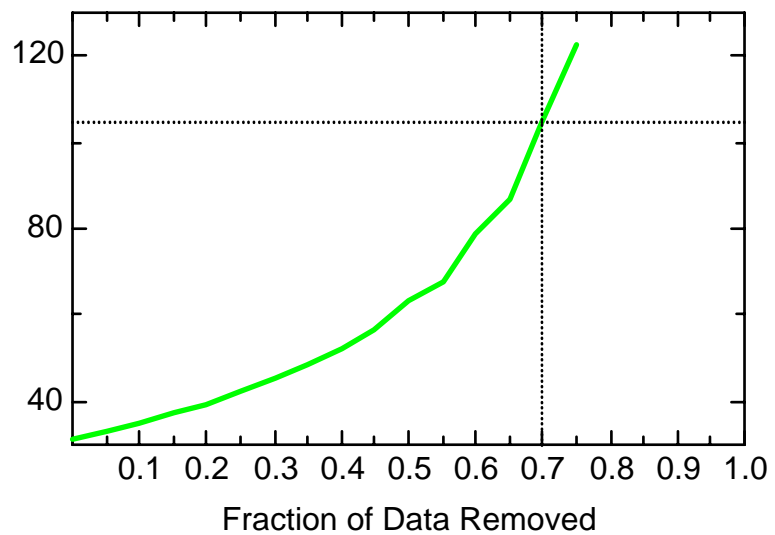
BZ: Well JPZ0342



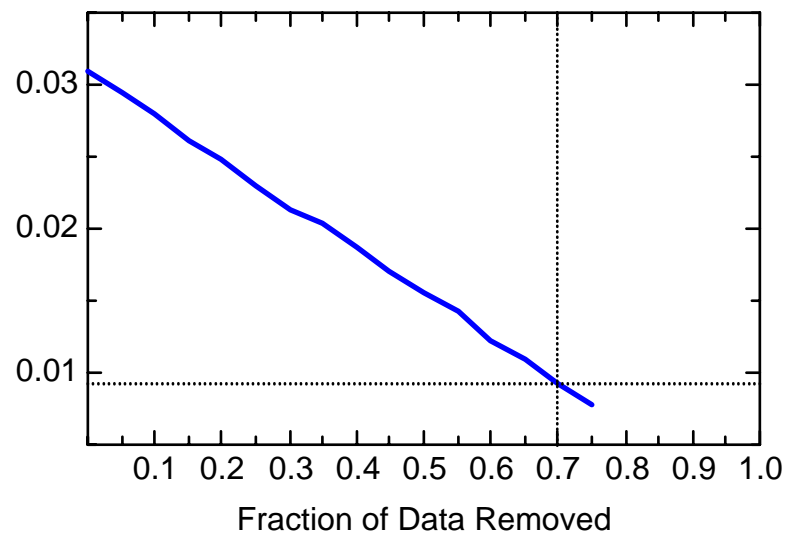
BZ: Well JPZ0342



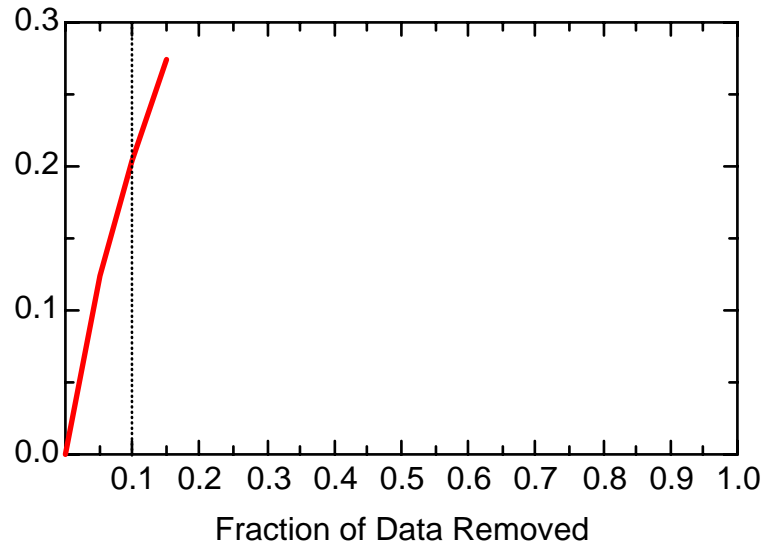
BZ: Well JPZ0342



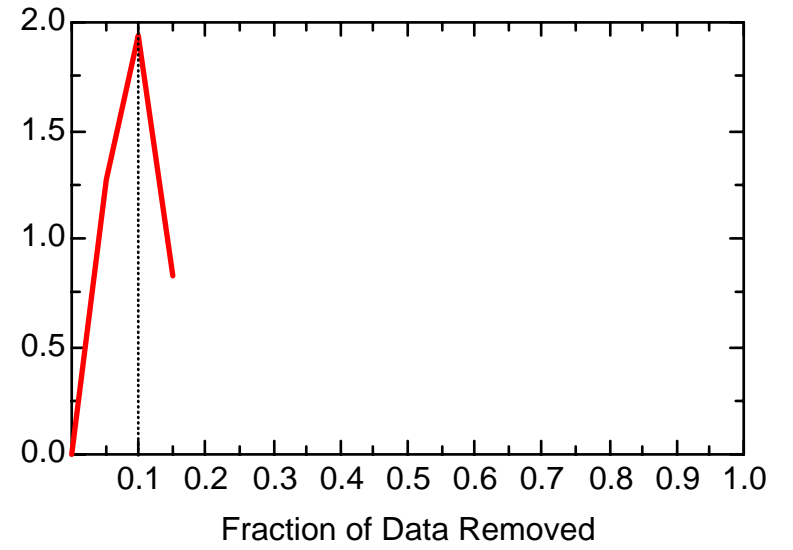
BZ: Well JPZ0342



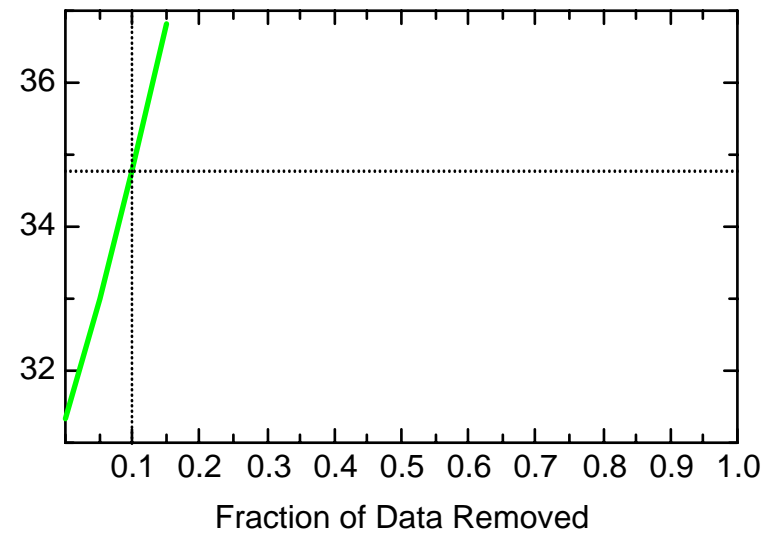
BZ: Well JPZ0343



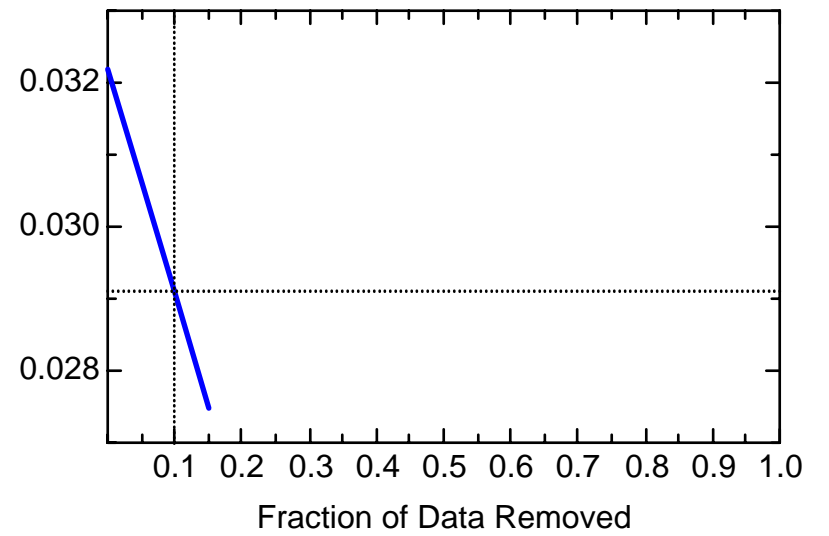
BZ: Well JPZ0343



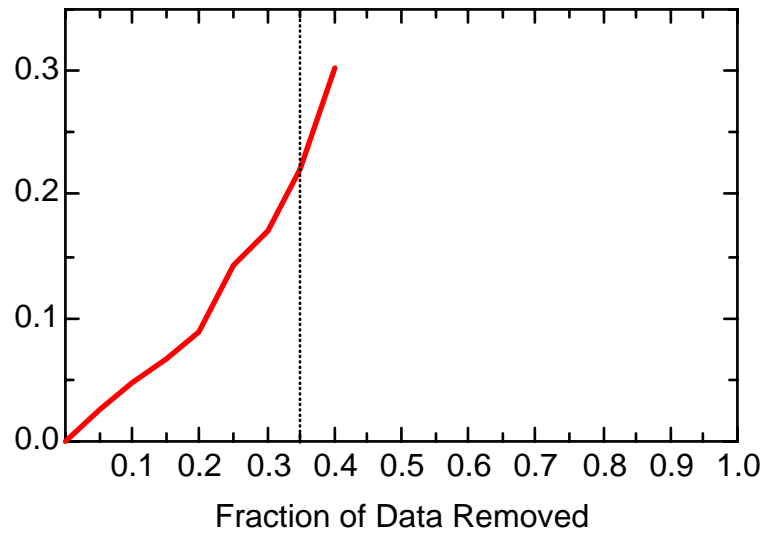
BZ: Well JPZ0343



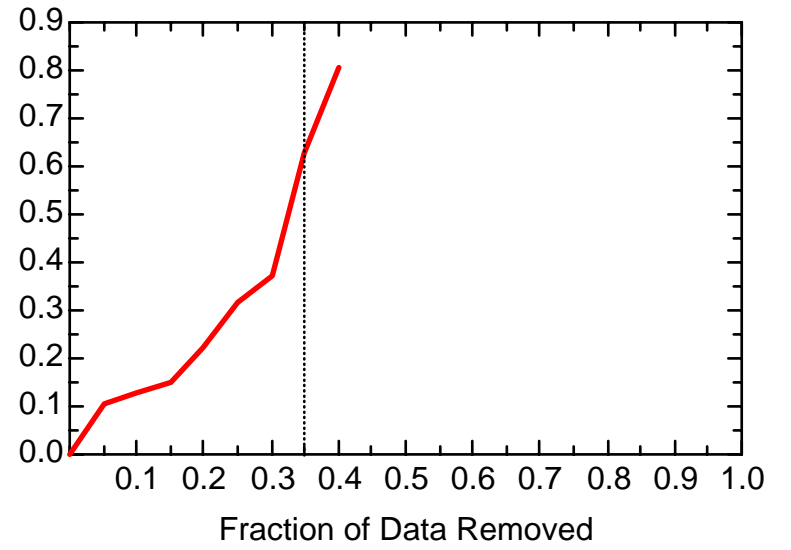
BZ: Well JPZ0343



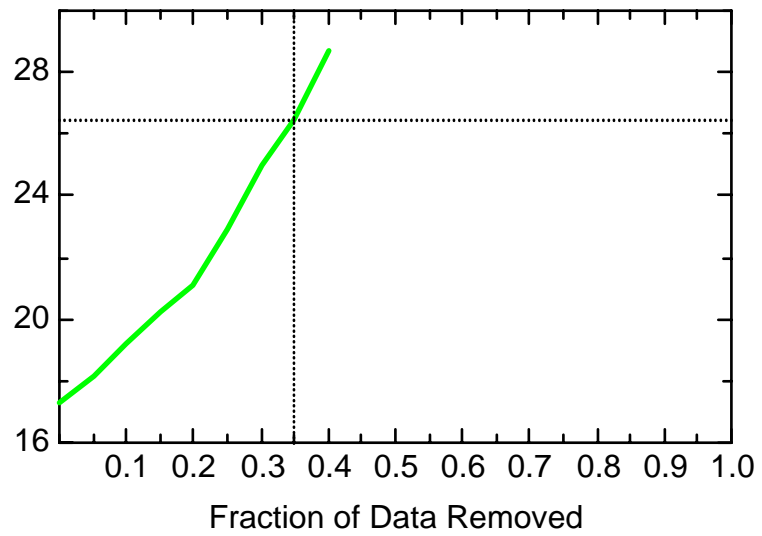
BZ: Well JPZ0348



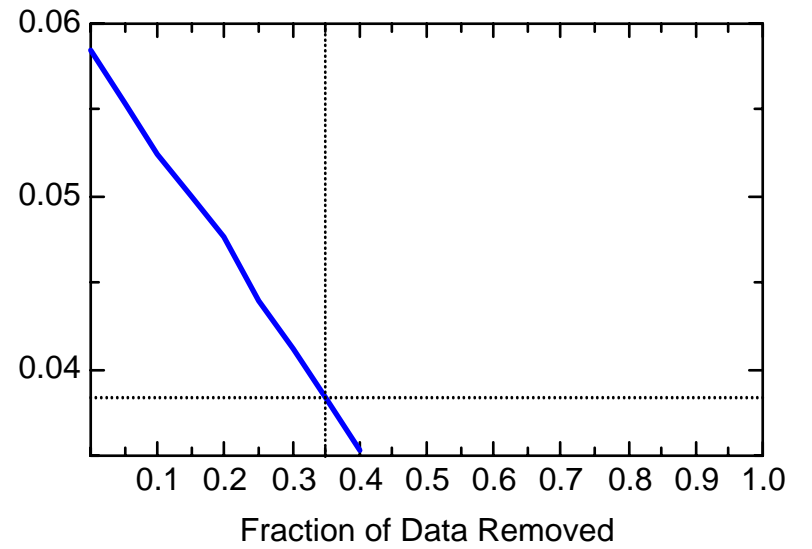
BZ: Well JPZ0348



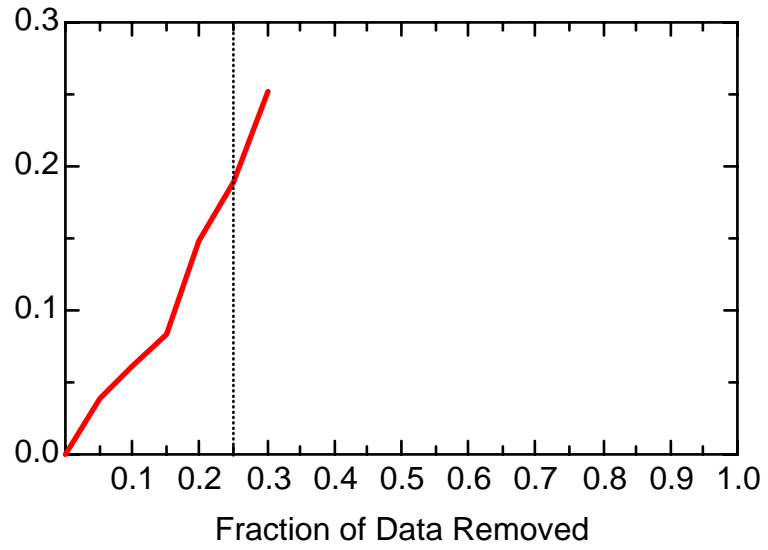
BZ: Well JPZ0348



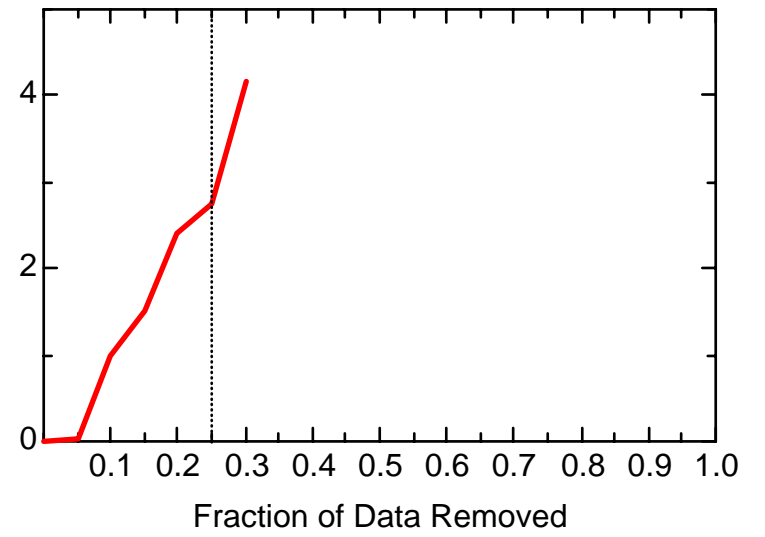
BZ: Well JPZ0348



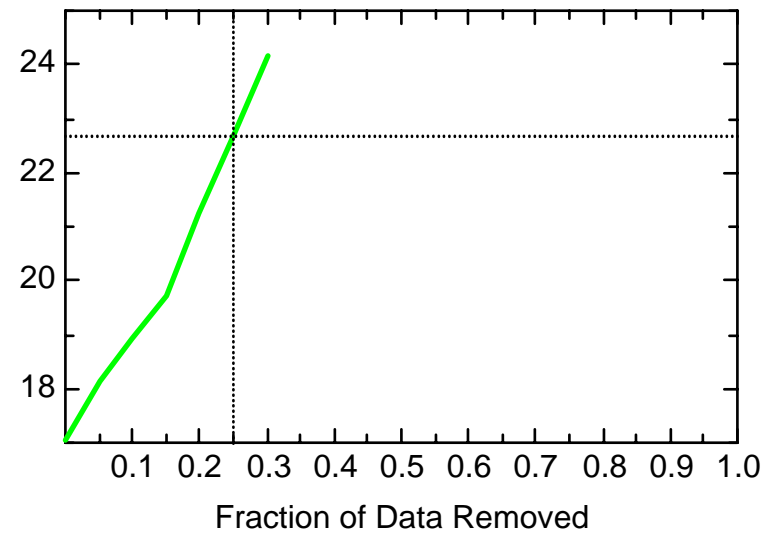
BZ: Well JPZ7312



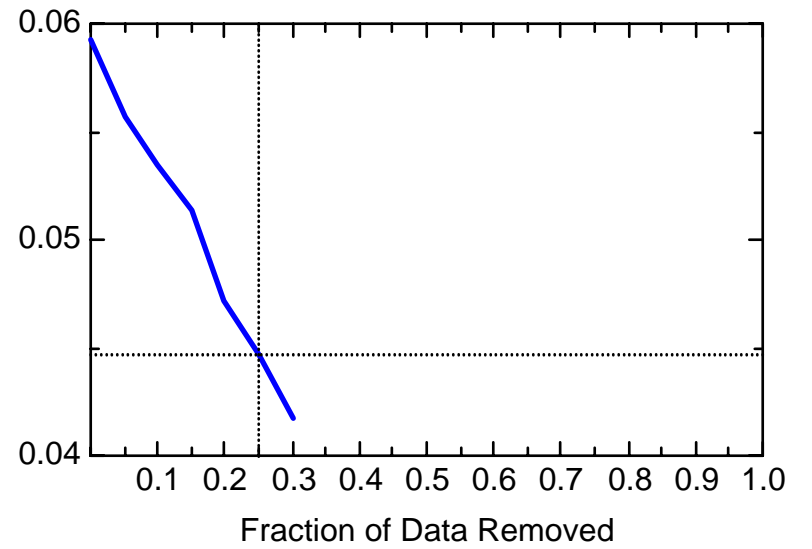
BZ: Well JPZ7312



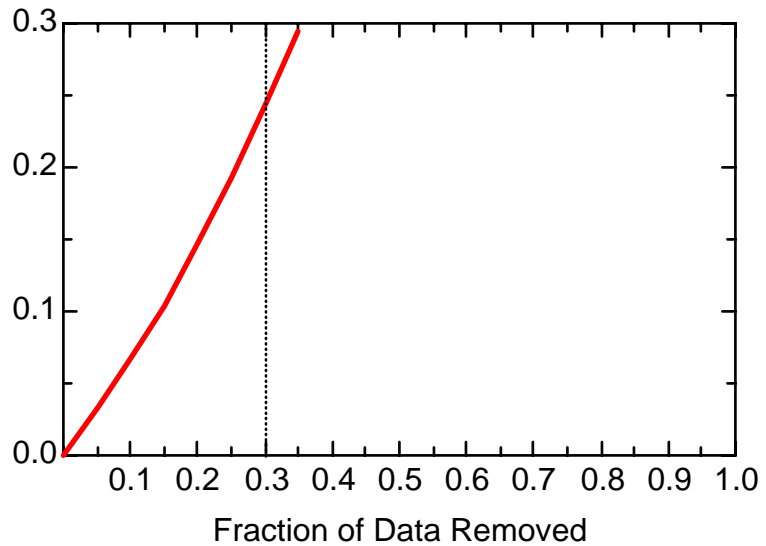
BZ: Well JPZ7312



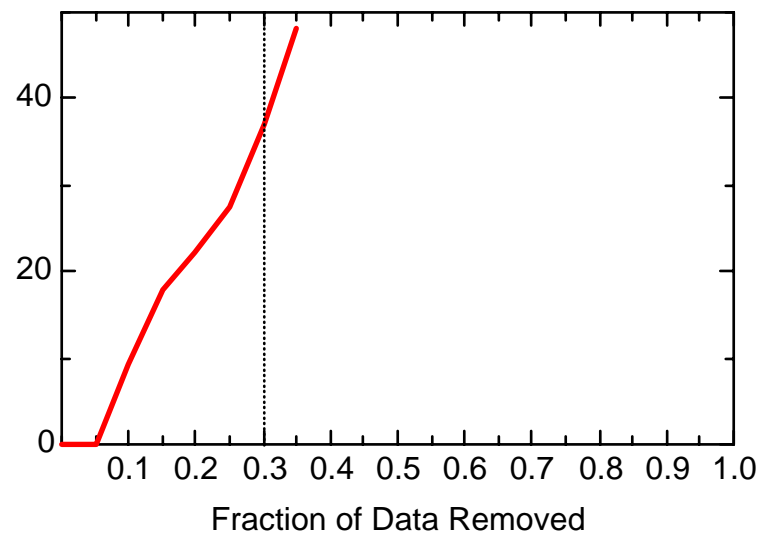
BZ: Well JPZ7312



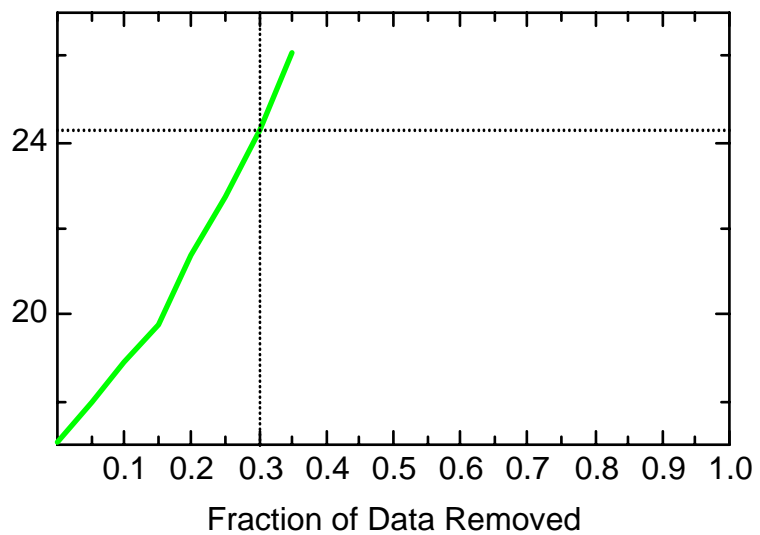
BZ: Well MMW0005



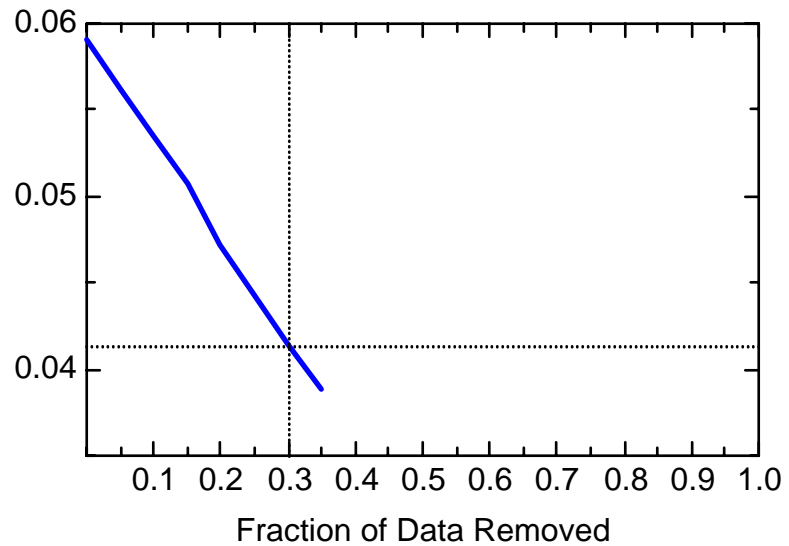
BZ: Well MMW0005



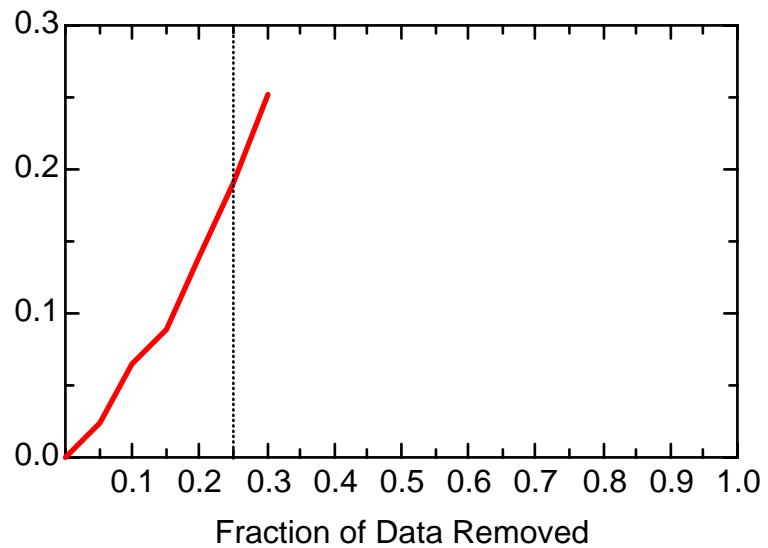
BZ: Well MMW0005



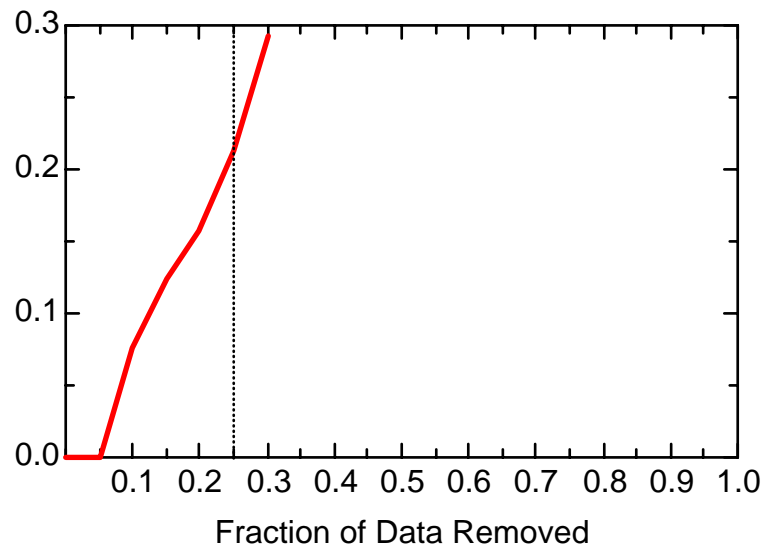
BZ: Well MMW0005



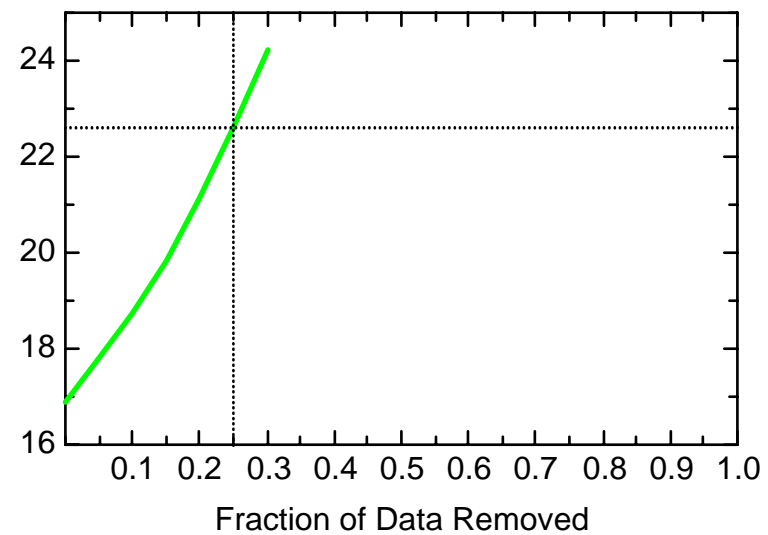
BZ: Well MMW0009



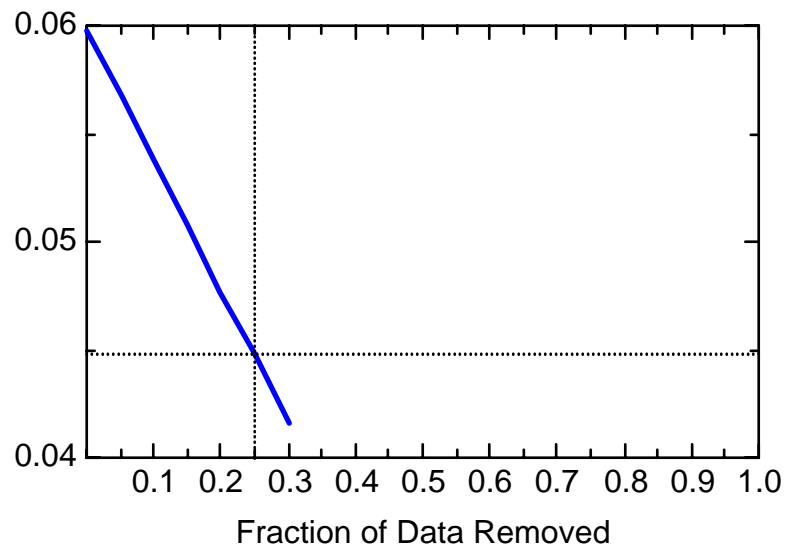
BZ: Well MMW0009



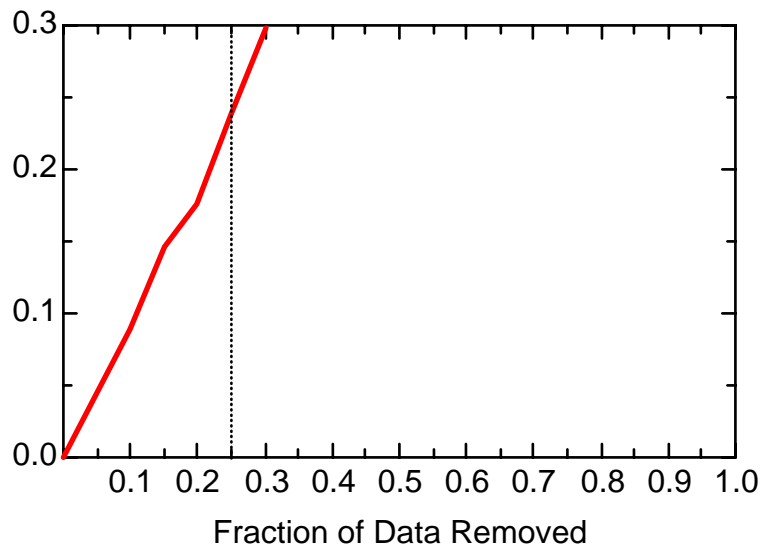
BZ: Well MMW0009



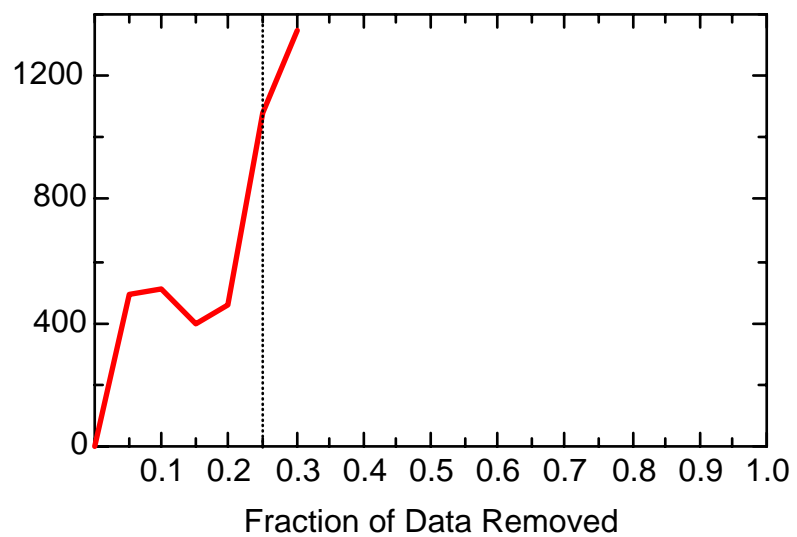
BZ: Well MMW0009



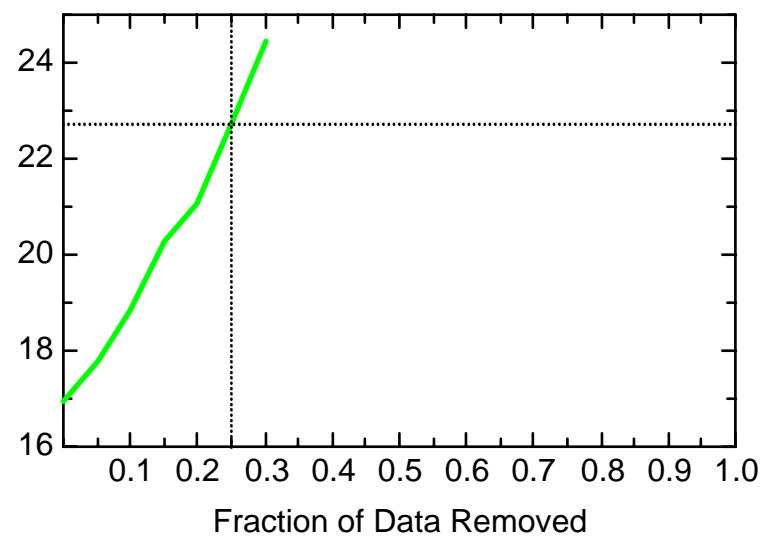
BZ: Well MMW1560



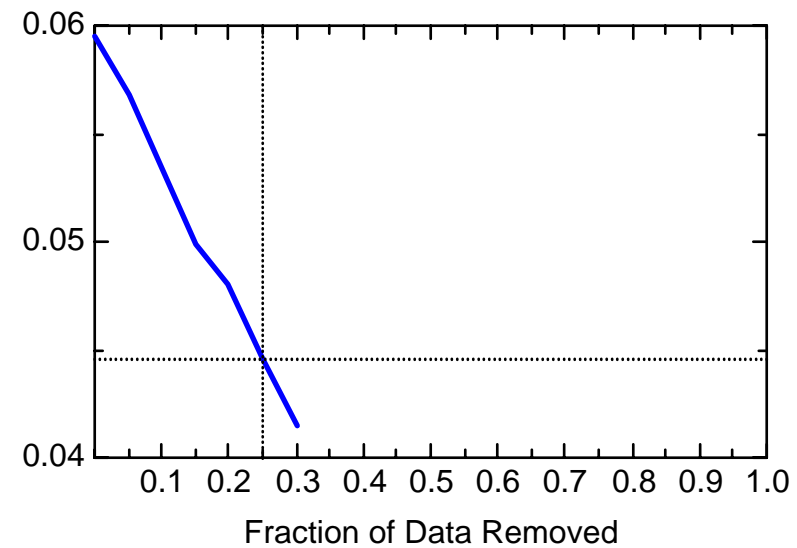
BZ: Well MMW1560



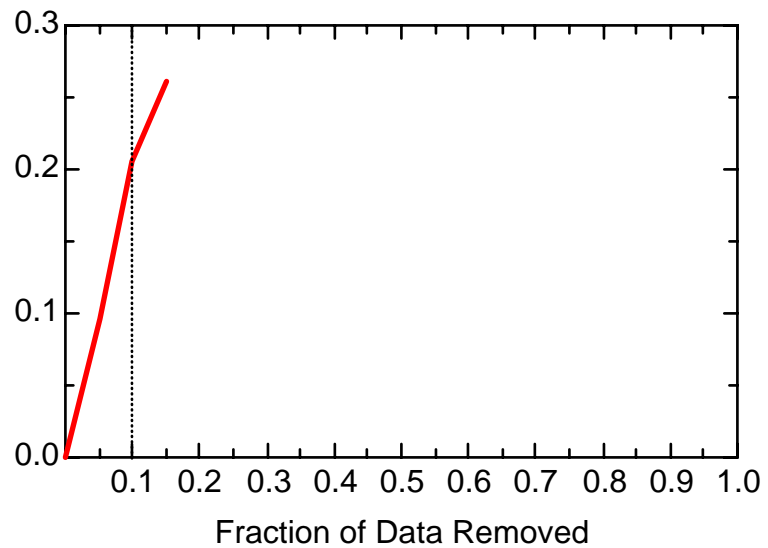
BZ: Well MMW1560



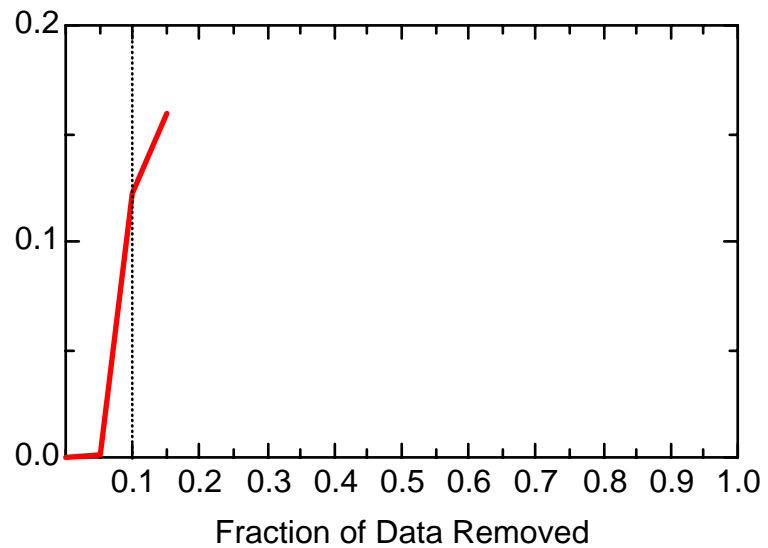
BZ: Well MMW1560



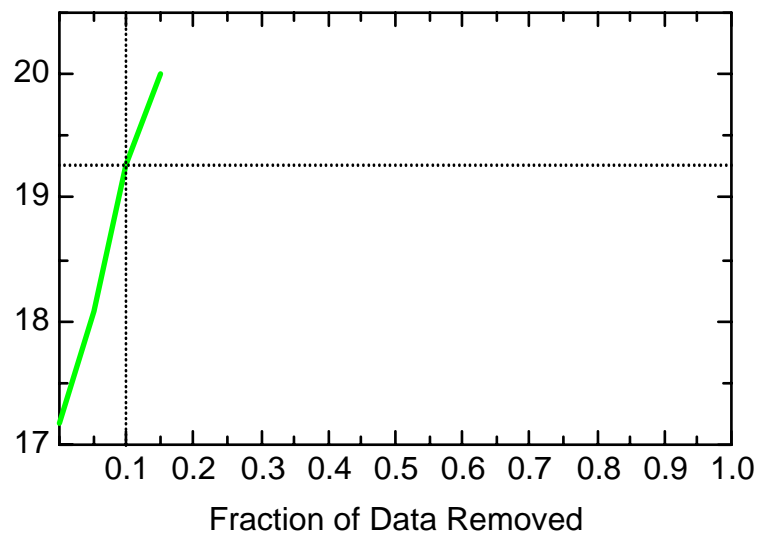
BZ: Well MMW7330



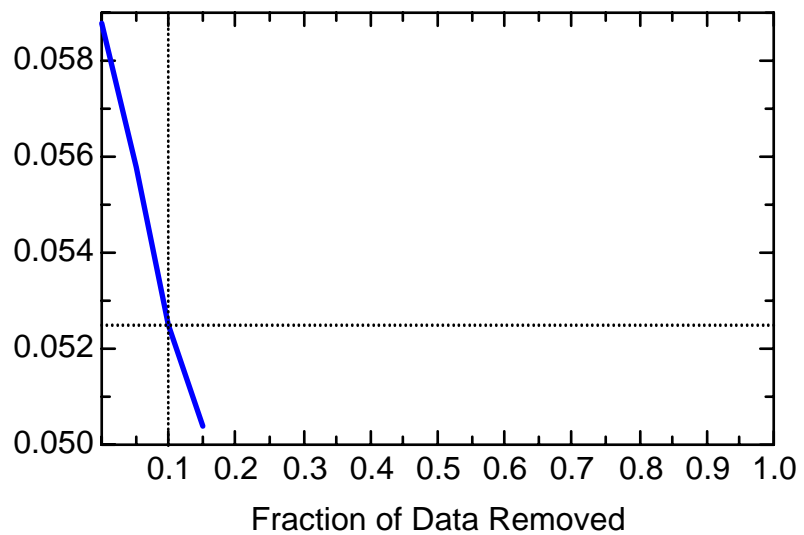
BZ: Well MMW7330



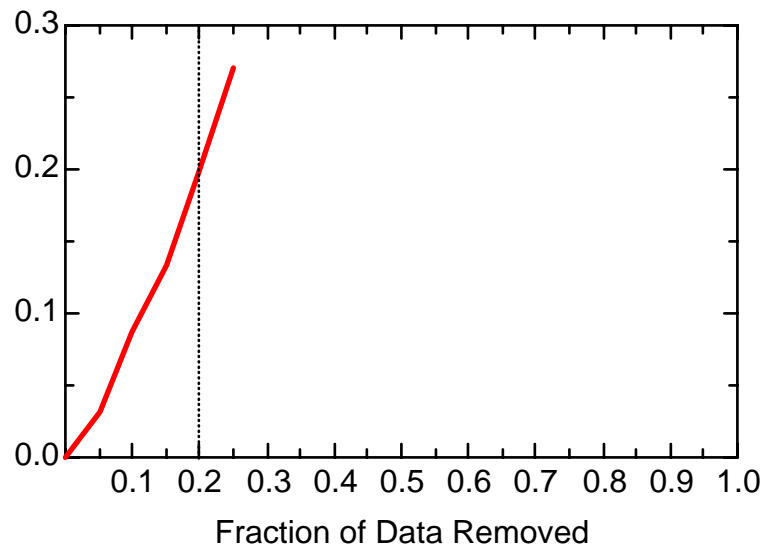
BZ: Well MMW7330



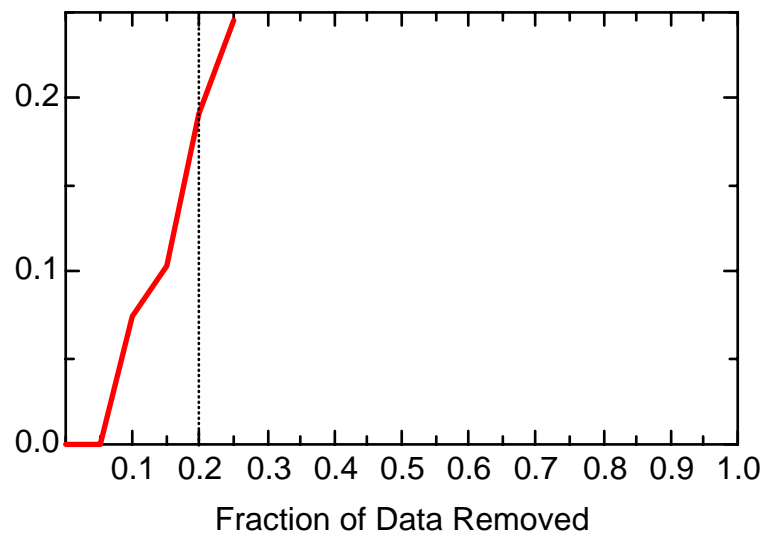
BZ: Well MMW7330



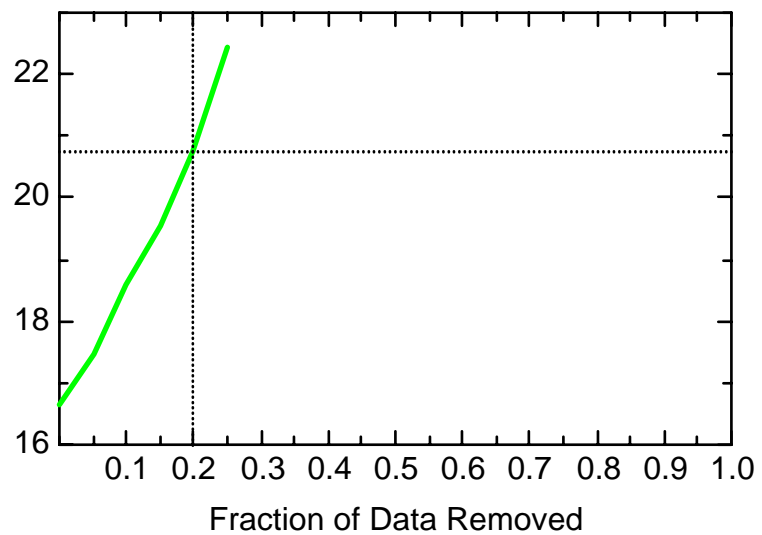
BZ: Well MMW8015



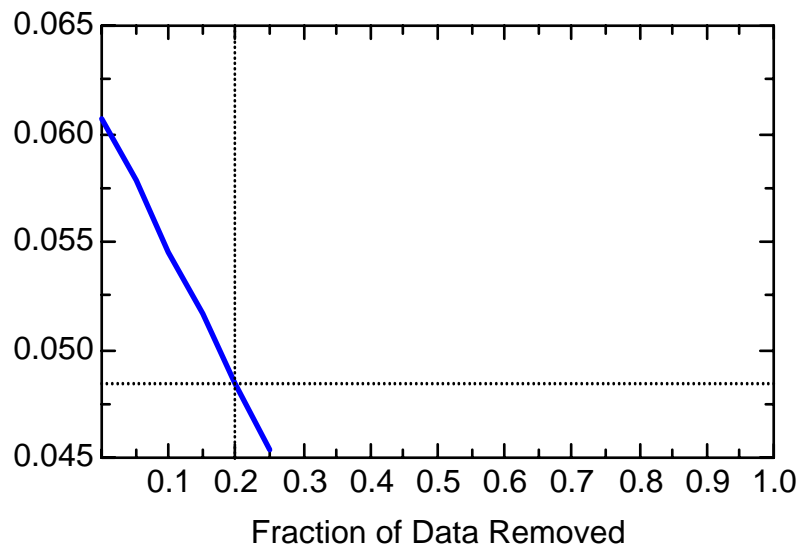
BZ: Well MMW8015



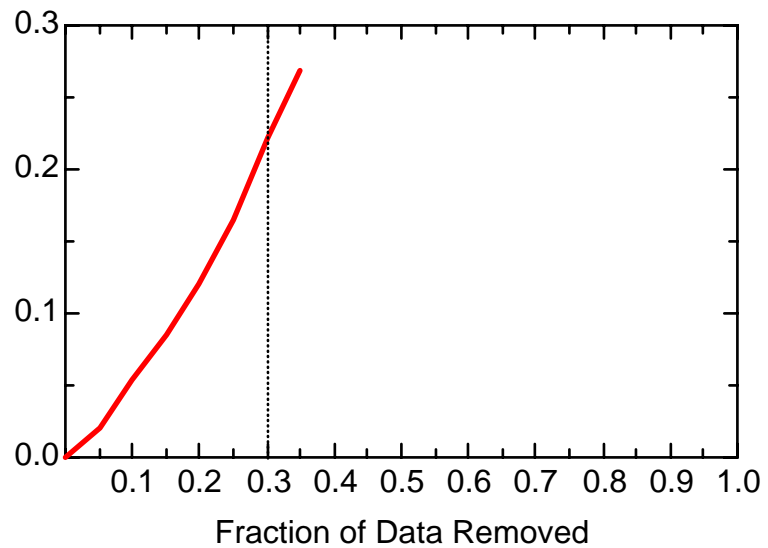
BZ: Well MMW8015



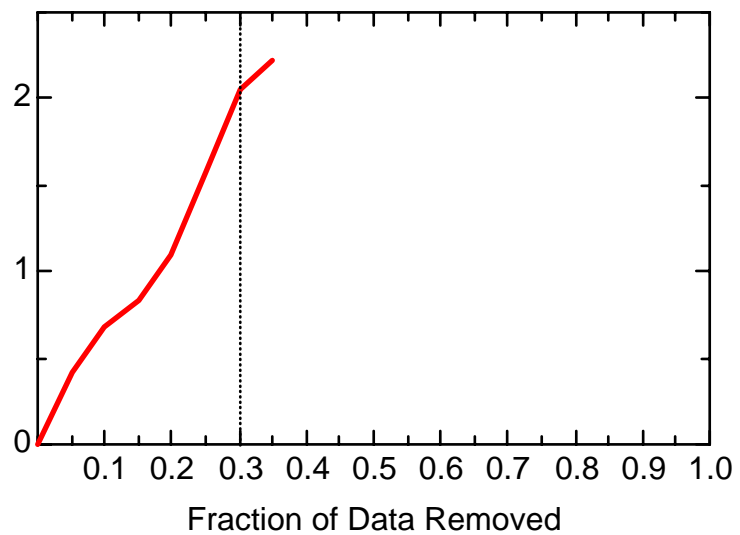
BZ: Well MMW8015



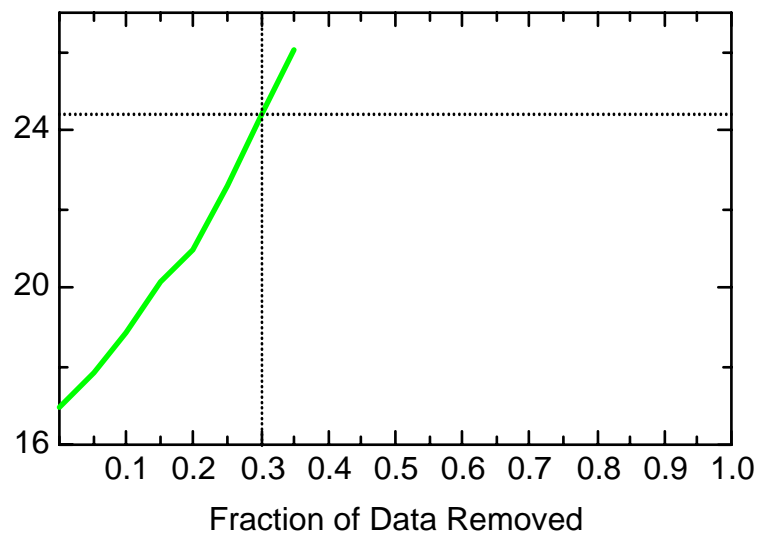
BZ: Well RFW1144



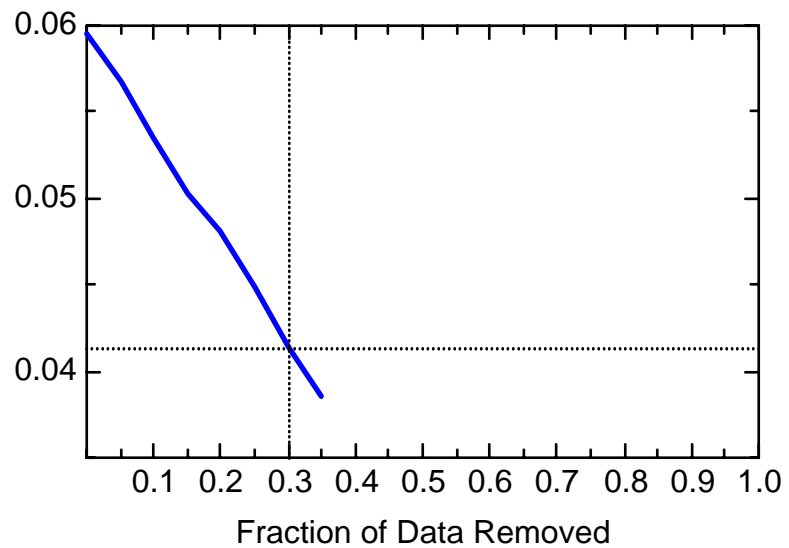
BZ: Well RFW1144



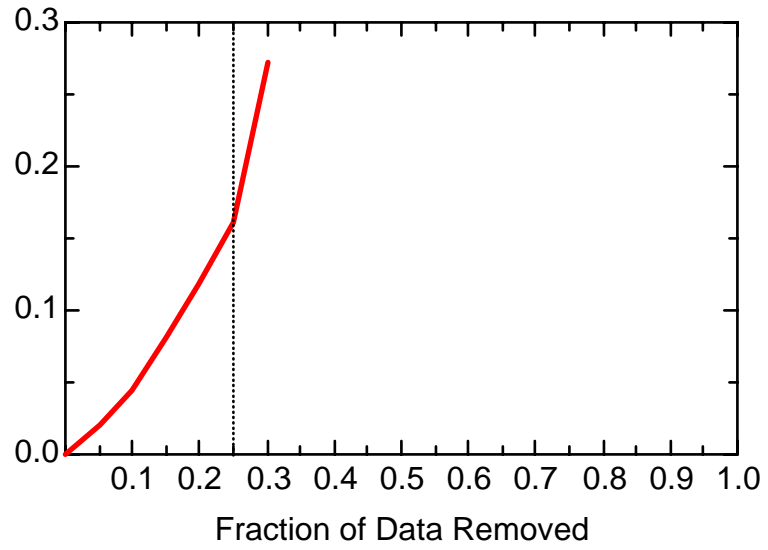
BZ: Well RFW1144



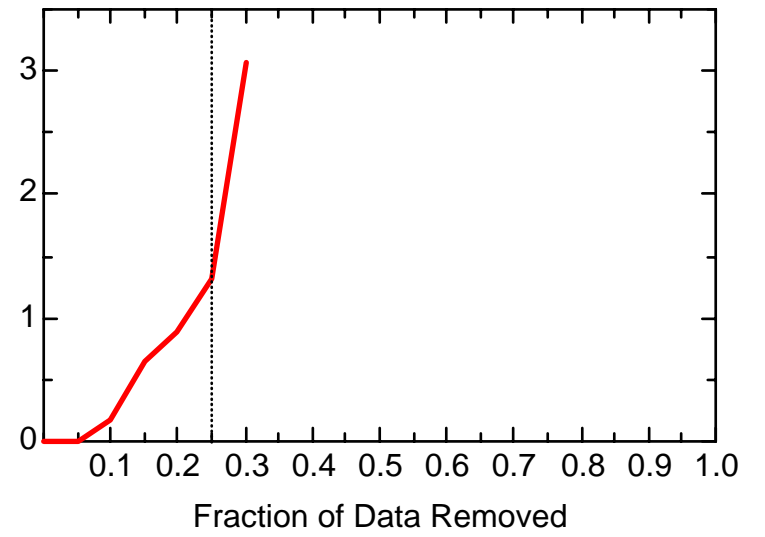
BZ: Well RFW1144



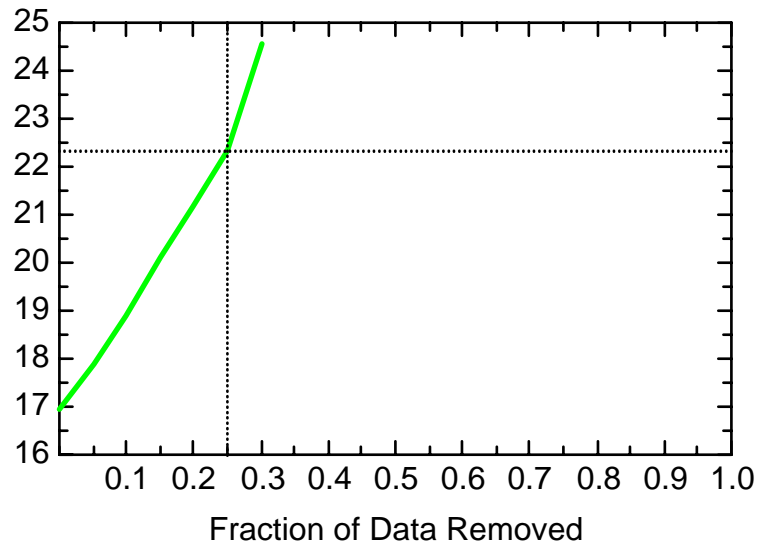
BZ: Well RFW1147



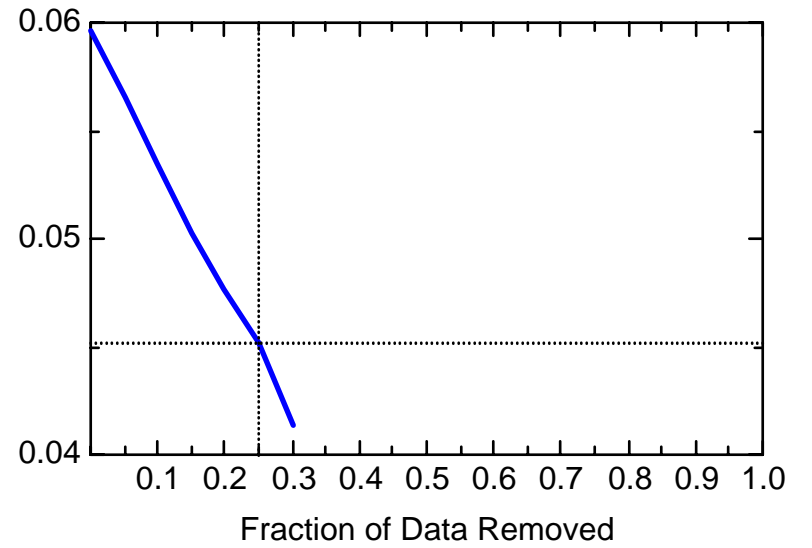
BZ: Well RFW1147



BZ: Well RFW1147



BZ: Well RFW1147



Appendix 3-3

Temporal Optimization

FE Iterative Fitting Results

Key to acronyms:

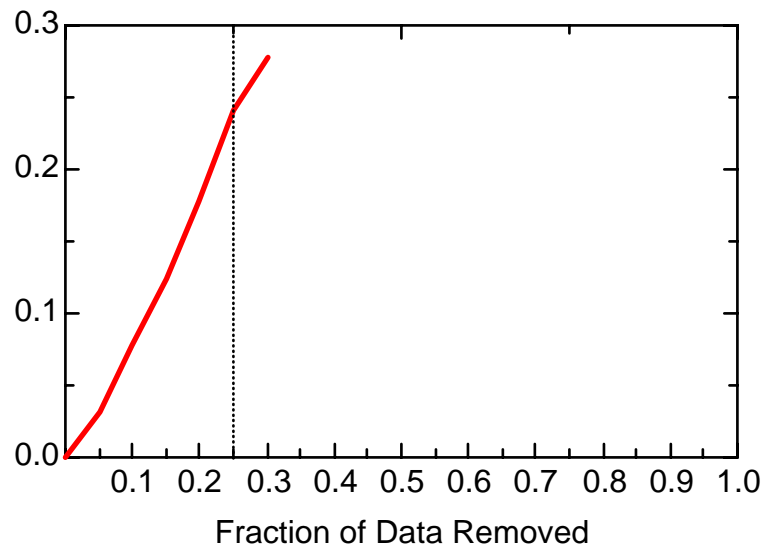
Fraction Outside Conf Bnds = Fraction of pointwise locally-weighted quadratic regression (LWQR) estimates from reduced data located beyond confidence bounds around LWQR fit on baseline data

Ave IQR of Iterative Fits = Mean interquartile range (averaged pointwise along the trend) of 500 LWQR fits computed on reduced dataset

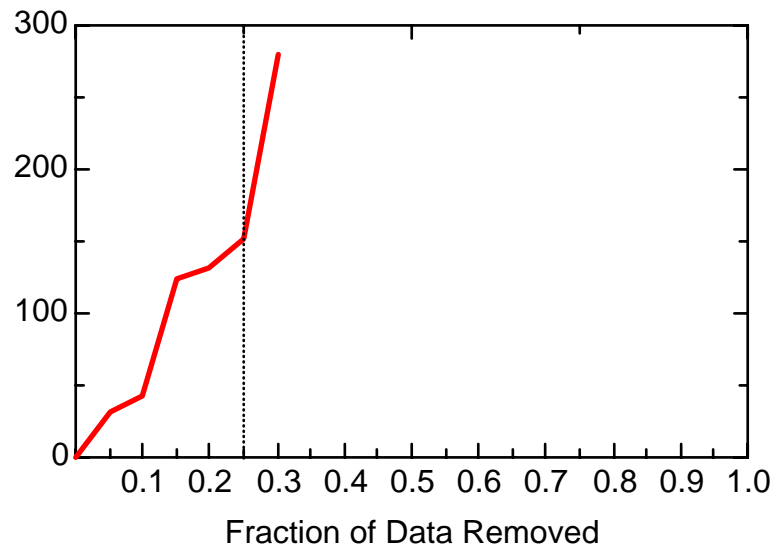
Opt Sampling Int = Optimal sampling interval, given fraction of data removed

Opt Num Samples/Week = Optimal weekly sampling frequency, given fraction of data removed

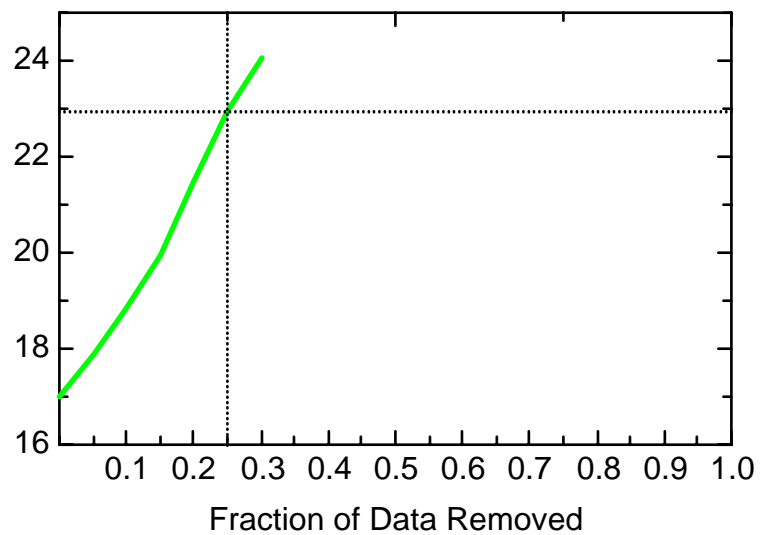
FE: Well 056MW02



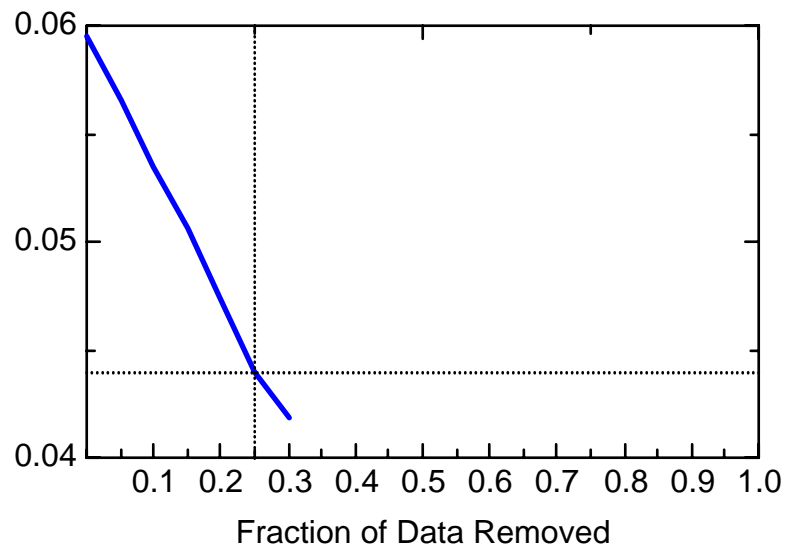
FE: Well 056MW02



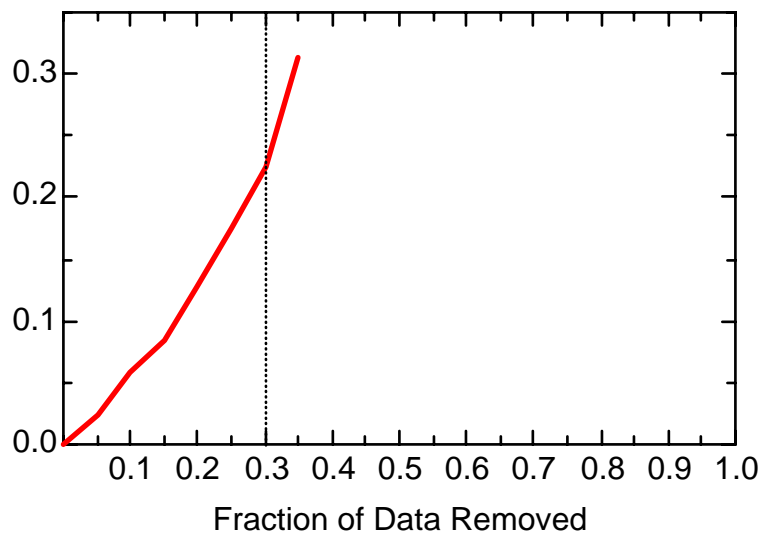
FE: Well 056MW02



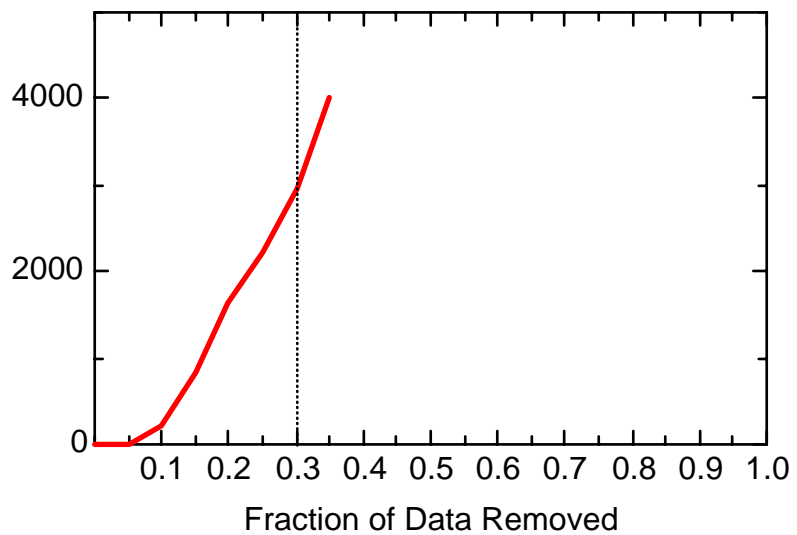
FE: Well 056MW02



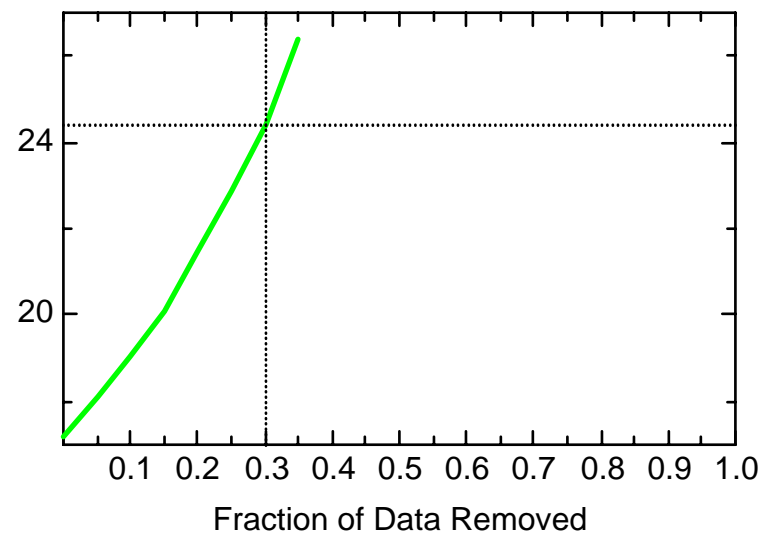
FE: Well 056MW04



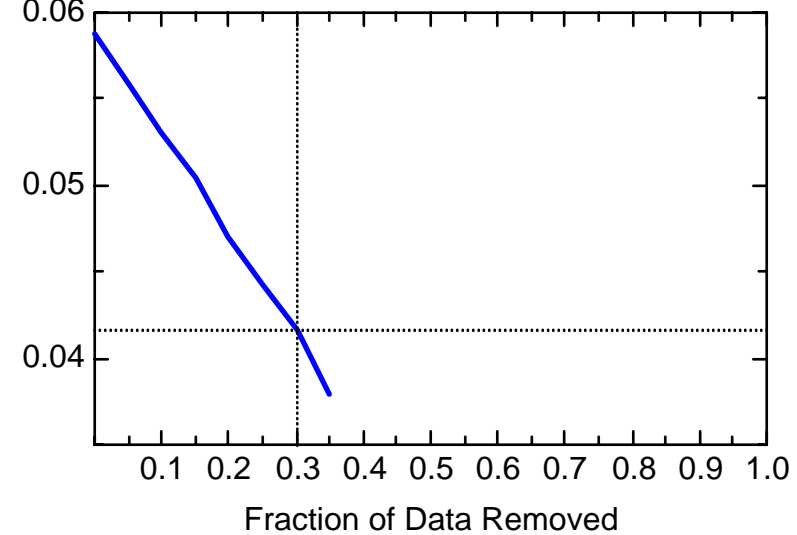
FE: Well 056MW04



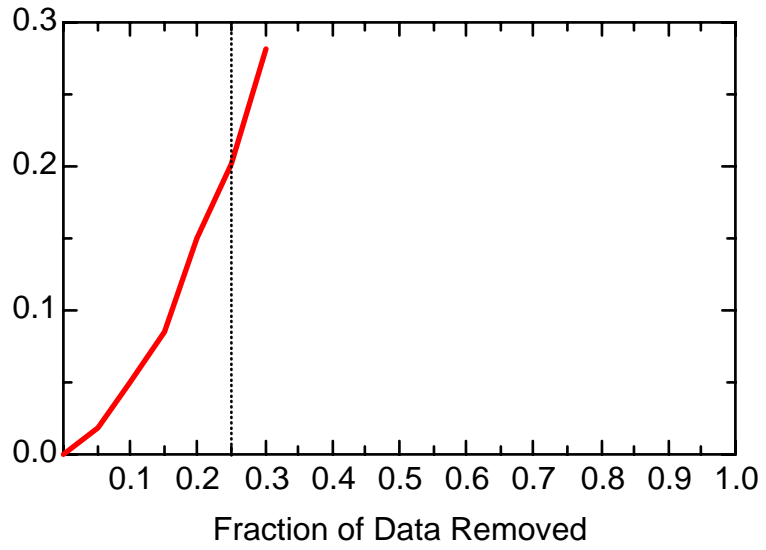
FE: Well 056MW04



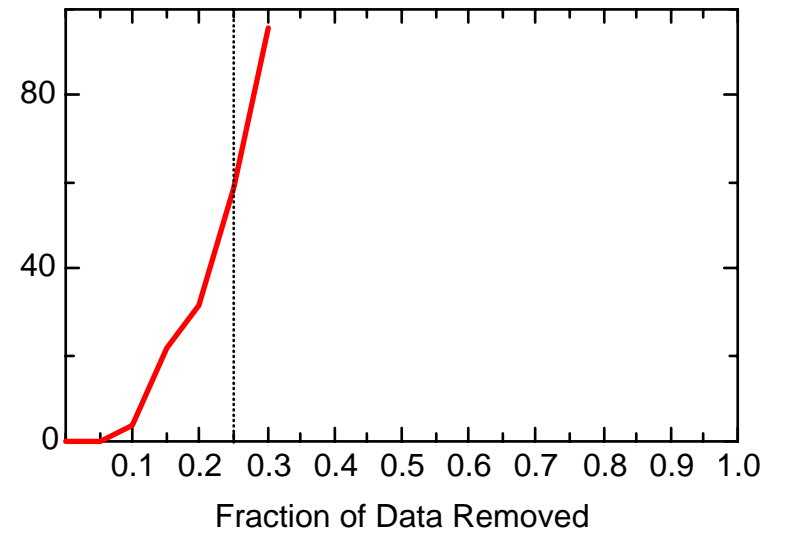
FE: Well 056MW04



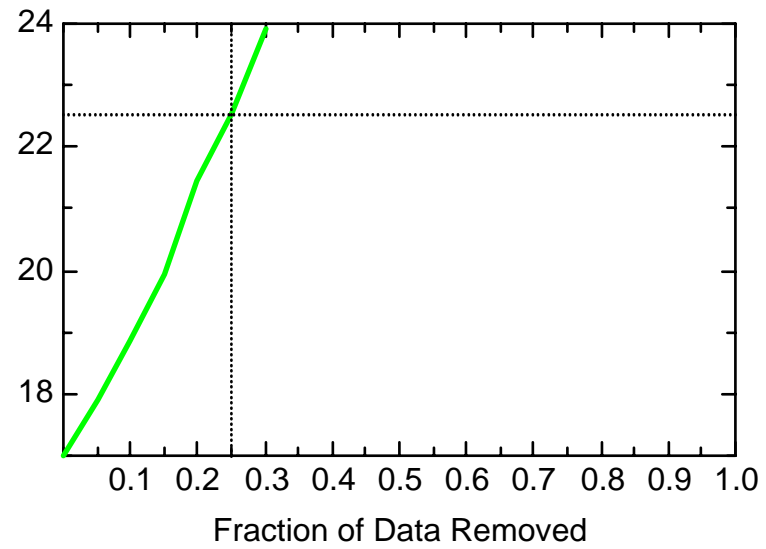
FE: Well AR25



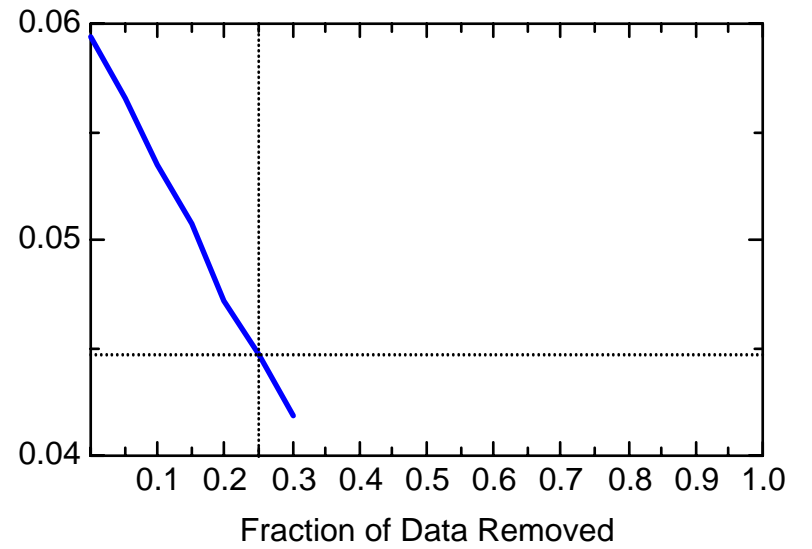
FE: Well AR25



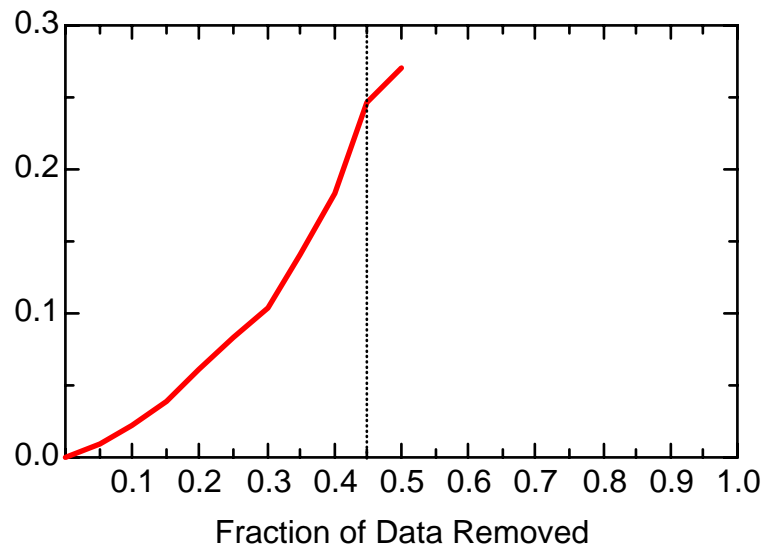
FE: Well AR25



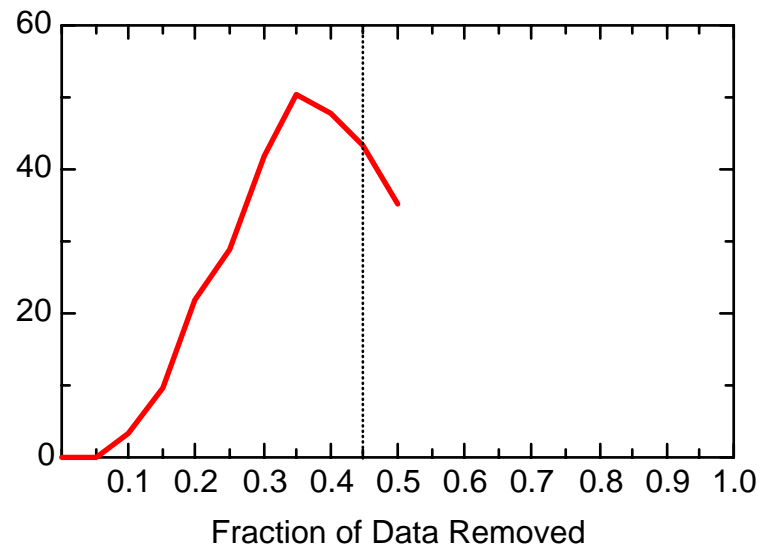
FE: Well AR25



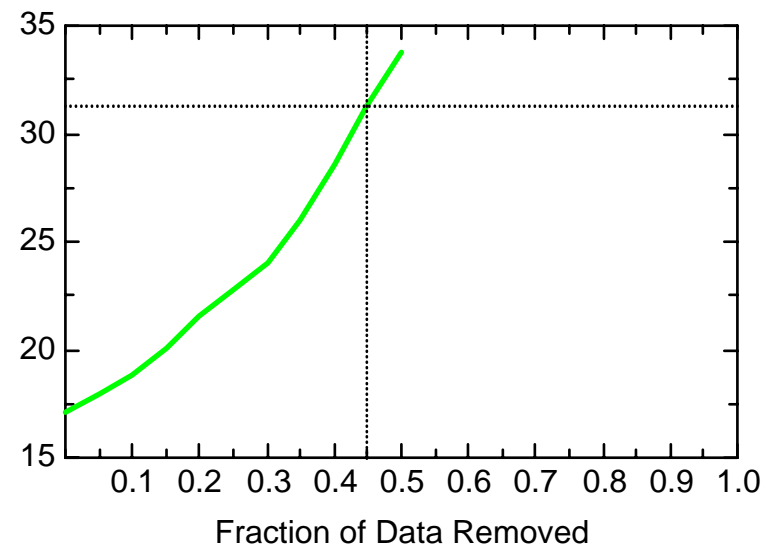
FE: Well FMW3413



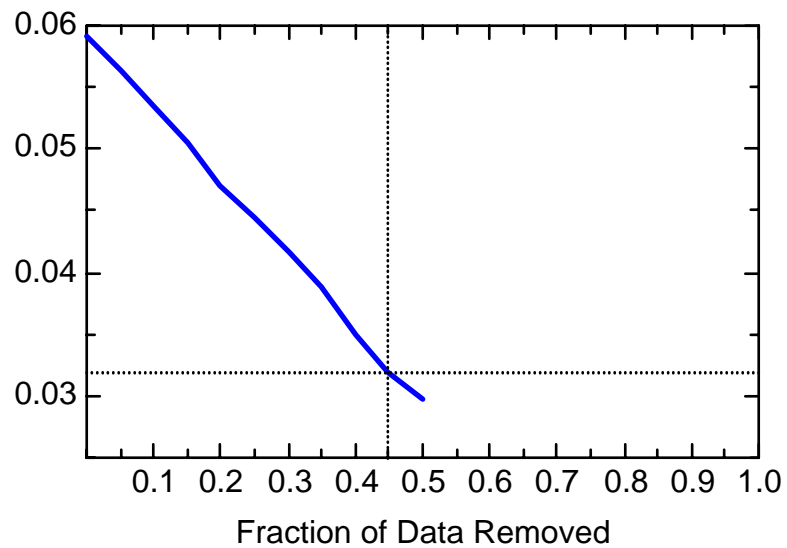
FE: Well FMW3413



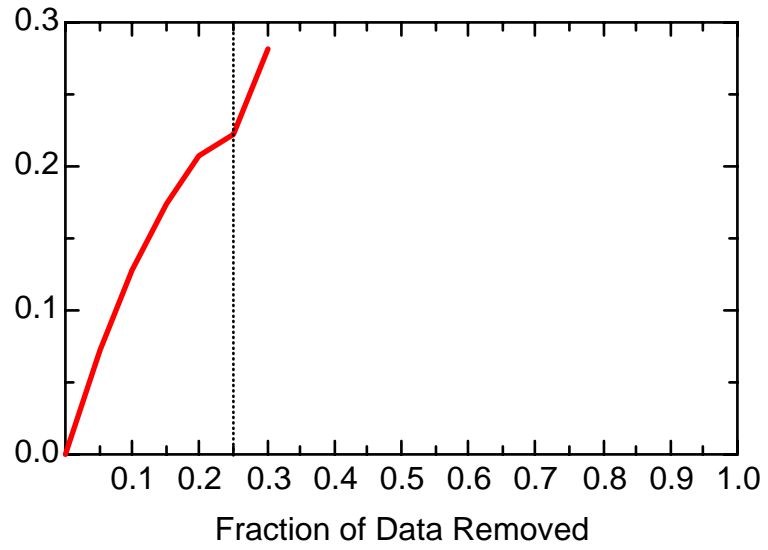
FE: Well FMW3413



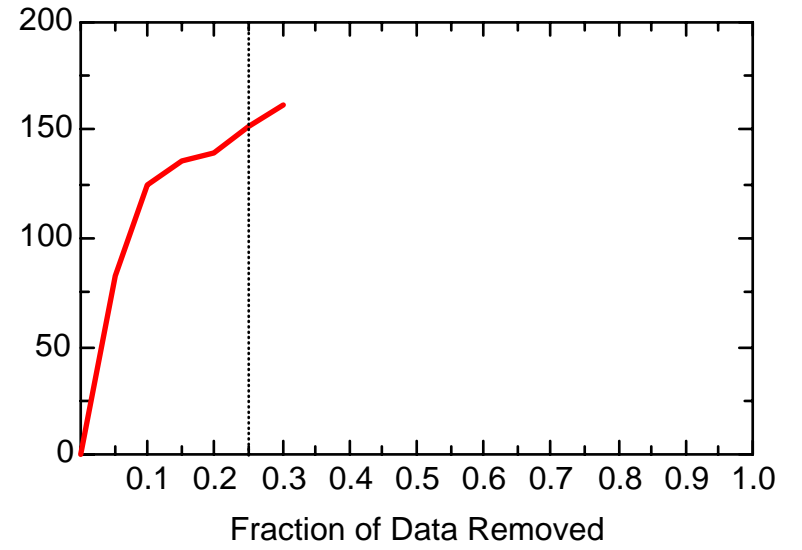
FE: Well FMW3413



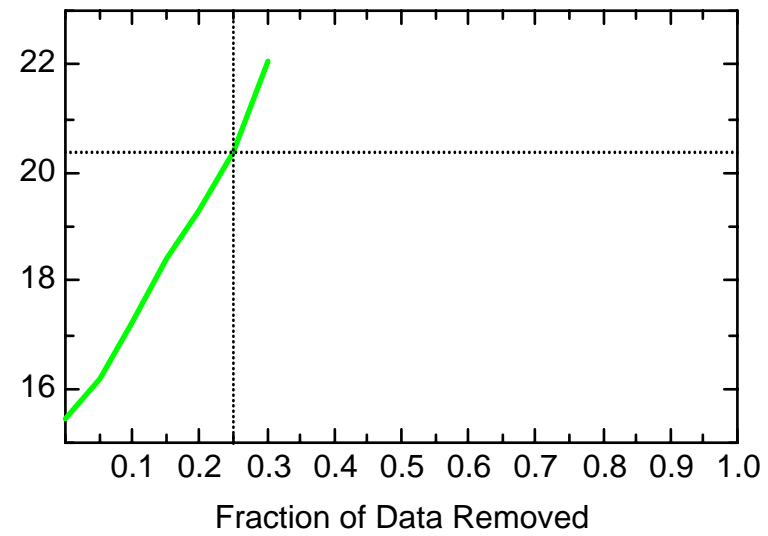
FE: Well JBW7101



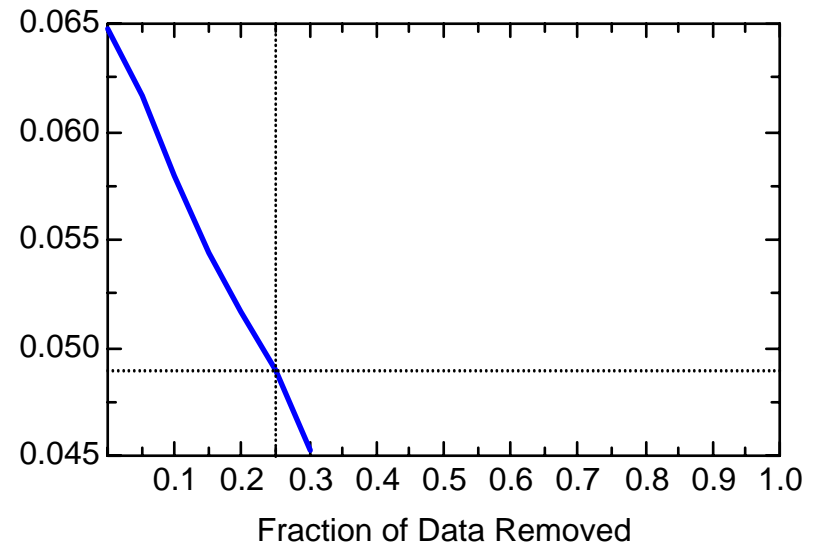
FE: Well JBW7101



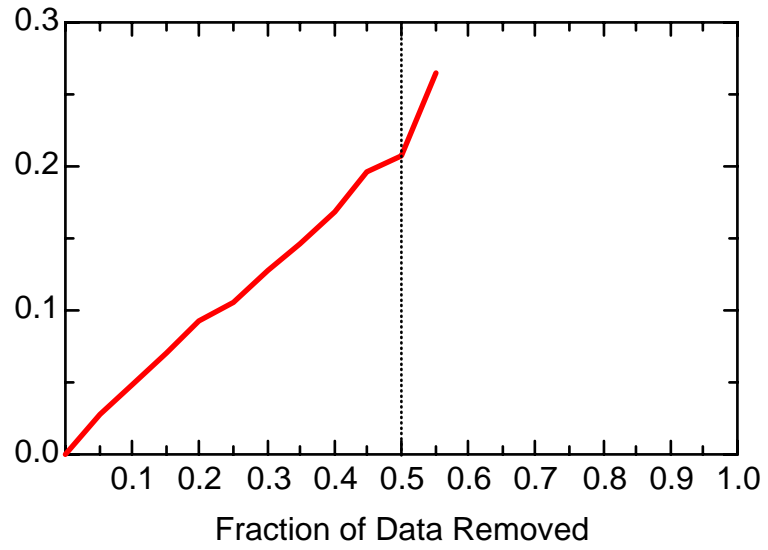
FE: Well JBW7101



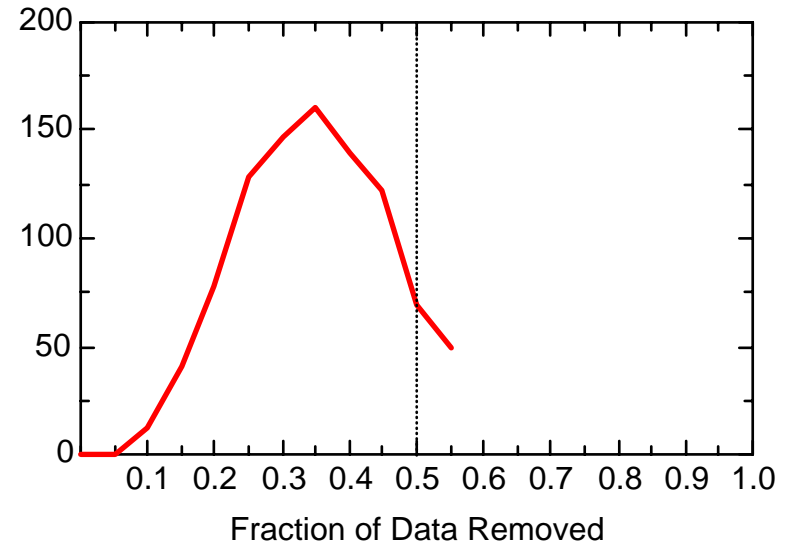
FE: Well JBW7101



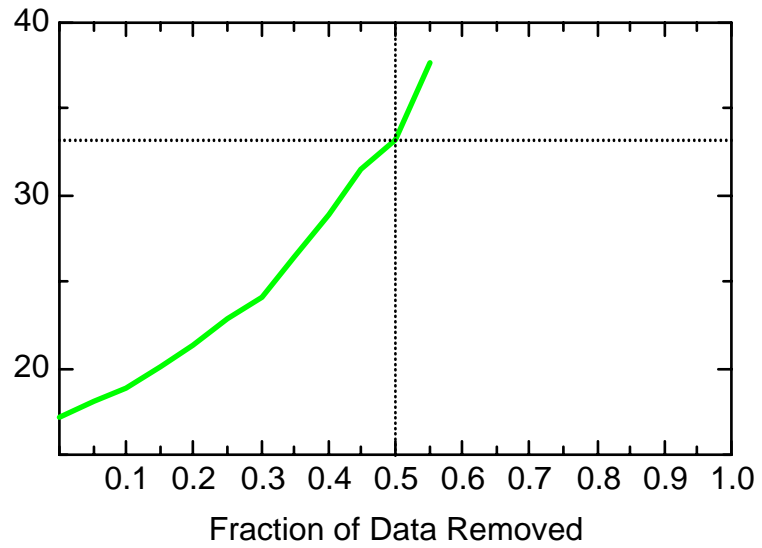
FE: Well JBW7102



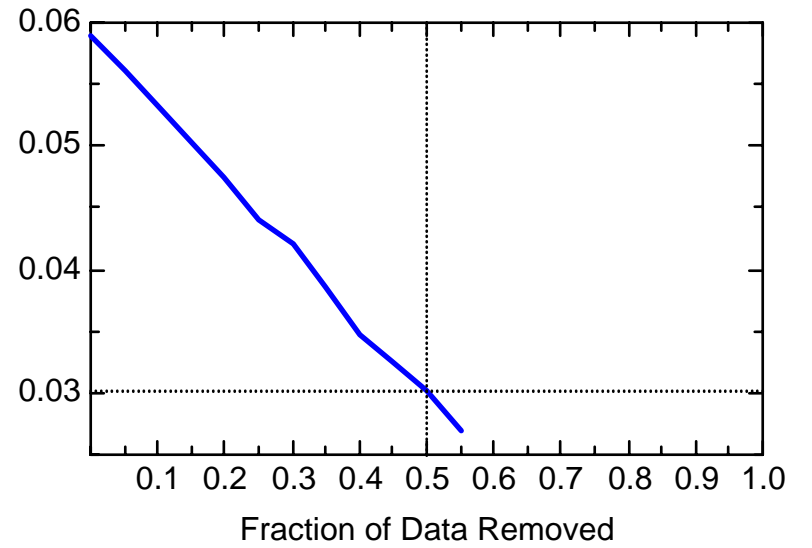
FE: Well JBW7102



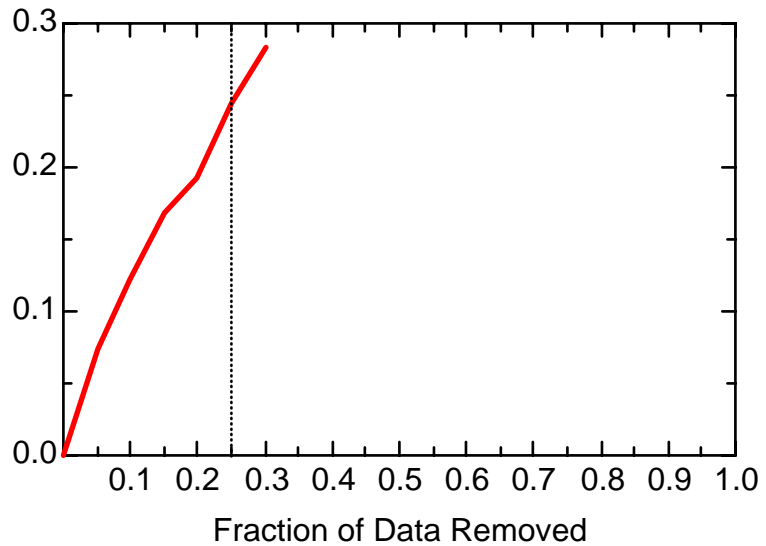
FE: Well JBW7102



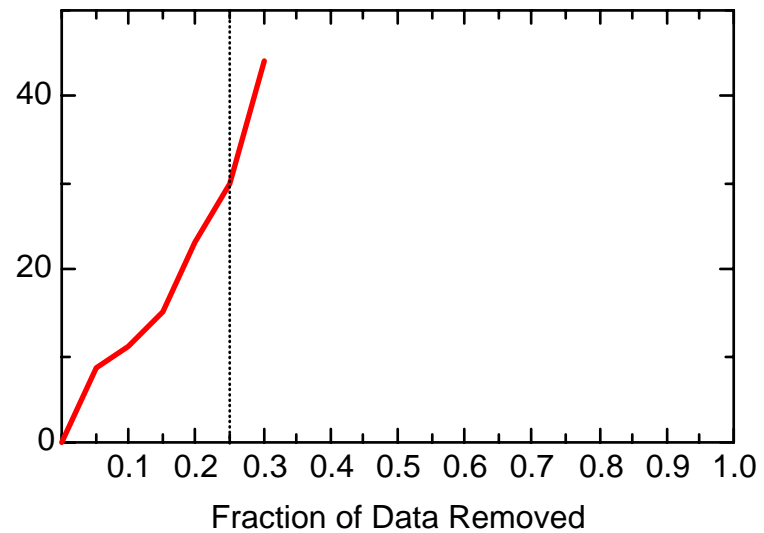
FE: Well JBW7102



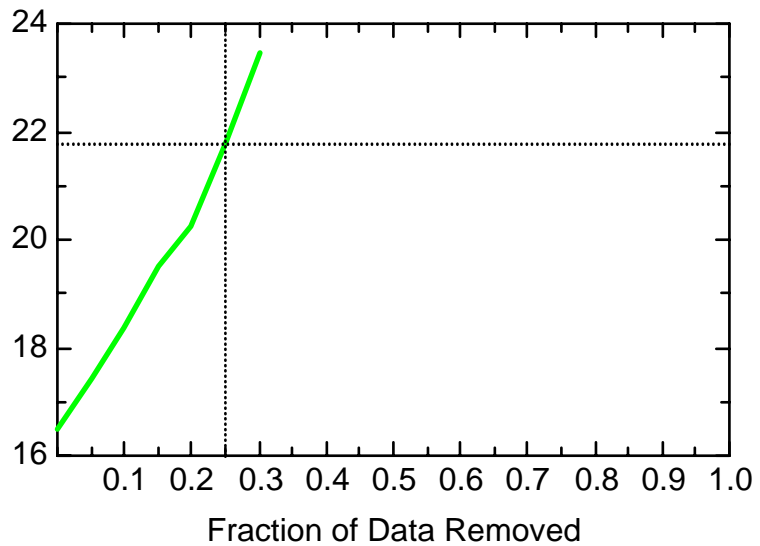
FE: Well JBW7106A



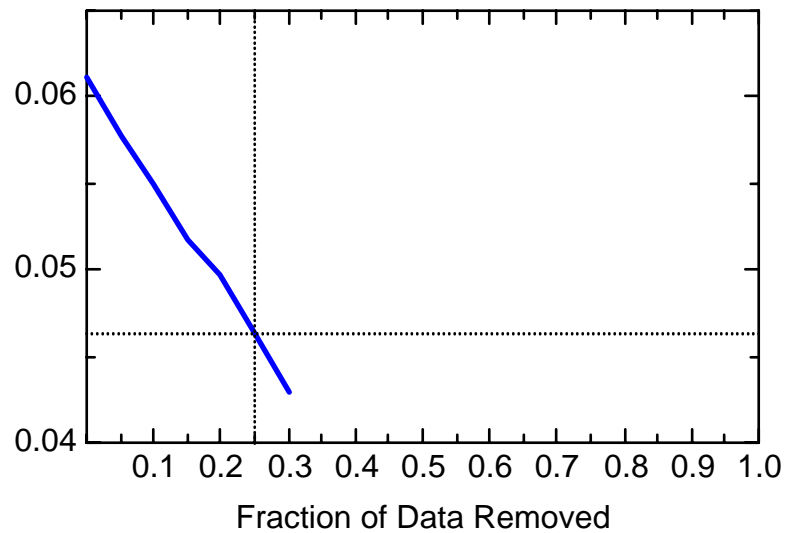
FE: Well JBW7106A



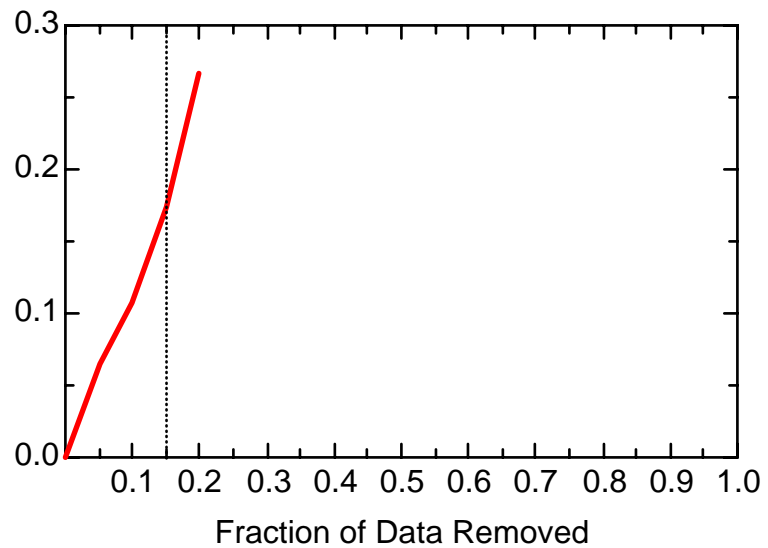
FE: Well JBW7106A



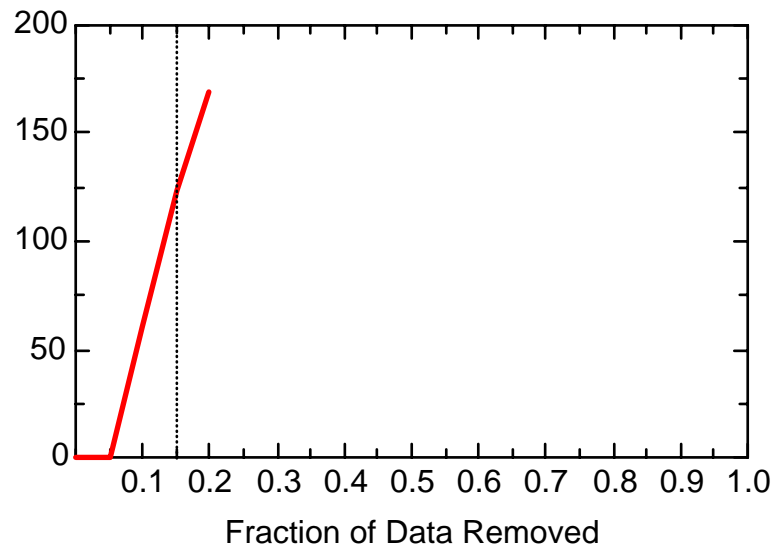
FE: Well JBW7106A



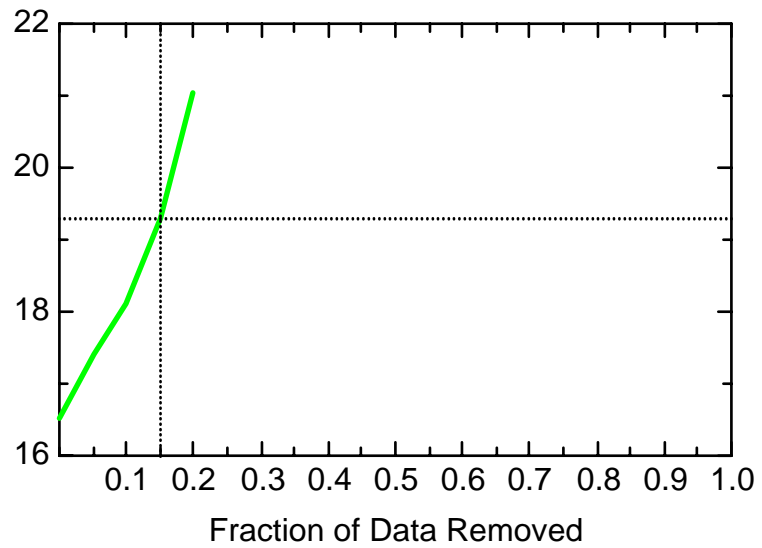
FE: Well JBW7106B



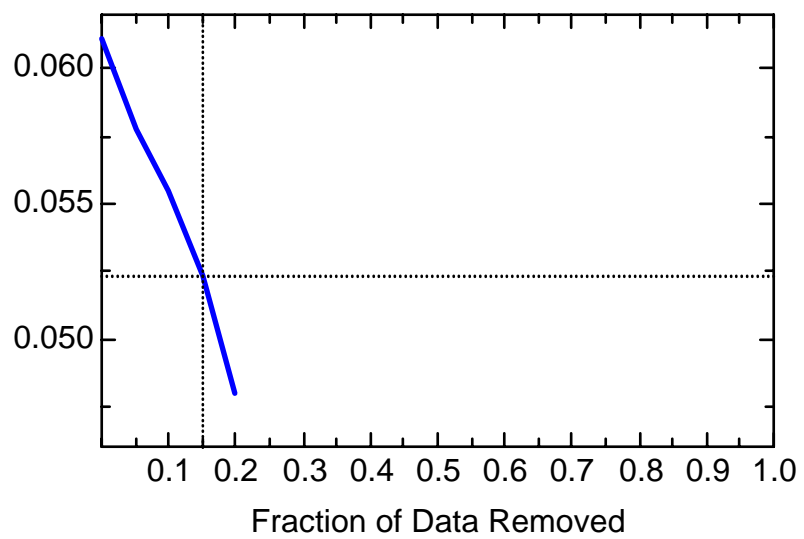
FE: Well JBW7106B



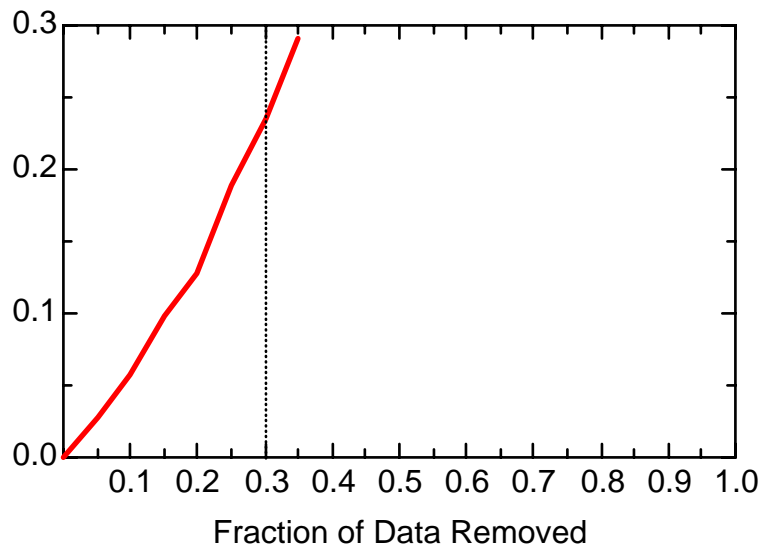
FE: Well JBW7106B



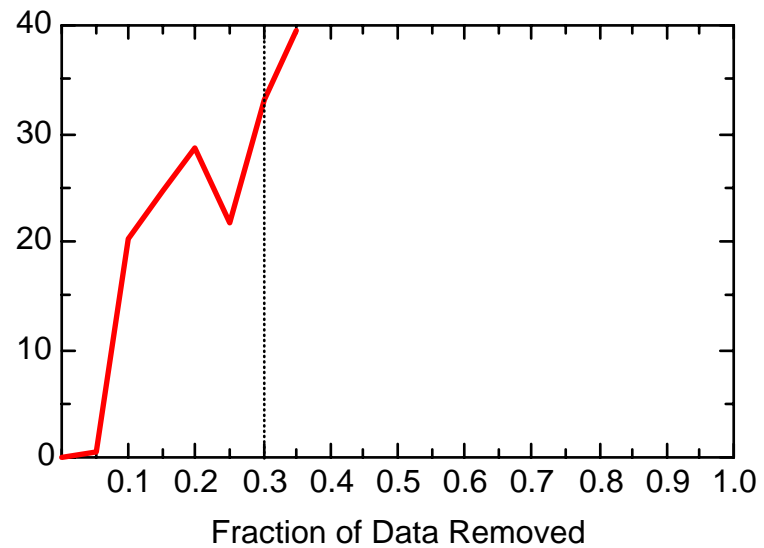
FE: Well JBW7106B



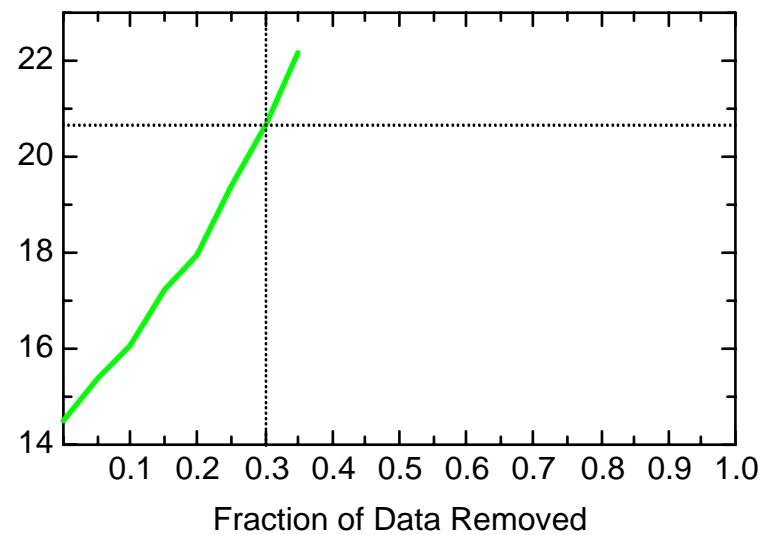
FE: Well JBW7203A



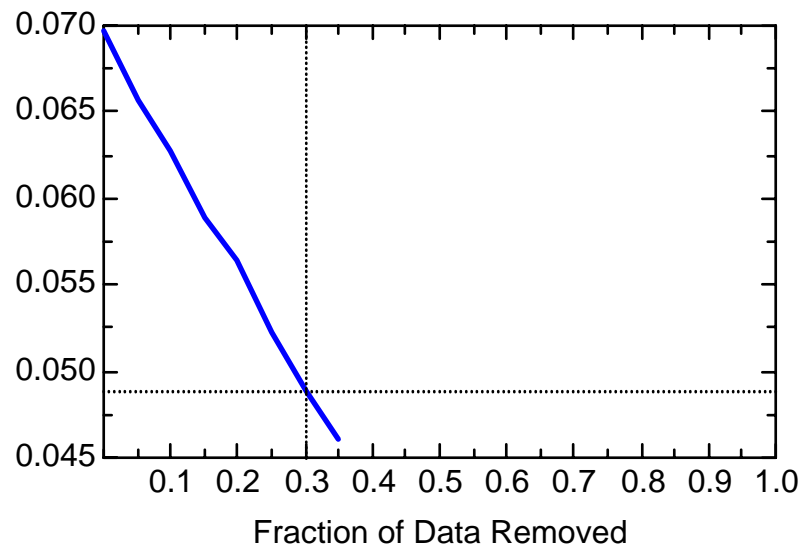
FE: Well JBW7203A



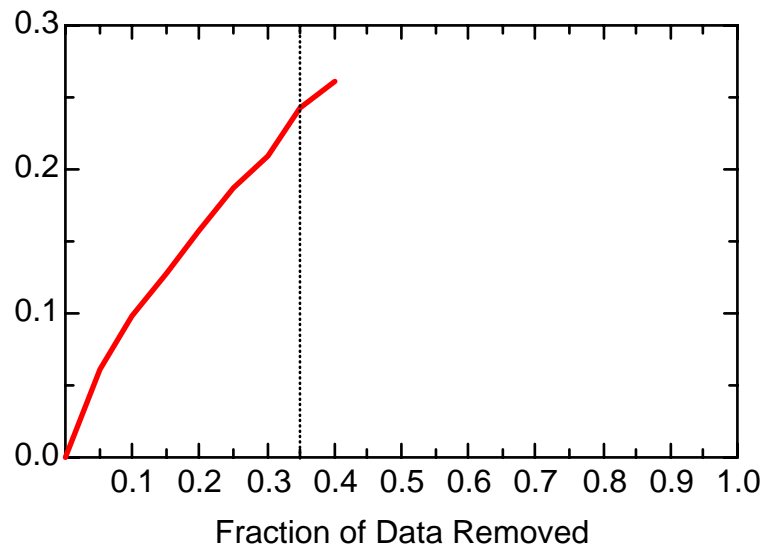
FE: Well JBW7203A



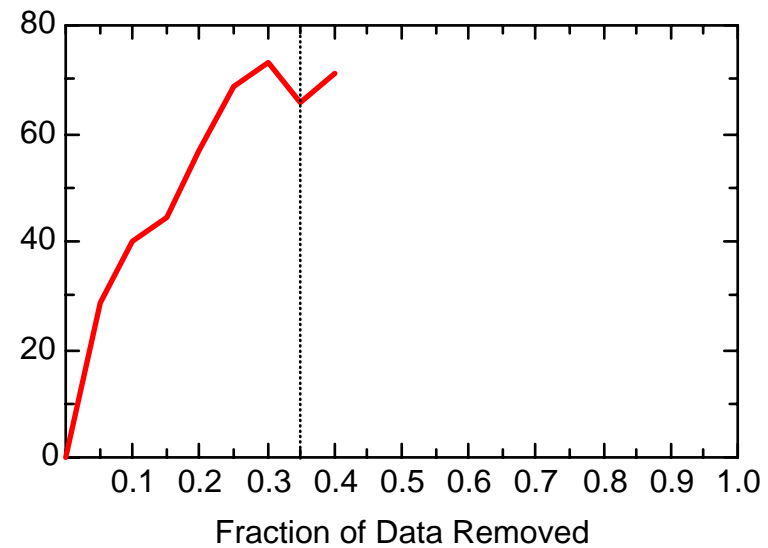
FE: Well JBW7203A



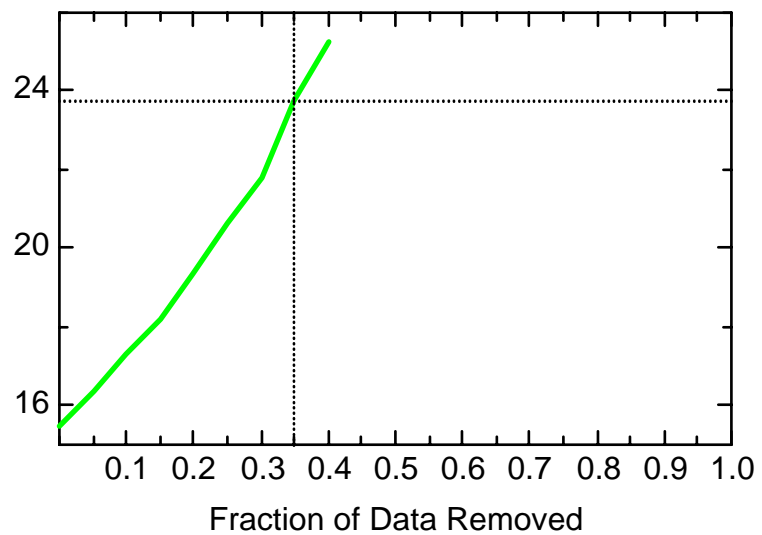
FE: Well JBW7203B



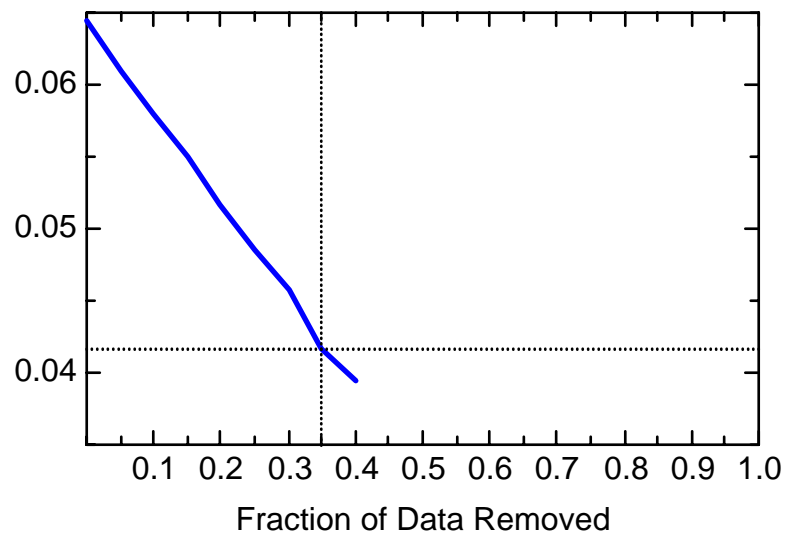
FE: Well JBW7203B



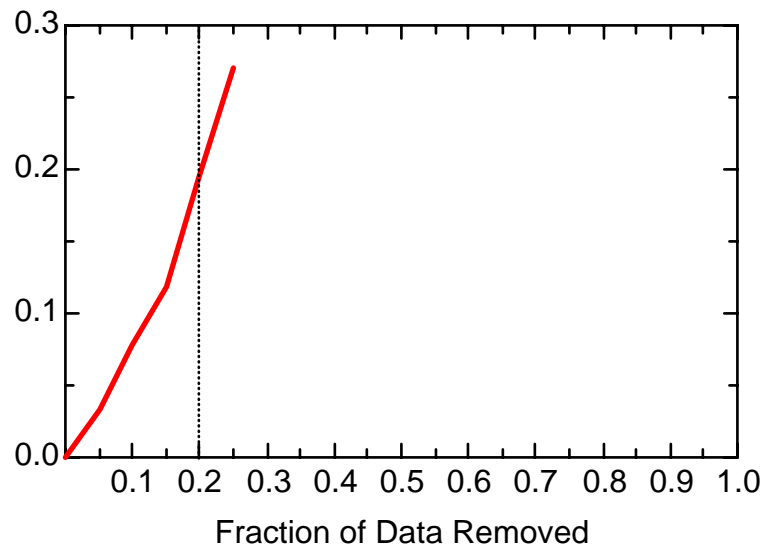
FE: Well JBW7203B



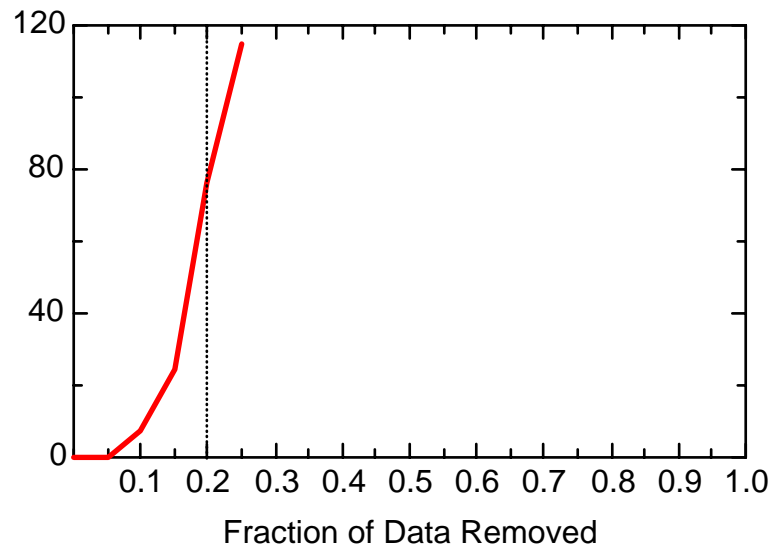
FE: Well JBW7203B



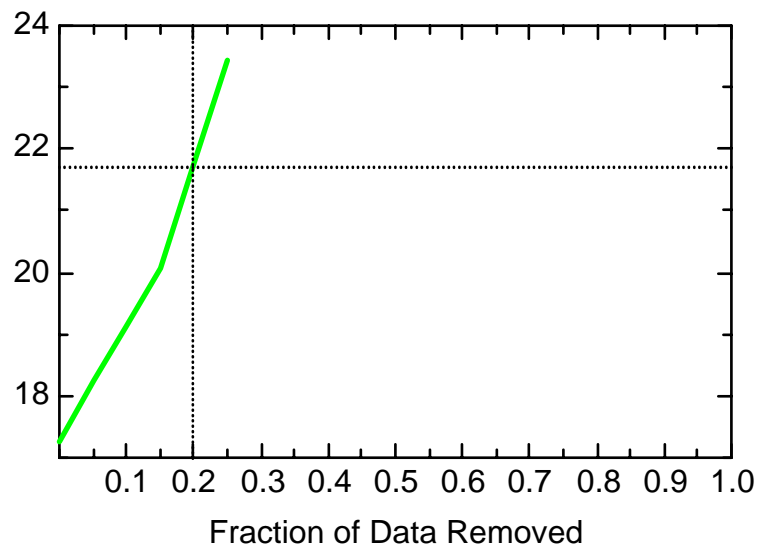
FE: Well JBW7204A



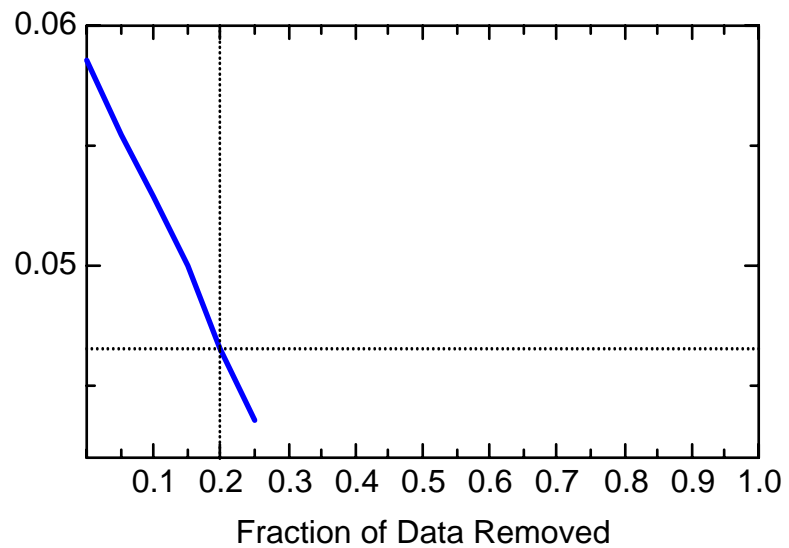
FE: Well JBW7204A



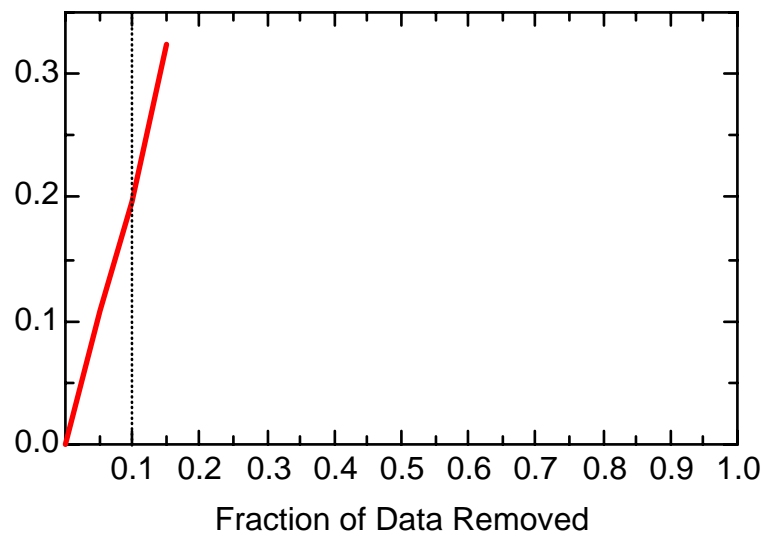
FE: Well JBW7204A



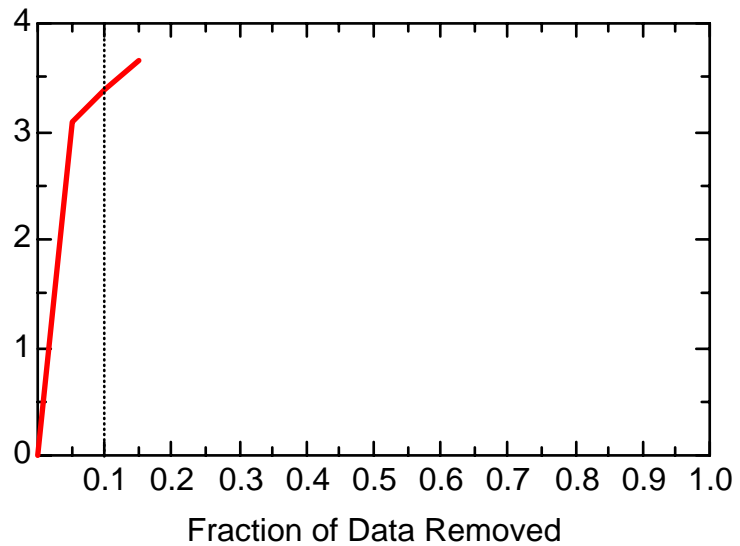
FE: Well JBW7204A



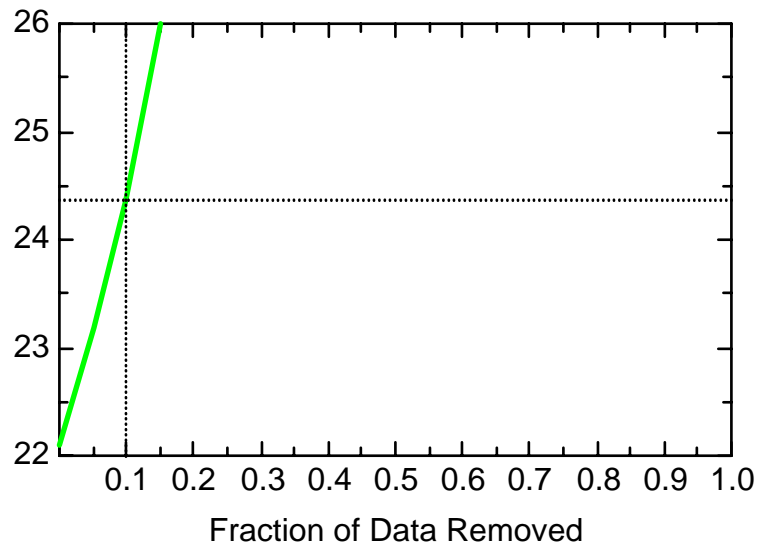
FE: Well JBW7212A



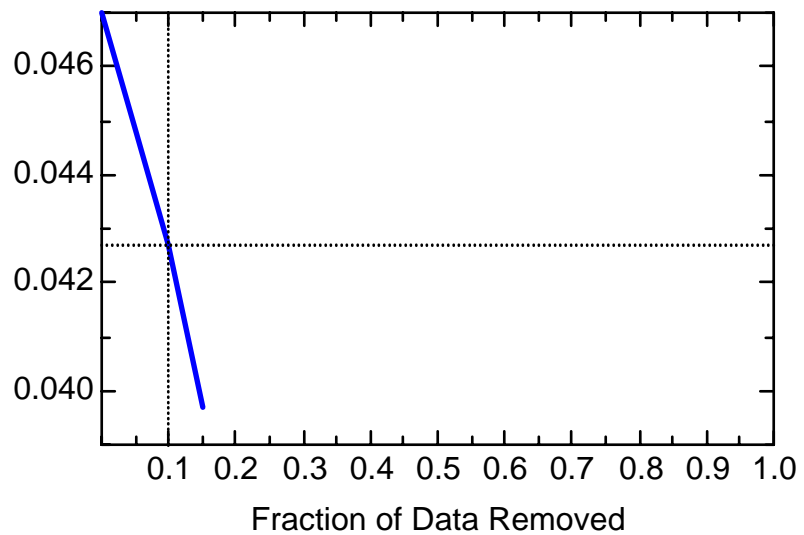
FE: Well JBW7212A



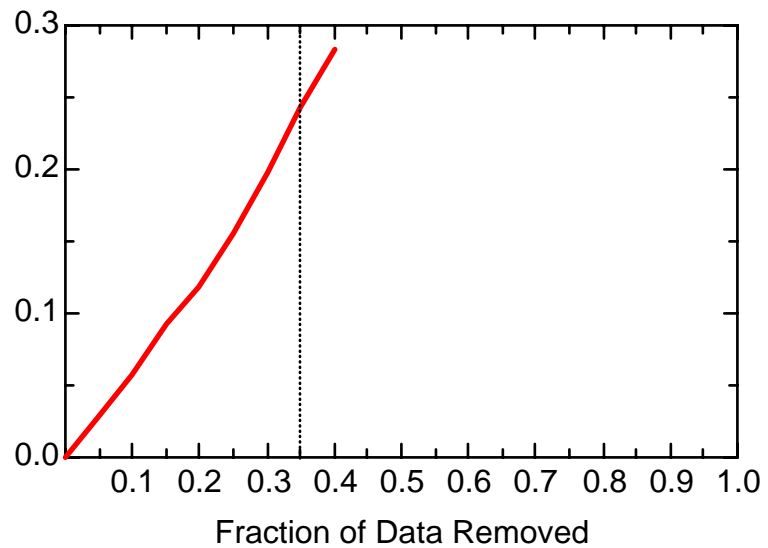
FE: Well JBW7212A



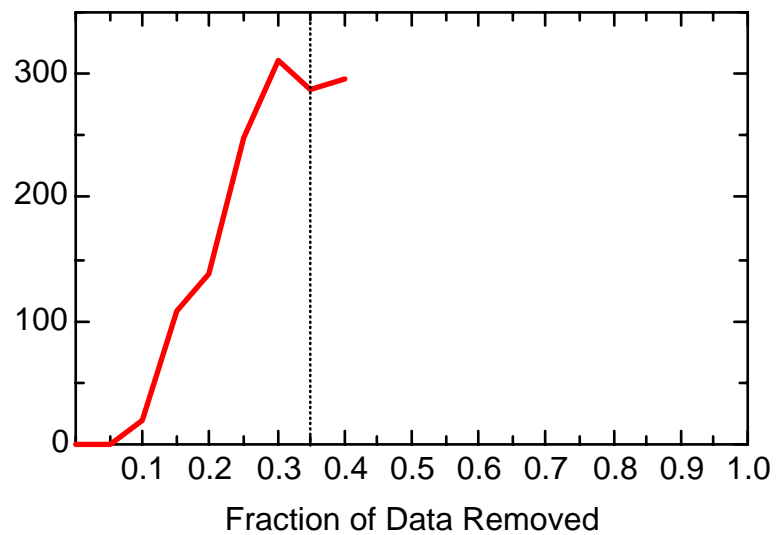
FE: Well JBW7212A



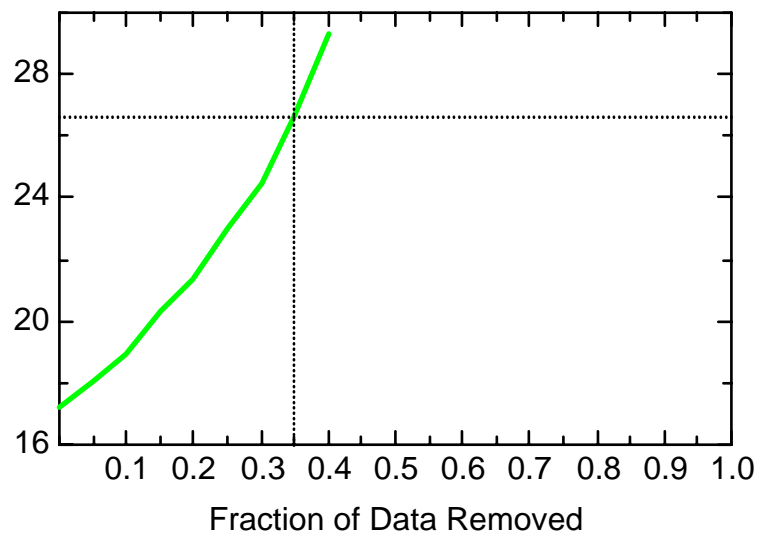
FE: Well JBW7212B



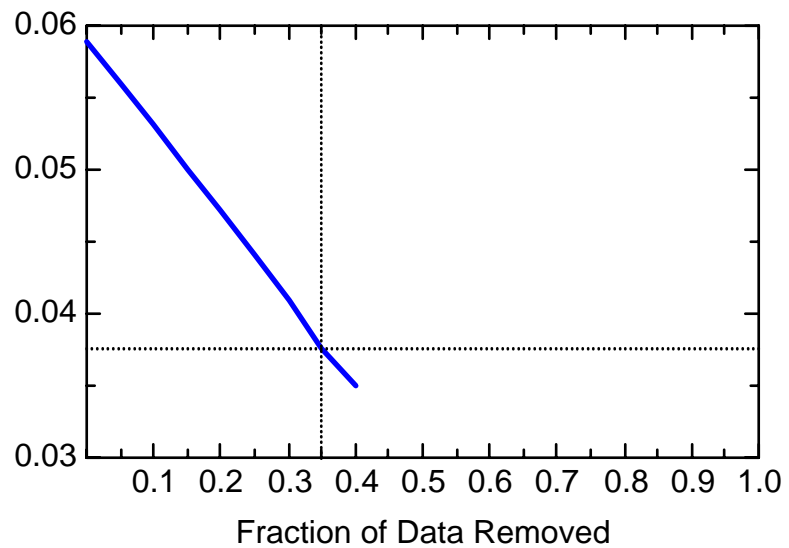
FE: Well JBW7212B



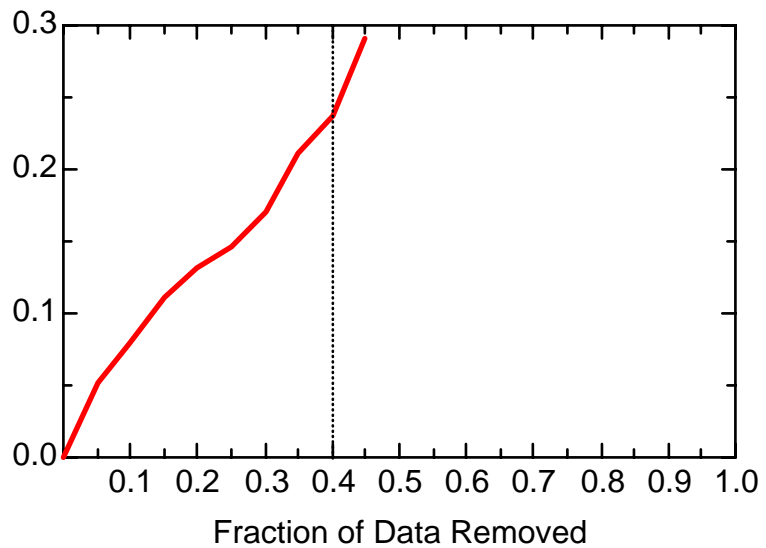
FE: Well JBW7212B



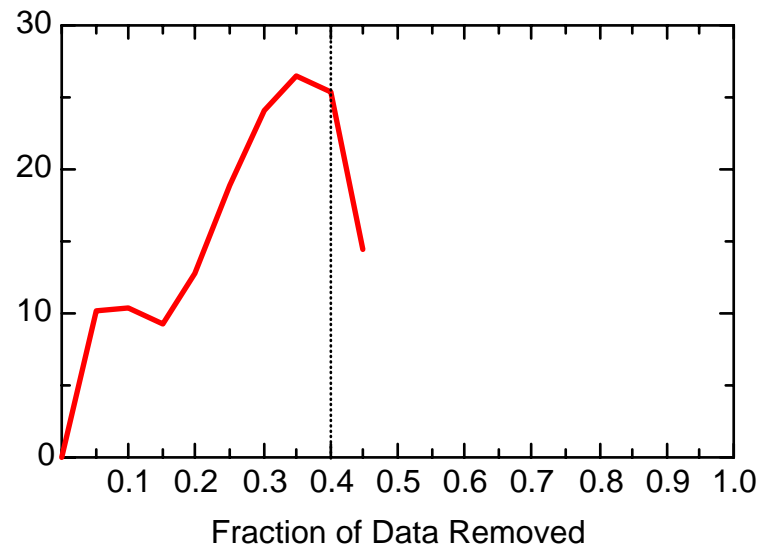
FE: Well JBW7212B



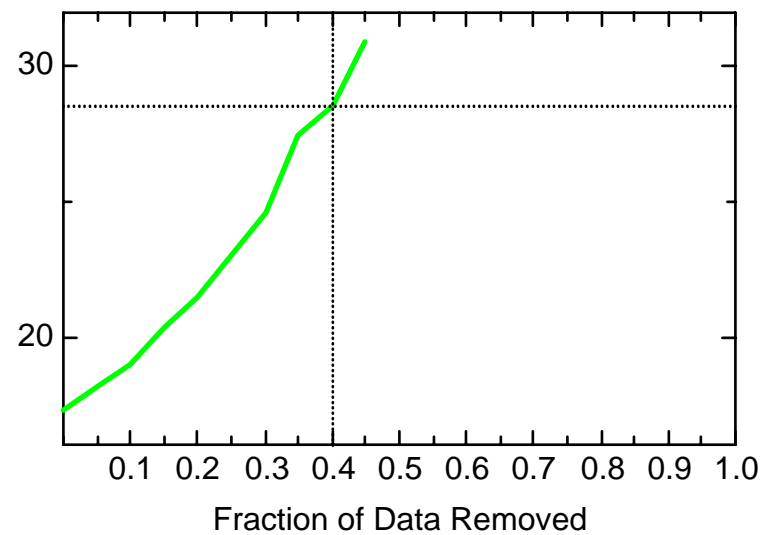
FE: Well JBW7213A



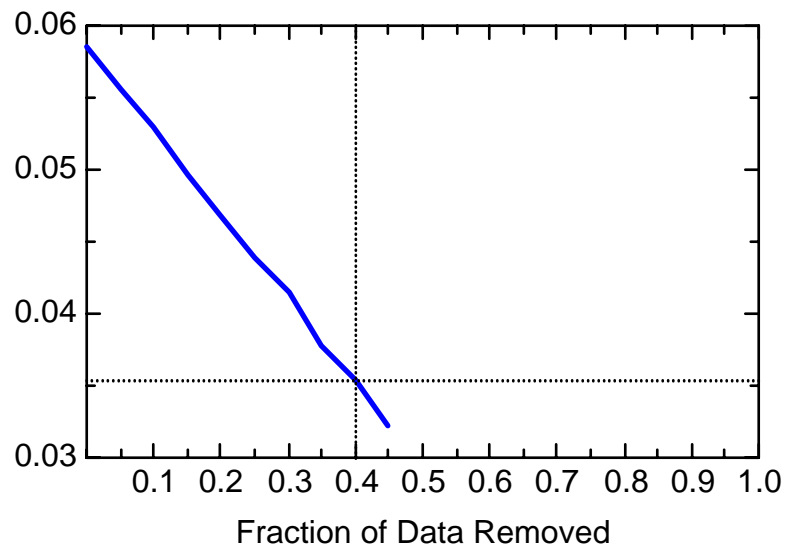
FE: Well JBW7213A



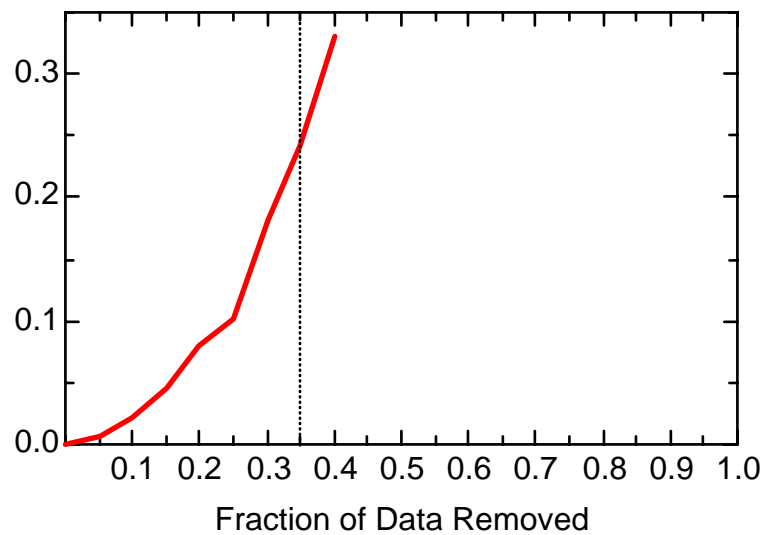
FE: Well JBW7213A



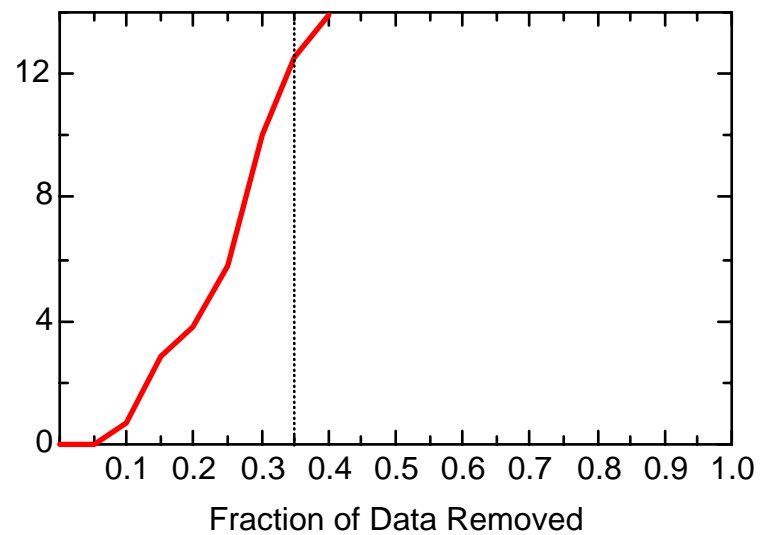
FE: Well JBW7213A



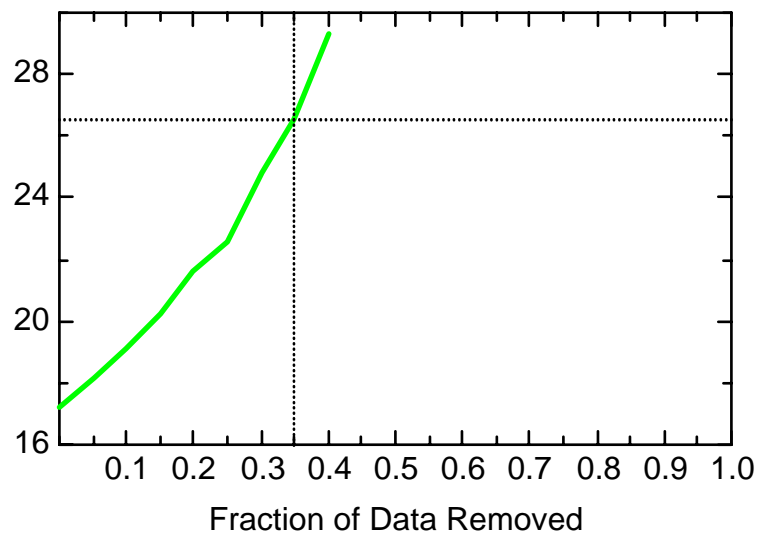
FE: Well JBW7213B



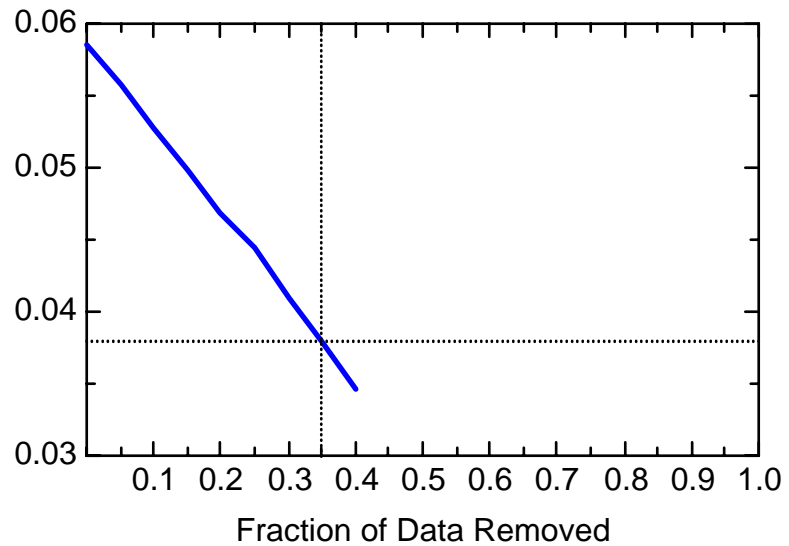
FE: Well JBW7213B



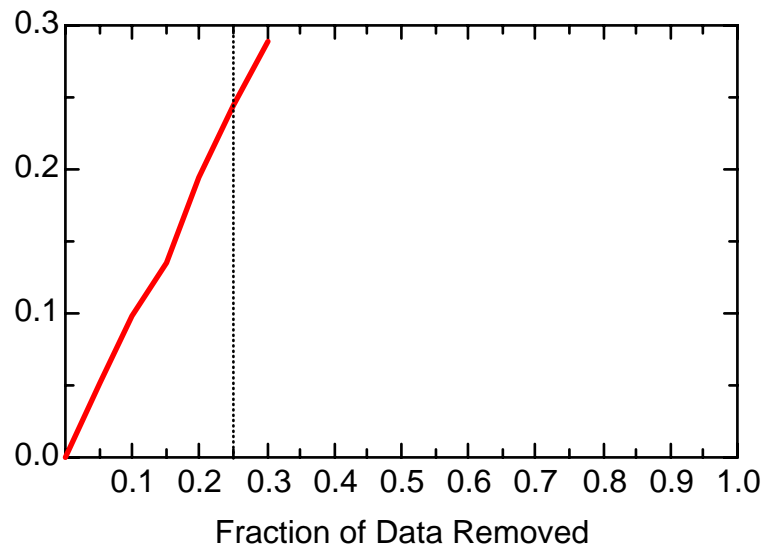
FE: Well JBW7213B



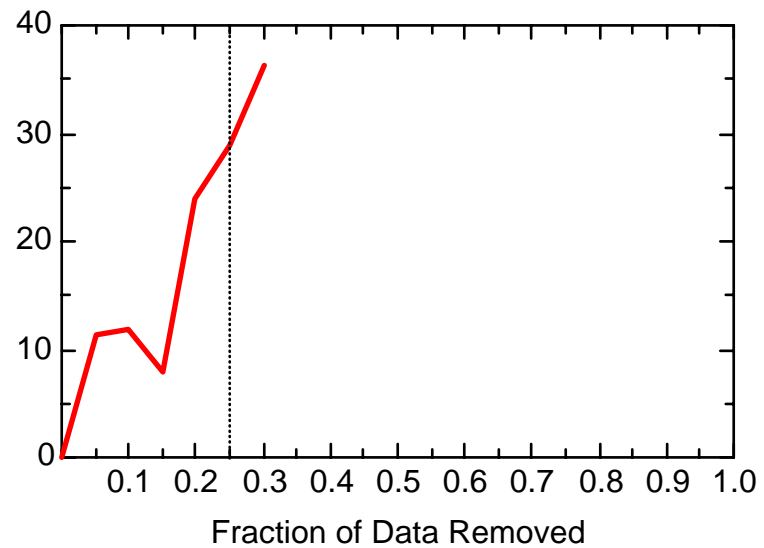
FE: Well JBW7213B



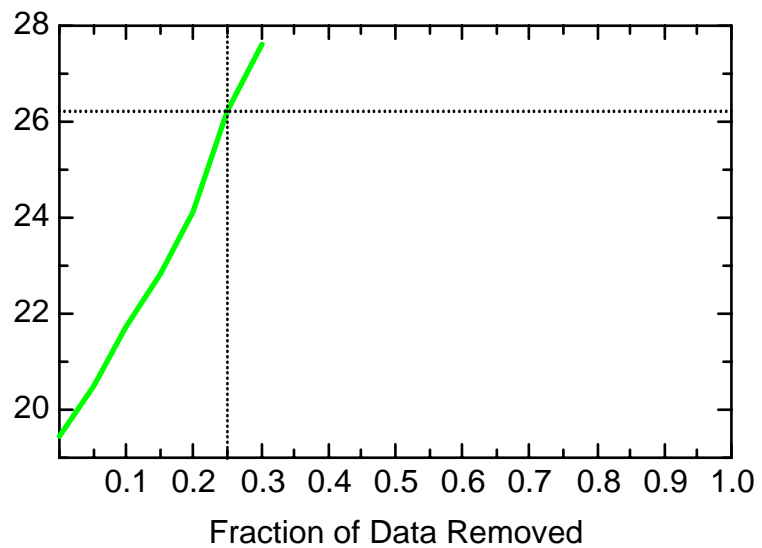
FE: Well JBW7215B



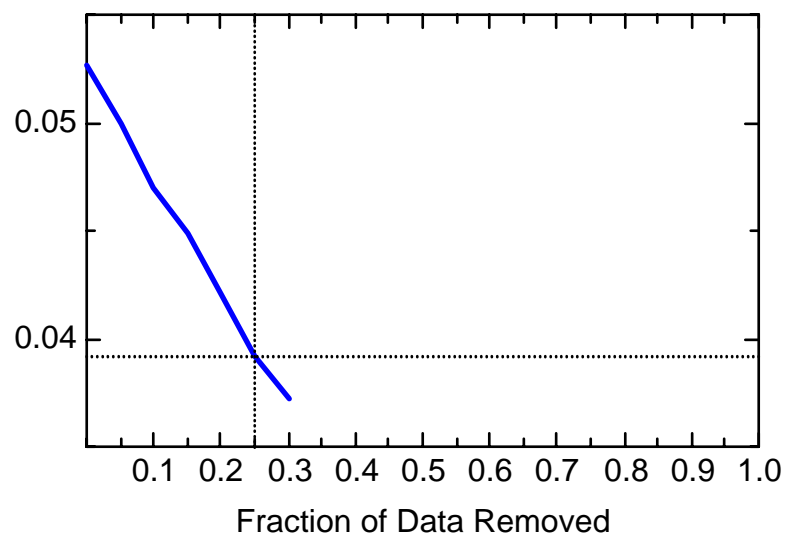
FE: Well JBW7215B



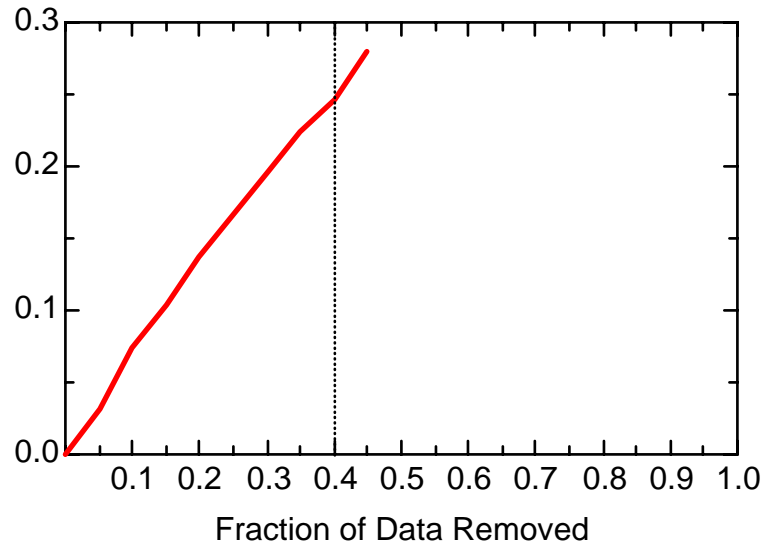
FE: Well JBW7215B



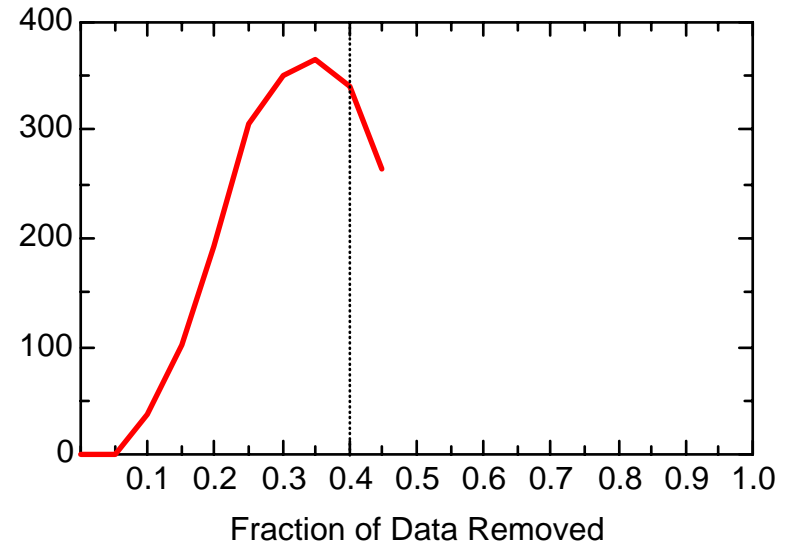
FE: Well JBW7215B



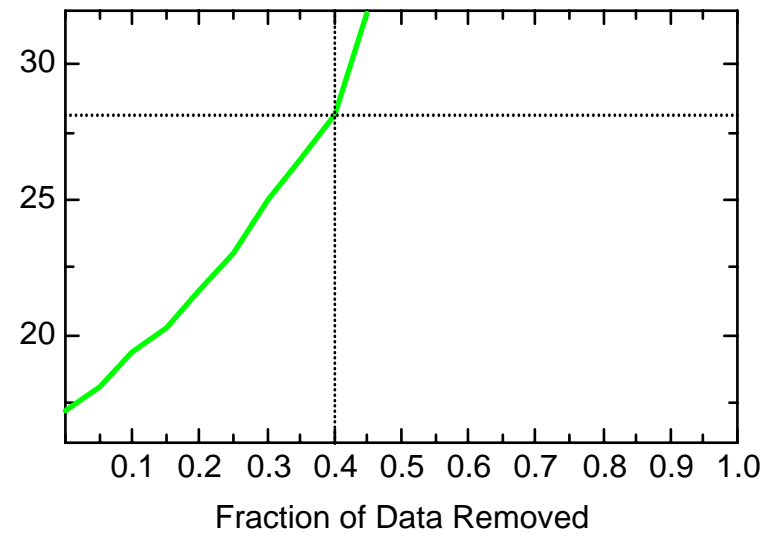
FE: Well JBW7317



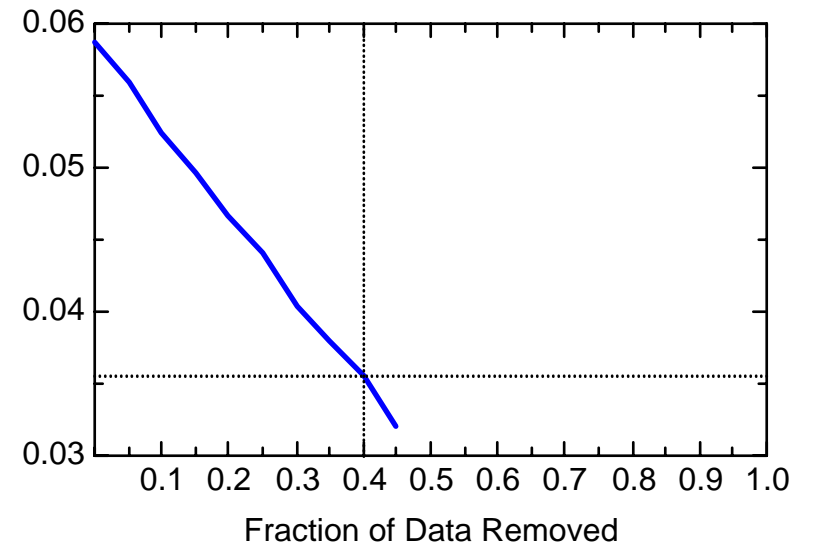
FE: Well JBW7317



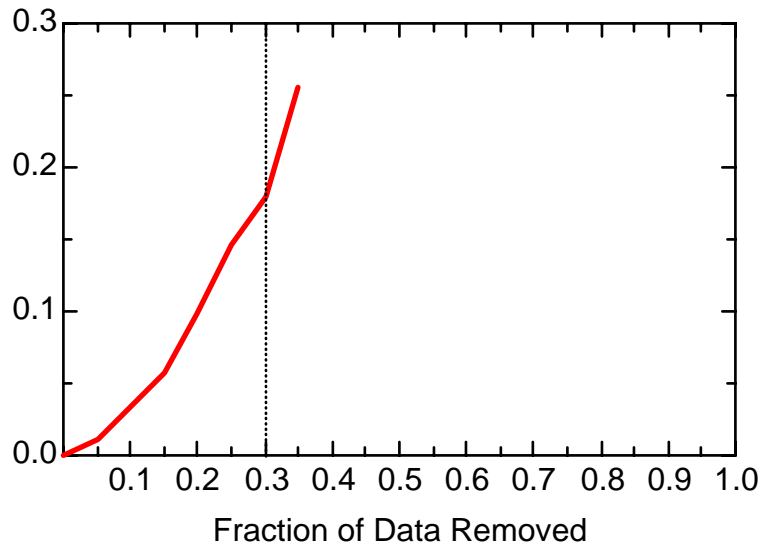
FE: Well JBW7317



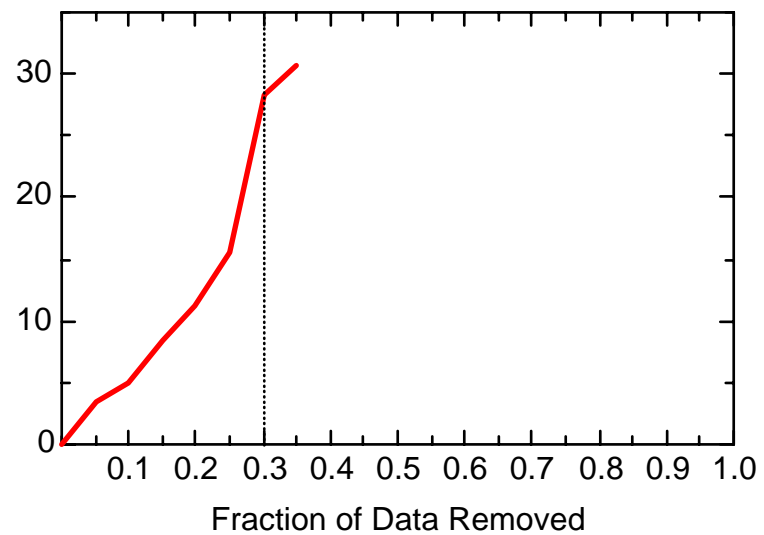
FE: Well JBW7317



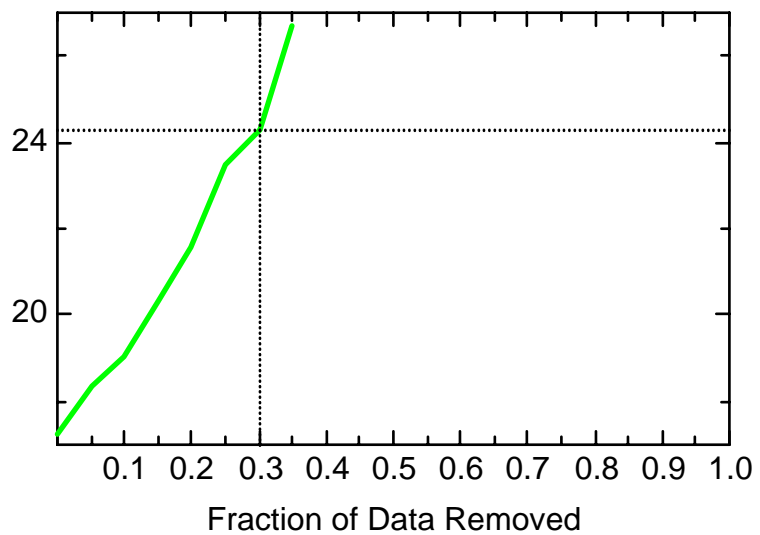
FE: Well JBW7326A



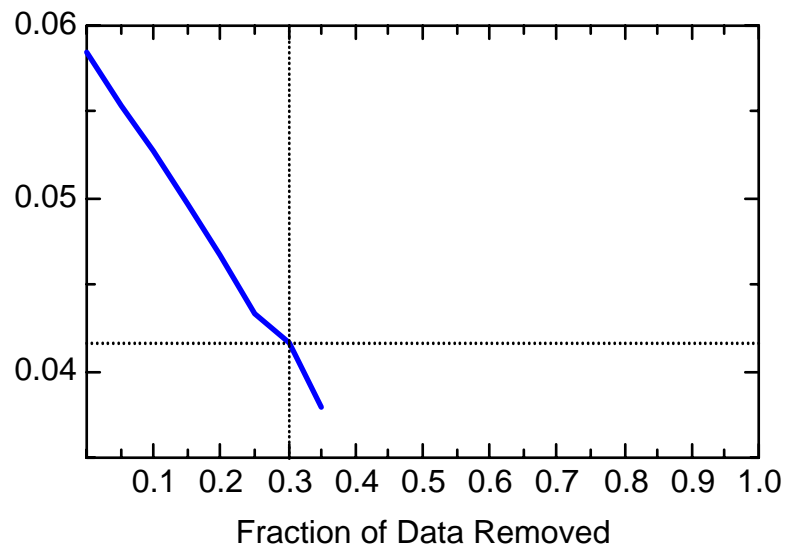
FE: Well JBW7326A



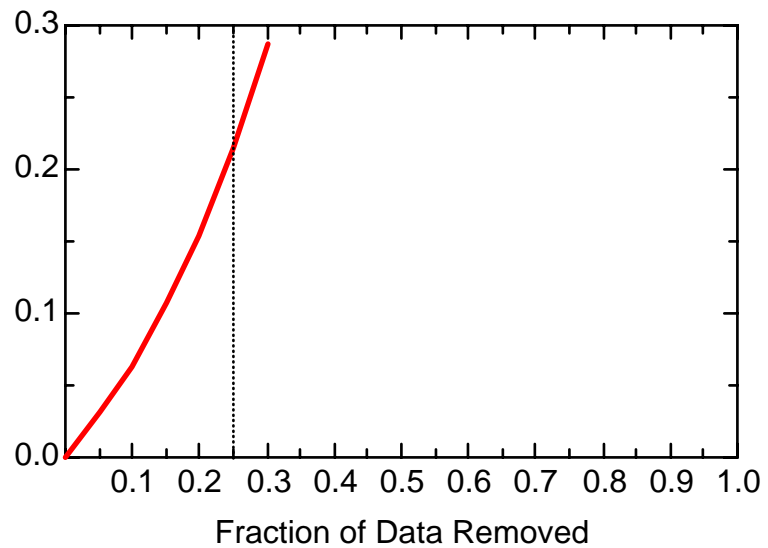
FE: Well JBW7326A



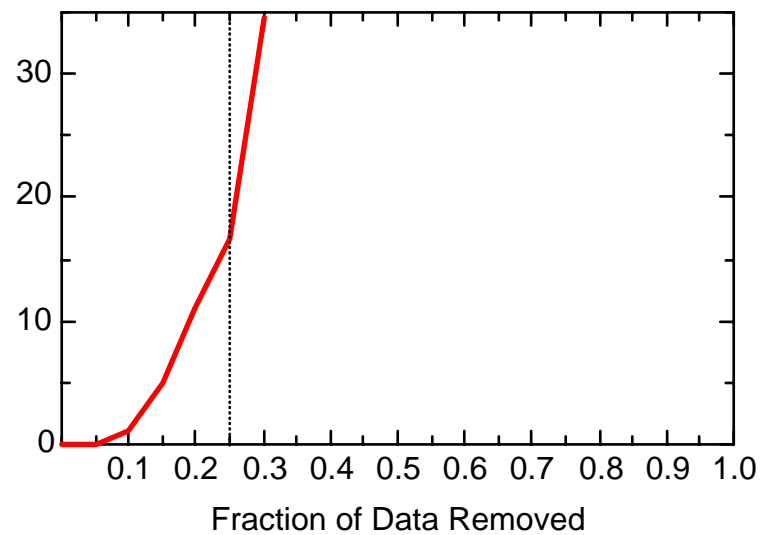
FE: Well JBW7326A



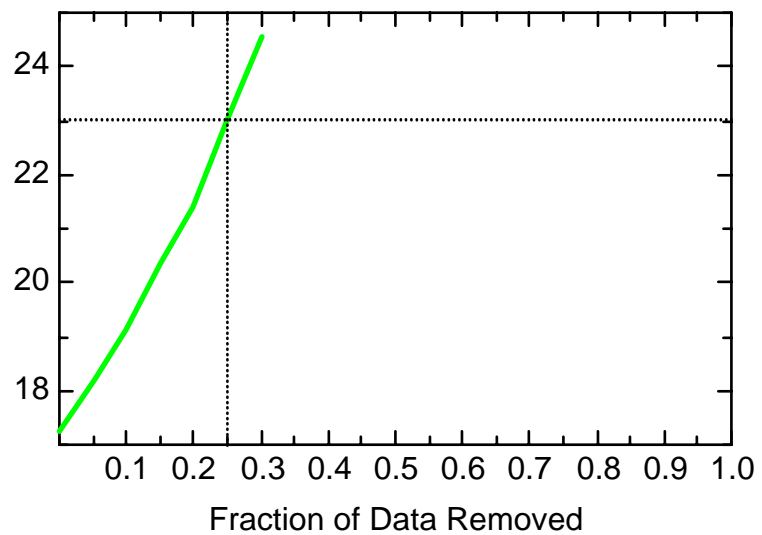
FE: Well JBW7326B



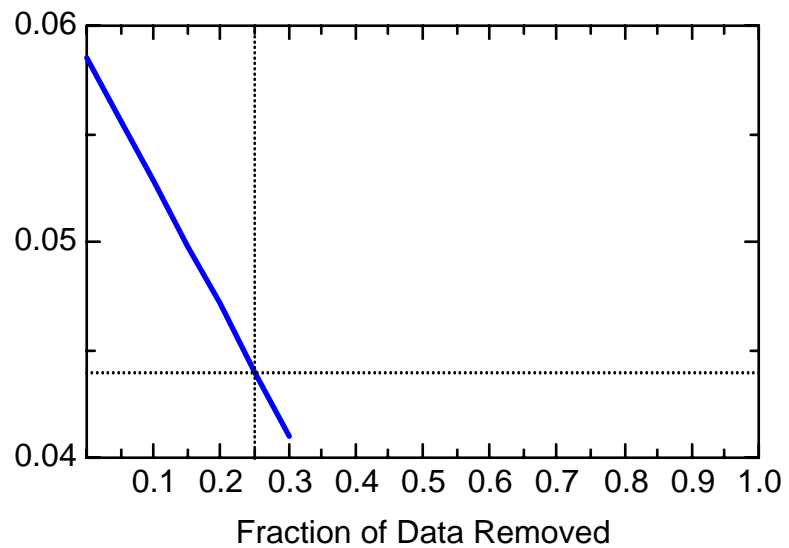
FE: Well JBW7326B



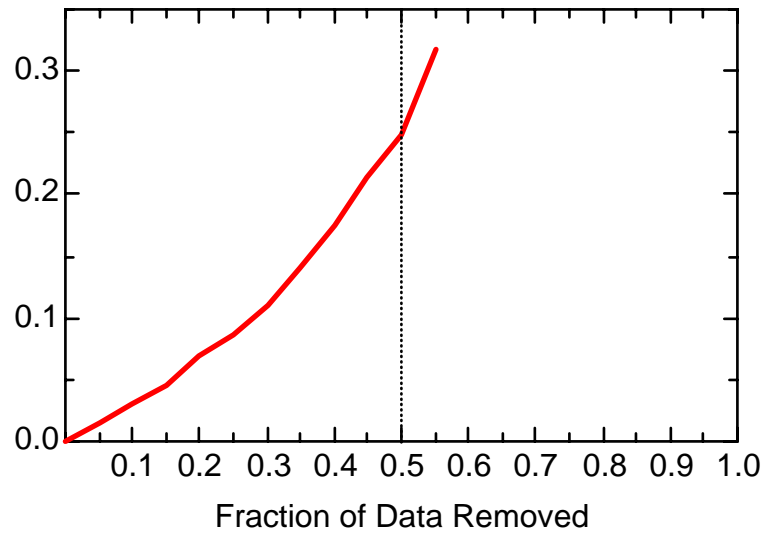
FE: Well JBW7326B



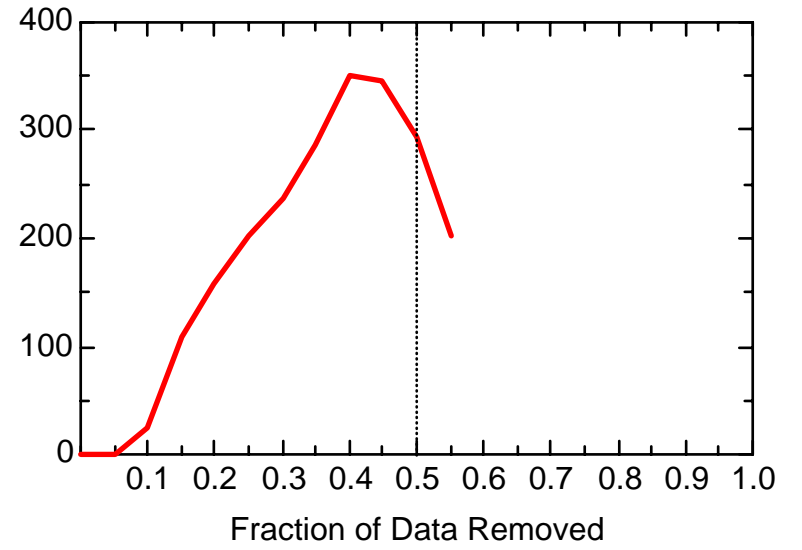
FE: Well JBW7326B



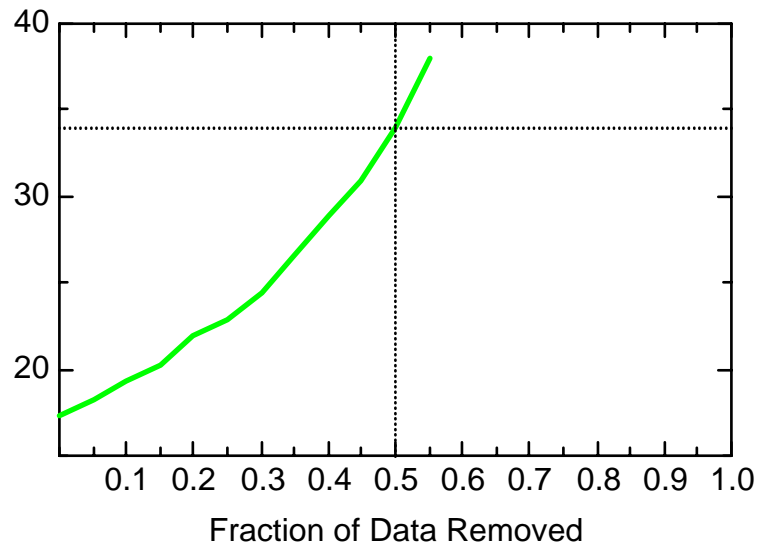
FE: Well JBW7328



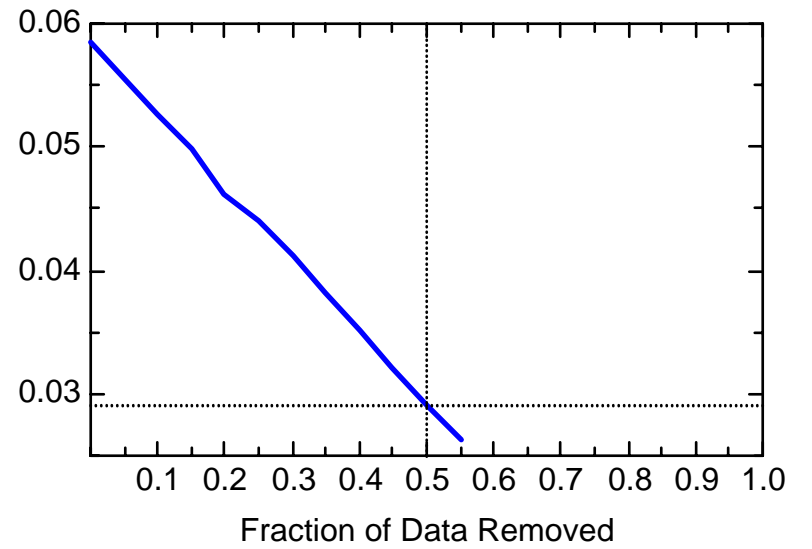
FE: Well JBW7328



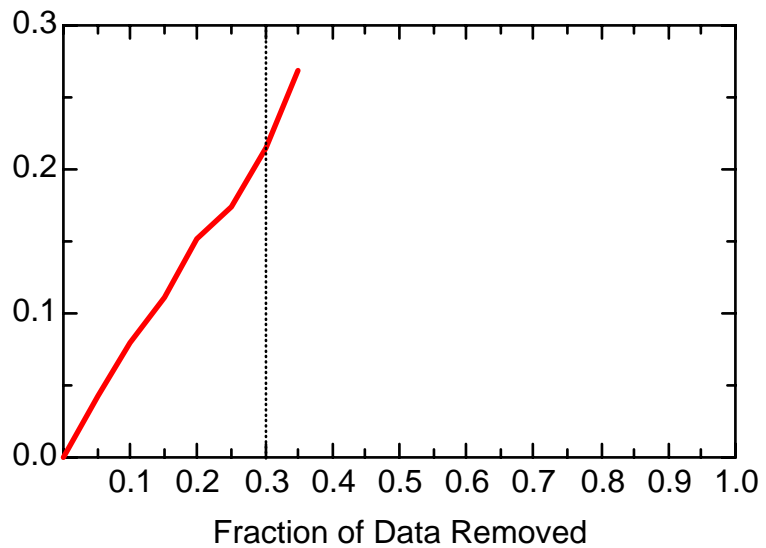
FE: Well JBW7328



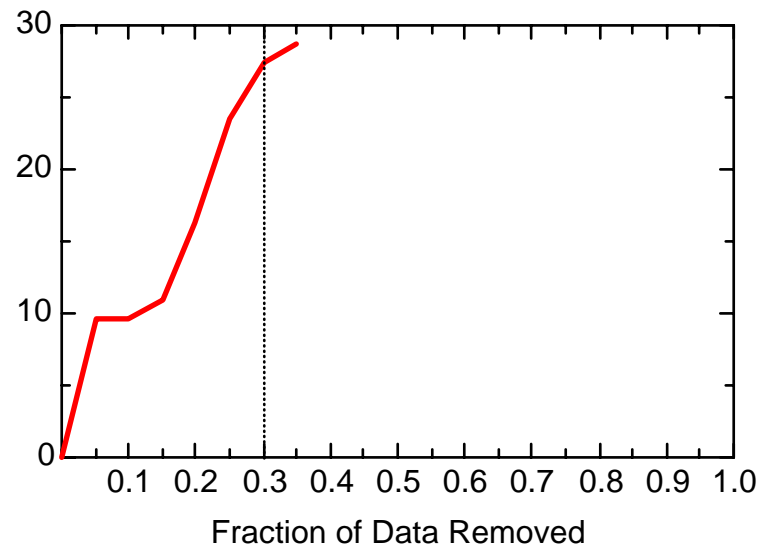
FE: Well JBW7328



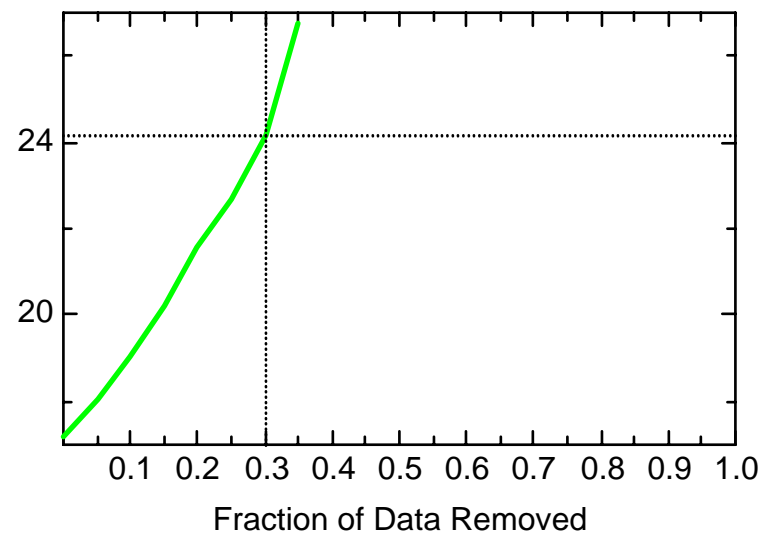
FE: Well JBW7330A



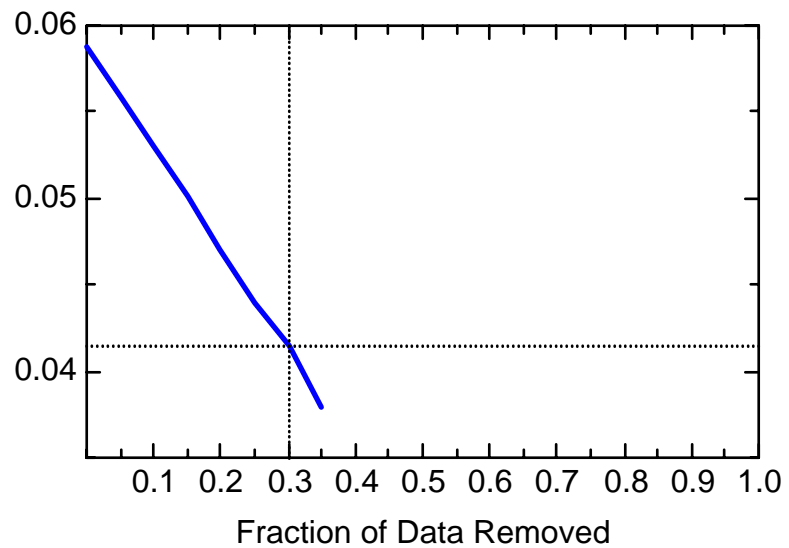
FE: Well JBW7330A



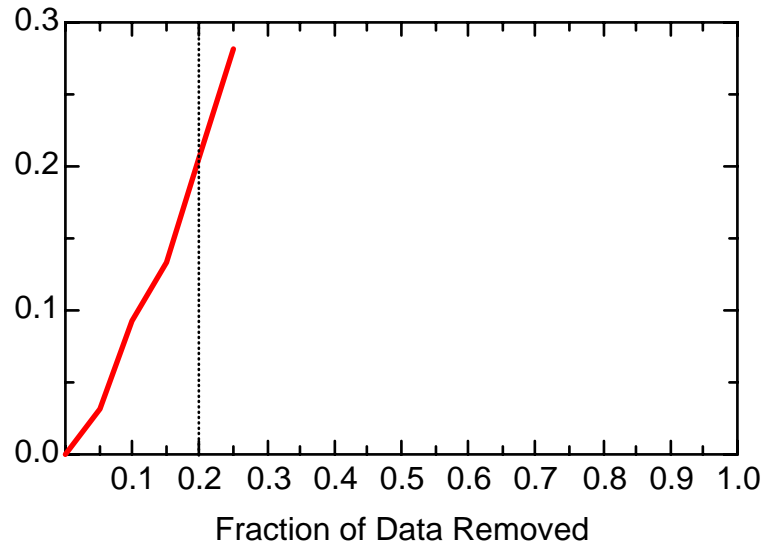
FE: Well JBW7330A



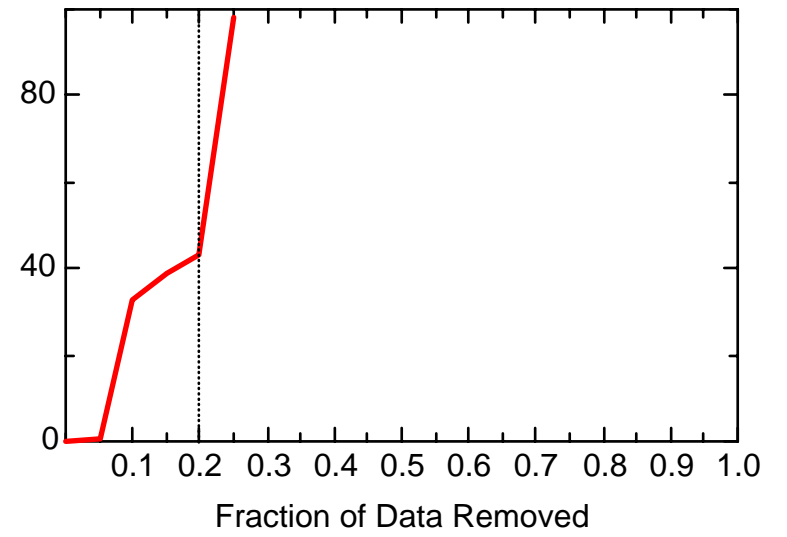
FE: Well JBW7330A



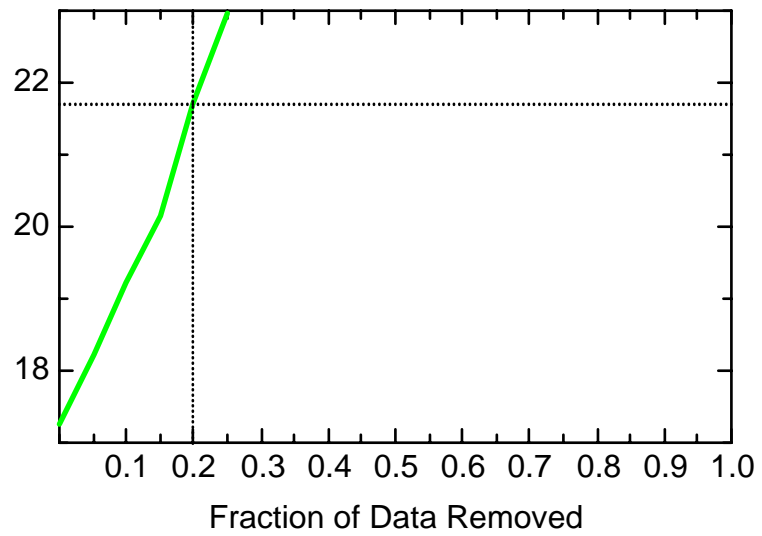
FE: Well JBW7333



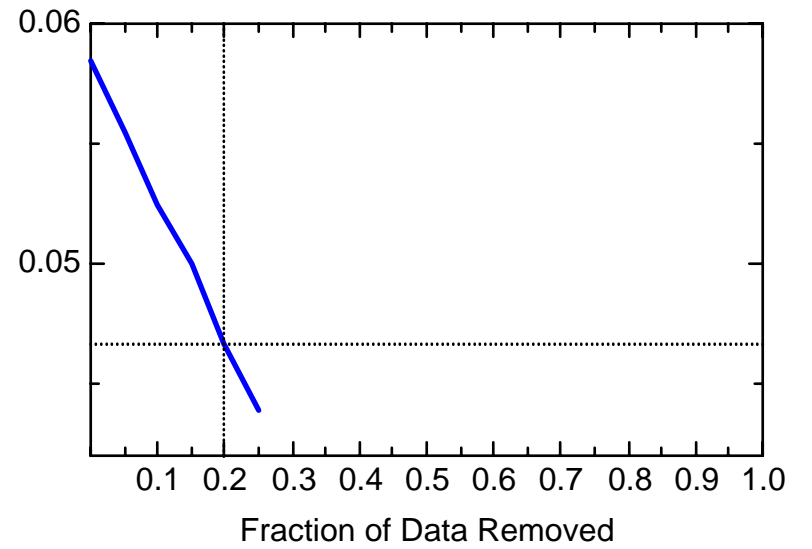
FE: Well JBW7333



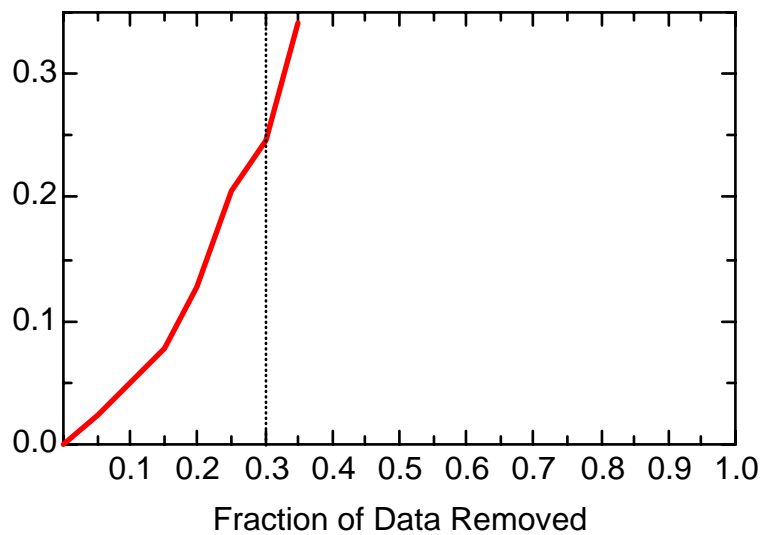
FE: Well JBW7333



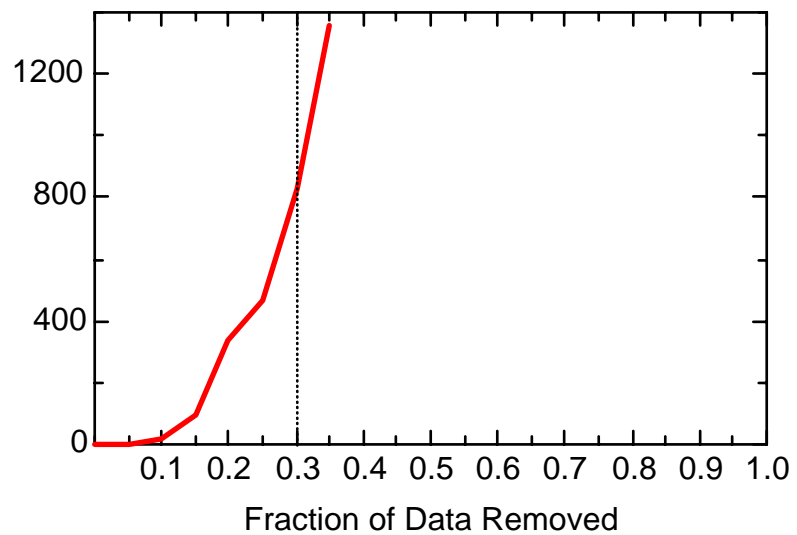
FE: Well JBW7333



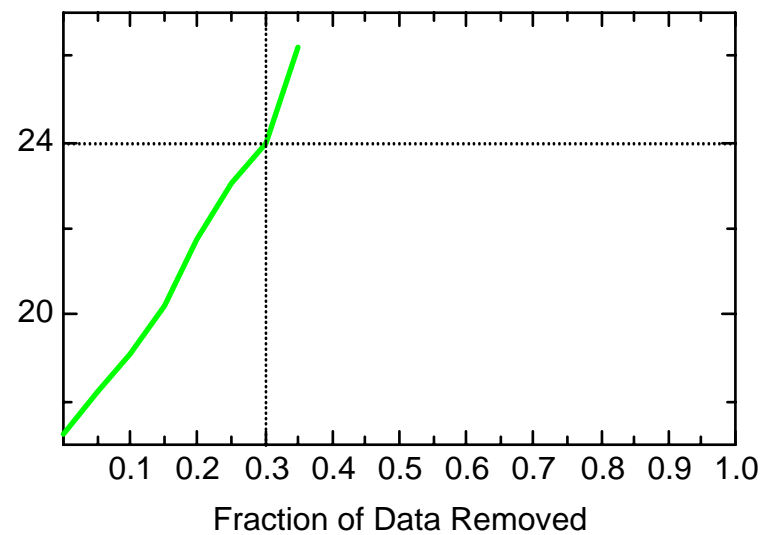
FE: Well JBW7338A



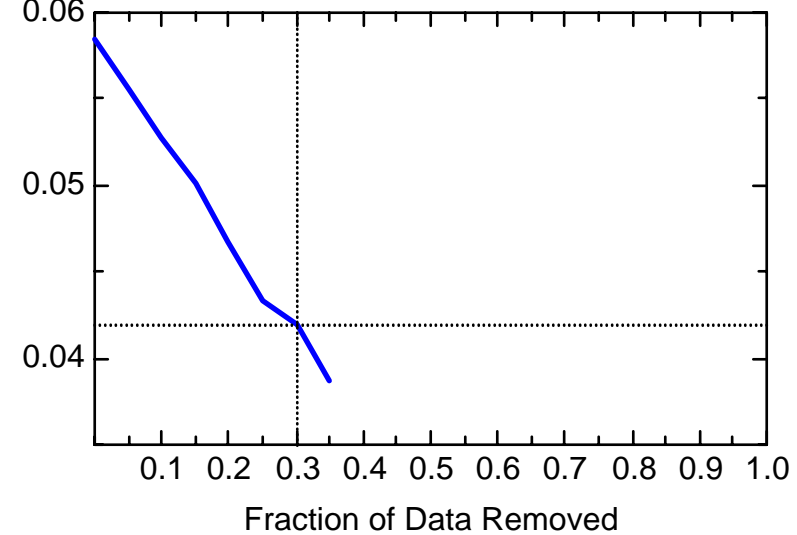
FE: Well JBW7338A



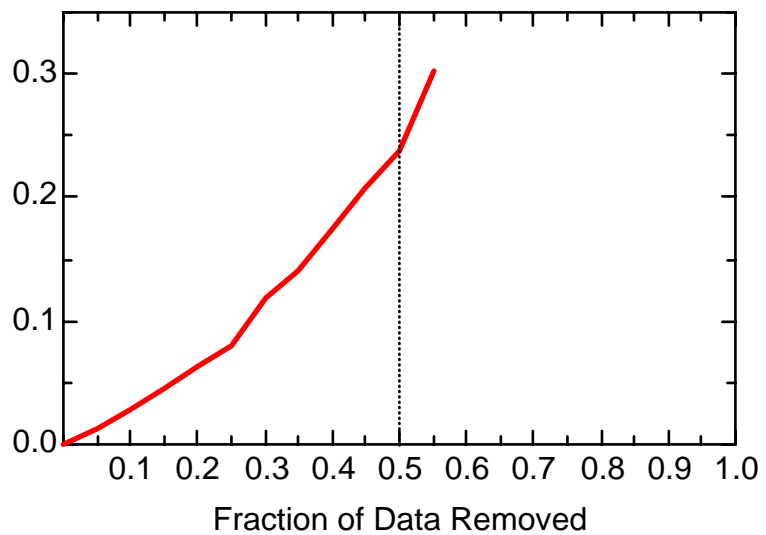
FE: Well JBW7338A



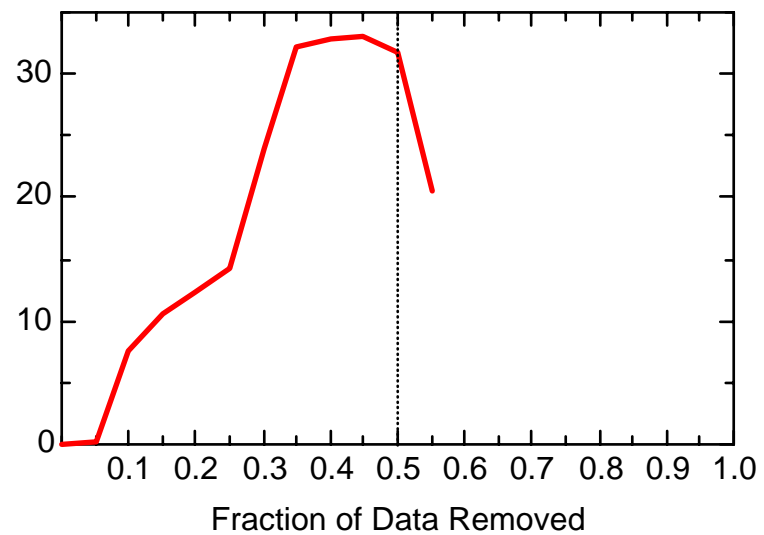
FE: Well JBW7338A



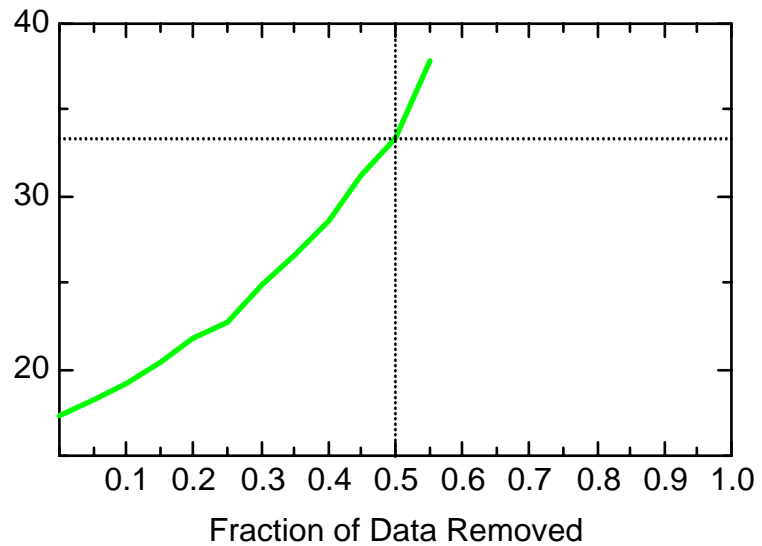
FE: Well JBW7338B



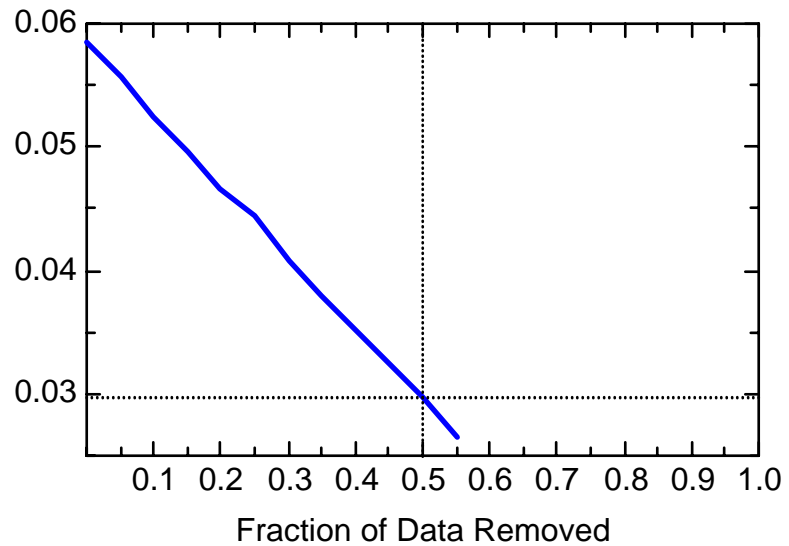
FE: Well JBW7338B



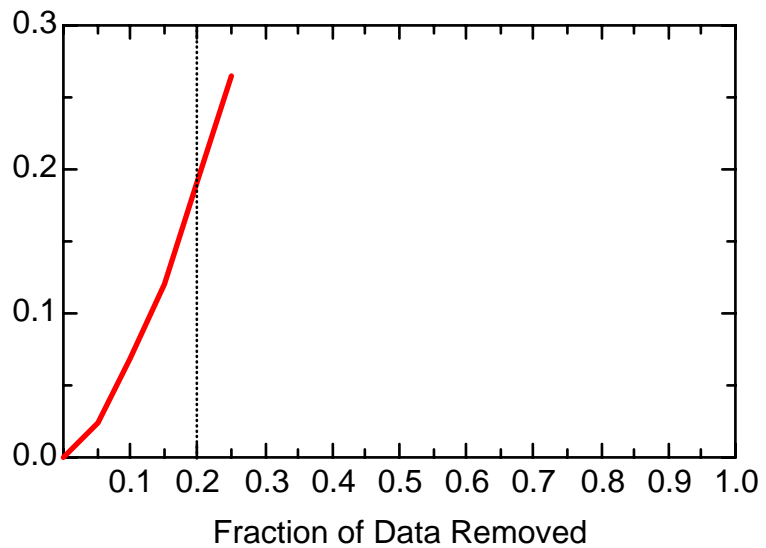
FE: Well JBW7338B



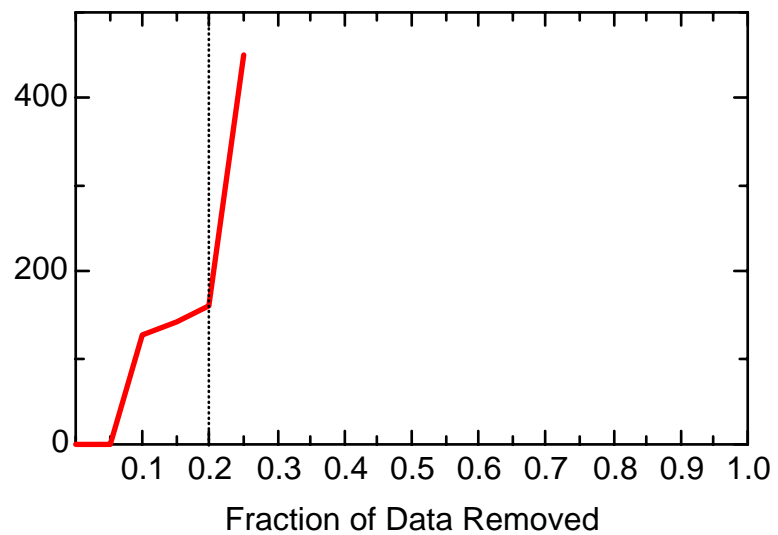
FE: Well JBW7338B



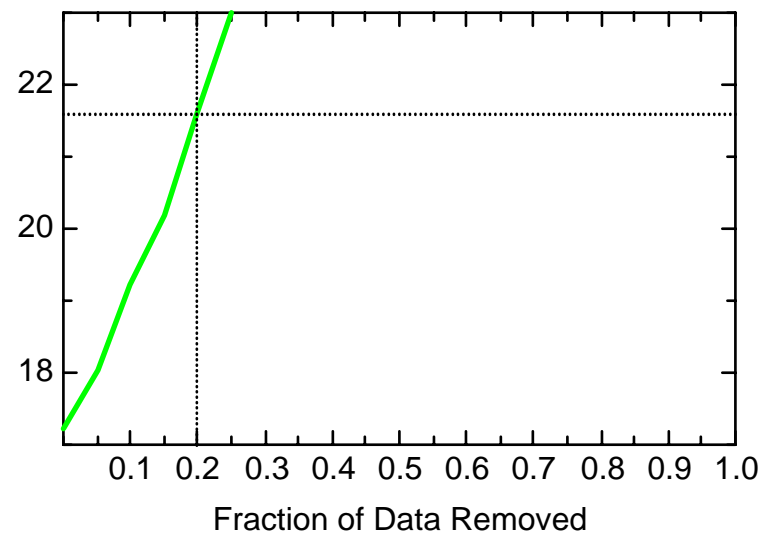
FE: Well JBW7340B



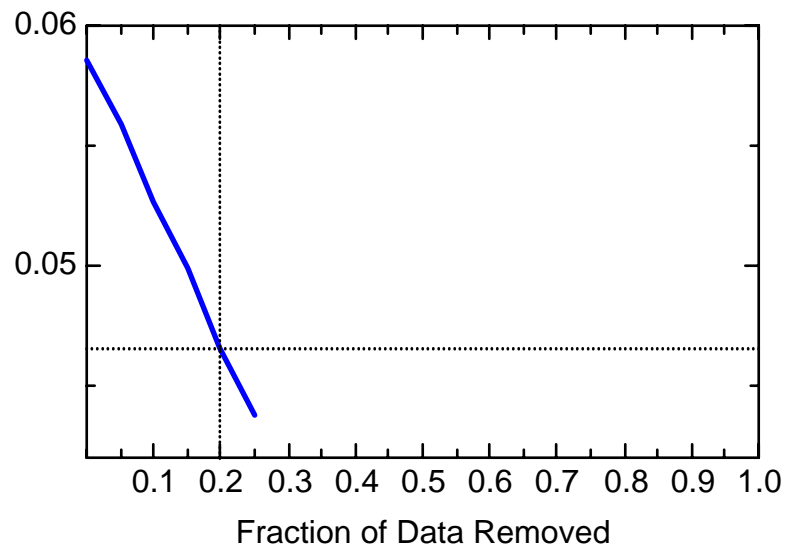
FE: Well JBW7340B



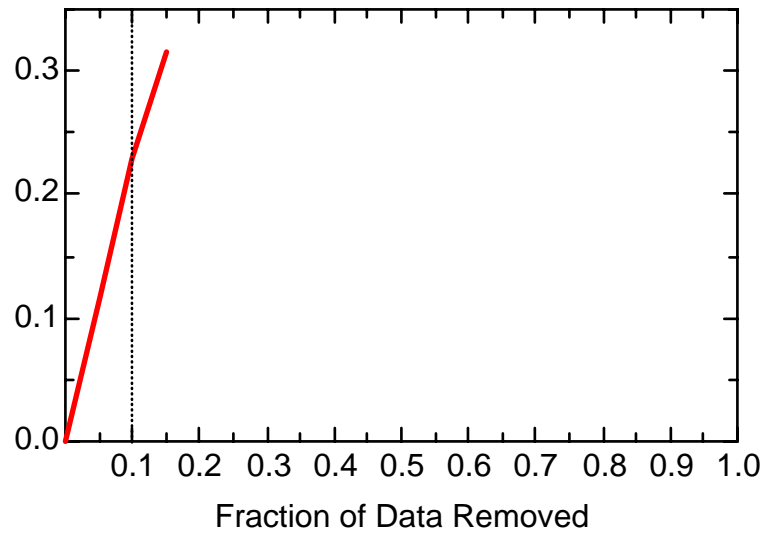
FE: Well JBW7340B



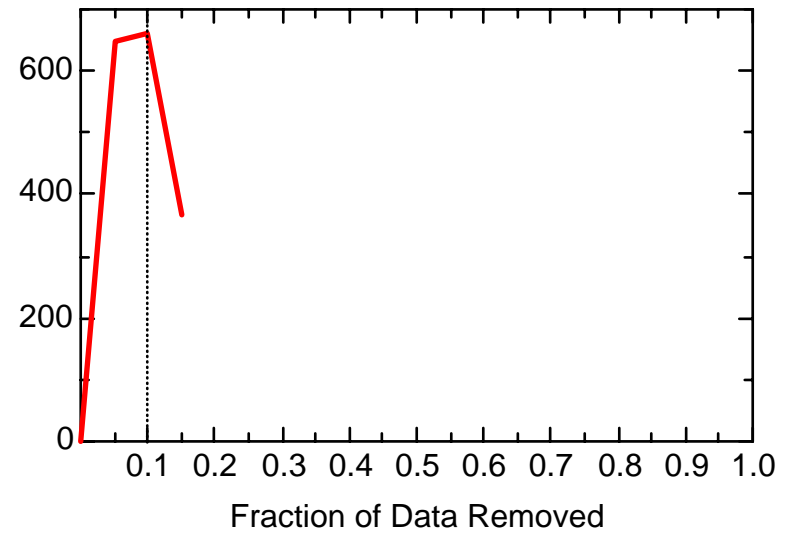
FE: Well JBW7340B



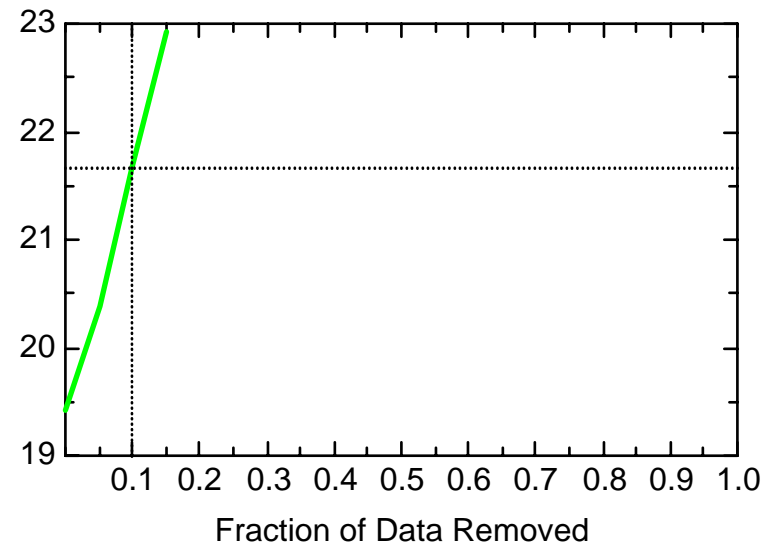
FE: Well JBW7344



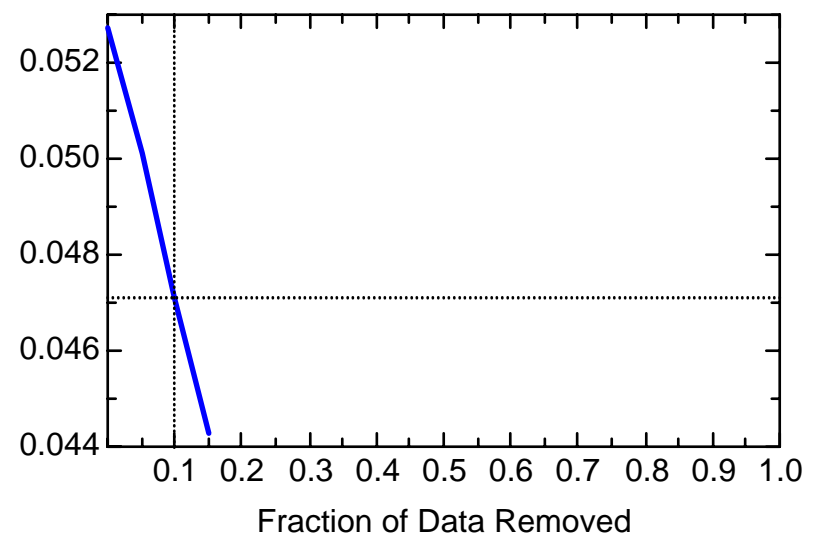
FE: Well JBW7344



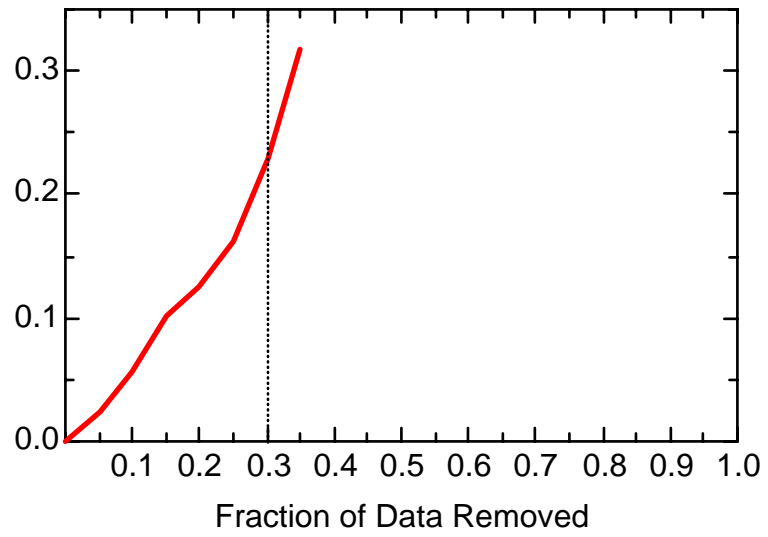
FE: Well JBW7344



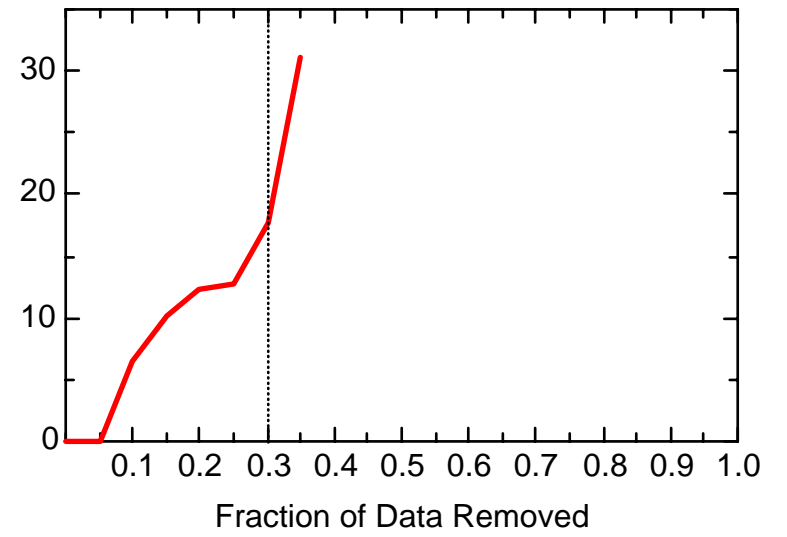
FE: Well JBW7344



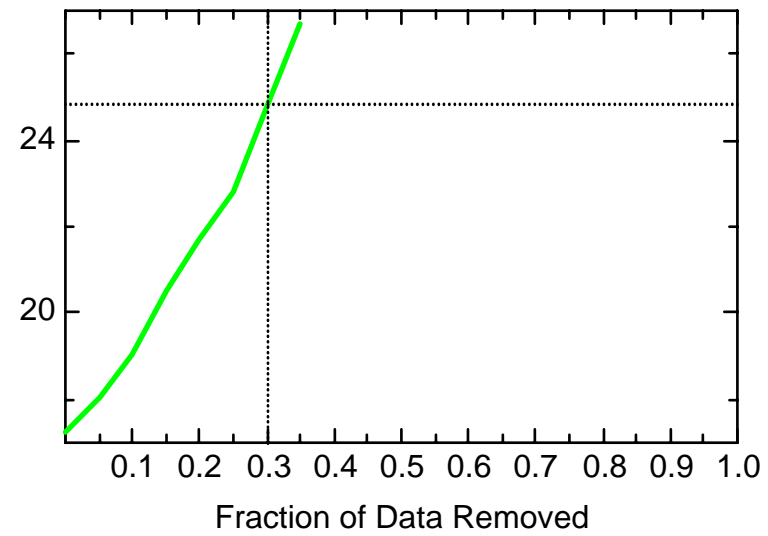
FE: Well JBW7345A



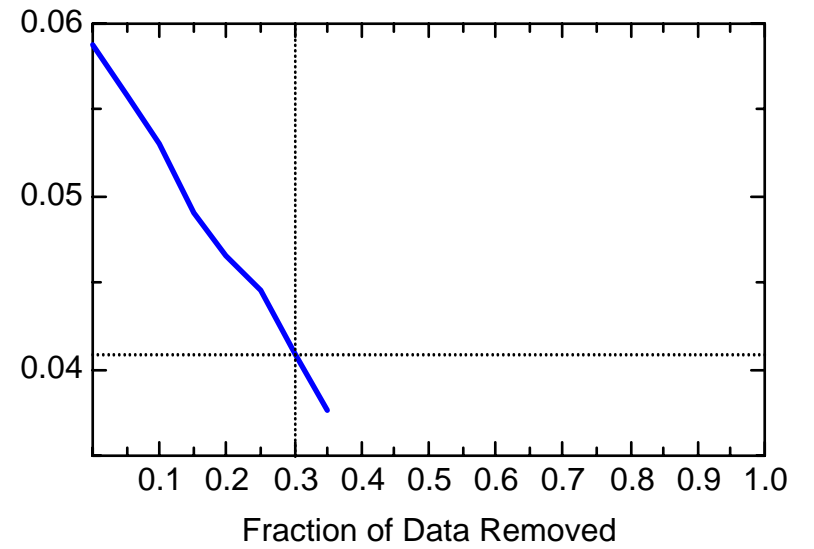
FE: Well JBW7345A



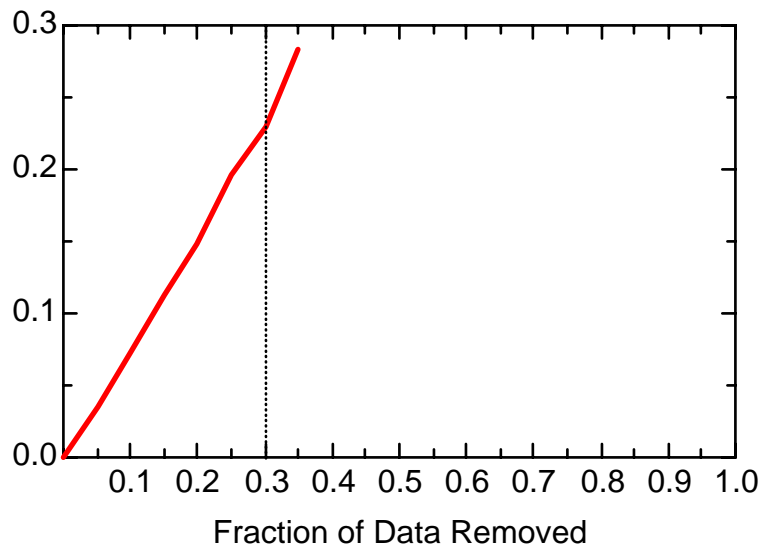
FE: Well JBW7345A



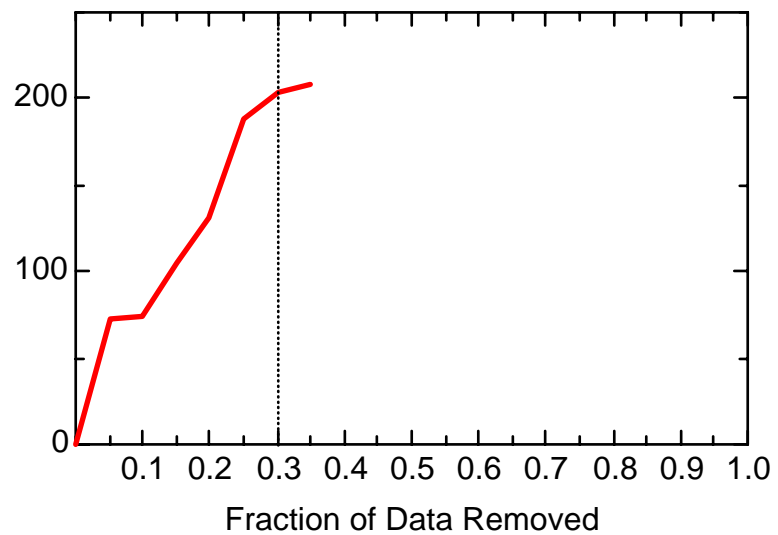
FE: Well JBW7345A



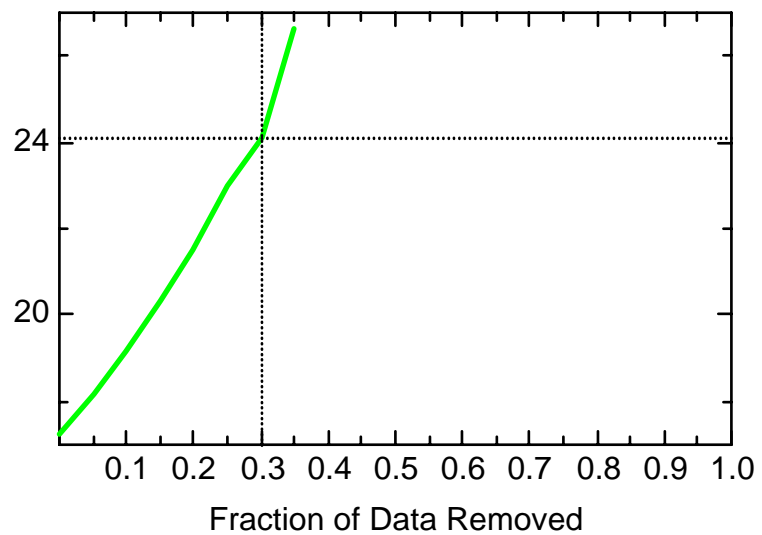
FE: Well JBW7347B



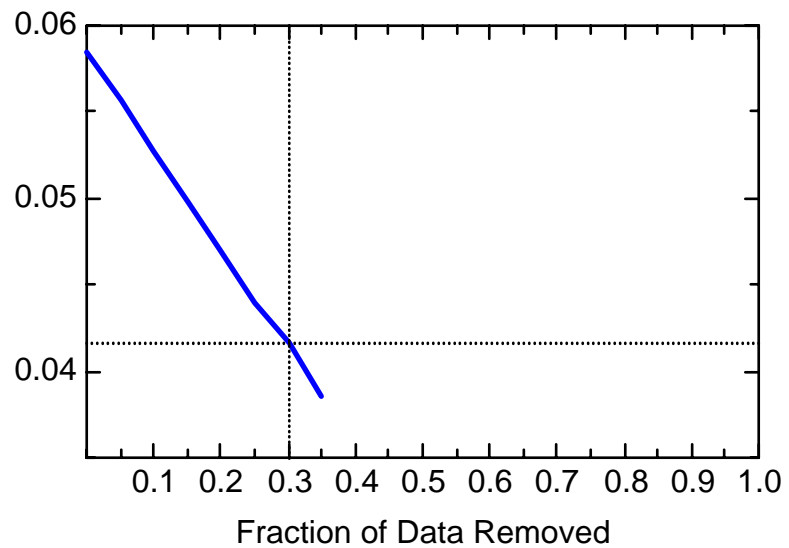
FE: Well JBW7347B



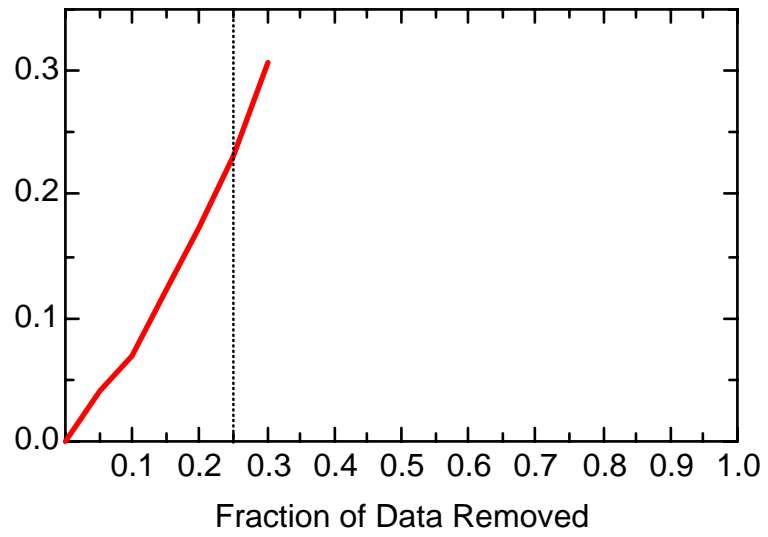
FE: Well JBW7347B



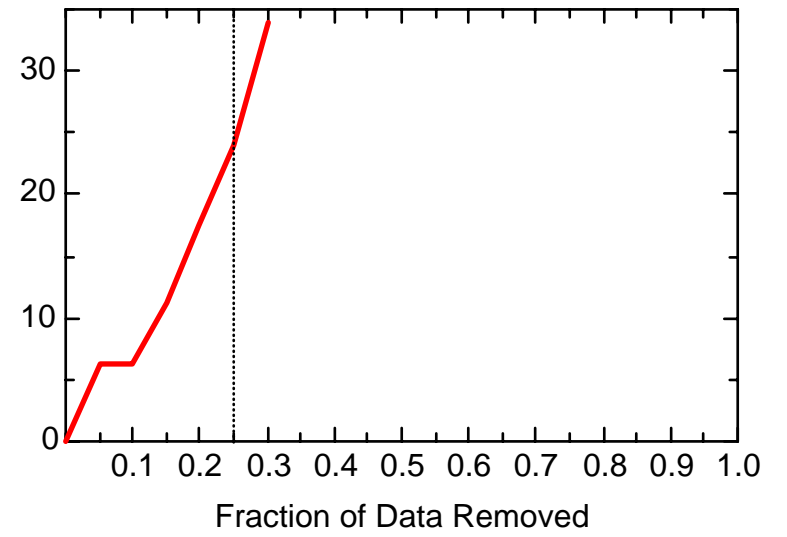
FE: Well JBW7347B



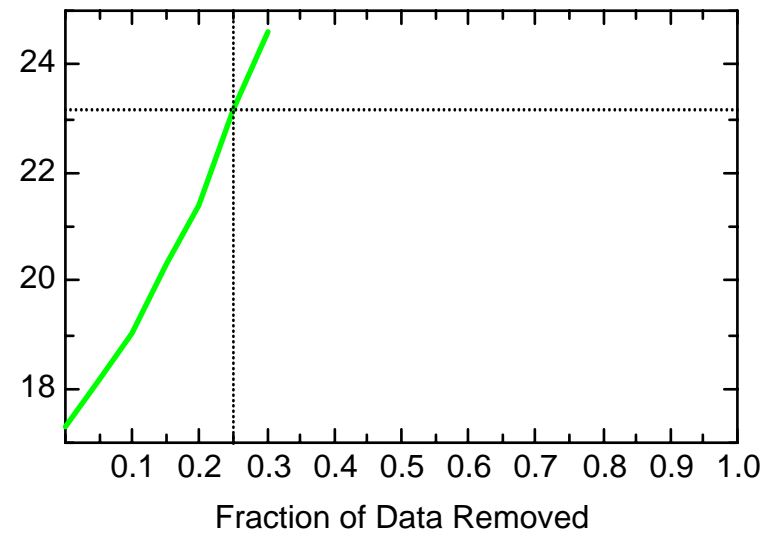
FE: Well JBW7348



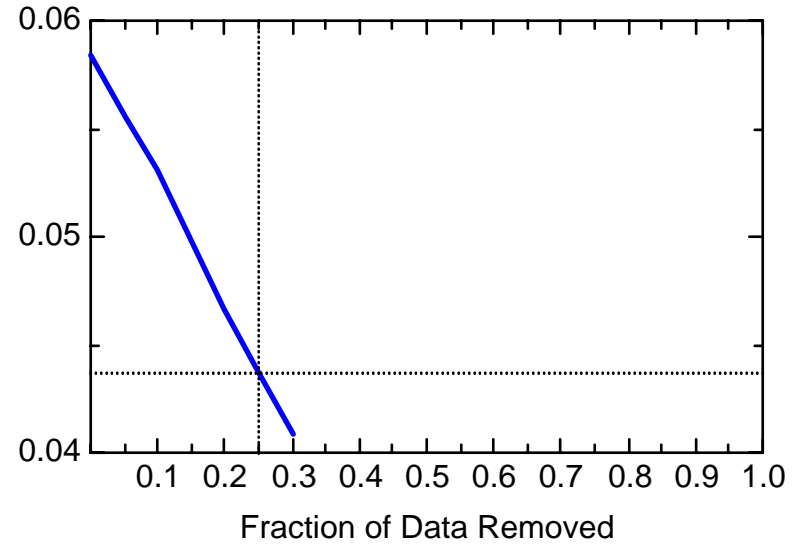
FE: Well JBW7348



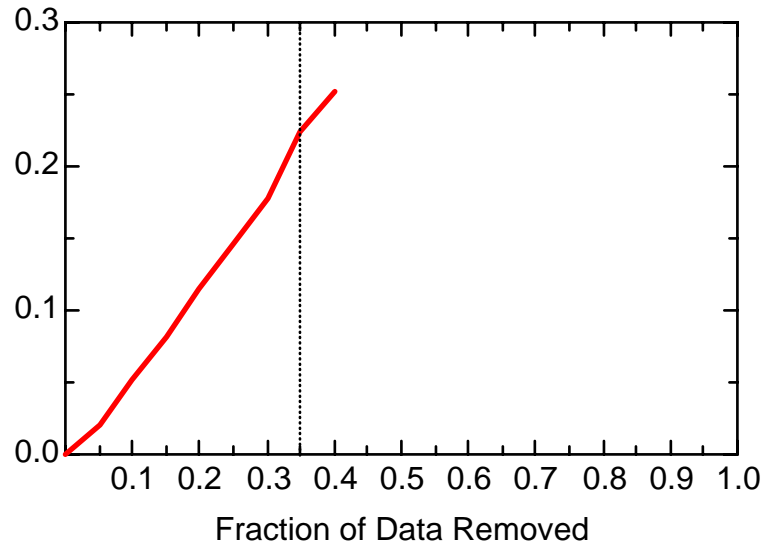
FE: Well JBW7348



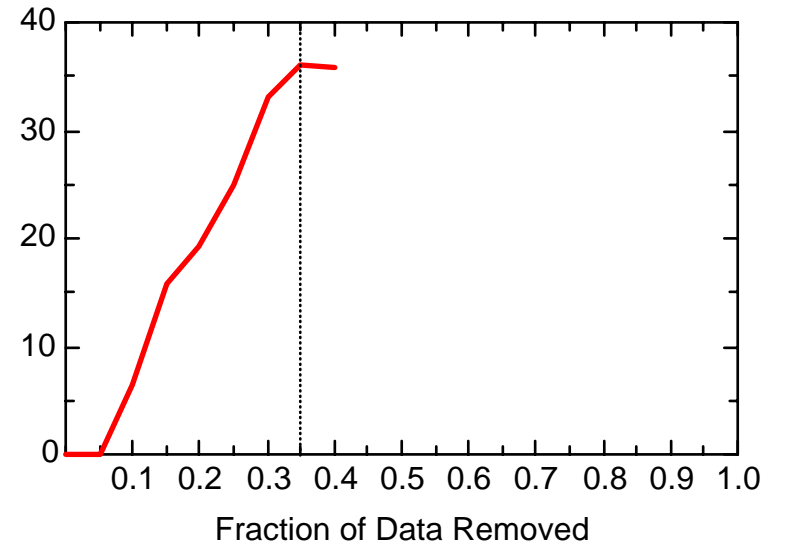
FE: Well JBW7348



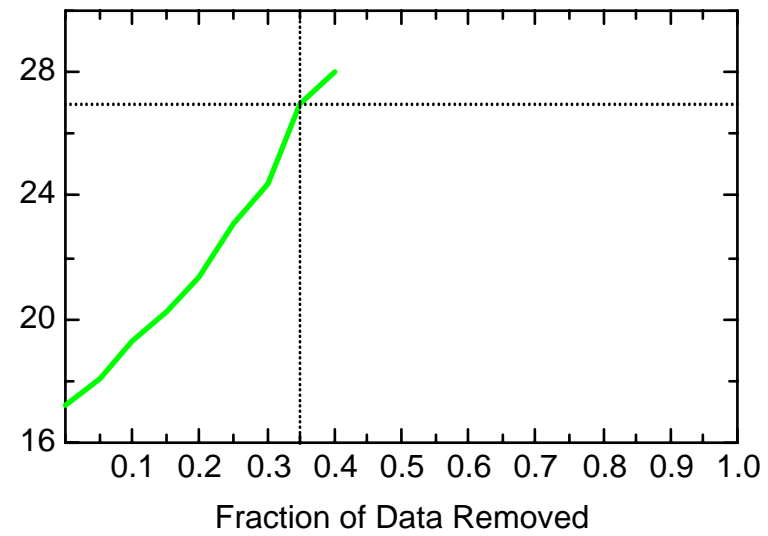
FE: Well JBW7350



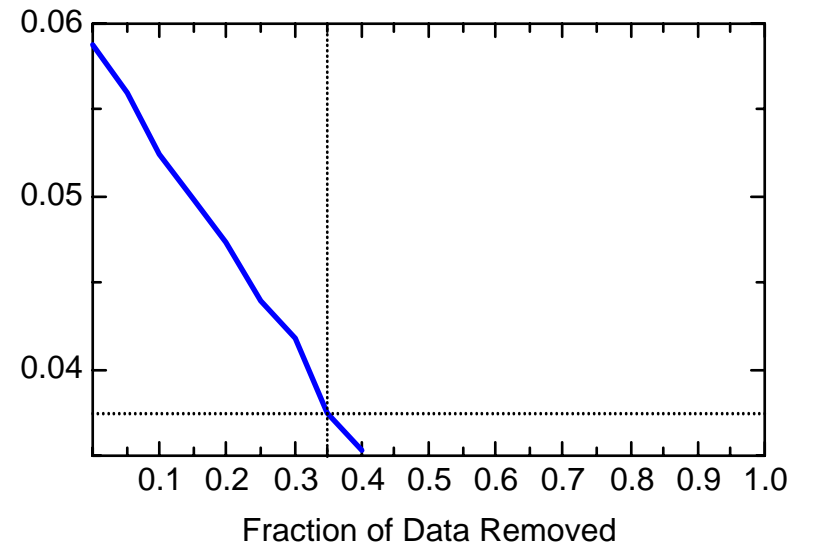
FE: Well JBW7350



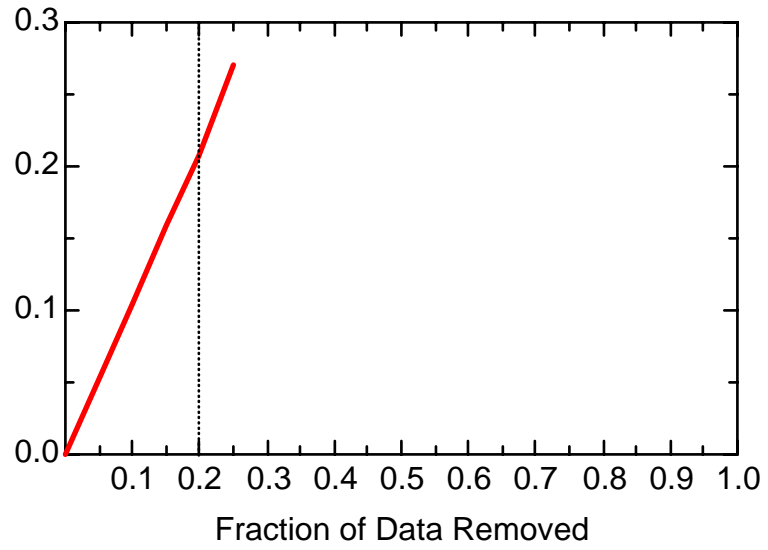
FE: Well JBW7350



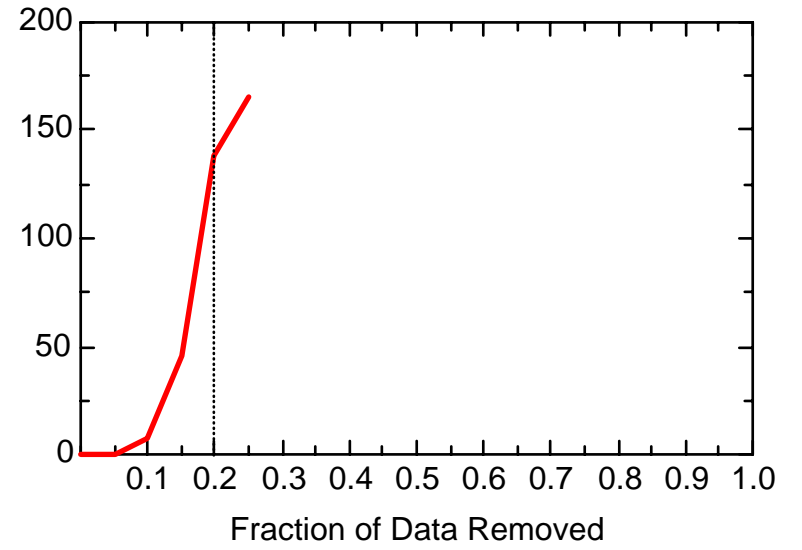
FE: Well JBW7350



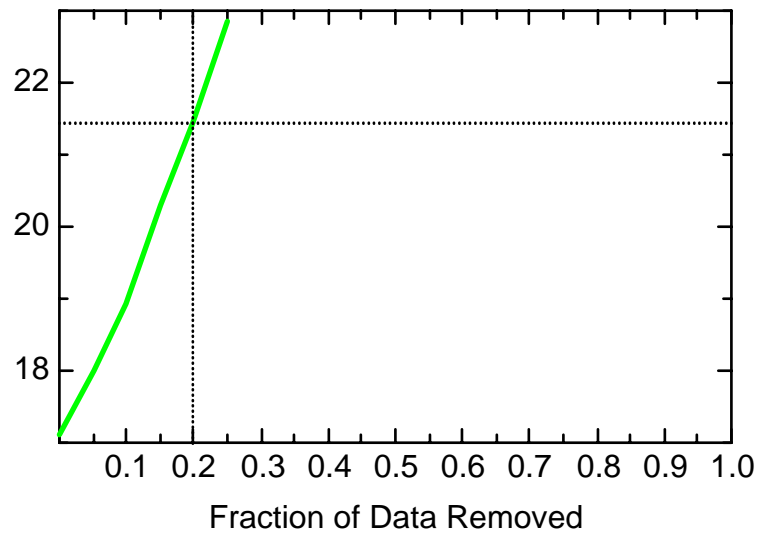
FE: Well JBW7806



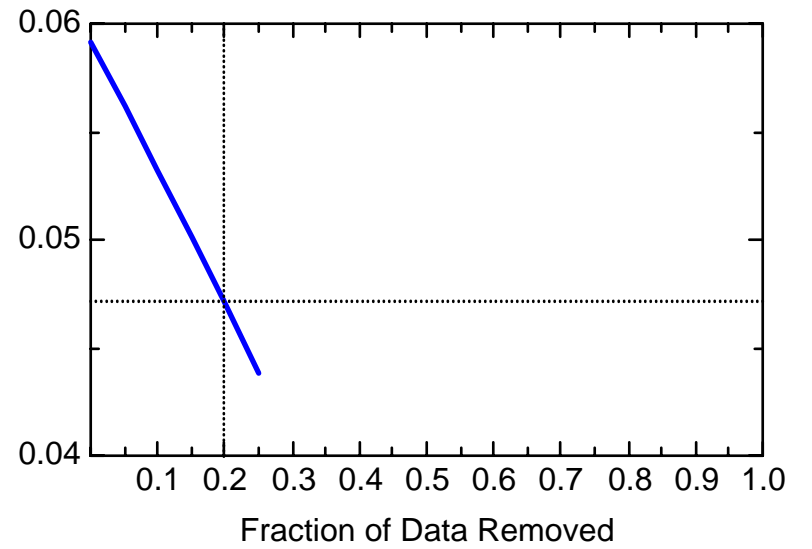
FE: Well JBW7806



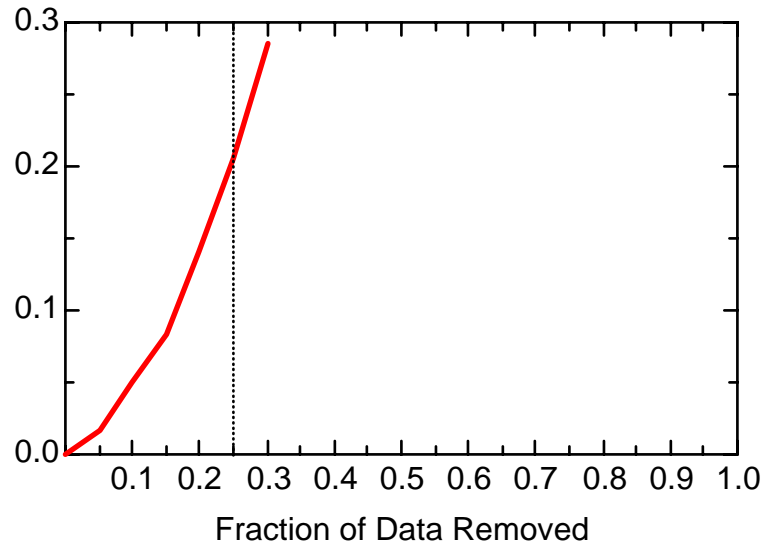
FE: Well JBW7806



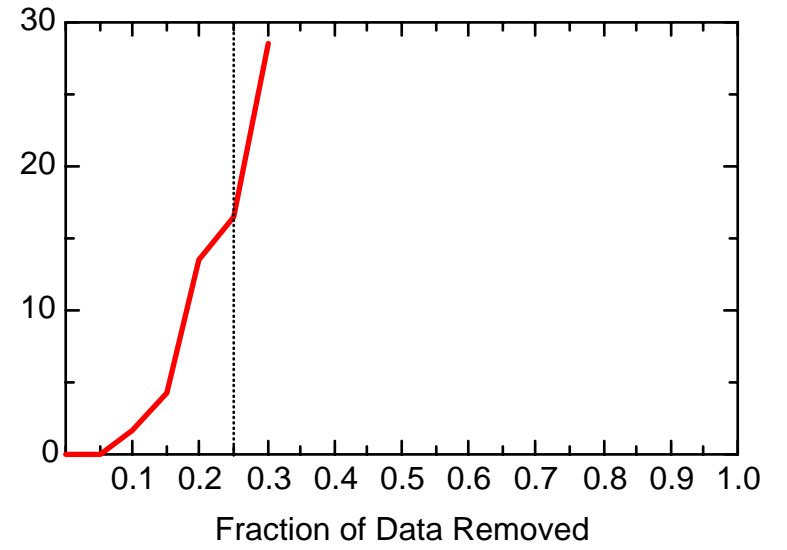
FE: Well JBW7806



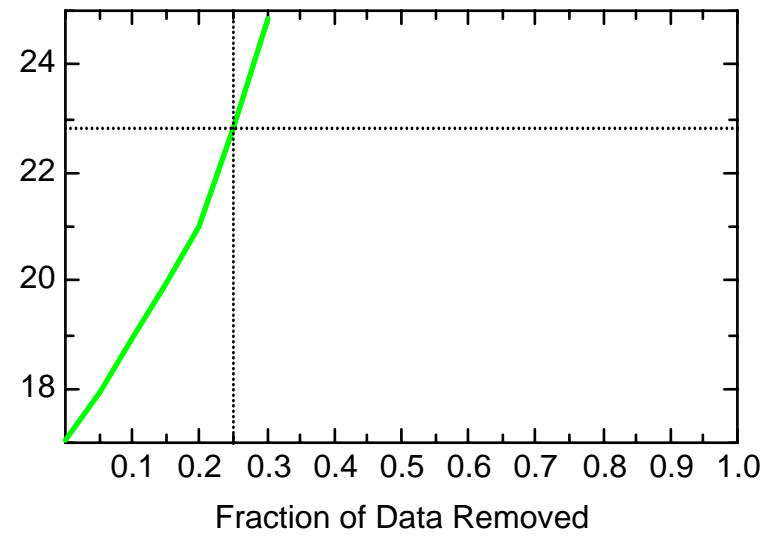
FE: Well JBW7809



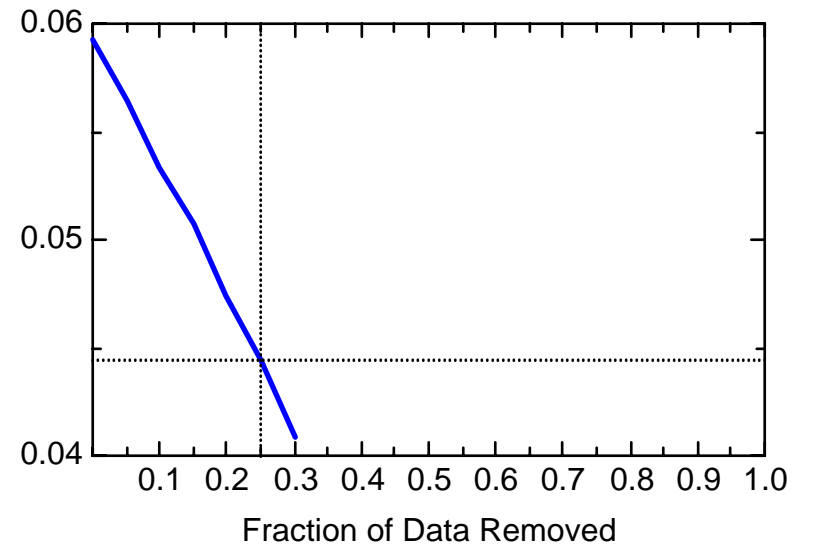
FE: Well JBW7809



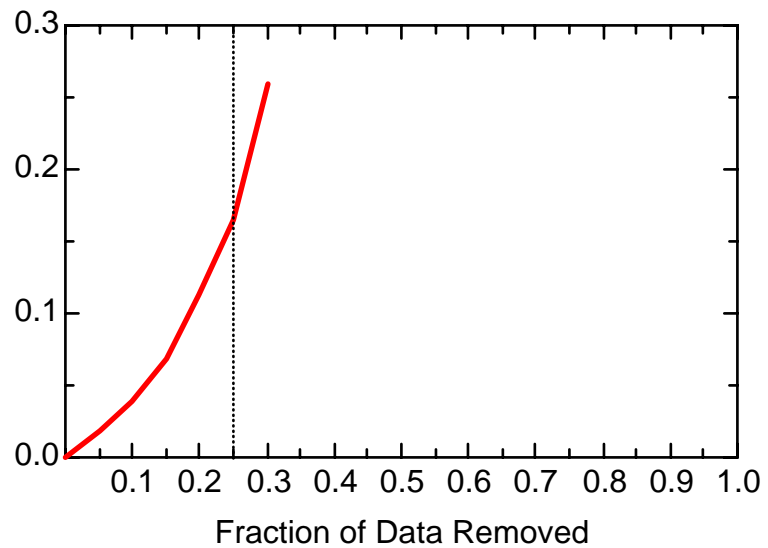
FE: Well JBW7809



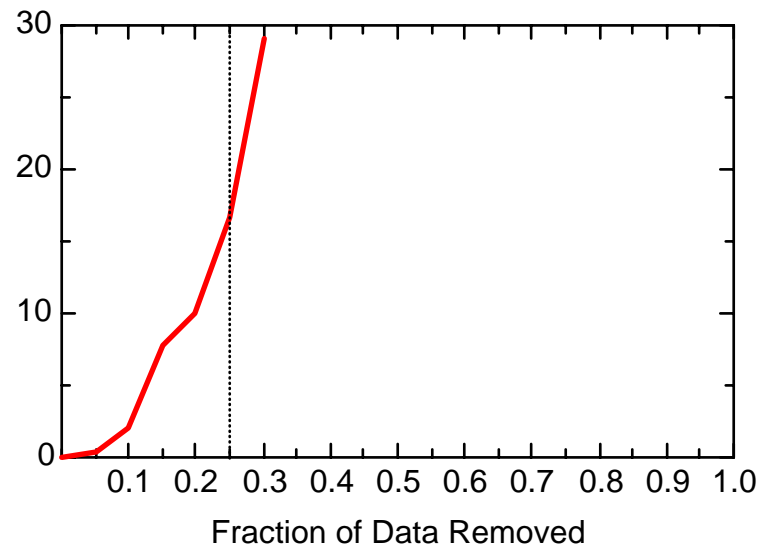
FE: Well JBW7809



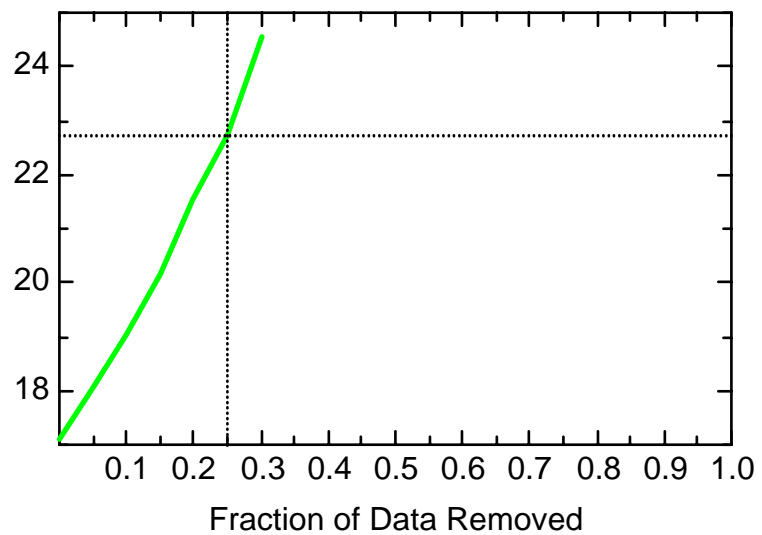
FE: Well JBW7812B



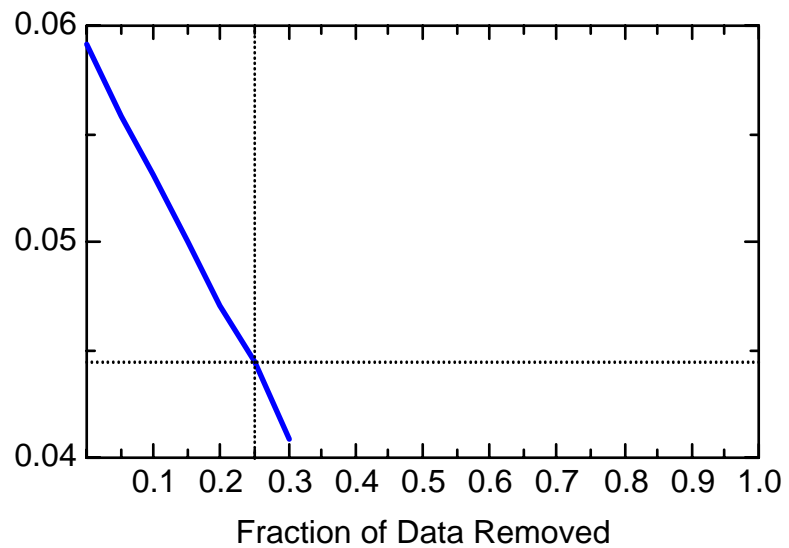
FE: Well JBW7812B



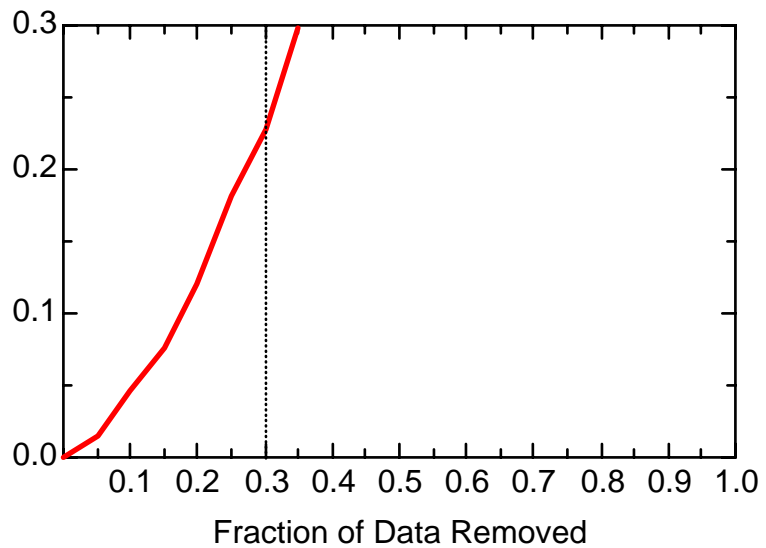
FE: Well JBW7812B



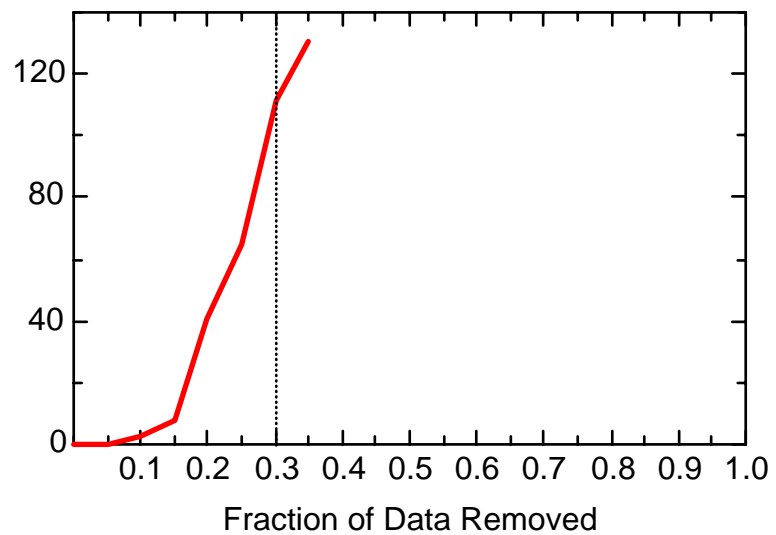
FE: Well JBW7812B



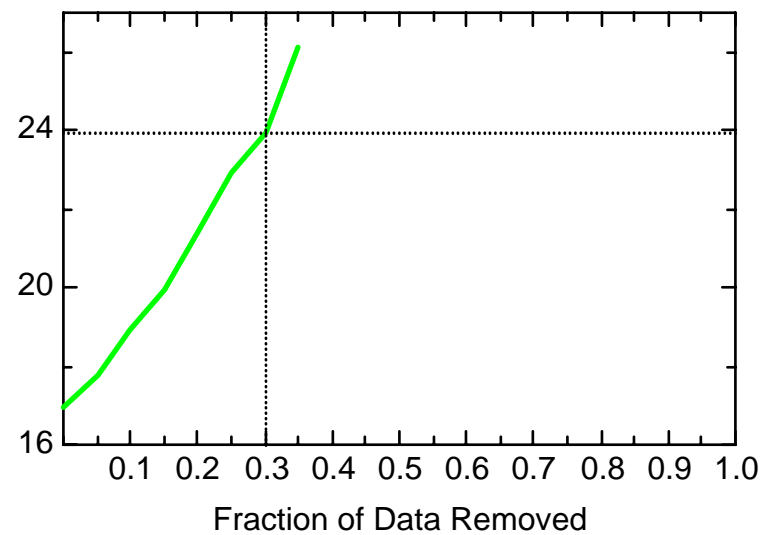
FE: Well JBW8003B



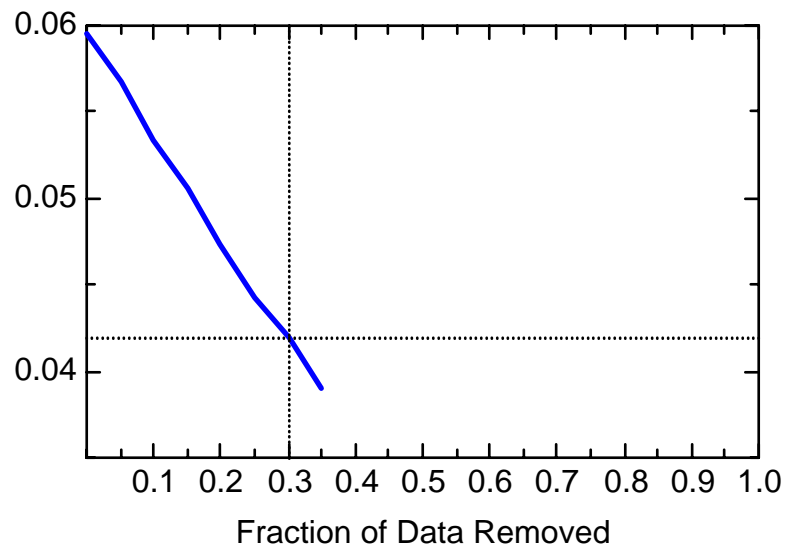
FE: Well JBW8003B



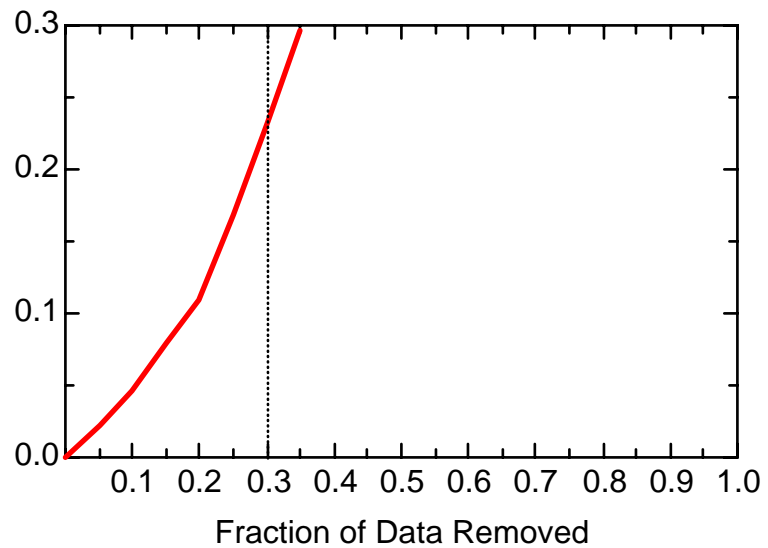
FE: Well JBW8003B



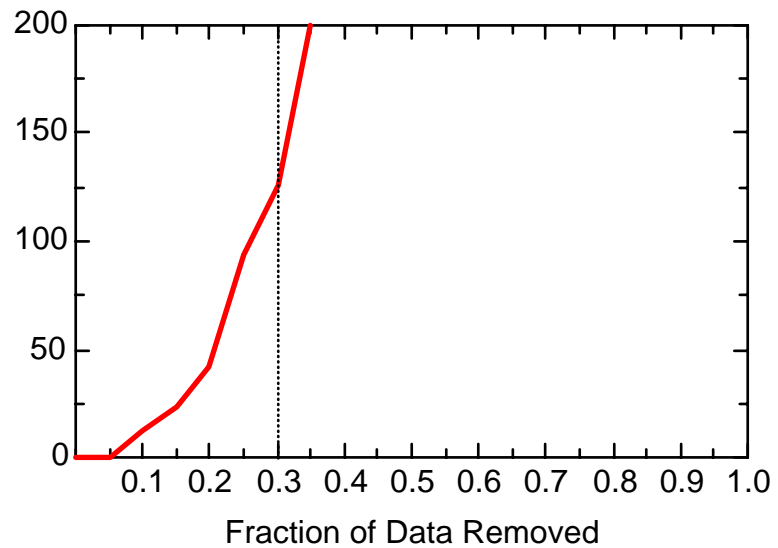
FE: Well JBW8003B



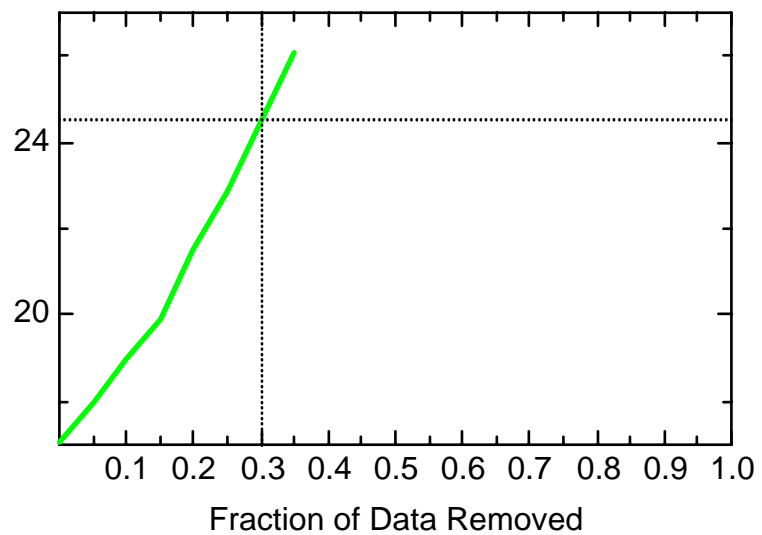
FE: Well JBW8004B



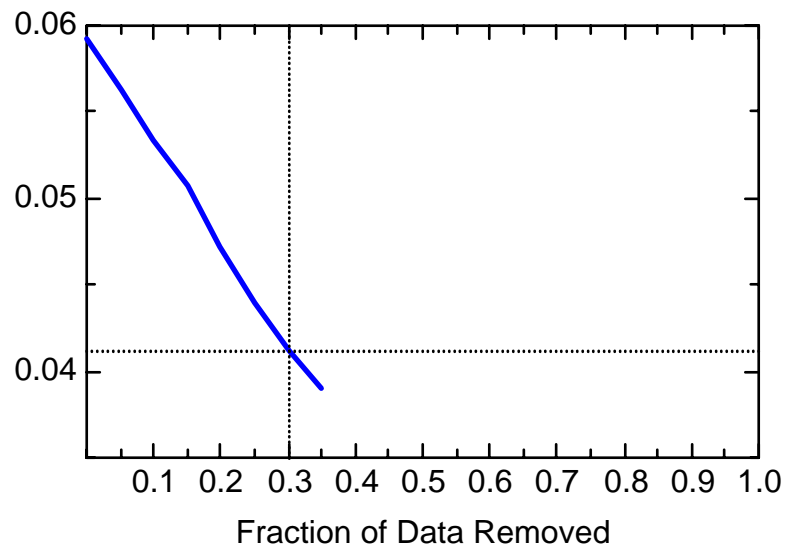
FE: Well JBW8004B



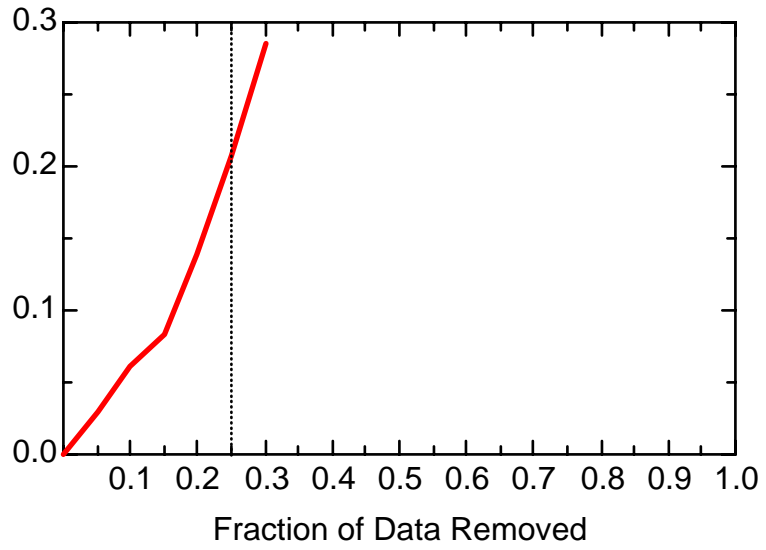
FE: Well JBW8004B



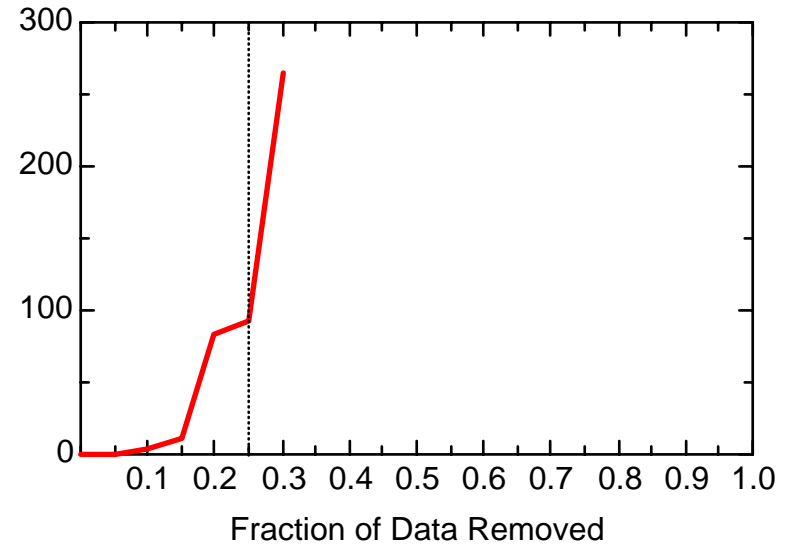
FE: Well JBW8004B



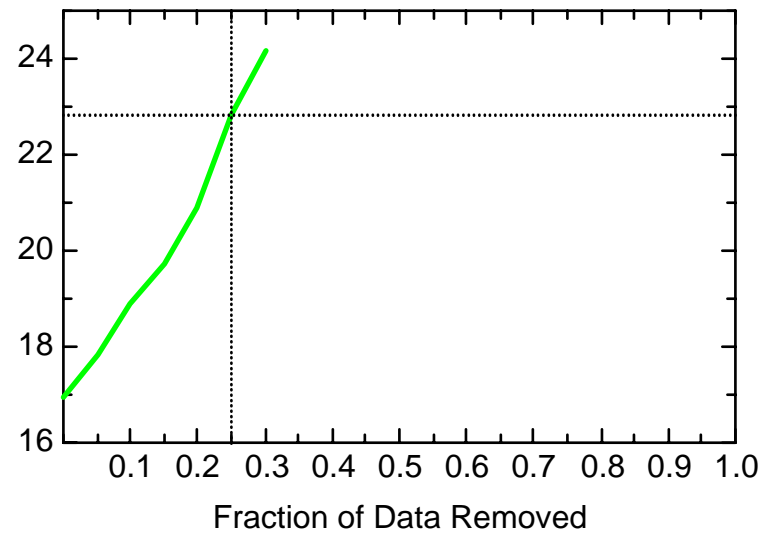
FE: Well JBW8009



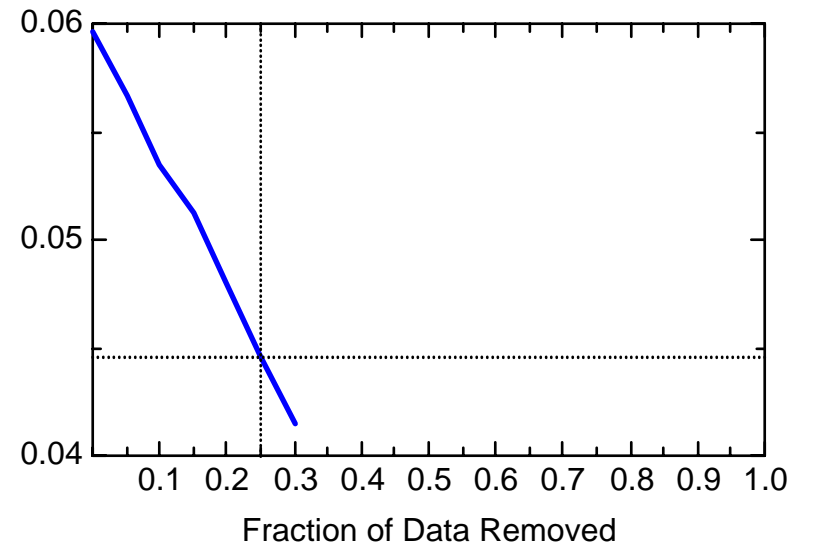
FE: Well JBW8009



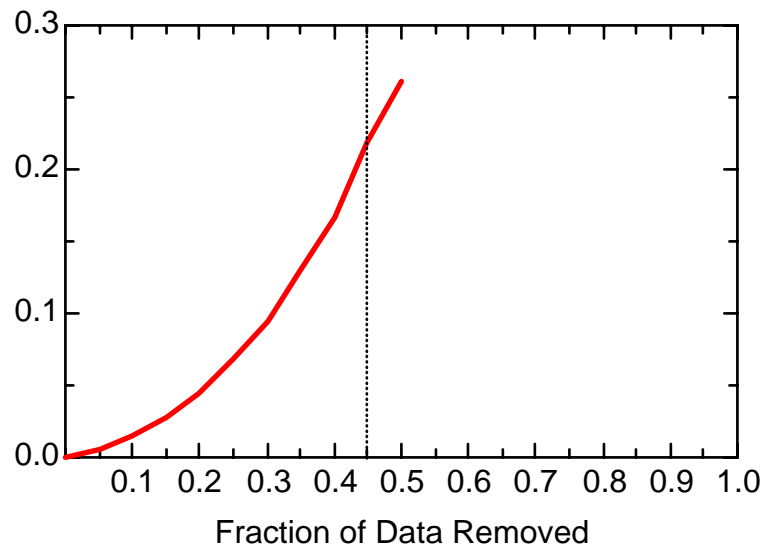
FE: Well JBW8009



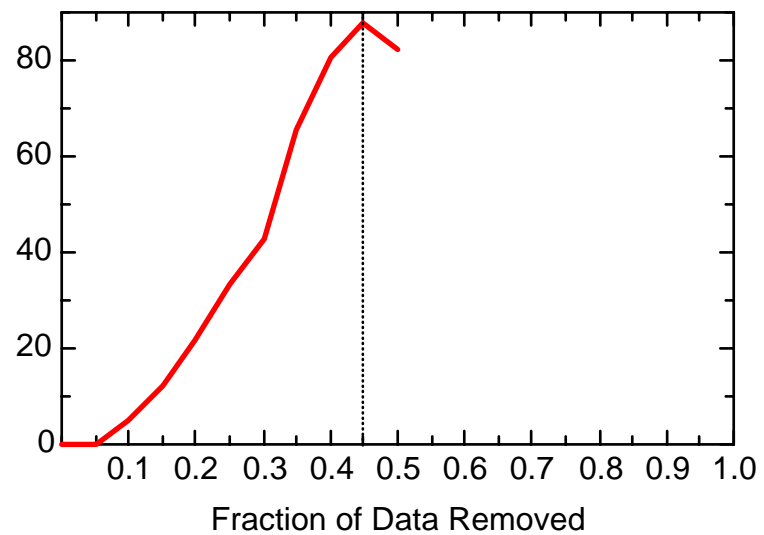
FE: Well JBW8009



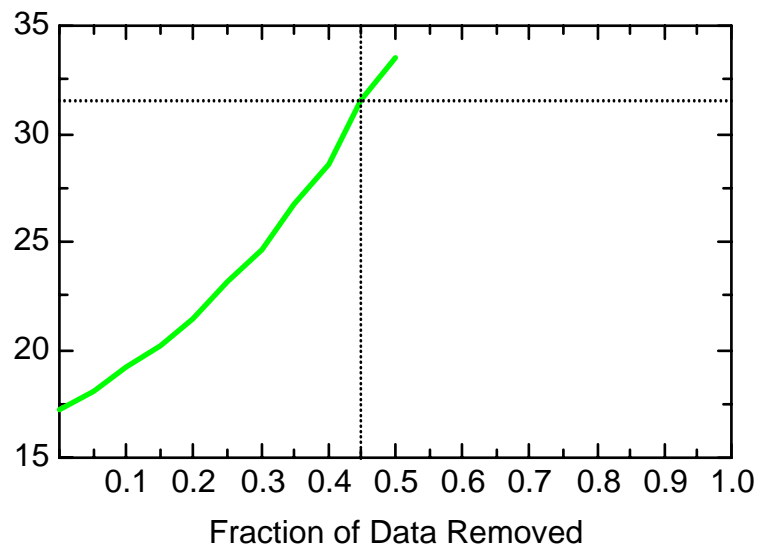
FE: Well JMW35X2



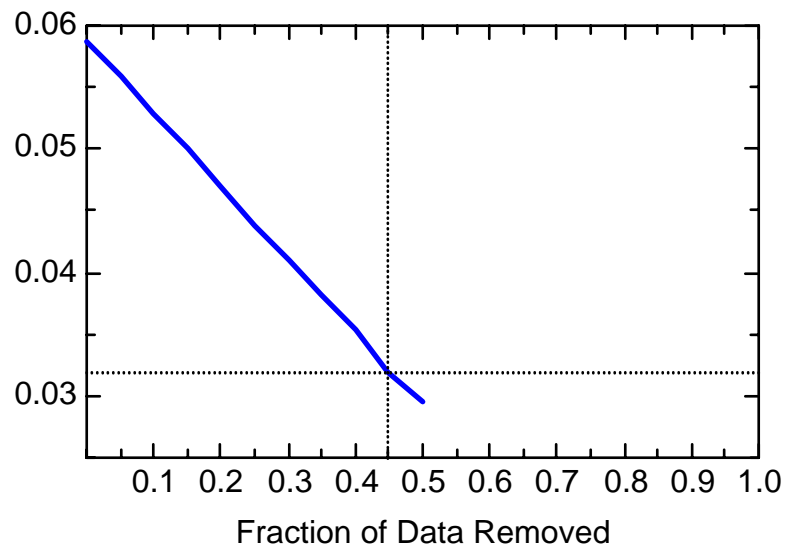
FE: Well JMW35X2



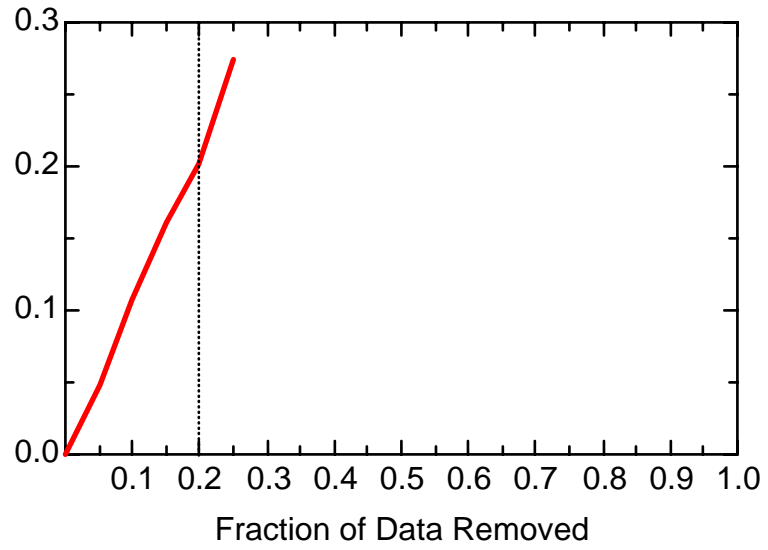
FE: Well JMW35X2



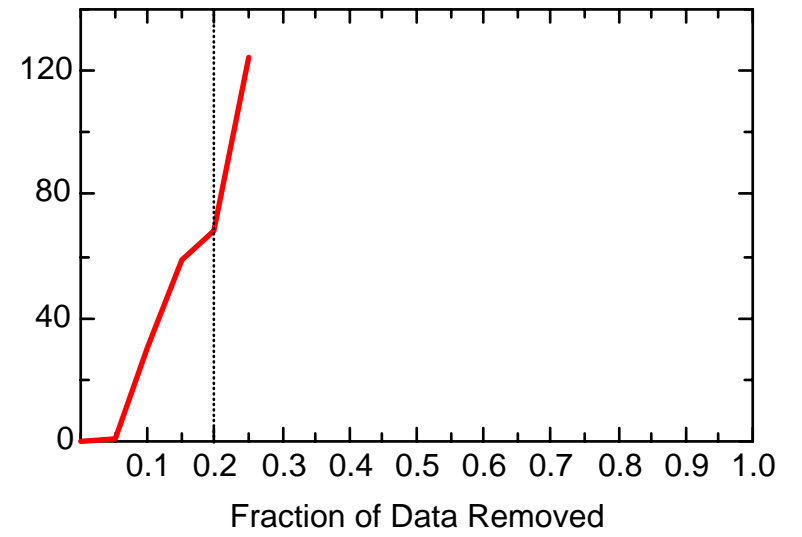
FE: Well JMW35X2



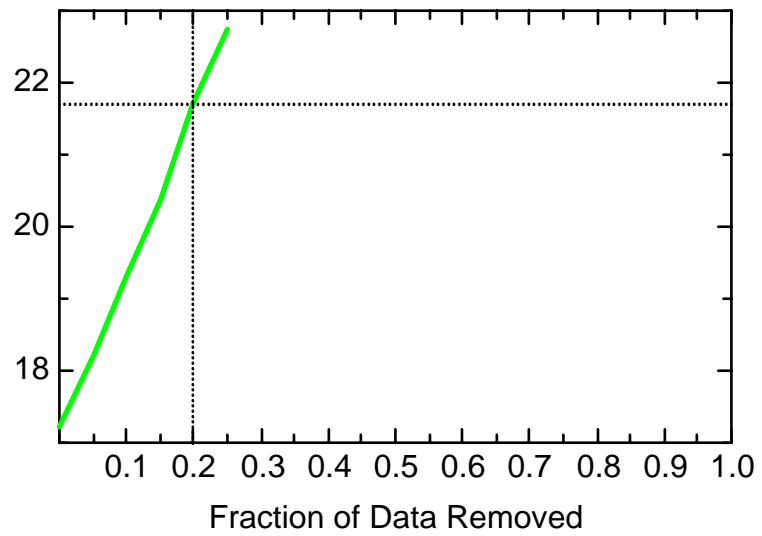
FE: Well JMW0301C



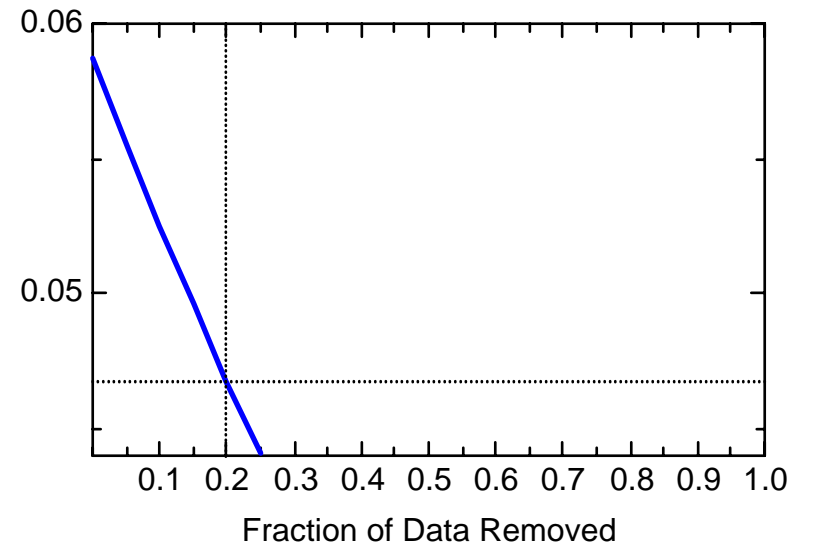
FE: Well JMW0301C



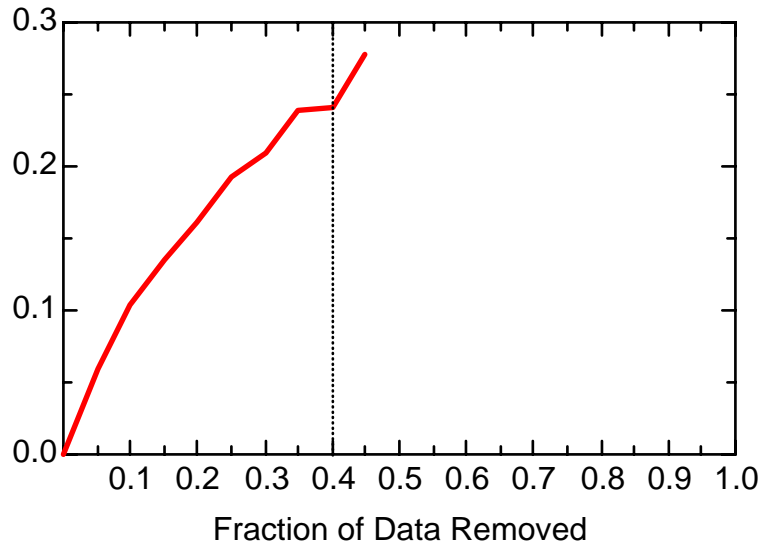
FE: Well JMW0301C



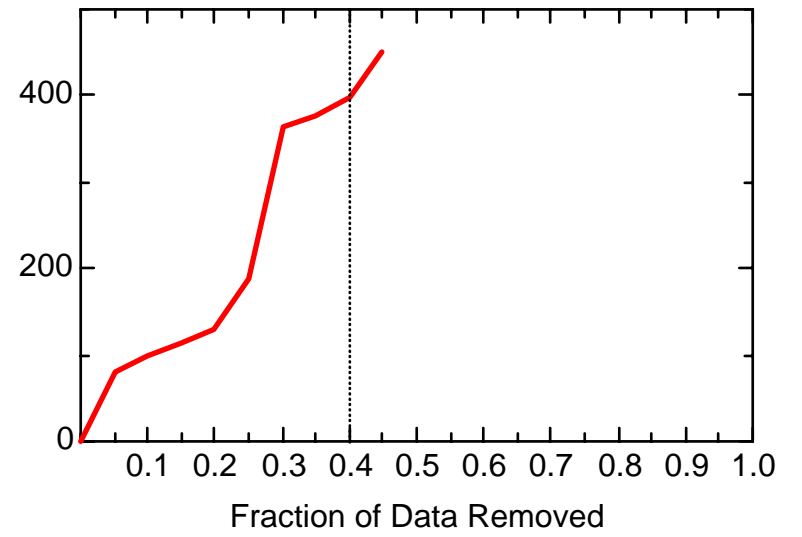
FE: Well JMW0301C



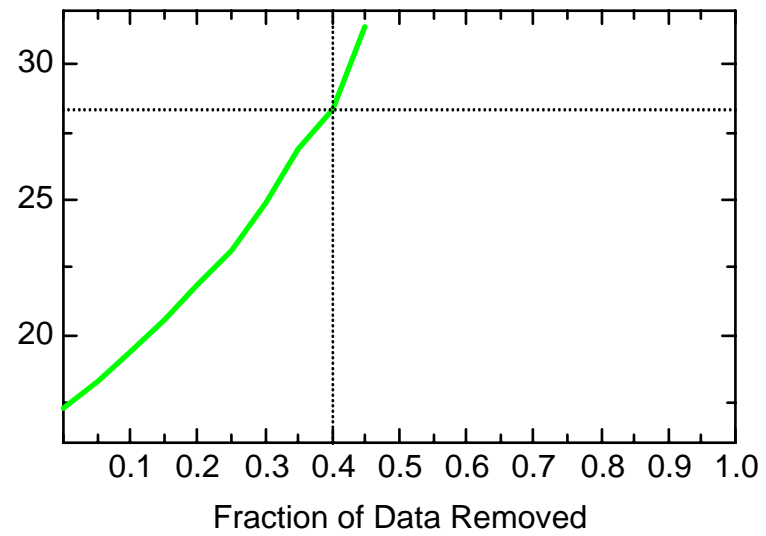
FE: Well JMW0503



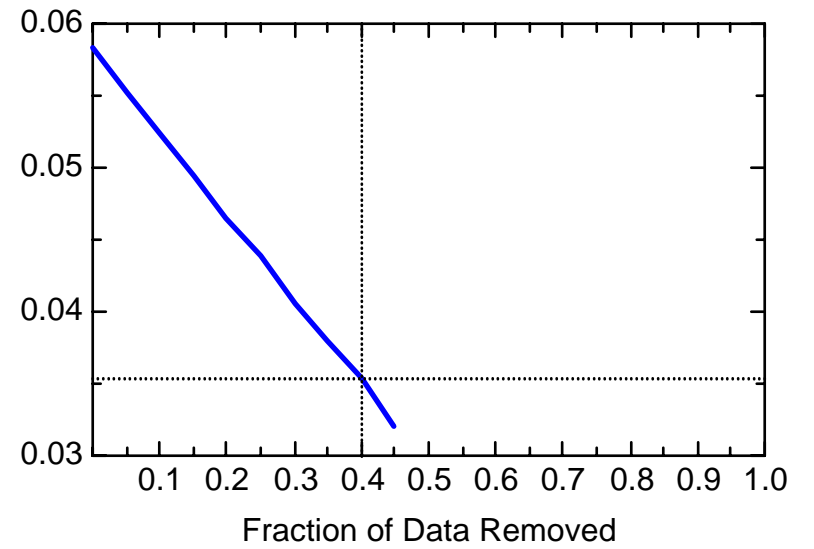
FE: Well JMW0503



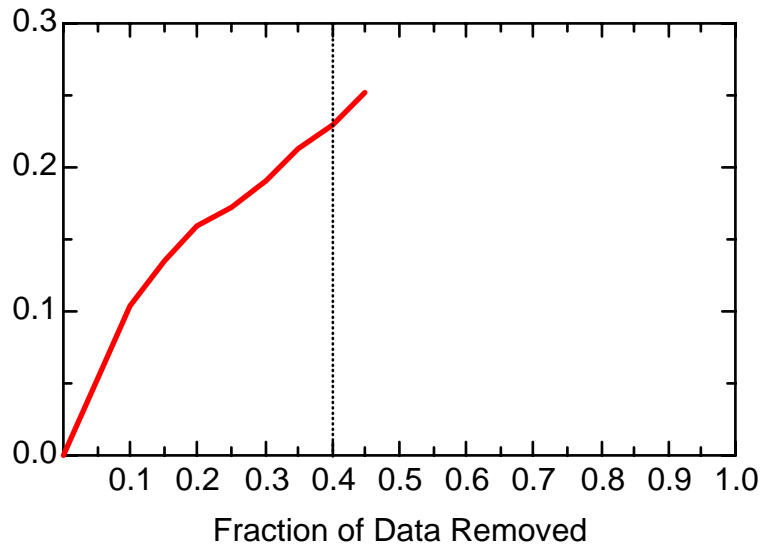
FE: Well JMW0503



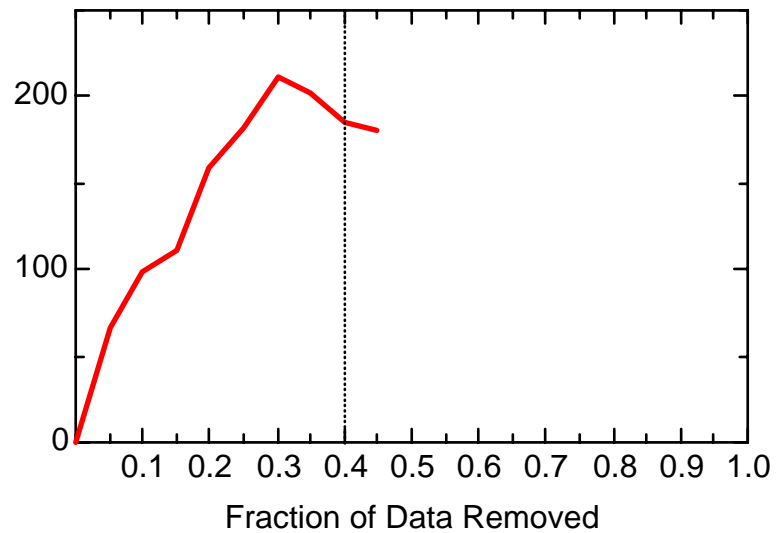
FE: Well JMW0503



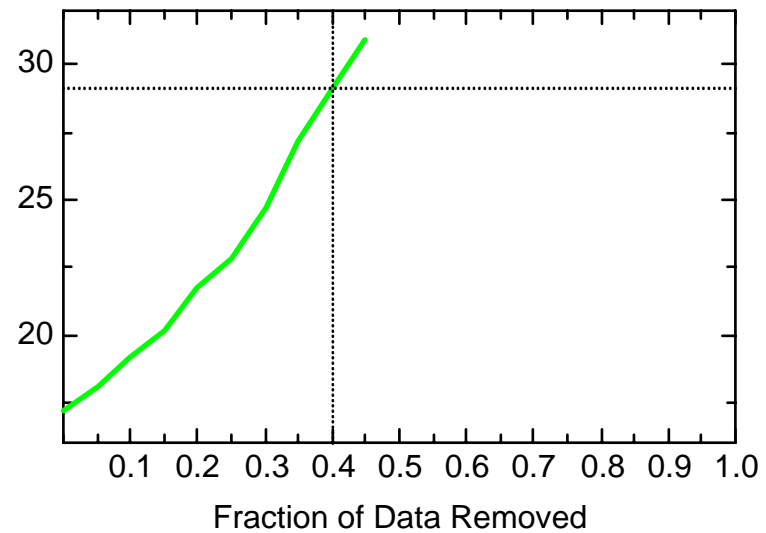
FE: Well JMW0505



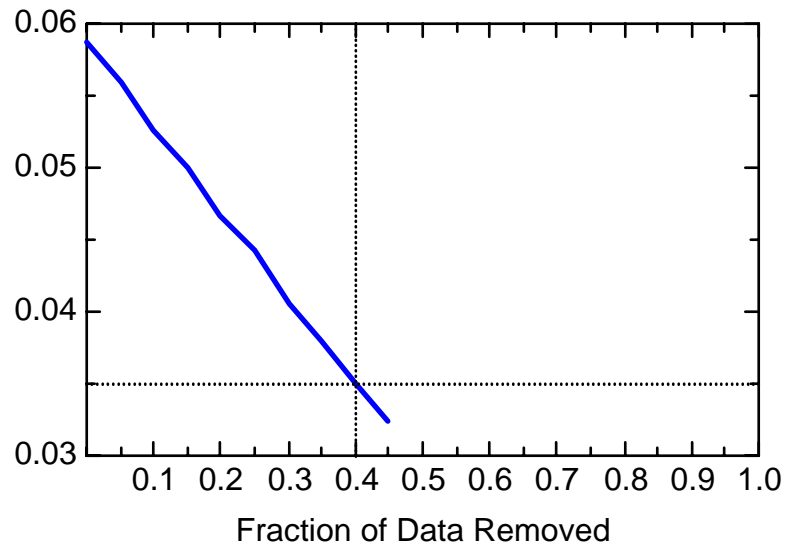
FE: Well JMW0505



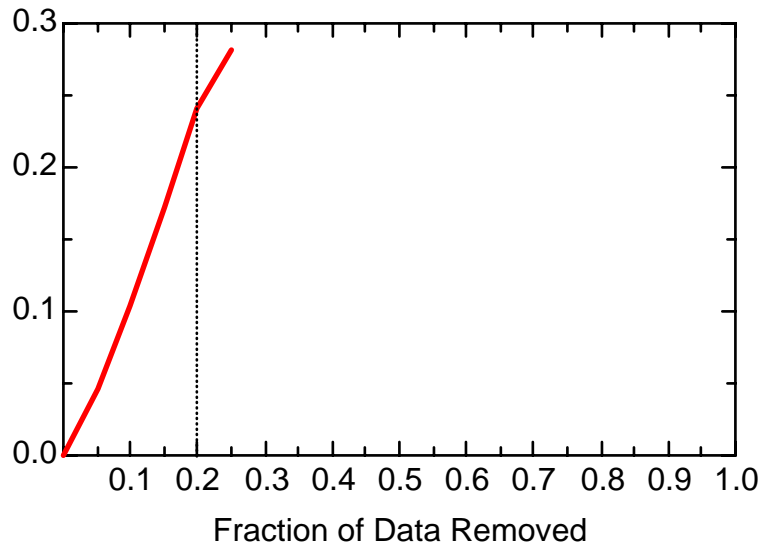
FE: Well JMW0505



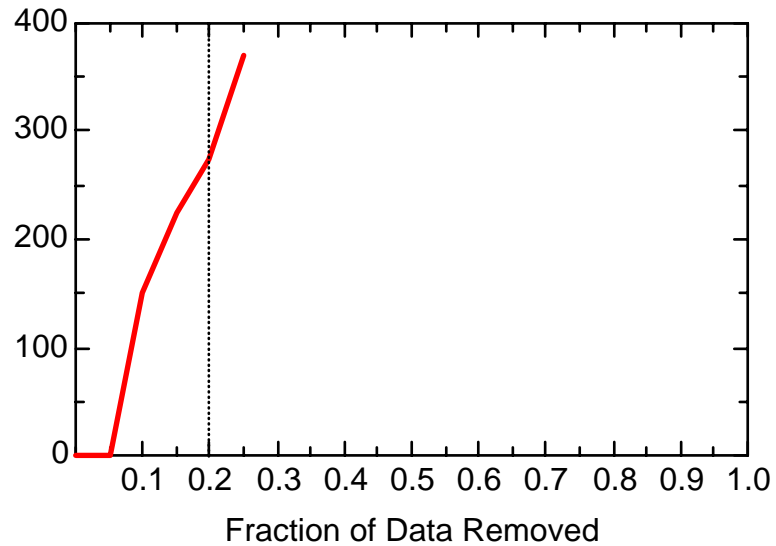
FE: Well JMW0505



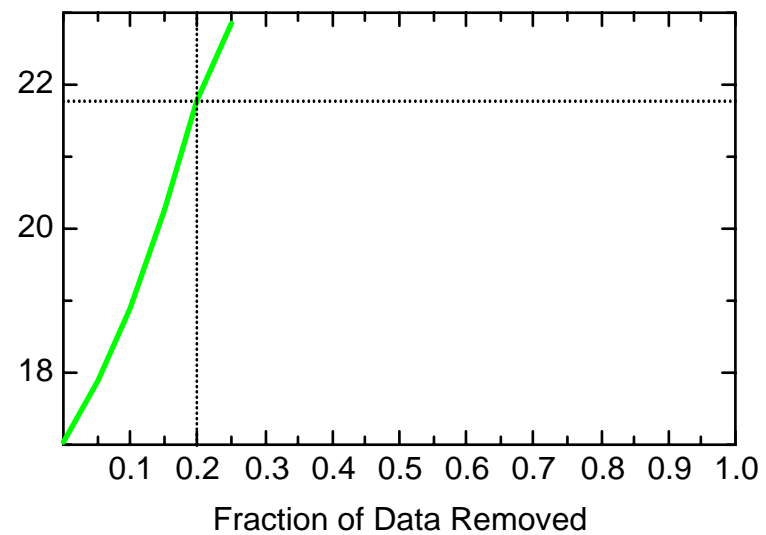
FE: Well JMW0542



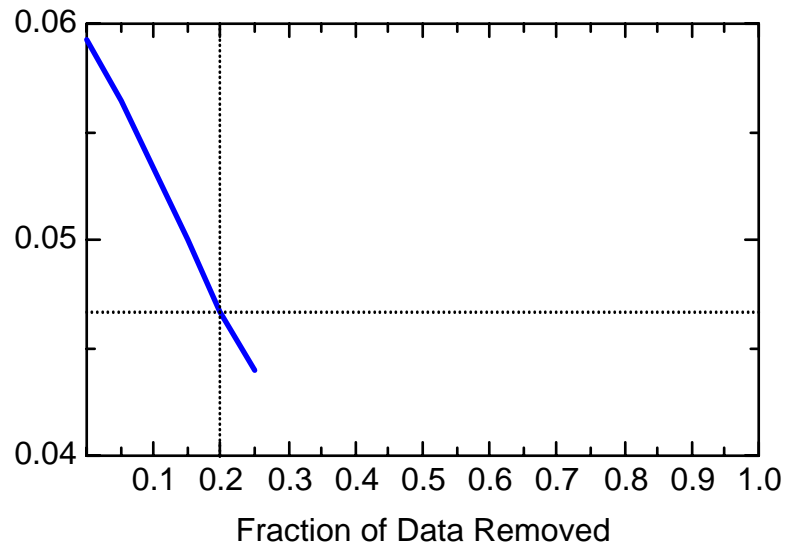
FE: Well JMW0542



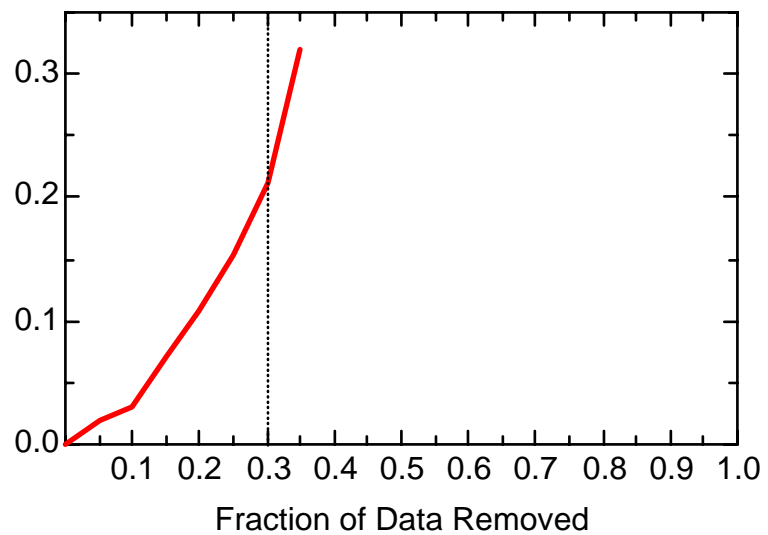
FE: Well JMW0542



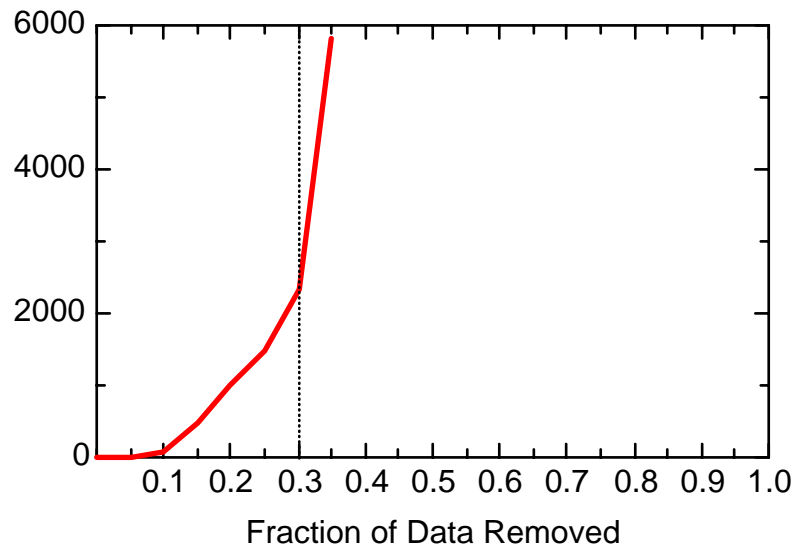
FE: Well JMW0542



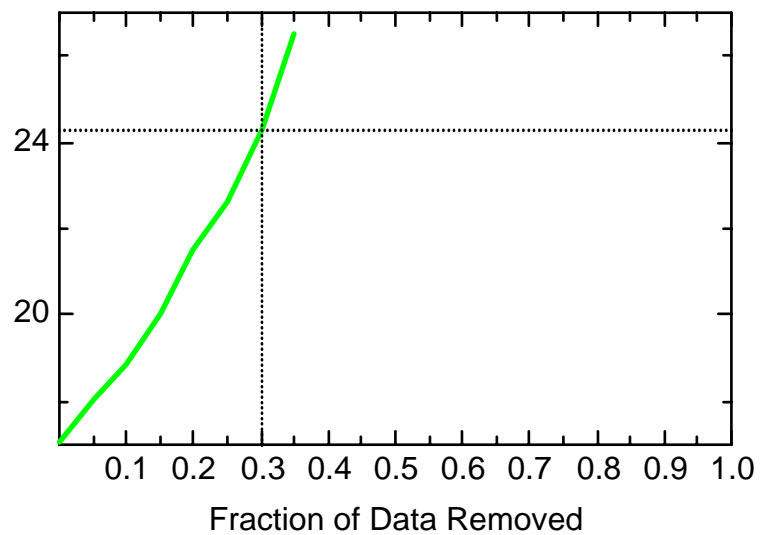
FE: Well JMW1103D



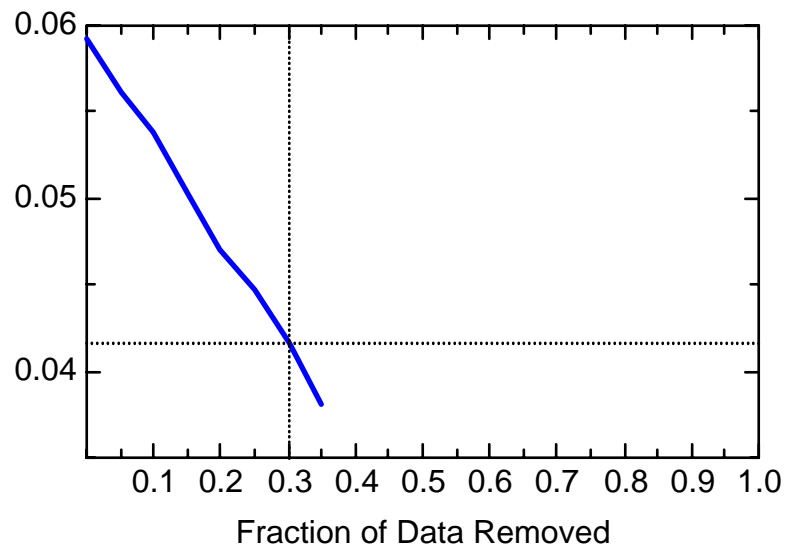
FE: Well JMW1103D



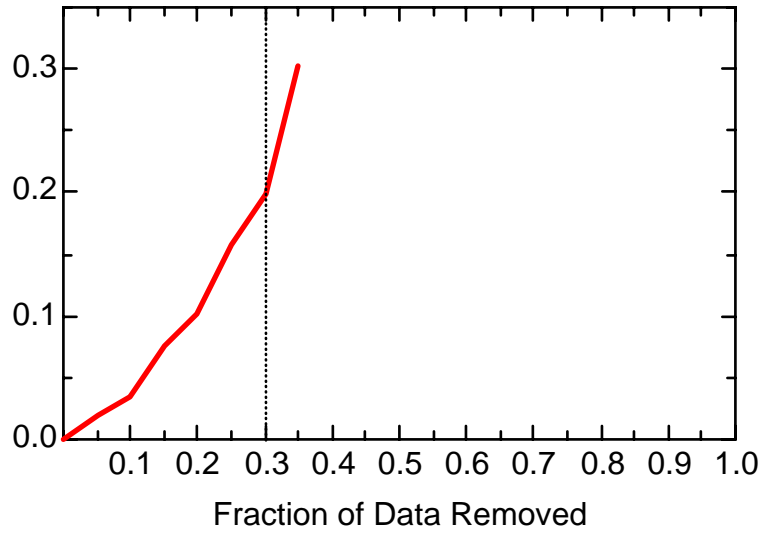
FE: Well JMW1103D



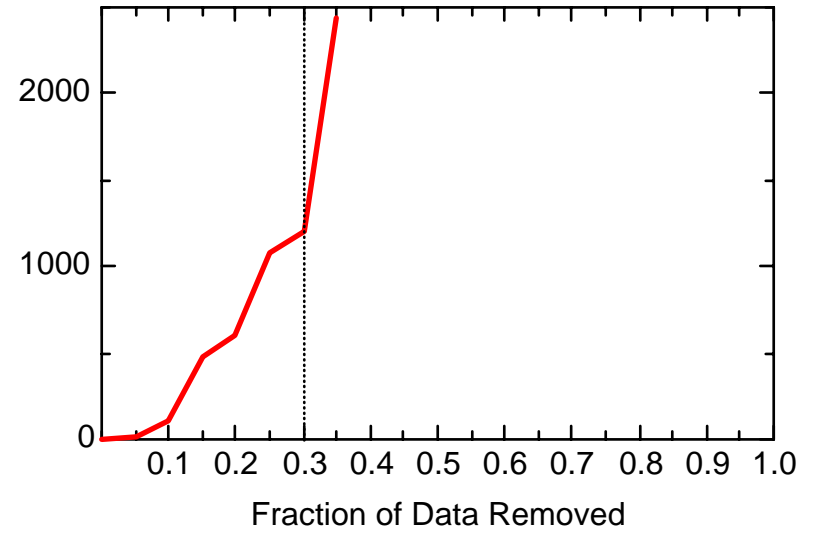
FE: Well JMW1103D



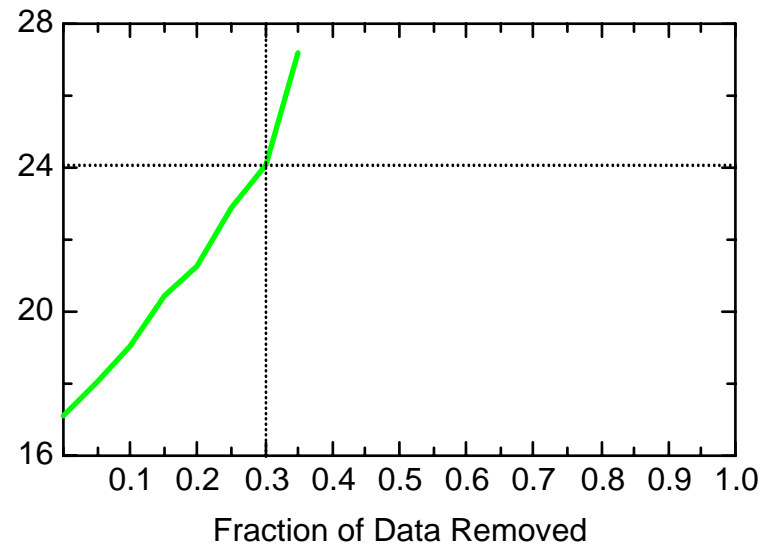
FE: Well JMW1564



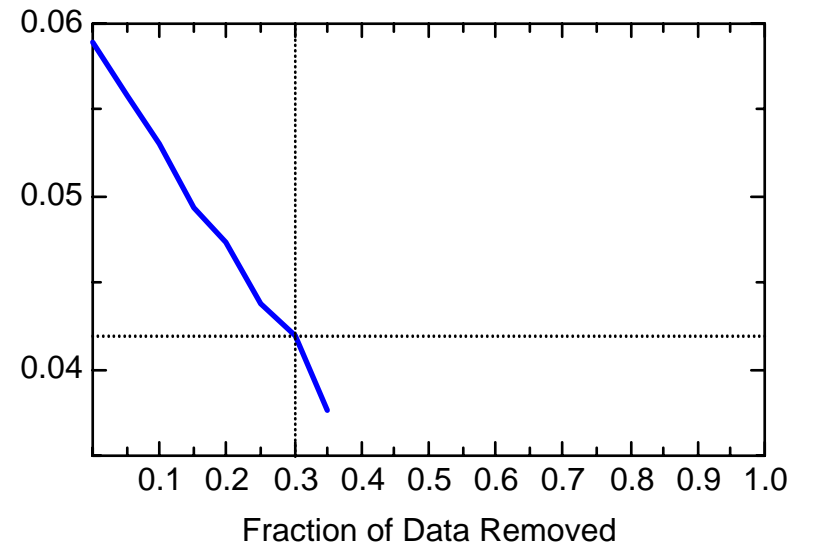
FE: Well JMW1564



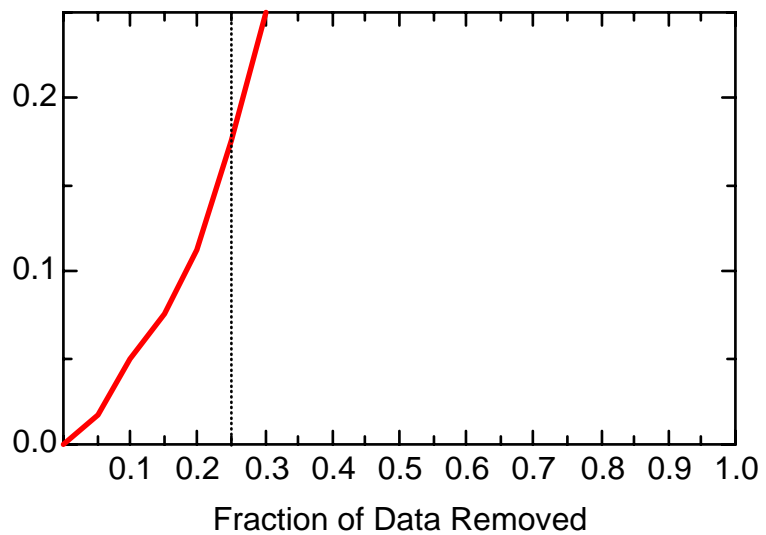
FE: Well JMW1564



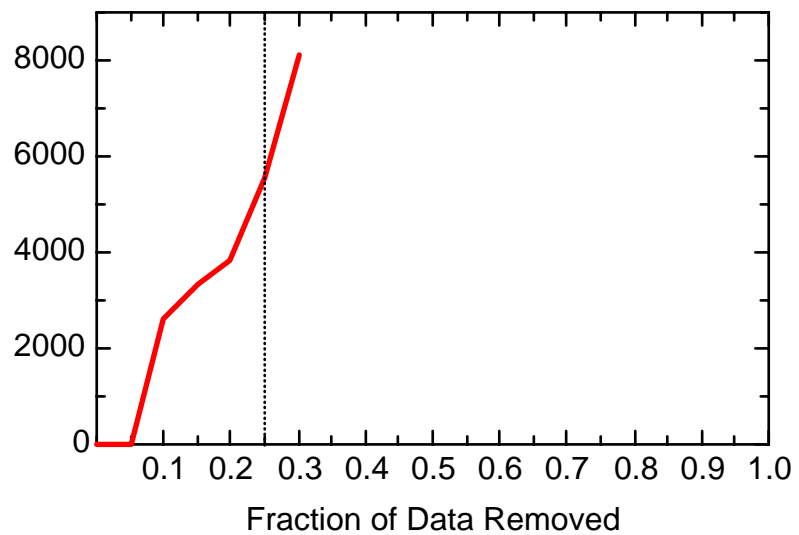
FE: Well JMW1564



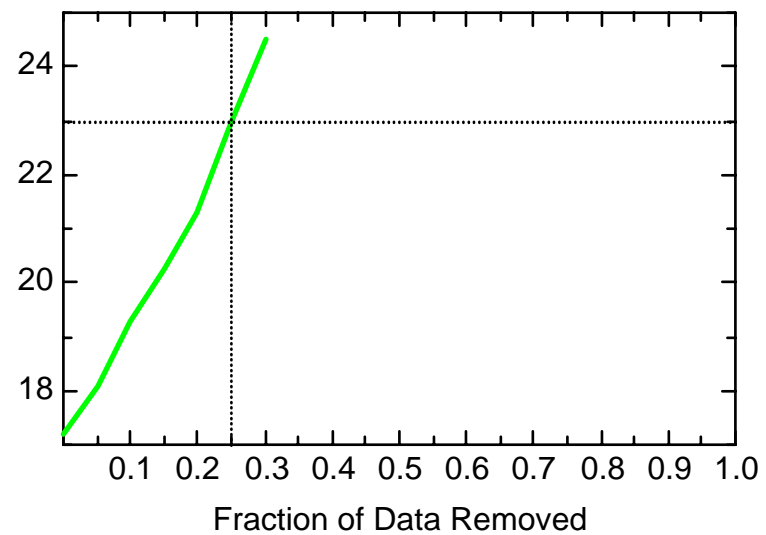
FE: Well JMW1565



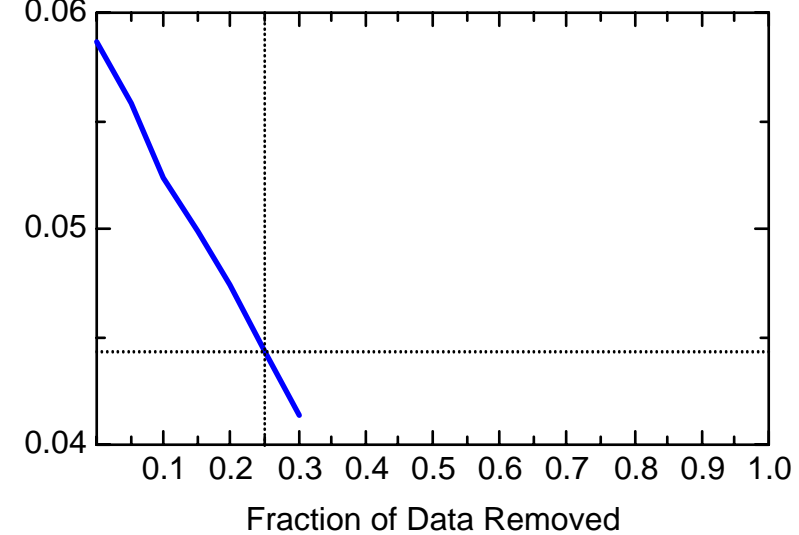
FE: Well JMW1565



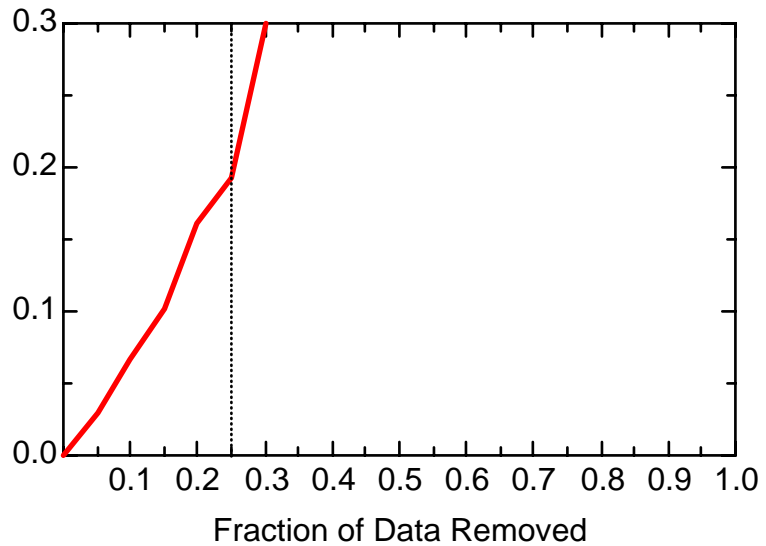
FE: Well JMW1565



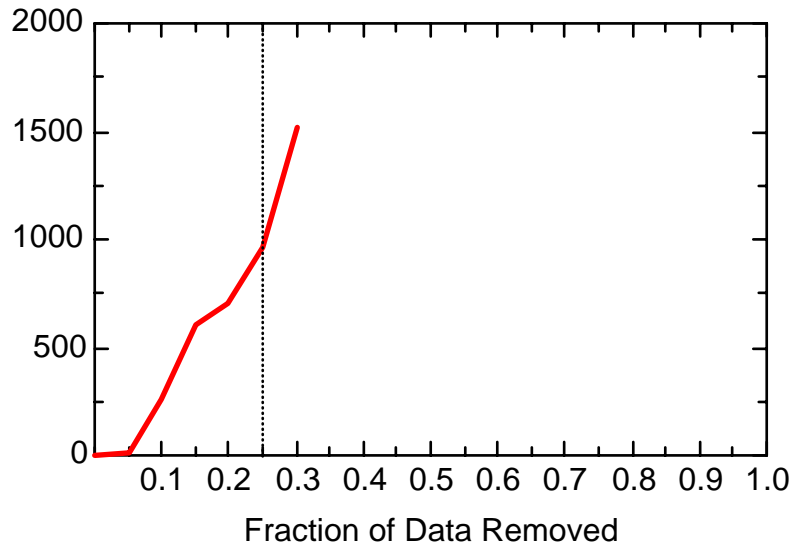
FE: Well JMW1565



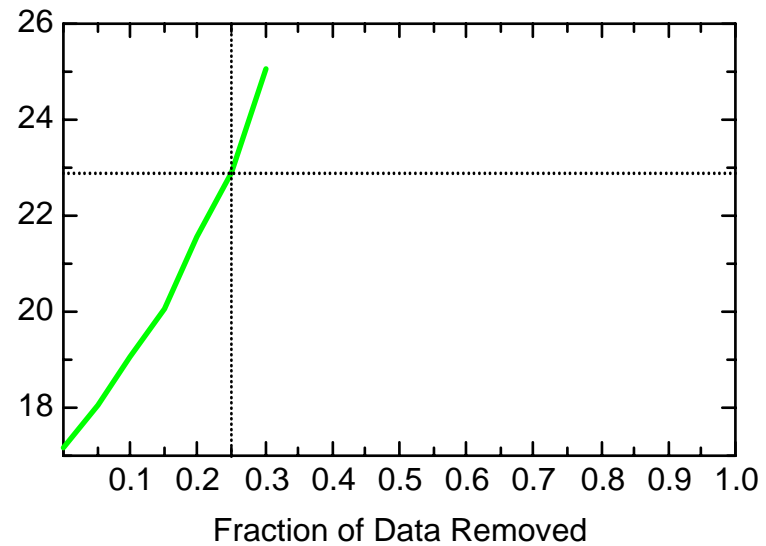
FE: Well JMW1860



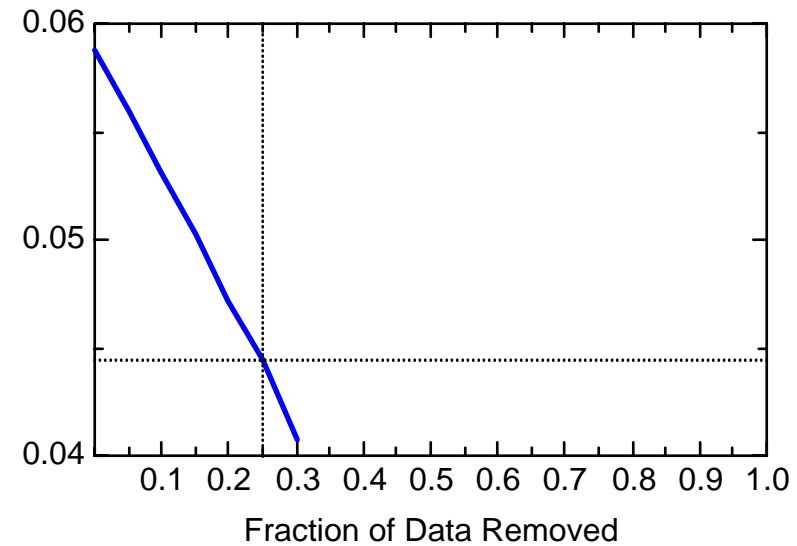
FE: Well JMW1860



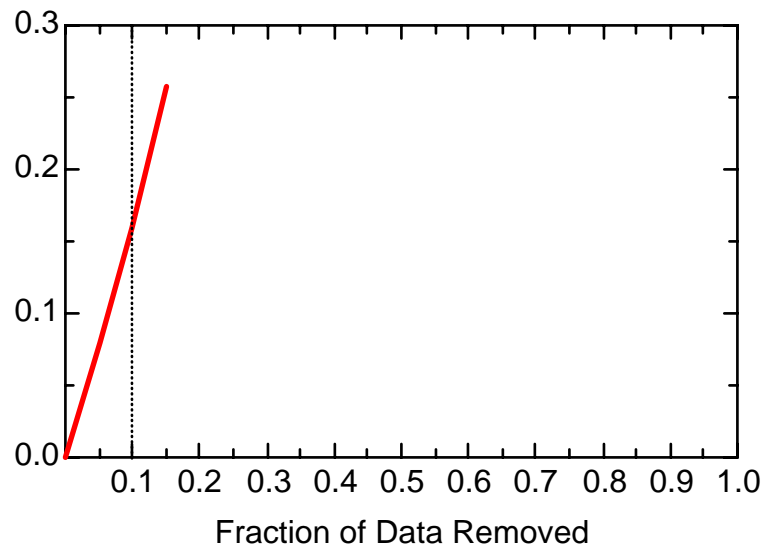
FE: Well JMW1860



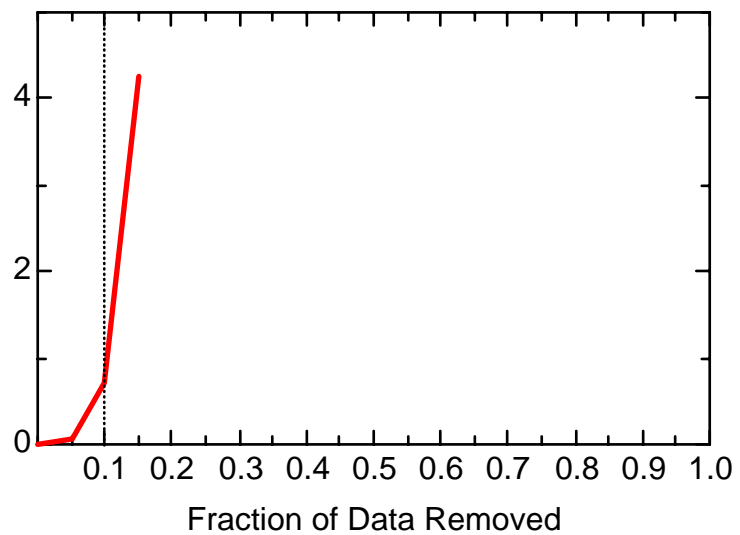
FE: Well JMW1860



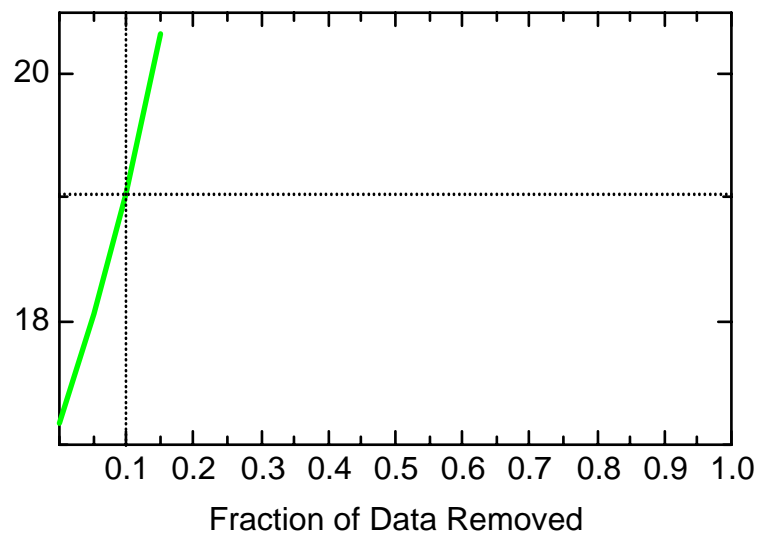
FE: Well JMW1881



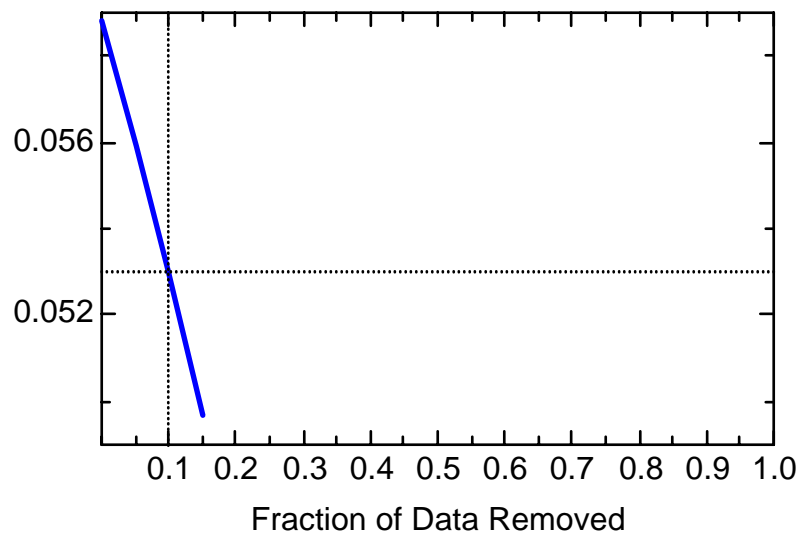
FE: Well JMW1881



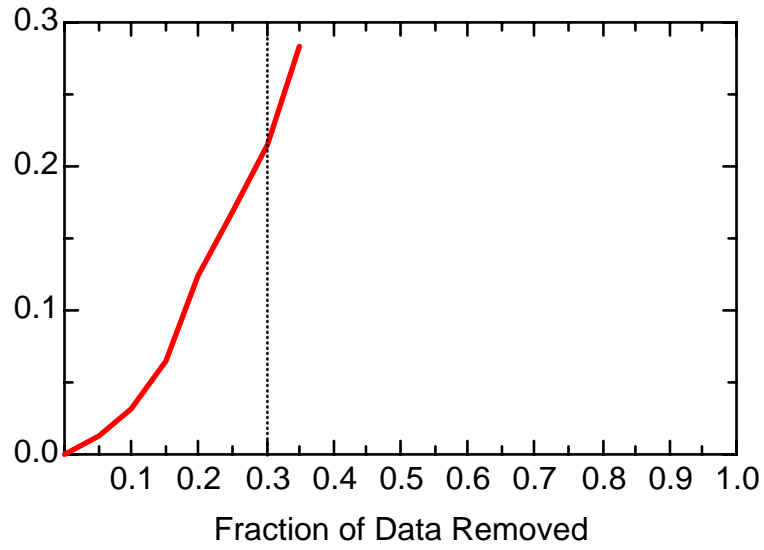
FE: Well JMW1881



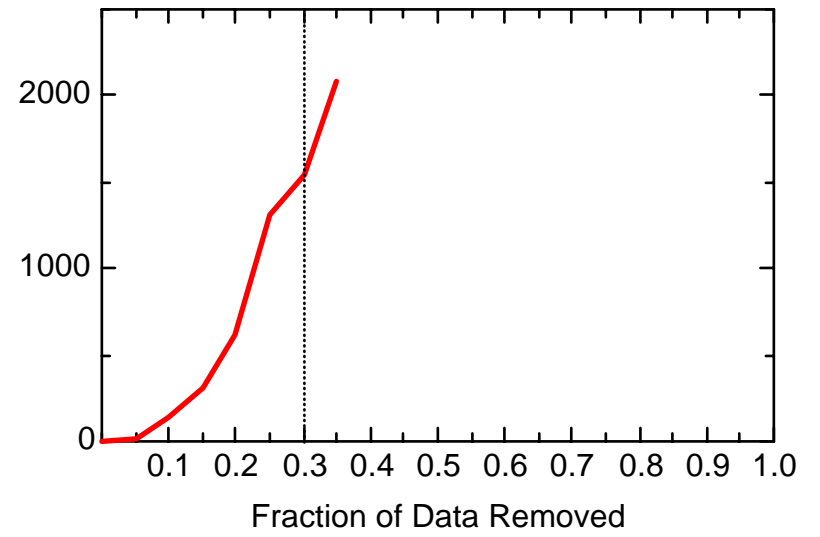
FE: Well JMW1881



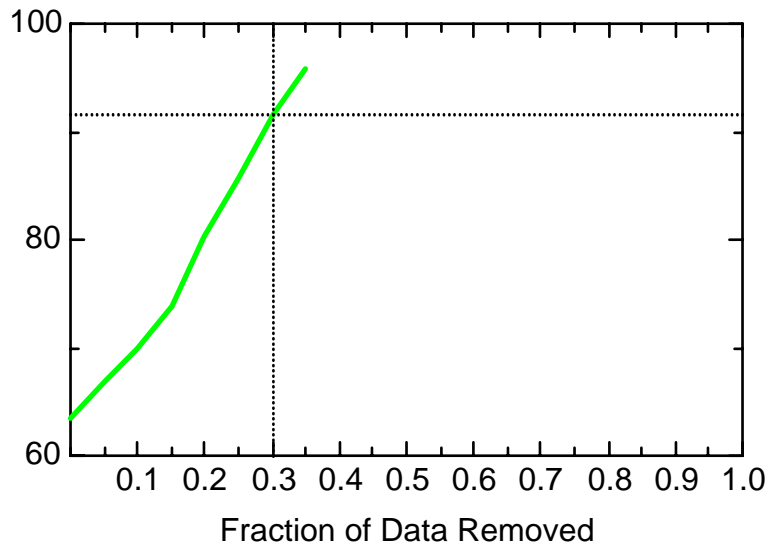
FE: Well JMW1960



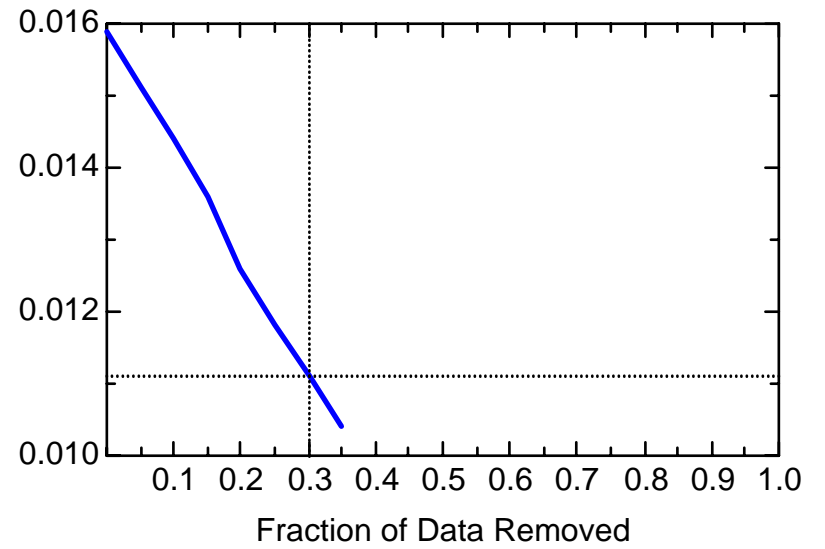
FE: Well JMW1960



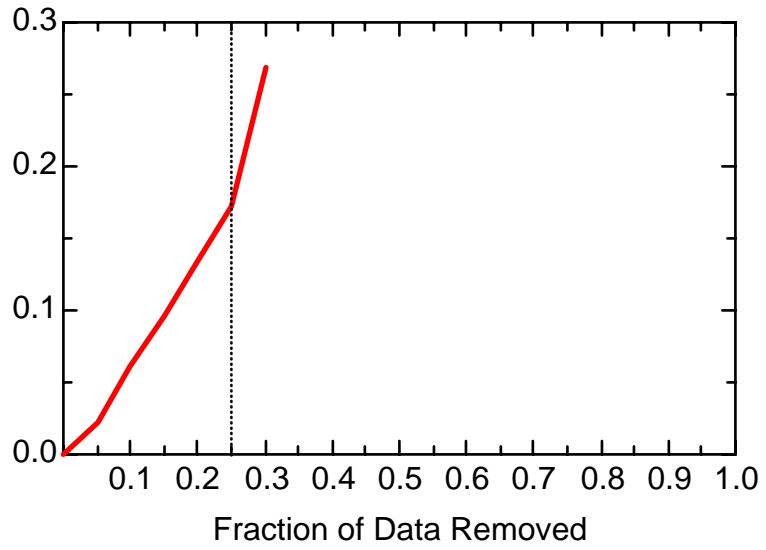
FE: Well JMW1960



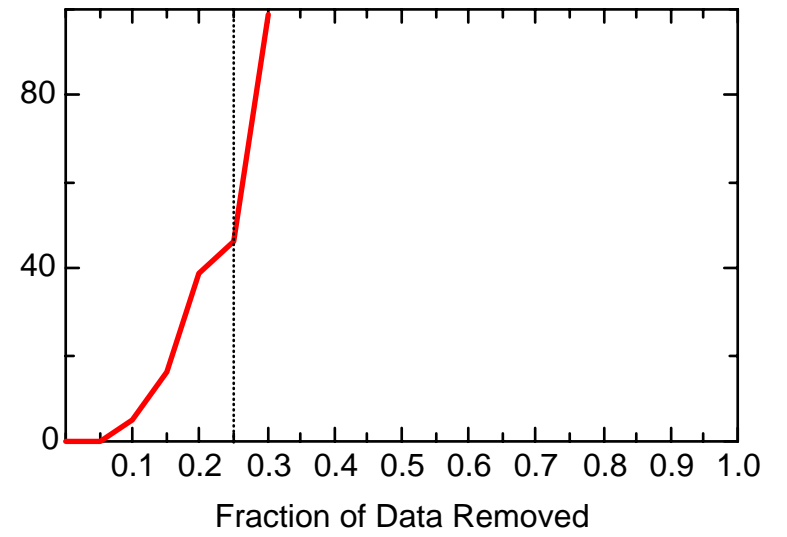
FE: Well JMW1960



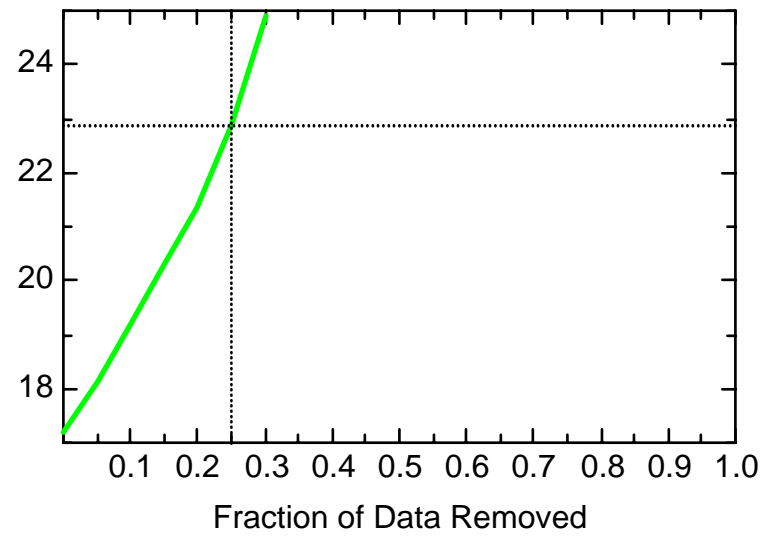
FE: Well JMW1963



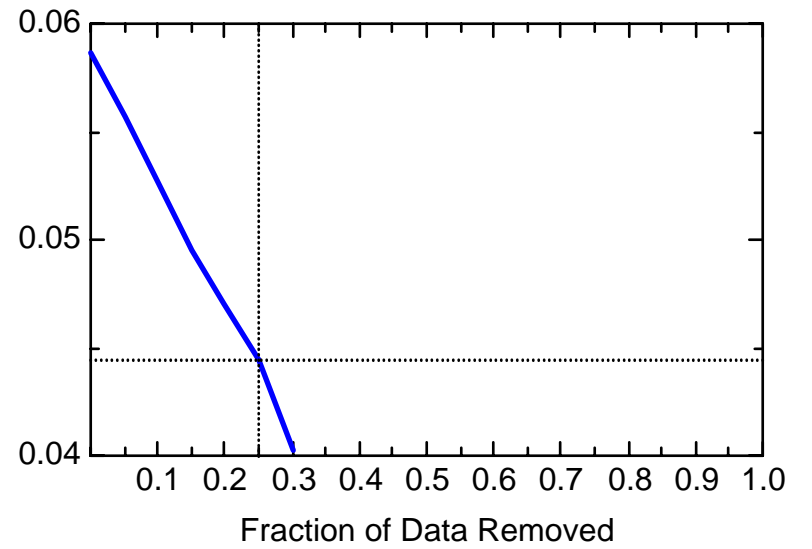
FE: Well JMW1963



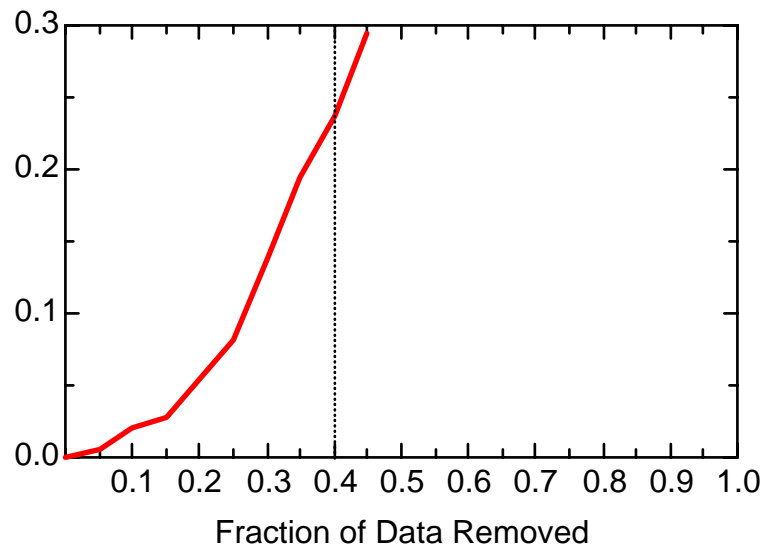
FE: Well JMW1963



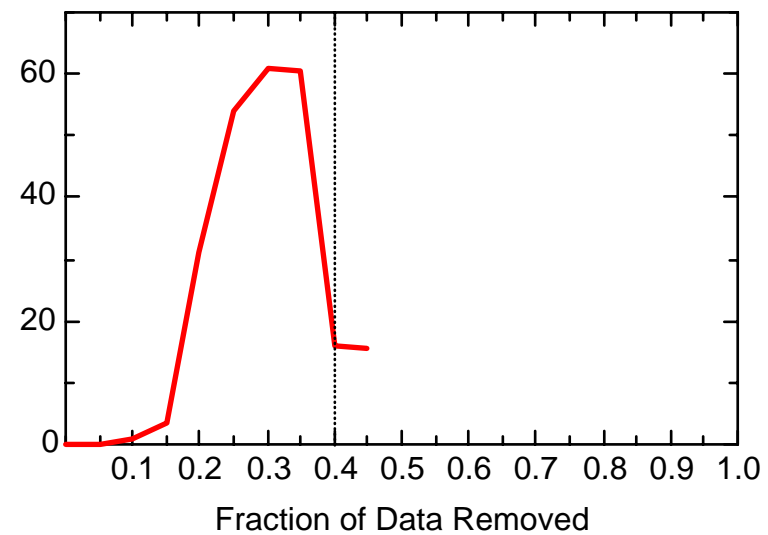
FE: Well JMW1963



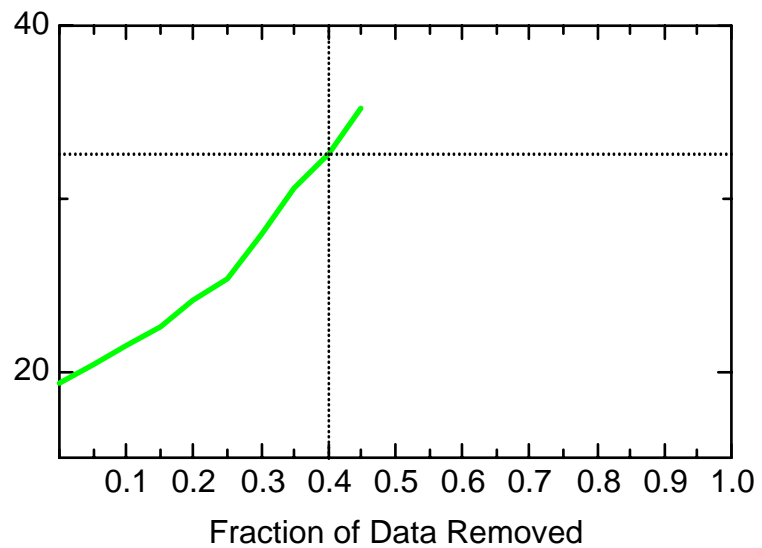
FE: Well JMW1964



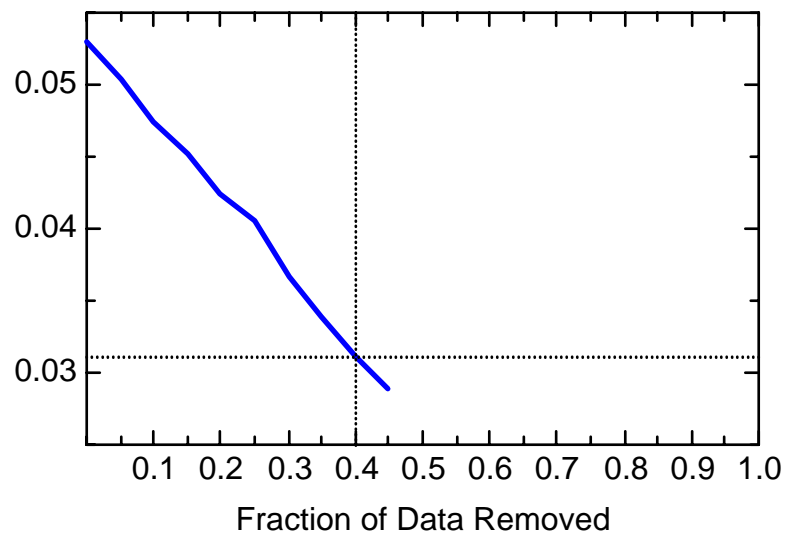
FE: Well JMW1964



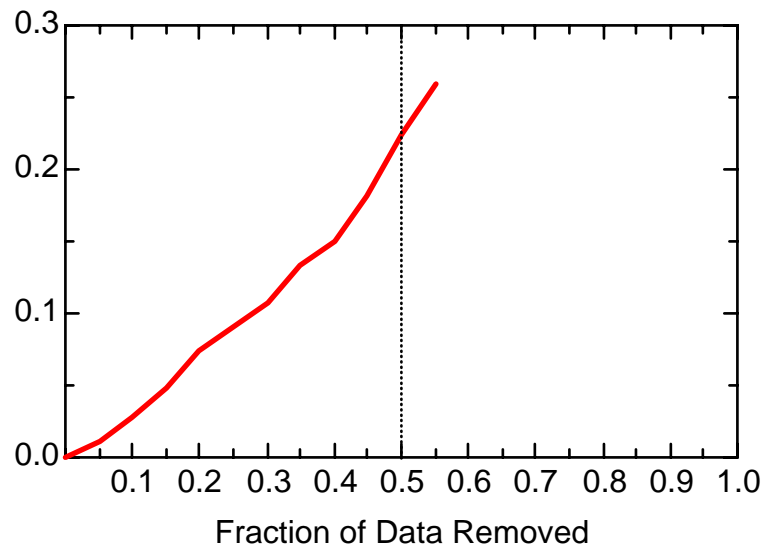
FE: Well JMW1964



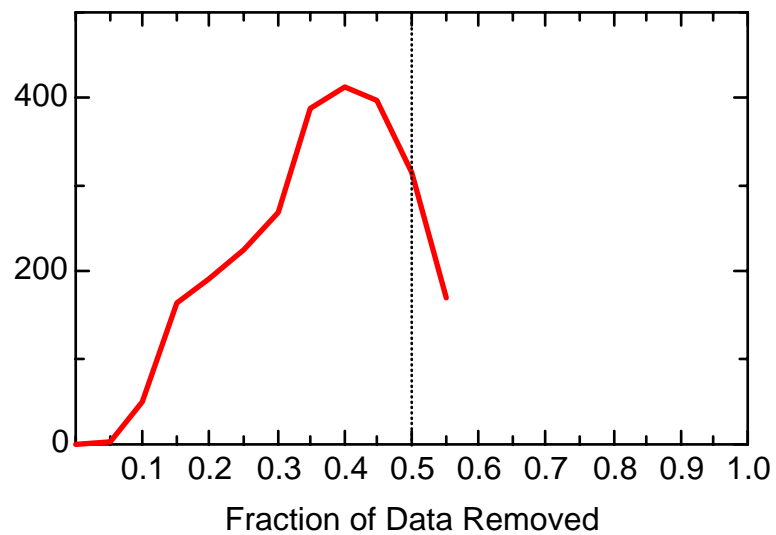
FE: Well JMW1964



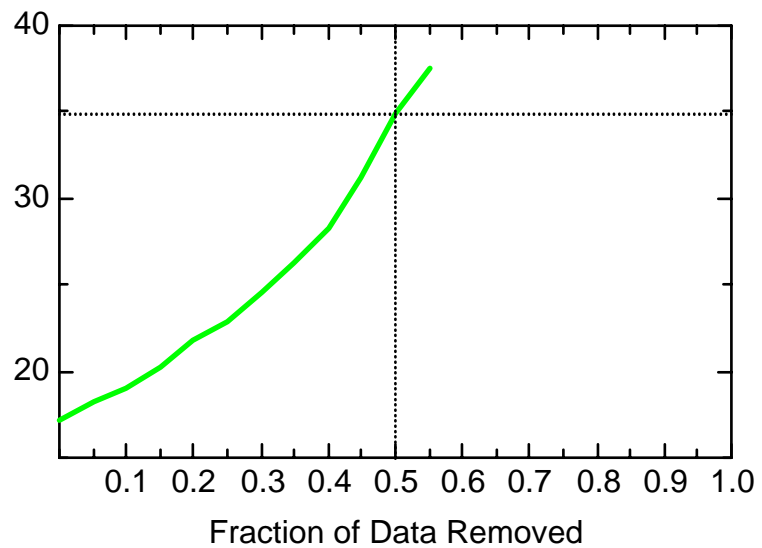
FE: Well JMW1966



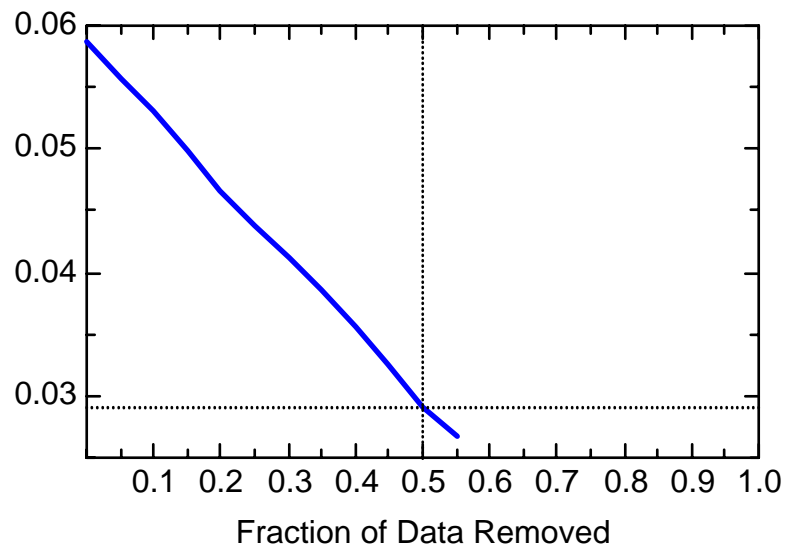
FE: Well JMW1966



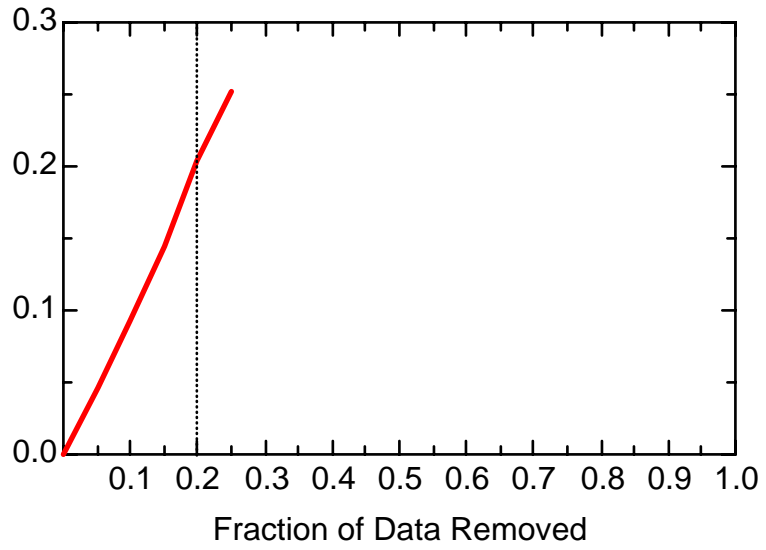
FE: Well JMW1966



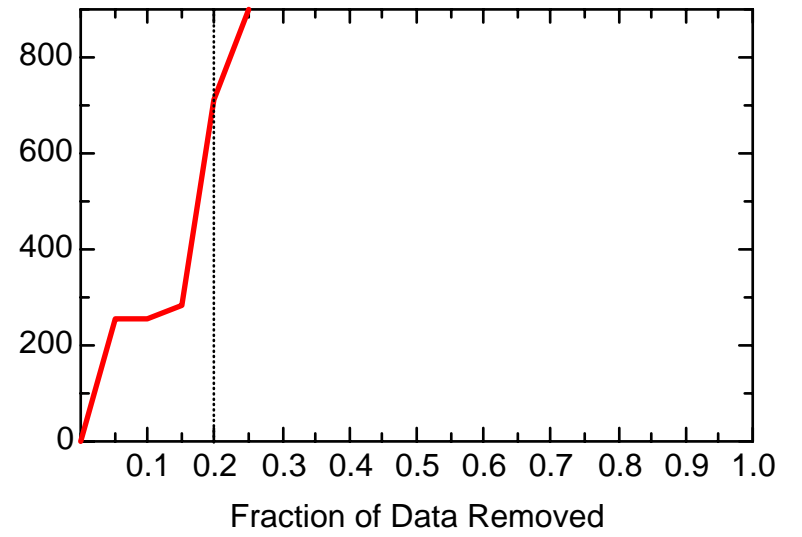
FE: Well JMW1966



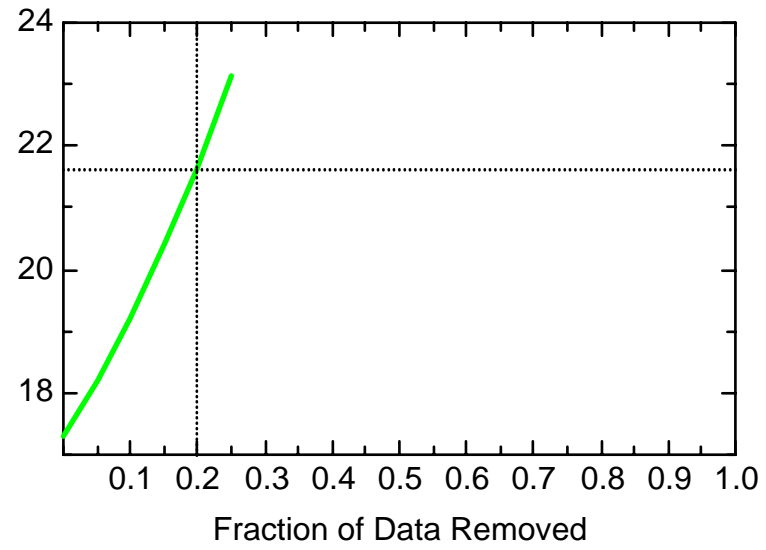
FE: Well JMW3202



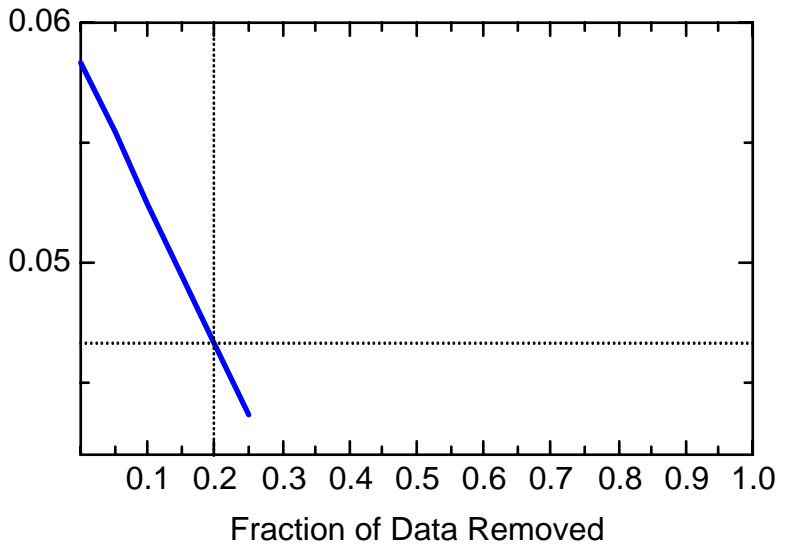
FE: Well JMW3202



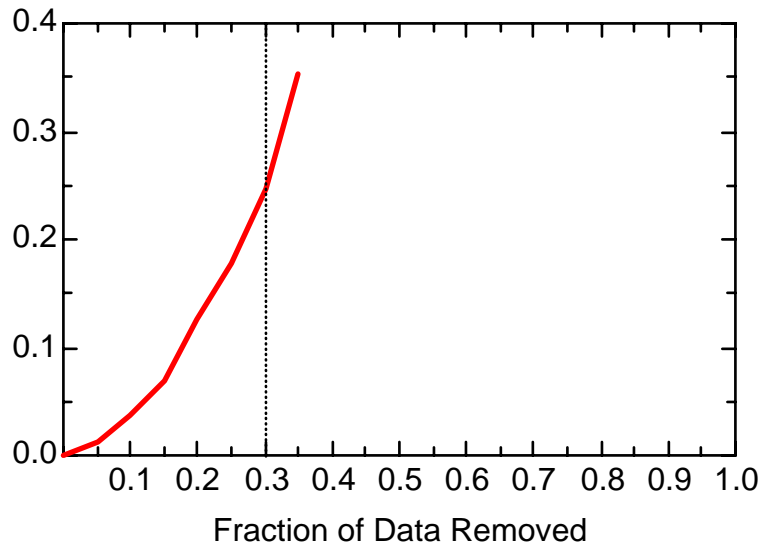
FE: Well JMW3202



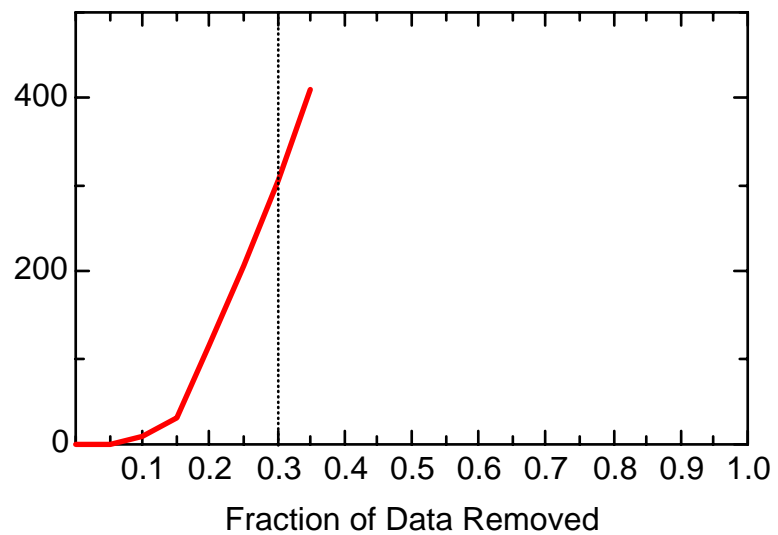
FE: Well JMW3202



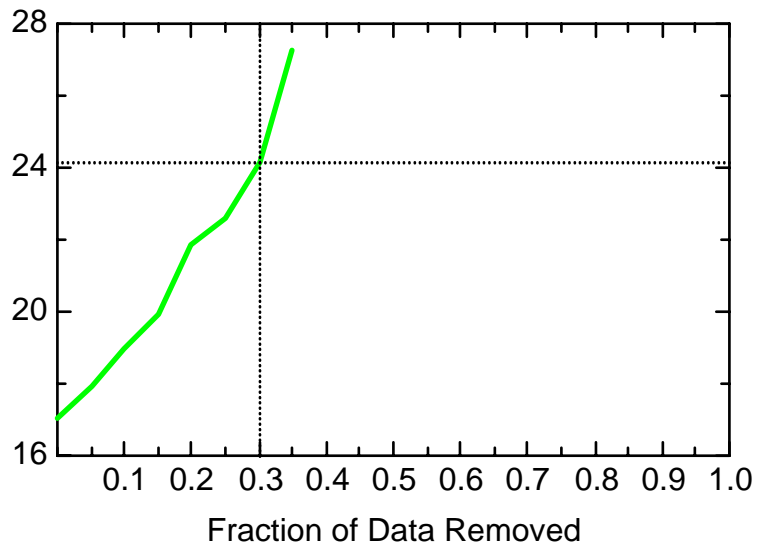
FE: Well JMW7332



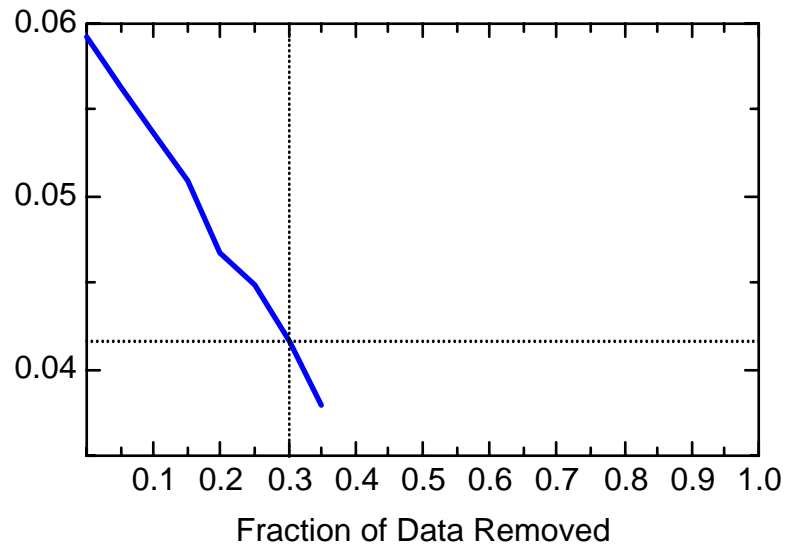
FE: Well JMW7332



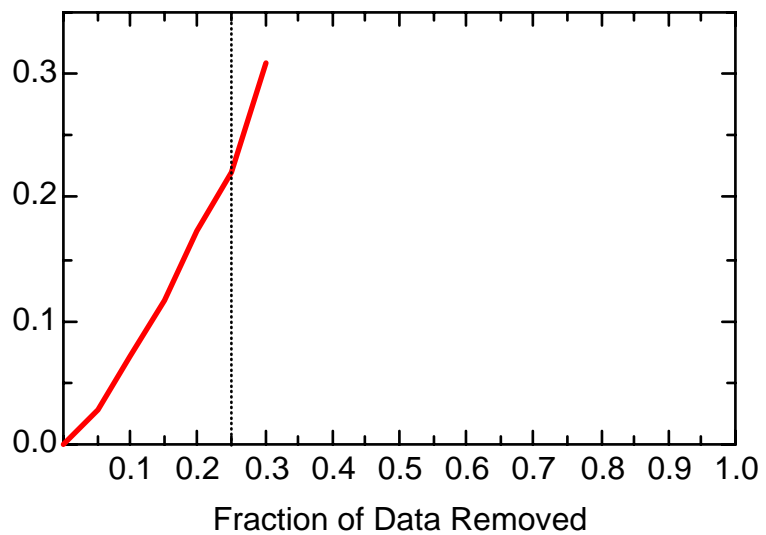
FE: Well JMW7332



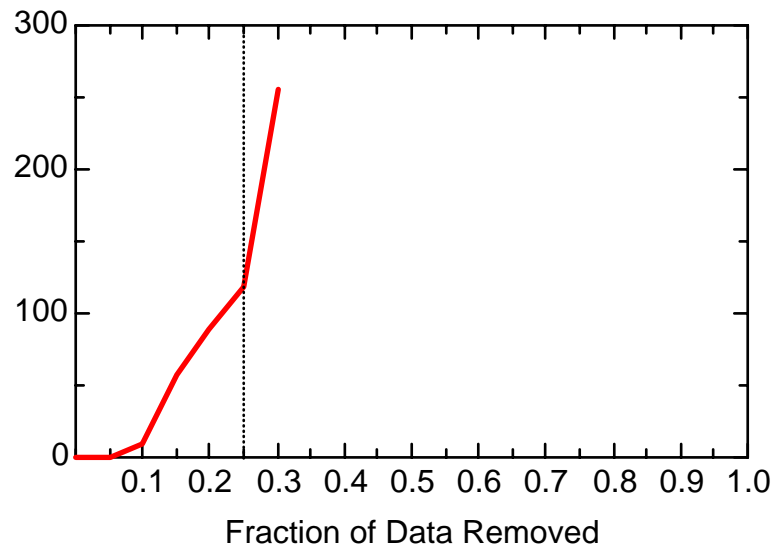
FE: Well JMW7332



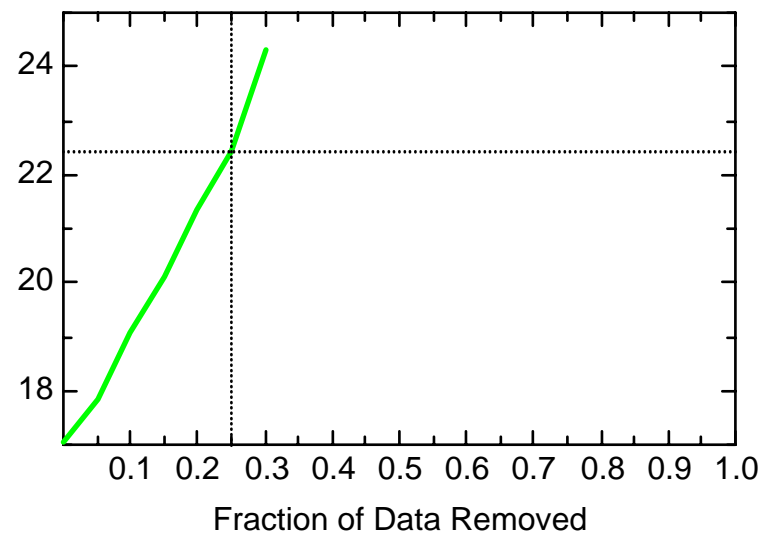
FE: Well JMW8011



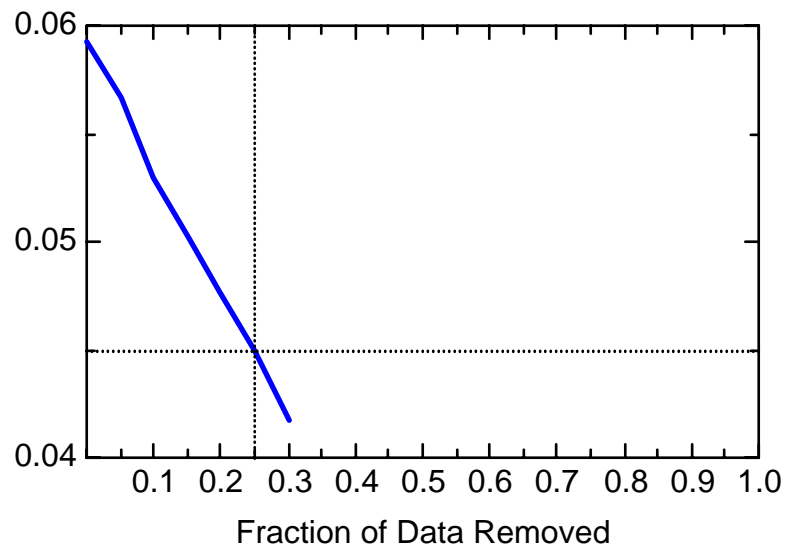
FE: Well JMW8011



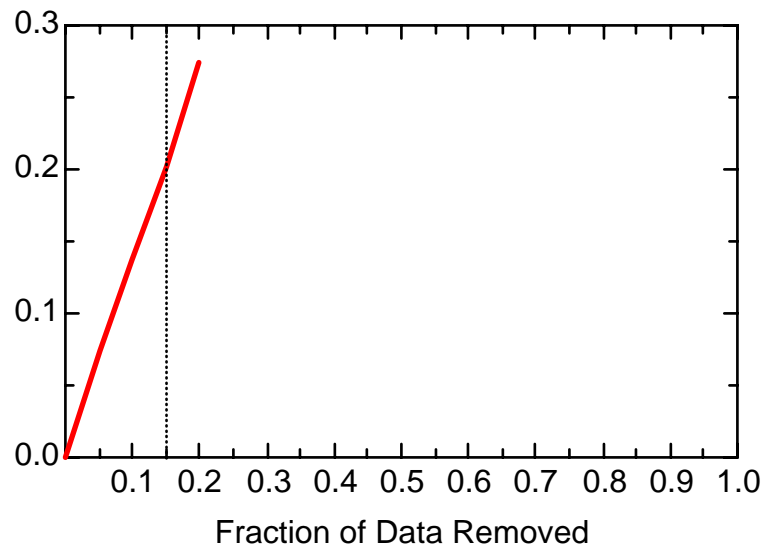
FE: Well JMW8011



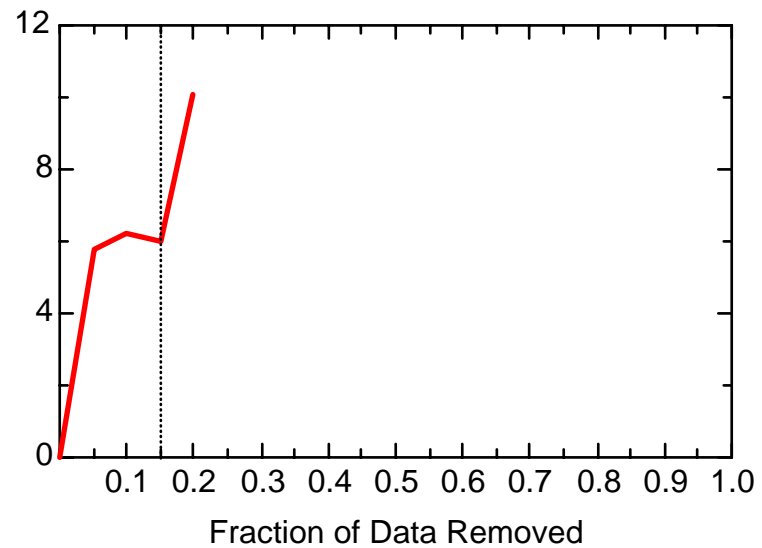
FE: Well JMW8011



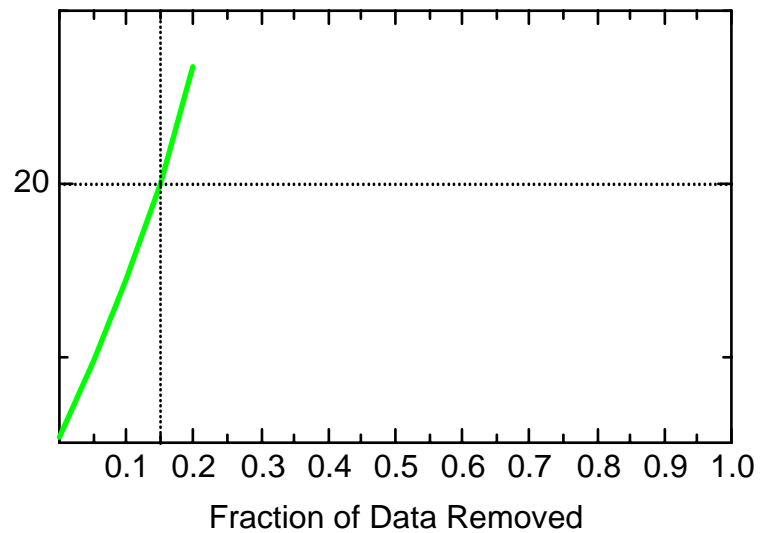
FE: Well JPZ0340



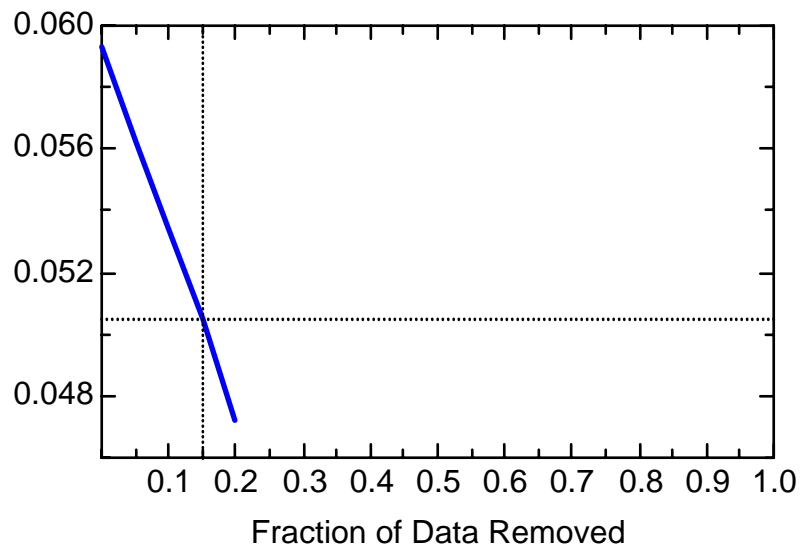
FE: Well JPZ0340



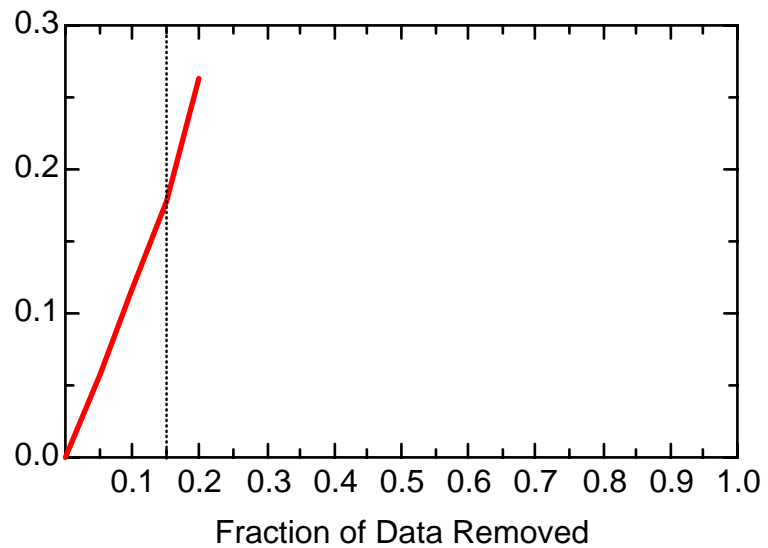
FE: Well JPZ0340



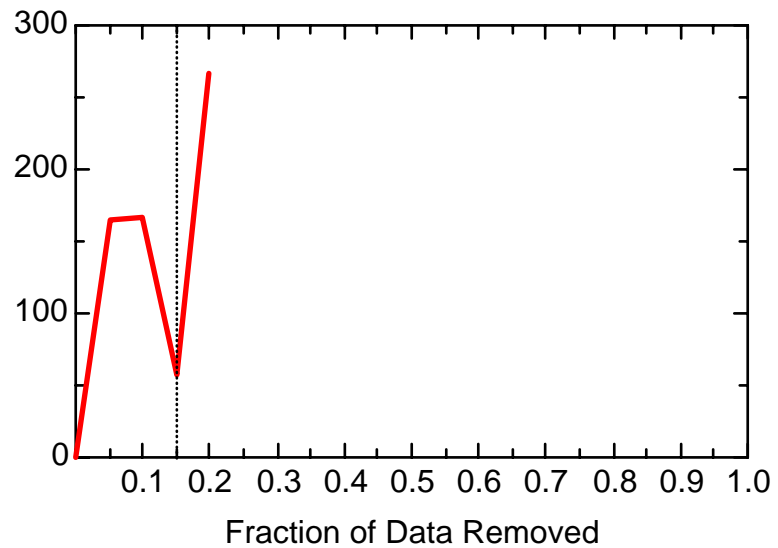
FE: Well JPZ0340



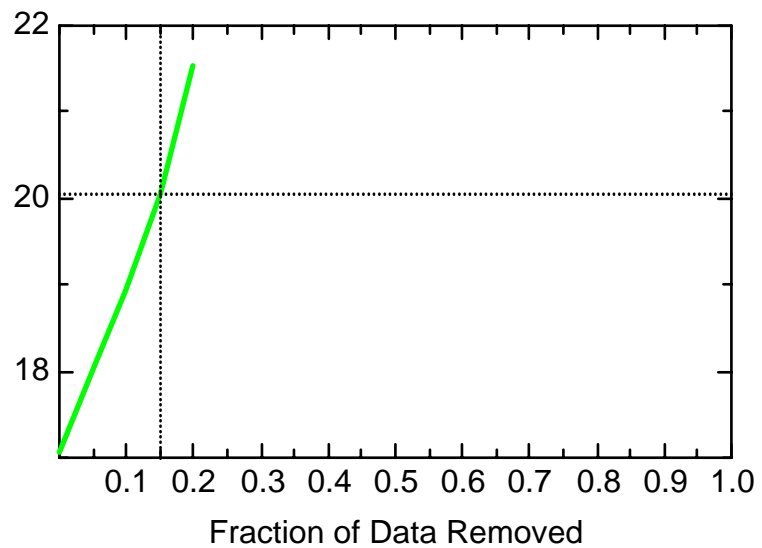
FE: Well JPZ0341



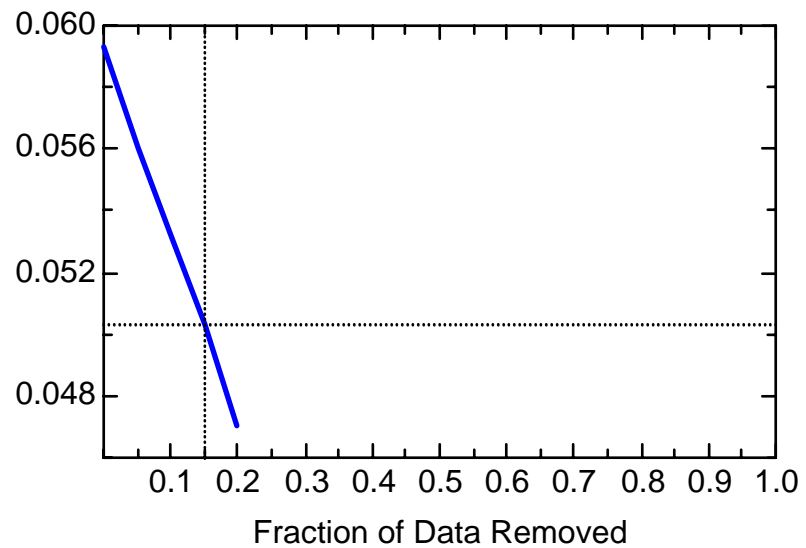
FE: Well JPZ0341



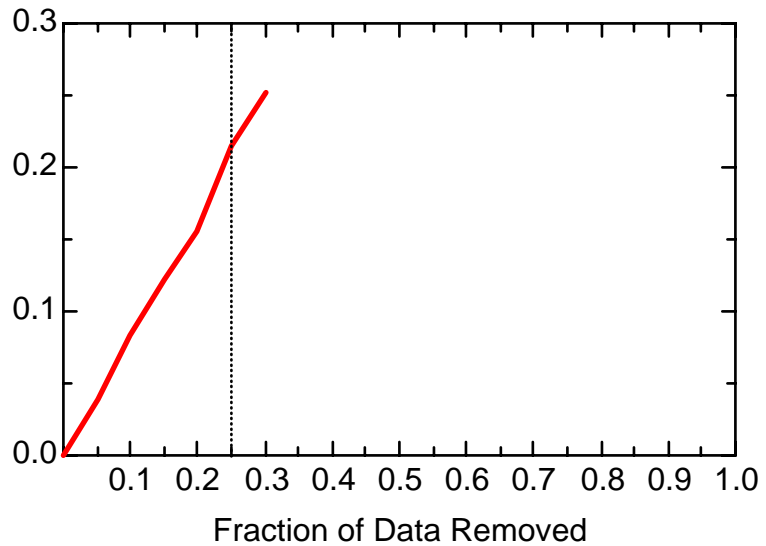
FE: Well JPZ0341



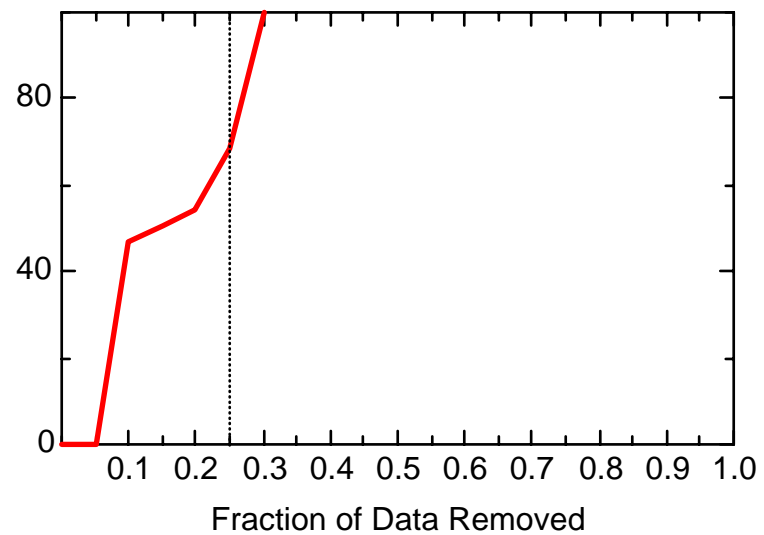
FE: Well JPZ0341



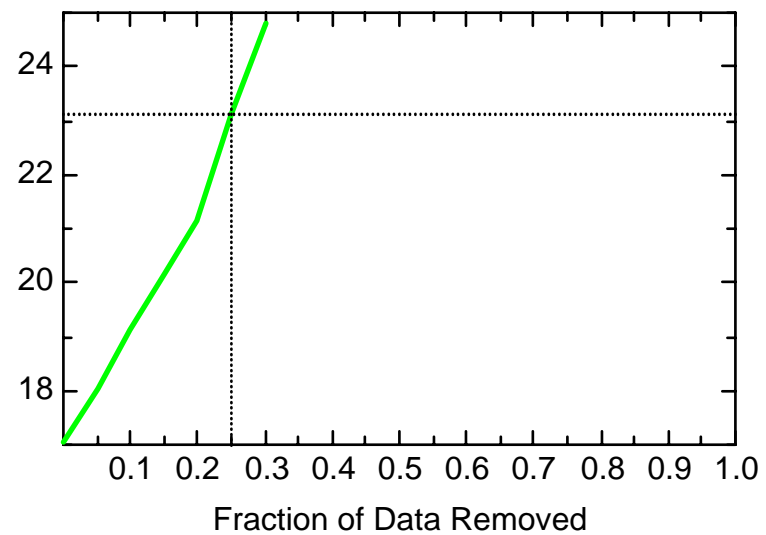
FE: Well JPZ0342



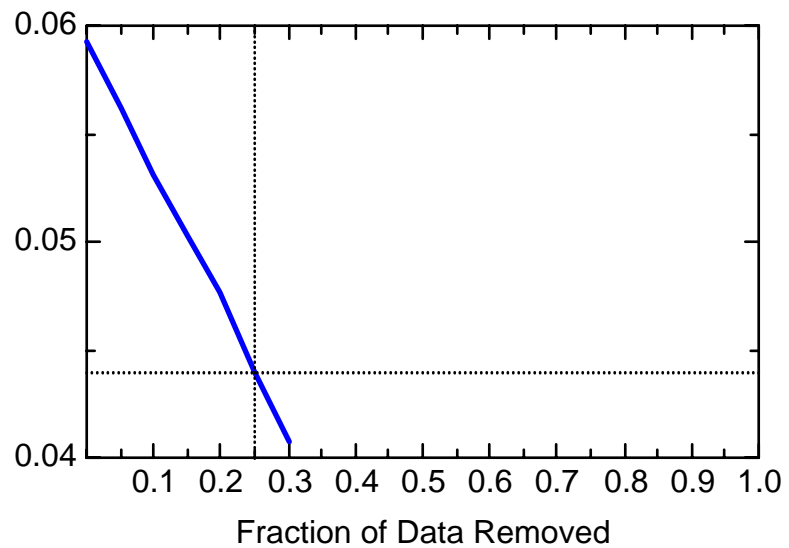
FE: Well JPZ0342



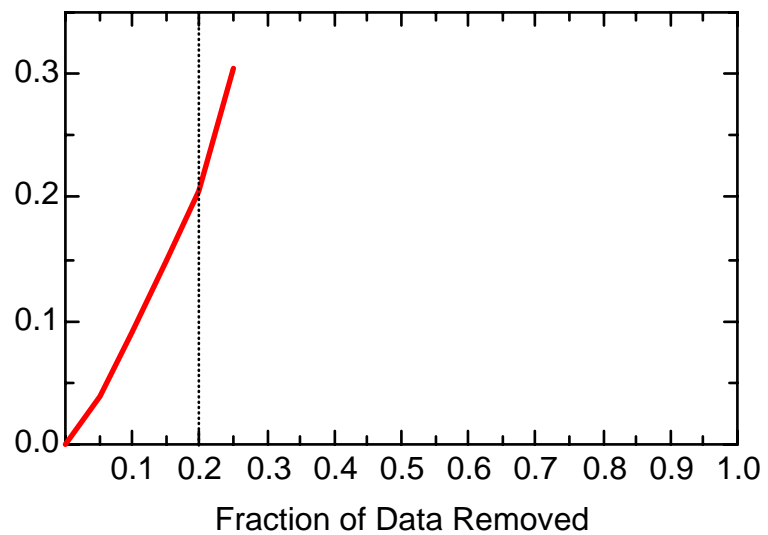
FE: Well JPZ0342



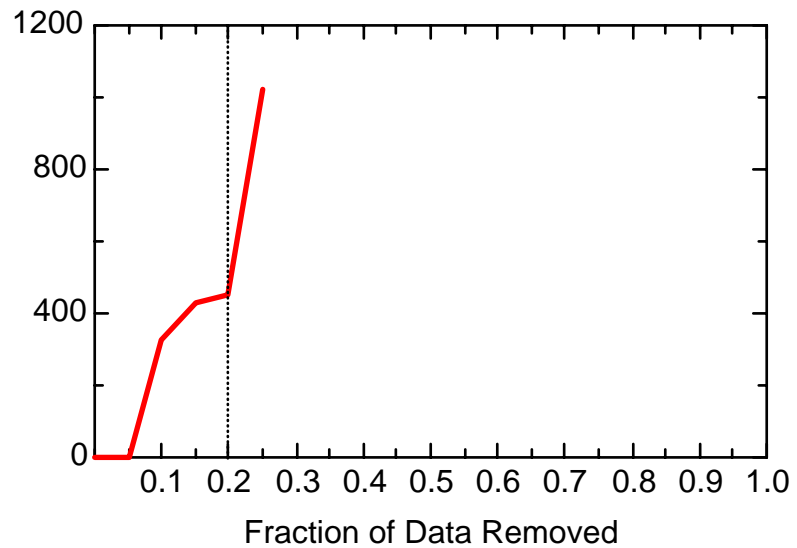
FE: Well JPZ0342



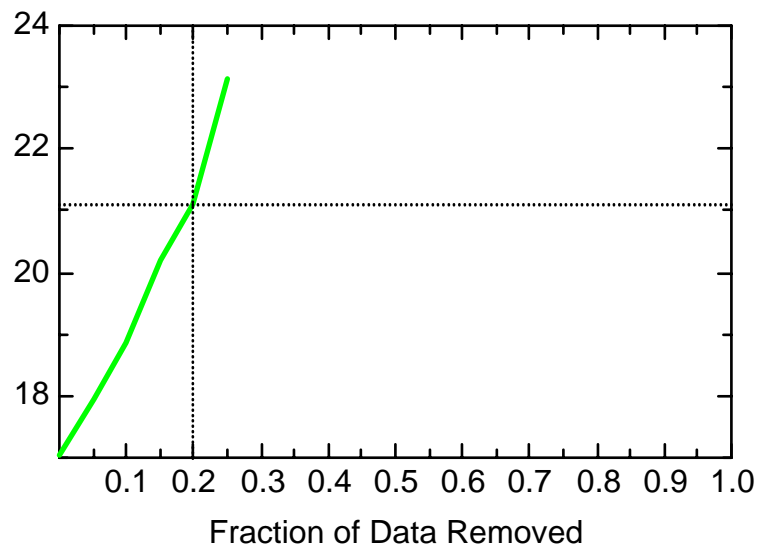
FE: Well JPZ0343



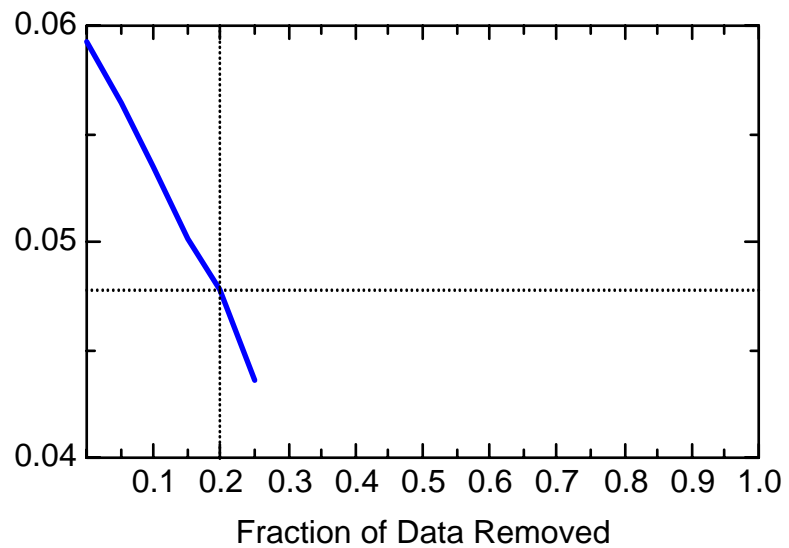
FE: Well JPZ0343



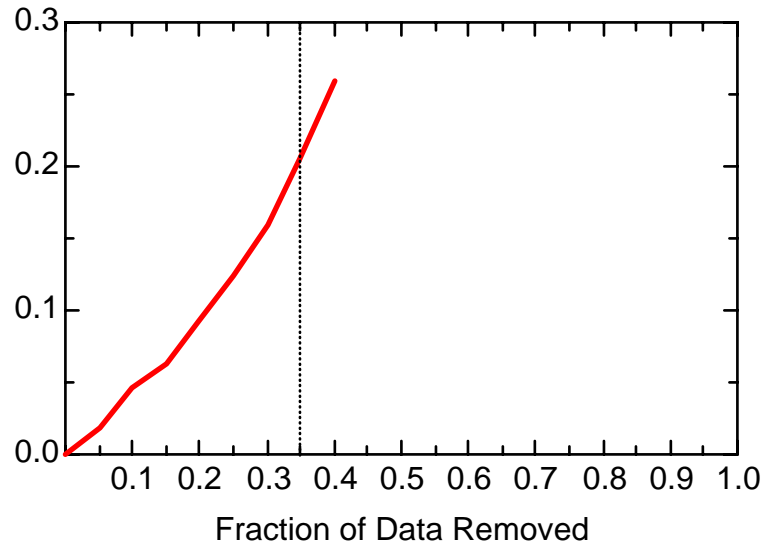
FE: Well JPZ0343



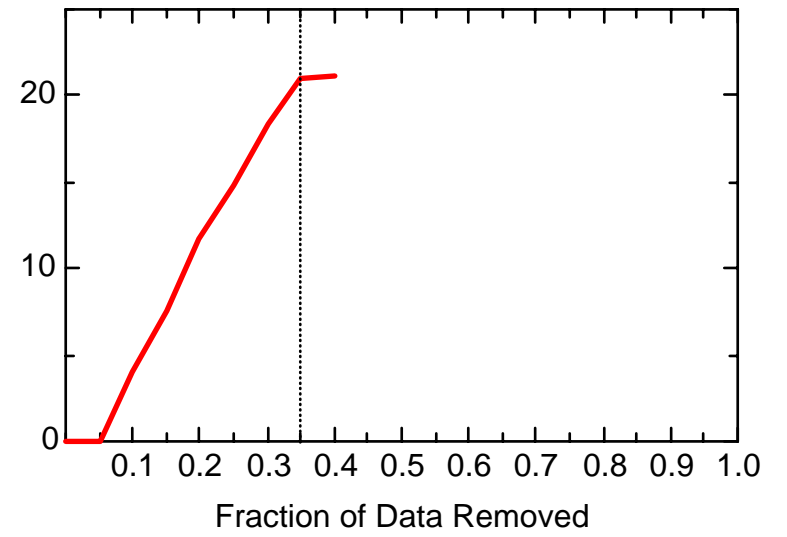
FE: Well JPZ0343



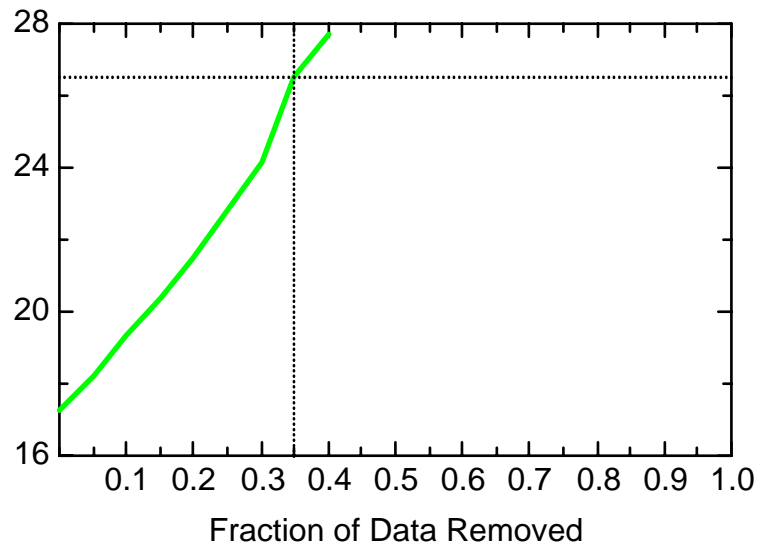
FE: Well JPZ0348



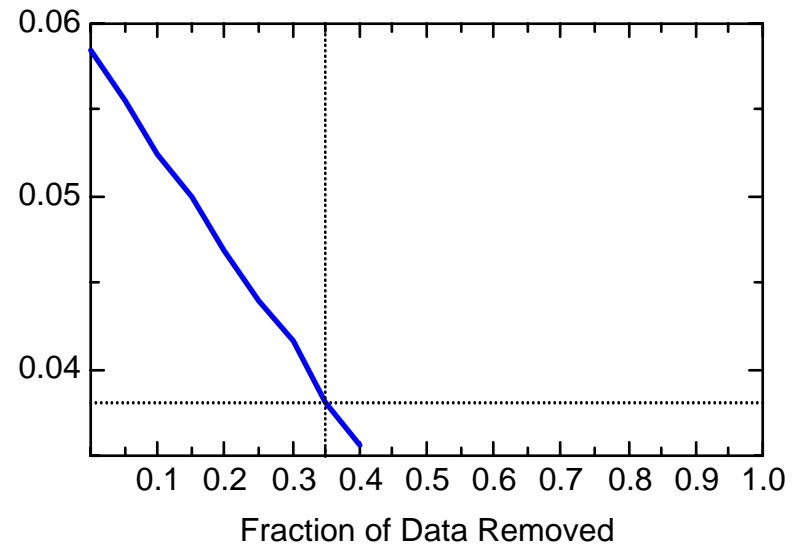
FE: Well JPZ0348



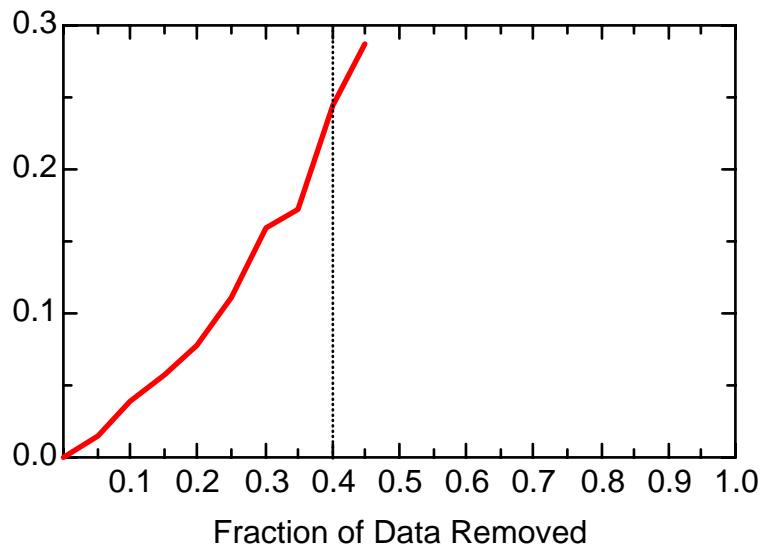
FE: Well JPZ0348



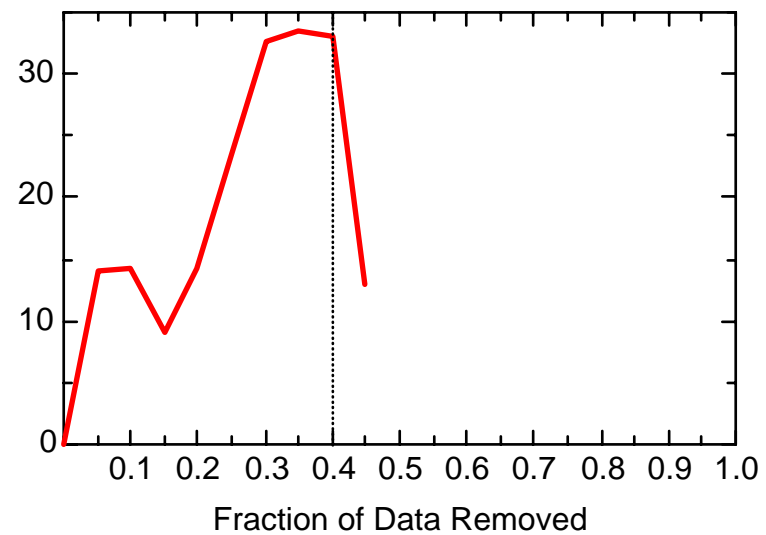
FE: Well JPZ0348



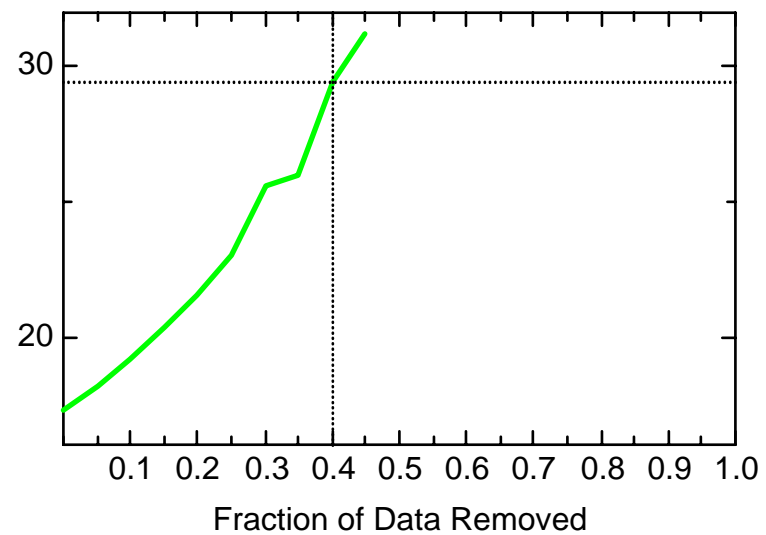
FE: Well JPZ0349



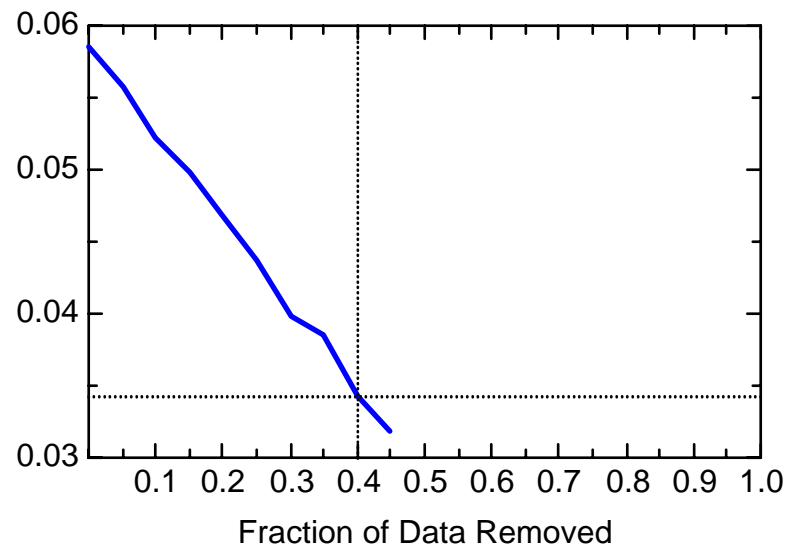
FE: Well JPZ0349



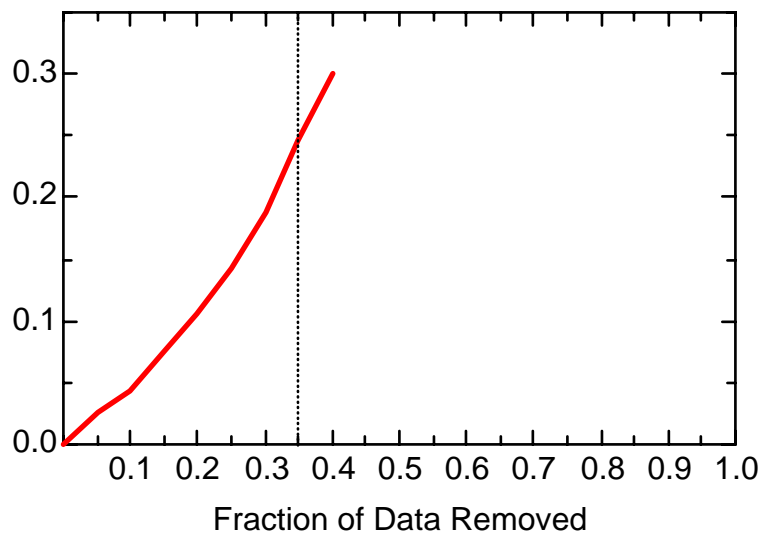
FE: Well JPZ0349



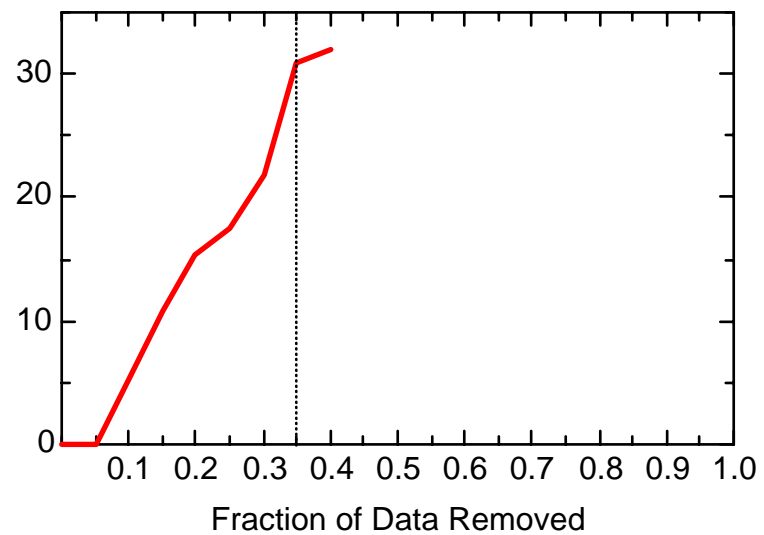
FE: Well JPZ0349



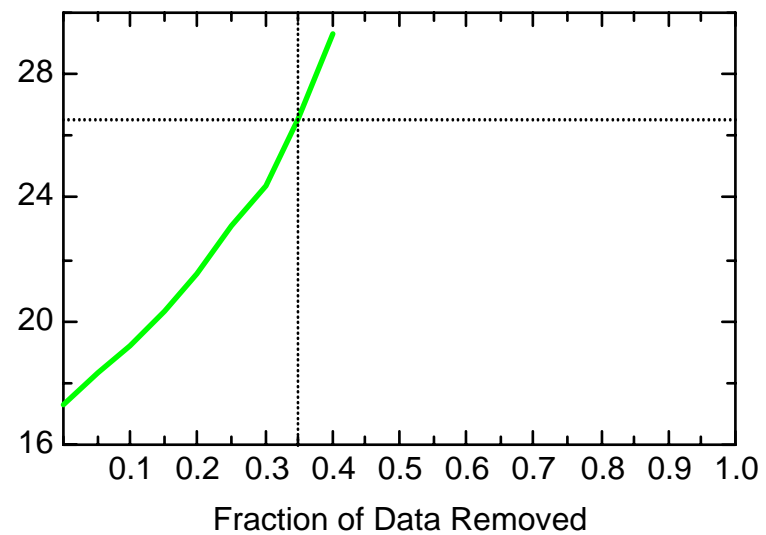
FE: Well JPZ1780



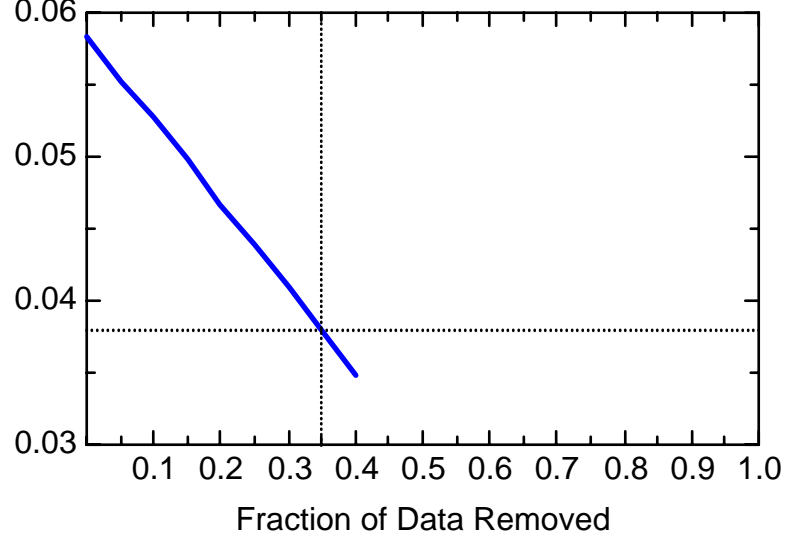
FE: Well JPZ1780



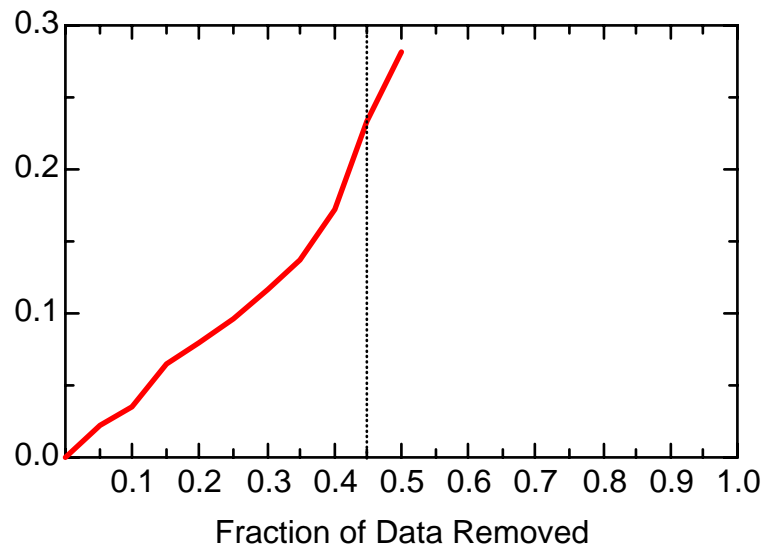
FE: Well JPZ1780



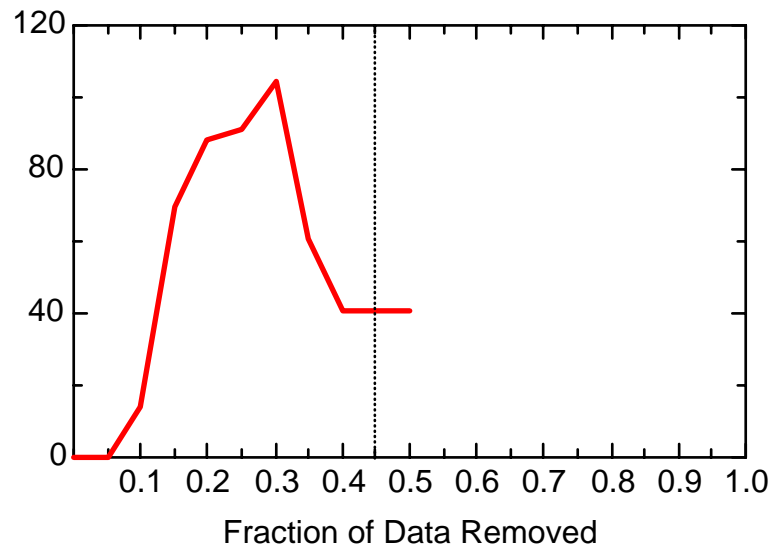
FE: Well JPZ1780



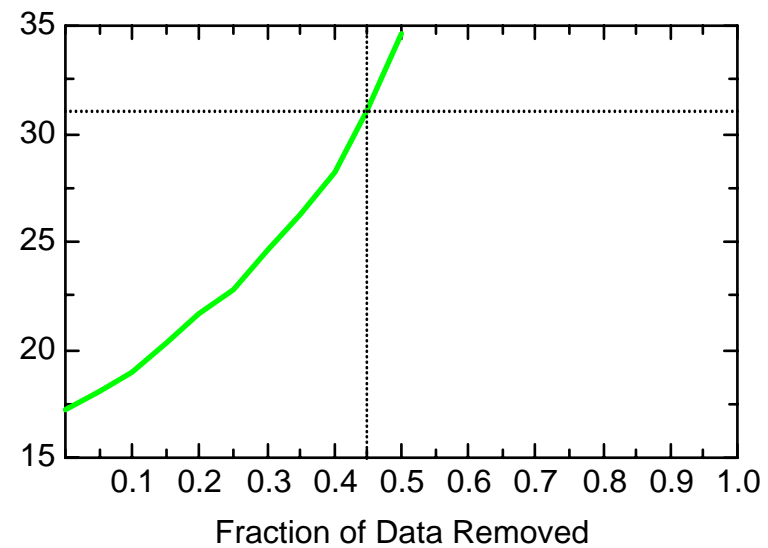
FE: Well JPZ7208



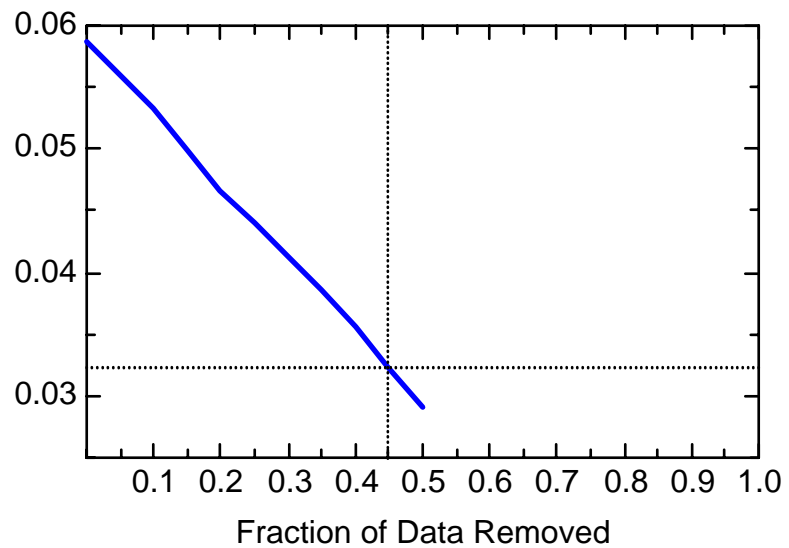
FE: Well JPZ7208



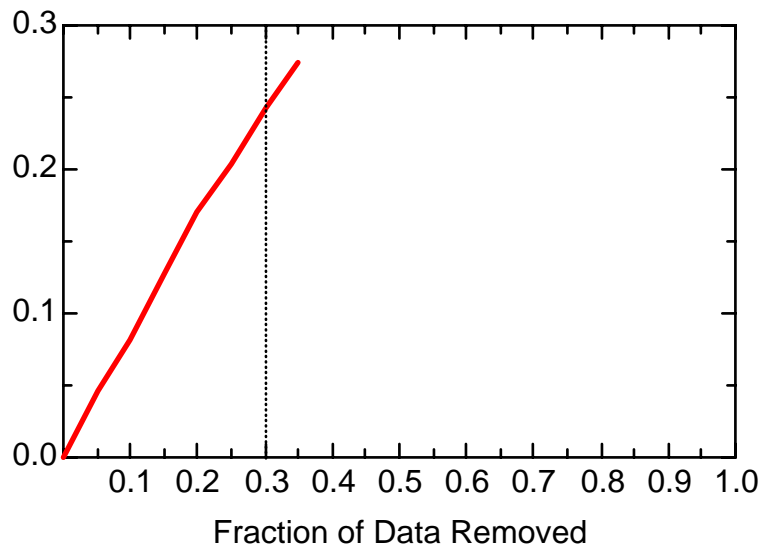
FE: Well JPZ7208



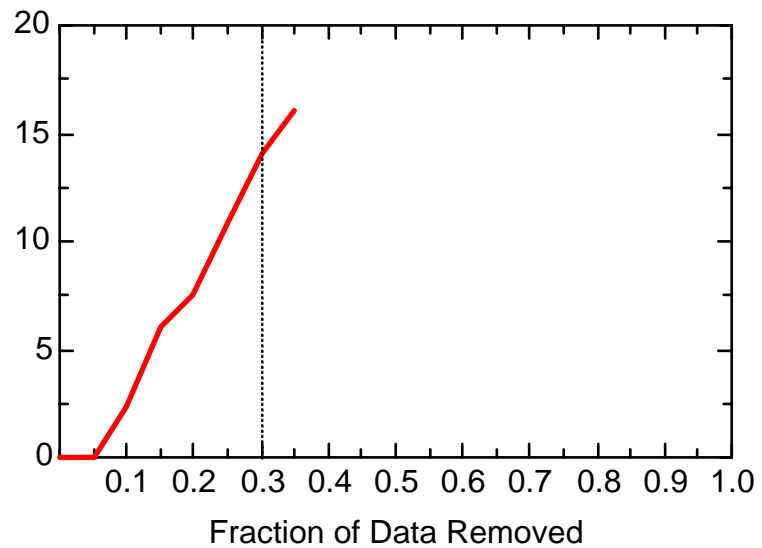
FE: Well JPZ7208



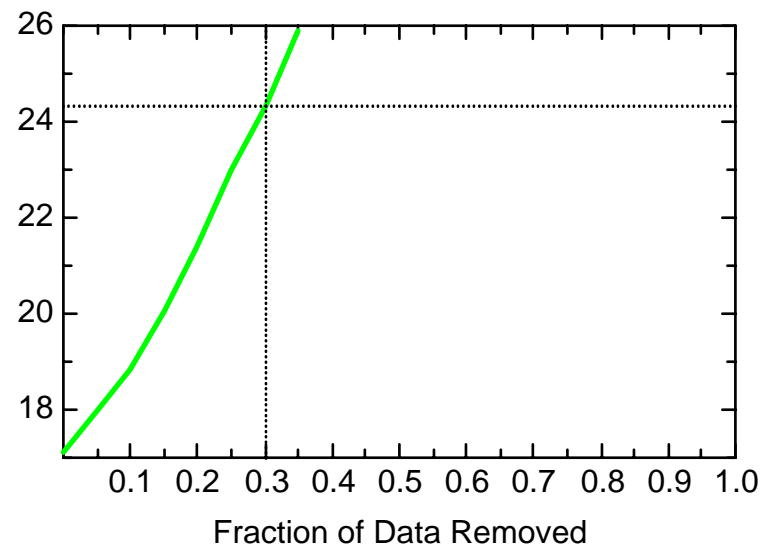
FE: Well JPZ7807



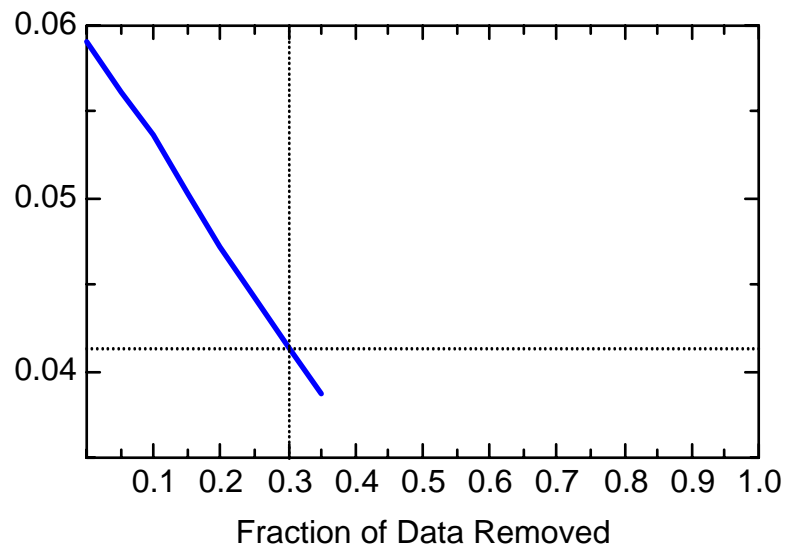
FE: Well JPZ7807



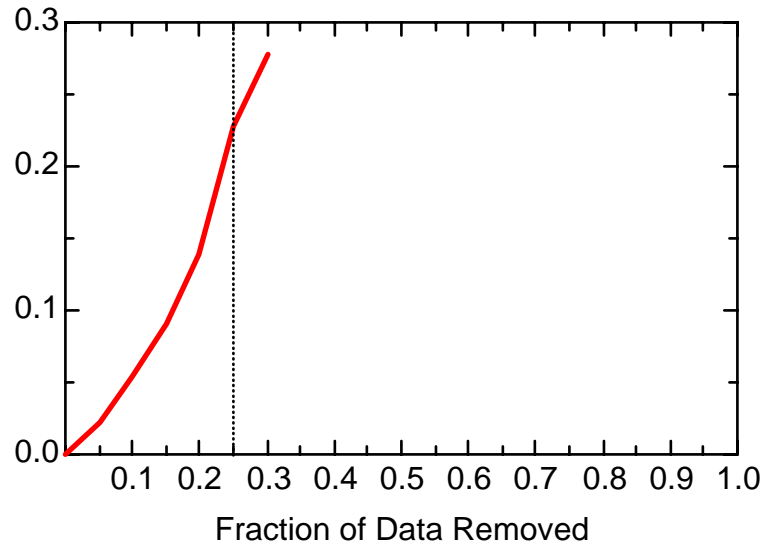
FE: Well JPZ7807



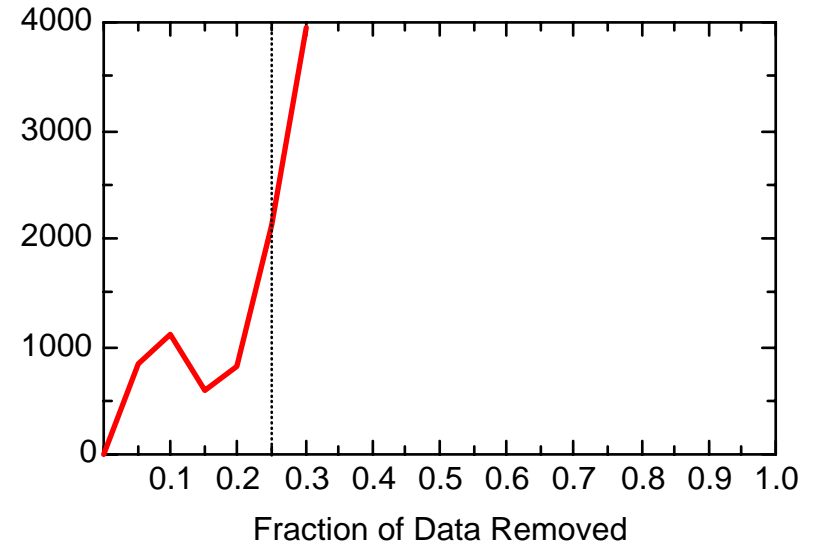
FE: Well JPZ7807



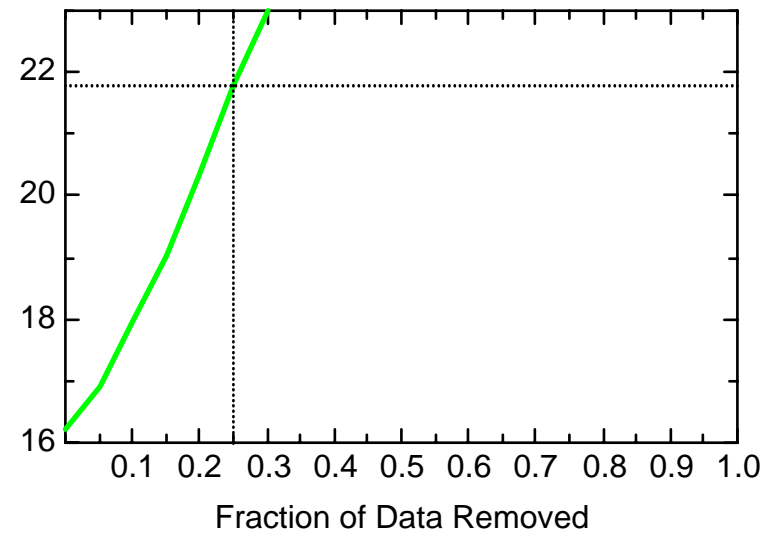
FE: Well MMW0005



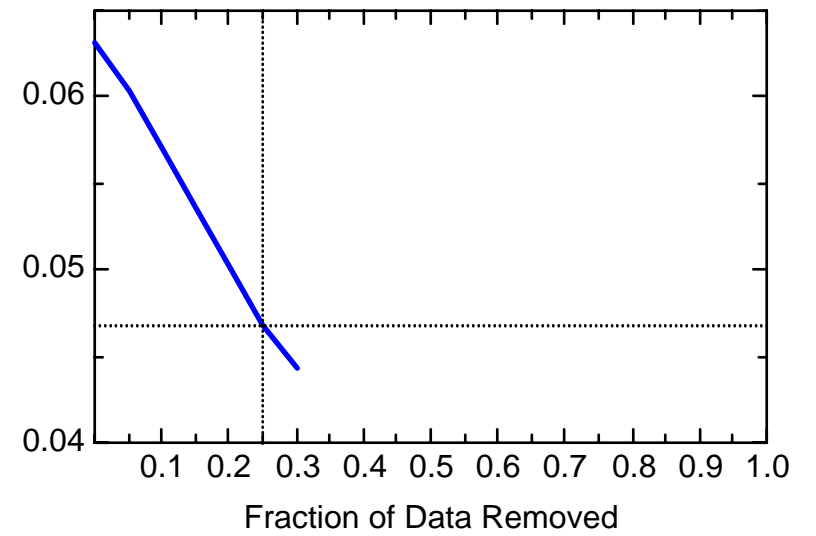
FE: Well MMW0005



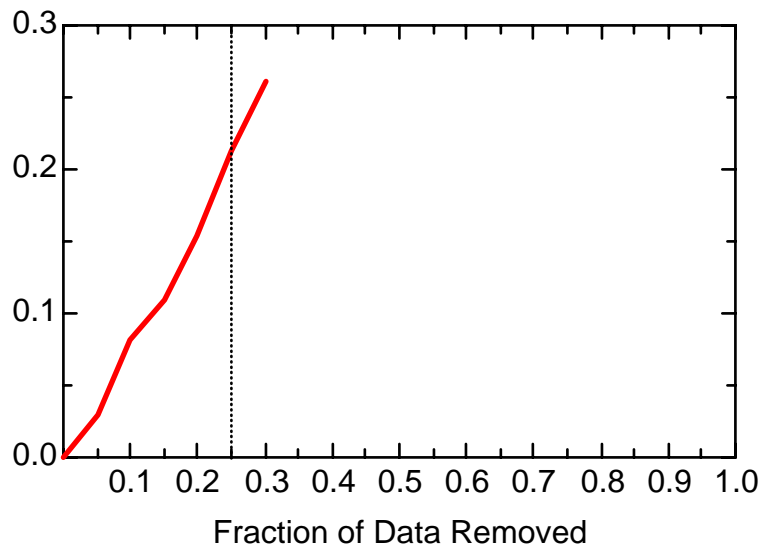
FE: Well MMW0005



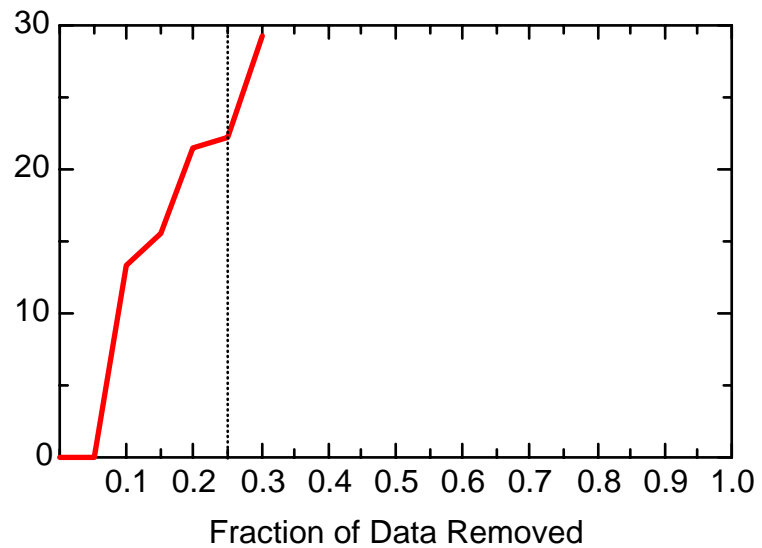
FE: Well MMW0005



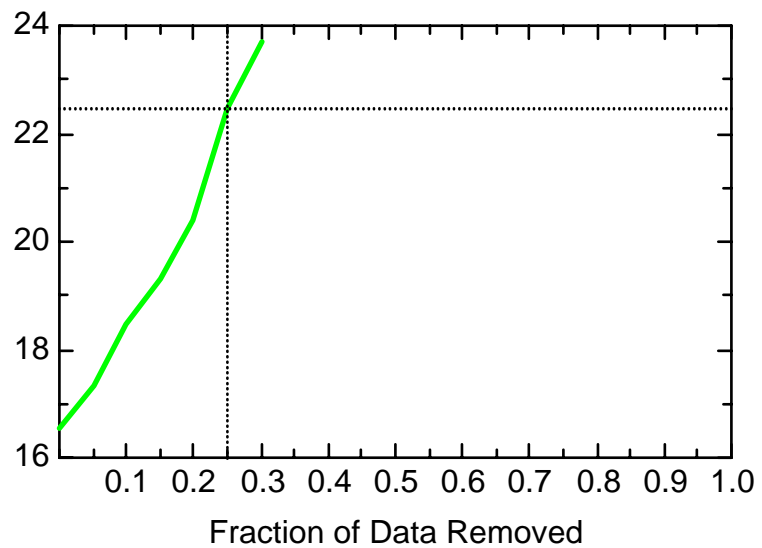
FE: Well MMW0007A



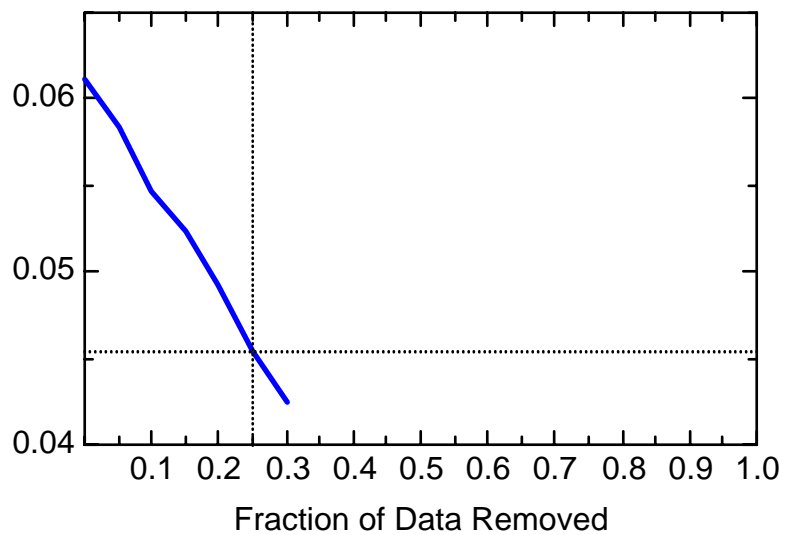
FE: Well MMW0007A



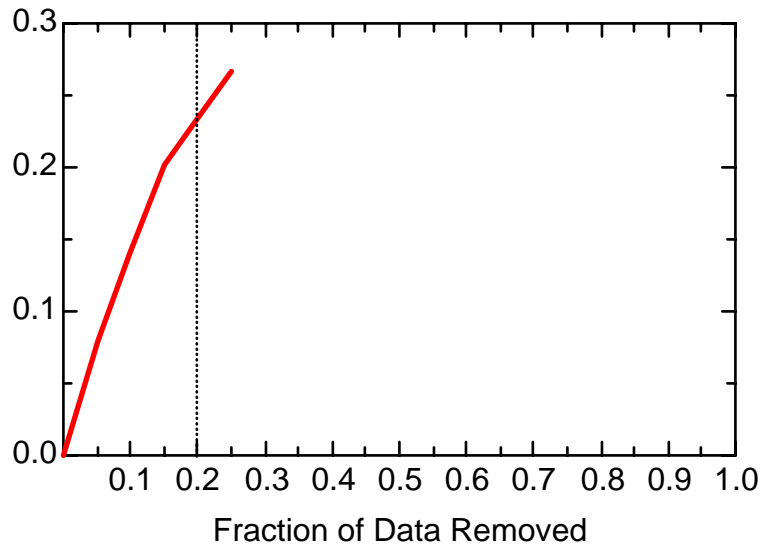
FE: Well MMW0007A



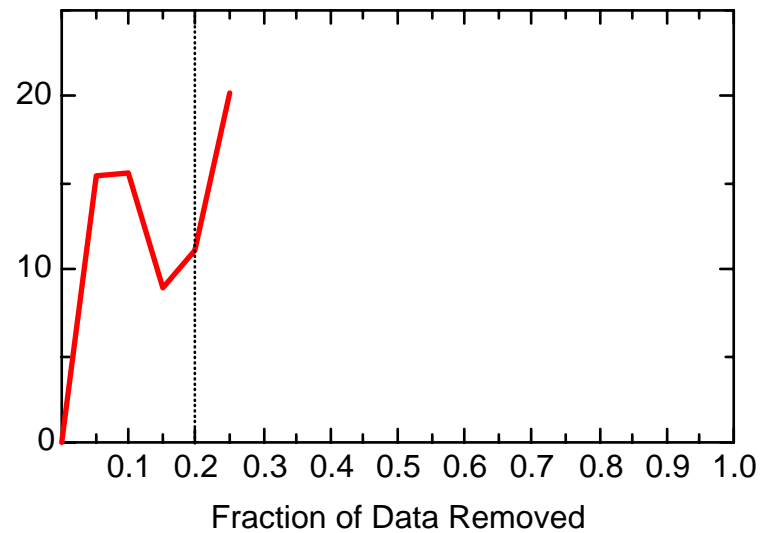
FE: Well MMW0007A



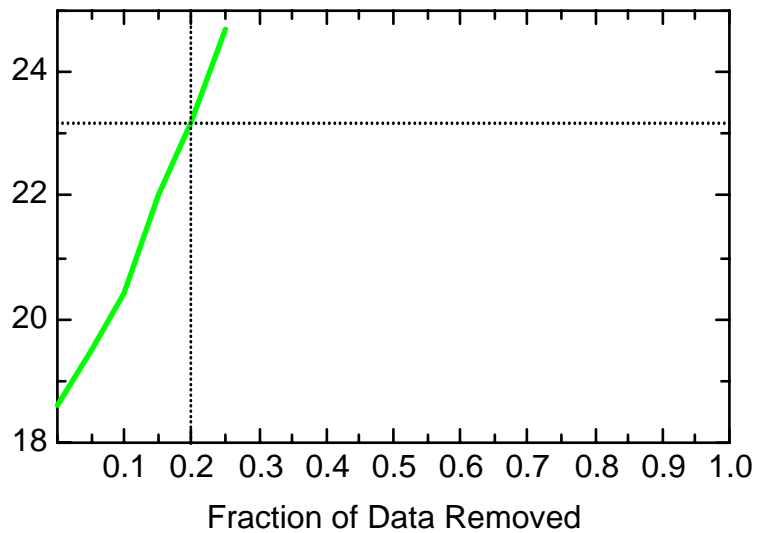
FE: Well MMW0007B



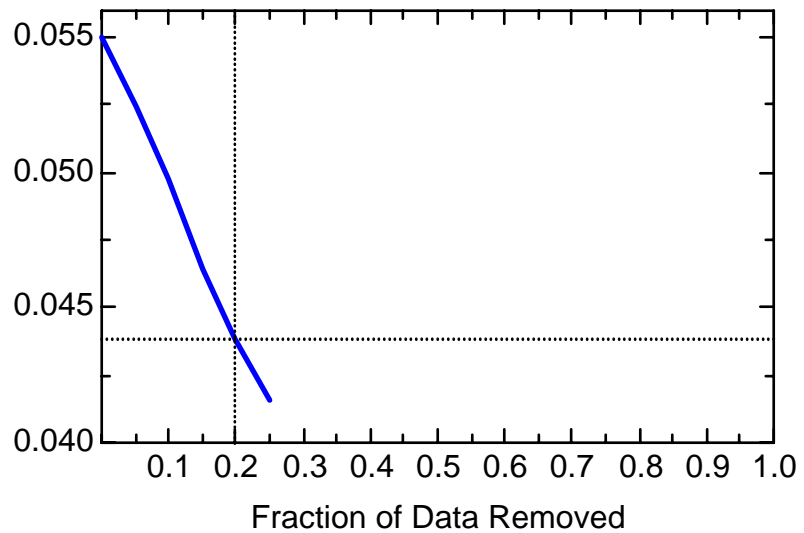
FE: Well MMW0007B



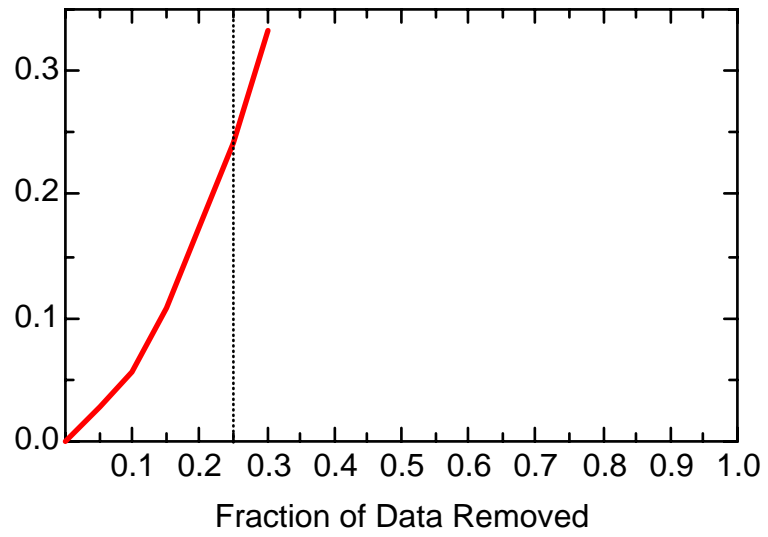
FE: Well MMW0007B



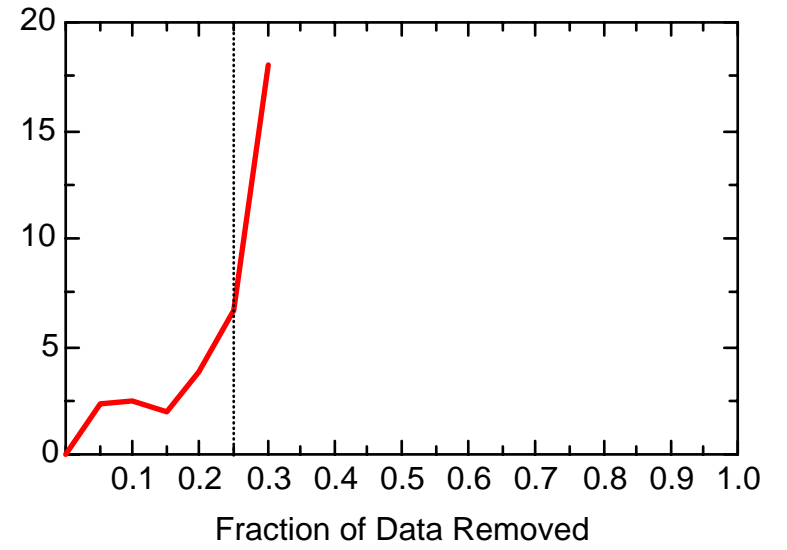
FE: Well MMW0007B



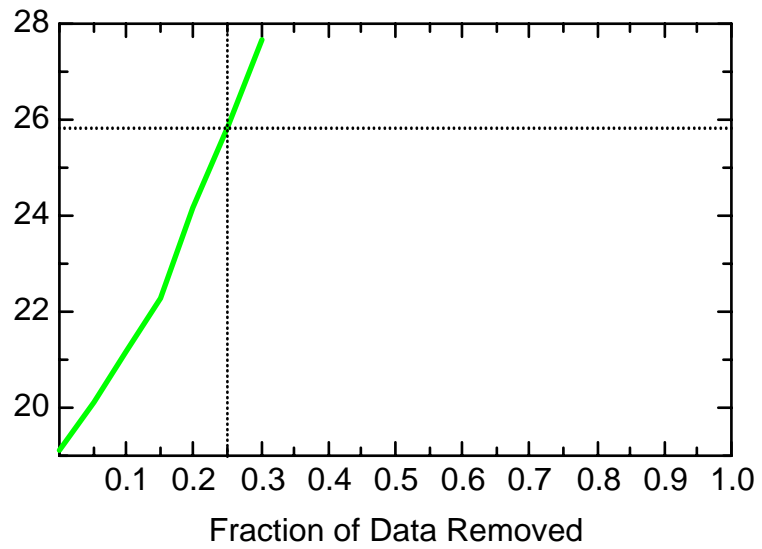
FE: Well MMW0008



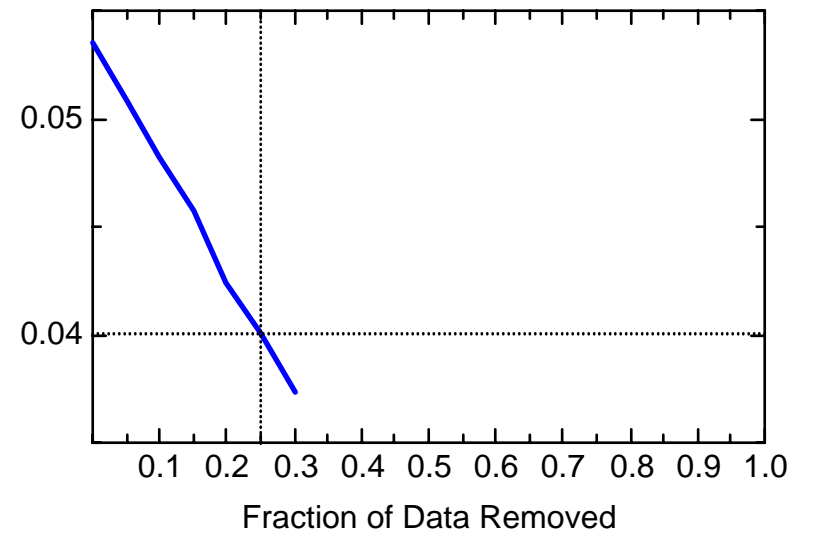
FE: Well MMW0008



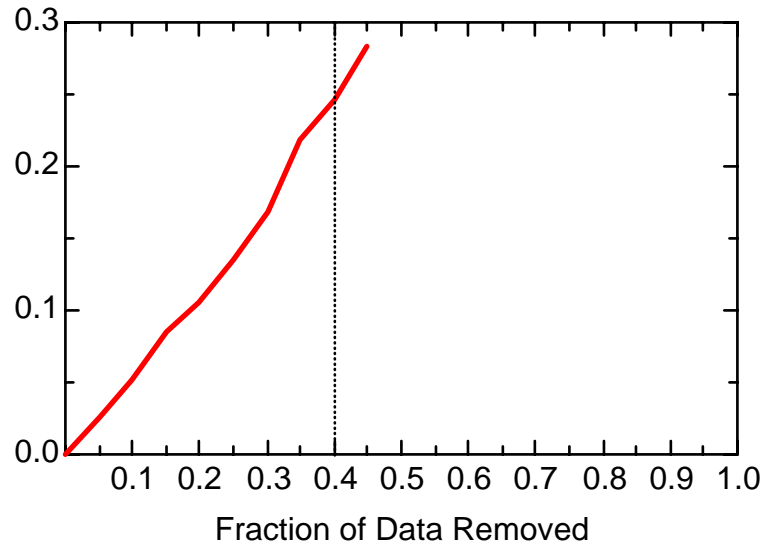
FE: Well MMW0008



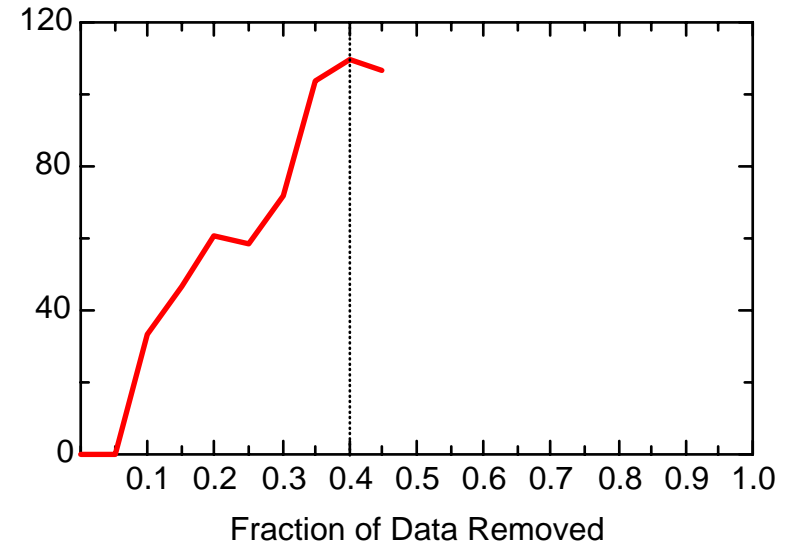
FE: Well MMW0008



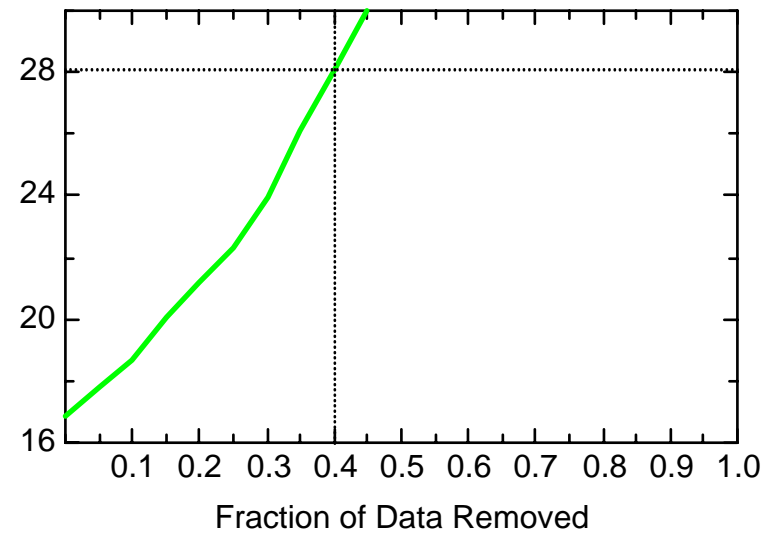
FE: Well MMW0009



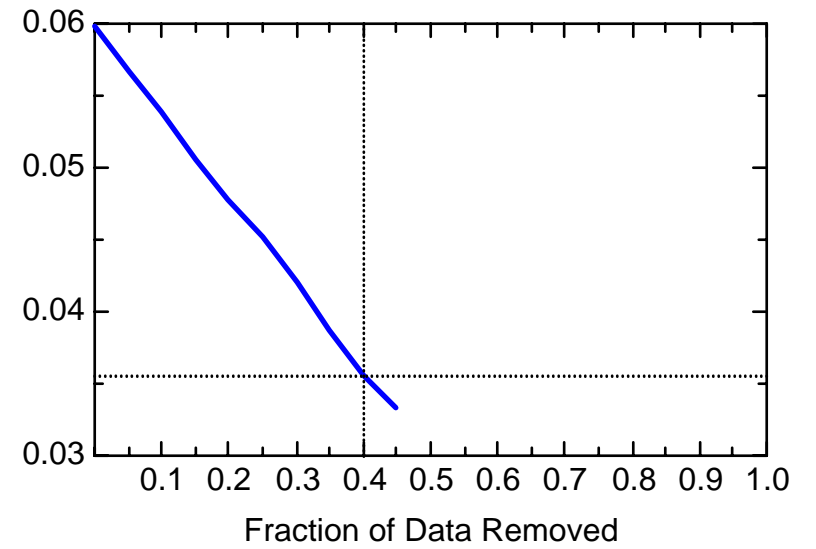
FE: Well MMW0009



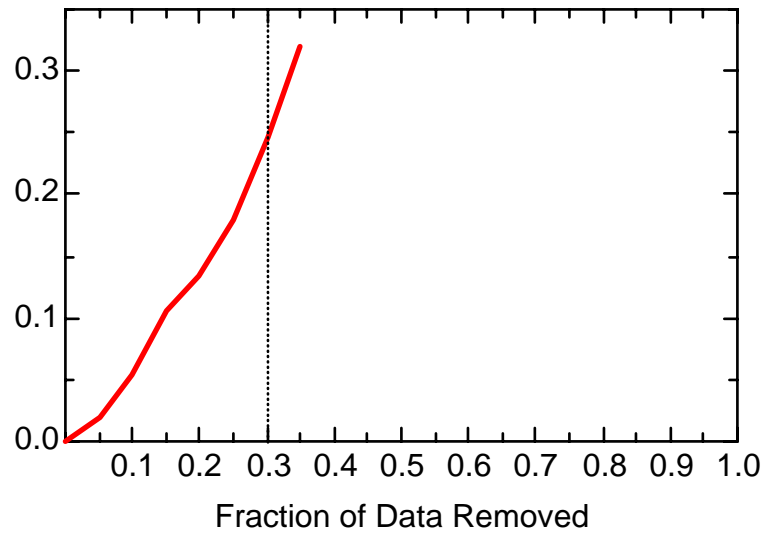
FE: Well MMW0009



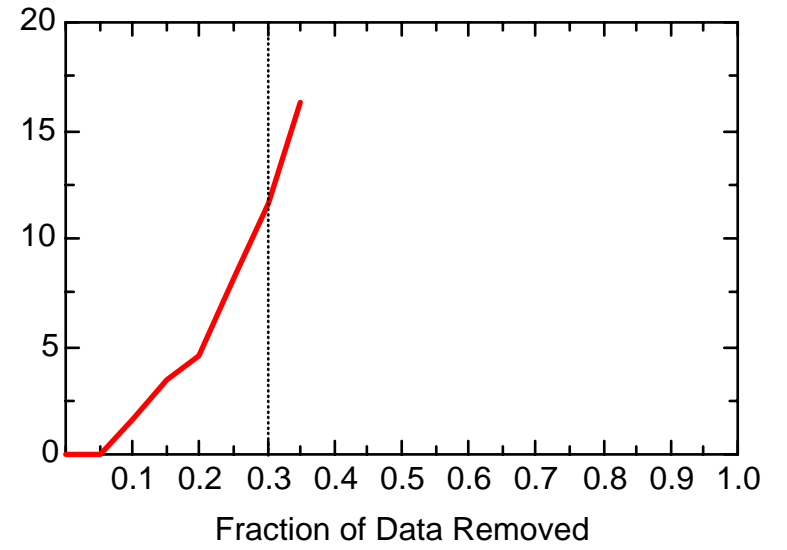
FE: Well MMW0009



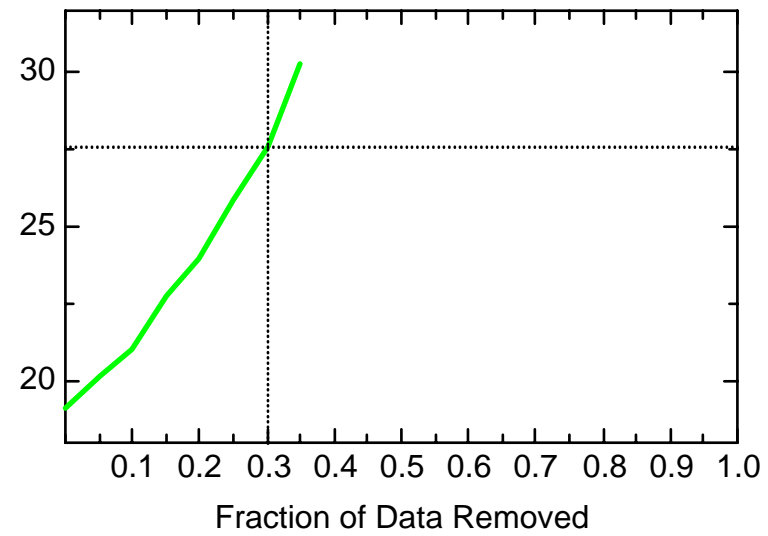
FE: Well MMW0010



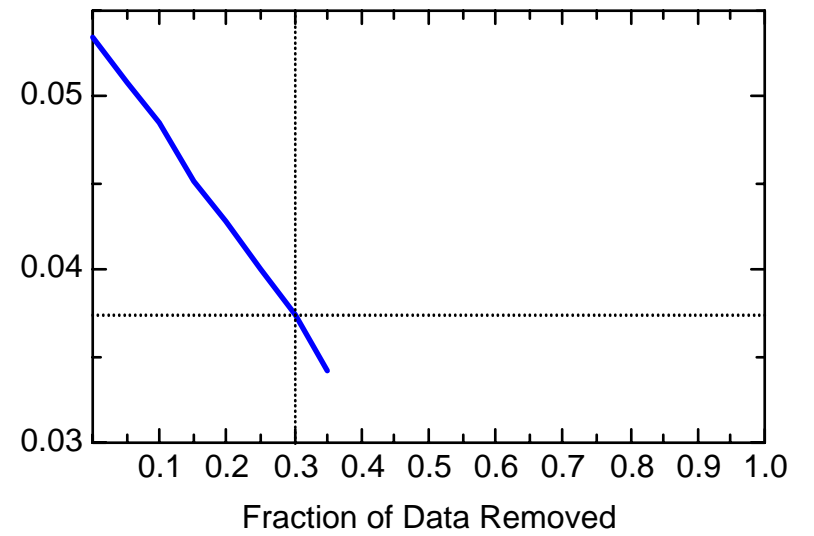
FE: Well MMW0010



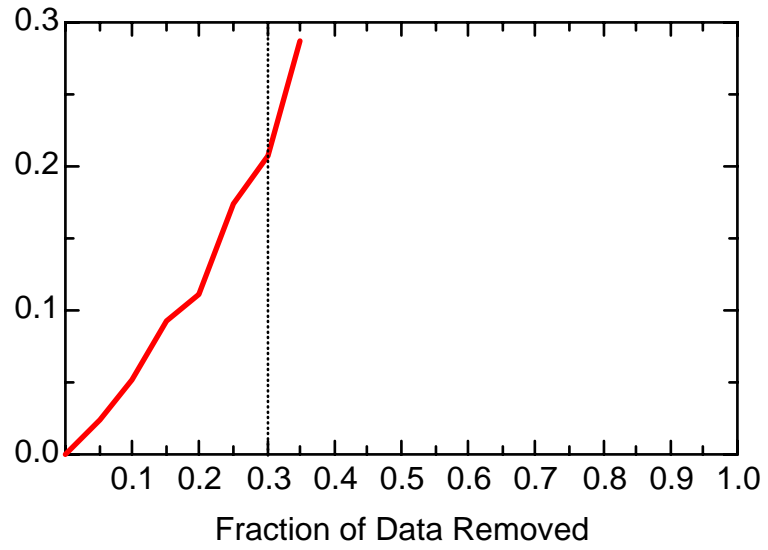
FE: Well MMW0010



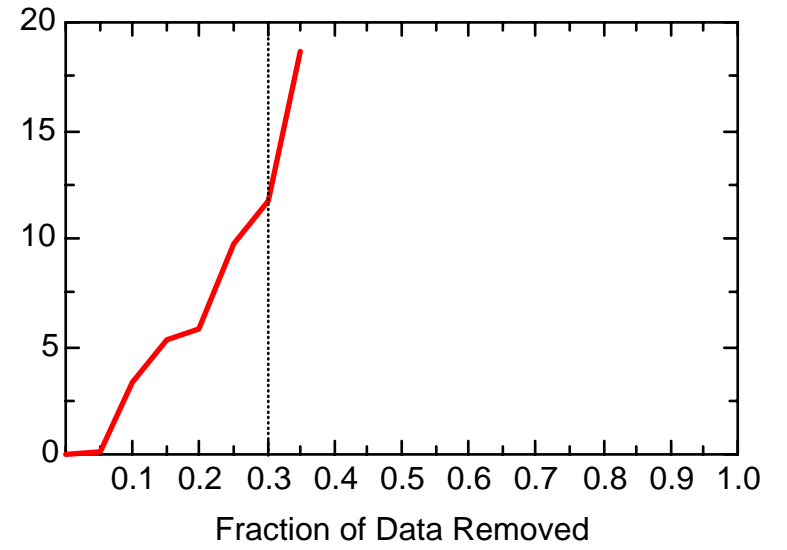
FE: Well MMW0010



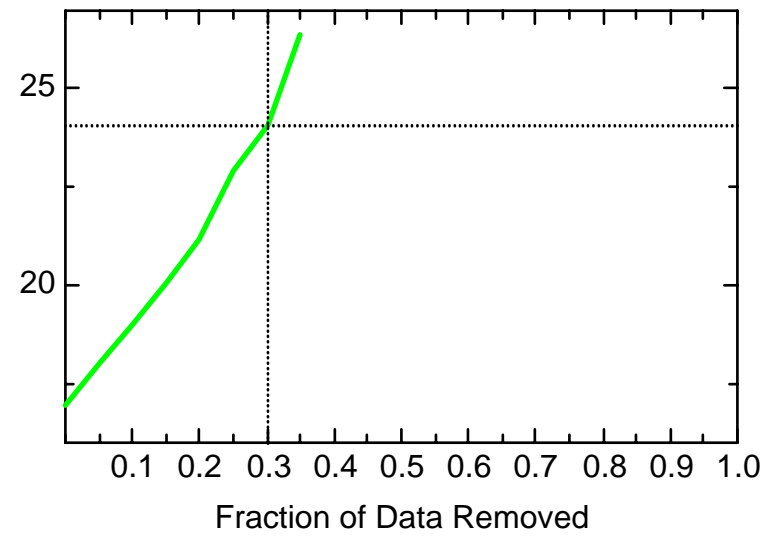
FE: Well MMW0011



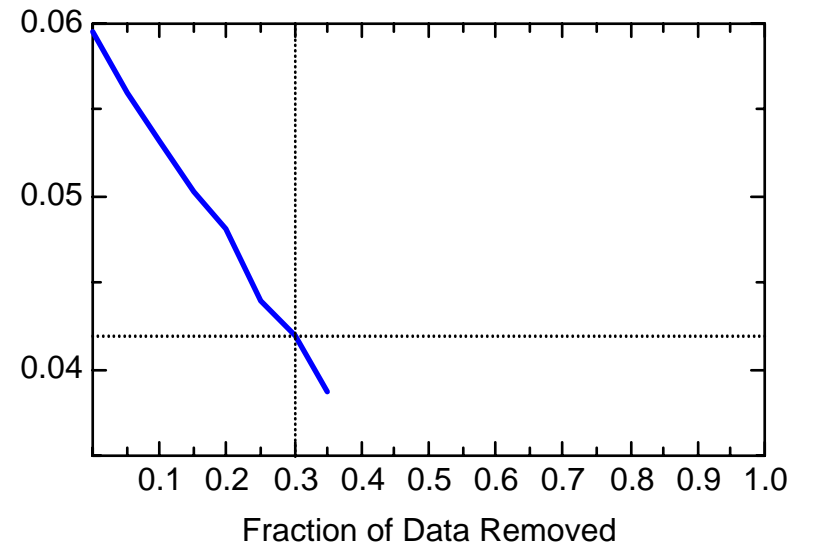
FE: Well MMW0011



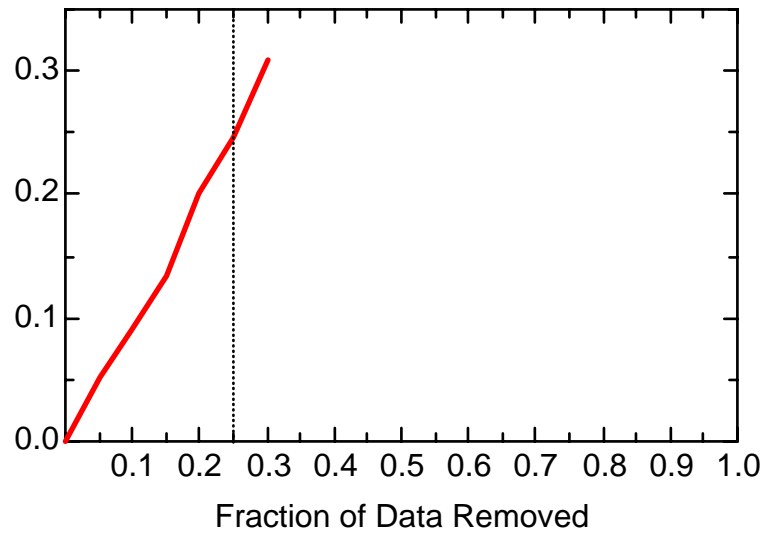
FE: Well MMW0011



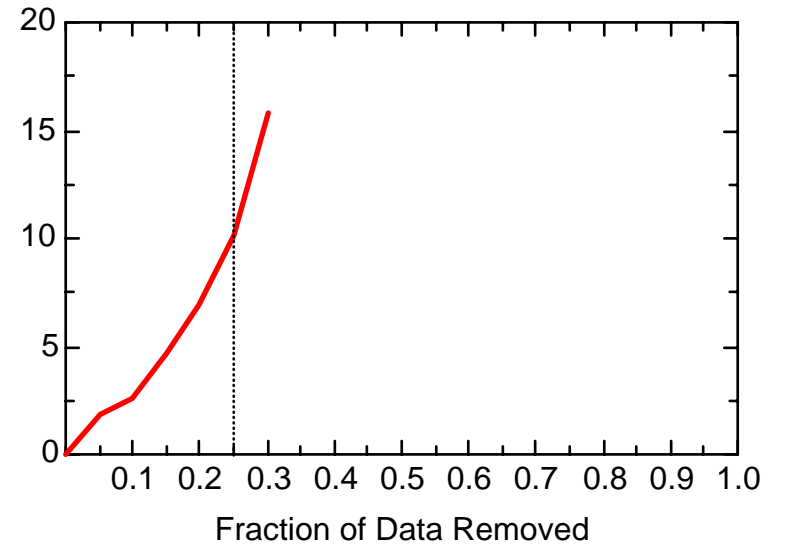
FE: Well MMW0011



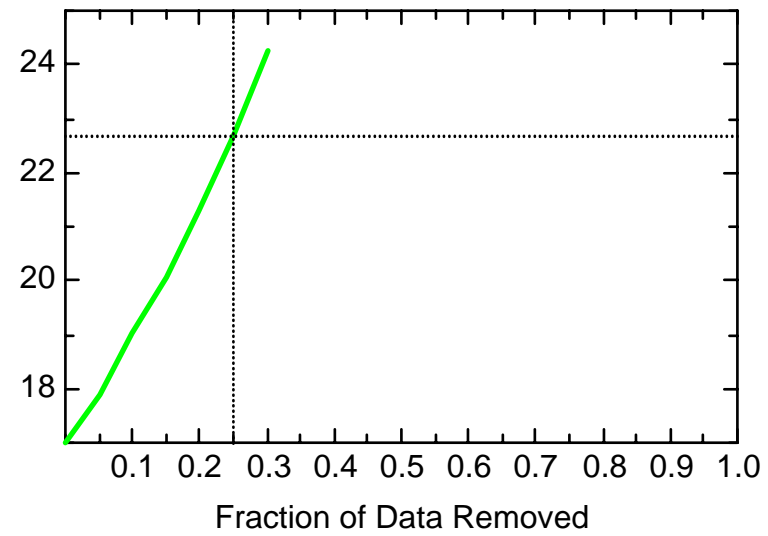
FE: Well MMW0012



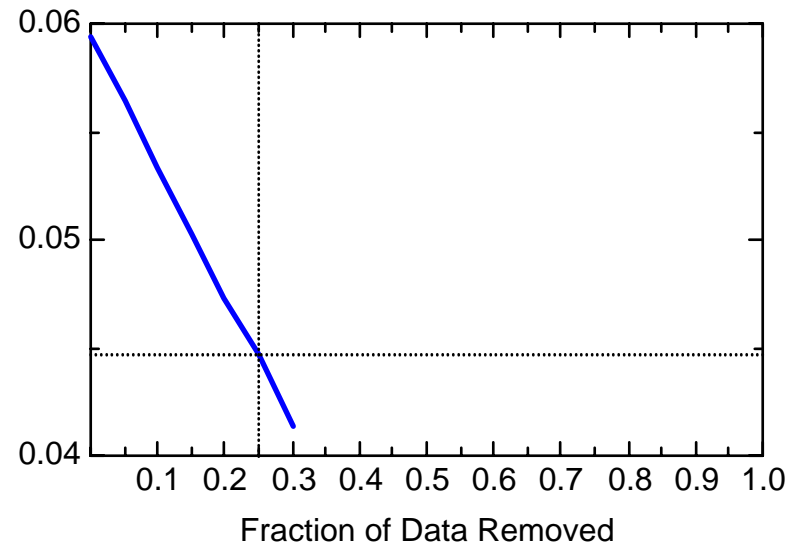
FE: Well MMW0012



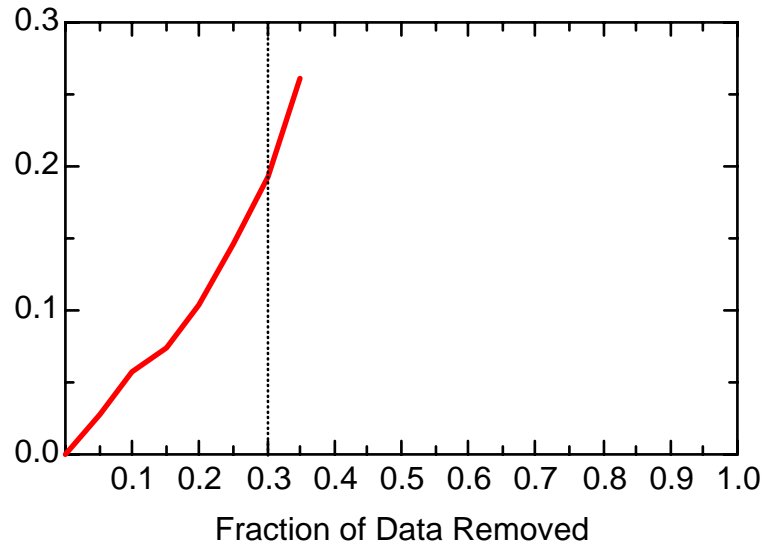
FE: Well MMW0012



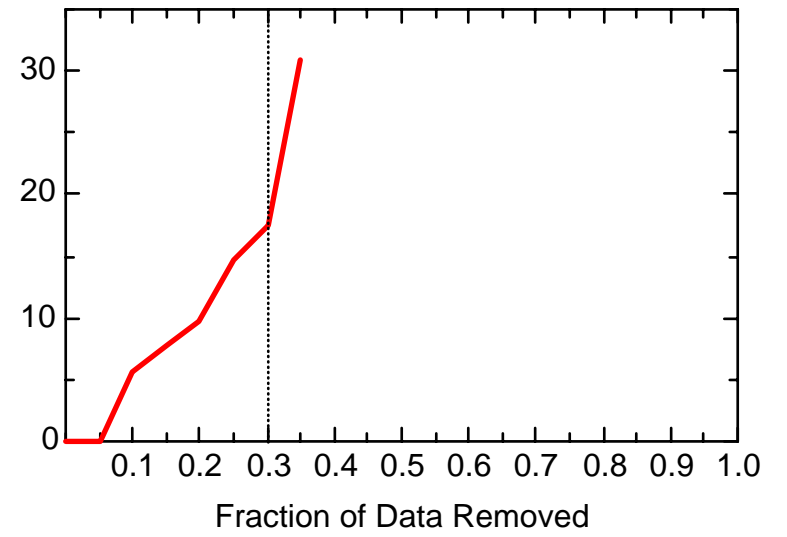
FE: Well MMW0012



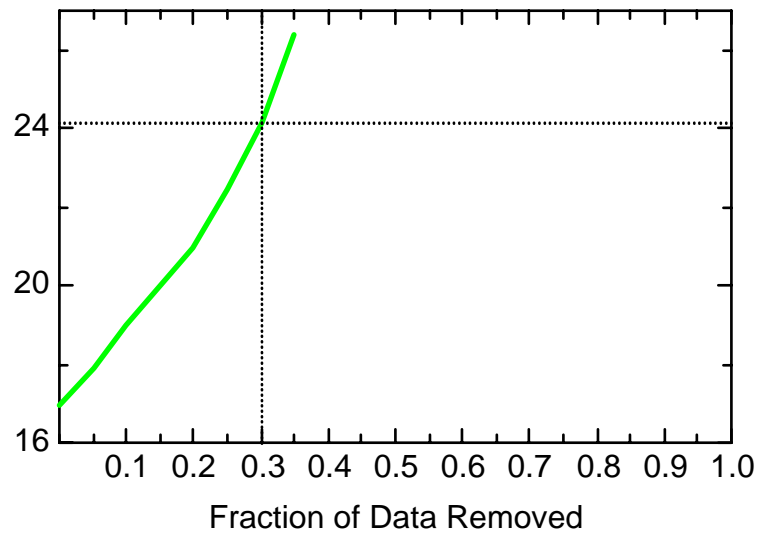
FE: Well MMW0013



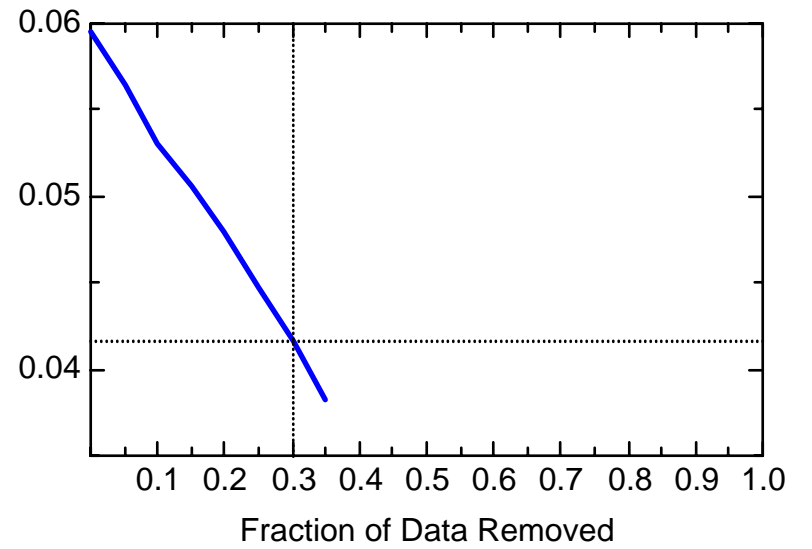
FE: Well MMW0013



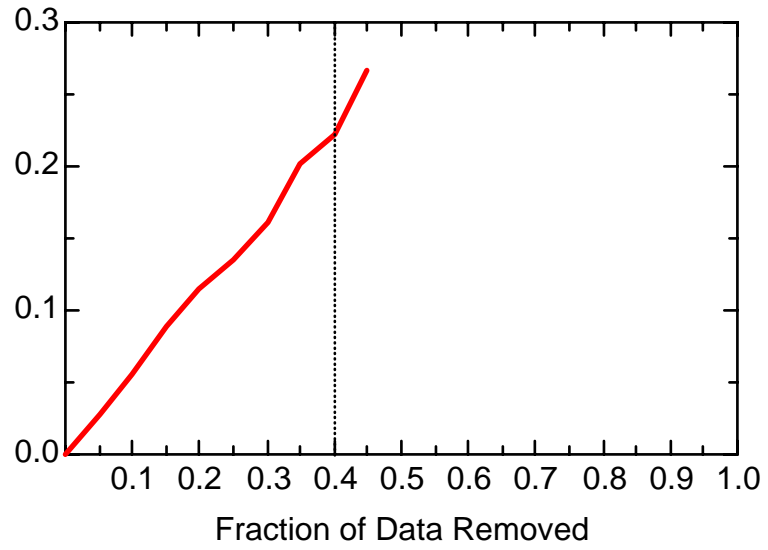
FE: Well MMW0013



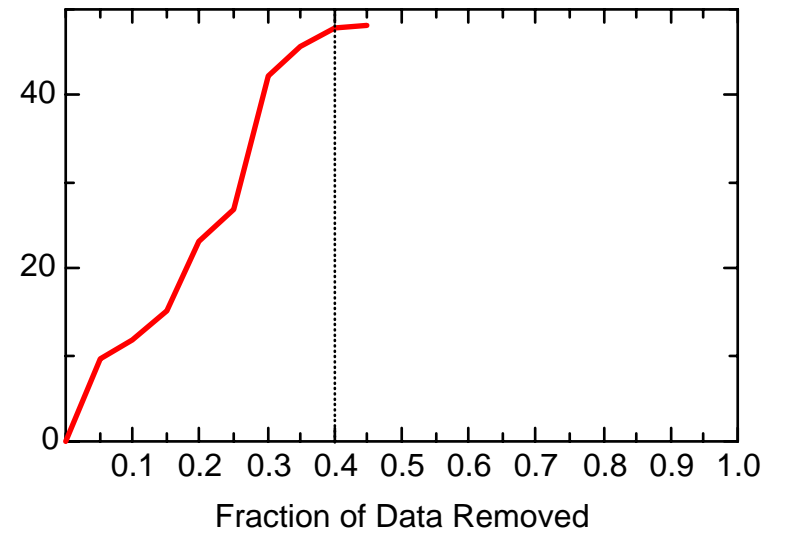
FE: Well MMW0013



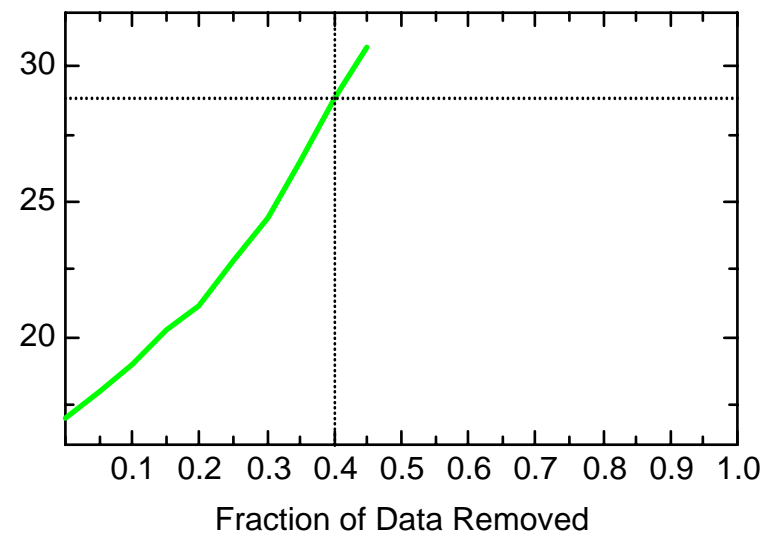
FE: Well MMW0016



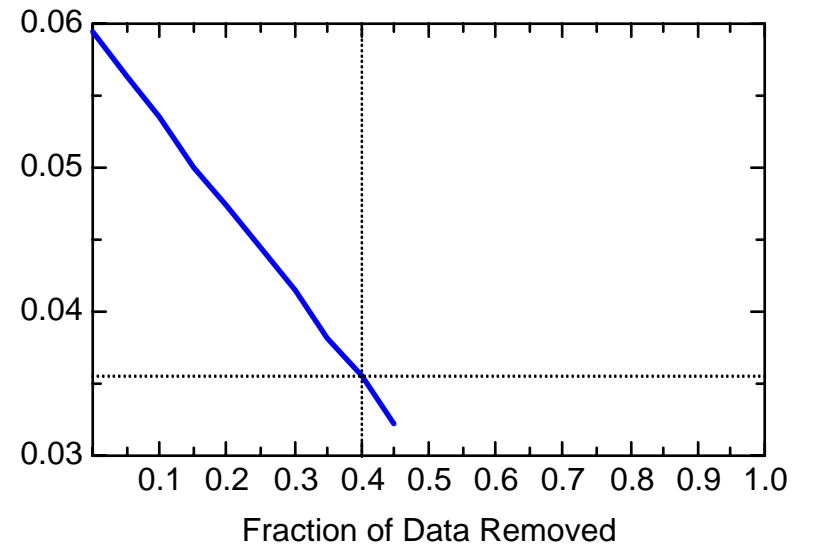
FE: Well MMW0016



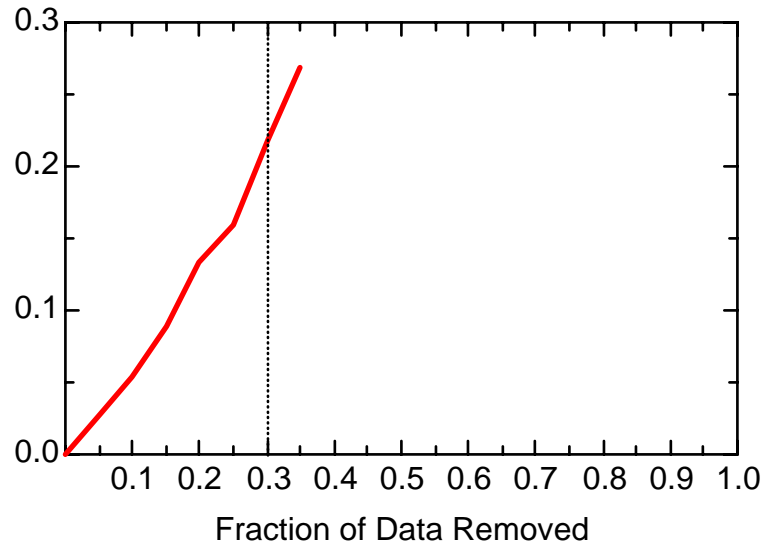
FE: Well MMW0016



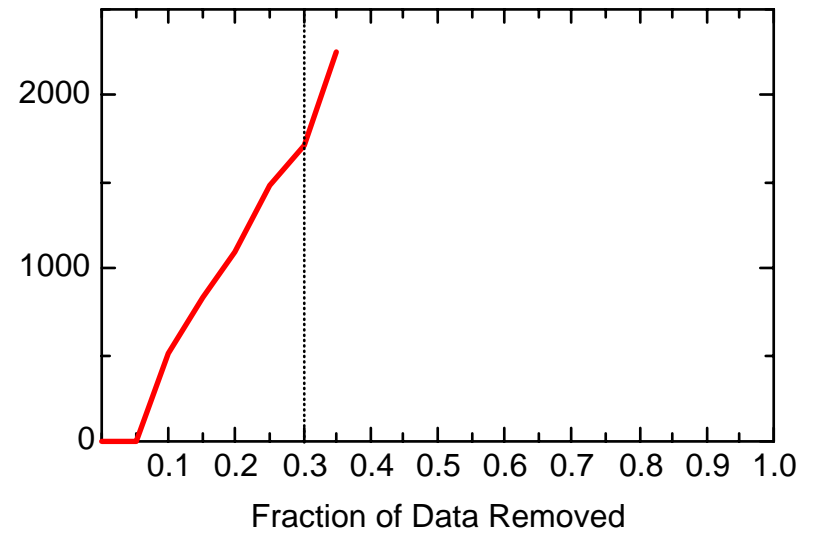
FE: Well MMW0016



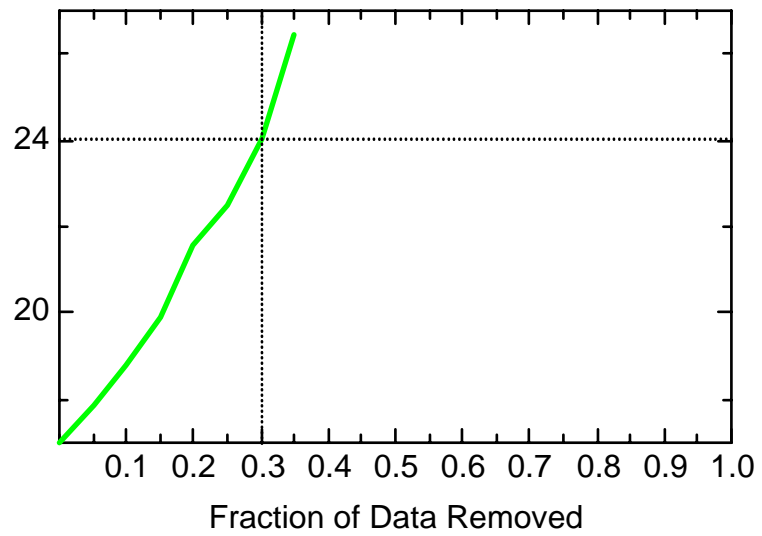
FE: Well MMW0017



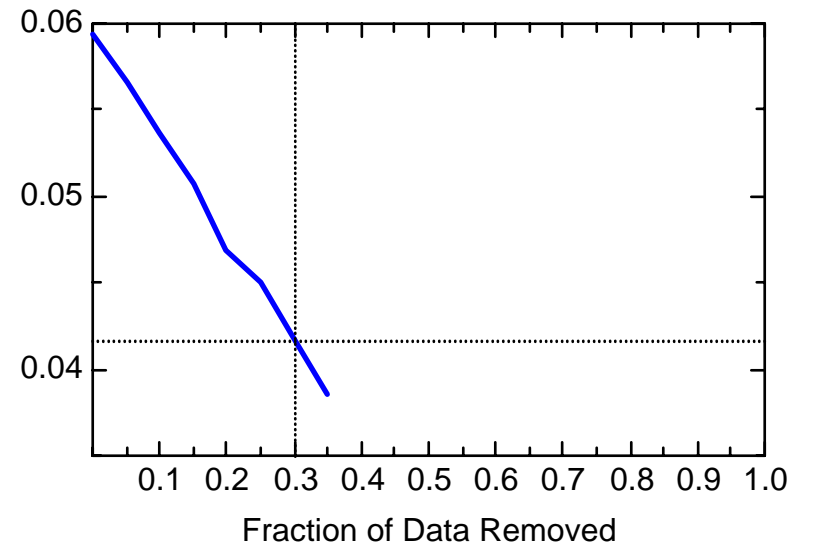
FE: Well MMW0017



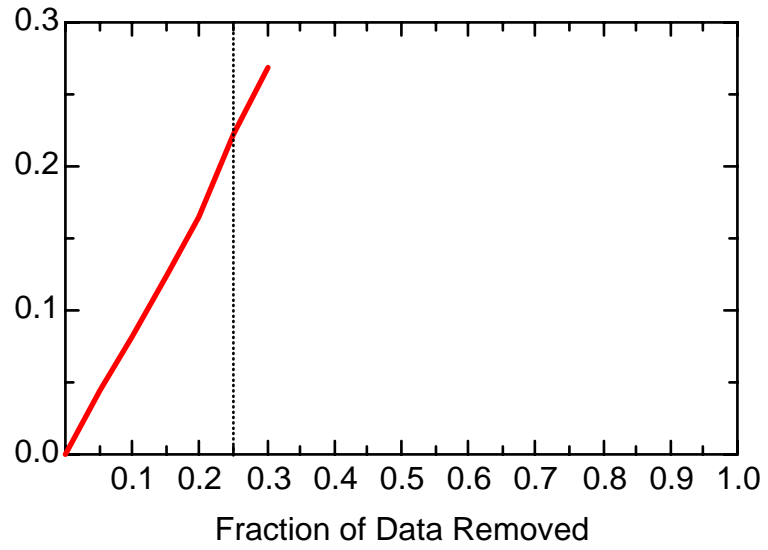
FE: Well MMW0017



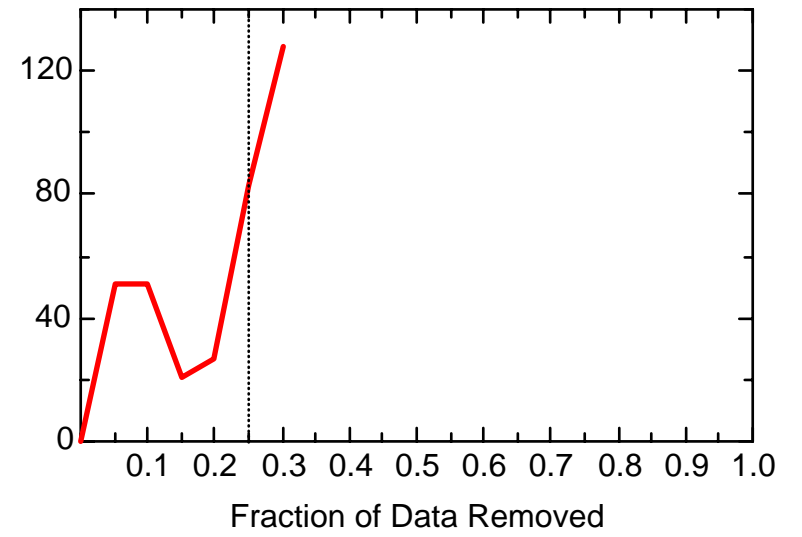
FE: Well MMW0017



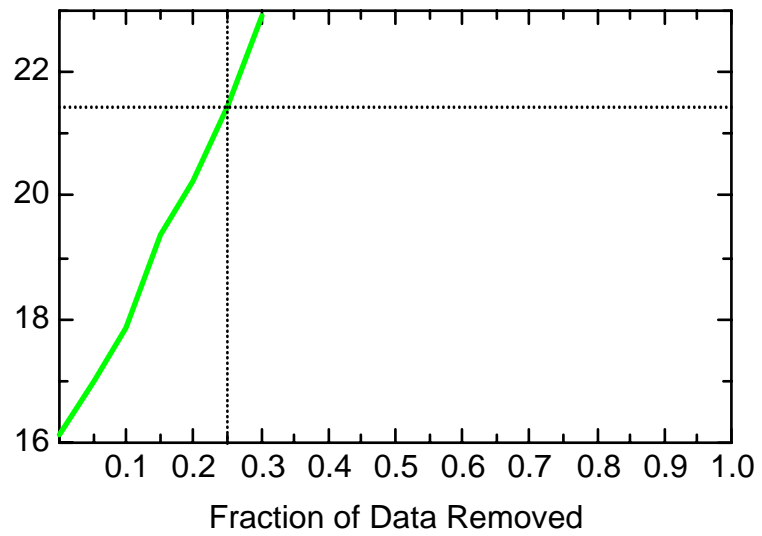
FE: Well MMW0019



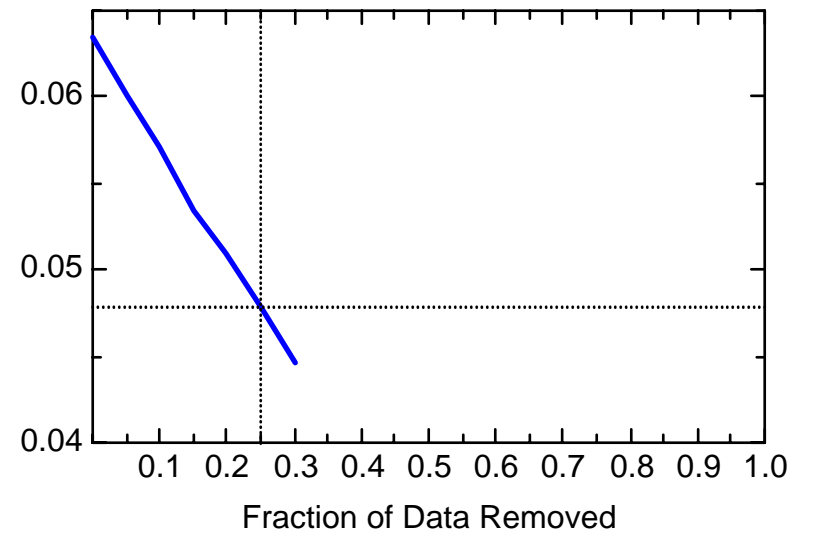
FE: Well MMW0019



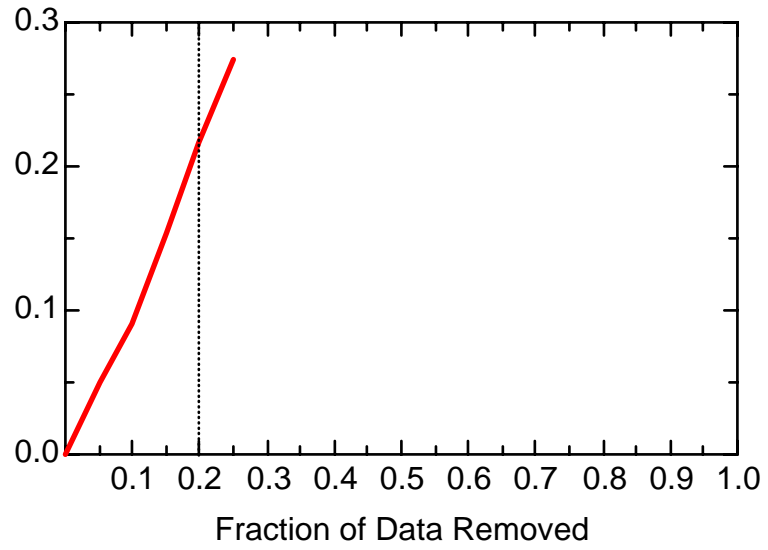
FE: Well MMW0019



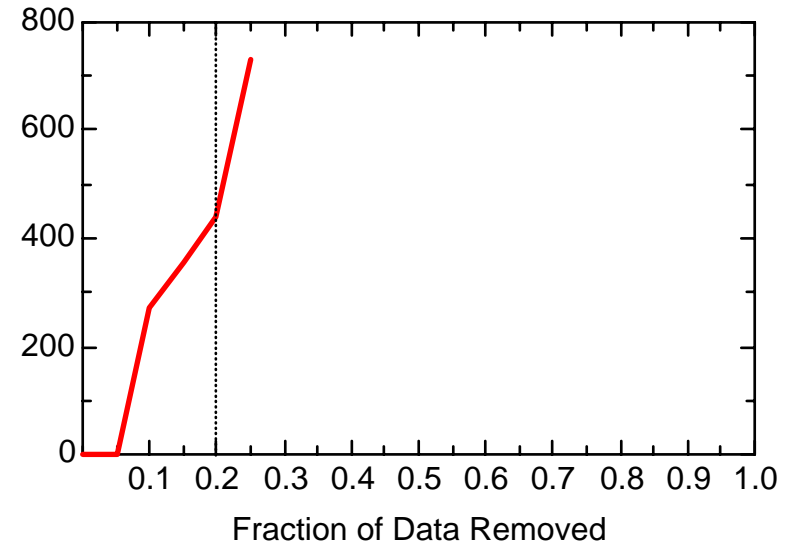
FE: Well MMW0019



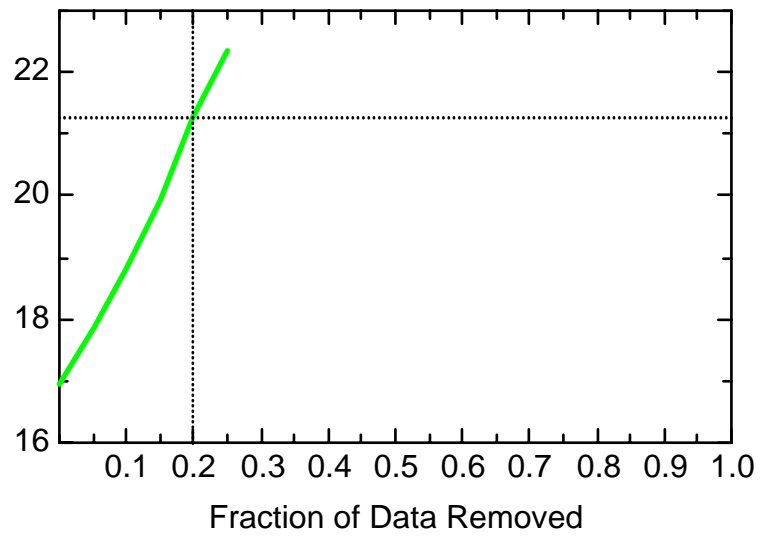
FE: Well MMW1560



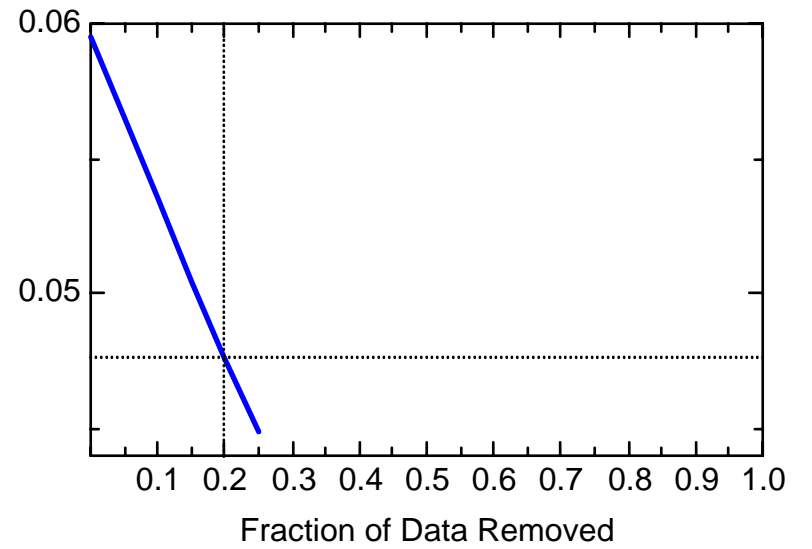
FE: Well MMW1560



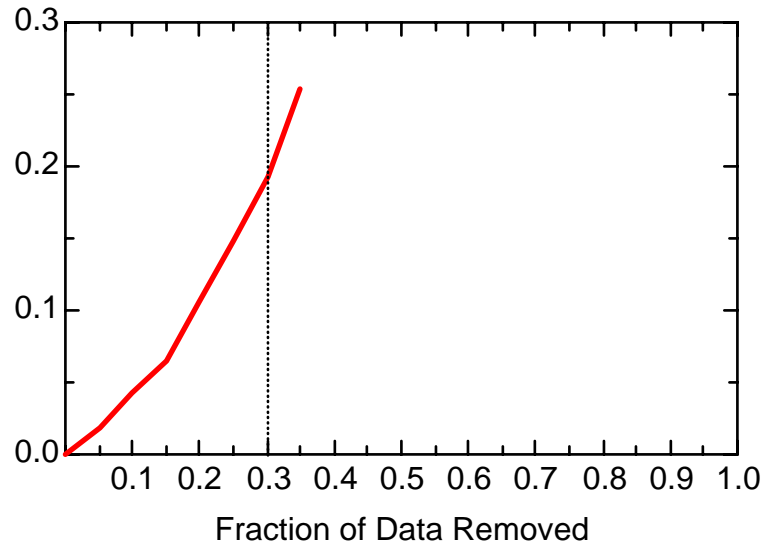
FE: Well MMW1560



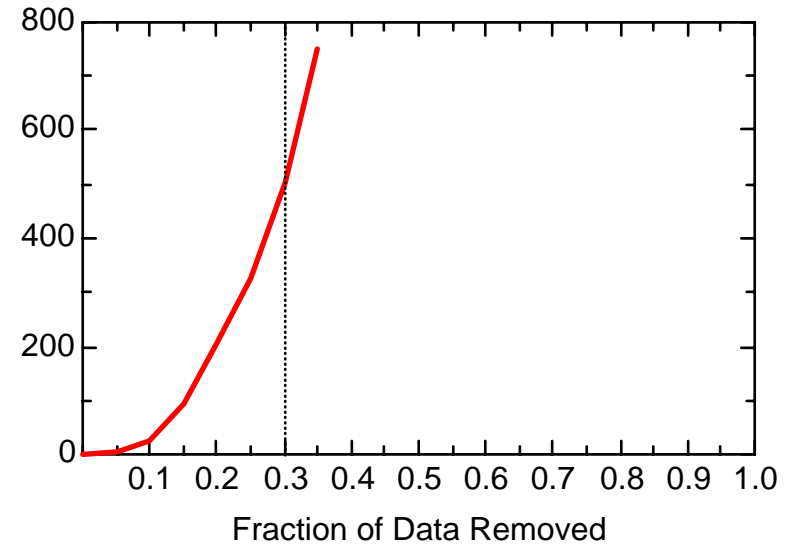
FE: Well MMW1560



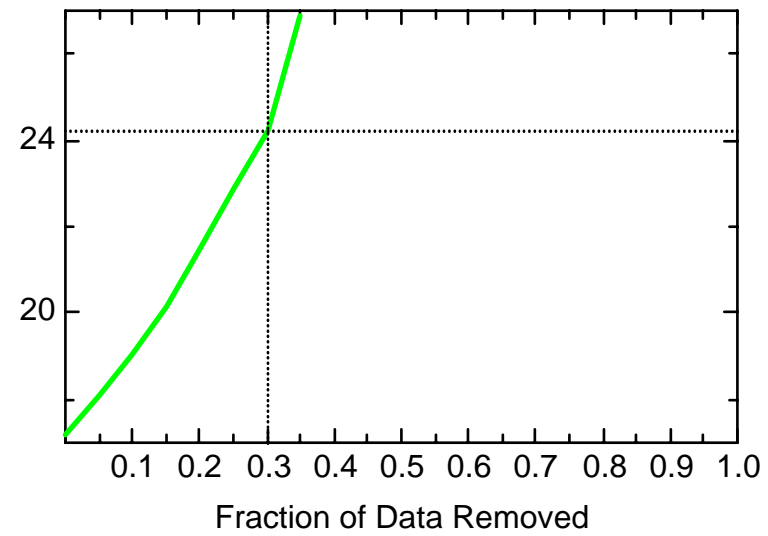
FE: Well MMW7330



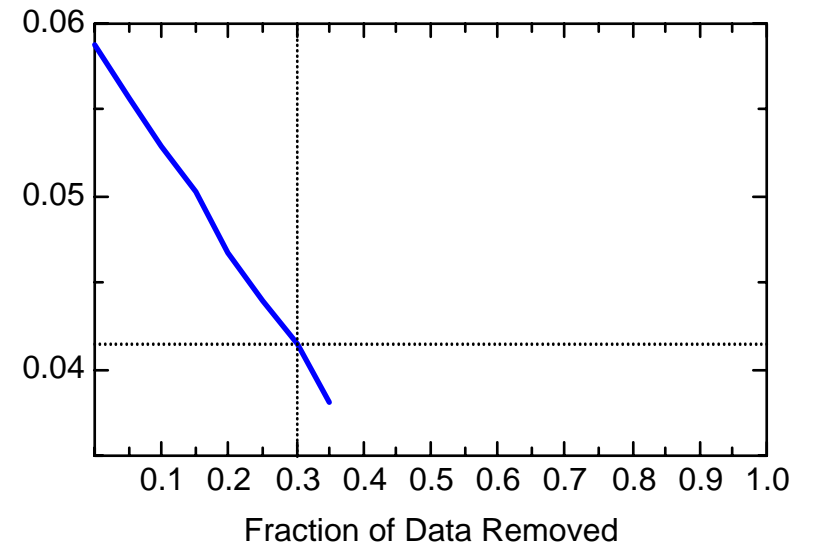
FE: Well MMW7330



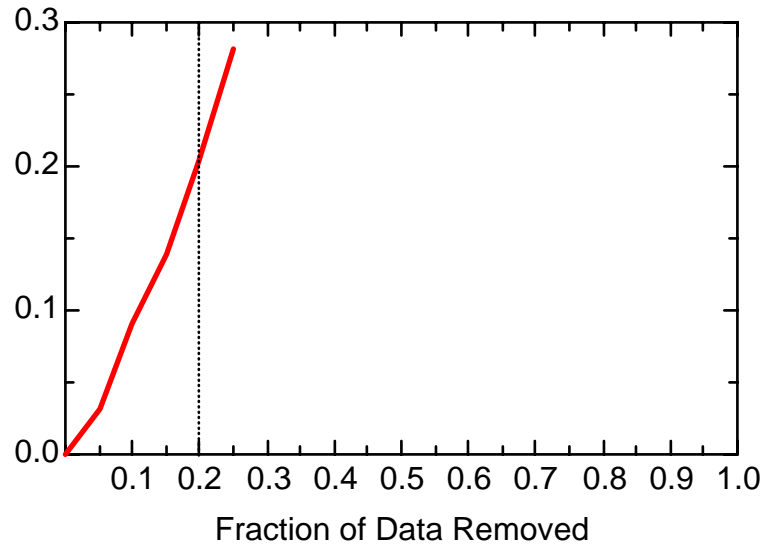
FE: Well MMW7330



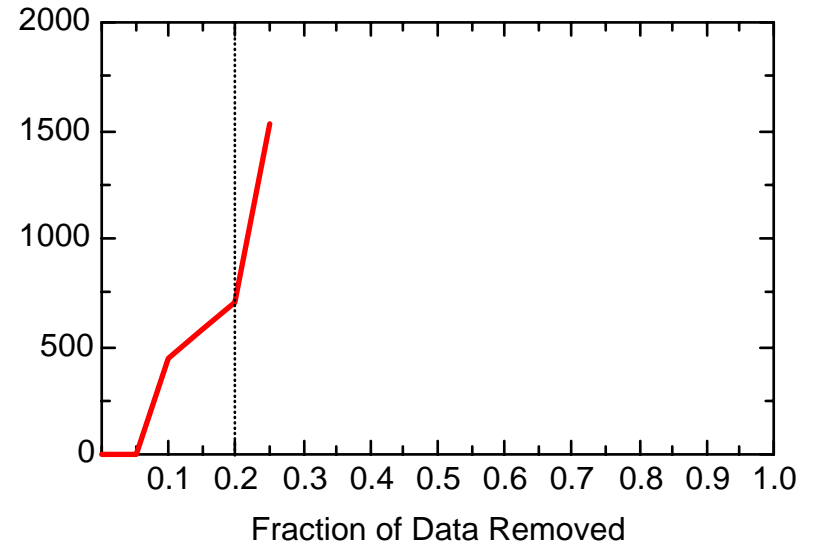
FE: Well MMW7330



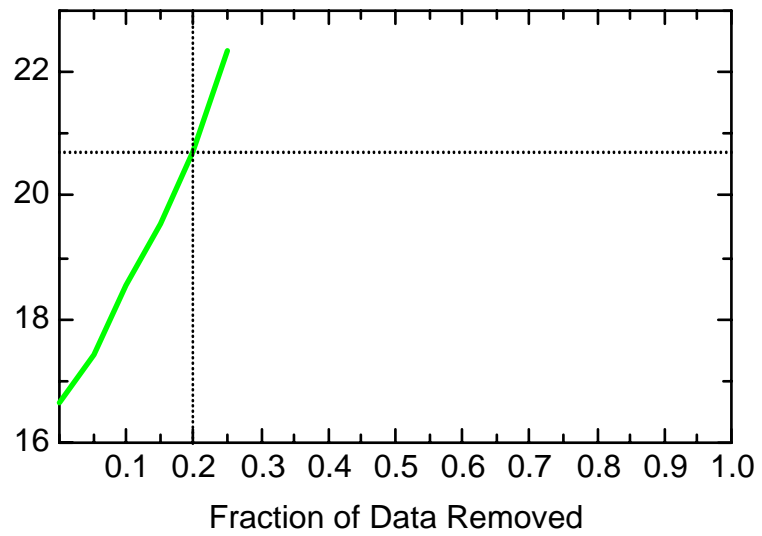
FE: Well MMW8015



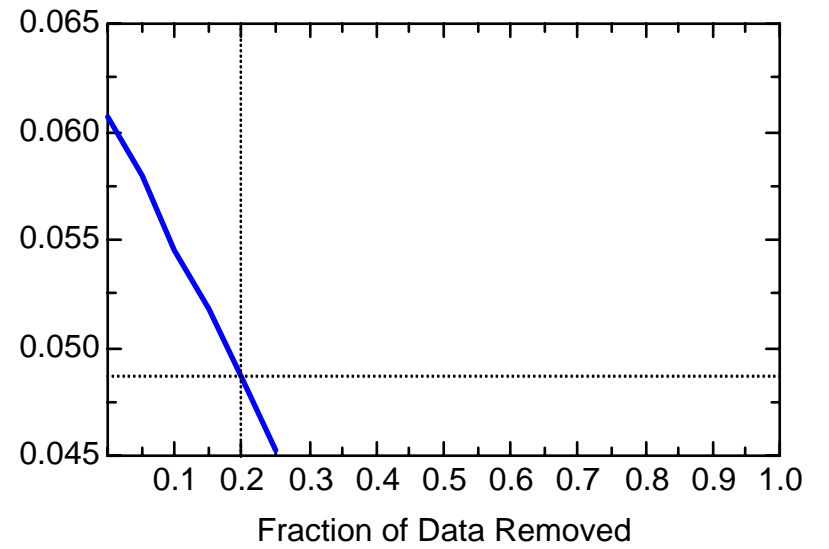
FE: Well MMW8015



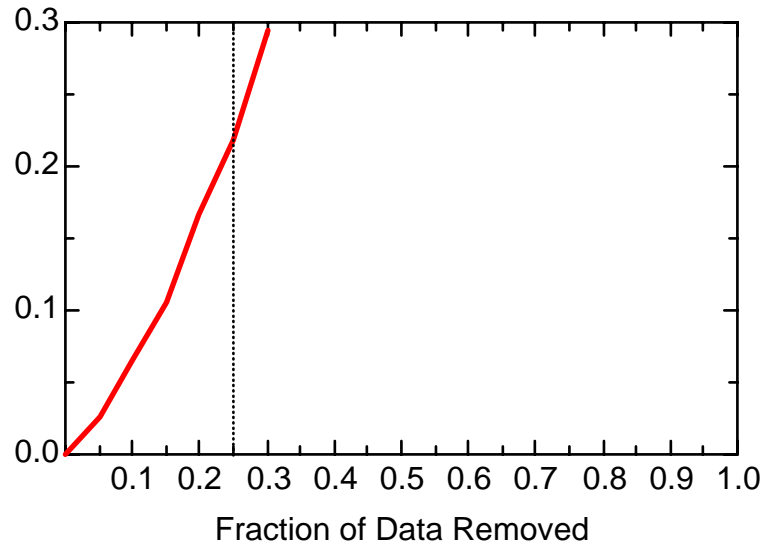
FE: Well MMW8015



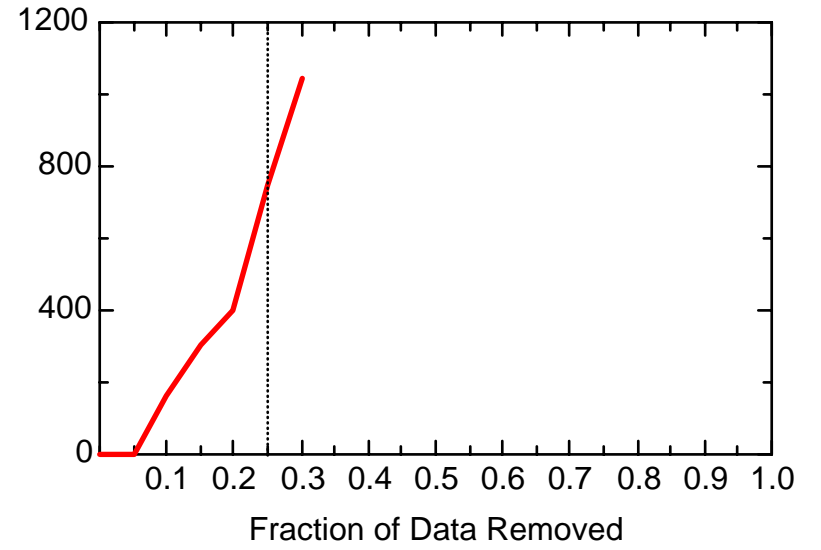
FE: Well MMW8015



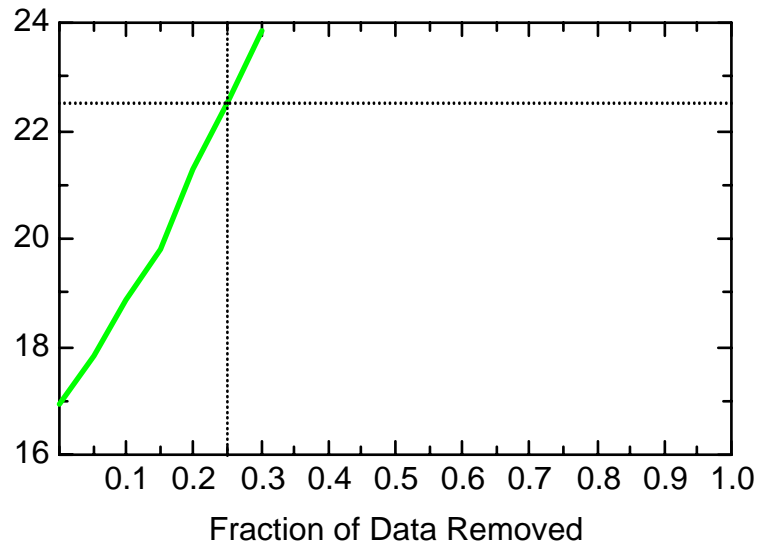
FE: Well RFW1144



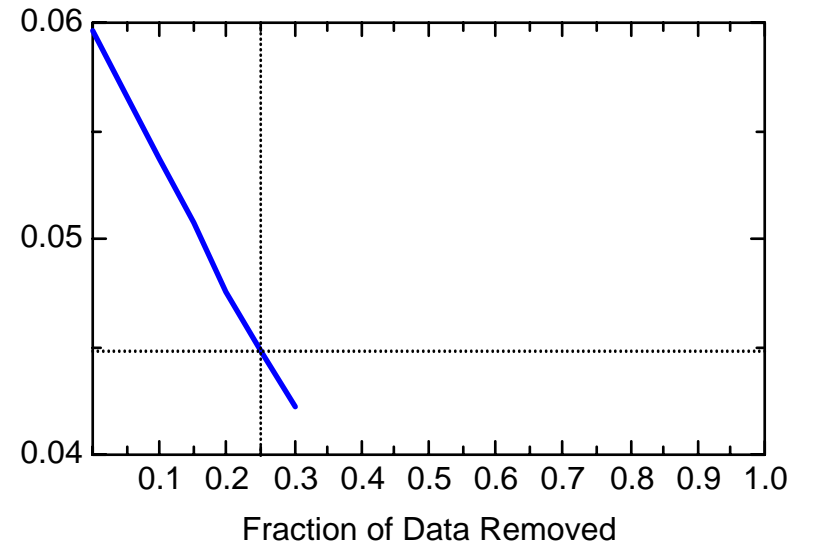
FE: Well RFW1144



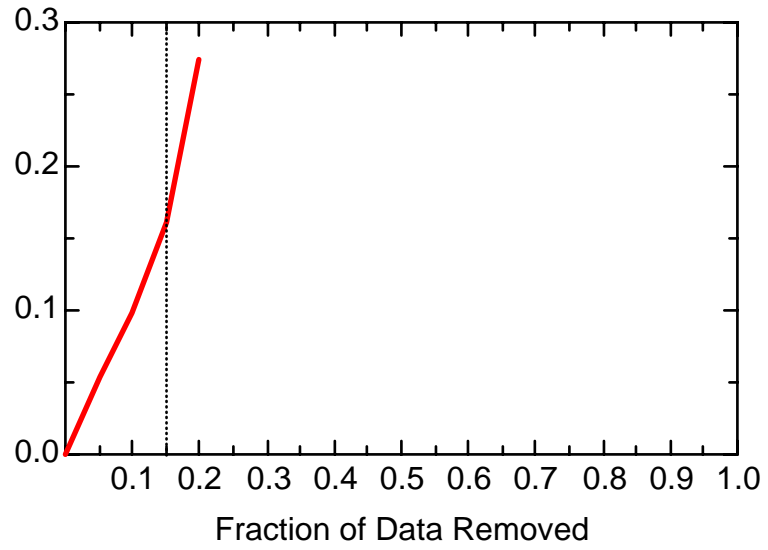
FE: Well RFW1144



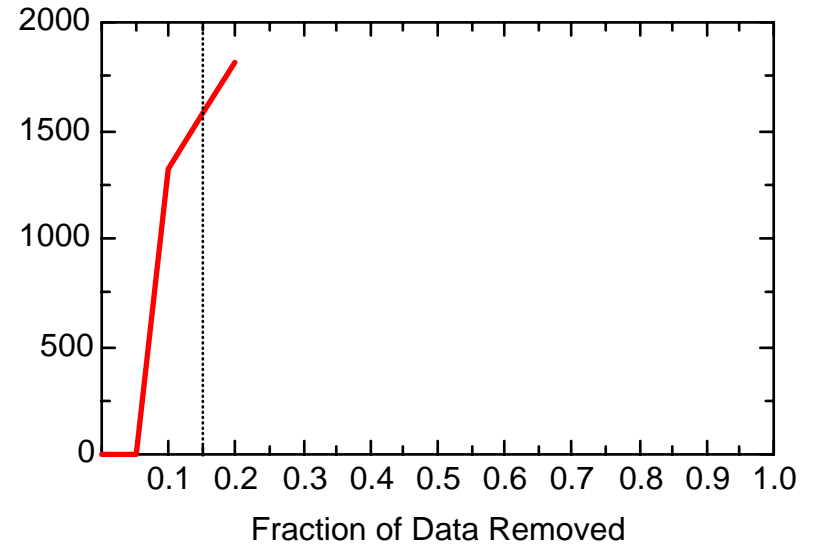
FE: Well RFW1144



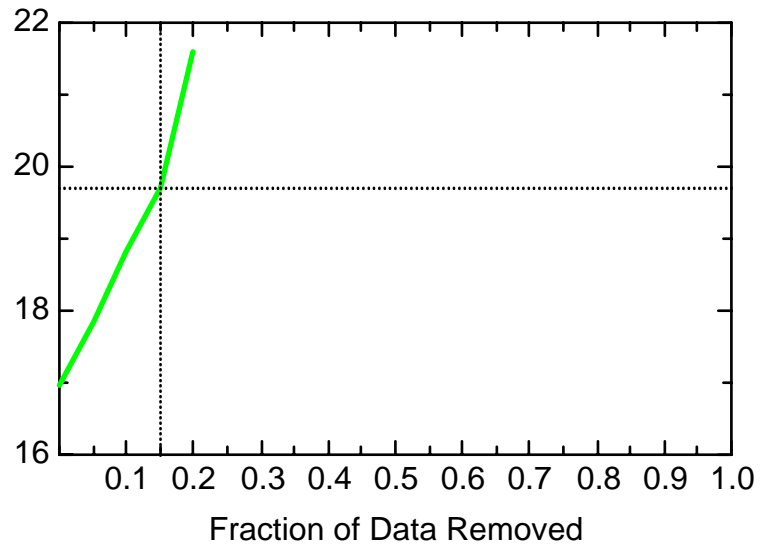
FE: Well RFW1147



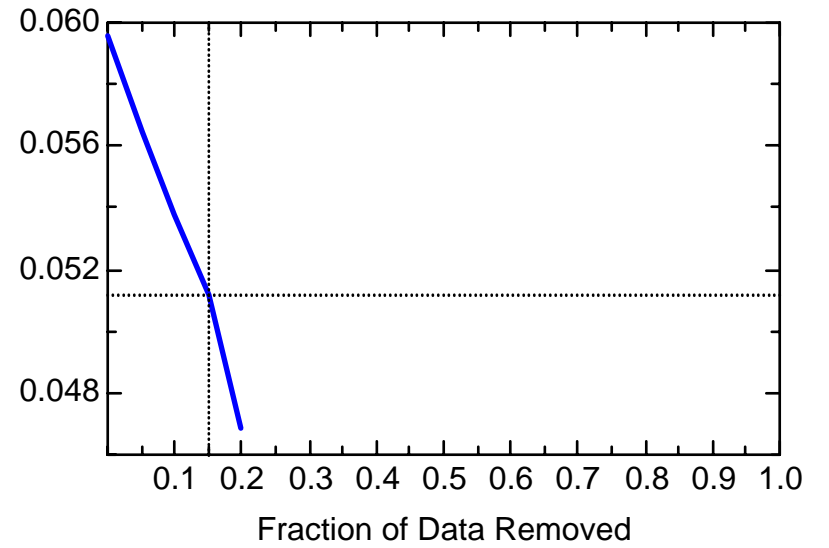
FE: Well RFW1147



FE: Well RFW1147



FE: Well RFW1147



Appendix 3-3

Temporal Optimization: MN Iterative Fitting Results

Key to acronyms:

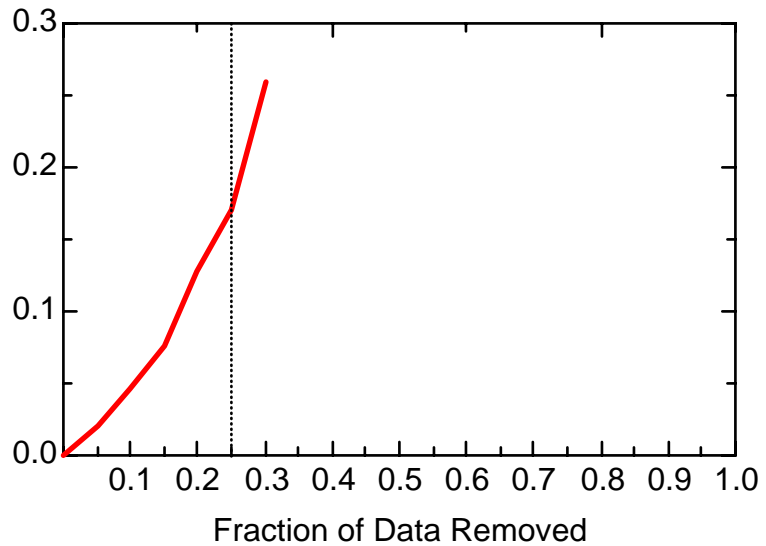
Fraction Outside Conf Bnds = Fraction of pointwise locally-weighted quadratic regression (LWQR) estimates from reduced data located beyond confidence bounds around LWQR fit on baseline data

Ave IQR of Iterative Fits = Mean interquartile range (averaged pointwise along the trend) of 500 LWQR fits computed on reduced dataset

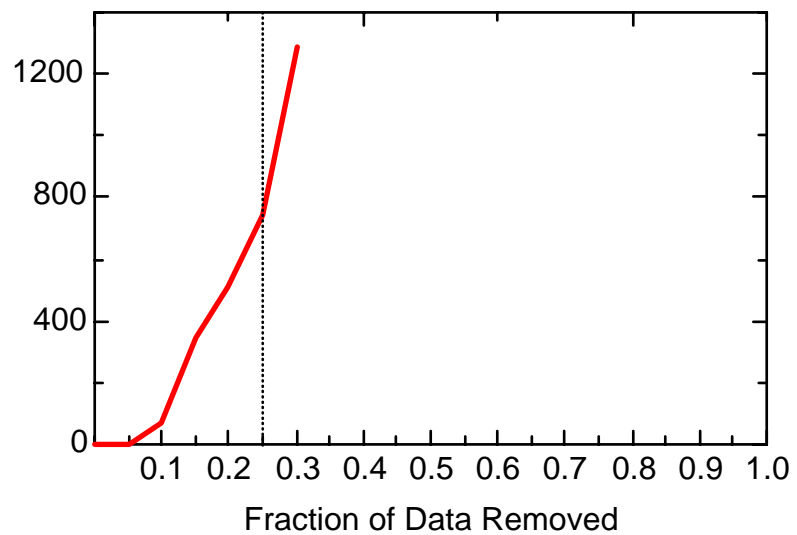
Opt Sampling Int = Optimal sampling interval, given fraction of data removed

Opt Num Samples/Week = Optimal weekly sampling frequency, given fraction of data removed

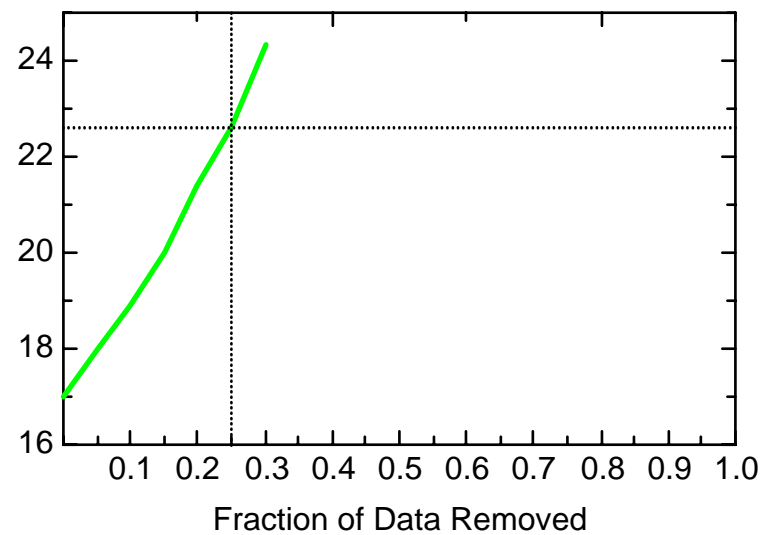
MN: Well 056MW02



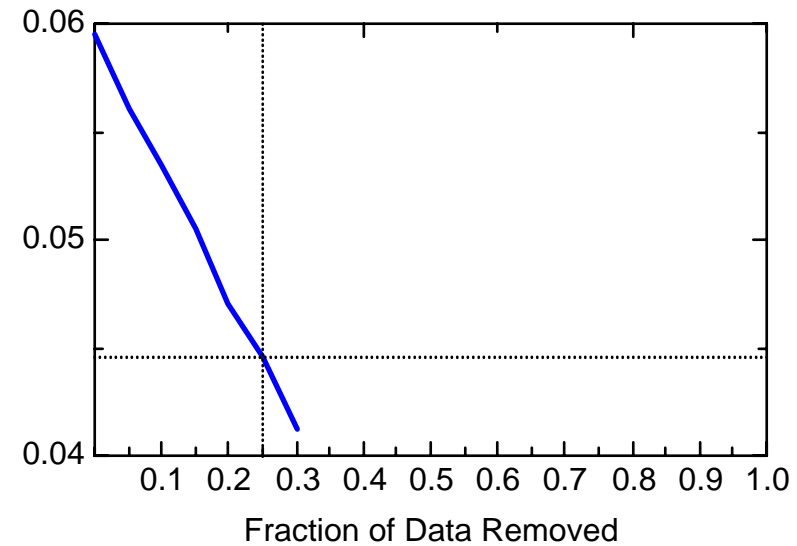
MN: Well 056MW02



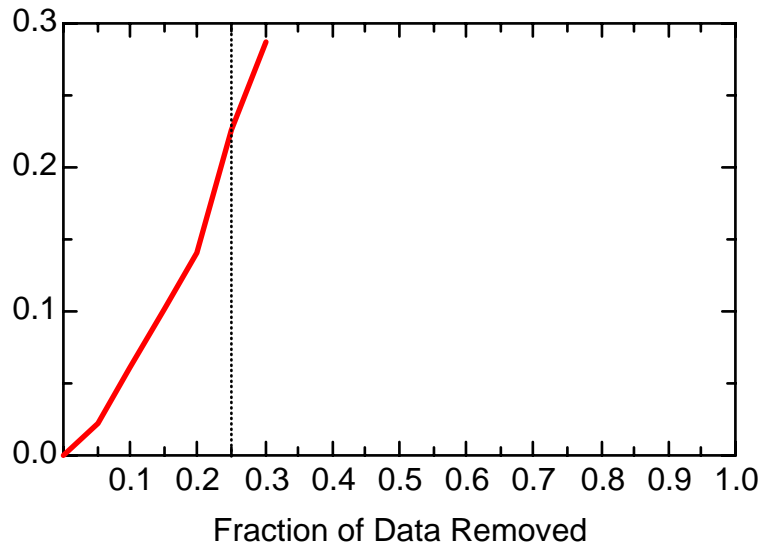
MN: Well 056MW02



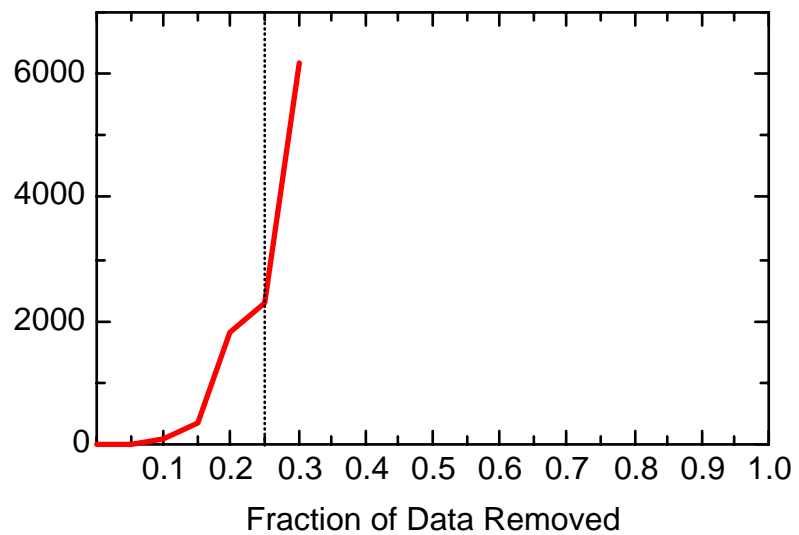
MN: Well 056MW02



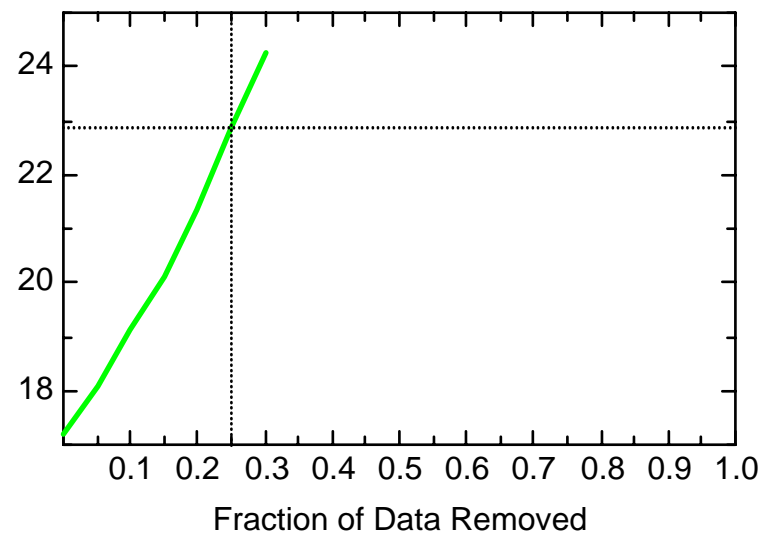
MN: Well 056MW04



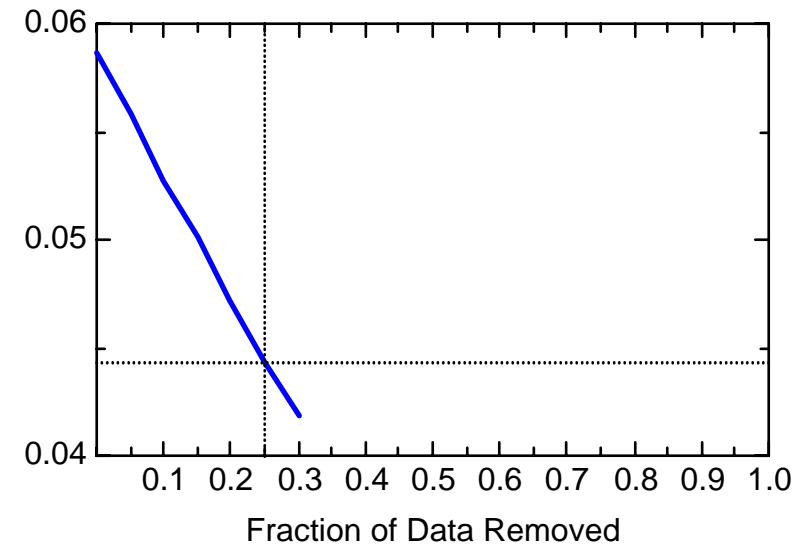
MN: Well 056MW04



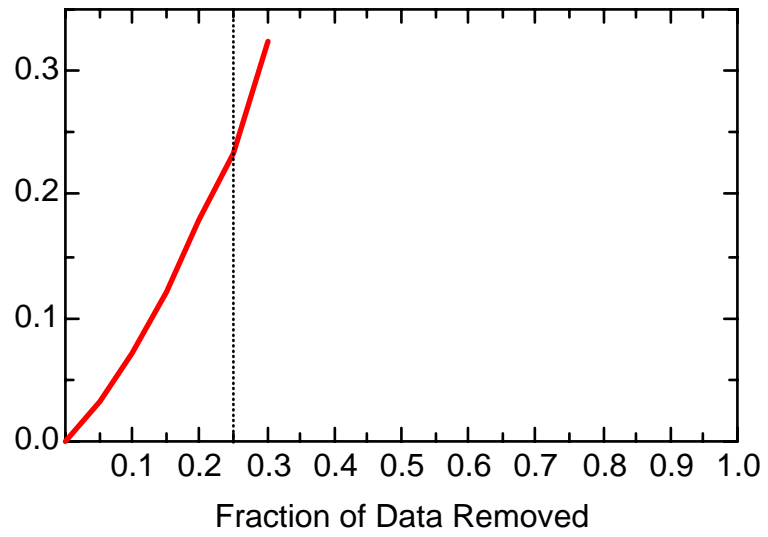
MN: Well 056MW04



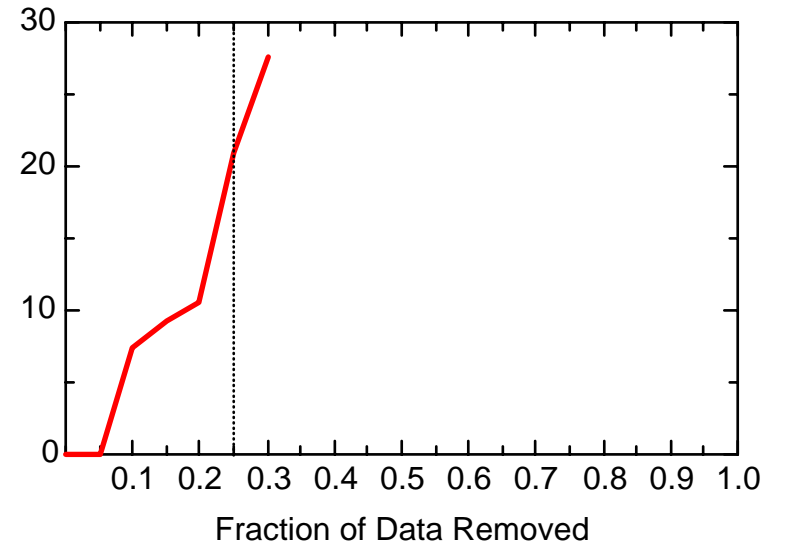
MN: Well 056MW04



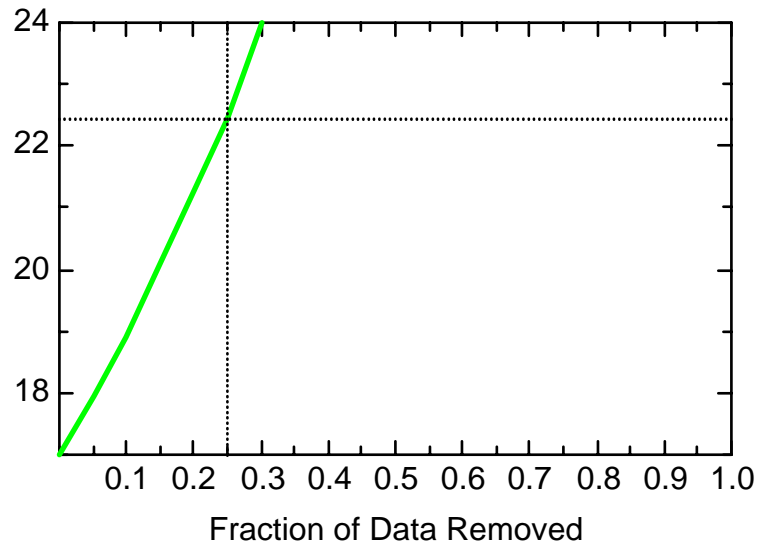
MN: Well AR25



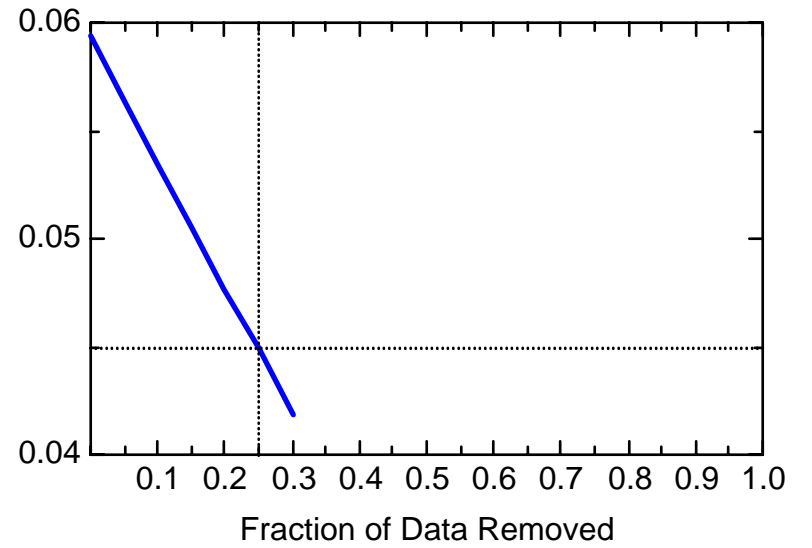
MN: Well AR25



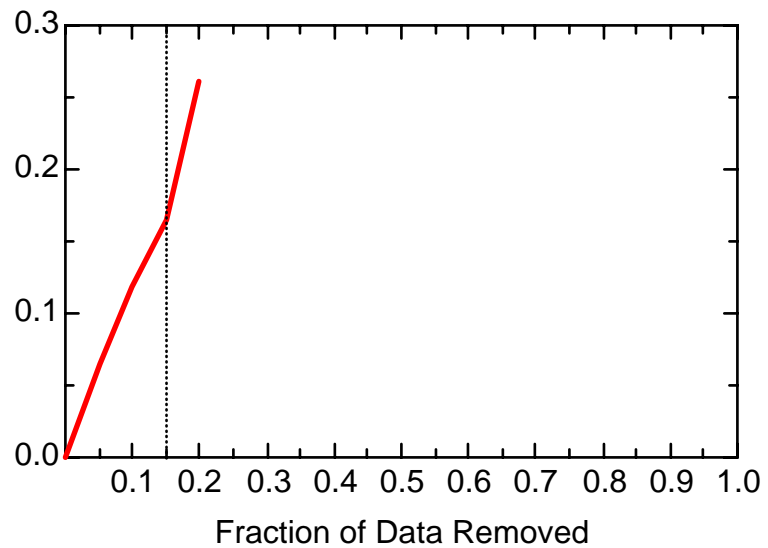
MN: Well AR25



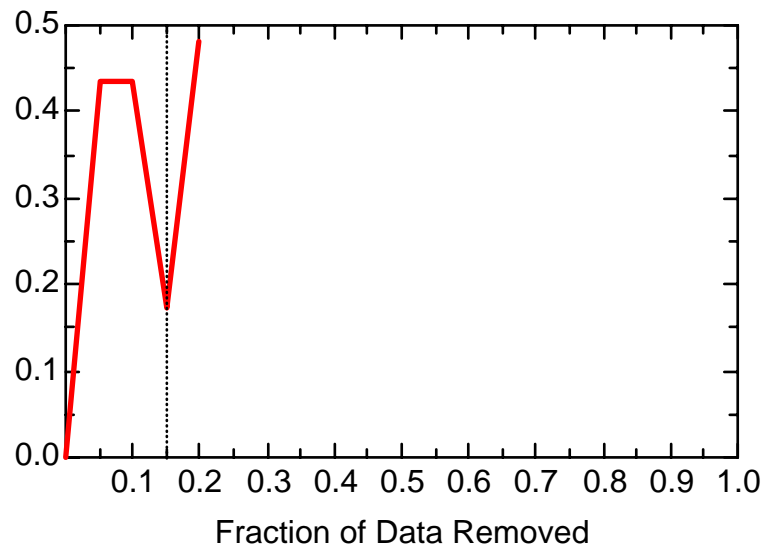
MN: Well AR25



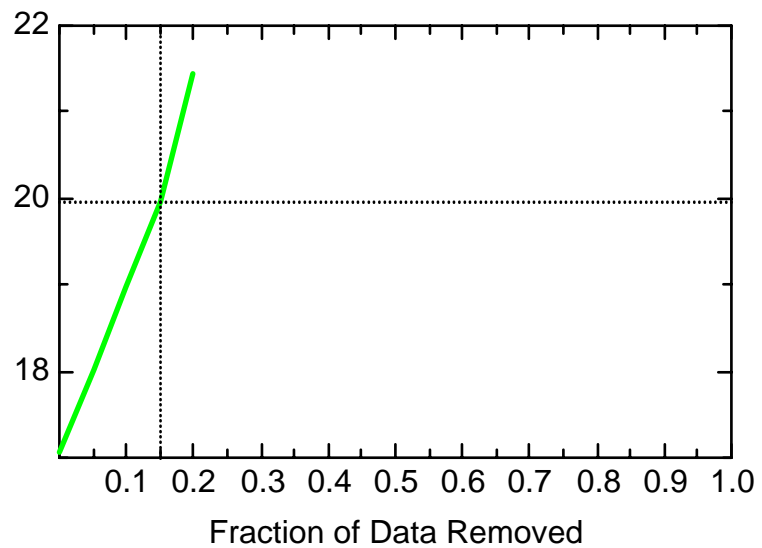
MN: Well FMW3413



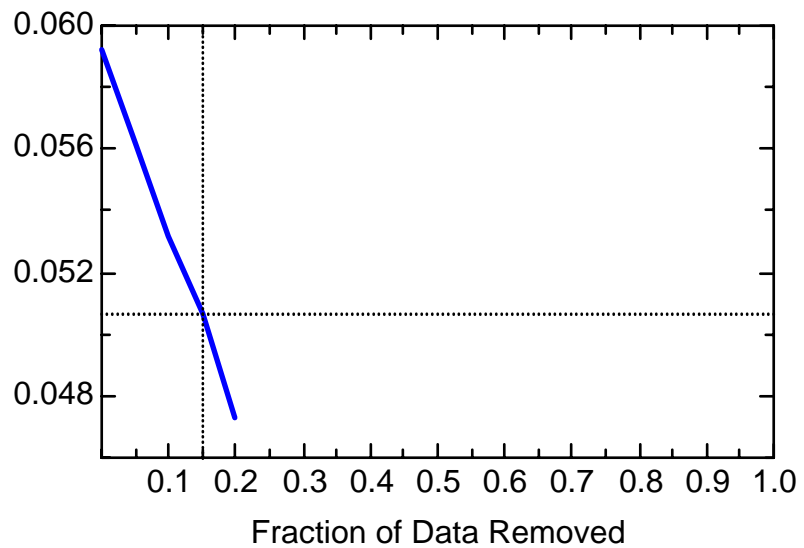
MN: Well FMW3413



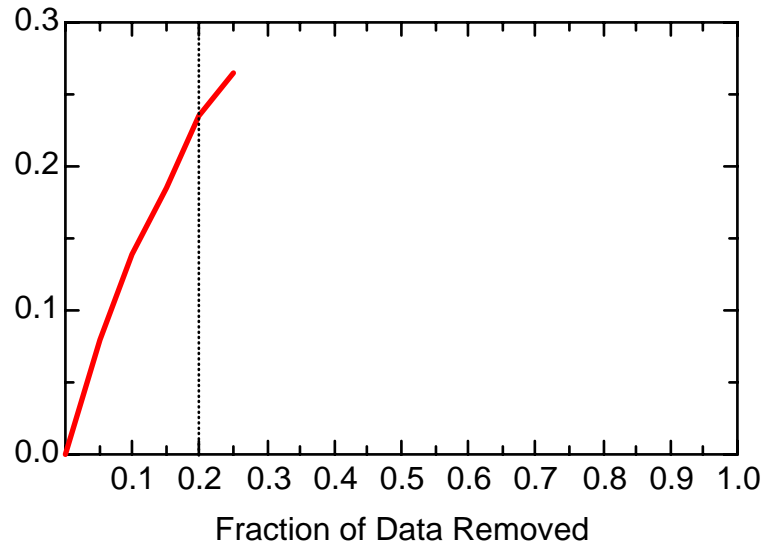
MN: Well FMW3413



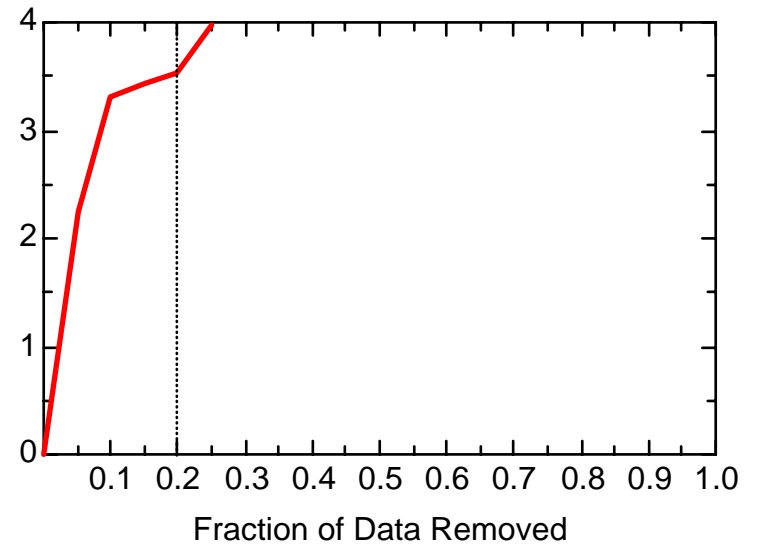
MN: Well FMW3413



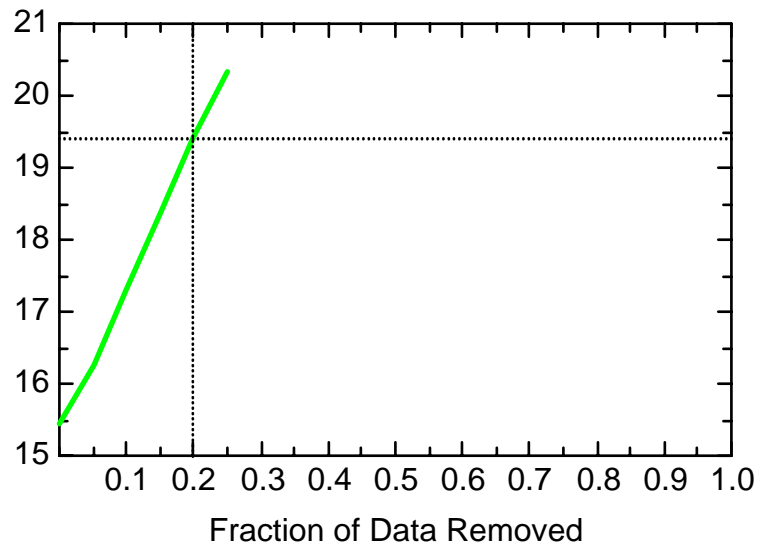
MN: Well JBW7101



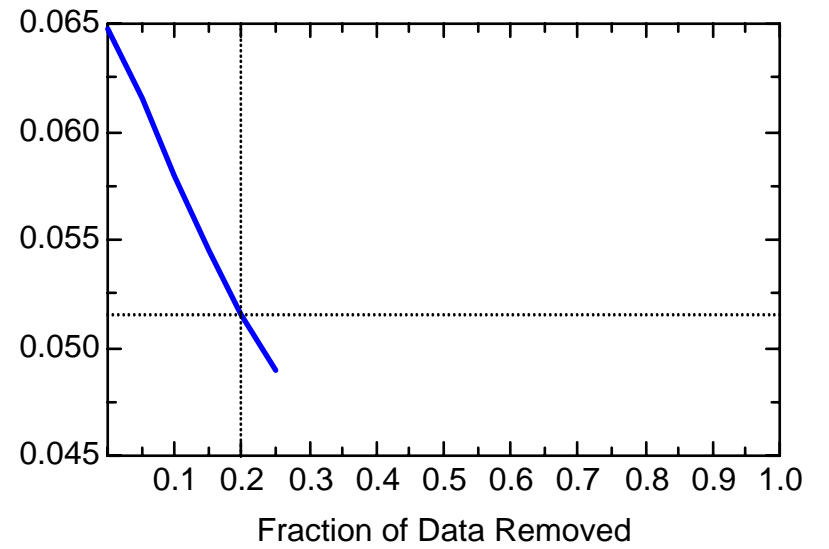
MN: Well JBW7101



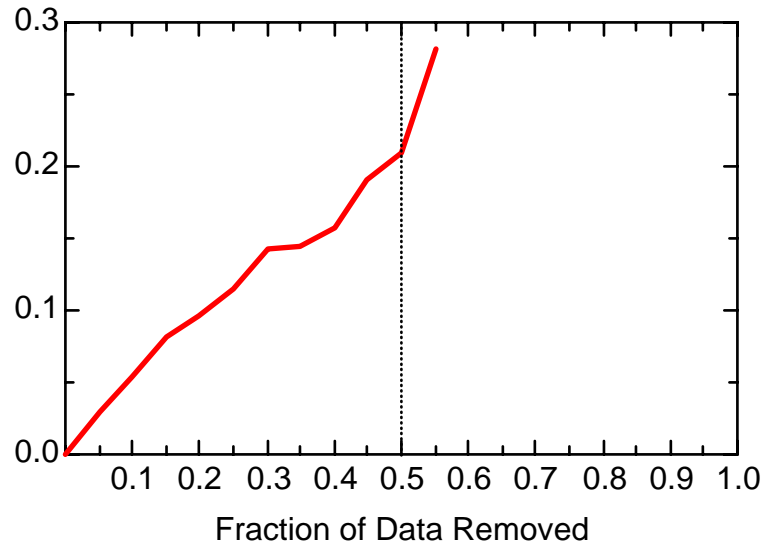
MN: Well JBW7101



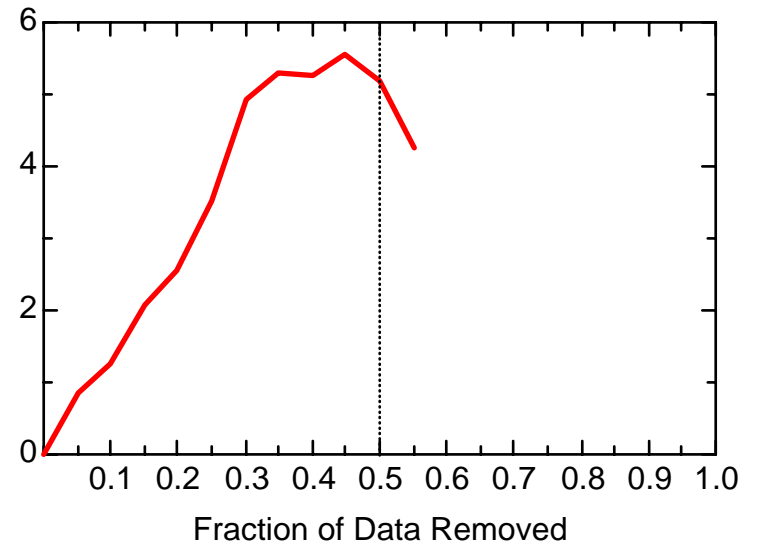
MN: Well JBW7101



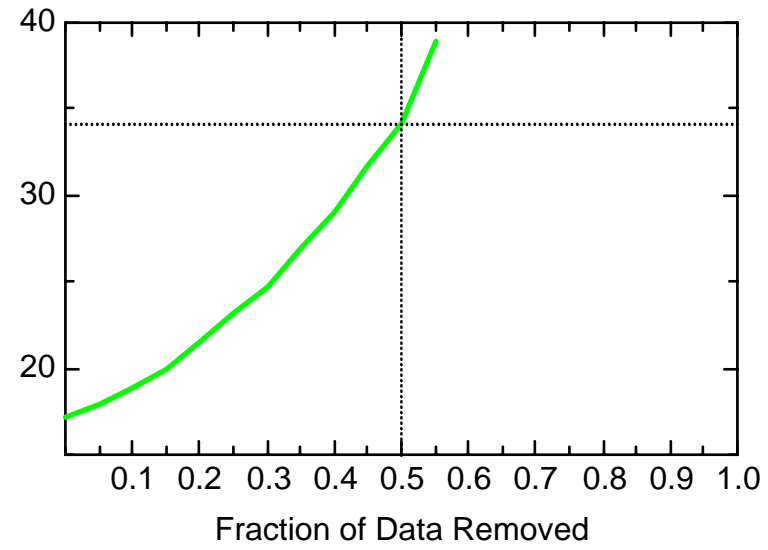
MN: Well JBW7102



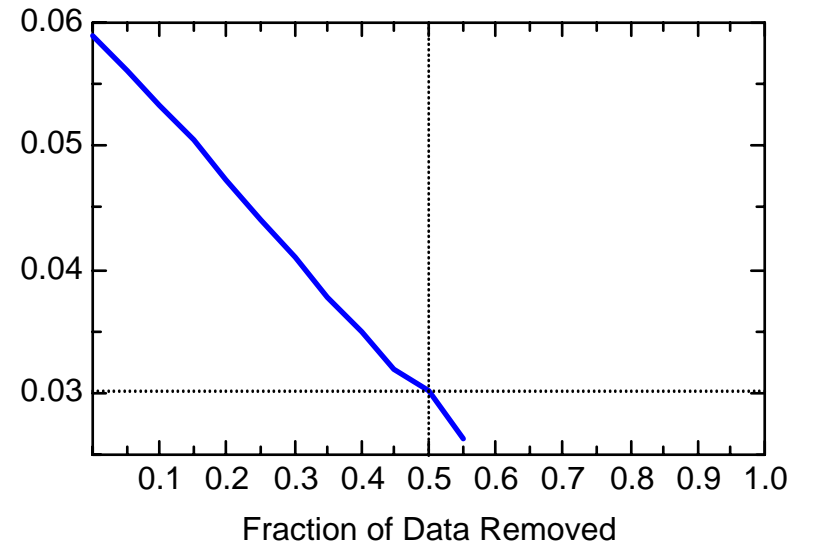
MN: Well JBW7102



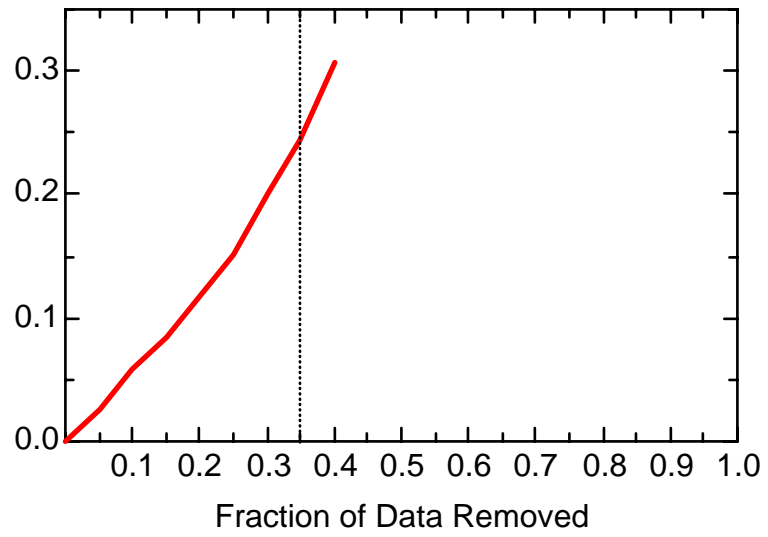
MN: Well JBW7102



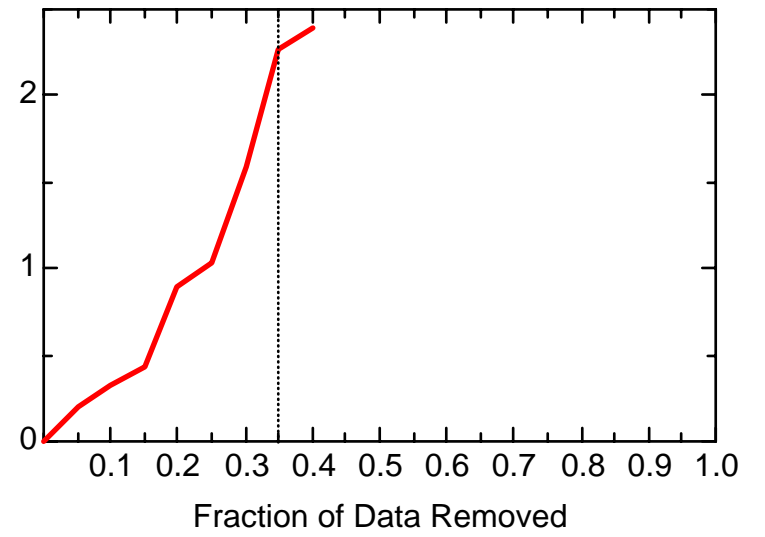
MN: Well JBW7102



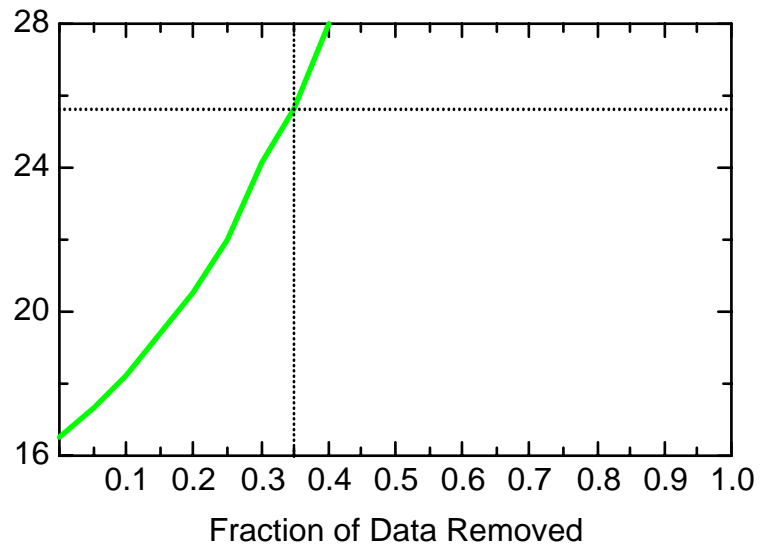
MN: Well JBW7106A



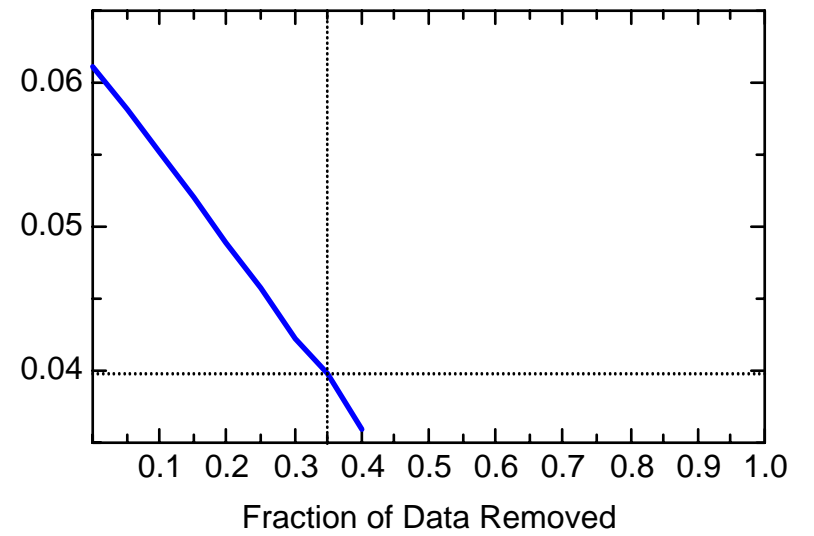
MN: Well JBW7106A



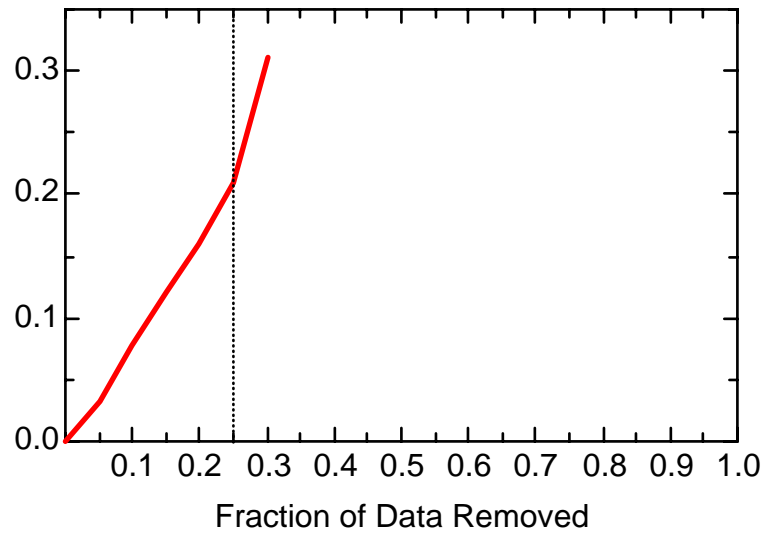
MN: Well JBW7106A



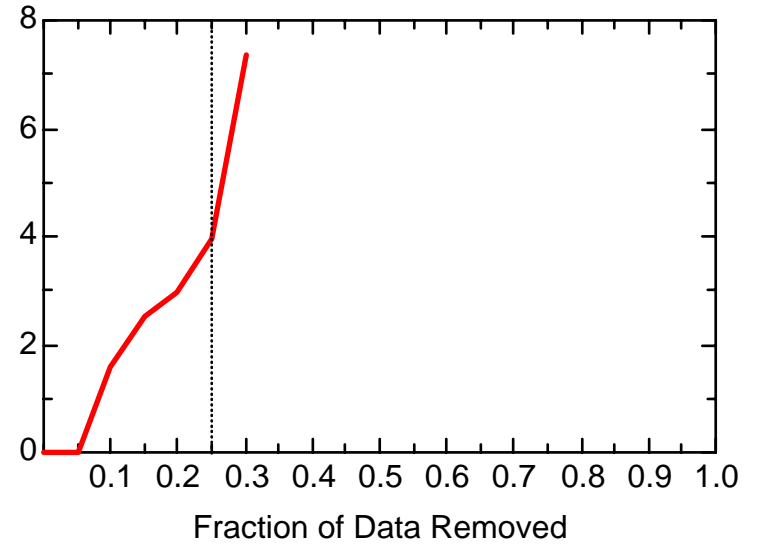
MN: Well JBW7106A



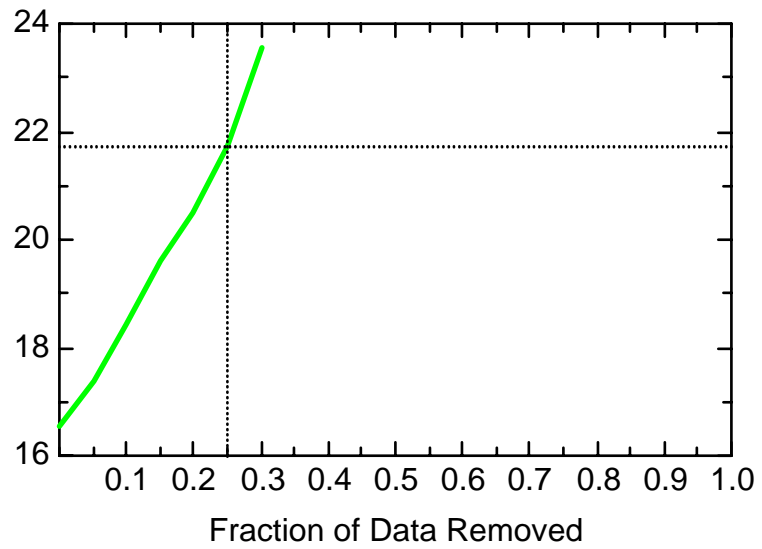
MN: Well JBW7106B



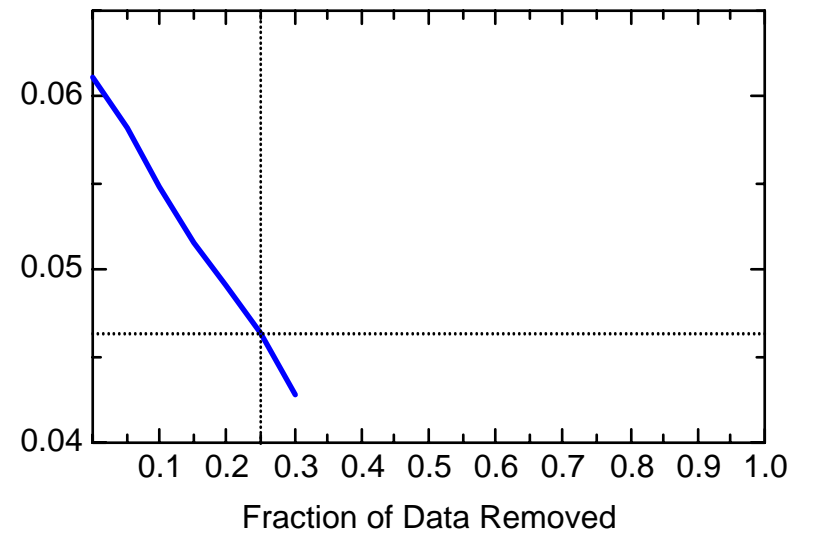
MN: Well JBW7106B



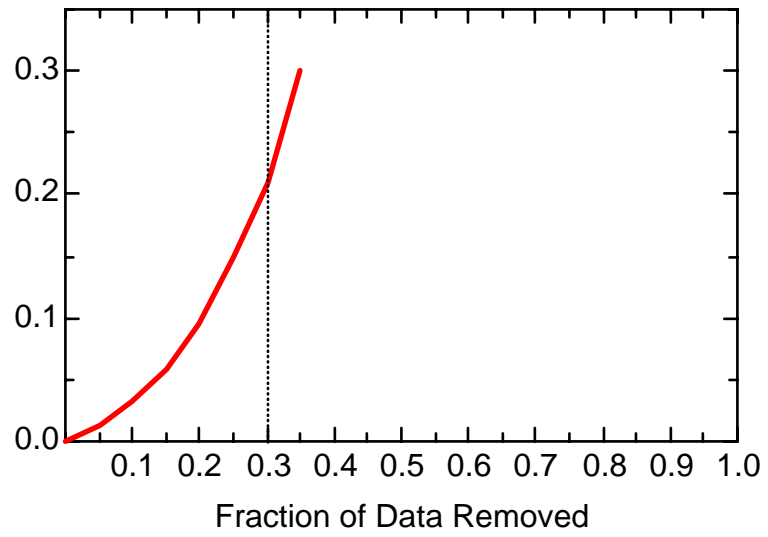
MN: Well JBW7106B



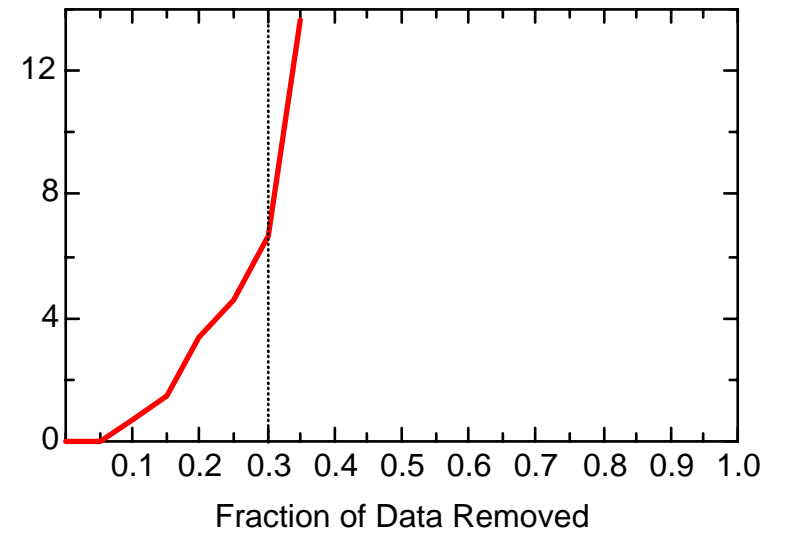
MN: Well JBW7106B



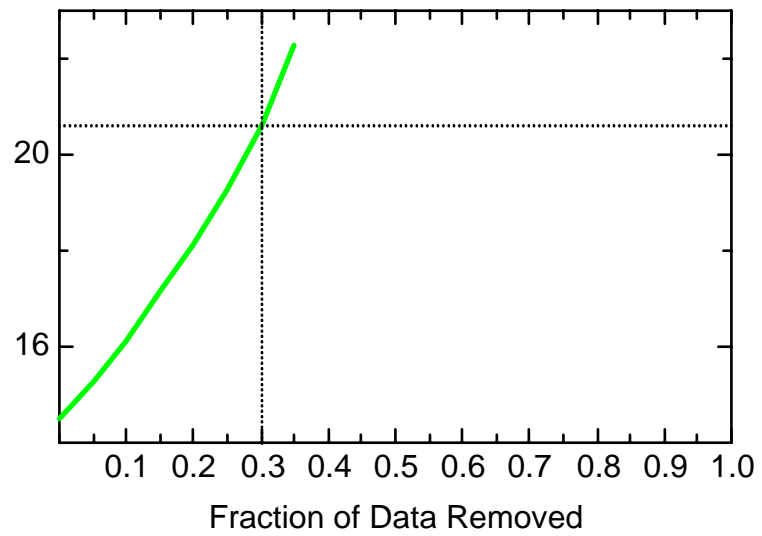
MN: Well JBW7203A



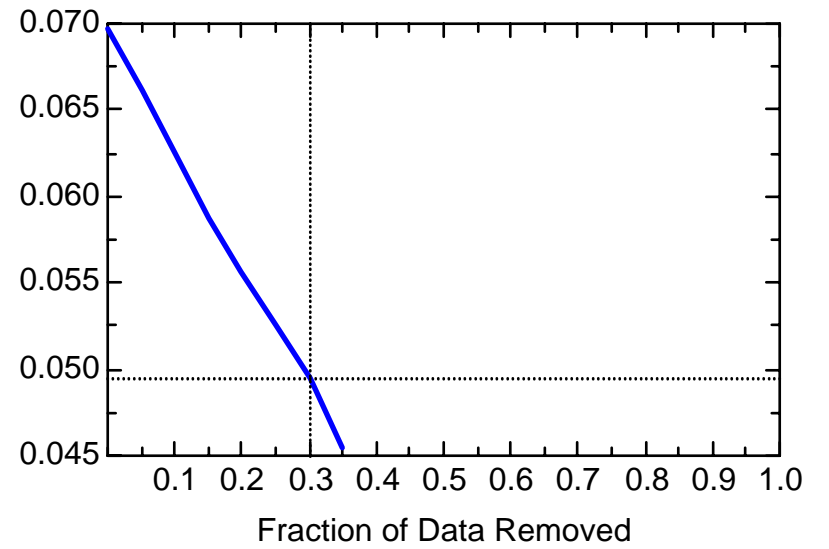
MN: Well JBW7203A



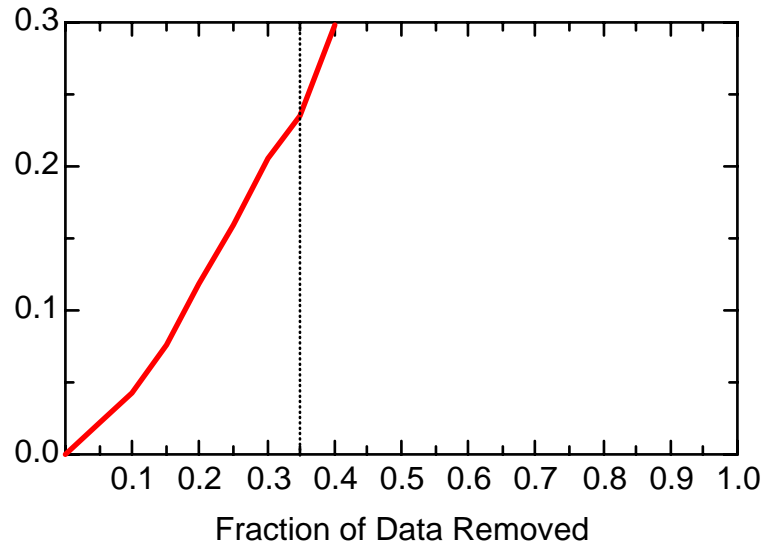
MN: Well JBW7203A



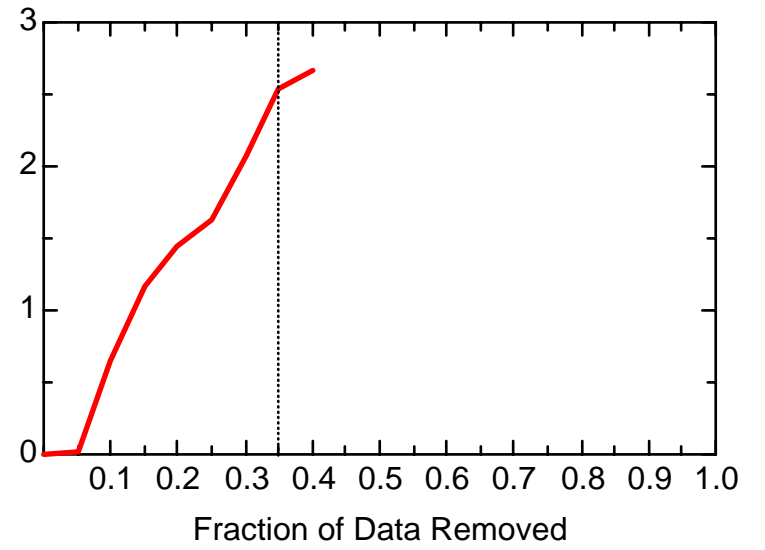
MN: Well JBW7203A



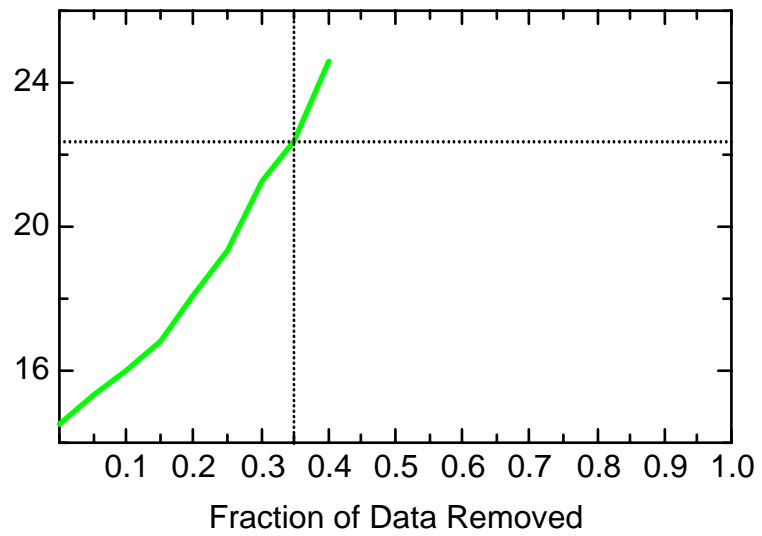
MN: Well JBW7203B



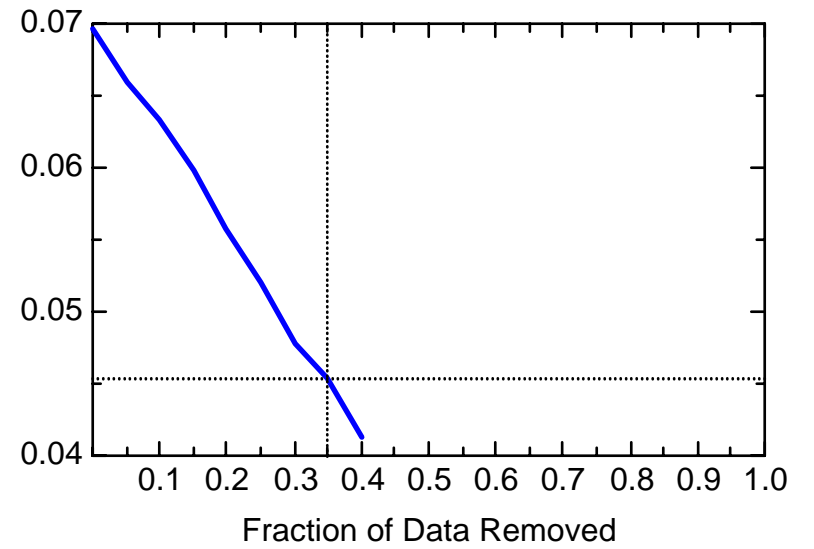
MN: Well JBW7203B



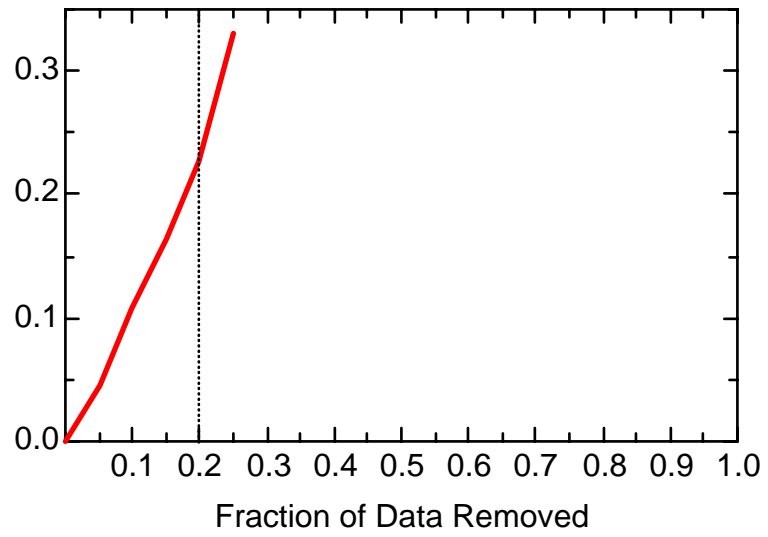
MN: Well JBW7203B



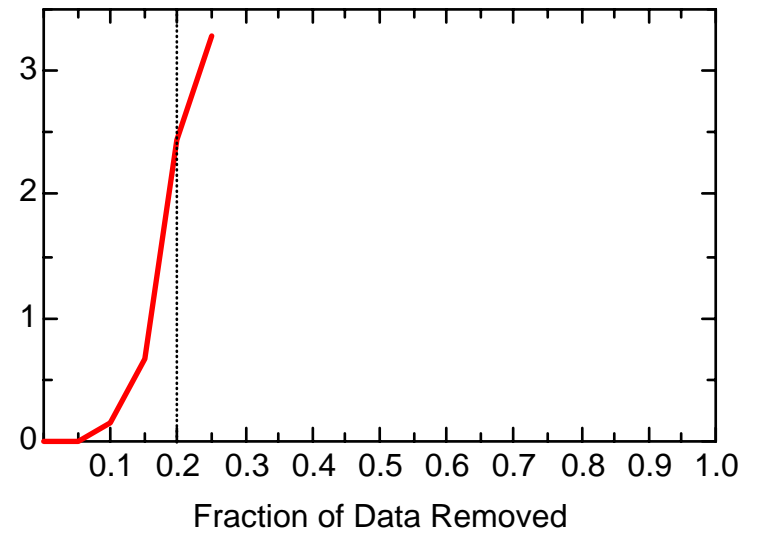
MN: Well JBW7203B



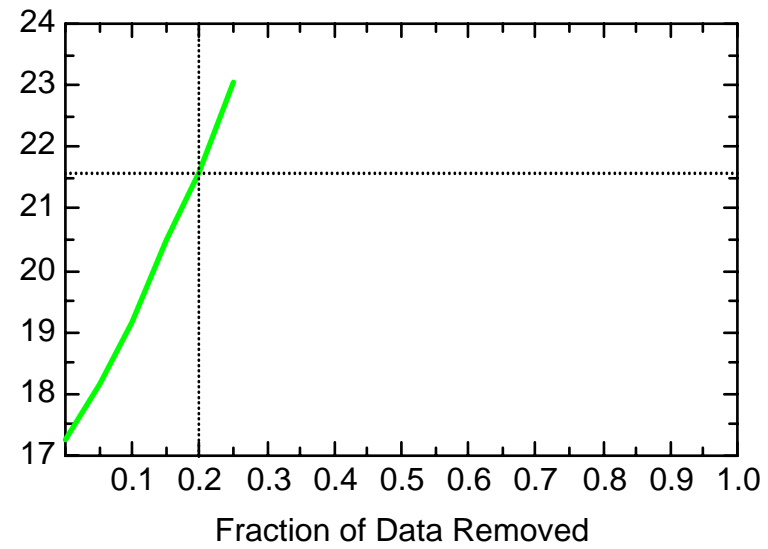
MN: Well JBW7204A



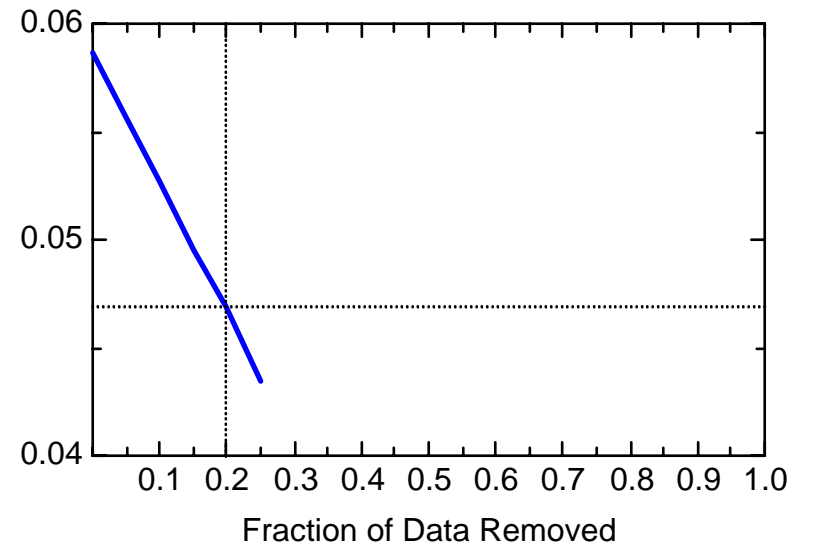
MN: Well JBW7204A



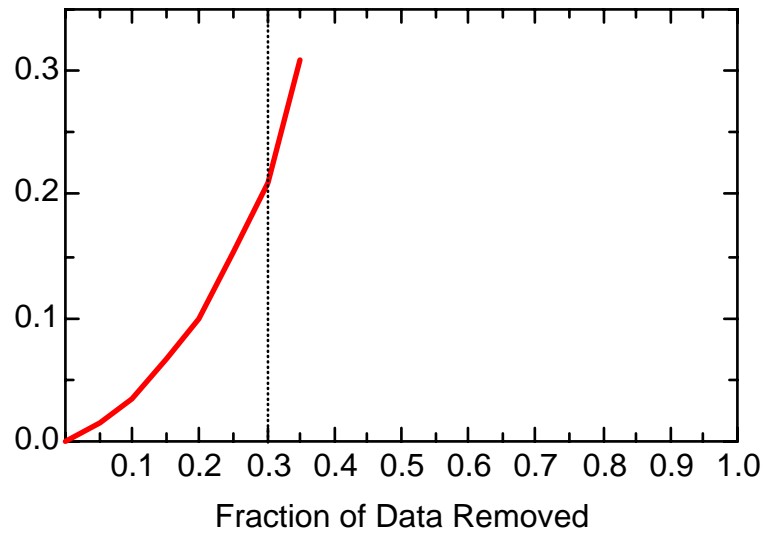
MN: Well JBW7204A



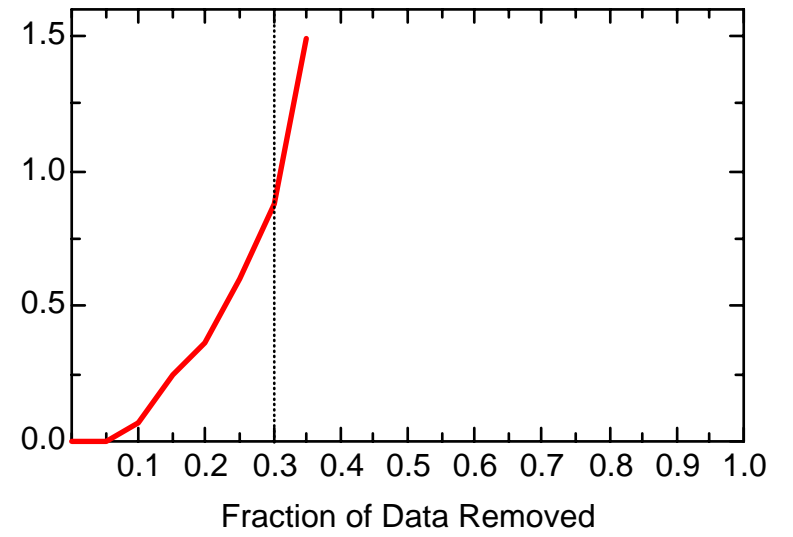
MN: Well JBW7204A



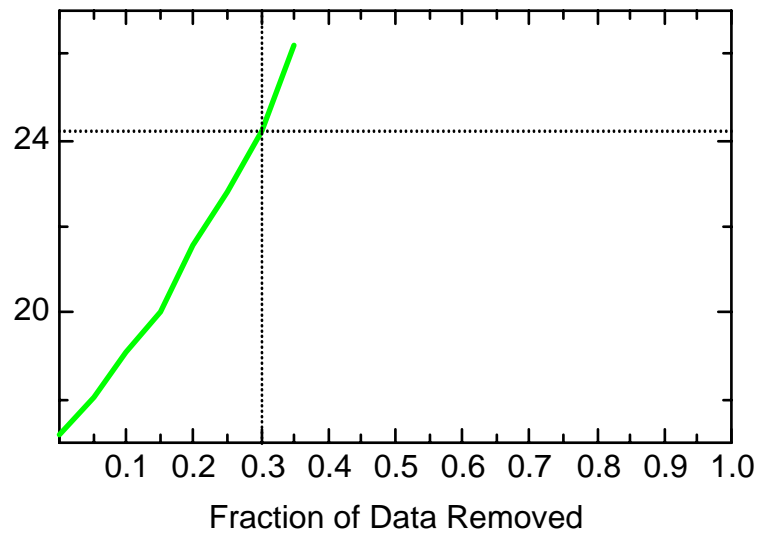
MN: Well JBW7212A



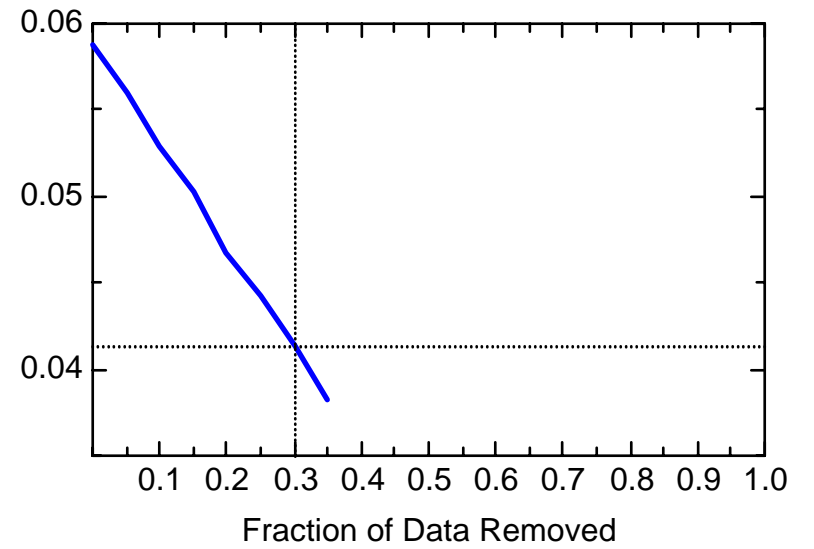
MN: Well JBW7212A



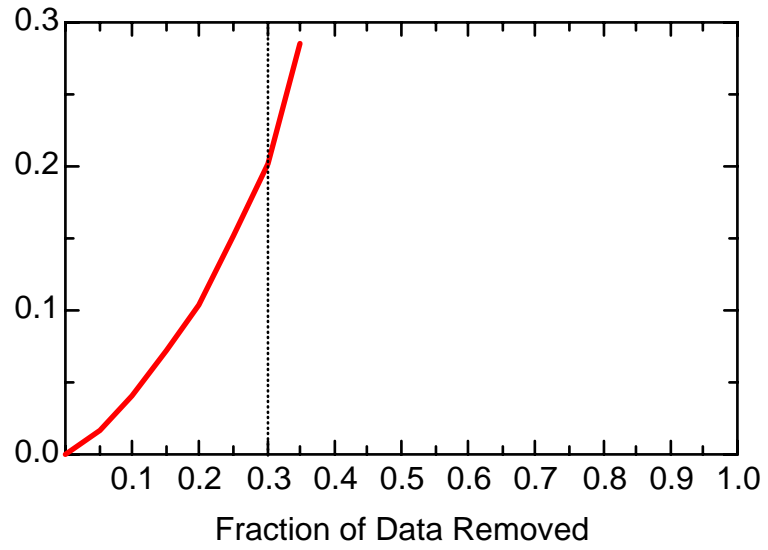
MN: Well JBW7212A



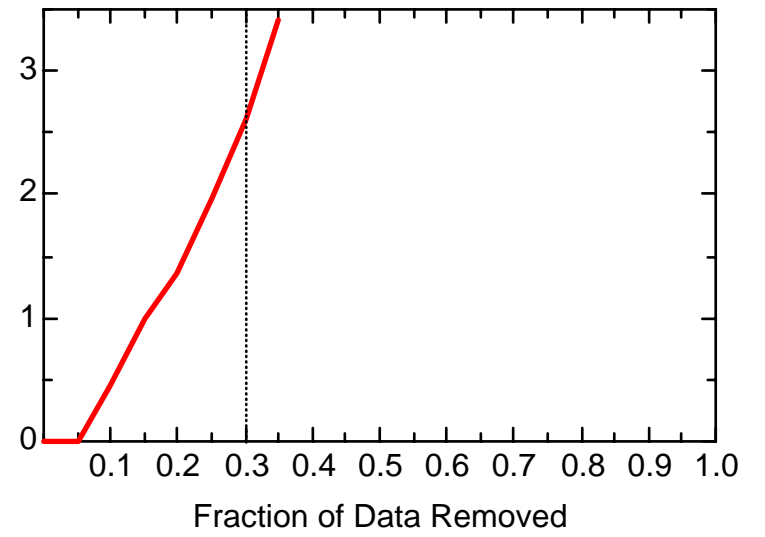
MN: Well JBW7212A



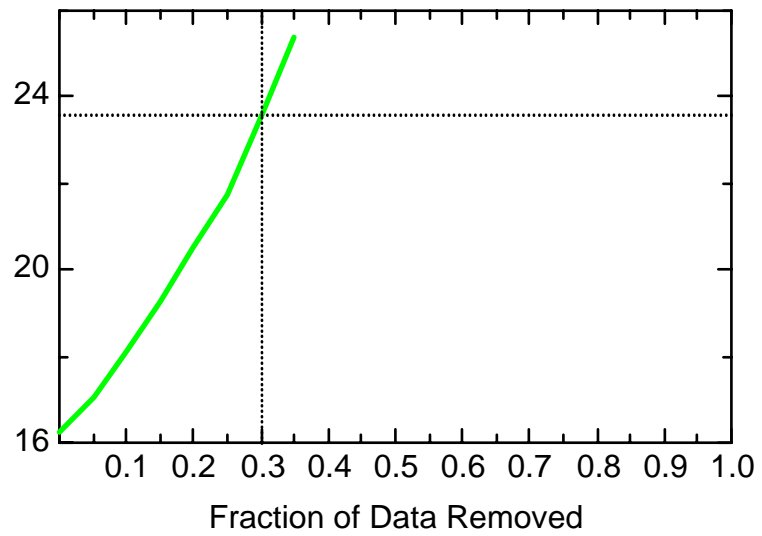
MN: Well JBW7212B



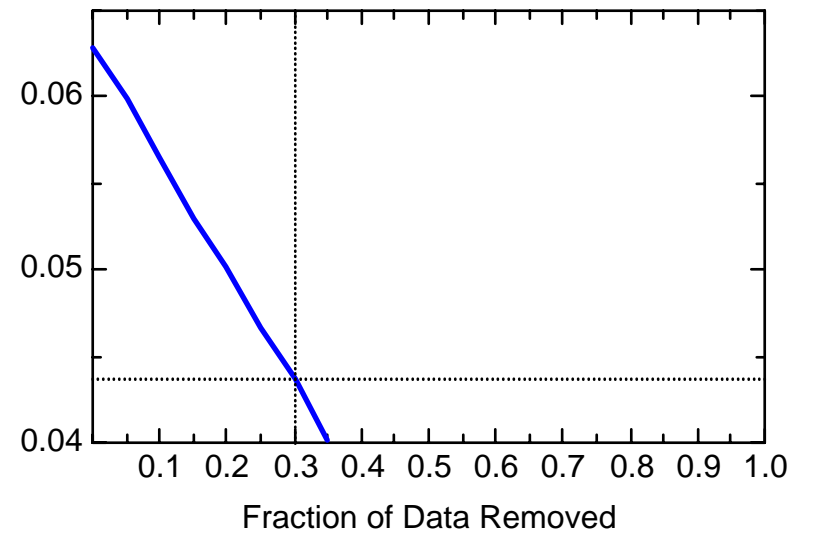
MN: Well JBW7212B



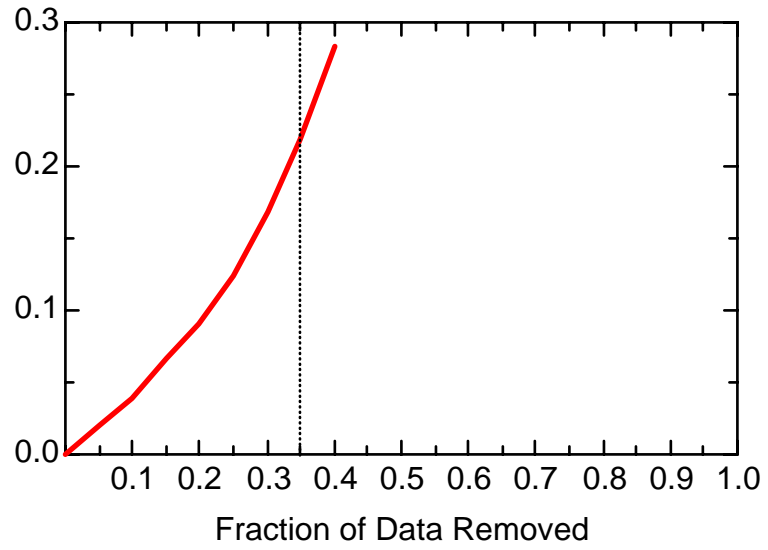
MN: Well JBW7212B



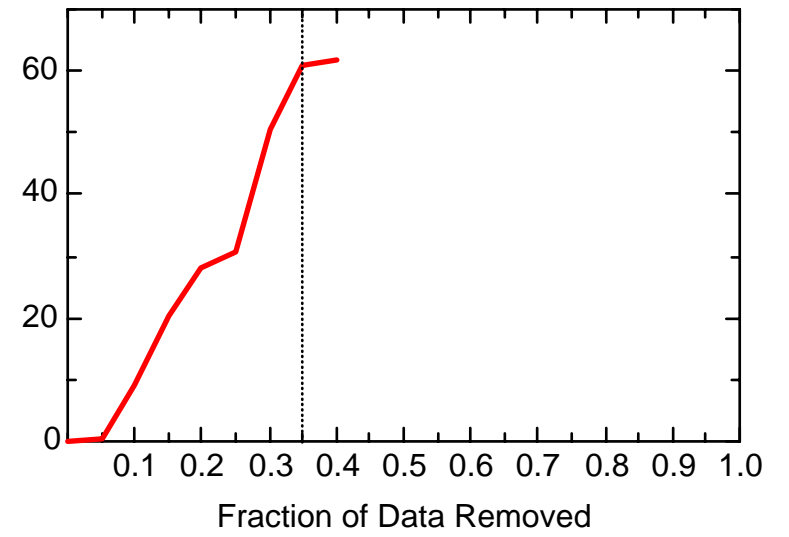
MN: Well JBW7212B



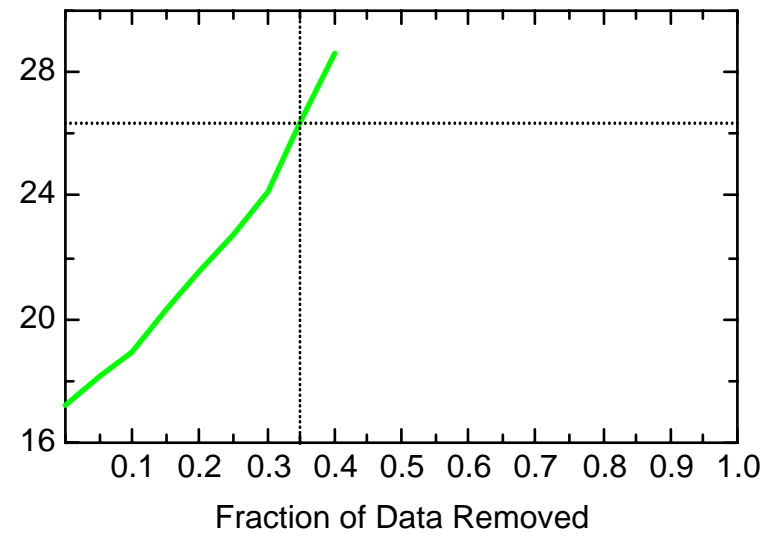
MN: Well JBW7213A



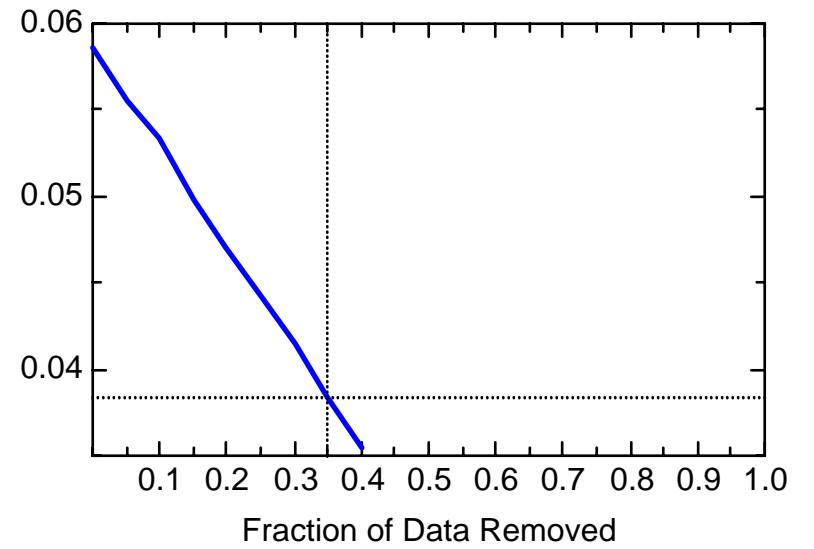
MN: Well JBW7213A



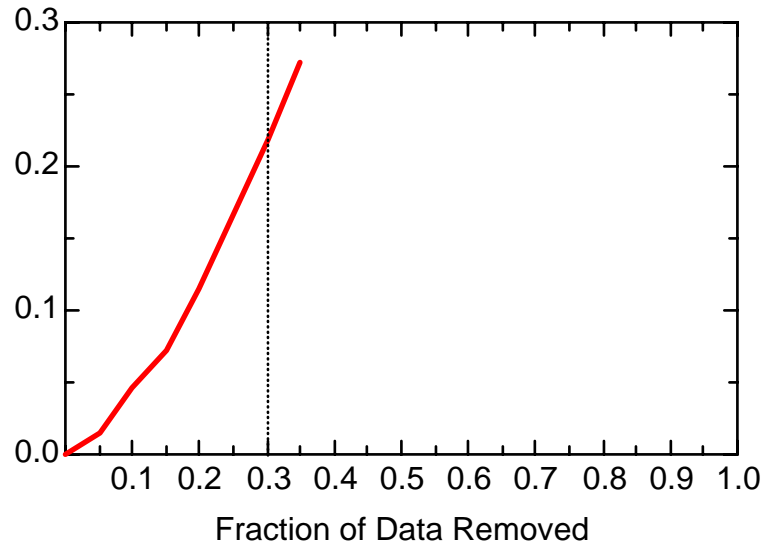
MN: Well JBW7213A



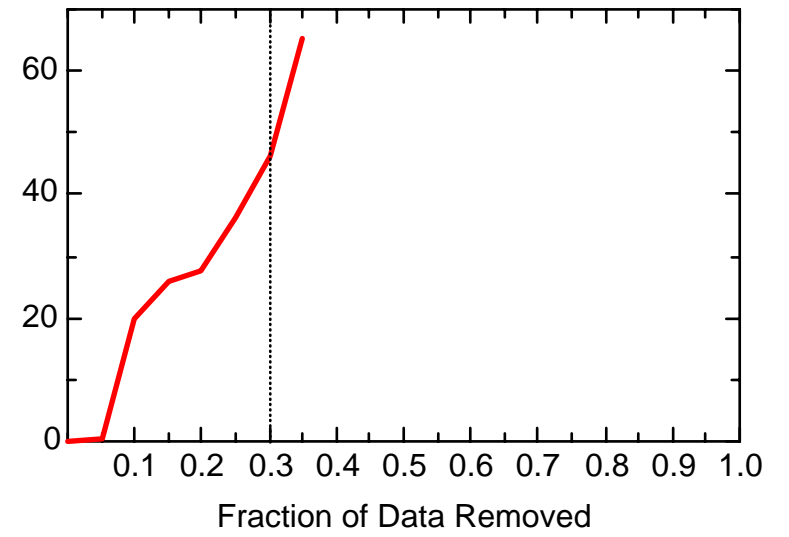
MN: Well JBW7213A



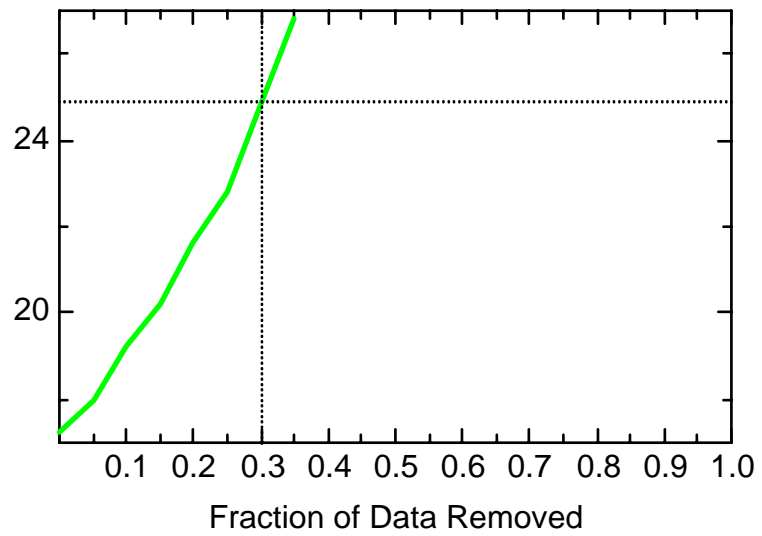
MN: Well JBW7213B



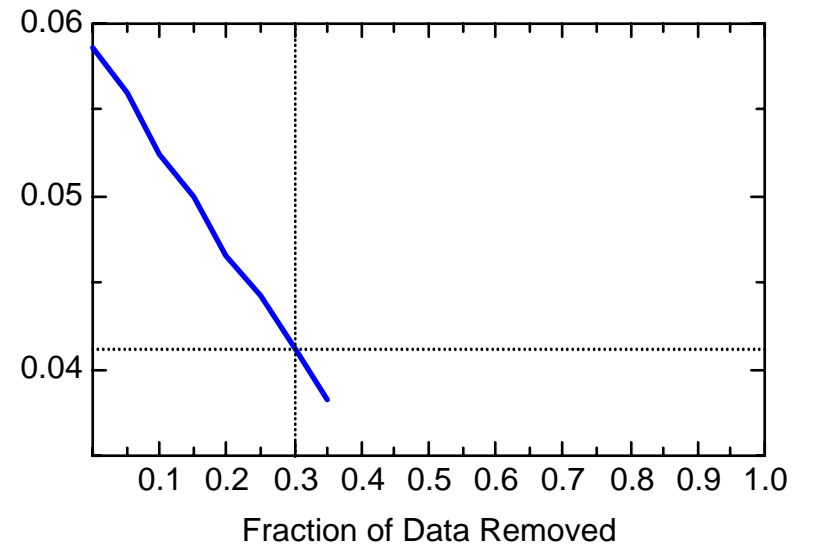
MN: Well JBW7213B



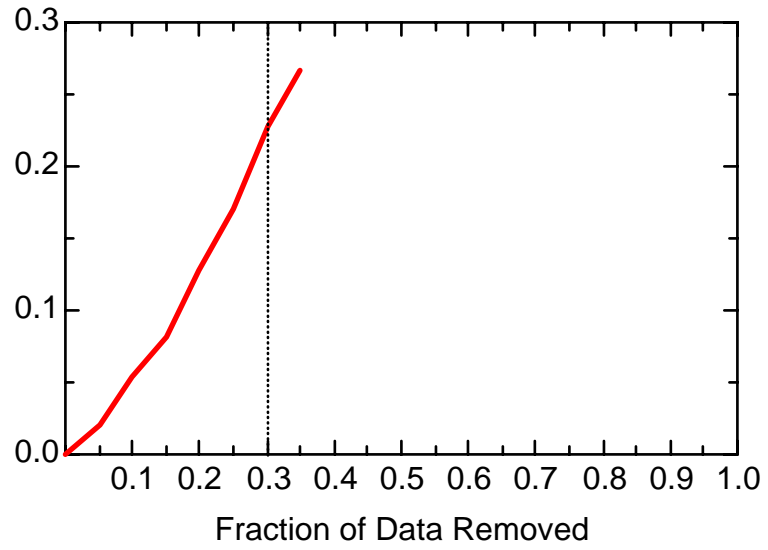
MN: Well JBW7213B



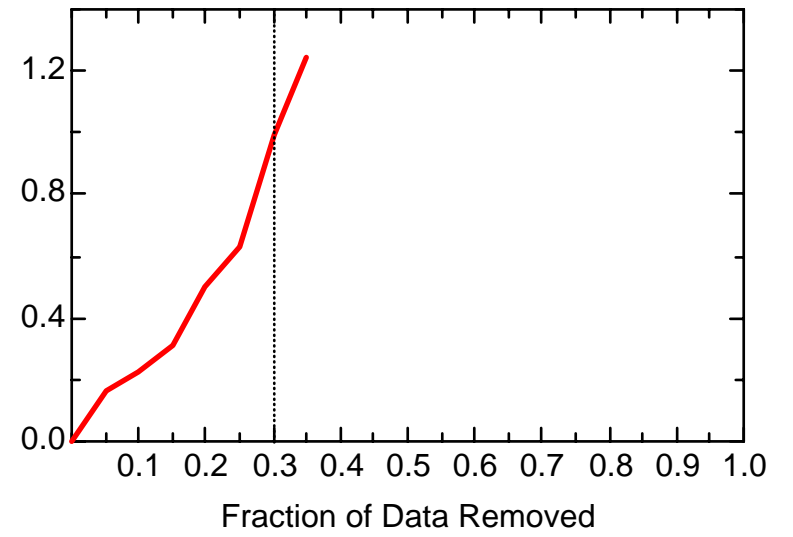
MN: Well JBW7213B



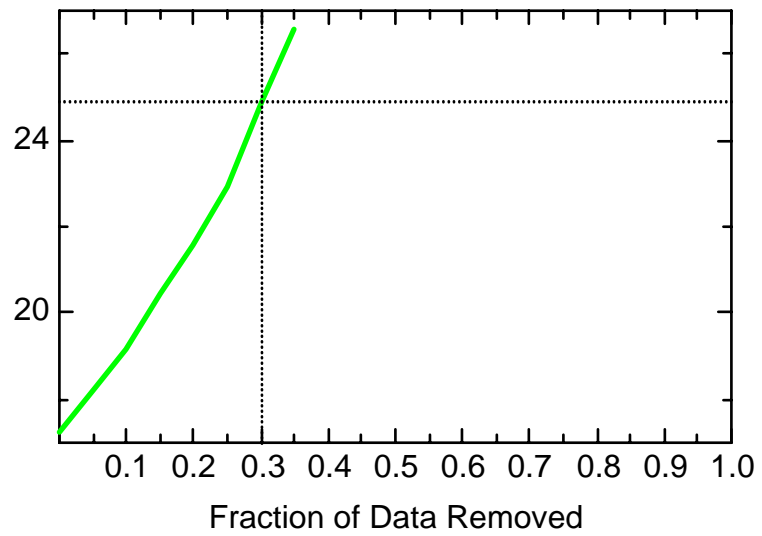
MN: Well JBW7215B



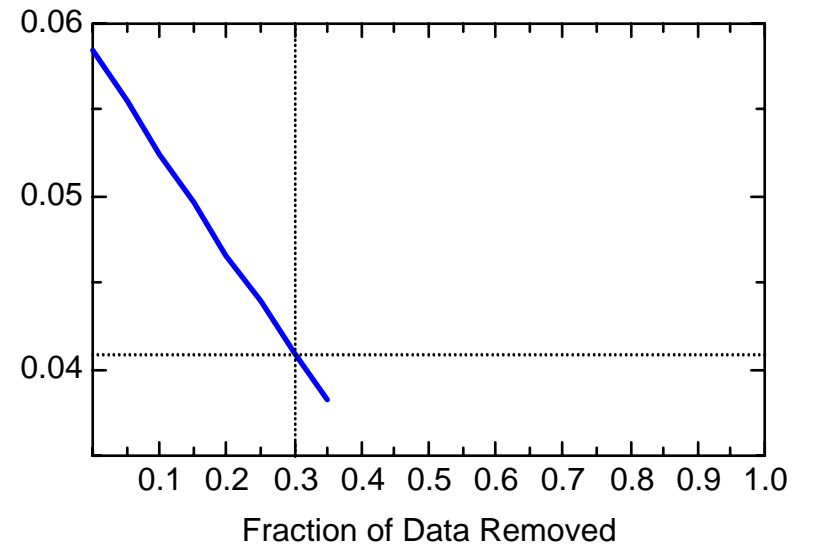
MN: Well JBW7215B



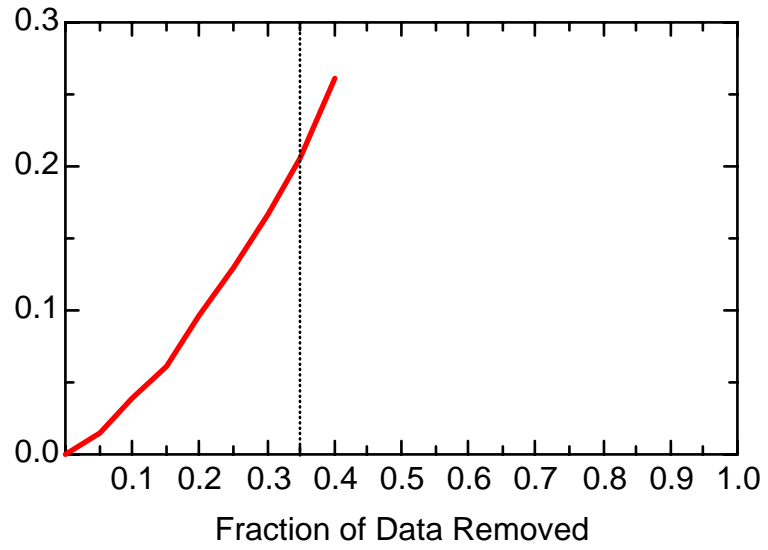
MN: Well JBW7215B



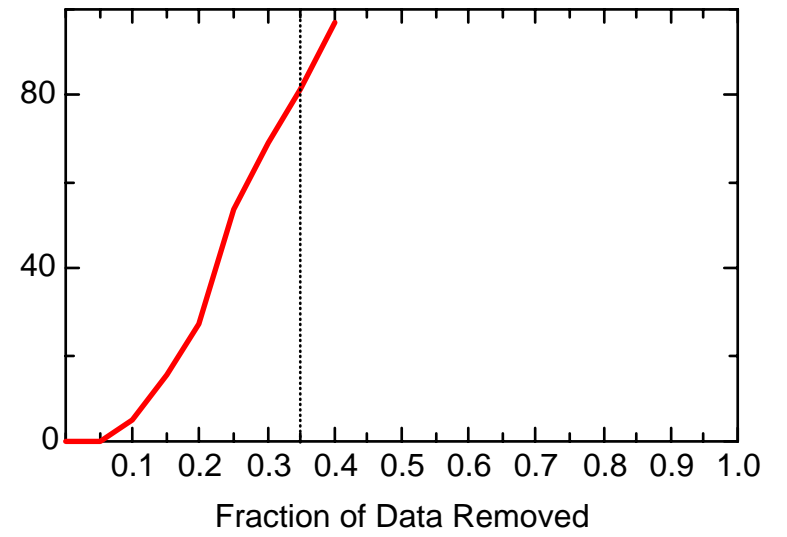
MN: Well JBW7215B



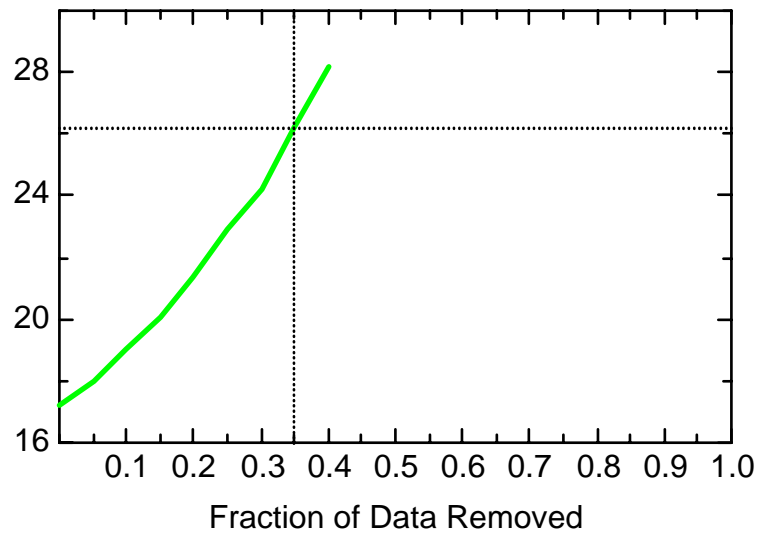
MN: Well JBW7317



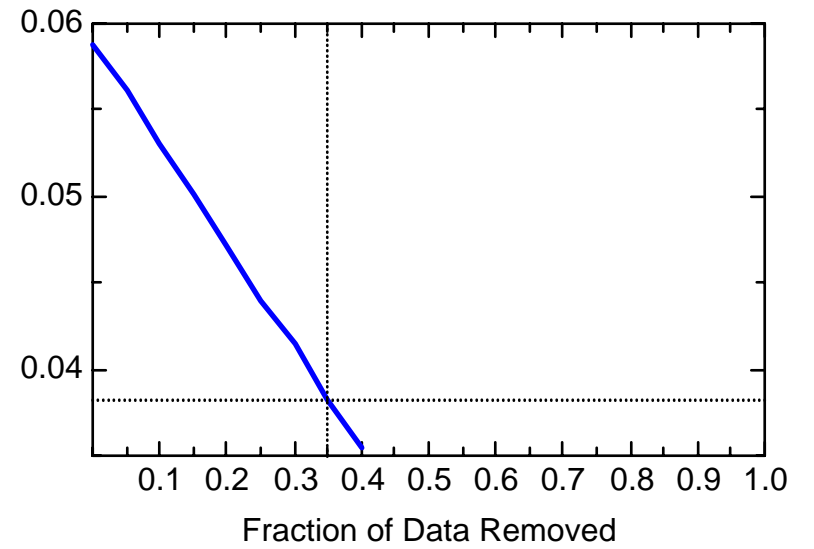
MN: Well JBW7317



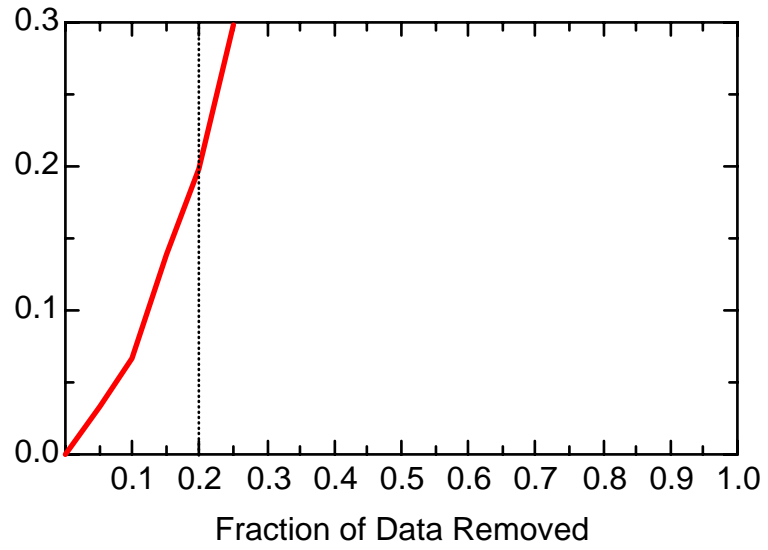
MN: Well JBW7317



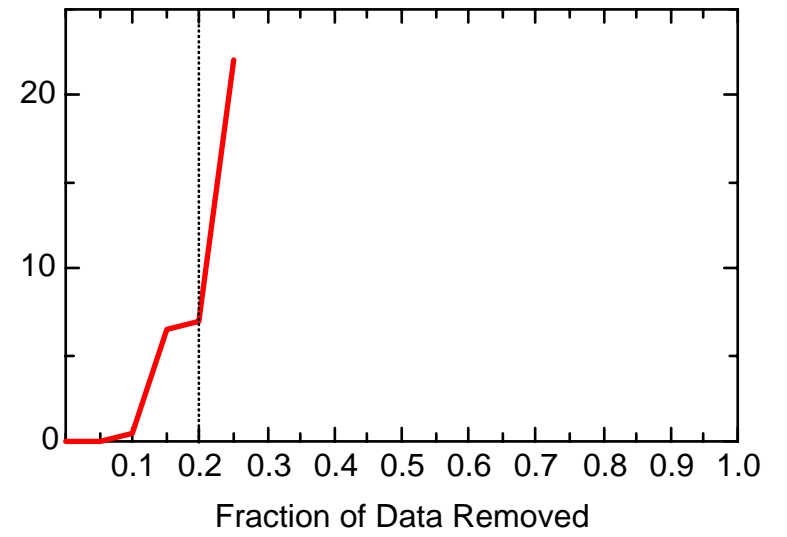
MN: Well JBW7317



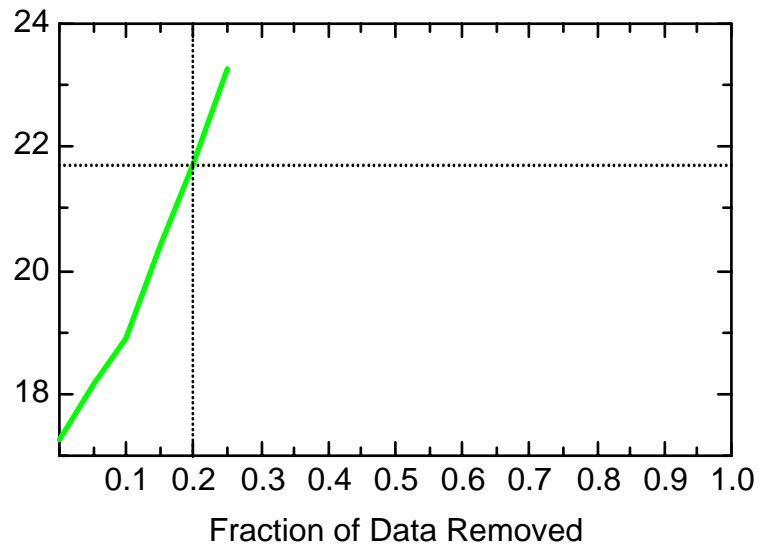
MN: Well JBW7326A



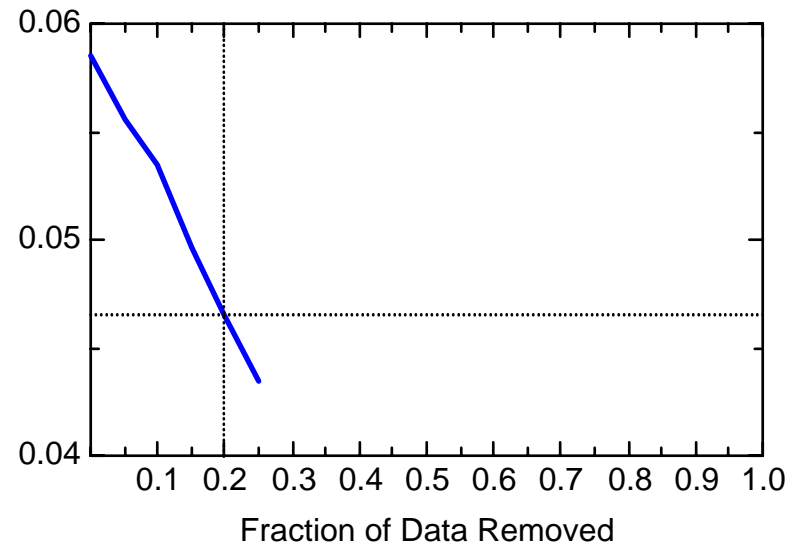
MN: Well JBW7326A



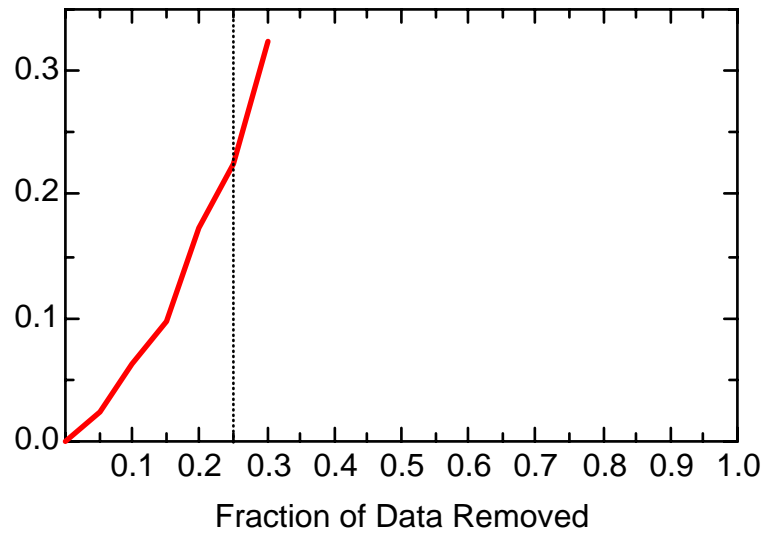
MN: Well JBW7326A



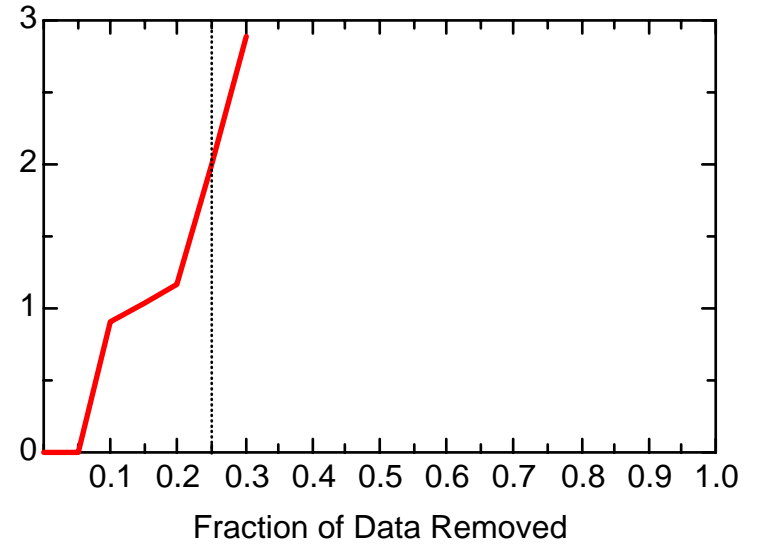
MN: Well JBW7326A



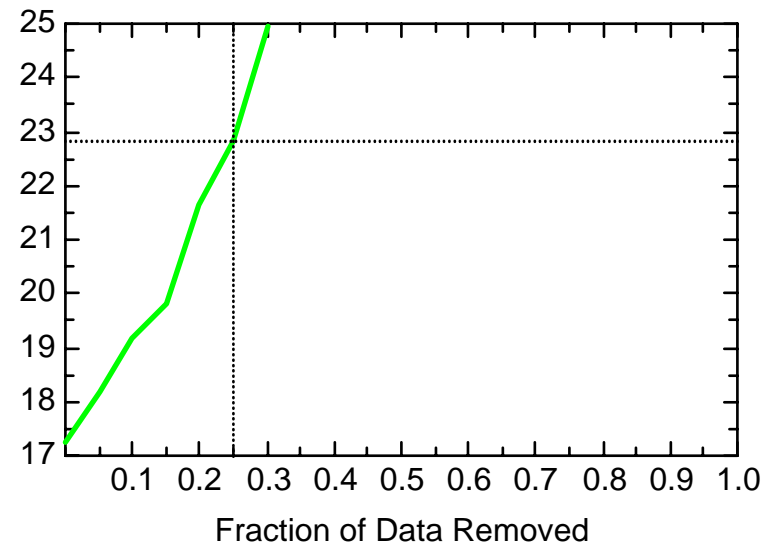
MN: Well JBW7326B



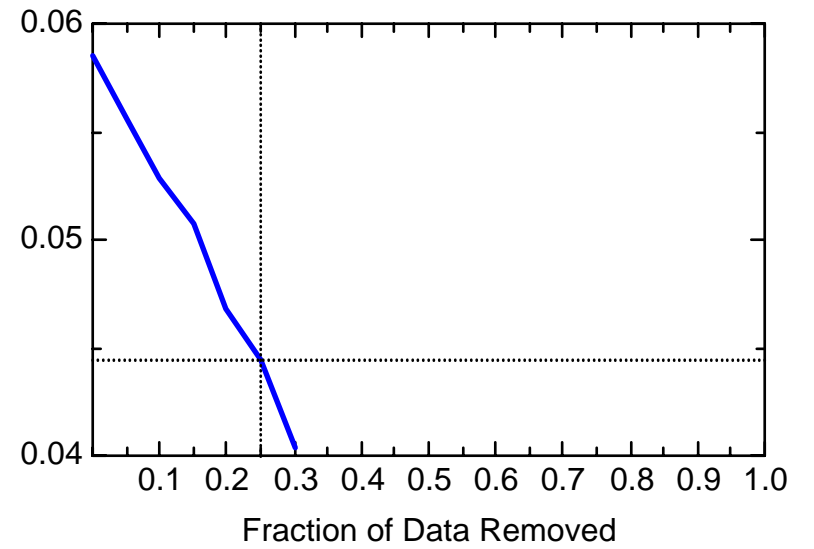
MN: Well JBW7326B



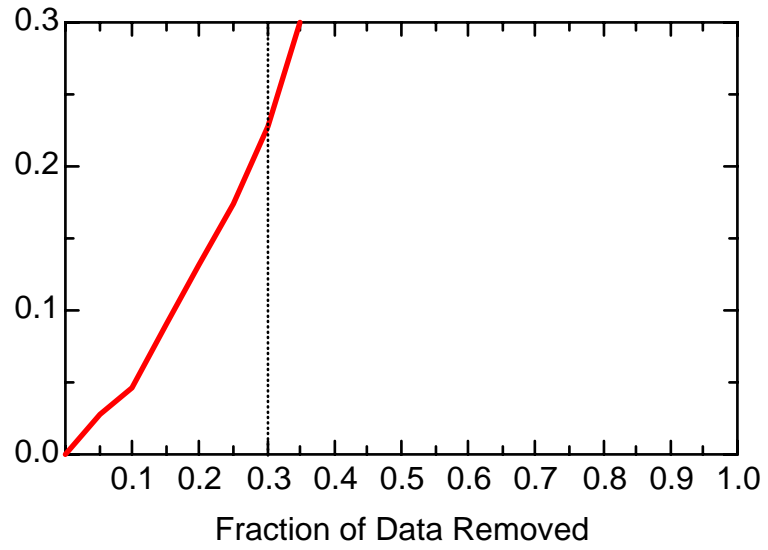
MN: Well JBW7326B



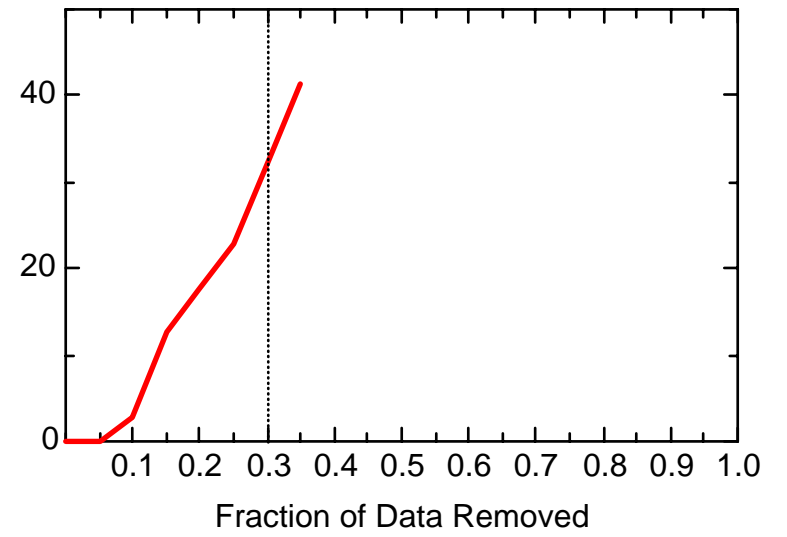
MN: Well JBW7326B



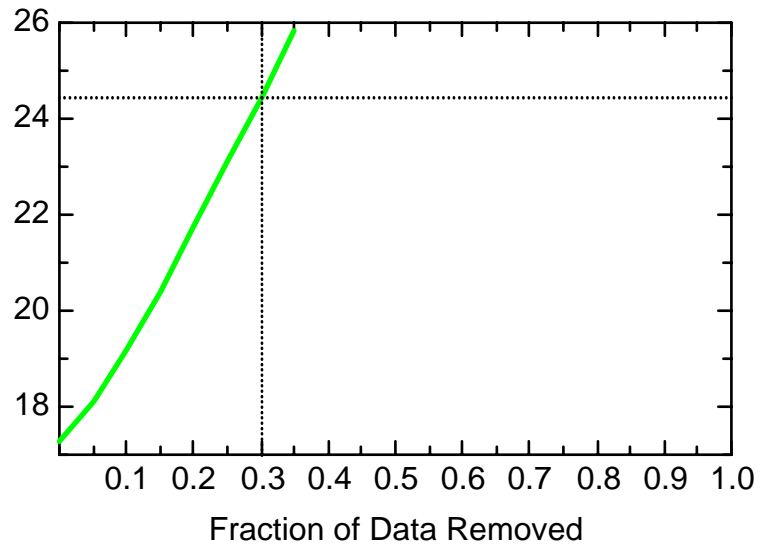
MN: Well JBW7328



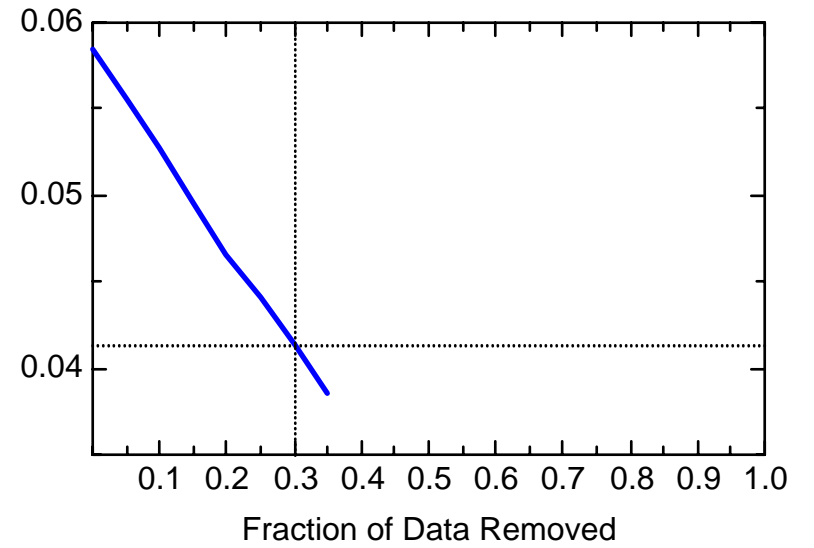
MN: Well JBW7328



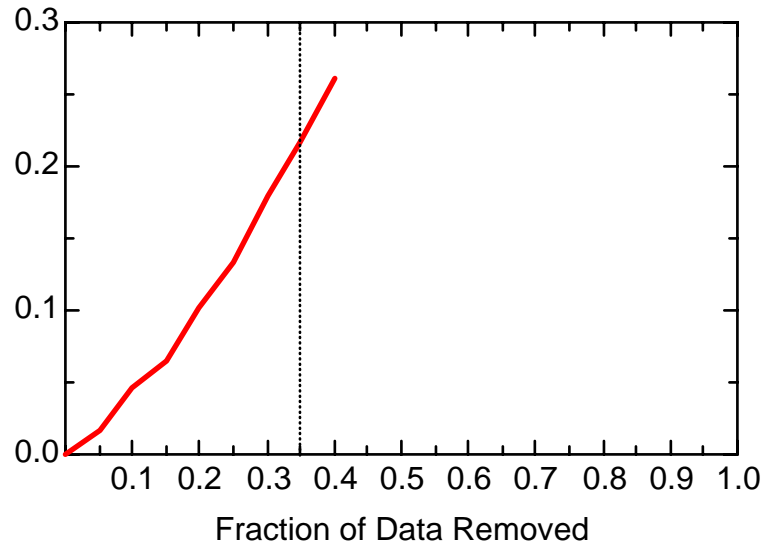
MN: Well JBW7328



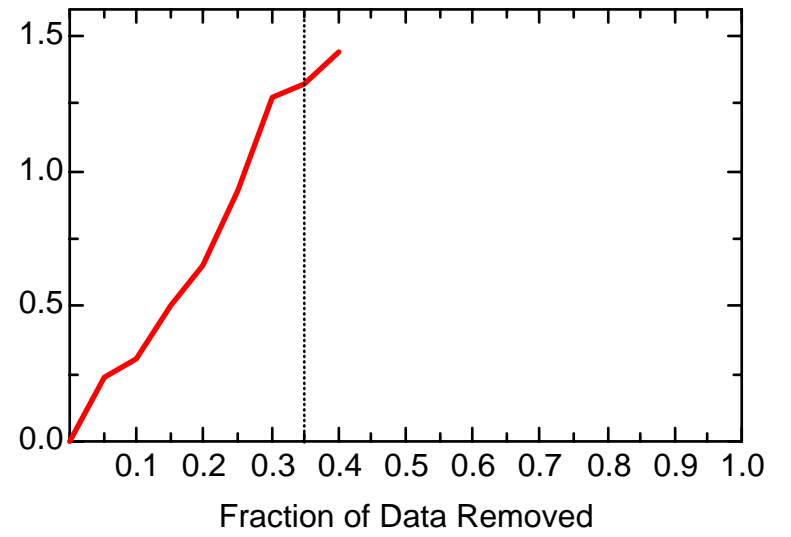
MN: Well JBW7328



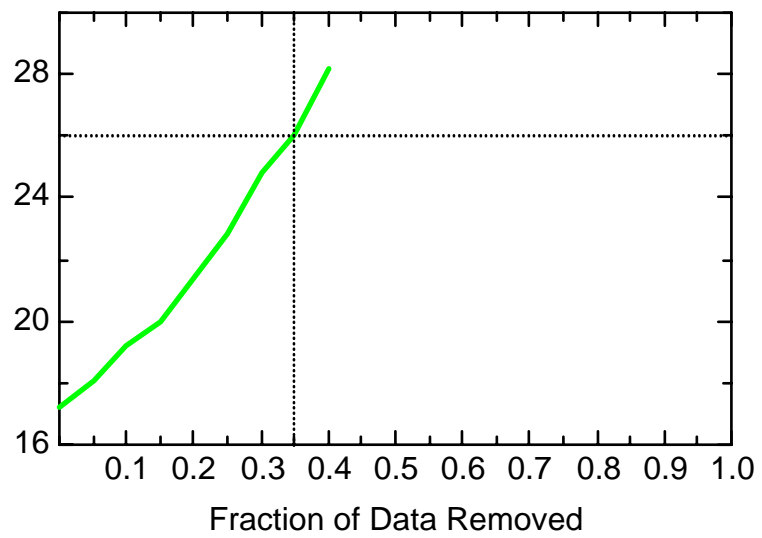
MN: Well JBW7330A



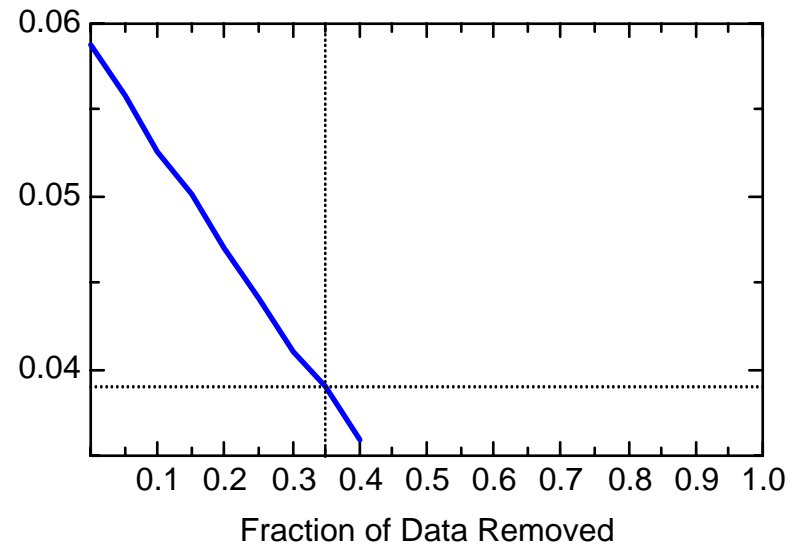
MN: Well JBW7330A



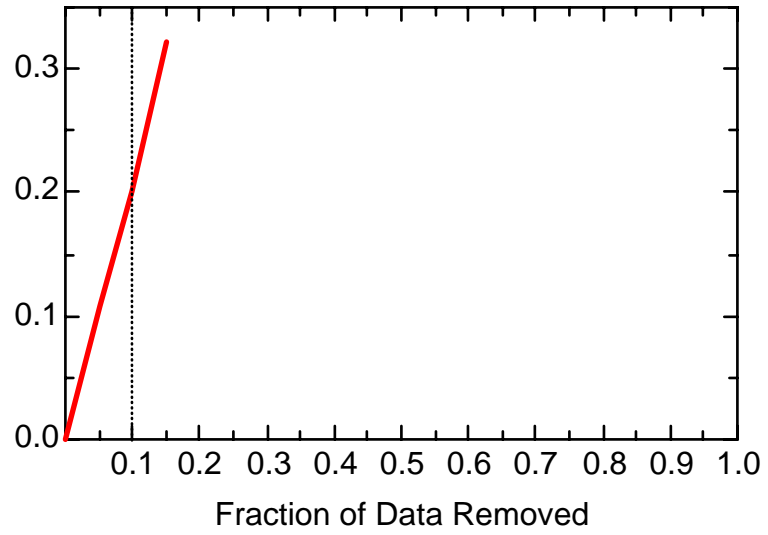
MN: Well JBW7330A



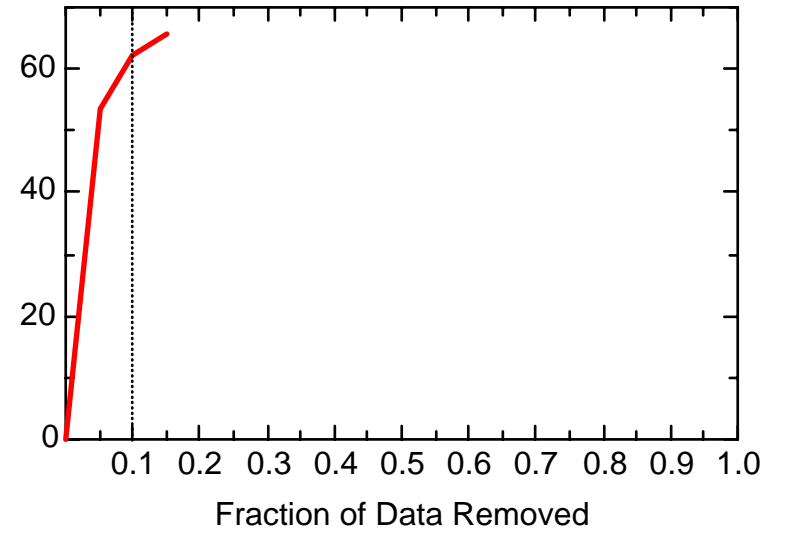
MN: Well JBW7330A



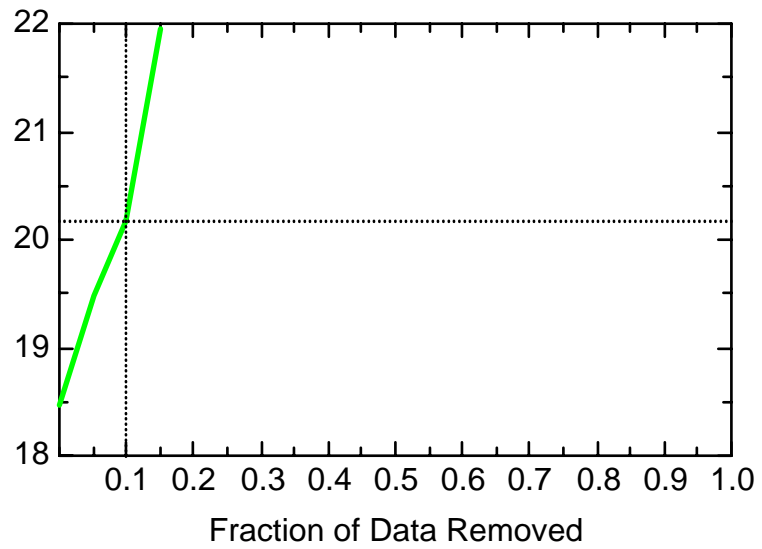
MN: Well JBW7333



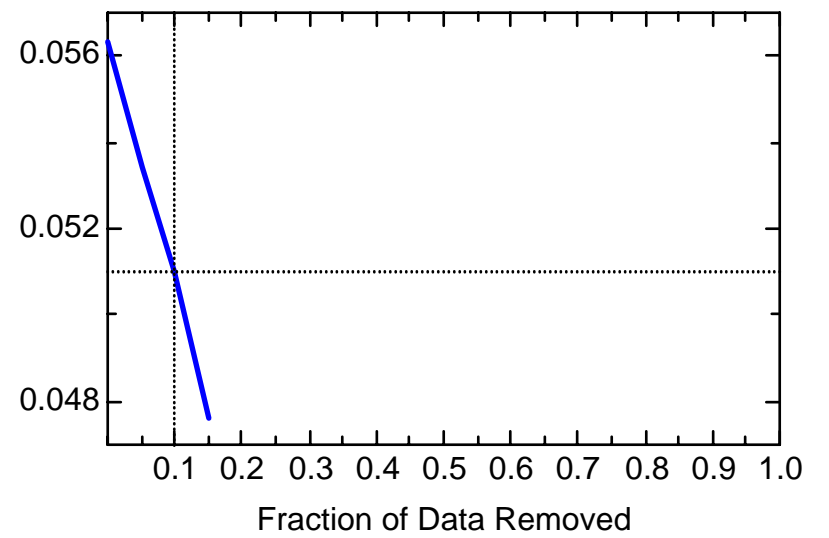
MN: Well JBW7333



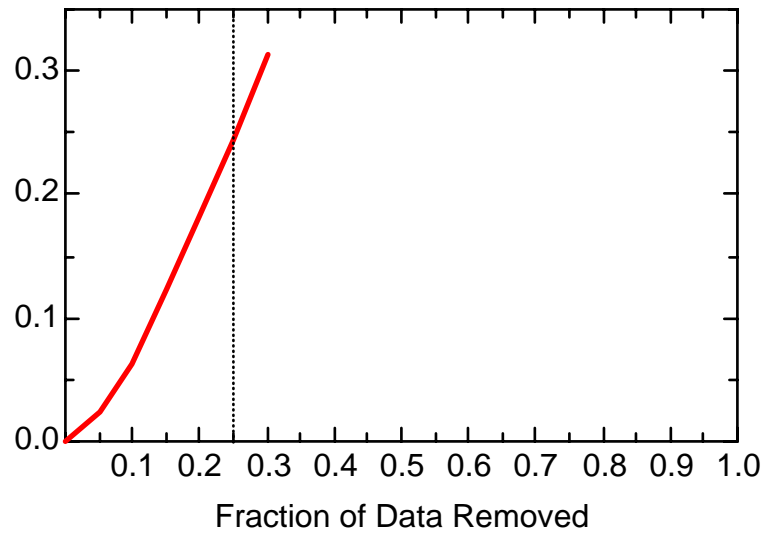
MN: Well JBW7333



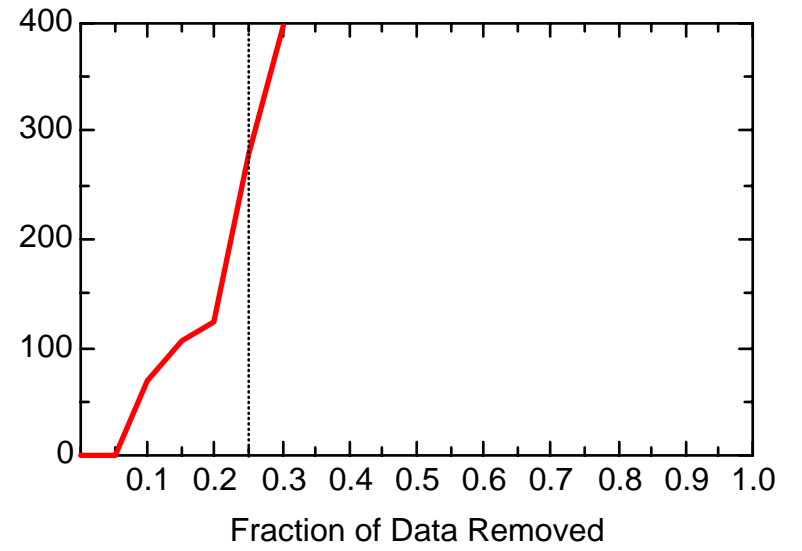
MN: Well JBW7333



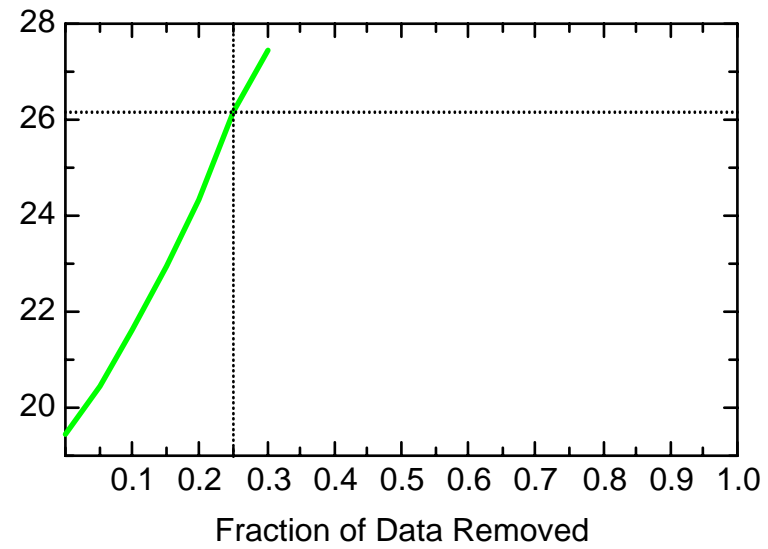
MN: Well JBW7338A



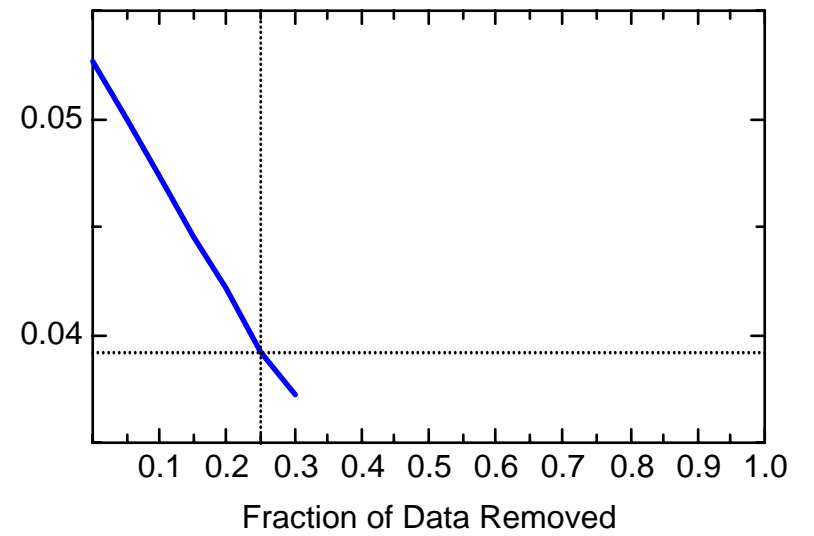
MN: Well JBW7338A



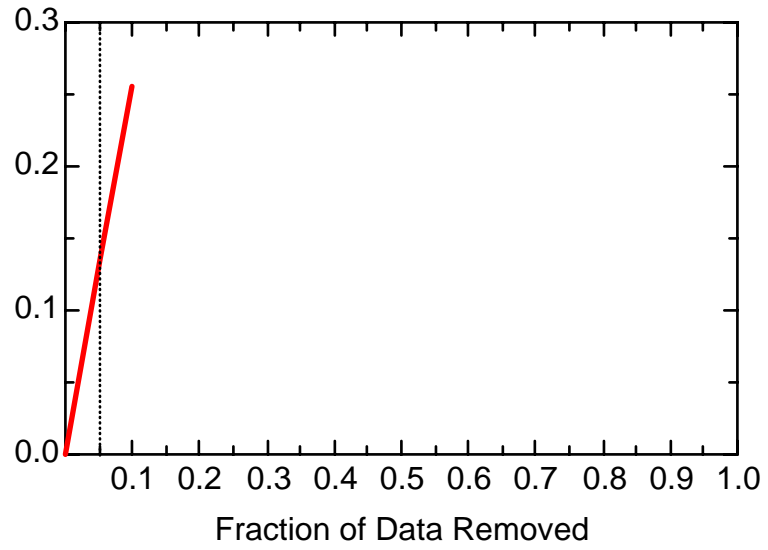
MN: Well JBW7338A



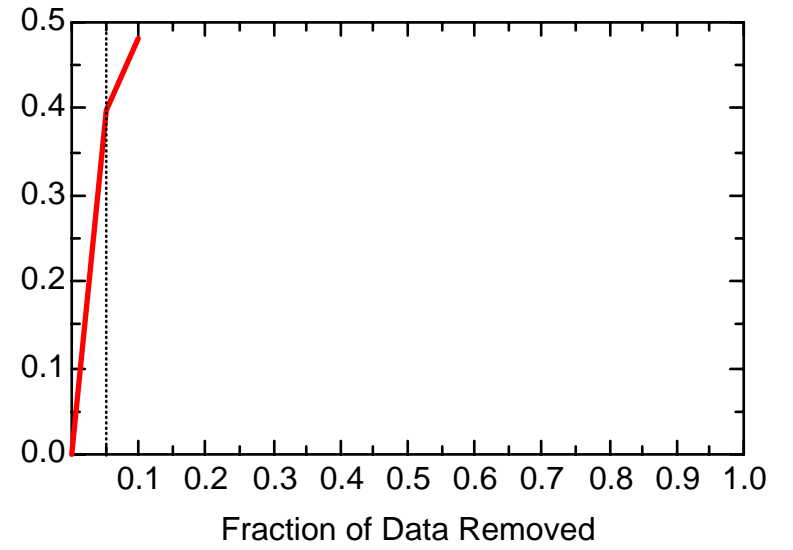
MN: Well JBW7338A



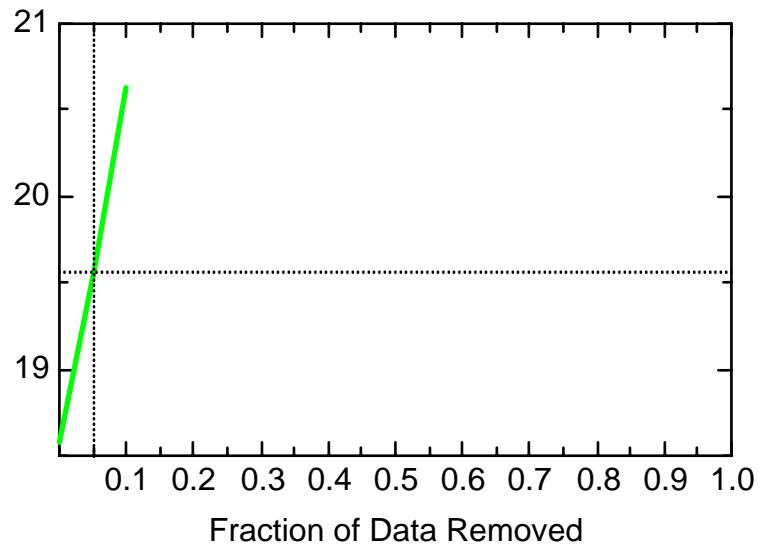
MN: Well JBW7338B



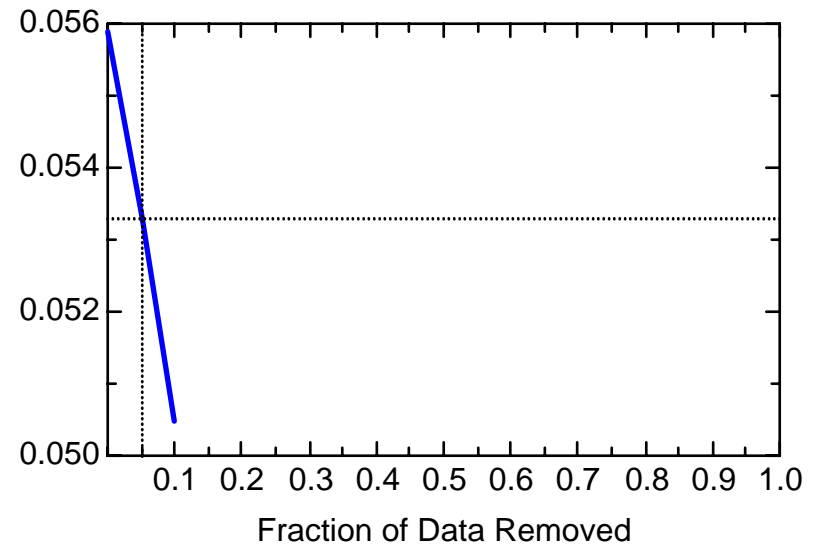
MN: Well JBW7338B



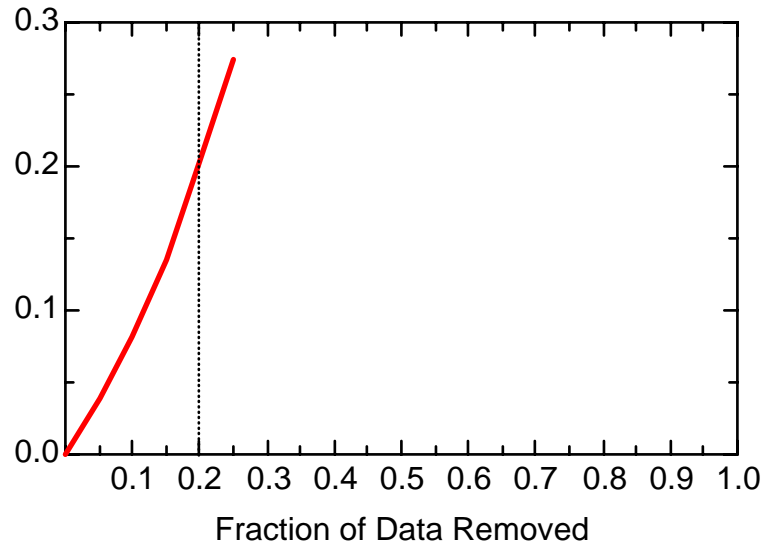
MN: Well JBW7338B



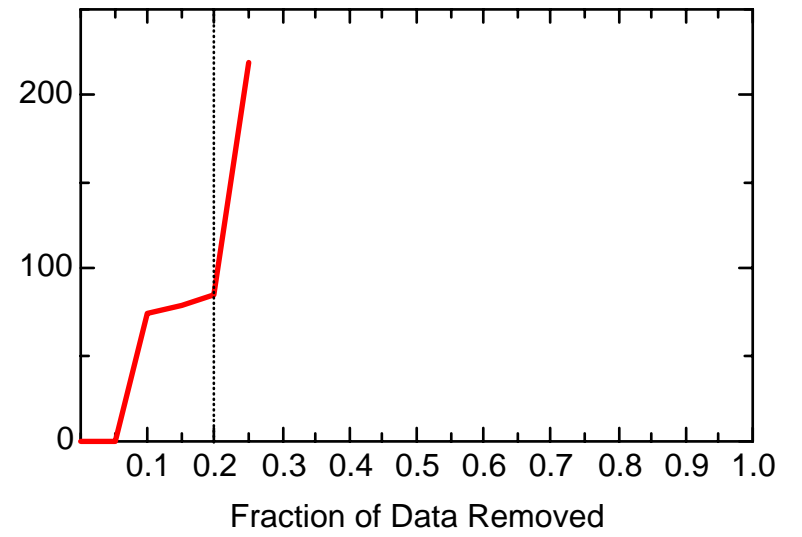
MN: Well JBW7338B



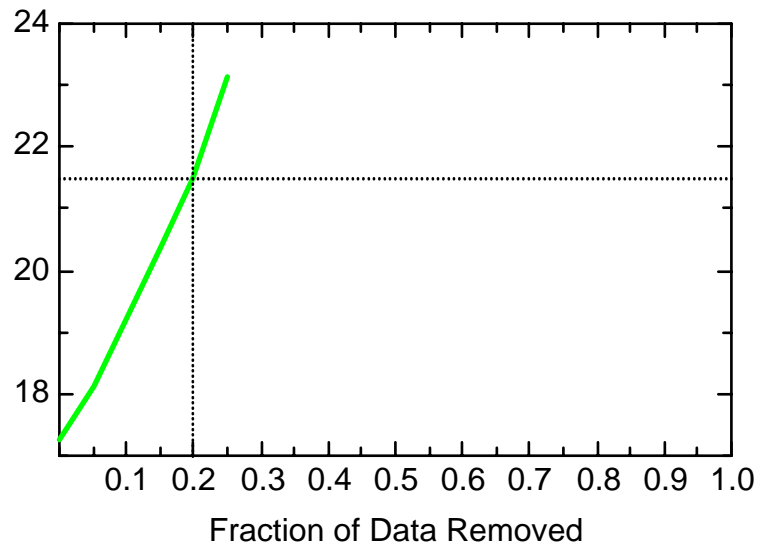
MN: Well JBW7340B



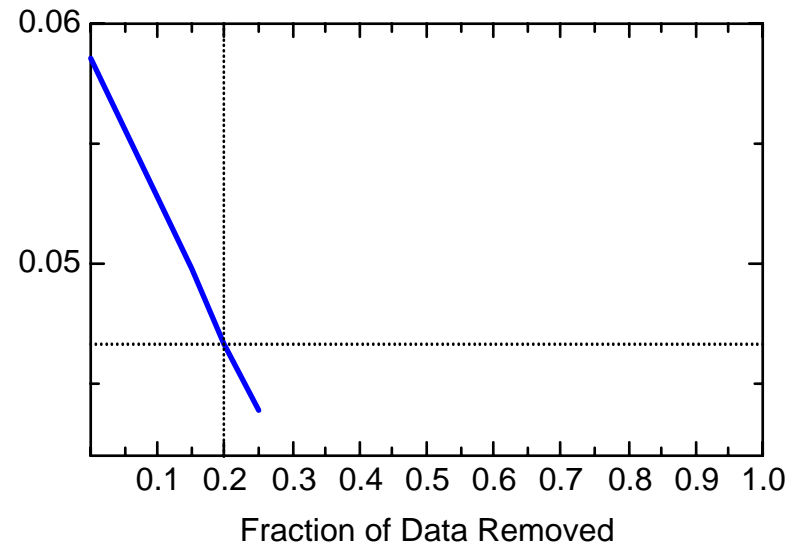
MN: Well JBW7340B



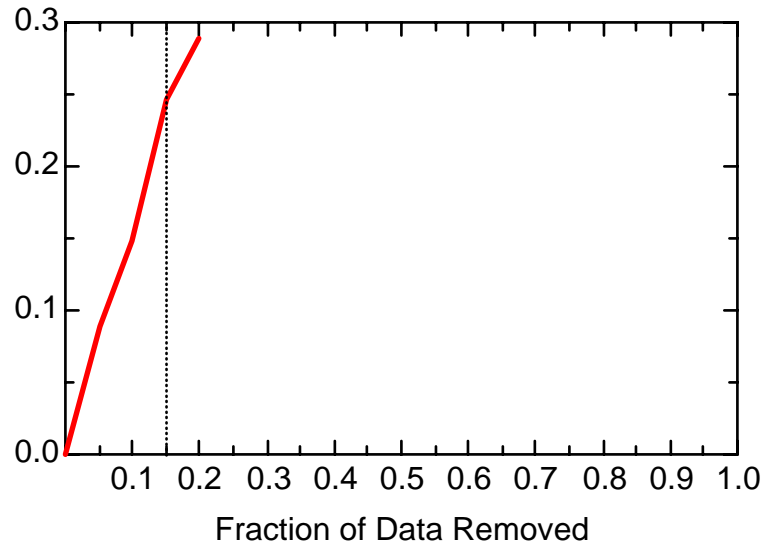
MN: Well JBW7340B



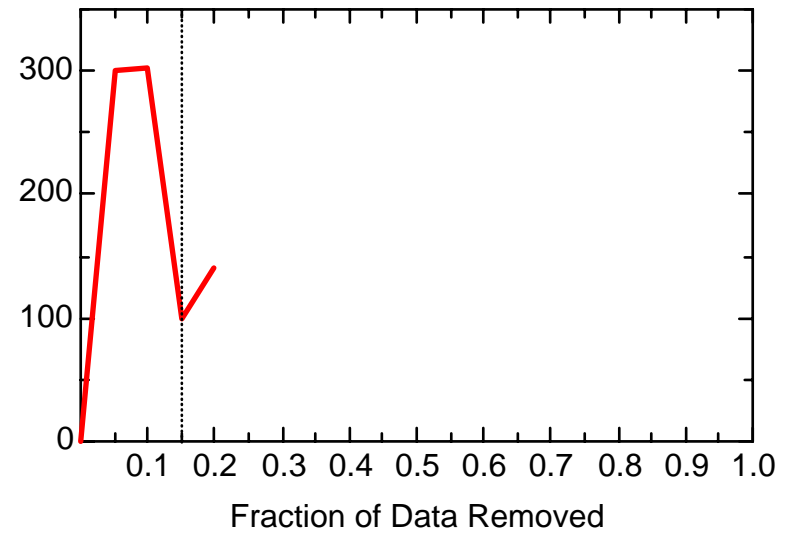
MN: Well JBW7340B



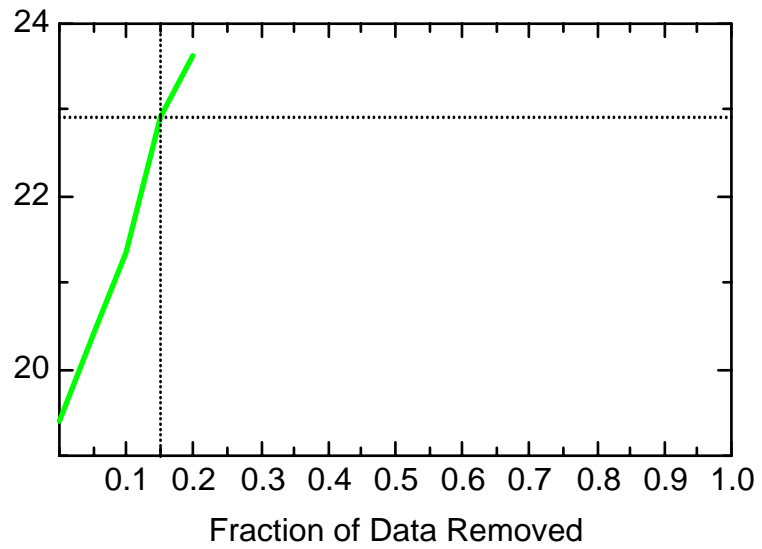
MN: Well JBW7344



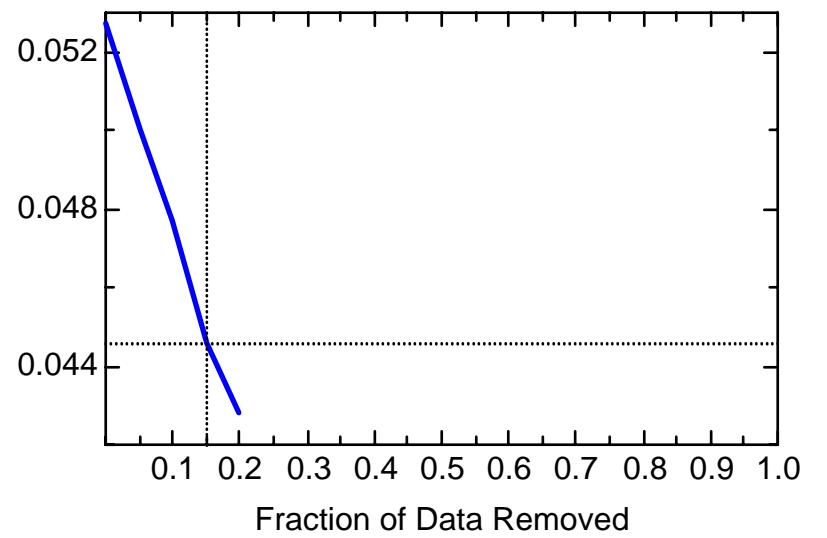
MN: Well JBW7344



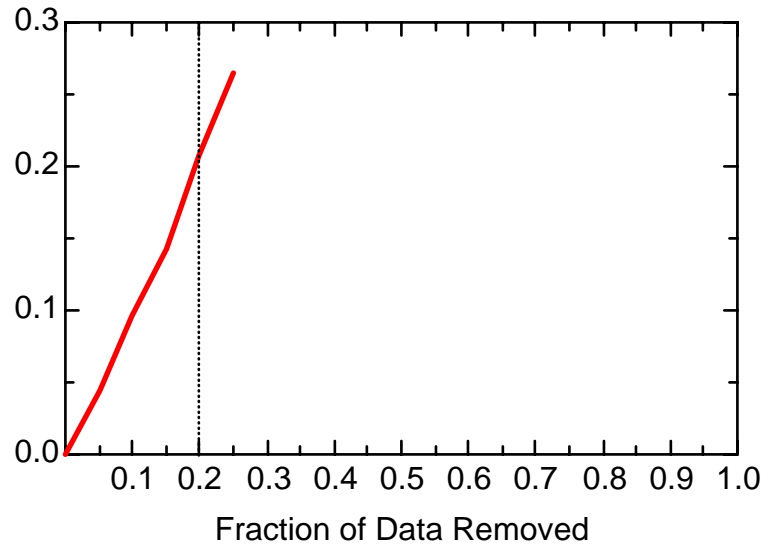
MN: Well JBW7344



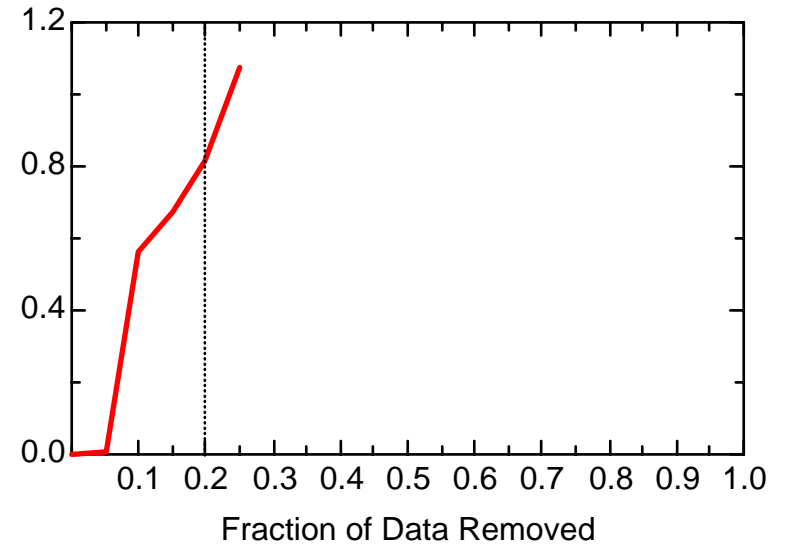
MN: Well JBW7344



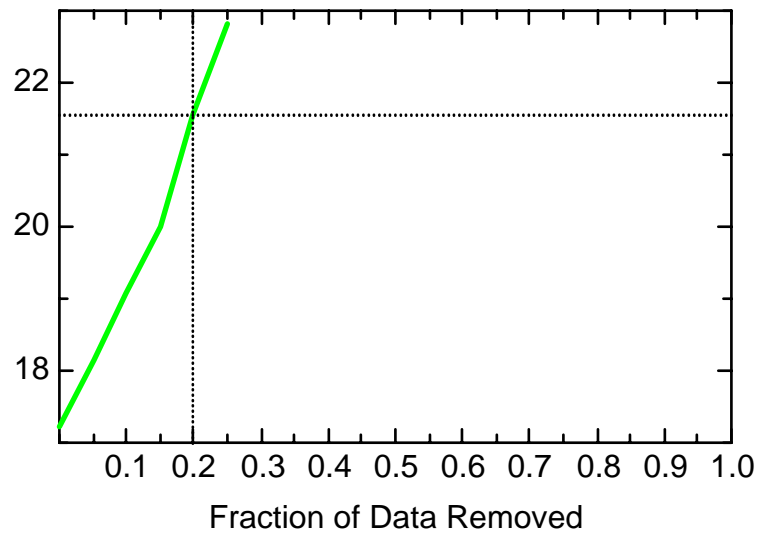
MN: Well JBW7345A



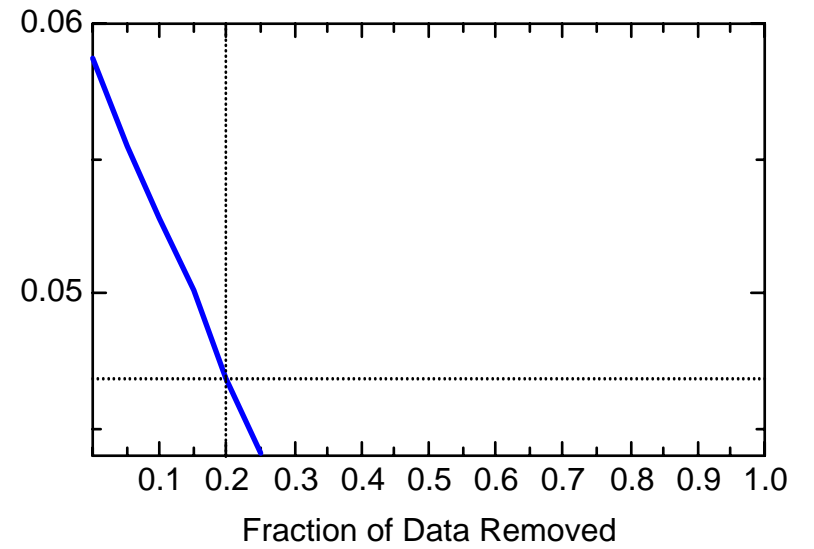
MN: Well JBW7345A



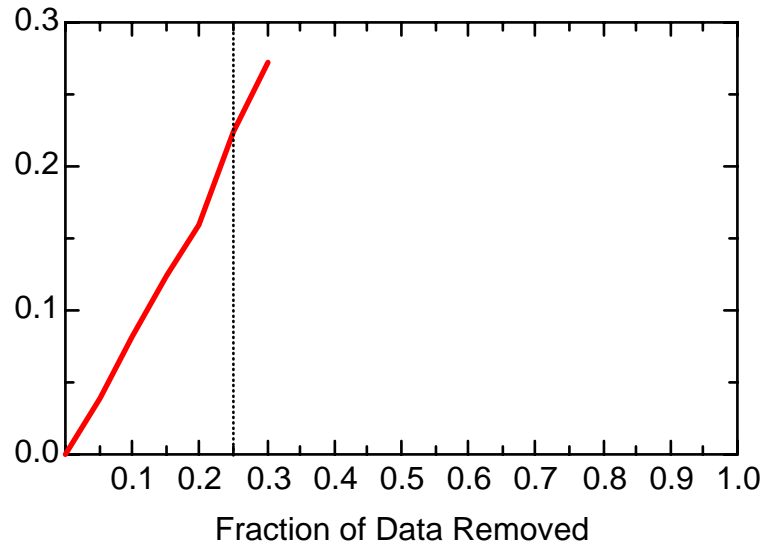
MN: Well JBW7345A



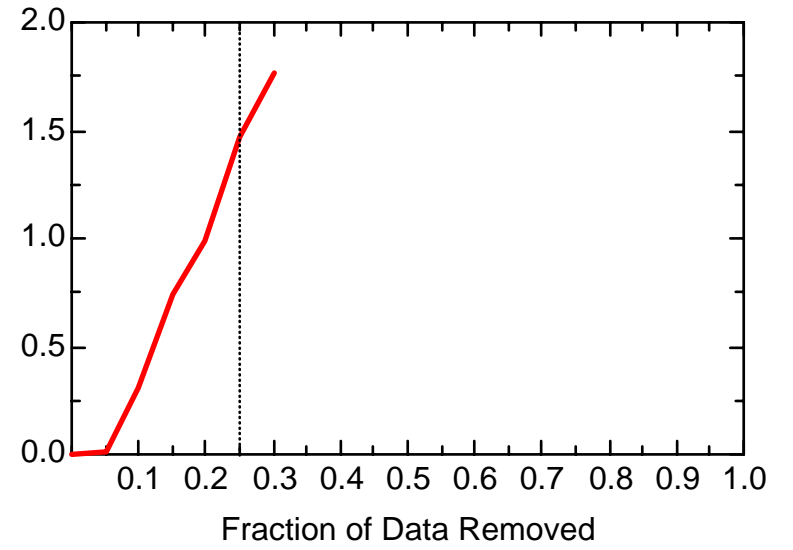
MN: Well JBW7345A



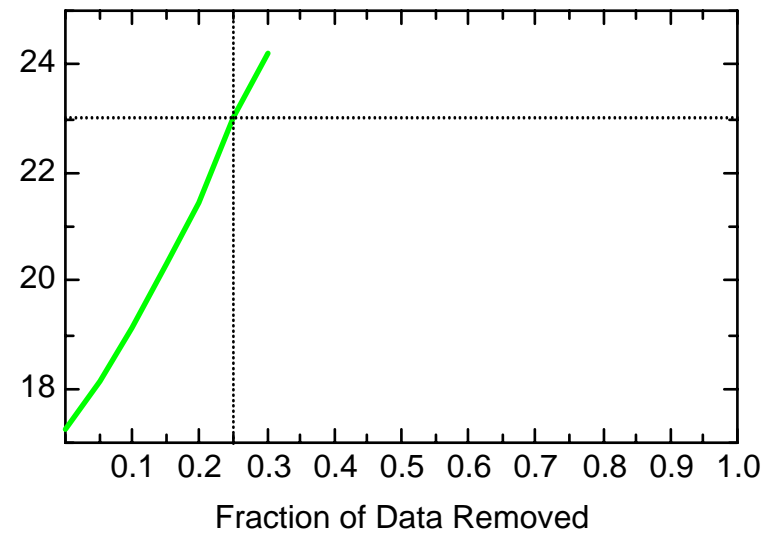
MN: Well JBW7347B



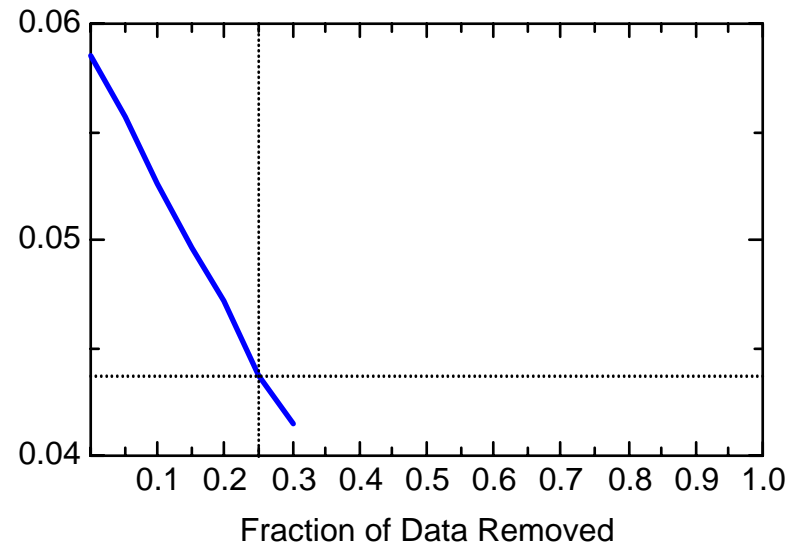
MN: Well JBW7347B



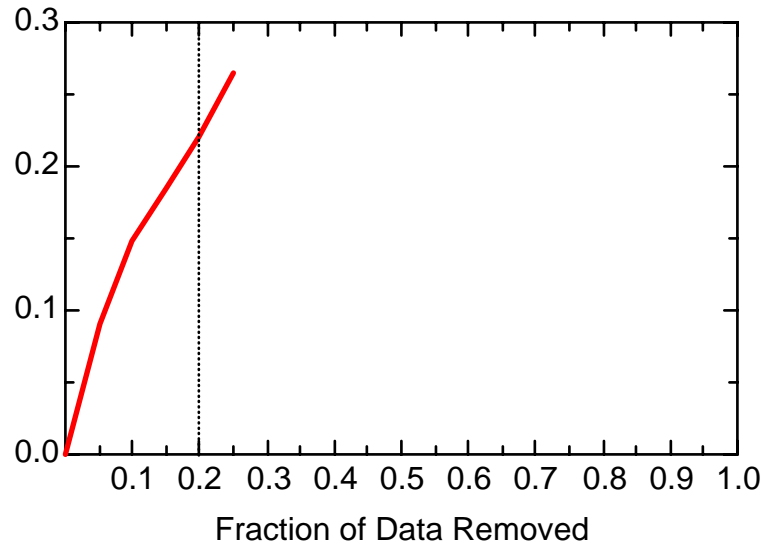
MN: Well JBW7347B



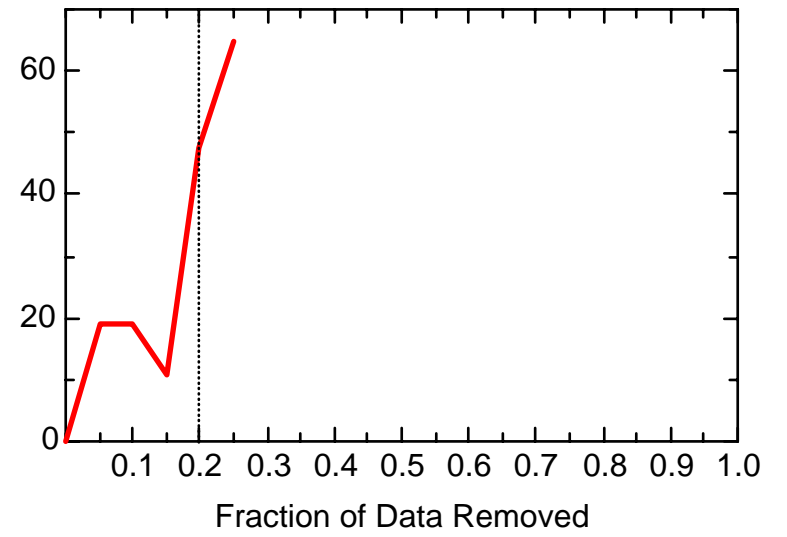
MN: Well JBW7347B



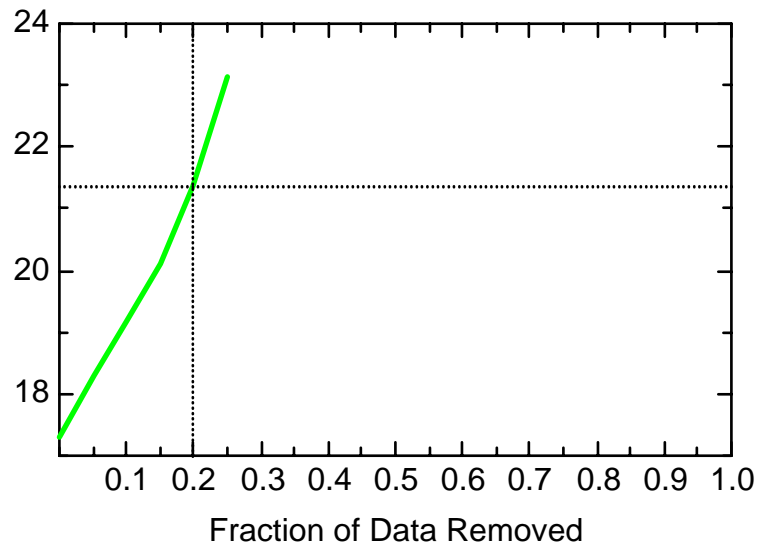
MN: Well JBW7348



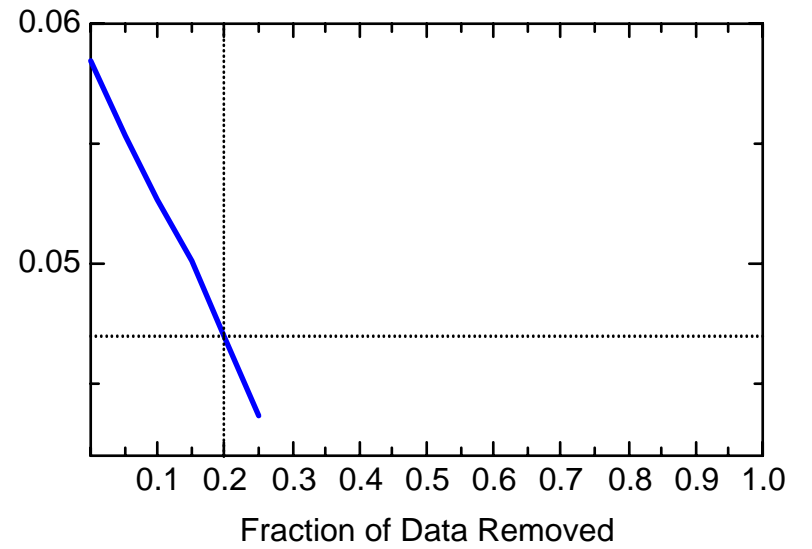
MN: Well JBW7348



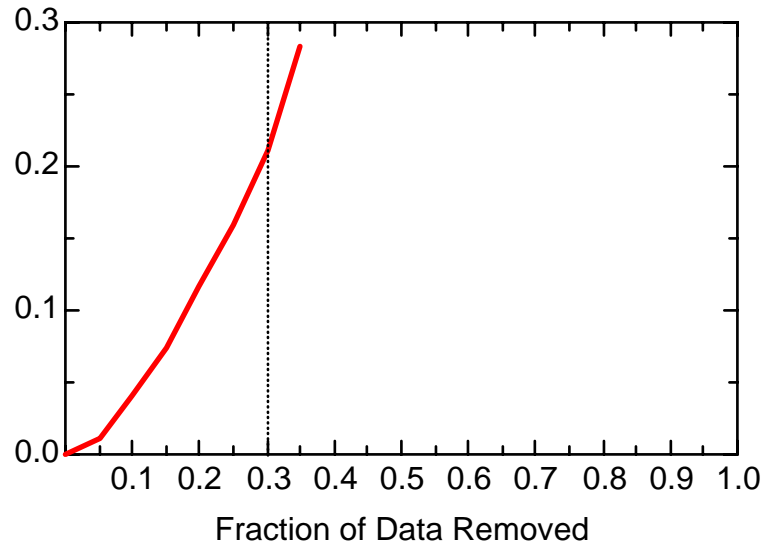
MN: Well JBW7348



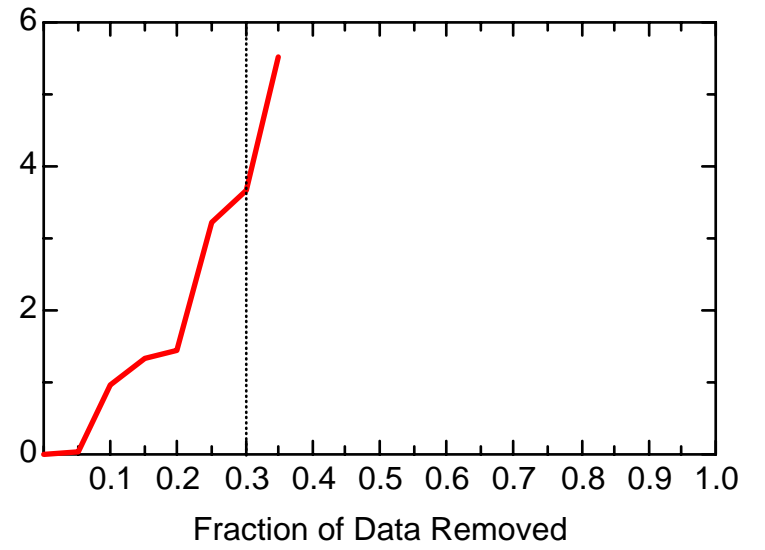
MN: Well JBW7348



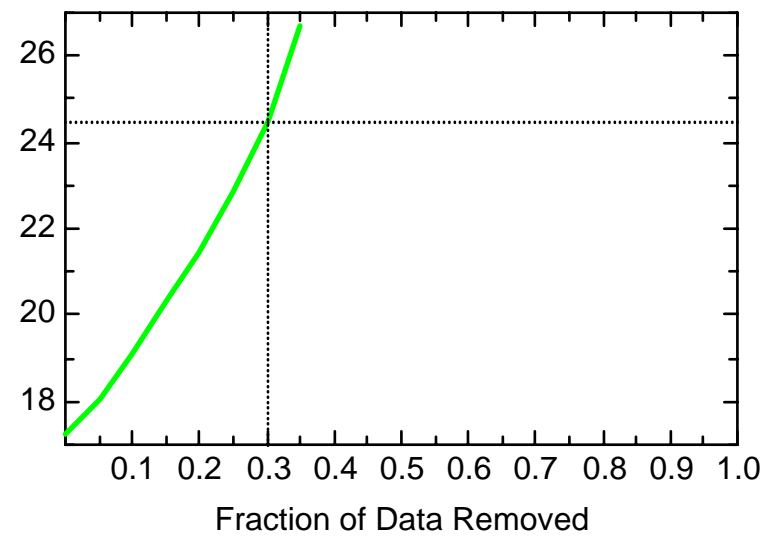
MN: Well JBW7350



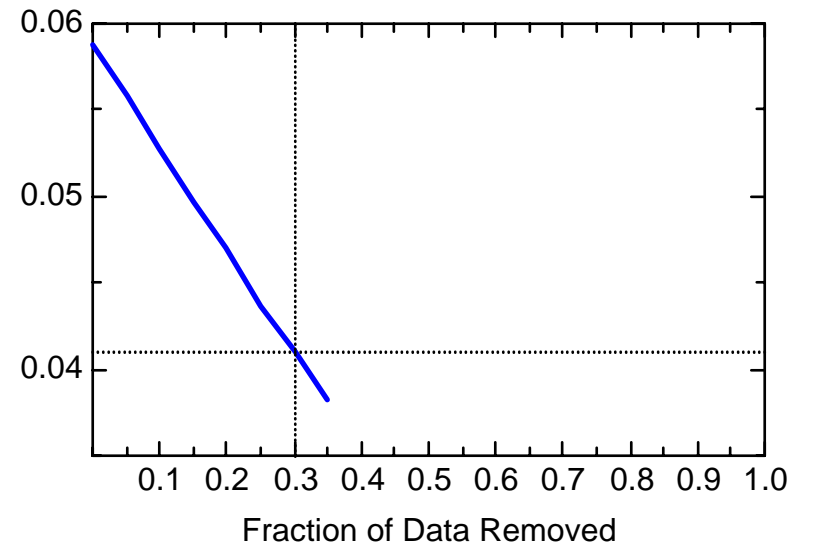
MN: Well JBW7350



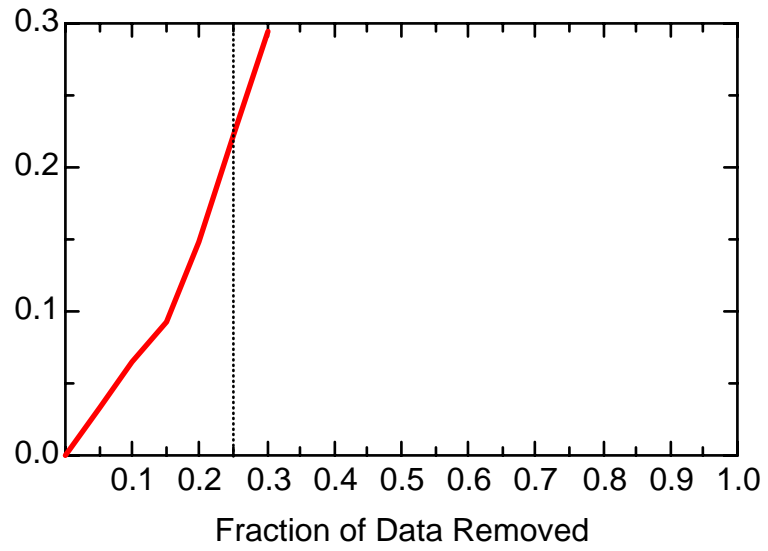
MN: Well JBW7350



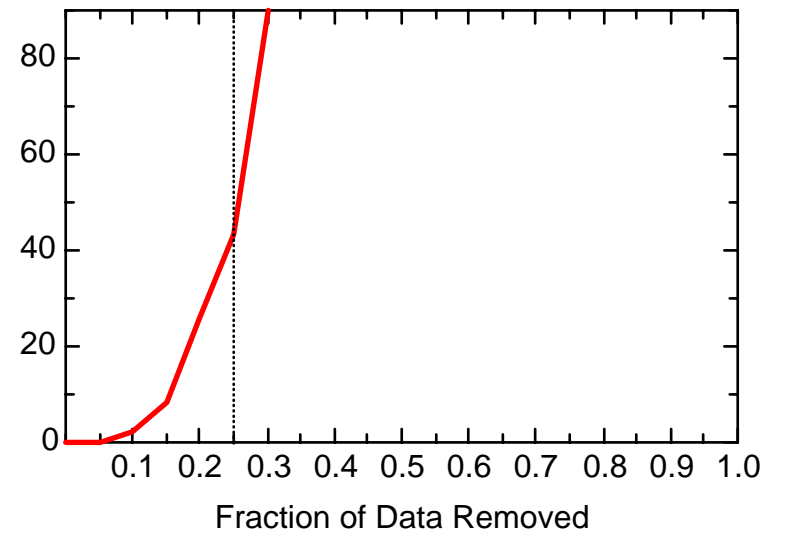
MN: Well JBW7350



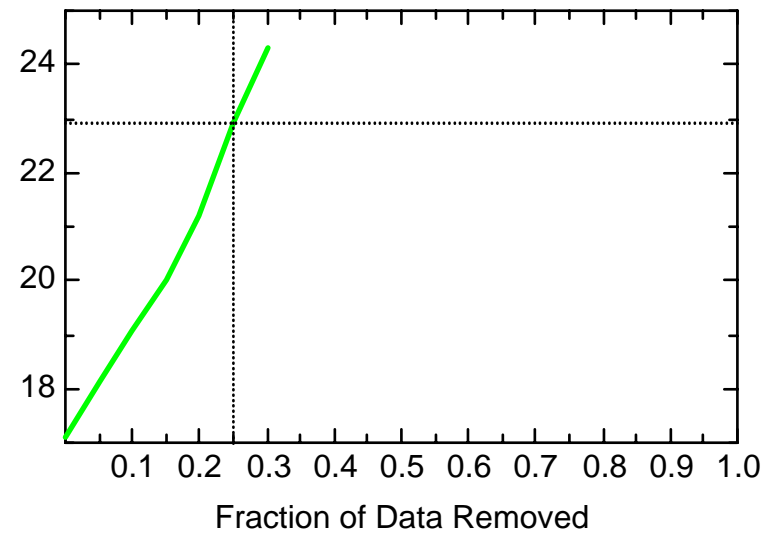
MN: Well JBW7806



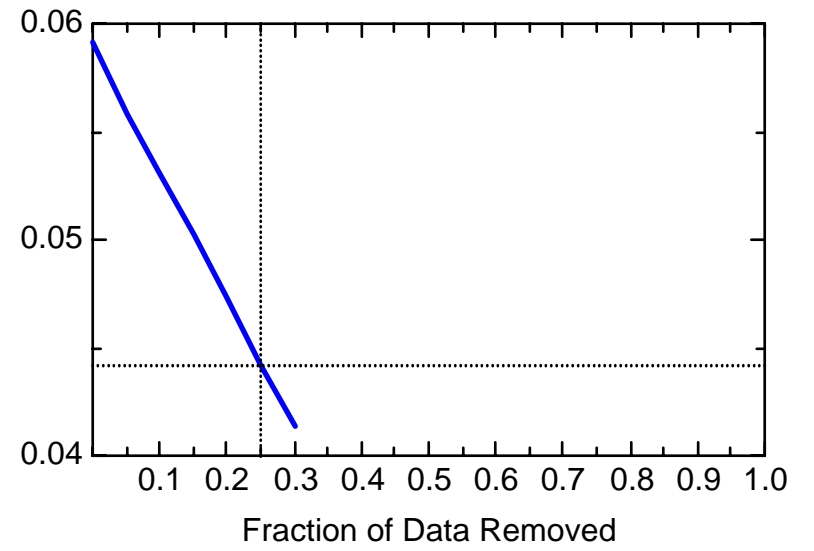
MN: Well JBW7806



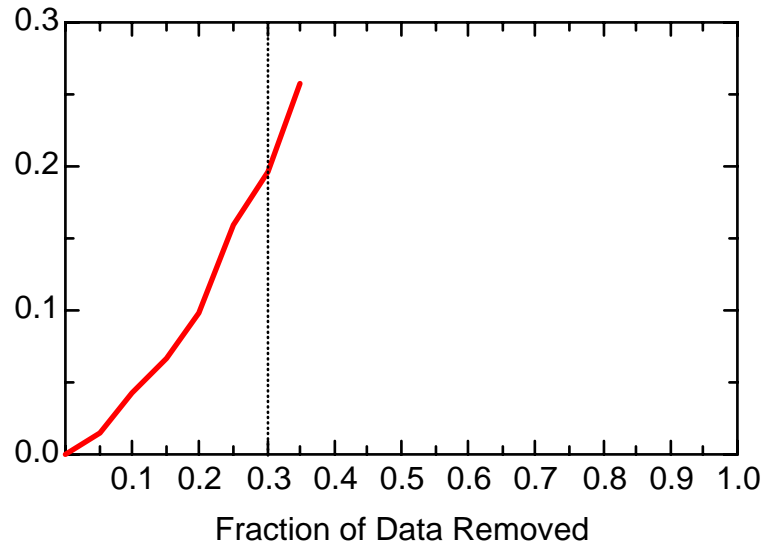
MN: Well JBW7806



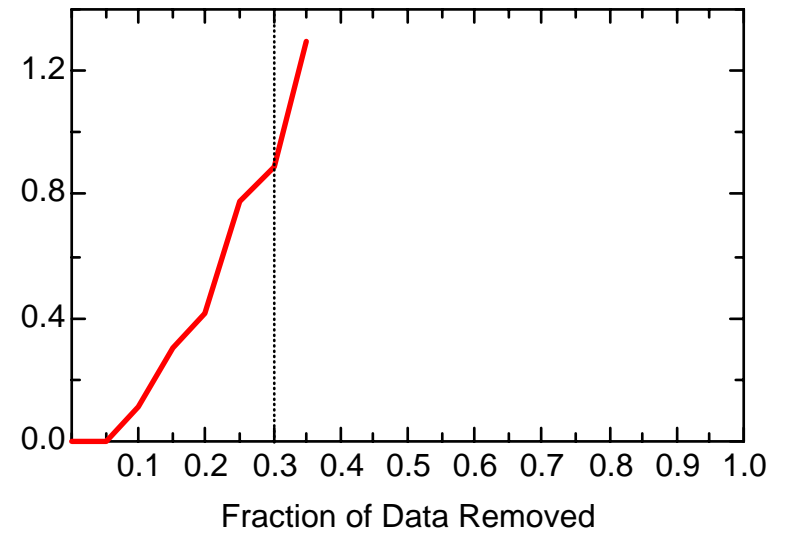
MN: Well JBW7806



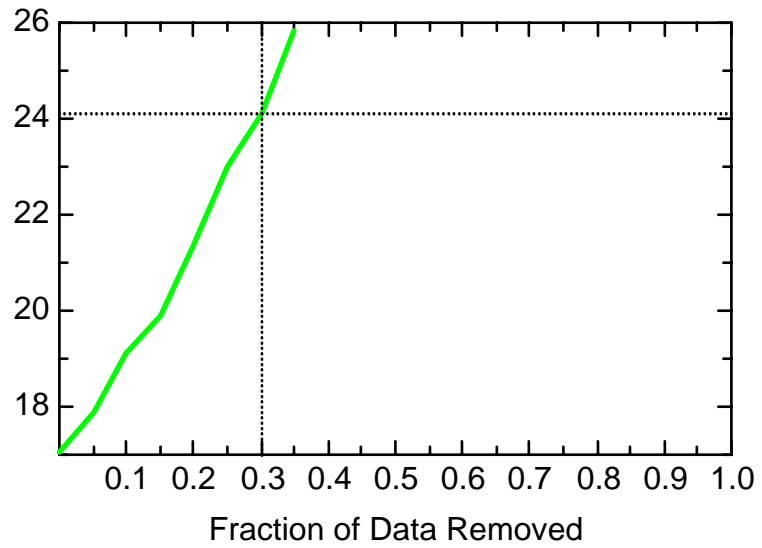
MN: Well JBW7809



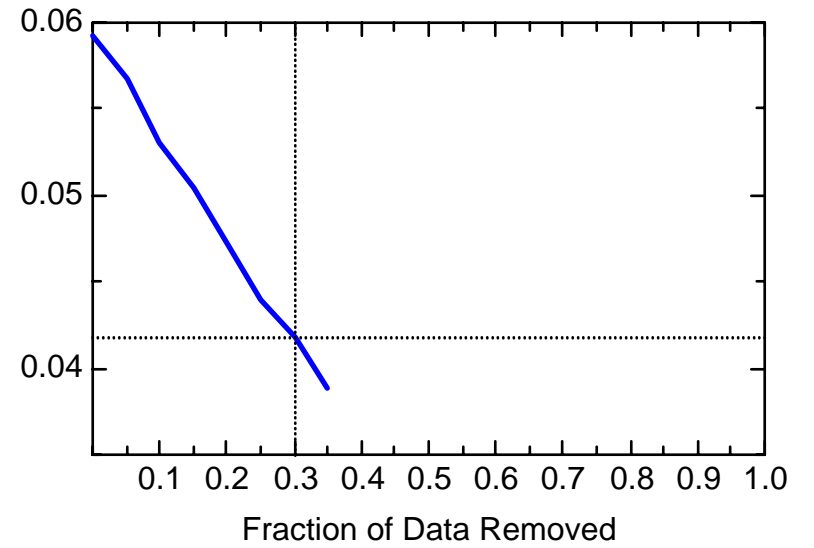
MN: Well JBW7809



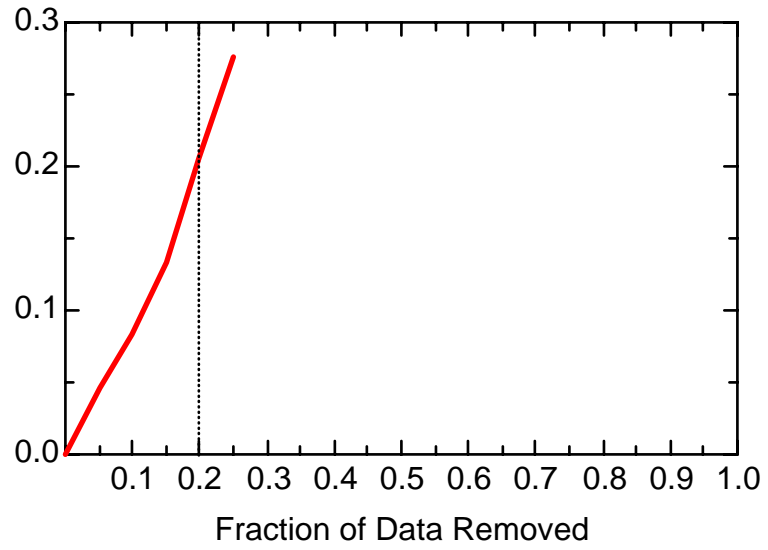
MN: Well JBW7809



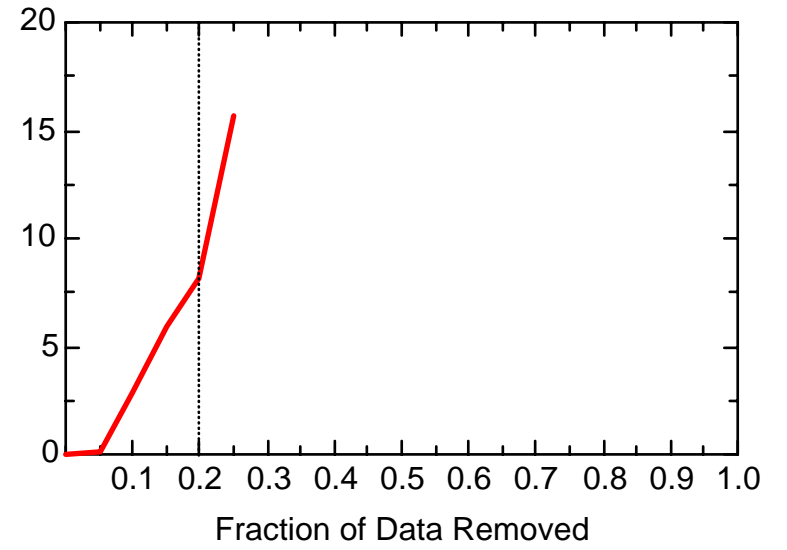
MN: Well JBW7809



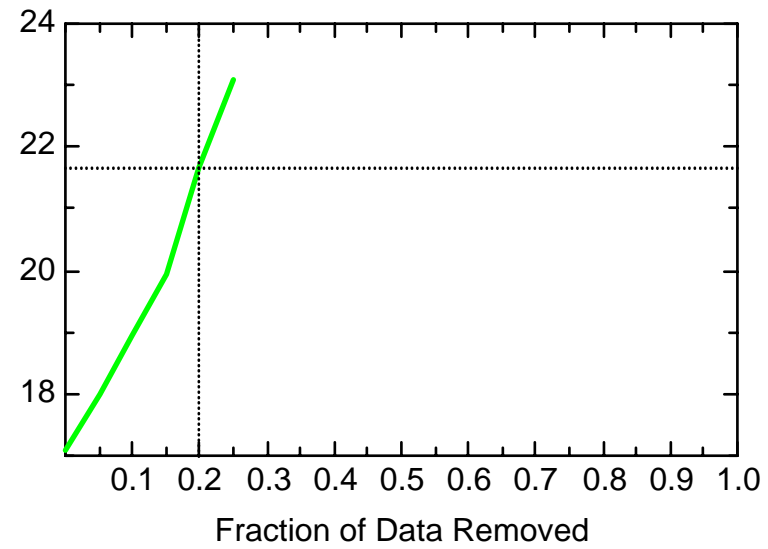
MN: Well JBW7812B



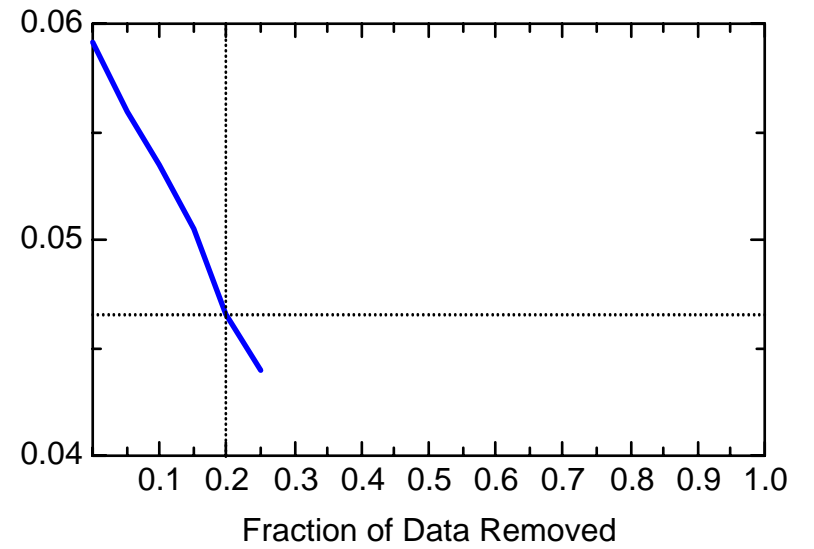
MN: Well JBW7812B



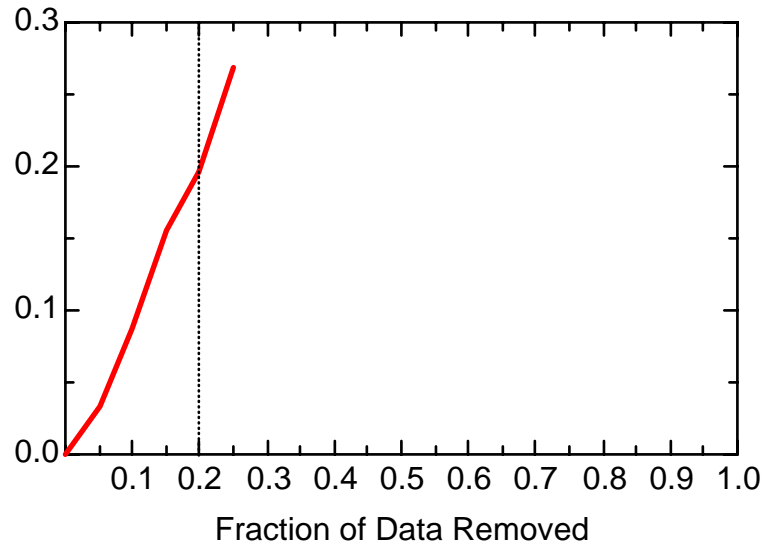
MN: Well JBW7812B



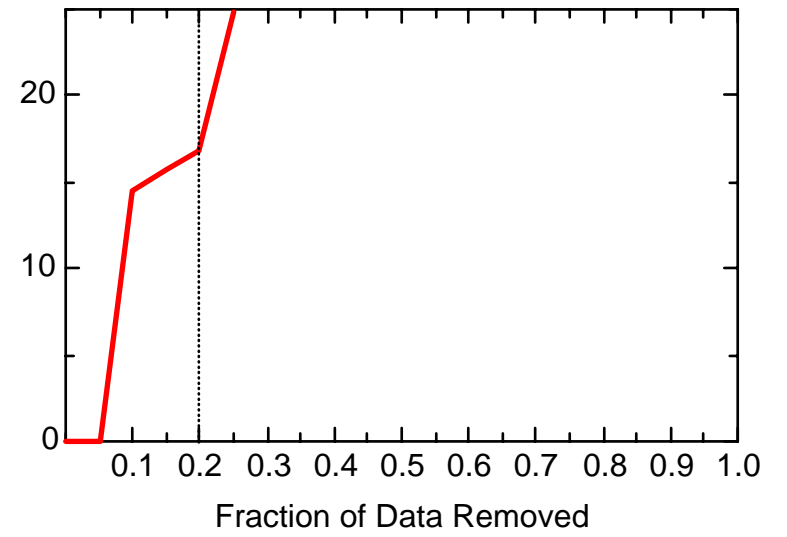
MN: Well JBW7812B



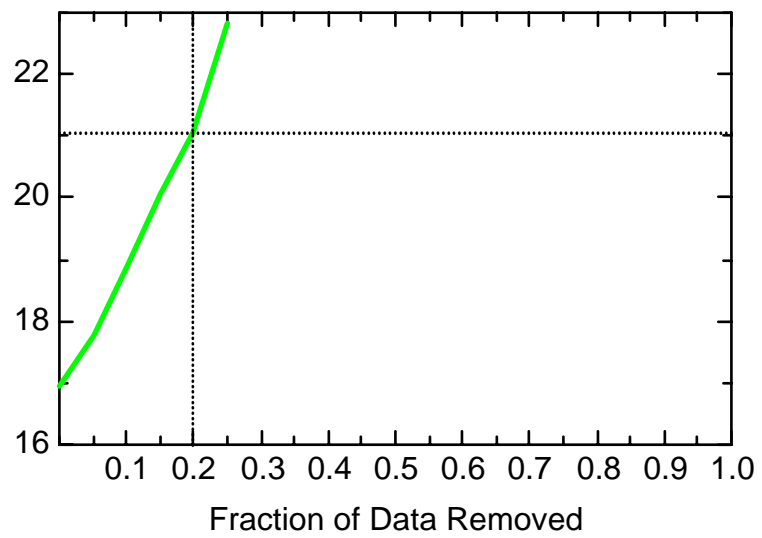
MN: Well JBW8003B



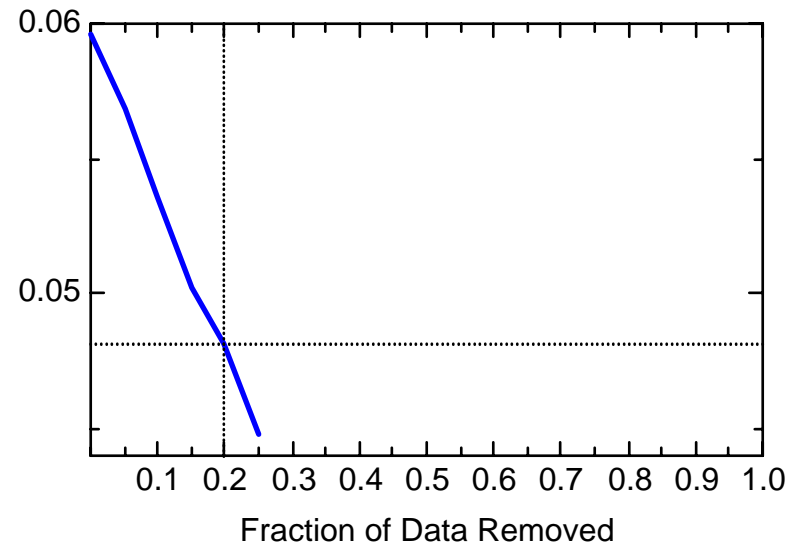
MN: Well JBW8003B



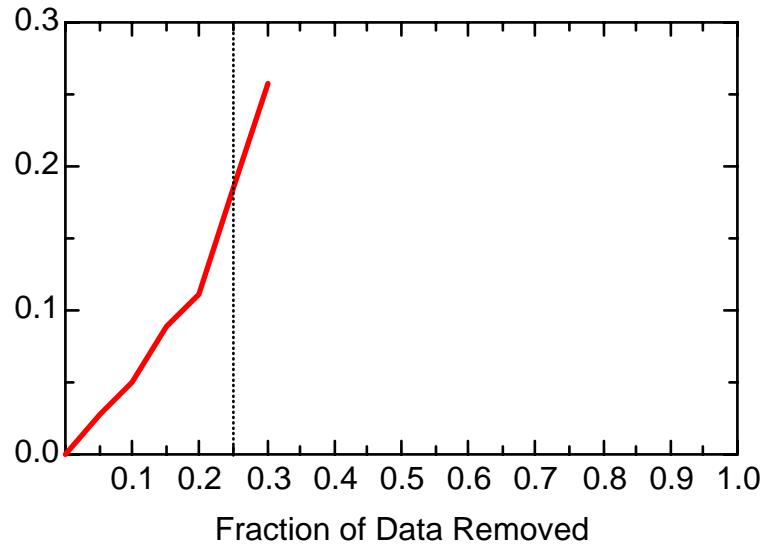
MN: Well JBW8003B



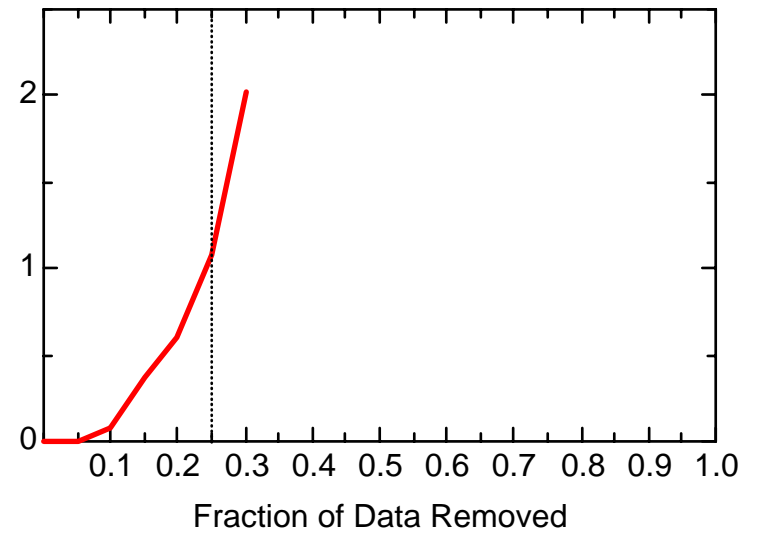
MN: Well JBW8003B



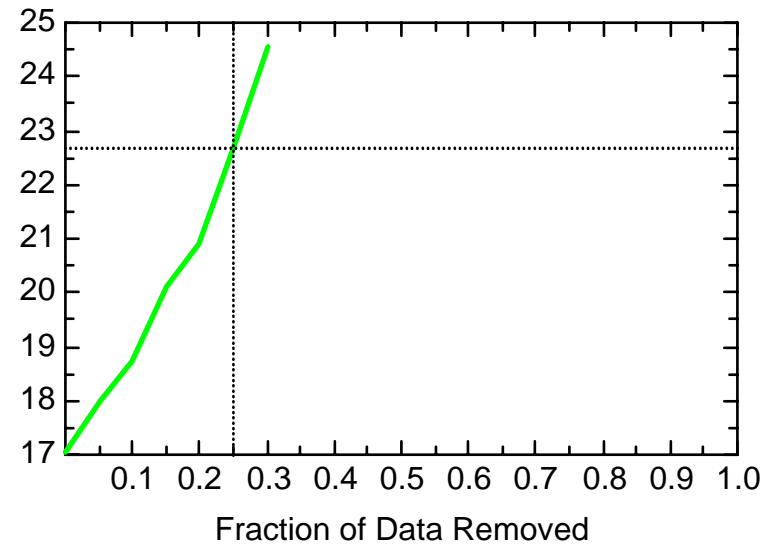
MN: Well JBW8004B



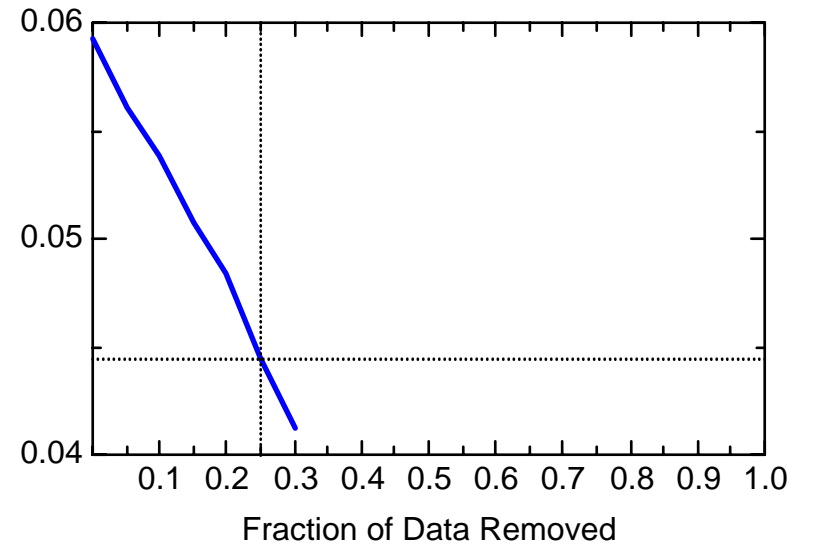
MN: Well JBW8004B



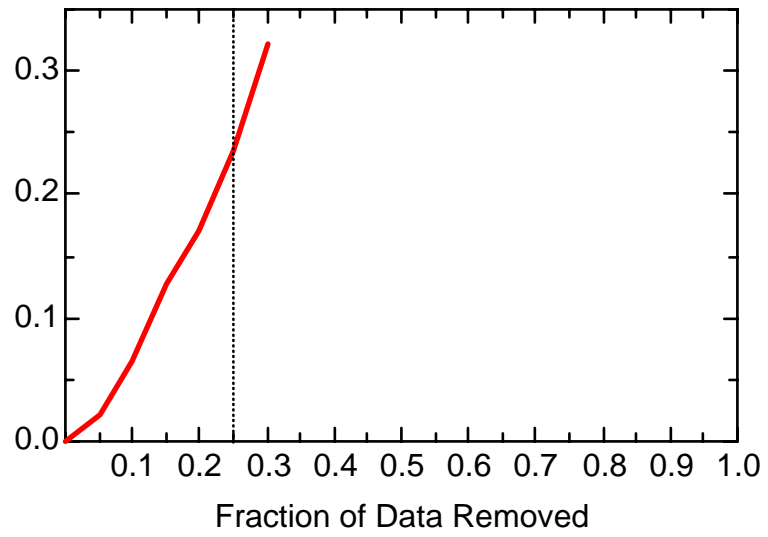
MN: Well JBW8004B



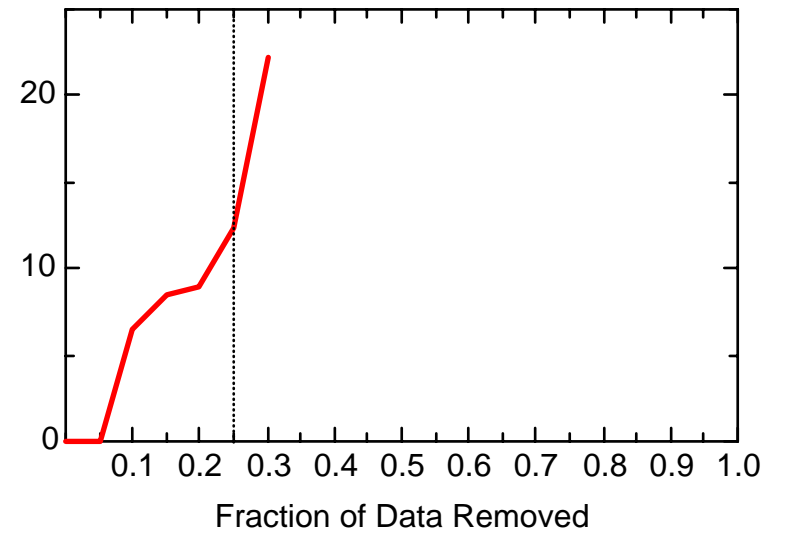
MN: Well JBW8004B



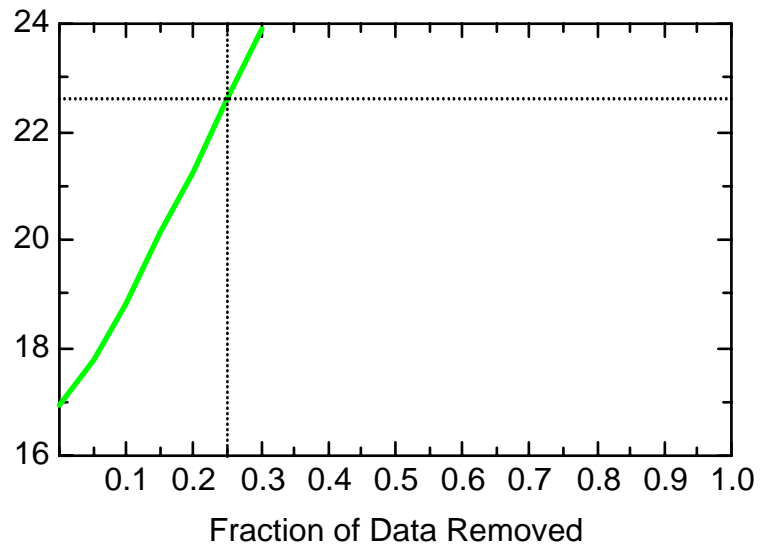
MN: Well JBW8009



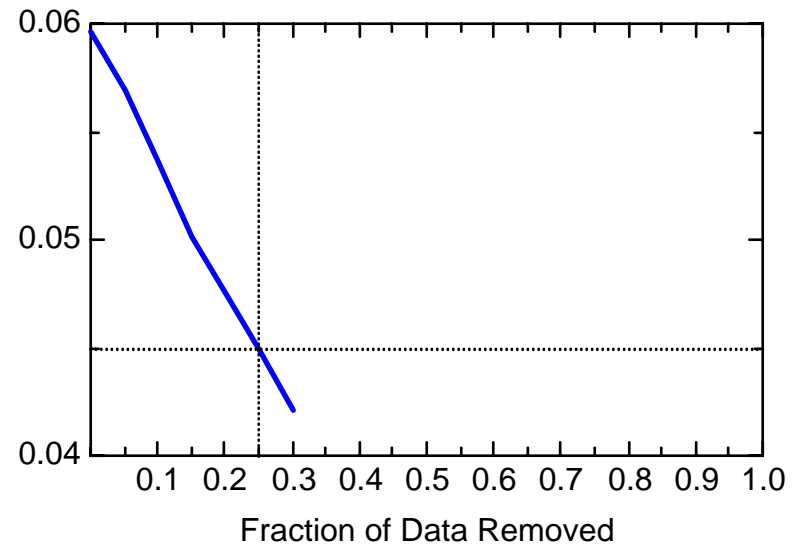
MN: Well JBW8009



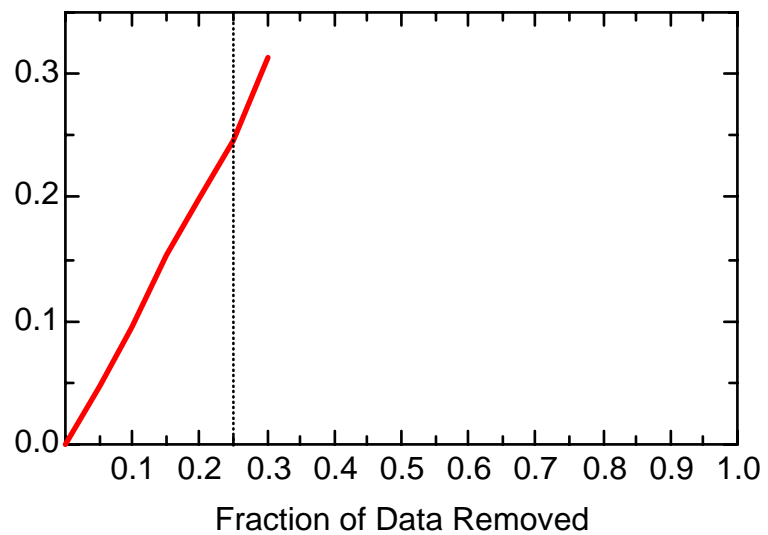
MN: Well JBW8009



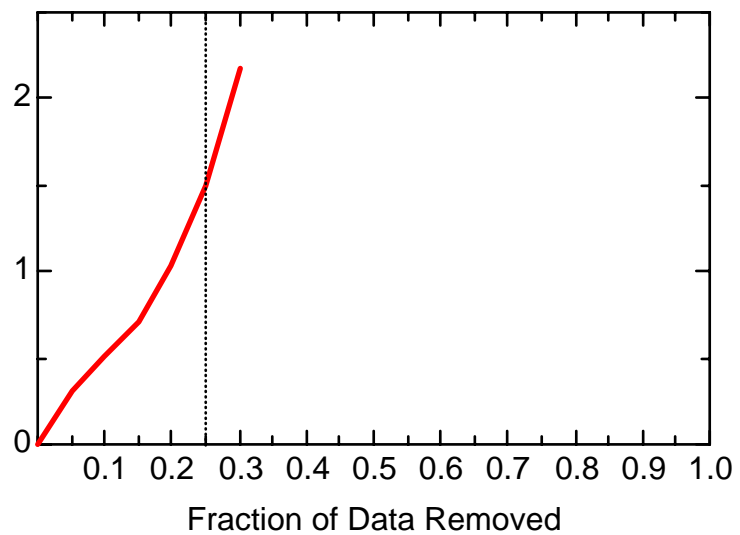
MN: Well JBW8009



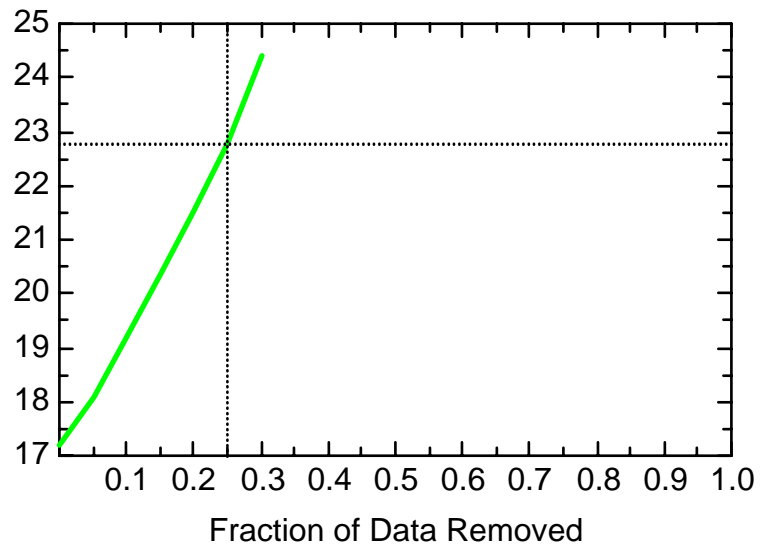
MN: Well JMW35X2



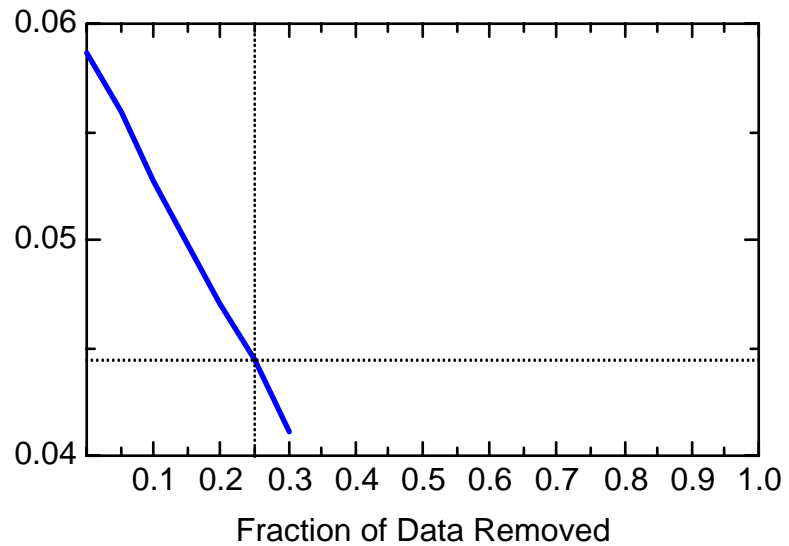
MN: Well JMW35X2



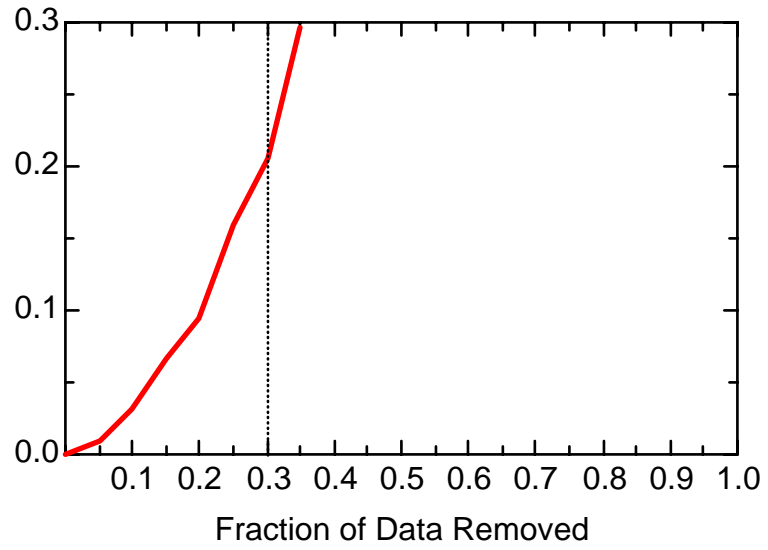
MN: Well JMW35X2



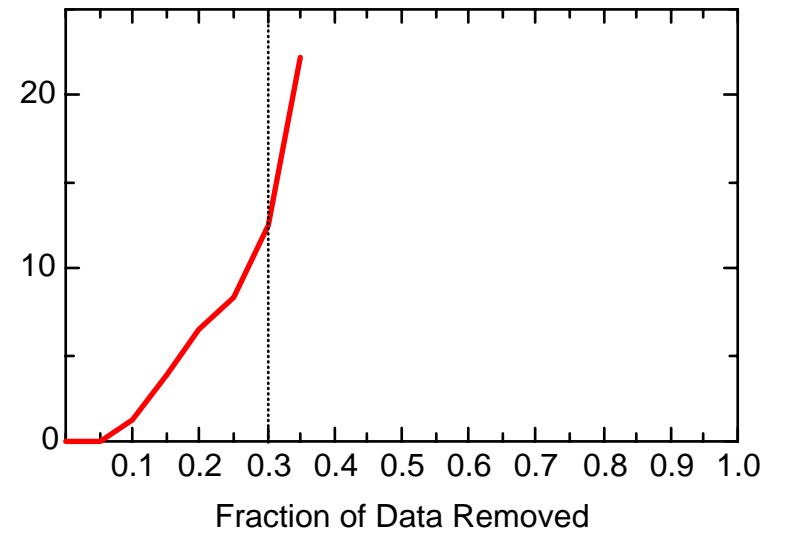
MN: Well JMW35X2



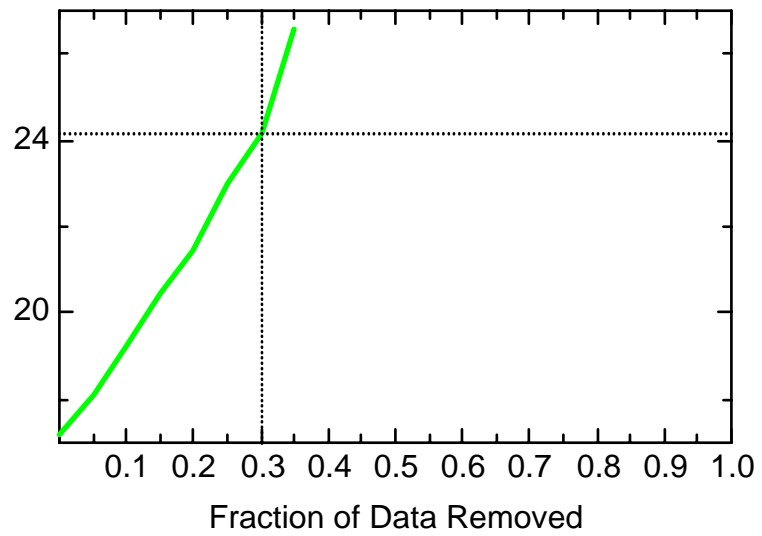
MN: Well JMW0301C



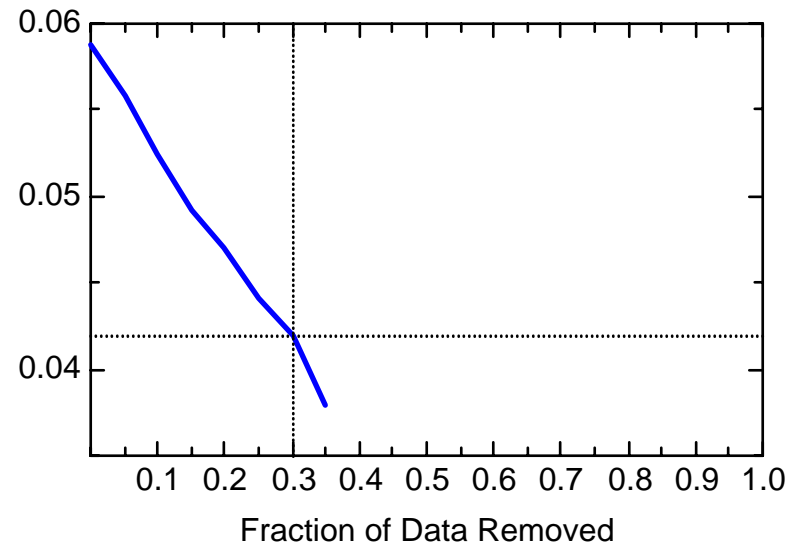
MN: Well JMW0301C



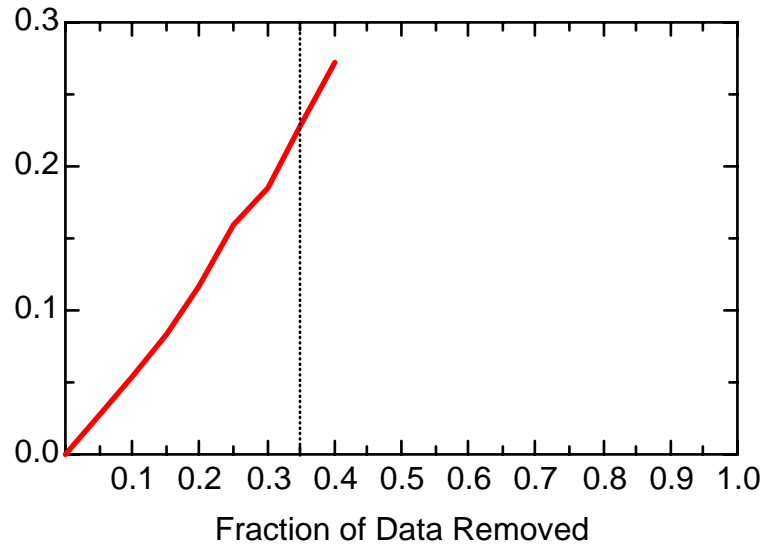
MN: Well JMW0301C



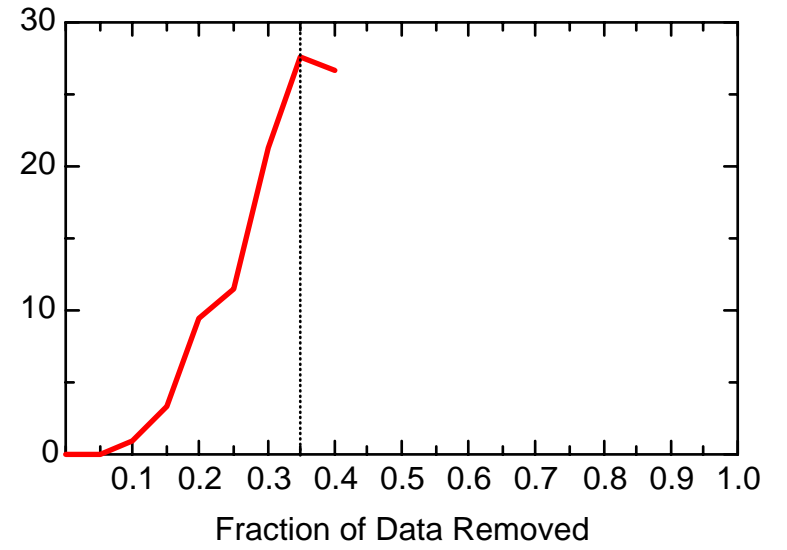
MN: Well JMW0301C



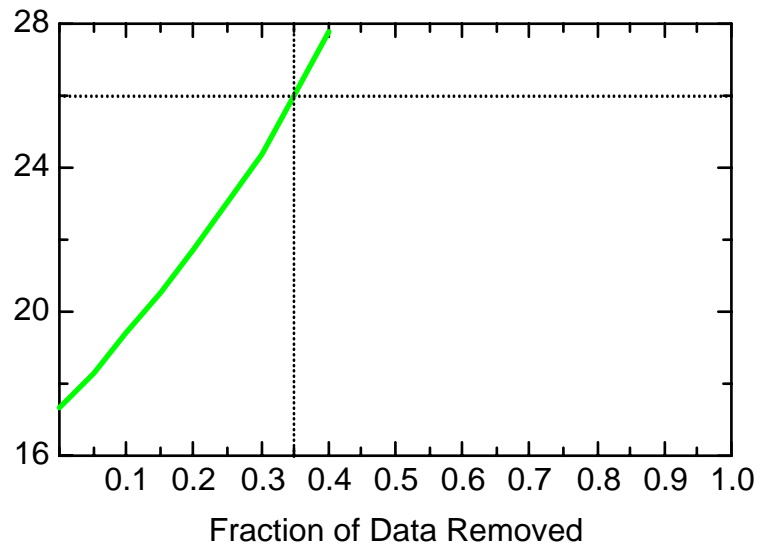
MN: Well JMW0503



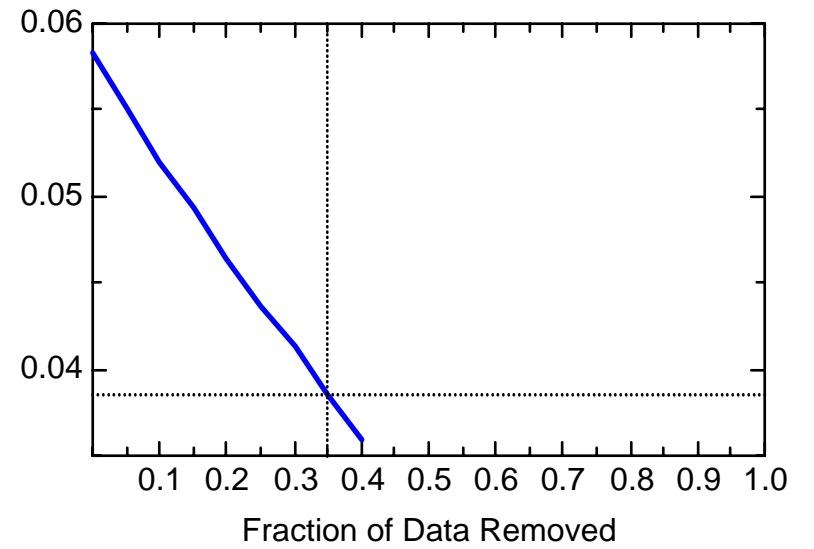
MN: Well JMW0503



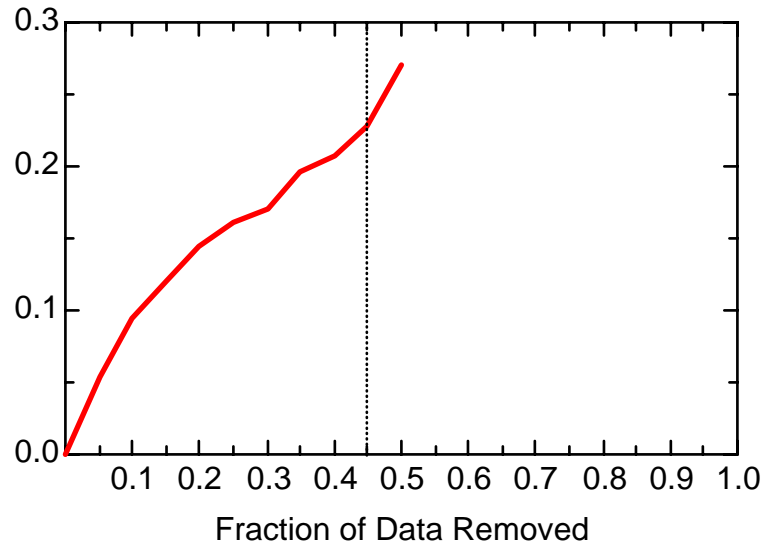
MN: Well JMW0503



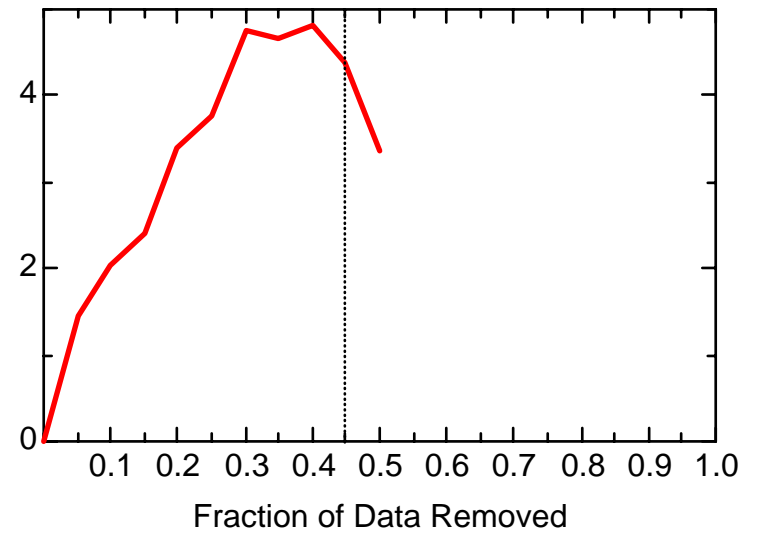
MN: Well JMW0503



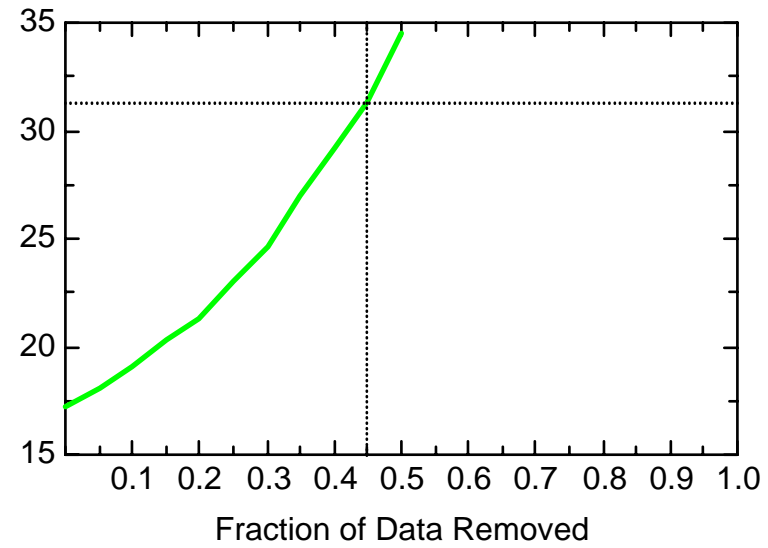
MN: Well JMW0505



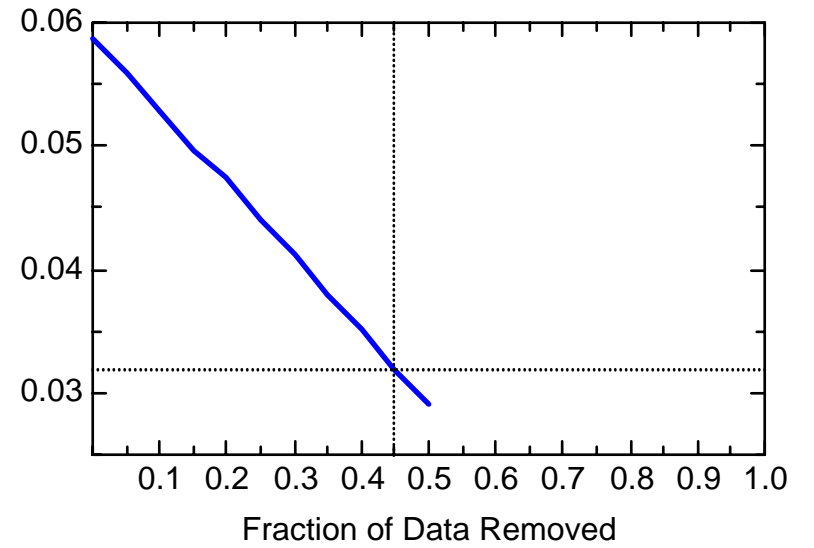
MN: Well JMW0505



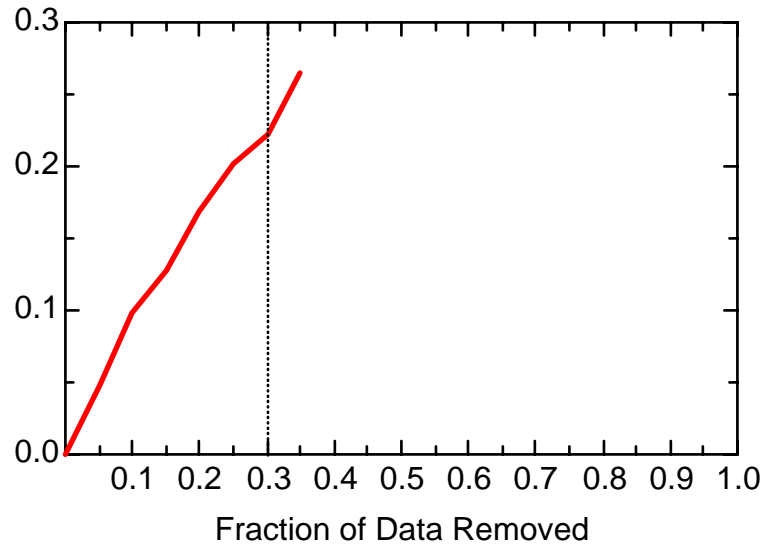
MN: Well JMW0505



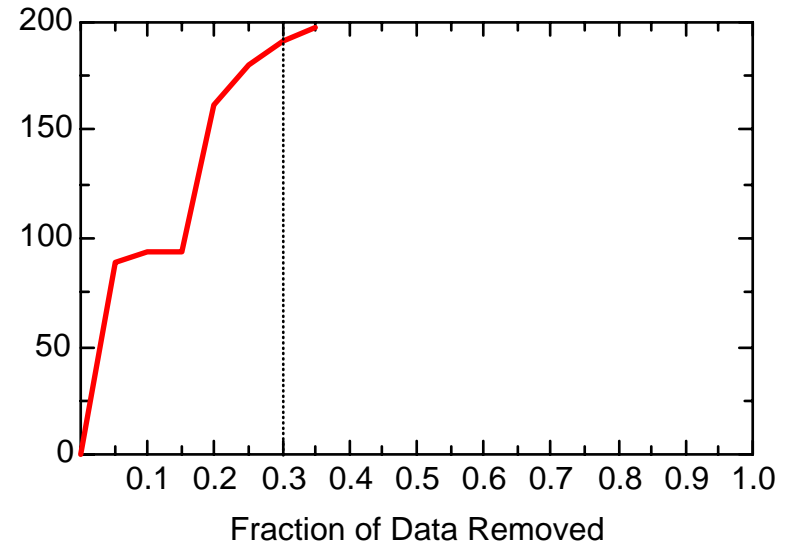
MN: Well JMW0505



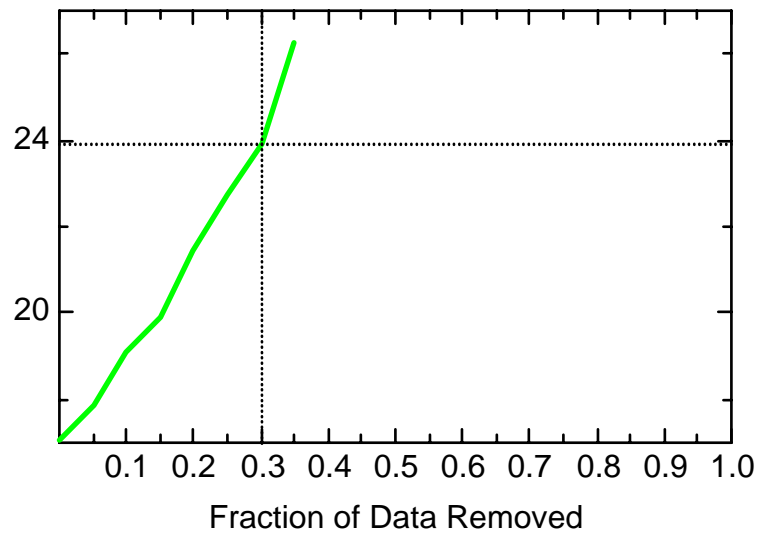
MN: Well JMW0542



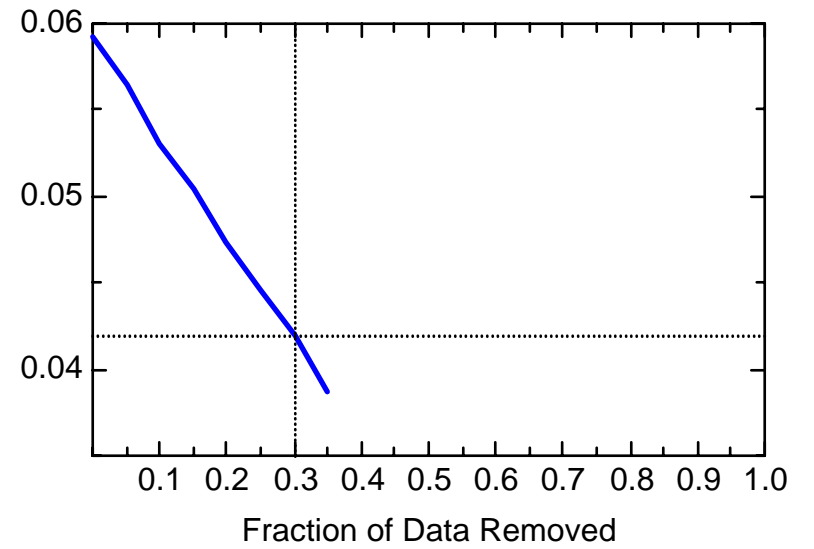
MN: Well JMW0542



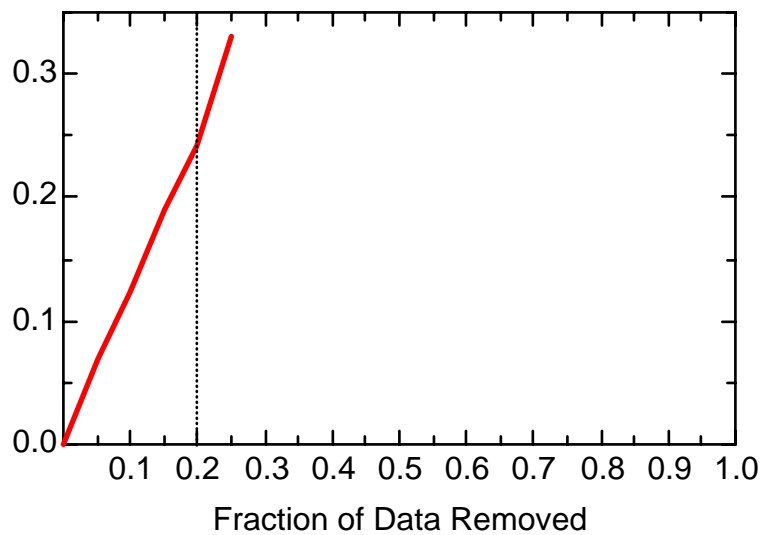
MN: Well JMW0542



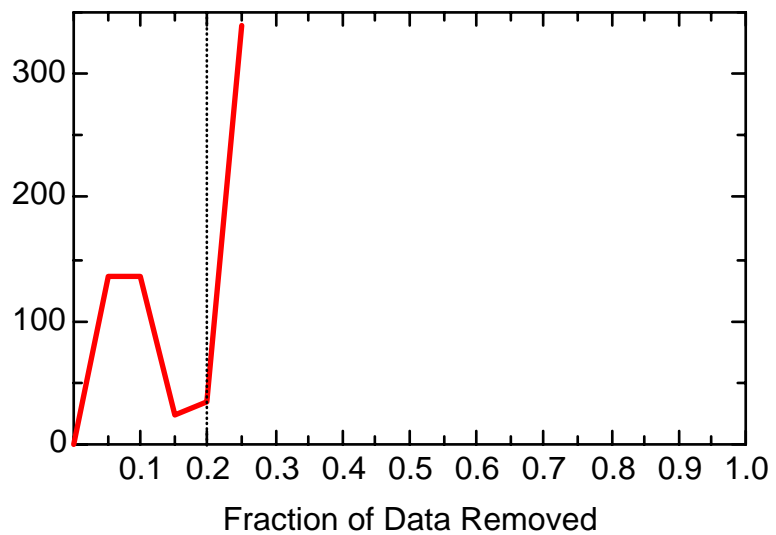
MN: Well JMW0542



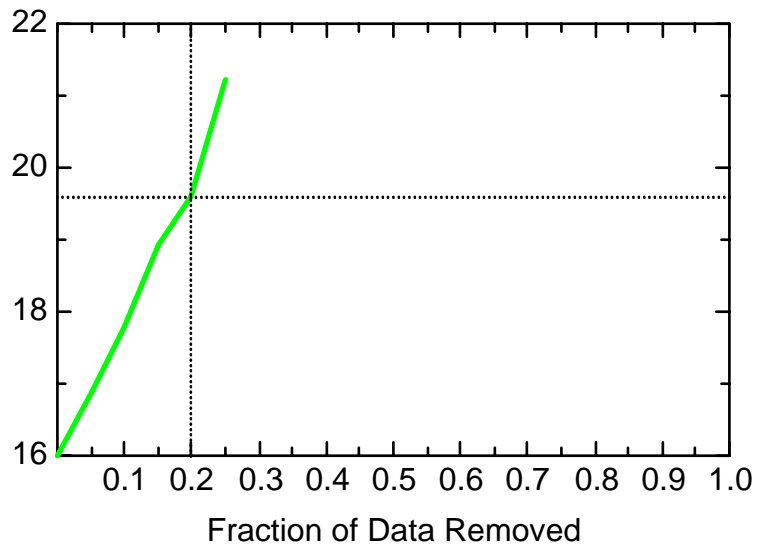
MN: Well JMW1103D



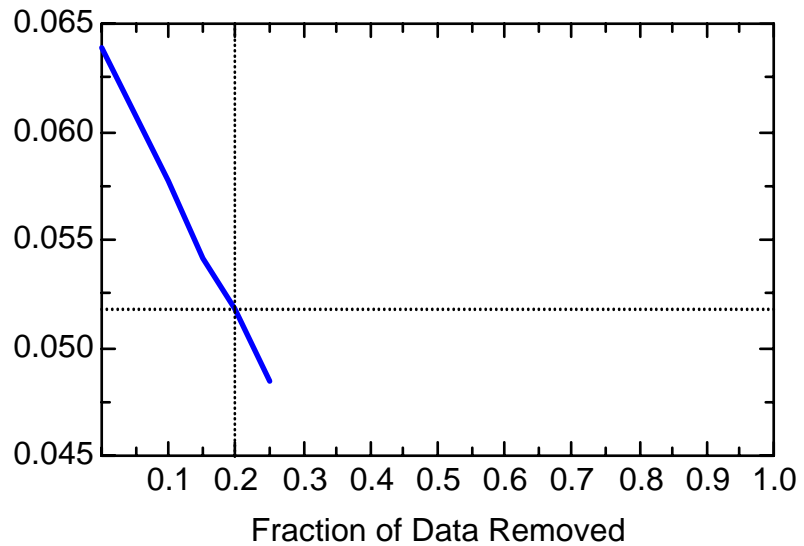
MN: Well JMW1103D



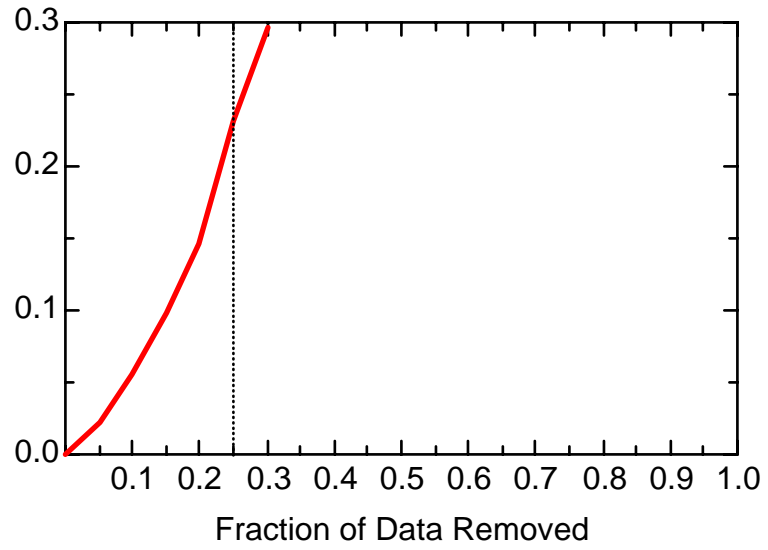
MN: Well JMW1103D



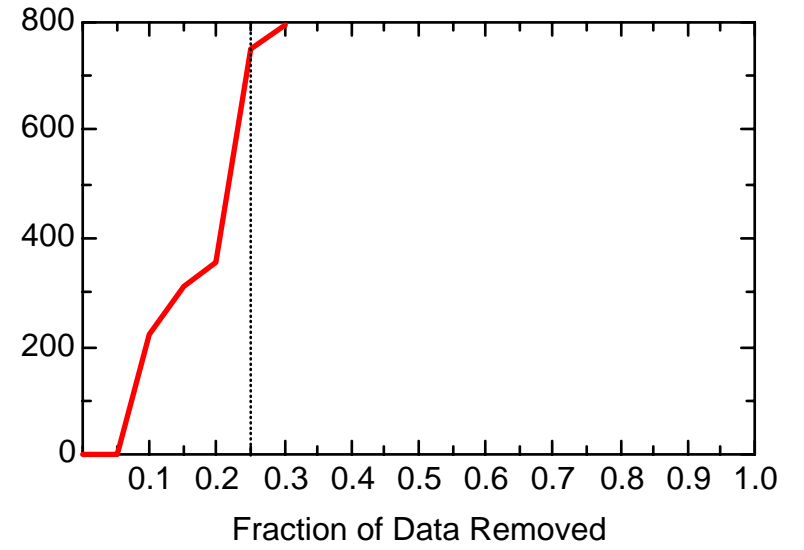
MN: Well JMW1103D



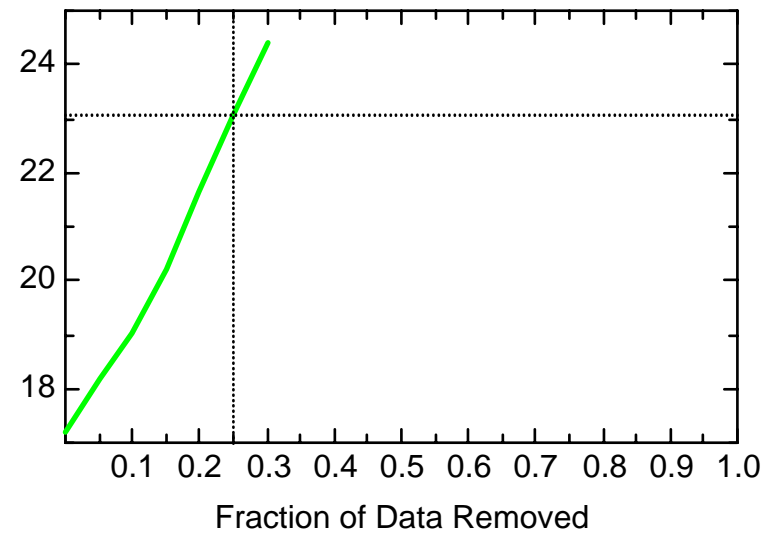
MN: Well JMW1565



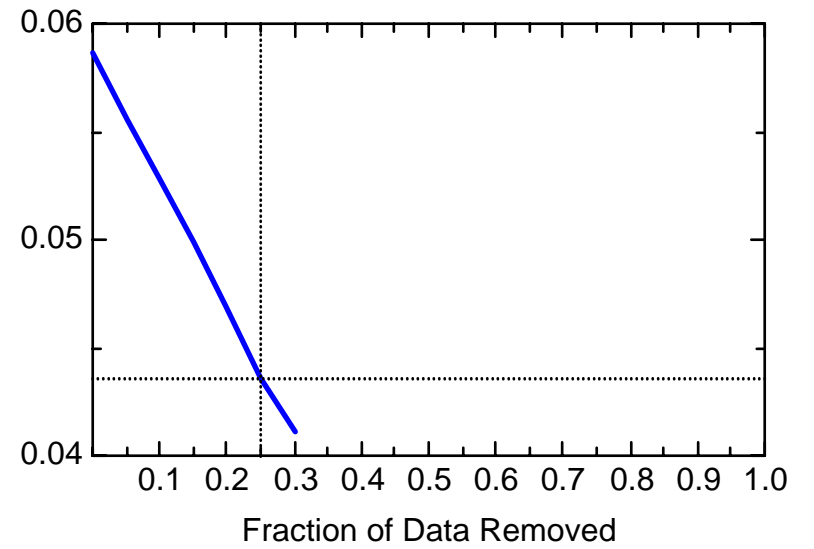
MN: Well JMW1565



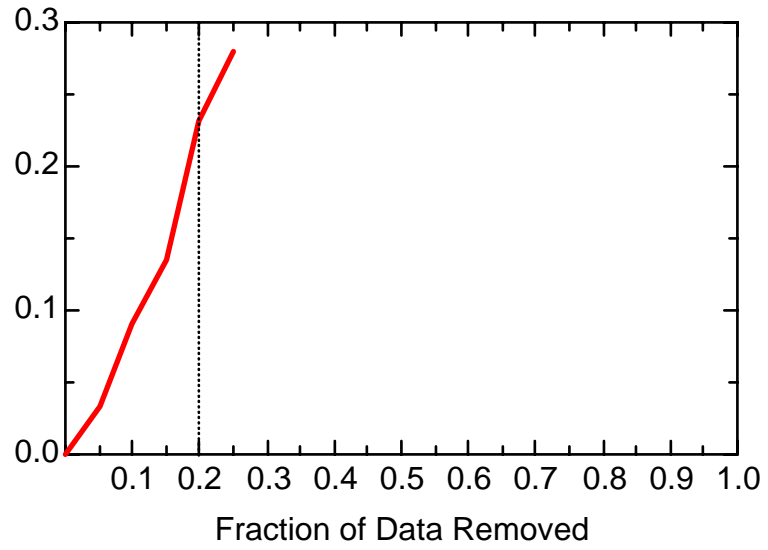
MN: Well JMW1565



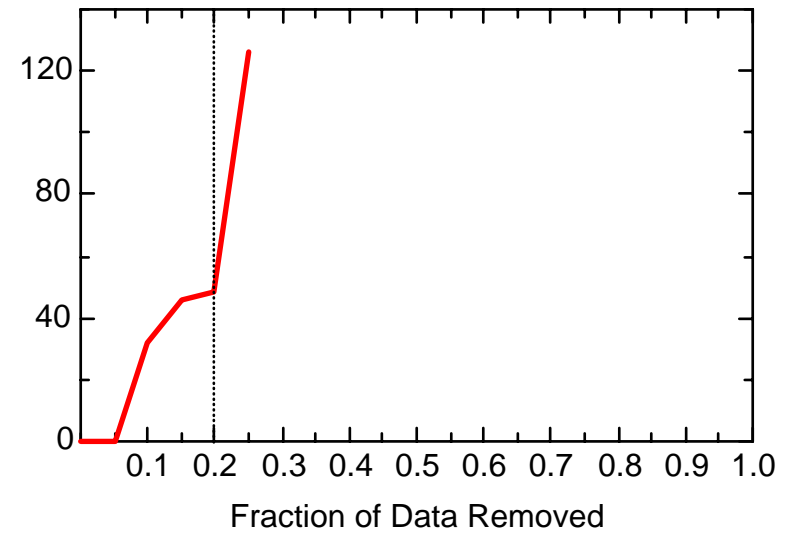
MN: Well JMW1565



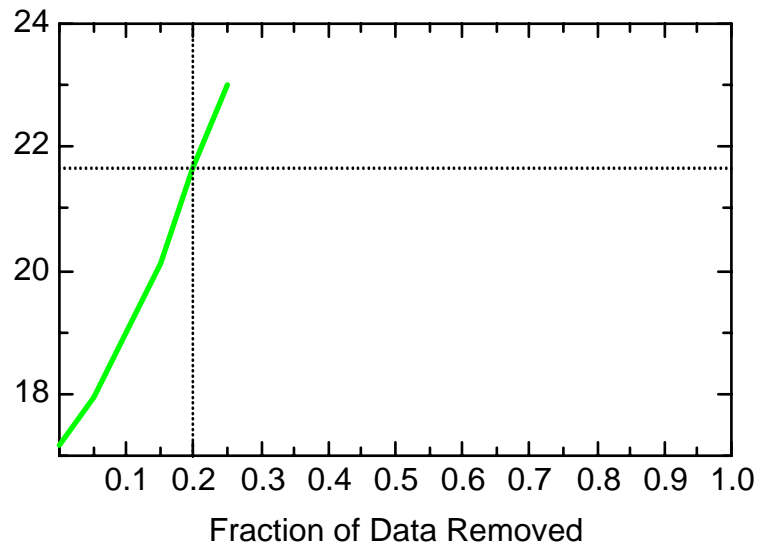
MN: Well JMW1860



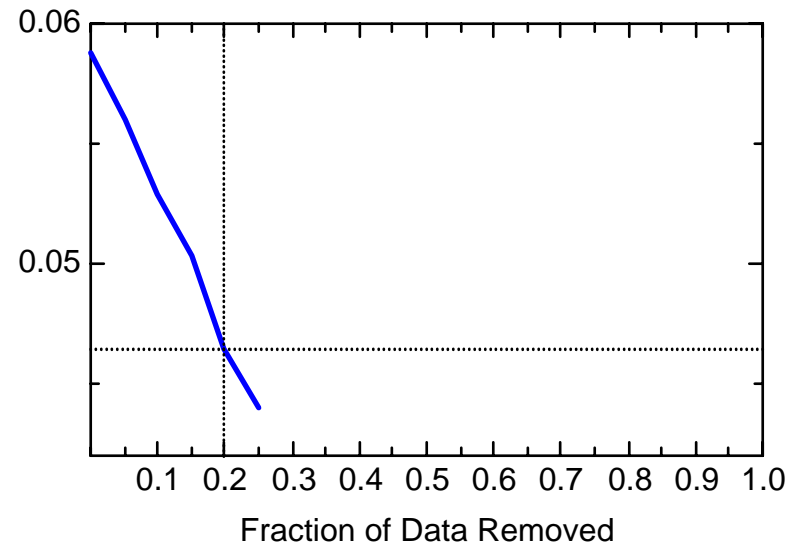
MN: Well JMW1860



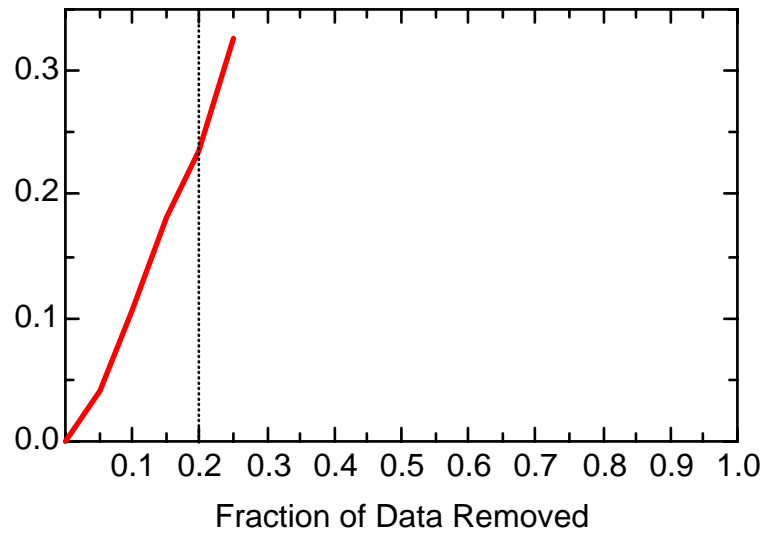
MN: Well JMW1860



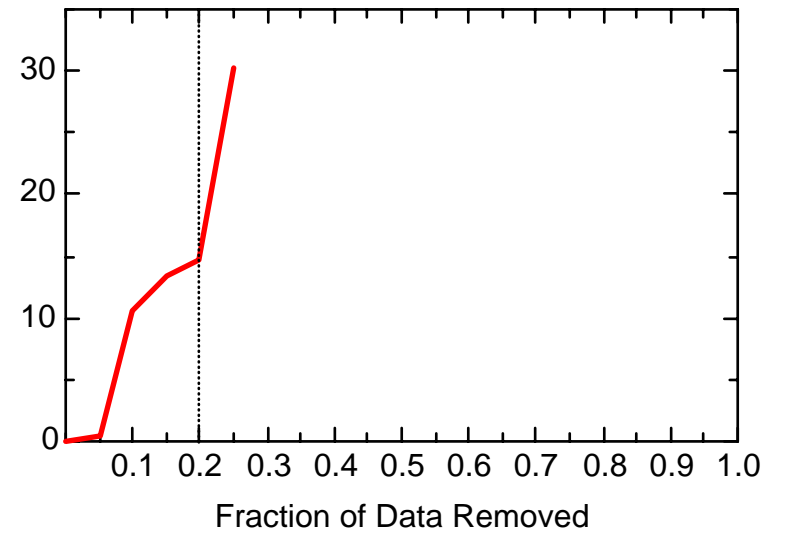
MN: Well JMW1860



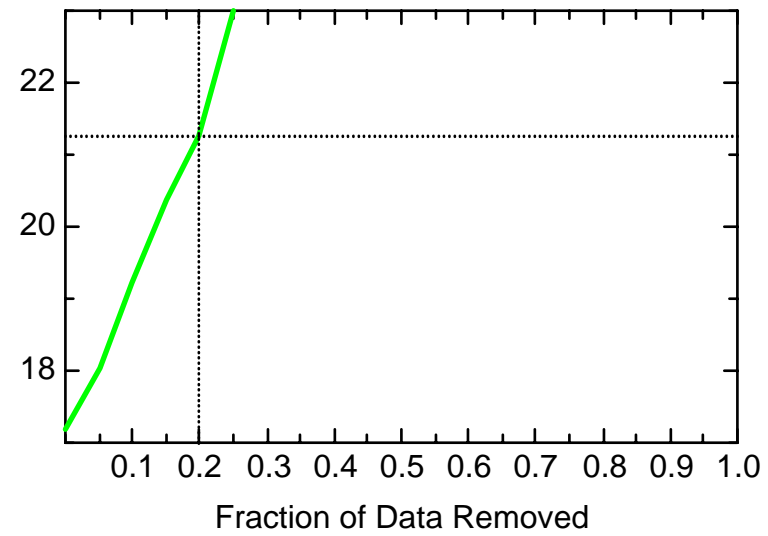
MN: Well JMW1881



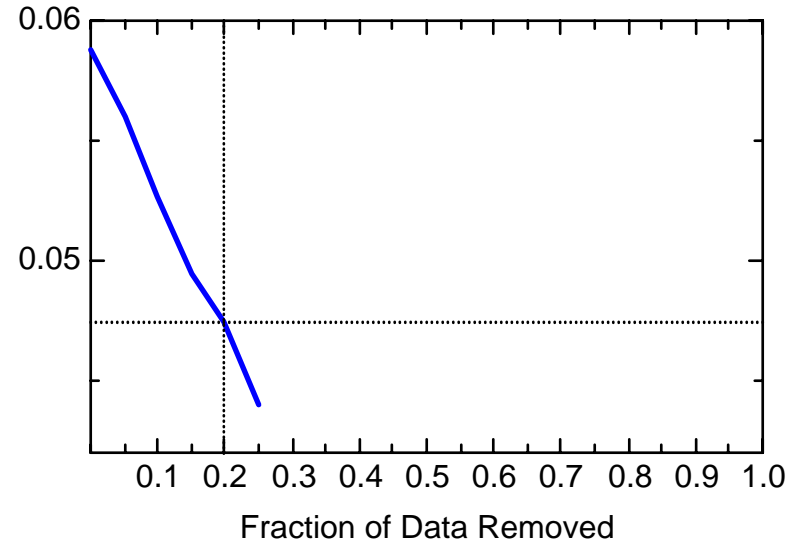
MN: Well JMW1881



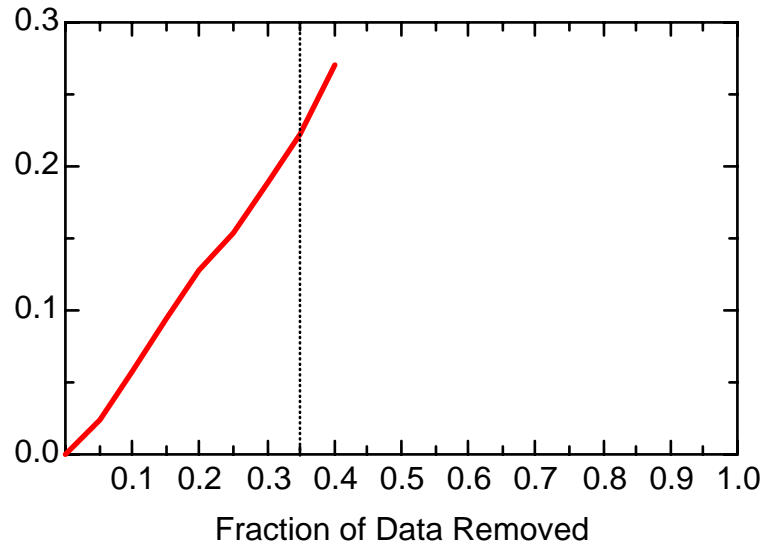
MN: Well JMW1881



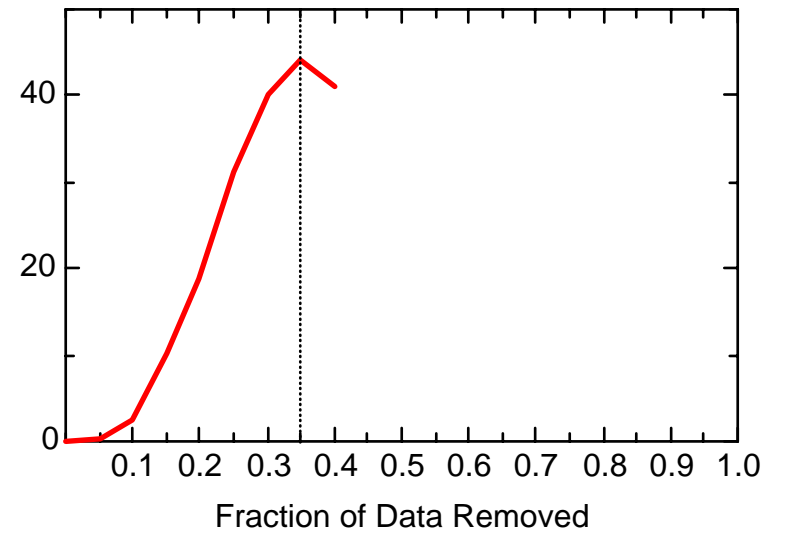
MN: Well JMW1881



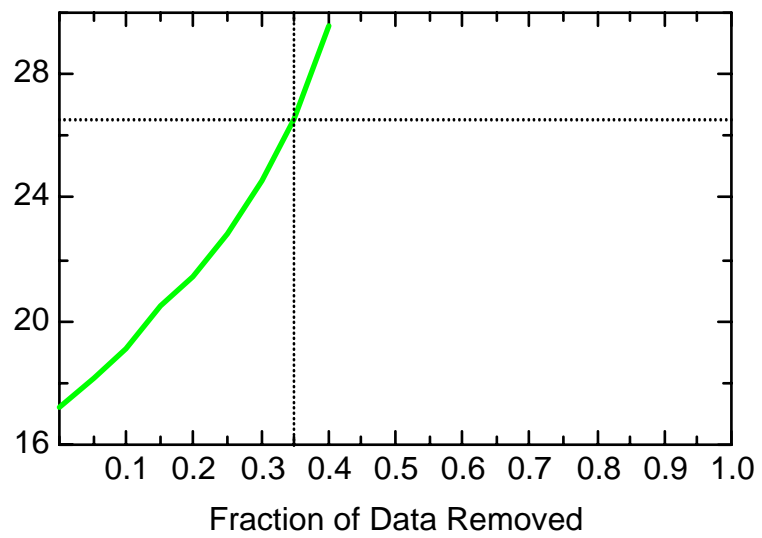
MN: Well JMW1963



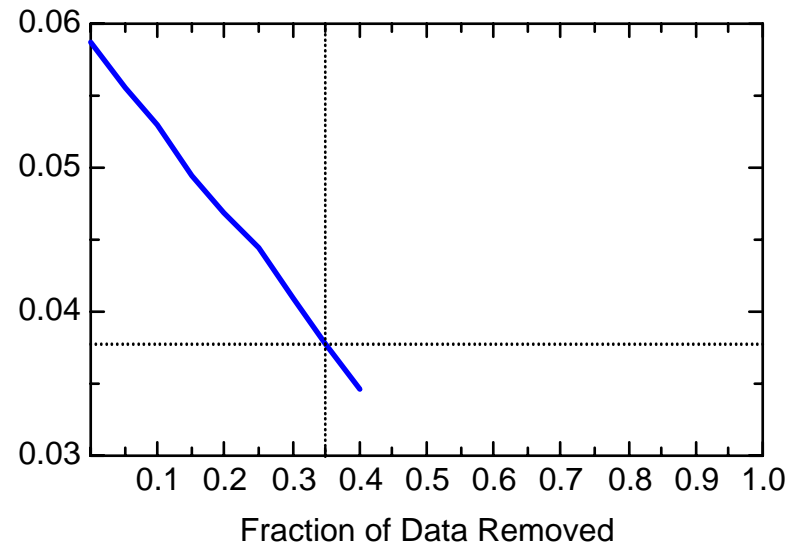
MN: Well JMW1963



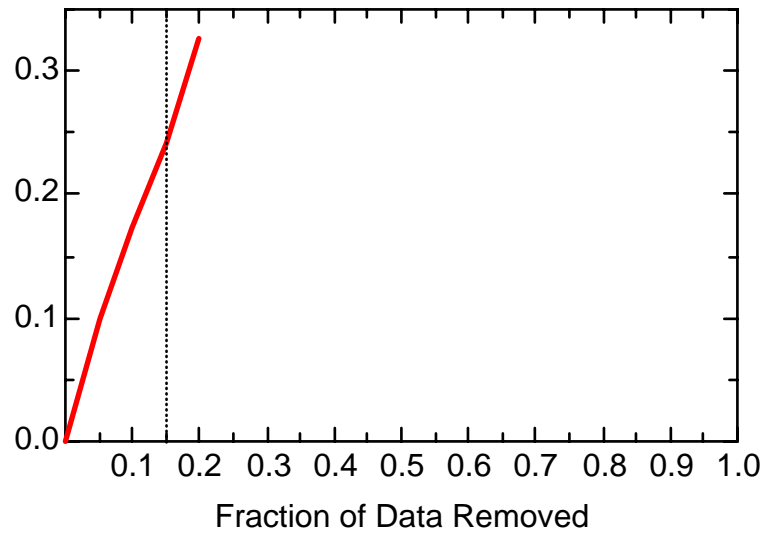
MN: Well JMW1963



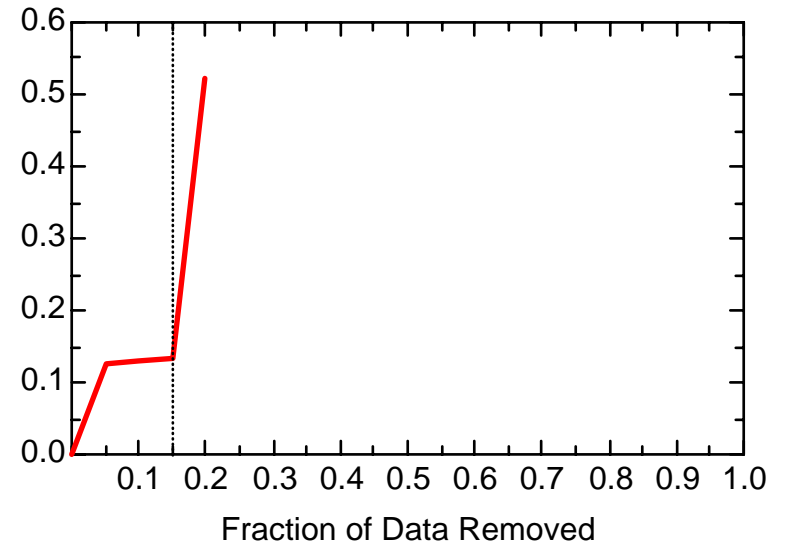
MN: Well JMW1963



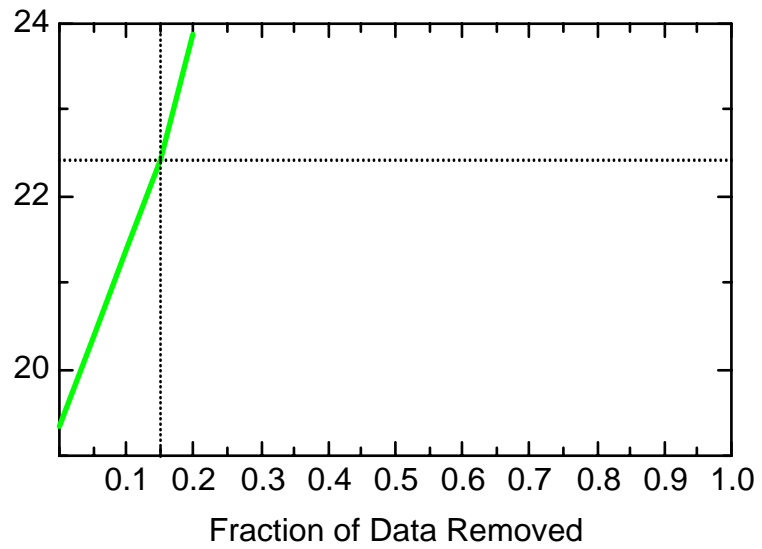
MN: Well JMW1964



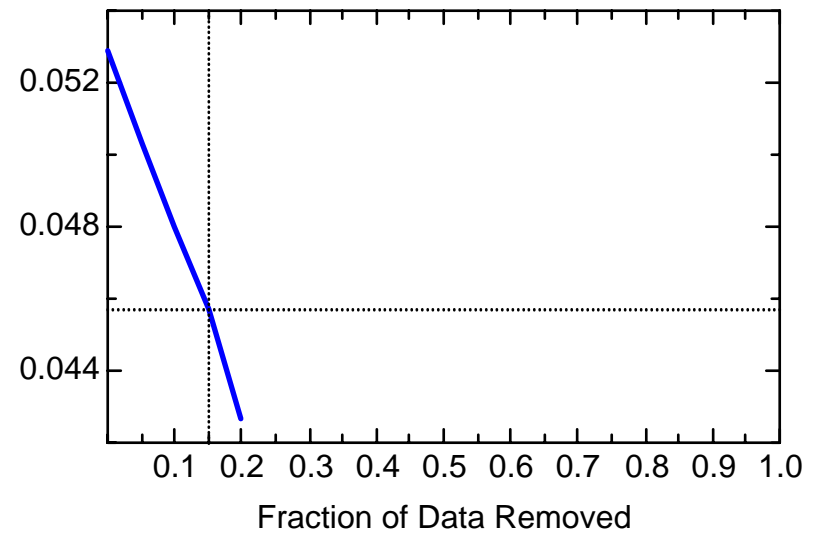
MN: Well JMW1964



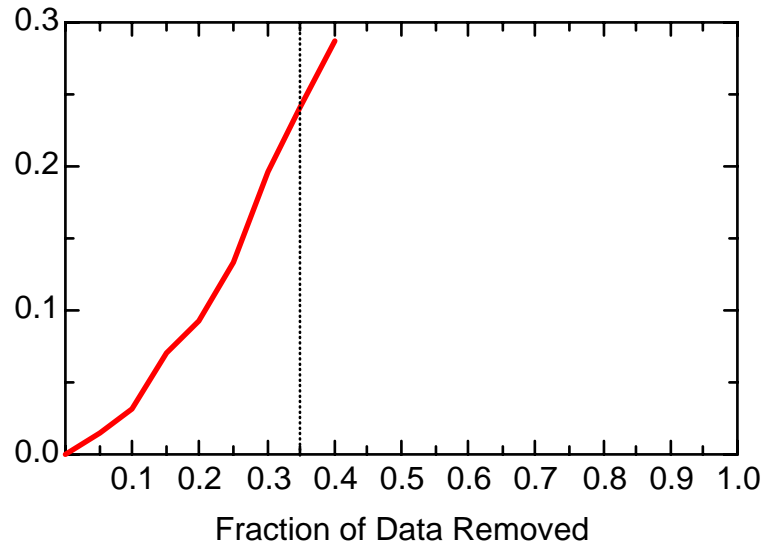
MN: Well JMW1964



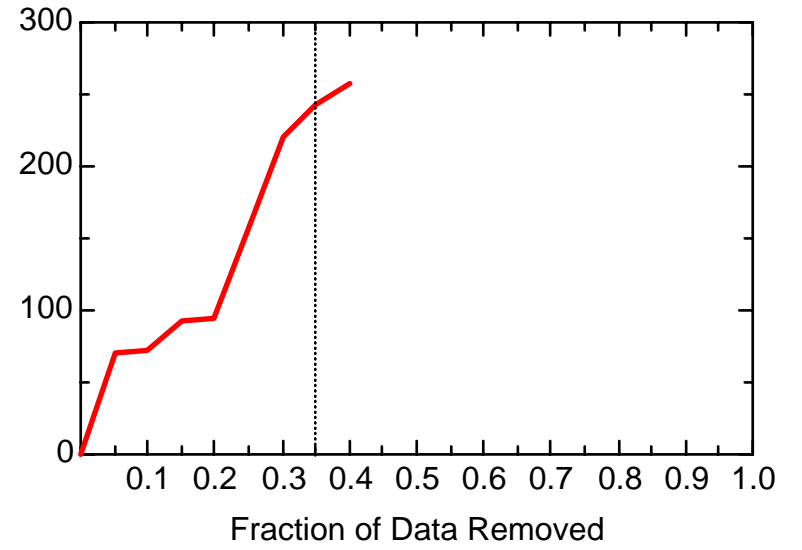
MN: Well JMW1964



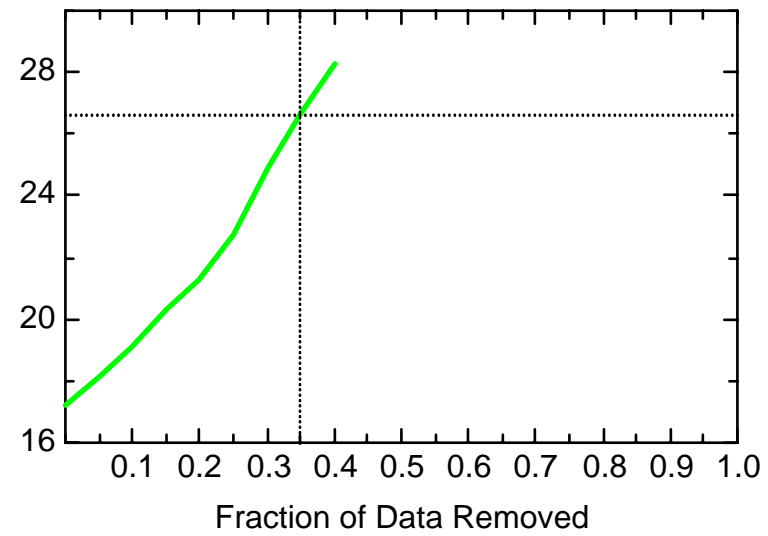
MN: Well JMW1966



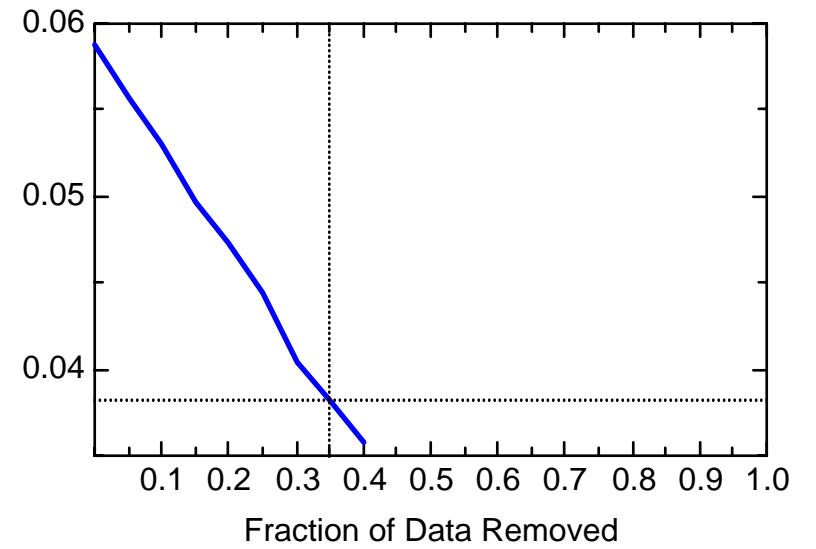
MN: Well JMW1966



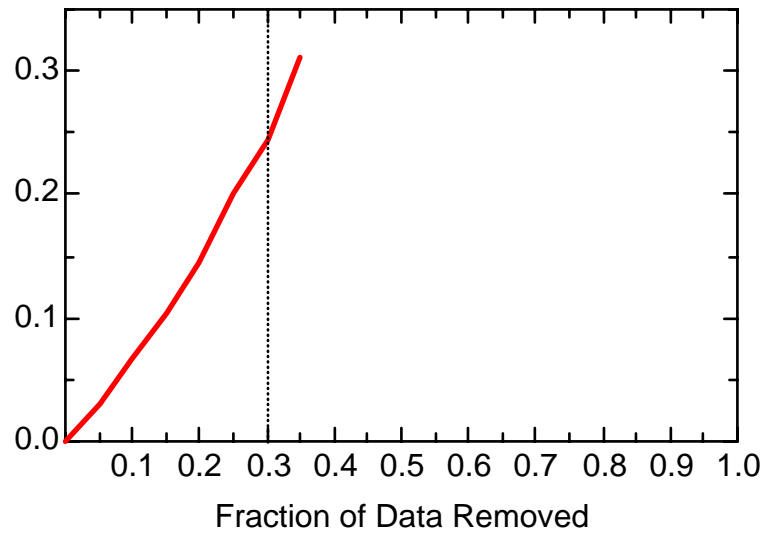
MN: Well JMW1966



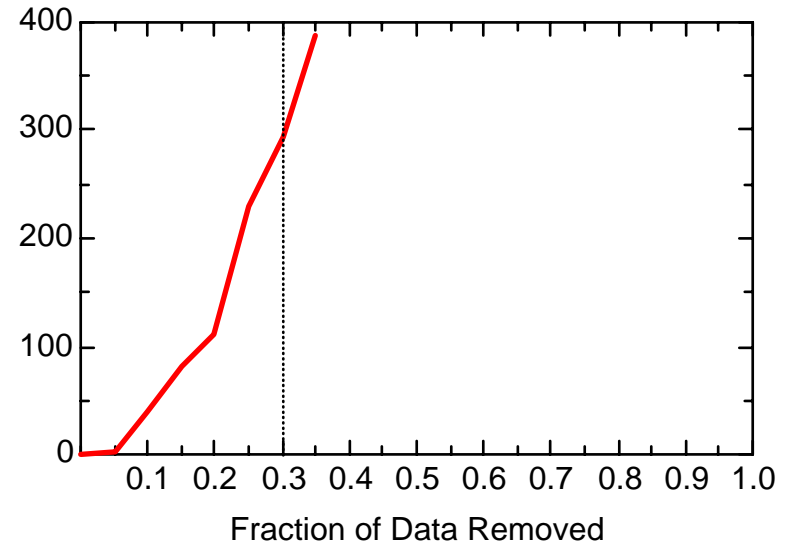
MN: Well JMW1966



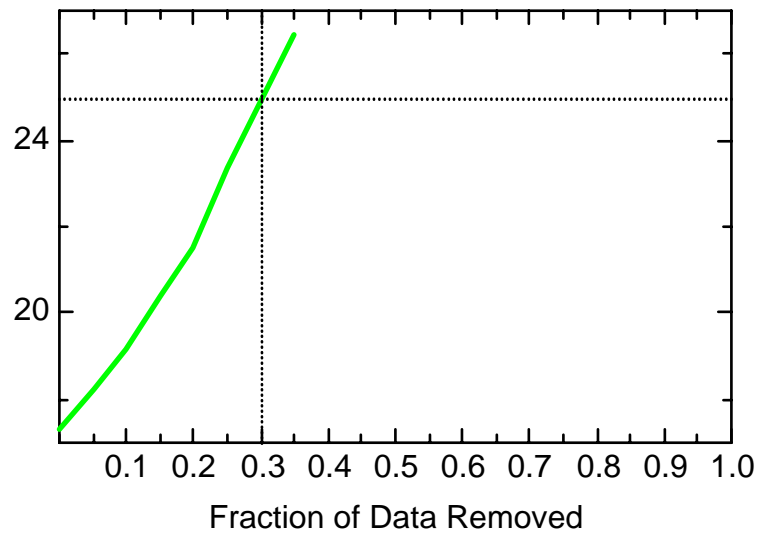
MN: Well JMW3202



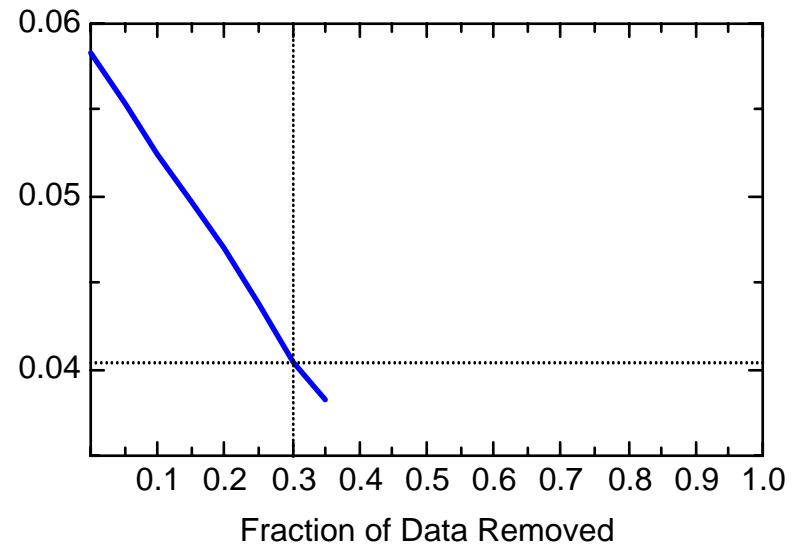
MN: Well JMW3202



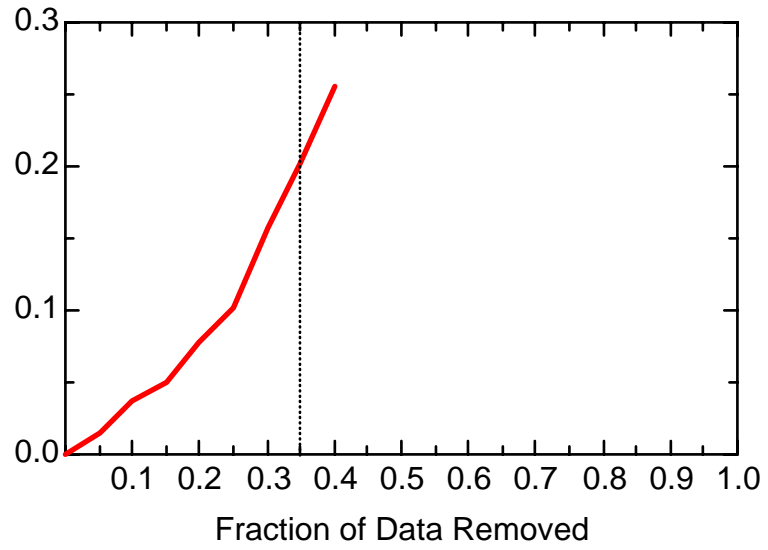
MN: Well JMW3202



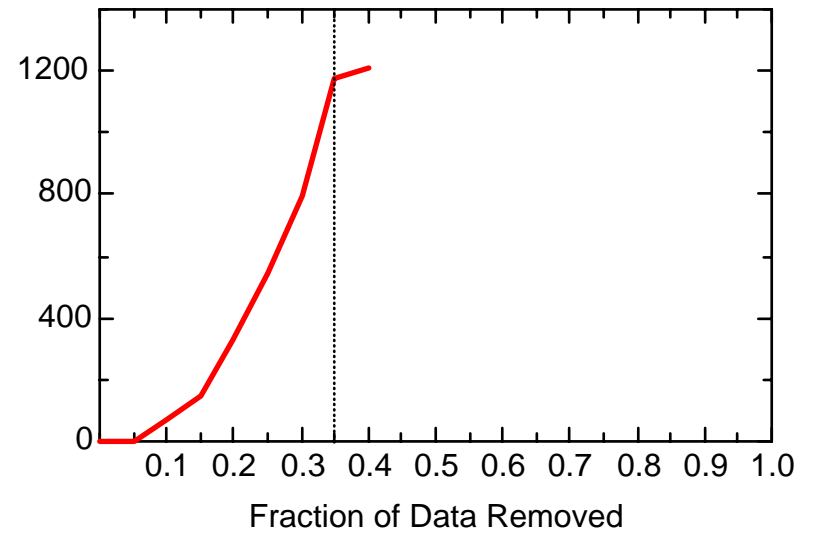
MN: Well JMW3202



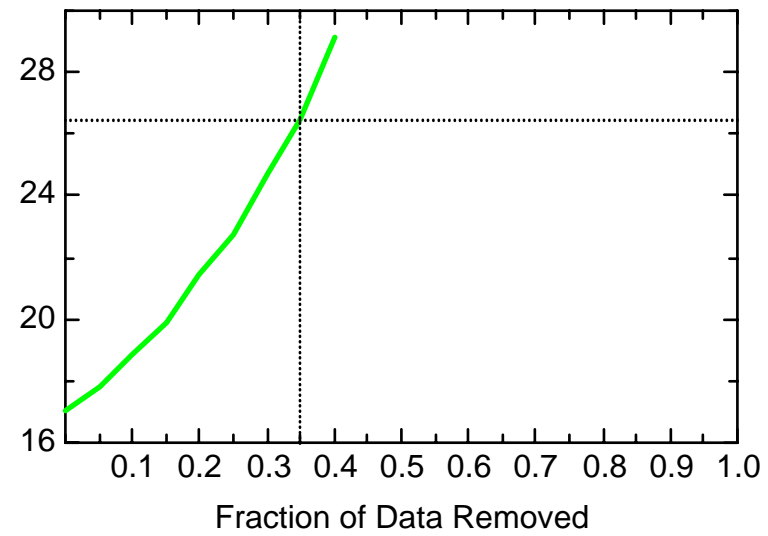
MN: Well JMW7332



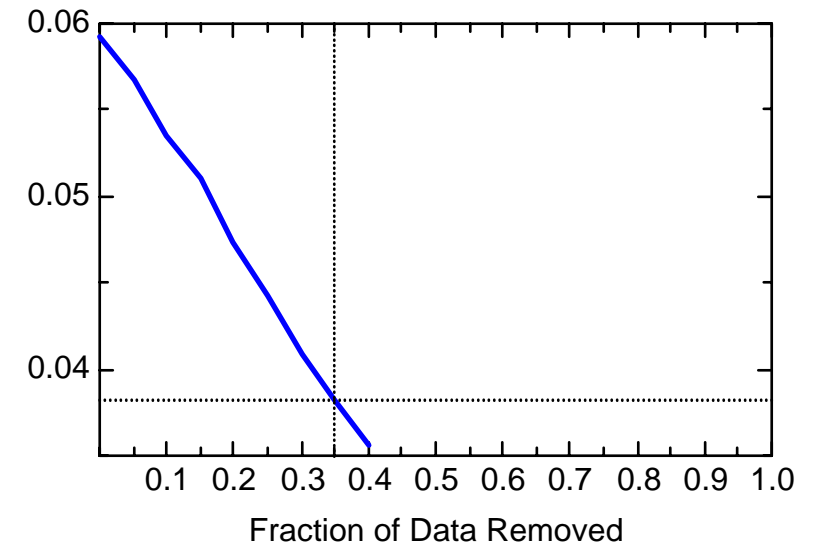
MN: Well JMW7332



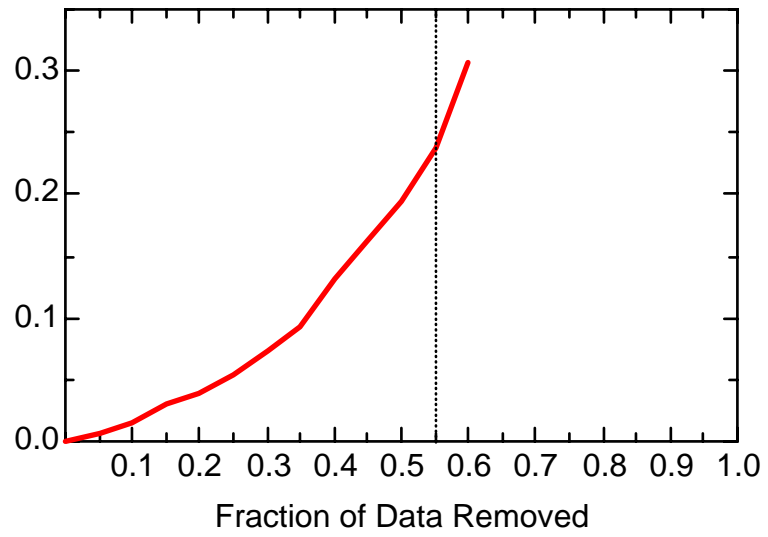
MN: Well JMW7332



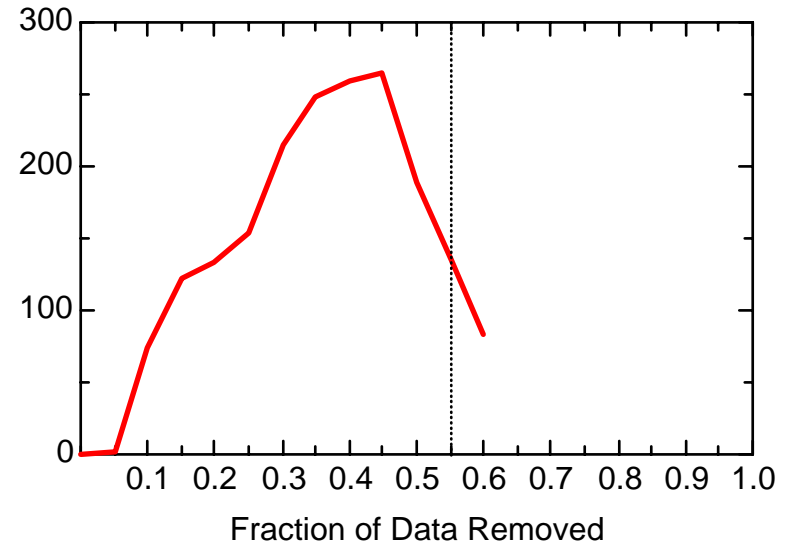
MN: Well JMW7332



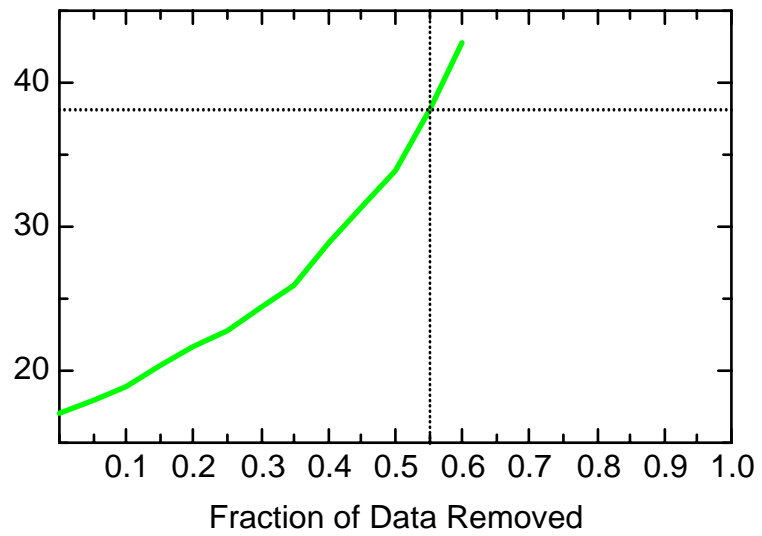
MN: Well JMW8011



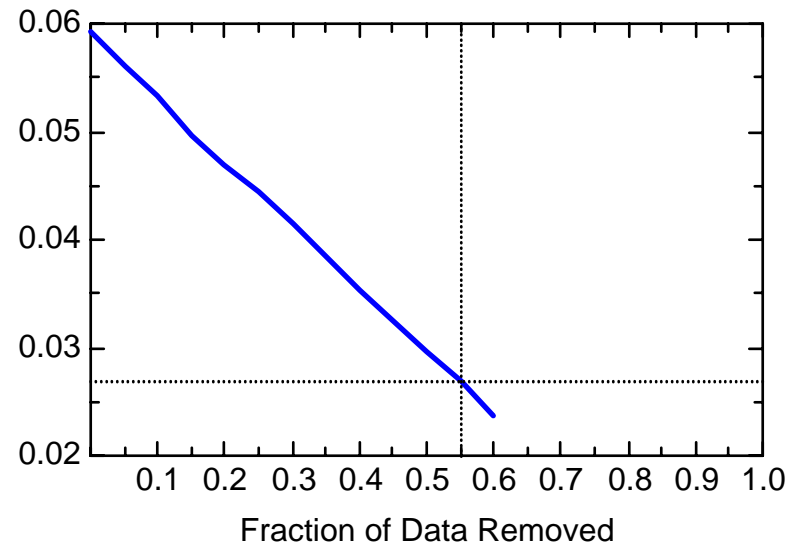
MN: Well JMW8011



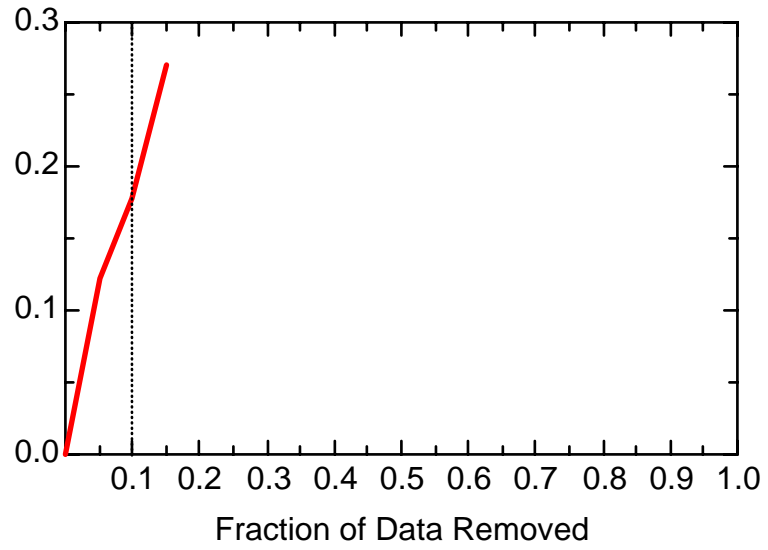
MN: Well JMW8011



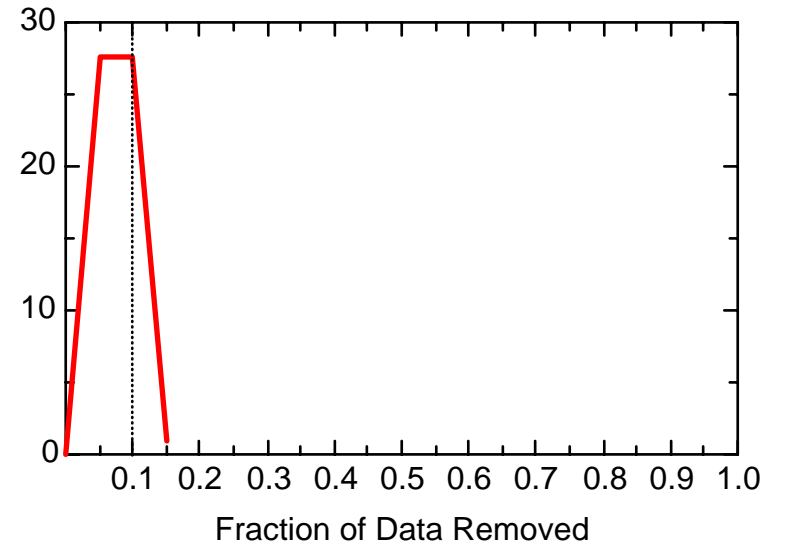
MN: Well JMW8011



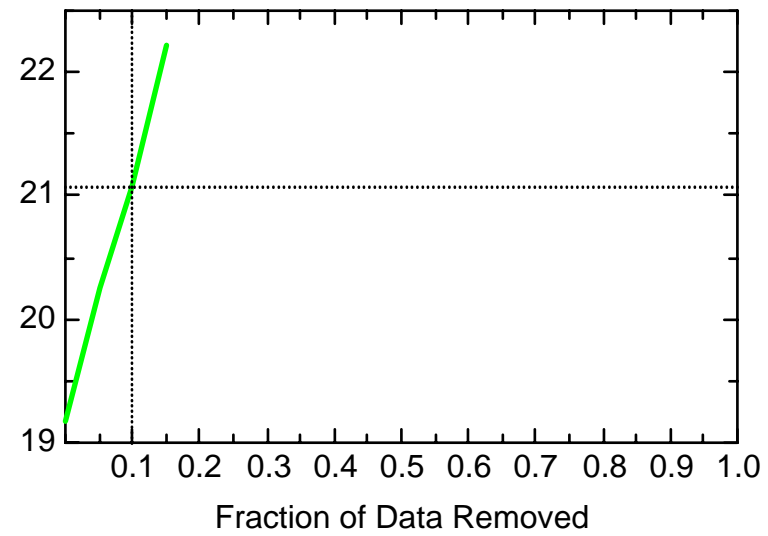
MN: Well JPZ0340



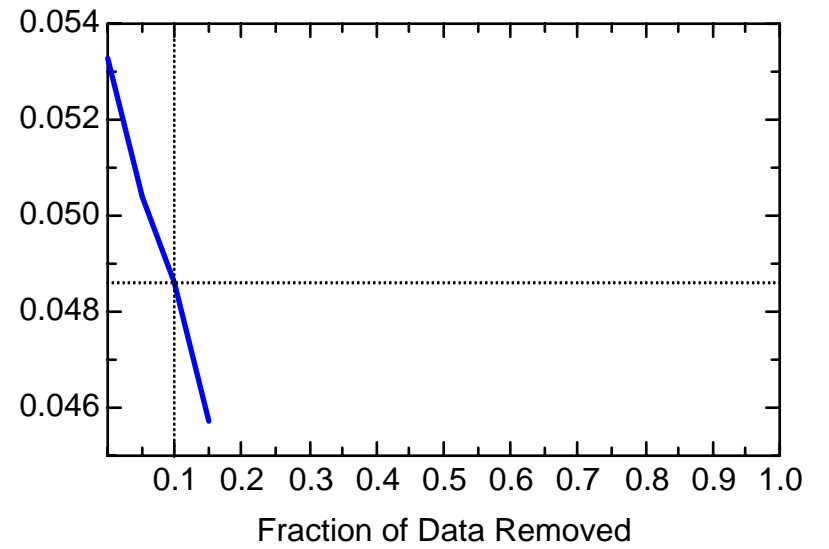
MN: Well JPZ0340



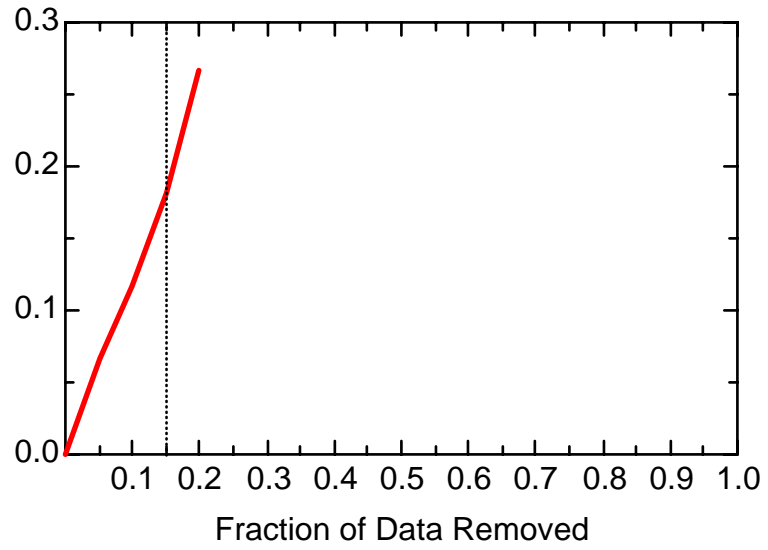
MN: Well JPZ0340



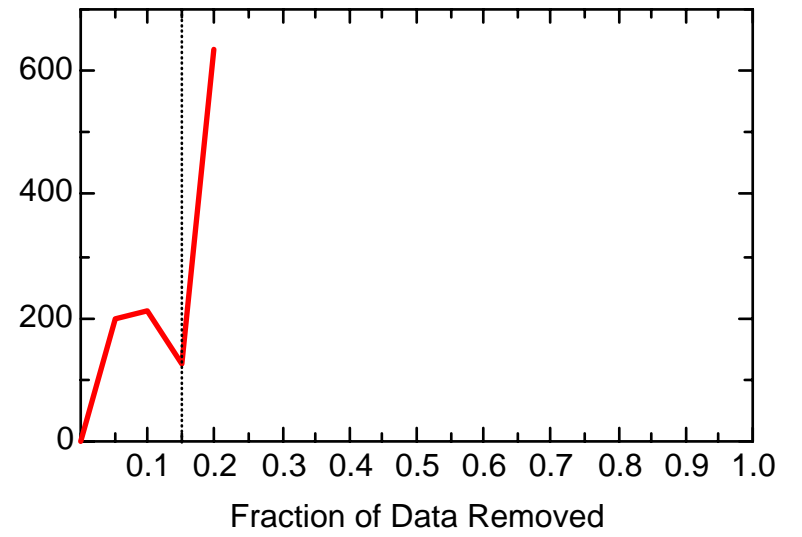
MN: Well JPZ0340



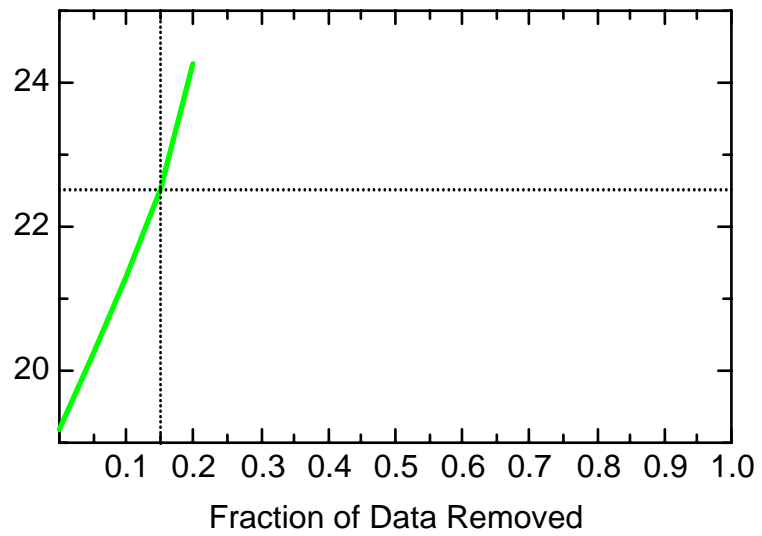
MN: Well JPZ0341



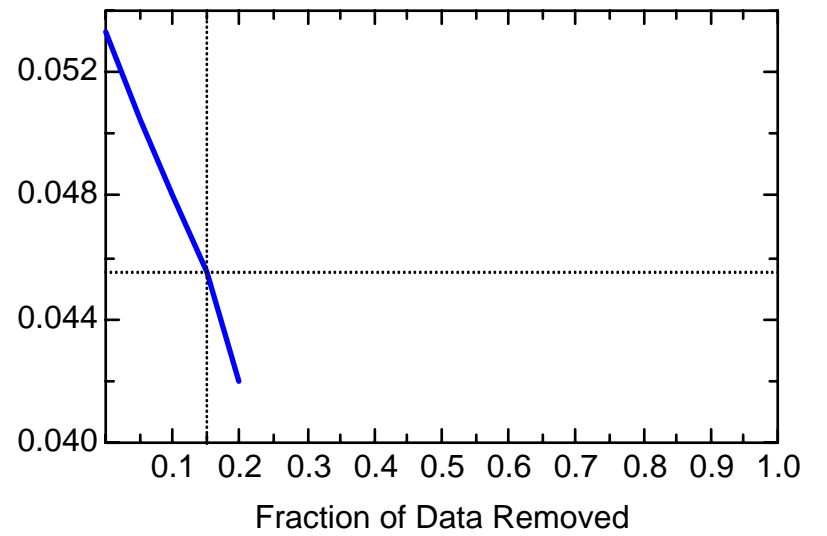
MN: Well JPZ0341



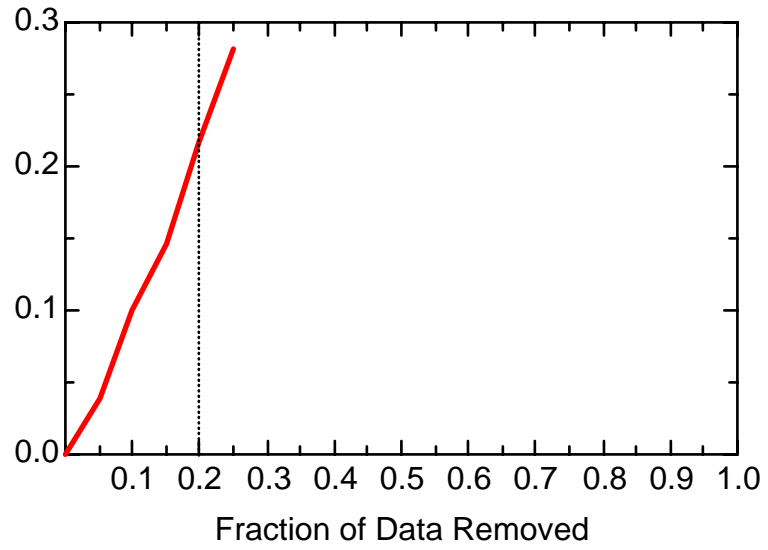
MN: Well JPZ0341



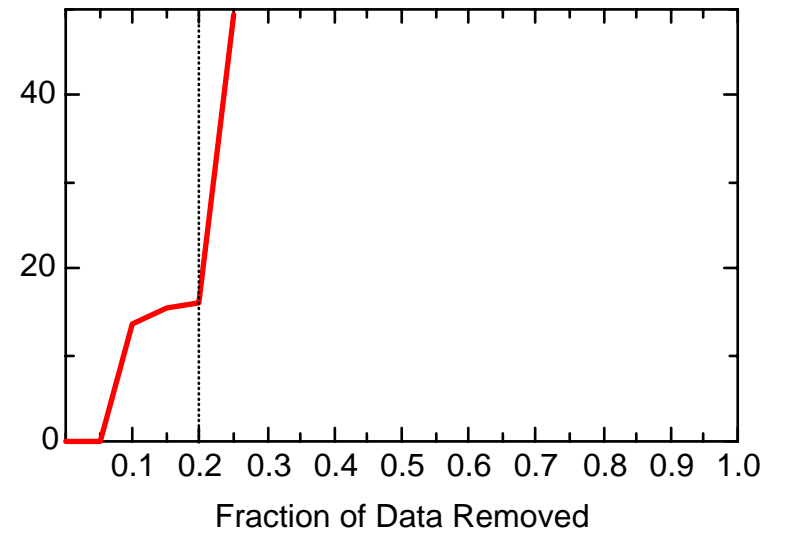
MN: Well JPZ0341



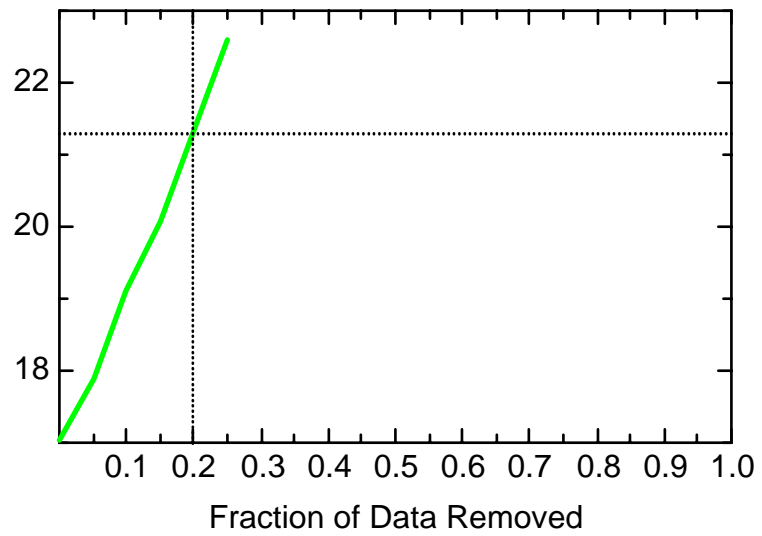
MN: Well JPZ0342



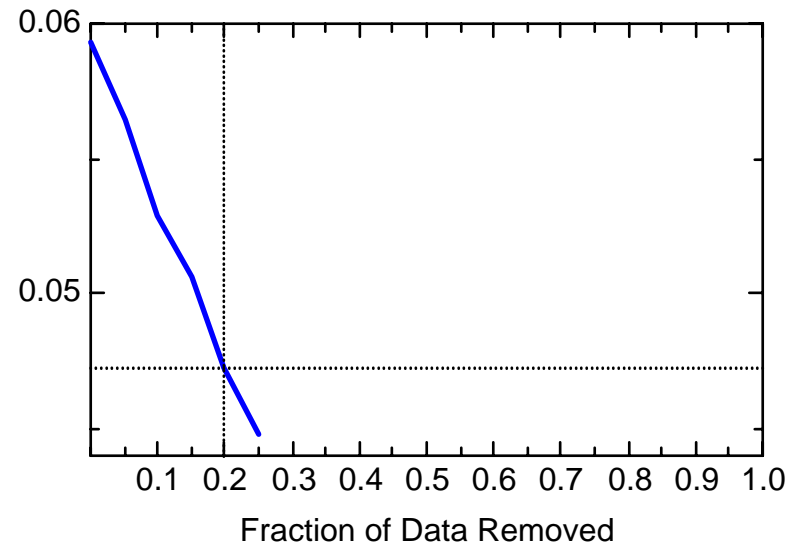
MN: Well JPZ0342



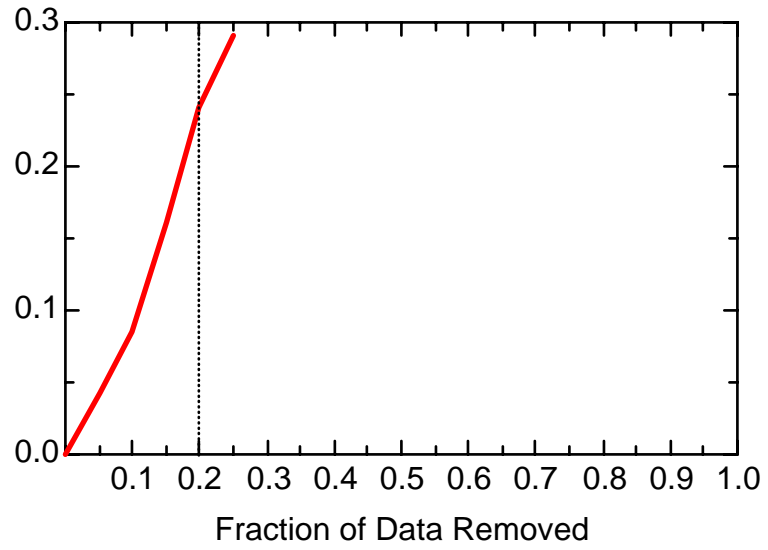
MN: Well JPZ0342



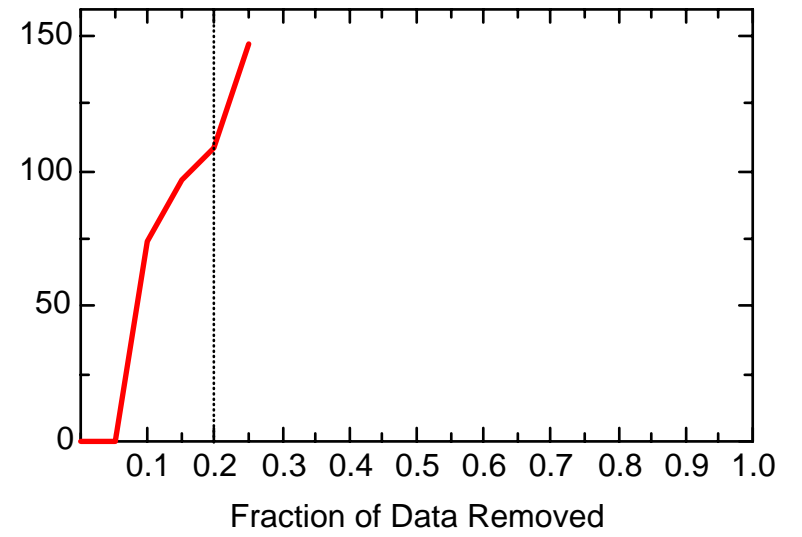
MN: Well JPZ0342



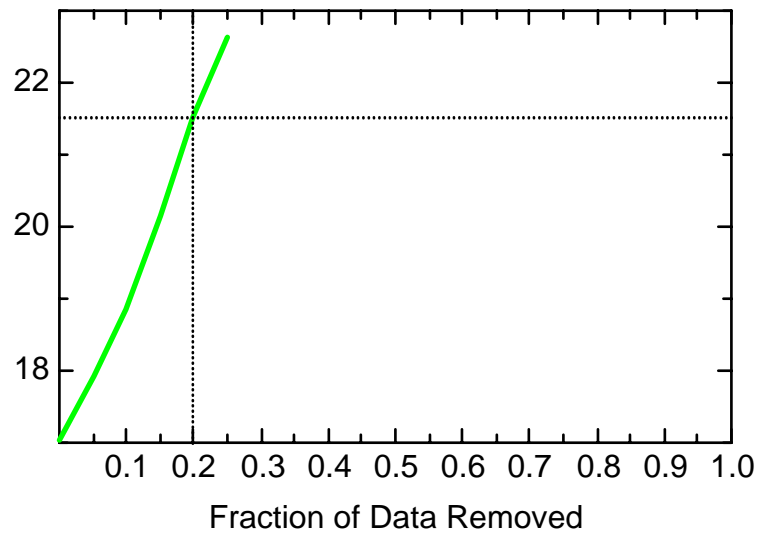
MN: Well JPZ0343



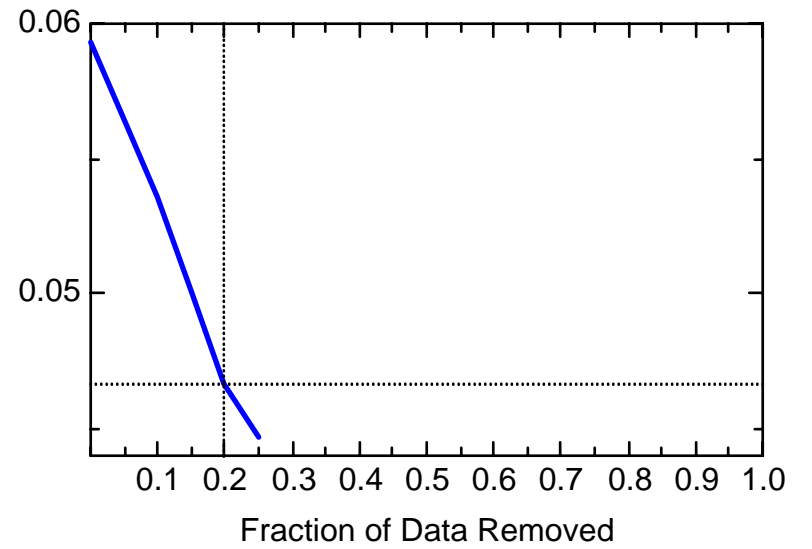
MN: Well JPZ0343



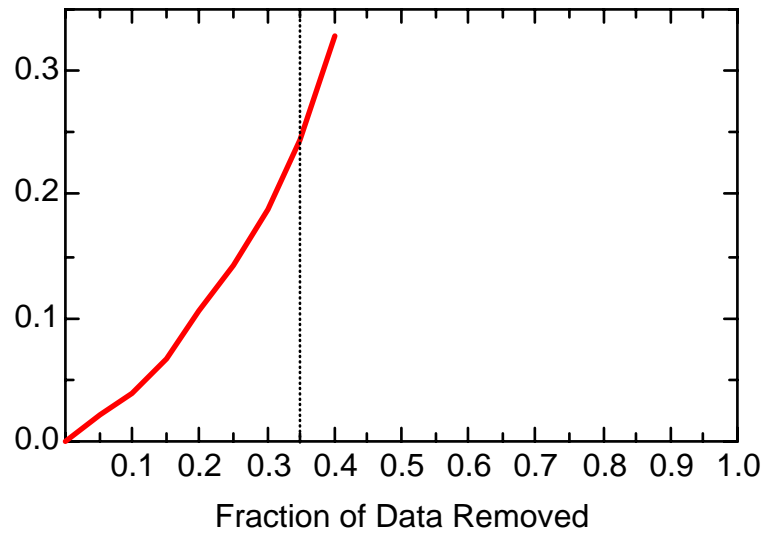
MN: Well JPZ0343



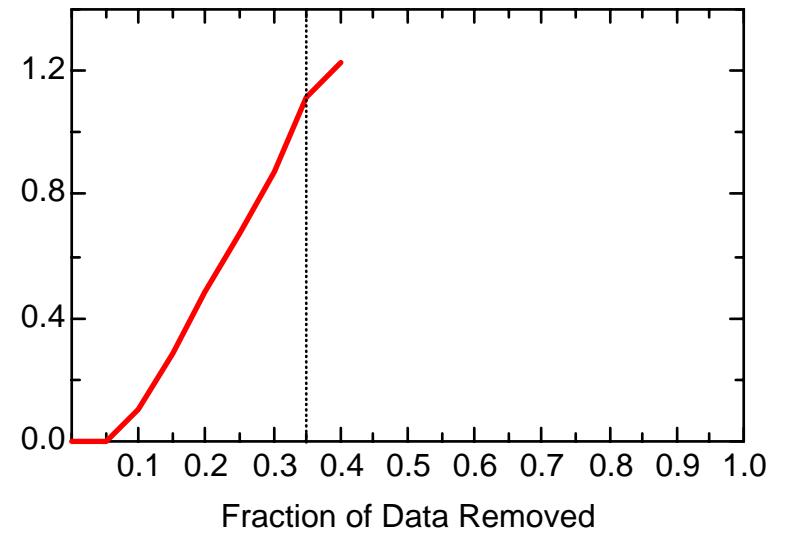
MN: Well JPZ0343



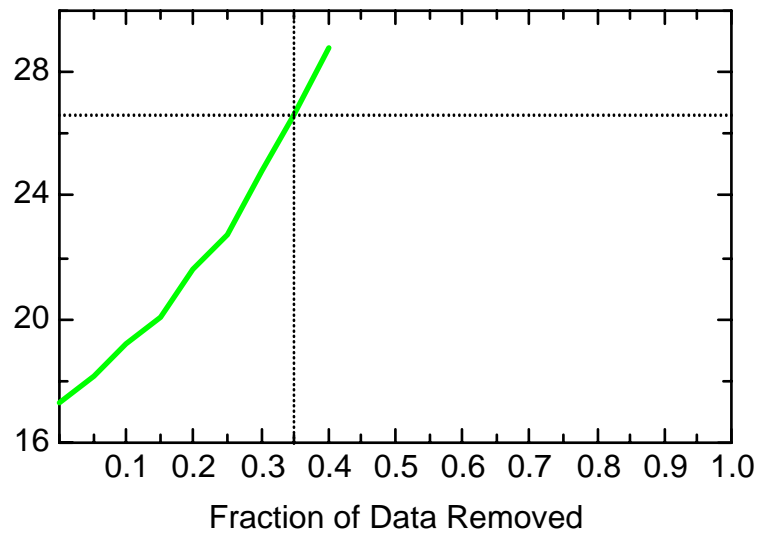
MN: Well JPZ0348



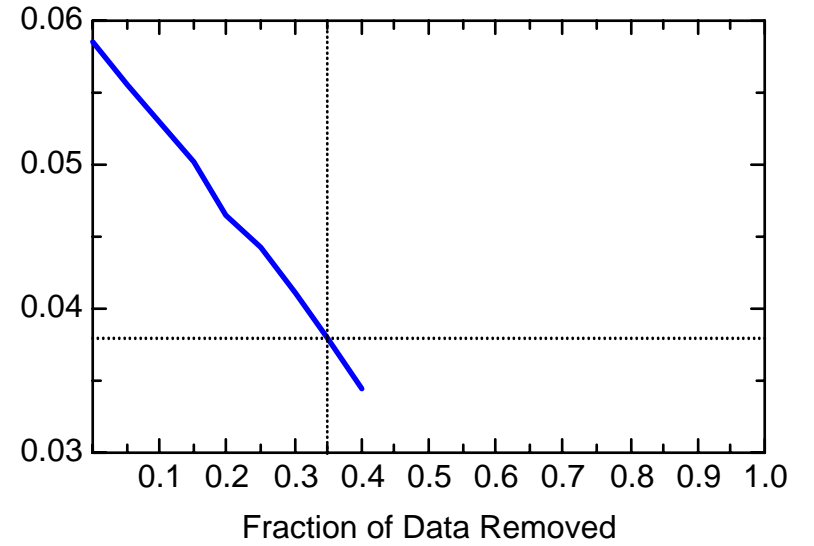
MN: Well JPZ0348



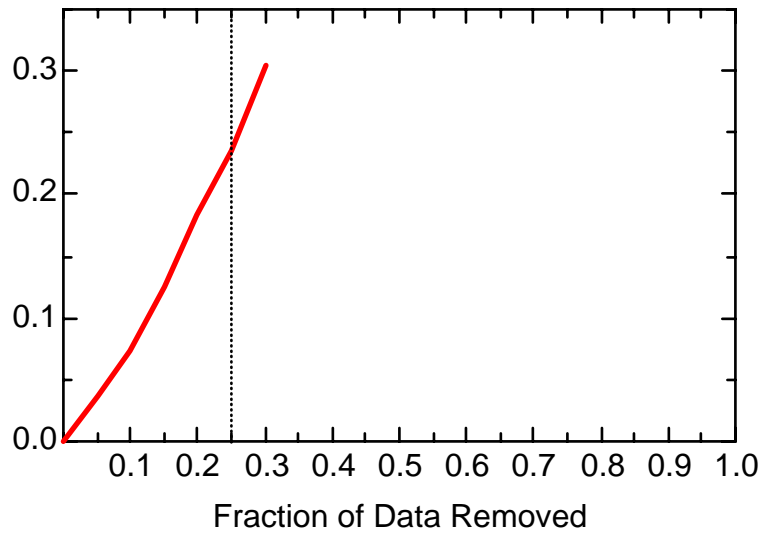
MN: Well JPZ0348



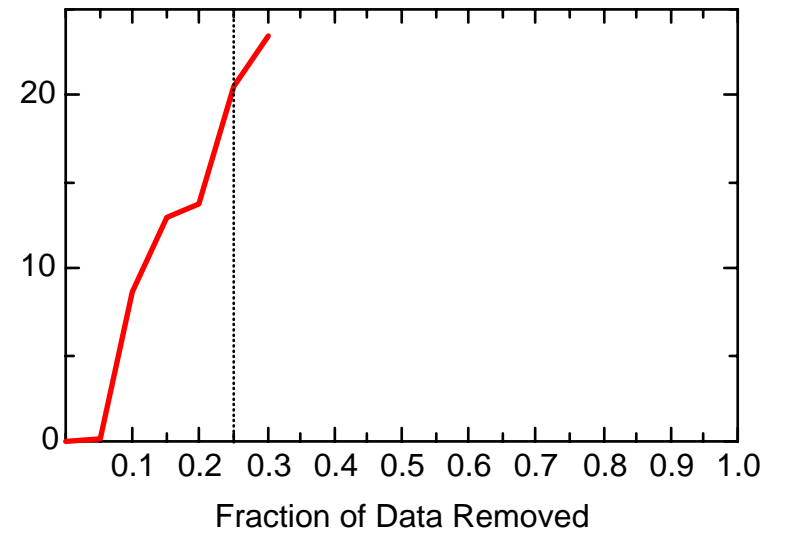
MN: Well JPZ0348



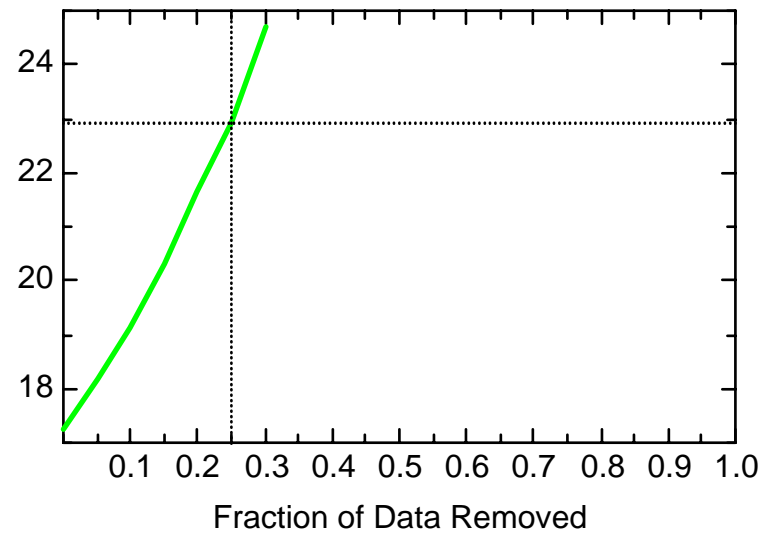
MN: Well JPZ0349



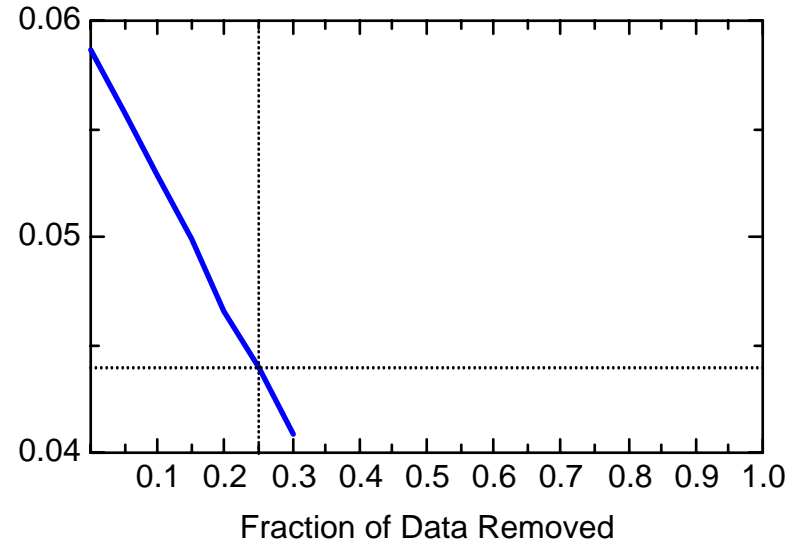
MN: Well JPZ0349



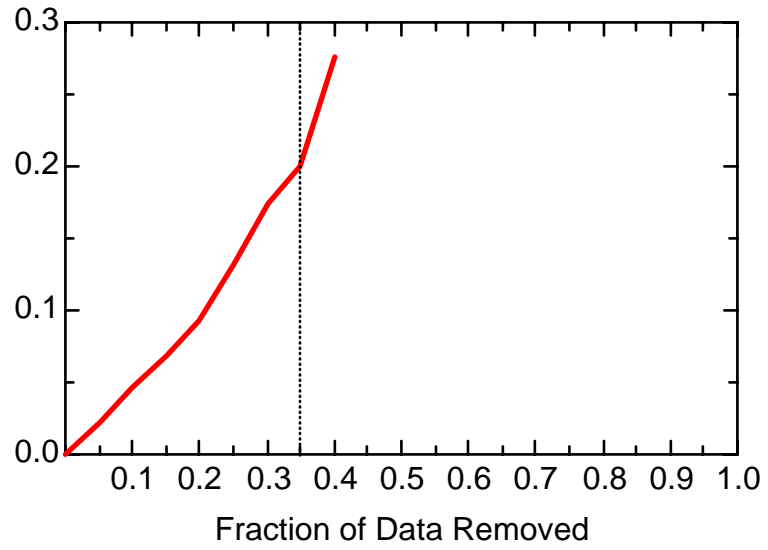
MN: Well JPZ0349



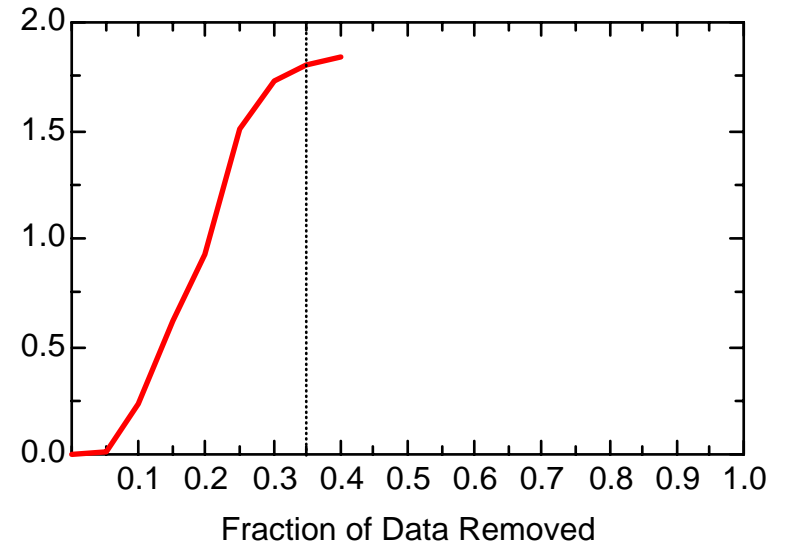
MN: Well JPZ0349



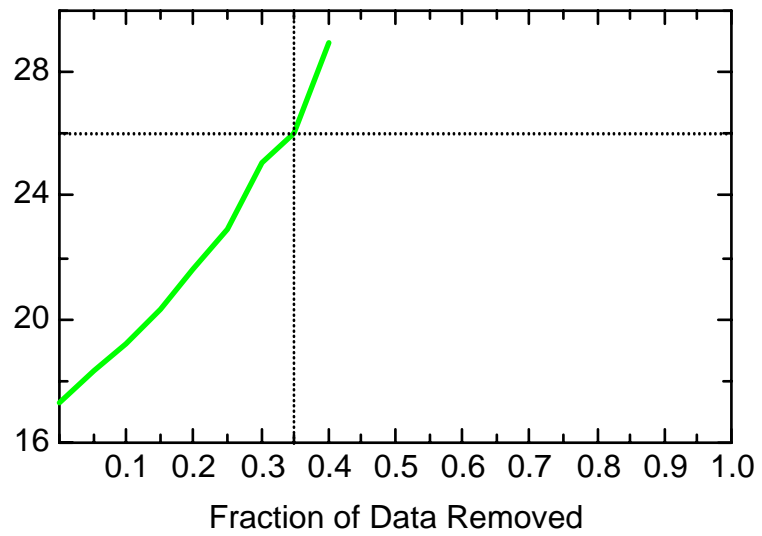
MN: Well JPZ1780



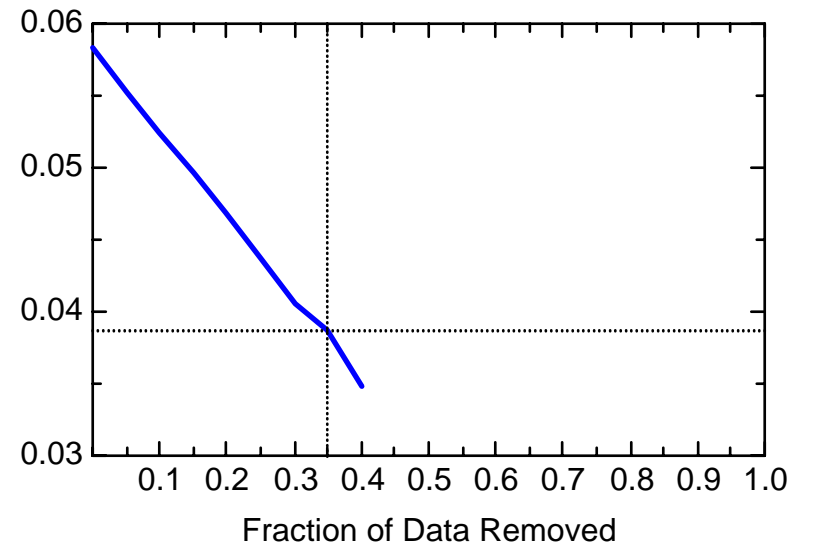
MN: Well JPZ1780



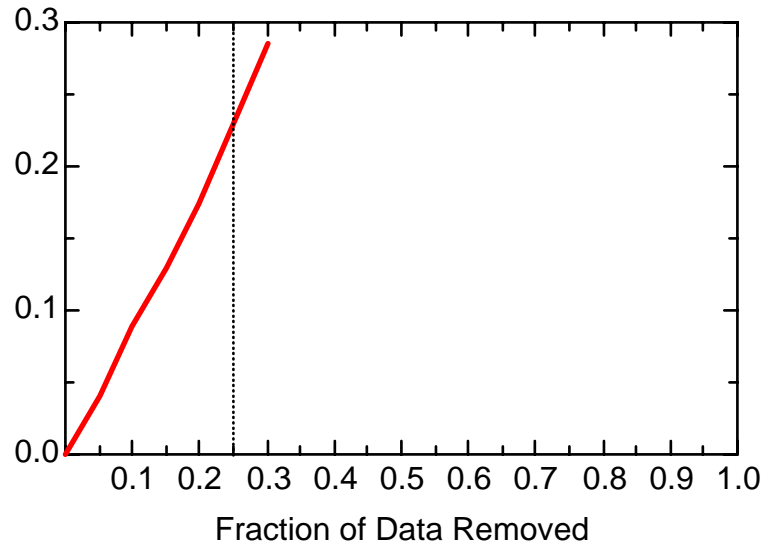
MN: Well JPZ1780



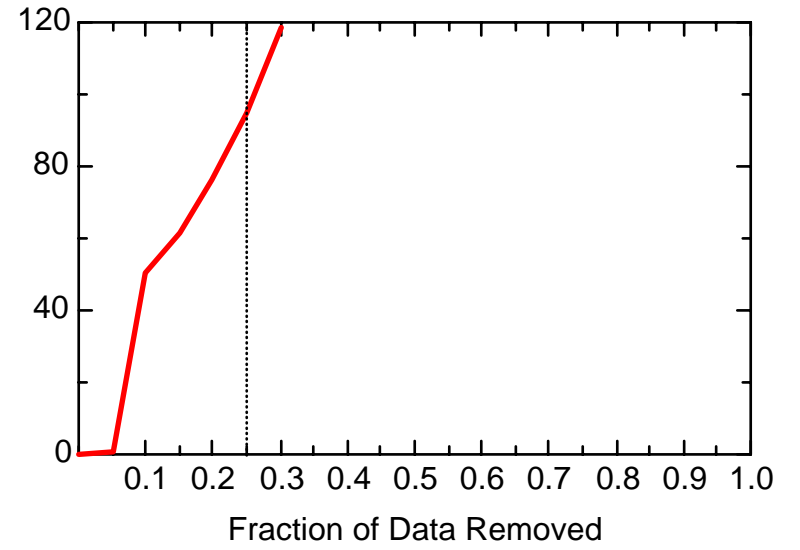
MN: Well JPZ1780



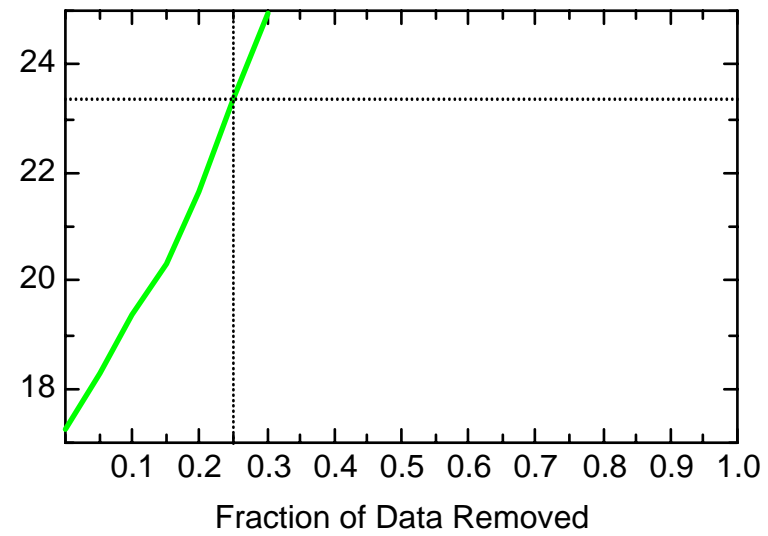
MN: Well JPZ7208



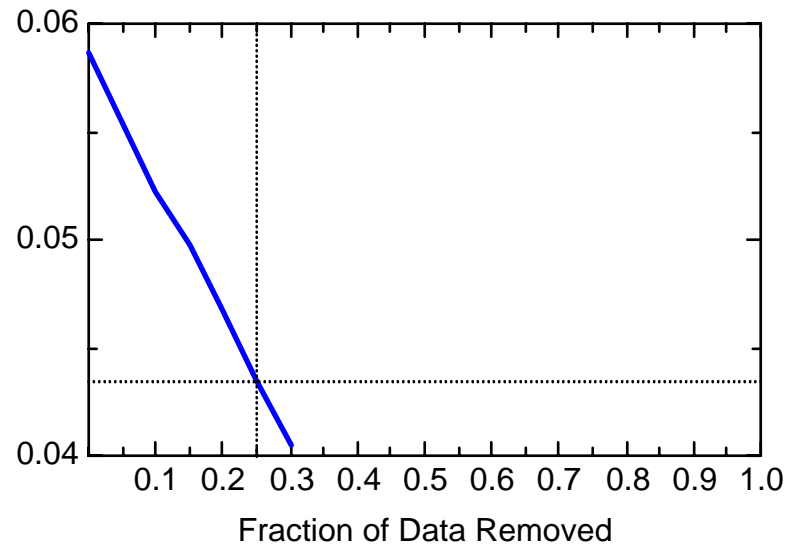
MN: Well JPZ7208



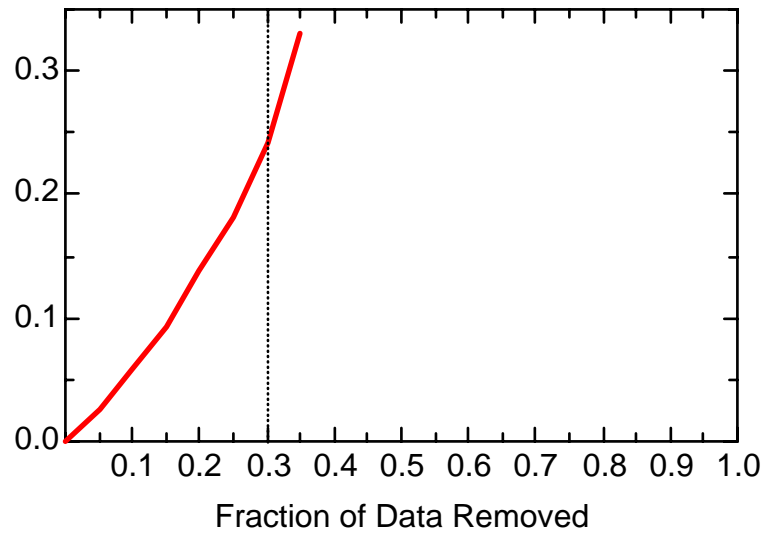
MN: Well JPZ7208



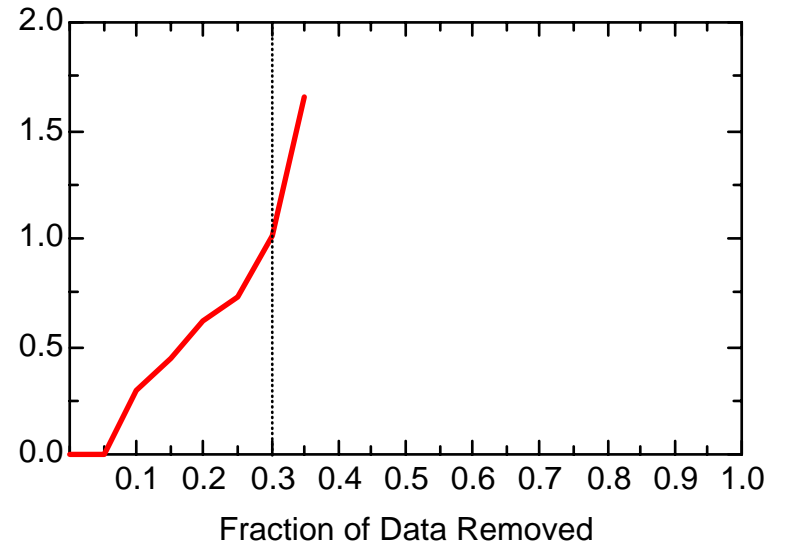
MN: Well JPZ7208



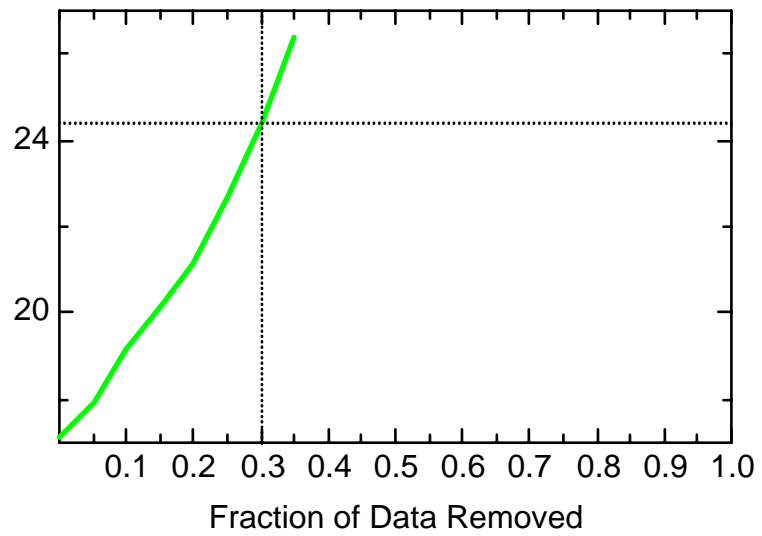
MN: Well JPZ7807



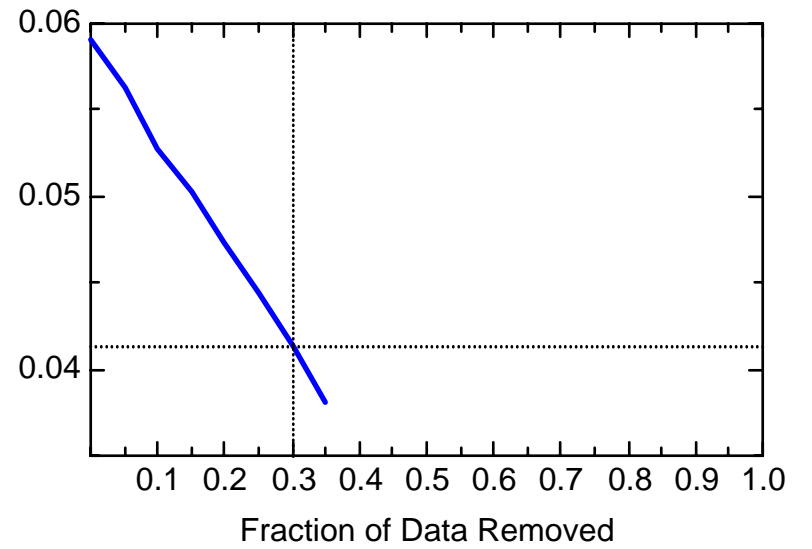
MN: Well JPZ7807



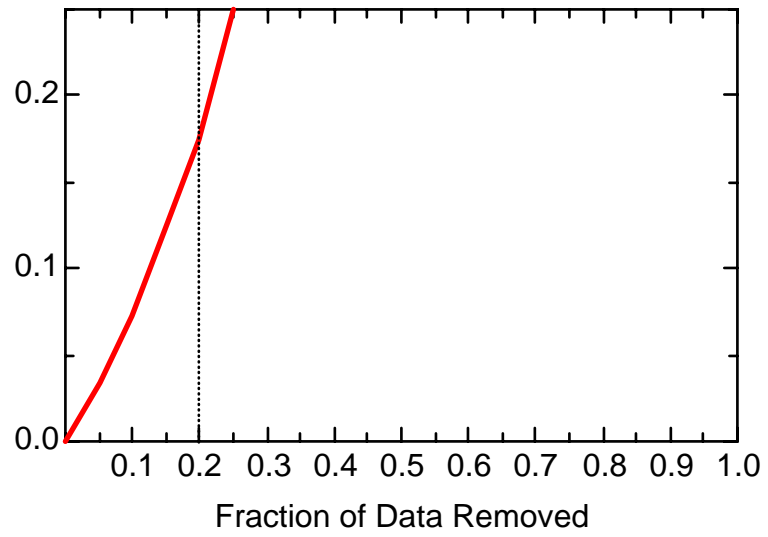
MN: Well JPZ7807



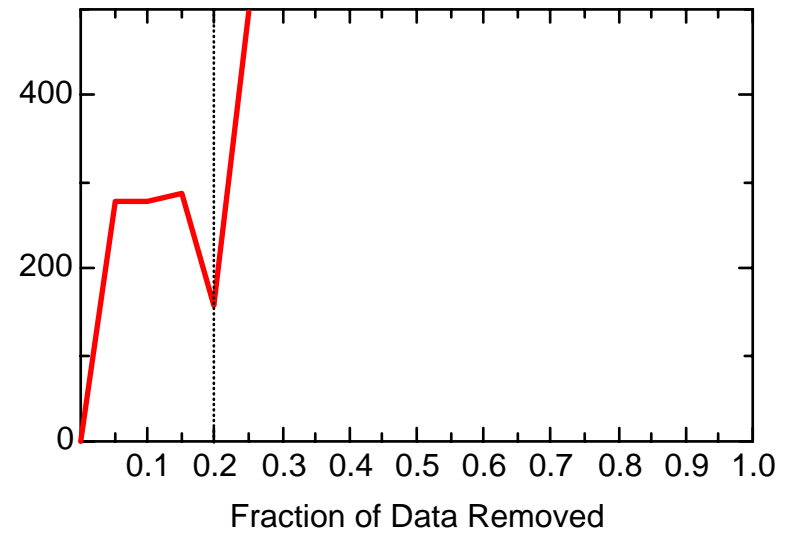
MN: Well JPZ7807



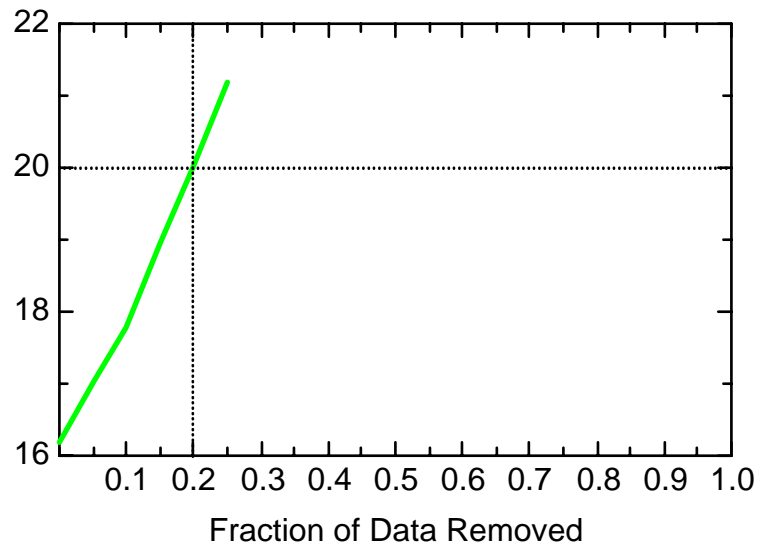
MN: Well MMW0005



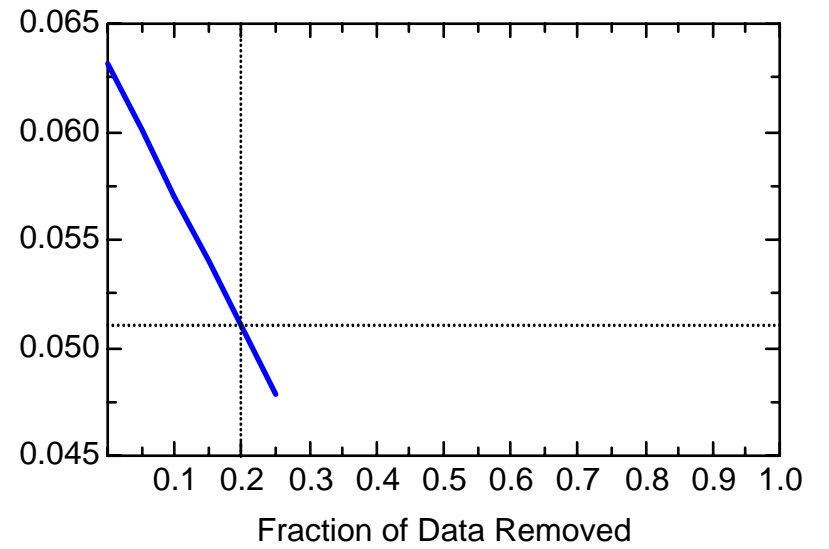
MN: Well MMW0005



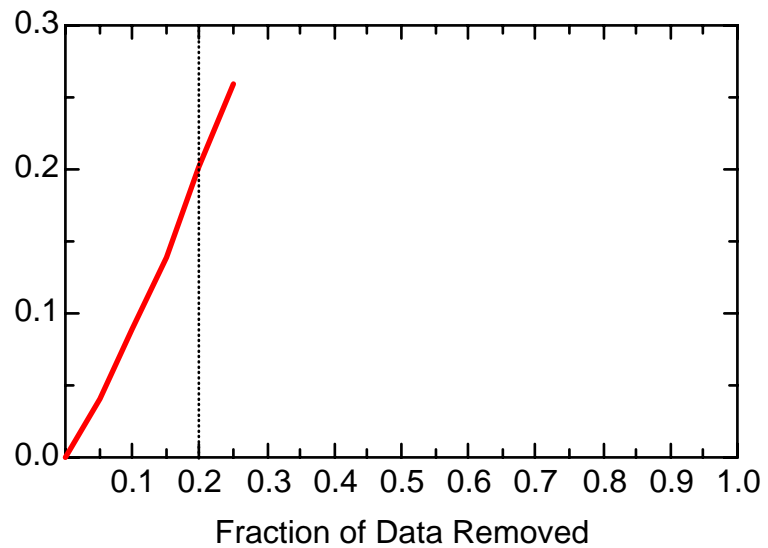
MN: Well MMW0005



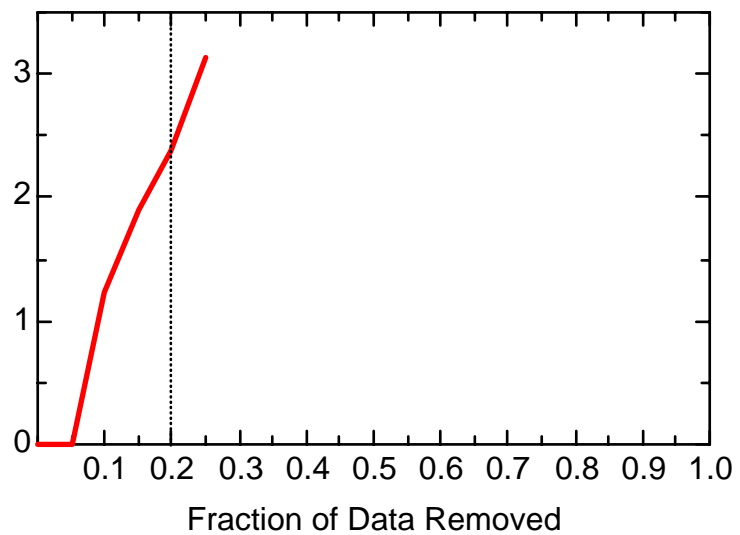
MN: Well MMW0005



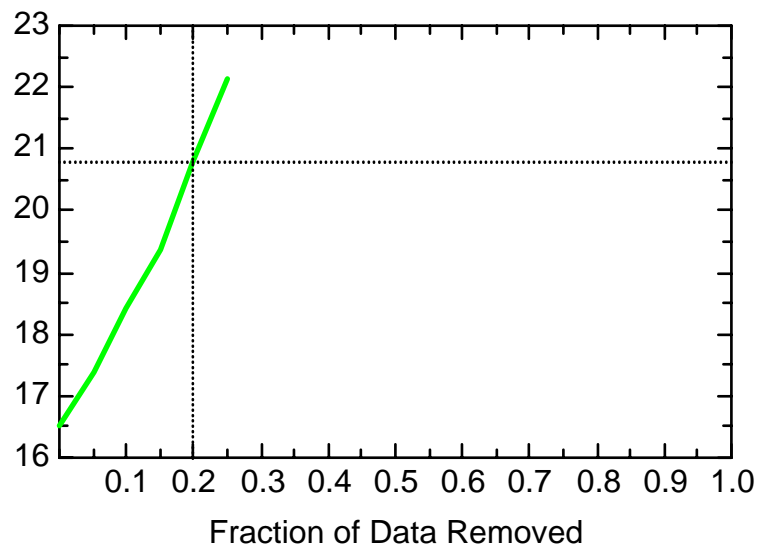
MN: Well MMW0007A



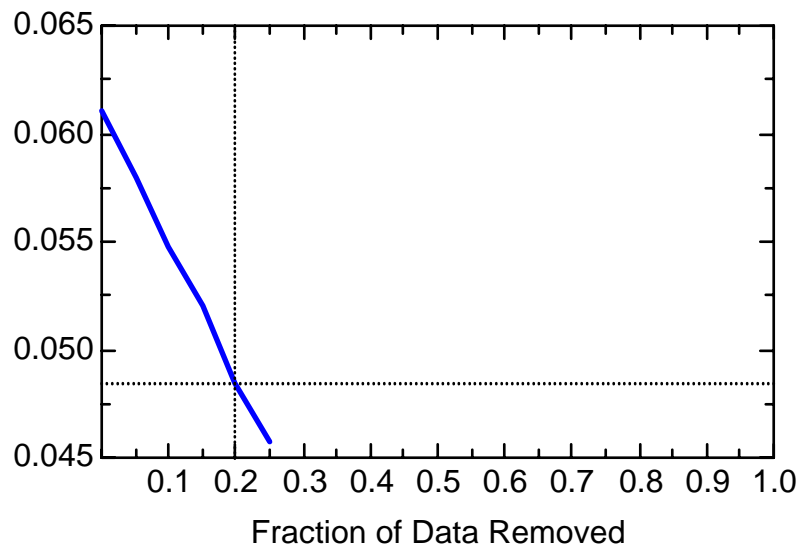
MN: Well MMW0007A



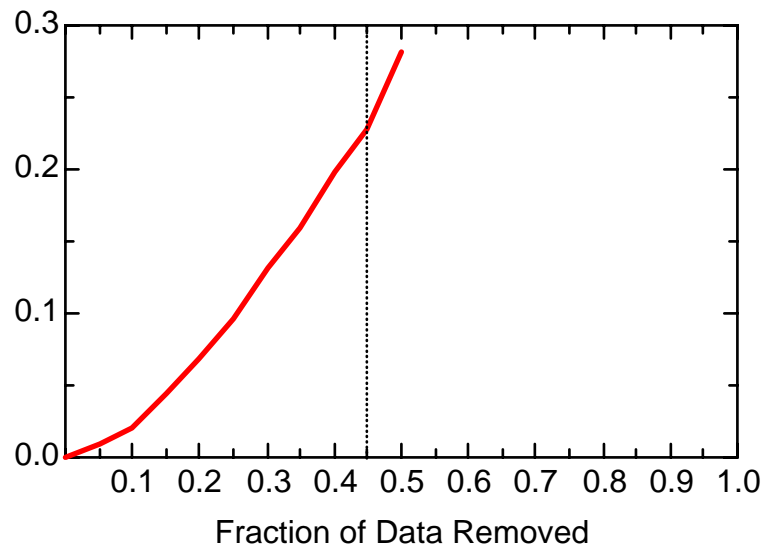
MN: Well MMW0007A



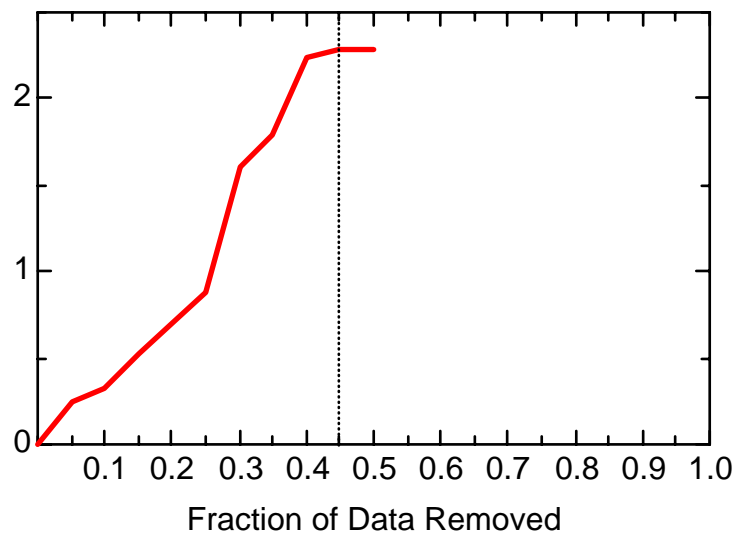
MN: Well MMW0007A



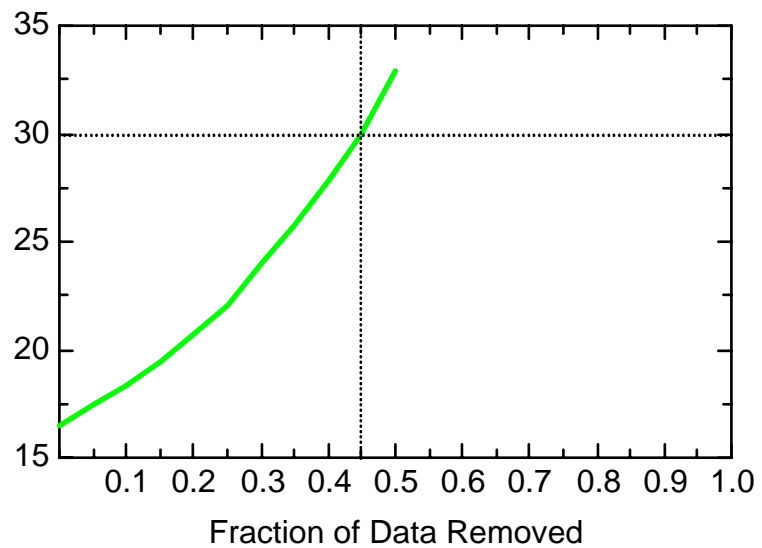
MN: Well MMW0007B



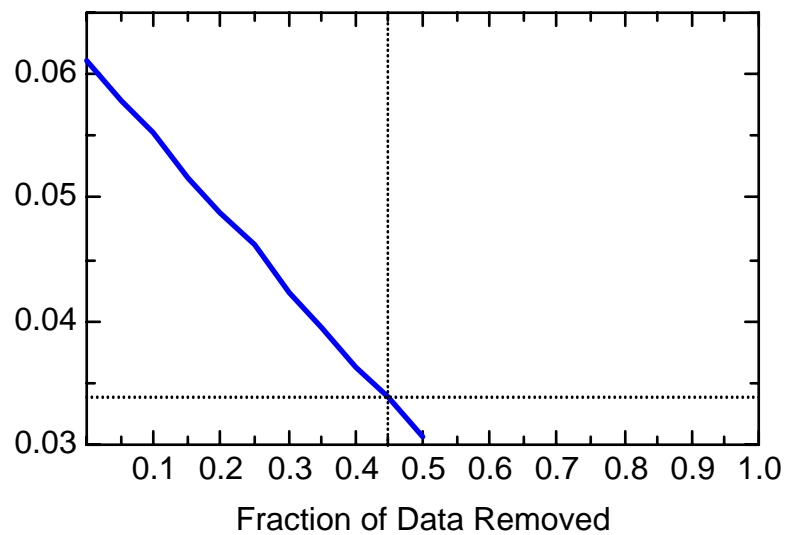
MN: Well MMW0007B



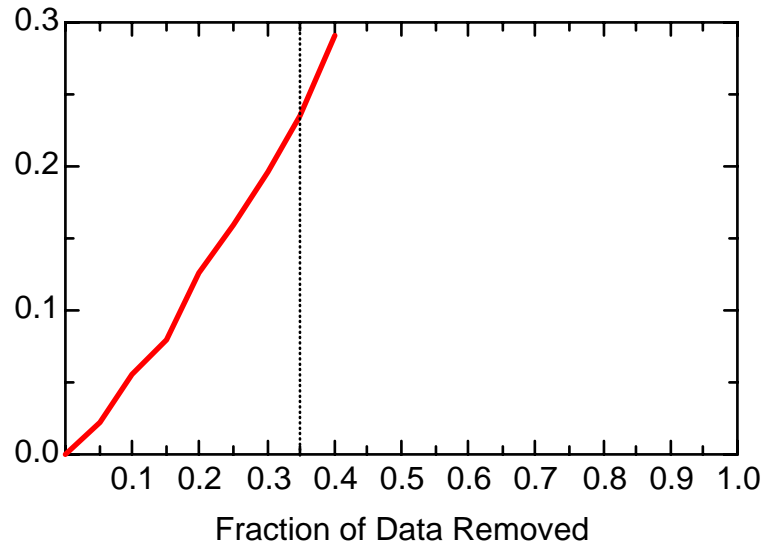
MN: Well MMW0007B



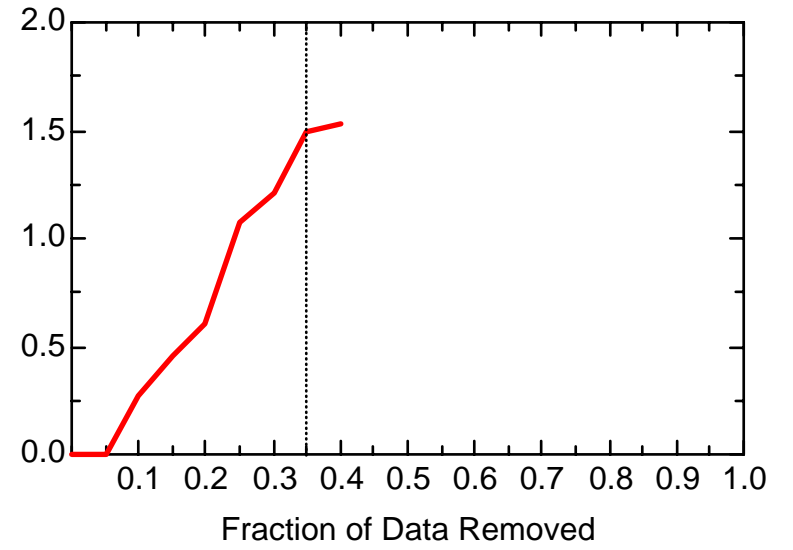
MN: Well MMW0007B



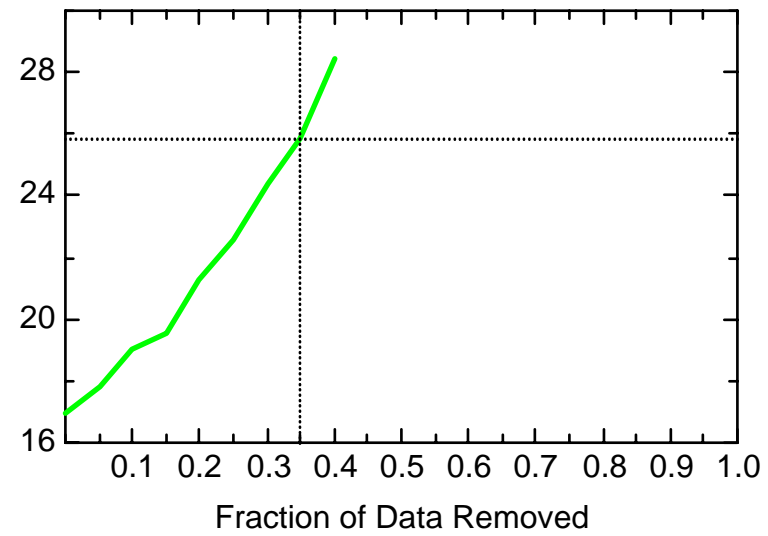
MN: Well MMW0008



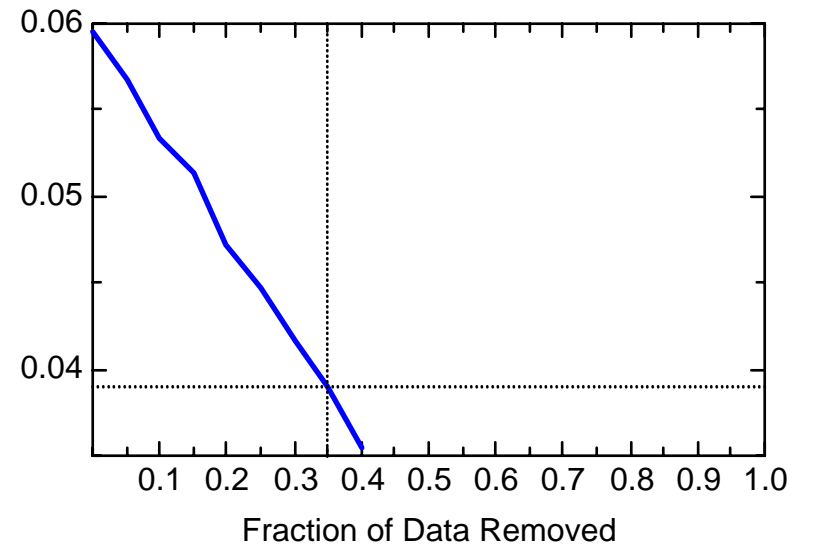
MN: Well MMW0008



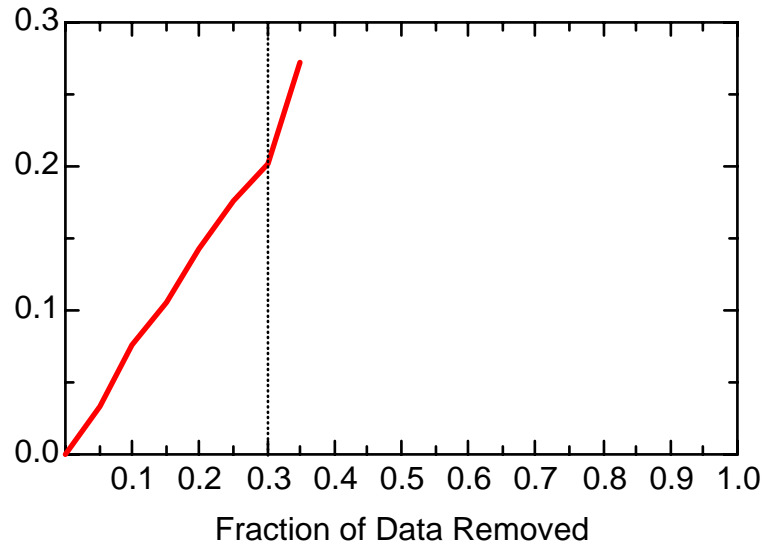
MN: Well MMW0008



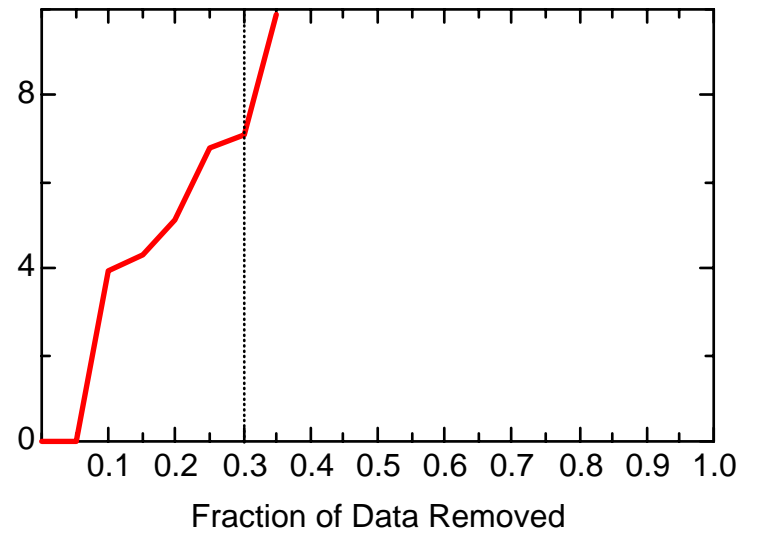
MN: Well MMW0008



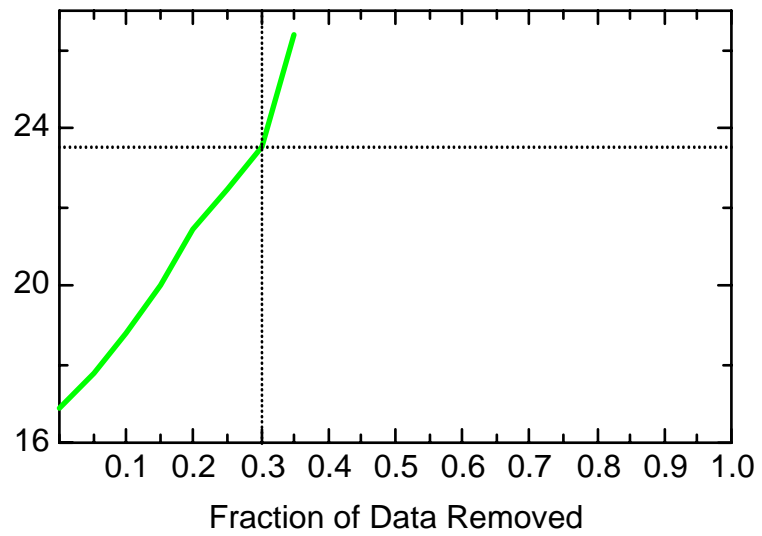
MN: Well MMW0009



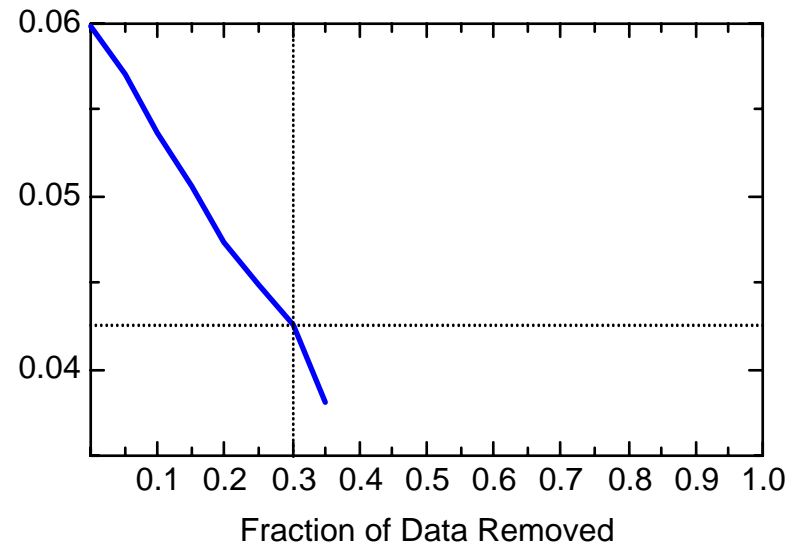
MN: Well MMW0009



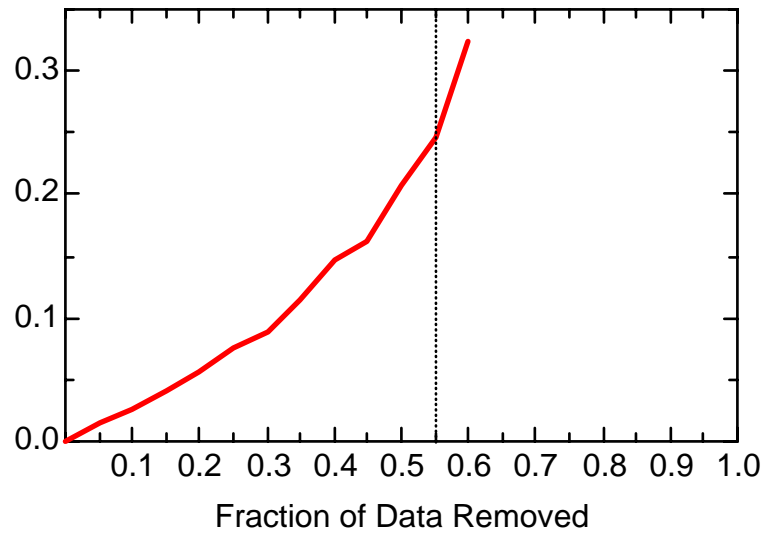
MN: Well MMW0009



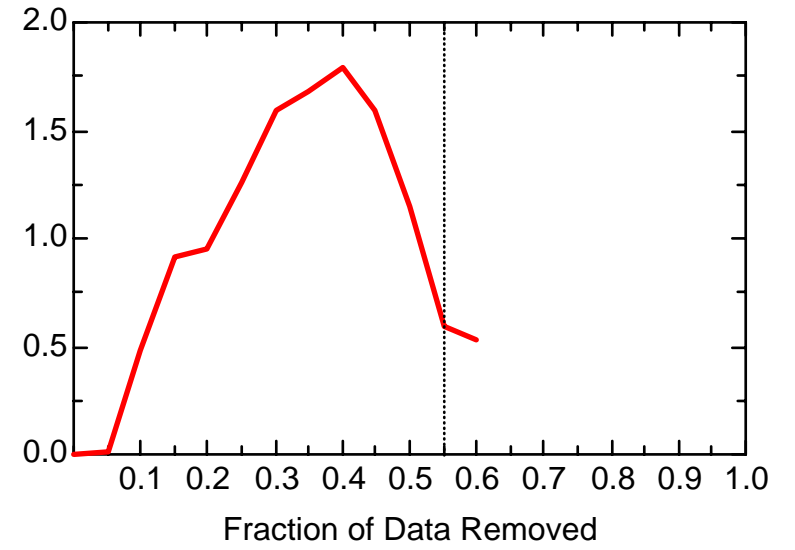
MN: Well MMW0009



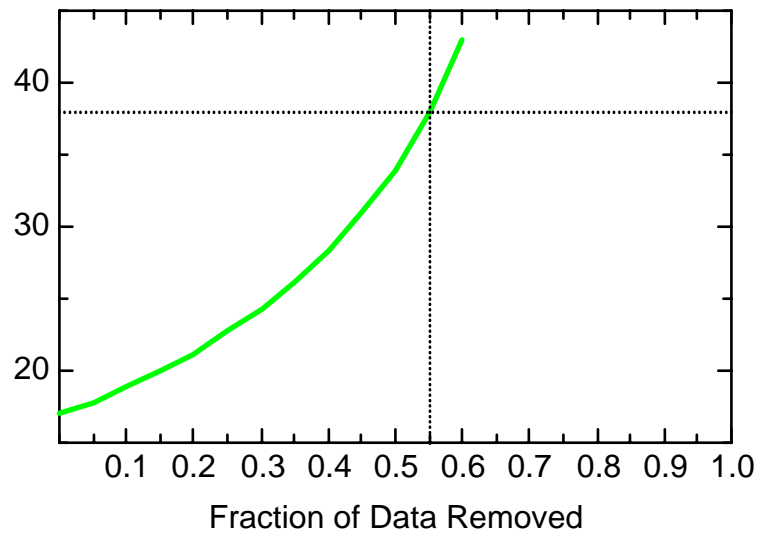
MN: Well MMW0010



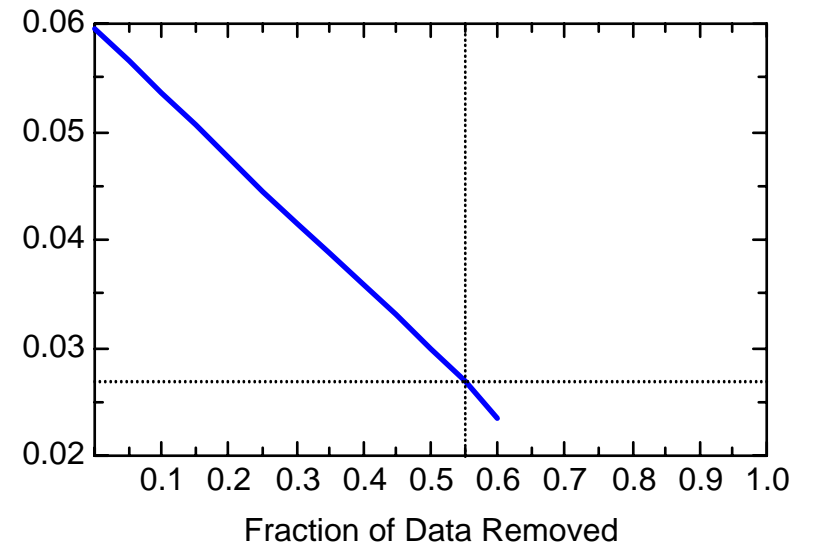
MN: Well MMW0010



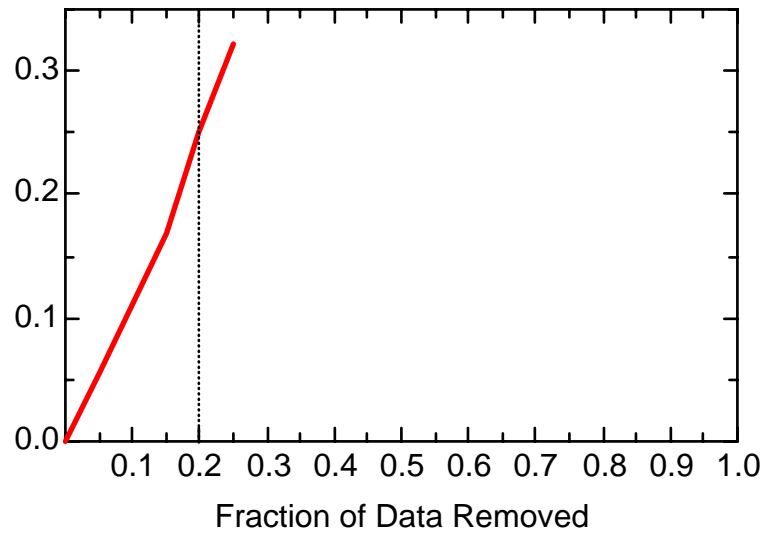
MN: Well MMW0010



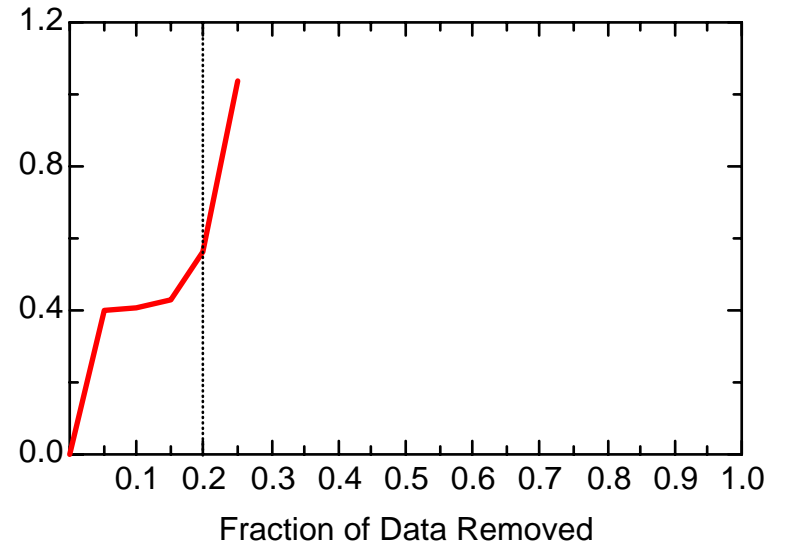
MN: Well MMW0010



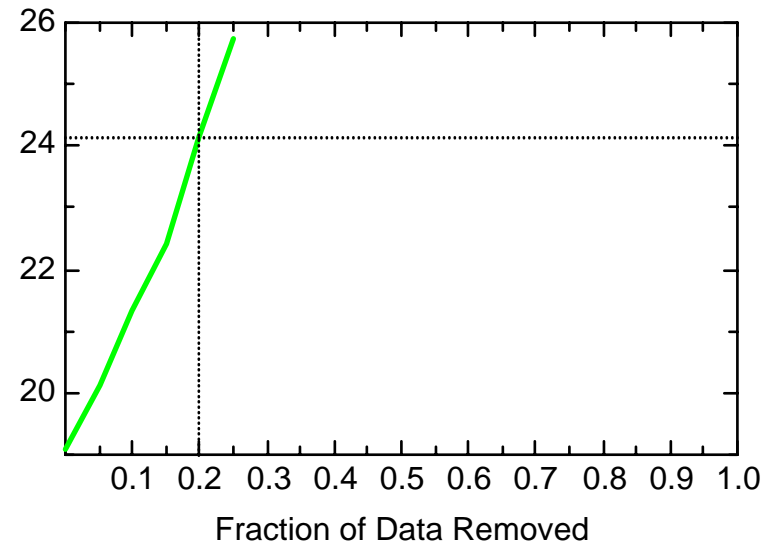
MN: Well MMW0011



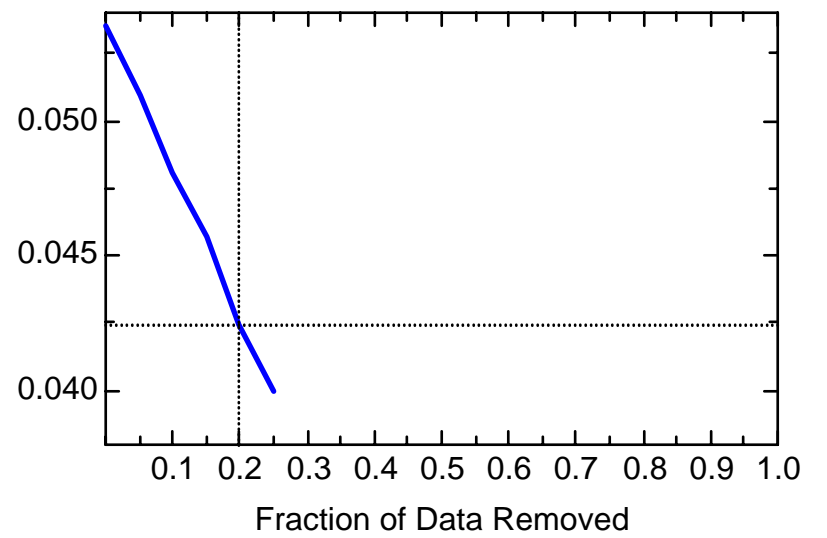
MN: Well MMW0011



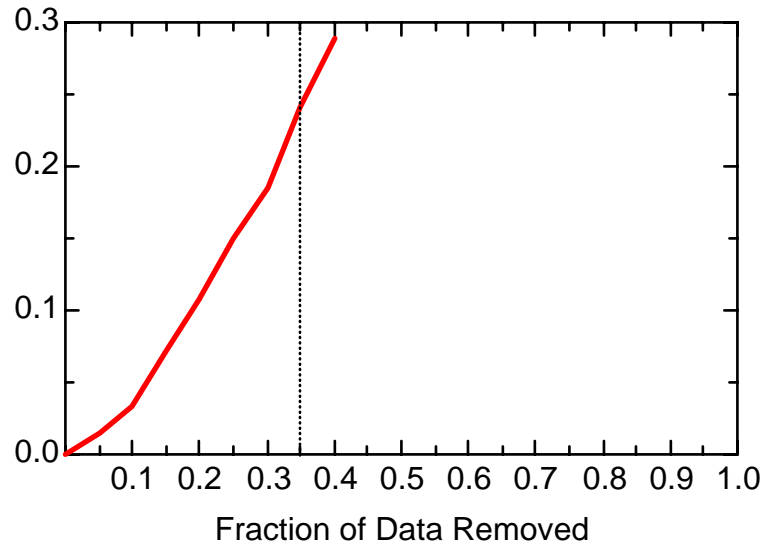
MN: Well MMW0011



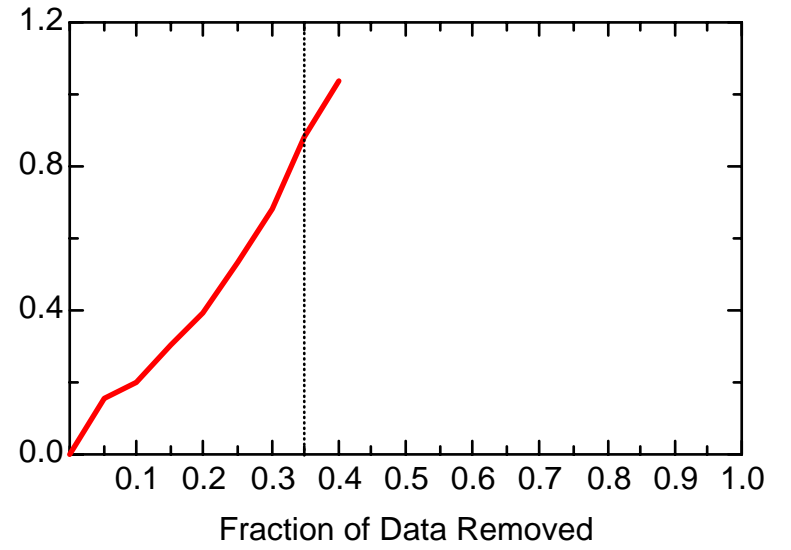
MN: Well MMW0011



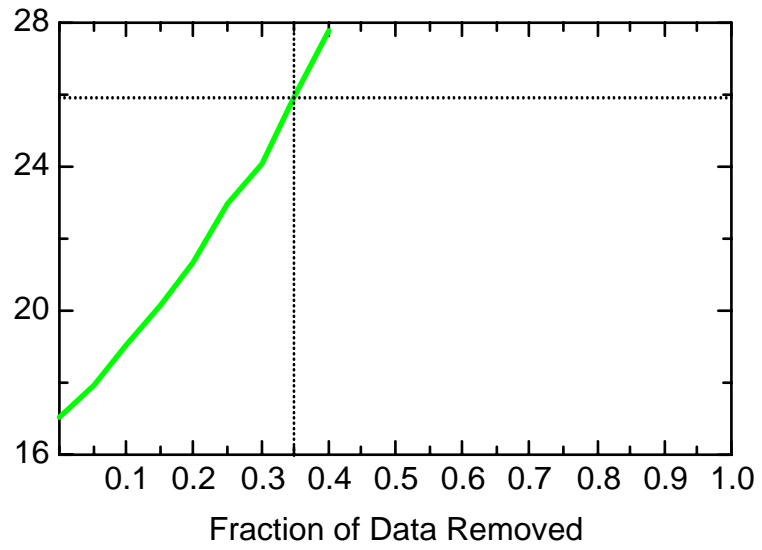
MN: Well MMW0012



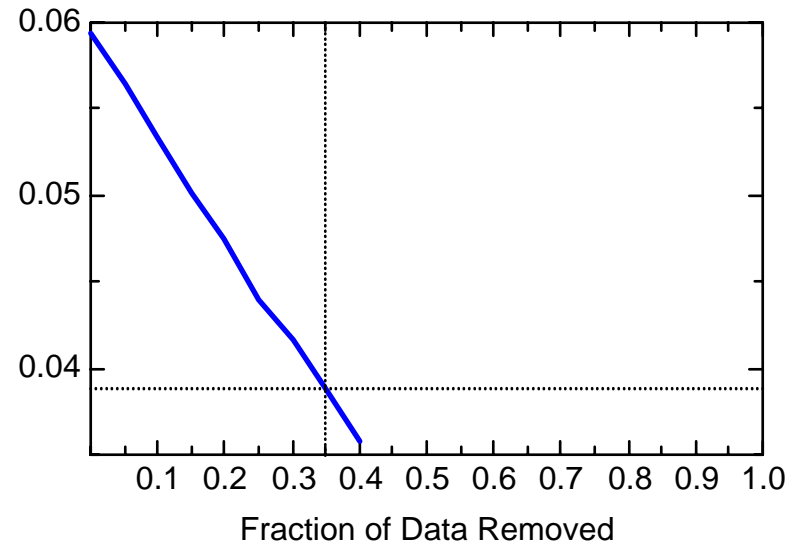
MN: Well MMW0012



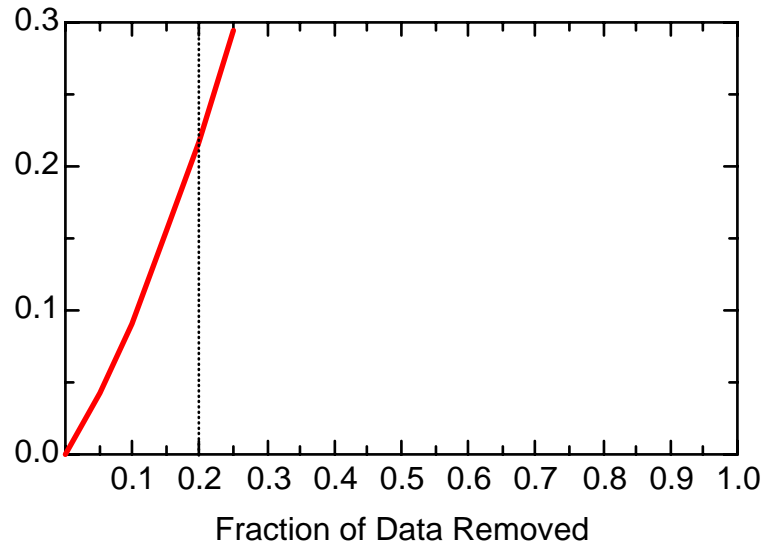
MN: Well MMW0012



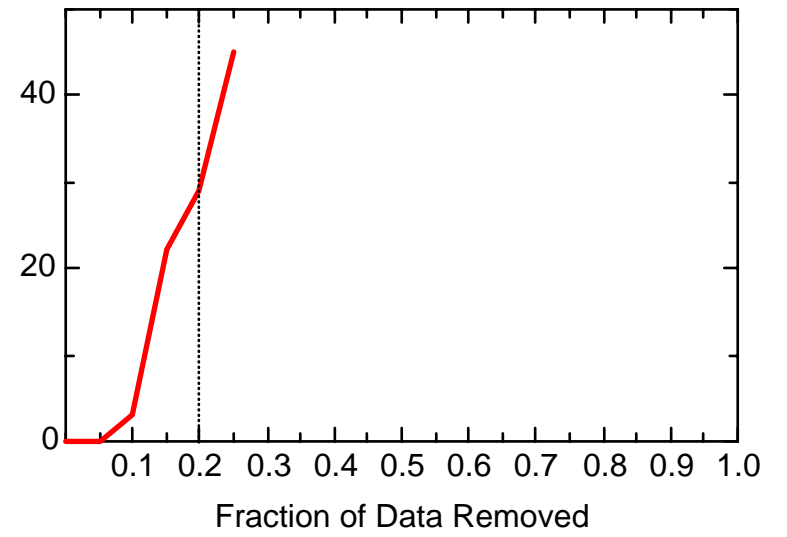
MN: Well MMW0012



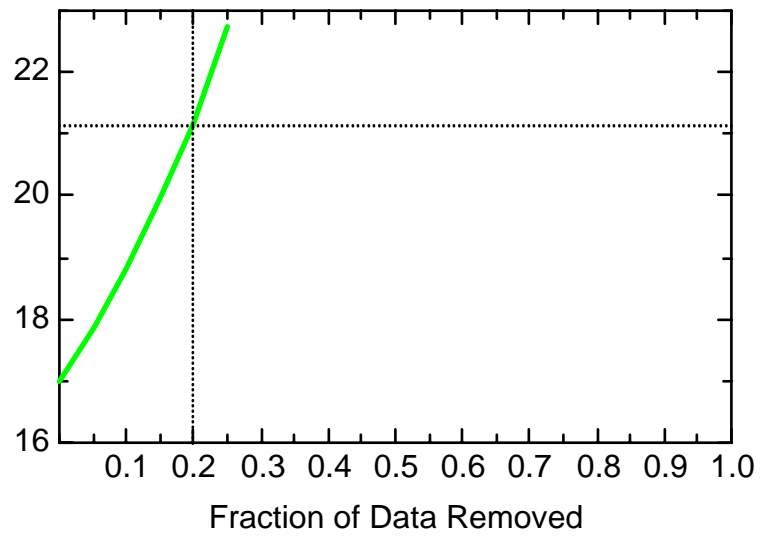
MN: Well MMW0013



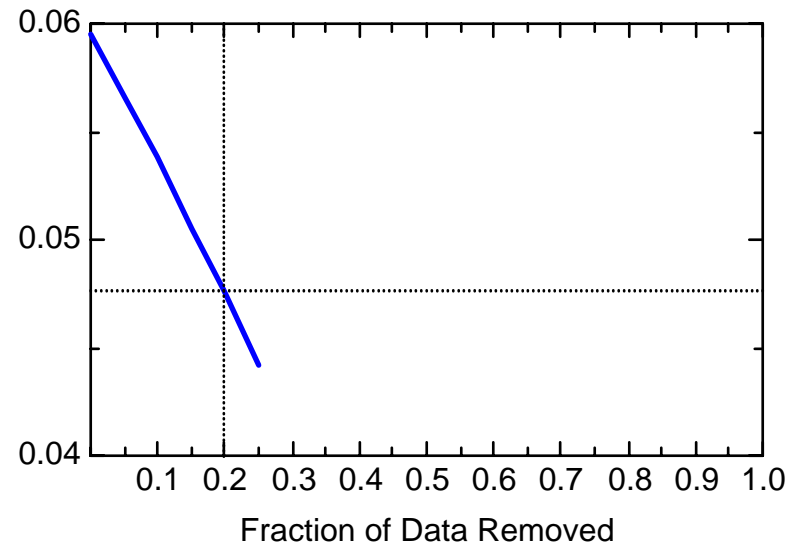
MN: Well MMW0013



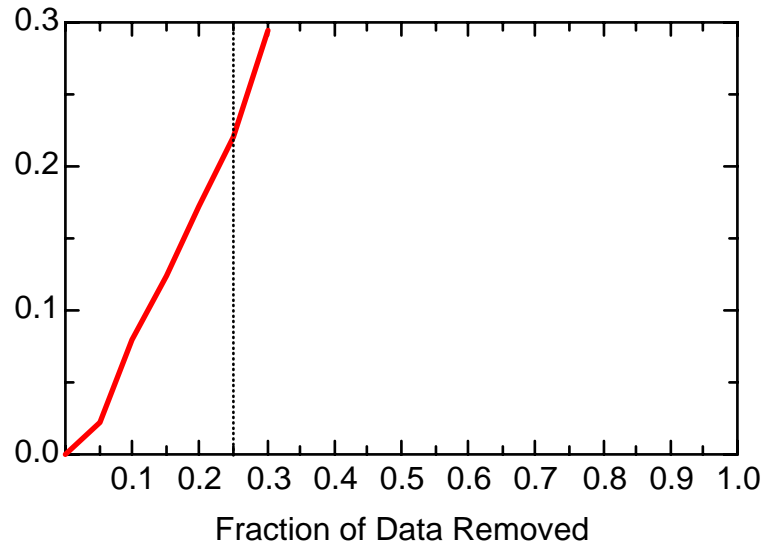
MN: Well MMW0013



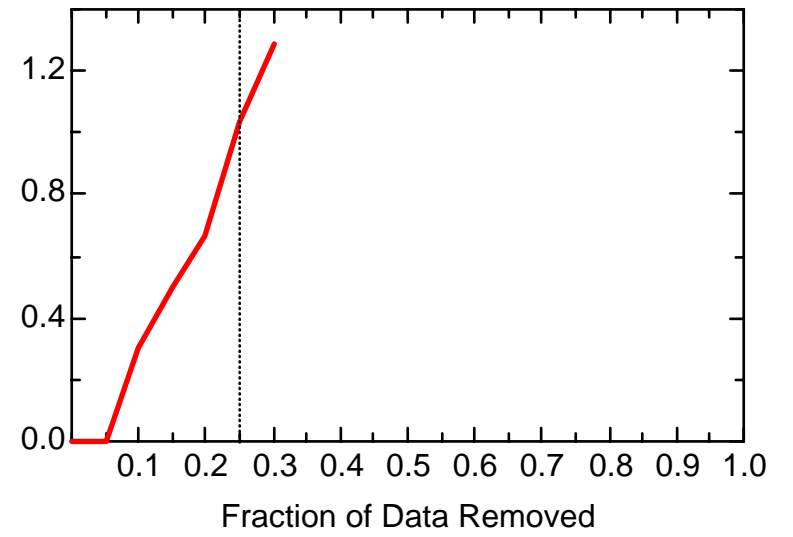
MN: Well MMW0013



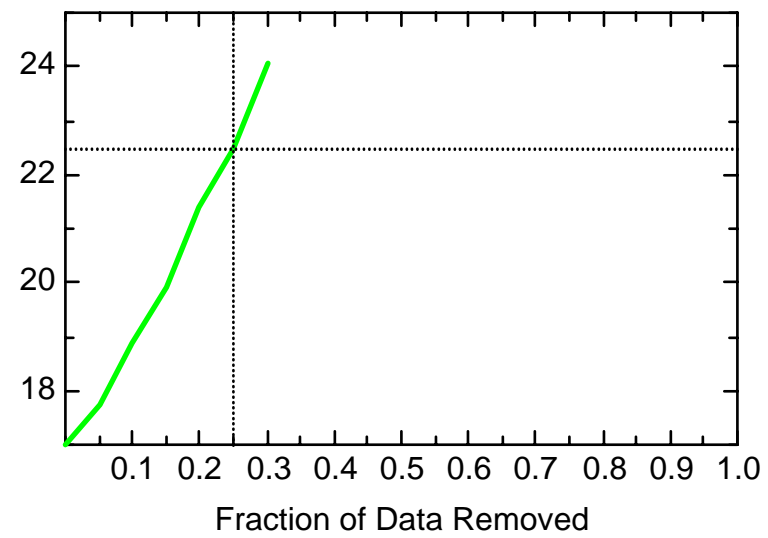
MN: Well MMW0016



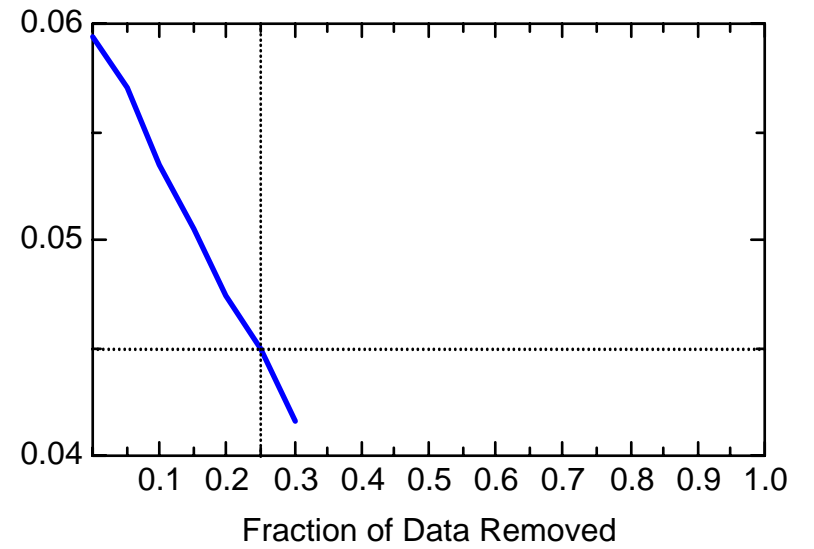
MN: Well MMW0016



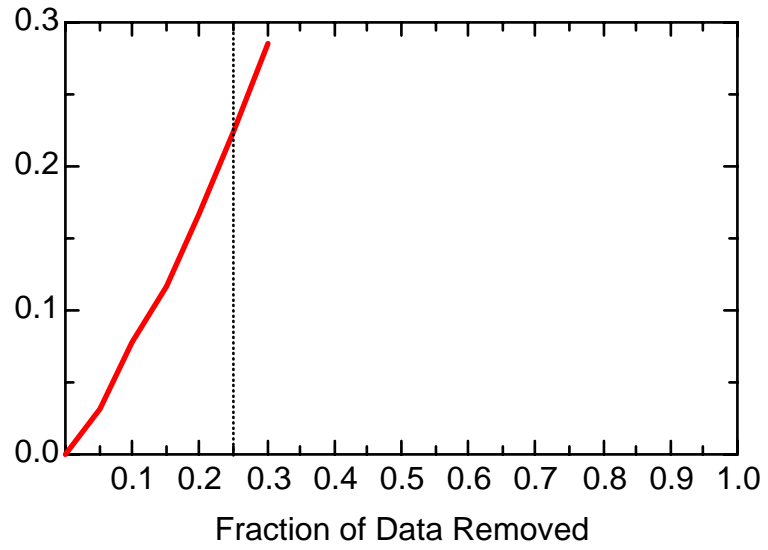
MN: Well MMW0016



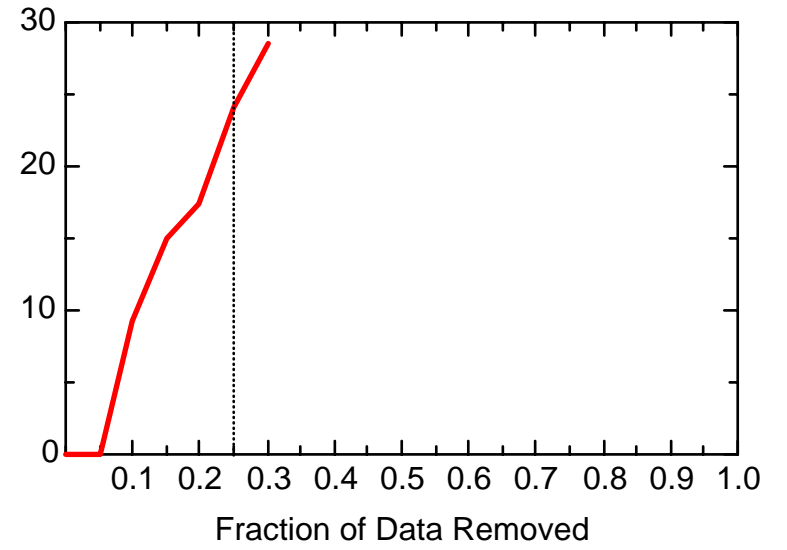
MN: Well MMW0016



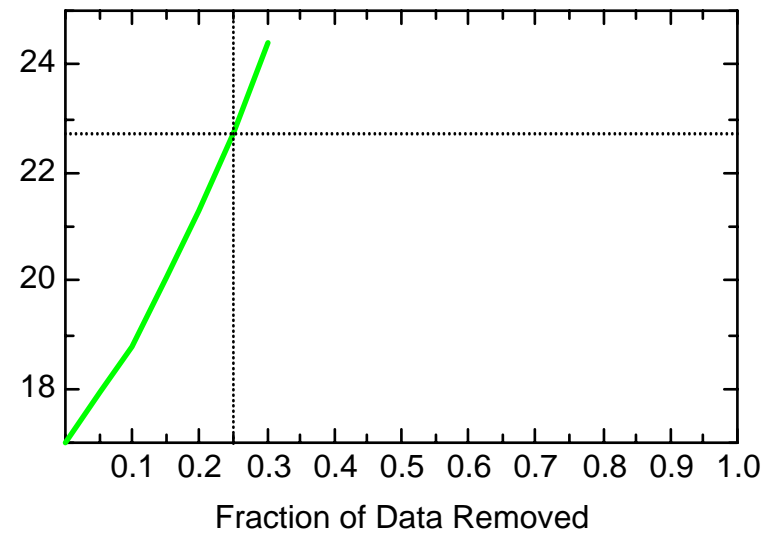
MN: Well MMW0017



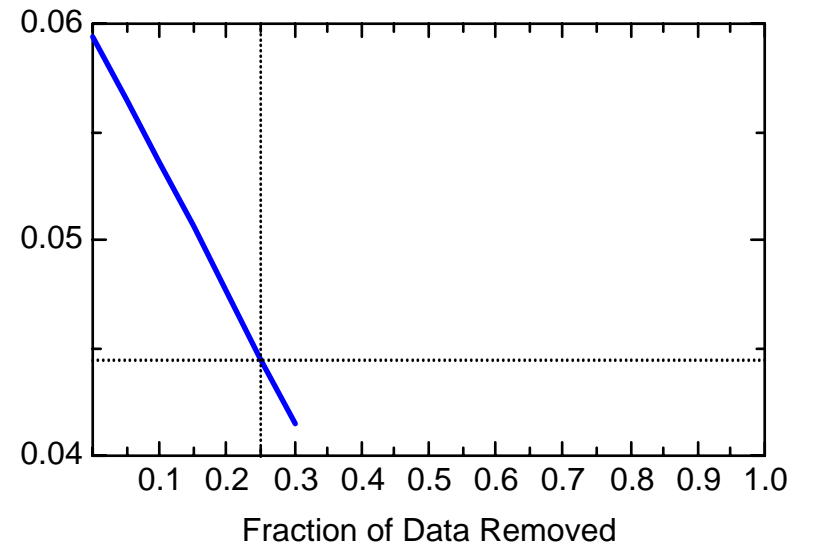
MN: Well MMW0017



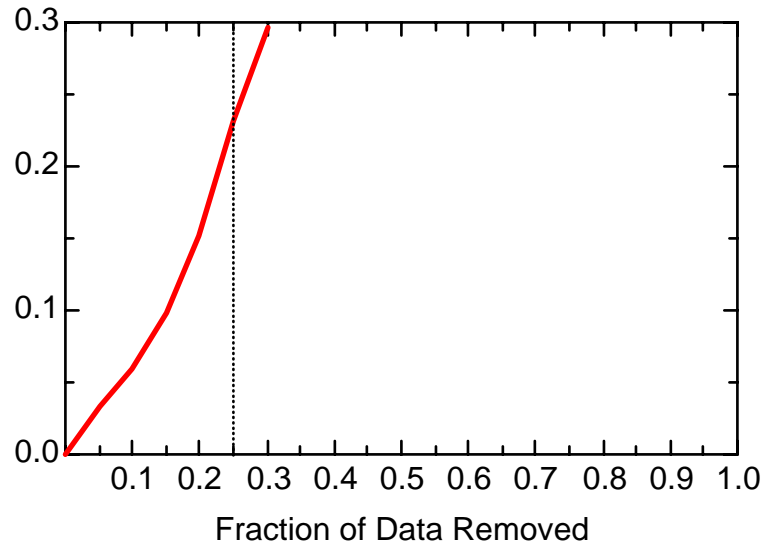
MN: Well MMW0017



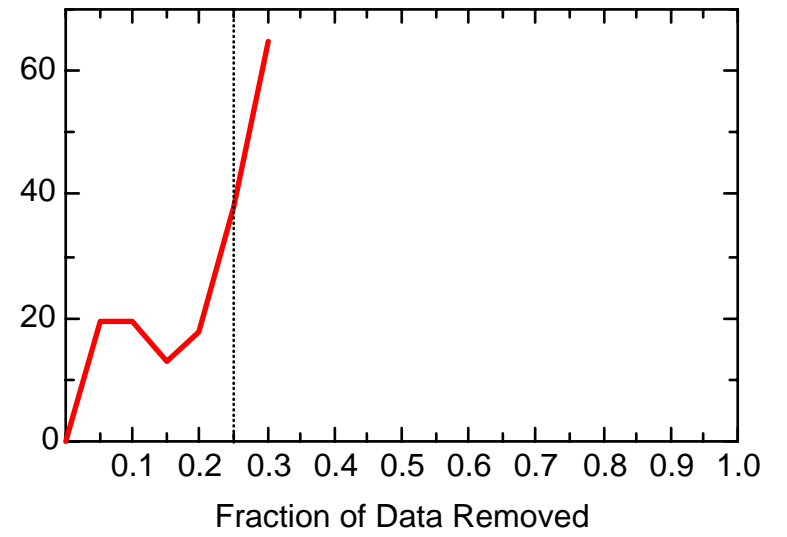
MN: Well MMW0017



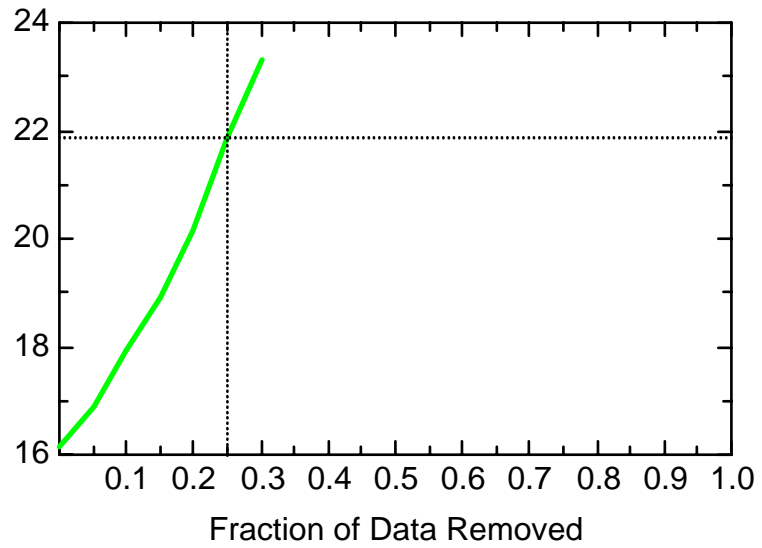
MN: Well MMW0019



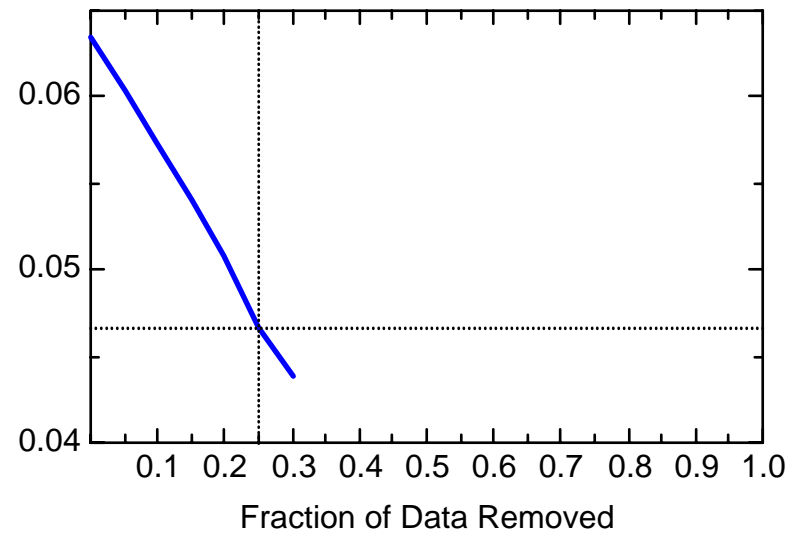
MN: Well MMW0019



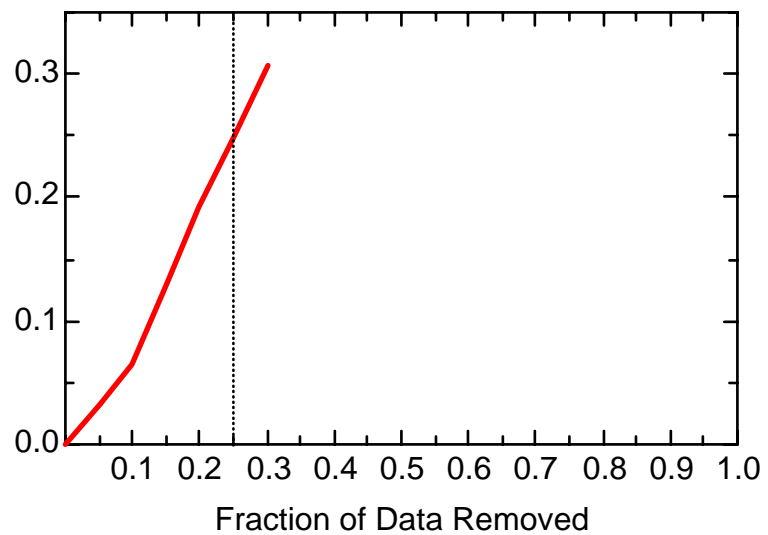
MN: Well MMW0019



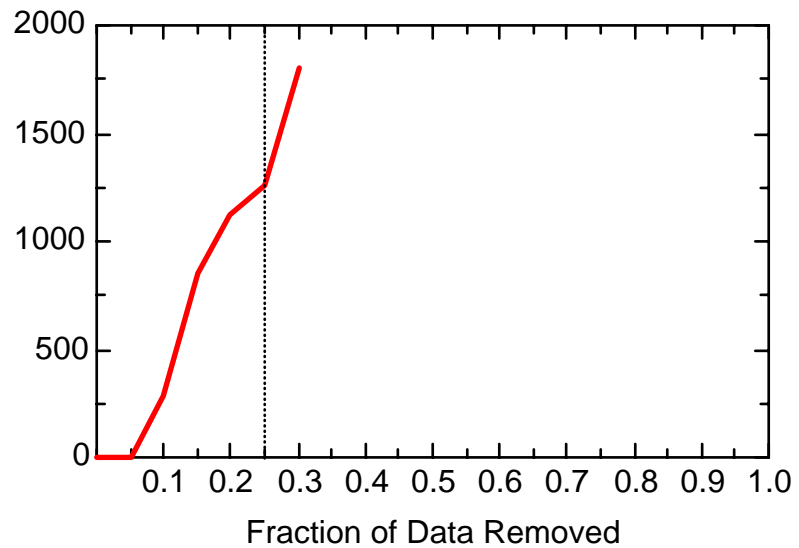
MN: Well MMW0019



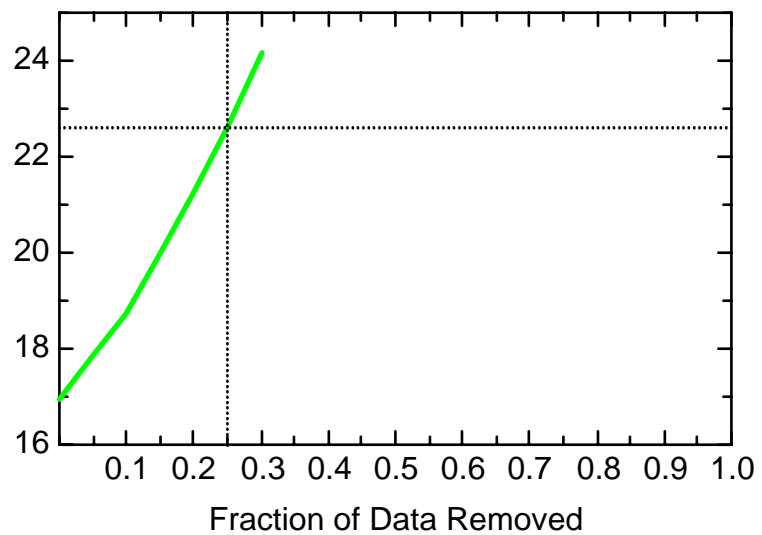
MN: Well MMW1560



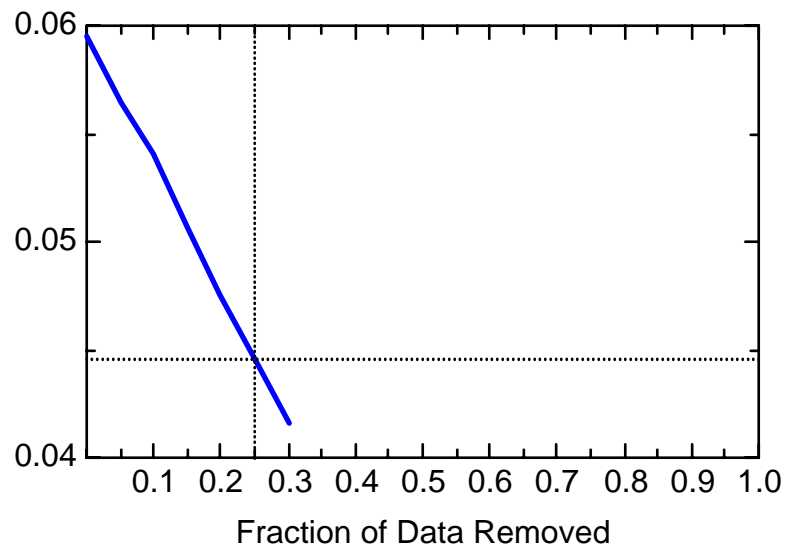
MN: Well MMW1560



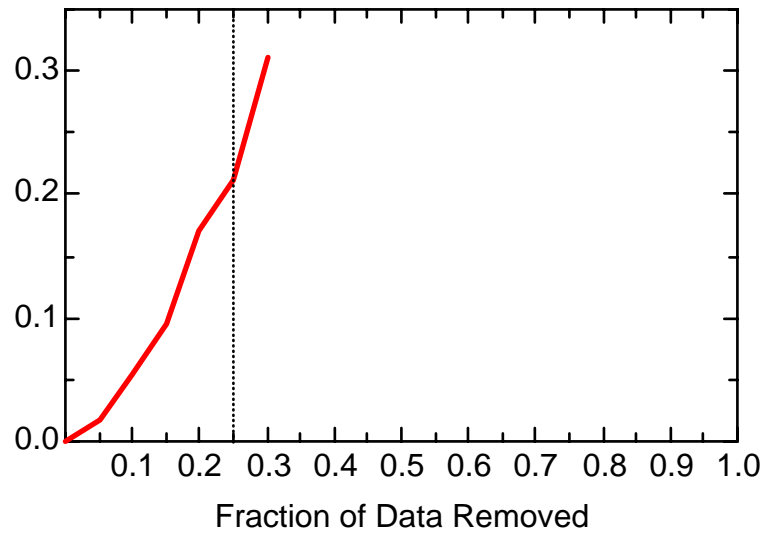
MN: Well MMW1560



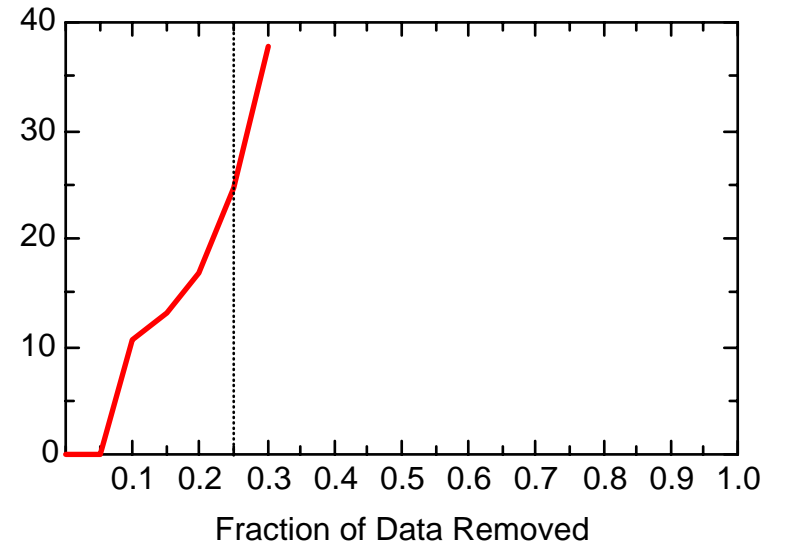
MN: Well MMW1560



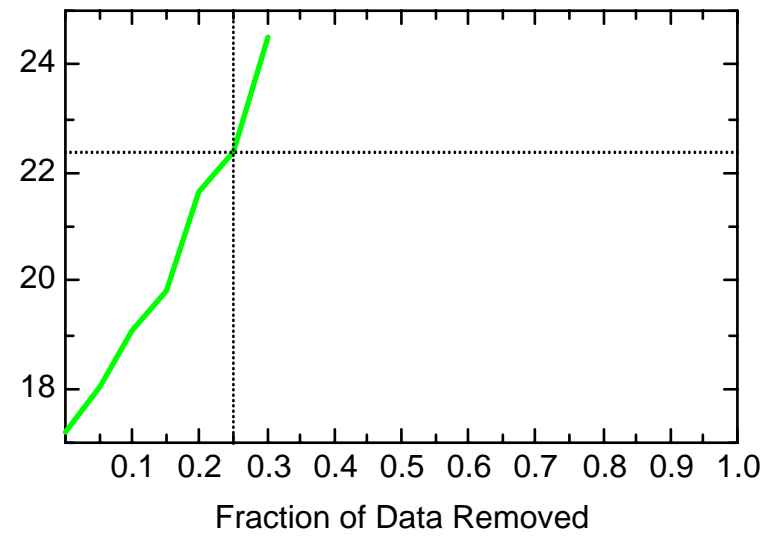
MN: Well MMW7330



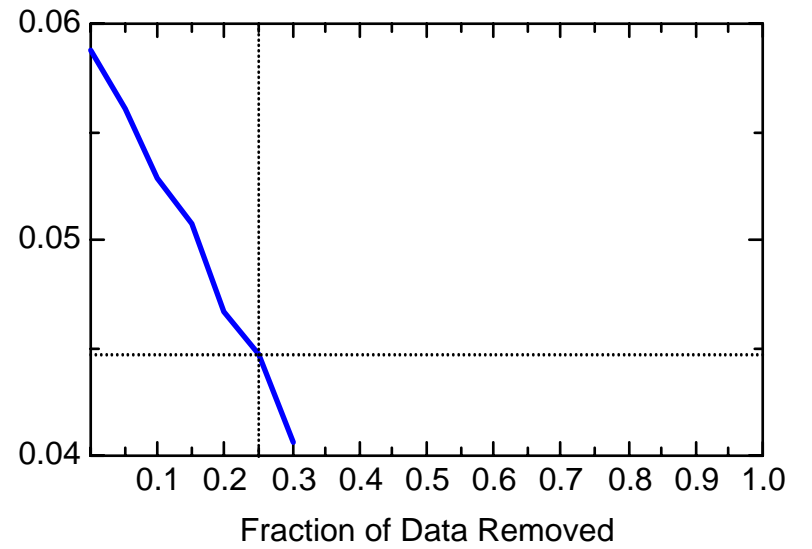
MN: Well MMW7330



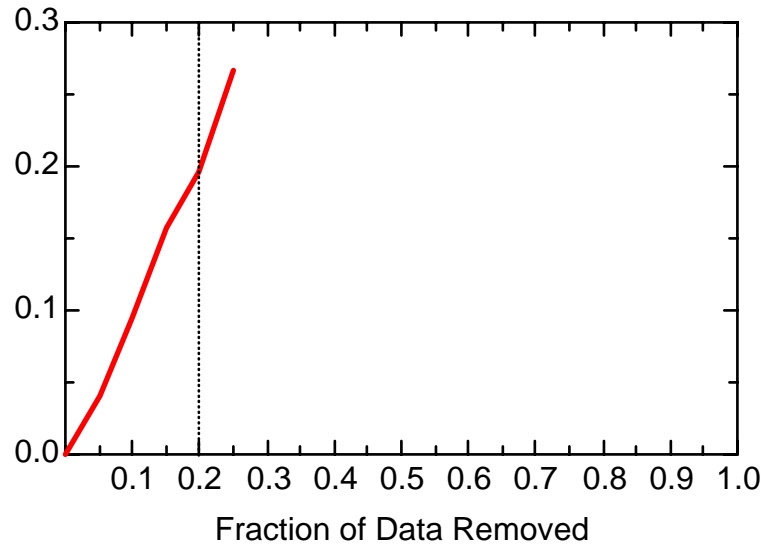
MN: Well MMW7330



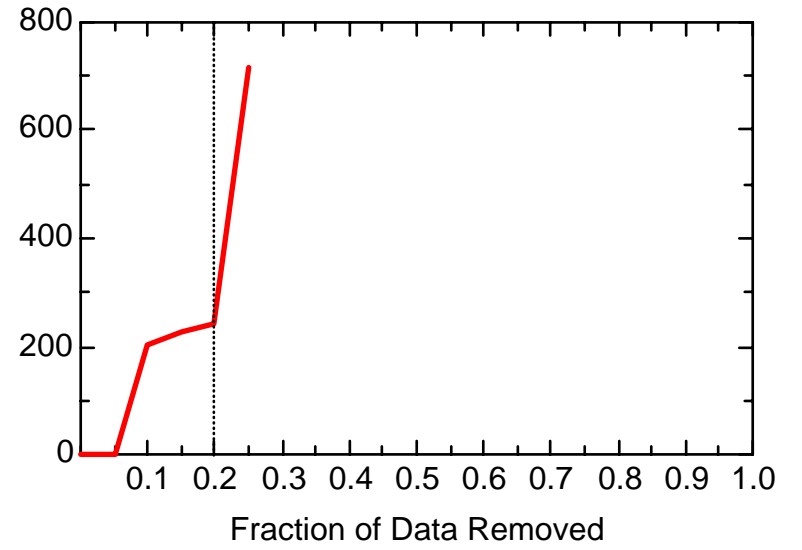
MN: Well MMW7330



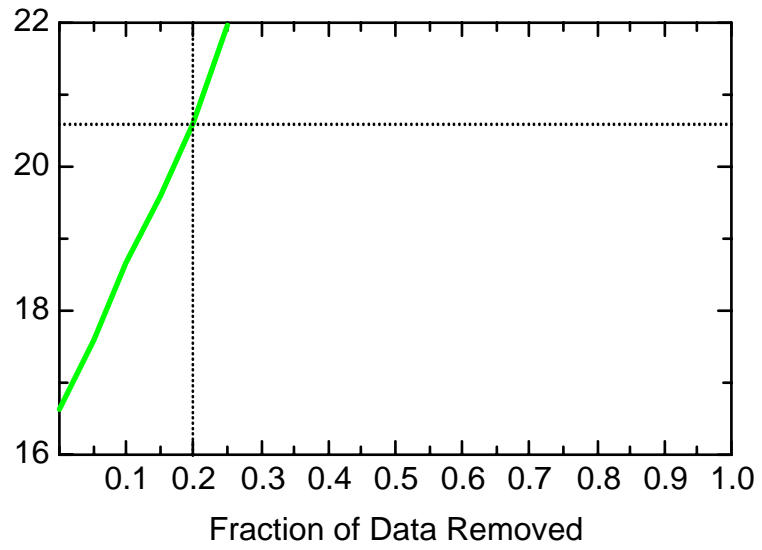
MN: Well MMW8015



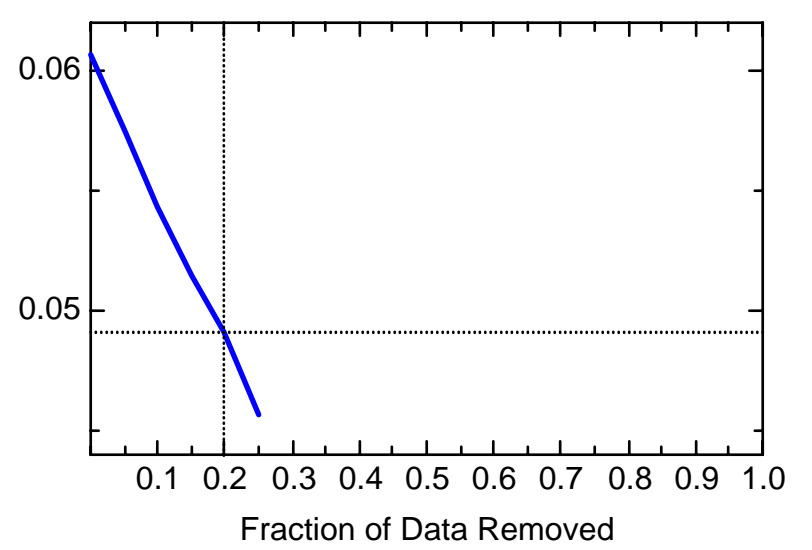
MN: Well MMW8015



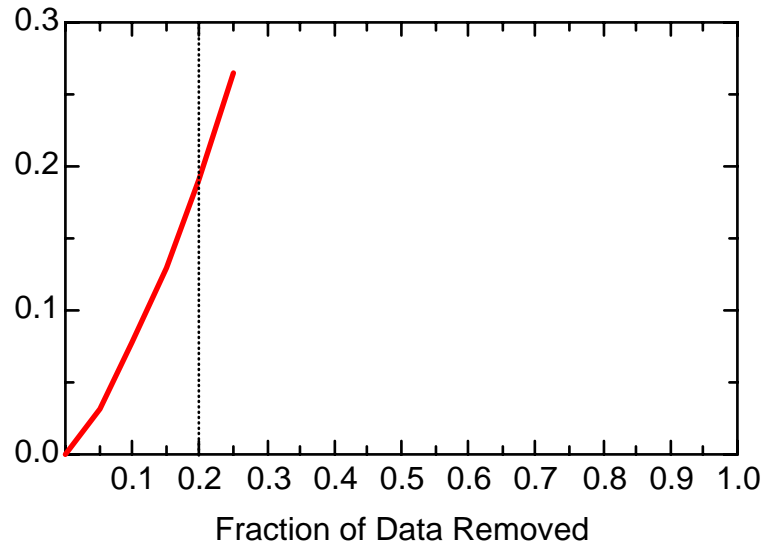
MN: Well MMW8015



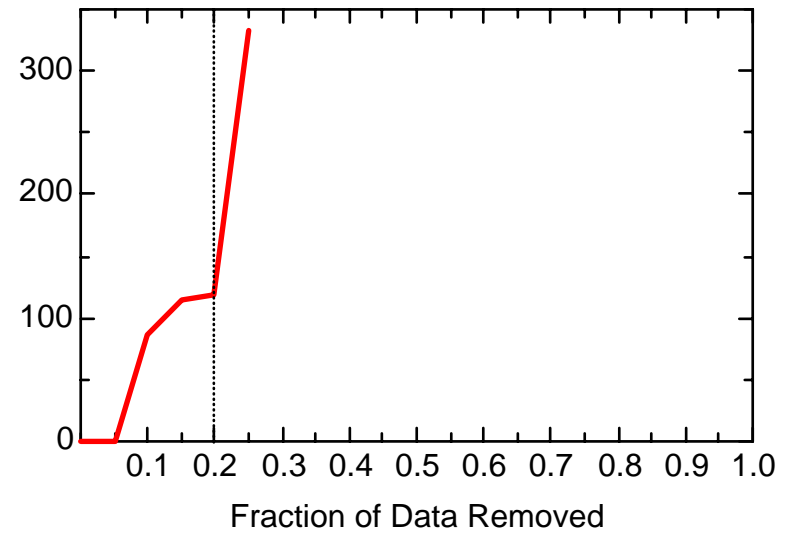
MN: Well MMW8015



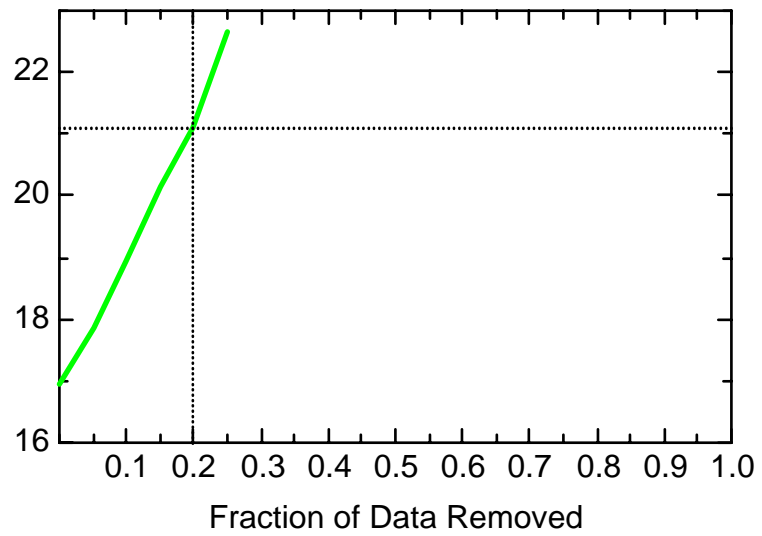
MN: Well RFW1144



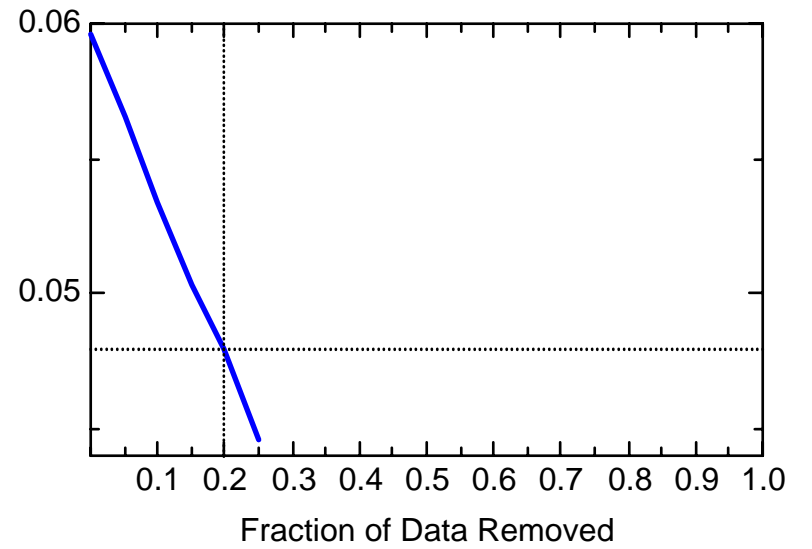
MN: Well RFW1144



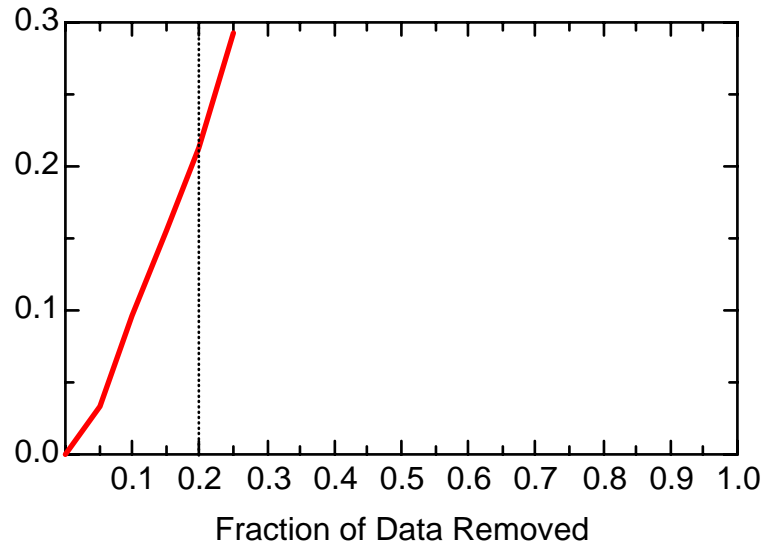
MN: Well RFW1144



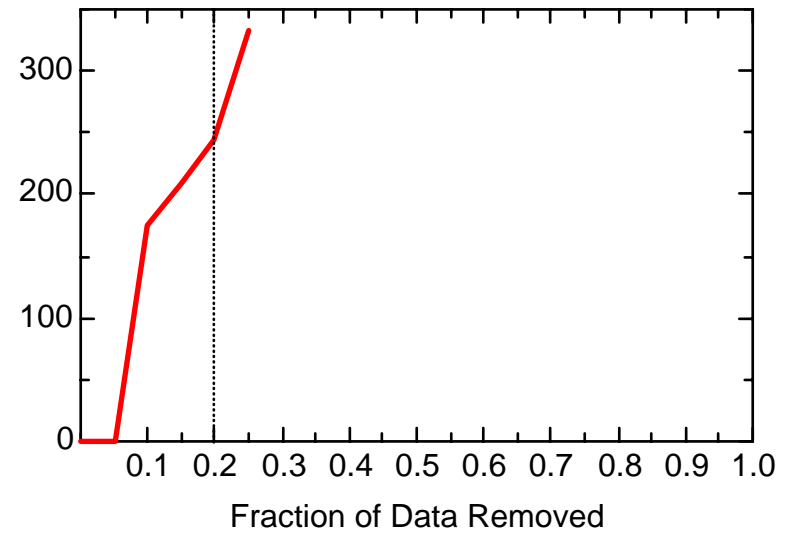
MN: Well RFW1144



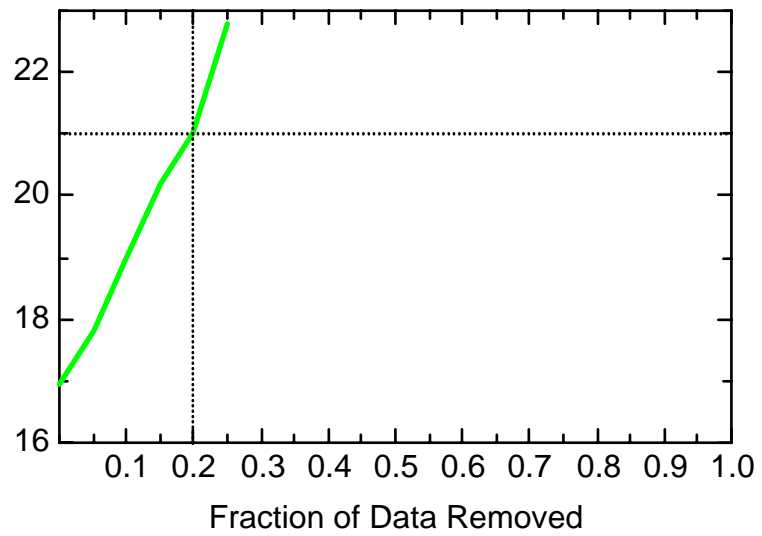
MN: Well RFW1147



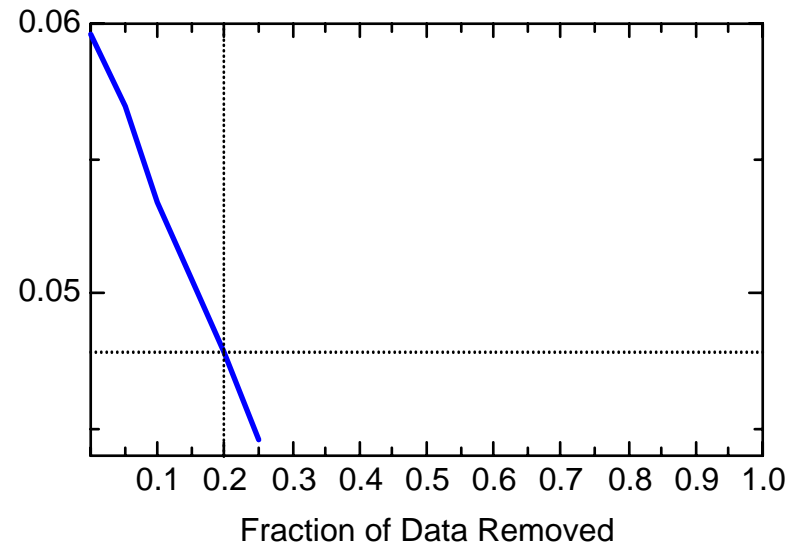
MN: Well RFW1147



MN: Well RFW1147

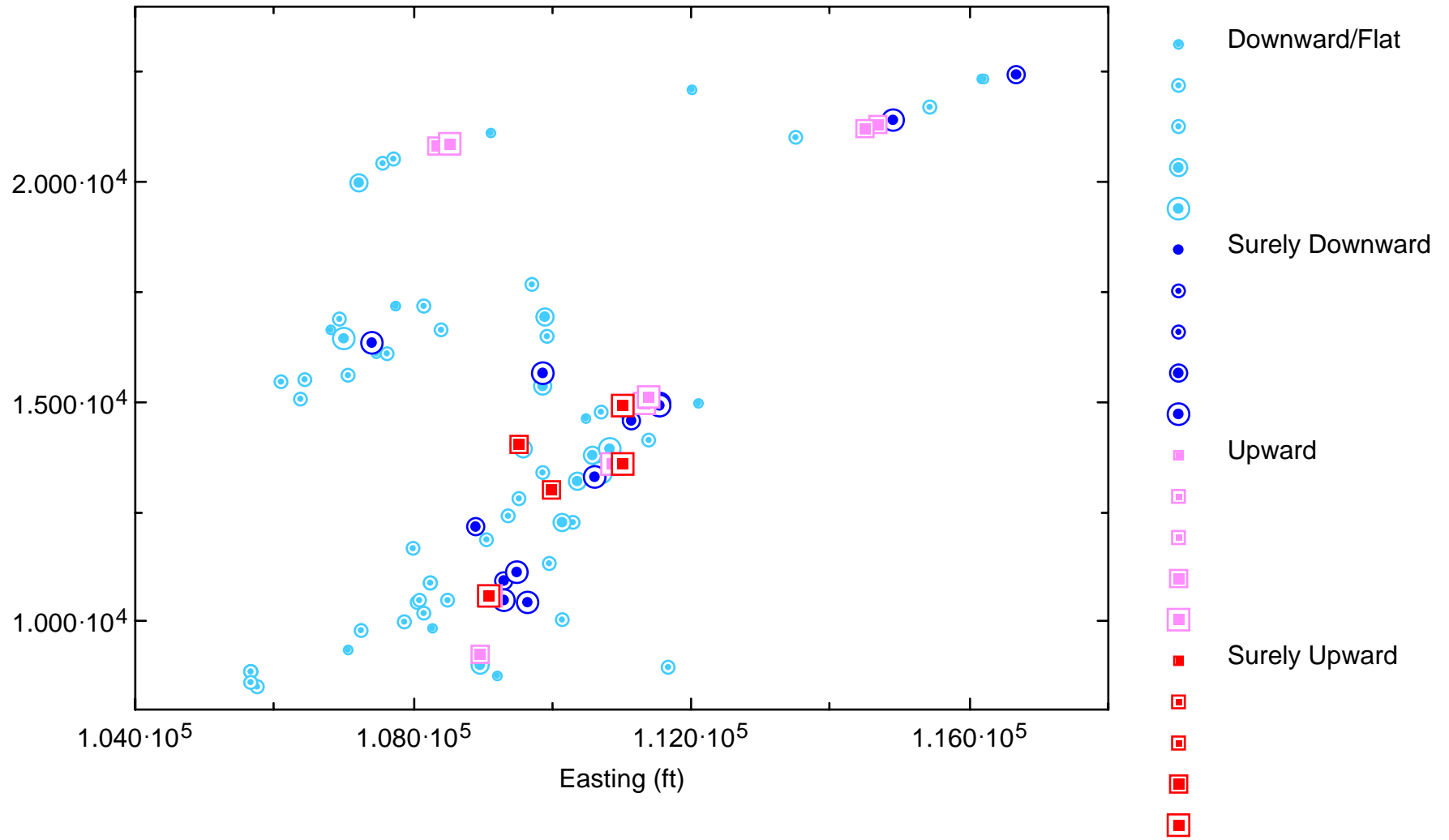


MN: Well RFW1147

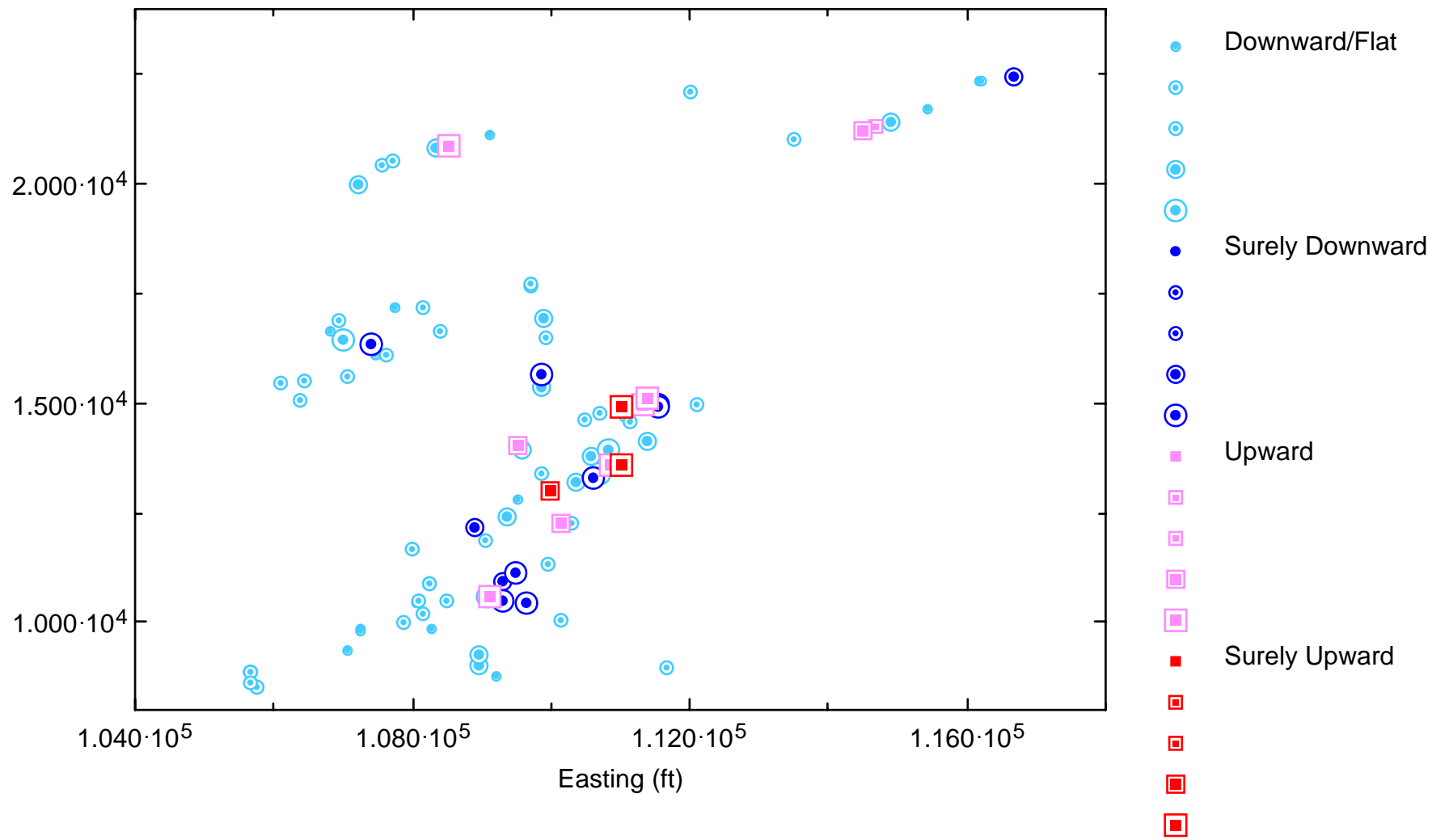


Appendix 3-4
Temporal Optimization:
Trend Maps

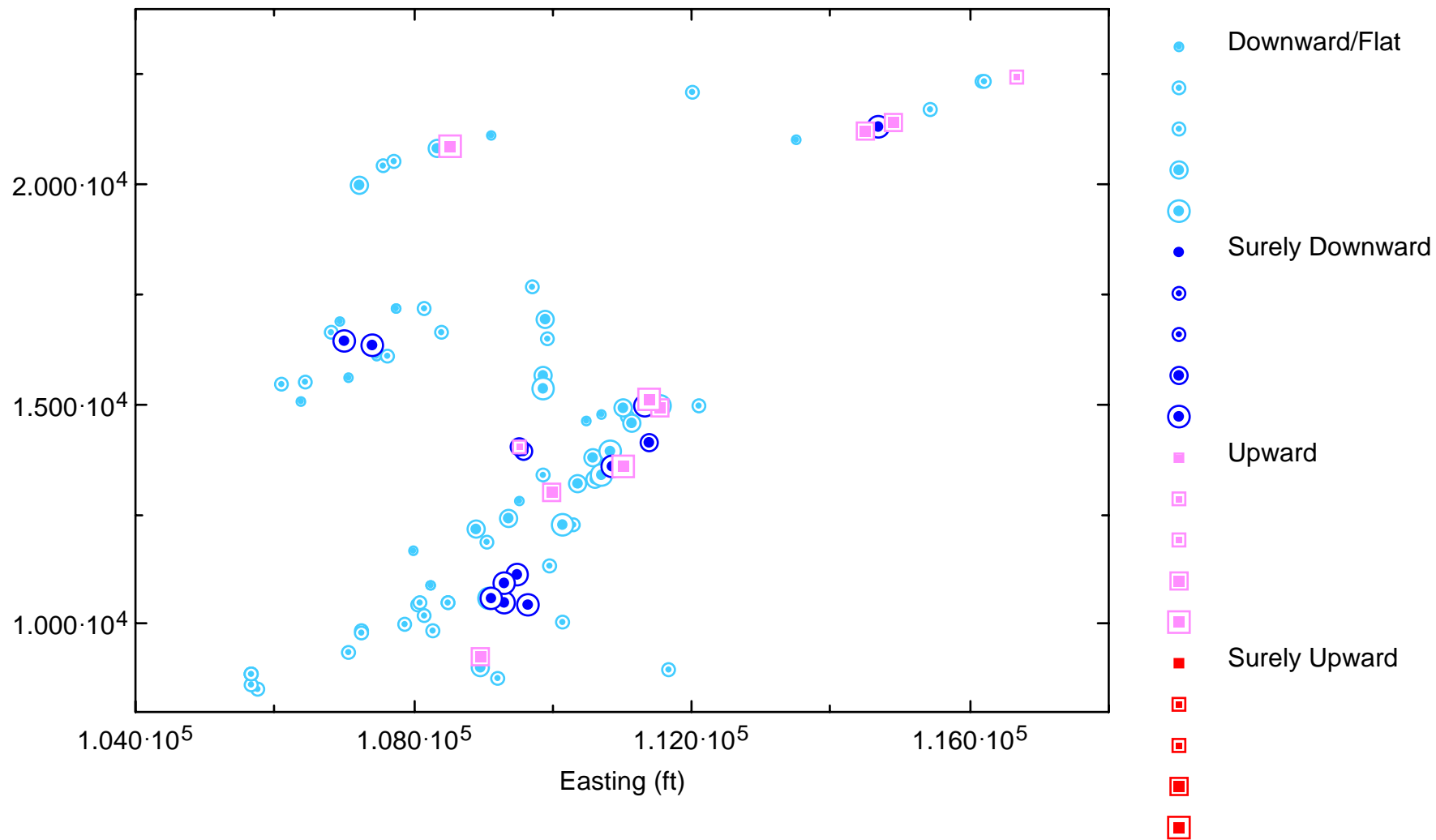
Post-Plot of Historical Median Trends for Bz



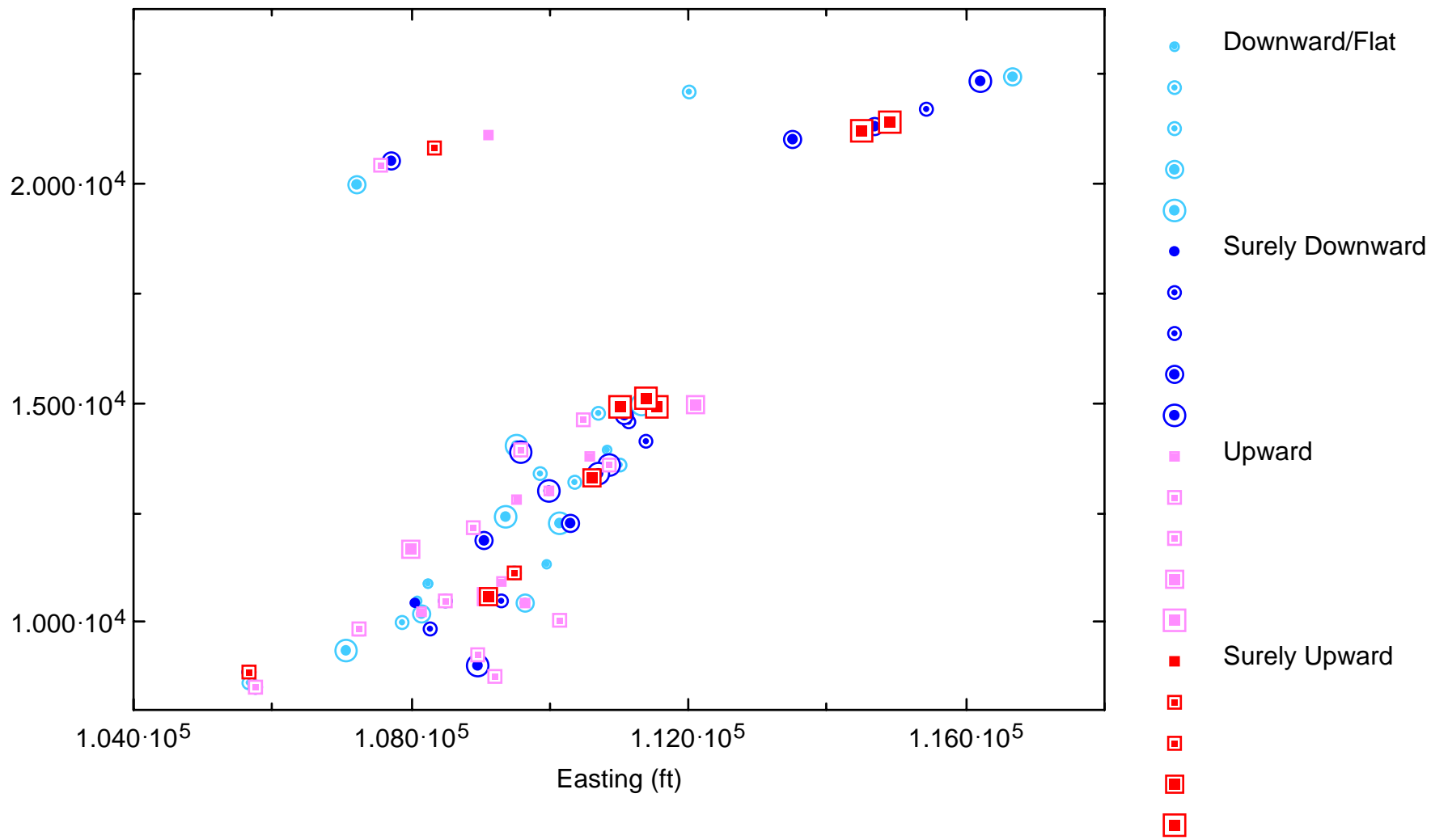
Post-Plot of Recent (Post-1999) Median Trends for BZ



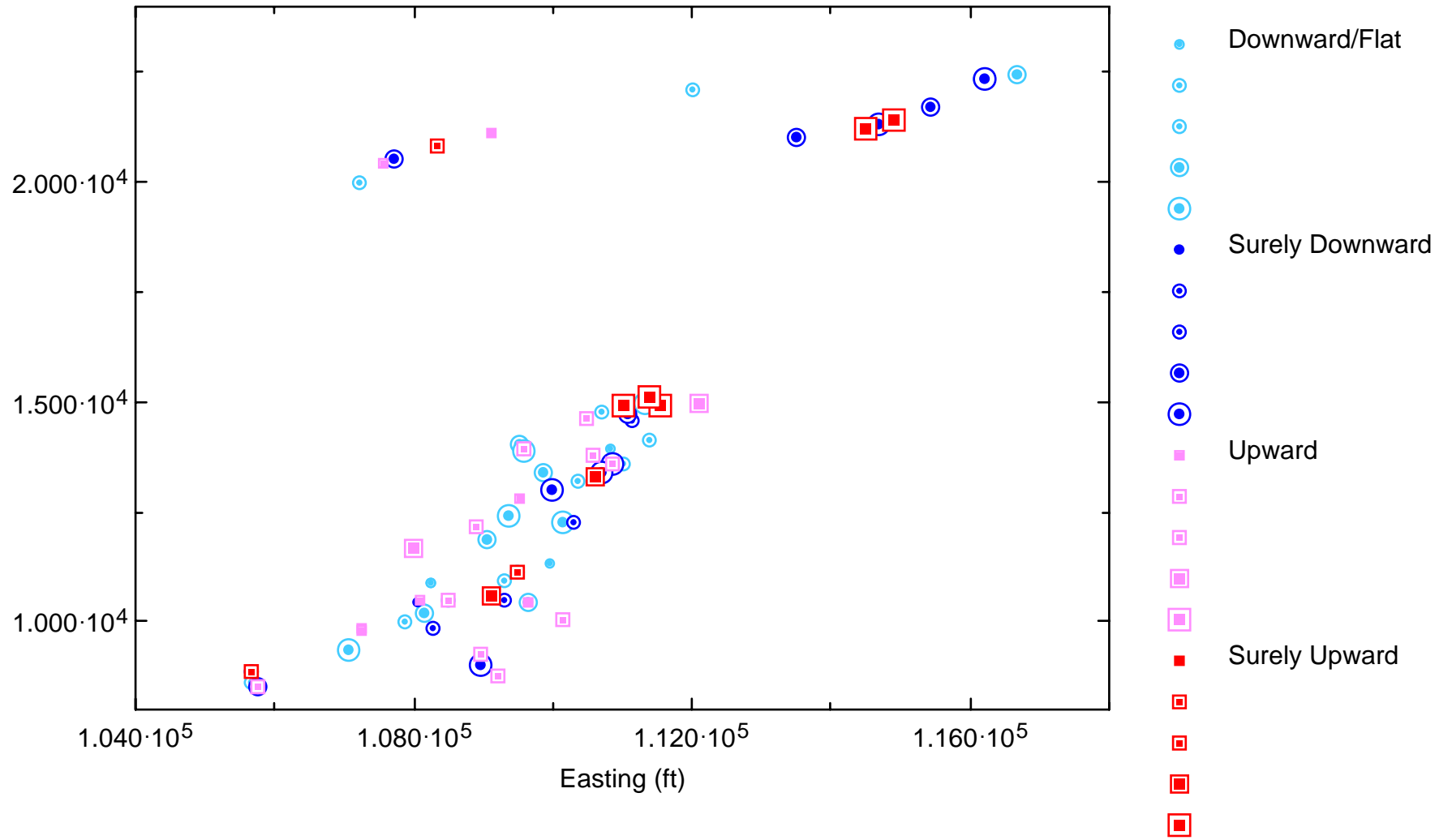
Post-Plot of New (Last 4 Sampling Events) Median Trends for BZ



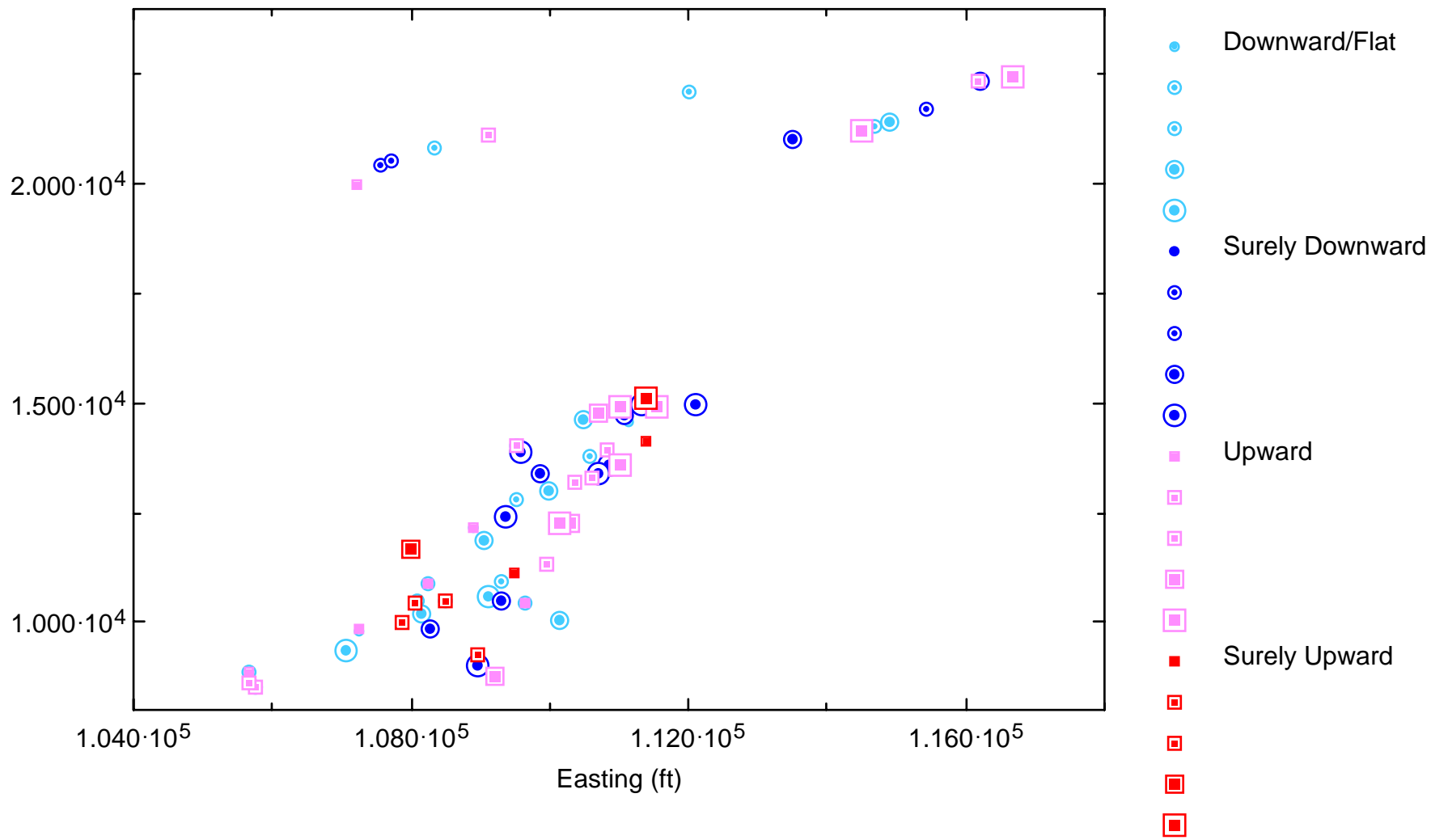
Post-Plot of Historical Median Trends for FI



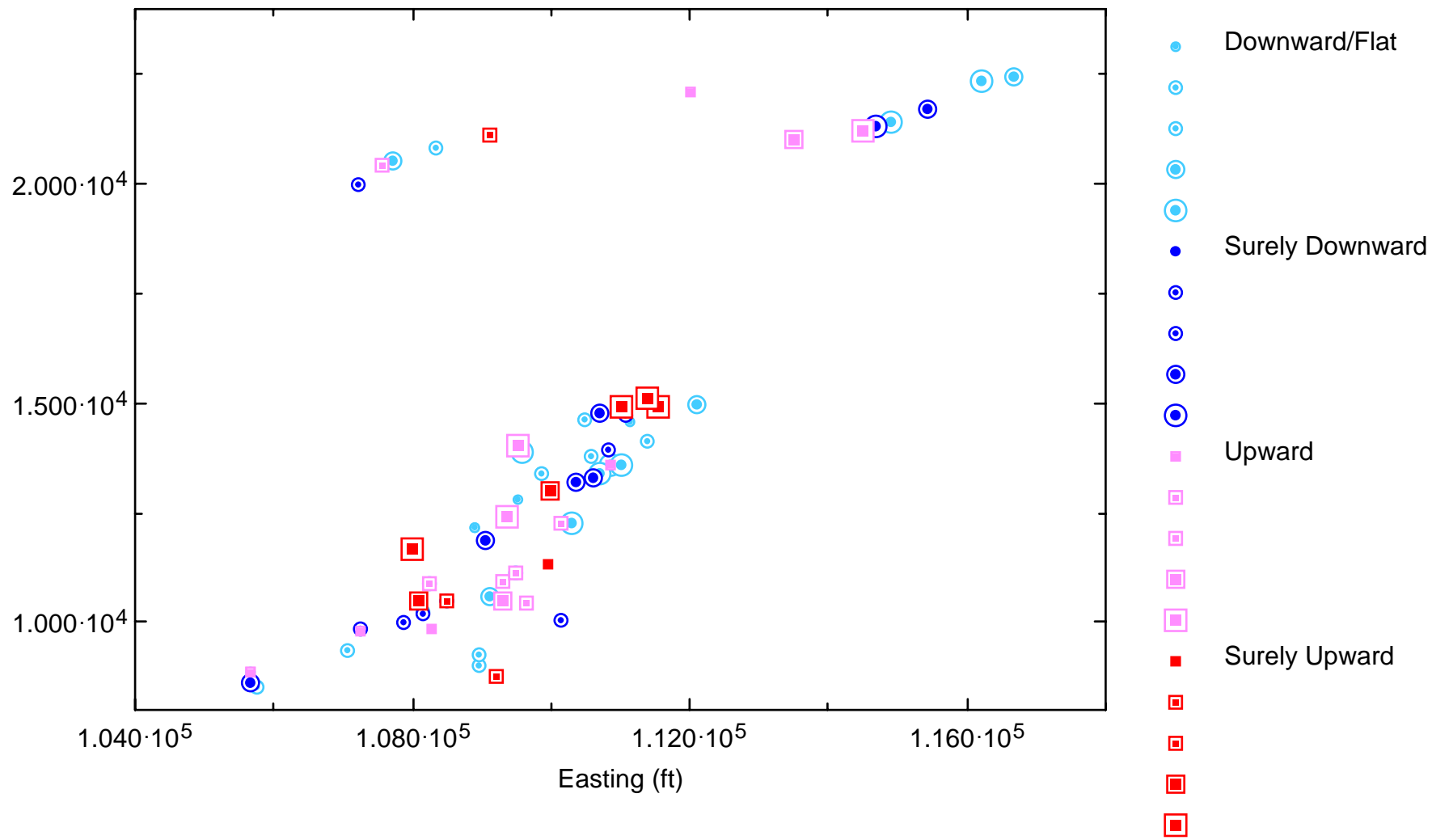
Post-Plot of Recent (Post-1999) Median Trends for FE



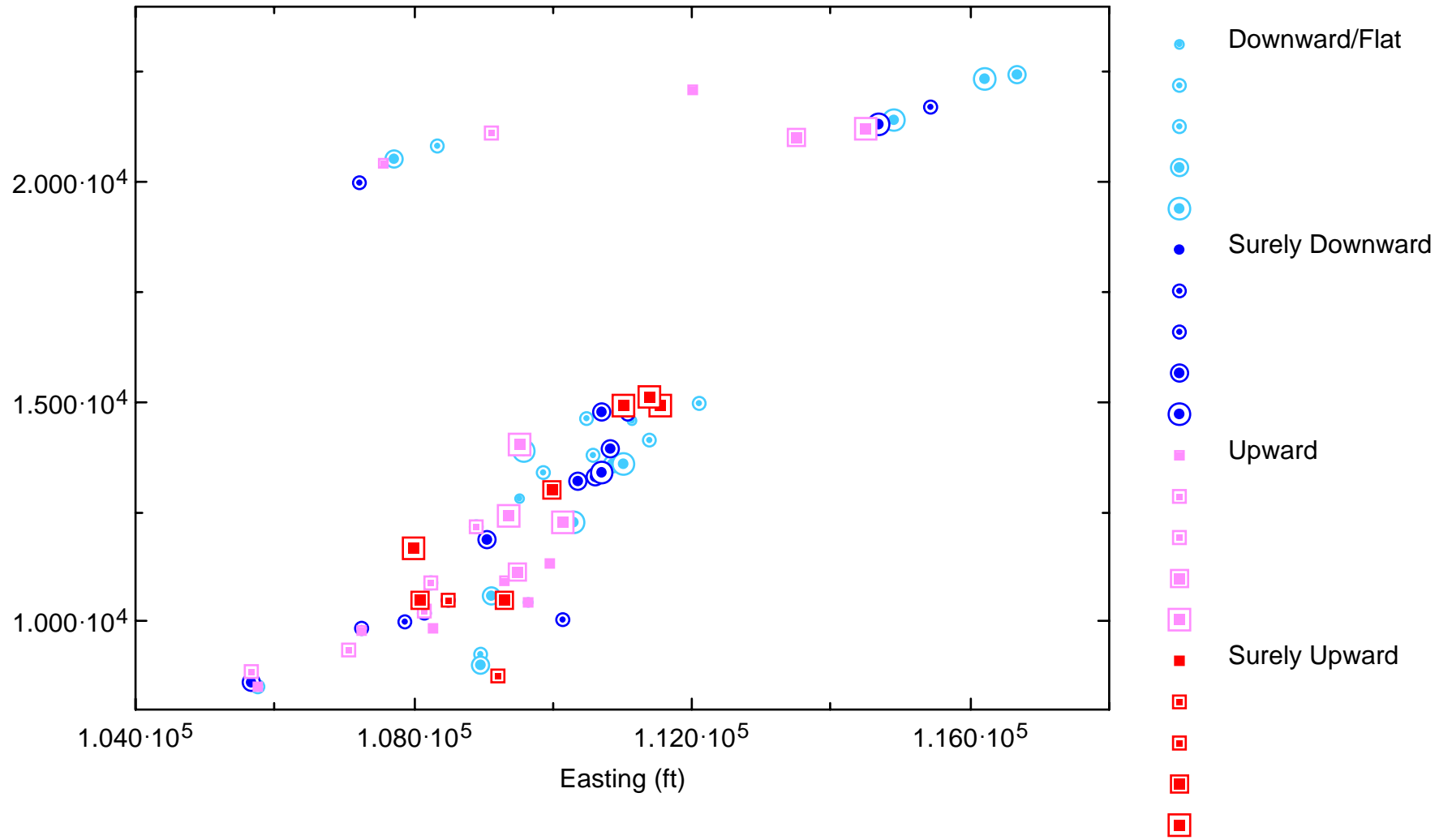
Post-Plot of New (Last 4 Sampling Events) Median Trends for FE



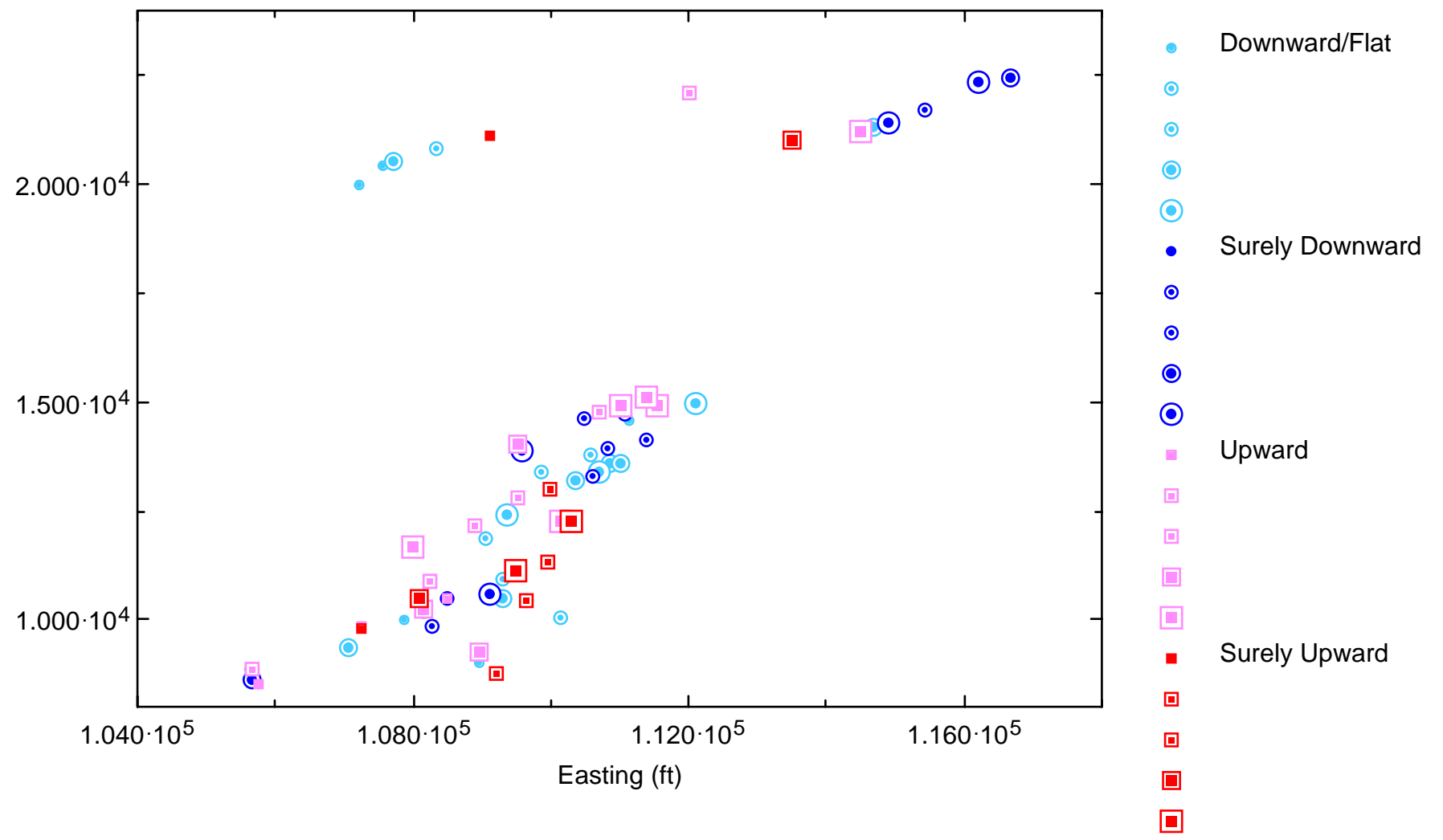
Post-Plot of Historical Median Trends for MR



Post-Plot of Recent (Post-1999) Median Trends for MN



Post-Plot of New (Last 4 Sampling Events) Median Trends for MN



Appendix 4-1

Spatial Optimization: Global Redundancy Measures

Key to acronyms:

REDUCED-VARPCT = Percentage of voxels with high local (node-specific) regression variances

AVE-IDIFF = Average difference between locally-weighted quadratic regression (LWQR) indicator estimates from reduced dataset and LWQR indicator estimates from base map

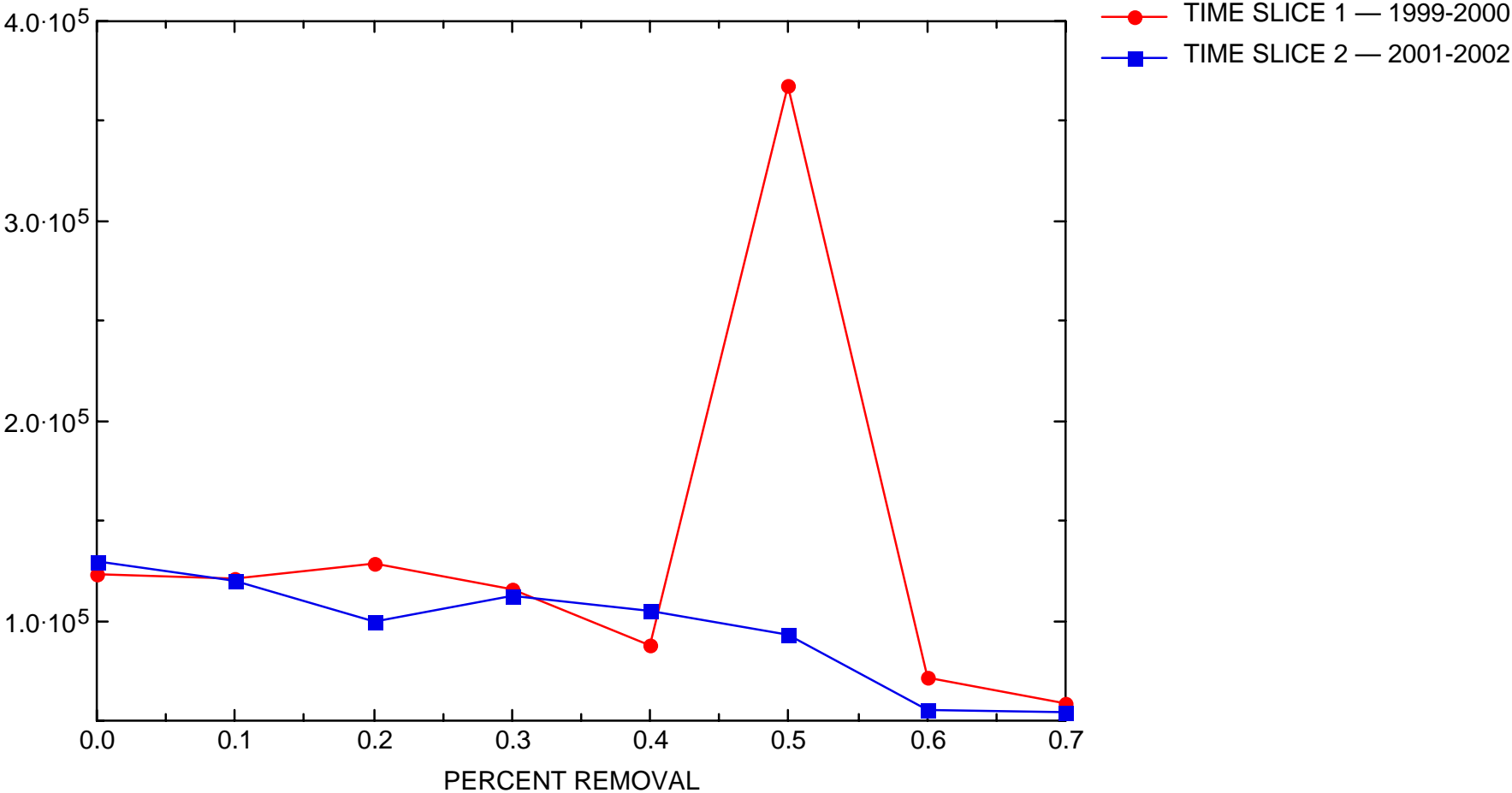
MEAN-MISCLASS = Percentage of voxels classified in opposite ways on base and reduced-data maps with respect to fixed standard (using LWQR mean concentration estimate)

TRIM-MISCLASS = Percentage of voxels classified in opposite ways on base and reduced-data maps with respect to fixed standard (using LWQR trimmed mean concentration estimate)

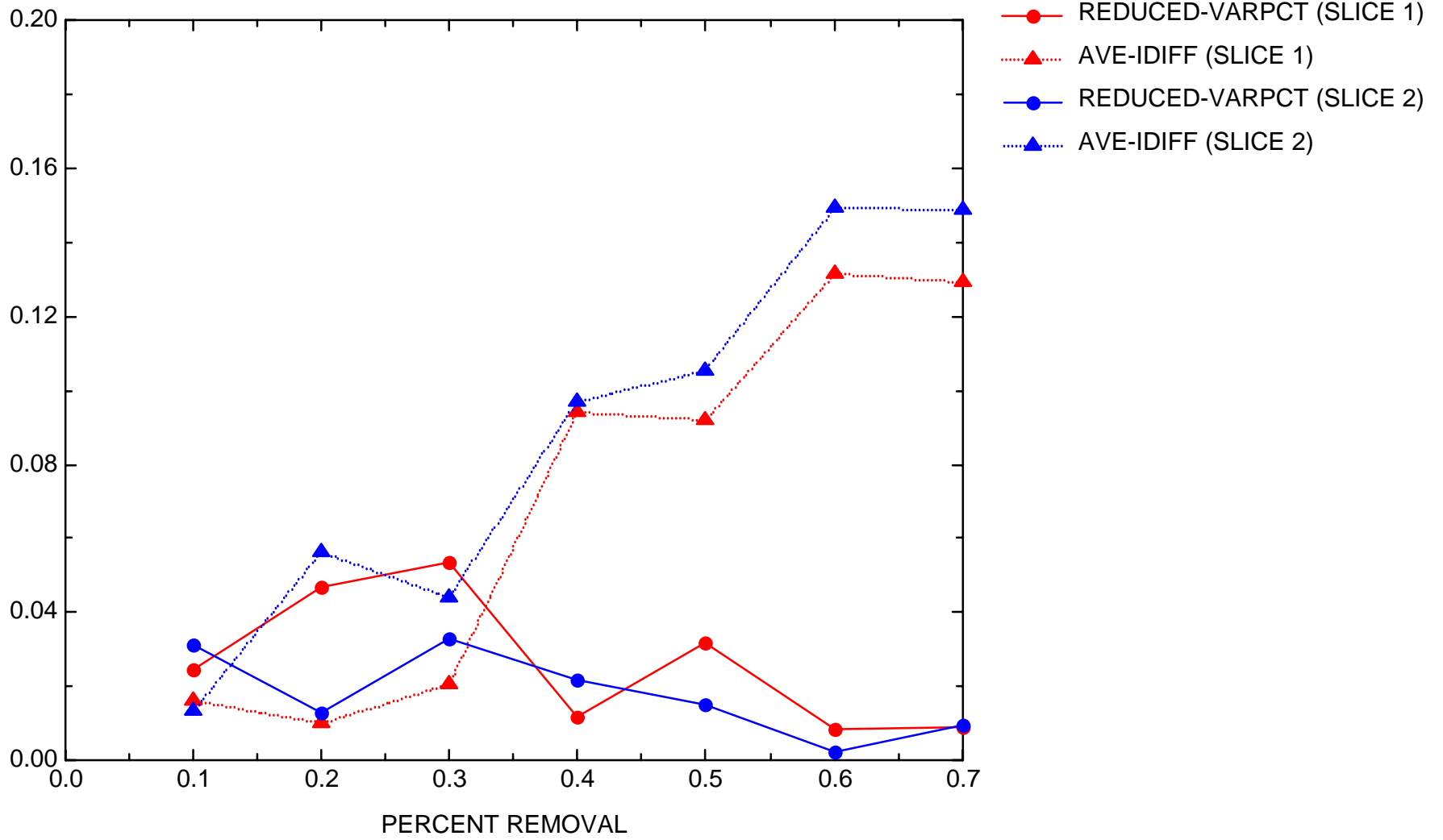
PCT-IDIFF = Percentage of voxels at which at least one reduced-data indicator estimate differs from corresponding base map indicator estimate by at least 0.5

BZ

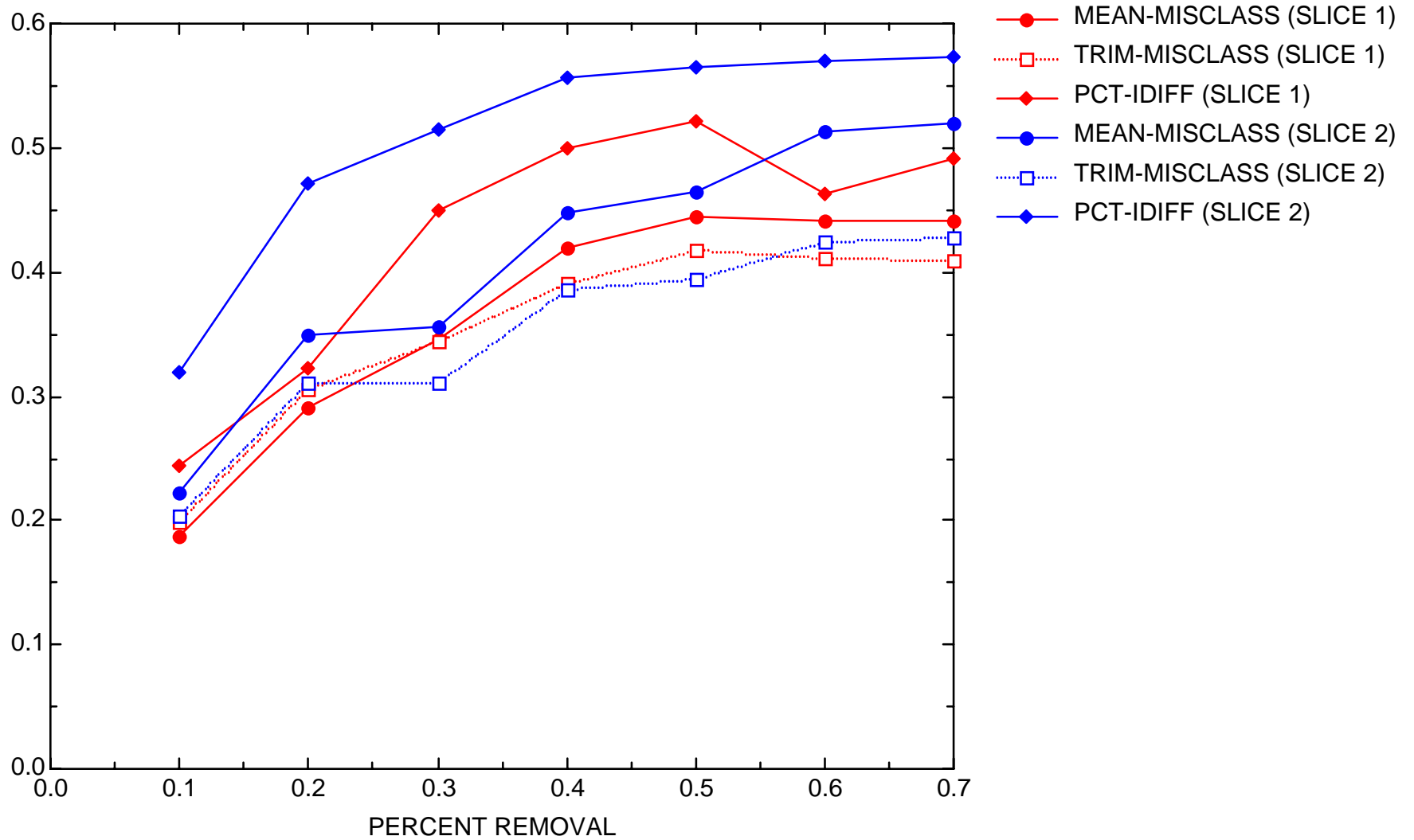
LORING AFB, SITE OU-12: BZ TRENDS IN GLOBAL VARIANCE



LORING AFB, SITE OU-12: BZ GLOBAL REDUNDANCY MEASURES, PART 1

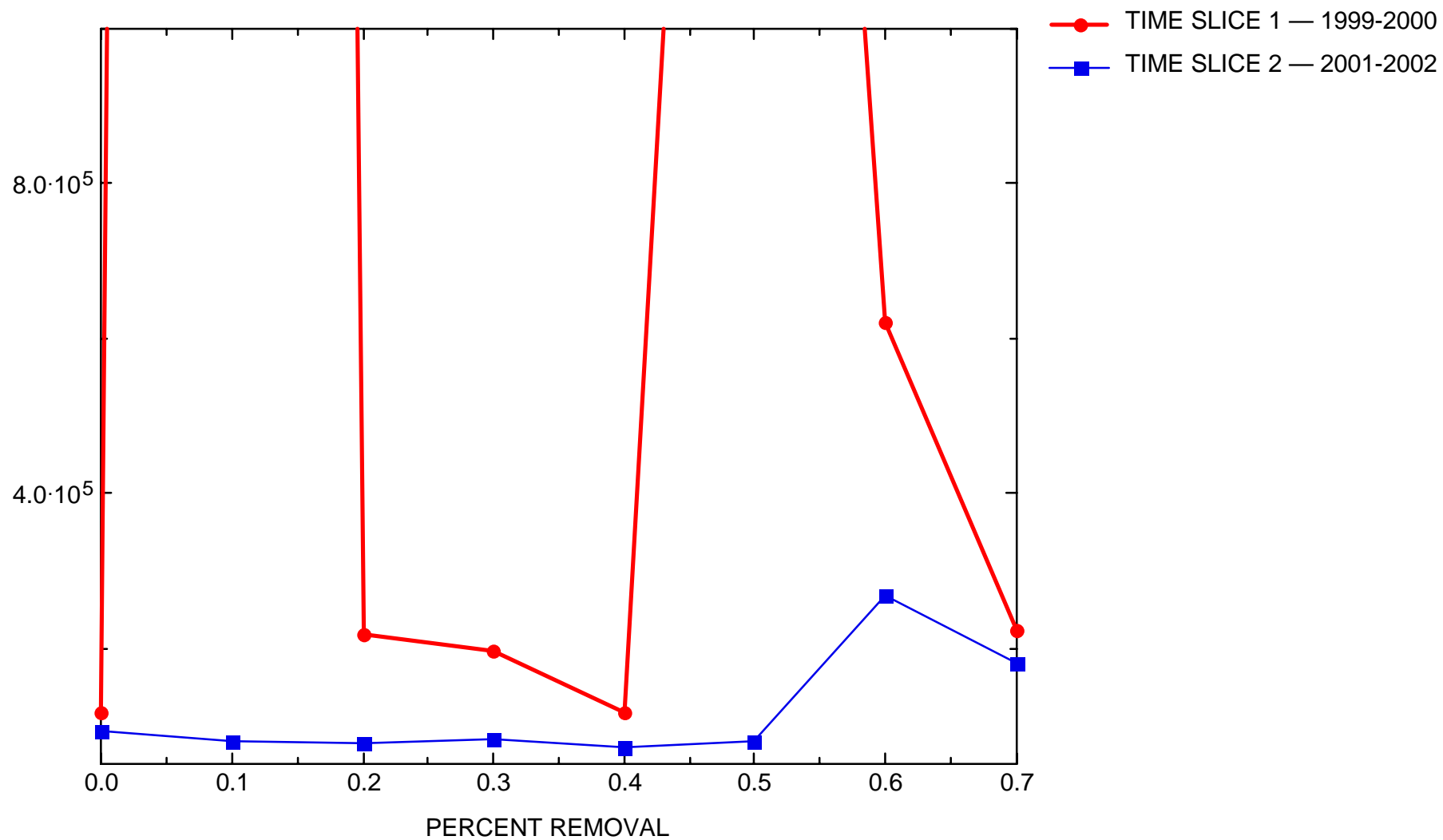


LORING AFB, SITE OU-12: BZ GLOBAL REDUNDANCY MEASURES, PART 2

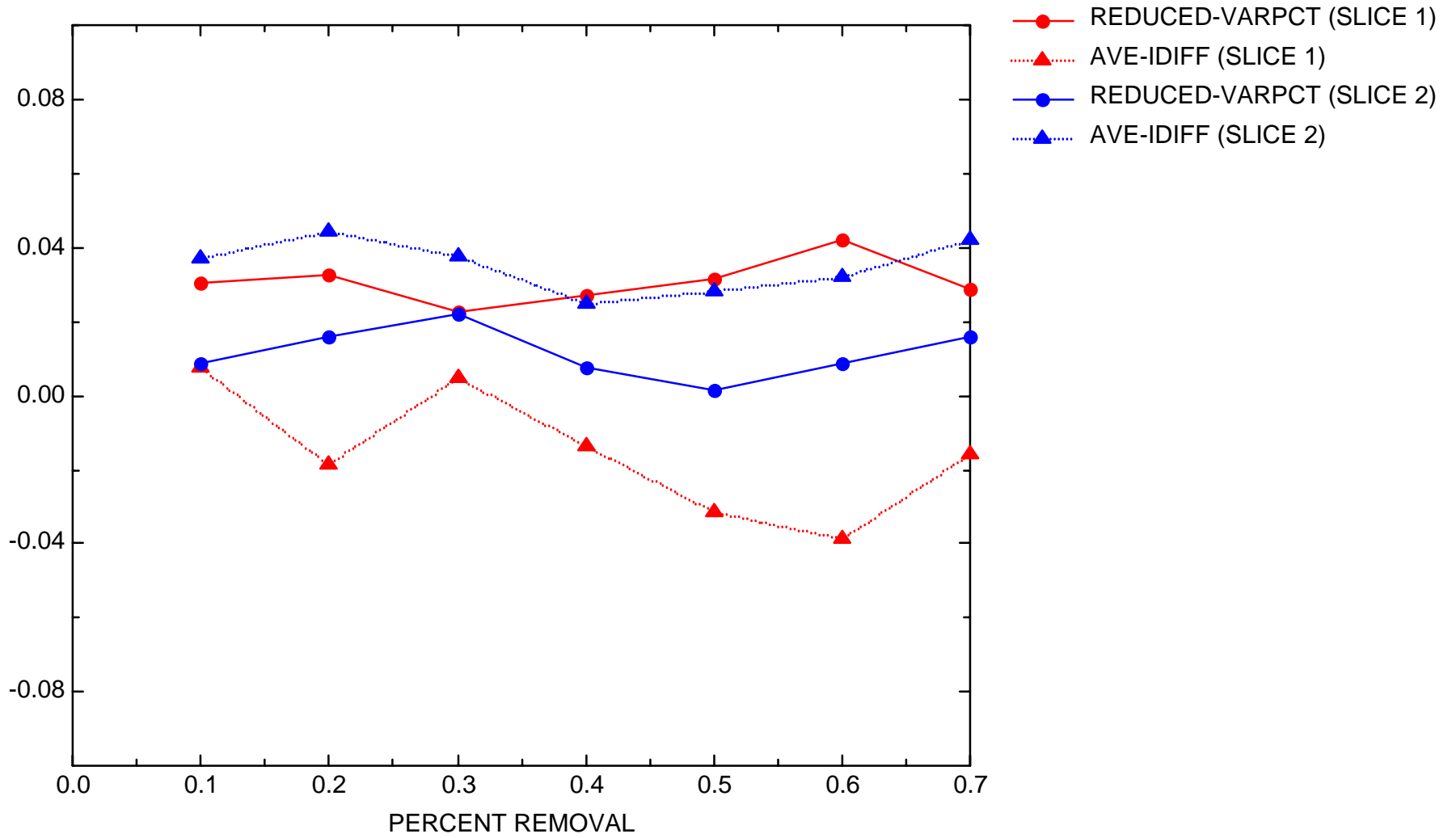


FE

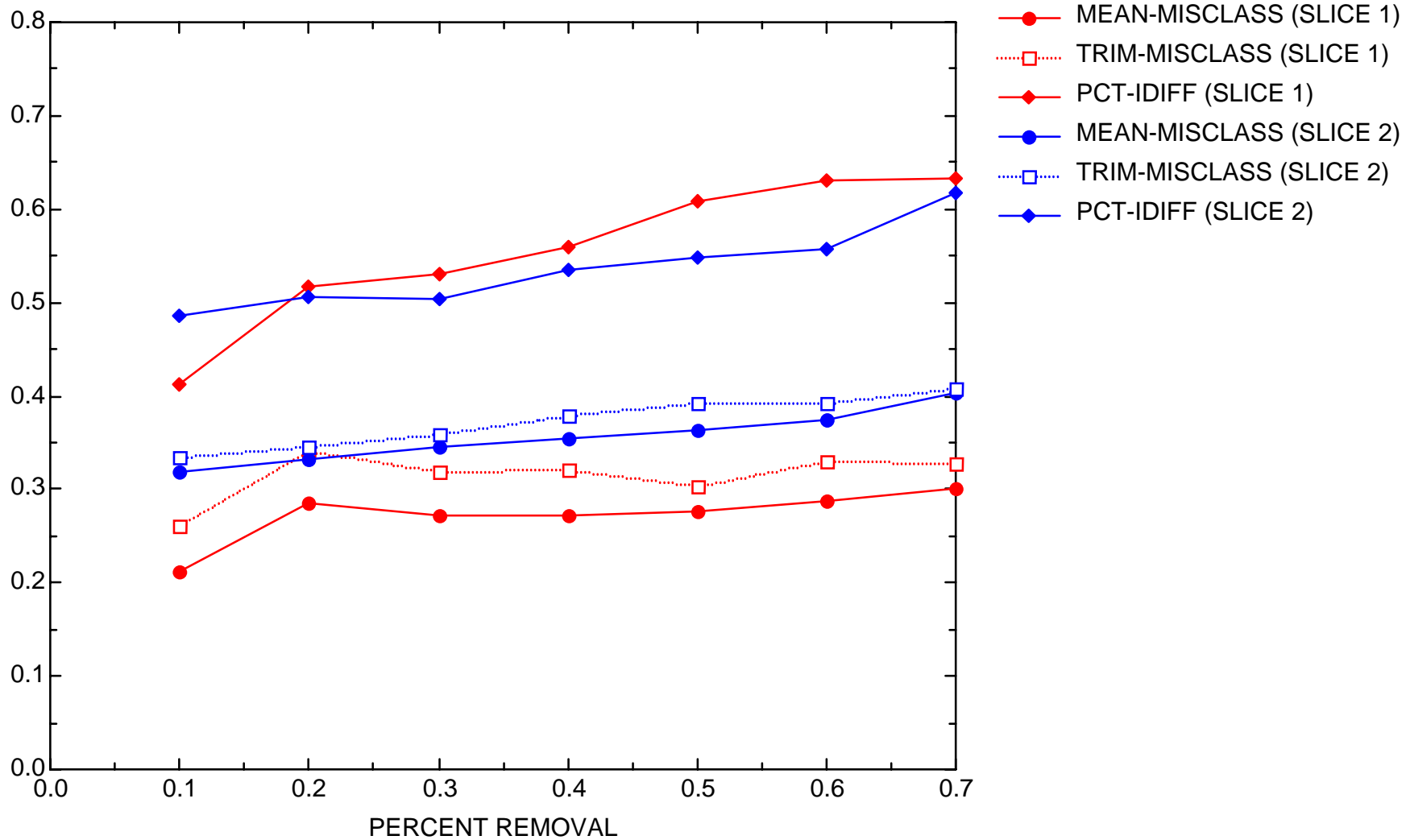
LORING AFB, SITE OU-12: FE TRENDS IN GLOBAL VARIANCE



LORING AFB, SITE OU-12: FE GLOBAL REDUNDANCY MEASURES, PART 1

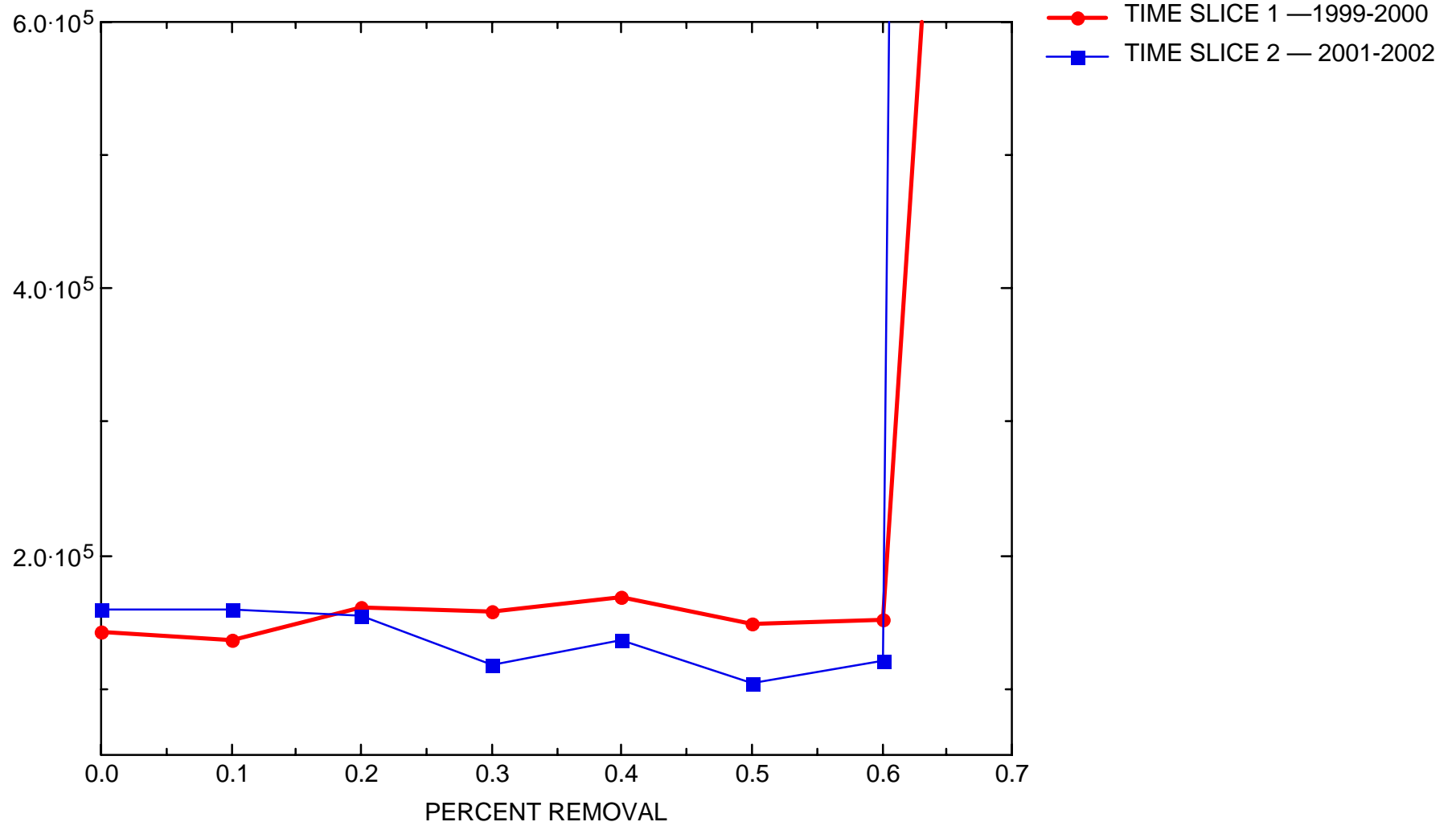


LORING AFB, SITE OU-12: FE GLOBAL REDUNDANCY MEASURES, PART 2

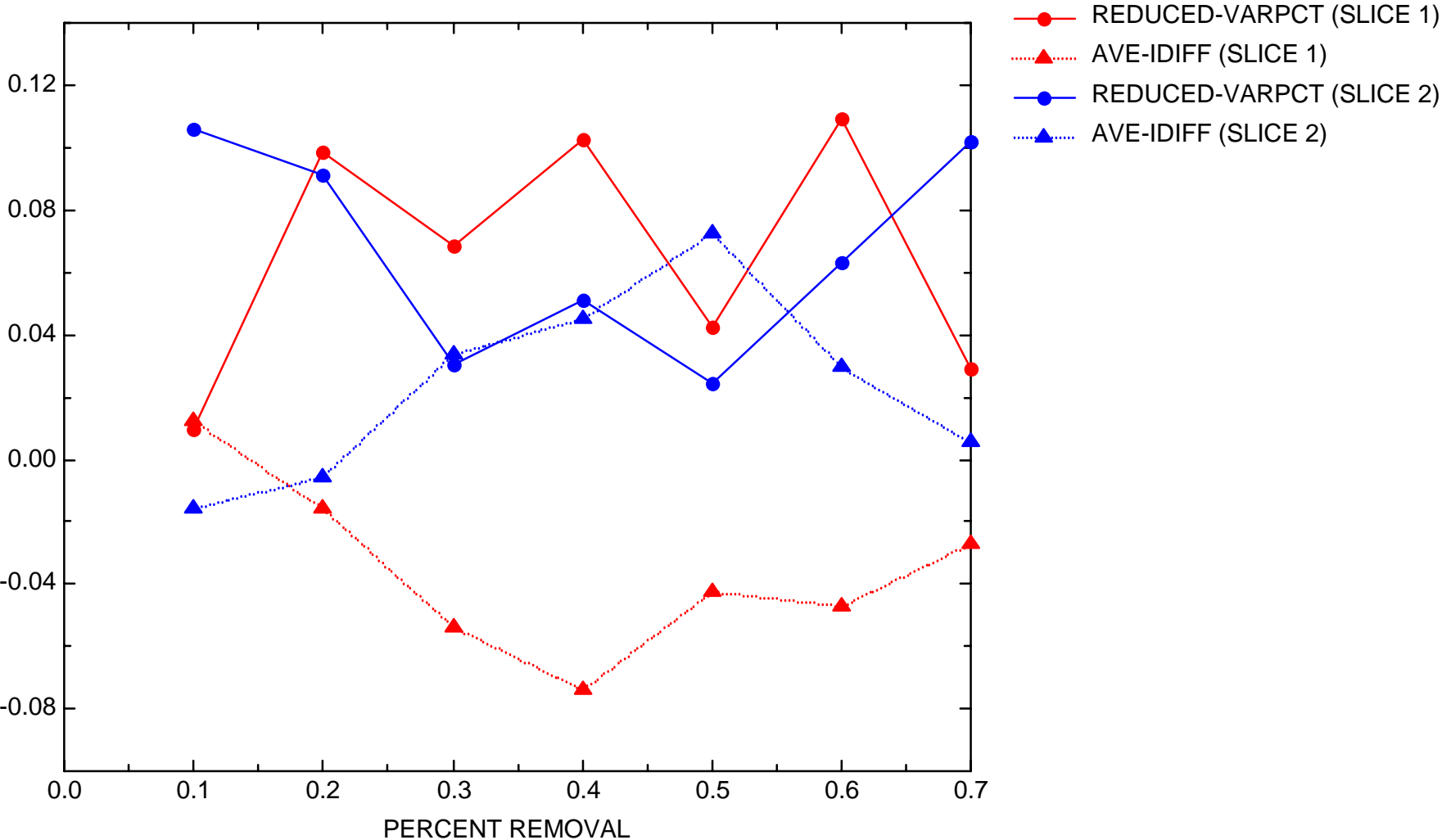


MIN

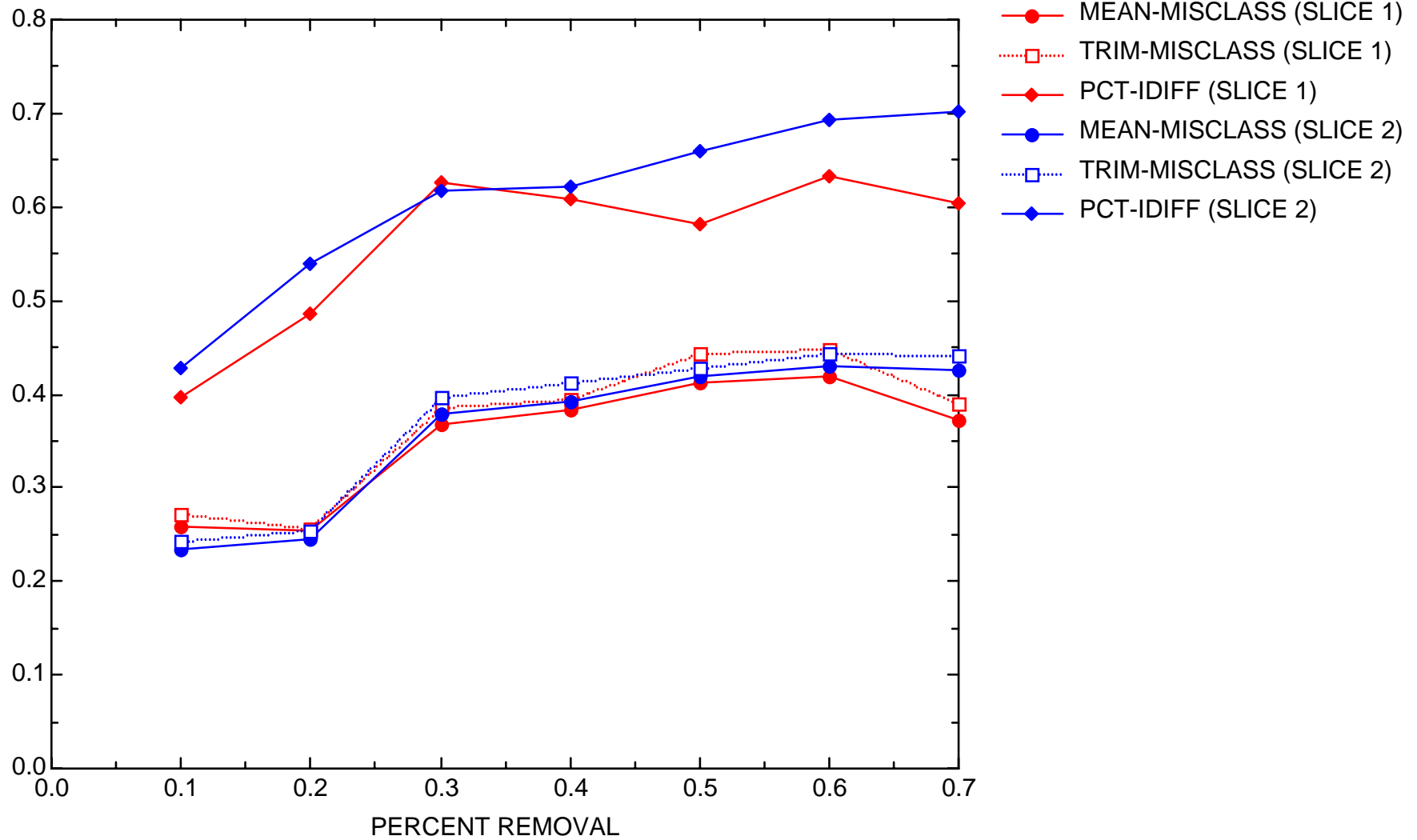
LORING AFB, SITE OU-12: MN TRENDS IN GLOBAL VARIANCE



LORING AFB, SITE OU-12: MN GLOBAL REDUNDANCY MEASURES, PART 1



LORING AFB, SITE OU-12: MN GLOBAL REDUNDANCY MEASURES, PART 2



Appendix 4-2

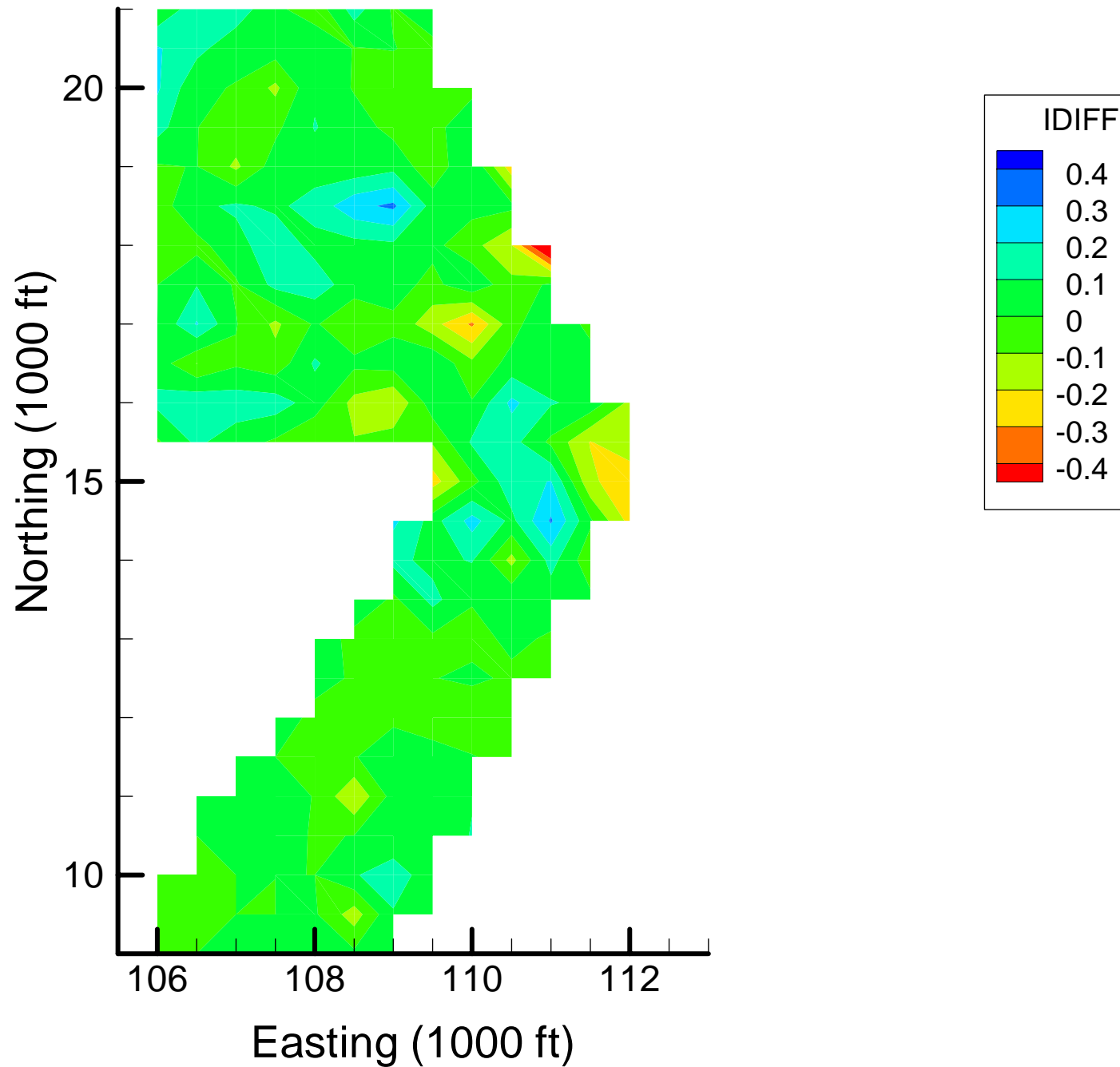
Spatial Optimization: BZ Indicator Difference Maps

Notes:

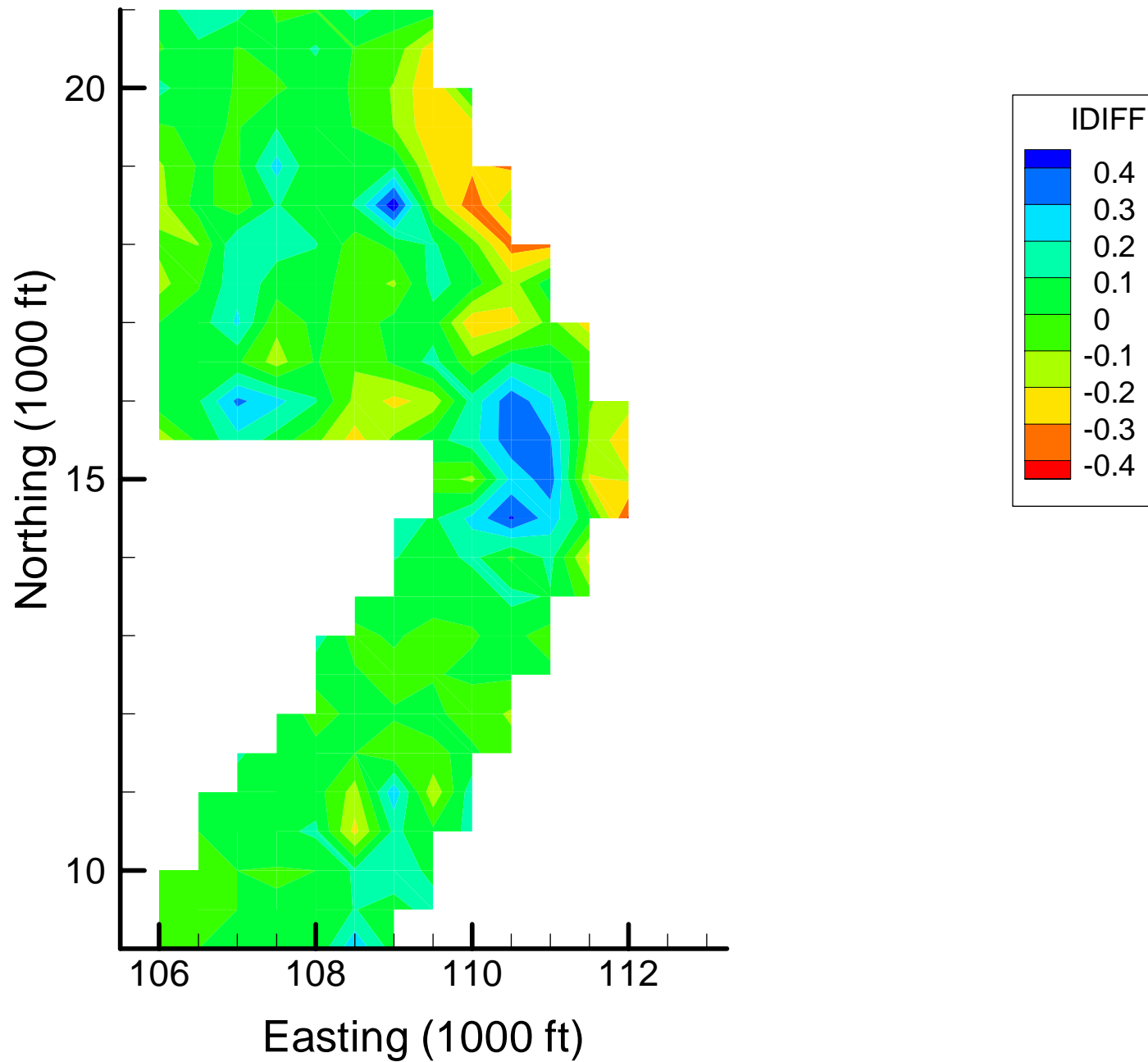
IDIFF = Difference between voxel-specific locally-weighted quadratic regression (LWQR) indicator estimates from reduced-data map to base map (averaged over depth)

Color scheme — red = overestimate compared to base map; blue = underestimate compared to base map

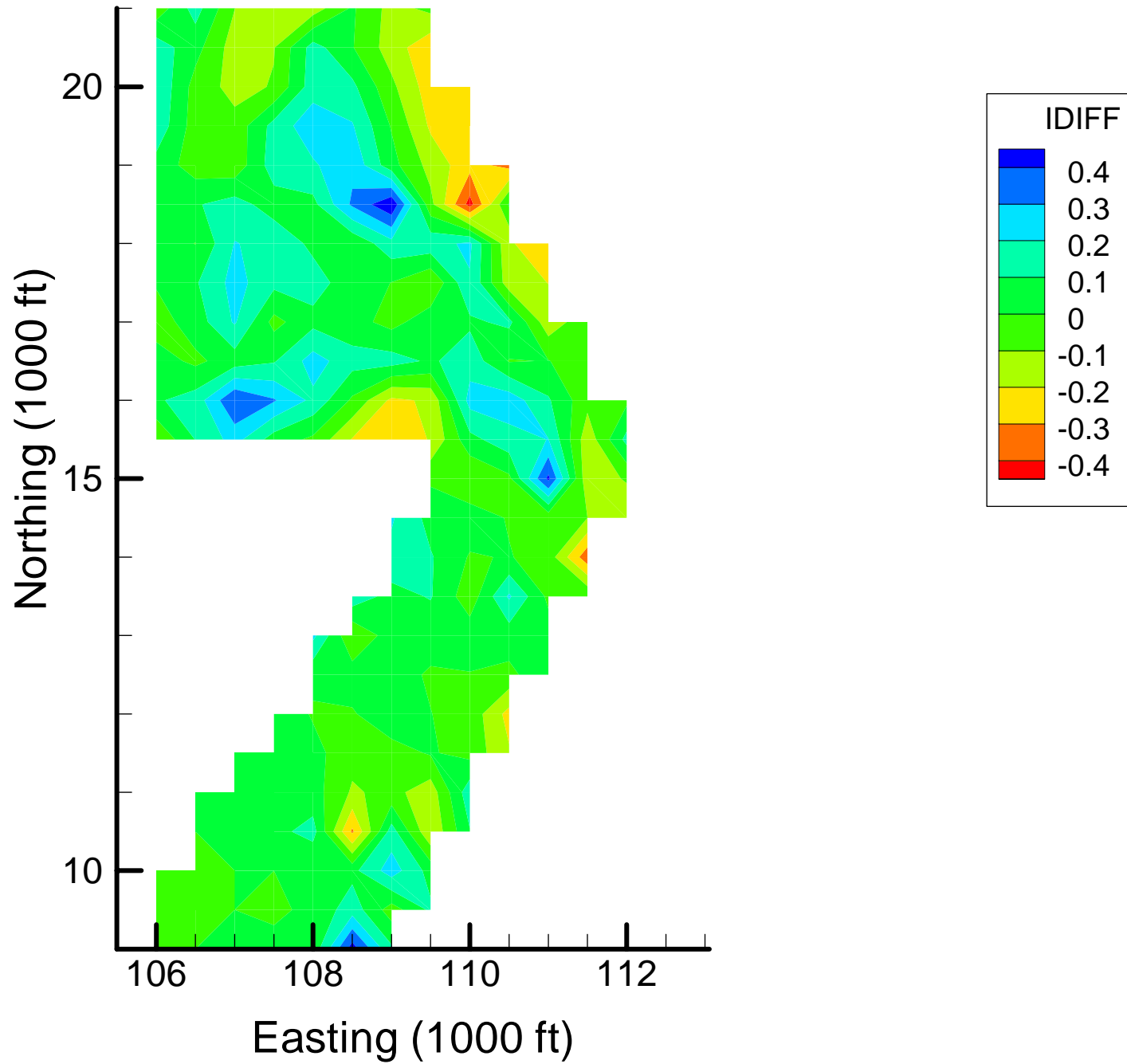
Site OU-12: Benzene Indicator Differences, 1999-2000, 10% Removal



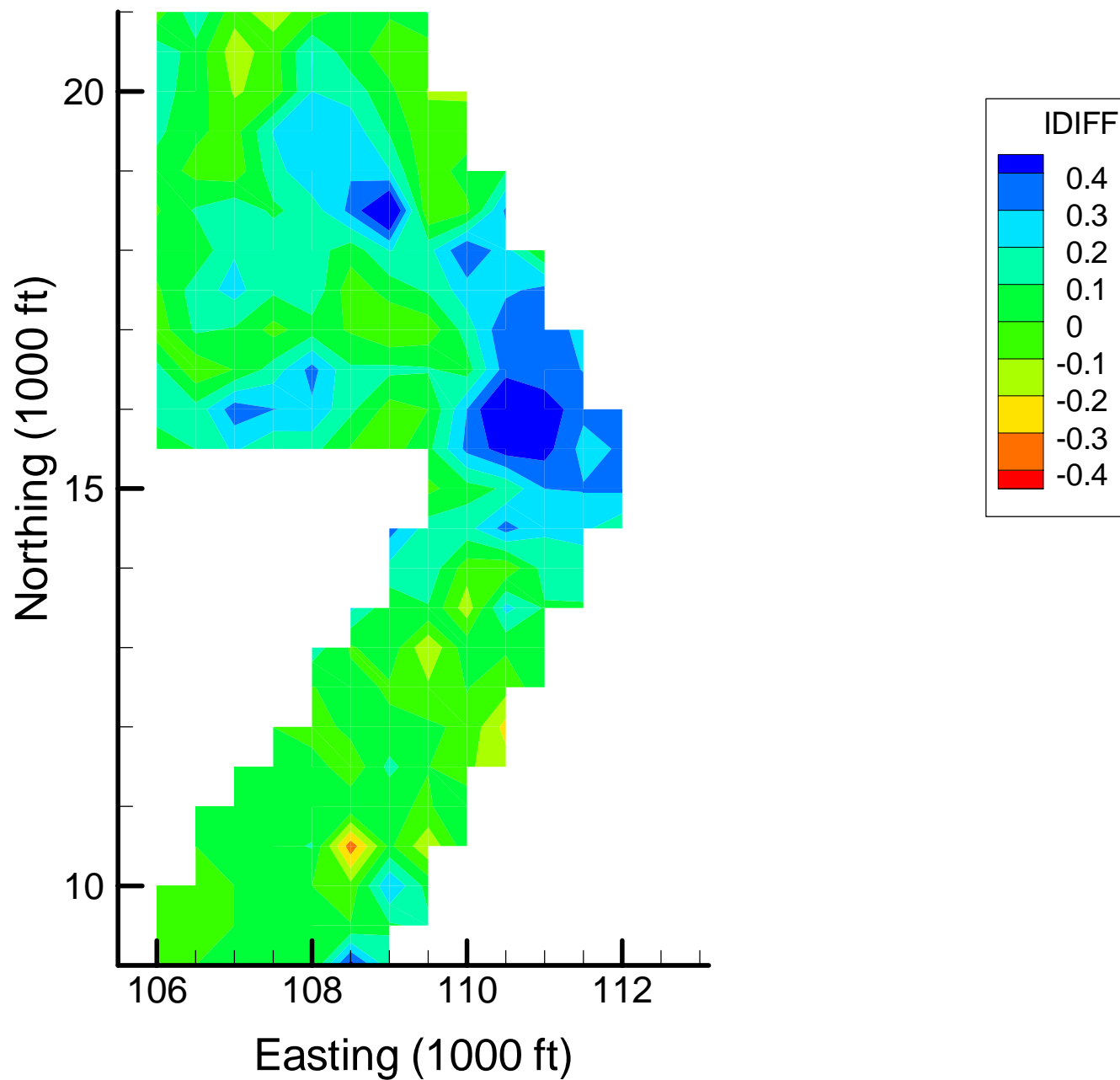
Site OU-12: Benzene Indicator Differences, 1999-2000, 20% Removal



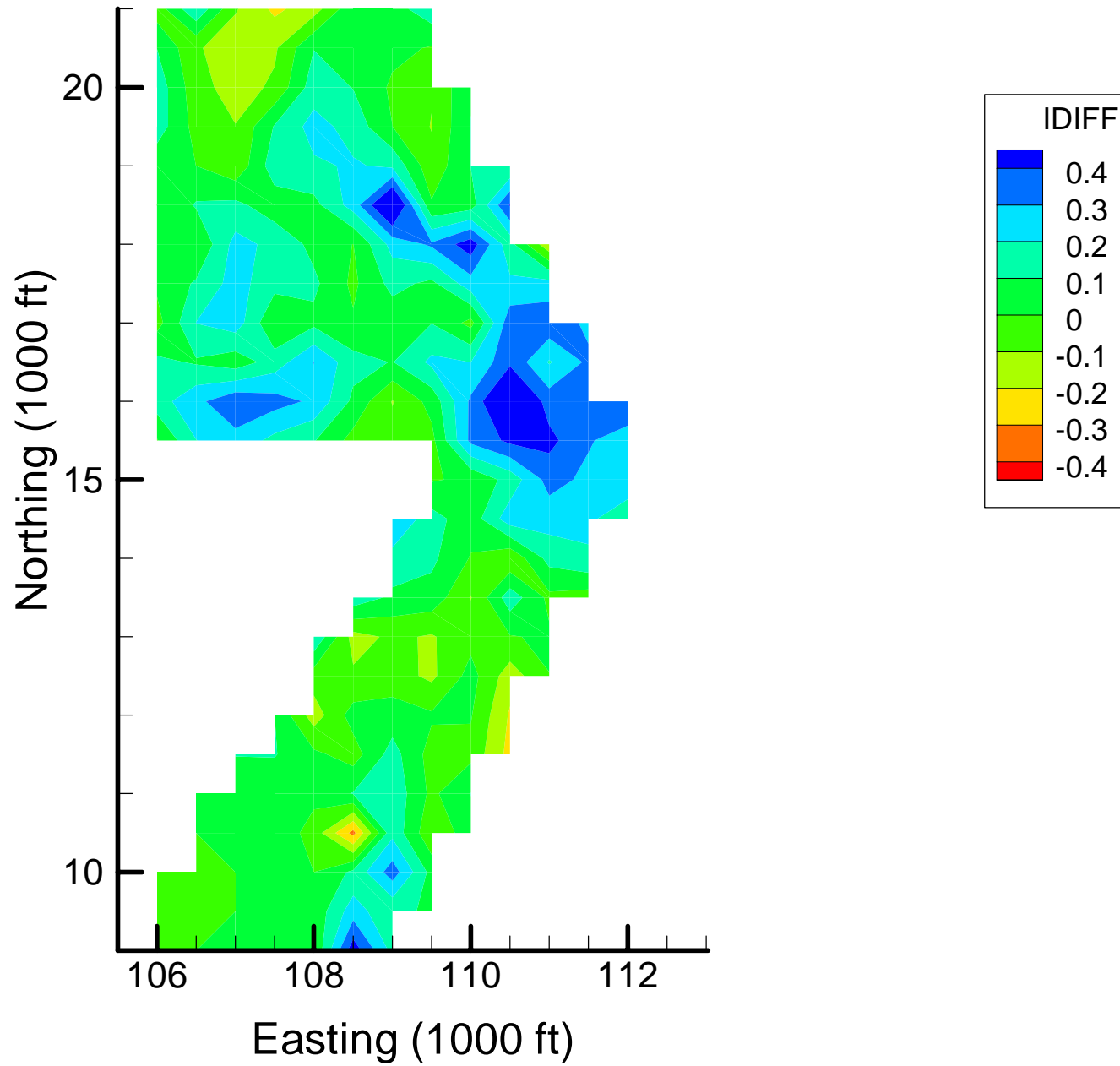
Site OU-12: Benzene Indicator Differences, 1999-2000, 30% Removal



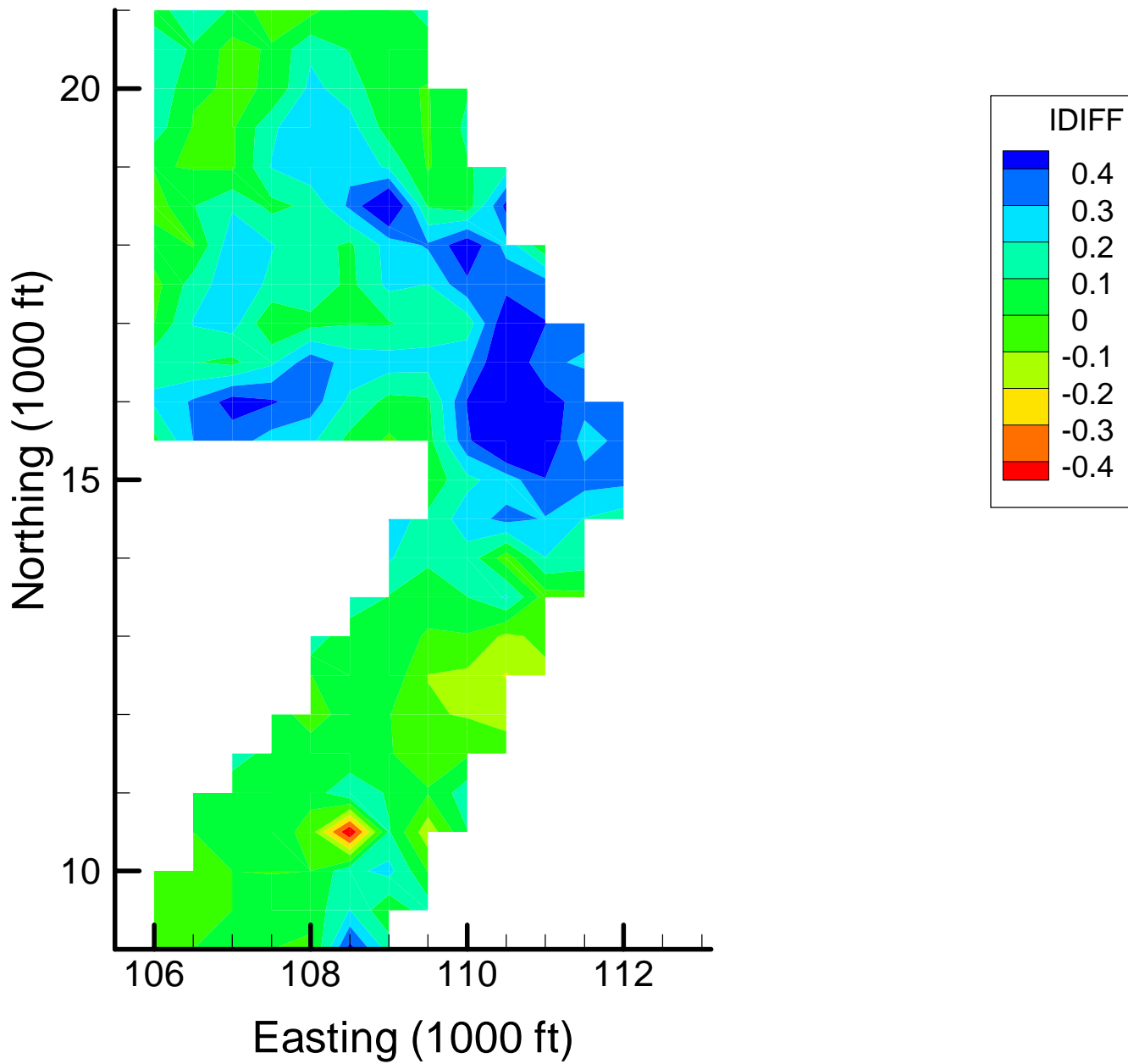
Site OU-12: Benzene Indicator Differences, 1999-2000, 40% Removal



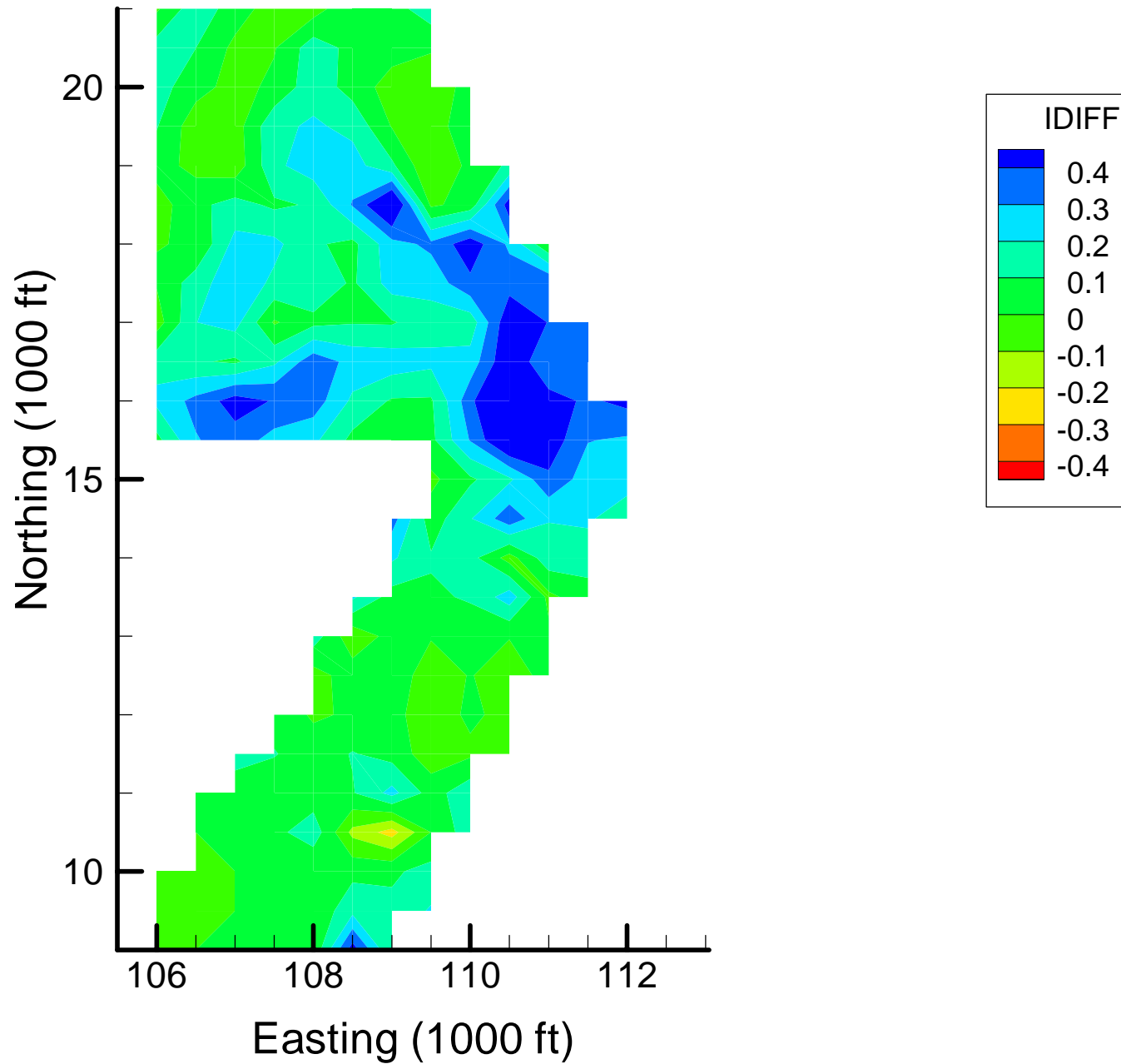
Site OU-12: Benzene Indicator Differences, 1999-2000, 50% Removal



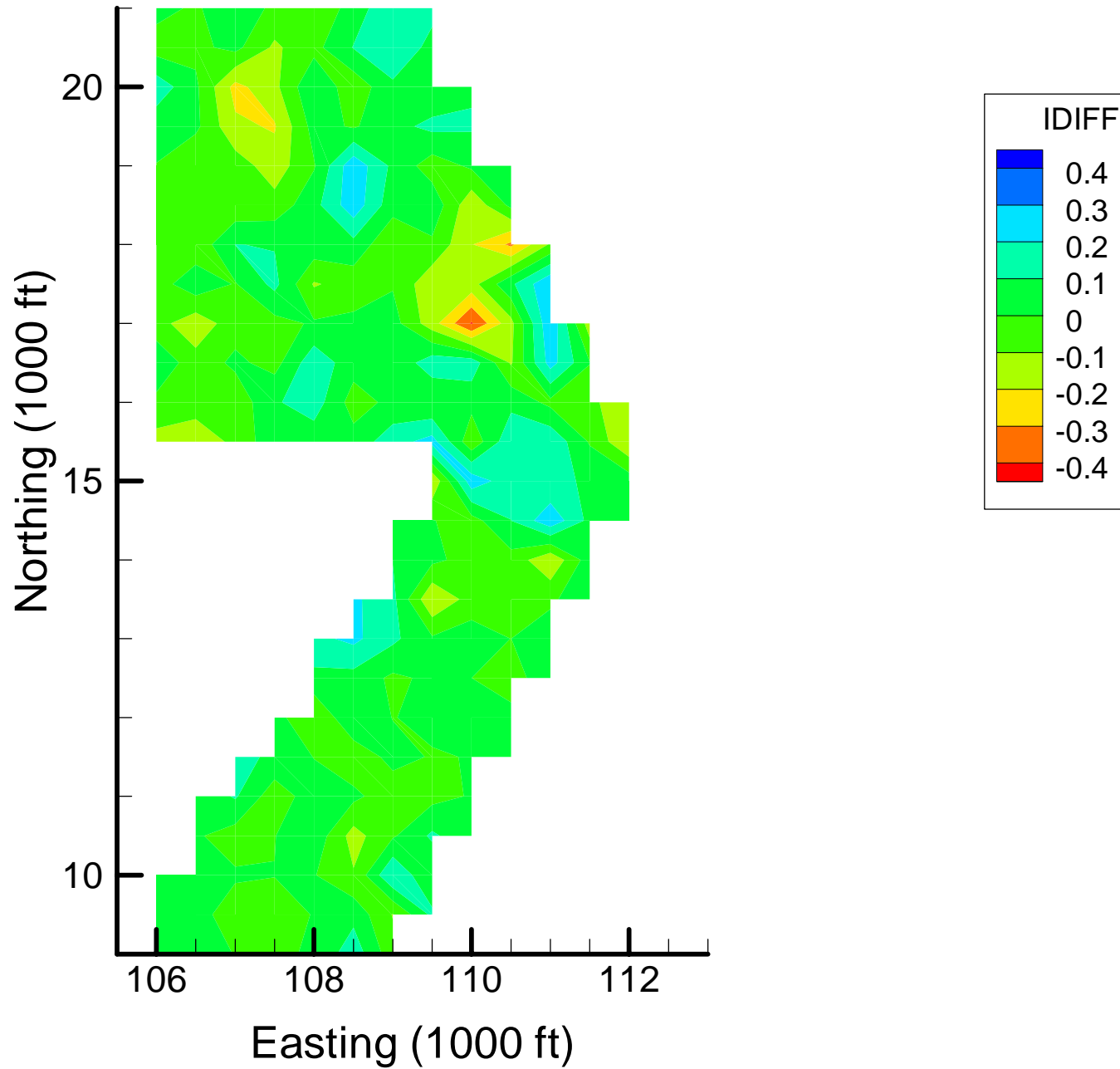
Site OU-12: Benzene Indicator Differences, 1999-2000, 60% Removal



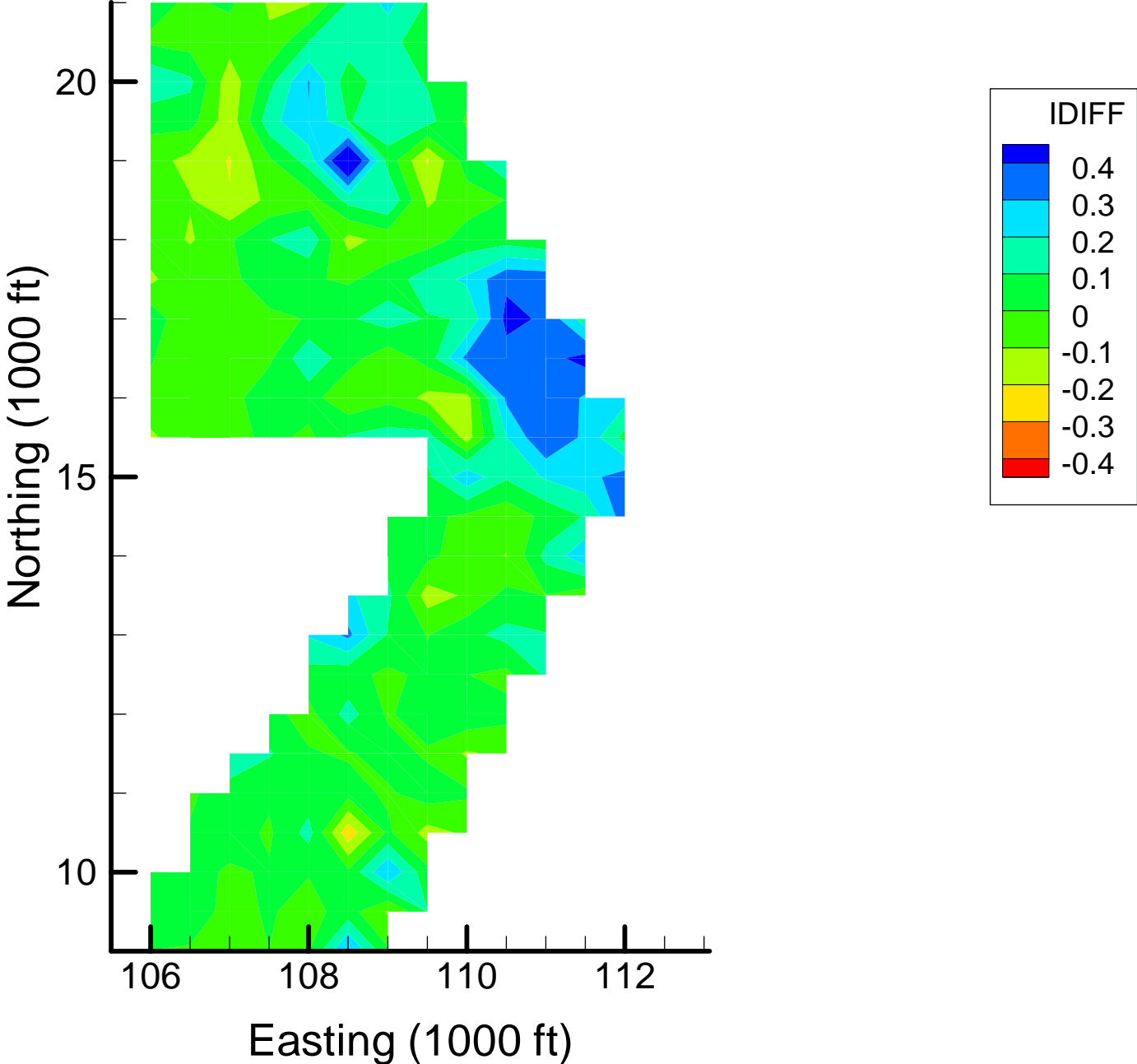
Site OU-12: Benzene Indicator Differences, 1999-2000, 70% Removal



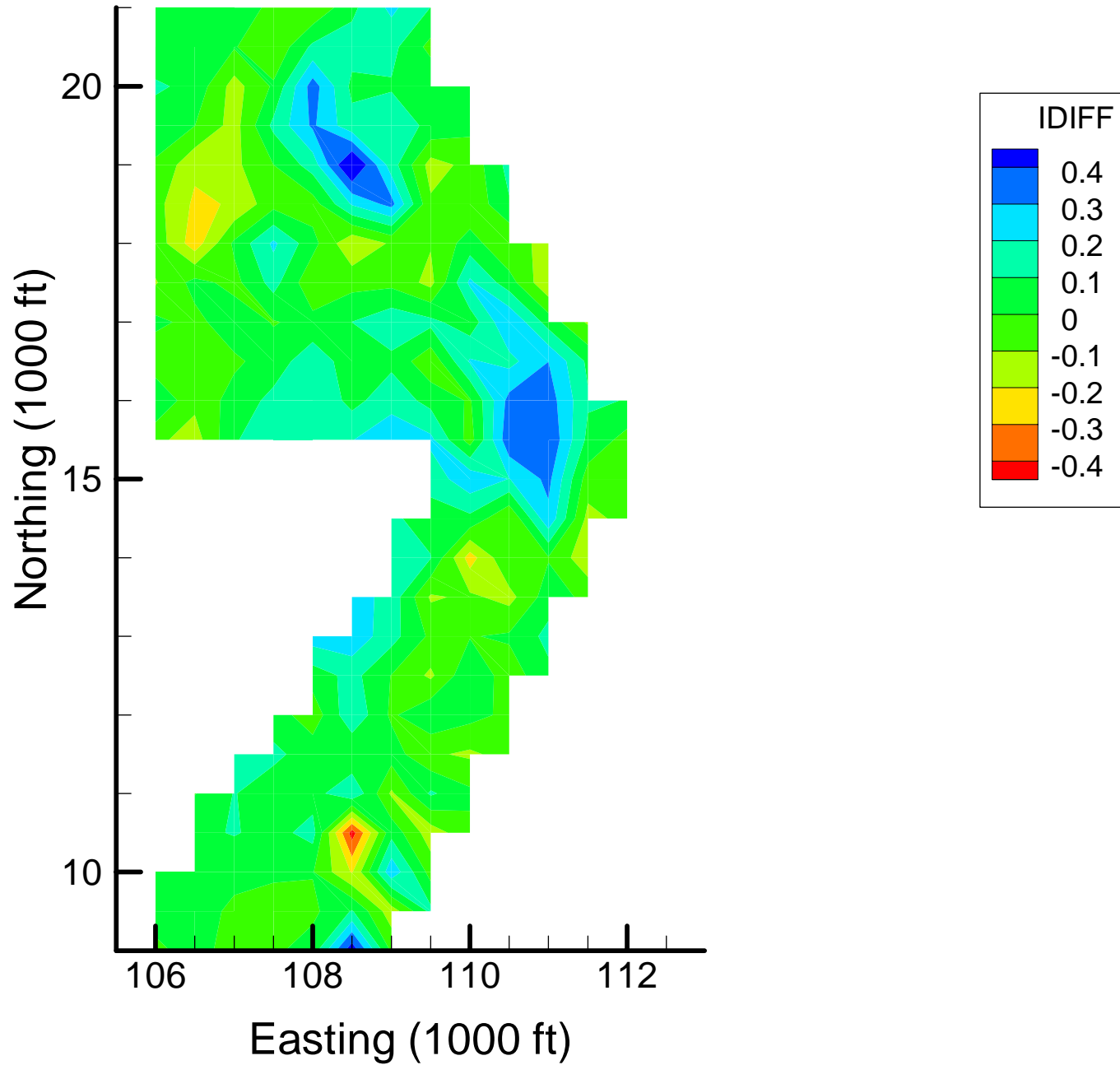
Site OU-12: Benzene Indicator Differences, 2001-2002, 10% Removal



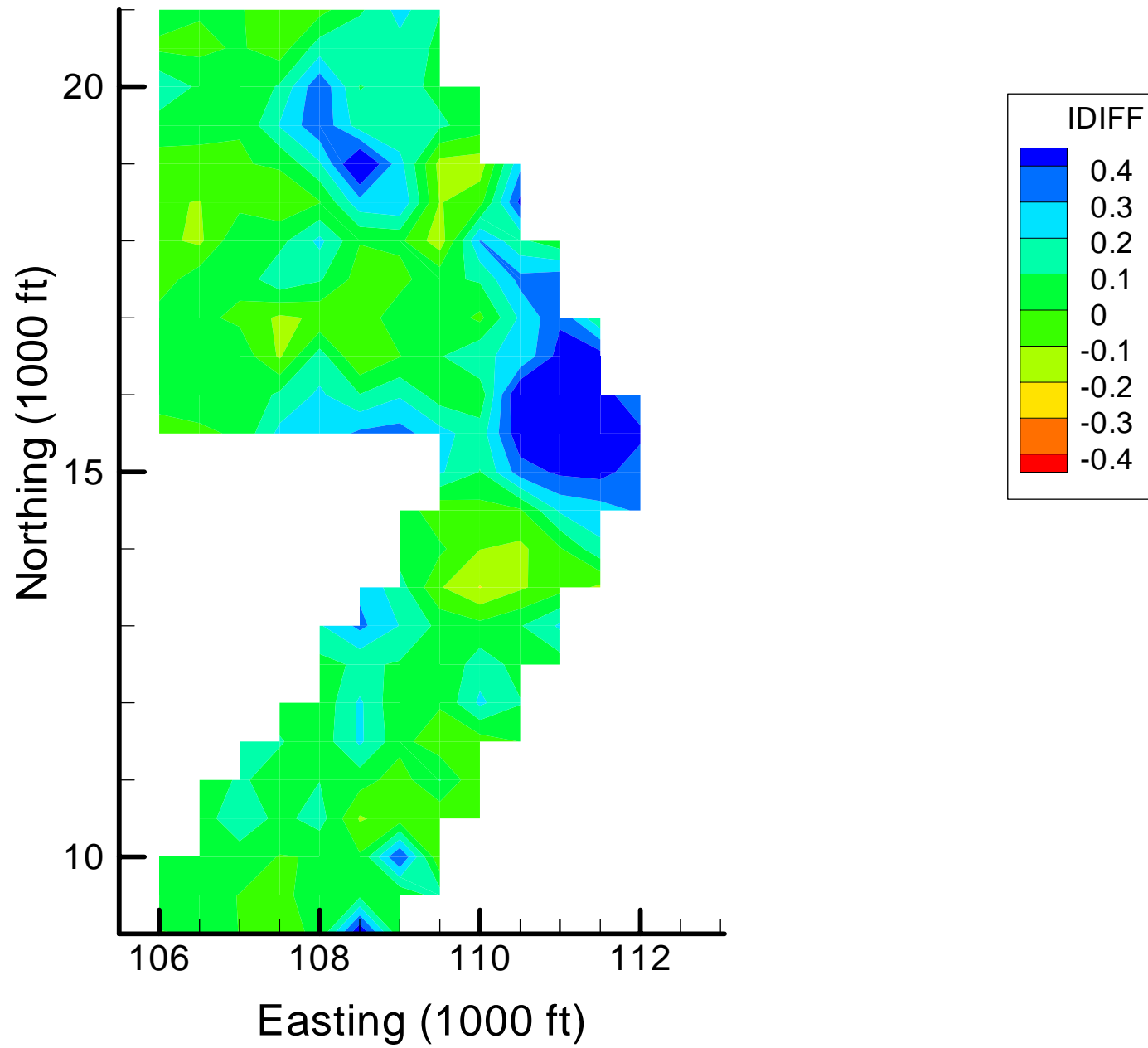
Site OU-12: Benzene Indicator Differences, 2001-2002, 20% Removal



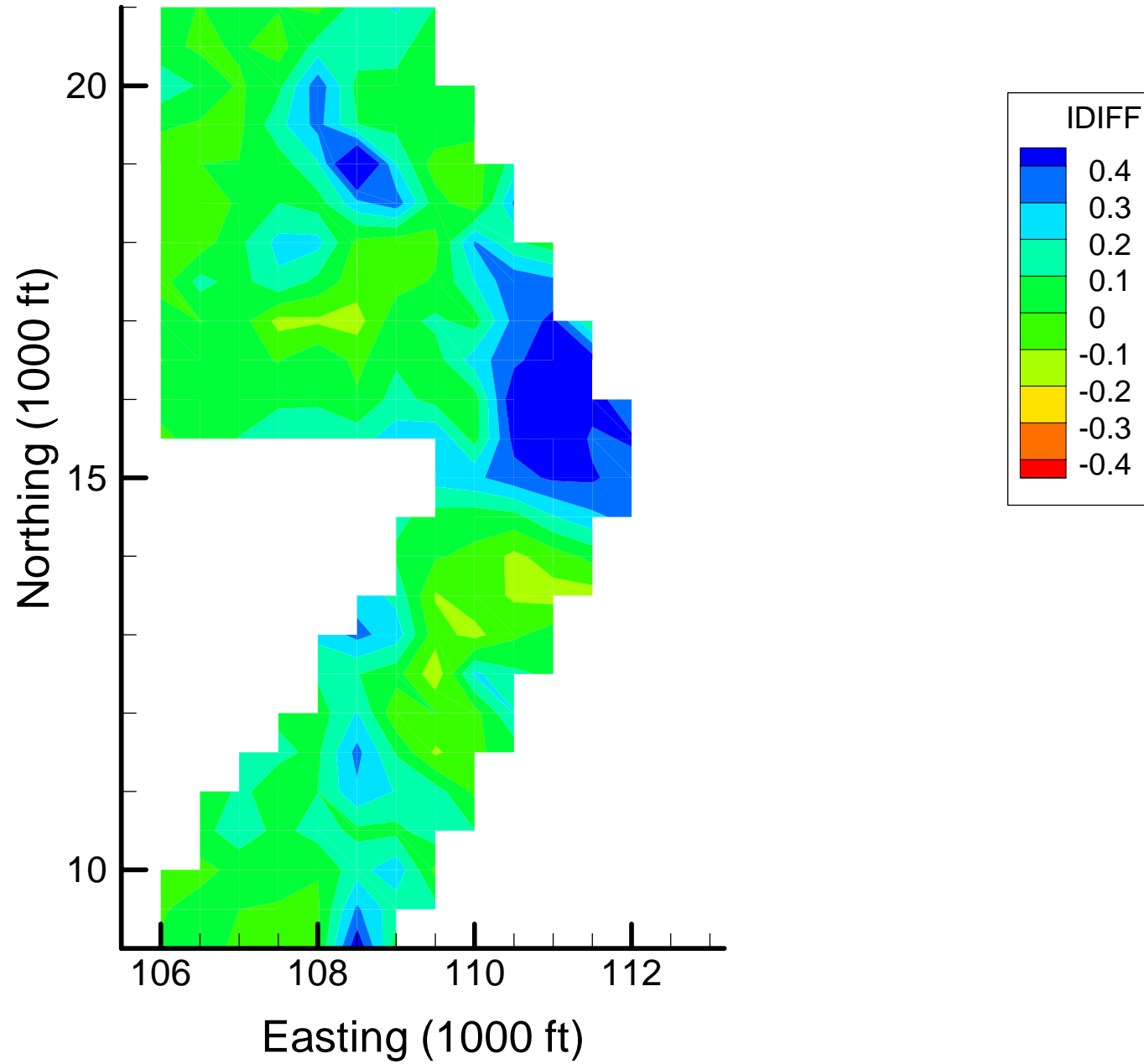
Site OU-12: Benzene Indicator Differences, 2001-2002, 30% Removal



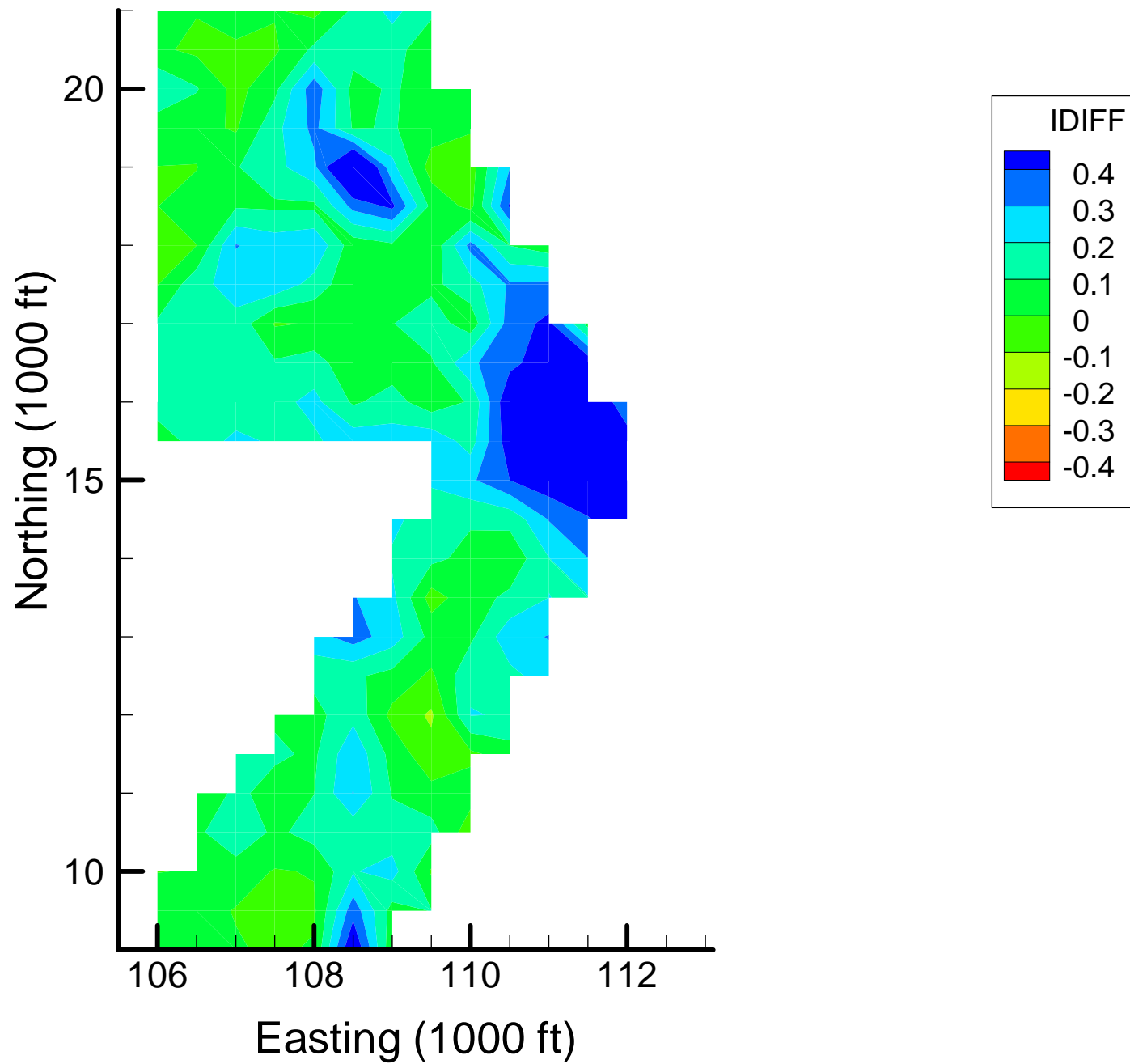
Site OU-12: Benzene Indicator Differences, 2001-2002, 40% Removal



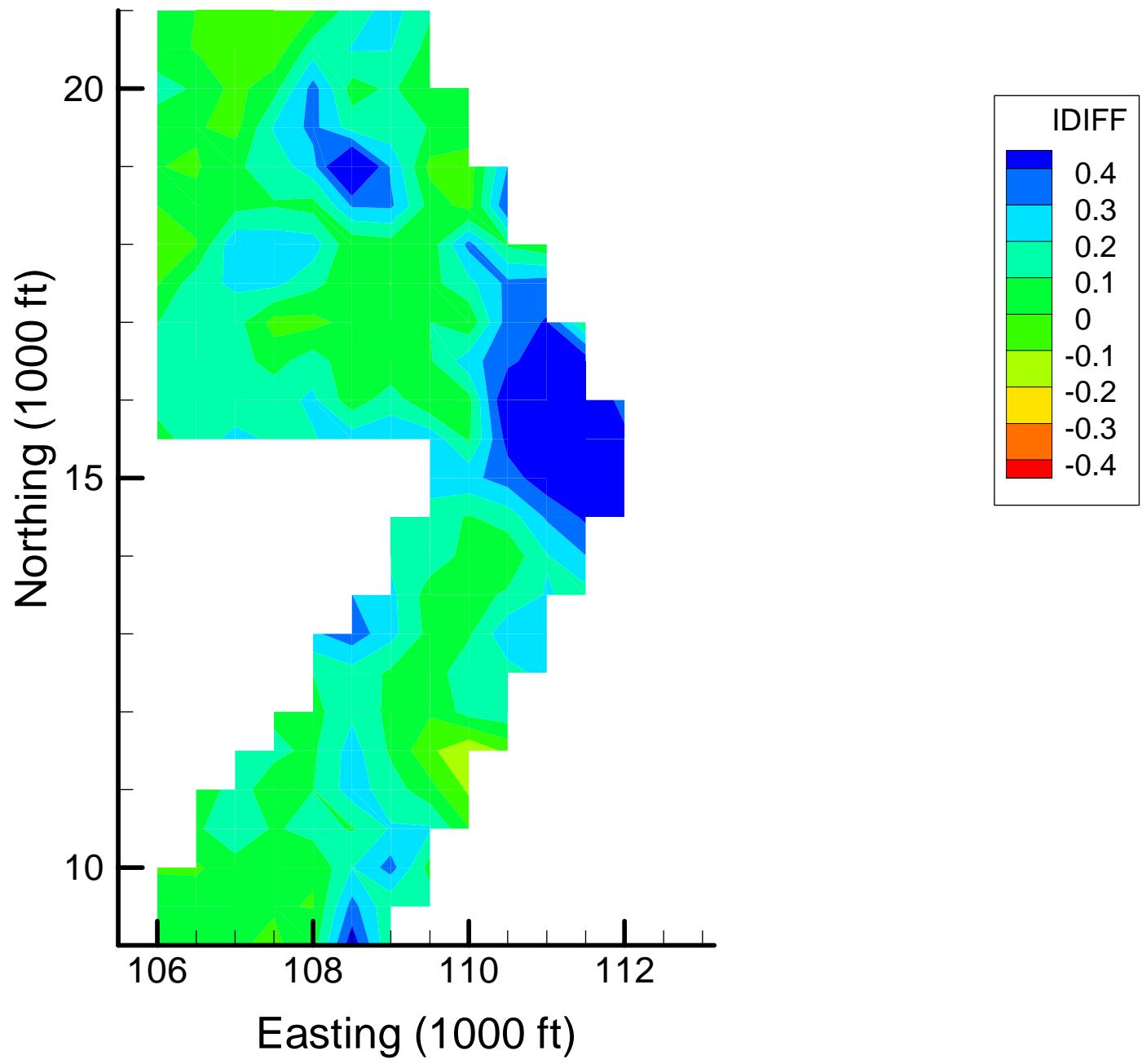
Site OU-12: Benzene Indicator Differences, 2001-2002, 50% Removal



Site OU-12: Benzene Indicator Differences, 2001-2002, 60% Removal



Site OU-12: Benzene Indicator Differences, 2001-2002, 70% Removal



Appendix 4-2

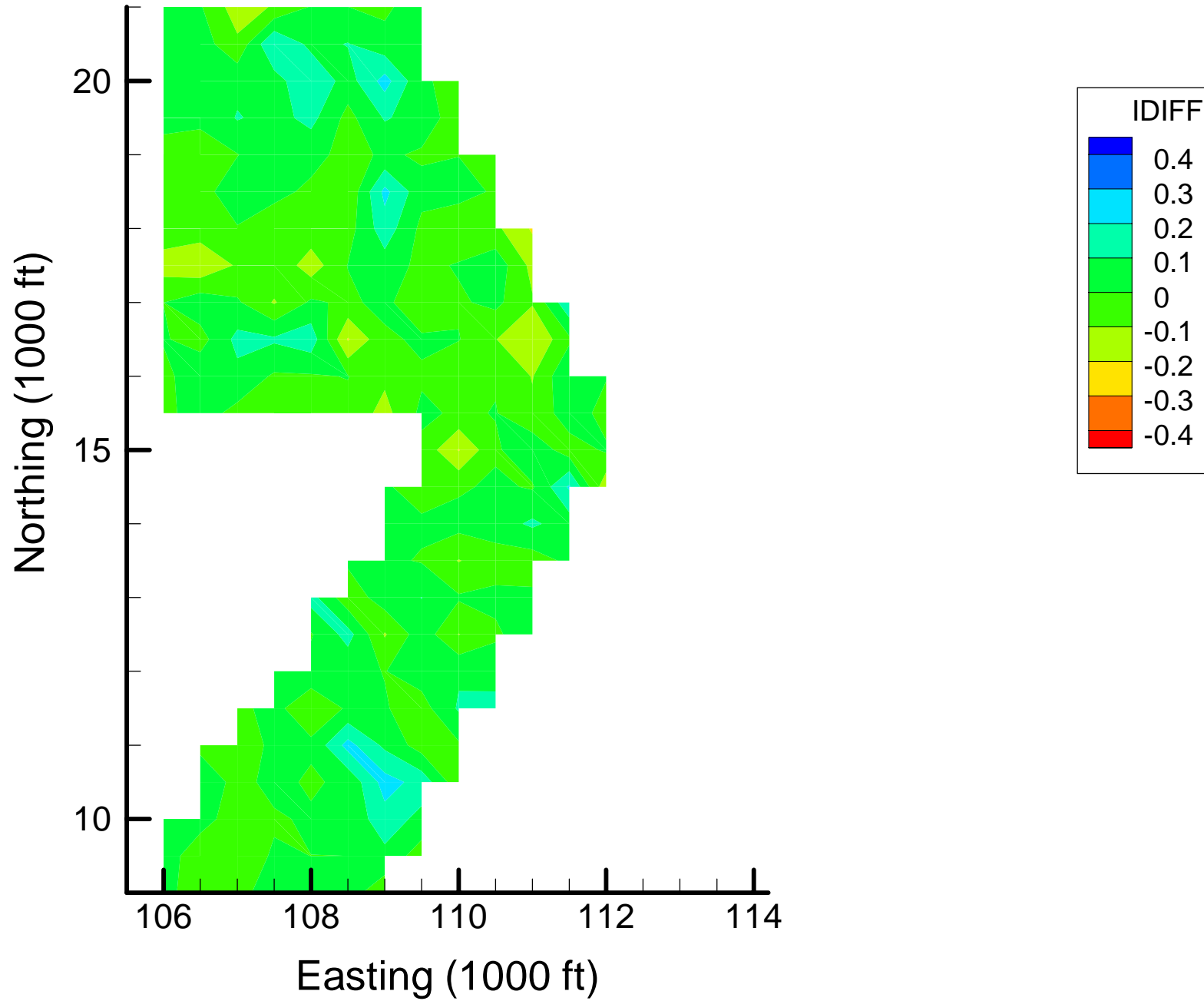
Spatial Optimization: FE Indicator Difference Maps

Notes:

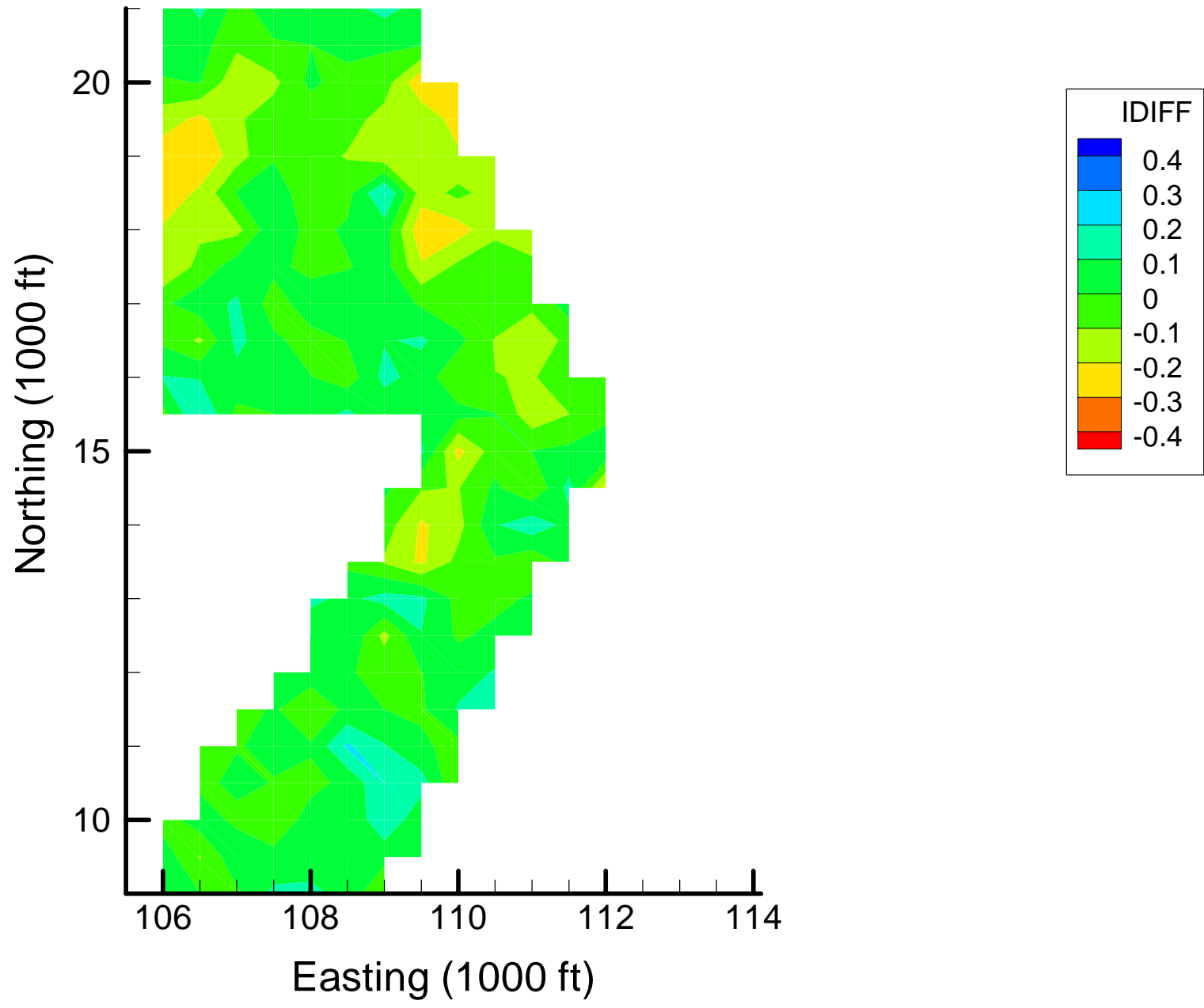
IDIFF = Difference between voxel-specific locally-weighted quadratic regression (LWQR) indicator estimates from reduced-data map to base map (averaged over depth)

Color scheme — red = overestimate compared to base map; blue = underestimate compared to base map

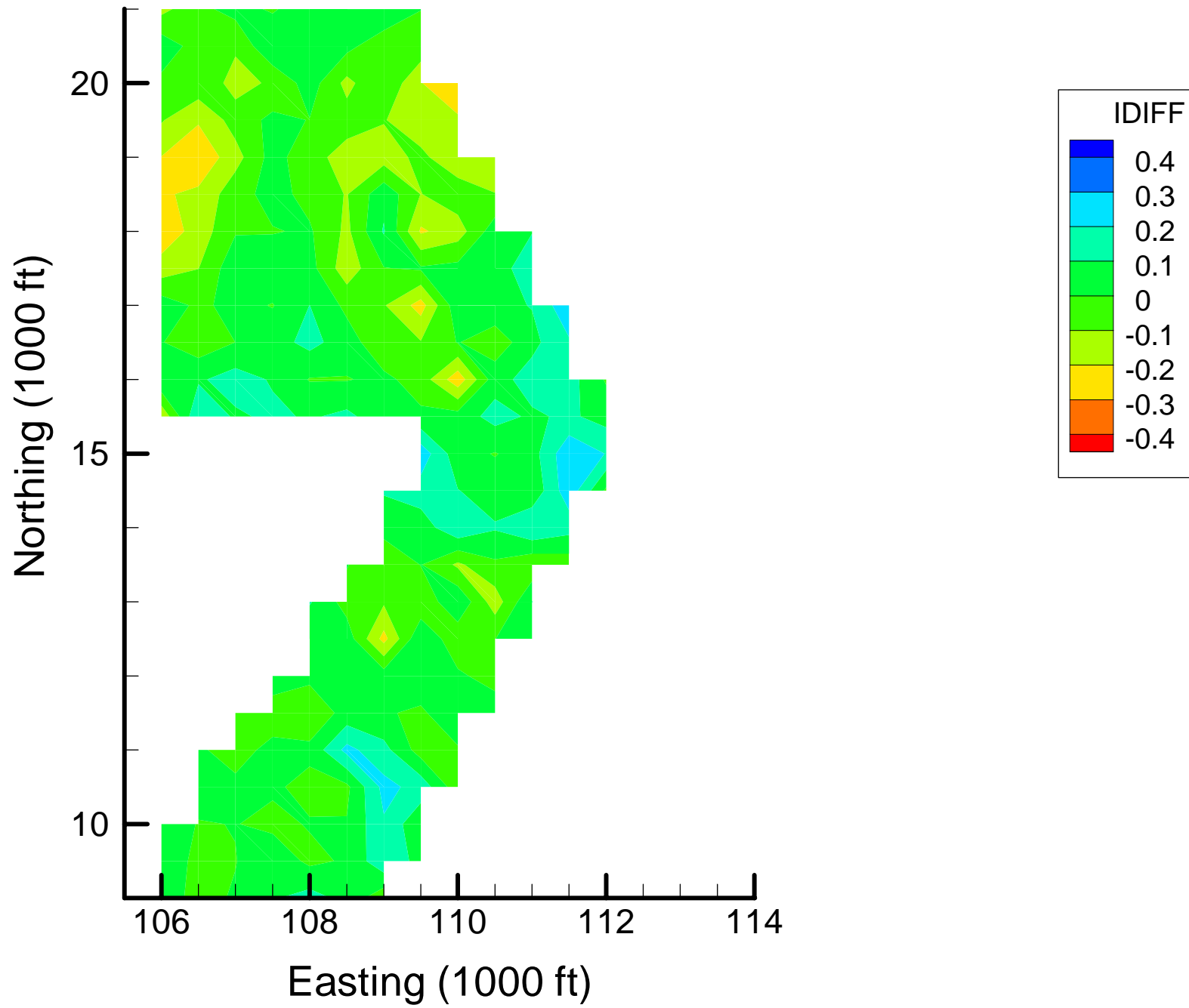
Site OU-12: Iron Indicator Differences, 1999-2000, 10% Removal



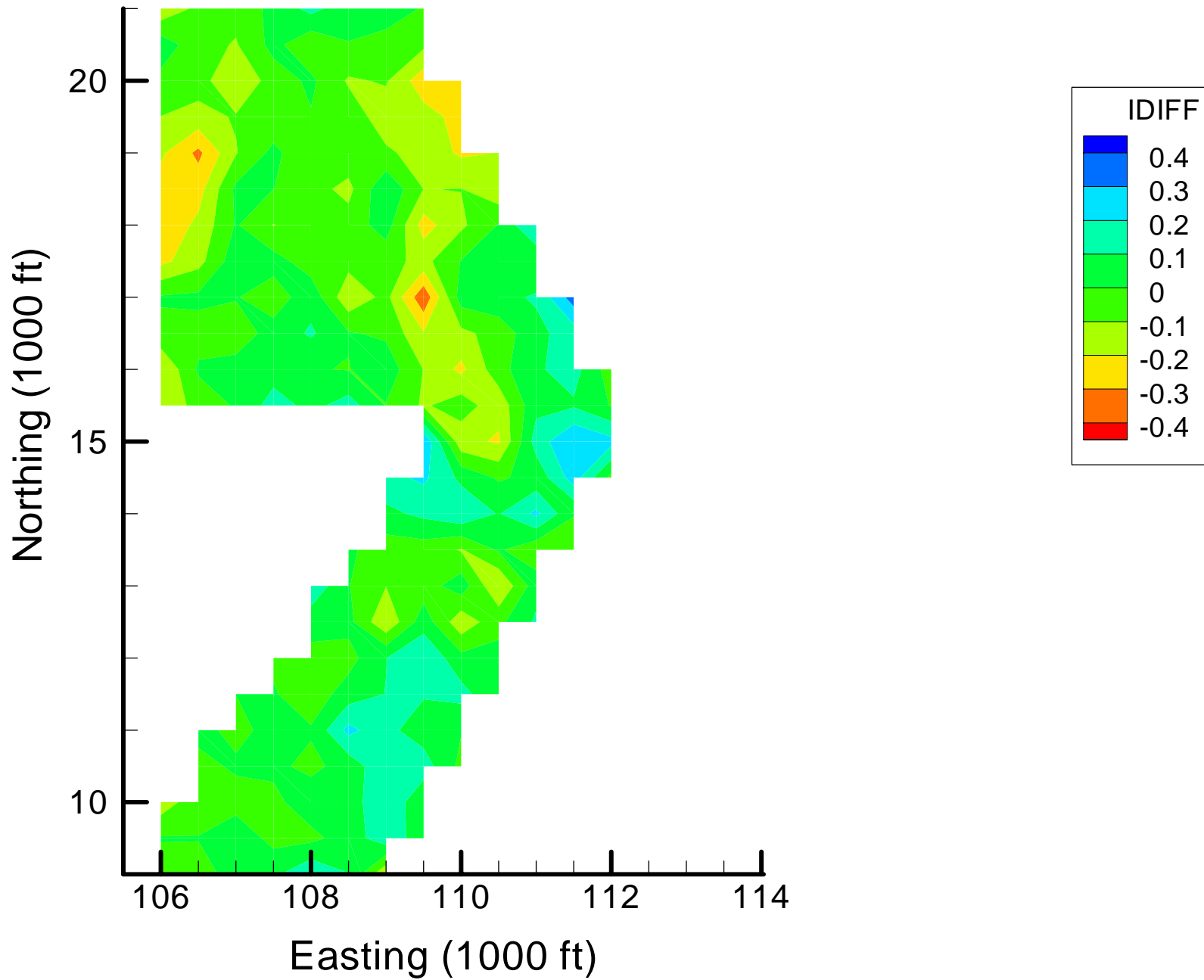
Site OU-12: Iron Indicator Differences, 1999-2000, 20% Removal



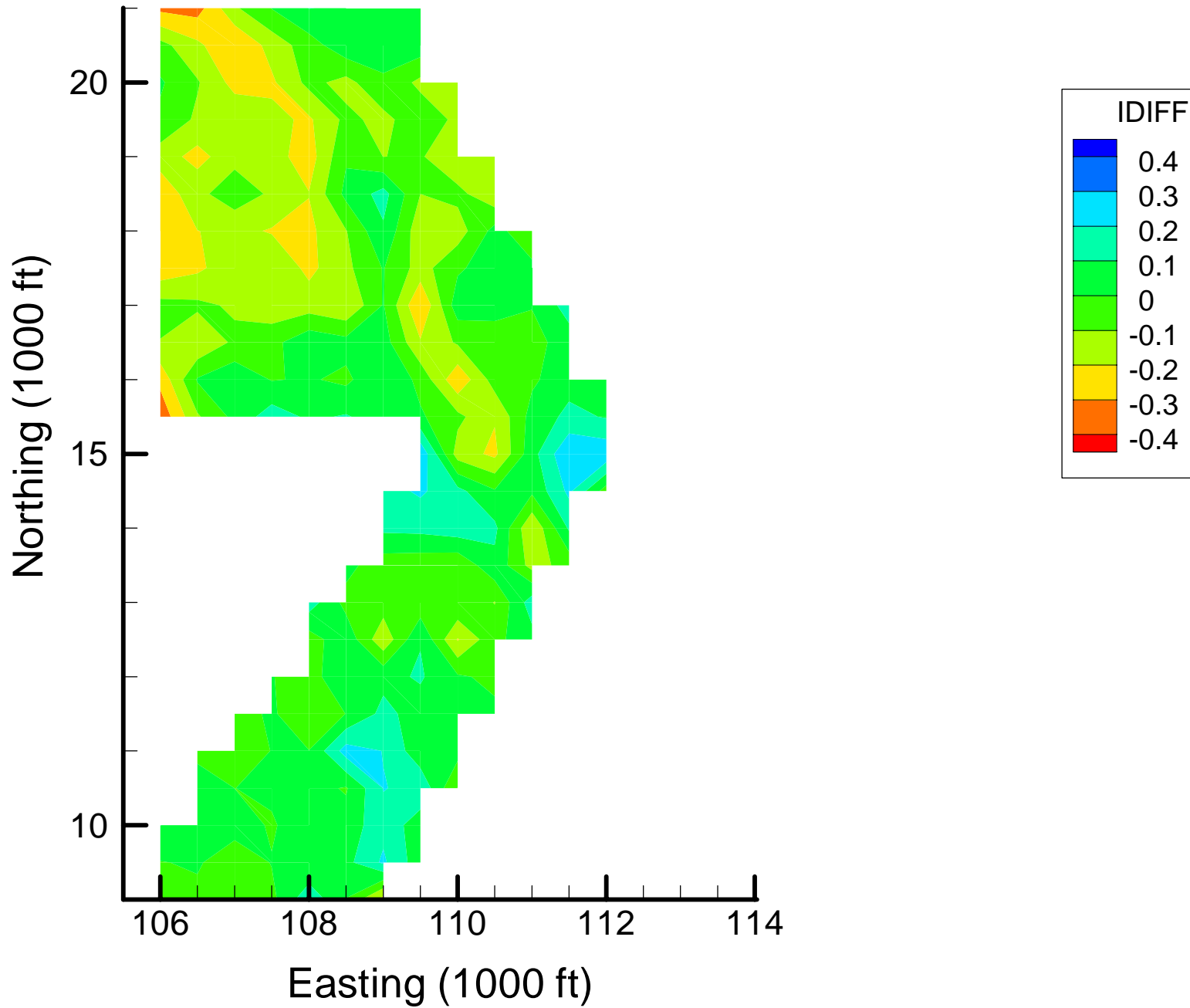
Site OU-12: Iron Indicator Differences, 1999-2000, 30% Removal



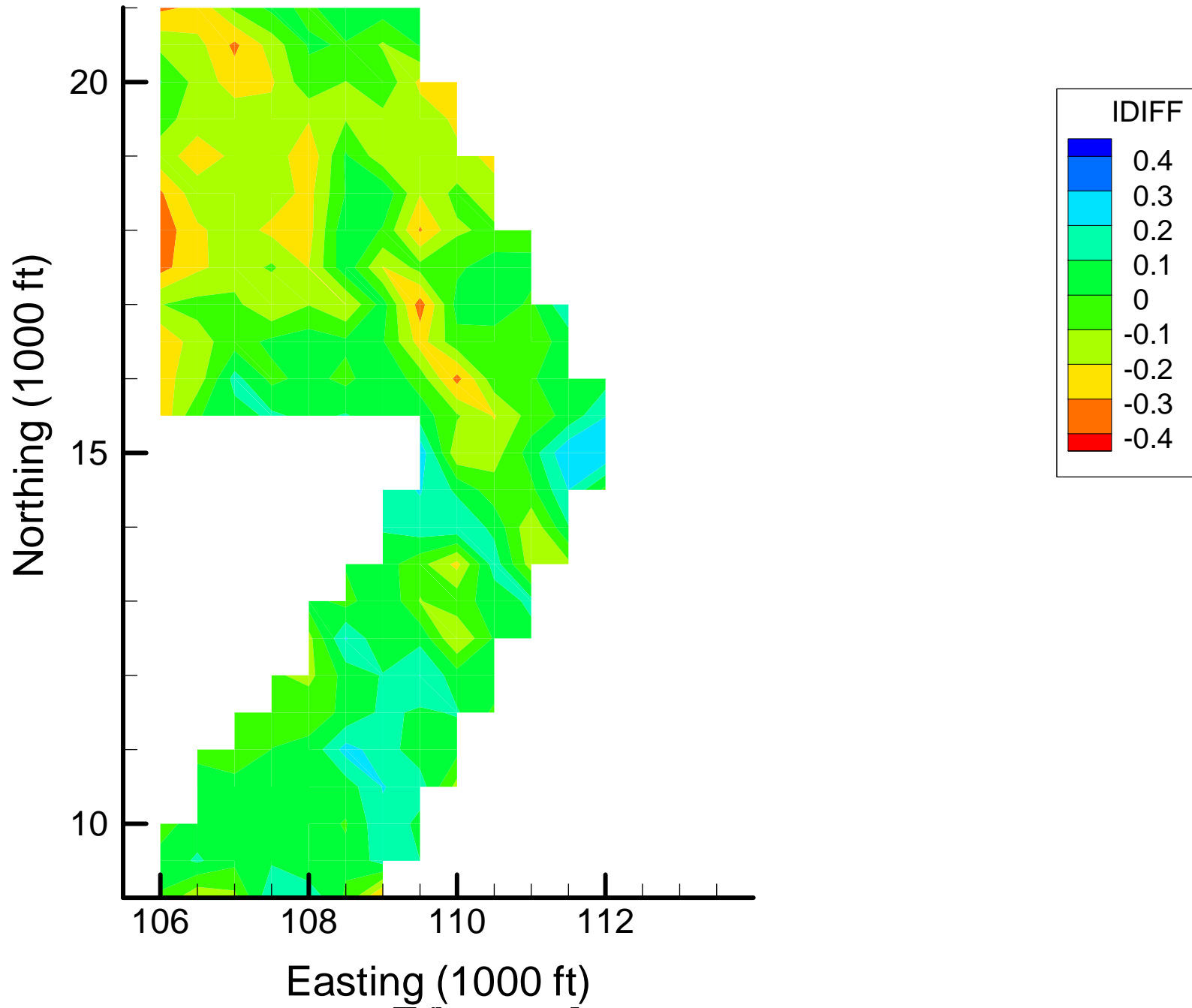
Site OU-12: Iron Indicator Differences, 1999-2000, 40% Removal



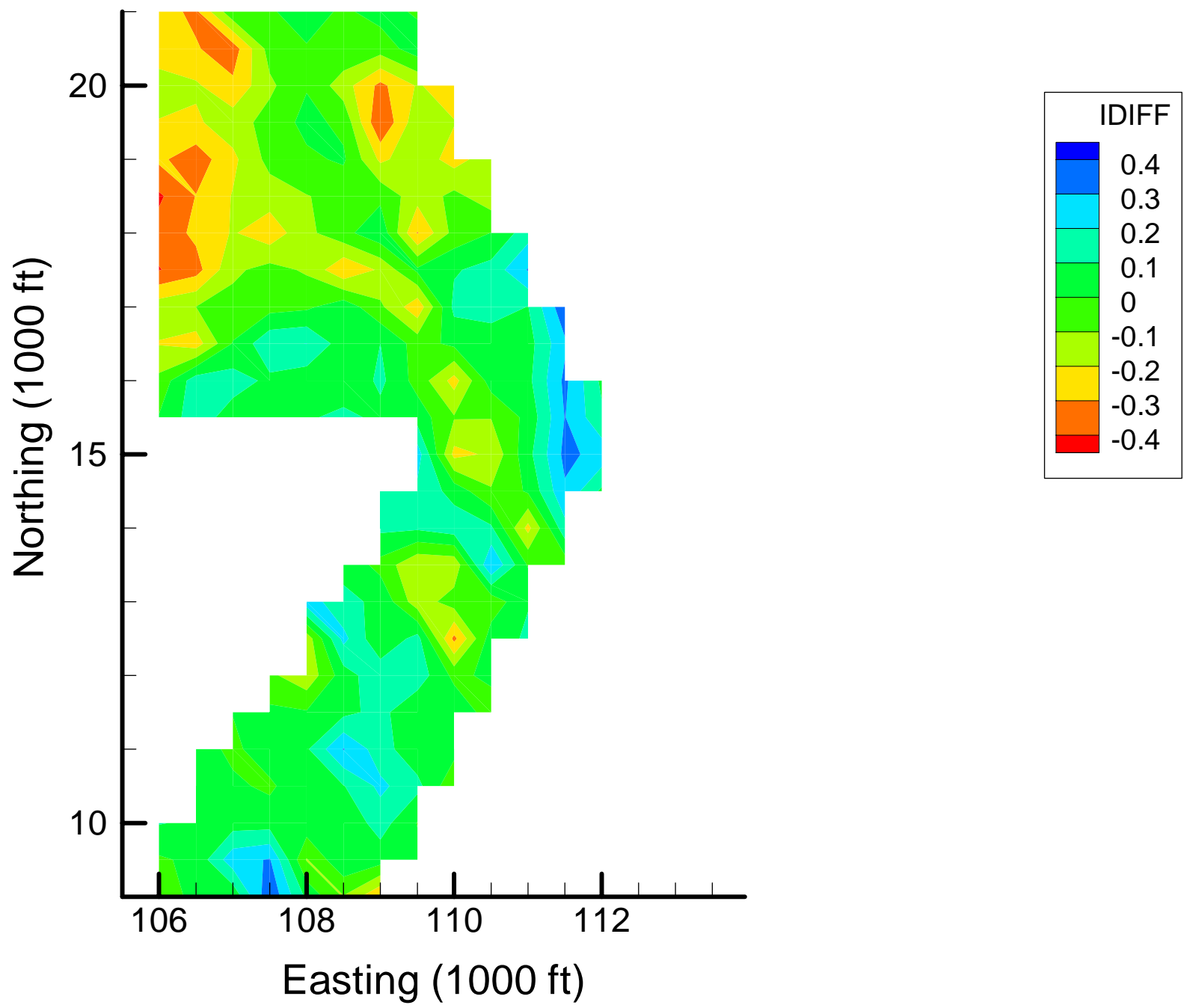
Site OU-12: Iron Indicator Differences, 1999-2000, 50% Removal



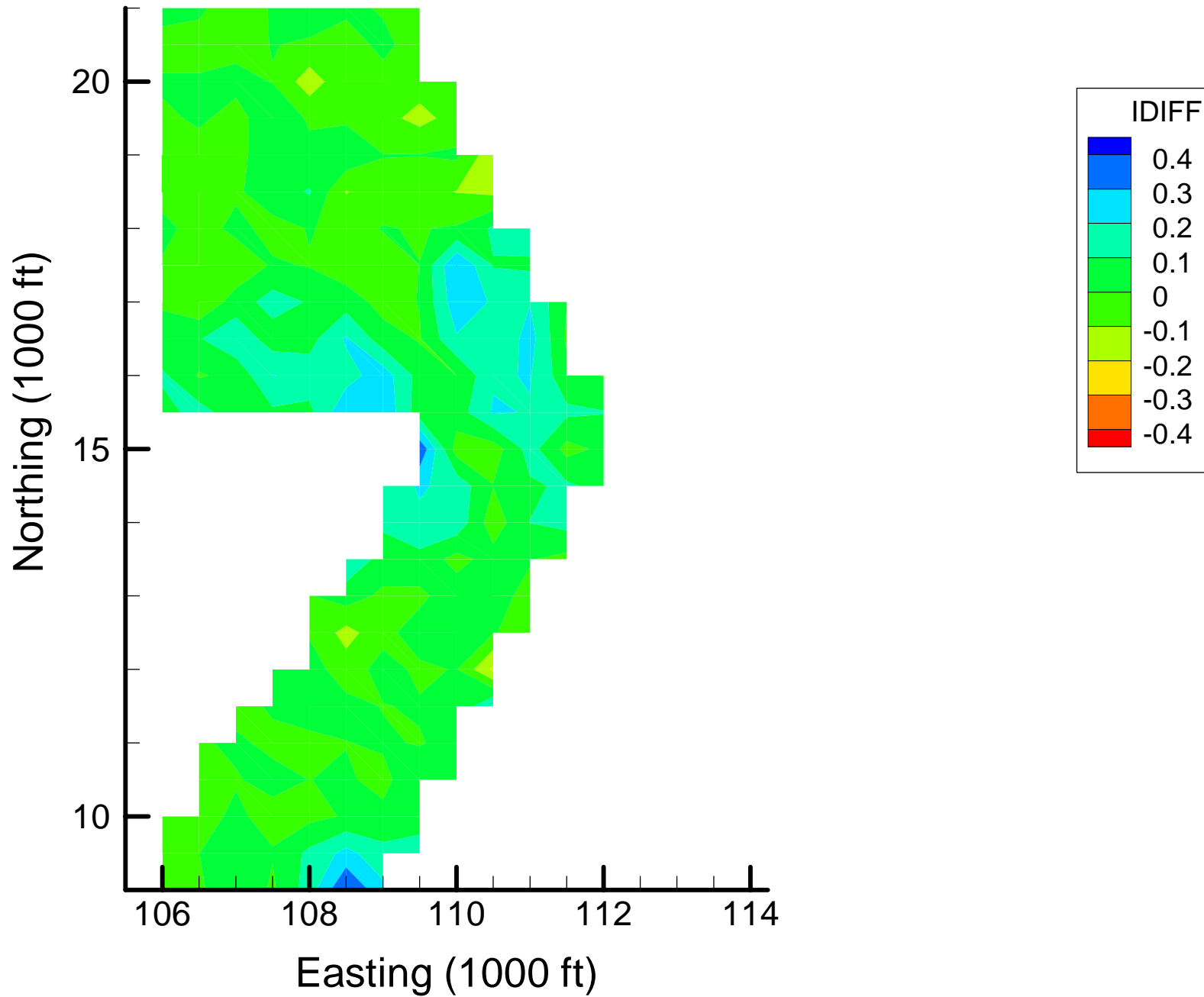
Site OU-12: Iron Indicator Differences, 1999-2000, 60% Removal



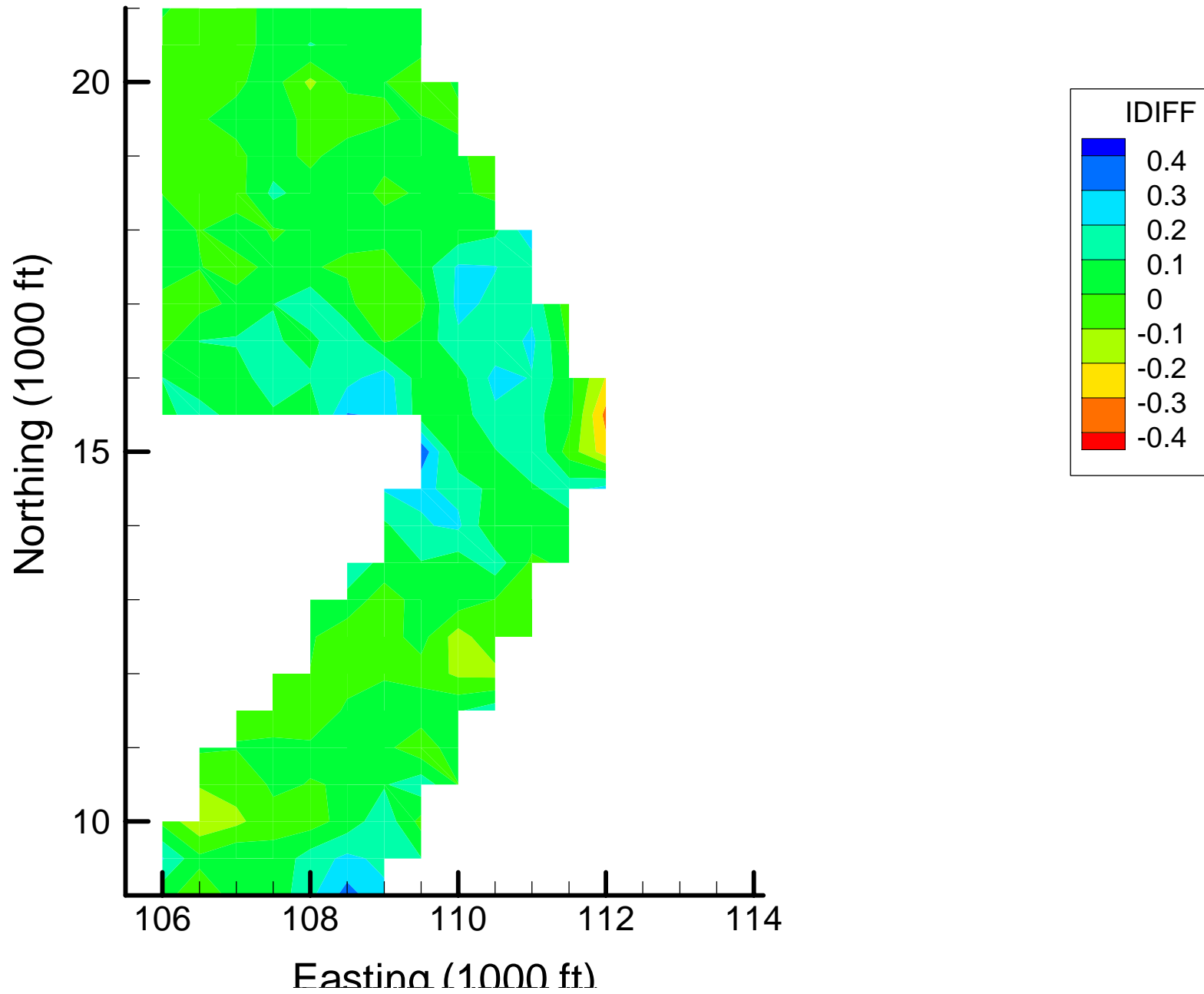
Site OU-12: Iron Indicator Differences, 1999-2000, 70% Removal



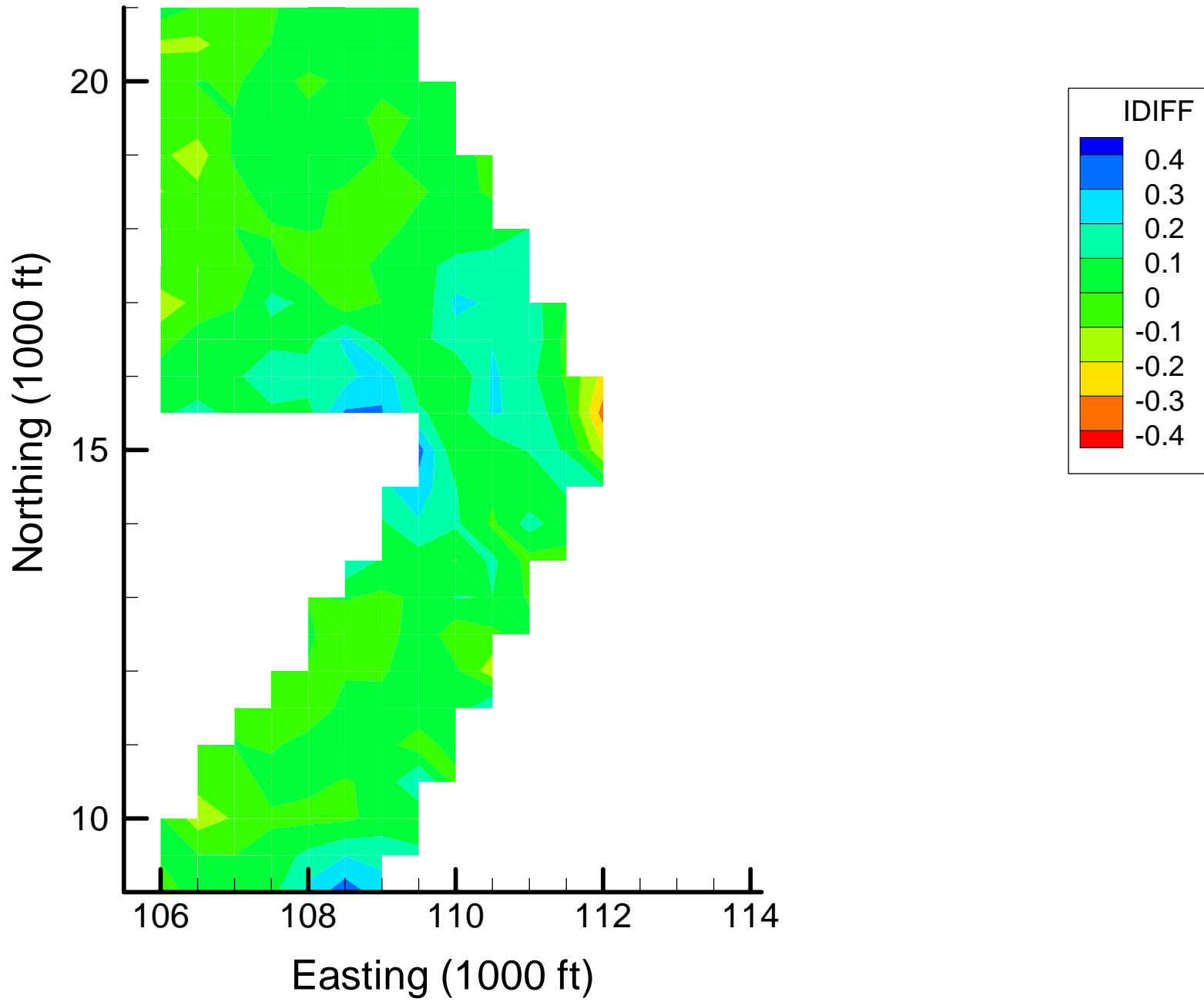
Site OU-12: Iron Indicator Differences, 2001-2002, 10% Removal



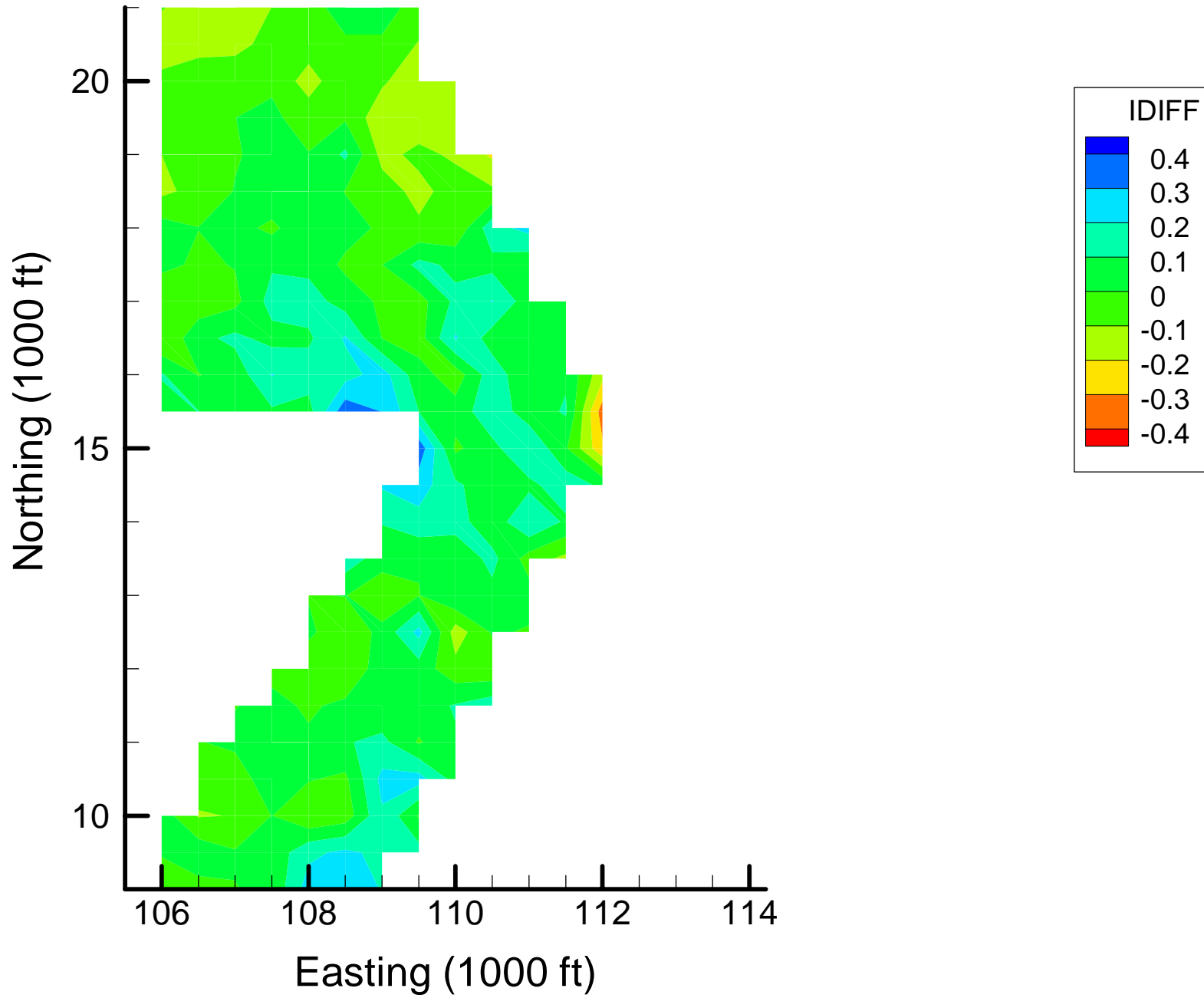
Site OU-12: Iron Indicator Differences, 2001-2002, 20% Removal



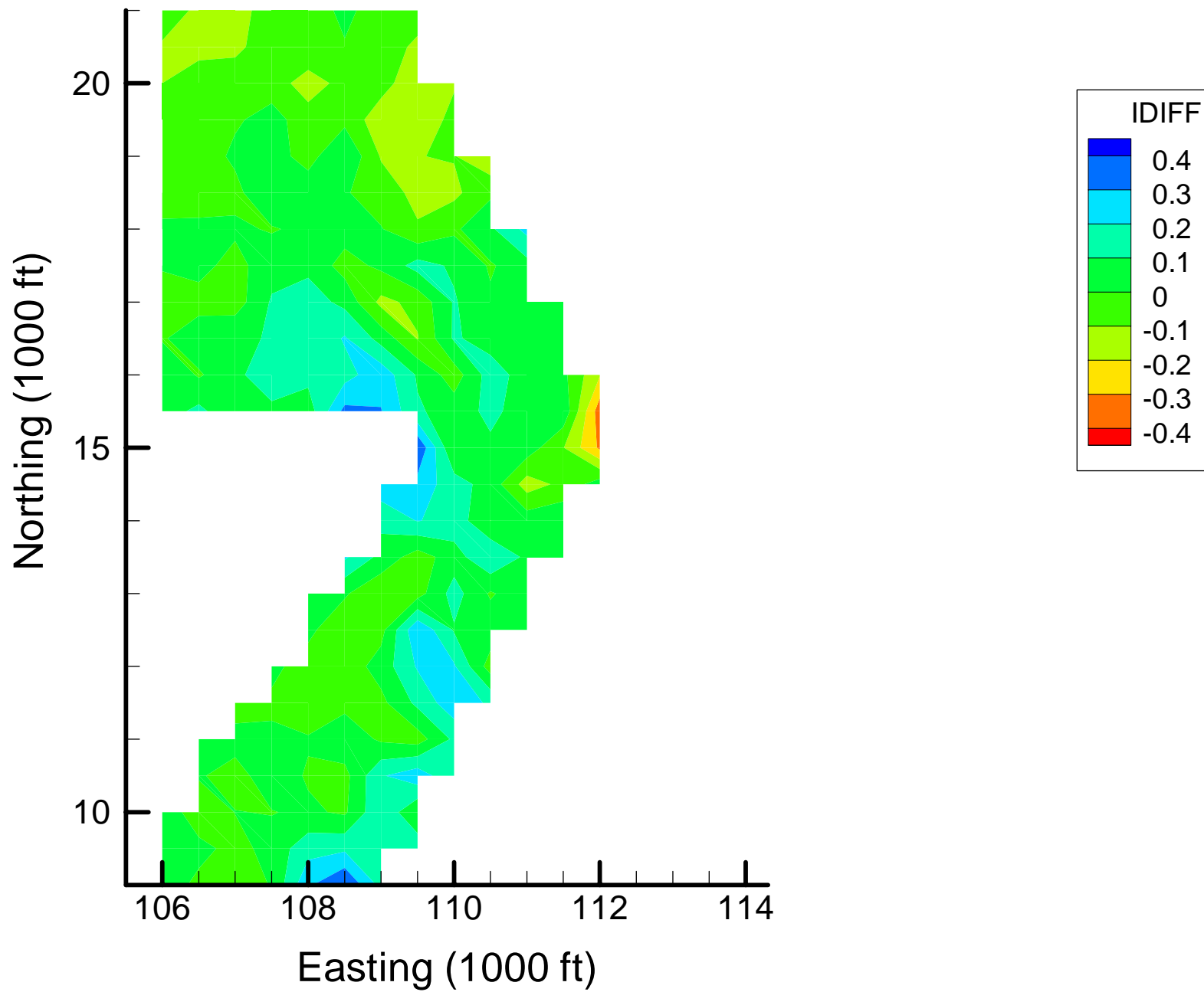
Site OU-12: Iron Indicator Differences, 2001-2002, 30% Removal



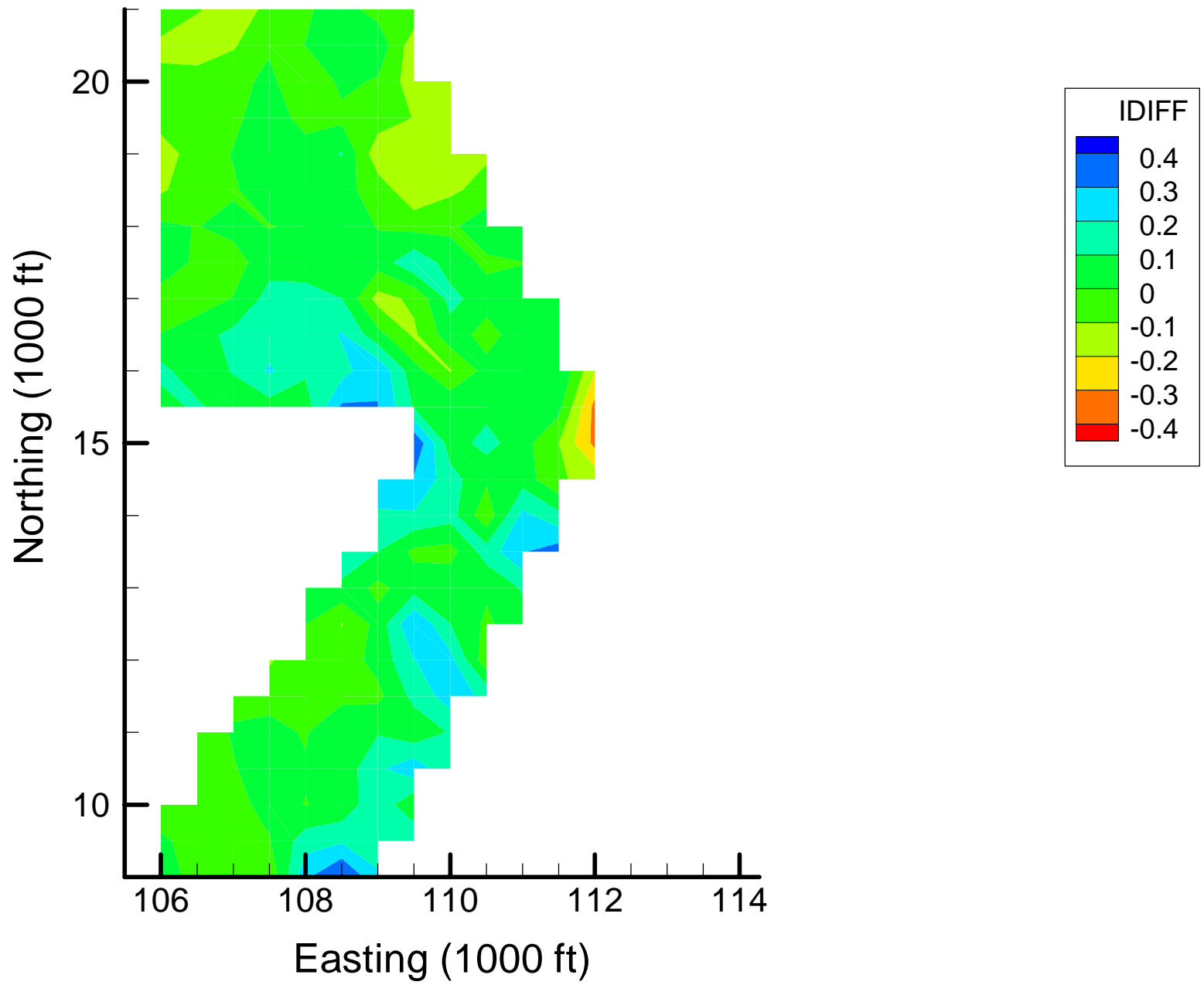
Site OU-12: Iron Indicator Differences, 2001-2002, 40% Removal



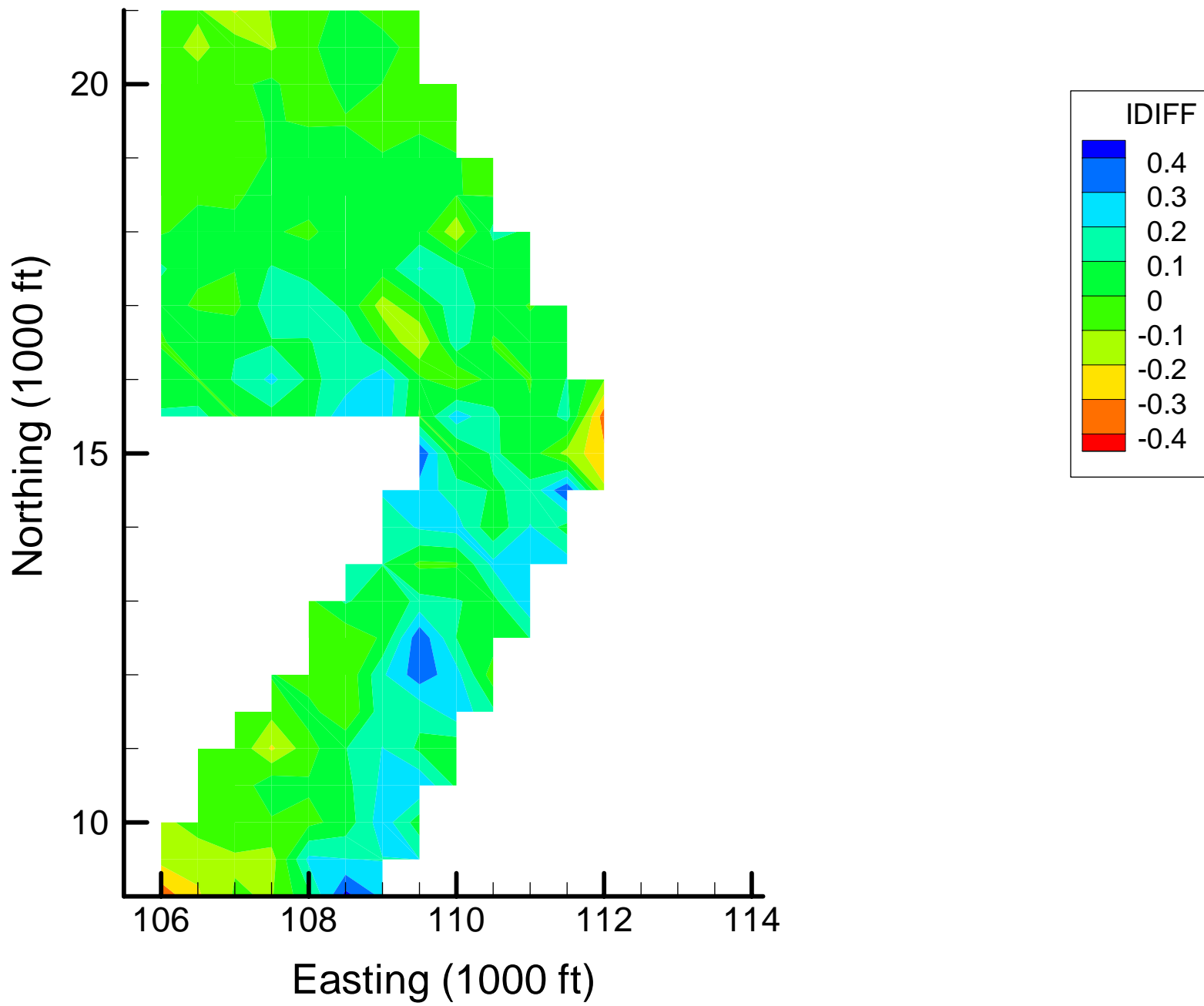
Site OU-12: Iron Indicator Differences, 2001-2002, 50% Removal



Site OU-12: Iron Indicator Differences, 2001-2002, 60% Removal



Site OU-12: Iron Indicator Differences, 2001-2002, 70% Removal



Appendix 4-2

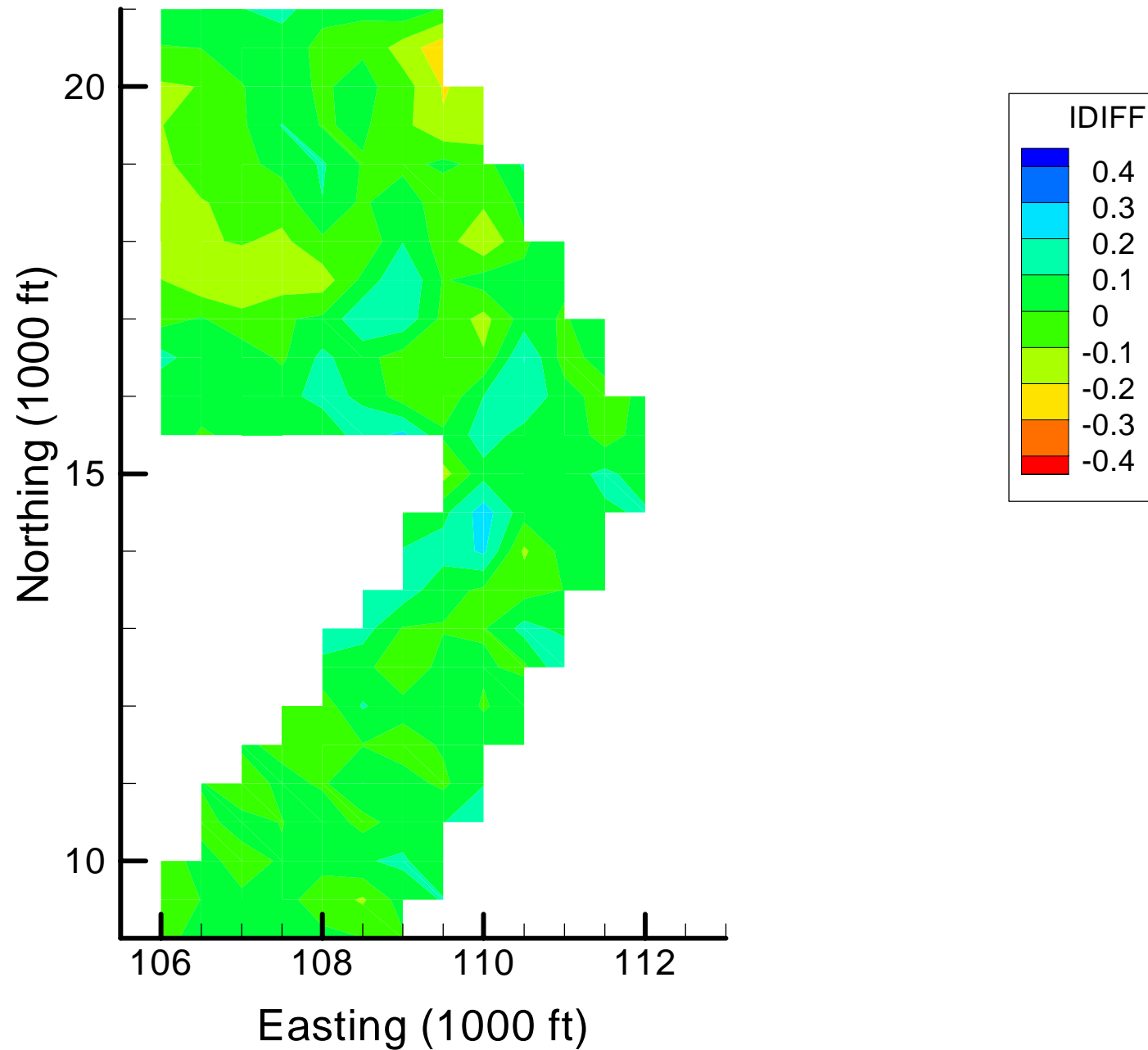
Spatial Optimization: MN Indicator Difference Maps

Notes:

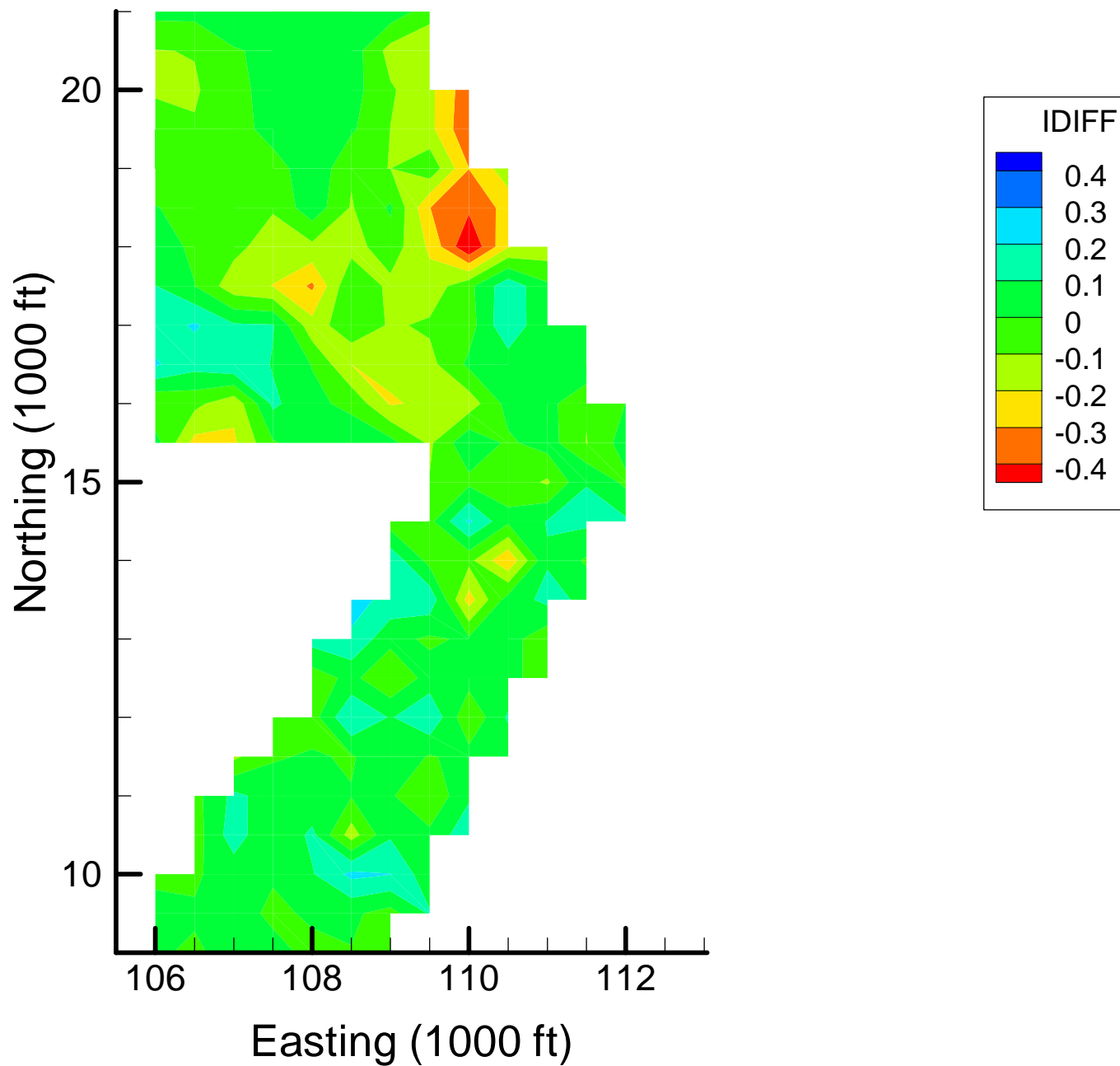
IDIFF = Difference between voxel-specific locally-weighted quadratic regression (LWQR) indicator estimates from reduced-data map to base map (averaged over depth)

Color scheme — red = overestimate compared to base map; blue = underestimate compared to base map

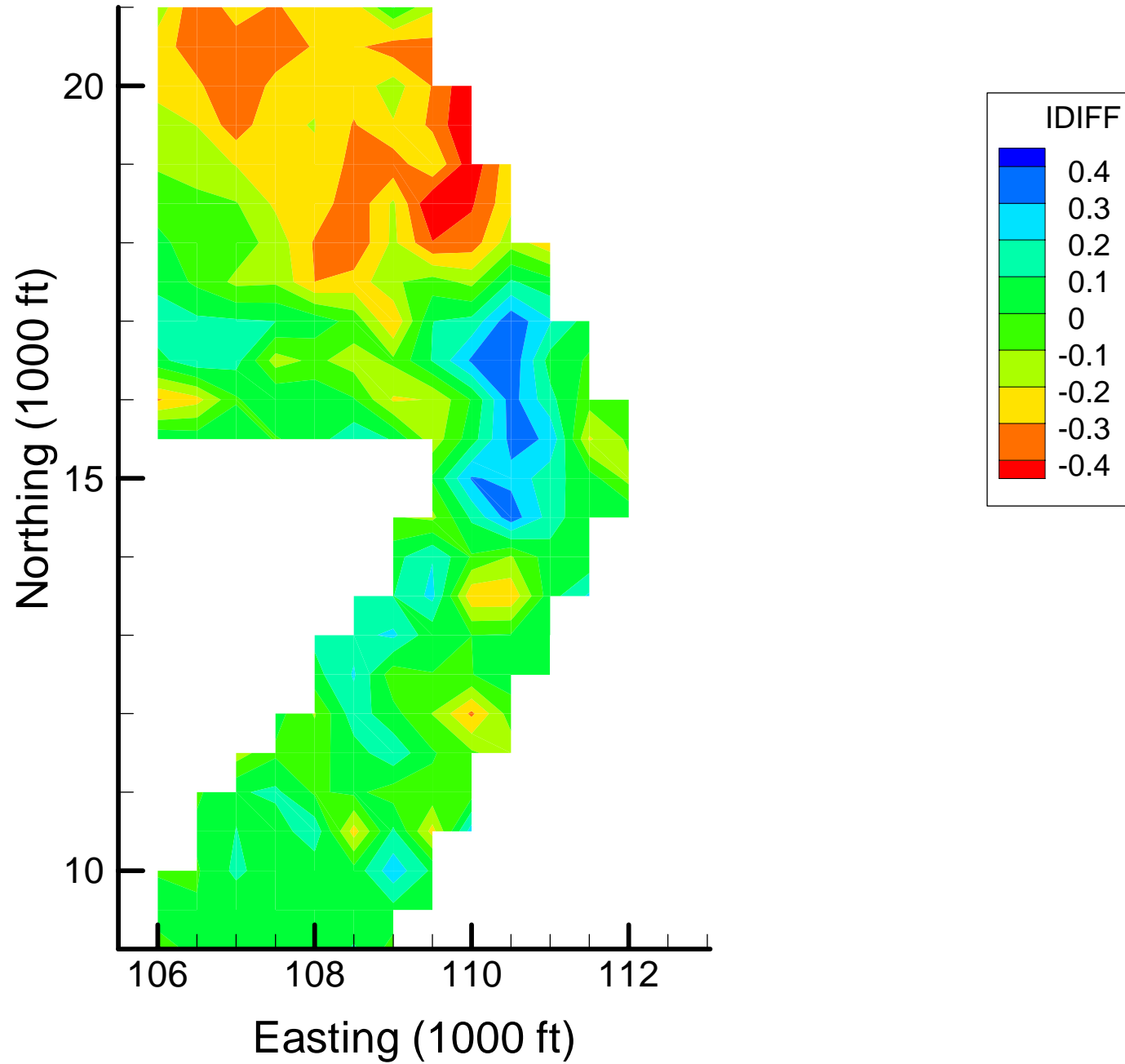
Site OU-12: MN Indicator Differences, 1999-2000, 10% Removal



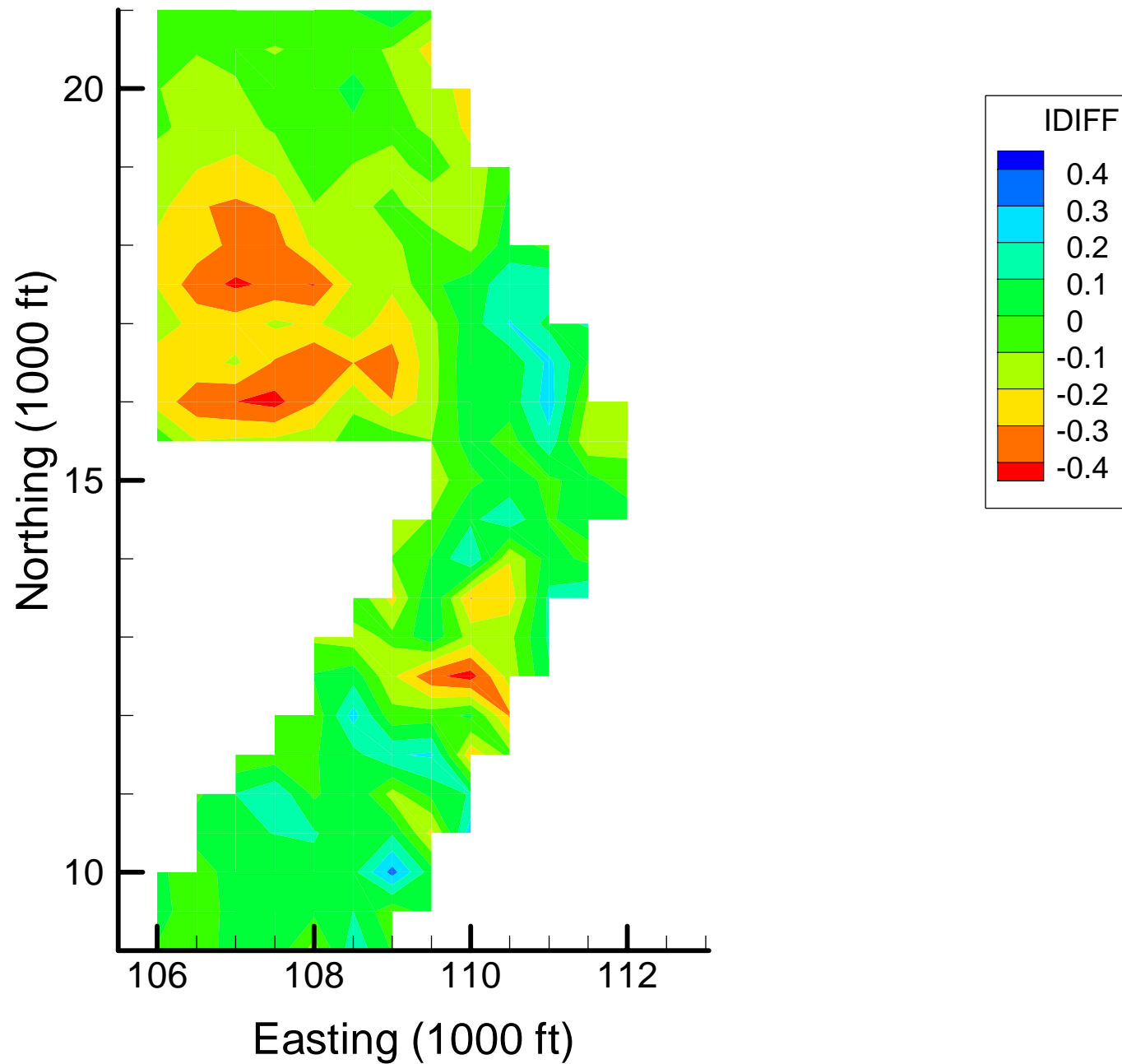
Site OU-12: MN Indicator Differences, 1999-2000, 20% Removal



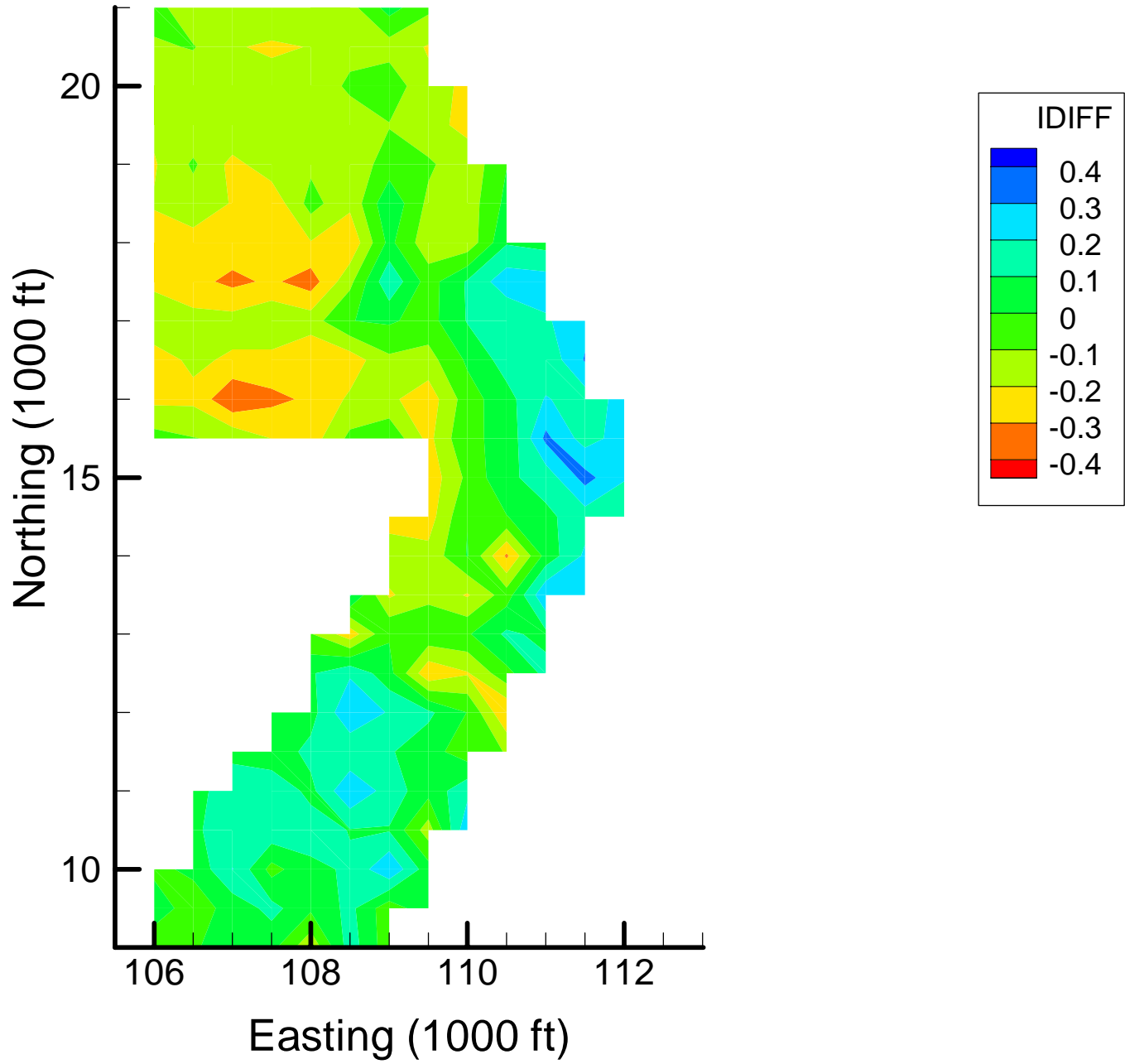
Site OU-12: MN Indicator Differences, 1999-2000, 30% Removal



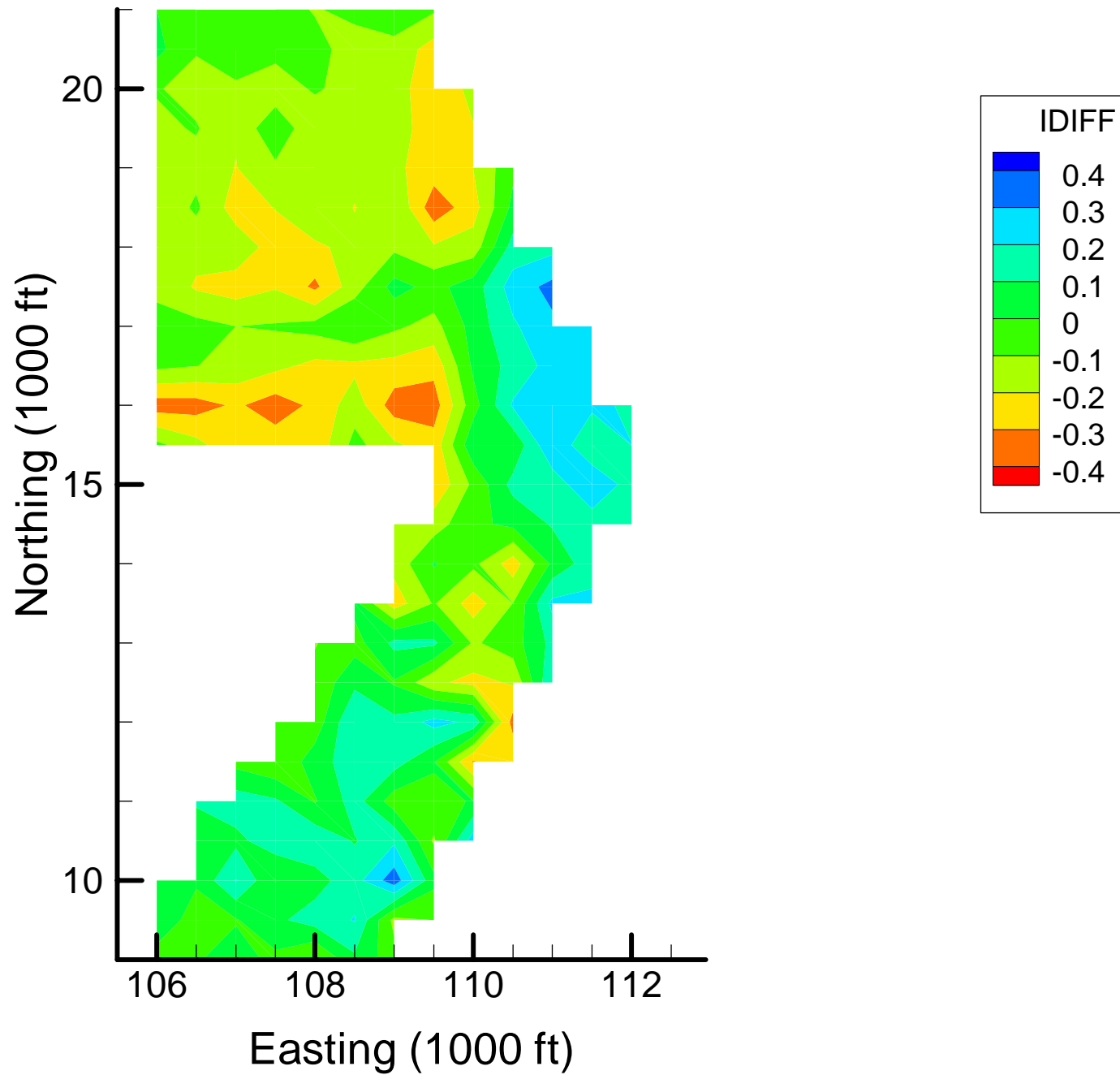
Site OU-12: MN Indicator Differences, 1999-2000, 40% Removal



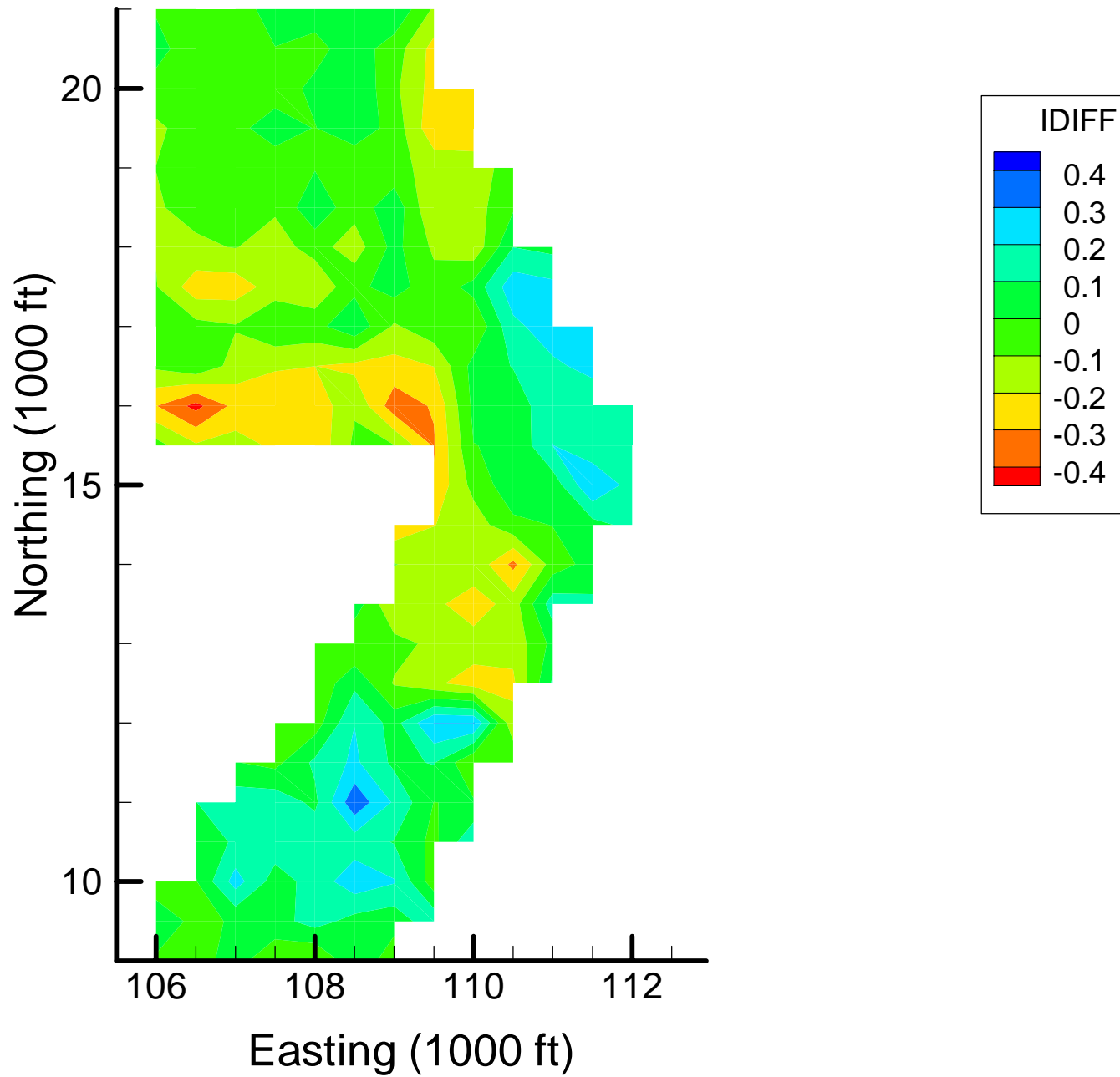
Site OU-12: MN Indicator Differences, 1999-2000, 50% Removal



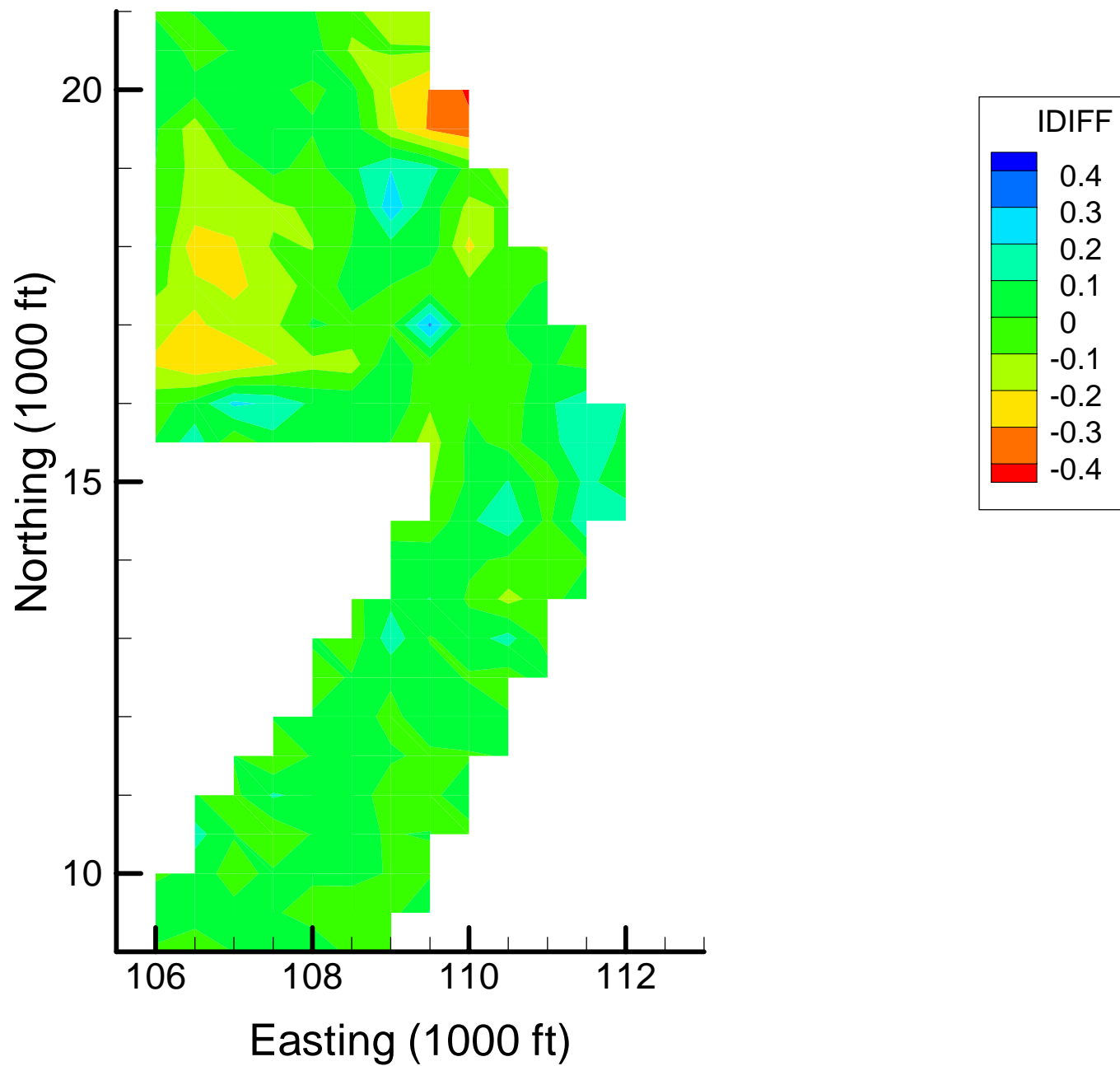
Site OU-12: MN Indicator Differences, 1999-2000, 60% Removal



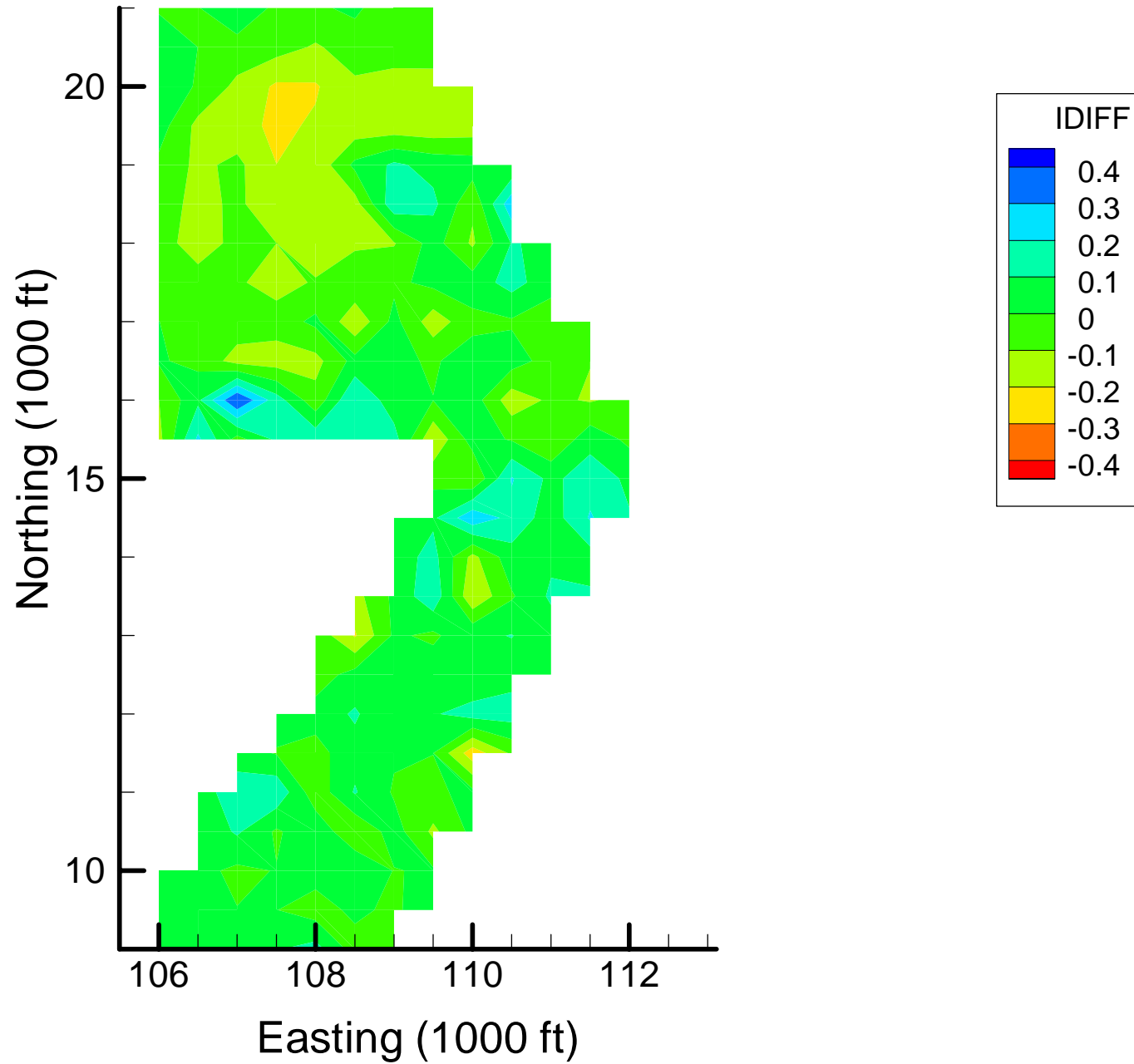
Site OU-12: MN Indicator Differences, 1999-2000, 70% Removal



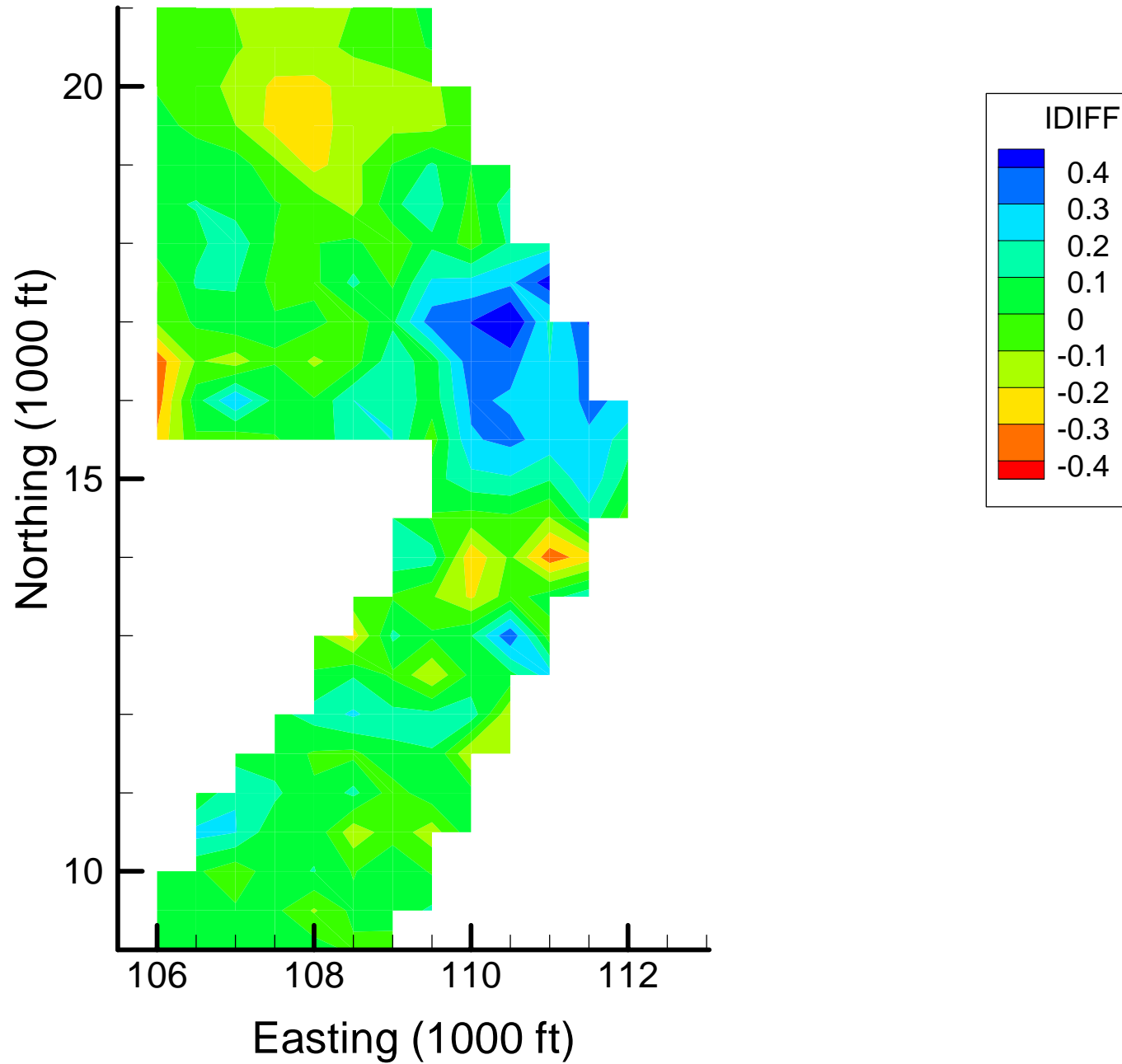
Site OU-12: MN Indicator Differences, 2001-2002, 10% Removal



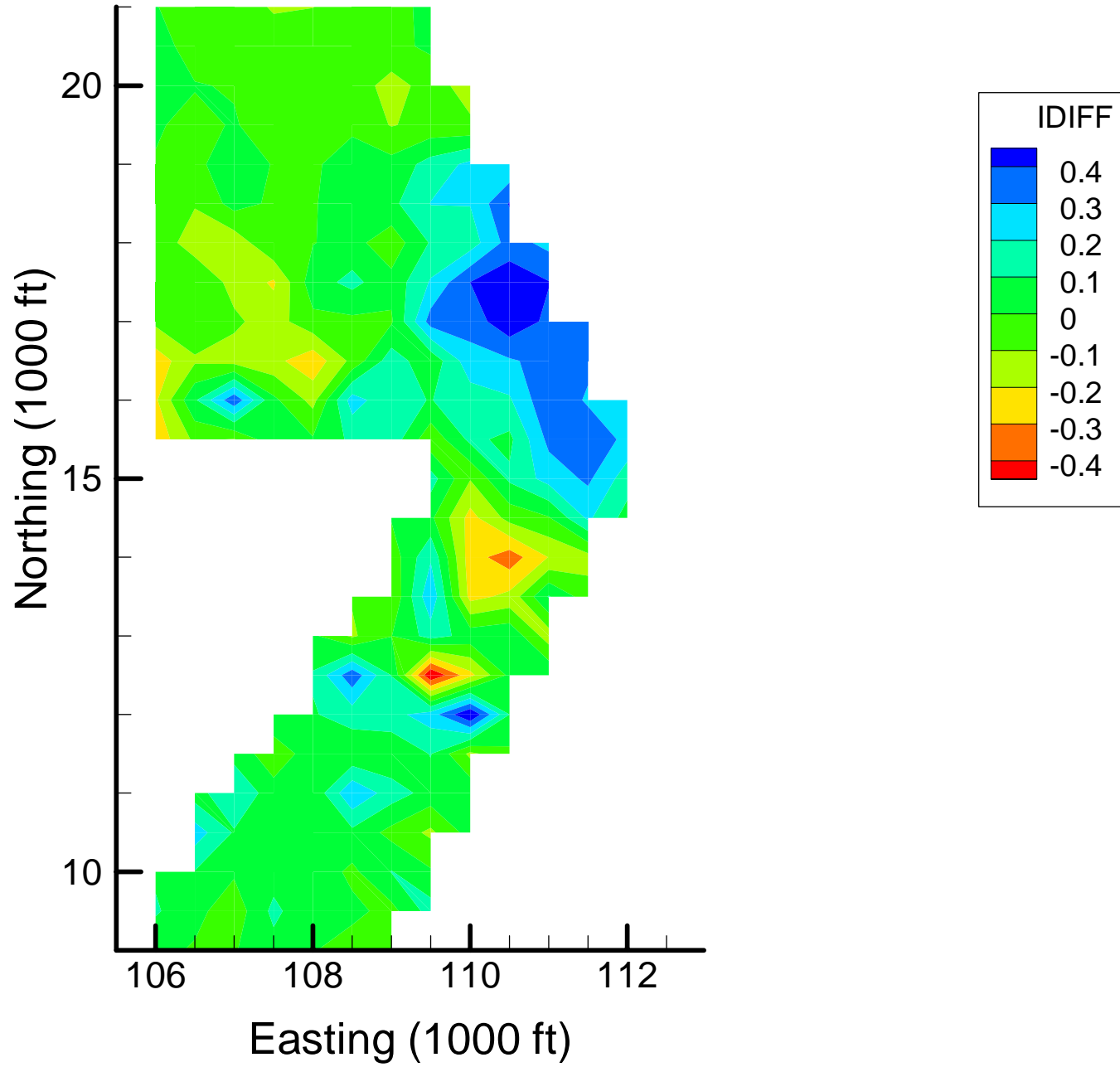
Site OU-12: MN Indicator Differences, 2001-2002, 20% Removal



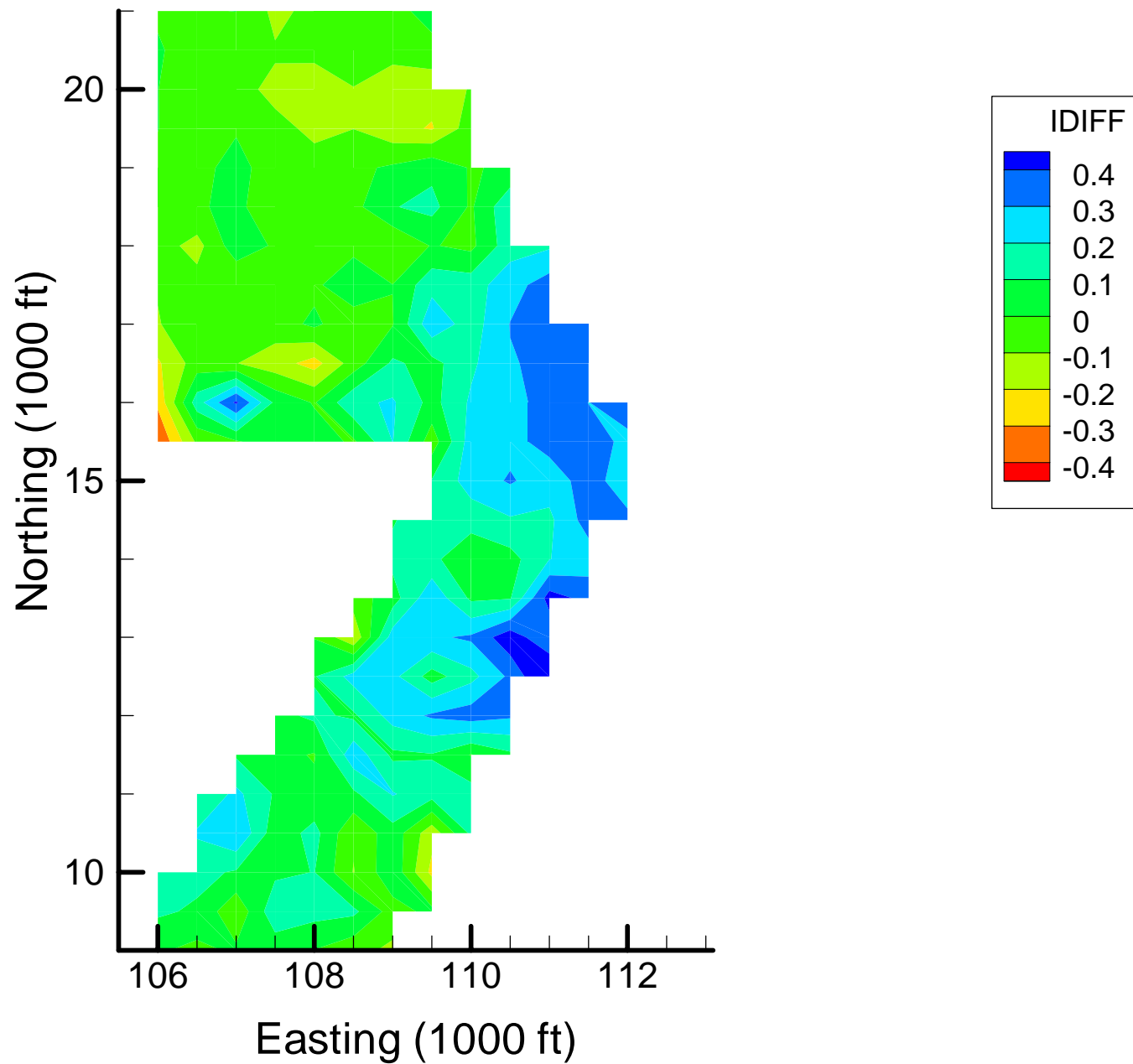
Site OU-12: MN Indicator Differences, 2001-2002, 30% Removal



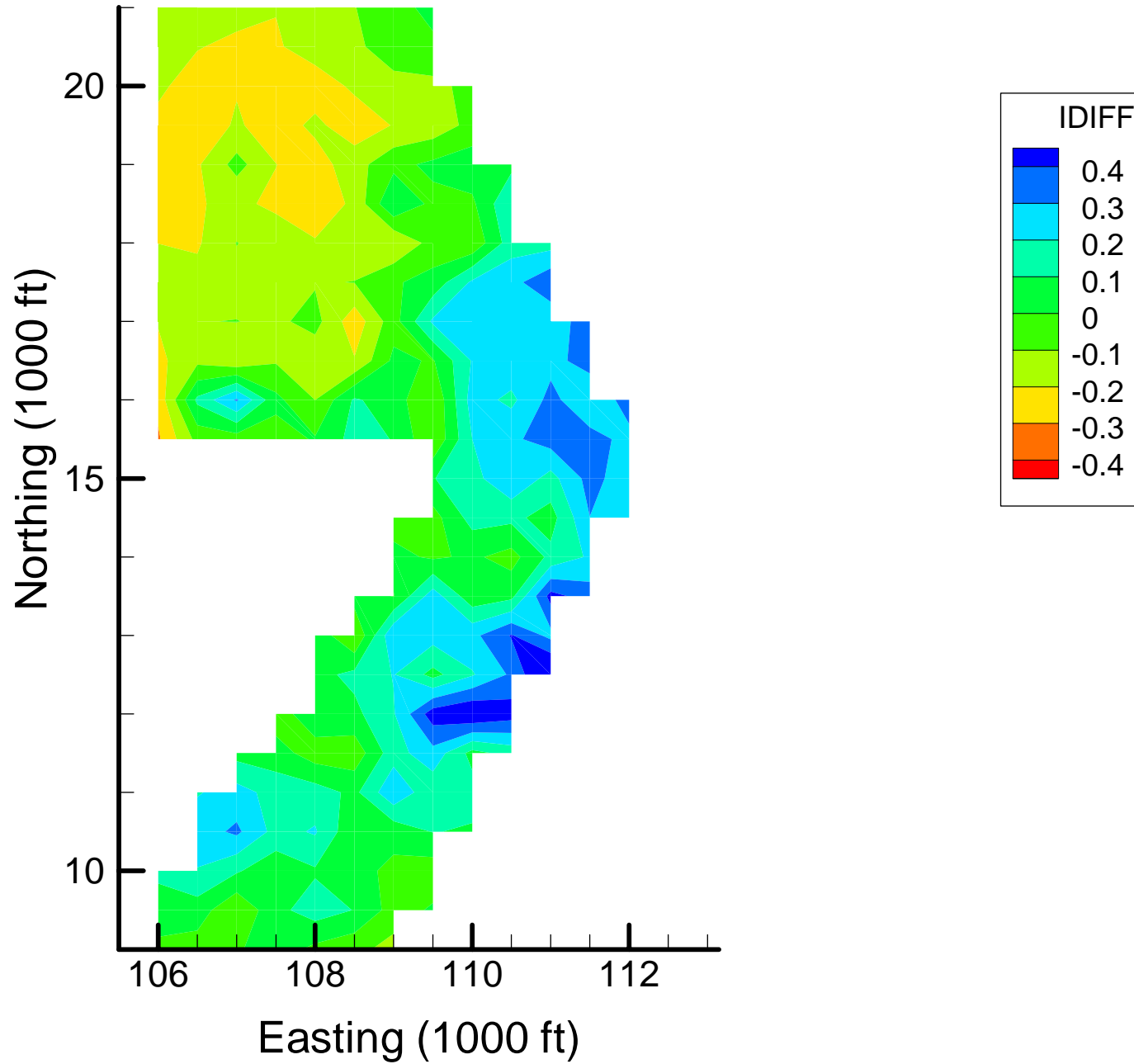
Site OU-12: MN Indicator Differences, 2001-2002, 40% Removal



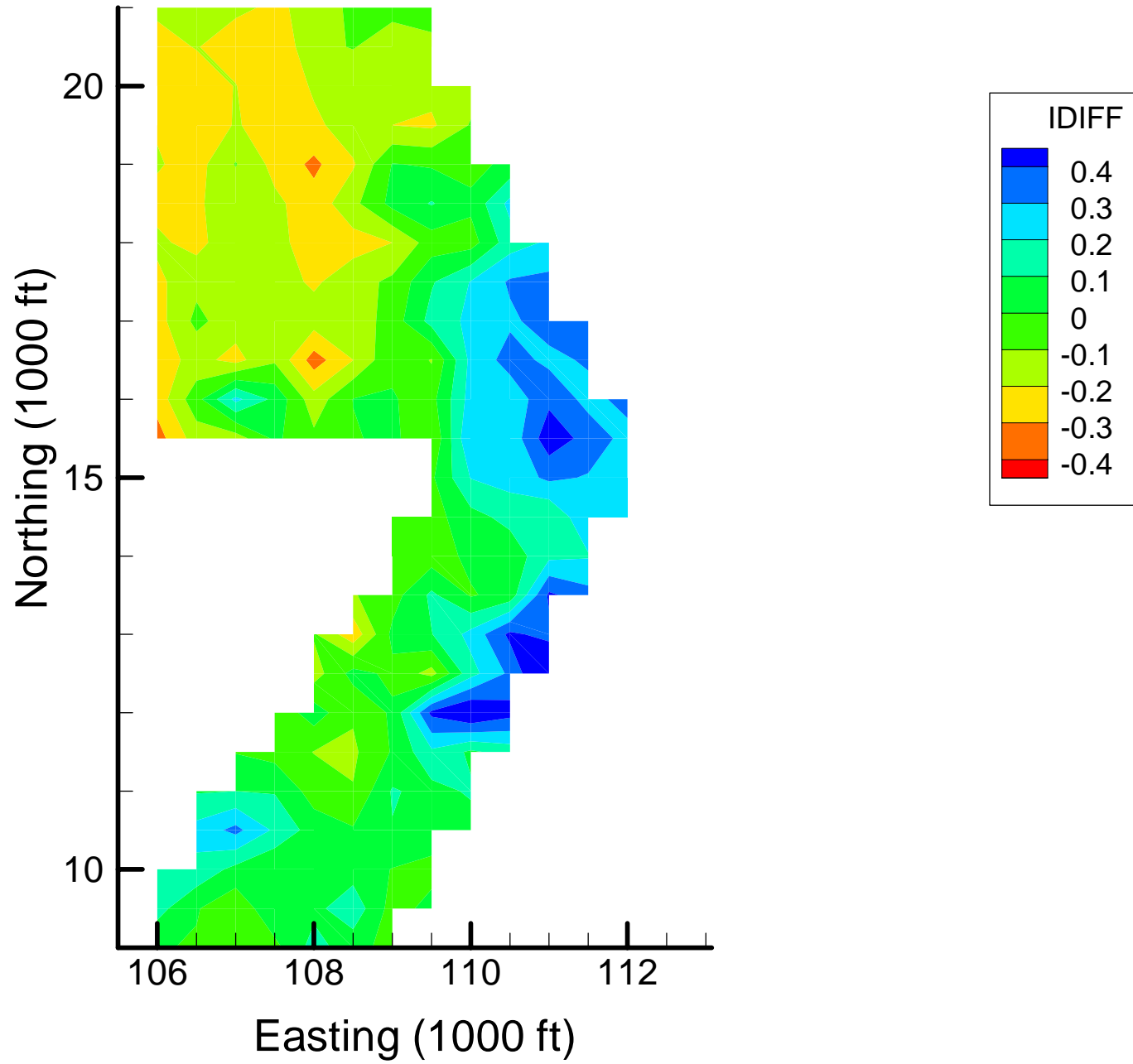
Site OU-12: MN Indicator Differences, 2001-2002, 50% Removal



Site OU-12: MN Indicator Differences, 2001-2002, 60% Removal



Site OU-12: MN Indicator Differences, 2001-2002, 70% Removal



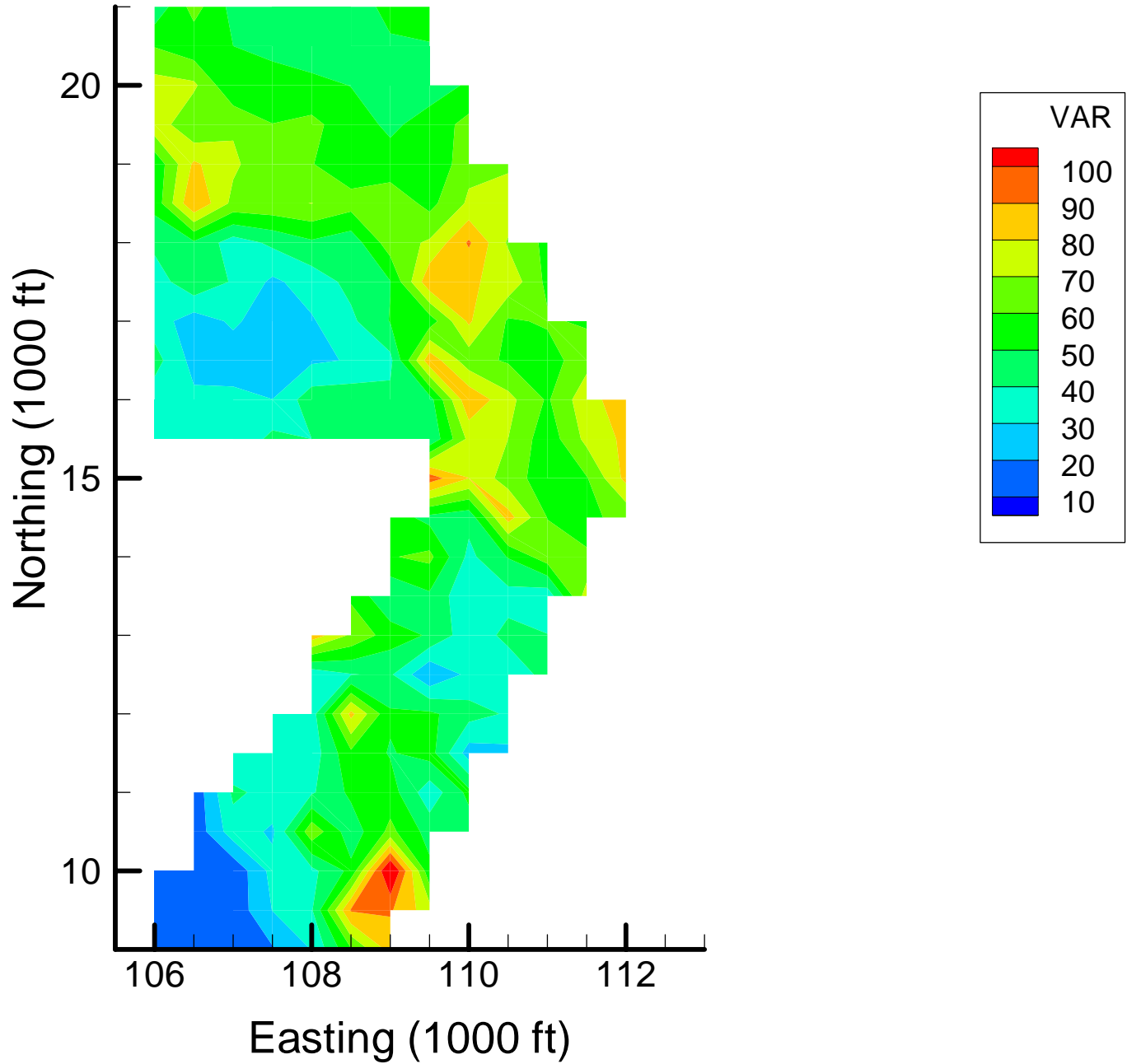
Appendix 4-3

Spatial Optimization: BZ Local Variance Maps

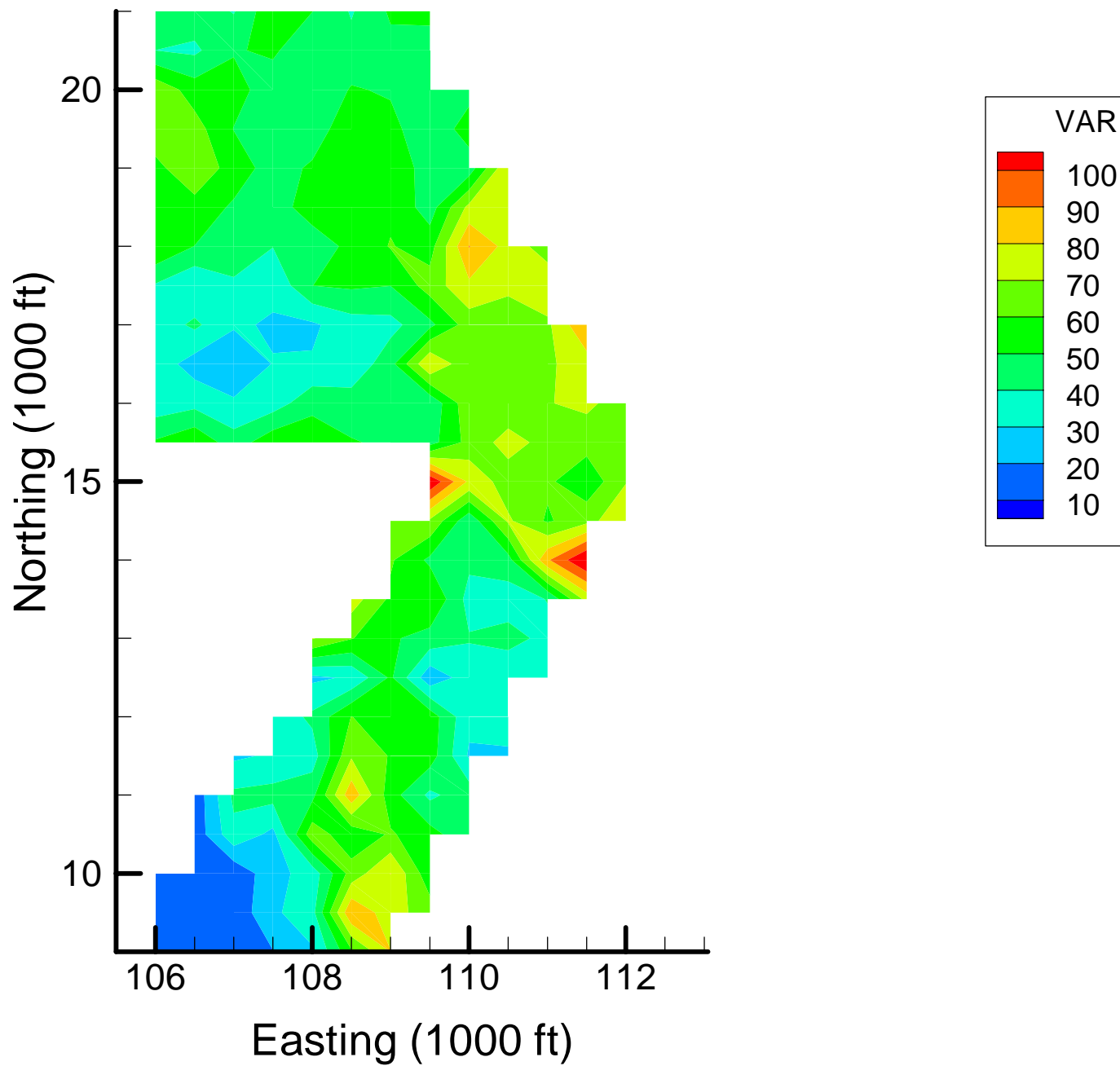
Notes:

VAR = Voxel-specific local variance estimates (averaged over depth, in ppb)

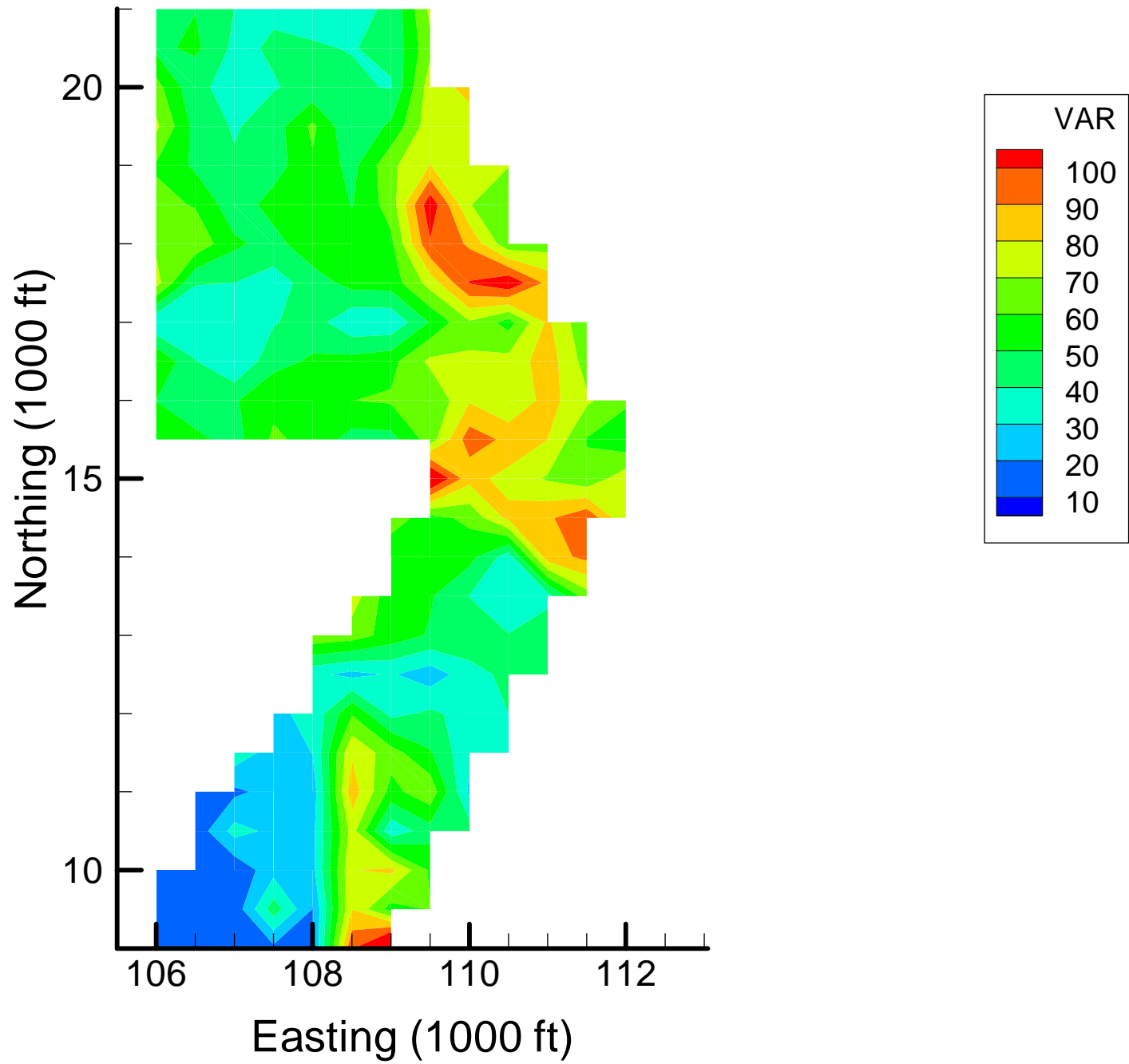
Site OU-12: Benzene Local Variances, 1999-2000, Base Map



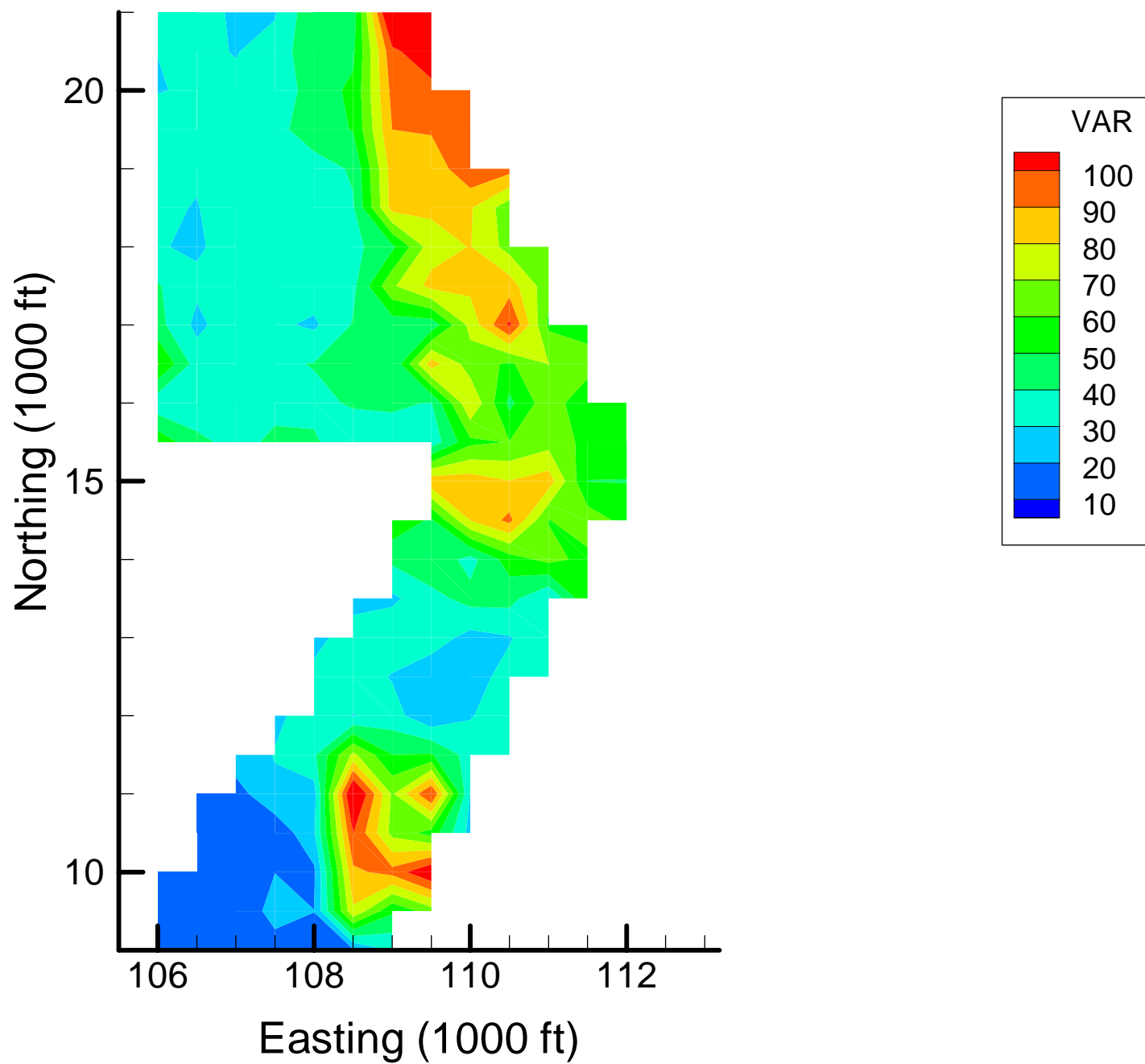
Site OU-12: Benzene Local Variances, 1999-2000, 10% Removal



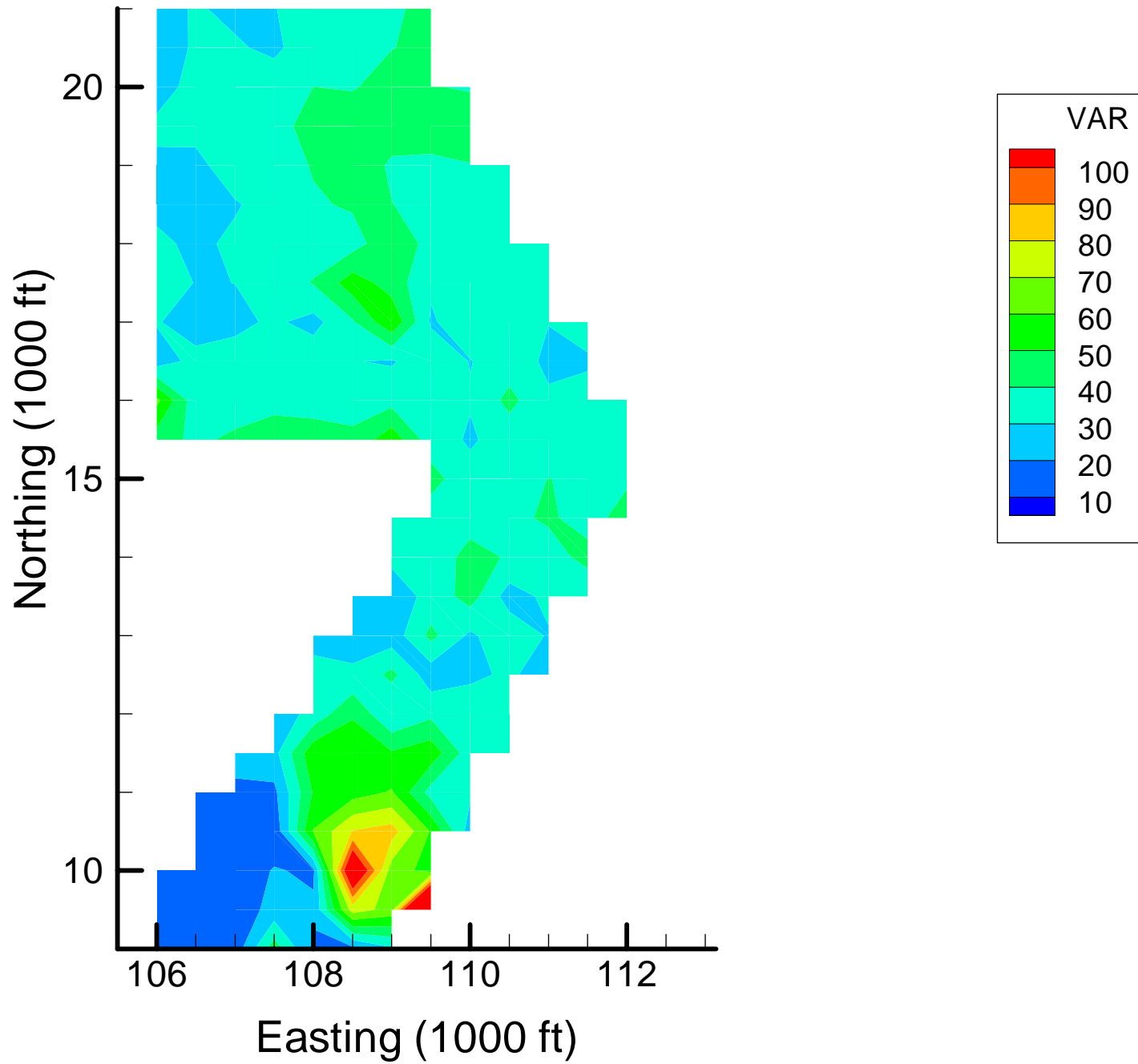
Site OU-12: Benzene Local Variances, 1999-2000, 20% Removal



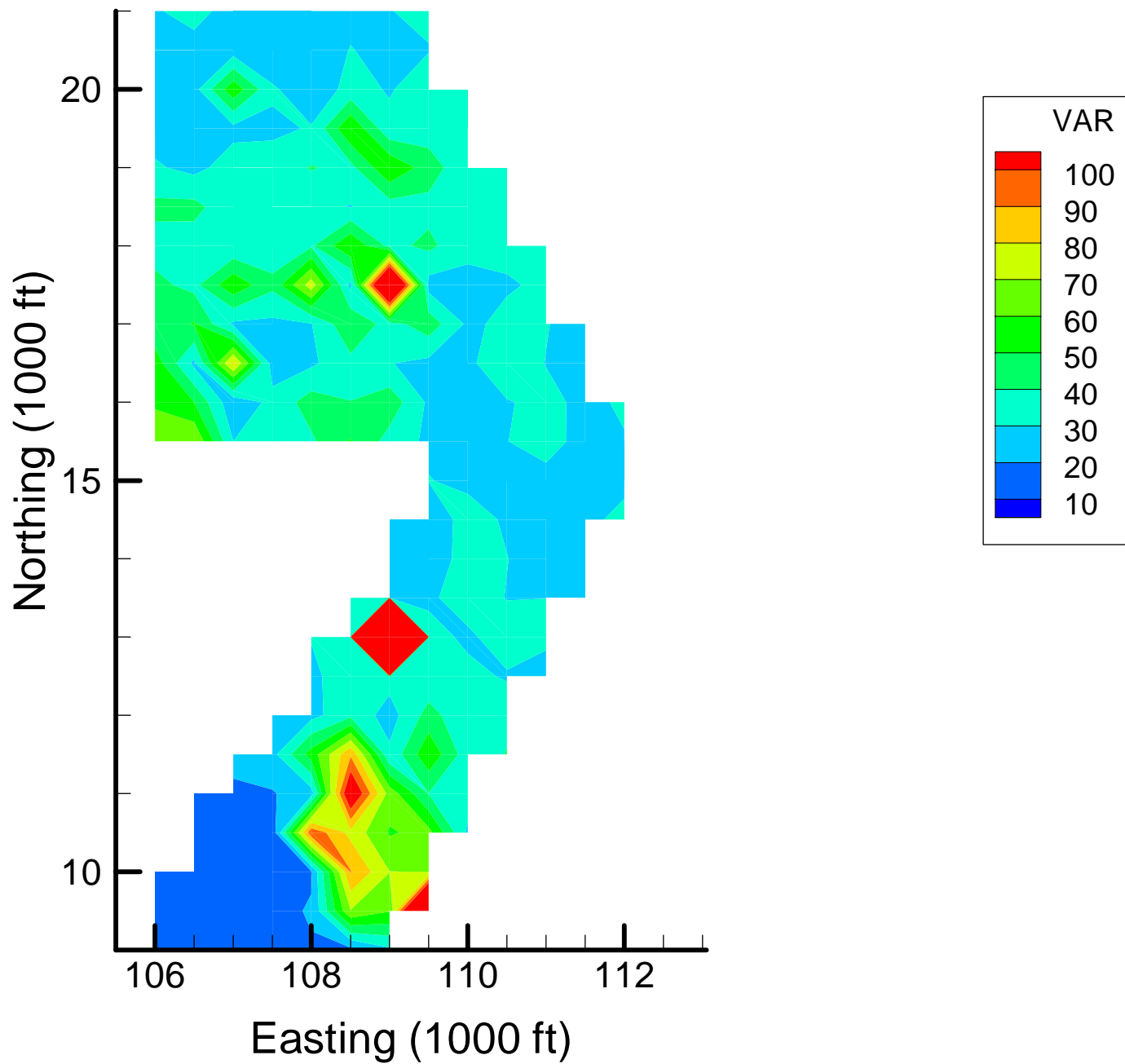
Site OU-12: Benzene Local Variances, 1999-2000, 30% Removal



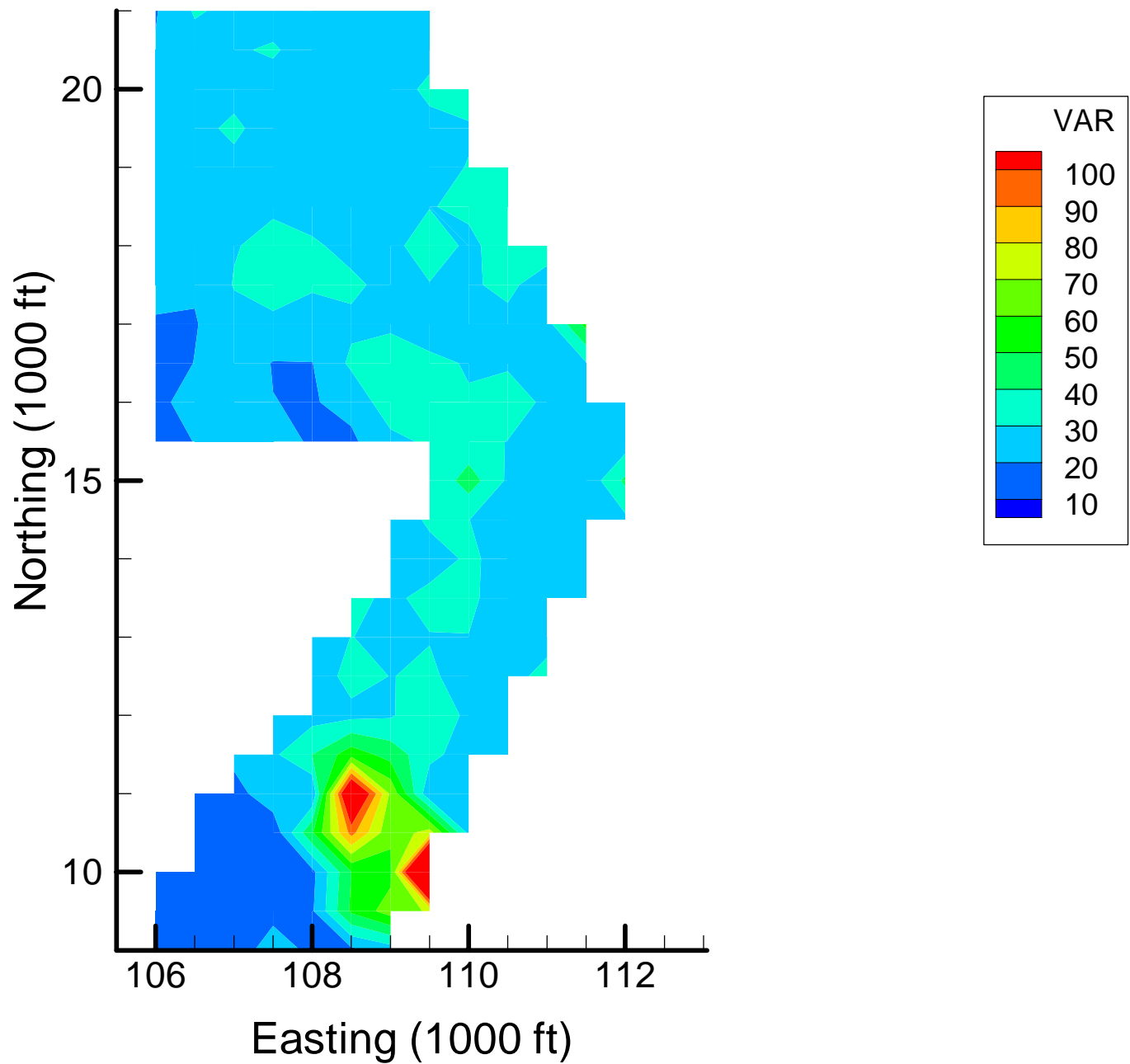
Site OU-12: Benzene Local Variances, 1999-2000, 40% Removal



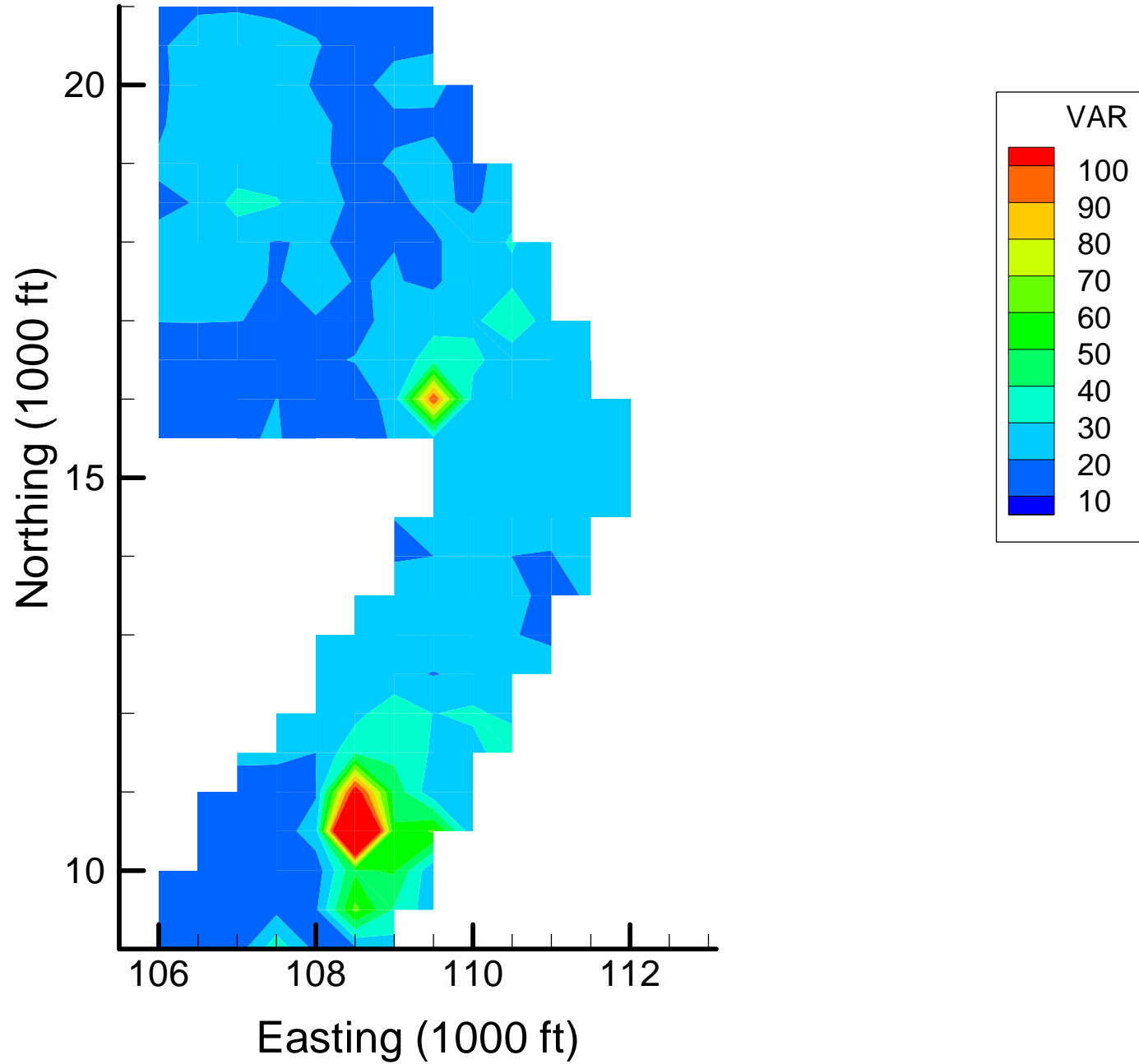
Site OU-12: Benzene Local Variances, 1999-2000, 50% Removal



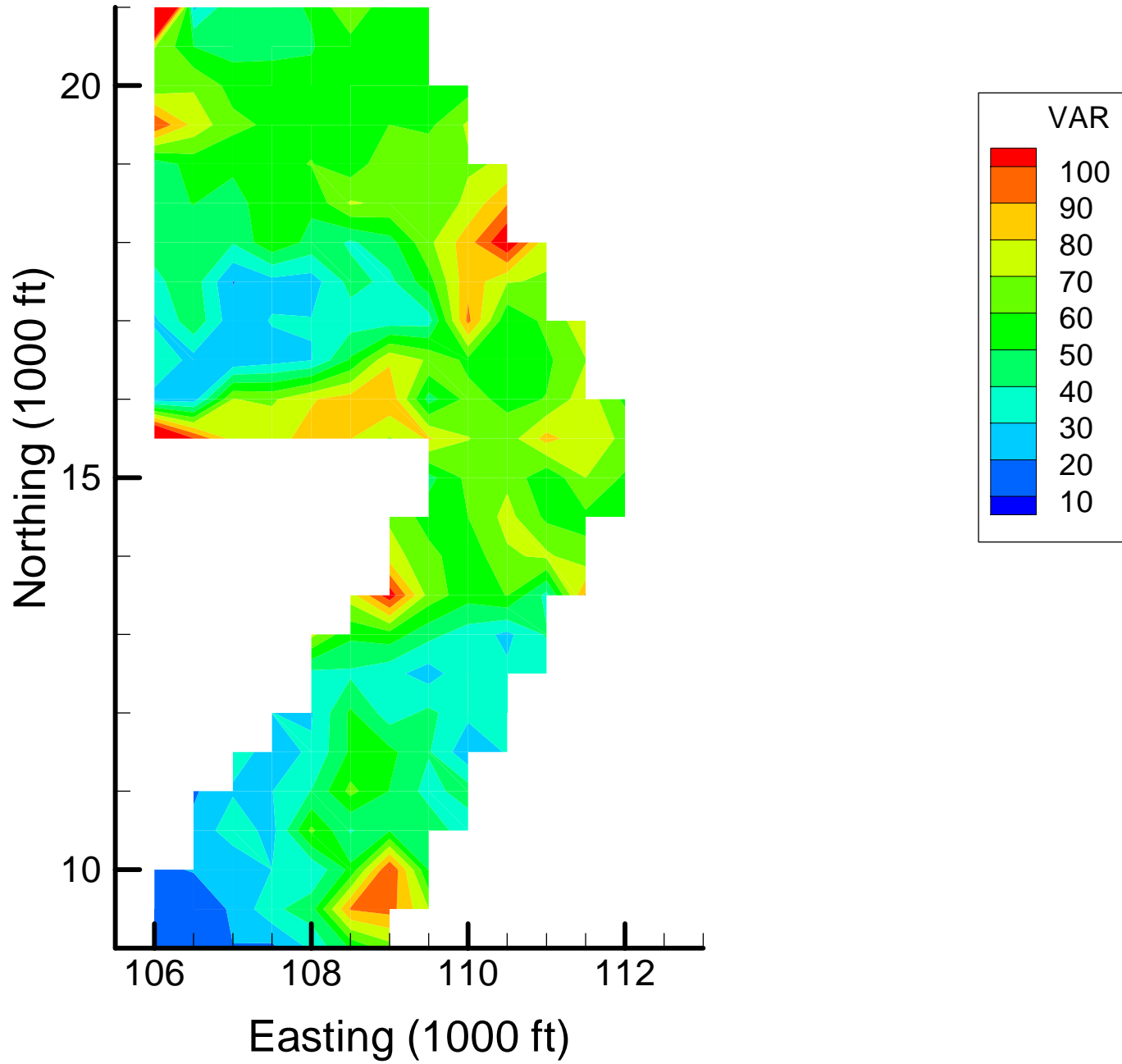
Site OU-12: Benzene Local Variances, 1999-2000, 60% Removal



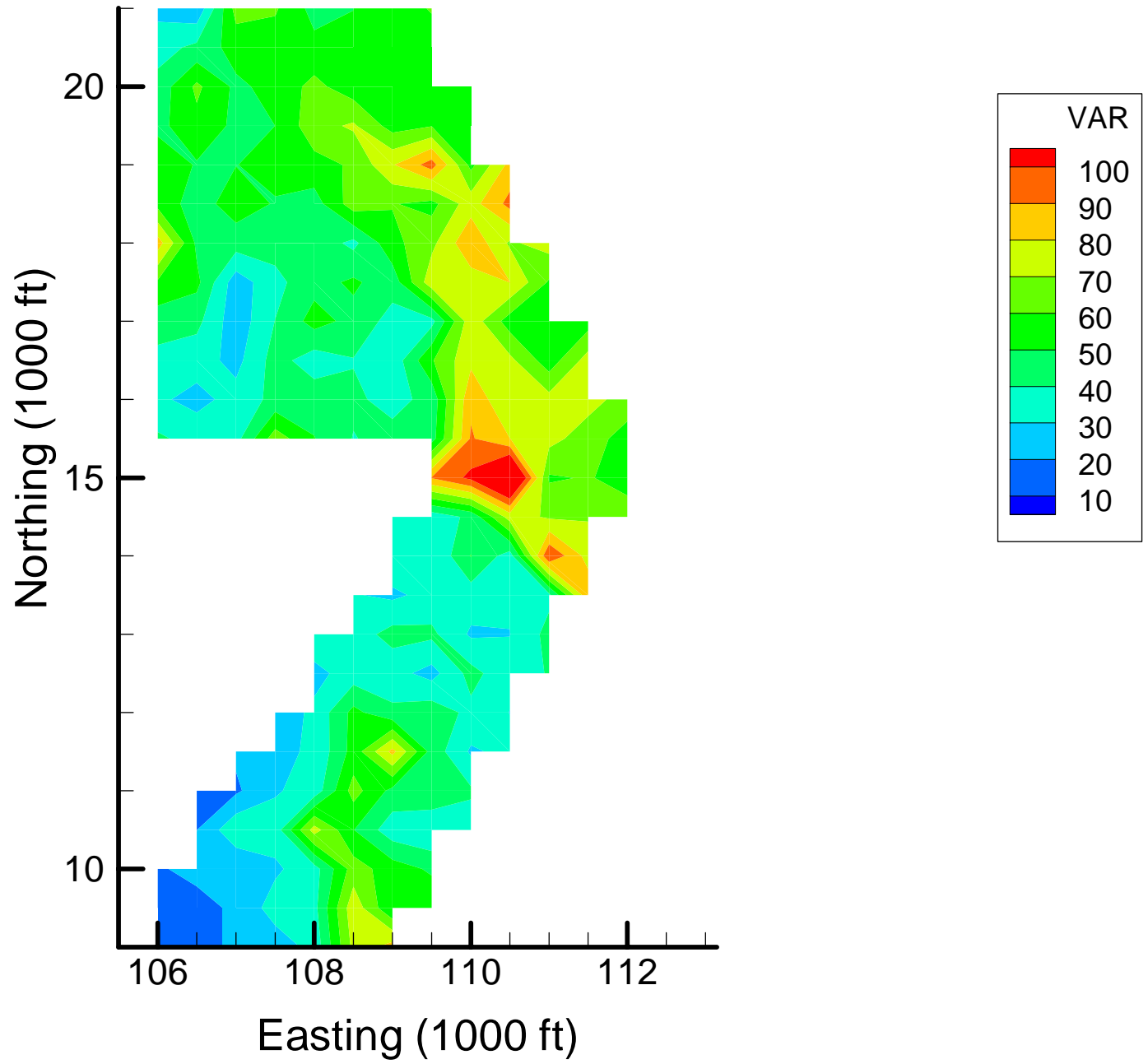
Site OU-12: Benzene Local Variances, 1999-2000, 70% Removal



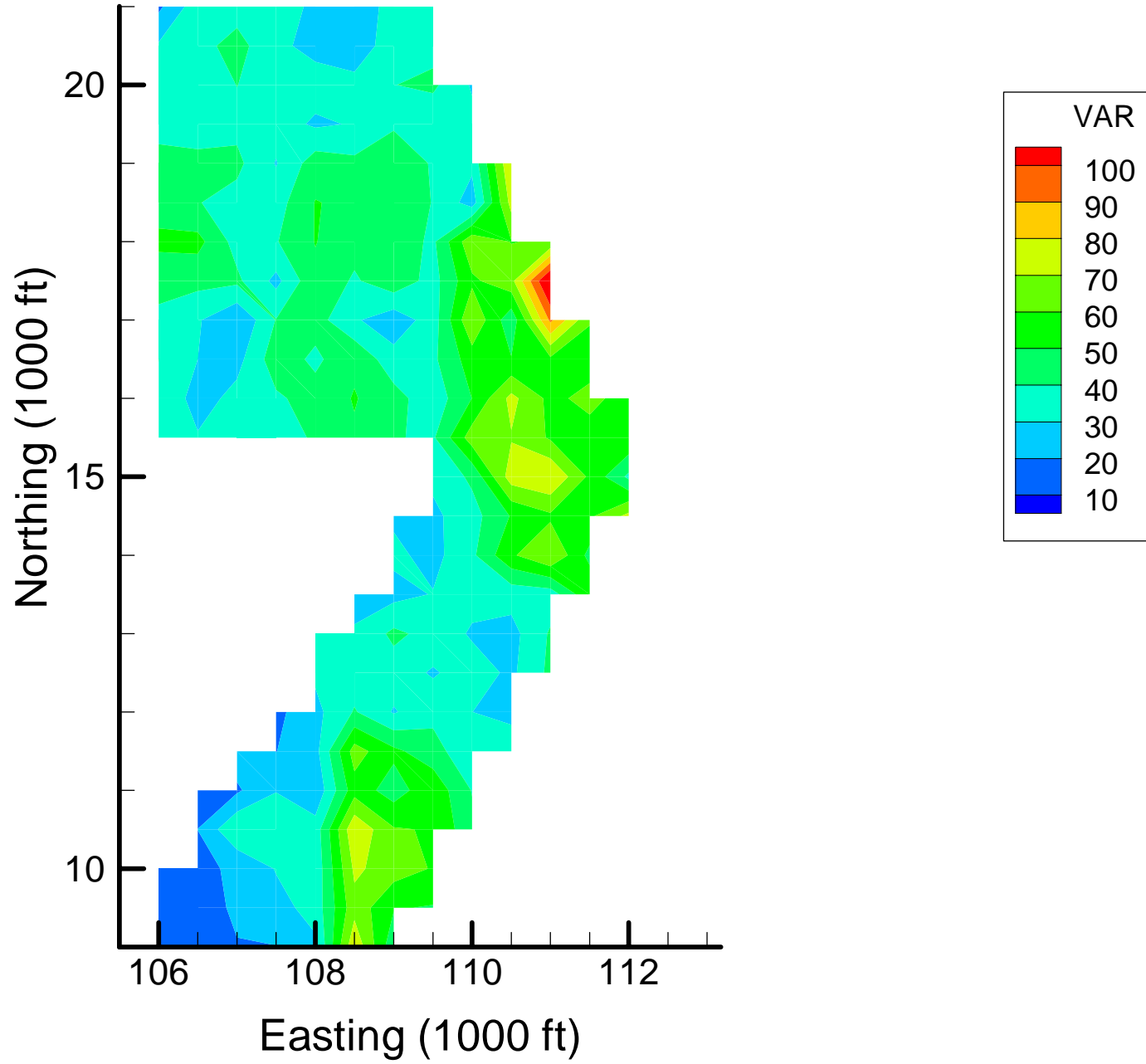
Site OU-12: Benzene Local Variances, 2001-2002, Base Map



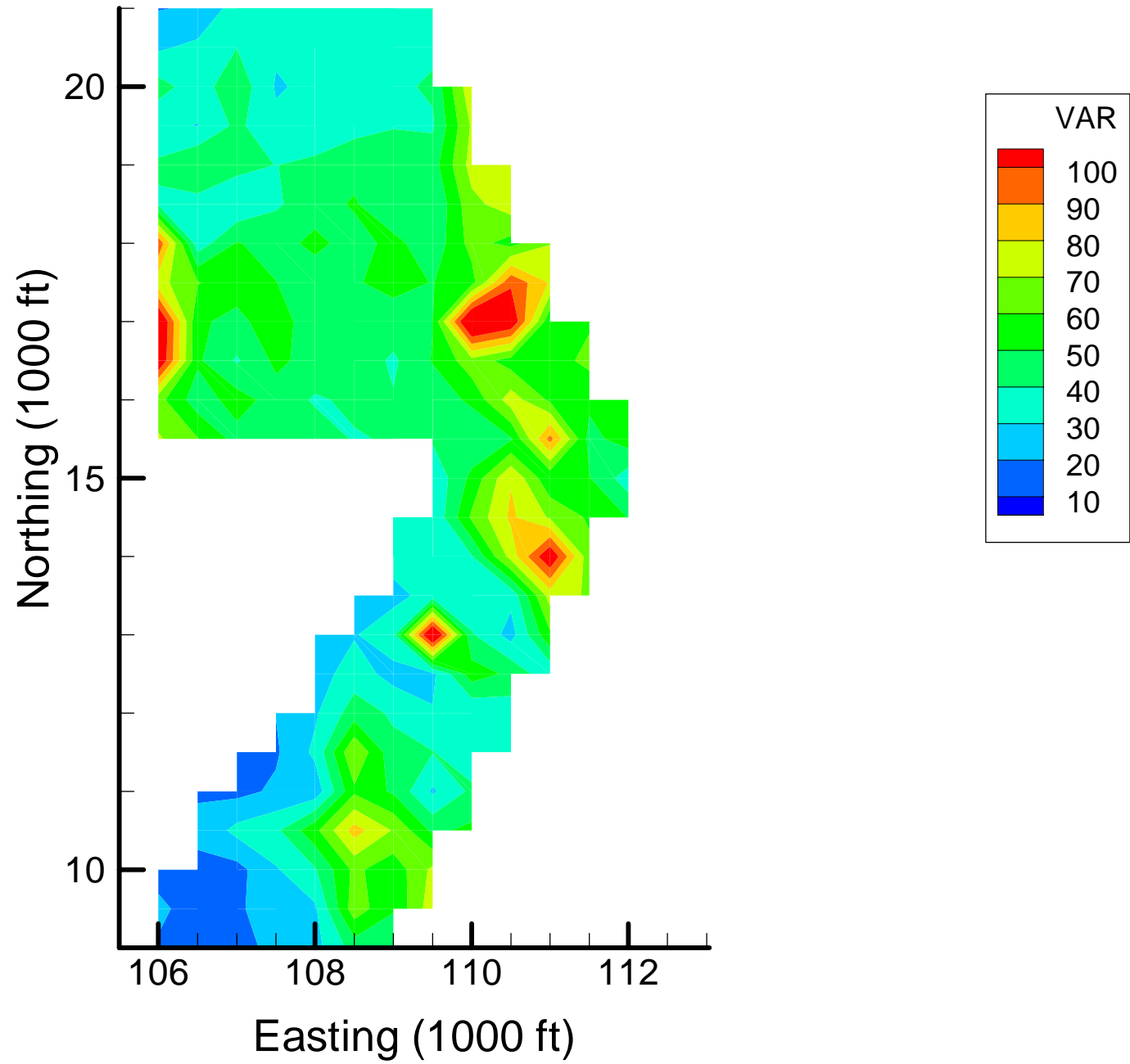
Site OU-12: Benzene Local Variances, 2001-2002, 10% Removal



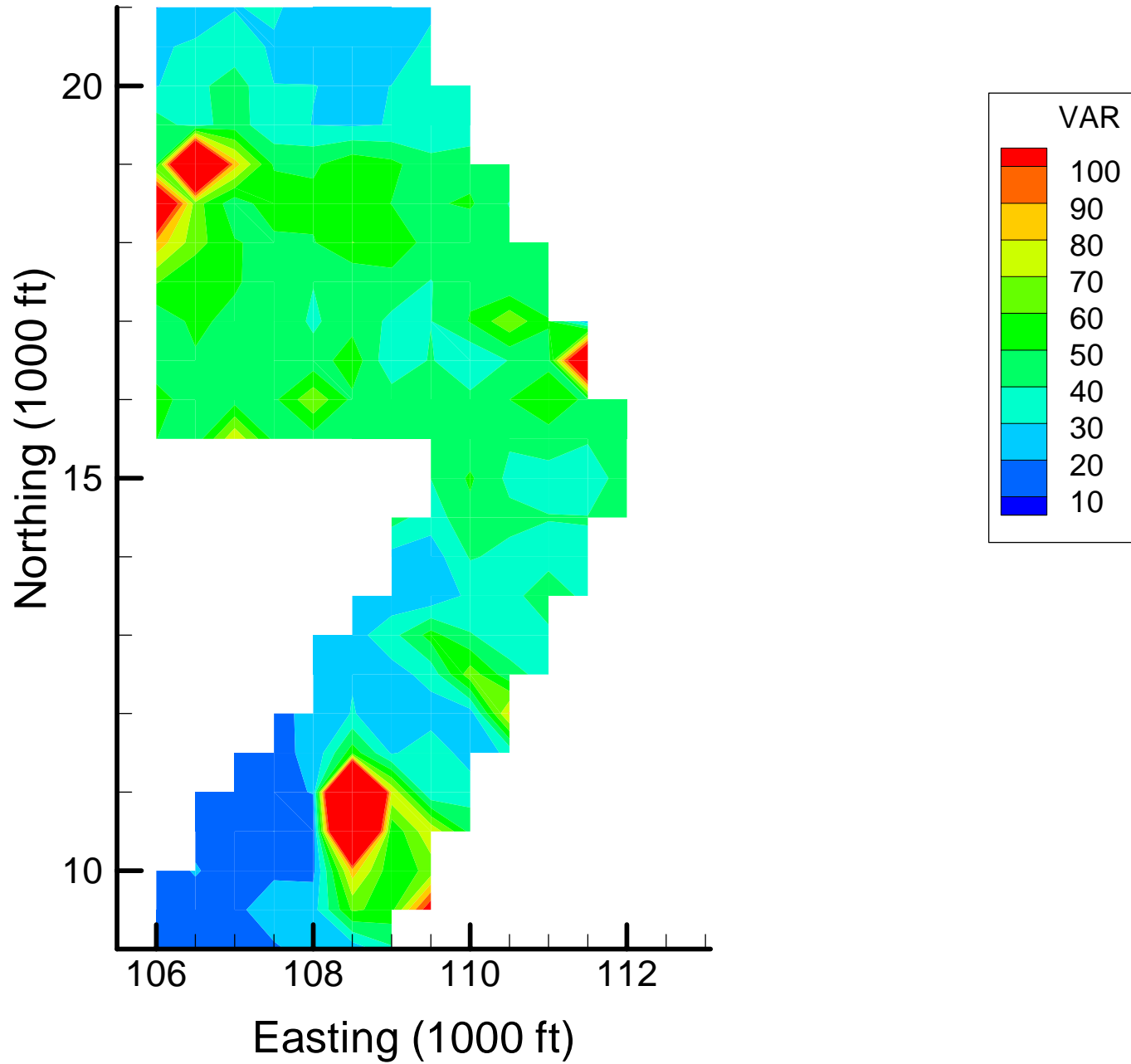
Site OU-12: Benzene Local Variances, 2001-2002, 20% Removal



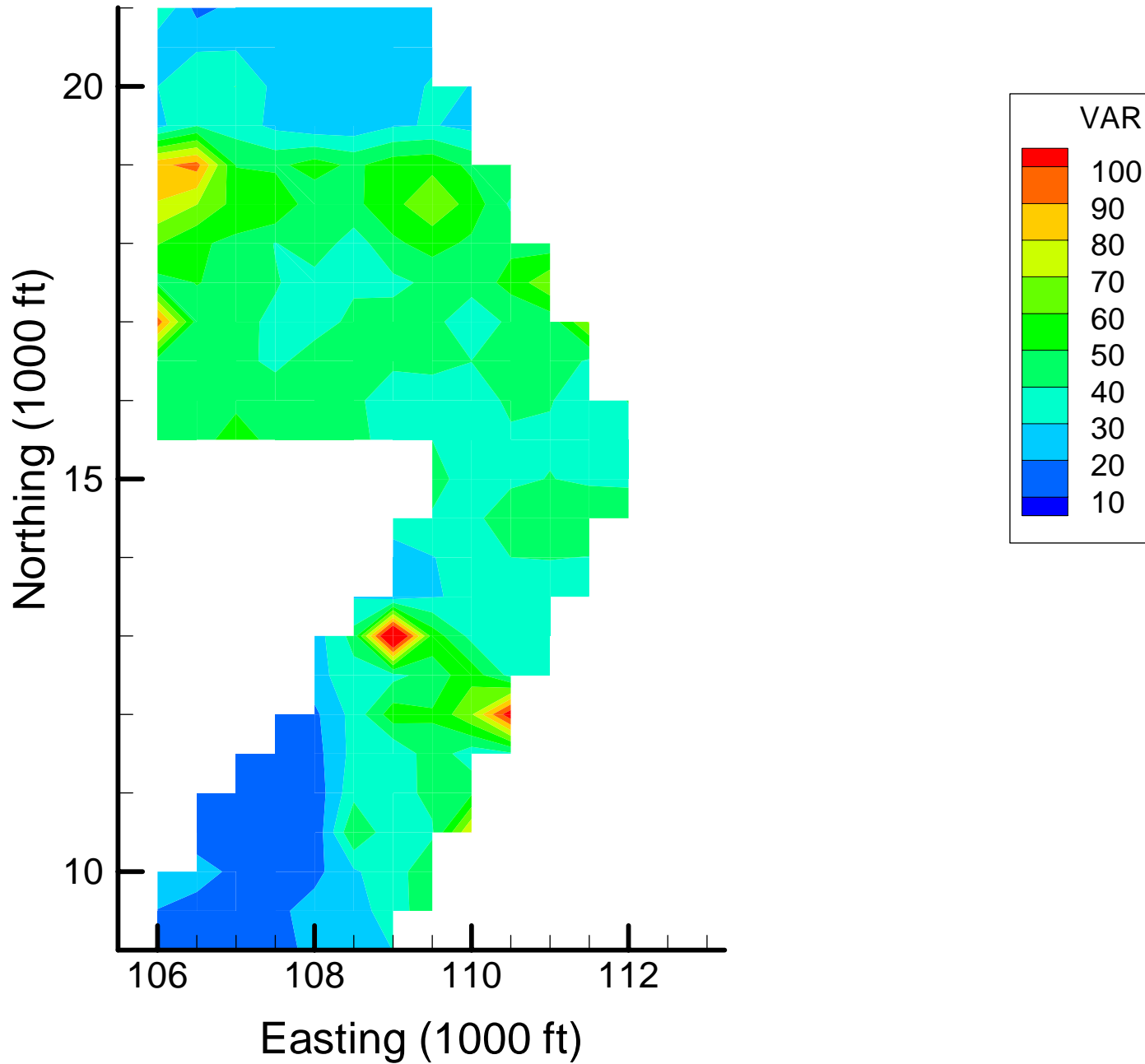
Site OU-12: Benzene Local Variances, 2001-2002, 30% Removal



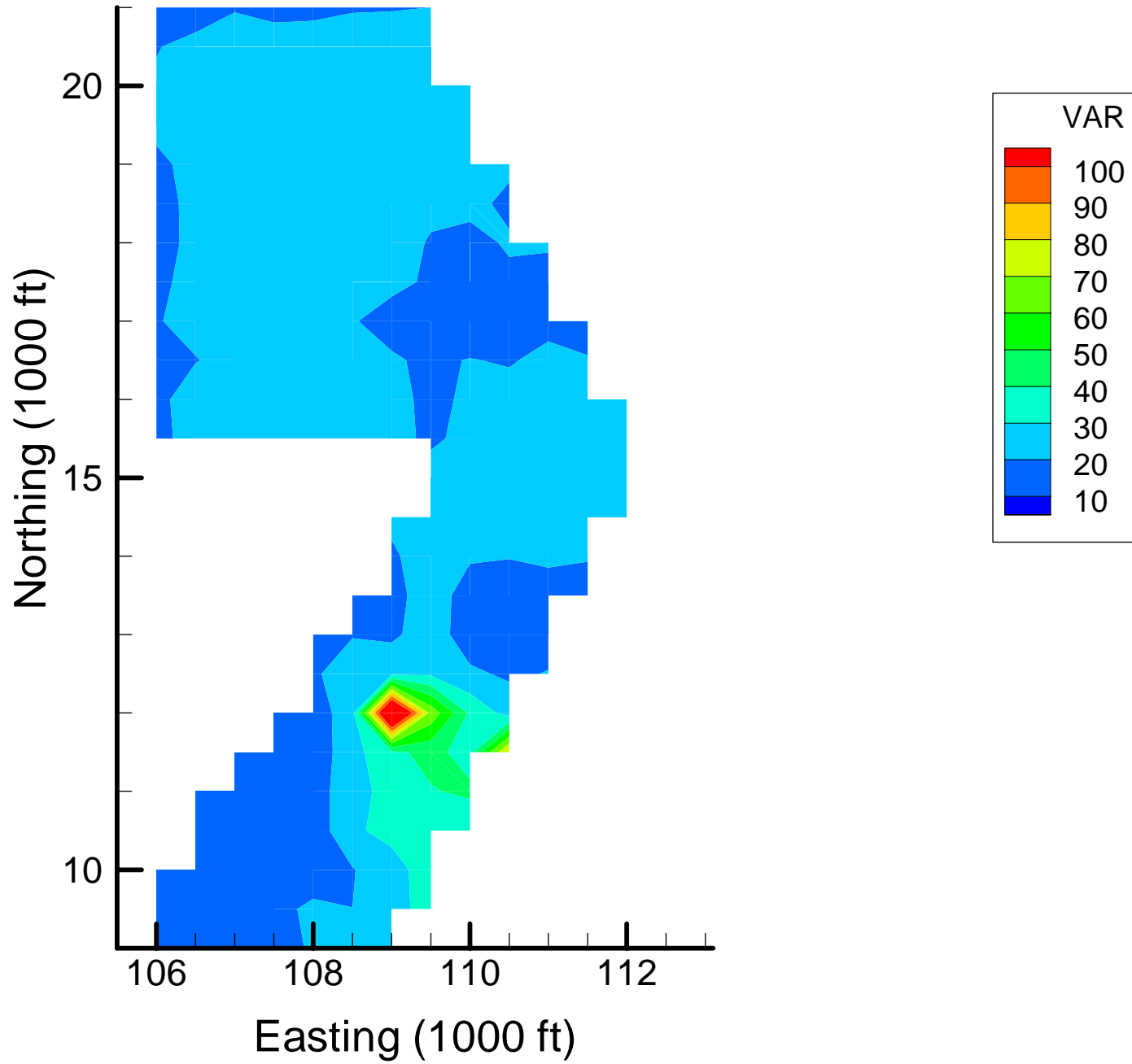
Site OU-12: Benzene Local Variances, 2001-2002, 40% Removal



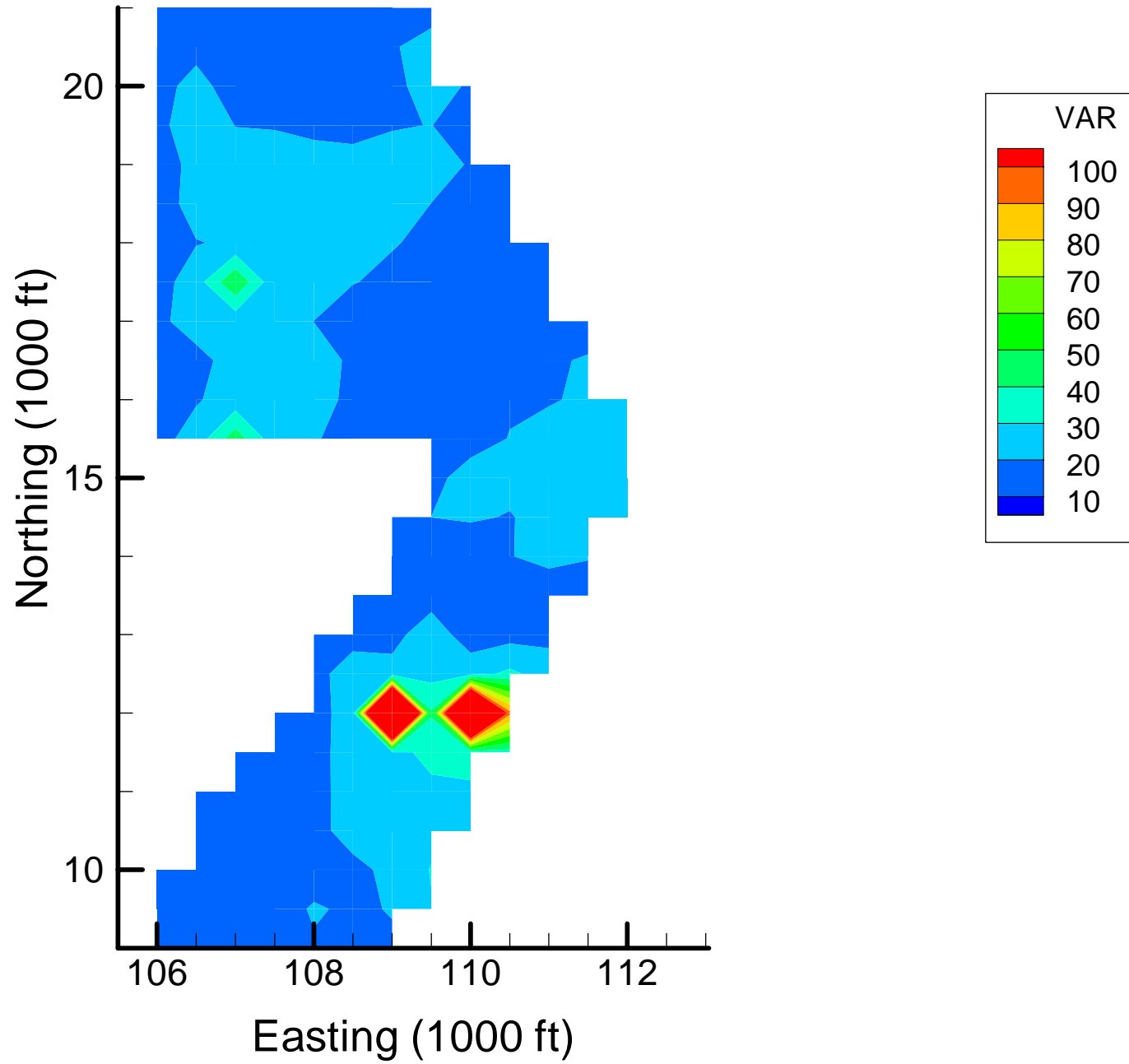
Site OU-12: Benzene Local Variances, 2001-2002, 50% Removal



Site OU-12: Benzene Local Variances, 2001-2002, 60% Removal



Site OU-12: Benzene Local Variances, 2001-2002, 70% Removal



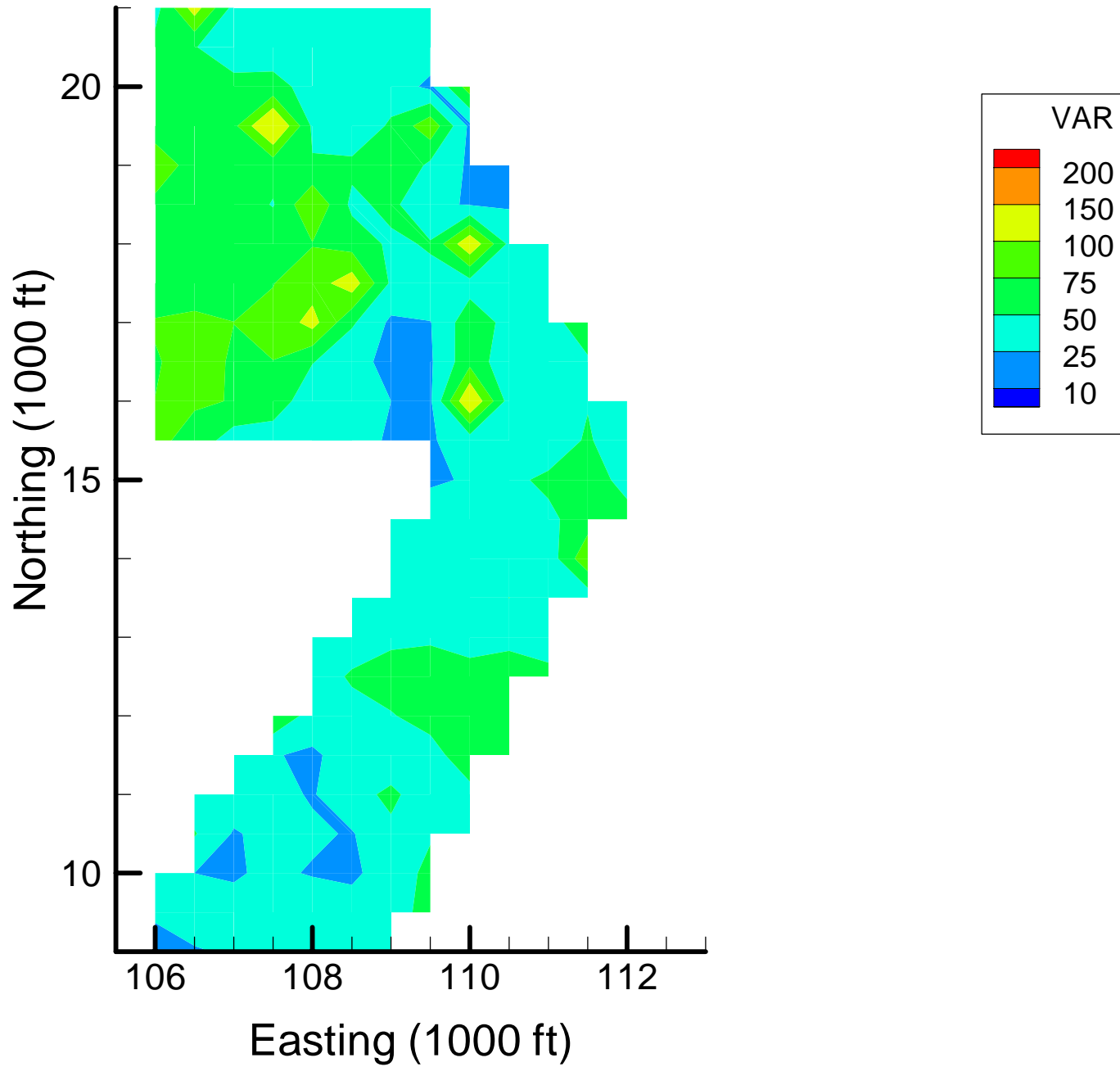
Appendix 4-3

Spatial Optimization: FE Local Variance Maps

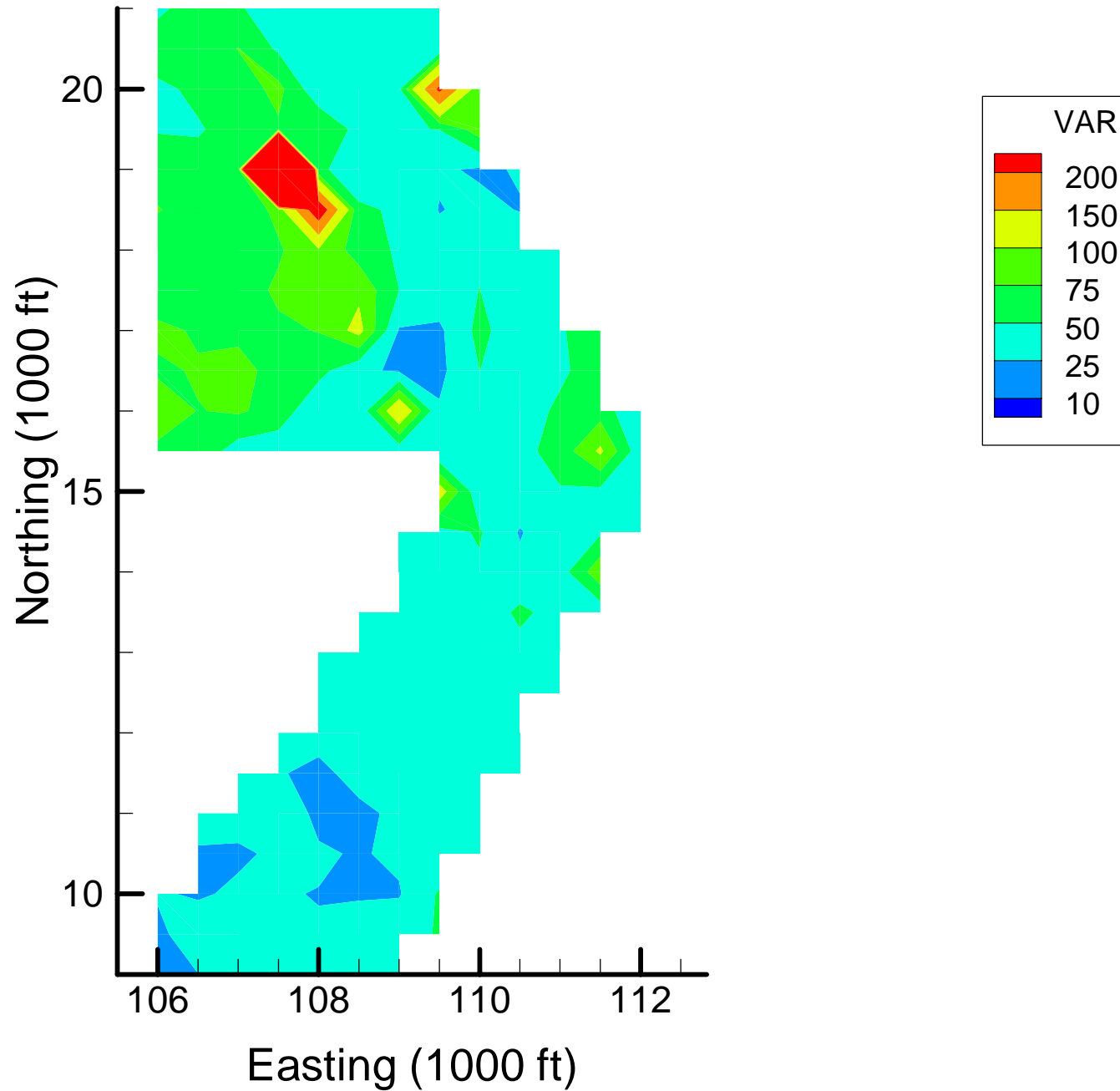
Notes:

VAR = Voxel-specific local variance estimates (averaged over depth, in ppb)

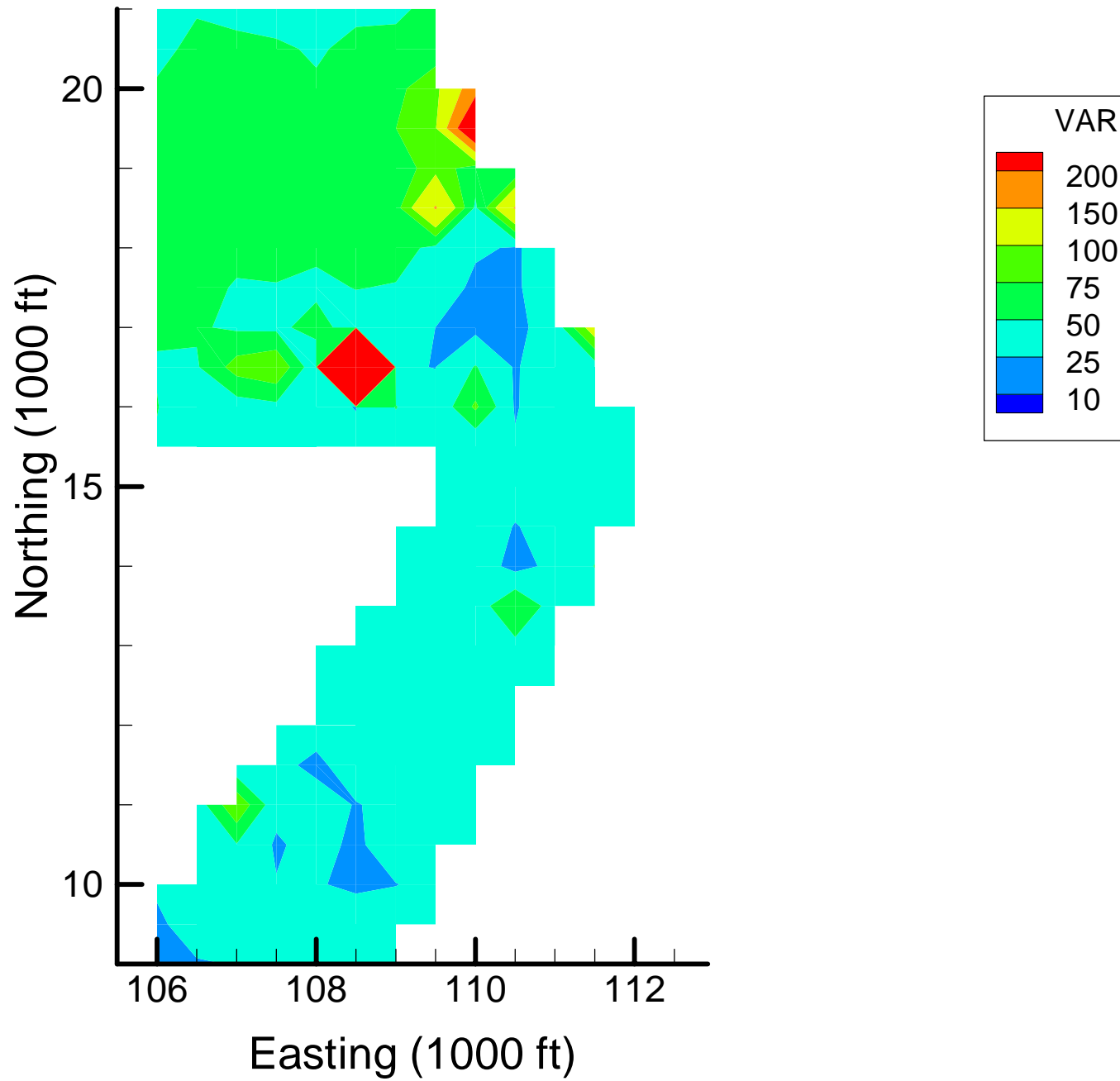
Site OU-12: FE Local Variances, 1999-2000, Base Map



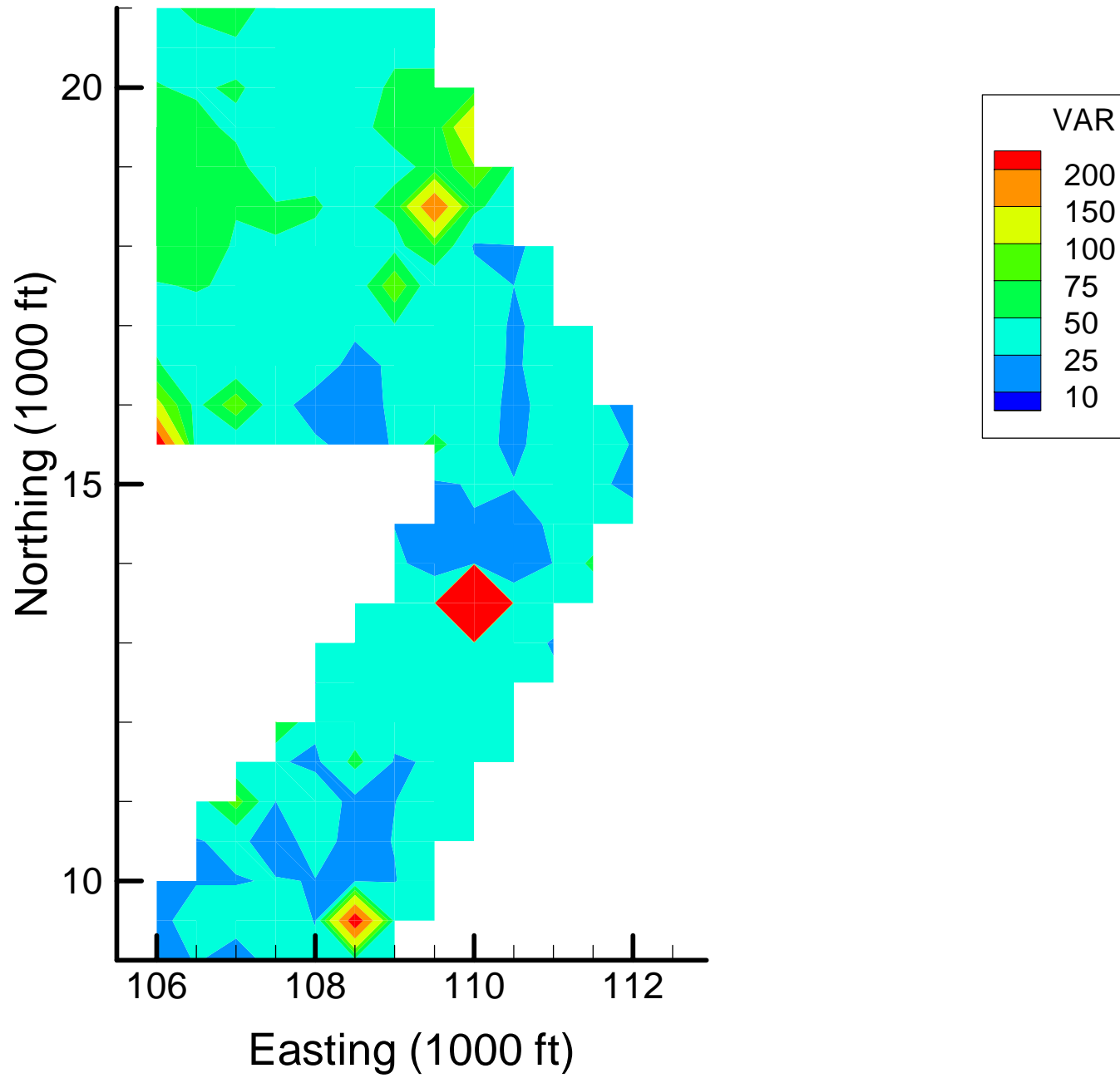
Site OU-12: FE Local Variances, 1999-2000, 10% Removal



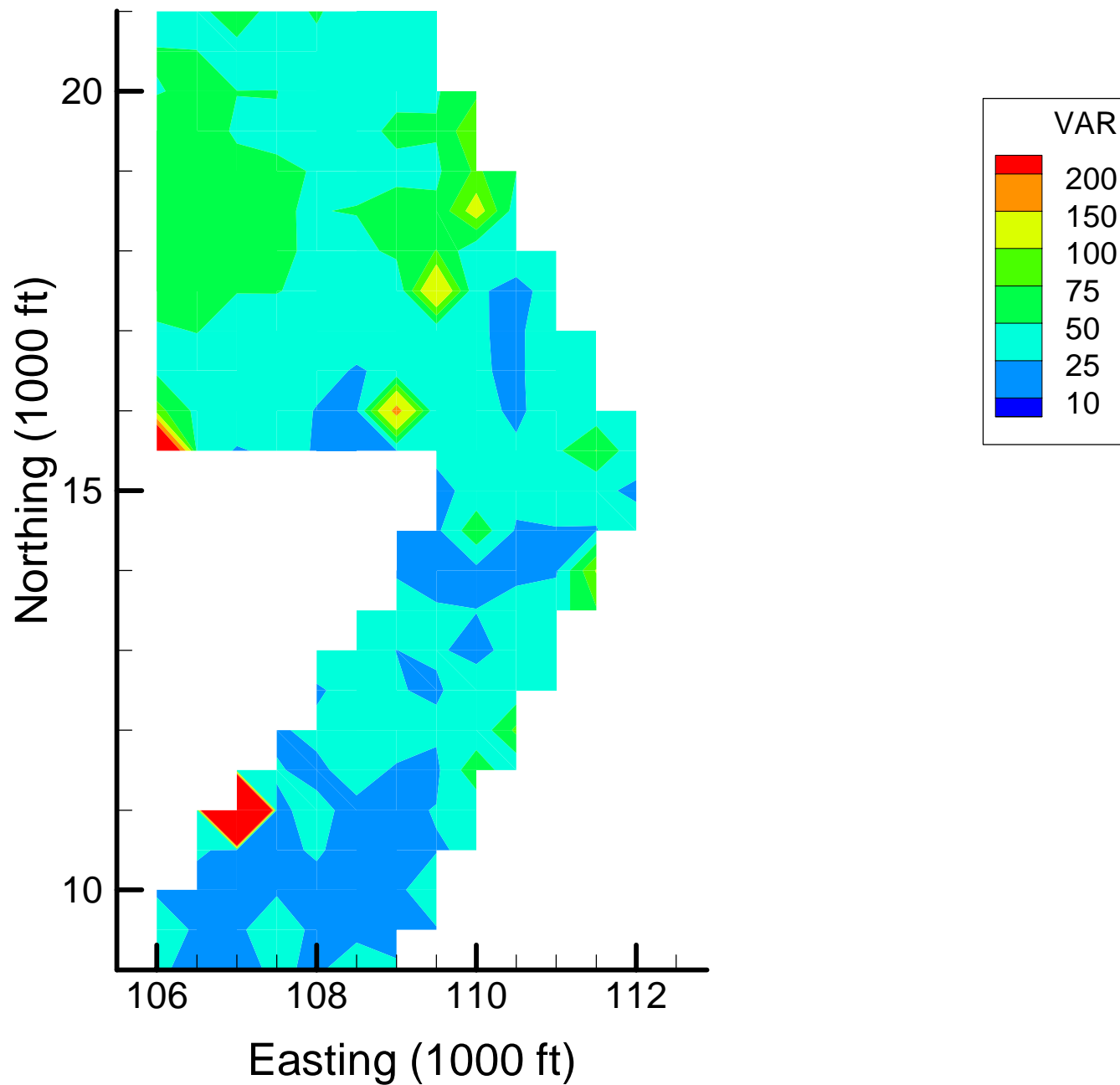
Site OU-12: FE Local Variances, 1999-2000, 20% Removal



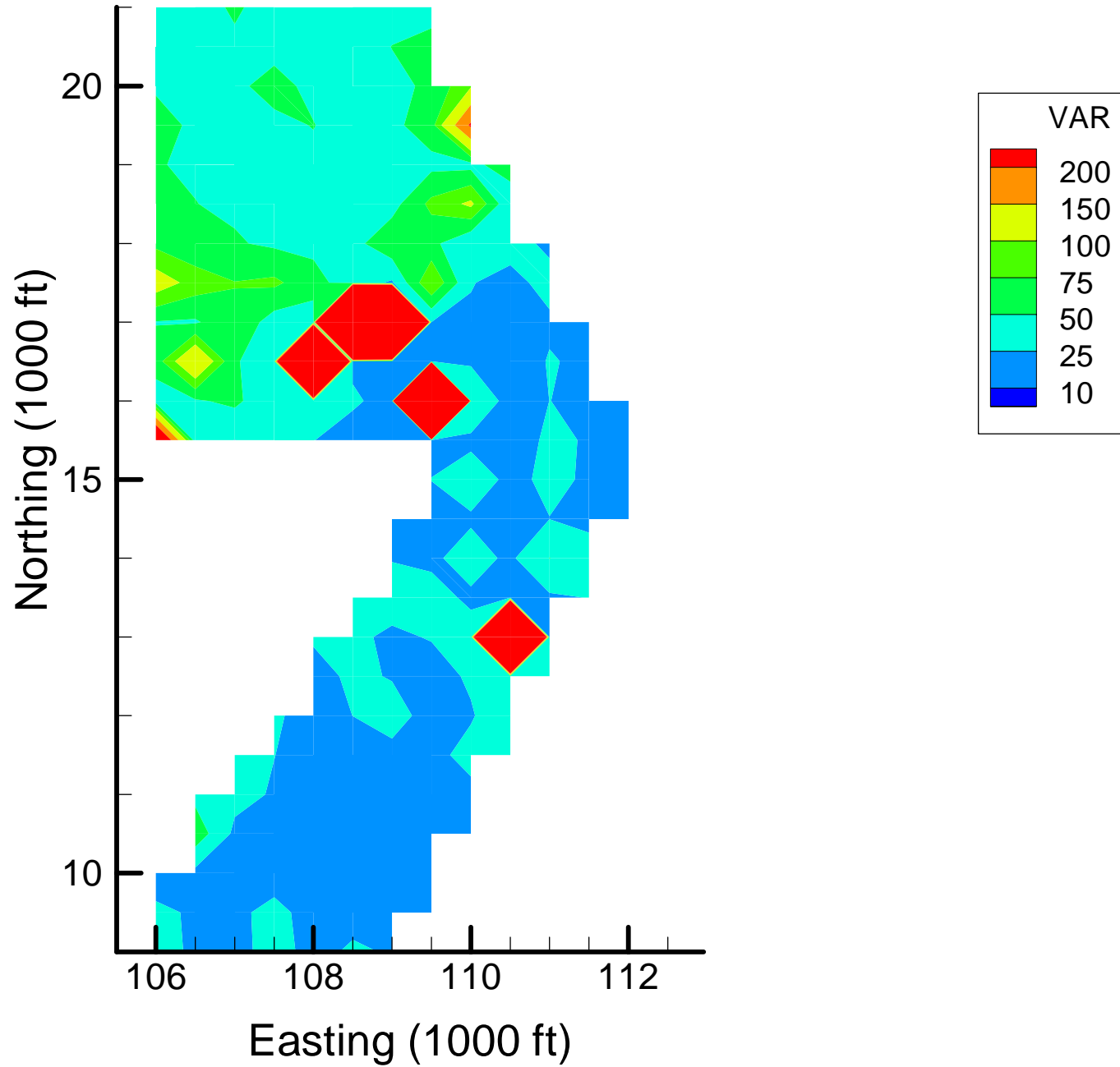
Site OU-12: FE Local Variances, 1999-2000, 30% Removal



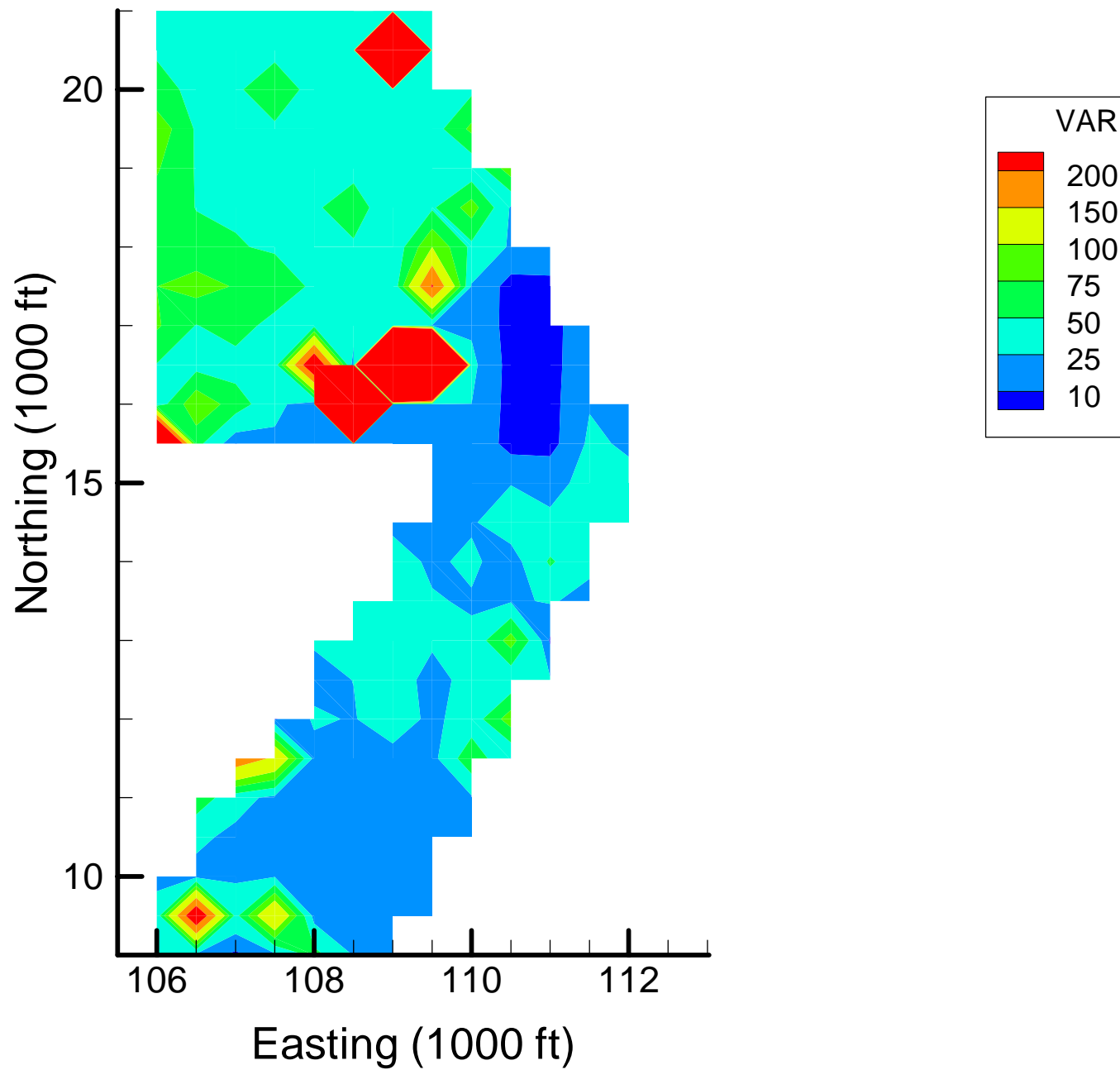
Site OU-12: FE Local Variances, 1999-2000, 40% Removal



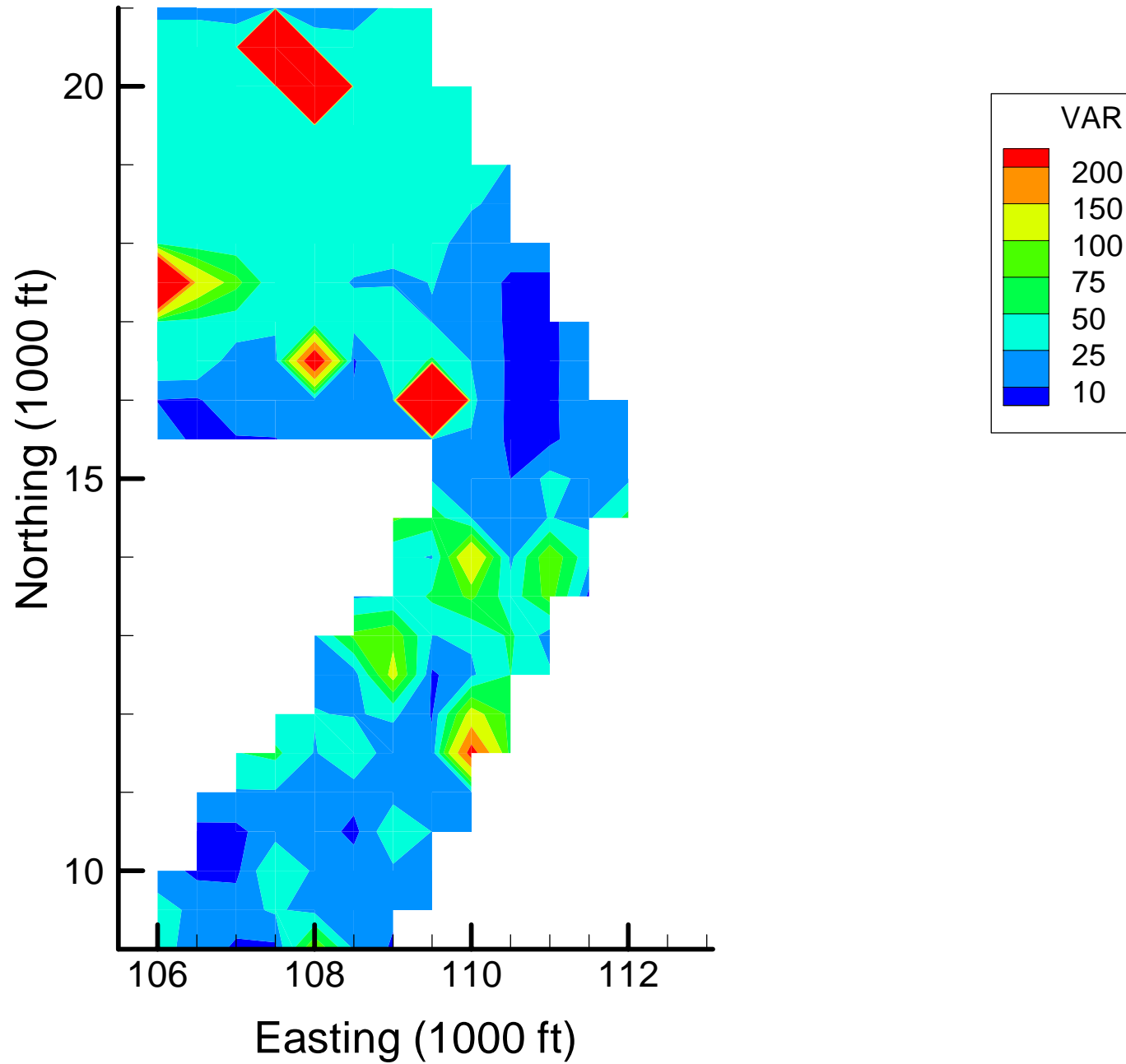
Site OU-12: FE Local Variances, 1999-2000, 50% Removal



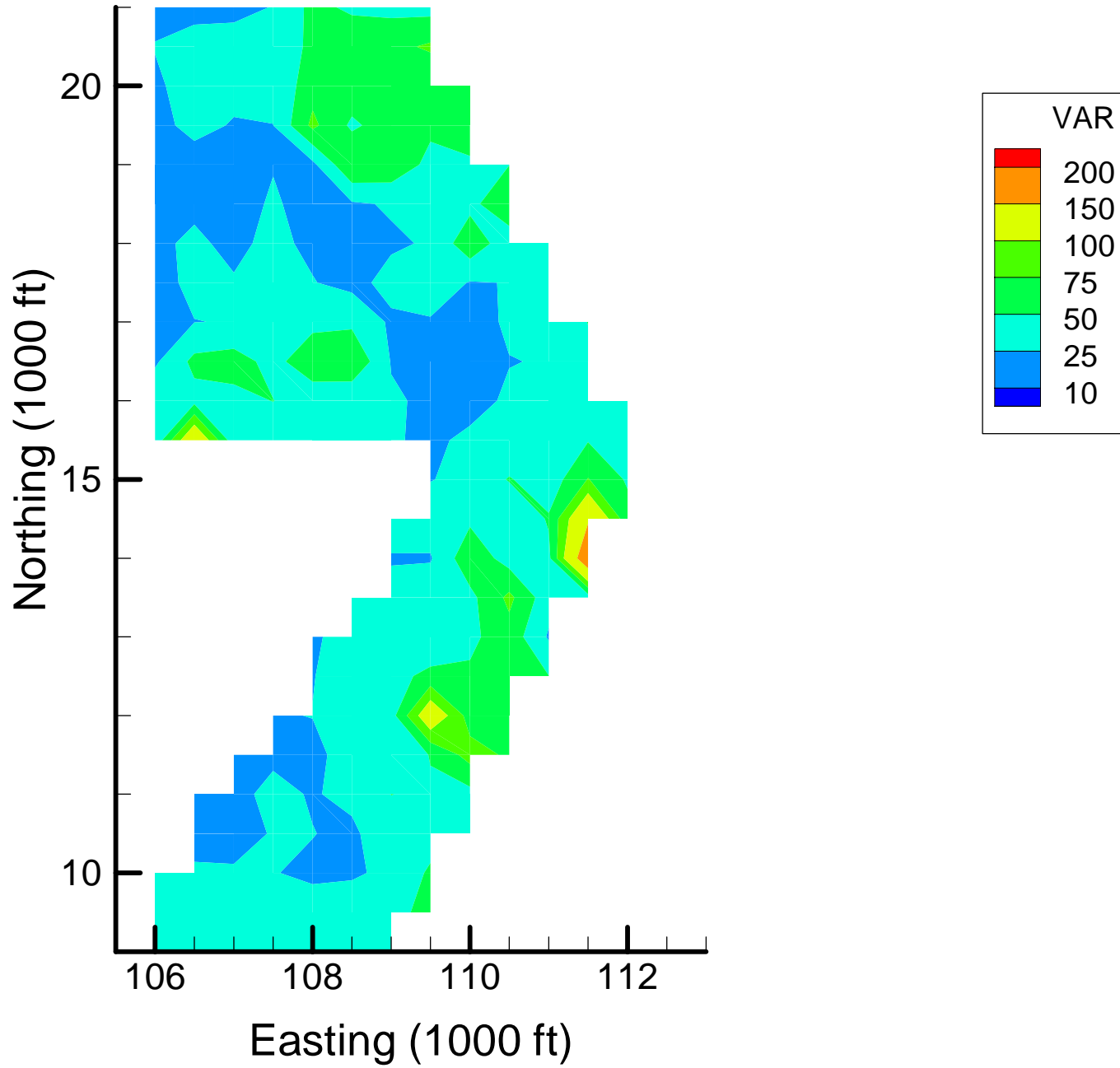
Site OU-12: FE Local Variances, 1999-2000, 60% Removal



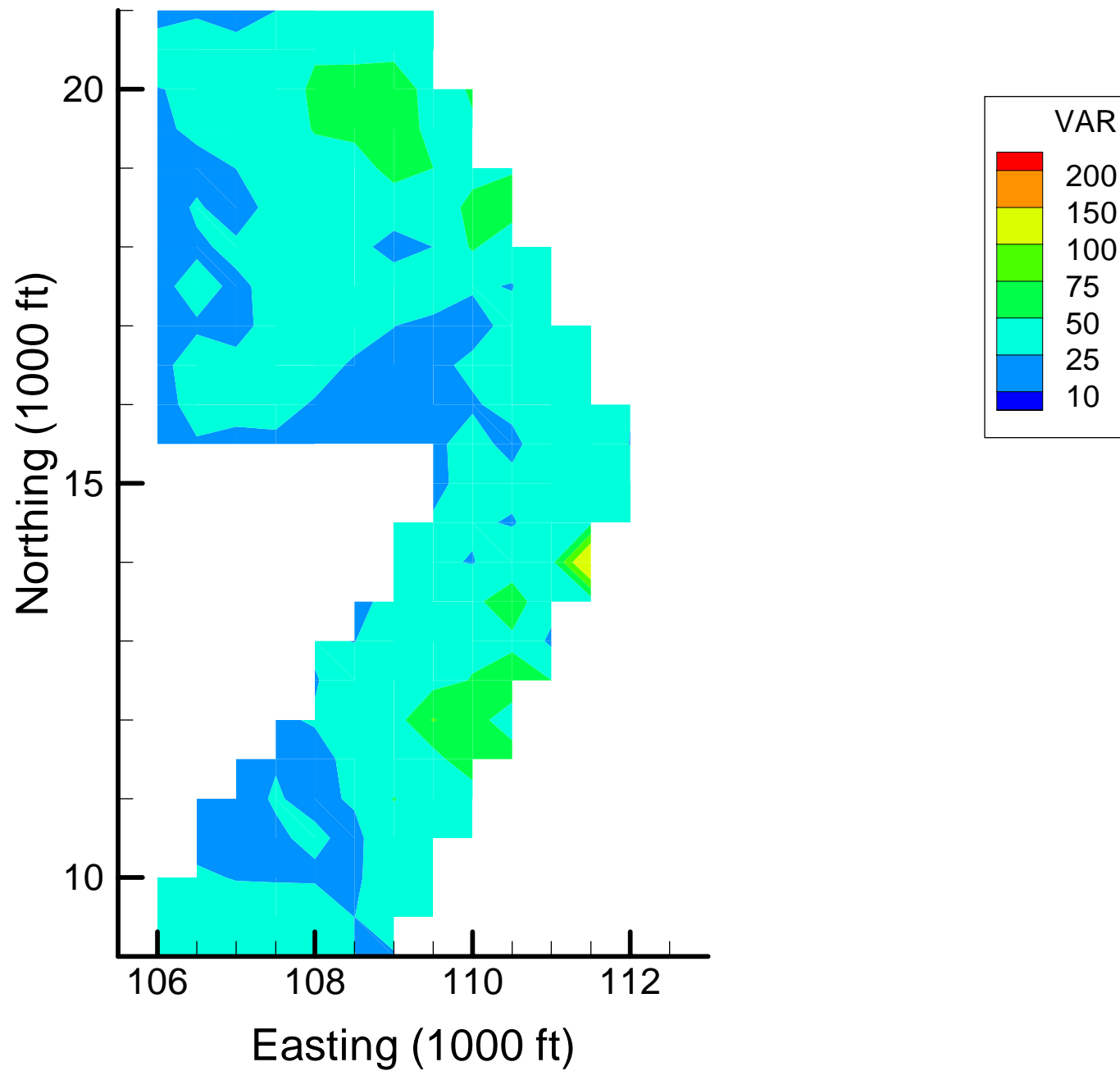
Site OU-12: FE Local Variances, 1999-2000, 70% Removal



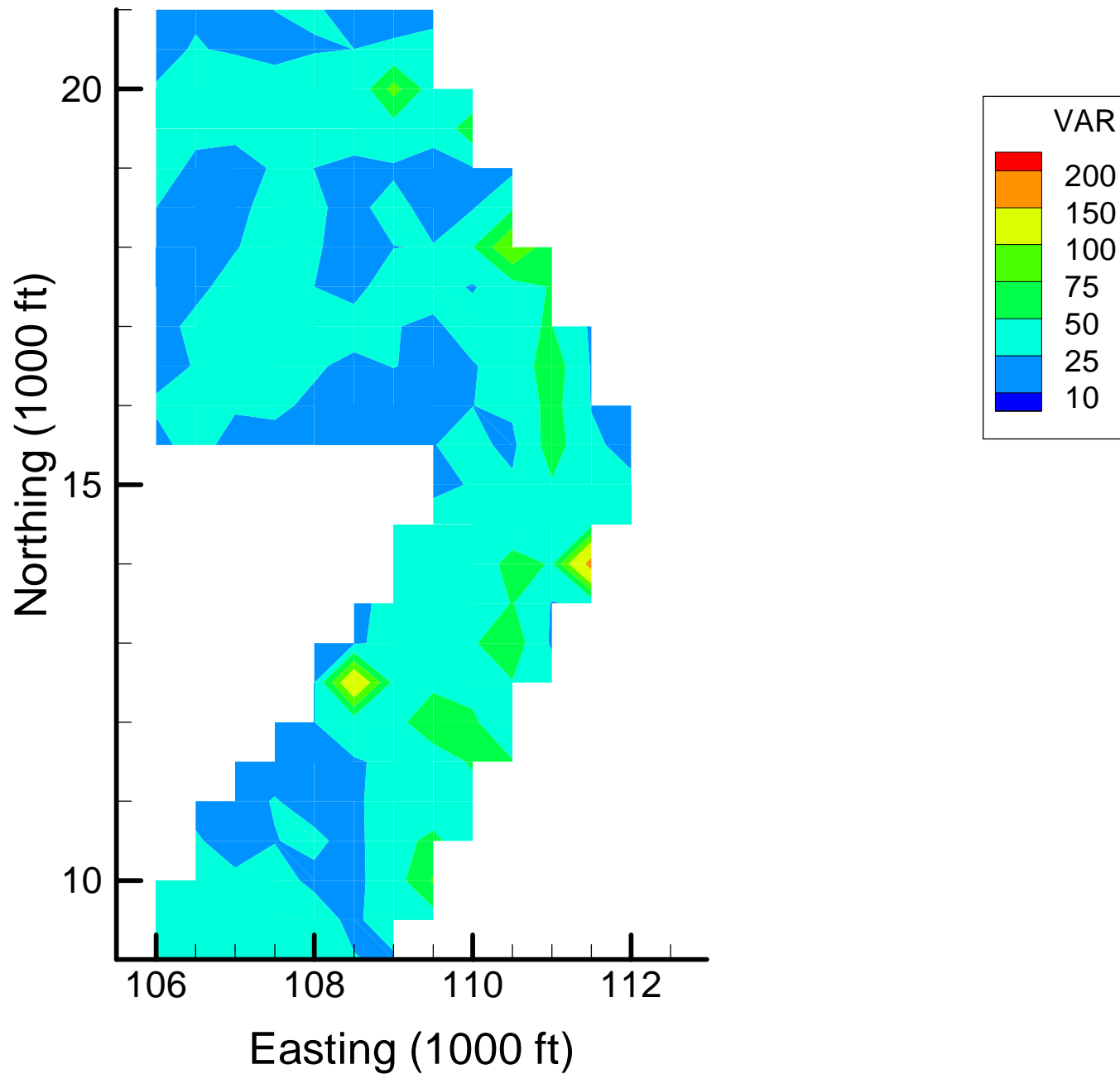
Site OU-12: FE Local Variances, 2001-2002, Base Map



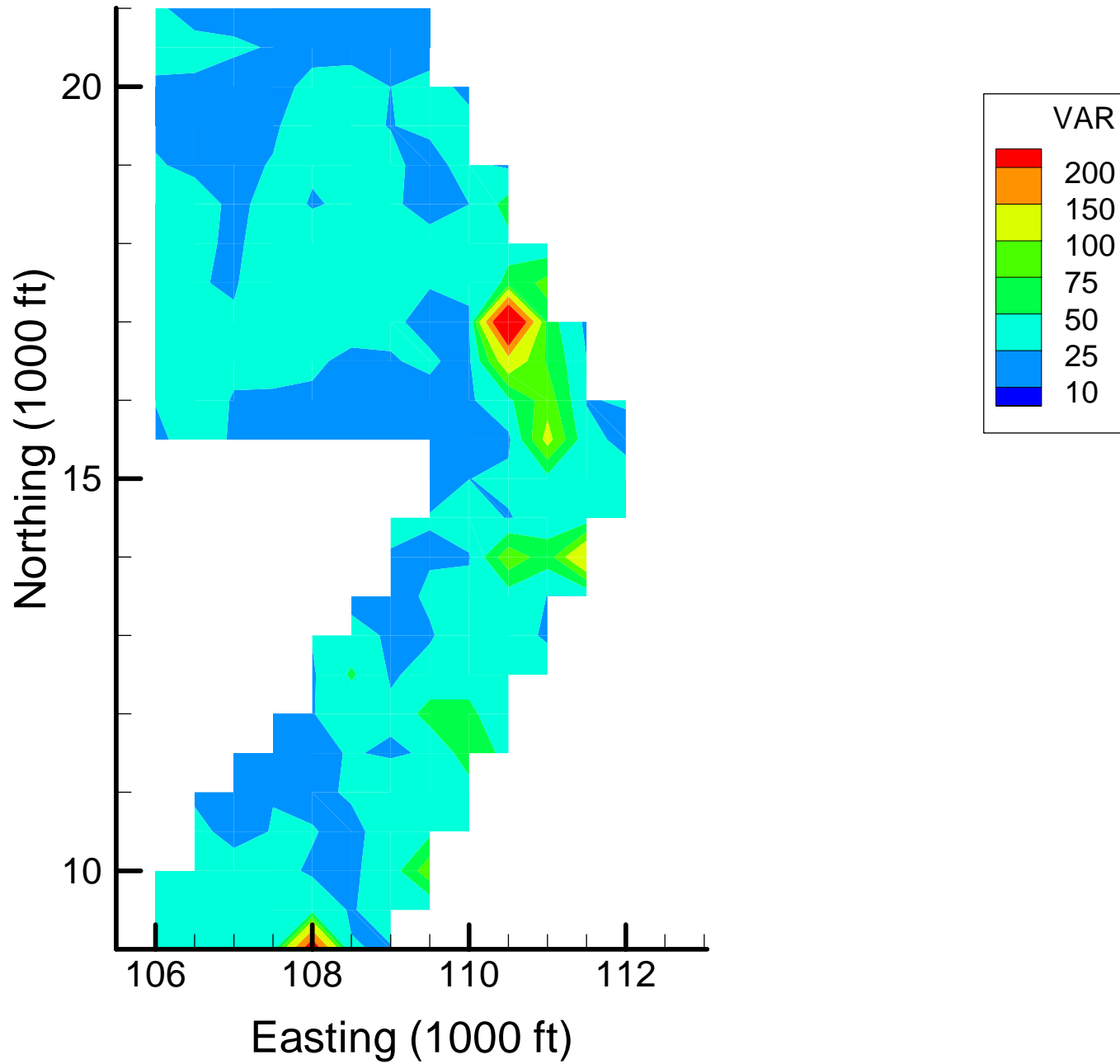
Site OU-12: FE Local Variances, 2001-2002, 10% Removal



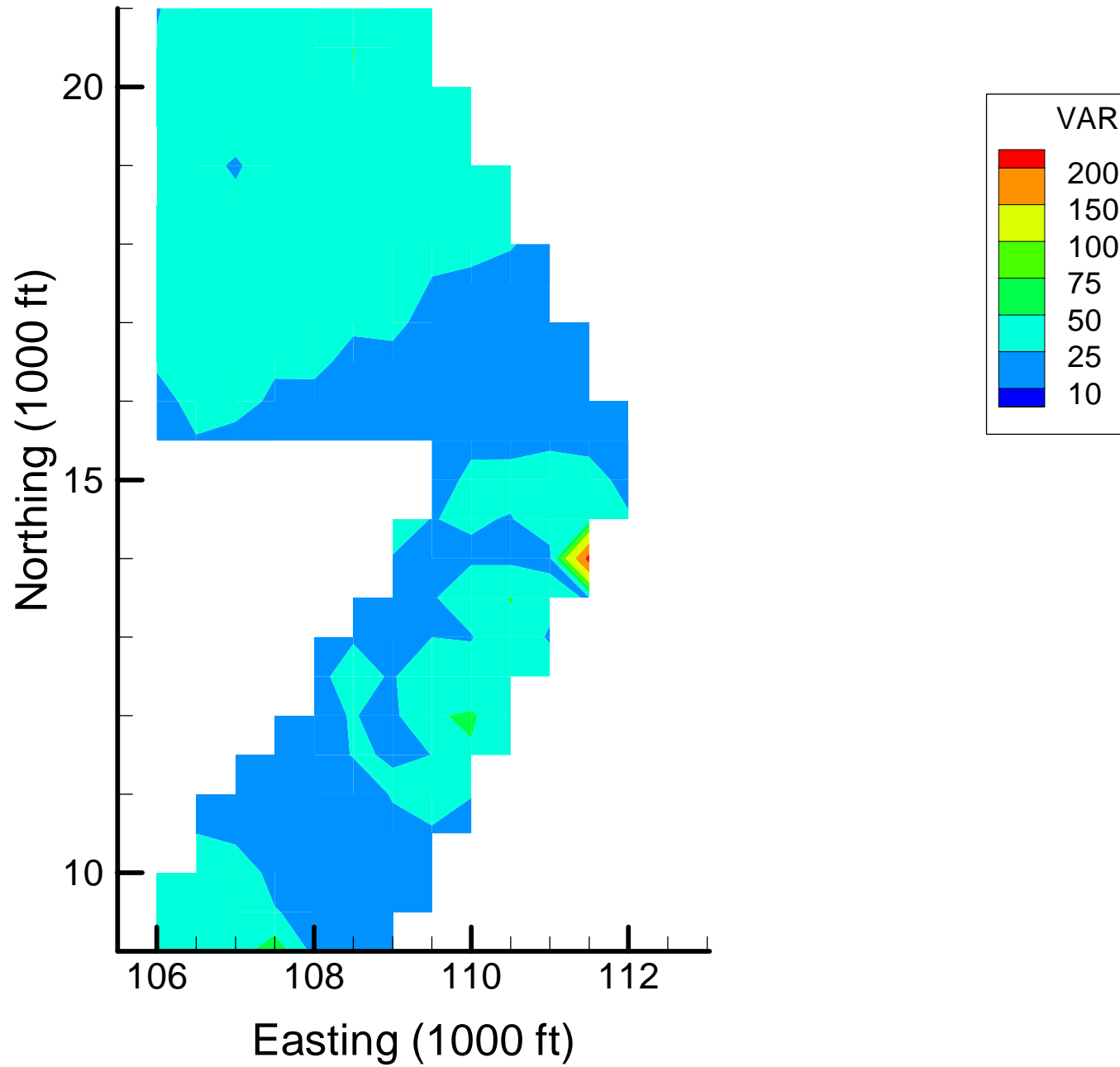
Site OU-12: FE Local Variances, 2001-2002, 20% Removal



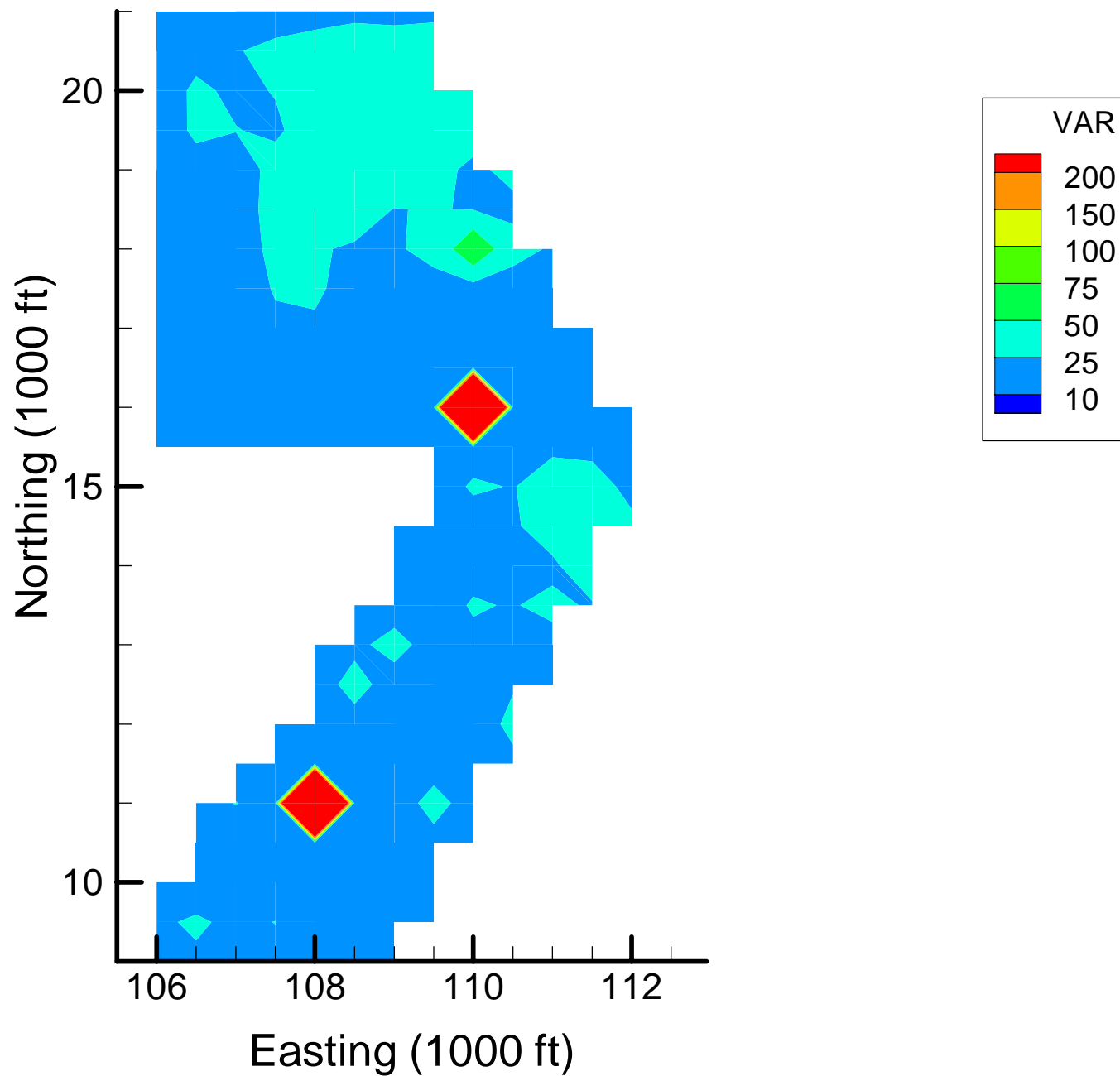
Site OU-12: FE Local Variances, 2001-2002, 30% Removal



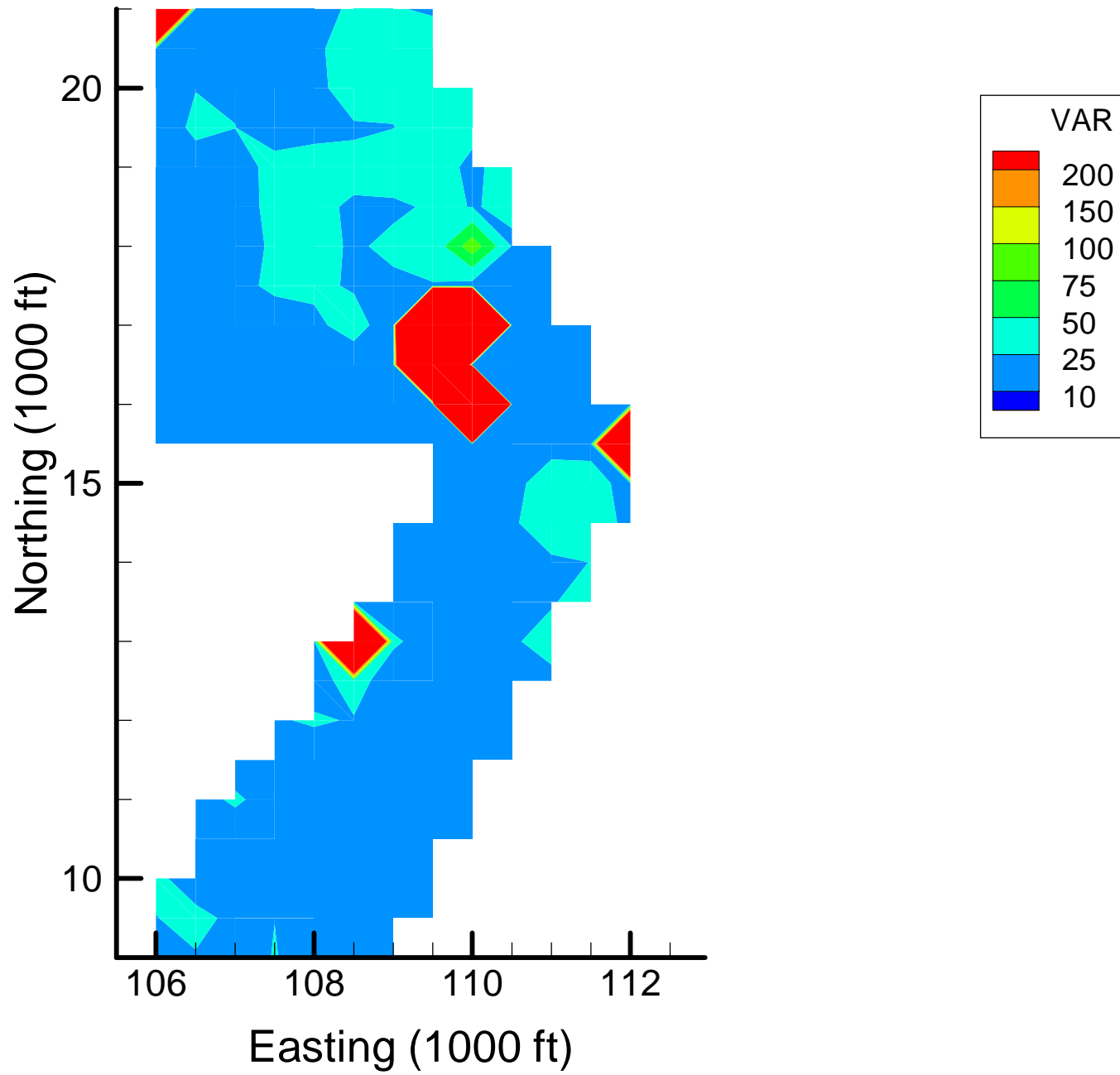
Site OU-12: FE Local Variances, 2001-2002, 40% Removal



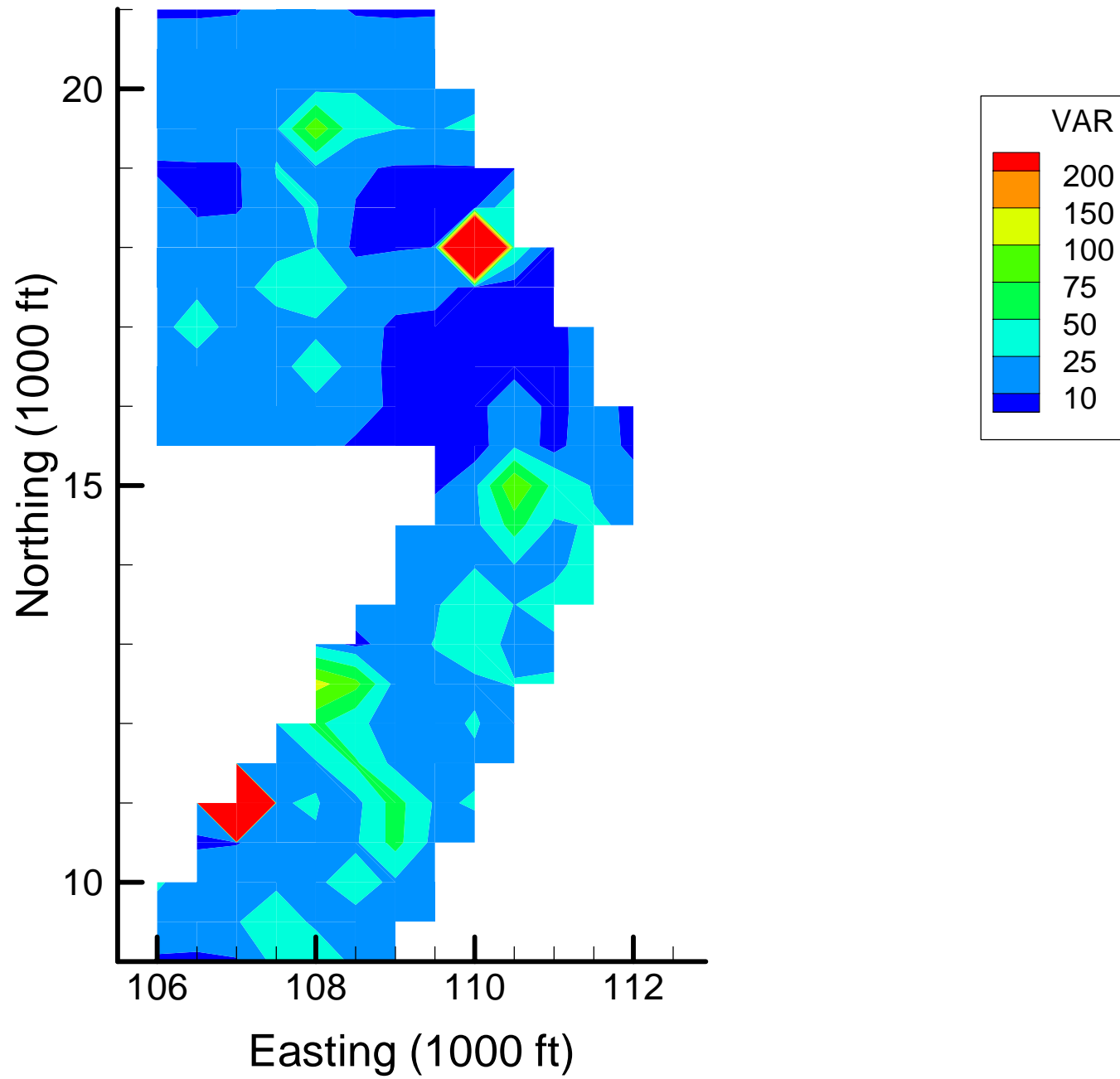
Site OU-12: FE Local Variances, 2001-2002, 50% Removal



Site OU-12: FE Local Variances, 2001-2002, 60% Removal



Site OU-12: FE Local Variances, 2001-2002, 70% Removal



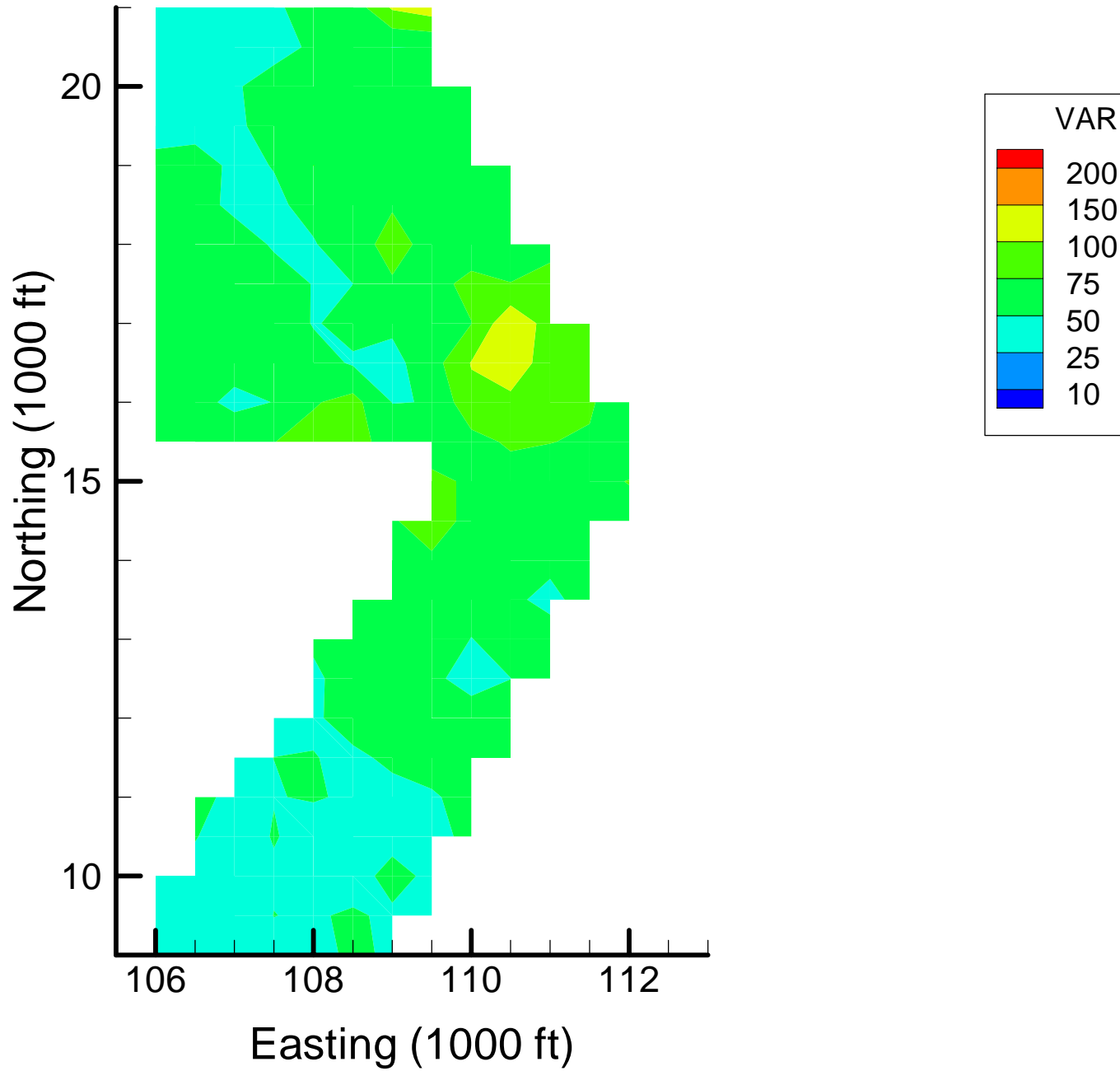
Appendix 4-3

Spatial Optimization: MN Local Variance Maps

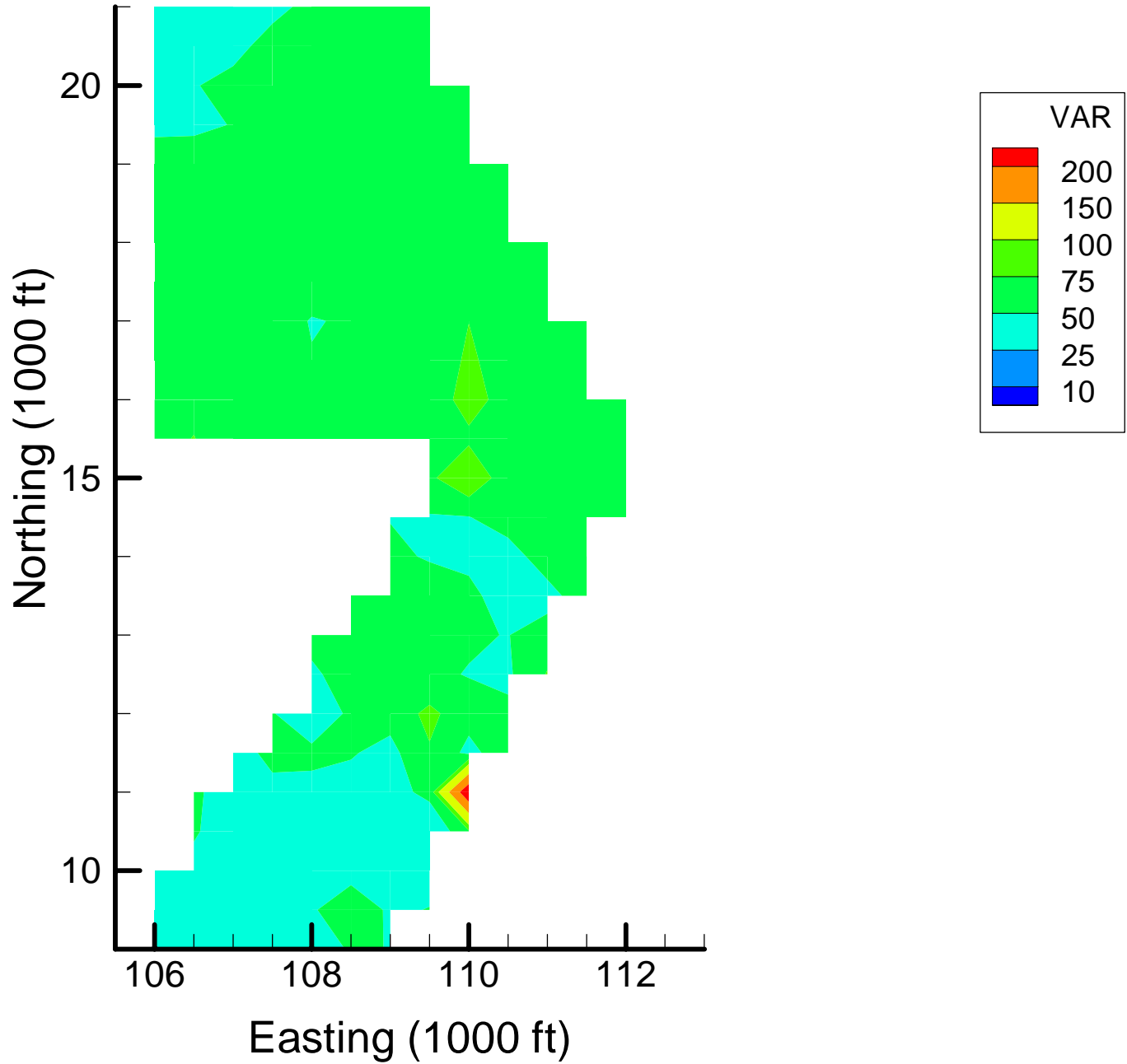
Notes:

VAR = Voxel-specific local variance estimates (averaged over depth, in ppb)

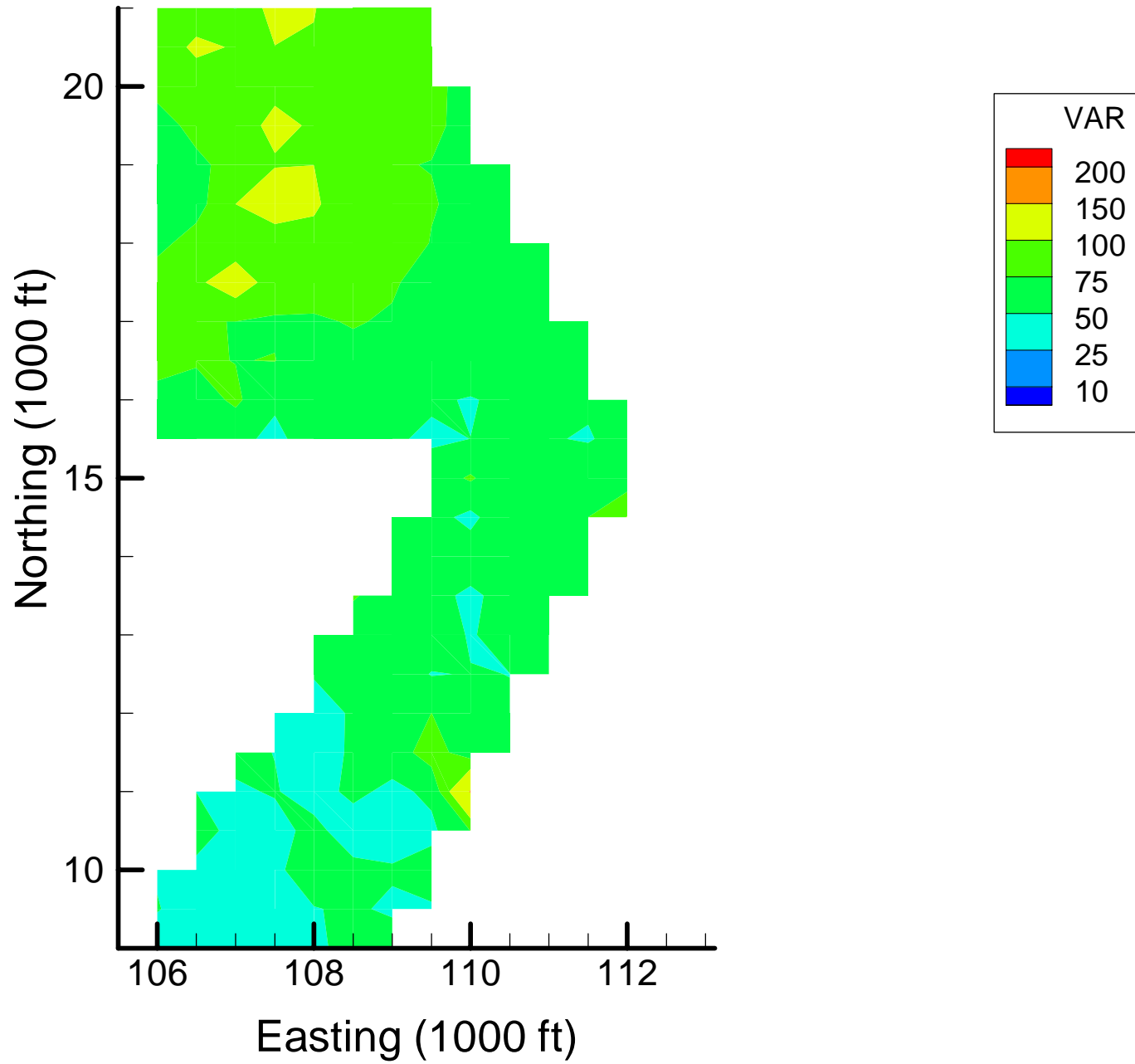
Site OU-12: MN Local Variances, 1999-2000, Base Map



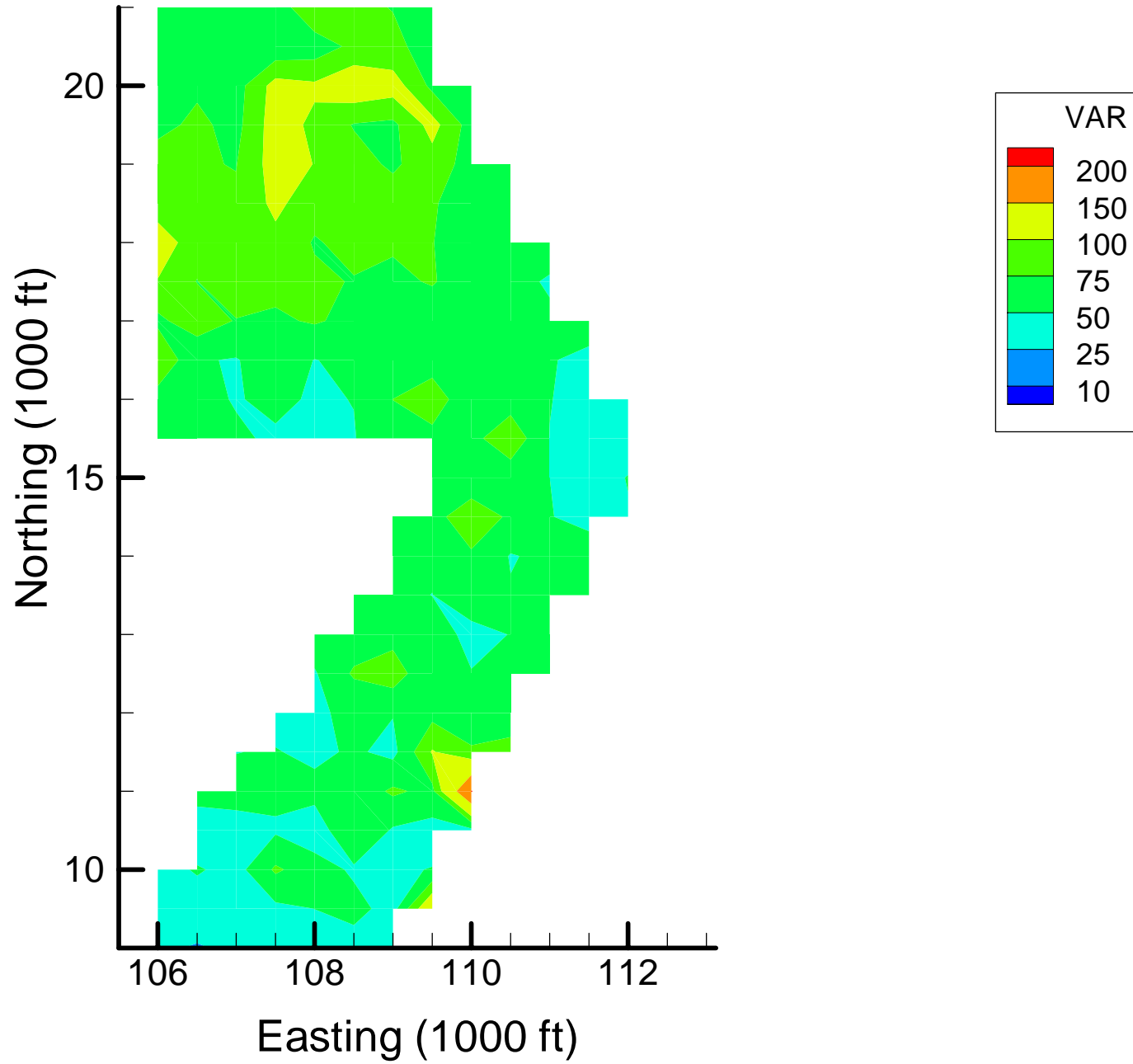
Site OU-12: MN Local Variances, 1999-2000, 10% Removal



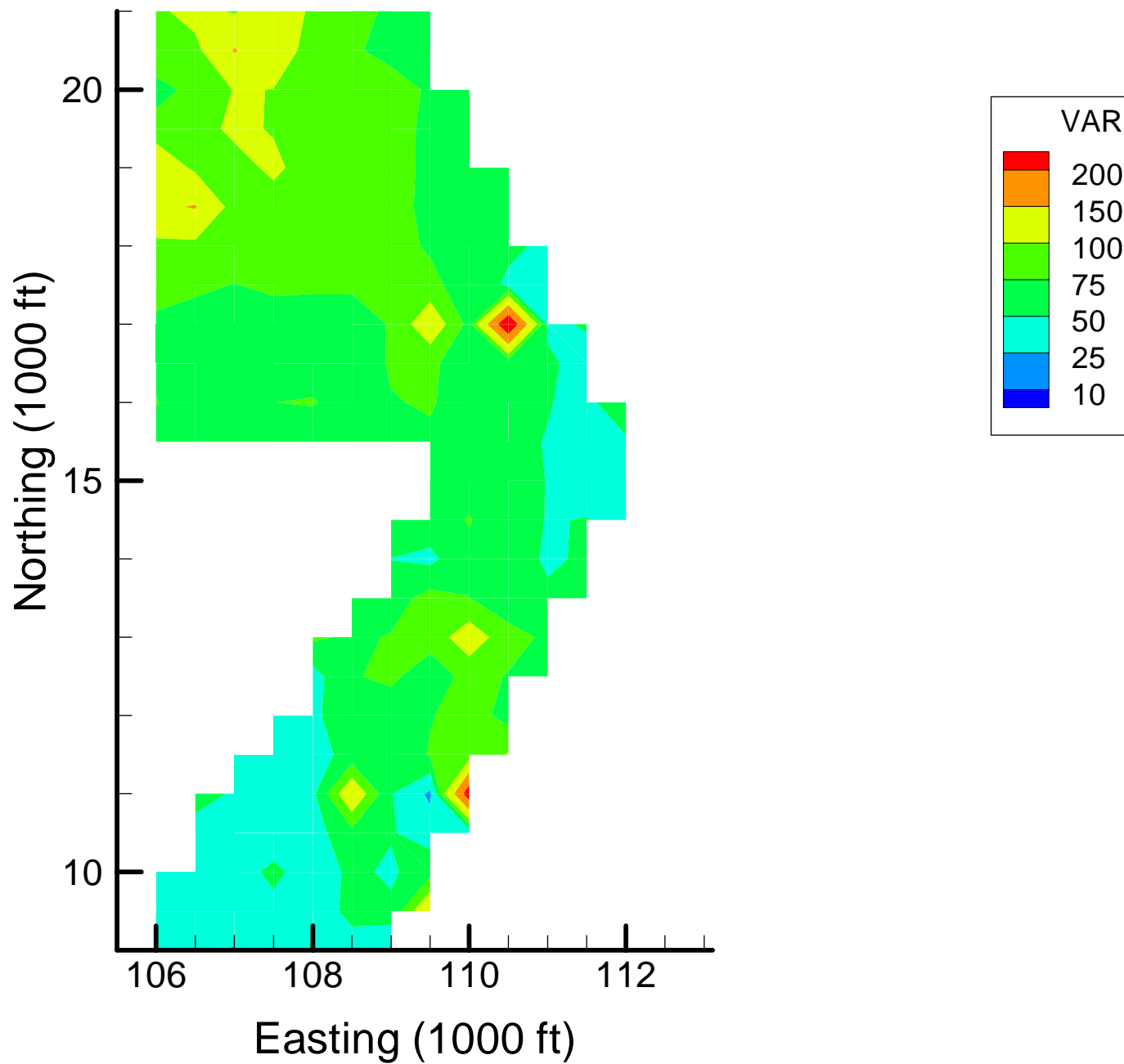
Site OU-12: MN Local Variances, 1999-2000, 20% Removal



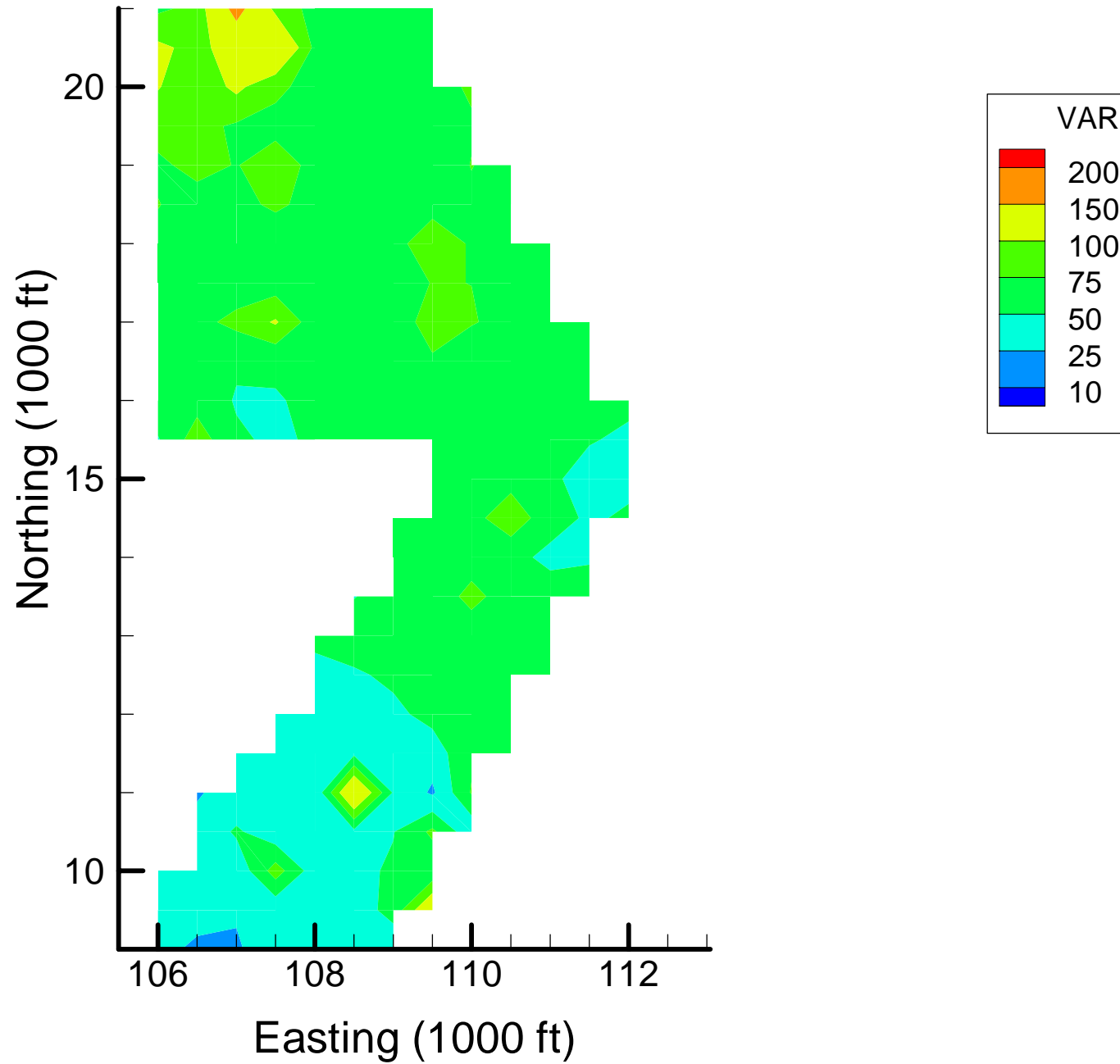
Site OU-12: MN Local Variances, 1999-2000, 30% Removal



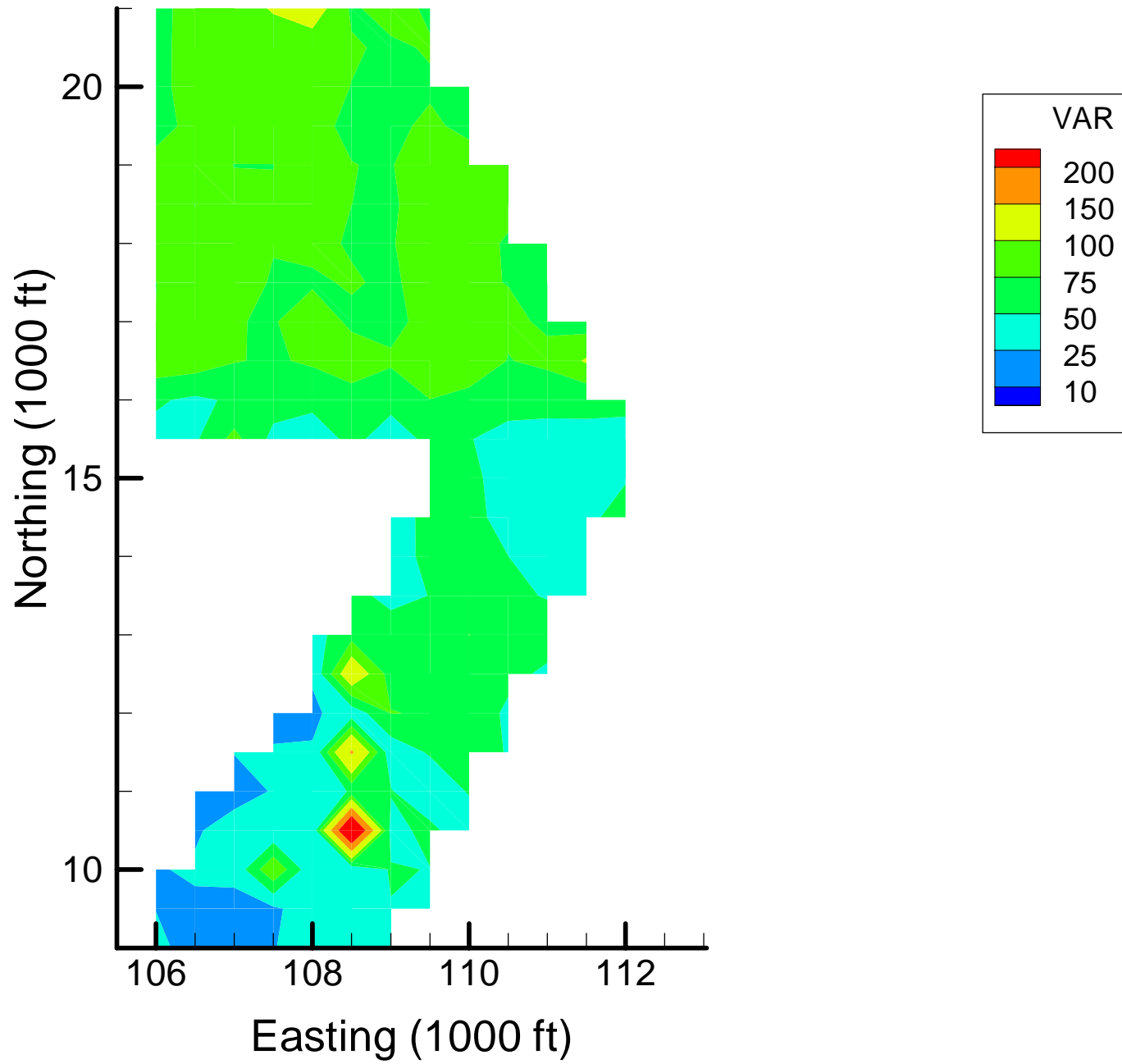
Site OU-12: MN Local Variances, 1999-2000, 40% Removal



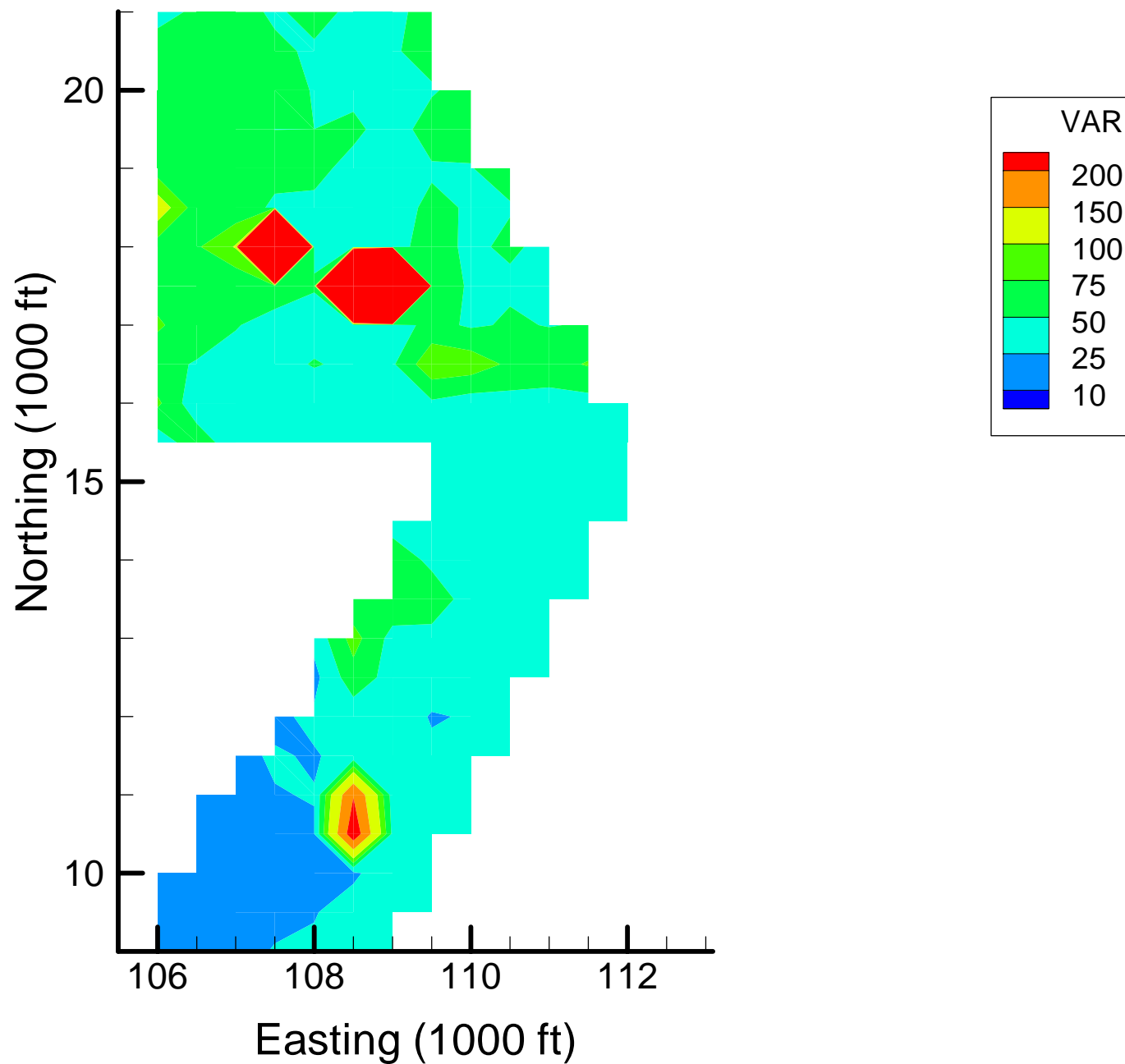
Site OU-12: MN Local Variances, 1999-2000, 50% Removal



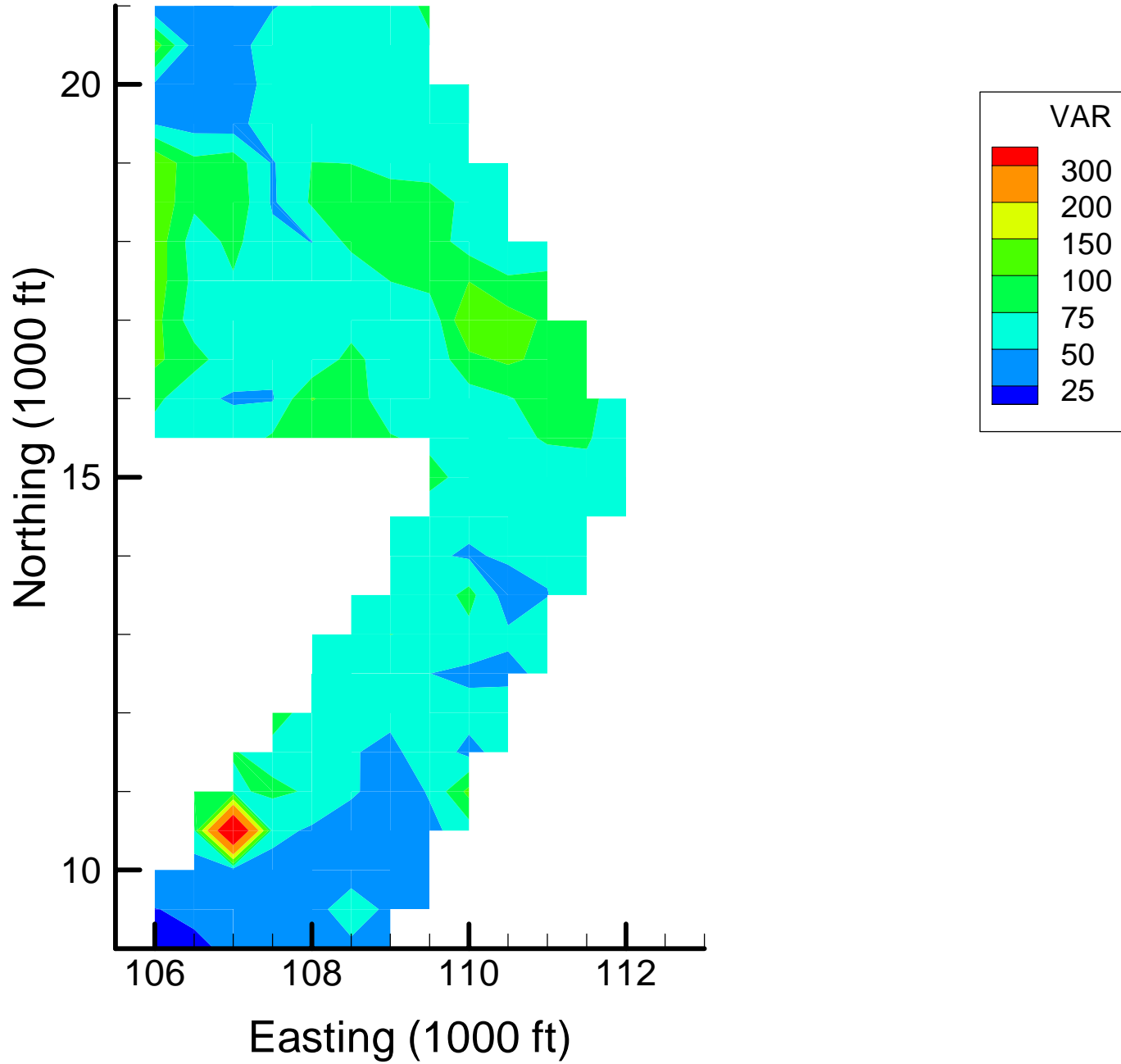
Site OU-12: MN Local Variances, 1999-2000, 60% Removal



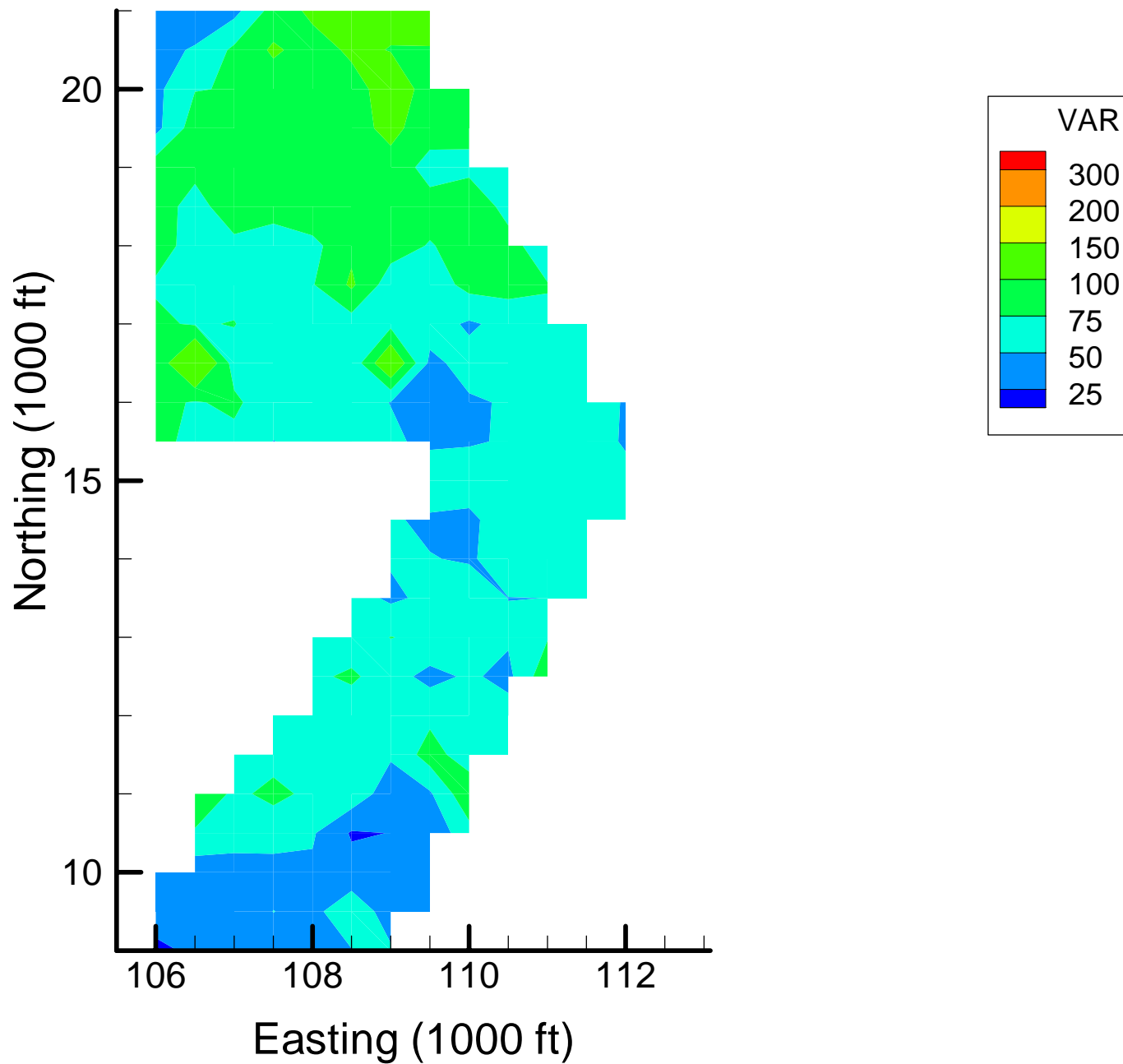
Site OU-12: MN Local Variances, 1999-2000, 70% Removal



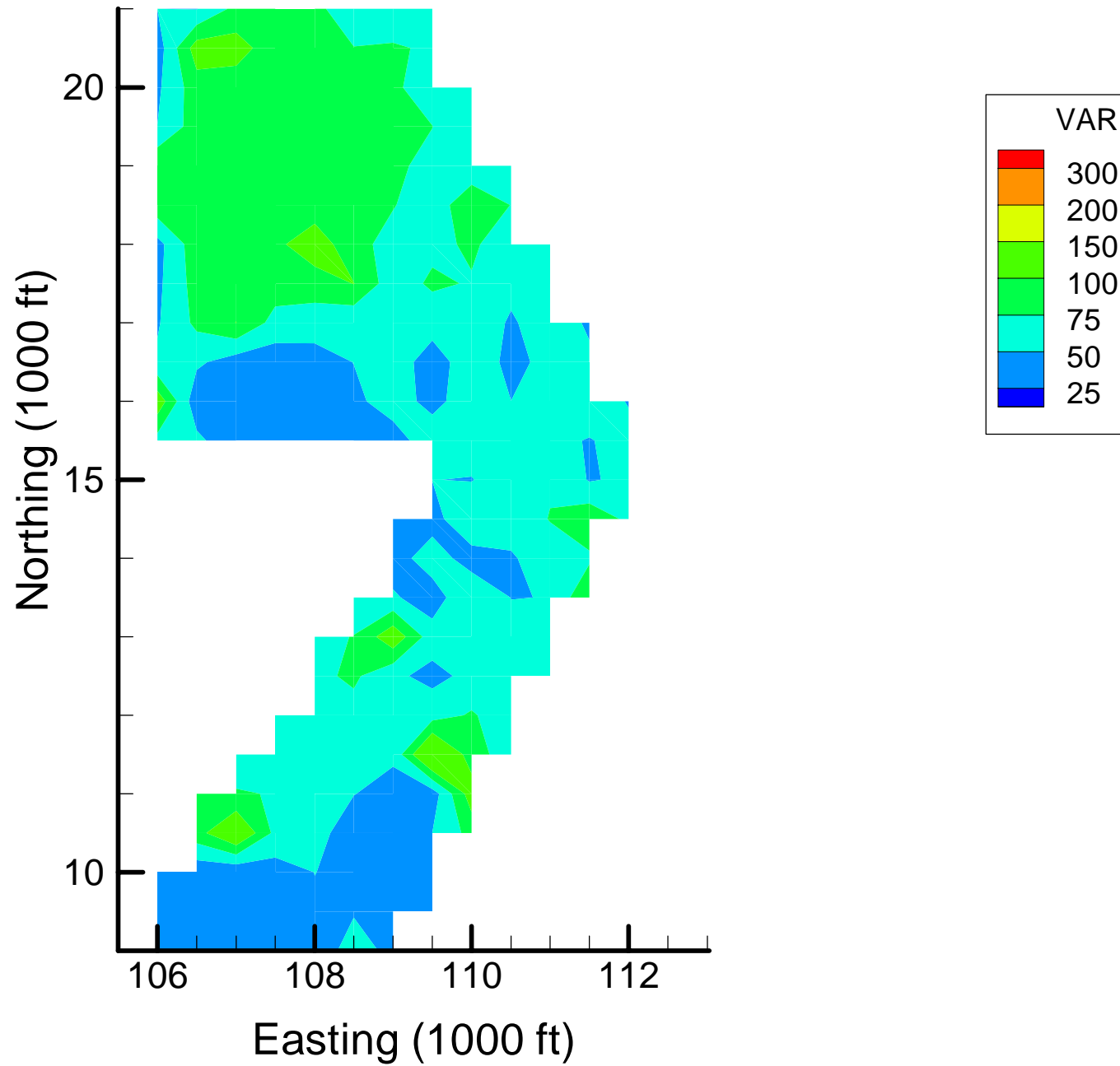
Site OU-12: MN Local Variances, 2001-2002, Base Map



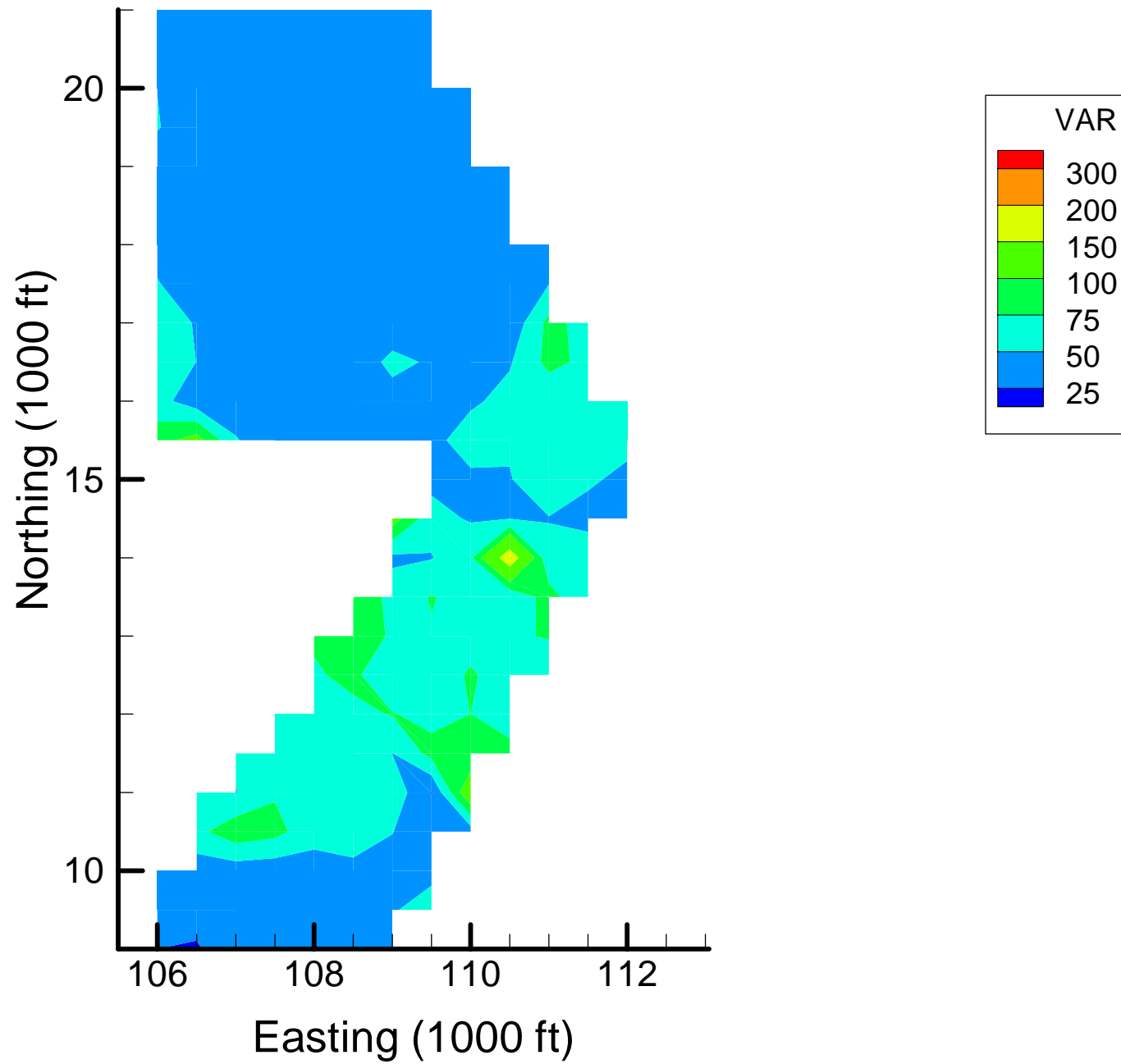
Site OU-12: MN Local Variances, 2001-2002, 10% Removal



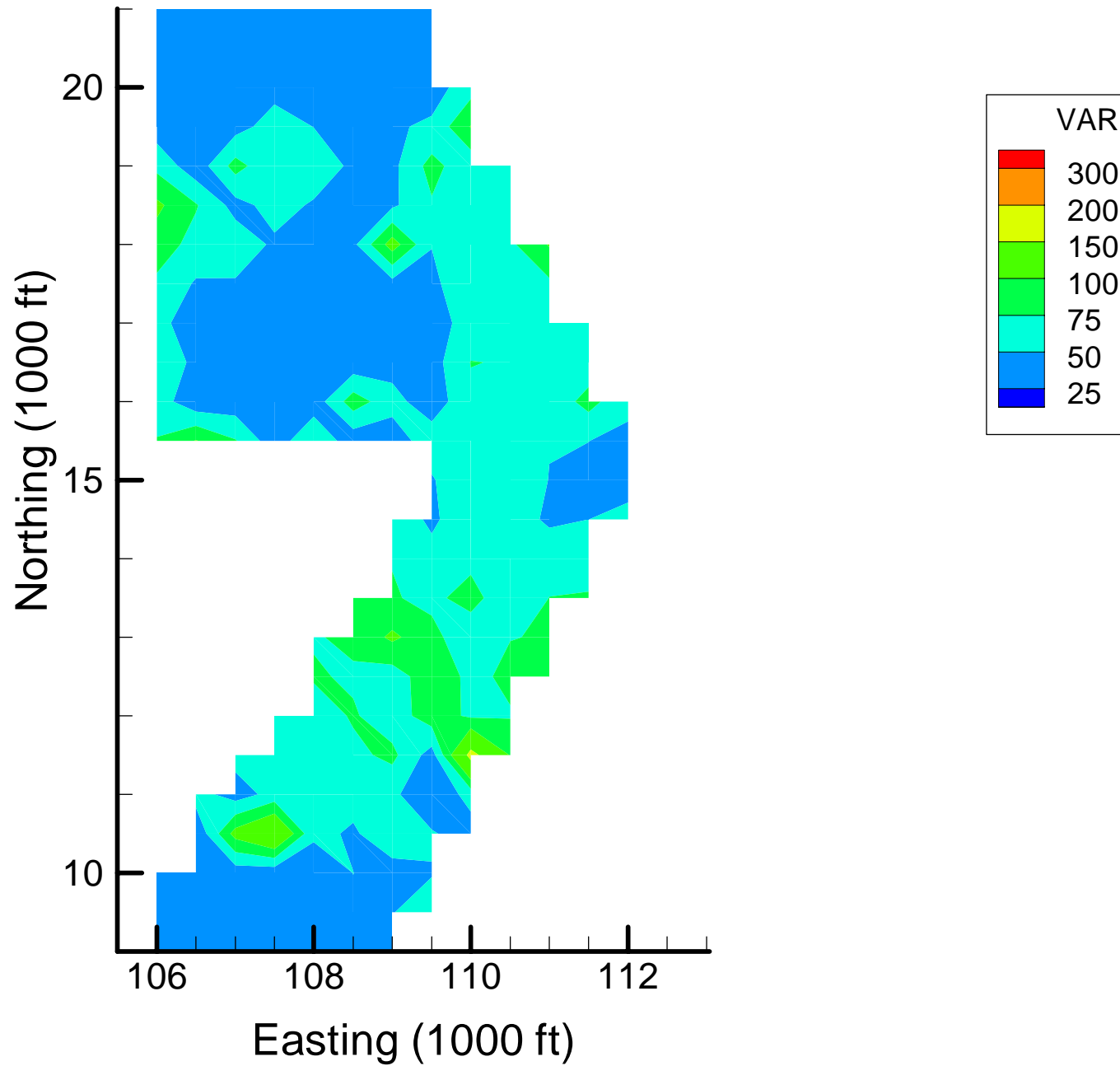
Site OU-12: MN Local Variances, 2001-2002, 20% Removal



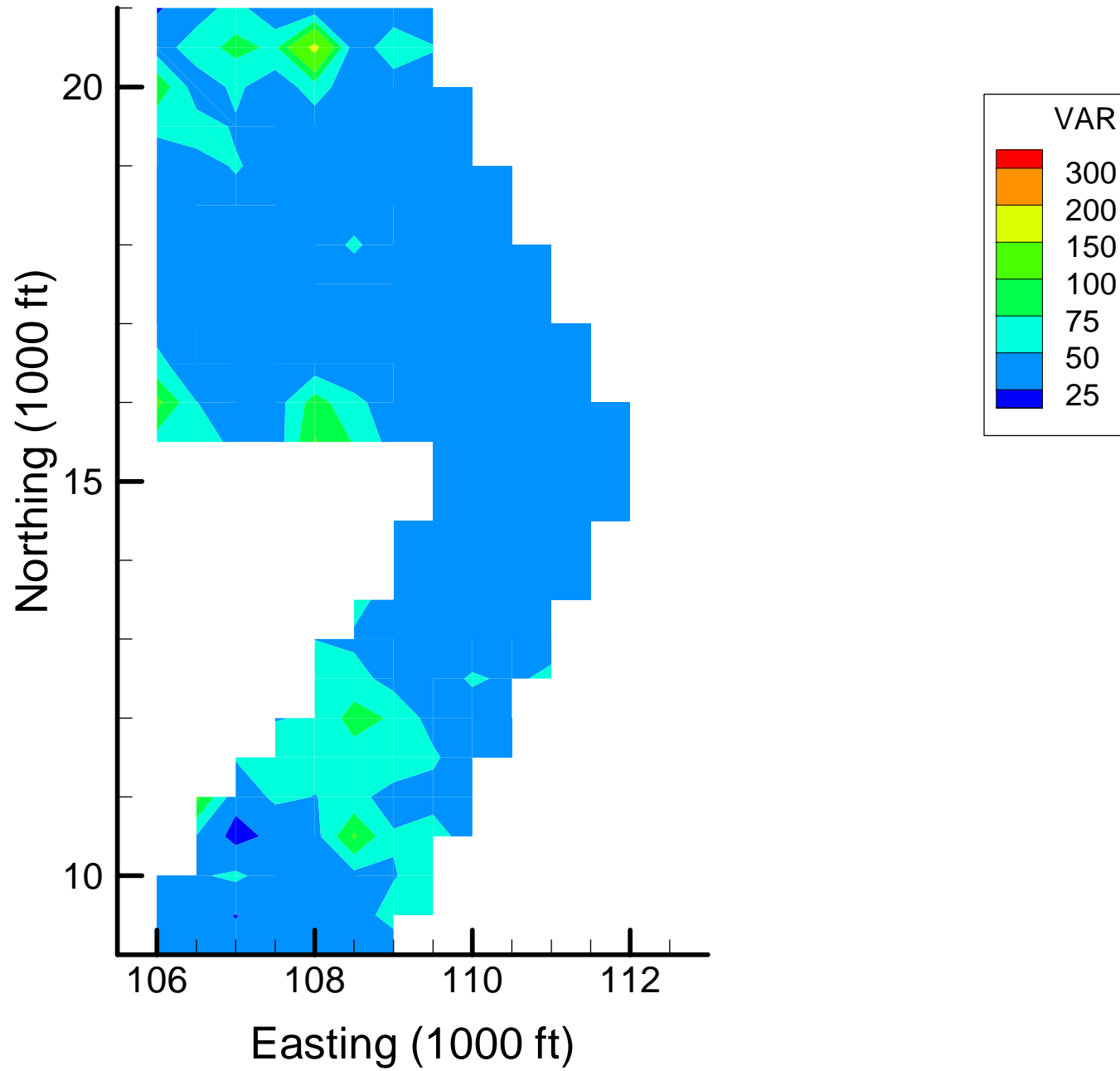
Site OU-12: MN Local Variances, 2001-2002, 30% Removal



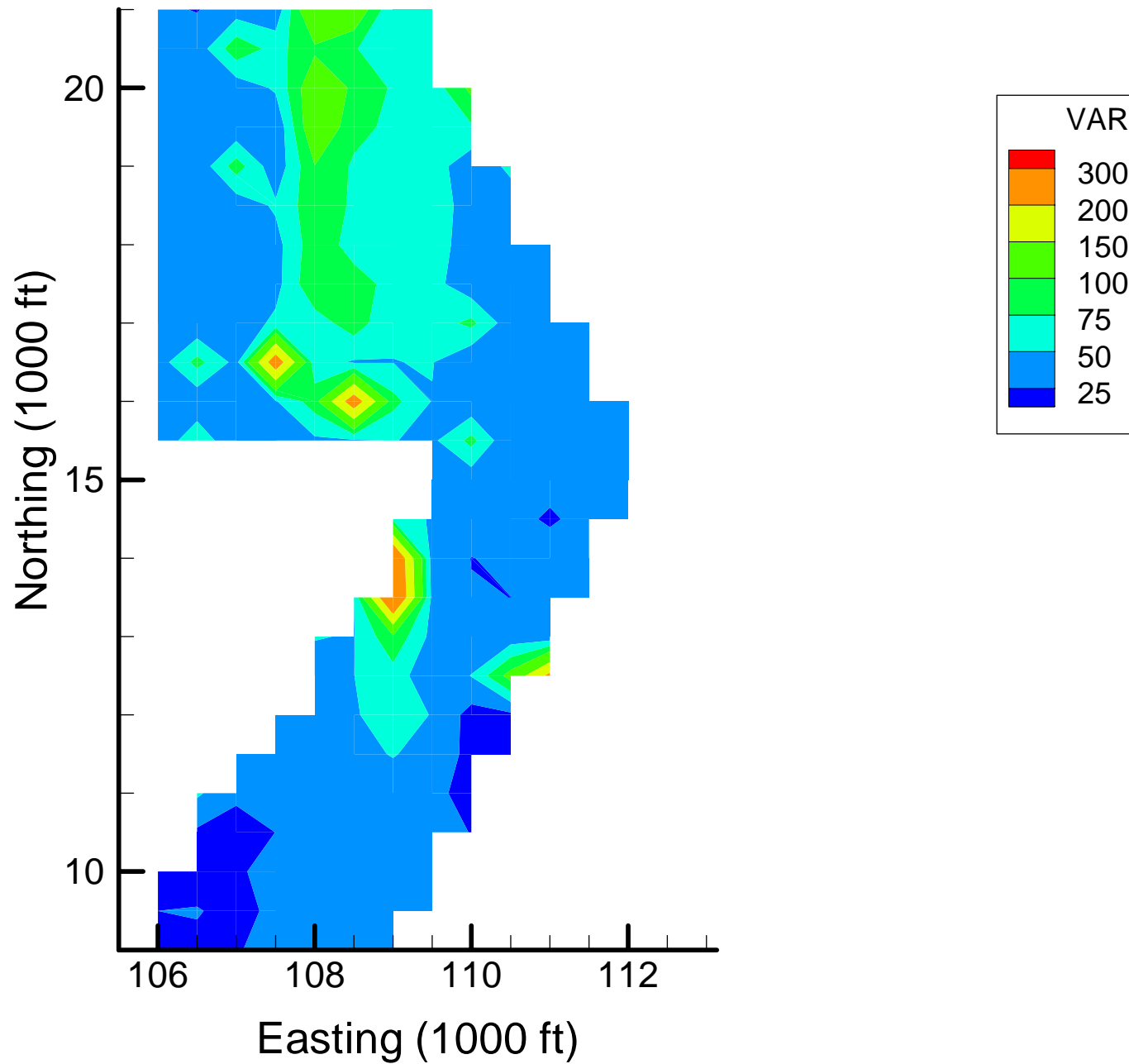
Site OU-12: MN Local Variances, 2001-2002, 40% Removal



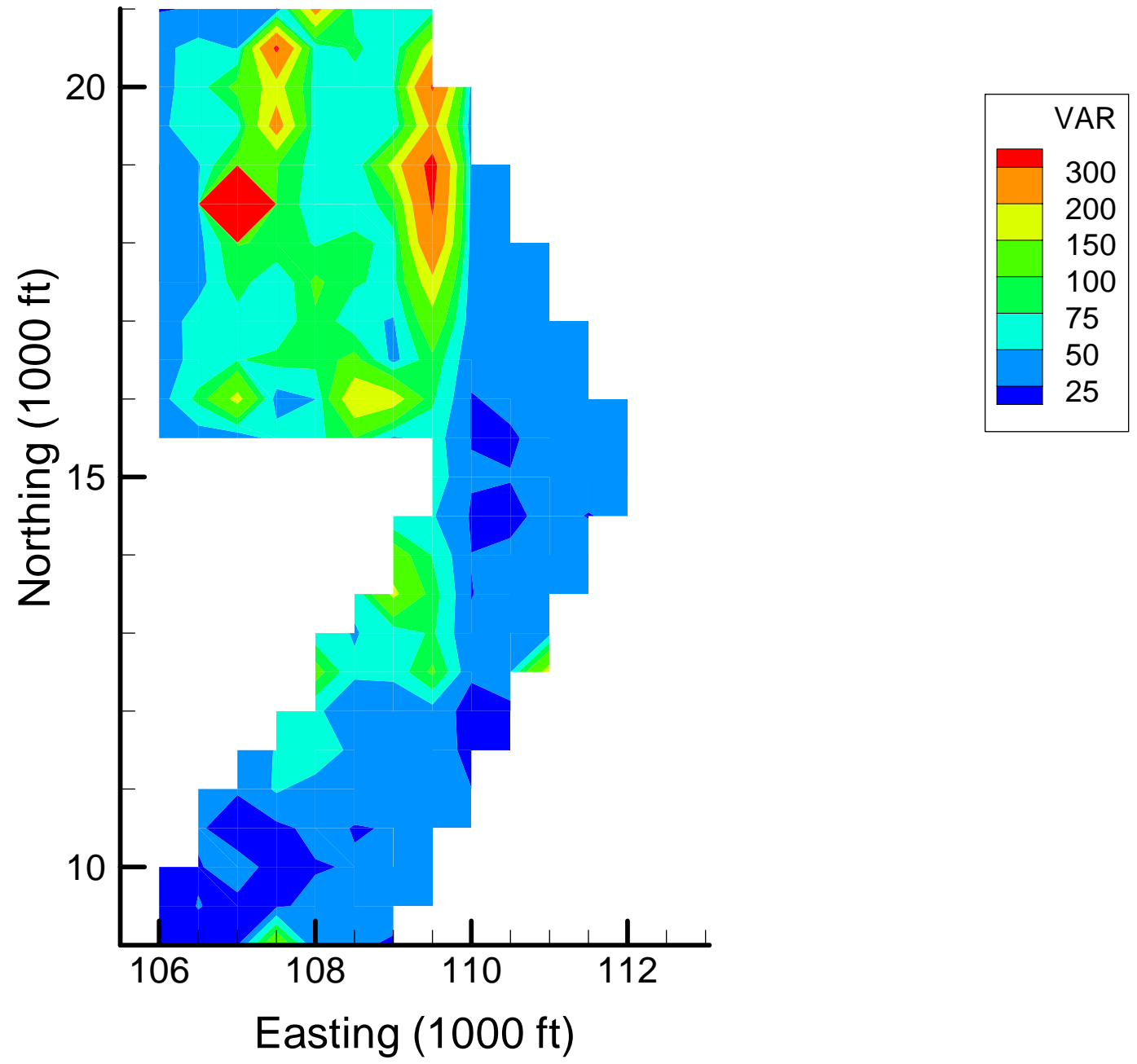
Site OU-12: MN Local Variances, 2001-2002, 50% Removal



Site OU-12: MN Local Variances, 2001-2002, 60% Removal



Site OU-12: MN Local Variances, 2001-2002, 70% Removal



Appendix 4-4

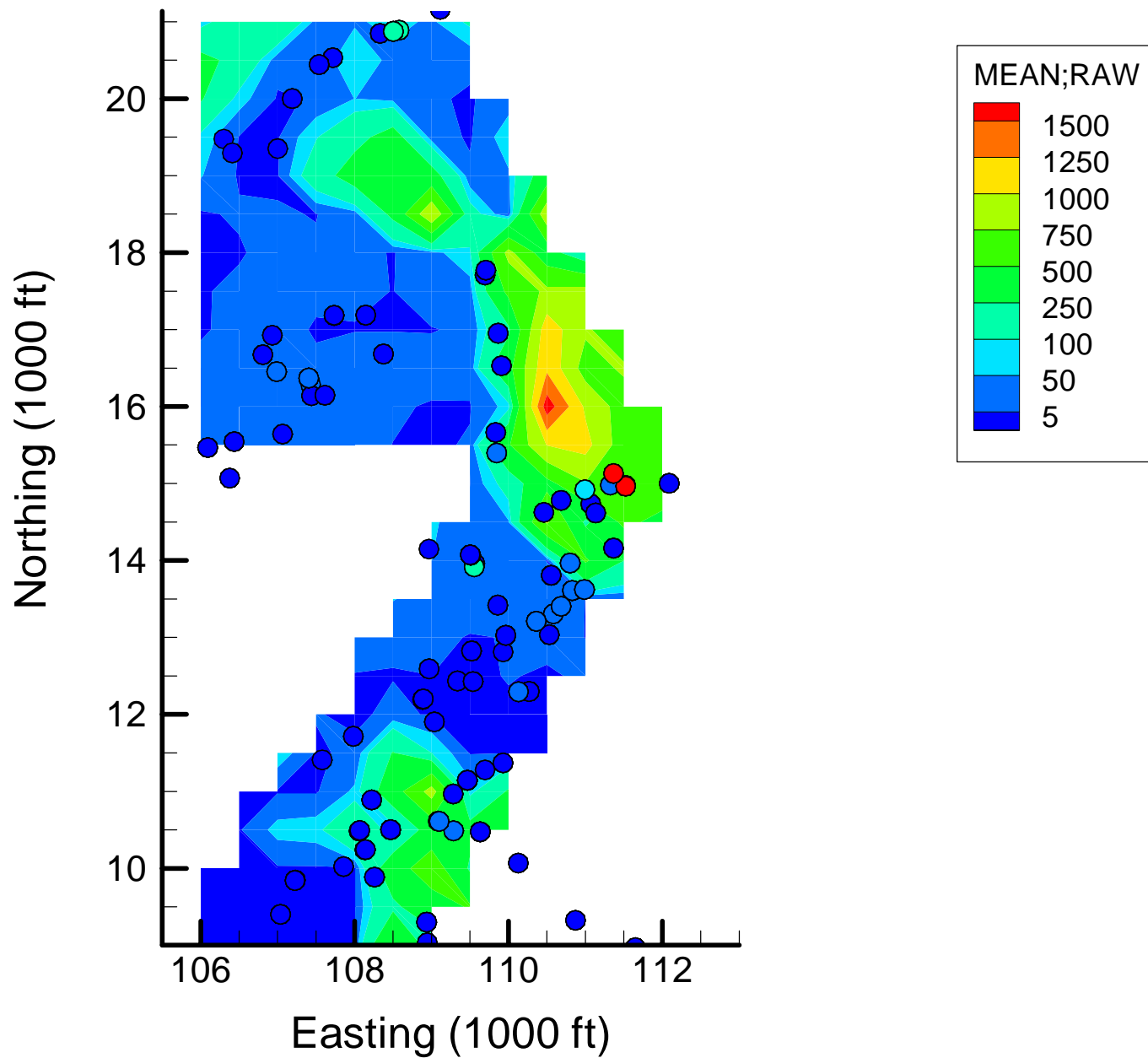
Spatial Optimization: BZ Base Concentration Maps

Notes:

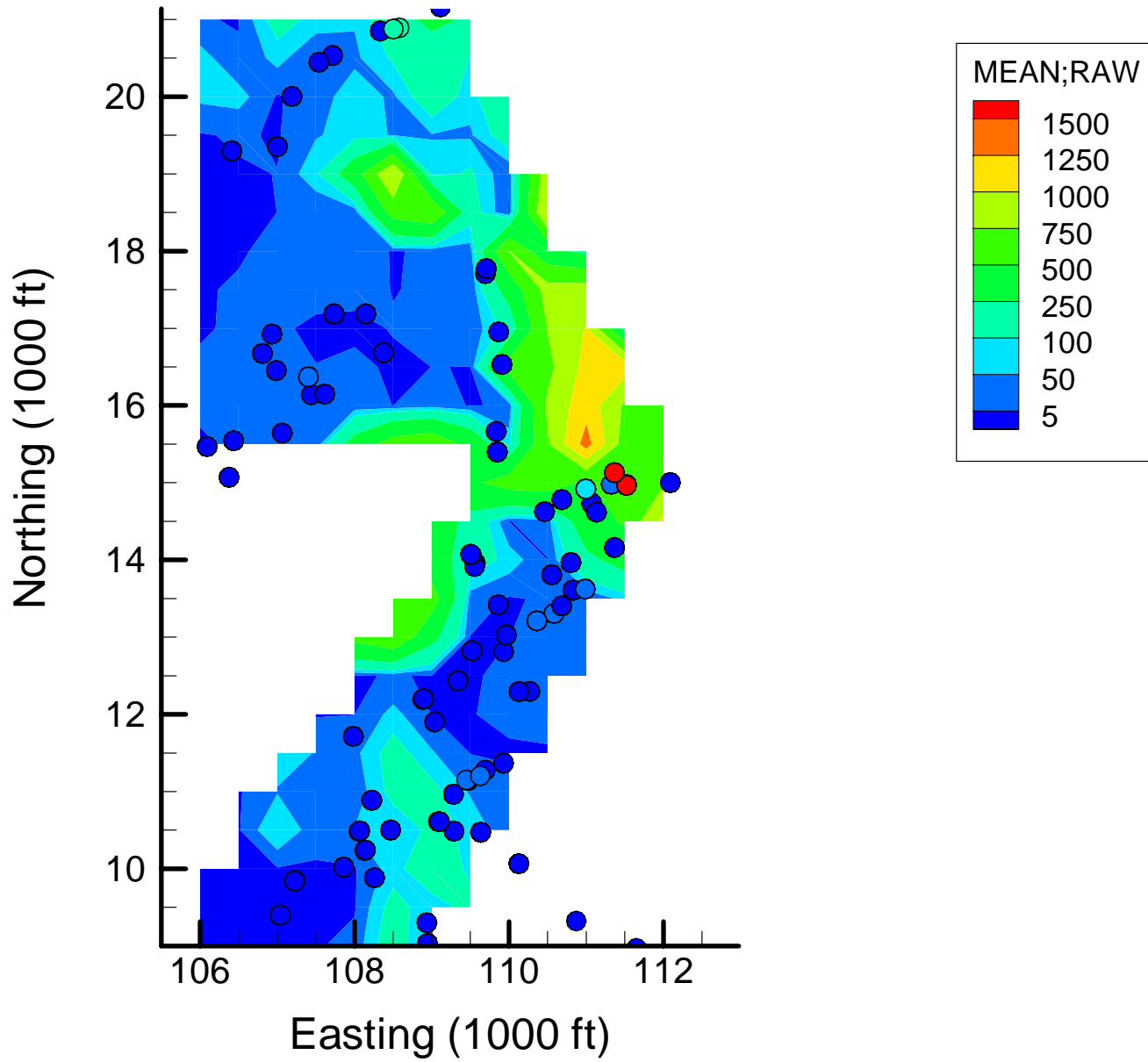
MEAN;RAW = Raw concentration values overlaid on mean locally-weighted quadratic regression (LWQR) estimates, in ppb

Base maps are constructed using all available concentration data

Site OU-12: Benzene Concentrations (ppb), 1999-2000, Base Map



Site OU-12: Benzene Concentrations (ppb), 2001-2002, Base Map



Appendix 4-4

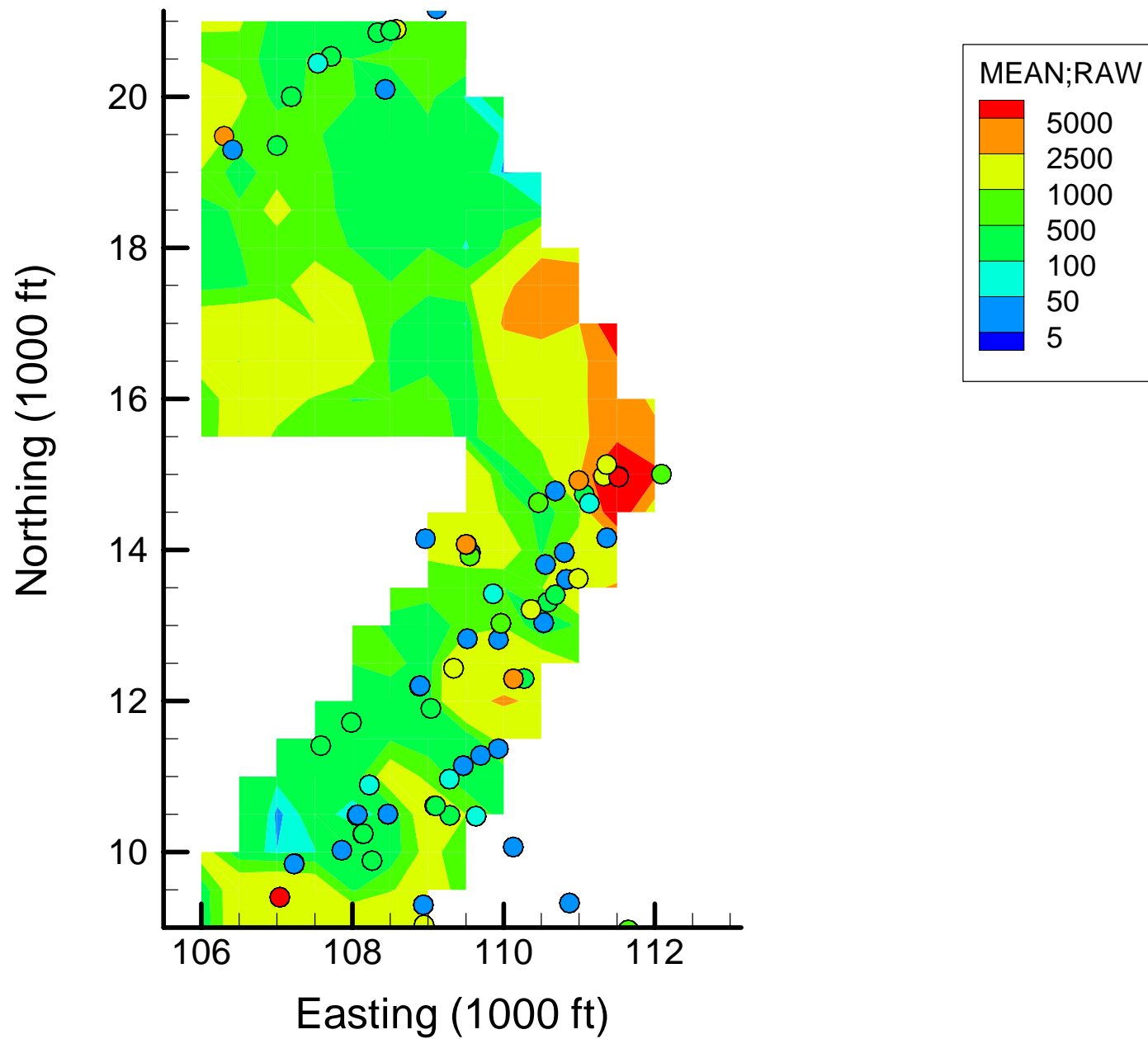
Spatial Optimization: FE Base Concentration Maps

Notes:

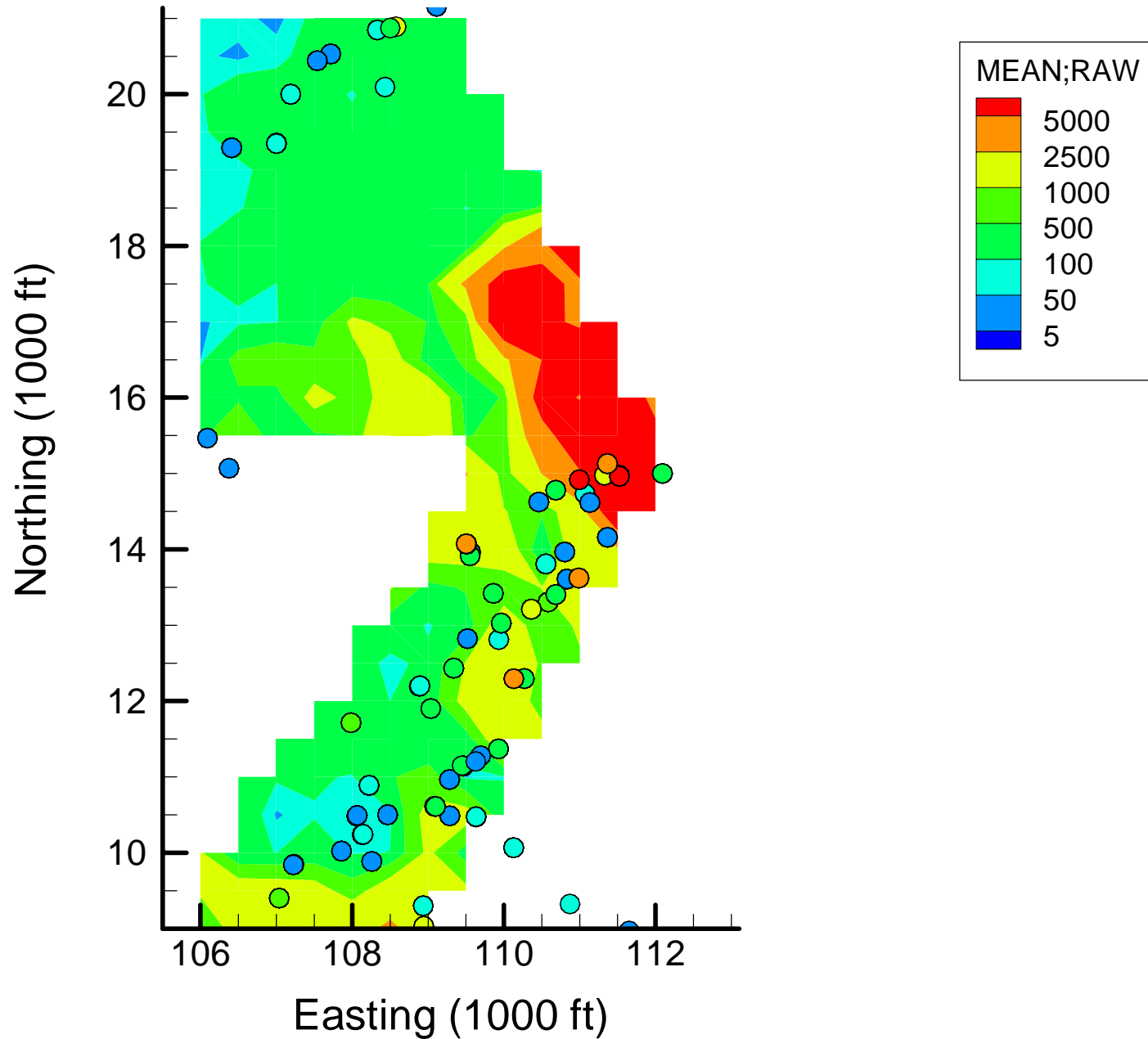
MEAN;RAW = Raw concentration values overlaid on mean locally-weighted quadratic regression (LWQR) estimates, in ppb

Base maps are constructed using all available concentration data

Site OU-12: FE Concentrations (ppb), 1999-2000, Base Map



Site OU-12: FE Concentrations (ppb), 2001-2002, Base Map



Appendix 4-4

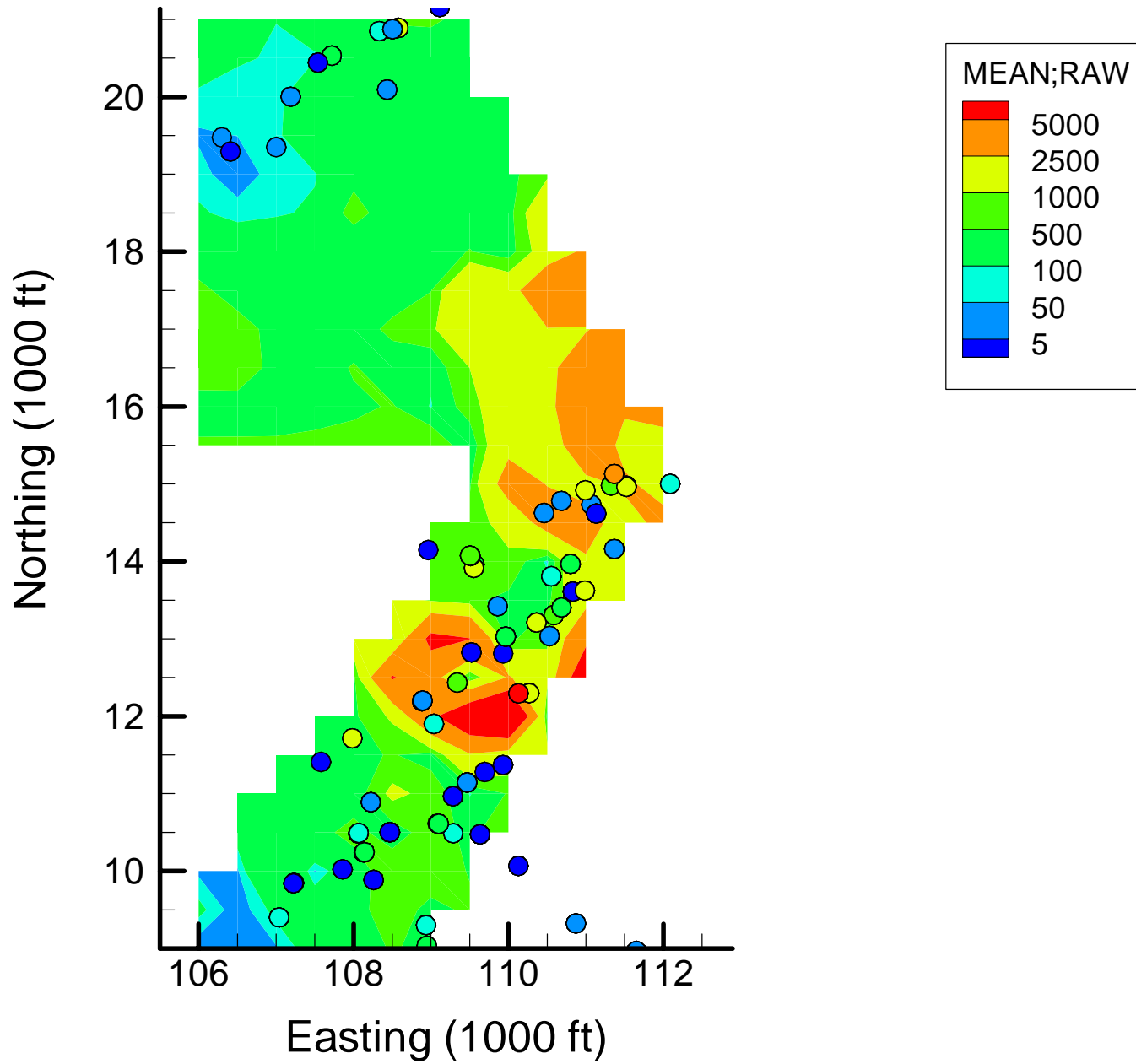
Spatial Optimization: MN Base Concentration Maps

Notes:

MEAN;RAW = Raw concentration values overlaid on mean locally-weighted quadratic regression (LWQR) estimates, in ppb

Base maps are constructed using all available concentration data

Site OU-12: MN Concentrations (ppb), 1999-2000, Base Map



Site OU-12: MN Concentrations (ppb), 2001-2002, Base Map

